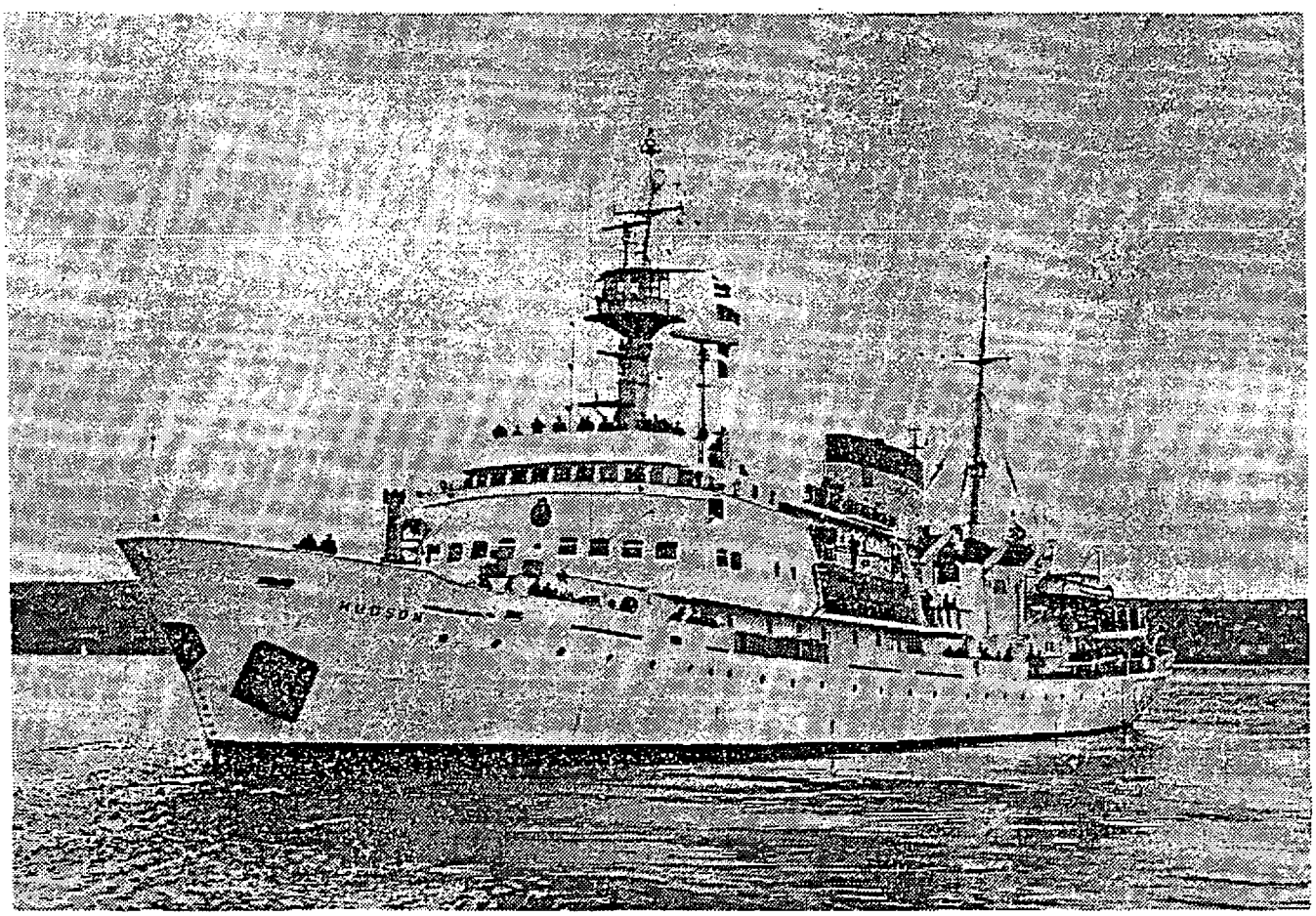
69050

THE HUDSON 70 EXPEDITION

THE

HUDSON 70

EXPEDITION

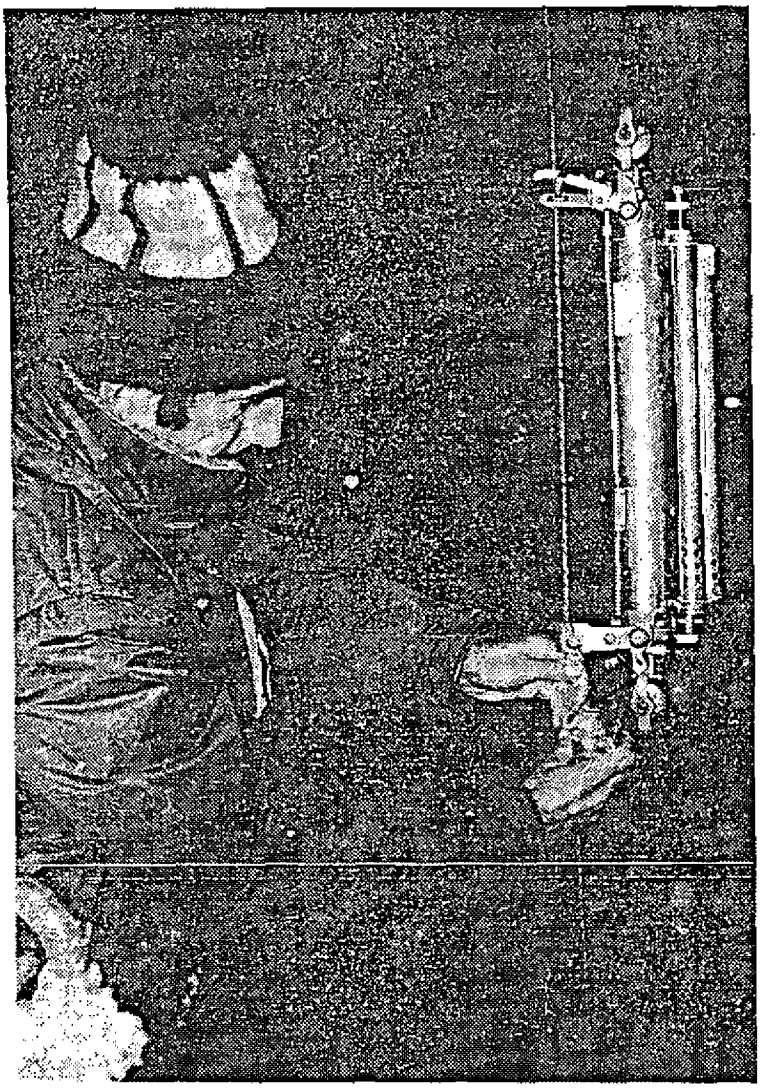


The expedition begins. It is 1535 hours on 19 November 1969 and CSS Hudson is bound for Rio de Janeiro on the first leg of her circumnavigation of the Americas.

ACKNOWLEDGEMENTS

This bound record of the scientific work and results from the HUDSON 70 Expedition was compiled by Robert F. Reiniger and Michael P. Latremouille with the valuable assistance of Ms. Joni Henderson, Mr. Art Cosgrove, Mr. Roger Belanger, Ms. Betty Sutherland, Dr. Allyn Clarke and Dr. Jim Elliott. Other contributors included Dr. R.M. Cameron, Dr. B.D. Loncarevic, Dr. C.D. Maunsell, Dr. B.R. Pelletier, Dr. C.T. Schafer, and Dr. S.P. Srivastava.

FOREWORD



Dr. Cedric R. Mann, leader of the Hudson 70 expedition.

In recognition of the pioneering scientific contributions and the influential leadership provided to Canadian oceanography by Dr. Cedric Robert Mann during the 60's, 70's, and 80's, a period of dynamic growth in Canadian oceanography, this document was compiled and presented to him on the occasion of his retirement from the Department of Fisheries and Oceans in January 1987.

A New Zealander who emigrated to Canada in 1949, Dr. Mann obtained a Ph.D. in physics from the University of British Columbia in 1953, then joined the Defence Research Board's (DRB's) Naval Research Establishment in Halifax where he helped develop Canada's first sonar system. It was in 1961, with the expansion of oceanography by the Department of Mines and Technical Surveys and the construction of the Bedford Institute of Oceanography (BIO), that he transferred from DRB to become one of the original BIO physical oceanographers. Throughout his career, he maintained an active interest in scientific endeavours in addition to playing a prominent role as a science manager in government. In this latter capacity he was

Senior Oceanographer from 1962 to 1965, then in 1965 head of a group that eventually became the Ocean Circulation Division of the Atlantic Oceanographic Laboratory (AOL), Director of AOL in 1975, Director-General of BIO in 1978, and Director-General of the Institute of Ocean Sciences, B.C., from 1979 until his retirement.

Throughout this period as oceanographer, he was a major influence in fostering constructive working relationships between government laboratories, local universities, international scientific organizations and other national laboratories, and served on numerous working groups and advisory boards.

His scientific interests focused on large-scale circulation, mixing, and water mass formation. The principal geographic areas of interest to him were those associated with the interaction between the Gulf Stream and Labrador Current, but over his career he collaborated in studies of Denmark Strait, Venezuela Basin, and Drake Passage. His scientific publications were not without controversy. There was and still is debate over the confirmation that the Gulf Stream extension across the Tail of the Bank is the genesis of the North Atlantic Current, a concept that is now considered correct.

Throughout his career, he had a knack for 'making things happen' in a quiet and unassuming way. The magnitude and breadth of the responsibilities he undertook is exemplified by the Hudson 70 Expedition, a project he guided from its inception. As is evident from this compilation of Hudson 70 material, numerous hours are required to organize the scientific community and funding agencies to put together the plan for such a mammoth project, conduct the various legs, and finally, from the efforts of many individual scientists, interpret the results. Behind this venture was the firm guiding hand of Dr. C.R. Mann. Throughout his career he propelled the oceanographic community like that invisible force in The Rime of the Ancient Mariner by S.T. Coleridge,

"... Slowly and smoothly went the ship,
Moved onward from beneath."

Thank you from your many colleagues.

J.A. Elliott
Director, AOL

TABLE OF CONTENTS

Acknowledgements....2
FOREWORD....3
Chronological Account....6
Captain and Chief Scientists....9
Shipboard Scientific Party....10
An Expedition to. . . (Initial Plan for HUDSON 70)....13
The HUDSON 70 Expedition....31

A. CRUISE REPORTS....35
Data collected during the HUDSON 70 Expedition....37
I and II. Halifax to Rio de Janeiro and Rio de Janeiro to Buenos Aires....83
III. Buenos Aires to Punta Arenas....97
IV. Punta Arenas to Valparaiso....117
V. Valparaiso to Tahiti....127
VI. Tahiti to Vancouver....135
VII. Victoria to Victoria....141
VIII. Victoria to Resolute Bay....163
IX. Resolute Bay to Halifax....177

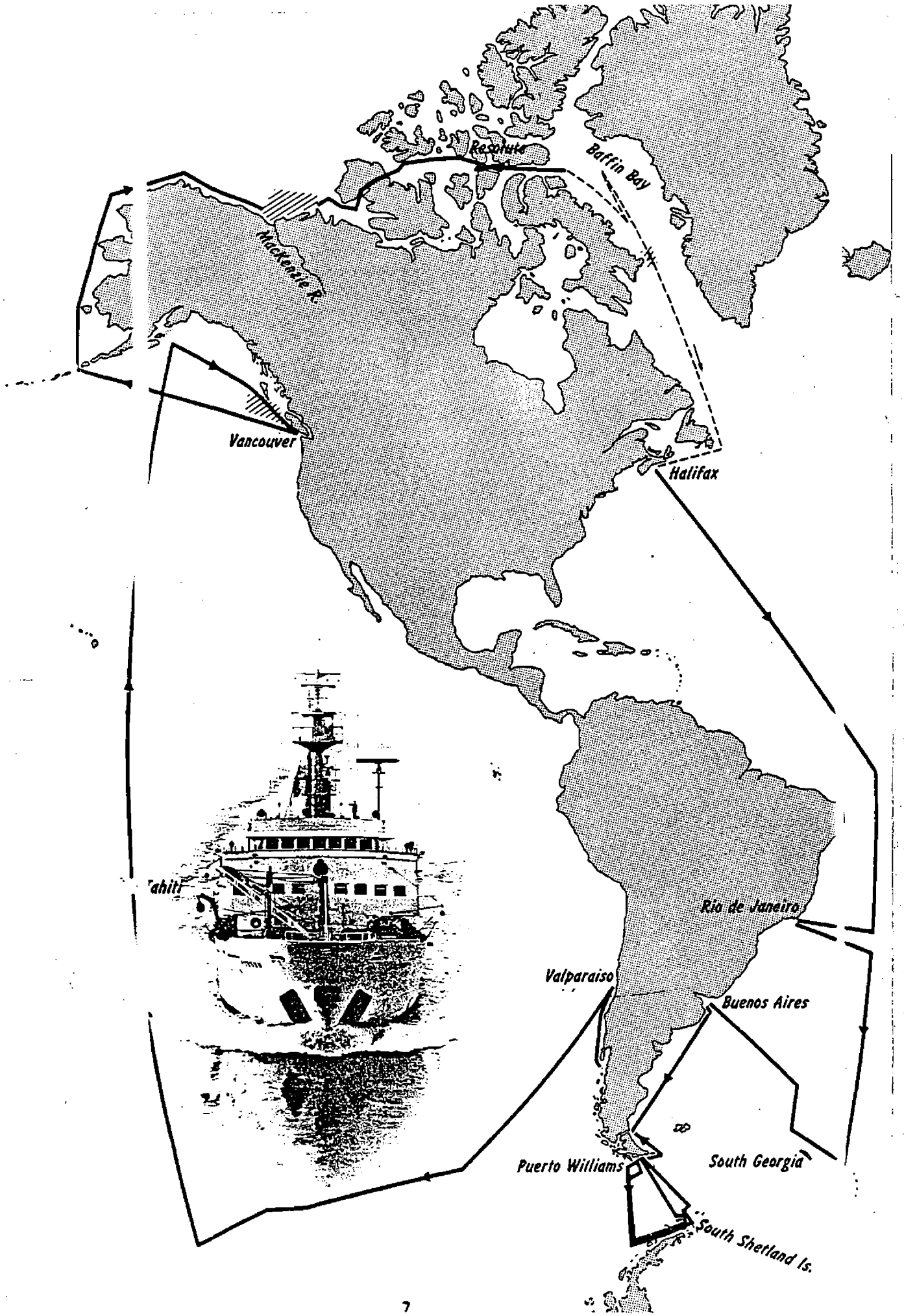
B. ATLAS OF PHYSICAL OCEANOGRAPHIC DATA....189

Atlas of physical oceanographic data for the South Atlantic Ocean, Drake Passage, Pacific Ocean, and Canadian Arctic - 1970....191

C. PUBLICATIONS FROM HUDSON 70....245

A bibliography of published papers....247
Publications....253

Phase	Departure	Date	Arrival	Date	Senior Scientist
I	Halifax, Nova Scotia	19 Nov. 1969	Rio de Janeiro, Brazil	20 Dec. 1969	Dr. C.R. Mann
II	Rio de Janeiro, Brazil	20 Dec. 1969	Buenos Aires, Brazil	16 Jan. 1970	Dr. C.R. Mann
III	Buenos Aires, Brazil	22 Jan. 1970	Punta Arenas, Argentina	23 Feb. 1970	Dr. C.R. Mann
IV	Punta Arenas, Argentina	1 March 1970	Valparaiso, Chile	7 Apr. 1970	Dr. G.L. Pickard
V	Valparaiso, Chile	15 Apr. 1970	Papeete, Tahiti	12 May 1970	Mr. R.C. Melanson
VI	Papeete, Tahiti	16 May 1970	Vancouver, British Columbia	12 June 1970	Dr. W.M. Cameron
VII	Victoria, British Columbia	12 July 1970	Victoria, British Columbia	5 Aug. 1970	Dr. C.D. Maunsell
VIII	Victoria, British Columbia	13 Aug. 1970	Resolute Bay, Northwest Territories	22 Sept. 1970	Dr. B.R. Pelletier
XI	Resolute Bay, Northwest Territories	30 Sept. 1970	Halifax, Nova Scotia	6 Oct. 1970	Dr. D.I. Ross


Resolute
Baffin Bay
Mackenzie R.
Vancouver
Halifax
Rio de Janeiro
Valparaiso
Buenos Aires
Puerto Williams
South Georgia
South Shetland Is.



Captain D. Butler



Dr. W. M. Cameron



Dr. C. R. Mann



Dr. C. D. Maunsell



Mr. R. C. Melanson



Dr. B. R. Pelletier



Dr. G. L. Pickard



Dr. D. I. Ross

SHIPBOARD SCIENTIFIC PARTY

for the

HUDSON 70 EXPEDITION

Ahumada, R.[21]
Atkinson, L.P.[9]
Barrett, D.L.[1]
Bary, B. Mck.[10]
Beamish, P.C.[4]
Beamish, R.J.[12]
Belanger, J.R.[1]
Belleguay, R.[5]
Bhattacharyya, P.J.[9]
Bertrand, W.[6]
Bluy, O.[7]
Bousfield, E.L.[3]
Brewers, P.G.[16]
Brown, R.G.B.[8]
Bruce, J.[1]
Burt, W.V.[18]
Cameron, W.M.[26]
Carson, B.D.[1]
Choi, C.I.[9]
Chase, K.L.[10]
Chuecas, L.A.[21]
Coady, V.[1]
Conover, R.J.[4]
Cooke, F.[11]
Cooke, R.C.[9]
Coote, A.R.[1]
Corbett, T.J.[1]
Corkum, P.L.[1]
Courtney, T.F.[1]
Davidson, R.[10]
Davis, E.[19]
Dean, J.P.[16]
Deevey, G.B.[9]
Densmore, C.D.[16]
Druhan, D.[1]
Duedall, I.W.[3]
Eaton, R.M.[1]
Edwards, R.L.[14]
Faber, D.J.[2]
Foote, T.R.[1]
Freeman, K.F.[4]
English, D.[10]
Garner, D.M.[1]
Gill, J.G.[7]
Gorveatt, M.[1]
Grant, A.B.[1]
Greifeneder, W.B.[1]
Harding, A.[27]
Havard, C.[6]
Haworth, R.T.[1]
Henderson, H.[1]
Hessler, R.R.
Hiltz, R.S.[1]
Hughes, M.[1]
Hyndman, R.[9]
Inostroza, H.M.[21]
Johnston, B.L.[1]
Keen, C.E.[1]
Lalli, C.M.[13]
Landry, L.P.[5]
Lewis, E.A.[1]
Lister, C.R.B.[19]
Loncarevic, B.D.[1]
MacDonald, R.[10]
MacLean, A.[9]
MacPherson, H.A.[7]
Manchester, K.S.[1]
Mann, C.R.[1]
Markham, J.W.[2]
Maunsell, C.D.[1]
McHughen, S.B.[1]
Melanson, R.C.[1]
Michael, A.D.[9]
Mills, E.L.[9]
Montaner, R.E.[22]
Muise, F.[1]
Murray, J.G.[1]
Nielsen, J.A.[1]
Paranjape, M.A.[4]
Parker, R.[6]
Pelletier, B.R.[1]
Pickard, G.L.[10]
Piechura, J.[1]
Pilote, J.M.R.[1]
Pinner, W.[15]
Pond, G.S.[18]
Prakash, A.[4]
Probert, P.[20]
Purdy, G.M.[1]
Rankin, D.[9]
Rebaudi, R.S.[25]
Reiniger, R.F.[1]
Rey, F.R.[21]
Rock, N.R.[24]

Rogers, G.[26]
Ross, D.I.[1]
Sacks, P.L.[16]
Schafer, C.T.[1]
Sharpe, J.H.[9]
Shearer, J.M.[1]
Sheldon, R.W.[4]
Shih, K.G.[1]
Silva, N.[23]
Smith, R.[11]
Solowan, P.A.[1]
Srivastava, S.P.[1]
Steele, J.P.[1]
Storm, M.P.[10]
Strad, J.[15]
Sutcliffe, W.H.[4]
Taylor, B.[1]
Thomlinson, A.[1]
Tiffin, D.[5]
Toom, H.[1]
Uccelletti, B.D.[22]
Vilks, G.[1]
Von Arx, W.[16]
Wadhams, P.[1]
Wagner, F.J.E.[1]
Wangersky, P.J.[9]
Watt, W.[9]
Whiteway, W.J.[1]
Winters, D.[1]
Wong, C.S.[5]
Woodside, J.M.
Yorath, C.[6]
Yoshinari, T.[9]
Zurbrigg, R.E.[12]

Footnotes

1 Atlantic Oceanographic Laboratory, Bedford Institute, Dartmouth, N.S.

2 National Research Council of Canada, Ottawa.

3 National Museum of Natural Sciences, Ottawa.

4 Marine Ecology Laboratory, Bedford Institute, Dartmouth, N.S.

5 Pacific Oceanographic Group, Nanaimo, B.C.

6 Geological Survey of Canada, Ottawa.

7 Defence Research Establishment Atlantic, Dartmouth, N.S.

8 Canadian Wildlife Service, Bedford Institute, Dartmouth, N.S.

9 Institute of Oceanography, Dalhousie University, Halifax, N.S.

10 Institute of Oceanography, University of British Columbia, Vancouver, B.C.

11 Queen's University, Kingston, Ontario.

12 University of Toronto, Toronto, Ontario.

13 McGill University, Montreal, Quebec.

14 Trent University, Peterborough, Ontario.

15 Highland Helicopter Ltd., Vancouver, B.C.

16 Wood's Hole Oceanographic Institution, Wood's Hole, Massachusetts.

[17] Scripps Institution of Oceanography, La Jolla, California.

[18] Oregon State University, Corvallis, Oregon.

[19] University of Washington, Seattle, Washington.

[20] Royal Navy.

[21] Universidad de Conception, Chile.

[22] Instituto Hidrografico, Chile.

[23] Universidad Catiolica, Valparaiso, Chile.

[24] I.O. Sao Paulo, Sao Paulo, Chile.

[25] Argentine Navy, Buenos Aires, Argentina.

[26] Marine Sciences Branch, Department of Energy, Mines and Resources, Ottawa.

[27] Hunting Ltd., U.K.



CANADA

DEPARTMENT OF ENERGY, MINES AND RESOURCES
MARINE SCIENCES BRANCH

MINISTÈRE DE L'ÉNERGIE DE MINES ET DES RESSOURCES
DIRECTION DES SCIENCES DE LA MER

ATLANTIC OCEANOGRAPHIC LABORATORY

BEDFORD INSTITUTE

LABORATOIRE OCEANOGRAPHIQUE DE L'ATLANTIQUE

INSTITUT de BEDFORD

Dartmouth, Nova Scotia
Canada

HUDSON 70

AN EXPEDITION TO THE SOUTH ATLANTIC SOUTHERN AND PACIFIC OCEANS

and the

CANADIAN ARCHIPELAGO

by

C. R. MANN

AUGUST, 1968

PROGRAMMED BY

THE CANADIAN COMMITTEE OF OCEANOGRAPHY

A Note to the Reader

This report describes the initial plan for the HUDSON 70 Expedition as prepared by Dr. C.R. Mann during the winter and summer of 1968. More than a year of preparations followed the publication of the report and the basic plan was modified accordingly. Much of the work done during HUDSON 70 did nevertheless follow the basic outline and therefore the report is included here as part of the official record of the expedition.

HUDSON 70

INTRODUCTION

HUDSON 70 is the title of a major, multi-disciplinary, oceanographic expedition planned for the C.S.S. Hudson for the period November, 1969, to October, 1970. The scientific work of the expedition, involving the fields of biological, chemical and physical oceanography, underwater acoustics, geodesy, geophysics, geology and hydrography, would be implemented as a series of operations in several areas around the Americas and on the tracks to and from these areas; see Cruise Track, Figure 1. It is largely composed of projects which have been under consideration for up to several years but which, singly, have not warranted taking a major research ship over the distances involved. By a process of collaborative assessment, selection and coordination, a program encompassing the projects of thirteen principal investigators has been devised which takes full and efficient advantage of the capabilities of the ship and provides, for many of the projects, a mutual interaction vital to the realization of their individual purposes. A chronological summary of the plan of work is given in Part I and a resume of the scientific background and objectives of the studies is given in Part II together with a list of the principal investigators.

The attainment of the far-reaching objectives for the expedition would contribute significantly to the solution of problems of interest to Canada and would be a substantial contribution to the International Oceanographic Decade planned for 1970-80. If completed as envisioned, it would not only break much new scientific ground in the world ocean but progress several outstanding projects on the continental margin of Canada and, incidentally, result in the first circumnavigation of the Americas.

Initial Plan for HUDSON 70...Published in 1968

PART I

The circumnavigation will be made clockwise as this places the ship in the areas of interest at the most favourable times of the year.

CHRONOLOGICAL ACCOUNT OF THE PROGRAM

PHASE I

Leave Halifax	19 November 1969
Arrive Rio de Janeiro	15 December, 1969

On leaving Halifax, the ship will proceed directly to Latitude 5°N, Longitude 30°W. Enroute, Gravity, Magnetics and Expendable Bathythermographs will be made underway. These will be continued throughout the cruise. Measurements of temperature, salinity, nitrate, phosphates, silicates, organic carbon and other chemical properties will be made at stations along the 30th meridian of longitude for the chemistry and physical oceanography programs.

Plankton hauls will be made for the program in micropaleontology.

Measurements will be made of the physical characteristics of the scattering layer.

Measurements of gravity and deflection of gravity vertical will be made for the program in geodesy.

Along selected sections of the track, underway seismic profiles will be obtained.

PHASE II

Leave Rio de Janeiro	20 December, 1969
Arrive South Georgia	9 January, 1970

The ship will proceed south along the 30th meridian and continue the measurements along the line of stations for the chemistry, physical oceanography and micropaleontology programs. At selected positions, cores will be made for the program in micropaleontology.

Trawls and plankton hauls will be made for the biological program in the Atlantic. The geodesy program will continue.

PHASE III

Leave South Georgia	11 January, 1970
Arrive Punta Arenas	26 January, 1970

Initial Plan for HUDSON 70...Published in 1968

A zig-zag track will be followed from South Georgia to the Drake Passage to delineate the shape of the Antarctic Convergence. At selected stations along this track, measurements for the programs commenced on the southerly line of stations will be continued.

A line of stations will be run across Drake Passage to provide information for planning the current measurements in Phase IV.

PHASE IV

Leave Punta Arenas	29 January, 1970
Arrive Punta Arenas	26 February, 1970

During this phase, current meters will be installed in Drake Passage to study the circumpolar current, and supporting measurements made of the distribution of temperature and salinity. The meters will be recovered at the end of the period.

Magnetic induction equipment will be installed in shallow water in the Magellan Passage area and recovered.

Bottom samples will be obtained off the Falkland Islands for studies of deep benthic fauna.

PHASE V

Leave Punta Arenas	1 March, 1970
Arrive Valparaiso	7 April, 1970

This phase of the cruise is devoted to studies of the Chilean Fjords. Temperature, salinity and chemical parameters will be measured and plankton hauls and bottom samples will be taken throughout the fjords to study their physical, chemical and biological characteristics.

PHASE VI

Leave Valparaiso	14 April, 1970
Arrive Vancouver	13 June, 1970

The ship will leave Valparaiso and proceed to a position as far south on the 140th. west meridian as possible. She will then proceed to run north through the South and North Pacific Oceans to Vancouver. A stop will be made in the Marquesas Islands.

Measurements of temperature and chemical properties of the water will be made on a series of 24 stations up the Pacific for the programs in chemical and physical oceanography. A closely spaced series of measurements will be made across the equatorial current.

Initial Plan for HUDSON 70...Published in 1968

Measurements of the physical characteristics of the scattering layer will be resumed and biological sampling will be conducted at the same time.

Measurements of gravity and deflection of vertical for geodesy will be continued from the Atlantic. This long south-to-north transect is the major part of the program.

Underway measurements of gravity and magnetics will be made for the geophysics program.

PHASE VII

Leave Vancouver	20 June, 1970
Arrive Victoria	1 August, 1970

During this six weeks, a detailed geophysical study will be made of the continental margin west of British Columbia.

PHASE VIII*

Leave Victoria	8 August, 1970
Arrive Resolute	6 September, 1970

The ship will proceed through the Bering Strait to the MacKenzie Delta. Cores and plankton hauls will be made enpassage. Cores and seismic studies will be made of the Delta. Enroute through the Northwest Passage reflection profiling will be done for sediment studies.

PHASE IX*

Leave Resolute	8 September, 1970
Arrive Halifax	13 October, 1970

A detailed survey of gravity, seismics and magnetics in Baffin Bay. A second ship will rendezvous with Hudson for two ship seismics.

The geology program will continue with cores and plankton hauls.

Ice potential stations will be occupied on the run south to Halifax.

*Phases VIII and IX will be undertaken only if the ice conditions in the Northwest Passage permit; if not, the ship will depart Victoria for Halifax via Panama Canal.

Initial Plan for HUDSON 70...Published in 1968

THE SCIENTIFIC OBJECTIVES AND BACKGROUND

Principal Investigators

Chemistry:	Prof. K. Park - Oregon State University
	Prof. P. Wangersky - Institute of Oceanography, Dalhousie University
Physical Oceanography:	Dr. C.R. Mann - Atlantic Oceanographic Laboratory, Bedford Institute
	Prof. W.S. Von Arx - Massachusetts Institute of Technology and Wood's Hole Oceanographic Institution
Biology:	Dr. L.M. Dickie - Marine Ecology Laboratory, Bedford Institute
	Dr. R.J. Conover - Marine Ecology Laboratory, Bedford Institute
Acoustics:	Dr. R.P. Chapman - Defence Research Establishment Atlantic
Geophysics:	Dr. B.D. Loncarevic - Atlantic Oceanographic Laboratory, Bedford Institute
	Dr. D.I. Ross - Atlantic Oceanographic Laboratory, Bedford Institute
Chilean Fjords:	Prof. G.L. Pickard - Institute of Oceanography, University of British Columbia
	Prof. R.J. Scagel - Institute of Oceanography, University of British Columbia
Geology:	Dr. B.R. Pelletier - Atlantic Oceanographic Laboratory, Bedford Institute
	Dr. G.A. Bartlett - Atlantic Oceanographic Laboratory, Bedford Institute

CHEMISTRY AND PHYSICAL OCEANOGRAPHY

These two programs will be discussed together as the chemistry relates to the large scale movements of water masses. The new techniques developed for chemical measurement allow much more precise definition of chemical features of the ocean than has been possible in the past. They also make it possible to study the different chemical parameters simultaneously. This has not been done extensively because of the labour involved using older techniques. As a result, features such as

dissolved nutrients have not been used as effectively as they could in the study of the movement of large water massaes. The north-south line in the South Atlantic runs through the deep waters moving into the North Atlantic from their source in the Antarctic, and is ideal for the purpose of studying these deep movements and for testing the new techniques. The studies along the line are related to part of the Biological program discussed later. The cruise will also provide the opportunity of comparing the chemical features of the Atlantic and Pacific using the same equipment, thus obviating the difficulties of intercalibration.

CHEMISTRY - K. PARK, P. WANGERSKY

1. Study of the distribution of dissolved and particulate organic matter in the deep layers of the ocean

The non-living particulate organic material suspended in the water column is the major source of food for the organisms living in the ocean depths. Evidence has now accumulated to suggest that a large part of this particulate material is derived from aggregation of dissolved organic materials, and that some sort of equilibrium exists between the dissolved and particulate fractions of the organic matter in the ocean.

The dissolved organic fraction must be largely released into a water mass while it is at or near the surface of the ocean. The distribution of dissolved organic carbon in near-surface waters would suggest that the greatest amounts of soluble carbon compounds are released in the very surface layer. Once the water mass has cooled and left the surface, the dissolved organic content should decrease as new particles are formed, replacing those eaten by the organisms of the deep sea.

Since the dissolved organic fraction is about ten times the size of the particulate fraction, the decrease brought about in this fashion is too small to be picked up by analytical methods in any single station. A series of stations is needed to sample the Antarctic Deep Water at varying distances from its origin. If the theory is correct, the dissolved organic carbon content of this water mass should vary inversely with the distance from the point of origin. The sampling program should be carried out in the South Atlantic and Pacific to give a relatively unambiguous picture of the water structures involved, and because the Antarctic is the source of the bottom water of the world oceans.

Similar studies will be carried out in the equatorial under-currents in both oceans. The water in these easterly flowing currents was last at the surface in the west. As biological life excretes inorganic carbon, the dissolved organic carbon should be diminished and the inorganic carbon should increase from west to east. Some measurements have shown a higher organic carbon in the case of the counter current than in the water on either side. Detailed and precise chemical sections across both undercurrents should be made to study this problem. Only one section can be made in each ocean during the cruise, but these will provide a comparison with the same equipment and will check whether the anomalous

distribution is correct.

2. Precise definition of the preformed and oxydative nutrients in the ocean - Silicates, Nitrates and Phosphates

Preformed nutrients are conservative properties of a water mass and are defined as the amount of inorganic nutrients which existed in the water before it sank from the surface layer. Oxidization or organic matter in situ changes the total inorganic nutrients but not preformed concentrations. The latter can be calculated by subtracting from the total quantity measured, the oxidative portion calculated from the oxygen distribution. Distributions of the preformed nutrients can then be used to study large scale movements of water masses. This technique is under study and has been applied with success to the Subarctic boundary in the Pacific. Suitable measurements are not available on an ocean wide scale. The two lines in the Atlantic and Pacific will provide data which can be used to study the northerly movement of the deep water masses from their source in the Antarctic. A considerable advantage of the cruise is that the measurements will be made in both oceans with the same new equipment.

Recent studies at Bedford Institute of the dissolved silica distribution through the Atlantic show that this particular nutrient may be very useful. The deep waters formed in the Antarctic have dissolved silica values as high as 150 mg atoms/litre. The silica content of the deep water flowing into the Atlantic through the passages between Greenland and Scotland by contrast is as low as 5 mg atoms/litre. This great contrast between the dissolved silica content of the source waters of the deep Atlantic makes studies of the movement and mixing of the water masses using dissolved silica as a tracer very profitable but considerably more data is needed on an ocean wide basis.

3. Determination of the Alkalinity to Salinity ratio

This ratio does not vary with the addition or removal of fresh water from the ocean. It does, however, change with the decomposition of organic and carbonate material from the skeletons of falling organisms. There should then be a gradual increase in the ratio related to the age of the deep water. This effect can be studied along the north-south lines. The changes are small and measurements need to be made over many hundreds of lines through the water masses.

The measurements of pH which are necessary for this work will also be used to study the effect of pH on the conductivity/chlorinity relationship. Recent work has shown that this effect could be important in relationship to the changes in chlorinity that are often used to study movement of water masses under the assumption that the chlorinity is a conservative property. The effect has not been measured on an ocean wide basis and it is important that it be done.

Initial Plan for HUDSON 70...Published in 1968

4. Transport of carbon into the air masses

There is evidence that carbon can be transported from the water into the air masses and that the carbon which escapes more than a few metres into the air is able then to rise to considerable distances in the atmosphere. This results from the large particles falling out in the first few metres. The cruise will provide an excellent opportunity to make the necessary measurements to study this effect. They must be conducted far from land and over a long enough period to obtain a meaningful sampling.

PHYSICAL OCEANOGRAPHY - C.R. MANN, W.M. VON ARX

1. Large scale deep water circulation and thermal microstructure

The present description of the large scale movement of water masses south to north is based on East-West sections, and on data obtained with conventional sampling techniques which yield data at discrete depths. These sections are spaced far apart and the resulting description of the south-north changes in the temperature and chemical properties is poor. The section in the Atlantic is designed to provide a detailed south-north description of the water masses. Temperature will be measured with newly developed equipment which gives a continuous record of temperature as a function of depth. This will enable a much more detailed examination to be made of the layering of the water masses than has been possible in the past.

Of importance in these studies are measurements of the thermal microstructure, or the occurrence of very thin layers the order of one to twenty metres thick. If these do occur, it is possible in some circumstances for the mechanism of the vertical transport of heat and salt to be different to that normally envisioned. This results in different rates of vertical diffusion of heat and salt. The section should determine whether this layering occurs in water moving north at intermediate depth and at the Arctic Convergence where the water mass converges and sinks below the surface. Besides providing information on the Arctic convergence, the section will be useful in studying the layering phenomena in a situation where a convergence is well developed, and not obscured by a complex current system as in the North Atlantic.

The cruise will also provide the opportunity to obtain measurements of the thermal microstructure in the two equatorial undercurrents where a strong shear occurs in both horizontal and vertical directions.

2. Deep circulation in the Argentine Basin

On the basis of theoretical studies, there should be a well defined deep current flowing north in the Argentine Basin, part of which may flow east in the northern part still as a relatively narrow current. The data obtained on west-east lines cannot be expected to show this. If the current exists, it should appear in the section to be run along the 30th meridian.

Initial Plan for HUDSON 70...Published in 1968

3. Flow of Antarctic Bottom Water North into the Argentine Basin

Recent evidence indicates that the bottom water from the Weddell Sea flows north around South Georgia and into the Argentine Basin through a very narrow channel. Estimates of the volume of this current place it as high as 90 million cubic metres per second. These estimates have been made on the basis of fragmentary data. The southern line together with a partial line in the vicinity of 36°W. long. will provide detailed sections across this current from which better estimates of the transport can be made. As this is the source of the bottom water of the whole Atlantic, a good estimate of the volume is of importance.

4. Current measurements in Drake Passage

As the oceanographer's ability to moor equipment in the open ocean has improved, it has been possible to commence attempting direct measurements of current velocities and hence of transports in critical areas of the ocean where knowledge of the volume of water transported is of importance. Present estimates of volumes are based on indirect computations from observations of temperature and salinity. This type of estimate without current meter data to support it, can be far from correct.

One of the important passages in the world ocean is the Drake Passage through which flows the Antarctic Circumpolar Current. Estimates of the volume transport of this current will be made by direct current measurement in the Drake Passage together with temperature and salinity sections which may then be compared with theoretical studies of this major ocean current.

As part of the geodesy program, an attempt will be made to measure the slope of the sea surface across the Passage. With this measurement, the barotropic current can be estimated, which together with the baroclinic component obtained from the temperature, salinity data gives an estimate of the transport which should agree with the estimate based on current meter measurements.

5. Definition of an equipotential surface of the oceans and measurements of the slope of the physical sea surface

The object of this experiment is to provide an equipotential or level-surface datum at sea. If such a surface can be obtained, it provides a reference which may be used to study ocean transport, tides, eustatic changes in sea level, the regimen of continental ice sheets and other effects, using microwave-laser altimetry from orbiting satellites. Essentially, the experiment is to define the shape of the geoid with precision sufficient for these purposes.

The shape of the geoid can be determined at sea by measurement of gravity with some uncertainty concerning the amplitudes of undulations which occur. These uncertainties can be removed if the angle between gravity vertical (which is normal to the geoid) and a vertical normal to

the spheroid can be measured. This can be accomplished with a system GEON (Gyro Erected Optical Navigation) developed by Von Arx at the Massachusetts Institute of Technology, which enables measurements of the deflection of vertical to be obtained. If accurate, gravity measurements are made simultaneously and satellite navigation is available for accurate positioning, the shape of the geoid may be found.

To undertake these measurements, long north-south transects and equatorial east-west transects are required in both oceans. It is proposed to assemble the system and make the north-south transects on the cruise.

A part of this program will be devoted to measurements of the tilt of the physical sea surface in certain areas. This has been dealt with in connection with the work in Drake Passage.

BIOLOGY - R.J. CONOVER, L.M. DICKIE

1. The chemical composition and physiology of submergent plankton species

The primary objective is to study the distribution, chemical composition and physiology of submergent plankton species in relation to the antarctic and subtropical convergences. The primary concern is with inhabitants of the antarctic intermediate water. It is thought that certain planktonic species which inhabit colder waters near the surface can be used as chronometers when these cold waters are introduced into the deeper ocean at zones of convergence. Such species would be herbivorous, fat-storing forms, which are unable to feed in deeper water because of the lack of suitable food but which would survive for some period of time, which we hope to determine, by subsisting on stored energy.

An acoustically controlled, telemetering plankton sampler, now being built, will enable sampling of a given stratum with considerable precision. The net can take three uncontaminated tows per haul and would be used to catch organisms from below, in and above the antarctic intermediate water.

A north-south plankton section or sections from well north of the subtropic convergence down to the antarctic convergence is necessary. Sampling will be in the upper 1500 metres (depending on water mass distribution) and accurate and immediate information about the vertical distribution of different water masses is required. The bathysonde observations made in the physical oceanographic program should be ideal for this purpose.

2. Biology of the scattering layer

Acoustic studies have shown the presence (over the world oceans) of layers of biological materials which scatter sound. Estimates of fish

densities in the layers show that they contain more organic material than any other source. Many aspects of these layers are not understood. Sampling by scientists in the Atlantic and Pacific show consistent differences in the size and species of the fish population of the scattering layer, however, it is not certain whether these are real or due to differences in sampling techniques and interpretation. In both oceans, a north-south distribution of size and species appears. This raises the question whether the biological life in the layers is influenced greatly by the distribution of water masses in the ocean or by the supply of nutrients. The nutrient distribution may itself be determined by the water mass distribution in any area.

To study these problems, sampling of the fish population in the scattering layers will be done along with the sound scattering experiments. These measurements together with the chemical and physical oceanography programs, will provide the first definitive description of the scattering layer in both oceans, with the same equipment, and of the environment in which the scattering layer occurs.

SOUND SCATTERING FROM MARINE ORGANISMS - R.P. CHAPMAN

In recent years, underwater acousticians and marine biologists have shown an increasing interest in reverberation from the ocean volume. The former are interested because sound scattered by marine organisms constitutes an important component of the sonar background; the latter are interested because underwater acoustics is a powerful tool for obtaining information on such organisms. The most effective marine scatterers of sound, at least at frequencies below a few tens of KHz, are resonant, indicating that they are bathypelagic fish or siphonosphores which use gas bladders to control their buoyancy.

In the deep ocean, marine organisms are found in horizontal layers in the depth interval between the sea surface and several hundred metres. Some experience diurnal migrations, rising towards the sea surface at sunset and returning to depth at sunrise. Because the scattering properties of such organisms depend on their depth and size, pronounced changes in the acoustic properties of scattering layers would be expected with time of day and location.

Since 1959, Defence Research Establishment Atlantic has been investigating the volume reverberation background in the North Atlantic; thirteen experiments have been carried out between Halifax and Puerto Rico, Halifax and Gibraltar, and St. John's and the Norwegian Sea. From these experiments, it appears that the acoustic properties of reverberation vary with the oceanographic province of water mass. It would be thus desirable to test this hypothesis in different ocean areas and water masses. The proposed cruise would be ideal for this purpose.

Two types of data are to be obtained:

(a) Scattering strength of the water column and its variation with location and time of day

This measurement requires a very simple experimental arrangement using an omnidirectional hydrophone and explosive. During the various "legs" of the cruise, it would be desirable to carry out this measurement two times per day, once in the period between two hours after sunset and two hours before sunrise and once in the period between two hours after sunrise and two hours before sunset.

(b) The resonant frequency and depth of scatters during a sunset migration

This requires a downward looking wideband array and point charge. From the data obtained, it will be possible to estimate the size and numbers of scatterers and how they behave; are they in schools and are they relatively complicated organisms capable of adjusting the size of their swim bladder during migration? A total of six charges will be fired equally spaced over the period from two hours before to two hours after sunset. If the handling procedure for this equipment could be so streamlined, it would also be desirable to carry out measurements with it as for (a) above.

GEOPHYSICS - B.D. LONCAREVIC, D.I. ROSS

1. Geophysics studies west of Vancouver Island

Canada is one of the few countries in the world which spans a continent. This provides Canadian Geophysicists with the opportunity of studying the geophysical structures on either side of a continent and to make progress in the understanding of theories such as that of Continental Drift. If the drift is westward, the east side of the continent goes with the ocean floor and the west side overrides it. This must result in a considerable difference in the geological and geophysical features from the shore to the abyssal plain (the continental margins).

Studies of gravity, seismics and magnetics and the assembly of the complex shipboard equipment for these measurements has proceeded at Bedford Institute for several years, and considerable information obtained about the east coast features of Canada.

2. Studies of Lancaster Sound and Baffin Bay

These studies will be a continuation of initial studies of magnetics in the area done by Bedford Institute. Baffin Bay should have a thin oceanic crust. There is some evidence that the crust is thick and Continental in character. To resolve this, a survey of the area using seismic and gravimetric techniques is necessary as well as magnetics. It is proposed that this be done as part of the Circumnavigation with the equipment assembled on Hudson. To carry out the seismic work, a second ship will rendezvous with Hudson in the area.

Initial Plan for HUDSON 70...Published in 1968

3. Underway gravity and magnetics

The world is largely covered with water and many of the geophysical measurements necessary for an understanding of its crust and interior must be made shipboard. Excepting for catastrophic events, changes in the crust occur slowly. This enables the geophysical community to gradually build a description of the crust from measurements made on separate cruises. From these measurements, there is evolving a picture of the ocean basins and their geophysical features. To contribute to this world-wide exploration, magnetics and gravity will be measured together with precision echo-sounding along all tracks. The latter will be a contribution to GEBCO. It is also hoped that underway seismic reflection and refraction equipment which is being tested on Hudson will be ready and seismic sections may be made on features of particular interest.

PHYSICAL, GEOLOGICAL AND BIOLOGICAL CHARACTERISTICS OF FJORDS OF SOUTHERN CHILE, AND MARINE BENTHONIC ALGAE OF SOUTHERN CHILE - G.L. PICKARD, R.S.SCAGEL

1. Chilean Fjords

The major fjord coasts in the world are those of Norway, Greenland, eastern Canada, western North America (British Columbia and Alaska), Chile and southern New Zealand. Many of the fjords in Norway were studied by Norwegian oceanographers in the earlier part of this century. The fjords of eastern Greenland are very difficult to access and have been little studied, while some study has been made of those in western Greenland. Some of the fjords in eastern Canada (Newfoundland and Baffin Island), have been studied by Dunbar and associates of McGill University. Almost all of the fjords in British Columbia have been investigated by Pickard and associates in British Columbia and recently this study has been extended to most of the larger fjords in southeast Alaska. (Some 50 scientific papers, 14 M.Sc. and 6 Ph.D. theses have resulted from these U.B.C. studies). The few fjords in southern New Zealand are currently being studied by the New Zealand Oceanographic Institute. Of the extensive fjord system in southern Chile, little oceanographic investigation has been made at all.

There are significant differences between the water property distributions in the fjords in the two most studied regions, Norway and British Columbia/Alaska. The differences stem in part from the smaller river runoff in Norway than in Northwest America, and in part from the shallow entrance sills that are more common in Norway than here. From the Chilean fjords, there is little information on river runoff but much could be inferred from the salinity and transparency distributions. From the available Chilean charts, shallow sills appear to be uncommon but the sounding detail is sparse and more measurements are needed, although salinity and oxygen distributions in the fjords would themselves give a very good indication of the existence or otherwise of sills.

Topographically, the Chilean fjords appear to be similar to those of British Columbia and southeast Alaska. The two systems differ in the oceanic regime outside. The British Columbia and Alaska fjords open to the relatively low salinity, warm north Pacific waters whereas those of Chile open on to the cold, more saline Antarctic waters of the Humboldt Current system. Many of the southern fjords of Chile have icebergs from glaciers in them, a feature which does not occur in British Columbia at all. Recent investigations in Alaska have shown that such "iceberg" fjords have markedly different oceanographic characteristics from those without icebergs. The flora and fauna of the chilean fjords and the character of the bottom deposits are unknown.

The cruise will provide the opportunity for a thorough study of the distribution of temperature, salinity and dissolved oxygen content of the waters of the fjords off the coast of Chile, and of the bottom sediments and plankton populations. The data will be used for the purpose of describing these fjords oceanographically and for comparison or contrast with those in other parts of the world, particularly in British Columbia and southeast Alaska. The basic objective is to obtain a better understanding of the water structure and circulation, sediment distribution and zooplankton species and distribution and of the determining factors, in deep fjord estuaries. The influence of icebergs on the oceanographic conditions will be studied by comparing fjords with these to those without. A secondary study, to be made photographically from the ship, would be of structural characteristics of the mountains around the fjords and of the tree line with respect to latitude and climatic factors.

2. Marine benthonic algae

Scagel and associates have made very extensive collections of marine benthonic algae along the east and north coast of the North Pacific to determine species distributions and relations to oceanographic characteristics such as water properties, substrate, exposure to waves, climate, etc. This direct collection is supported by specimens obtained on exchange from other coasts of the North Pacific and North Atlantic, and from a collection from the western Indian Ocean. A major gap in the U.B.C. collection and others is of material from the Pacific coast of South America, particularly that of southern Chile.

Recently, after negotiations with the Chilean Navy, two students made some collections in the northern and southern extremities of the Chilean fjord region. The transportation facilities actually made available fell far short of what had been expected (only 10 days collecting was done in about 90 days) and the expedition resulted in very limited results.

Collections will be made to study distributions of marine benthonic algae along the coast of southern Chile, in association with oceanographic measurements, for comparison with corresponding distributions in the north Pacific which have been determined in U.B.C. investigations. The anticipated result is a better understanding of the factors governing the distribution of algae species.

Initial Plan for HUDSON 70...Published in 1968

GEOLOGY - B.R. PELLETIER, G.A. BARTLETT

1. Studies of the nature and structure of the underlying geological formations in the McKenzie Delta and Arctic Archipelago

Studies in the Queen Elizabeth Islands and the Arctic Continental Shelf have shown a massive vertical migration of the sea floor with respect to sea level. In these areas, the sea floor is depressed to a depth of 900 metres in contrast to the depths of 200 metres which is usual for Continental Shelves throughout the world. Old beaches in these areas have been found occurring 350 metres above sea level which may be dated to 9000 years. These measurements indicate vertical movement of the order of 1000 metres in a time period the order of 10,000 years.

It is proposed to collect cores while the ship is in the Arctic and to study the fauna and sediments in them. From these, it is hoped that geological events can be distinguished which will lead to an understanding of the Arctic climate in the past, particularly events as described below.

2. Sedimentation in the Arctic Delta

A part of the geological work in recent years has been of the Arctic sedimentary transport from the watershed into the deeper basins of the Arctic channels. From this has developed principles of sedimentation in Arctic waters, a knowledge of the source areas and the character of the sediments associated with them.

The cruise affords the opportunity to study the disposal of these sediments over a wide area and it is planned to carry these studies throughout the channels of the Archipelago as the ship transits.

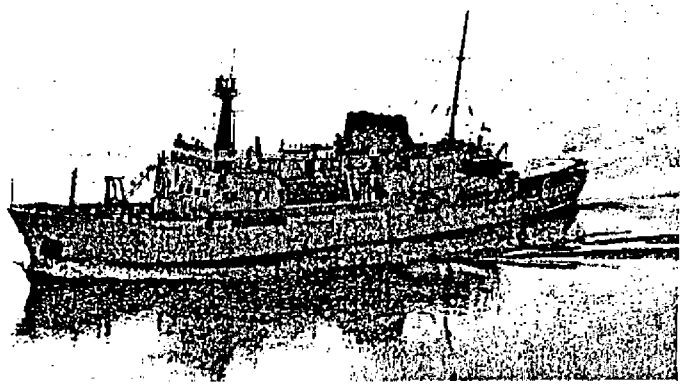
3. Micropaleontology

An accumulating body of evidence throughout the world's oceans shows a relationship between assemblages of planktonic foraminifera and currents and water masses. In fact, there is evidence that these assemblages may change markedly in a few miles as an oceanographic boundary is crossed. To understand this phenomena and to describe it correctly, a much better sampling is required of the foraminifera on an ocean wide scale with physical oceanographic measurements being made at the same time. Bedford Institute has begun a collection of this material in the Atlantic and it is proposed to extend the sampling to the South Atlantic and Arctic during the cruise.

In addition to the foraminifera collection, cores will be made in certain areas. By relating the assemblages in the cores to those associated with the present current systems, it is possible, in part, to understand the past history of ocean currents.

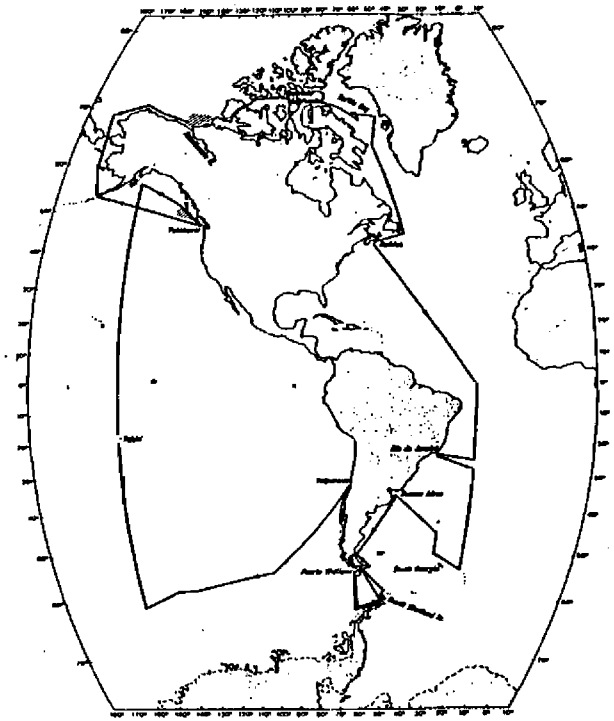
The Hudson 70 Expedition

One of the major projects undertaken by the Bedford Institute in 1969 and 1970 was an oceanographic expedition around North and South America on the CSS *Hudson*. The aims of the expedition were to make a significant contribution to the exploration of the world's oceans at the beginning of the International Oceanographic Decade and to continue the exploration of the Canadian continental shelf. A preliminary scientific program was drawn up in January 1968 which was then reviewed and revised during the following summer as requests to take part in the expedition were received from many scientists from laboratories across Canada and the United States. By August the major part of the program was finalized and the expedition was given the name 'HUDSON 70'. Following authorization by the Minister of Energy, Mines and Resources, and a year of hectic preparation, the *Hudson* sailed south from Halifax on the 19th of November 1969. Eleven months later, October 16, 1970, she arrived back in Halifax having completed her scientific work and become the first ship ever to circumnavigate the Americas.



Hudson silhouetted against a low sun in the Beaufort Sea.

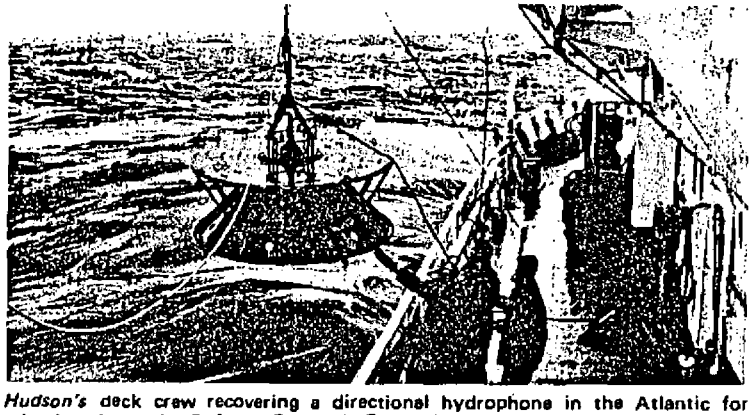
The first leg of the voyage took the *Hudson* down the South Atlantic Ocean to the vicinity of South Georgia with a call at Rio de Janeiro enroute. Acousticians, biologists, chemists, geologists and physical oceanographers made up the scientific party, most of whom sought samples for studies of oceanwide distributions. The long transect of the South Atlantic provided the opportunity to collect on this scale. As the ship proceeded south, plankton hauls were made at different depths from the surface to 1500 metres; the acoustic characteristics of the deep scattering layer were mapped and mid-water trawls made to sample the fish in it; sea water samples were collected for chemical analysis; and measurements were made of the size and distribution of particulate matter at the sea surface. Experiments were conducted on the feeding habits of plankton and on the process of photosynthesis, and the sounds emitted by whales were recorded whenever they were sighted. Altogether the ship was very busy with every square foot of laboratory space occupied and a full 12 hours required at each station to make all the collections and observations. Christmas day was celebrated in the middle of the south Atlantic with Christmas dinner, and a station..



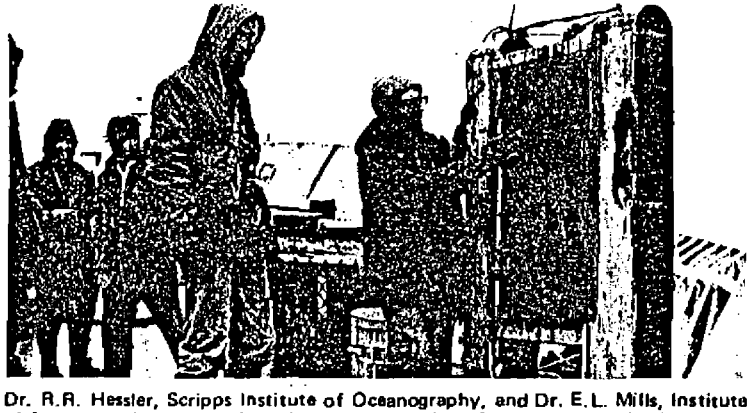
Hudson's track and main ports of call.

From the vicinity of south Georgia, *Hudson* sailed to Buenos Aires, then south to work between South America and Antarctica. Four buoys, each carrying three current meters and three temperature recorders were laid across the Drake Passage and recovered after 11 days. Recovery of the current meters, all of which worked except one, was a major achievement as the recorders contribute the first comprehensive set of direct current measurements across this important passage. A set of mud samples for a study of the emergence of benthic fauna in polar regions was collected in the bays of the South Shetland Islands. Sea water samples for trace element analysis were collected in

the deep waters of Drake Passage. While *Hudson* was laying the current meters and collecting the mud samples a launch party left at Puerto Williams, a Chilean Naval Base, to collect fresh and salt water invertebrates and intertidal algae in the coastal channels of Tierra del Fuego. Of the collection of invertebrates, about one-third are probably new to science. An unexpected discovery was a primitive species of beach flea which has changed little in 100 million years.



Hudson's deck crew recovering a directional hydrophone in the Atlantic for scientists from the Defence Research Establishment Atlantic. The hydrophone was used with explosive sources to study scattering from layers of fish at depths up to 1000 metres.



Dr. R.R. Hessler, Scripps Institute of Oceanography, and Dr. E.L. Mills, Institute of Oceanography, Dalhousie University, recovering a benthic sled in the Antarctic. The sled collects a sample of mud for studies of bottom fauna.

From Puerto Williams the *Hudson* sailed to Punta Arenas and then carried a party of Canadian and Chilean scientists to study the physical oceanography, chemistry, and biological life of the Chilean fjords. These fjords whose marine characteristics were unexplored, extend nearly 100 miles along Chile's southern coast. Thirty-three fjords were visited and it was found they could be classified into three groups: northern, middle and southern. The northern group has clear surface water and high productivity; the middle group has less saline and very silty surface water (due to rock flour from glaciers); and the southern group, opening off the Strait of Magellan, has subsurface water of markedly different characteristics from the others, indicating that it might have its origin in the Atlantic rather than the Pacific. Besides affording the opportunity to study and compare Chilean and west coast Canadian fjords, the expedition provided valuable information that Chilean oceanographers can use to plan further work.

Valparaiso was reached on April 15. Here most of the biologists and chemists who had taken part in the South Atlantic leg of the expedition rejoined the ship to continue their work in the Pacific. Magnetometry and gravimetry were added to the observations, the latter to calculate the slope of the sea surface from Antarctica to Alaska to provide a base measurement for the determination of ocean currents by satellite observations. The track provided the longest continuous gravity line along any meridian. An unexpected deep trench with adjacent peaks was found in the South Pacific; this indicates that the Pacific has not moved as a single block and that more trenches may be found in future surveys.

As the ship approached Vancouver, the only serious setback of the voyage occurred due to fatigue in a cover plate of one of the main engines. Repairs to engines reduced the time available for the



Dr. B.D. Loncarevic, Assistant Director, Atlantic Oceanographic Laboratory, standing watch on the geophysics console in the Beaufort Sea. Gravimetry, magnetometry and bathymetry were recorded automatically.

geophysics program off the coast of British Columbia from six to four weeks. Despite the delay, the *Hudson* with the CNAV *Endeavour* carried out most of the planned two-ship geo-physical survey over the continental shelf and slope between Vancouver Island and the Queen Charlottes. The object of the survey, comprised of gravimetry, magnetometry, bathymetry, seismic profiling, heat flow measurements and coring, was to study Continental Drift; the results support the hypothesis that the ocean floor is drifting away from the mainland. In the Explorer Trench a record high heat flow, measured in cooperation with the University of Washington, showed the trench to be an active zone of rifting, explaining some of the earthquake activity on the west coast.

On August 13 the *Hudson* left Victoria to work in the Beaufort Sea, travel through the Northwest Passage to Baffin Bay, and return to Halifax. Four weeks were spent in the Beaufort Sea as part of a two-ship program of geology and hydrography with the Bedford Institute's other major ship, the CSS *Baffin*, which had come west through the Panama Canal and gone into the Beaufort Sea two weeks earlier. The team of geologists and geophysicists on the *Hudson* obtained an extensive sampling of the sediments on the Beaufort Sea shelf, together with reflection profiles and gravity measurements. The discovery of extensive bands of coarse sands 30 to 60 metres below sea



Dr. G. Vilks, Atlantic Oceanographic Laboratory, recovering a plankton net for the micropaleontology program. The plankton collection for this program was made through all four oceans visited.

level, probably representing relic beaches, and of sediment-filled depressions in the earth's crust will contribute greatly to an understanding of the geological history of the Canadian Arctic. Samples of foraminifera and plankton obtained in the water masses of the Beaufort Sea, and through the Prince of Wales Strait into Baffin Bay form the most comprehensive single collection through the archipelago. A major part of the collection will be retained at the National Museum, Ottawa, as the basis of a description of specimen types and as a national reference. The foraminifera collection is of considerable interest because from it, together with information from cores, much can be learned about the past history of the Arctic Ocean.

The Northwest Passage was traversed between September 22 and September 30. Transcending the rounding of Cape Horn, this was the most exciting part of the voyage, particularly as it had been left so late in the season with the risk of being caught in the ice for the winter. The passage was made through the Prince of Wales Strait, with the *Hudson* and the *Baffin* proceeding independently to its northern end where they were met by the ice-breaker, the *John A. MacDonald*. The three ships sailed in convoy through heavy ice in Viscount Melville Sound to Resolute where a jubilant party celebrated the west-to-east journey and the virtual success of the rounding of the Americas.

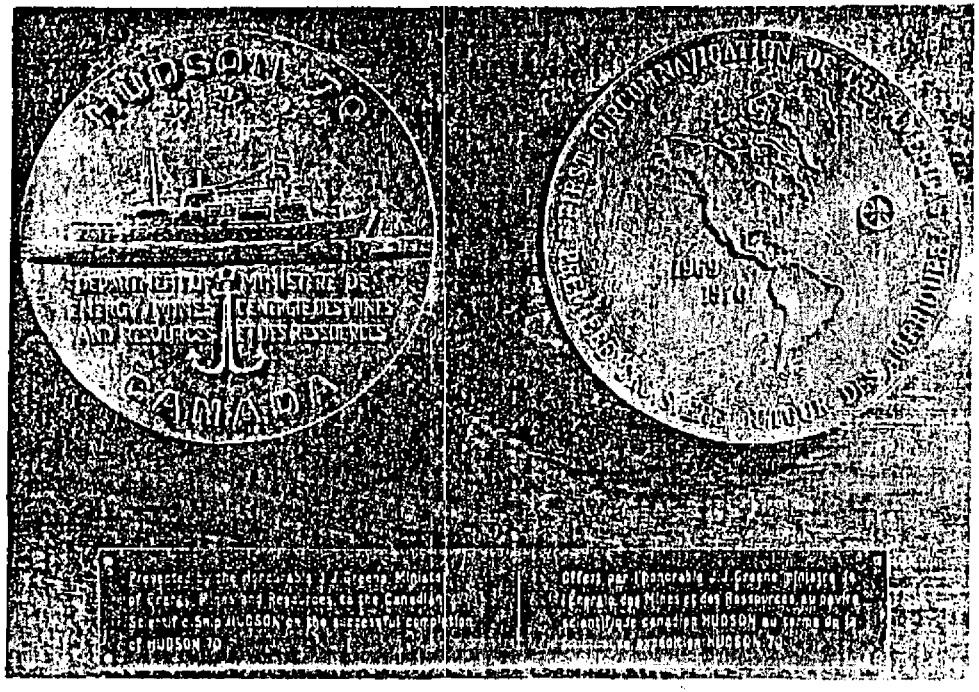
It seemed a fitting end that the final major experiment of the voyage, to determine whether the crust beneath Baffin Bay was continental or oceanic, should be successful. The United States Coastguard Cutter, the *Edisto*, with a party from the Bedford Institute aboard, joined the *Hudson* in Baffin Bay to act as shot-ship for a seismic refraction profile of the crust beneath the Bay. This was one of the few experiments where an analysis could be completed quickly on board. The profile proved conclusively that Baffin Bay has an oceanic structure and settled one of the important questions about the geology of the eastern Arctic. From Baffin Bay, the *Hudson* sailed for Halifax arriving home on the 16th of October, 1970.

By any measure, this expedition was a success. The *Hudson* sailed 55,000 miles, carried 122 scientific staff during the course of her voyage, and generated an impressive statistic of samples and observations. All of the scientific program was completed and most of the scientists collected many more samples than they had set out to obtain. Much of the credit goes to the crew of the ship, to Captain D. Butler, who completed the circumnavigation, and to Captain F. Mauger, who was captain during the west coast survey. HUDSON 70 was a collaborative venture and its success was due in large part to the efforts and cooperation of the Chief Scientists each of whom organized their own part of the program. They are listed below:

C.R. Mann*	Halifax to Punta Arenas

G.L. Pickard†	Punta Arenas to Valparaiso
R.C. Melanson*	Valparaiso to Tahiti
W.M. Cameron Δ	Tahiti to Vancouver
C.D. Maunsell*	West Coast Survey
B.R. Pelletier*	Vancouver to Resolute
D.I. Ross*	Resolute to Halifax

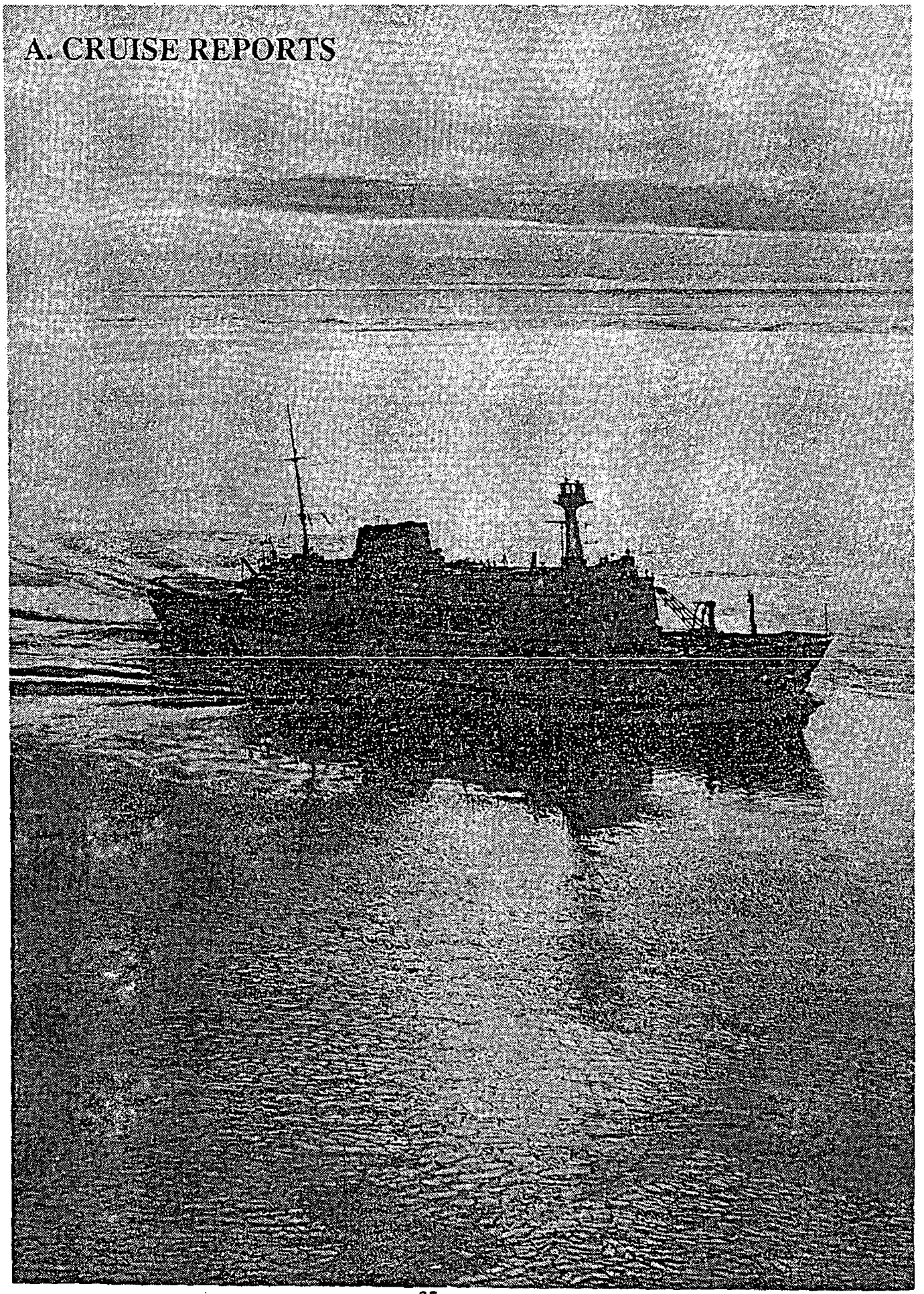
C.R. Mann



Plaque of the commemorative medal for HUDSON 70. Medals were presented to all participants.

* Atlantic Oceanographic Laboratory
† University of British Columbia
Δ Director, Marine Sciences Branch, Energy, Mines and Resources.

A. CRUISE REPORTS



DATA COLLECTED DURING

THE HUDSON 70 EXPEDITION

INDEX OF ABBREVIATIONS

A.S.L.O.	Acoustic Scattering Layer Observations
A.CO^2 S.	Air CO^2 Samples
A. C14 S.	Air C14 Samples
A.D.G.	Anchor Dredge Grabs
B.L.	Bathysonde Lowerings
B.S.T.	Biological Sled Trawl
B.B. 9060 STD C.	Bissett Berman 9060 S.T.D. Casts
B.S.N.	Bottle Station Number
B.S.	Bottom Samples
C.S.	Camera Stations
C.-B.T.	Clarke-Bumpus Tows
C. Stn.	Collection Station
C.	Cores
C.M.M.	Current Meters Moored
C.M.R.	Current Meters Recovered
D.M.P.T.	Deep Multiple Plankton Tows
D.P.T.	Deep Plankton Tows
E.S.H.	Epibenthic Sled Hauls
I.-S. C-14 I.	In-Situ C-14 Incubation
I.K.T.	Issac Kidd Trawl
I.K.T.H.	Issac Kidd Trawl Hauls
K. & N.C.	Knudsen & Nisken Casts
K.C.	Knudsen Casts
Lat.	Latitude
Long.	Longitude
M.-O.P.H.	Multi-Oblique Plankton Hauls
N.O.	Nephelometer Observations
N.	Nutrients
O.B.T.	Oblique Biological Tow
O.P.T.	Oblique Plankton Tows
R. of W.S.	Recording of Whale Sounds
R.D.	Rock Dredges
S.W. CO^2 S.	Sea Water CO^2 Samples
S.D.	Sediment Dredges
S.H.	Shallow Hydro
S.M.G.	Smith McIntyre Grabs
S.#	Station Number
S.B.T.	Surface Biological Tows
S.P.T.	Surface Plankton Tows
S. Temp.	Surface Temperature
S.T.N.N.	Surface Tows Neuston Net
Temp.	Temperature
U./W./T.	Underwater Television
V.V.G.	Van Veen Grabs
V.B.T.	Vertical Biological Tows
V.P.H.	Vertical Plankton Hauls
V.P.T.	Vertical Plankton Tows

"HUDSON 70"

November 19, 1969 - January 14, 1970

Area:- Halifax, Nova Scotia to Puerto Williams, Chile, S.A.

Soundings - G.E.B.C.O.:	-	16155 km
Gravity Records:	-	3800 km
Magnetics:	-	4200 km

1) Oxygens were analyzed by the Carpenter modification of the Winkler method using 60 ml sampler bottles.

2) On some stations, samples were withdrawn for dissolved helium and helium isotope studies.

3) In the Atlantic, total dissolved CO_2 and CO_2 in the air were also determined on most stations.

S.#	Lat.	Long.	Date	S.P.T.	V.P.T.	O.P.T.	D.M.P.T.	D.P.T.	S.T.M.N.	I.K.T.	K.&N.C.	B.L.	C.	A.S.L.O.	R.ofW.S.	I.-S.C-141.	S.H.	B.S.N.
1	02°31.00N	31°35.00W	29 11 69												X			
2	00°01.79N	29°58.27W	30 11 69	X	X					X	X	X		X				1
3	00°51.00S	30°00.00W	01 12 69		X				X									
4	02°28.76S	30°04.28W	01 12 69	X	X					X	X	X		X		X		2
5	03°31.90S	30°07.10W	02 12 69		X				X									
6	04°54.73S	30°00.50W	02 12 69	X	X					X	X			X		X		3
7	06°04.20S	30°00.50W	02 12 69		X				X					X				
8	07°27.06S	30°03.17W	03 12 69	X	X					X	X	X		X		X		4
9	08°30.77S	30°01.99W	04 12 69		X					X				X				
10	09°58.58S	30°02.77W	04 12 69	X	X					X	X	X		X		X		5
11	10°58.78S	29°58.88W	05 12 69		X					X				X				
12	12°25.48S	30°06.83W	05 12 69	X	X					X	X	X		X		X		6
13	13°28.70S	30°02.40W	05 12 69		X					X				X				
14	14°54.74S	30°06.54W	06 12 69	X	X					X	X	X		X		X		7
15	15°47.19S	29°59.03W	06 12 69		X				X		I			X				
16	17°31.57S	30°01.23W	07 12 69	X	X						X	X	X	X		X		8
17	18°19.48S	30°03.68W	07 12 69		X					X								
18	20°00.19S	30°00.23W	08 12 69	X	X						X	X		X		X		9

S.#	Lat.	Long.	Date	S.P.T.	V.P.T.	O.P.T.	D.M.P.T.	D.P.T.	S.T.M.N.	I.K.T.	K.&N.C.	B.L.	C.	A.S.L.O.	R.ofW.S.	I.-S.C-141.	S.H.	B.S.N.
19	20°02.64S	30°31.34W	08 12 69										X					
20	20°07.50S	30°28.00W	09 12 69		X				X	X				X				
21	22°30.16S	29°58.12W	09 12 69	X	X						X	X						10
22	23°21.00S	29°55.00W	09 12 69		X									X				
23	25°01.45S	30°01.55W	10 12 69	X	X					X	X	X		X		X		11
24	24°52.51S	30°07.89W	10 12 69		X									X				
25	24°36.59S	32°30.62W	11 12 69		X					X				X				
26	24°21.35S	32°36.21W	11 12 69											X				
27	24°17.29S	32°43.47W	11 12 69		X									X				
28	24°13.36S	35°02.99W	12 12 69		X							X	X	X				
29	27°31.58S	30°07.01W	23 12 69	X	X	X				X	X	X		X				12
30	29°59.89S	29°58.82W	24 12 69	X	X	X	X				X	X		X				13
31	31°10.25S	29°58.00W	24 12 69		X				X	X								
32	32°25.05S	30°09.60W	25 12 69	X	X	X	X				X			X				14
33	34°59.65S	30°04.70W	26 12 69	X	X	X	X				X	X	X	X				15
34	37°28.42S	29°59.20W	27 12 69	X	X	X	X				X	X		X				16
35	38°39.50S	29°59.80W	28 12 69	X	X					X								
36	39°54.98S	29°52.99W	28 12 69	X	X	X	X			X	X	X		X				17

	S.#	Lat.	Long.														
37	42°29.91S	29°57.53W	29 12 69	X	X	X	X				X	X		X			18
38	43°39.70S	29°52.50W	29 12 69	X	X					X							
39	45°07.29S	29°58.67W	30 12 69	X	X	X	X			X	X	X		X			19
40	46°04.17S	29°53.99W	30 12 69	X	X									X			
41	47°34.55S	29°53.44W	31 12 69	X	X	X		X			X	X		X			20
42	48°20.06S	29°51.94W	31 12 69		X							X					
43	49°03.39S	29°48.65W	01 01 70	X	X	X					X			X			21
44	49°07.27S	29°38.33W	01 01 70		X		X			X		X					
45	50°33.32S	29°35.36W	02 01 70	X	X	X	X			X	X	X		X			22
46	52°03.72S	30°03.67W	03 01 70	X	X	X		X			X	X	X				23
47	52°30.23S	29°50.60W	04 01 70											X			
48	53°27.22S	29°59.48W	04 01 70	X	X	X	X				X	X		X			24
49	53°52.92S	29°49.12W	05 01 70		X					X							
50	54°54.83S	29°23.16W	05 01 70	X	X	X	X				X	X		X			25
51	53°32.58S	33°56.26W	06 01 70	X	X		X			X							
52	51°27.91S	39°57.27W	08 01 70	X	X	X	X			X	X	X	X	X			26
53	50°19.80S	39°54.10W	08 01 70												X		
54	49°58.99S	39°57.76W	08 01 70	X	X	X					X						27

S.#	Lat.	Long.	Date	S.P.T.	V.P.T.	O.P.T.	D.M.P.T.	D.P.T.	S.T.N.N.	I.K.T.	K.&N.C.	B.L.	C.	A.S.L.O.	R.ofW.S.	I.-S.C-141	S.H.	B.S.N.
55	48°58.93S	39°52.42W	09 01 70	X	X	X					X	X		X				28
56	47°58.90S	39°59.55W	10 01 70		X	X					X			X				29
57	47°03.28S	40°04.62W	11 01 70		X	X		X			X			X				30
58	45°41.67S	40°38.33W	11 01 70	X	X		X		X		X							
59	45°10.62S	41°10.75W	12 01 70	X	X									X				
60	44°12.44S	42°45.95W	12 01 70	X	X			X		X				X				
61	41°46.48S	46°26.37W	13 01 70	X	X		X				X			X				31
62	41°40.83S	46°52.06W	14 01 70	X	X					X				X				

"HUDSON 70"

January - February - 1970

Intertidal Marine Life Survey:-

Hudson 70 Expedition

Cape Horn Region, South America,

by the National Museum of National Sciences,

Ottawa, Ontario

Puerto Williams Launch Party, Isla Navarino and Vicinity,

Magallanes (Cape Horn Region) Chile.

Vessel:- Diesel Launch "REDHEAD" from C.S.S. "HUDSON"

Stn. #	Latitude	Longitude	Date	C. Stn.	Temp.	S. Temp.
F1	54°57.00S	67°40.00W	29 01 70	X	X	
F2	54°56.00S	67°37.00W	30 01 70	X		
F3	54°56.00S	67°37.00W	30 01 70	X	X	
F4	54°56.00S	67°37.00W	30 01 70	X		
F5	54°56.00S	67°37.00W	30 01 70	X	X	
F6	54°56.00S	67°38.50W	31 01 70	X	X	
F7a	54°51.00S	68°48.00W	01 02 70	X		
F7b	54°51.00S	68°48.00W	02 02 70	X		X
F8	54°52.00S	68°46.00W	02 02 70	X		
F9	54°56.00S	68°49.00W	02 02 70	X		X
F10a	55°03.00S	68°10.00W	02 02 70	X	X	
F10b	55°03.00S	68°10.00W	03 02 70	X	X	
F11	55°04.00S	68°10.50W	03 02 70	X	X	
F12	55°05.50S	67°04.50W	05 02 70	X	X	
F13	55°05.00S	67°04.50W	05 02 70	X	X	
F14	55°09.00S	67°04.00W	05 02 70	X		
F15	55°13.00S	66°52.00W	05 02 70	X		
F16	55°18.00S	66°49.00W	06 02 70	X	X	
F17	55°07.00S	66°50.00W	07 02 70	X	X	
F18	55°07.00S	68°12.00W	10 02 70	X		
F19	55°16.00S	67°49.00W	10 02 70	X	X	
F20	55°16.00S	67°49.50W	10 02 70	X	X	
F21	55°15.00S	67°57.00W	10 02 70	X	X	
F22	55°11.00S	67°55.00W	11 02 70	X		
F23	55°14.50S	67°45.00W	11 02 70	X		X

Stn. #	Latitude	Longitude	Date	C. Stn.	Temp.	S. Temp.
F24	55°14.50S	67°44.50W	11 02 70	X		
F25	55°14.50S	68°12.00W	14 02 70	X	X	
F26	55°23.50S	68°07.00W	14 02 70	X		
F27	55°31.50S	68°05.00W	14 02 70	X	X	
F28	55°32.00S	68°01.50W	15 02 70	X	X	
F29	55°30.00S	67°40.00W	15 02 70	X		
F30	55°12.50S	67°06.00W	16 02 70	X	X	
F31	54°56.00S	68°17.00W	19 02 70	X		
F32	54°56.00S	68°23.50W	19 02 70	X		
F33	54°56.00S	67°38.00W	20 02 70	X		
F34	52°54.00S	70°17.00W	22 02 70	X	X	

"HUDSON 70"

January 29, 1970 - February 18, 1970

Area: Puerto Williams - Drake Passage - Punta Arenas

Soundings - G.E.B.C.O.:- 4755 km

Stn. #	Lat.	Long.	Date	S.P.T.	V.P.H.	K.&N.C.	B.L.	E.S.H.	A.D.G.	S.M.G.	C.M.M.	C.M.R.	N.O.	V.P.T.	B.S.N.
63	54°54.58S	67°35.42W	29 01 70					X							
64	55°36.91S	67°11.80W	29 01 70	X				X							
65	55°42.59S	66°57.52W	29 01 70	X				X							
66	57°11.55S	65°59.72W	29 01 70	X											
67	57°48.62S	68°18.51W	31 01 70			X							X	X	32
68	57°49.15S	68°19.60W	31 01 70								X				
69	60°04.50W	68°04.00W	01 02 70		X						X				
70	60°16.30S	67°59.62W	02 02 70	X	X	X							X		33
71	61°59.00S	67°33.30W	02 02 70								X				
72	62°07.21S	67°32.98W	03 02 70		X	X							X		34
73	63°28.05S	67°07.00W	03 02 70								X				
74	63°34.07S	66°47.62W	04 02 70		X	X		X	X				X		35
75	62°38.98S	60°25.93W	05 02 70	X				X							
76	62°29.10S	59°44.30W	05 02 70	X				X		X					
77	62°12.90S	58°40.60W	05 02 70	X				X		X					
78	62°19.30S	57°51.20W	06 02 70			X							X	X	36
79	62°06.80S	58°25.00W	06 02 70			X		X		X					37
80	61°47.50S	58°43.20W	07 02 70					X							

Stn. #	Lat.	Long.	Date	S.P.T.	V.P.H.	K.&N.C.	B.L.	E.S.H.	A.D.G.	S.M.G.	C.M.M.	C.M.R.	N.O.	V.P.T.	B.S.N.
81	56°41.07S	68°27.44W	10 02 70	X			X								
82	57°02.06S	68°25.36W	10 02 70		X		X								
83	57°33.51S	68°15.66W	11 02 70		X	X									38
84	58°01.38S	68°17.61W	11 02 70		X		X					X			
85	58°28.25S	68°06.15W	11 02 70			X								X	39
86	58°58.44S	68°03.37W	12 02 70				X								
87	59°29.65S	67°57.72W	12 02 70			X									40
88	60°01.63S	67°54.59W	12 02 70		X		X					X			
89	60°32.09S	67°45.60W	12 02 70	X	X	X									41
90	61°02.18S	67°43.28W	13 02 70	X	X		X								
91	61°30.97S	67°29.01W	13 02 70		X	X									42
92	61°58.34S	67°35.14W	13 02 70	X	X		X					X			
93	62°28.16S	67°17.75W	13 02 70	X	X	X									43
94	62°59.56S	67°13.45W	14 02 70		X		X								
95	63°30.62S	67°06.22W	14 02 70		X	X						X			44
96	63°59.61S	66°57.37W	14 02 70		X		X								
97	64°20.00S	66°58.00W	14 02 70	X	X		X								
98	62°57.80S	60°39.00W	15 02 70	X	X	X	X								45

Stn. #	Lat.	Long.	Date	S.P.T.	V.P.H.	K.&N.C.	B.L.	E.S.H.	A.D.G.	S.M.G.	C.M.M.	C.M.R.	N.O.	V.P.T.	B.S.N.
99	61°50.00S	55°39.00W	15 02 70	X	X			X							
100	60°53.57S	57°46.03W	17 02 70		X	X									46
101	60°23.28S	56°42.61W	18 02 70			X							X	X	47
102	54°59.00S	66°51.00W	19 02 70						X	X					
103	55°32.00S	67°27.00W	20 02 70						X	X					

"HUDSON 70"

March 1, 1970 - April 7, 1970

Area: Chilean Fjords and passages from Punta Arenas to Puerto Montt and Ocean Sections along 42°S, 81°W and 31°S to Valparaiso.

Soundings:- G.E.B.C.O.:-

Fjords:	-	4042 km
Pacific:	-	1792 km
Total:	-	5834 km

In this phase of the cruise, some stations were done from lifeboats or launches. Nutrients are listed separately as they were not done at each and every station.

Stn. #	Lat.	Long.	Date	B.B. 9060 STD C.	K.C.	N.	B.S.	C.-B.T.	I.K.T.H.	V.P.H.	O.P.T.	V.P.I.	B.S.N.
104	53°38.40S	70°12.50W	03 03 70	X	X	X		X		X		X	48
105	53°56.00S	70°14.50W	03 03 70	X	X	X							49
106	54°08.00S	70°07.00W	04 03 70	X	X	X							50
107	54°14.50S	69°46.0W	04 03 70	X	X	X		X	X	X			51
108	54°19.00S	69°26.80W	04 03 70	X	X	X							52
109	54°24.50S	69°12.50W	04 03 70	X	X	X	X						53
110	53°29.20S	70°37.20W	04 03 70	X	X	X		X	X	X		X	54
111	53°51.00S	71°38.00W	06 03 70		X	X							55
112	53°17.00S	72°22.80W	06 03 70	X	X	X							56
113	53°12.50S	72°05.0W	06 03 70	X	X	X		X		X		X	57
114	53°10.00S	71°54.10W	06 03 70		X	X							58
115	53°04.10S	71°38.50W	06 03 70	X	X	X							59
116	52°59.00S	71°29.50W	06 03 70	X	X	X	X						60
117	52°53.30S	71°20.50W	06 03 70		X	X							61
118	53°21.40S	73°01.30W	07 03 70	X	X	X							62
119	53°07.80S	73°25.00W	07 03 70	X	X	X		X				X	63
120	53°08.00S	72°57.50W	07 03 70		X	X							64
121	53°11.20S	72°49.70W	07 03 70	X	X	X	X	X				X	65

Stn. #	Lat.	Long.	Date	B.B. 9060 STD C.	K.C.	M.	B.S.	C.-B.T.	I.K.T.H.	V.P.H.	O.P.T.	V.P.T.	B.S.N.
122	52°58.80S	72°55.80W	07 03 70		X								66
123	52°54.10S	72°55.60W	07 03 70		X								67
124	52°52.30S	72°57.70W	07 03 70		X								68
125	53°02.70S	72°57.00W	07 03 70	X	X	X		X		X		X	69
126	53°07.70S	73°08.80W	08 03 70	X	X	X		X	X	X		X	70
127	52°54.10S	73°56.10W	08 03 70	X	X	X		X	X	X		X	71
128	52°49.80S	73°37.50W	08 03 70	X	X	X		X				X	72
129	52°46.20S	73°30.60W	08 03 70	X	X	X	X						73
130	52°42.30S	73°25.70W	08 03 70	X	X	X				X		X	74
131	52°43.50S	73°18.50W	08 03 70	X	X	X	X			X			75
132	52°48.70S	73°20.5W	09 03 70	X	X	X							76
133	52°01.50S	73°46.20W	09 03 70	X	X	X		X	X				77
134	52°01.10S	73°36.50W	09 03 70		X	X	X						78
135	52°06.50S	73°28.60W	09 03 70	X	X	X		X		X		X	79
136	52°10.00S	73°23.10W	09 03 70	X	X	X							80
137	52°06.50S	73°16.20W	09 03 70	X	X								81
138	51°59.50S	73°18.10W	09 03 70	X	X			X		X		X	82
139	51°52.50S	73°18.00W	09 03 70	X	X		X						83
140	51°37.50S	72°46.6W	11 03 70		X								84

Stn. #	Lat.	Long.	Date	B.B. 9060 STD C.	K.C.	N.	B.S.	C.-B.T.	I.K.T.H.	V.P.H.	O.P.T.	V.P.T.	B.S.N.
141	51°36.70S	72°49.10W	11 03 70		X								85
142	51°53.00S	72°42.20W	12 03 70		X	X	X			X		X	86
143	51°56.50S	72°52.40W	12 03 70		X								87
144	52°01.80S	72°57.20W	12 03 70	X	X	X		X		X		X	88
145	51°36.60S	73°59.8W	12 03 70	X	X	X							89
146	50°52.20S	74°14.80W	13 03 70	X	X								90
147	50°51.60S	74°02.50W	13 03 70	X	X	X		X	X	X		X	91
148	50°49.50S	73°53.50W	13 03 70	X	X								92
149	50°45.50S	73°47.80W	13 03 70	X	X			X		X		X	93
150	50°39.80S	73°47.10W	13 03 70	X	X								94
151	50°54.80S	73°49.20W	13 03 70	X	X					X		X	95
152	50°31.80S	73°59.50W	13 03 70	X	X								96
153	50°29.50S	74°05.30W	13 03 70	X	X		X	X	X			X	97
154	50°28.20S	74°14.20W	14 03 70	X	X								98
155	50°23.60S	74°24.60W	14 03 70	X	X			X		X		X	99
156	50°20.00S	74°34.10W	14 03 70	X	X								100
157	50°20.40S	74°49.50W	14 03 70	X	X			X	X	X	X		101
158	50°01.70S	74°55.20W	14 03 70	X	X								102
159	50°20.50S	74°49.80W	14 03 70	X									

Stn. #	Lat.	Long.	Date	O.B. 9060 STD C.	K.C.	N.	B.S.	C.-B.T.	I.K.T.H.	V.P.H.	O.P.T.	V.P.T.	B.S.N.
160	50°12.50S	74°11.00W	14 03 70		X								103
161	50°08.00S	74°13.60W	14 03 70		X								104
162	50°04.10S	74°19.00W	14 03 70		X								105
163	49°59.40S	74°26.20W	14 03 70	X	X			X	X	X		X	106
164	49°33.50S	74°14.10W	15 03 70	X	X								107
165	49°31.10S	74°08.10W	15 03 70	X	X			X	X	X	X		108
166	49°26.10S	74°08.70W	15 03 70	X	X								109
167	49°20.20S	74°06.80W	15 03 70	X	X		X			X		X	110
168	49°17.00S	74°06.10W	15 03 70									X	
169	48°43.00S	74°26.70W	15 03 70	X	X			X	X	X		X	111
170	48°42.50S	74°11.00W	15 03 70		X								112
171	48°43.80S	74°18.00W	15 03 70		X								113
172	48°25.60S	74°32.60W	16 03 70	X	X			X	X	X		X	114
173	48°00.80S	74°41.40W	16 03 70	X	X			X	X	X		X	115
174	47°56.40S	74°29.70W	16 03 70	X				X		X	X		116
175	48°06.20S	74°17.40W	16 03 70	X	X								117
176	48°09.50S	74°15.50W	16 03 70	X	X								118
177	48°11.20S	73°20.00W	16 03 70		X		X	X		X		X	119
178	48°07.30S	73°18.60W	16 03 70	X	X								120

Stn. #	Lat.	Long.	Date	B.B. 9060 STD C.	K.C.	N.	B.S.	C.-B.T.	I.K.T.H.	V.P.H.	O.P.T.	V.P.T.	B.S.N.
179	48°11.80S	73°27.40W	17 03 70	X	X								121
180	48°08.20S	73°34.80W	17 03 70	X	X			X		X		X	122
181	48°02.80S	73°43.20W	17 03 70	X	X								123
182	48°01.30S	73°50.90W	17 03 70	X	X	X		X	X	X		X	124
183	47°58.50S	74°07.30W	17 03 70	X	X		X						125
184	48°00.00S	74°17.40W	17 03 70	X	X								126
185	48°00.00S	73°19.00S	17 03 70	X	X								127
186	47°59.70S	73°25.80W	17 03 70	X	X			X		X	X		128
187	47°58.70S	73°31.70W	17 03 70	X	X		X						129
188	47°54.20S	73°36.40W	17 03 70	X	X			X	X	X		X	130
189	47°52.50S	73°47.90W	18 03 70	X	X								131
190	47°49.70S	73°44.90W	18 03 70	X	X	X		X		X		X	132
191	47°45.60S	73°46.00W	18 03 70	X	X		X						133
192	47°41.80S	73°43.70W	18 03 70	X	X	X		X		X		X	134
193	47°51.50S	73°59.40W	18 03 70	X	X								135
194	47°47.80S	74°15.60W	18 03 70	X	X	X							136
195	47°49.20S	74°32.00W	18 03 70	X	X								137
196	47°45.60S	74°43.70W	18 03 70	X	X								138
197	47°34.50S	74°54.10W	18 03 70	X	X			X	X	X		X	139

Stn. #	Lat.	Long.	Date	B.B. 9060 STD C.	K.C.	N.	B.S.	C.-B.T.	I.K.T.H.	V.P.H.	O.P.T.	V.P.T.	B.S.N.
198	46°55.00S	74°14.40W	19 03 70	X	X	X							140
199	46°50.60S	74°19.50W	19 03 70		X								141
200	46°49.20S	74°29.10W	19 03 70		X	X							142
201	46°49.00S	74°36.50W	19 03 70		X		X						143
202	47°10.00S	74°19.00W	19 03 70	X	X	X		X	X		X		144
203	47°11.40S	74°10.00W	19 03 70		X								145
204	47°09.60S	74°03.50W	19 03 70		X								146
205	47°18.80S	74°06.30W	19 03 70		X								147
206	47°34.50S	74°54.10W	19 03 70	X									
207	47°00.40S	75°47.50W	20 03 70	X	X	X			X				148
208	45°45.00S	75°40.20W	20 03 70	X	X	X			X				149
209	45°50.00S	74°30.60W	20 03 70	X	X			X		X		X	150
210	45°44.60S	73°59.20W	20 03 70		X		X			X		X	151
211	45°52.10S	73°37.10W	20 03 70	X	X					X		X	152
212	46°08.00S	73°39.50W	21 03 70		X	X							153
213	46°14.50S	73°41.50W	21 03 70		X					X		X	154
214	46°19.50S	73°43.50W	21 03 70		X	X	X						155
215	46°02.50S	73°25.10W	21 03 70	X	X	X							156

Stn. #	Lat.	Long.	Date	B.B. 9060 STD C.	K.C.	H.	B.S.	C.-B.T.	I.K.T.H.	V.P.H.	O.P.T.	V.P.T.	S.T.	B.S.N.
216	46°06.30S	73°27.50W	21 03 70	X	X		X	X	X	X		X		157
217	46°12.30S	73°32.50W	21 03 70	X	X	X								158
218	46°18.10S	73°36.60W	21 03 70	X	X		X	X		X		X		159
219	46°08.40S	73°58.50W	21 03 70		X	X								160
220	46°14.60S	74°15.40W	21 03 70		X	X								161
221	46°13.00S	74°07.30W	21 03 70		X	X								162
222	45°58.20S	73°39.40W	21 03 70		X									163
223	45°21.20S	73°39,00W	22 03 70	X	X									164
224	45°27.10S	73°31.20W	22 03 70	X	X		X	X		X		X		165
225	45°39.40S	73°33.20W	22 03 70	X	X									166
226	45°48.50S	73°33.50W	22 03 70	X	X		X							167
227	45°44.60S	73°27.10W	22 03 70		X									168
228	45°41.60S	73°23.70W	22 03 70		X									169
229	45°40.00S	73°17.50W	22 03 70		X									170
230	45°22.20S	73°25.70W	22 03 70	X	X									171
231	45°18.40S	73°17.40W	22 03 70	X	X		X	X	X	X		X		172
232	45°17.70S	73°09.70W	23 03 70	X	X									173
233	45°22.60S	73°04.40W	23 03 70	X	X	X								174

Stn. #	Lat.	Long.	Date	B.B. 9060 STD C.	K.C.	N.	B.S.	C.-B.T.	I.K.T.H.	V.P.H.	O.P.T.	V.P.T.	S.T.	B.S.N.
234	45°26.20S	72°57.20W	23 03 70	X	X	X	X	X				X		175
235	45°24.50S	72°51.50W	23 03 70	X	X	X								176
236	45°22.00S	73°04.70W	23 03 70	X										
237	45°18.00S	73°17.40W	24 03 70	X										
238	45°26.00S	73°33.00W	24 03 70	X										
239	45°20.50S	73°39.70W	24 03 70	X										
240	45°07.50S	73°39.00W	24 03 70	X	X		X	X						177
241	44°49.20S	73°29.50W	24 03 70	X	X									178
242	44°17.40S	73°11.70W	24 03 70	X	X									179
243	44°18.30S	73°01.60W	24 03 70	X	X		X	X		X		X		180
244	44°23.30S	72°55.30W	24 03 70	X	X		X							181
245	44°26.80S	72°45.70W	24 03 70	X	X	X		X		X		X		182
246	44°25.50S	72°37.00W	24 03 70	X	X	X								183
247	44°33.20S	72°44.10W	25 03 70	X	X		X							184
248	44°38.20S	72°45.10W	25 03 70	X	X	X		X		X				185
249	44°45.60S	72°49.40W	25 03 70	X	X									186
250	44°49.00S	72°55.70W	25 03 70	X	X	X	X							187
251	44°54.50S	73°04.20W	25 03 70	X	X			X	X	X				188

Stn. #	Lat.	Long.	Date	B.B. 9060 STD C.	K.C.	N.	B.S.	C.-B.T.	I.K.T.H.	V.P.H.	O.P.T.	V.P.T.	S.T.	B.S.N.
252	44°56.80S	73°15.00W	25 03 70	X	X		X							190
253	44°27.10S	73°29.60W	25 03 70	X	X		X	X	X	X				190
254	44°12.80S	73°25.50W	25 03 70	X	X									191
255	43°55.10S	73°24.30W	25 03 70	X	X	X	X	X		X				192
256	43°44.60S	74°19.60W	26 03 70	X										
257	43°45.50S	75°11.70W	26 03 70	X	X	X			X					193
258	43°33.30S	73°23.80W	26 03 70	X	X									194
259	43°18.40S	73°17.60W	26 03 70	X	X			X		X				195
260	43°00.30S	73°01.30W	26 03 70	X	X		X							196
261	42°27.00S	72°58.60W	27 03 70	X	X		X	X		X				197
262	42°28.30S	72°48.60W	27 03 70	X	X									198
263	42°30.00S	72°42.80W	27 03 70	X	X									199
264	42°32.50S	72°37.40W	27 03 70	X	X		X			X				200
265	42°34.40S	72°33.20W	27 03 70	X	X									201
266	42°10.10S	72°41.50W	27 03 70	X	X									202
267	42°11.50S	72°32.30W	27 03 70	X	X		X	X		X				203
268	42°19.10S	72°31.30W	27 03 70	X	X									204
269	42°23.50S	72°28.80W	27 03 70	X	X		X	X		X				205

Stn. #	Lat.	Long.	Date	B.B. 9060 STD C.	K.C.	N.	B.S.	C.-B.T.	I.K.T.H.	V.P.H.	O.P.T.	V.P.T.	S.T.	B.S.N.
270	42°27.80S	72°29.00W	27 03 70	X	X									206
271	42°06.80S	72°29.50W	27 03 70	X	X									207
272	42°03.50S	72°28.30W	28 03 70	X	X			X		X				208
273	41°59.70S	72°30.40W	28 03 70	X	X									209
274	42°03.30S	72°32.10W	28 03 70	X	X	X		X		X				210
275	42°07.50S	72°48.00W	28 03 70	X	X		X	X		X				211
276	42°04.20S	73°09.20W	28 03 70	X	X	X								212
277	41°48.70S	72°55.60W	28 03 70	X	X									213
278	41°43.10S	72°45.20W	28 03 70	X	X		X							214
279	41°35.50S	72°49.50W	28 03 70	X	X									215
280	41°43.00S	72°38.00W	28 03 70	X	X		X	X		X		X		216
281	41°42.60S	72°30.80W	28 03 70	X	X									217
282	41°40.80S	72°24.30W	28 03 70	X	X	X	X	X		X				218
283	41°35.40S	72°20.50W	29 03 70		X									219
284	41°31.10S	72°19.80W	29 03 70	X	X		X	X		X				220
285	41°25.30S	72°18.10W	29 03 70		X									221
286	41°40.60S	74°14.10W	31 03 70	X										
287	41°39.00S	75°02.10W	01 04 70	X										

Stn. #	Lat.	Long.	Date	B.B. 9060 STD C.	K.C.	N.	B.S.	C.-B.T.	I.K.T.H.	V.P.H.	O.P.T.	V.P.T.	S.T.	B.S.N.
288	41°38.80S	76°00.00W	01 04 70	X										
289	41°40.00S	77°00.00W	01 04 70	X	X									222
290	41°39.50S	78°00.00W	01 04 70	X										
291	41°40.00S	79°00.00W	01 04 70	X										
292	41°39.50S	79°59.80W	02 04 70	X										
293	41°39.30S	80°58.50W	02 04 70	X	X									223
294	41°00.00S	80°59.00W	02 04 70	X										
295	40°01.20S	80°59.40W	02 04 70	X										
296	38°58.30S	81°00.10W	02 04 70	X										
297	38°00.00S	81°00.00W	03 04 70	X	X				X					224
298	37°00.00S	80°58.50W	03 04 70	X										
299	35°58.10S	80°57.80W	03 04 70	X										
300	35°03.10S	81°01.30W	03 04 70	X										
301	33°57.70S	81°00.00W	04 04 70	X										
302	33°30.00S	81°00.00W	04 04 70	X	X									225
303	33°31.9S	80°08.30W	04 04 70	X										
304	33°30.80S	79°00.80W	04 04 70	X										
305	33°30.90S	78°01.00W	05 04 70	X										

Stn. #	Lat.	Long.	Date	B.B. 9060 STD C.	K.C.	N.	B.S.	C.-B.T.	I.K.T.H.	V.P.H.	O.P.T.	V.P.T.	S.T.	B.S.N.
306	33°24.50S	77°00.00W	05 04 70	X	X									226
307	33°19.00S	76°00.60W	05 04 70	X										
308	33°16.00S	75°01.90W	05 04 70	X										
309	33°09.50S	74°00.00W	05 04 70	X										
310	33°05.00S	73°00.00W	06 04 70	X										
311	32°58.50S	72°01.40W	06 04 70	X										

"HUDSON 70"

April 15, 1970 - June 6, 1970

Area:- Valparaiso to Vancouver

Soundings - G.E.B.C.O.: - 19920 km

Gravity Records: - 19920 km

Magnetics: - 19920 km

1) Oxygens were analyzed by the Carpenter modification of the Winkler method using 60 ml sampler bottles.

2) Normally, nutrient samples were withdrawn from Knudsen bottles into 25 ml polyethelene tubes and preserved for a few hours in a refrigerator after the addition of 2 drops of chloroform. They were then analyzed in an auto analyzer.

1) Normally, the samples taken from the Nisken bottles were used by Dr. P.J. Wangersky for determination of nitrogen, argon, dissolved and particulate organic carbon, and ratios of major ions.

2) On some stations, samples were withdrawn for helium and helium isotope studies.

Stn. #	Lat.	Long.	Date	S.P.T.	V.P.T.	O.P.T.	A.S.L.O.	K.M.C.	C.	A. CO^2 S.	A.C14 S.	S.W. CO^2 S.	B.S.N.
312	59°39.70S	126°14.00W	24 04 70									X	
313	60°14.80S	136°10.30W	25 04 70									X	
314	61°16.20S	141°30.80W	26 04 70									X	
315	62°55.80S	149°57.90W	27 04 70	X	X	X	X	X		X	X	X	227
316	59°54.20S	149°56.30W	28 04 70		X	X	X	X		X	X	X	228
317	54°55.70S	149°49.7W	29 04 70	X	X		X	X		X	X	X	229
318	49°55.90S	150°01.30W	01 05 70	X	X	X	X	X		X	X	X	230
319	44°54.90S	150°01.70W	02 05 70	X	X		X	X		X	X	X	231
320	39°59.60S	150°01.40W	04 05 70	X	X		X	X		X	X	X	232
321	35°00.0S	149°59.90W	05 05 70	X	X	X	X	X		X	X	X	233
322	29°58.40S	149°58.20W	07 05 70	X	X	X	X	X	X	X	X	X	234
323	24°50.10S	150°00.70W	09 05 70	X	X	X	X	X		X	X	X	235
324	19°57.80S	150°02.90W	10 05 70	X	X	X	X	X	X	X	X	X	236
325	16°37.00S	150°02.00W	11 05 70				X		X				

Stn. #	Lat.	Long.	Date	M.-O.P.H.	S.P.T.	V.P.H.	K.N.C.	B.L.	A.S.L.O.	C.	A. CO^2 S.	A. C14 S.	S.W. CO^2 S.	B.S.N.
326	15°03.10S	149°59.70W	17 05 70		X	X	X		X		X	X	X	237
327	09°50.00S	150°01.50W	19 05 70	X	X	X	X	X	X		X	X	X	238
328	04°59.30S	150°08.30W	20 05 70	X	X	X	X	X	X			X	X	239
329	00°03.60S	149°52.20W	22 05 70	X	X	X	X	X	X		X	X	X	240
330	04°47.40N	150°00.20W	23 05 70	X	X	X	X		X		X		X	241
331	10°05.10N	150°03.80W	25 05 70	X	X	X	X	X	X		X	X	X	242
332	16°02.80N	150°05.70W	26 05 70	X	X	X	X		X		X	X	X	243
333	22°09.80N	149°58.90W	28 05 70	X	X	X	X		X		X	X	X	244
334	28°50.20N	149°57.30W	30 05 70	X	X	X	X		X	X	X	X	X	245
335	35°56.70N	149°54.50W	01 06 70	X		X	X		X		X		X	246
336	42°48.60N	149°51.90W	03 06 70	X	X	X	X		X		X	X	X	247
337	49°09.00N	150°00.40W	04 06 70	X	X	X	X		X		X	X	X	248
338	54°25.00N	150°04.60W	06 06 70	X	X	X	X		X	X	X	X	X	249

"HUDSON 70"

July 12, 1970 - August 8, 1970

Geophysical Survey off the Coast of British Columbia

Soundings - G.E.B.C.O.:	- 6933 km
Gravity Records:	- 6933 km
Magnetics:	- 6933 km
Reflection Profiling:	- 1675 km
Seismic Refraction:	- 621 km

Stn. #	Latitude	Longitude	Date	Heat Flow Stn. #	Camera Stn.	Coring Stn.	Velocimeter Stn.
339	50°58.00N	131°54.70W	15 07 70	1			
340	51°34.70N	134°20.70W	19 07 70	2			
341	51°43.80N	130°00.40W	26 07 70				X
342	49°58.60N	129°32.60W	29 07 70	4			
343	50°01.60N	129°43.00W	29 07 70	5			
344	50°04.40N	129°46.40W	30 07 70	6			
345	50°07.70N	129°49.80W	30 07 70	7		X	
346	50°07.70N	130°01.80W	30 07 70	8			
347	50°13.20N	130°09.20W	30 07 70	9			
348	50°15.30N	130°17.80W	30 07 70	10			
349	50°21.00N	130°06.60W	31 07 70	11			
350	50°45.90N	130°36.60N	01 08 70	12			
351	50°39.50N	130°33.00W	02 08 70	13			
352	50°16.60N	130°17.70W	03 08 70		X		

"HUDSON 70"

August 14, 1970 - September 30, 1970

Esquimalt to Resolute

Soundings G.E.B.C.O.:	- 9653 km
Gravity Records:	- 9653 km
Magnetics:	- 9653 km
Reflection Profiling: (done in Beaufort Sea Area)	- 2194 km

Stn. #	Latitude	Longitude	Date	S.P.T.	V.P.T.	S.B.T.	V.B.T.	V.V.G.	R.D.	C.	C.S.	K. & N.C.	B.S.T.	U./W/T.	O.B.T.
353	49°56.40N	128°56.20W	14 08 70	X	X					X					
354	54°02.50N	161°41.40W	19 08 70	X	X					X					
355	54°58.00N	165°21.00W	20 08 70		X										
356	57°05.00N	166°24.00W	20 08 70		X										
357	59°21.00N	167°38.00W	21 08 70		X										
358	61°40.00N	168°47.00W	21 08 70		X										
359	63°01.00N	169°10.00W	22 08 70		X										
360	67°02.30N	168°23.00W	22 08 70		X										
361	67°38.00N	167°44.00W	23 08 70		X										
362	69°44.00N	164°59.00W	23 08 70		X										
363	70°44.00N	161°03.00W	23 08 70		X										
364	71°23.30N	156°57.19W	24 08 70		X	X									
365	71°26.50N	156°30.50W	24 08 70					X							
366	70°54.50N	151°08.50W	25 08 70		X										

Stn. #	Latitude	Longitude	Date	S.P.T.	V.P.T.	S.B.T.	V.B.T.	V.V.G.	S.D.	C.	C.S.	K. & N.C.	B.S.T.	U./W/T.	O.B.T.
367	70°33.61N	147°26.43W	25 08 70		X										
368	70°07.00N	141°14.00W	26 08 70		X										
369	69°38.00N	138°45.00W	26 08 70			X	X	X		X					
370	69°45.00N	138°34.00W	26 08 70			X		X		X					
371	69°28.00N	138°48.00W	26 08 70			X		X		X					
372	69°36.00N	138°24.00W	26 08 70			X		X							
373	69°40.00N	138°14.00W	26 08 70			X	X	X							
374	70°27.50N	138°57.00W	27 08 70		X	X	X	X							
375	70°19.00N	138°47.50W	27 08 70	X	X	X	X	X		X					
376	70°12.50N	138°40.0W	27 08 70			X		X							
377	70°06.50N	138°31.00W	27 08 70		X	X	X	X		X					
378	69°57.50N	138°27.00W	27 08 70			X		X							

Stn. #	Latitude	Longitude	Date	S.P.T.	V.P.T.	S.B.T.	V.B.T.	V.V.G.	S.D.	C.	C.S.	K.C.	B.S.T.	U./W.T.	O.B.T.	B.S.N.
379	69°50.50N	138°18.00W	27 08 70	X	X	X	X	X		X						
380	69°56.00N	138°54.80W	27 08 70		X	X	X	X								
381	69°53.20N	139°05.00N	27 08 70			X		X					X			
382	70°29.70N	139°00.40W	28 08 70	X	X	X	X									
383	70°22.00N	139°05.50W	28 08 70	X	X	X	X	X								
384	70°15.50N	139°12.30W	28 08 70	X	X	X	X	X								
385	70°08.40N	139°15.90W	28 08 70	X	X	X	X	X	X		X	X				250
386	69°54.20N	139°28.10W	28 08 70	X	X	X	X	X			X					
387	69°42.00N	139°42.10W	28 08 70		X	X	X	X								
388	71°31.30N	138°11.00W	29 08 70	X	X	X				X						
389	70°59.80N	138°14.70W	30 08 70	X	X	X	X			X						
390	70°37.00N	139°29.00W	30 08 70	X	X	X	X	X		X		X				251
391	70°22.00N	139°42.00W	30 08 70	X	X	X	X	X		X		X				252
392	70°10.30N	139°52.60W	30 08 70	X	X	X	X	X		X		X				253
393	69°59.30N	140°15.70W	30 08 70	X	X	X	X	X		X		X				254
394	69°42.00N	140°38.00W	30 08 70	X	X	X	X	X		X		X				255
395	69°11.00N	137°57.00W	31 08 70	X	X	X	X	X		X						
396	69°22.10N	138°04.80W	31 08 70	X	X	X	X	X		X						

Stn. #	Latitude	Longitude	Date	S.P.T.	V.P.T.	S.B.T.	V.B.T.	V.V.G.	S.D.	C.	C.S.	K.C.	B.S.T.	U./W.T.	O.B.T.	B.S.N.
397	69°33.00N	138°11.80W	31 08 70	X	X	X	X	X		X						
398	70°30.50N	138°19.50W	01 09 70	X	X	X	X	X								
399	70°19.80N	138°11.00W	01 09 70	X	X	X	X	X								
400	70°10.50N	137°59.50W	01 09 70	X	X	X	X	X								
401	70°01.00N	137°57.00W	01 09 70	X	X	X	X	X								
402	69°47.00N	137°32.00W	01 09 70	X	X	X	X	X								
403	69°36.00N	137°20.00W	01 09 70	X	X	X	X	X								
404	69°27.00N	137°10.00W	01 09 70	X		X	X	X								
405	70°29.80N	137°49.00W	02 09 70	X	X	X	X	X		X						
406	70°21.50N	137°33.00W	02 09 70	X	X	X	X	X	X	X						
407	70°08.20N	137°15.80W	02 09 70	X	X	X	X	X		X	X					
408	69°58.00N	137°00.00W	02 09 70	X	X	X	X	X		X						
409	69°51.00N	136°48.00W	02 09 70;	X		X	X	X			X					
410	69°44.70N	136°37.30W	02 09 70	X		X	X	X	X							
411	69°58.50N	137°07.60W	03 09 70							X				X		
412	70°45.70N	137°04.00W	04 09 70	X	X	X	X	X								
413	70°32.00N	136°40.00W	04 09 70	X	X	X	X	X								
414	70°18.00N	136°15.00W	04 09 70	X	X	X	X	X								

Stn. #	Latitude	Longitude	Date	S.P.T.	V.P.T.	S.B.T.	V.B.T.	V.V.G.	S.D.	C.	C.S.	K.C.	B.S.T.	U./W.T.	O.B.T.	B.S.N.
415	70°10.60N	135°54.50W	04 09 70	X	X	X	X	X								
416	70°00.60N	135°39.10W	04 09 70	X	X	X	X	X								
417	70°50.85N	136°17.92W	05 09 70	X	X	X	X	X		X						
418	70°42.50N	135°52.00W	05 09 70	X	X	X	X	X		X						
419	70°37.60N	135°49.40W	05 09 70	X	X	X	X	X		X						
420	70°26.00N	135°27.00W	05 09 70		X	X	X	X		X						
421	70°17.60N	135°11.00W	05 09 70		X	X	X	X		X						
422	70°08.00N	134°54.00W	05 09 70			X		X		X						
423	70°41.30N	134°41.50W	06 09 70	X	X	X	X	X				X				256
424	70°26.50N	134°17.50W	06 09 70	X	X	X	X	X				X				257
425	70°17.00N	134°00.00W	06 09 70	X	X	X	X	X				X				258
426	71°31.98N	135°57.48W	07 09 70	X	X	X	X			X						
427	70°57.40N	135°03.40W	07 09 70	X	X	X	X	X		X		X				259
428	70°52.35N	134°57.00W	07 09 70	X	X	X	X	X				X				260
429	70°46.50N	134°50.00W	07 09 70	X	X	X	X	X				X				261
430	70°08.50N	132°47.90W	08 09 70			X	X	X		X						
431	70°14.50N	132°06.10W	08 09 70			X	X	X			X			X		
432	70°07.00N	131°35.00W	08 09 70			X	X	X	X							

Stn. #	Latitude	Longitude	Date	S.P.T.	V.P.T.	S.B.T.	V.B.T.	V.V.G.	S.D.	C.	C.S.	K.C.	B.S.T.	U./W.T.	O.B.T.	B.S.N.
433	70°00.00N	132°32.00W	08 09 70			X	X	X	X							
434	69°52.00N	133°19.50W	08 09 70			X	X	X								
435	70°02.00N	133°45.80W	08 09 70			X	X	X								
436	71°12.00N	134°22.50W	09 09 70	X	X	X	X	X		X						
437	71°01.00N	134°07.00W	09 09 70	X	X	X	X	X		X						
438	70°56.00N	133°59.50W	09 09 70	X	X	X	X	X		X						
439	70°47.00N	133°47.00W	09 09 70	X	X	X	X	X		X						
440	70°38.00N	133°29.00W	09 09 70	X	X	X	X	X		X						
441	70°24.00N	133°09.00W	09 09 70	X	X	X	X	X		X						
442	71°18.50N	133°23.50W	10 09 70	X	X	X	X	X								
443	71°09.50N	133°07.00W	10 09 70	X	X	X	X	X								
444	71°02.80N	132°59.50W	10 09 70	X	X	X	X	X								
445	70°56.20N	132°47.00W	10 09 70	X	X	X	X	X								
446	71°01.20N	132°53.20W	10 09 70							X	X			X		
447	70°45.20N	132°27.60W	10 09 70	X	X	X	X	X								
448	70°31.80N	132°10.00W	10 09 70	X	X	X	X	X								
449	70°52.00N	128°33.00W	12 09 70	X	X	X	X	X		X						
450	70°41.00N	128°19.00W	12 09 70	X	X	X	X	X	X	X	X			X		

Stn. #	Latitude	Longitude	Date	S.P.T.	V.P.T.	S.B.T.	V.B.T.	V.V.G.	S.D.	C.	C.S.	K.C.	B.S.T.	U./W.T.	O.B.T.	B.S.N.
451	70°29.80N	129°22.80W	12 09 70	X		X	X	X	X						X	
452	70°38.70N	129°39.40W	12 09 70	X	X		X	X				X				262
453	71°25.70N	132°06.00W	12 09 70	X	X	X	X	X		X						
454	71°14.14N	131°54.76W	12 09 70	X	X	X	X	X		X						
455	71°03.50N	131°42.70W	13 09 70		X			X		X						
456	70°56.50N	131°24.70W	13 09 70		X	X	X	X		X						
457	70°41.30N	130°52.10W	13 09 70		X	X	X	X		X						
458	70°31.80N	130°41.60W	13 09 70		X	X	X	X		X						
459	70°22.40N	130°31.00W	13 09 70		X	X	X	X	X	X						
460	71°26.75N	130°53.90W	14 09 70		X		X	X				X				263
461	71°16.60N	130°37.60W	14 09 70	X	X		X	X				X				264
462	71°07.00N	130°17.80W	14 09 70	X	X	X	X	X				X				265
463	70°56.80N	130°03.60W	14 09 70	X	X	X	X	X				X				266
464	70°50.00N	129°52.00W	14 09 70		X		X	X				X				267
465	71°25.20N	129°27.30W	15 09 70	X	X	X	X	X		X						
466	71°17.50N	129°10.60W	15 09 70	X	X	X	X	X		X						
467	71°07.90N	128°59.10W	15 09 70	X	X	X	X	X		X						
468	71°01.00N	128°49.50W	15 09 70	X	X		X	X	X	X					X	

Stn. #	Latitude	Longitude	Date	S.P.T.	V.P.T.	S.B.T.	V.B.T.	V.V.G.	S.D.	C.	C.S.	K.C.	B.S.T.	U./H.T.	O.B.T.	B.S.N.
469	69°56.50N	134°33.00W	18 09 70			X	X	X	X	X		X				268
470	69°51.00N	135°20.00W	19 09 70			X	X	X	X	X		X				269
471	71°34.30N	127°41.80W	20 09 70	X	X	X	X	X								
472	71°38.00N	129°50.00W	20 09 70							X						
473	71°15.80N	127°57.60W	23 09 70	X	X	X	X	X		X		X				270
474	71°02.00N	125°44.00W	23 09 70	X	X	X	X	X		X		X				271

Stn. #	Latitude	Longitude	Date	S.P.T.	V.P.T.	S.B.T.	V.B.T.	V.V.G.	R.D.	C.	C.S.	K.C.	B.S.T.	U./W.T.	O.B.T.	B.S.N.
475	70°49.80N	123°30.50W	23 09 70	X	X	X	X	X		X		X				272
476	71°20.00N	119°24.00W	24 09 70	X	X	X	X	X		X		X				273
477	71°59.00N	119°30.00W	24 09 70	X	X	X	X	X		X		X				274
478	72°30.00N	118°39.00W	24 09 70	X	X	X	X	X		X		X				275
479	73°01.00N	117°12.00W	24 09 70	X	X	X	X	X		X		X				276
480	73°24.20N	115°04.00W	25 09 70	X	X	X	X	X		X		X				277
481	73°48.10N	113°45.50W	25 09 70	X	X	X	X	X		X		X				278
482	74°39.00N	108°10.50W	26 09 70	X	X	X	X	X		X		X				279
483	74°41.80N	105°15.50W	27 09 70	X	X	X	X	X		X		X				280
484	74°47.90N	101°35.20W	27 09 70	X	X	X	X	X		X		X				281
485	74°53.00N	98°03.00W	28 09 70	X	X	X	X			X		X				282
486	74°13.90N	95°29.70W	28 09 70	X	X	X	X	X		X		X				283
487	74°28.00N	92°32.00W	29 09 70	X	X	X	X	X		X		X				284
488	74°28.60N	90°04.00W	29 09 70	X	X	X	X	X				X				285
489	74°22.80N	90°08.00W	29 09 70	X	X	X	X	X				X				286
490	74°16.80N	90°17.00W	29 09 70	X	X	X	X	X		X		X				287
491	74°11.00N	90°12.00W	29 09 70	X	X	X	X	X				X				288
492	74°02.50N	90°30.00W	29 09 70	X	X	X	X					X				289
493	74°16.00N	88°01.50W	30 09 70	X	X	X	X					X				290

"HUDSON 70"

October 1, 1970 - October 16, 1970

Area:- Resolute to Halifax
(Covering - Eastern Arctic - Baffin Bay - Labrador Sea)

Soundings - G.E.B.C.O.:	- 4570 km
Gravity Records:	- 4570 km
Magnetics:	- 4570 km
Seismic Reflection Profiling:	- 770 km
Reversed Seismic Refraction:	- 250 km

Stn. #	Latitude	Longitude	Date	S.P.T.	V.P.T.	C.	K.C.	B.S.N.
494	74°10.80N	84°58.00W	01 10 70	X	X			
495	74°01.00N	79°56.00W	01 10 70	X	X		X	291
496	72°13.00N	69°50.00W	04 10 70	X	X	X	X	292
497	71°02.00N	64°54.00W	05 10 70	X	X	X	X	293
498	72°17.50N	66°02.00W	06 10 70	X	X	X	X	294
499	72°16.00N	67°40.00W	06 10 70	X	X		X	295
500	71°00.90N	59°48.80W	08 10 70	X	X		X	296
501	69°00.00N	59°39.50W	09 10 70	X	X		X	297
502	67°11.90N	59°22.20W	09 10 70	X	X		X	298
503	64°45.40N	58°28.30W	10 10 70	X	X		X	299
504	62°25.00N	57°06.00W	10 10 70	X	X		X	300
505	57°37.00N	55°01.90W	11 10 70	X	X		X	301
506	52°46.90N	53°15.50W	12 10 70	X	X			
507	50°13.00N	52°26.50W	13 10 70	X	X			
508	48°32.20N	52°12.40W	13 10 70	X	X			

A T L A N T I C O C E A N O G R A P H I C L A B O R A T O R Y

B E D F O R D I N S T I T U T E

"HUDSON 70"

INTERIM CRUISE REPORT

A. HALIFAX TO RIO DE JANEIRO

B. RIO DE JANEIRO TO BUENOS AIRES

C.R. MANN

CRUISE NO. 69-050

CRUISE REPORT NO. 69-050

"HUDSON 70" - INTERIM CRUISE REPORT

A. HALIFAX TO RIO DE JANEIRO

Local Cruise Designation:	69-050
CODC Reference Number:	10-69-050
Vessel:	C.S.S. HUDSON
Dates:	19 November to 20 December 1969
Area:	Halifax to Rio de Janeiro
Responsible Agency:	Atlantic Oceanographic Laboratory Bedford Institute
Personnel:	Ship's Master, Captain D.W. Butler
Scientific Staff:	
C.R. Mann Chief Scientist	Atlantic Oceanographic Laboratory Bedford Institute
R.C. Melanson Assistant Chief Scientist	Atlantic Oceanographic Laboratory Bedford Institute
B.D. Carson	Atlantic Oceanographic Laboratory Bedford Institute
A.R. Coote	Atlantic Oceanographic Laboratory Bedford Institute
T.J. Corbett	Atlantic Oceanographic Laboratory Bedford Institute
A.B. Grant	Atlantic Oceanographic Laboratory Bedford Institute
R.S. Hiltz	Atlantic Oceanographic Laboratory Bedford Institute
J. Piechura	Atlantic Oceanographic Laboratory Bedford Institute
P. Wadhams	Atlantic Oceanographic Laboratory Bedford Institute
P.C. Beamish	Marine Ecology Laboratory Bedford Institute
I.W. Duedall	Marine Ecology Laboratory Bedford Institute

Scientific Staff (Continued):

K. Freeman	Marine Ecology Laboratory Bedford Institute
L.P. Atkinson	Institute of Oceanography Dalhousie University
Chung I. Choi	Institute of Oceanography Dalhousie University
R.C. Cooke	Institute of Oceanography Dalhousie University
W. Watt	Institute of Oceanography Dalhousie University
O. Bluy	Defence Research Establishment Atlantic Dartmouth, Nova Scotia
J.G. Gill	Defence Research Establishment Atlantic Dartmouth, Nova Scotia
R. Smith	Queen's University Kingston, Ontario
R.J. Beamish	University of Toronto Toronto, Ontario

Summary:

Surface Plankton Tows	21
Vertical Plankton Hauls	25
Isaacs Kidd Midwater Trawls	13
Surface Tows - Neuston Net	4
Knudsen and Niskin Casts (Surface to Bottom)	11
Bathysonde Lowerings	12
Expendable Bathythermographs Used	90
Cores Taken	3
Acoustic Scattering Layer Observations	21
In-Situ C^{14} Incubation Experiments (Including 4-bottle Niskin Cast)	10

Summary (continued):

Miles of Soundings (GEBCO)	4463
Miles of Gravity Records (approximate)	3800
Miles of Magnetics (approximate)	4200
Recordings of Whale and Dolphin Sounds	2

Narrative:

C.S.S. Hudson left Halifax for Rio de Janeiro at 1535 hours, 19 November, 1969, on the first leg of her cruise to circumnavigate the Americas. The following report covers activities up to the time of departure from Rio de Janeiro.

On leaving Halifax, a great circle route was followed to 0° Lat., 30° Long., the position of the first of a line of stations extending along 30°W Long. in the South Atlantic. Gravity, magnetics, and bathymetry were recorded enroute to the first station, and from then on between stations until 250 miles from Cape Frio. Gravity was measured with an Askania gravimeter, magnetics with a Barringer magnetometer, and bathymetry using an Alpine precision depth recorder with a Gifft receiver. As much as possible of the data were processed on board by computer. All the magnetic data were reduced to give the earth's magnetic field but it was not possible to process the gravity data due to lack of time. The bathymetric data were copied onto plotting sheets. The positions of the oceanographic stations and of other stops for observations were also recorded on these sheets.

A herd of sperm whales was sighted on 29 November 1969; the ship was stopped and records of their sounds were made. The ship arrived at 0° Lat., 30°W Long., on 30 November, 1969, and commenced the sampling program for chemistry, biology, acoustics, and physical oceanography. As the chemists could not analyze water samples from more than one station each day, it was decided to do one station each day at which all samples were taken. This allowed two or three hours extra time each night as each complete station took 12 hours and the ship could steam between stations in 9 hours. From 0° Lat. one station each day was occupied every $2\frac{1}{2}$° of latitude along the 30°W meridian and the work at Station 11, the last station before making for Rio de Janeiro, was completed on 10 December, 1969. Usually, each station consisted of scattering-layer observations; vertical and surface plankton tows; two casts, one deep and one shallow, of Knudsen and Niskin bottles on the same wire; a bathysonde cast; and an Isaacs Kidd haul. The scattering layer observations were made with a 1 lb. explosive sound-source, a directional receiving system consisting of a hydrophone in an inverted cone, and an omnidirectional receiving system. Four to five charges were fired at each station.

Each night the ship was stopped at about 2130 hours, depending on the

program, and an additional set of scattering layer observations made and a vertical plankton tow taken. On occasion, a Neuston net was towed to catch surface fish and the Isaacs Kidd net was hauled at night instead of early in the day.

A series of three cores was obtained where the water was shallower than 4,000 metres, as this was the deepest that a core could be taken. Mostly soft mud was recovered and the core on two occasions went into its maximum depth so that 57 and 60 foot cores were obtained.

Experiments to study primary production were made at each station. This required lowering 4 sets of small bottles attached to a line to 120 metres, and allowing them to sit in position for four hours at midday. As the experiment had to be conducted while doing other work, it could not be done from the ship. A lifeboat was put out and the string of bottles lowered from the lifeboat. This worked very well except that the lifeboat tended to drift away from the ship and the bottles could not be brought inboard quickly enough for processing. Eventually the lifeboat was tethered to the bow of the ship by a long nylon line and allowed to drift away with the wind about 200 metres.

The newly installed sea-water loop was used to collect samples of sea water for a study of productivity by measuring the uptake of C^{14}, and a series of samples obtained for measurement of chlorophyll, RNA, ATP, and particulate carbon.

On completing the sampling program at the 11 stations laid out at every $2\frac{1}{2}^{o}$ of latitude in the original plan, the ship made for Rio de Janeiro. There was additional time available enroute to Rio and this was used for scattering-layer observations and plankton hauls.

The ship arrived in Rio de Janeiro on 14 December, 1969, with the first phase of Hudson 70 completed. While in Rio, permission was obtained to capture a dolphin. Recordings of sounds from the dolphins in the bay were made and one dolphin was captured and frozen for return to Halifax for identification. The ship remained in Rio until 20 December, 1969, when she departed for the southern part of the Atlantic.

B. RIO DE JANEIRO TO BUENOS AIRES

Local Cruise Designation:	69-050
CODC Reference Number:	10-69-050
Vessel:	C.S.S. HUDSON
Dates:	20 December 1969 to 16 January 1970
Area:	Rio de Janeiro to Buenos Aires with operations in vicinity of South Georgia.
Responsible Agency:	Atlantic Oceanographic Laboratory Bedford Institute
Personnel:	Ship's Master, Captain D.W. Butler
Scientific Staff:	
C.R. Mann Chief Scientist	Atlantic Oceanographic Laboratory Bedford Institute
R.C. Melanson Assistant Chief Scientist	Atlantic Oceanographic Laboratory Bedford Institute
B.D. Carson	Atlantic Oceanographic Laboratory Bedford Institute
A.R. Coote	Atlantic Oceanographic Laboratory Bedford Institute
A.B. Grant	Atlantic Oceanographic Laboratory Bedford Institute
R.S. Hiltz	Atlantic Oceanographic Laboratory Bedford Institute
G. Vilks	Atlantic Oceanographic Laboratory Bedford Institute
P. Wadhams	Atlantic Oceanographic Laboratory Bedford Institute
P.C. Beamish	Marine Ecology Laboratory Bedford Institute
R.J. Conover	Marine Ecology Laboratory Bedford Institute

Scientific Staff (continued):

I.W. Duedall	Marine Ecology Laboratory Bedford Institute
K. Freeman	Marine Ecology Laboratory Bedford Institute
A. Prakash	Marine Ecology Laboratory Bedford Institute
L.P. Atkinson	Institute of Oceanography Dalhousie University
Mrs. G.B. Deevey	Institute of Oceanography Dalhousie University
J.H. Sharpe	Institute of Oceanography Dalhousie University
P. Wangersky	Institute of Oceanography Dalhousie University
O. Bluy	Defence Research Establishment Atlantic Dartmouth, Nova Scotia
J.G. Gill	Defence Research Establishment Atlantic Dartmouth, Nova Scotia
R. Smith	Queen's University Kingston, Ontario
Mrs. C.M. Lalli	McGill University Montreal, Quebec
R.E. Zurbrigg	University of Toronto Toronto, Ontario

Summary:

Surface Plankton Tows	36
Vertical Plankton Hauls	32
Oblique Plankton Tows	18
Deep Multiple Plankton Tows	15
Isaacs Kidd Midwater Trawls	14
Knudsen and Niskin Casts (Surface to Bottom)	20

Summary (continued):

Bathysonde Lowerings	16
Expendable Bathythermographs Used	162
Cores Taken	3
Acoustic Scattering Layer Observations	23
Recording of Whale Sounds	1
Miles of Soundings (GEBCO)	3270

Narrative:

At noon on 20 December, 1969, C.S.S. Hudson left Rio de Janeiro for the southernmost regions of the Atlantic Ocean. The general plan was to continue the sampling at stations running south along the 30°W meridian that had been started before entering Rio. This line of stations was to terminate at 55°S Lat., to the east of South Georgia. A second line of stations running north along 40°W meridian was then to be worked after which the ship was to steam for Buenos Aires.

The ship arrived at the first station on 23 December, 1969, and commenced a program of casts of Knudsen and Niskin bottles for the chemical and physical oceanographic studies, and various plankton tows for biological programs. Measurement of gravity and the earth's magnetic field was terminated in Rio and not carried on further south. The program on station became heavier than during the Halifax to Rio de Janeiro transit because of the increase in the number of plankton tows. Each station took approximately 12 hours to complete and consisted of a deep and shallow cast of Knudsen and Niskin bottles on the same wire, two vertical plankton tows from 200 metres, an oblique tow (underway) at 200 metres, a deep tow with three nets on one wire (usually done from the Telecon winch) with the deepest net at 1000 metres or deeper, an Isaacs Kidd haul, a surface plankton tow, and a streaming of hydrophones for observation of the scattering layer. When time permitted, and this was not often, additional tows and observations of the scattering layer were made between stations.

On running down the 30th meridian, one station was occupied each day. This was more time consuming than running the 90 miles between stations as quickly as possible but was adopted because the two teams of chemists could not complete their analysis, and the biologists could not sort plankton and conduct the experiments that they were performing faster than one station each day. Still, more data were acquired than originally anticipated when it was thought only every second station could be fully processed.

On 29 December, 1969, after Station 18, the sub-tropical convergence was crossed and Antarctic plankton forms began to appear in the tows.

On 2 January, 1970, at Station 22, large icebergs appeared 11 miles south on the radar. After leaving the station, the ship crossed the Antarctic convergence in the vicinity of the icebergs and the surface temperature dropped to 1.5°C. While steaming on the night of the 2 January, 1970, many icebergs appeared on the radar, and on one occasion, when visibility was poor due to fog, the ship had to go astern to avoid a growler too low to show on the radar screen. Due to the density of icebergs and growlers, it was decided to stop at night. As there were only six hours of darkness and the stations were only 60 miles apart, this did not slow up the program greatly.

On completing the stations down the 30th meridian, the ship headed for 51°30'S Lat., 40°W Long. to start a line of five stations running north along the 40th meridian, across the south edge of the Argentine Basin. In view of the work up to this time, it was decided to run these stations as fast as possible to allow time for more work in the Argentine Basin. Also, a message had been received from Bedford Institute that the fire extinguishers had to be overhauled in Buenos Aires, and it was learned from the agent in Punta Arenas that Hudson had to call at Possession Bay for clearance before proceeding to Puerto Williams after leaving Buenos Aires. This made it desirable to attempt to reach Buenos Aires a day early and to leave on the afternoon of 21 January, 1970, instead of the morning of 22 January, 1970, so that Puerto Williams could be reached by 27 January, 1970, as originally planned.

The five stations along 40°W Long. were completed on 11 January, 1970, and the ship steamed for Buenos Aires. As a line of soundings was listed on the latest bathymetric chart of the oceans along the direct track, the ship steamed 60 miles north before heading for the pilot station at the mouth of the Rio de la Plata, so as to provide a new set of soundings for GEBCO.

During the run in, a station was occupied on the western side of the Argentine Basin, and Isaacs Kidd and plankton hauls made at several positions on the way across. The scientific program was terminated on the evening of 13 January, 1970. Hudson arrived in Buenos Aires at 0800 hours on 16 January, 1970.

The two groups of chemists onboard determined oxygen, phosphate, nitrate, silicate, pH, alkalinity, argon, nitrogen, and total carbonate from sea-water samples taken from the surface to bottom at each station. Samples were also collected for determination of particulate organic carbon, major-ion ratios, and helium isotope analyses. At Station 25, in the South Sandwich Trench, a special cast of Niskin bottles was made to 7400 metres to collect samples for determination of dissolved organic carbon at depths greater than 5000 metres.

The biological program consisted of a series of tows of nets at various depths from the surface to about 2000 metres. Some difficulty was experienced south of the Antarctic Convergence with steaming and recovery of the nets. Generally, the wind speed was 30-40 knots in this area and the motion of the ship caused slackening of the wire and snarls

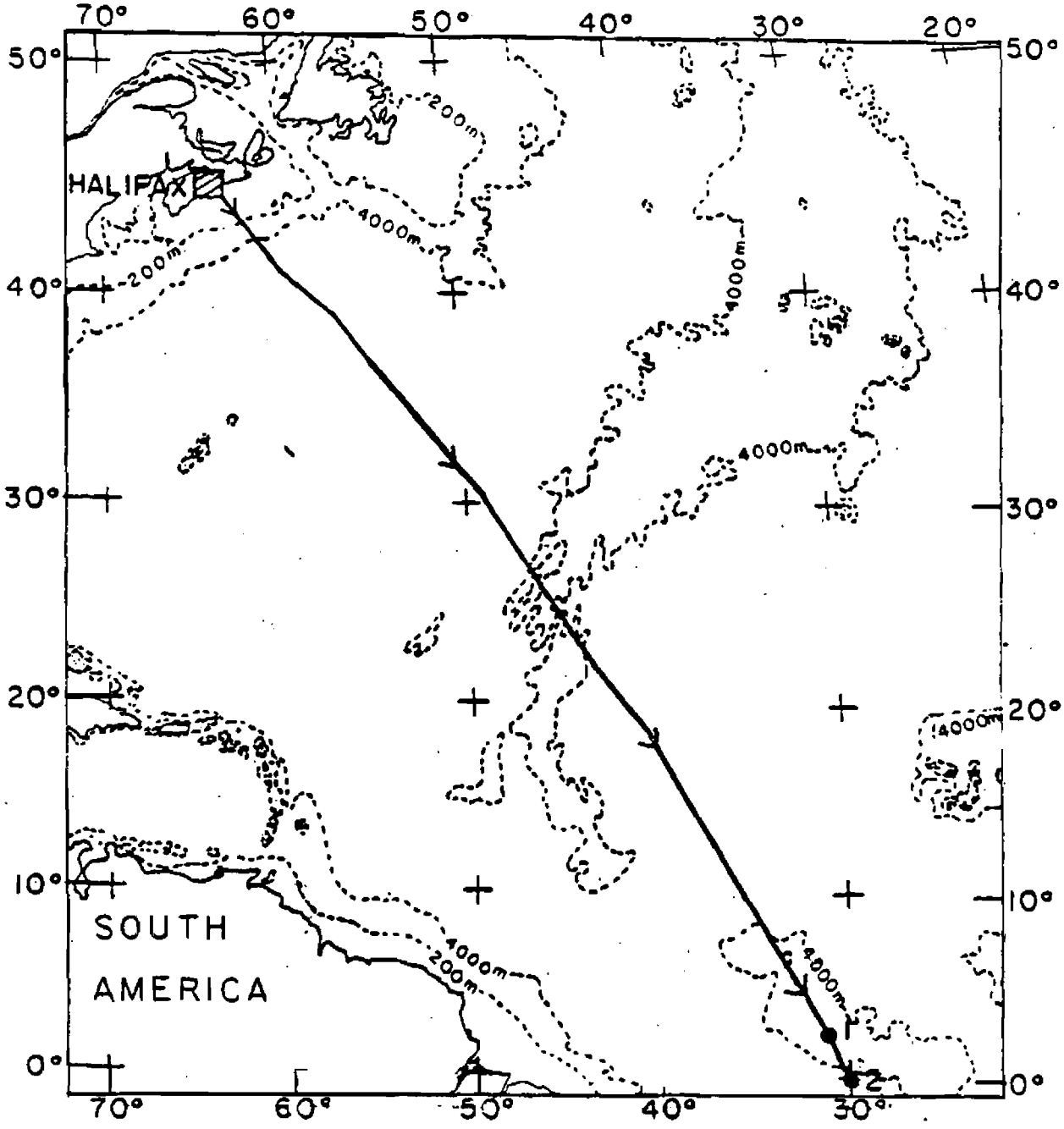
in it. The nets also flapped badly in the wind and tore on occasion.

At several stations, it was not possible to tow the Isaacs Kidd net. Some preliminary identification was done onboard and feeding experiments carried out. Surface samples were collected using the sea-water loop for the study of productivity of surface water started on the run from Halifax to Rio de Janeiro. In addition to the determination of chlorophyll, RNA, ATP, and particulate carbon, a Coulter Counter was operated after leaving Rio to give a count of particulate matter of various sizes. A preliminary examination shows a correlation with the water-mass structure. Three cores were obtained.

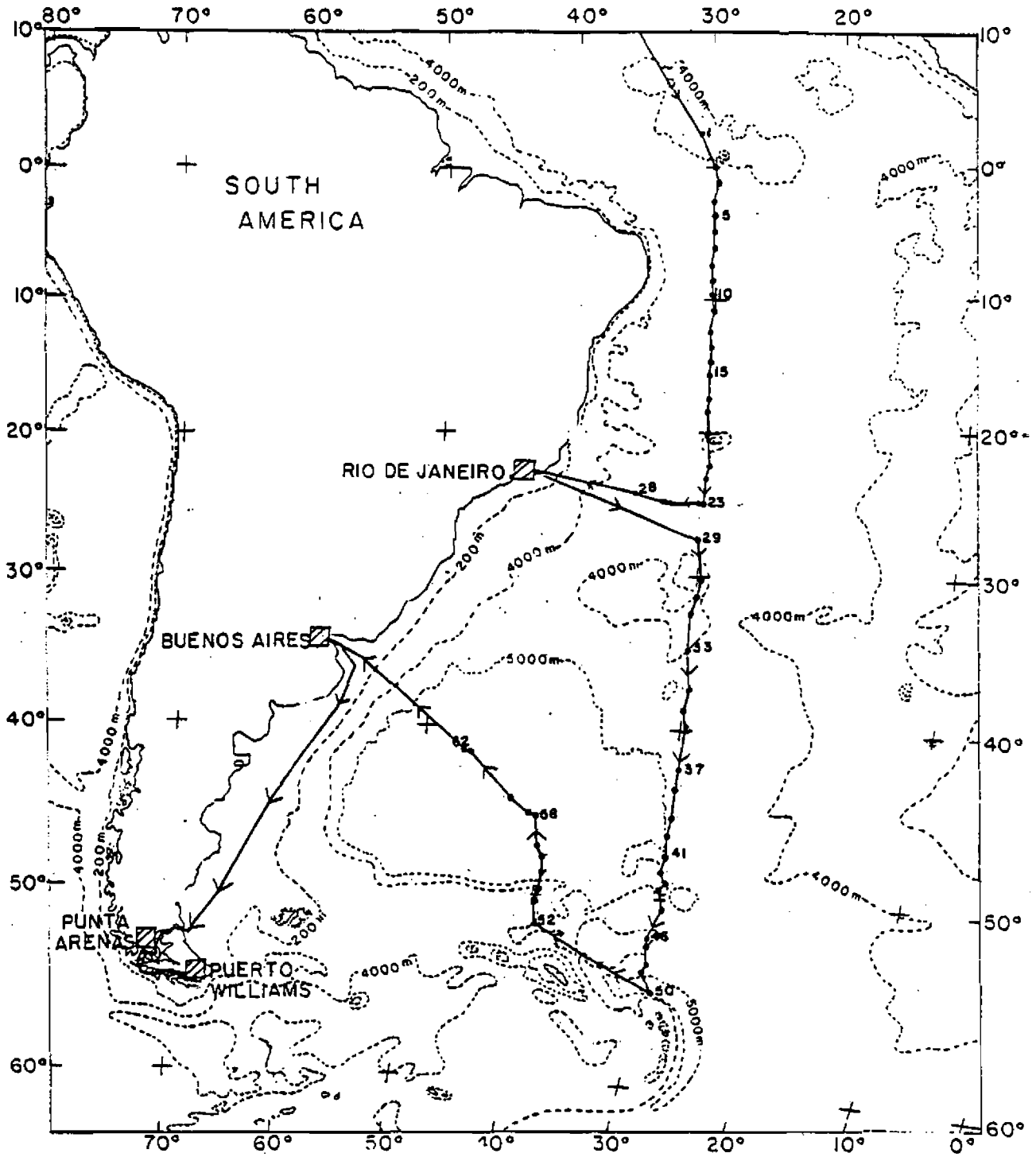
Measurements of sound scattering from the scattering layer were continued as on the Halifax to Rio leg. It was not possible to operate the directional receiving system in the southernmost areas as the seas made steaming and recovery of the directional hydrophone in the cone-reflector hazardous, with possible loss of the cone. The omnidirectional receiving system was operated at all stations.

Whales were sighted on occasion although in the vicinity of South Georgia none were seen. A recording of sounds from whales, tentatively identified as Fin whales, was made in the vicinity of Station 26. A large number of pilot whales came near the ship at Station 29 but no good recordings were obtained. After leaving Station 30, pictures were obtained of a spectacular striped dolphin which could not be identified from reference pictures aboard.

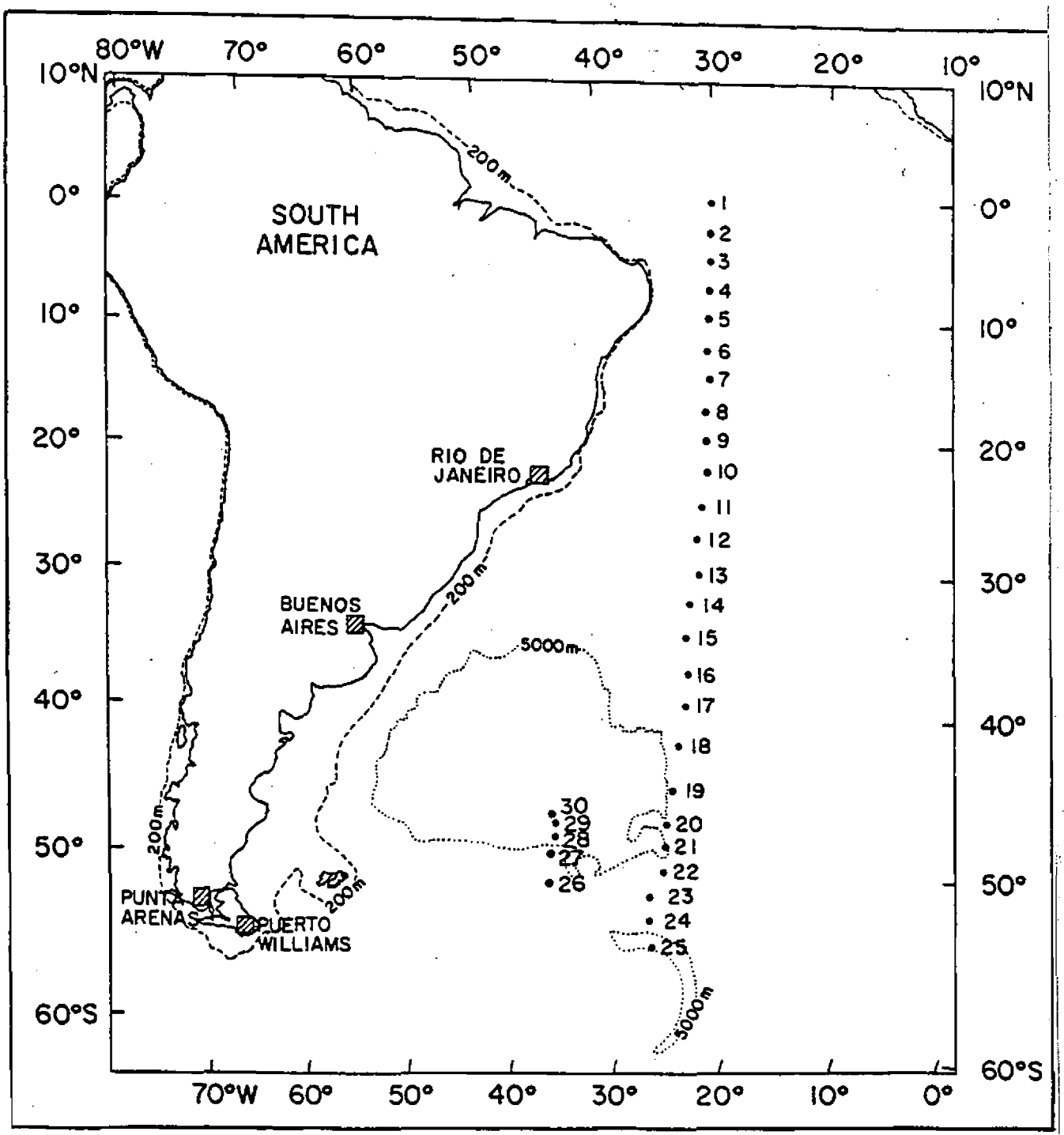
As the skies were overcast, the satellite navigation system proved invaluable. On one station near the Antarctic Convergence that took 14 hours, the ship was found to drift 23 miles.



The first two stations of the HUDSON 70 Expedition on the Halifax to Rio de Janeiro leg (Phase I).



Cruise stations occupied on the first two legs of HUDSON 70: Halifax to Rio de Janeiro (Phase I) and Rio de Janeiro to Buenos Aires (Phase II).



Oceanographic bottle stations during the first two phases of HUDSON 70

A T L A N T I C O C E A N O G R A P H I C L A B O R A T O R Y

B E D F O R D I N S T I T U T E

"HUDSON 70"

INTERIM CRUISE REPORT

BUENOS AIRES TO PUNTA ARENAS

C.R. MANN

CRUISE NO. 69-050

CRUISE REPORT NO. 69-050

"HUDSON 70" - INTERIM CRUISE REPORT

BUENOS AIRES TO PUNTA ARENAS

Local Cruise Designation:	69-050
CODC Reference Number:	10-69-050
Vessel:	C.S.S. HUDSON
Dates:	22 January to 23 February 1970
Responsible Agency:	Atlantic Oceanographic Laboratory Bedford Institute
Personnel:	Ship's Master, Captain D.W. Butler
Scientific Staff:	
C.R. Mann Chief Scientist	Atlantic Oceanographic Laboratory Bedford Institute
T.R. Foote Asst. Chief Scientist	Atlantic Oceanographic Laboratory Bedford Institute
B.D. Carson	Atlantic Oceanographic Laboratory Bedford Institute
A.B. Grant	Atlantic Oceanographic Laboratory Bedford Institute
J.G. Murray	Atlantic Oceanographic Laboratory Bedford Institute
P. Wadhams	Atlantic Oceanographic Laboratory Bedford Institute
J.M.R. Pilote	Atlantic Oceanographic Laboratory Bedford Institute
S.B. McHughen	Atlantic Oceanographic Laboratory Bedford Institute
E.A. Lewis	Atlantic Oceanographic Laboratory Bedford Institute
R.F. Reiniger	Atlantic Oceanographic Laboratory Bedford Institute
I.W. Duedall	Marine Ecology Laboratory Bedford Institute

Scientific Staff (continued):

A.D. Michael	Institute of Oceanography Dalhousie University
E.L. Mills	Institute of Oceanography Dalhousie University
R. Smith	Queen's University Kingston, Ontario
F. Cooke	Queen's University Kingston, Ontario
E.L. Bousfield	National Museum of Natural Sciences Ottawa, Ontario
J.W. Markham	National Research Council Halifax, Nova Scotia
P.L. Sacks	Woods Hole Oceanographic Institution Woods Hole, Massachusetts
P.G. Brewer	Woods Hole Oceanographic Institution Woods Hole, Massachusetts
R.L. Edwards	Trent University Peterborough, Ontario
R.R. Hessler	Scripps Institution of Oceanography La Jolla, California
N.R. Rock	I.O. Sao Paulo Sao Paulo, Brazil
R.S. Rebaudi	Argentine Navy Buenos Aires

Summary:

Surface Plankton Tows	16
Vertical Plankton Tows	34
Knudsen and Niskin Casts	16
Bathysonde Lowerings	10
Expendable Bathythermographs	32
Current Meter Moorings	4
Epibenthic Sled Hauls	11

Summary (continued):

Anchor Dredge Grabs	1
Smith McIntyre Grabs	3
Bird Count Watches	23
Nephelometer Lowerings	8
Miles of Soundings (GEBCO)	3700

Launch Operations - Isla Navarino:

Marine and fresh-water invertebrate animals: About 20,000 specimens collected at 33 collecting stations.

Intertidal Marine Algae: About 500 samples.

Narrative:

At 1015 on 22 January, C.S.S. Hudson left Buenos Aires for Puerto Williams, the Drake Passage, and the Bransfield Strait. An Argentine oceanographer, Lt. S. Rebaudi, and a Brazilian oceanographer, Dr. N. Rock, joined the vessel for this part of the voyage. Hudson entered the Strait of Magellan on 26 January and sailed west through the Strait to Punta Arenas where she stood offshore to allow transfer of personnel ashore. She then proceeded to Puerto Williams through the Islands of Tierra del Fuego, approaching Puerto Williams from the west, through the Beagle Channel, on the evening of the 27 January.

The ship was made welcome by the Commandante and his staff. Drs. Bousfield, Markham and Coxwain, F. Durnford, were put ashore with the launch 'Redhead' to remain at Puerto Williams and collect algae and molluscs around the shores of Isla Navarino while Hudson worked in the Drake Passage. The Chilean navy very kindly provided quarters for them and a naval officer went with them in the launch and guided them around the Islands.

Hudson left Puerto Williams on 28 January and took a dredge sample of the sea bed to start the collection of bottom fauna and after rounding Navarino Island, collected more samples in the vicinity of Cape Horn.

Leaving Cape Horn on 30 January, Hudson proceeded south to start laying buoys carrying current meters and temperature recorders across the Drake Passage. At the first position, a bathymetric survey showed an uneven bottom with several hundred metres between crest and trough. The current meters could not be laid here and the location was shifted 60 miles west where an acceptably flat area was found. Even so, undulations of 50 metres in the topography made an uncertainty of 25 metres in the depth at which the subsurface float would settle as the length of line between float and anchor had to be cut before laying. The first of four buoys was laid on the afternoon of 31 January. The subsurface float was set at 150 metres and carried three current meters, one at 100 metres from the bottom, one at a depth of 1500 metres, and one at a

depth of 150 metres. Temperature recorders were located in the mooring immediately below the current meters. Hudson proceeded across the Passage towards Anvers Island laying three more sets of current meters and buoys enroute. A rough bottom at the second mooring position caused problems as in the first mooring; at the two southern locations, the bottom was smooth and gently rising to the south and the buoys were laid without difficulty.

Enroute across the Passage, Knudsen bottle casts and plankton hauls were made at four locations. Lowerings of a nephelometer to study turbidity in the water column were made. These showed clear water throughout the deeper part of the water column with no sign of the deep nepheloid layer of the Atlantic. Five one litre Niskin bottles were set in the knudsen bottle casts to collect water samples for trace element analysis.

Having completed laying the current meters on 4 January, a start was made on the collection of benthic fauna in the Bransfield Strait area using sleds and dredges to obtain samples from the surface of the sea floor. A haul was made north of Anvers Island in depths of 1500 metres. Hudson then sailed into the Bransfield Strait and samples were collected in southern bays of the South Shetland Islands where mud was known to occur. South Bay, Discovery Bay, and Marion Cove were visited on 5 February. The ship entered Admiralty Bay, King George V Island, on 6 February and remained in the bay during the day. A landing was made in the vicinity of the old base of the Falkland Islands Dependencies Survey.

On leaving King George V Island, a heavy storm was encountered and Hudson moved north to obtain a lee north of the Island where bottom samples were obtained on 7 January. As one of the party was ill, the ship headed for Puerto Williams arriving early on 9 January. The ill member of the party was put ashore and contact was made with the launch party who needed repairs to the 'Redhead'. These were made and Hudson left Puerto Williams during late afternoon, for the Drake Passage.

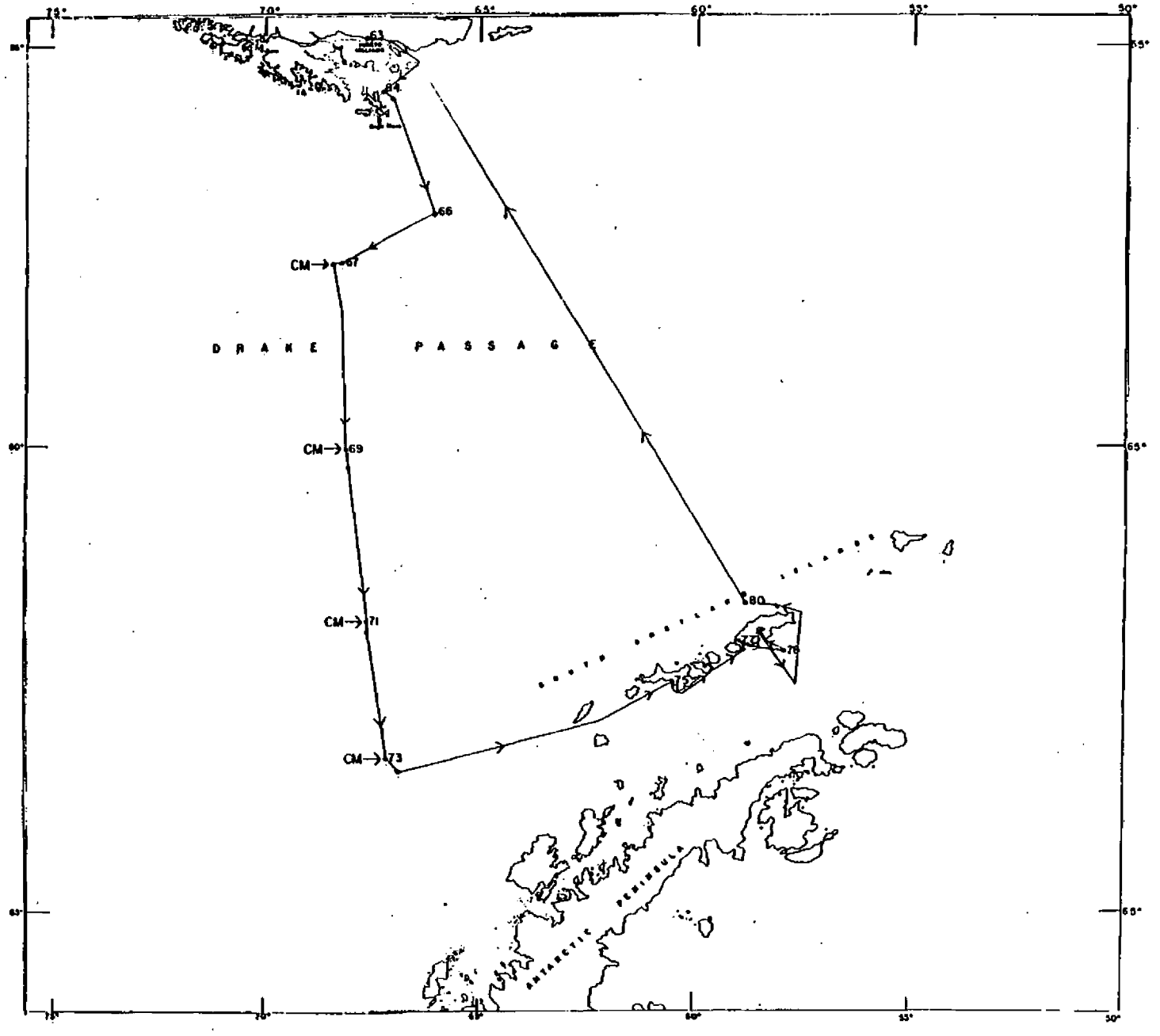
From 10 to 14 January, a series of Knudsen bottle casts and bathysonde lowerings was made as the ship proceeded south along the line that the current meters were laid on. The current meters were recovered as the ship moved south. All acoustic releases operated on command and the buoys and meters were recovered without incident. Calm weather helped the recovery but fog caused difficulty in sighting the buoys after they had surfaced. The radio beacons mounted on the buoys proved very useful as the ship could be guided to them by D/F.

After recovering the current meters. Bransfield Strait was again entered to complete the collection of bottom samples at the eastern end of the Strait. A call was made at Deception Island enroute on 15 February. Hudson cleared the Bransfield Strait on 16 January, collected some sea water samples north of Elephant Island, and made for Puerto Williams. A bottom sample was obtained at the entrance to the Beagle Channel.

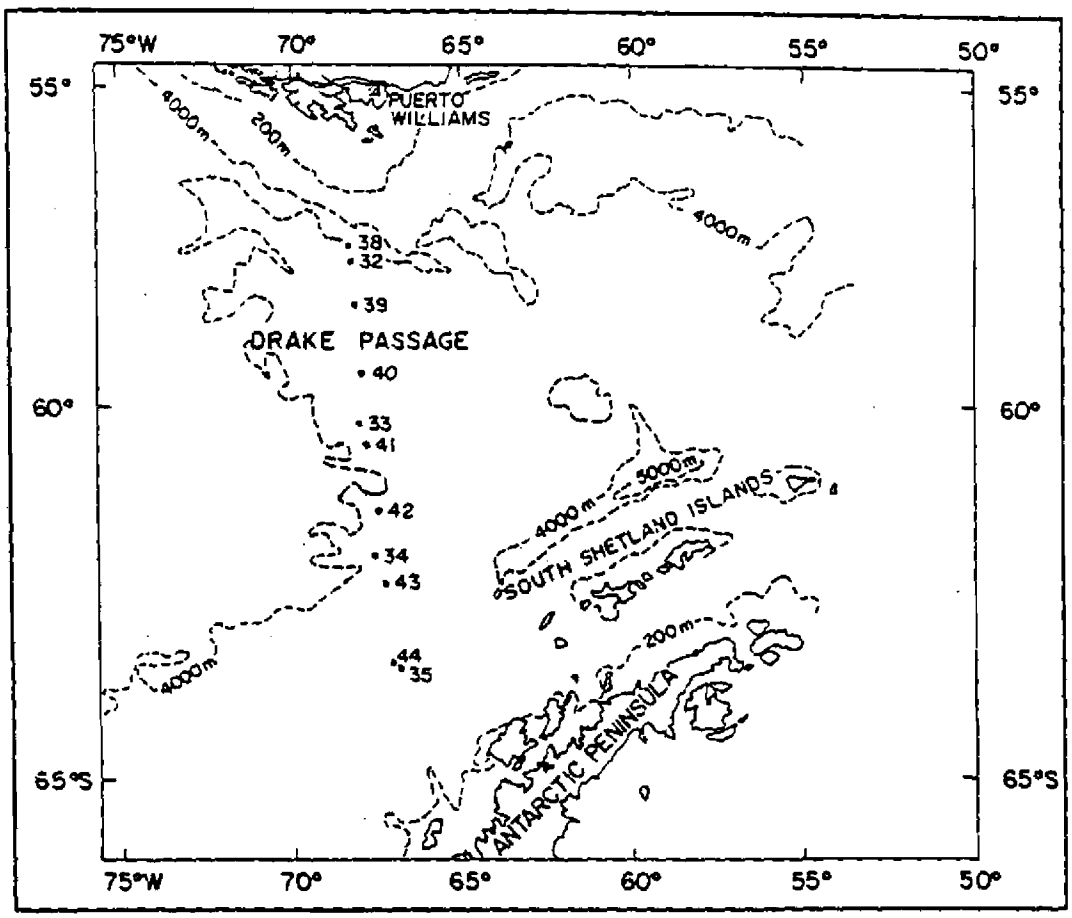
On arrival at Puerto Williams on 20 February, the launch party was taken aboard. Their expedition had proven very successful. Leaving

Puerto Williams in the late afternoon, Hudson made for the area south of Isla Navarina where a final bottom sample was obtained; she then sailed, via the Magellan Strait, for Punta Arenas arriving on 23 February 1970.

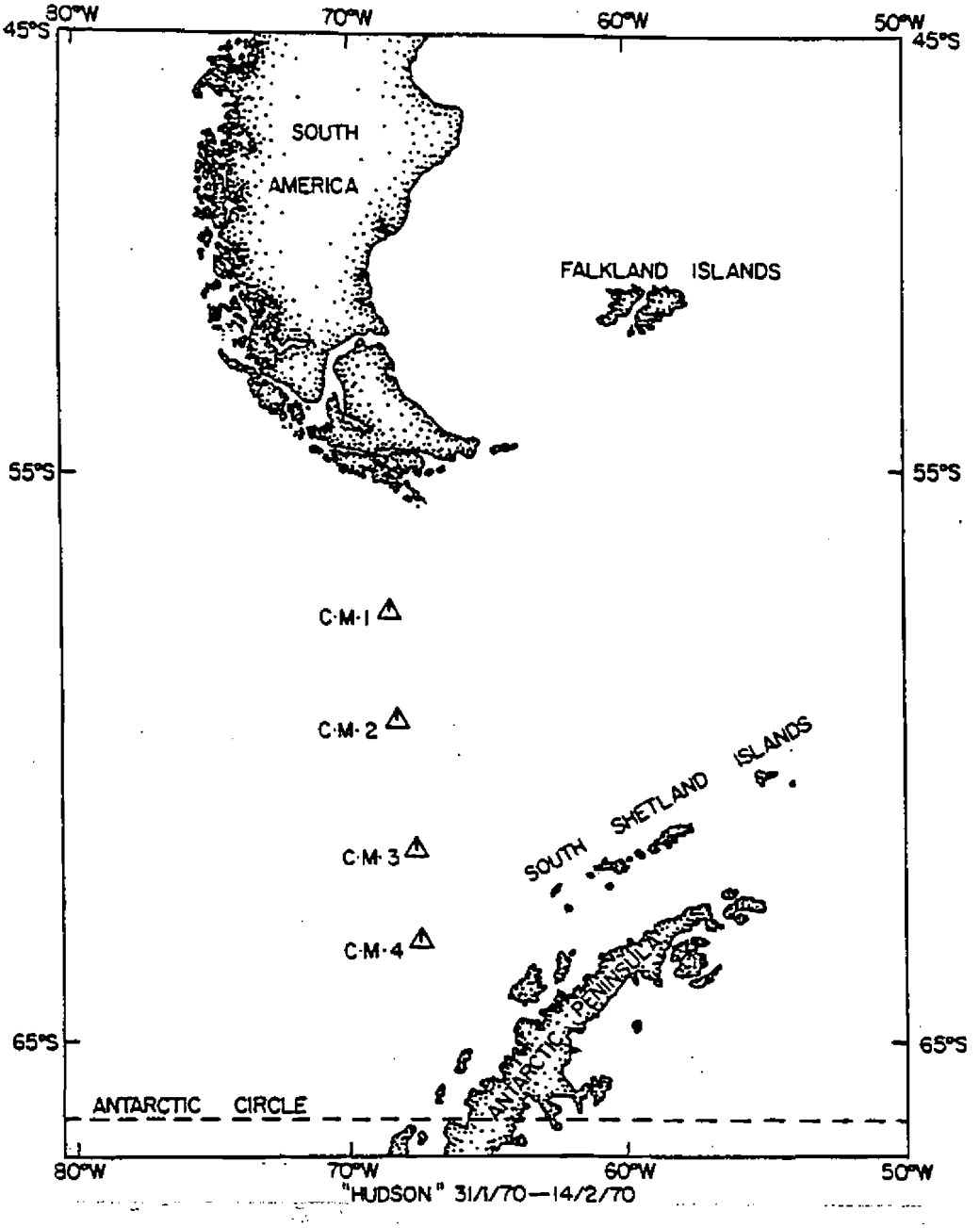
The collection of molluscs and algae for Bousfield and Markham, a series of sea bed samples for Mills and Hessler, water samples and nephelometer lowerings for Brewer and Sacks, plankton samples for Edwards, and current meter measurements and water samples for chemical analysis by AOL staff had all been obtained. In addition, some ardent bird watching by F. Cooke provided new information on the bird life in the area. The scientific program of this phase of Hudson 70 was completed to the satisfaction of all staff.



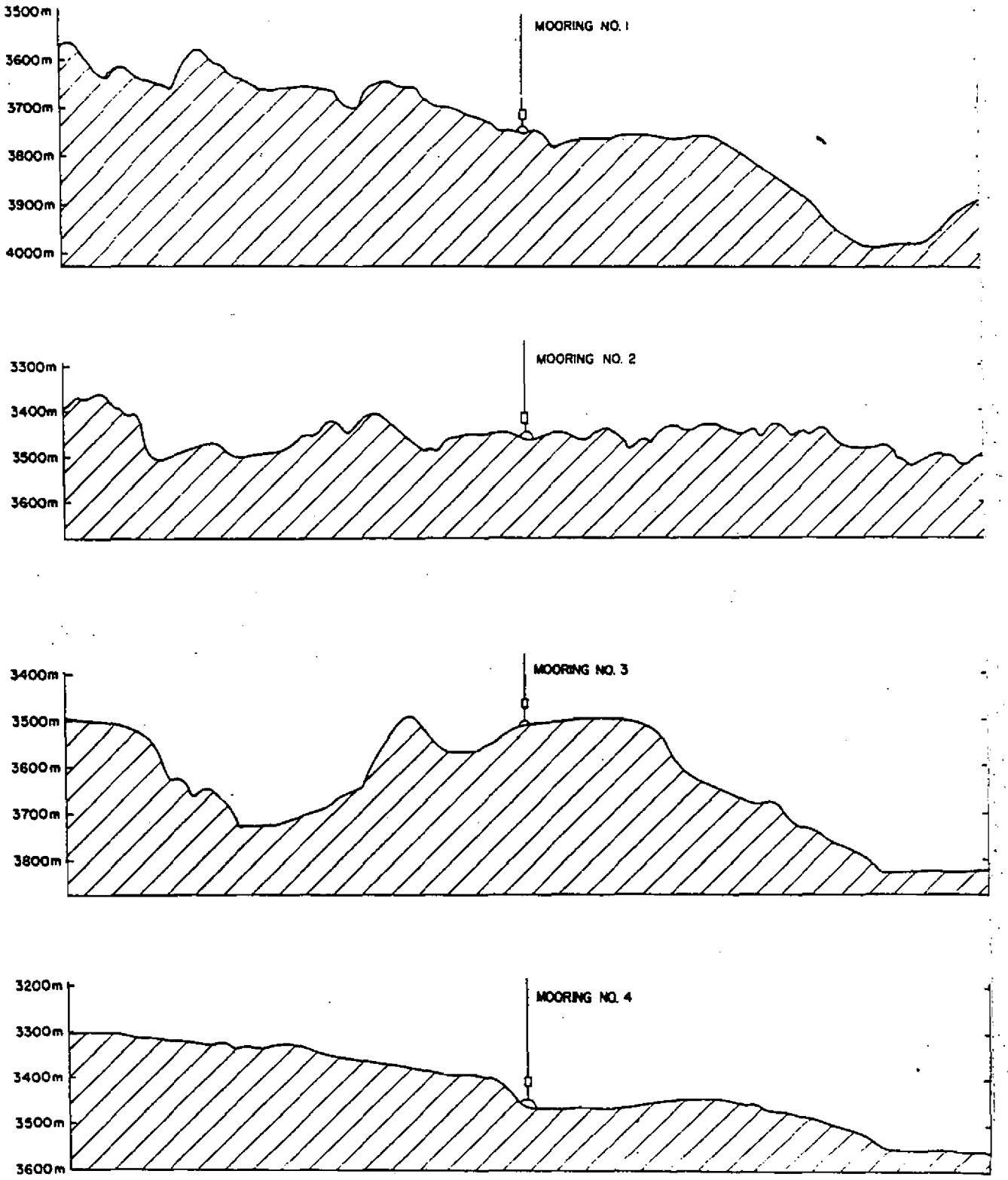
Track plot and cruise station numbers occupied in Drake Passage in the Buenos Aires to Punta Arenas leg (Phase III).



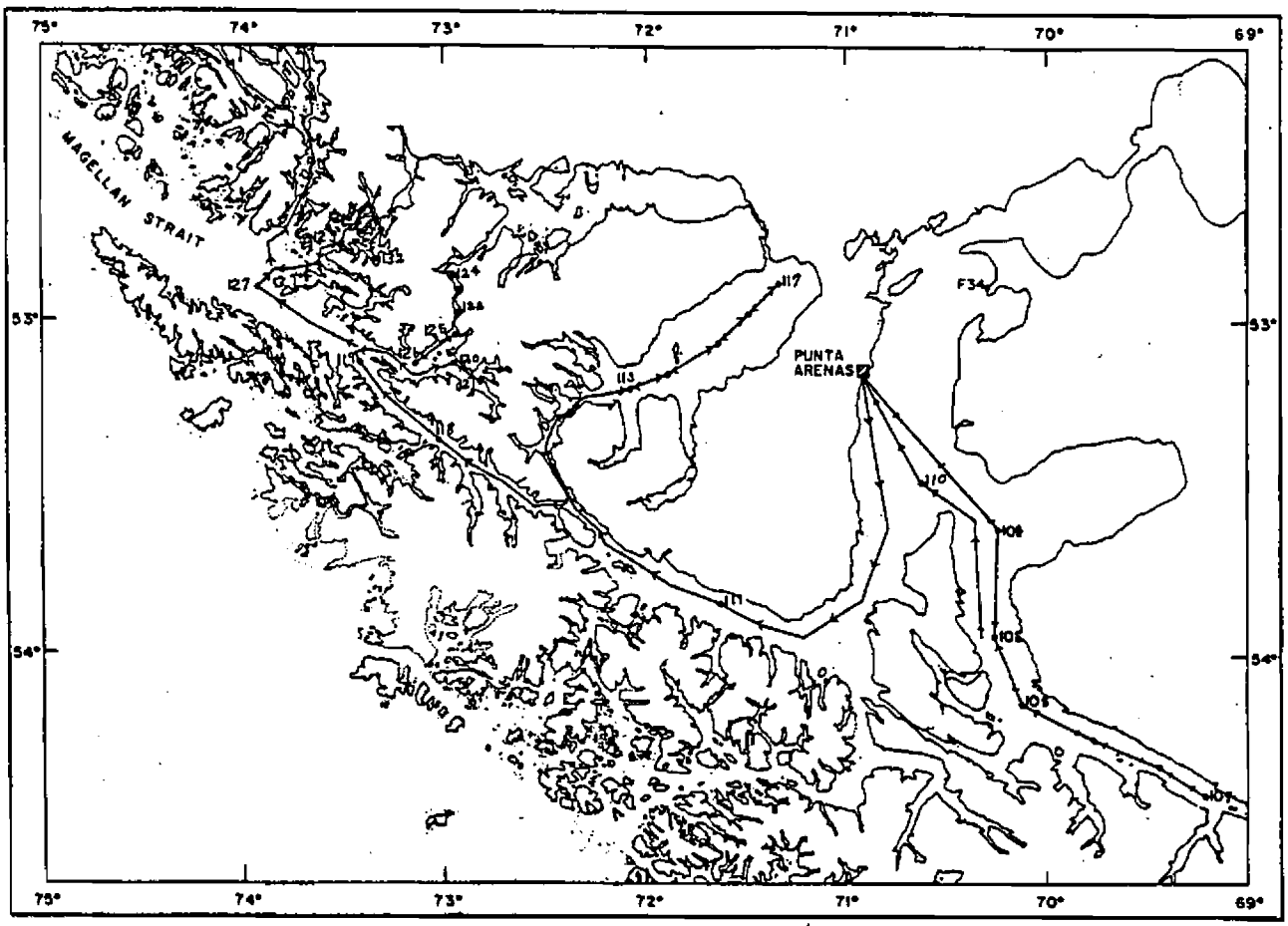
Oceanographic bottle stations during Phase III.



Current meter stations during Phase III.



Current meter depth contours in Drake Passage, Phase III.



Coastal stations occupied during Phase III of HUDSON 70.

APPENDIX A

LAUNCH OPERATIONS - ISLA NAVARINO

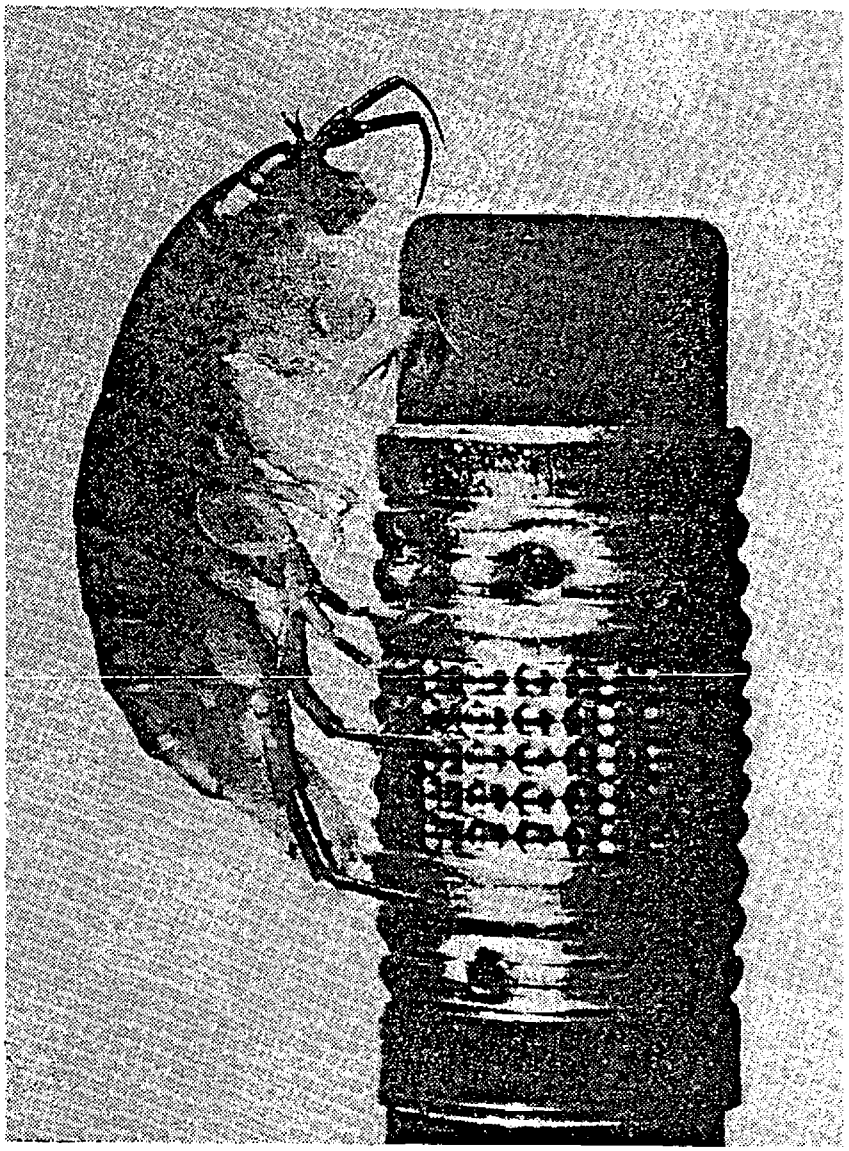
E.L. Bousfield

The three and one half week period 29 January to 19 February was spent in the Beagle Channel and Isla Navarino region. The main field operations were based at the southern Chilean naval base of Puerto Williams located near the mid-point of the north coast of Isla Navarino, on Beagle Channel. Through the courtesy of the Chilean Naval Department, comfortable living quarters and meals were provided for the two scientists and coxswain while staying in Puerto Williams between cruises. Particularly helpful in providing facilities and hospitality were the base Commandant, Raul Consina, and Lieutenant Commander Louis Parga. Lt. Augusto Tapia, on loan to the launch party, proved a most helpful and competent advisor during the work cruises, particularly in maintaining radio contact with remote island outposts where suitable nightly accommodation could be arranged.

Six field cruises were conducted from the Hudson's diesel launch, 'Redhead', which has a top speed of about 10 knots and a cruising range of about 200 miles. Seven hundred nautical miles were logged by the 30-foot launch during visits to 33 collecting stations. About 60 lots of marine and freshwater invertebrate animals, particularly crustaceans and molluscs (20,00+ specimens) were collected by means of light dredges and hand nets. In addition, Dr. James Markham, University of British Columbia, obtained more than 500 samples of intertidal marine algae. Highlights of the six launch cruises were recorded on 35 mm colour transparencies and 16 mm colour motion film. These include sequences on remarkable marine birds and mammals of these yet-unspoiled, sparsely populated, subantarctic islands.

The launch performed reasonably well and enabled the field party to accomplish all major objectives. Its shallow draft and echo sounder made the vessel particularly suitable for work in rocky, kelp-clogged, inshore waters. However, its living quarters were somewhat restrictive for four men, and the stern deck area proved rather small for dredging operations. The electric winch lacked variable speed control and the wire snapped several times in lifting the loaded dredge out of water. The side-mounted main pulley could not be swivelled and thus was not usable during actual bottom dredging. However, despite such operational limitations, the iron-frame dredge yielded excellent biological specimens until it was lost overboard near Seno Grandi. The 16-foot wooden dory could not be used because of the cut-away stern, which shipped water when the outboard motor was turned on. Ship-to-shore transportation was therefore provided by a small inflatable dinghy that required some practice for successful two-man use! A broken valve in the water-cooling system of the launch would have halted cruise operations on 9 February but for the timely unscheduled return of the Hudson to Puerto Williams that very day! The launch continued to lose revolutions in subsequent cruises, dropping to a maximum of about 1600 r.p.m. by final pick-up date. However, the launch could be used for

work even in head winds up to 20 m.p.h. or run down-wind even above 30 m.p.h. Meteorological conditions were unusually favourable, with tail-winds, light winds, or calm prevailing for more than 80% of the cruise time. The fact that really severe (gale) winds set in only after we departed Puerto Williams reinforces the suspicion that good fortune may be the most important single ingredient in successful completion of a field project!



The Cape Horn Beach Flea on the End of a Pencil.

HUDSON 70 EXPEDITION. PUERTO WILLIAMS LAUNCH PARTY. JANUARY-FEBRUARY, 1970
ISLA NAVARINO AND VICINITY, MAGALLANES (CAPE HORN REGION), CHILE.

Personnel:

Dr. E.L. Bousfield, Chief Zoologist, National Museum of Natural Sciences, Ottawa

Dr. James W. Markham, Phycologist. National Research Council of Canada, Halifax

Mr. Frank Durnford, Coxswain, C.S.S. Hudson

Lt. Augusto Tapia, Armada de Chile, Puerto Williams

Vessel: Diesel launch 'Redhead' from C.S.S. Hudson

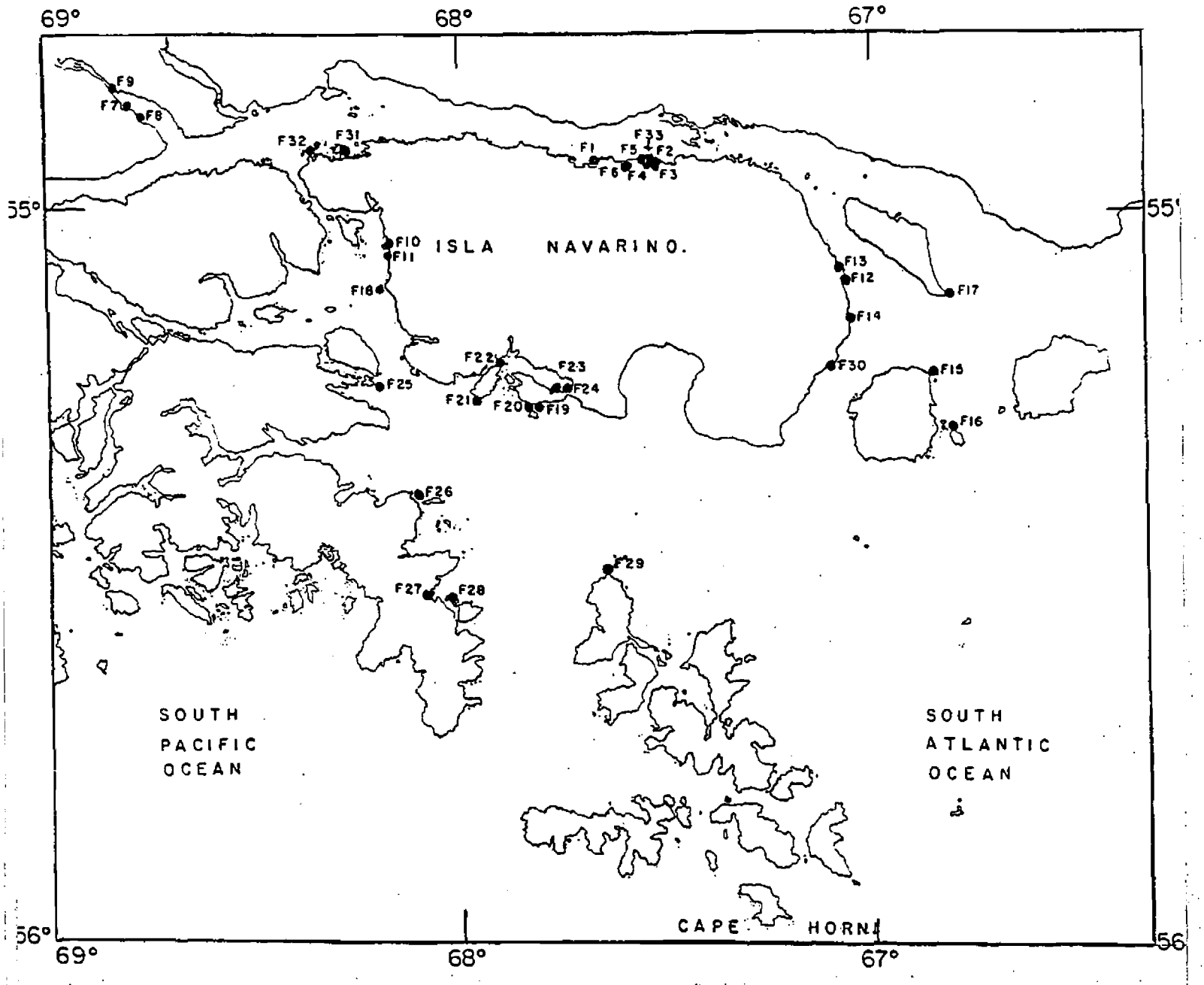
COLLECTION STATIONS

Stn. #	Date	Locality	Position	Temp. °C.	Salinity ppt	Collected Materials
F1	29 01 70	Punta Robalo, Isla Navarino	54°57'S 67°40'W	12.5	30.0	Intertidal; Inv., algae
F2	30 01 70	Puerto Williams, E. Shore at Stream Mouth	54°56'S 67°37'W	---	brackish	Intertidal; Inv., fishes
F3	30 01 70	Puerto Williams E. FW stream, near mouth	54°56'S 67°37'W	8.0	fresh	Supra-tidal; Inv., fishes
F4	30 01 70	Puerto Williams East, Notofagus forest	54°56'S 67°37'W	---	----	Terr; cryptozoic Inv., lich
F5	31 01 70	Puerto Williams Hbr.	54°56'S 67°37.5W	9.8	----	Dredge, 30-40 ft.;

Stn. #	Date	Locality	Position	Temp. °C.	Salinity ppt	Collected Materials
		Isla Navarino		(surface)	----	Inv.; algae
F6	31 01 70	Seno Lauta, Puerto	54°56.5S 67°38.5W	10.5	----	Intertidal; Inv.
F7a	01 02 70	Caleta Ferrari, Bahia Yendegaia, Tierra del	54°51'S 68°48'W	---	----	HW. Level; terr Inv.
F7b	02 02 70	" " "	" "	4.0 (surf)	nearly fresh	Intertidal; Inv., algae
F8	02 02 70	Bahia Contreras, near mouth of Bahia Yendegaia	54°52'S 68°46'W	---	----	Intertidal; inv., algae
F9	02 02 70	Mouth of Yendegaia R.	54°56'S 68°49'W	3.0 (surf)	fresh	LW and Subtidal Inv.
F10a	02 02 70	Caleta Wulaia, Isla Navarina	55°03'S 68°10'W	5.0	fresh	Mouth of small stream; Inv.
F10b	03 02 70	Caleta Wulaia, Isla at wharf	55°03'S 68°10'W	5.0	fresh	Surface dipnet; squid
F11	03 02 70	Punta Wulaia, Isla Navarino	55°04'S 68°10.5W	9.5	31.4	Intertidal; Inv., algae
F12	05 02 70	Banco de las Tacas, Isla Navarino (East)	55°05.5S 67°04.5W	9.5	----	Intertidal & Dredged. Inv. and algae
F13	05 02 70	Laguna Roja, Banca de las Tacas	55°05'S 67°04.5'W	9.0	fresh	Bottom Inv.
F14	05 02 70	Playa Aaron, Isla Navarino (East)	55°09'S 67°04'W	---	----	Intertidal; Inv.

Stn. #	Date	Locality	Position	Temp. °C.	Salinity ppt	Collected Materials
F15	05 02 70	Playa Lennox, Isla Lennox (N.E.)	55°13'S 66°52'W	---	----	Intertidal; Inv.
F16	06 02 70	Islotes Mamones, off Isla Lennox	55°18'S 66°49.5'W	10.2	32.3	Intertidal; Inv., algae
F17	07 02 70	Cabo Maria, Isla Picton	55°07'S 66°50'W	10.0	32.4	Intertidal; Inv., algae
F18	10 02 70	Off Isla Troude Seno Ponsonby	55°07'S 68°12'W	abt.	----	Surface Dipnet; Inv.
F19	10 02 70	Peninsula Scott, E. beach, I. Navarino	55°16'S 67°49'W	10.5	----	Intertidal; invertebrates
F20	10 02 70	Peninsula Scott, W. Beach, I. Navarino	55°16'S 67°49.5'W	13.0	----	Intertidal; Inv.
F21	10 02 70	Isla Bertrand, South Point, S. Navarino	55°15'S 67°57'W	10.5	----	Intertidal; algae, Inv.
F22	11 02 70	Seno Grandi, off N. end Isla Bertrand	55°11'S 67°55'W	---	----	Dredged, 70-75 ft.; Inv. and algae.
F23	11 02 70	Seno Grandi, W. of Head Island	55°14.5'S 67°45'W	10.5 (surf)	----	Dredged, 40 ft.; Inv., algae
F24	11 02 70	Seno Grandi E. of Head Island	55°14.5'S 67°44.5'W	---	----	Dredged, 25 ft.; Inv., algae
F25	14 02 70	Isla Green, off Peninsula Pasteur, Isla Hoste	55°14.5'S 68°12'W	10.0	31.9	Intertidal; Inv., algae
F26	14 02 70	Small Island NW of Packsaddle I., Peninsula Hardy, I. Hoste	55°23.5'S 68°07'W	---	----	Intertidal; kelp, shells (clams)

Stn. #	Date	Locality	Position	Temp. °C.	Salinity ppt	Collected Materials
F27	14 02 70	Bahia Orange, Isla Hoste; at stream mouth	55°31.5'S 68°05'W	10.5	brackish	Intertidal; Inv., algae
F28	15 02 70	Isla Bullock, E. side Peninsula Hardy	55°32'S 68°01.5'W	10.0	32.1	Intertidal; Inv., algae
F29	15 02 70	Isla Grevy, N. end beach	55°30'S 67°40'W	---	----	Intertidal; Inv., Obs.
F30	16 02 70	"Tern I." near Punta Yawl, Isla Navarino	55°12.5'S 67°06'W	10.5	----	Intertidal; Inv., algae
F31	19 02 70	Puerto Navarino, Isla Navarino	54°56'S 68°17'W	---	----	Shallow rake; crabs
F32	19 02 70	Isla Tongo, Islas Whaits, Canal Beagle	54°56'S 68°23.5'W	8.5	30.5	Intertidal; Inv., algae
F33	20 02 70	Puerto Williams Harbour	54°56'S 67°38'W	---	----	Trap, 30 m. crabs
F34	22 02 70	Punta Percy, Tierra del Fuego	52°54'S 70°17'W	11 appr.	----	Intertidal; Inv., algae



Intertidal marine life stations near Isla Navarino occupied during Phase III of HUDSON 70.

A T L A N T I C O C E A N O G R A P H I C L A B O R A T O R Y

B E D F O R D I N S T I T U T E

"HUDSON 70"

INTERIM CRUISE REPORT

PUNTA ARENAS TO VALPARAISO

G.L. PICKARD

CRUISE NO. 69-050

CRUISE REPORT NO. 69-050

"HUDSON 70" - INTERIM CRUISE REPORT

PUNTA ARENAS TO VALPARAISO

Local Cruise Designation:	69-050
Code Reference Number:	10-69-050
Vessel:	C.S.S. Hudson
Dates:	1 March 1970 to 7 April 1970
Area:	Chilean Fjords and passages from Punta Arenas to Puerto Montt and ocean sections along 42°S, 81°W and 33°S to Valparaiso.
Responsible Agency:	University of British Columbia Vancouver, British Columbia
Personnel:	Ship's Master, Captain D.W. Butler
Scientific Staff:	
G.L. Pickard Chief Scientist	Institute of Oceanography Vancouver, British Columbia
B. McK. Bary Asst. Chief Scientist	Institute of Oceanography Vancouver, British Columbia
M.P. Storm	Institute of Oceanography Vancouver, British Columbia
D. English	Institute of Oceanography Vancouver, British Columbia
W.V. Burt	Oregon State University Corvallis, Oregon
G.S. Pond	Oregon State University Corvallis, Oregon
R.G. Brown	Canadian Wildlife Service
H.M. Inostroza	Universidad de Concepcion, Chile
L.A. Chuecas	Universidad de Concepcion, Chile
R. Ahumada	Universidad de Concepcion, Chile
R.E. Montaner	Instituto Hidrografico, Chile

Scientific Staff (continued):

B.D. Uccelletti	Instituto Hidrografico, Chile
F.R. Rey	Universidad de Chile, Valparaiso
N. Silva	Universidad Catiolica, Valparaiso
I.W. Duedall	Marine Ecology Laboratory Bedford Institute
P. Wadhams	Atlantic Oceanographic Laboratory Bedford Institute
J.M.R. Pilote	Canadian Hydrographic Service

Summary:	Fjords		Pacific		Total
Knudsen Casts (T,S,O_2)	175	+	5	=	180
Nutrients	65	+	-	=	65
Bissett/Berman 9060 STD Casts	147	+	26	=	173
Bathythermograph Casts	151	+	3	=	154
Bottom Samples	41	+	-	=	41
Vertical Plankton Hauls	58	+	-	=	58
Oblique & Vertical Plankton Tows	65	+	-	=	65
Clarke-Bumpus Tows	58	+	-	=	58
Isaacs Kidd Trawl Hauls	27	+	1	=	28
Acoustic Scattering Observations	58	+	-	=	58
Soundings - GEBCO Miles	2210	+	980	=	3190
Bird Identification and Counts (all day stations)					

Purpose of Cruise:

The prime purpose was to obtain data on the water characteristics and plankton in the fjords of the southern coast of Chile, an area not previously investigated oceanographically, to add to the fund of knowledge on fjord estuaries and to permit comparison with other fjord regions, particularly on the west coast of North America. Oceanographic observations in the open oceans between 42°S and 33°S were also planned.

The general intention was to make observations at as many stations as possible in as many fjords as time permitted, together with stations in the south-north passages and at openings to the Pacific through the Island Archipelagoes.

Narrative:

The start was scheduled for 1 March from Punta Arenas, Chile, but was delayed until 2030 hours on 5 March awaiting the arrival of the second pilot, two being required for extended passages in Chilean waters. (The unusual length of this cruise had been something of a deterrent to pilots volunteering for the duty.) The four-day wait was used, in part, to complete the study of the first inlet, Seno del Almirantazgo. This also served as a shakedown for the scientific staff enabling them to get to know each other and to develop familiarity with equipment and procedures.

As it was planned to work continuously, as far as possible, three watches were organized to carry out the bottle casts for temperature, salinity, oxygen, and nutrient observations, BT casts, and STD casts for temperature and salinity profiles to 500 m. Two watches of two were organized for the plankton studies at about one half of the total stations to be occupied. Counts of sea birds were made at stations to obtain quantitative estimates of species numbers.

On leaving Punta Arenas on 5 March, CSS Hudson proceeded Pacific-ward along the Strait of Magellan, taking stations in the passages enroute to Otway Water where stations in a 50-60 knot wind tested the new group's abilities. The proposed boat expedition to the connecting Skyring Water was cancelled because of the probability that the weather would continue too severe for the boat operations. Continuing north, the ship occupied stations in Golfo Xaultegua on 7 March while the sounding launch operated in Canal Gajardo. While the launch was being hoisted, one of the falls broke and the boat was severely damaged. Inspection revealed that the lifting wire was corroded at a babbitt joint; similar corrosion was found on the falls for the second launch, making it imprudent to attempt to lower either of them again.

The consequent unavailability of both launches was a severe blow to our plans, as we had been relying on using them to precede Hudson in the many unsounded fjords which it was planned to study. As it would be imprudent for Hudson to sail in those areas without the sounding launches ahead, it was decided that the ten unsounded fjords would have to be deleted from the ship's programme, but that, when daylight and weather permitted, efforts would be made to get some oceanographic information in some of them using a lifeboat and hand winch. On 8 March, stations were occupied in some reaches of Bahia Beaufort, the innermost stations being omitted because of lack of soundings. Several glaciers had been seen earlier but it was here that evidene of their runoff of meltwater became apparent by the reduced salinity and increased silt content of the surface waters. The ship continued north by Smyth Channel to Canal las Montagnes for stations terminating at nightfall before the inlet head. Here the glaciers were more numerous, some coming down close to sea level. The appearance of the glacier fronts and the areas of light rock

surrounding many of the glacier caps on mountains suggest that most of them are at present retreating. On 10 March, the ship passed through the narrow Canal Kirke and across Golfo Almirante Montt to Puerto Natales where a day was spent while two stations were made from the lifeboat in Seno Ultima Experanza in the uncomfortable conditions of a 20-25 knot wind, short steep waves and cold water coming aboard. Numerous Chileans visited Hudson informally and a reception was held for local dignitaries. On 12 March, the ship completed stations in this area and continued north for Estero Asia and Bahia San Andres on 13 March. Glaciers were very numerous in this area and there were many bergy bits in Estero Asia.

On 14 March, while the ship worked in Trinidad and Concepcion Passages, the lifeboat was sent into Europa Inlet and stations were taken until ice prevented further travel toward the inlet head. On the following day in Eyre Channel, there was considerable ice during the night stations and near the head there was so much accumulation of ice against the ship when on station that the bathythermograph was retrieved with difficulty and further work there abandoned. The flow of ice past the ship clearly indicated the estuarine outflow. The water was extremely silty with 'rock flour' from extensive glaciers visible further up the inlet.

After passing English Narrows in sunshine and flat calm, contrasting with the usual weather in the region, and passing two wrecks perched sedately on rocks, two stations were made from the lifeboat in Iceberg Inlet which lived up to its name.

On 16 March, we entered the extensive Canal Baker area and were struck by the considerable siltiness of the water even at the mouth some 60 miles from the glacial inflow from very large glaciers near the head. Another conspicuous feature of this region was the almost complete absence of bird life, in contrast to regions further south, and small plankton catches.

On 18 March, after several days of good weather, we emerged into Golfo de Penas to 40-50 knot winds and 6-8 foot swells and were told that this represented good weather in this area. On the next day, stations were taken from the lifeboat in Seno Jesuitas and Seno Julian, the latter showing the first evidence of low oxygen conditions yet encountered. From here, the ship sailed outside, taking open sea stations, to Bahia Anna Pink on 20 March.

After some work in the wide but very shallow Golfo Elefantes, the ship worked in Estuario Francisco while the lifeboat was in Estuario Puelma. The lack of silt in these northern area waters was in noticeable contrast to the southern regions, the glaciers from here north being generally smaller and terminating higher at 2000-3000 feet above sea level. The general character of the scenery changed from the spectacular abrupt barren rock hills with scrubby trees of the southern regions to dense woods from sea level to mountain tops in this northern region.

On 22 March, the ship worked north up Golfo Elefantes, stations were taken in Estero Quitralco from the lifeboat, the last of the boat

expeditions that, while they provided limited data from regions judged inaccessible to the ship, were tiring and, at times, miserable in rain and wind because of lack of shelter.

On 23 March, the ship worked up Seno Aysen to Checabuco where the ship anchored for 12 hours to catch up on chemical work and for a short break ashore in brilliant sunshine, the first for a week there and the warmest day for the ship for a couple of months. Two hours after Checabuco stations were being taken in a 40 knot wind and heavy rain; by morning on 24 March, it was calm and dry again in Canal Jacaf where the clearest water so far was noted.

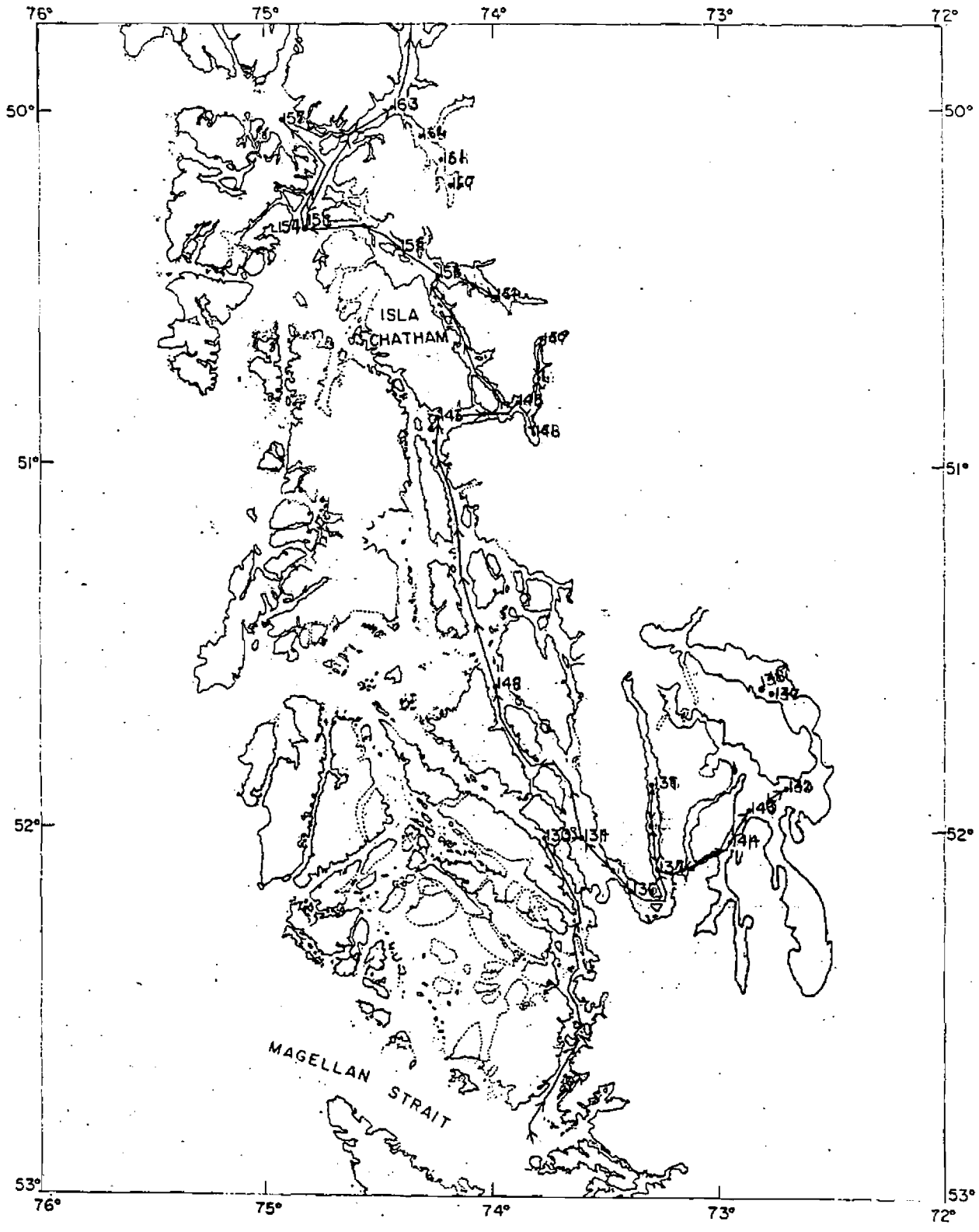
On 25 March, work in Canal Puyuguapi was completed and the ship worked up the Canal Moraleda and to the Pacific west of Isla Guafo for an open sea station.

On 26 March, we returned to Golfo Corcovado and Golfo de Ancud for the last group of inlets. Fjordo Renihue, Estero Comau, Canal Hornopiern, and Estero Reloncavi. Considerable numbers of medusae, one to two feet in diameter and 10-15 feet long, interfered with bottle casts, clogged plankton nets, and rendered it impractical to use the Isaacs Kidd mid-water trawl in this region. In the valleys ashore, areas of cultivated land were noted and fishermen came out to sell mussels on several occasions. The only silty water here was in the upper 20 miles or so of Reloncavi, appearing to be brownish alluvial silt rather than white glacial rock flour. The last station of the fjord series was taken on 29 March and the ship proceeded to Puerto Montt where two of the scientific staff left.

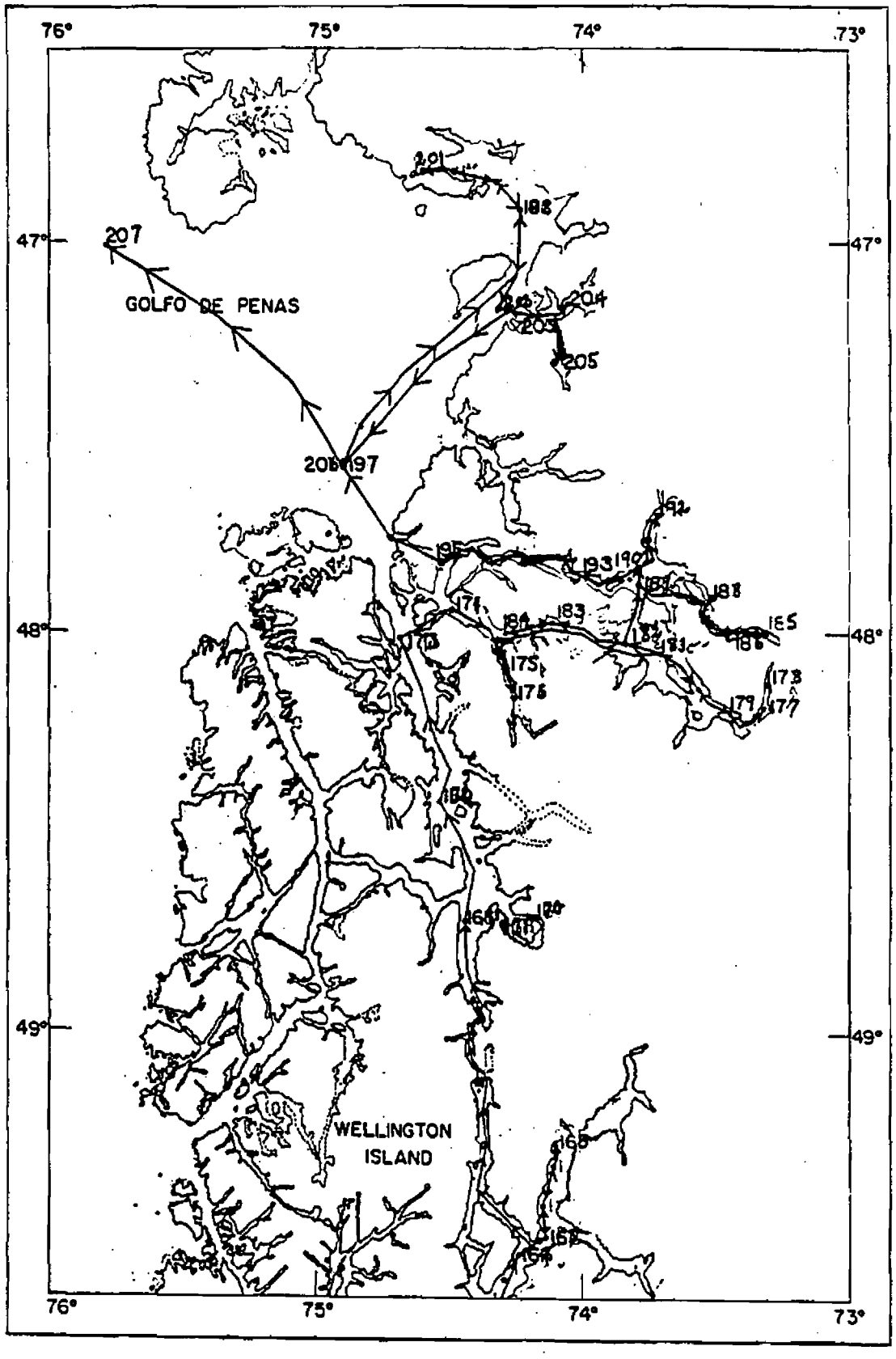
On 31 March, C.S.S. Hudson left Puerto Montt for Canal Chacao to drop one of the pilots at Ancud and then proceeded west along 41°40'S to make a section across the Humboldt Current with STD casts every 45 miles and bottle casts at 77°and 81°W. The change from the green-blue water of the Humboldt Current to the cobalt blue of Pacific water was noticeable. Turning north along 81°W, into a steep swell and strong wind, STD casts were made every 60 miles and bottle casts at 38°and 33°30'S. The ship turned east for a second section across the Humboldt Current with STD casts every 50 miles and a bottle cast at 77°W.

On 4 April, we anchored for a few hours in Cumberland Bay in Isla Robinson Crusoe of the Juan Fernandex Islands, an open anchorage but attractive in the sun with its backdrop of steep wooded mountains. Visits were paid to the community of a few hundred persons subsisting chiefly on a lobster fishery. Large numbers of very tame colorful fish were seen when skin diving in the clear water of the Bay. In the afternoon, the ship continued east and the last station of this phase of the cruise was taken 15 miles off Valparaiso at 0200 hours on 6 April.

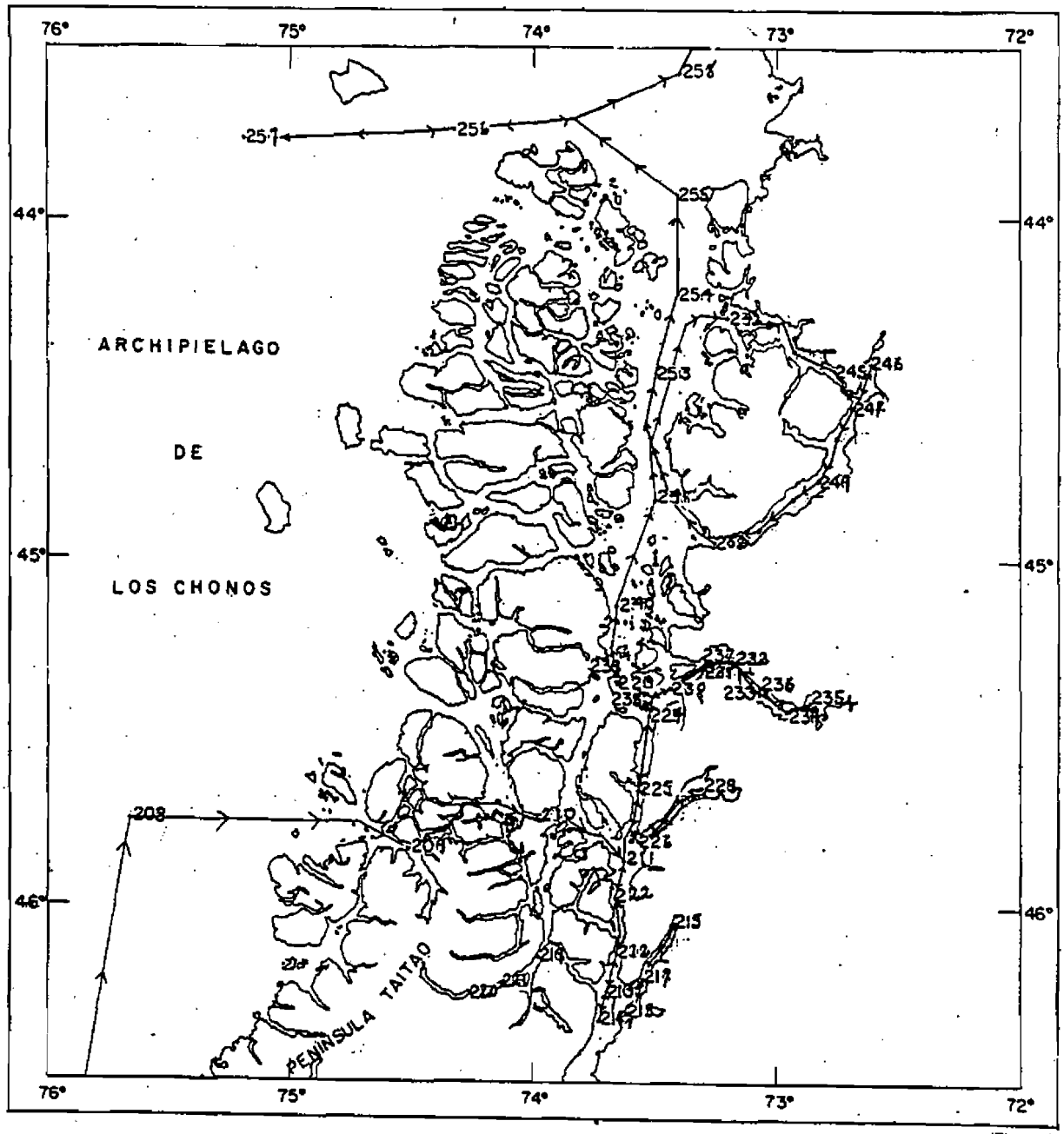
On 7 April, the ship entered Valparaiso to complete Phase V of the Hudson 70 cruise.



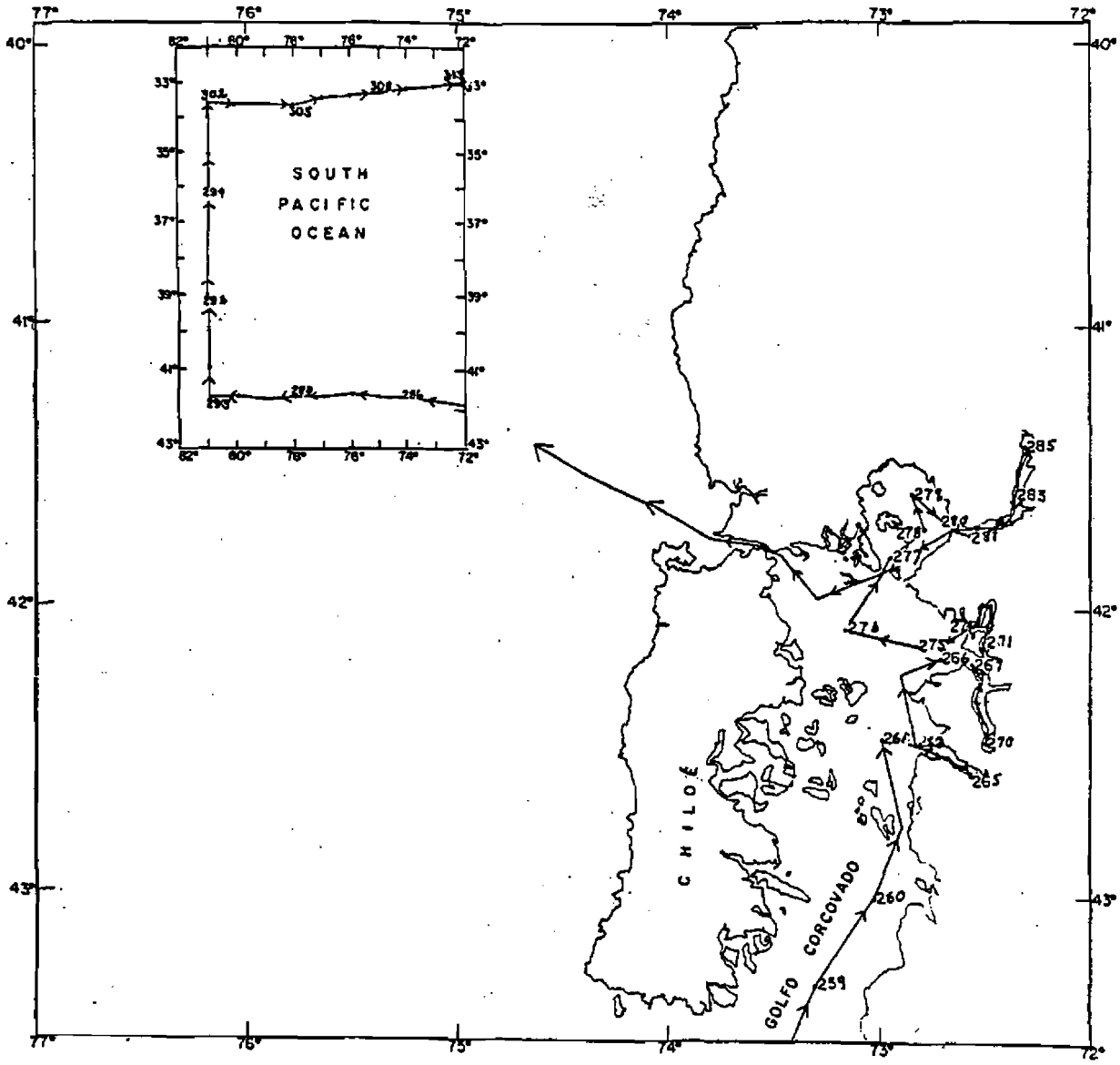
Cruise station numbers during Phase IV of HUDSON 70, Punta Arenas to Valparaiso.



Cruise station numbers during PHASE IV of HUDSON 70, Punta Arenas to Valparaiso.



Cruise station numbers during Phase IV of HUDSON 70, Punta Arenas to Valparaiso.



Cruise station numbers during Phase IV of HUDSON 70, Punta Arenas to Valparaiso.

A T L A N T I C O C E A N O G R A P H I C L A B O R A T O R Y

B E D F O R D I N S T I T U T E

"HUDSON 70"

INTERIM CRUISE REPORT

VALPARAISO, CHILE TO PAPEETE, TAHITI

R.C. MELANSON

CRUISE NO. 69-050

CRUISE REPORT NO. 69-050

"HUDSON 70" - INTERIM CRUISE REPORT

VALPARAISO, CHILE TO PAPEETE, TAHITI

Local Cruise Designation:	69-050
CODE Reference Number:	10-69-050
Vessel:	C.S.S. Hudson
Dates:	15 April to 12 May 1970
Area:	Valparaiso to Papeete, Tahiti
Responsible Agency:	Atlantic Oceanographic Laboratory Bedford Institute
Personnel:	Ship's Master, Captain D.W. Butler
Scientific Staff:	
R.C. Melanson Chief Scientist	Atlantic Oceanographic Laboratory Bedford Institute
R.T. Haworth Assistant Chief Scientist	Atlantic Oceanographic Laboratory Bedford Institute
A.R. Coote	Atlantic Oceanographic Laboratory Bedford Institute
I.W. Duedall	Atlantic Oceanographic Laboratory Bedford Institute
M. Hughes	Atlantic Oceanographic Laboratory Bedford Institute
P. Wadhams	Atlantic Oceanographic Laboratory Bedford Institute
W.B. Greifeneder	Atlantic Oceanographic Laboratory Bedford Institute
P.L. Corkum	Atlantic Oceanographic Laboratory Bedford Institute
W.H. Sutcliffe	Marine Ecology Laboratory Bedford Institute
R.W. Sheldon	Marine Ecology Laboratory Bedford Institute

Scientific Staff (continued):

M.A. Paranjape	Marine Ecology Laboratory Bedford Institute
P.J. Wangersky	Institute of Oceanography Dalhousie University
J. Sharpe	Institute of Oceanography Dalhousie University
T. Yoshinari	Institute of Oceanography Dalhousie University
C.S. Wong	Pacific Oceanographic Group
R. Belleguay	Pacific Oceanographic Group
W. von Arx	Woods Hole Oceanographic Institution
J.P. Dean	Woods Hole Oceanographic Institution
C.D. Densmore	Woods Hole Oceanographic Institution
O. Bluy	Defence Research Establishment Atlantic Dartmouth, Nova Scotia
J.G. Gill	Defence Research Establishment Atlantic Dartmouth, Nova Scotia
R. Smith	Queen's University Kingston, Ontario

Summary:

Surface Plankton Tows	25
Vertical Plankton Tows	14
Oblique Plankton Tows	18
Knudsen and Niskin Casts (Surface to Bottom)	10
Special Deep Niskin Casts	3
Expendable Bathythermographs	240
Cones	1
Acoustic Scattering Layer Observations	19

Summary (continued):

Soundings - G.E.B.C.O.	11,800
Gravity and Magnetics (Kilometres)	11,800

Narrative:

The C.S.S. Hudson commenced Phase V of the Hudson 70 cruise at 1140, 15 April, when departure was made from Valparaiso, Chile. The departure was to have been made a day earlier, however a one day delay was caused by difficulties encountered with the offshore fueling arrangements.

The cruise to the first atation of the Phase (consecutive #277), Latitude 65°S, Longitude 150°W, was laid out along the great circle route. However, because of not being able to obtain meteorological reports on weather or ice conditions, it was decided to alter to the rhumb line course at 0000 April 22, therefore, passing further north than the previous course would have placed us, and thus avoiding any unpredicted concentrations of ice. The rhumb line course was held until 0000 April 25, when the course was again altered to due West to avoid ice. Because of heavy weather, the ship's speed was slowed considerably so it was decided, because time was so critical at this stage, to proceed to Latitude 63°S, Longitude 150°W, and observe the first station.

Gravity, magnetics, and bathymetry were commended just outside the 3 mile territorial limit of South America, and carried through in continuous profiles to just off Tahiti. Expendable bathythermographs were commenced at Latitude 40°S and taken every two hours along the route. Continuous analog recordings were made of the temperature and salinity.

The first station was observed at Latitude 63°S, Longitude 150°W; the second station (#278) was observed at Latitude 60°S, Longitude 150°W, and stations observed thereafter at 5° intervals along meridian 150°W to Latitude 20°S. An intermediate station was observed at Latitude 16°37'S, Longitude 150°W, prior to our call at Tahiti. The main stations consisted of a shallow and deep cast, plankton tows, and acoustic reverberations. However, at stations 277, 278, and 284, special deep Niskin casts were made for Dr. Clarke of McMaster University, who is interested in the helium isotopes of sea water. At station 284, 286, and 287, cores of 27½', 37' and 22' respectively were obtained.

Most of the equipment functioned very well; however, there were a few malfunctions.

a) Bathysonde - Both units were tried, however no success was had until station 287. Readings collected on the Tahiti to Vancouver Phase will have to be corrected following calibration of the instrument.

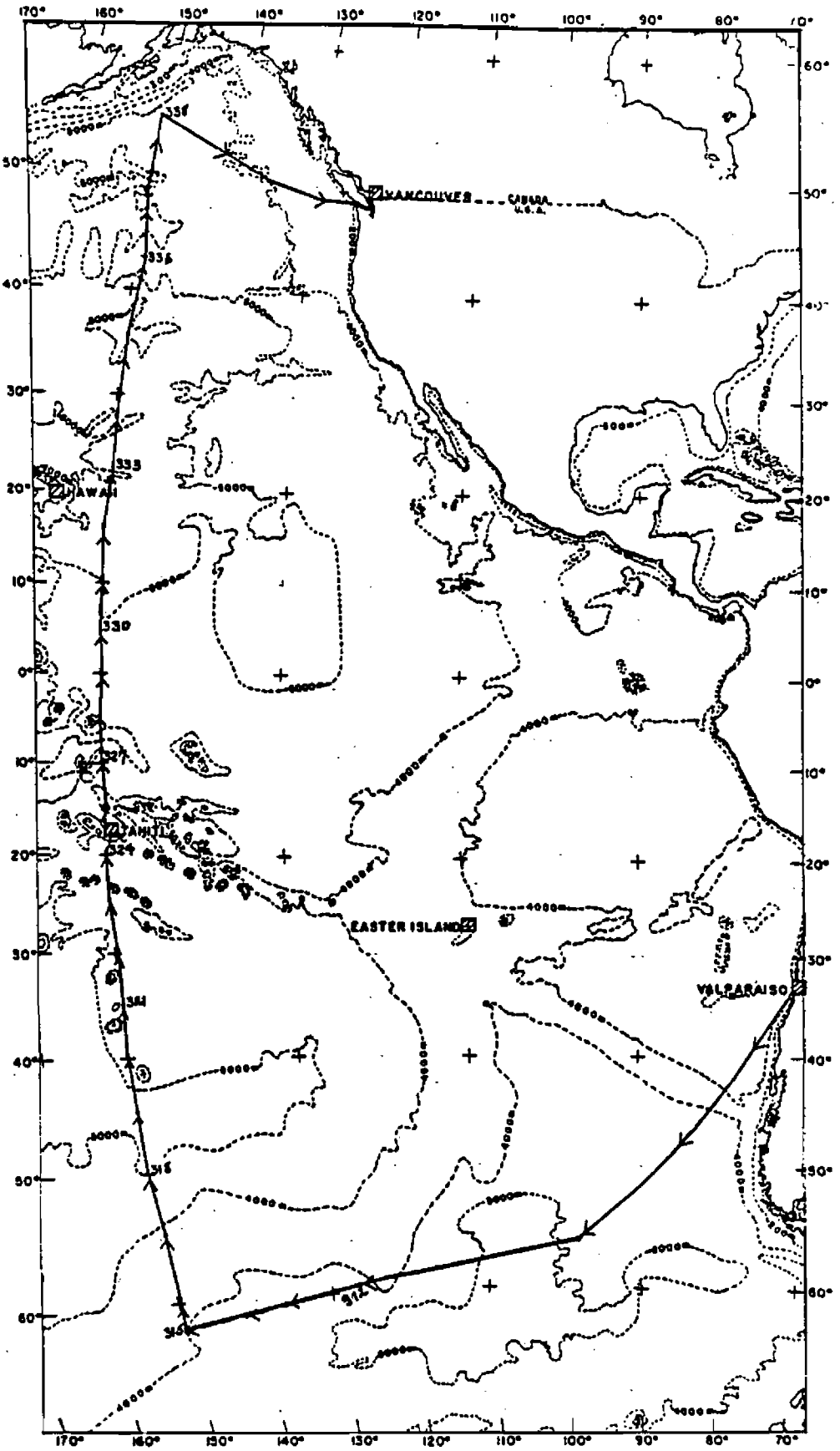
b) Benthos Multi-Plankton Net - This system was tried on three or four different occasions but with little success. It would appear that the power supply is inadequate to make the system operate to depths greater than 500 metres.

c) Acoustic Cone - Unfortunately, the Defence Research Establishment Atlantic cone was lost on station 278, when the ship surged and snapped both lines.

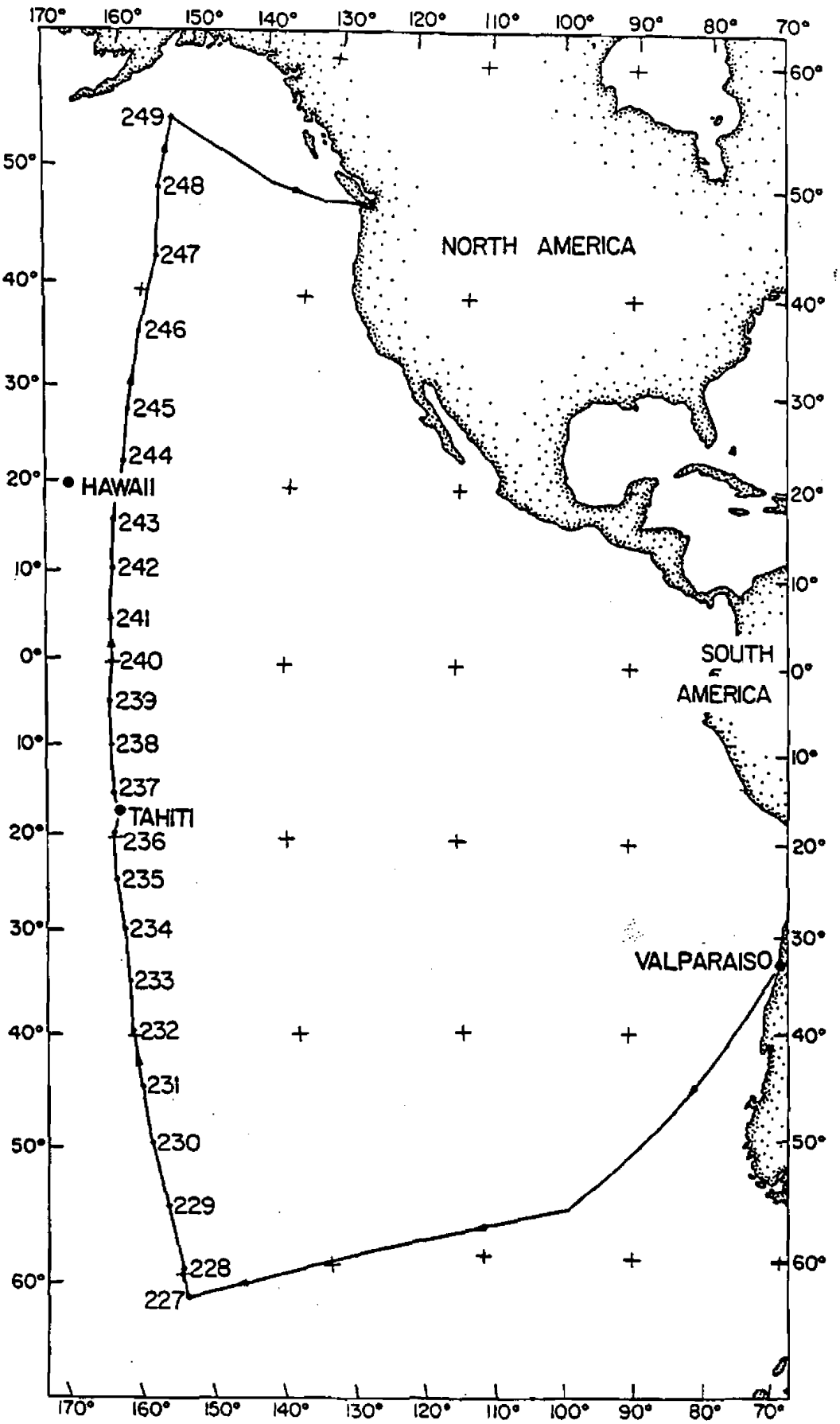
d) Salt Water Loop - Problems were encountered with the small plastic centrifugal pump, in that the pump was too fragile for the job. As a last resort, a bronze pump was substituted and operated trouble free through the remainder of the cruise. Dr. Sutcliffe discontinued using the loop following pump substitution when an experiment, loop vs. bucket sample, indicated the bronze impeller was having an adverse effect on his organic particulate count.

This Phase was very straightforward, with a great amount of data being collected. A program was drawn up for each station giving activities and times, and adhered to as closely as possible. The chemists and biologists were busy most of the time either collecting samples, processing, or preserving for return to the laboratories. The geophysical program progressed exceptionally well both in the collection of data and in the implementation of the stringent navigation requirements. GEBCO data were processed daily and a major contribution to the charts will result.

The ship arrived at Papeete, Tahiti at 0930 on 12 May, one day ahead of schedule. This was due to the fairly good weather and fair wind enjoyed on the run north. The responsibilities of senior scientists were turned over to Dr. W.M. Cameron on 14 May for the next Phase, Tahiti to Vancouver.



Cruise track and station numbers during Phases V and VI of HUDSON 70, Valparaiso to Tahiti and Tahiti to Vancouver.



Oceanographic bottle stations occupied during Phase V and VI of HUDSON 70.

A T L A N T I C O C E A N O G R A P H I C L A B O R A T O R Y

B E D F O R D I N S T I T U T E

"HUDSON 70"

INTERIM CRUISE REPORT

PAPEETE, TAHITI, TO VANCOUVER, B.C.

W.M. CAMERON

CRUISE NO. 69-050

CRUISE REPORT NO. 69-050

"HUDSON 70" - INTERIM CRUISE REPORT

PAPEETE, TAHITI, TO VANCOUVER, B.C.

Local Cruise Designation:	69-050
CODC Reference Number:	10-69-050
Vessel:	C.S.S. HUDSON
Dates:	16 May to 12 June 1970
Area:	Papeete, Tahiti, to Vancouver, B.C.
Responsible Agency:	Atlantic Oceanographic Laboratory Bedford Institute
Personnel:	Ship's Master, Captain D.W. Butler

Scientific Staff:

W.M. Cameron Chief Scientist	Marine Sciences Branch, Ottawa
P.J. Wangersky Assistant Chief Scientist	Dalhousie University Halifax, Nova Scotia
A.R. Coote	Atlantic Oceanographic Laboratory Bedford Institute
I.W. Duedall	Atlantic Oceanographic Laboratory Bedford Institute
J. Woodside	Atlantic Oceanographic Laboratory Bedford Institute
Lt. Comdr. P. Probert	Royal Navy
P. Wadhams	Atlantic Oceanographic Laboratory Bedford Institute
W.B. Greifeneder	Atlantic Oceanographic Laboratory Bedford Institute
P.L. Corkum	Atlantic Oceanographic Laboratory Bedford Institute
A. Prakash	Marine Ecology Laboratory Bedford Institute
M.A. Paranjape	Marine Ecology Laboratory Bedford Institute

Scientific Staff (continued):

C.T. Schafer	Atlantic Oceanographic Laboratory Bedford Institute
J. Sharpe	Dalhousie University
T. Yoshinari	Dalhousie University
C.S. Wong	Pacific Oceanographic Group
R. Belleguay	Pacific Oceanographic Group
W. von Arx	Wood's Hole Oceanographic Institution
J.P. Dean	Wood's Hole Oceanographic Institution
C.D. Densmore	Wood's Hole Oceanographic Institution
O. Bluy	Defence Research Establishment, Atlantic
J.G. Gill	Defence Research Establishment, Atlantic
K.F. Freeman	Marine Ecology Laboratory Bedford Institute
R. Smith	Queen's University
D. Winters	Atlantic Oceanographic Laboratory Bedford Institute
H. Henderson	Atlantic Oceanographic Laboratory Bedford Institute

Narrative:

The C.S.S. Hudson commenced Phase VI of the HUDSON 70 cruise at 0925 hours when the vessel cleared Papeete. The first station of Phase VI was commenced at 2237 hours May 16th.

The routine carried out by the scientific staff was effectively a continuation of the program commenced at station #277, in Phase V. Stations intended to be five degrees latitude apart were occupied with bottle casts, plankton tows, and acoustic reverberation measurements. Gravity, magnetics, and bathymetry were recorded while under way.

Plankton tows were collected with a modified Benthos Multiple Plankton Sampler fitted with 200-micron mesh nets. This type of net is suitable for studying the vertical distribution of planktonic foraminifera because samples can be obtained from specific depth ranges. The device was initially submerged to a depth of 25 m and towed at a speed of about 1.5 knots for 15 minutes. Two additional tows were made during each cast at 350 and 750 m depths respectively. The samples

collected represent planktonic specimens resident in the 0-200, 200-500, and 500-1000 m water layers respectively (Table 1). It is assumed, however, that the concentration of planktonic foraminifera is roughly constant in the water layers and that there is no appreciable diurnal change in the faunal population. The volume of water filtered through the nets was monitored using a Tsurumi-Seiki-Kosakusho flow meter attached to one side of the sampler frame. It was integrated with a Benthos Model 1023 acoustic telemeter. The samples were washed from each net and preserved in 10% formalin solution buffered with hexamethylene tetramine.

The high seawater temperatures near the Equator reduced the ship's engines efficiencies, and the heavy set during stations retarded the speed of advance. It was decided to open the spacing between the stations north of Latitude 10 degrees. This insured appropriate chemistry and biological sampling without reducing the high quality of the geophysics line.

The last bottle station on the north-south line of 150°W., was at 55°N. The geophysics sampling continued north to 57°30'N. Underway geophysical observations continued during the run southwest to Victoria, discontinuing at 48°35'N., 125°W.

The Hudson put in at Victoria to arrange for service to a main generator and proceeded to Vancouver, berthing at the CPR dock at 0810 hours 12th. June.

Table 1 Sampling Depths and General Faunal Details

STA.	DATE	LOCATION LAT. N-S	LOCATION LONG. W	D. of T.(m)	V. of W.F.(m^3)	S.D.(%)	A.A.(1000m^3)	S. to S.R.	P. of K.
1	2	3	4	5	6	7	8	9	10
				0-190	194.2	50.00	8205	547.00	03.01
327	May 8	10°S	150°W	190-460	67.5	30.00	0623	69.22	04.76
				460-760	295.6	30.00	0231	25.6	08.82
				0-200	261.8	53.33	7975	498.44	06.90
328	May 20	5°S	150°W	200-435	878.3	23.33	0036	05.14	06.66
				765-0	730.5	20.00	0057	09.50	04.76
329	May 21	0°	150°	0-800	2483.1	46.66	5487	417.64	16.61
330	May 23	5°N	150°	0-800	1638.5	66.66	3187	159.35	12.77
				0-190	409.6	53.33	1727	107.94	04.52
331	May 24	10°N	150°W	190-460	595.4	53.33	1547	96.81	11.95
				460-750	532.0	46.66	0599	42.78	07.54
				0-170	565.8	63.33	2010	105.79	02.29
332	May 26	15°N	150°W	170-450	426.5	43.33	0156	012.00	09.09
				450-780	553.2	40.00	0481	40.08	06.01
				0-180	384.2	63.33	2319	122.05	04.70
333	May 28	22°N	150°W	180-440	426.5	40.00	0343	28.58	04.11
				440-1050	447.6	26.66	0060	07.50	14.29
				0-160	506.7	36.66	0273	24.81	05.80
334	May 30	29°N	150°W	160-475	536.3	40.00	0263	21.91	05.63
				475-1030	532.1	36.66	0067	06.91	05.88
335	May 31	36°N	150°	0-320	777.0	40.00	0112	09.33	09.30
				0-900	1554.0	30.00	0244	01.39	08.60
				0-185	443.4	30.00	1342	149.11	12.75
336	June 2	43°N	150°W	185-850	2010.1	36.66	0746	67.81	14.44
				185-0	304.0	30.00	0810	90.00	12.19
337	June 4	49°N	150°W	0-1050	3606.4	20.00	1538	256.33	22.19
				0-190	629.2	20.00	0906	151.00	60.48
338	June 5	55°N	157°W	100-700	2326.8	26.66	0241	030.13	36.80
				100-0	312.5	20.00	1439	239.83	43.55

Sta. - Station
D. of T.(m) -Depth of Tows(m)
V. of W.F.(m^3) -Volume of Water Filtered(m^3)
S.D.(%) -Species Diversity(%)

A.A. (1000m^3) - Absolute Abundance (100 m^3)
S. to S.R. - Specimen to Species Ratio
P. of K. - Percentage of Kummerform

A T L A N T I C O C E A N O G R A P H I C L A B O R A T O R Y

B E D F O R D I N S T I T U T E

"HUDSON 70"

INTERIM CRUISE REPORT

VICTORIA, B.C., TO VICTORIA, B.C.

C.D. MAUNSELL

CRUISE NO. 69-050 (HUDSON)

CRUISE REPORT NO. 69-050

"HUDSON 70" - INTERIM CRUISE REPORT

VICTORIA, B.C., TO VICTORIA, B.C.

Local Cruise Designation:	69-050
CODC Reference Number:	10-69-050
Vessel:	C.S.S. Hudson
Dates:	12 July to 5 August 1970
Area:	Victoria, B.C., to Victoria, B.C.
Responsible Agency:	Atlantic Oceanographic Laboratory Bedford Institute
Personnel:	Ship's Master, Captain F.W. Mauger

Scientific Staff:

C.D. Maunsell Chief Scientist	Atlantic Oceanographic Laboratory Bedford Institute
S.P. Srivastava Assistant Chief Scientist	Atlantic Oceanographic Laboratory Bedford Institute
D.I. Ross	Atlantic Oceanographic Laboratory Bedford Institute
C.E. Keen	Atlantic Oceanographic Laboratory Bedford Institute
K.G. Shih	Atlantic Oceanographic Laboratory Bedford Institute
D.L. Barrett	Atlantic Oceanographic Laboratory Bedford Institute
P. Wadhams	Atlantic Oceanographic Laboratory Bedford Institute
T.J. Corbett	Atlantic Oceanographic Laboratory Bedford Institute
T. Courtney	Atlantic Oceanographic Laboratory Bedford Institute
V. Coady	Atlantic Oceanographic Laboratory Bedford Institute

Scientific Staff (continued):

D. Druhan	Atlantic Oceanographic Laboratory Bedford Institute
P.A. Solowan	Atlantic Oceanographic Laboratory Bedford Institute
J.P. Steele	Atlantic Oceanographic Laboratory Bedford Institute
H. Toom	Atlantic Oceanographic Laboratory Bedford Institute
B. Taylor	Atlantic Oceanographic Laboratory Bedford Institute
D. Tiffin	Marine Sciences Branch, Vancouver
L.P. Landry	Marine Sciences Branch, Victoria
C.R.B. Lister	University of Washington, U.S.A.
E. Davis	University of Washington, U.S.A.
A. MacLean	Dalhousie University Halifax, Nova Scotia
M. Purdy	Imperial College, London

Summary:

Gravity, Magnetics, and Bathymetry (G.E.B.C.O.) Data	6933 km
Seismic Reflection Profiling	1675 km
Reversed Seismic Refraction Lines	621 km
Heat Flow Stations	13
Dredging Stations	17

Purpose of Cruise:

The British Columbia coastal leg of HUDSON 70 was designed to apply the geophysical techniques developed at the Bedford Institute and elsewhere to the region west of the southern portion of the Queen Charlotte Islands and of Queen Charlotte Sound. The northern termination of the Juan de Fuca Ridge and the area surrounding the Explorer Trench as well as the existence of the Queen Charlotte Islands Fault were investigated. The program included: bathymetric, gravity,

and magnetic measurements; continuous seismic reflection profiling along selected tracks; two-ship seismic refraction profiling; heat flow measurements at 13 stations; and bottom sampling using dredges.

Narrative and Experiments Conducted:

At 0930 on 12 July 1970, C.S.S. Hudson left Victoria, B.C. to begin the seventh leg of the HUDSON 70 expedition. A day later, C.N.A.V. Endeavour also left Victoria and joined Hudson on 15 July at 52°N, 134°W to conduct the planned seismic refraction experiment. In the sections below, the scientific experiments conducted during the cruise are described. The dredging operation conducted by C.N.A.V. Endeavour is described in Appendix A.

(a) Geophysical Survey---

The ship's tracks along which gravity, magnetic and bathymetric measurements were made are shown in the accompanying chart. Gravity values were measured using two gravimeters: a Graf-Askania Model GSS2-17 mounted on a gyro-stabilized platform and a D4e vibrating string gravimeter also mounted on the same gyro-stabilized platform. The latter was designed and built at the Wood's Hole Oceanographic Institution.

A cross coupling computer was mounted on the platform to measure the cross coupling error for the Askania gravimeter. The total magnetic field was measured using a proton precision magnetometer built by Barringer Research Corporation. The sensing element (fish) of the magnetometer was towed 700 feet astern to minimize the magnetic effect of the ship.

In order to get the precise gravity value in the survey area, it was essential to know the drift of the gravimeter for the duration of the survey. Both gravimeters were calibrated before and after the cruise at Victoria, B.C. (see Appendix B).

Most instruments worked extremely well throughout the cruise except for the Askania Gravimeter Chart recorder which was found to be non-linear in half of its span. Thus a major part of the gravity was recorded on the linear portion of the chart recorded. This gave unwanted gaps in the gravity map of the area. However, the second gravimeter worked well and we hope to get continuous gravity values from this gravimeter's recordings. The PDP-8 computer worked well for majority of the time, but needed constant maintenance.

(b) Navigation---

Primary navigation during the cruise was provided by satellite navigation and dead reckoning. An ITT 4007AB satellite navigation receiver with an on-line PDP-8 computer was used on C.S.S. Hudson to obtain satellite fixes and the conventional bridge dead reckoning was supplemented by data from a Sperry E/M log and gyro repeater

automatically recorded by the BIODAL data logging system. In addition, an attempt was made to use the Motorola RPS equipment recently purchased to obtain accurate range and bearing on C.N.A.V. Endeavour during the seismic refraction experiment. Endeavour carried a Magnavox 702CA satellite receiver and punch lent by Earth Physics Branch (EMR) to enable subsequent accurate positioning of tracks. No computer was installed on Endeavour but pertinent information was passed by radio to enable fixes to be computed on board Hudson. On three occasions when a rendezvous between the two ships was arranged, data from the Magnavox receiver was passed to Hudson for fix computations.

The RPS system required for accurate relative positioning of the two ships during the seismic refraction experiment proved disappointing. The range obtained was less than expected even after resighting the transponder on Endeavour to provide an unobstructed line of sight. However, the experiment was worthwhile in that it indicated that modifications were required for future use and demonstrated the limits of the equipment for deep sea relative navigation.

As the satellite fixes obtained by Endeavour were not available for the control of her lines, requiring computation by the PDP-8 aboard Hudson, she had to rely on poor Loran-A and dead reckoning for track and control. In this respect, the bathymetry chart of the area compiled by Jacqueline Mammerick of Scripps Institution proved extremely useful, particularly in locating station sites for dredging, etc. With aid of the satellite fixes computed on Hudson, the majority of tracks on which Endeavour had collected useful information and all station sites were computed and plotted by the end of the survey period.

(c) Seismic Reflection Profiling---

Seismic profiling was performed with Hudson steaming at about 6 knots. A Bolt Model 1500 air gun with pulse shaper was used as the sound source. It was fixed every 16 seconds at a peak pressure of about 1700 psi. The signals were recorded on magnetic tape and also on an Alpine recorder and an EPC dry paper recorder. The hydrophone array was 400 feet long, in four 100 foot sections. A slacking winch was used to reduce the noise at the eel.

During the cruise, 916 n.m. of reflection data were collected. Most of the track lines cross the continental margin. These were obtained to supplement the gravity and magnetic measurements, to determine the behaviour of the oceanic crust in the vicinity of the continental margin and to determine the depth and nature of the sediments on the shelf and slope. About two days were spent collecting reflection data around the refraction shooting circle to obtain the depth to oceanic basement so that corrections could be applied to the refraction arrival times.

(1) - On continental Shelf near Vancouver Island (48°16'N, 123°52'W to 48°45'N, 126°02'W)

(2) - As for (1) (49°13.5'N, 127°08'W to 49°18'N, 127°13'W)

(3) - As for (1) (50°47'N, 129°18'W to 50°41'N, 130°37'W)

(4) - Two traverses of continental margin off Queen Charlotte Islands (52°10'N, 133°58'W to 52°06'W, 131°24'W to 52°00'N, 131°12'W to 52°01'N, 132°31'W)

(C) - Along refraction circle

(5) - Across Moresby Channel (51°11', 133°35' to 50°21', 131°38')

(6) - Across continental margin north of Vancouver Island (50°21'N, 131°25'W to 51°19'N, 129°29'W)

(7) - Across continental margin to Paul Revere Ridge (50°26'N, 128°19'W to 49°42'N, 129°29'W)

(8) - Across continental margin near Vancouver Island (48°34'N 126°53'W to 49°01'N 126°12'W)

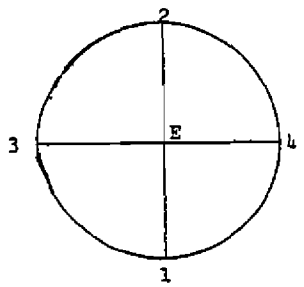
NOTE: The positions are the ends of the line.

(d) The Seismic Refraction Experiment---

The seismic refraction experiment was designed to measure the anistropy of the mantle P wave velocity. C.S.S. Hudson was used as the receiving station and C.N.A.V. Endeavour as the shooting ship. Two reversed lines, each about 50 miles long were completed, one in the east-west and one in the north-south direction. A 'circle' of shots was then performed, with Hudson in the centre of the circle, approximately at the intersection of the two reversed lines. A radar transponder buoy was moored near Hudson's position from which her drift was determined. The sketch below shows approximately the short lines and the positions taken up by Hudson.

1. 51°12.21'N 134°00.51'W
2. 52°02.9'N 133°56.7'W
3. 51 °32.4'N 134°22.7'W
4. 51°30.32'N 133°07.39'W

E. 51°29.0'N 133°51.0'W



The above positions are satellite fixes. Hudson drifted several miles at each of these stations during the shooting.

It was essential that the azimuth from shot to receiver be determined for each shot around the circle. The two ship Radar Positioning System did not provide sufficient range to be useful. Therefore, Endeavour's position was determined by satellite fixes. These should provide values

of azimuth accurate to + or -2° which is sufficiently precise for this experiment.

The experiment started on July 15 and finished on July 21. A total of 201 explosive shots were fired ranging in size from 50 to 600 lb. The shooting was very successful and there were few misfires. During the reversed lines, shots were fired at intervals of 5 to 20 minutes with charge sizes up to 300 lb. Six-hundred pound shots fired every 30 minutes were used during most of the circle. The charges necessary to obtain good first arrivals were larger than we had anticipated and therefore the shot spacing was larger than we had expected. The 2,000 cu. in. air gun was tried at the beginning of the experiment. We had hoped to use it instead of small explosive charges at close ranges. However, it would not seal and after two hours, and further attempts were not made to use it.

After the refraction experiment was completed, Hudson tried to retrace Endeavour's circle while reflection profiling to measure variations in the depth to basement, which be used to correct the travel times. A part of the time, the two tracks were not sufficiently close for accurate corrections to be applied but otherwise the attempt was successful.

On July 26, a sound velocimeter station was completed within the circle. The velocity of sound in sea water was measured down to 2900 m. The surface velocity is 1.495 km/sec. The position of this station is 51°43.8'N, 135°00.4'W.

Preliminary results suggest that the mantle exhibits a high P wave velocity in the E-W direction - about 8.5 km/sec and a lower velocity - about 8.1 km/sec in the N-S direction. The thickness of layer 3 is about 4.5 km and its velocity, 6.7 km/sec. In general, first arrivals from layer 2 were not observed.

(e) Heat-Flow and Bottom Photography---

Thirteen heat flow stations were attempted and 12 produced useful results. A list of the values and an index map of the Explorer Trough stations are included here. Two measurements were obtained in the northern survey area, one on a ridge extending from the continental rise and one in the refraction anisotropy circle. The rise measurement is normal and the value in the circle, at 2.68, would be considered somewhat high by most workers. However, the oceanic crust in the region is relatively young and is covered by a substantial accumulation of sediments presumably built up over a long period. Measurements in Cascadia basin, another heavily sedimented area, suggest that rapid sedimentation can seal off the oceanic basement for hydrothermal circulation, and thus result in observed conductive heat flow consistent with reasonable boundary layer cooling models. The circle measurement therefore does not indicate that the crust in the area is necessarily abnormal. The presence or relative absence of hydrothermal circulation in the upper crustal layers should not have a significant effect on the mantle interface.

The most important part of the heat flow work was a profile across the northern end of the Explorer Trough and some stations in subsidiary troughs to the north. Application of the plate tectonics concept to the west coast region north of Cape Mendocino suggests that the East Pacific Rise, after disappearing into the Gulf of California, is offset by the San Andreas fault and reappears as the Gorda and Juan de Fuca ridges. The Queen Charlotte fault has the correct orientation

STATION	LATITUDE* N	LONGITUDE* W	DEPTH** fm	HEAT FLOW ucal/cm^2-sec	ESTIMATED ACCURACY
HF-1	50 58.0'	131 54.7'	1403	1.1	.06
HF-2	51 34.7'	134 20.7'	1751	2.7	.05
HF-3	49 58.6'	129 32.6'	1111	3.8	.04
HF-5	50 1.6'	129 43.0'	1253	8.4	.3
HF-6	50 4.4'	129 46.4'	1742	1.3	.08
HF-7	50 7.7'	129 49.8'	1480	1.9	.2
HF-8	50 7.5'	130 1.8'	1116	6.6	.2
HF-9	50 13.2'	130 9.2'	1287	4.7	.07
HF-10	50 15.3'	130 17.8'	1300	1.5	.3
HF-11	50 21.0'	130 6.6'	1413	16.8	.4
HF-12	50 45.9'	130 36.6'	1310	4.8	.1
HF-13	50 39.5'	130 33.0'	1308	4.0	.06
Camera-3	50 16.6'	130 17.7'	1304		

*Location by satellite navigation.
**Depth in uncorrected fathoms.

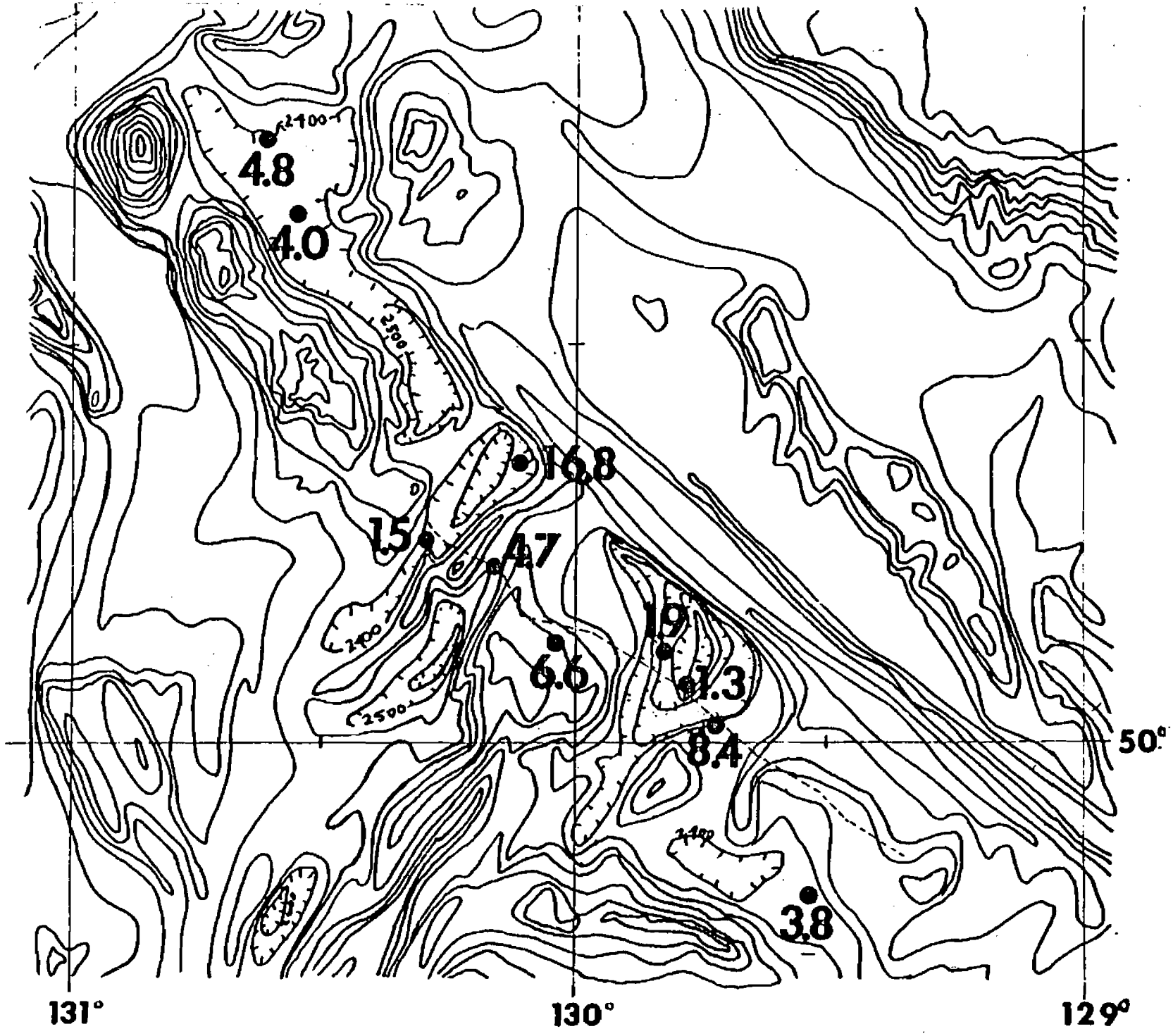
to terminate the rise system and lead the relative plate motion through complications in Alaska into the Aleutian trench. Therefore, the Explorer Trough should be the last expression of the East Pacific Rise spreading center with the possible exception of a small trough northwest of it which has the correct orientation to lead the spreading into the Queen Charlotte Fault. The heat flow stations were sited in an attempt to find out whether thermal anomalies confirm the spreading or not.

Seven stations were occupied across the two trough-like features which terminate at the Paul Revere ridge, a piece of ocean floor

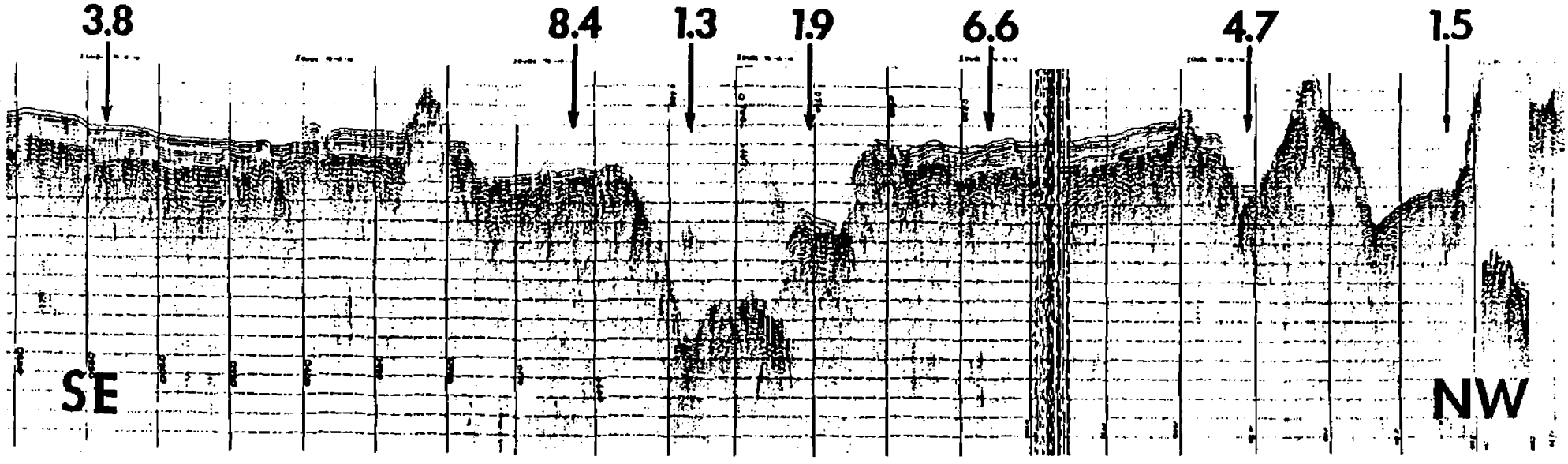
strongly upwarped and dipping northwest away from the trough zone. The stations follow UBC airgun profile 70-16-14 which was used to locate sediment and index the general structure. Two values in the southeasterly trough are low but the trough is flanked by high heat flows on both sides (8.4 and 6.6). A moderately high value (4.7) is observed on a ridge near the northwesterly, or main, trough but another relatively low value is indicated for the valley itself by a partial penetration station (2.4 for 60 cm of sediment). The presence of a large seamount immediately beyond the valley terminated the profile, and the important symmetry station for this trough is missing. However, a measurement was made where the northwestern trough abuts the Paul Revere ridge and produced a record value of 16.8. In short, the heat flow evidence suggests that both troughs are, or have recently been spreading centres and that the low values obtained in the troughs on the profile are the result of the well known but little understood, "valley effect".

Two measurements were made in the subsidiary trough leading northeast from the Paul Revere fault line. Owing to navigational problems they are not sited as was intended and, being approximately equal, do not confirm or deny the existence of spreading this trough. A heat flow of 4½ is rather high, but in view of the other measurement on the same fault line and the undisturbed sediment pond seen by UBC profile 70-16-21, we would guess that active spreading is not occurring. The diffuseness of the earthquake epicenters south of the Queen Charlotte Islands may be real and indicate that the ocean floor between Explorer Trough and the main transform fault is still undergoing general shear.

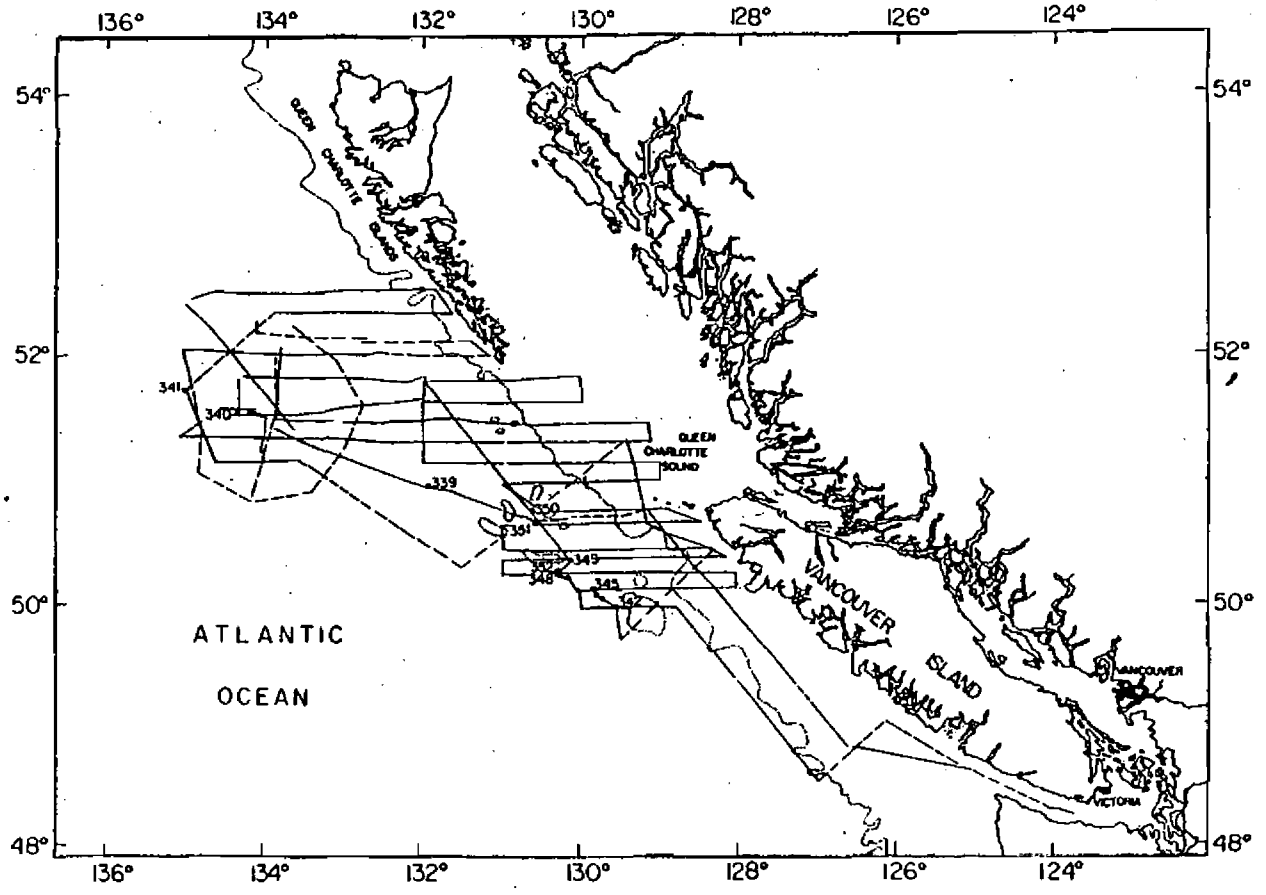
A new underwater cine-camera was brought on the cruise in an attempt to observe the bottom condition in Explorer Trough. Although the instrument had been thoroughly tested in the laboratory, the cold room and in Puget Sound, the pulsed thallium iodide light did not operate on the first two lowerings. Through a decision to modify the firing relay, it was discovered that the relay coil wire was broken in manufacture at one terminal and evidently became a sensitive thermometer after bumping to Victoria in the truck. The third and final lowering produced pictures, but without the expected test of exposure levels, we are not surprised that they are severely underexposed over much of the film. The station was sited close to the partial penetration heat flow measurement in Explorer Trough, whose gently undulating floor has an unusual acoustic signature at this point. The film has not, at this writing, been viewed through a projector, but it appears that the valley floor is a generally flat lava flow covered by some sediment through which rocks outcrop occasionally. The heat flow measurement is therefore likely to be reasonably representative of the conductive surface flow but major hydrothermal vents may not have been covered by the amount of sediment present.



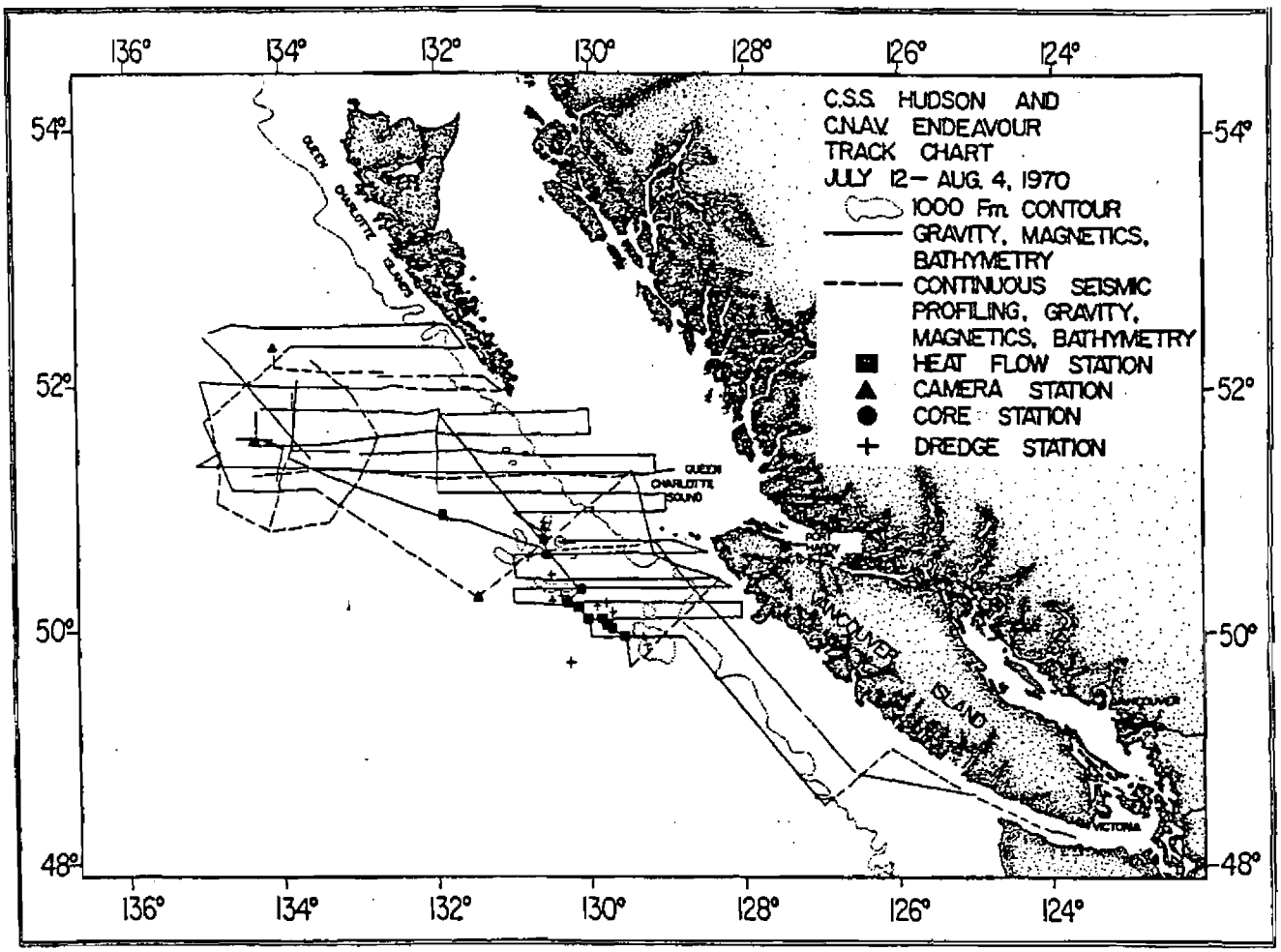
Map of the generalised bathymetry and heat flow values across the northern Explorer Trench system. Heat flow values are in μcal/cm^2/sec. The dashed line here shows the track of the seismic profile (see next



A continuous seismic profile with heat flow values across the northern Explorer Trench system. The profile is indexed on the preceding illustration and is from the University of British Columbia's airgun profile 70-16-



Cruise station numbers for C.S.S. Hudson and C.N.A.V. Endeavour on Phase VII (Victoria to Victoria) of HUDSON 70.



Track chart and types of data collected at stations on Phase VII of HUDSON 70.

Appendix A

Local Cruise Designation:	69-050
Code Reference Number:	10-69-050
Vessel:	C.N.A.V. Endeavour
Dates:	13 July to 4 August 1970
Area:	Victoria, B.C., to Victoria, B.C.
Responsible Agency:	Atlantic Oceanographic Laboaratory Bedford Institute
Personnel:	Ship's Master, Captain T. Bowles
Scientific Staff:	
K.S. Manchester Senior Scientist	Atlantic Oceanographic Laboratory Bedford Institute
F. Muise	Atlantic Oceanographic Laboratory Bedford Institute
J. Nielsen	Atlantic Oceanographic Laboratory Bedford Institute
A. Thomlinson	Atlantic Oceanographic Laboratory Bedford Institute
R. Hyndman (July 13-24)	Dalhousie University Halifax, Nova Scotia
D. Rankin (July 13-24)	Dalhousie University Halifax, Nova Scotia
K.L. Chase (July 25-August 4)	University of British Columbia
R. MacDonald (July 13-25)	University of British Columbia
R. Davidson	University of British Columbia
W. Bertrand	University of British Columbia
R. Parker	Department of Energy, Mines and Resources, Ottawa, Ontario
G. Rogers	Marine Sciences Branch, Ottawa, Ontario

Summary:

The Endeavour acted as the shooting ship with the C.S.S. Hudson as the receiving ship in completing reversed seismic crustal refraction lines: this portion of the work is described in the preceding cruise report on the Victoria to Victoria leg of HUDSON 70.

Following the seismic refraction experiment, the Endeavour carried out seismic profiling and dredging over the Explorer Trench - Paul Revere Ridge area and neighbouring seamounts, between 49°30' and 51°00'N and 129°00' and 131°00'W. Our intent herein is to report upon the dredging operation conducted from July 26 to August 4, 1970.

Purposes:

Our objective in dredging was to obtain outcrop specimens that could permit:

(1) Determination of relationships between lithology, magnetic properties, and age of basalts from different magnetic anomalies within the Explorer Trench area.

(2) Resolution of stratigraphic and structural relationships between greywackes, siltstones and mudstones, and serpentinite on Paul Revere Ridge. All three rock types were recovered in a single earlier (1969) dredge haul midway along the ridge. The need to resolve the stratigraphy and structure of Paul Revere Ridge is the more pressing because this ridge marks an abrupt northern termination of pronounced magnetic anomalies that characterize the adjacent Explorer Trench area.

(3) Petrographic and age-determinations of basalts of the Dellwood Range of seamounts and, to the northeast, the Dellwood Knolls. The aim was to determine whether or not this portion of the sea-floor is spreading.

Methods and Recovery:

Equipment consisted of chain-bag dredges supplied by the Bedford Institute. At each site (selected with the aid of a bathymetric chart (Mammerickx, 1969, Special Chart No. 1, Scripps Institution of Oceanography), echo-sounder profiles, and continuous seismic profiles), the dredge was lowered from the ship's bow. When the metered wire length indicated the dredge to be on the bottom, the ship moved slowly astern, paying out additional wire in amounts of approximately 50% of the water depth, to permit dredging with wire angles ranging from 0° to 45°. At all sites, we attempted to place the dredge low topographically and to dredge in the "uphill" direction. Beginning depths for dredging ranged from 1475 m on a seamount to 3200 m in Explorer Trench. Dredge-site locations and depths are listed in the accompanying table.

Locations and Depths of Dredge Sites

Dredge Site	Location of Start of dredge haul °N Lat.	°W Long.	Geographic Feature	Depth (m) From	To
1	Dredge did not touch bottom				
2	50°53.7'	130°35.0'	Dellwood Knolls (N.W.)	1900	1500
3	50°46.0'	130°24.0'	Dellwood Knolls (S.E.)	1900	1500
4	50°14.1'	130°15.4'	Explorer Trench	2500	2000
5	49°55.7'	129°20.7'	Paul Revere Ridge (South slope)	1800	1700
6	49°58.0'	129°17.7'	Paul Revere Ridge (crest)	1600	1500
7	50°17.9'	130°24.6'	Dellwood Range (S.E. end)	2000	1900
8	50°27.2'	130°32.5'	S.E. Dellwood Seamount	1475	1300
9	50°36.0'	130°45.5'	Middle Dellwood Seamount	1800	1500
10	50°14.5'	129°49.9'	Paul Revere Ridge (crest)	1800	1700
11	50°14.2'	129°54.7'	Paul Revere Ridge (S. slope)	2300	2200
12	Approx. 50°10.0'	Approx. 129°45'	Paul Revere Ridge (S. slope)	2200	2000
13	Approx. 49°46'	Approx. 130°18'	Explorer Trench (E. Wall)		
14	"	"	" "		
15	"	"	" "	2100	2000
16	Approx. 50°13'	Approx. 130°14'	Explorer area (N.W. Part)	2100	1900
17	Approx. 50°5.5'	129°44.5'	Explorer area (N.E. deep)	3200	2400

The method of dredging from the bow was time-consuming and inconvenient as it necessitated hoisting the dredge between the well-deck and the bow by crane, and attendant attaching and detaching of the winch wire at the beginning and end of each haul. Moreover, lack of lighting foreward of the ship precluded dredging with safety after dark, and under some wind and sea conditions the ship was incapable of maintaining the desired heading while steaming astern.

Despite the admittedly inefficient dredging technique, dictated by the ship's gear, in only 3 out of a total of 17 attempts, the dredge returned empty. As indicated in the second table, recovery ranged from a single fragment to several hundred pounds of rock in the other 14 hauls.

Dredge Hauls

Dredge Site	Recovery (Weights are estimates, descriptions are preliminary and tentative.)
1	Nil - dredge apparently did not reach bottom.
2	250 lbs. 90% angular fragments of vesicular pillow basalt, many with fresh glassy rind; 10% pebble size glacial erratics of dioritic to granitic composition.
3	100 lbs. 40% glacial boulders and cobbles, 60% pillow basalt. Generally thin manganese coating but one sample with 2 cm. thick crust of manganese oxides.
4	125 lbs.; fresh, ropey, vesicular basalt with glassy rind.
5	One 13 cm fragment of porous, low density, manganiferous mudstone.
6	600 lbs.; 10% glass sponges, infilled with clay and manganese oxide; 25% glacial pebbles and cobbles; 65% basalt with weathered, palagonitized glassy rind.
7	500 lbs.; mainly vesicular pillow basalt some with glassy rind. No glacial erratics.
8	600 lbs.; one large glacial boulder (80 lbs.) and few glacial pebbles and cobbles; remainder is vesicular pillow basalt. Many large samples with weathered glassy rind, some with manganese coating about 2 mm thick.
9	400 lbs.; 20% glacial pebbles and cobbles and iron oxide-stained volcanic ash; 75% basalt with manganese oxide coating to 3 cm thick. 5% manganese nodule fragments. Weathered glassy rind on some basalt fragments.
10	One glacial cobble of intrusive rock.
11	100 lbs.; vesicular olivine basalt, apparently from weathered talus, coated with manganese oxides.
12	300 lbs.; 50% green, partly serpentinized rock (basalt and/or peridotite); 50% greywacke and interbedded mudstone and siltstone, contorted and sheared, containing carbonized plant fragments and lenses of coal up to 8 mm thick. Uniform weathering of all sides of most rock fragments indicates a probable talus-slope as their source.

13	Nil
14	Nil
15	200 lbs.; pillow basalt with palagonitized glassy rind; one glacial cobble.
16	650 lbs. pillow basalt with glassy rind.
17	One angular fragment of fresh, dark green volcanic rock.

APPENDIX B

CALIBRATION OF GRAVIMETERS

The two gravimeters were calibrated at Graving Dock, Esquimalt, Victoria, B.C. before and after the cruise. The results of these calibrations are given in the following tables:

Note that the drift rates of the Askania Gravimeters depend on the MSD value considered in their compilations. A drift of -7.7 mgal results if the high MSD 6700 is used and of -12.9 mgal if the low MSD 6300 is used. The difference between the two is significant. What causes this non-linearity is not clear at the moment.

Variations in VSA readings

Time/Day	Old MSD	New MSD	Gravity VCO	C.C. VCO	Gravity CHART	C.C. Chart	VSA
0800/193	6300	6700	66777	65444	88.2	66.5	980969.5
0830/193	6700	6300	60991	65278	10.7	64.3	980970.7
0900/193	6300	6700	66769	65430	88.0	66.3	980970.2
0930/193	6700	6300	60987	65281	10.7	64.3	980970.0
1000/193	6300	6700	66766	65438	87.9	66.3	980969.5
1030/193	6700	6300	60989	65293	10.7	64.4	980970.5
1100/193	6300	6700	66764	65403	87.9	66.4	980969.4
1130/193	6700	6300	60985	65297	10.7	64.4	980970.2
1200/193	6300	6700	66760	65454	87.8	66.5	980970.5
1230/193	6700	6300	60987	65299	10.7	64.5	980970.4

Place: Esquimalt Graving Dock, Victoria, B.C.

Base Gravity: - 980976.1 mgal
Roll: - 0.5
Pitch: - 6.8
Lamp Current: - 165 ma
Erection: - Fast

Time Constant: - 6 sec.
Room Temp.: - 13.3°C.
Internal Temp.: - 40°C.
Sea State: - 1
Lower Spring: - 2100

Gravimeter Calibration after the Survey

Time/Day	Old MSD	New MSD	Gravity VCO	C.C. VCO	Gravity CHART	C.C. Chart	VSA
1820/218	6300	6700	66399	65484	83.0	66.7	980963.6
1900/218	6700	6300	60768	65257	07.7	63.7	980964.4
1940/218	6300	6700	66399	65460	83.0	66.4	980961.2
2020/218	6700	6300	60767	65229	07.7	63.4	980966.3
2100/218	6300	6700	66397	65403	83.0	66.0	980966.0
2140/218	6700	6300	60772	65220	07.7	63.4	980964.7
2220/218	6300	6700	66400	65417	82.9	63.0	980969.7
2300/218	6700	6300	60769	65211	07.7	63.0	980969.7

Place: Esquimalt Graving Dock, Victoria, B.C.

Base Gravity: - 980976.1
Roll: - +4.0
Pitch: - -6.5
Lamp Current: - 164 ma
Erection: - Normal

Time Constant: - 6 sec.
Room Temp.: - 13.3°C.
Internal Temp.: - 40°C.
Sea State: - 0
Lower Spring: - 2100

Drift Rate Calculation

For MSD = 6700, Average VCO = 60769.0

Computed gravity value of the vax station = 980968.4 using the calibration constants based on calibration performed on day 193. Measured gravity value of the base station = 980976.1

For MSD = 6300, Average VCO = 66397.75

Computed gravity value = 980963.2 based on calibration constant obtained on day 193; hence the drift for MSD = 6700 is -7.7 mgal and for MSD = 6300 is -12.9 mgal.

VSA Mean Gravity Values obtained at Graving Doc, Esquimalt, Victoria, B.C.

Time Interval	No. of Data	Mean Gravity	Standard Dev.
2021/191 - 0245/192	10	980970.6	.42
1540/192 - 2005/192	7	980969.2	1.03
0800/193 - 1230/193	10	980970.1	.45
1721/217 - 2314/217	10	980967.3	2.01
0146/218 - 0446/218	2	980969.3	.30
1820/218 - 2340/218	9	980964.7	2.59
0840/219 - 1000/219	11	980965.4	2.57

The total drift of the VSA gravimeter is the difference of the mean gravity values between day 193 and 217. Hence, the drift rate was obtained as -0.116 mgal/date. This is close to the drift correction rate -0.1 mgal/day used in the computation of VSA free air gravity.

A T L A N T I C O C E A N O G R A P H I C L A B O R A T O R Y

B E D F O R D I N S T I T U T E

"HUDSON 70"

INTERIM CRUISE REPORT

VICTORIA TO RESOLUTE BAY

B.R. PELLETIER

CRUISE NO. 69-050

CRUISE REPORT NO. 69-050

"HUDSON 70" - INTERIM CRUISE REPORT

VICTORIA, B.C., TO RESOLUTE BAY, DISTRICT OF FRANKLIN

Local Cruise Designation:	69-050
CODC Reference Number:	10-69-050
VESSEL:	C.S.S. HUDSON
Dates:	226 273 14 August - 30 September 1970
Areas:	(a) Northwest Pacific Ocean (b) Chukchi Sea (c) Beaufort Sea (d) Northwest Passage (Canadian Arctic Archipelago)
Responsible Agency:	Atlantic Oceanographic Laboratory Bedford Institute
Personnel:	Ship's Master, Captain D.W. Butler
Scientific Staff:	
B.R. Pelletier Chief Scientist	Atlantic Oceanographic Laboratory Bedford Institute
G. Vilks Assistant Chief Scientist	Atlantic Oceanographic Laboratory Bedford Institute
C.J. Yorath	Geological Survey of Canada, Calgary
C.J. Havard	Geological Survey of Canada, Calgary
D.J. Faber	National Museum of Canada, Ottawa
F.J.E. Wagner	Atlantic Oceanographic Laboratory Bedford Institute
W.J. Whiteway	Atlantic Oceanographic Laboratory Bedford Institute
J. Bruce	Atlantic Oceanographic Laboratory Bedford Institute
M. Gorveatt	Atlantic Oceanographic Laboratory Bedford Institute
W. Pinner	Highland Helicopter Ltd., Vancouver
J. Strad	Highland Helicopter Ltd., Vancouver

Scientific Staff (continued):

B.D. Loncarevic	Atlantic Oceanographic Laboratory Bedford Institute
J.R. Belanger	Atlantic Oceanographic Laboratory Bedford Institute
B.D. Carson	Atlantic Oceanographic Laboratory Bedford Institute
J. Shearer	Atlantic Oceanographic Laboratory Bedford Institute
R. Smith	Queens University, Kingston
A. Harding	Hunting Ltd., U.K.
C.R. Mann	Atlantic Oceanographic Laboratory Bedford Institute
H.A. MacPherson	Defence Research Establishment, Atlantic
P. Wadhams	Atlantic Oceanographic Laboratory Bedford Institute
H. Henderson	Atlantic Oceanographic Laboratory Bedford Institute
K.G. Shih	Atlantic Oceanographic Laboratory Bedford Institute
G.M. Purdy	Atlantic Oceanographic Laboratory Bedford Institute
V.F. Coady	Atlantic Oceanographic Laboratory Bedford Institute

Summary:

Soundings G.E.B.C.O.	9653 km
Gravity Records	9653 km
Magnetics	9653 km
Seismic Reflection Profiling	2194 km
Side Scan Sonar	1200 km
Surface Plankton Tows	94

Vertical Plankton Tows	116
Surface Biological Tows	117
Vertical Biological Tows	113
Van Veen Grabs	116
Sediment Dredges	11
Cores	71
Camera Stations	7
Knudsen Casts	41
Biological Sled Trawls	1
Underwater Television Stations	4
Oblique Biological Tows	2

Narrative:

On the morning of 14 August 1970, Hudson proceeded northwest out of Victoria, B.C., to begin Phase VIII of her journey around the Americas. All scientific hands for the Arctic voyage were aboard, exclusive of a few personnel who joined the ship in the Beaufort Sea. While steaming across the Pacific Ocean, some coring and station work was undertaken as part of a shakedown for the staff; also, these people were instructed in watchkeeping duties on the satellite navigator and the geophysical console. On the second day out, an emergency call was received from divers in trouble and Hudson altered course to render assistance as a doctor with experience in diving medicine was aboard. However, the Canadian Air Force participated shortly after so Hudson was relieved of her rescue mission.

During the next few days, heavy seas troubled the ship. Gear had to be made even more secure because of the heavy rolling and pitching of the vessel. For a few hours, the ship hove to until all moorings were checked. At times, seas poured over the foredeck. On 20 August at 1232 hours, an explosion occurred in a generator but at 1300 hours the ship was underway again as Captain Butler decided to continue on course. This action was crucial because it avoided abandoning HUDSON 70 and her circumnavigation of the Americas. The remainder of her passage to the Arctic Ocean through the Aleutian Islands was unimpeded. Along this track from Victoria, the acoustical records revealed the precipitous edge of the Pacific Continental Shelf and numerous rectilinear ridges and troughs comprising fracture zones in the ocean floor.

During the afternoon of 21 August, the ship anchored in the lee of St. Lawrence Island to replace a hatch cover over the sounding well of the variable depth transducer and thus be prepared for steaming through Arctic ice. She proceeded north through Bering Strait, with Siberia to

port and Alaska to starboard. In this region, on 22 August at 1700 hours, Hudson made her first crossing of the Arctic Circle and this message was piped to the ship's company. In the wheelhouse, the bridge log at the end of the watch read: "Navigation lights checked. Cloudy and clear. Vessel steady."

In the Chukchi Sea, loose floating ice was encountered that confined the steaming route to the coastal shipping lane lying within a few kilometres of shore. Proceeding on a northeasterly course along this coast, the ship was literally flagged down by a priest and an Inuit party in an outboard motor boat, who asked for assistance in the search for three walrus hunters from a nearby village who went missing on the ice. At this time, the U.S. Coast Guard and Alaskan State Police had contacted the ship, and later thanked the captain for his help. They relieved Hudson from the search. Hudson left Wainwright on 23 August.

Off Point Barrow, Alaska, the ship met with heavy ice; however, once clear, Hudson steamed down the coast past Barter Island toward Canadian territorial waters and arrived off Herschel Island on 26 August. Here, J.M. Shearer and A. Harding, who had been carrying out seismic profiling and side-scan sonar surveying in the Beaufort Sea from C.S.S. Richardson were picked up by helicopter and joined Hudson immediately. Two others, B.D. Loncarevic and J.R. Belanger, also joined the ship from Herschel Island, having come aboard in the helicopter. That day, the fog was too thick to permit safe flying for any distance over the ocean, so Hudson steamed within sight of land thereby bringing the airport to the pilot. From here, business commenced.

The plan was to run geophysical lines in the evening along 14 transects across the shelf, and along one tie line to the transects at mid-shelf locations parallel to the coast. During the day, station work would be carried out according to the schedule of operations prepared in the prior evening. (See accompanying example - next page.) By this means, all hands were alerted to the equipment and duties required, as well as the location and time for the work to be undertaken. The geophysical work revealed the form and structure of the seabed and continental shelf, while the bottom sampling recovered material that indicated the nature of the sediments and animals on the seafloor itself. Old beaches and ancient river valleys were located, but other significant discoveries were to come. The revelation of deep and profuse ice-scouring of the sea bed to water depths of 60 m and the existence of dozens of underwater ice-cored mounds (the so-called pingos) occurring 35 to 100 km from shore presented a two-fold obstacle in the safe development of resources and the secure protection of the environment.

New concepts on the water mass, particularly its microstructure, continued to develop from ocean-sampling operations. The relationship of the ocean to biology on the one hand, and sedimentology on the other were recorded and studied. Soon, it was learned that radically different life zones existed in the ocean; for example, planktonic foraminifera were offshore dwellers strictly speaking, and muddy sediments were deposited or transported mainly inshore where such faunal life was inhibited from growing.

WORKING SCHEDULE FOR SEPTEMBER 9, 1970

Continue Geophysical Survey along cross line X-9 to 0730 hours at 71:12N, 134:25W. Retrieve gear and steam to sampling station.

STATION NO. 407

Arrive on station 0800 hours, 71:12N, 134:25W
Operations:- Vertical Plankton Tow 864
- Surface Plankton Tow 849
- Vertical Biological Tow 860
- Surface Biological Tow 867
- Core (40 foot barrel) 833
- Van Veen Grab 864

STATION NO. 408

Arrive on station 1030 hours; 71:01N, 134:10W
Operations:- Vertical Plankton Tow 865
- Surface Plankton Tow 850
- Vertical Biological Tow 861
- Surface Biological Tow 866
- Core (40 foot barrel) 834
- Van Veen Grab 865

STATION NO. 409

Arrive on station 1230 hours; 70:55N, 133:55W
Operations:- Vertical Plankton Tow 866
- Surface Plankton Tow 851
- Vertical Biological Tow 862
- Surface Biological Tow 869
- Core (20 foot barrel) 835
- Van Veen Grab 866

STATION NO. 410

Arrive on station 1415 hours; 70:47N, 133:45W
Operations:- Vertical Plankton Tow 867
- Surface Plankton Tow 852
- Vertical Biological Tow 863
- Surface Biological Tow 870
- Core (20 foot barrel) 836
- Van Veen Grab 867

STATION NO. 411

Arrive on station 1615 hours; 70:36.5N, 133:30W
Operations:- Vertical Plankton Tow 868
- Surface Plankton Tow 853
- Vertical Biological Tow 864
- Surface Biological Tow 871
- Core (20 foot barrel) 837
- Van Veen Grab 868

STATION NO. 412

Arrive on station 1815 hours; 70:24N, 133:10W
Operations:- Vertical Plankton Tow 869
- Surface Plankton Tow 854
- Vertical Biological Tow 865
- Surface Biological Tow 872
- Core (20 foot barrel) 838
- Van Veen Grab 869

Steam to tie line C and commence Geophysical Survey 3 miles west of cross line X-9 at 1930 hours; 70:21.5N, 133:20W. Continue survey along tie line C to cross line A-10 at 70:31N, 132:20W and alter course to north and proceed along cross line A-10.
Operations:- Stream Seismic gear, Side Scan Sonar, Hydrophones and Magnetometer
- Watchkeeping on Geophysical Console and Satellite Navigation

B.R. Pelletier

B.R. Pelletier, Senior Scientist

The work proceeded daily in an unbroken routine, punctuated only by ice-reconnaissance helicopter flights. At times, parties visited shore in order to sample coastal features or examine geological formations inland. A brief respite from daily operations was gained when the oil barge arrived off Tuktoyaktuk in order to refuel Hudson for the remainder of the cruise to Dartmouth, N.S. The crews of both ships entertained for several hours in typical fashion while at anchor. In the late evening of 10 September, the oil barge cast her lines off and returned to harbour. Again, the work proceeded with daily regularity, while samples and records were examined and then stowed until the ship reached home port. The survey lines were quickly reduced in number in this race against the onset of winter. And now, the pace was beginning to tell physically, but the success of the work kept all spirits buoyed.

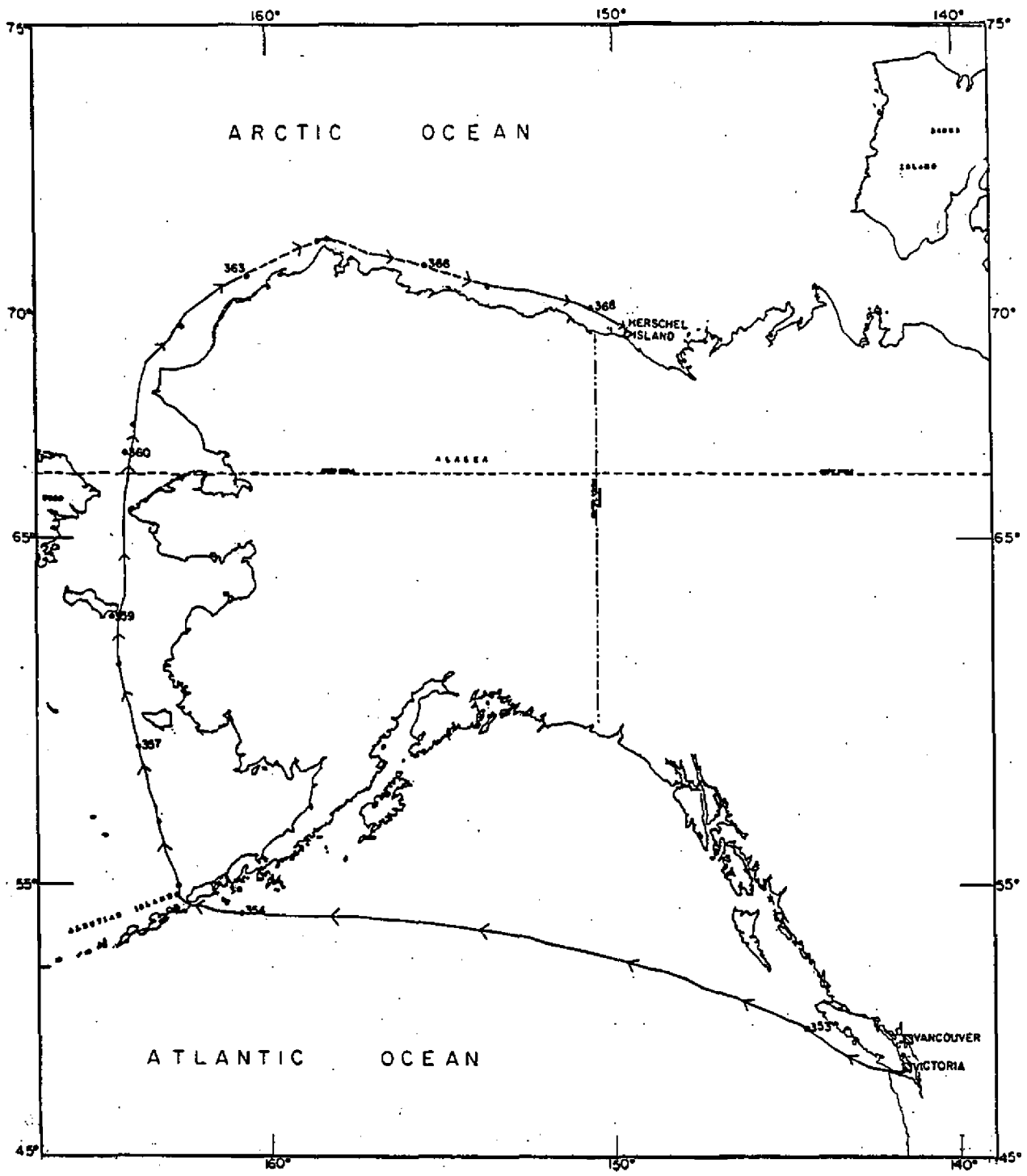
During the four weeks spent in the Beaufort Sea, sea conditions were unusually good. Only once, in early September, was the work routine interrupted when gale force winds required the ship to hove to for the night. However, the survey continued on course the next morning, but drifting pack ice indicated that the polar pack was moving south into the survey area.

At the start of the survey, the geophysical lines were run to points about 200 km offshore. Here, the presence of the polar pack ice prevented further surveying to the north. All through September, snow flurries continued and the ice began moving shoreward on a latitude-wide basis. By the third week in September, Hudson was restricted to surveying at locations over the shelf-slope break at distances of only 70 to 100 km from shore. New ice was forming in the Archipelago's channels as well, and old ice was blocking much of the proposed route in the Northwest Passage. Decisions would soon have to be made on the time to vacate the Arctic Ocean and on a choice of the route to take for the eastbound passage through the Arctic islands. On the latter count, the ship could proceed north through Prince of Wales Strait, or she could sail the alternate southern route along the mainland. In the evening of 22 September, after a personnel change at Tuktoyaktuk and a media crew joined the ship, Hudson sailed out of the Beaufort Sea to begin work in Amundsen Gulf.

The seafloor of Amundsen Gulf was once an outlet for tongues of ice that were spawned from the great continental ice sheets. Thousands of years earlier, rivers flowed in valleys that had been oriented by massive dislocations in the earths crust more than 20 or 30 millions of year ago. Such was the nature of the undersea features that Hudson's tracks would cover. Here, while the new ice was forming and snow falling steadily, Hudson began her transect of the Northwest Passage. To the north, heavy sea ice had been moving south all week so that choke points to navigation were expected between Banks and Cornwallis islands. With the prospect of CCGS Sir John A. MacDonald steaming from Resolute Bay in order to escort both Baffin and Hudson, it was decided to carry out station work en route. This was done during the night, and at 0740 on the morning of 25 September, Hudson reached the northern end of Prince of Wales Strait. At this point, the ship reached a major milestone in her journey around the world, but the ships terse log merely read: "Completed station work. Set course toward Sir John A.MacDonald. Overcast with frequent snow flurries".

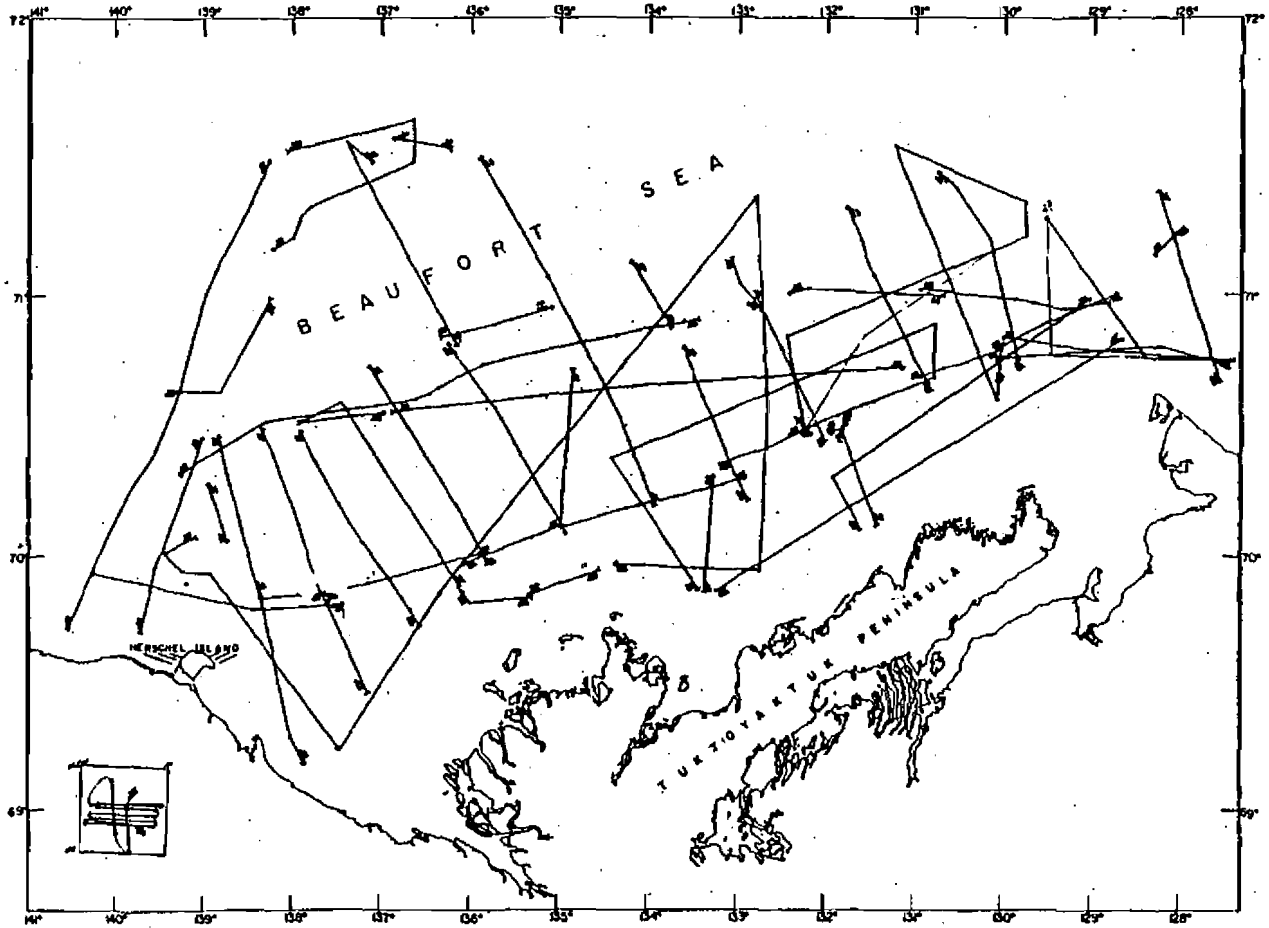
Over the next few days on the passage to Resolute, the ship was stopped several times by heavy ice. On one occasion, she rode up onto a particularly hard floe and slid off one side thereby heeling to port so abruptly and steeply that her guardrail almost touched the broken sea ice. Work continued, though in order to maintain the ocean and biological stations around the Americas, the geophysical surveying had to be abandoned. At evening, the ship stopped in the thick commonly 10/10 ice pack, with heavy snow falling and new ice forming constantly. From the sounding records, old watersheds were observed, which had been submerged throusands of years ago. Even the passage of ancient glaciers could be deduced. The station work continued over Barrow Strait and Lancaster Sound. From an onboard analysis of the plankton tows and cores, it was noted that some species failed to move westerly from Baffin Bay and the Atlantic Ocean. This migration was inhibited by the stronger residual current emerging from the Arctic Ocean.

At 0800 on 30 September, the helicopter began moving personnel, equipment and supplies between Resolute and Hudson. Meanwhile, a shore party comprising Bosun Joe Avery, Photographer Roger Belanger, and Chief Scientist B.R. Pelletier erected a plaque commemorating HUDSON 70 at the most northerly point of the cruise. Phase VIII had ended, and a new scientific staff was in place. At dinner in the evening before the ship lay at anchor off Resolute, the old scientific staff toasted the ship's company and wished them good sailing for the final leg of HUDSON 70 and the voyage home.

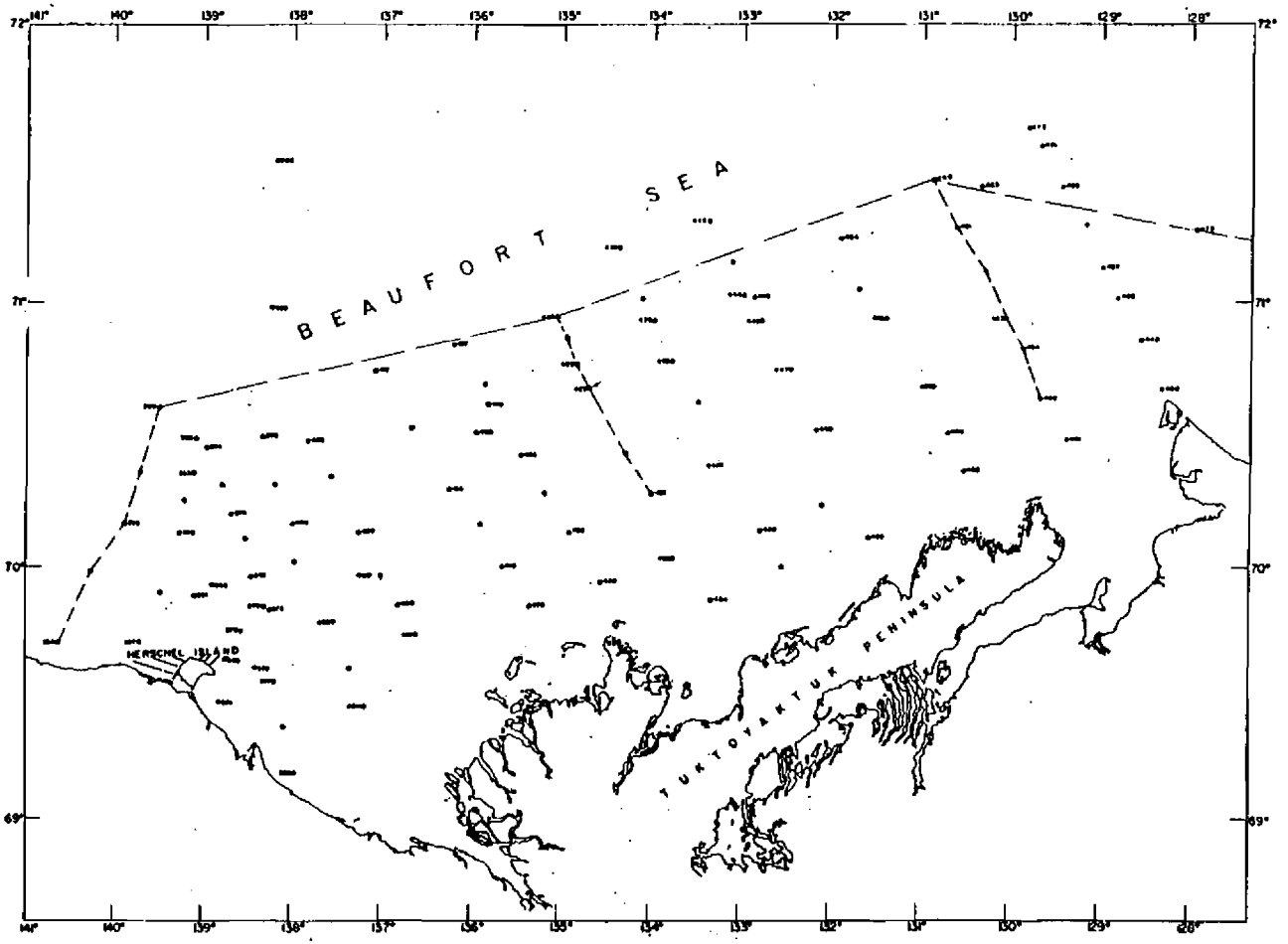


Track chart and cruise station numbers for Phase VIII

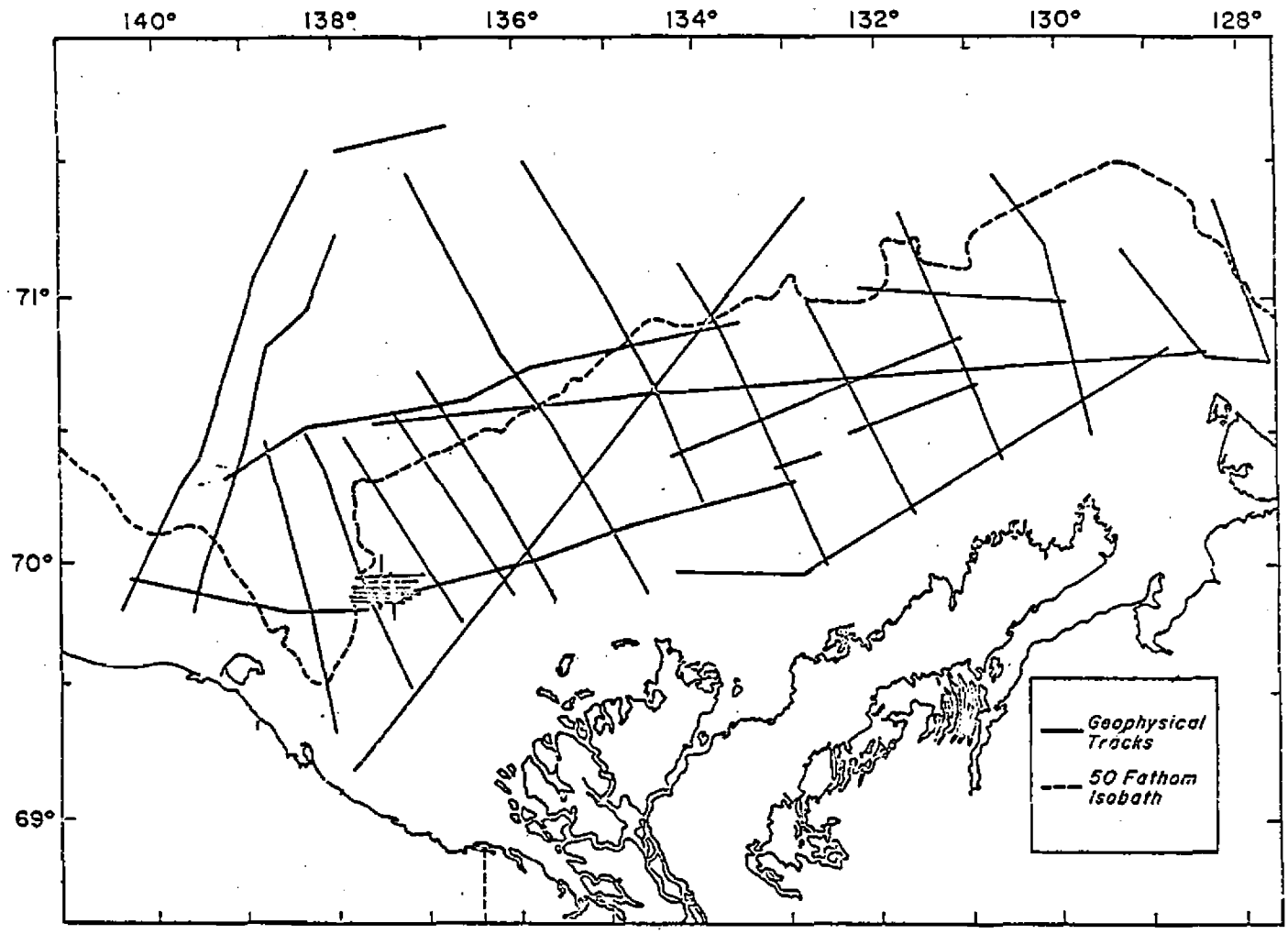
(Victoria to Resolute Bay) of HUDSON 70.



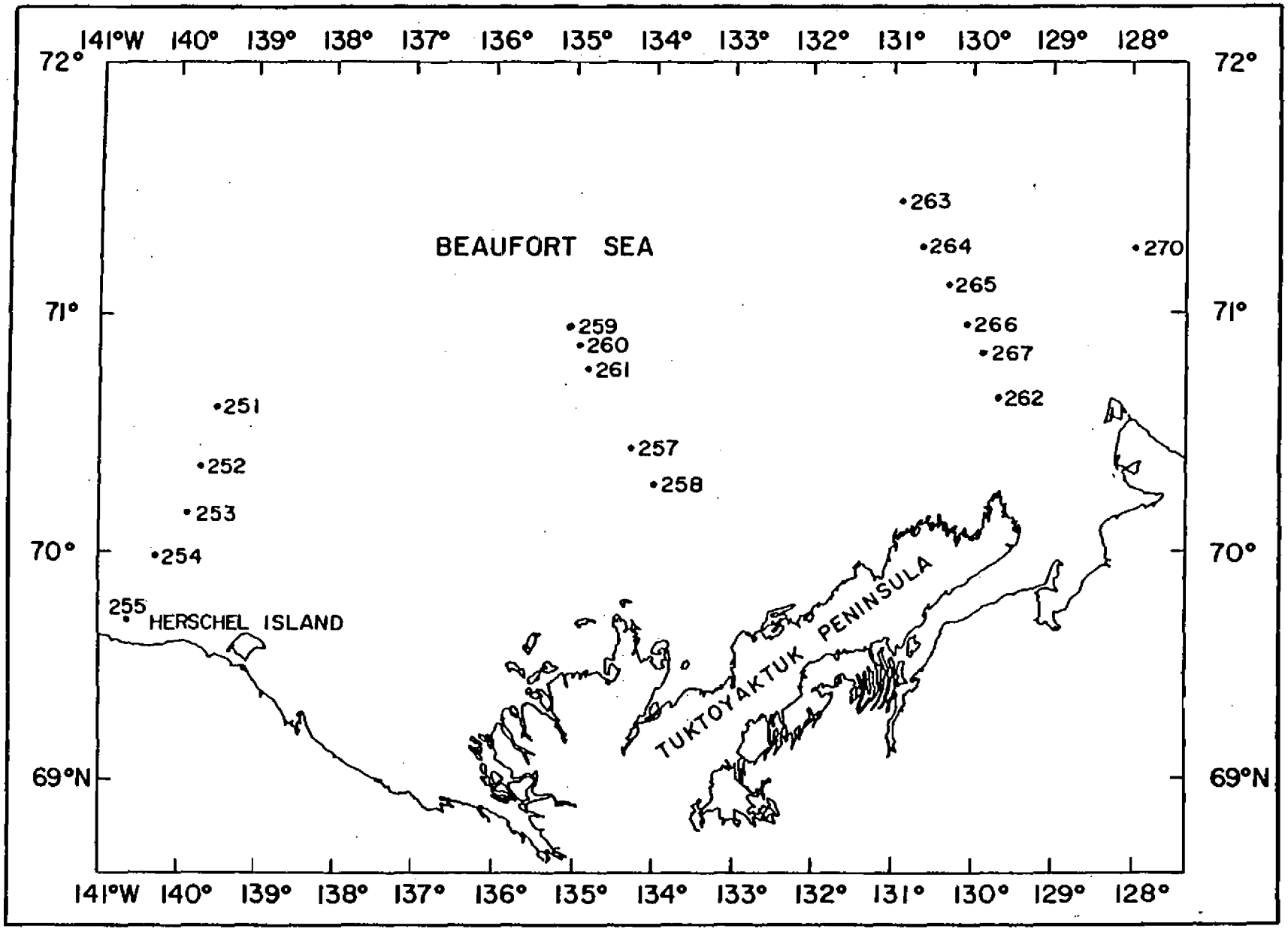
Cruise tracks and stations in the Beaufort Sea during Phase VIII. Note that cruise stations are more clearly depicted in the next illustration.



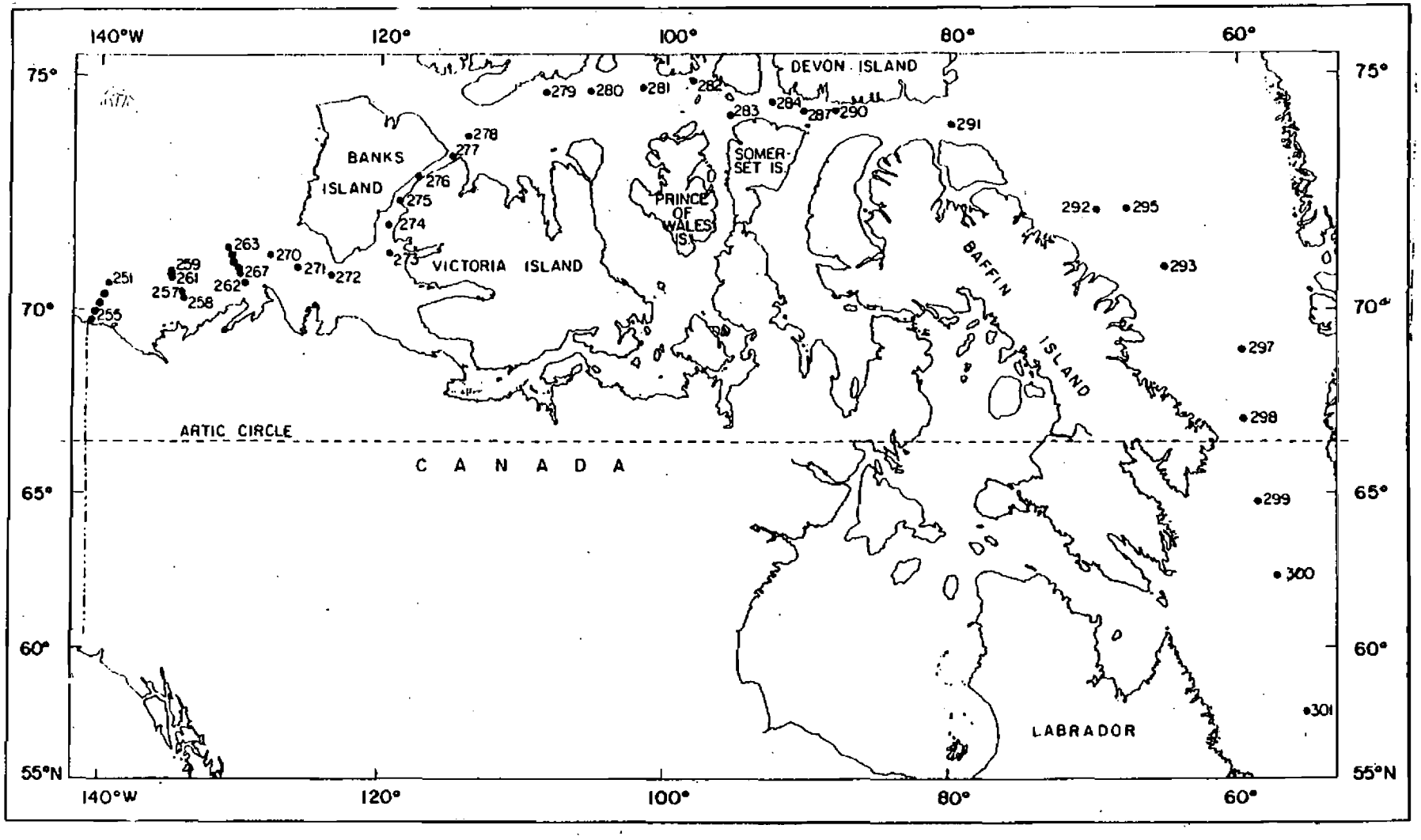
Cruise stations in the Beaufort Sea during Phase VIII.



Geophysical tracks in the Beaufort Sea during Phase VIII.



Oceanographic bottle stations occupied in the Beaufort Sea during Phase VIII.



Oceanographic bottle stations occupied in the western Arctic region during Phase VIII of HUDSON 70.

A T L A N T I C O C E A N O G R A P H I C L A B O R A T O R Y

B E D F O R D I N S T I T U T E

"HUDSON 70"

INTERIM CRUISE REPORT

EASTERN ARCTIC - BAFFIN BAY, LABRADOR SEA

D.I. ROSS

CRUISE NO. 69-050

CRUISE REPORT NO. 69-050

"HUDSON 70" - INTERIM CRUISE REPORT

EASTERN ARCTIC - BAFFIN BAY, LABRADOR SEA

Local Cruise Designation:	69-050
CODC Reference Number:	10-69-050
Vessel:	C.S.S. Hudson
Dates:	30 September to 16 October 1970
Area:	Eastern Arctic - Baffin Bay, Labrador Sea
Responsible Agency:	Atlantic Oceanographic Laboratory Bedford Institute
Personnel:	Ship's Master, Captain D.W. Butler

Scientific Staff:

D.I. Ross Senior Scientist	Atlantic Oceanographic Laboratory Bedford Institute
C.R. Mann	Atlantic Oceanographic Laboratory Bedford Institute
B.R. Pelletier	Atlantic Oceanographic Laboratory Bedford Institute
C.E. Keen	Atlantic Oceanographic Laboratory Bedford Institute
D.L. Barrett	Atlantic Oceanographic Laboratory Bedford Institute
R.M. Eaton	Atlantic Oceanographic Laboratory Bedford Institute
D.M. Garner	Atlantic Oceanographic Laboratory Bedford Institute
P. Wadhams	Atlantic Oceanographic Laboratory Bedford Institute
G.M. Purdy	Atlantic Oceanographic Laboratory Bedford Institute
J.A. Nielsen	Atlantic Oceanographic Laboratory Bedford Institute

Scientific Staff (continued):

T.F. Courtney	Atlantic Oceanographic Laboratory Bedford Institute
H. Henderson	Atlantic Oceanographic Laboratory Bedford Institute
J. Bruce	Atlantic Oceanographic Laboratory Bedford Institute
V. Coady	Atlantic Oceanographic Laboratory Bedford Institute
P.A. Solowan	Atlantic Oceanographic Laboratory Bedford Institute
K.S. Manchester	Atlantic Oceanographic Laboratory Bedford Institute
B.L. Johnson	Atlantic Oceanographic Laboratory Bedford Institute
P.J. Bhattacharyya	Dalhousie University Halifax, Nova Scotia
H. MacPherson	Department of National Defense Halifax, Nova Scotia
R. Parker	Department of Energy, Mines and Resources, Ottawa, Ontario

Summary:

Seismic Reflection Profiling	420 nm
Reversed Seismic Refraction Line	137 nm
Gravity, Magnetics, and Bathymetry Data	2500 nm
Core Stations	3
Bottle Casts	10
Plankton Tows	15

Purpose of Cruise:

1. To investigate the structure of Baffin Bay and its relation to continental Canada and Greenland.

2. To complete the continuous transect of plankton tows and bottle

Purpose of Cruise (continued):

casts from the Pacific through the Arctic Ocean commenced on the earlier phase of the cruise.

3. To obtain geophysical data on one of two parallel lines run by Hudson and Baffin through Davis Strait and Labrador Sea.

Narrative:

At 1500 on 30 September, C.S.S. Hudson left Resolute Bay on the last phase of HUDSON 70. Ice conditions in Barrow Strait and western Lancaster Sound prevented the streaming of equipment for the first 20 hours although they presented no problem to the passage of the ship. Gravity data obtained was very poor along the entire line in Lancaster Sound because of course changes to avoid heavy ice. Plankton tows and bottle casts were obtained at two stations (85°W and 80°W) in the Sound.

Once clear of the heavy ice, the magnetometer and seismic reflection gear were streamed and the ship proceeded at 6 knots along a line out of Lancaster Sound and into the deep water of northern Baffin Bay. Apart from minor problems with the seismic equipment resulting from having been packed away since Victoria, all equipment operated well until the magnetometer fish was lost in a string of ice across the entrance to Lancaster Sound. This resulted in a loss of magnetic data on the remainder of the line into the Bay while a new fish could be spliced onto the existing cable.

A regular daily R/T schedule was set up with C.S.S. Baffin, participating with Hudson during this phase (AOL Cruise Report) to discuss progress of work on lines proposed in earlier discussions and to consider any changes to the program that might be desirable. On 2 October, contact was made with USCGC Edisto. Edisto was to act as shooting ship during the seismic refraction work scheduled for 5 to 8 October and was to embark two persons from Bedford Institute and the Department Seismic Shooter at Frobisher Bay on 2 October (Appendix A). A regular R/T schedule was set up for communication with Edisto and the rendezvous of the two ships was set for midnight on 4 October.

The easterly line out from Lancaster Sound into northern Baffin Bay was terminated on the evening of 3 October in 660 fathoms of water and the ship proceeded SSW across the area east of Bylot Island surveyed by C.S.S. Dawson earlier in the summer (AOL Cruise Report) as far south as 72°10'N. Seismic reflection data were collected along the northern half of this line at 6 knots. Magnetic, gravity, and bathymetry data were collected along the entire line, the second half at 12 knots.

There remained some 36 hours at the end of the line before the rendezvous with Edisto which had by now been shifted till the early morning of the 5th. Hudson therefore steamed four miles west across the 100 fathom depth on the edge of Baffin Island and then proceeded to run a further seismic reflection line across the shelf edge of Baffin Island out into the deep Bay at the same time collecting gravity, magnetic, and

bathymetry data to correlate with the reflection records. The reflection record on this line showed a deeply dipping faulted boundary of the Baffin Island gneiss structure at a depth of 160 fathoms and a distance of 27 miles from the nearest coast. The feature correlated exceedingly well with anomalies on the gravity and magnetic records. These anomalies were typical of those found along the continental margins of eastern North America. This line into the Bay was terminated at a depth of 1020 fathoms. After retrieving the gear, a core station was taken prior to proceeding at 12 knots on a southeasterly course to the edge of the ice lying along the centre of the Bay at approximately 65°W then south through 4/10th ice to rendezvous with Edisto at 71°N, 65°W.

After its rendezvous with Edisto, Hudson took a second core station and proceeded to prepare the seismic refraction cable for streaming. An attempt was made to lay the refraction cable in a comparatively clear area within the ice finger lying through the central Basin. This proved disastrous as the drift of the ice proved far greater than that of the ship resulting in the ice pack drifting onto the ship and causing serious problems with the streamed cable within a period of two hours. At least 12 hours listening period was required to complete the line so attempts to keep station at this point were abandoned and Hudson and Edisto streamed northwest 42 miles to clear water on the western side of the ice edge.

The refraction cable was successfully streamed in the early afternoon and Edisto commenced shooting along a line bearing 350° from two miles north of Hudson. A total of 54 shorts was fired and received along the 37 nm line, the shorts ranging from 50 lb. charges while the two ships were close, to 500 lb. charges towards the end of the line.

The first line was completed at midnight on 5 October and after recovering the cable, Hudson proceeded towards the northern end of the line so that it could be reversed the following day. On meeting up with the Edisto again, a core, plankton, and bottle station was taken while waiting for daylight to lay the cable. Daybreak showed a number of growlers and small icebergs in the vicinity of the station so the two ships steamed west seven miles before laying the cable and commencing the reversed line. Shooting recommenced by 10 a.m. with Edisto steaming along the reciprocal course of the previous day. The only problems encountered were due to charge misfires resulting from a new type of booster supplied by C.I.L. and the line was completed by late afternoon. This completed the refraction work with Edisto. The two ships met for the last time three hours later to transfer the Departmental personnel onto Hudson. Edisto then left for Boston while Hudson continued with its program.

The seismic refraction work proved extremely successful. Three layers were detected between the surface sediment column and the mantle with a total thickness of 6 km. Velocities of 3.34, 5.85, and 7.14 km/sec were obtained for the three layers. Although some dip of the individual layers was indicated, the overall dip of the mantle interface was very small. The measured mantle velocity was 8 km/sec at a depth of approximately 8 km below the surface of the sea floor. The work proved conclusively that Baffin Bay has an oceanic structure.

Having proved Baffin Bay to be oceanic, it then became important to try to get a complete reflection line across the Bay to pick up any evidence of a buried oceanic ridge and to look at the transition from oceanic to continental type structure on both sides of the Bay. We had already obtained a line out from Baffin Island so it was sensible to continue this line across to the Greenland side. Hudson therefore steamed west to pick up this line as close as possible to where it had been left off as time permitted, and then proceeded east at 6 knots recording reflection, magnetic, gravity, and bathymetry data. The line was continued across the central Bay and broad deep shelf area off the west coast of Greenland terminating in 120 fathoms of water some 25 miles west of Svartenhuk Peninsula. This line showed a remarkable difference between the east and west sides of the Bay and also evidence of a deep rugged reflector in the central area. On the Greenland side there was no marked evidence of the transition from oceanic to continental structure so apparent off Baffin Island. Instead, the deep shelf appeared to consist of considerable thickness of gently dipping sediment beds exhibiting a very broad positive gravity anomaly of around 70 mgals.

At the conclusion of the line, Hudson turned SW towards 71°N, 60°W to rendezvous with Baffin when the Hudson's helicopter exchanged one slightly used teletype for one apparently operational magnetometer fish and cable. The latter was to replace the repaired cable and fish being used by Hudson which had been giving considerable noise spikes during operations at full speed. During the rendezvous, a further plankton tow and bottle cast station was taken.

After parting company, both ships then started the long trip home--Hudson proceeding due south along longitude 60°W with Baffin some 15 miles to the west until latitude 66°N then along a course 160° through Labrador Sea to the northeast continental margin of Newfoundland. Six plankton tows and bottle casts were taken along the track to complete the transect from the Pacific through the Arctic Ocean and Baffin Bay to the Labrador Sea. Gravity, magnetic, and bathymetry data were collected along the entire length of this line.

Hudson rounded Cape Race, Newfoundland, mid-day on 13 October and proceeded across the southern Grand Banks, Laurentian Channel, and Scotian Shelf to the Dominion Observatory gravity range located 50 miles south of Halifax. Two traverses of the NW-SE range line were run before heading back to Halifax to arrive on schedule off Georges Island on 16 October.

APPENDIX A

Local Cruise Designation:	69-050 (HUDSON 70)
Code Reference Number:	10-69-050
Vessel:	USCGC Edisto
Dates:	2 October to 6 October 1970
Area:	Davis Strait and Baffin Bay
Responsible Agency:	Atlantic Oceanographic Laboratory Bedford Institute
Personnel:	Ship's Master, Captain Brazier
Scientific Staff:	
K.S. Manchester	Atlantic Oceanographic Laboratory Bedford Institute
B.L. Johnston	Atlantic Oceanographic Laboratory Bedford Institute
R. Parker	Department of Energy, Mines & Resources, Ottawa, Ontario

Summary:

The Edisto acted as the shooting ship with the C.S.S. Hudson as receiving ship in completing a reversed seismic crustal refraction line in central Baffin Bay. Fifty-four explosive charges were set off ranging in size from 33 lb. to 750 lb.

Equipment and Methods Used on the Ship:

Nitrone S.M. super explosive manufactured by C.I.L. was supplied in 33 lb. and 50 lb. cans. These cans were strapped together using conventional 3/4" steel strapping to make up the required charge size of up to 750 lb. The charges were ignited by using three feet of C.I.L. black Clover safety fuse, a standard blasting cap, and a nitrone S.M. booster. The fuse was lit using a conventional 12 volt automobile cigarette lighter and the charge was allowed to roll down a conveyor over the side of the ship into the water. The charge usually exploded about one minute and fifteen seconds after it hit the water. Ship's speeds of six to twelve knots were used depending on the charge size. The time of each shot was accurately determined by using a chronometer, U.V. recorder, and a time break oscillator (T.B.O.). The direct shock wave from each explosion was picked up by a geophone on the deck of the ship. This signal from the geophone caused a tone that was being generated by

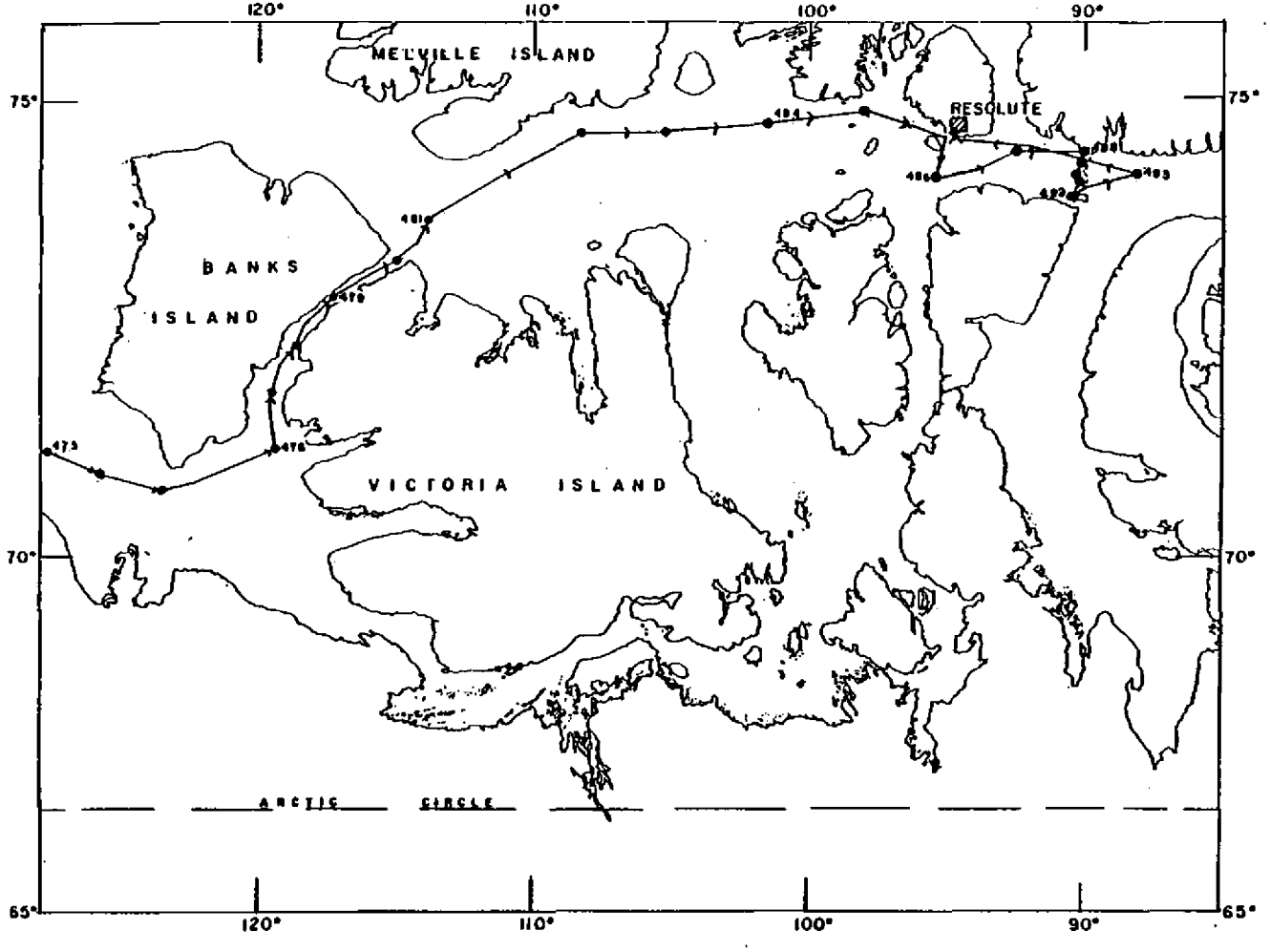
the T.B.O. and transmitted by radio to the receiving ship to be cut off for fifteen seconds. The time that the tone was cut off was the shot instant with only a convection for the shooting ship's distance from the explosion needing to be applied. As a precaution in case of T.B.O. or radio failure, the geophone signal of each shop was also recorded simultaneously on the U.V. recorder with a chronometer time signal and a time standard signal such as W.W.V. or C.H.U. The ship's position and the depth of water at each shot point was also recorded in a log.

Discussion and Comments:

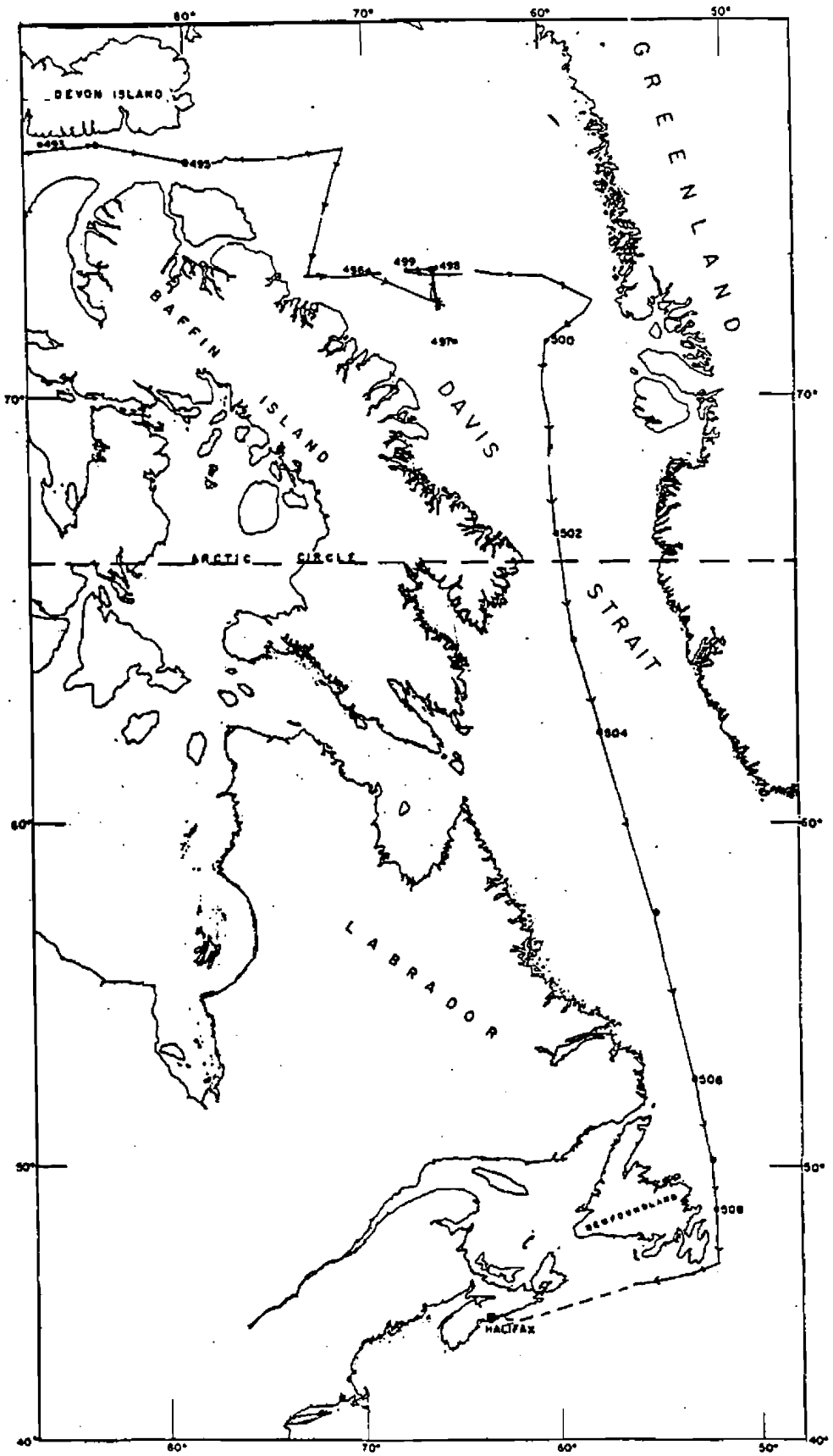
The use of the USCGC Edisto as a shooting ship in the Arctic was very satisfactory. The facilities were excellent and the ship's crew very helpful. Seventy-two charges were made up and put over the side; however, only fifty-four of these exploded with the others being misfires. This can be attributed to either the wrong type of boosters or a newly designed booster that is unsatisfactory for this purpose. Previously, the boosters were encased in copper and we would average about 1% misfires. The boosters we had this time were encased in plastic and we had about a 30% misfire average. As everything was similar to previous experiments except the booster, it is logical to state the booster was at fault. Most of the misfires were in charges over 150 lb. in size which apparently sink faster and greater water pressure is encountered before the charge explodes. This was partially remedied by using one-half pound TNT blocks and three pound C-3 demolition charges in place of the boosters. In the future, it should be mandatory that a few hundred pounds of geogel explosive should be available in case the boosters supplied do not work.

Preliminary Results:

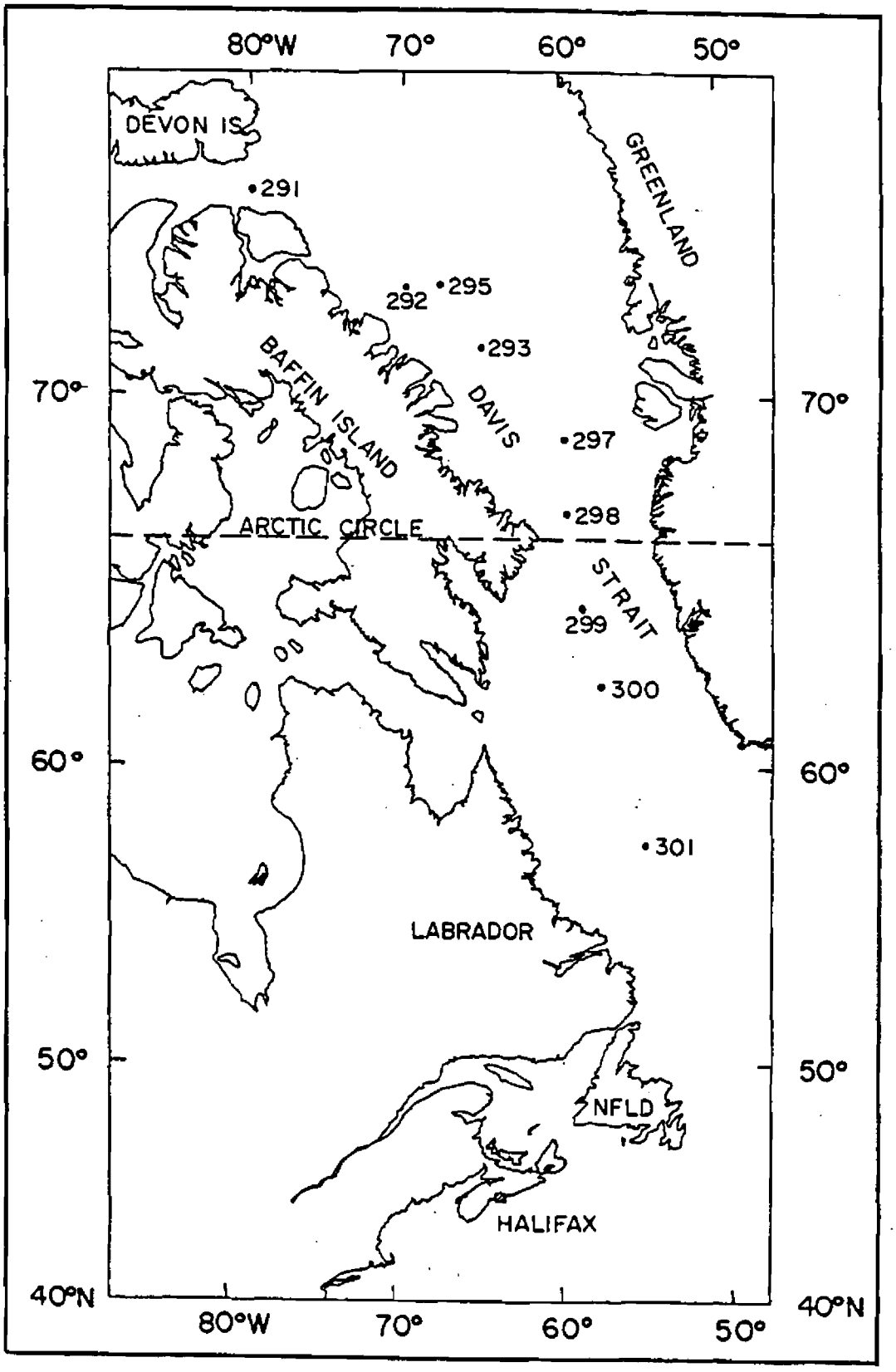
The preliminary results of this crustal refraction experiment indicate that there is a rather typical oceanic type crust underlying central Baffin Bay.



Cruise track and stations occupied up to Resolute during HUDSON 70.

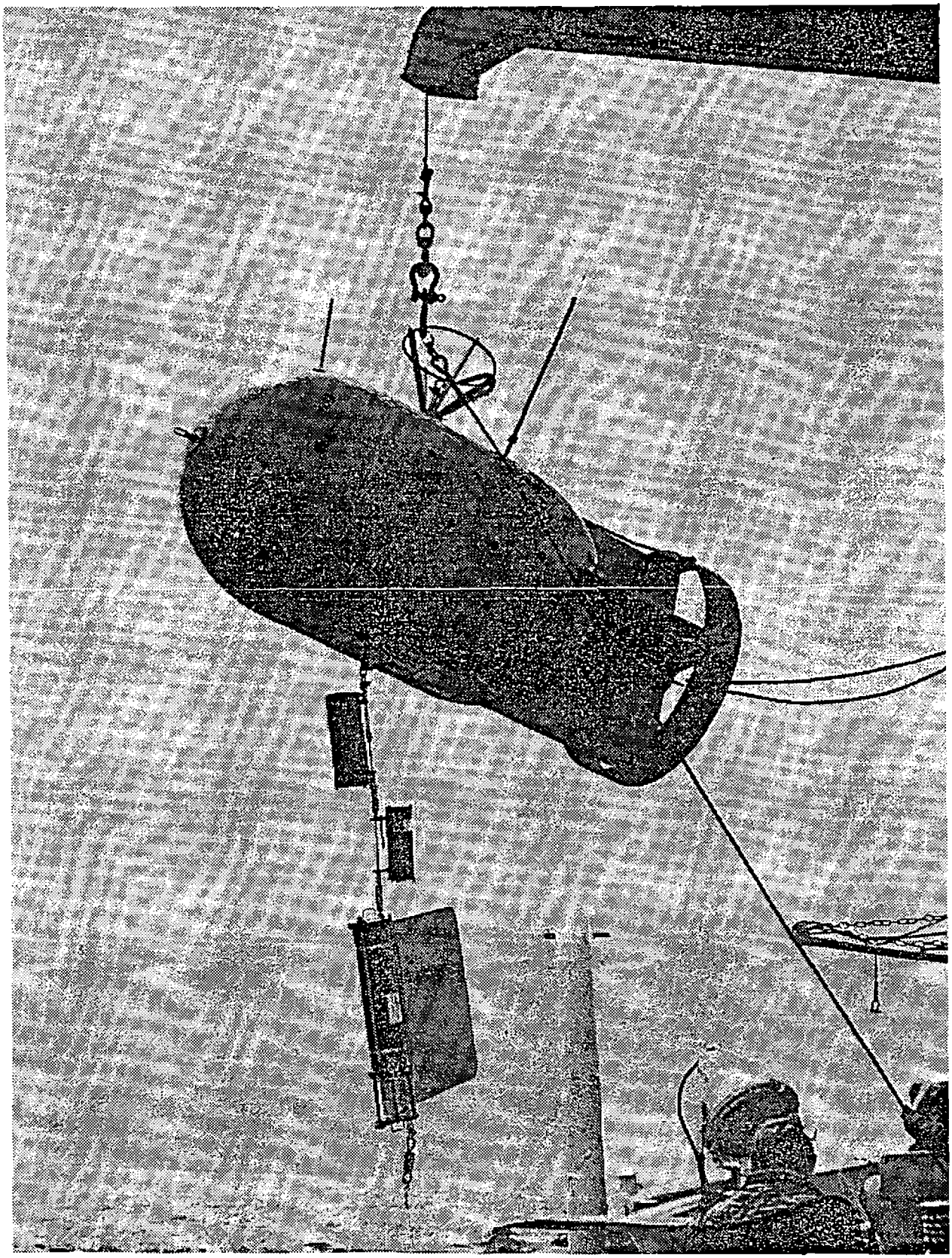


Cruise track and station numbers during the final Phase (IX) of HUDSON 70 Resolute Bay to Halifax (BIO).



Oceanographic bottle stations occupied during the final phase of HUDSON 70

B. ATLAS OF PHYSICAL OCEANOGRAPHIC DATA



Fisheries and Oceans
Ocean Science and Surveys Atlantic

Pêches et Océans
Sciences et levés océaniques Atlantique

Atlas of Physical Oceanographic Data for the South Atlantic Ocean, Drake Passage, Pacific Ocean, and Canadian Arctic-1970

L. Bellefontaine, J. Pritchard, and B. Reiniger

Atlantic Oceanographic Laboratory
Ocean Science and Surveys, Atlantic
Department of Fisheries and Oceans

Bedford Institute of Oceanography
P.O. Box 1006
Dartmouth, Nova Scotia
Canada B2Y 4A2

November 1982

Canadian Technical Report of Hydrography and Ocean Sciences No. 14

Canada

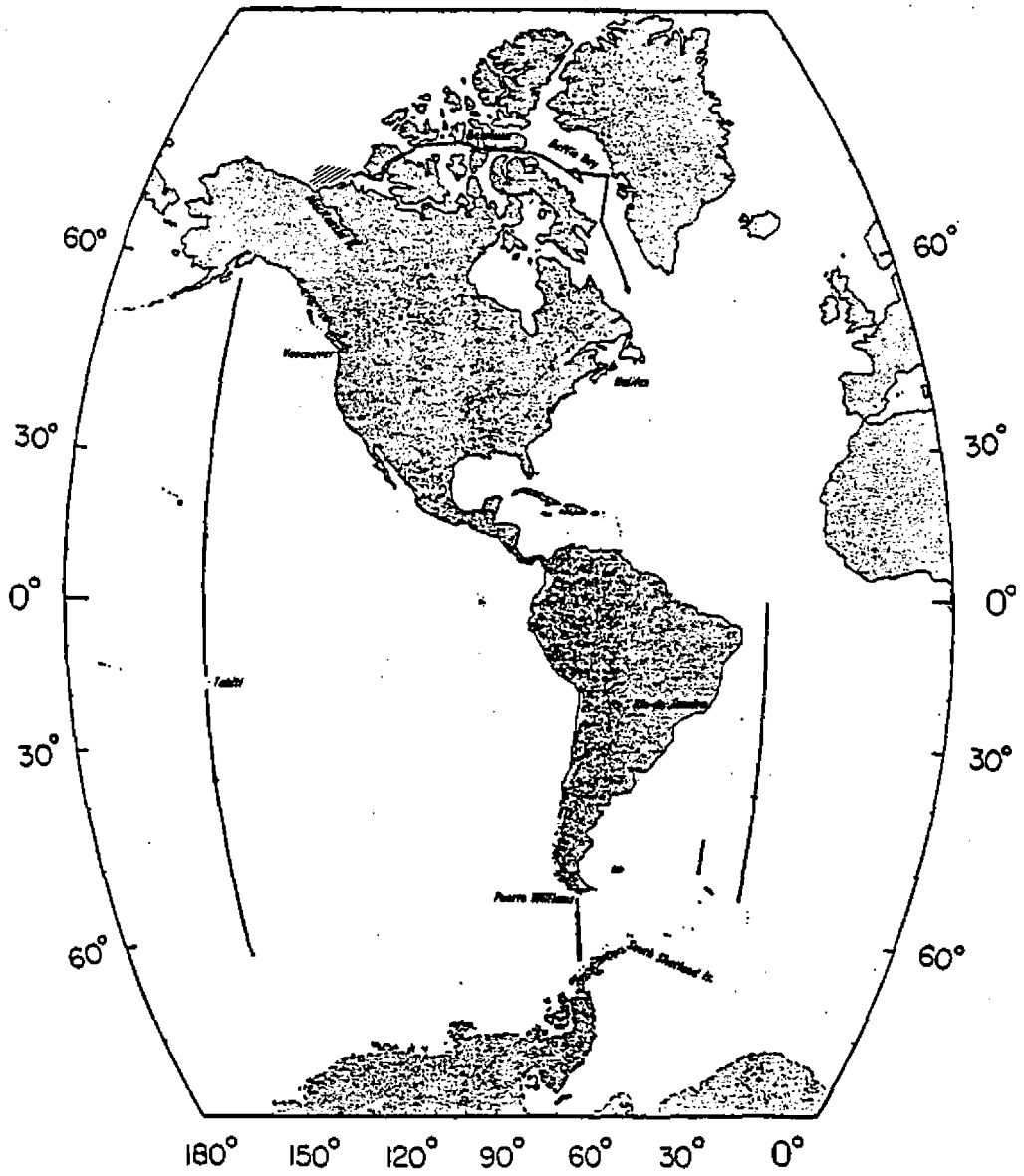
©Minister of Supply and Services Canada 1982

Cat. No. Fs 97-18/14E ISSN 0711-6764

Correct citation for this publication:

Bellefontaine, L., Pritchard, J., and Reiniger, R. 1982. Atlas of physical oceanographic data for the South Atlantic Ocean, Drake Passage, Pacific ocean, and Canadian Arctic - 1970. Can. Tech. Rep. Hydrogr. Ocean Sci. 14: 121 p.

EXPÉDITION HUDSON 70 EXPEDITION



CIRCUMNAVIGATION OF THE AMERICA'S
"CSS HUDSON"

NOVEMBER 19 1969 – OCTOBER 16 1970

ABSTRACT

Bellefontaine, L., Pritchard, J., and Reiniger, R. 1982. Atlas of physical oceanographic data for the South Atlantic Ocean, Drake Passage, Pacific Ocean, and Canadian Arctic - 1970. Can. Tech. Rep. Hydrogr. Ocean Sci. 14: 121 p.

Physical oceanographic data gathered in the South Atlantic, Drake Passage, Pacific Ocean, Western and Eastern Arctic and Arctic waters from November 19, 1969, to October 16, 1970, are presented as vertical sections. Data from current meters moored in Drake Passage from January 1970 to February 1970 are presented in various graphical displays including time series, progressive vector, and stick plots.

RÉSUMÉ

Bellefontaine, L., Pritchard, J., and Reiniger, R. 1982. Atlas of physical oceanographic data for the South Atlantic Ocean, Drake Passage, Pacific Ocean, and Canadian Arctic - 1970. Can. Tech. Rep. Hydrogr. Ocean Sci. 14: 121 p.

Présentation en sections verticales de données recueillies dans l'Atlantique Sud, le Détroit de Drake, l'océan Pacifique, l'Ouest et l'Est de l'Arctique et les eaux de l'Arctique, du 19 novembre 1969 au 16 octobre 1970.

On présente les données obtenues de courantographes amarrés dans le Détroit de Drake en janvier et février 1970 sous diverses formes graphiques, dont des séries chronologiques, des diagrammes de vecteurs progressifs et de vecteurs sous forme de bâtonnets.

ACKNOWLEDGEMENTS

The data presented in this atlas were gathered during the "HUDSON 70" cruise, which was led and co-ordinated by Dr. C.R. Mann. The authors wish to thank the staff of the Ocean Circulation Division, who took part in the data collection, also the personnel of both Ocean Circulation and Coastal Oceanography Data Processing Units who assisted in the analysis. We also acknowledge the contributions of Plansearch Inc. of Dartmouth, Nova Scotia under contract FP806-0-F095 for the preparation and drafting of the major part of the atlas.

PREFACE

INTRODUCTION

This publication contains prepared material derived from data collected during the voyage of the CSS HUDSON from Nov. 19, 1969 to Oct. 16, 1970. The voyage which involved circumnavigating both N. & S. America is known generally as 'HUDSON 70'.

The data is presented in two parts, firstly, selected sections of temperature, salinity, dissolved oxygen, and nutrients, and secondly, current meter data from Drake Passage during January and February 1970.

All the physical oceanographic data presented in this atlas are archived by the Marine Environment Data Service (MEDS) Department of Fisheries and Oceans, Ottawa, except the current meter data which are available from the Atlantic Oceanographic Laboratory.

This atlas does not represent the entire data collection from this cruise.

BOTTOM PROFILES

A precision graphic recorder was operated more or less continuously on the cruise, and bottom profiles have been drawn on most of the sections. The soundings were corrected using Mathews Tables, and are archived by the Oceanic Bathymetry and GEBCO Unit, Dept. of Environment, Ottawa.

For sections where no continuous positioning and/or soundings were available, only soundings at the stations are used, which in some instances are connected by a single line.

TEMPERATURE

All temperatures are expressed in degrees Celsius. Those at the surface were obtained by collecting a sample of water in a metal bucket and measuring its temperature with a mercury-in-glass thermometer accurate to ±0.1°C. Subsurface temperatures were measured with Richter and Wiese or Yoshino reversing thermometers. They are considered accurate to ±0.02°C.

SALINITY

Salinity determinations were made with an "Auto-Lab" inductive salinometer. They are considered accurate to ± 0.004°/₀₀. The salinities were calculated using the UNESCO (1966) tables.

OXYGEN

Dissolved oxygen content was determined by the Carpenter modification of the Winkler method using 60 ml sample bottles. The precision of the measurement are estimated to be ±0.06 ml/l.

NUTRIENTS

The nutrient components of sea water; silicate, nitrate and phosphate were determined by continuous flow analysis using a Technicon Auto Analyzer I. The methods used and statistical data for this cruise are described in Automatic Analysis at Sea (Coote, Duedall and Hiltz, 1971)*. The coefficient of variation was 0.6% for a single silicate determination and 6% for phosphate determination derived from varied CSK standards. The precision for nitrate though not determined would have been between those values.

* Coote A.R., I.W. Duedall and R.S. Hiltz. 1971. Automated Analysis at Sea. In Technicon International Congress 1970 Volume III, Industrial Analysis & Thurman Associates, Suite 1610, Congress Bldg., Miami, Florida, 33132.

T A B L E O F C O N T E N T S

INSIDE COVER SHEET ..... (iii)

ABSTRACT & ACKNOWLEDGEMENTS ..... (iv)

PREFACE ..... (v)

LIST OF TABLES ..... (vi)

LIST OF FIGURES ..... (vii)

PART (1) OCEANOGRAPIC SECTIONS

1.1 South Atlantic ..... (2)

1.2 South Atlantic ..... (6)

1.3 Drake Passage ..... (10)

1.4 South & North Pacific ..... (14)

1.5 Beaufort Sea ..... (18)

1.6 Arctic Sections ..... (22)

1.7 Davis Strait ..... (26)

PART (2) CURRENT MEASUREMENTS

2.1 Explanation ..... (28)

2.2 Positional Detail ..... (30)

2.3 Analysis ..... (33)

List of Tables

Page

Part 1 Physical Oceanographic Coverage in Sections ..... (1)

Part 2 Details of Moorings in Drage Passage ..... (30)

List of Figures

Part 1 Oceanographic Sections .....

Fig. 1 South Atlantic - Section Line (Stations 1-25) ..... (2)

2 Temperature and Salinity Sections ..... (3)

3 Oxygen and Silicate Sections ..... (4)

4 Phosphate and Nitrate Sections ..... (5)

5 South Atlantic - Section Line (Stations 26-30) ..... (6)

6 Temperature and Salinity Section ..... (7)

7 Oxygen and Silicate Sections ..... (8)

8 Phosphate and Nitrate Sections ..... (9)

9 Drake Passage - Section Line (Stations 35-38) ..... (10)

10 Temperature and Salinity Section ..... (11)

11 Oxygen and Silicate Section ..... (12)

12 Nitrate Section ..... (13)

13 South & North Pacific - Section Line (Stations 227-249) . (14)

14 Temperature and Salinity Section ..... (15)

15 Oxygen and Silicate Section ..... (16)

16 Phosphate and Nitrate Section ..... (17)

17 Beaufort Sea - Section Lines ..... (18)

18 Temperature and Salinity Section (Stations 251-255) ..... (19)

19 Temperature and Salinity Section (Stations 259-258) ..... (20)

20 Temperature and Salinity Section (Stations 263-262) ..... (21)

Fig. 21 Arctic Section (Stations 251-295) ..... (22)

22 Temperature and Salinity Section ..... (23)

23 Arctic Section (Station 285-289) ..... (24)

24 Temperature and Salinity Section ..... (25)

25 Davis Strait Section Line (Stations 295-301) ..... (26)

26 Temperature and Salinity Sections ..... (27)

Part 2 Current Measurements .....

Fig. 27 Operational & Statistical Detail ..... (28-29)

28 Current meter locations ..... (31)

29 Typical current meter mooring ..... (31)

30 Bathymetric Section of Drake Passage ..... (32)

31 U and V Components of current meter data ..... (33)

32 Current meter data - Station 1 ..... (34-36)

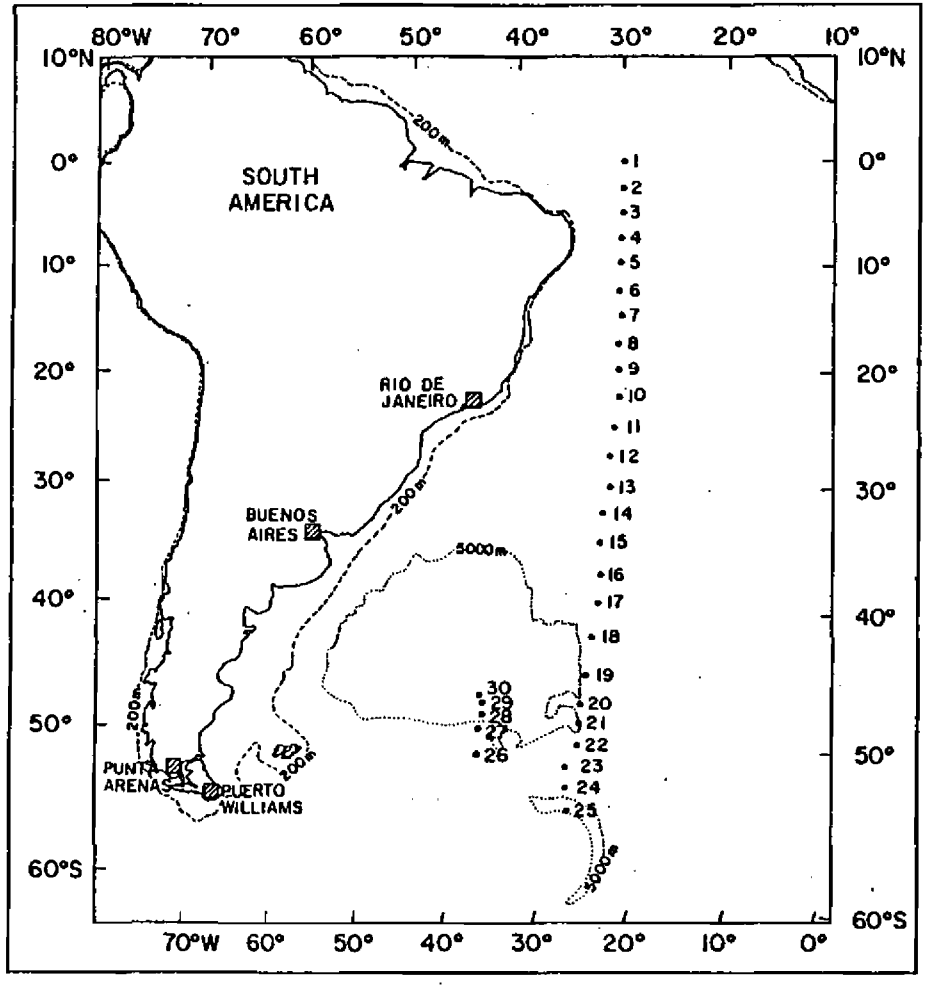
33 Current meter data - Station 2 ..... (37-39)

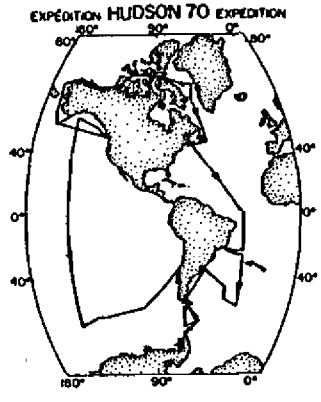
34 Current meter data - Station 3 ..... (40-42)

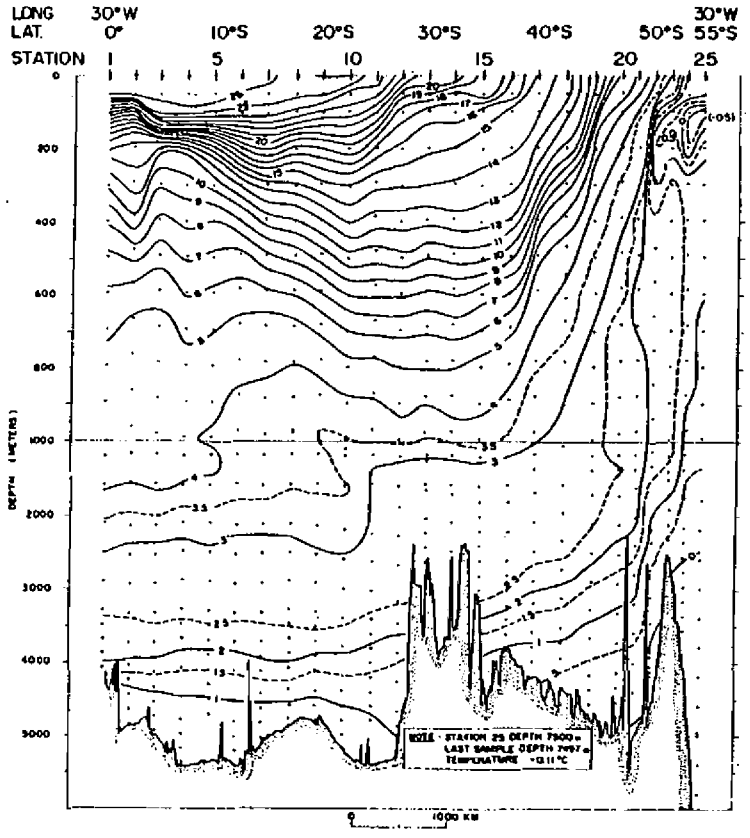
35 Current meter data - Station 4 ..... (43-45)

SECTION LOCATION	STATION NUMBERING	TEMPERATURE	SALINITY	DISSOLVED OXYGEN	SILICATE	PHOSPHATE	NITRATE
SOUTH ATLANTIC	1-25	X	X	X	X	X	X
SOUTH ATLANTIC	30-26	X	X	X	X	X	X
DRAKE PASSAGE	38-35	X	X	X	X		X
S. & N. PACIFIC	227-249	X	X	X	X	X	X
BEAUFORT SEA	251-255	X	X				
BEAUFORT SEA	259-258	X	X				
BEAUFORT SEA	263-262	X	X				
ARCTIC SECTION	251-295	X	X				
BARROW STRAIT	285-289	X	X				
DAVIS STRAIT	295-301	X	X				

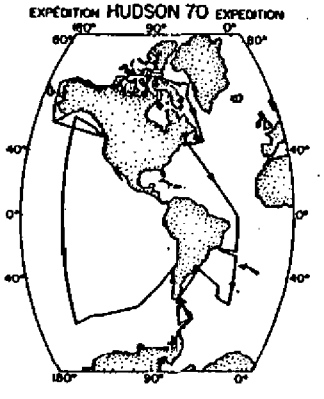
A summary indicating the sections for which data was collected and is presented in this publication

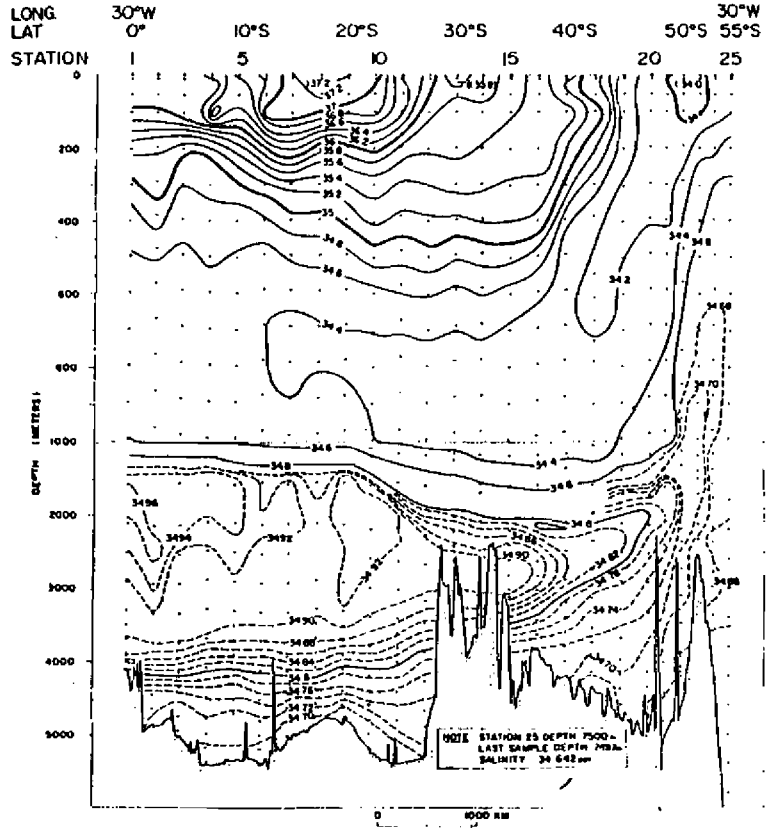

80°W
70°
60°
50°
40°
30°
20°
10°
10°N
0°
10°
20°
30°
40°
50°
60°S
SOUTH AMERICA
RIO DE JANEIRO
BUENOS AIRES
PUNTA ARENAS
PUERTO WILLIAMS
200 m
5000 m
1
2
3
4
5
6
7
8
9
10
11
12
13
14
15
16
17
18
19
20
21
22
23
24
25
26
27
28
29
30


EXPÉDITION HUDSON 70 EXPEDITION

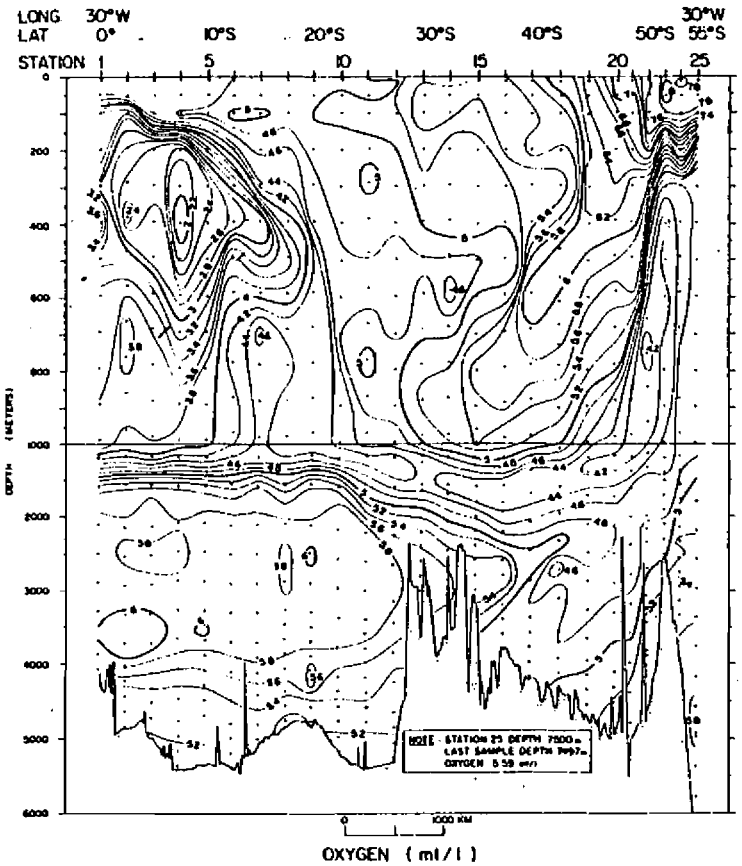


TEMPERATURE (°C)

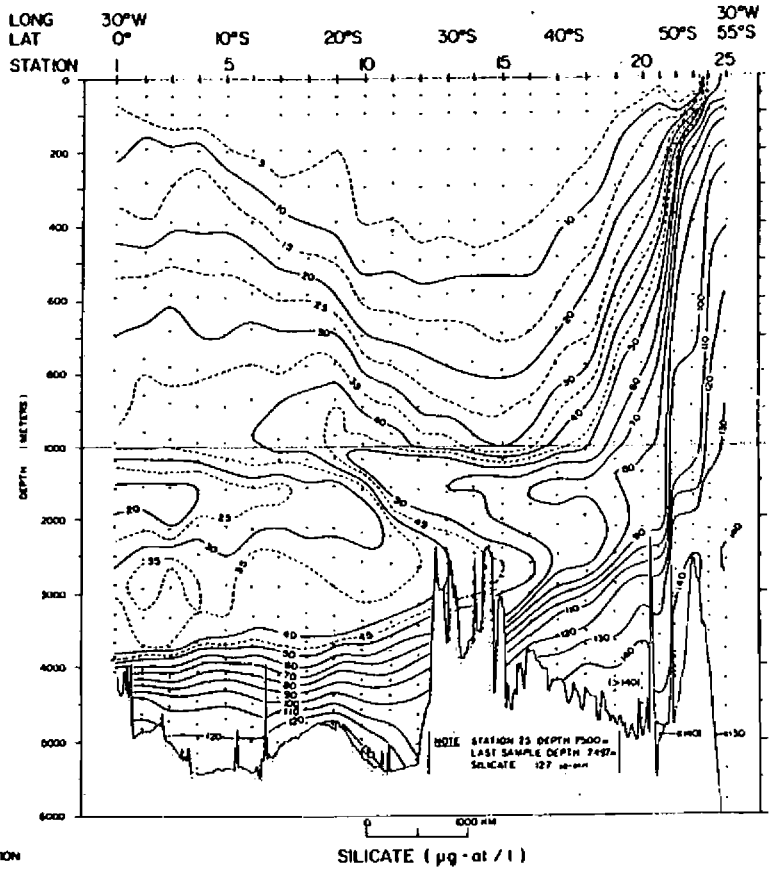




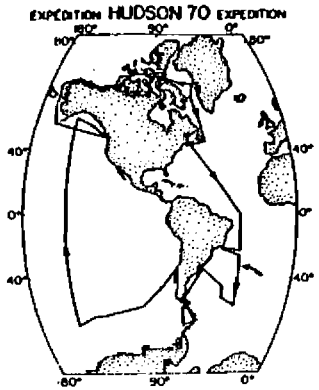
SALINITY (ppt)

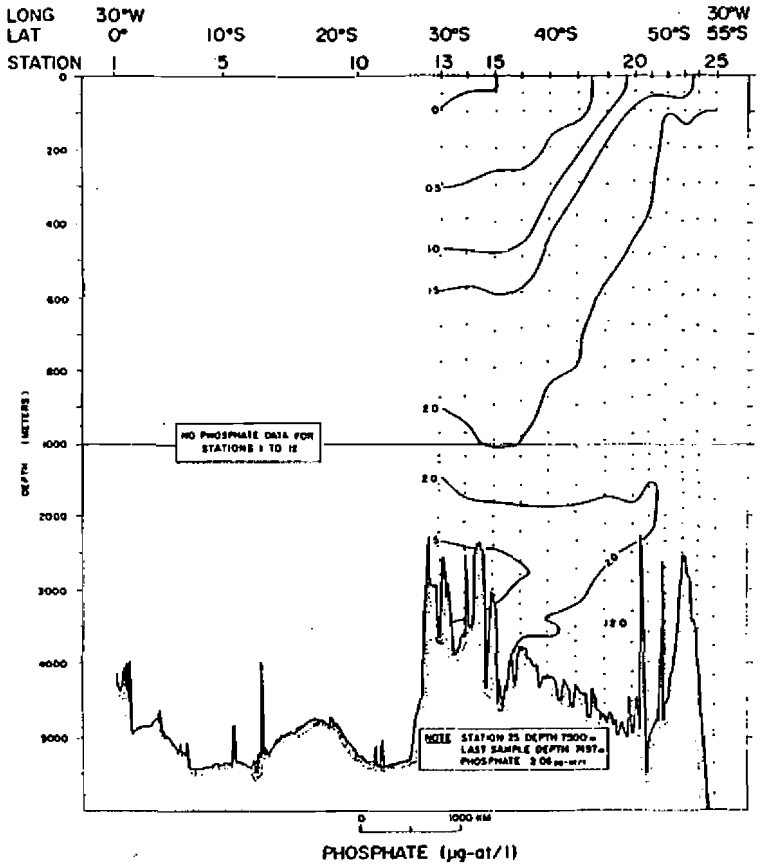


OXYGEN (ml / l)

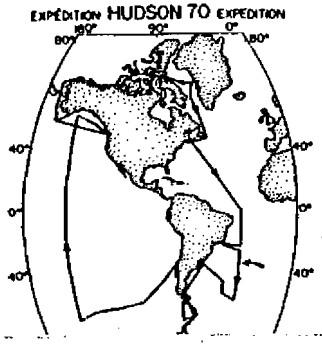


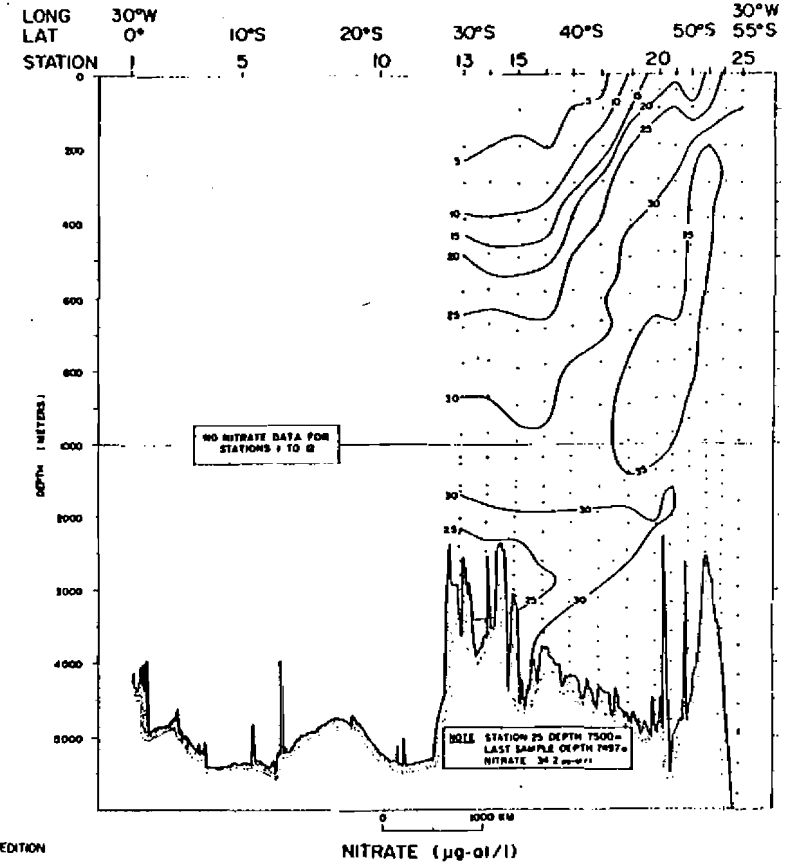
SILICATE (µg - at / l)



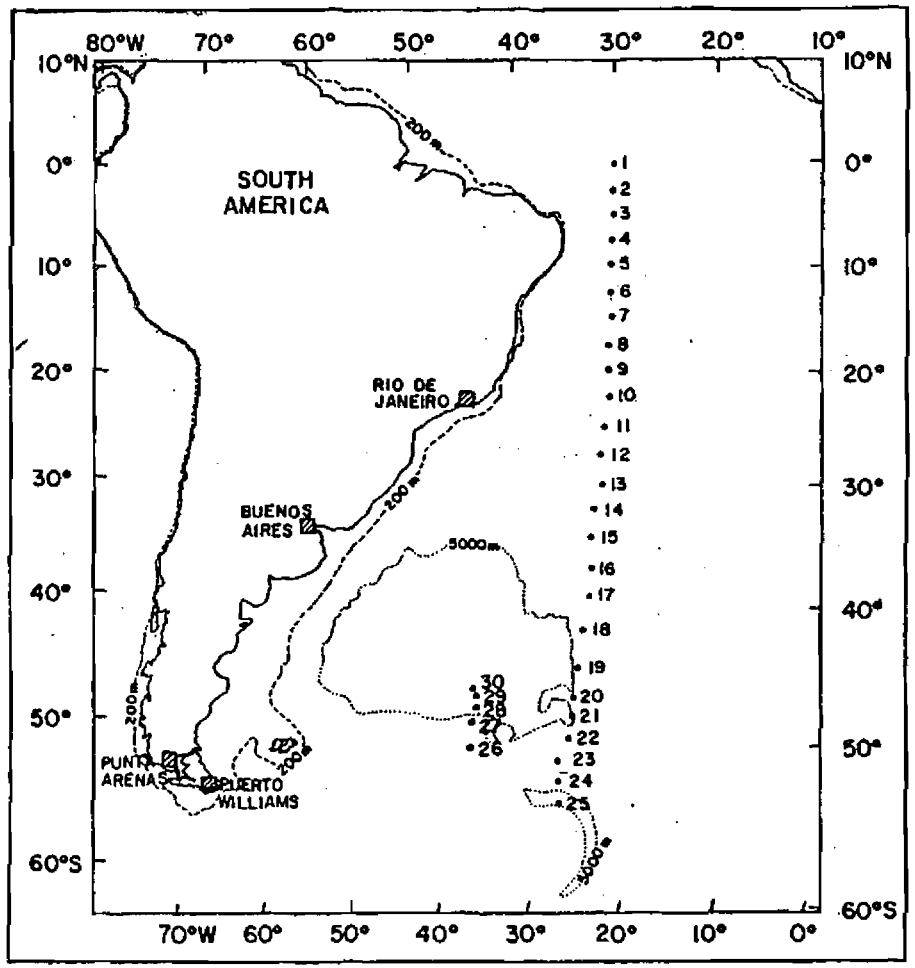


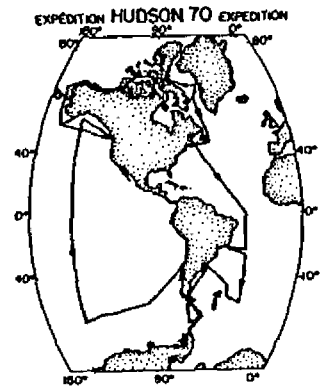
PHOSPHATE (µg-at/l)

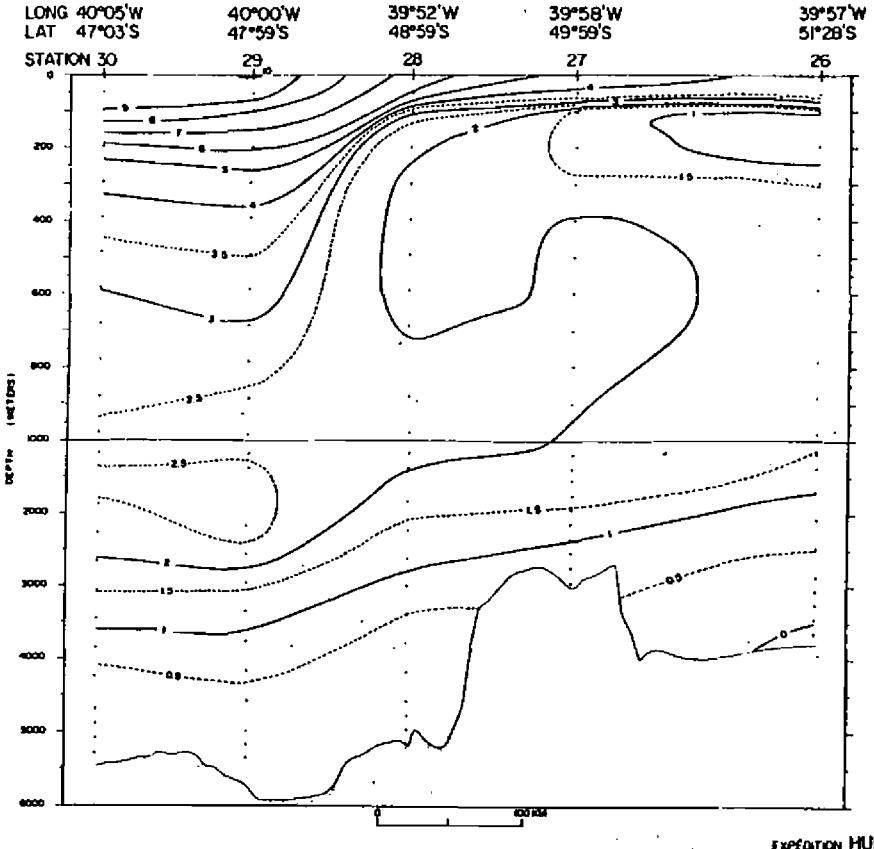




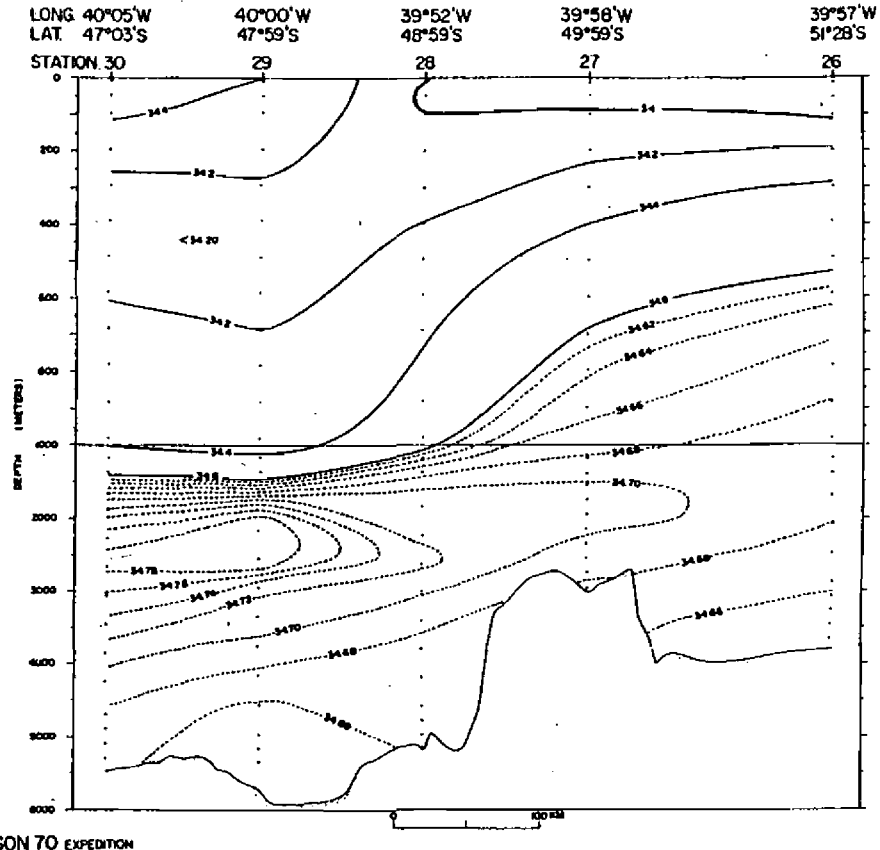
NITRATE (µg-at/l)


80°W
70°
60°
50°
40°
30°
20°
10°
10°N
0°
10°
20°
30°
40°
50°
60°S
SOUTH AMERICA
RIO DE JANEIRO
BUENOS AIRES
PUNTA ARENAS
PUERTO WILLIAMS
200 m
5000 m
1
2
3
4
5
6
7
8
9
10
11
12
13
14
15
16
17
18
19
20
21
22
23
24
25
26
27
28
29
30

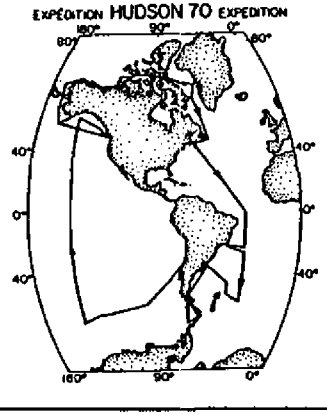

EXPEDITION HUDSON 70 EXPEDITION

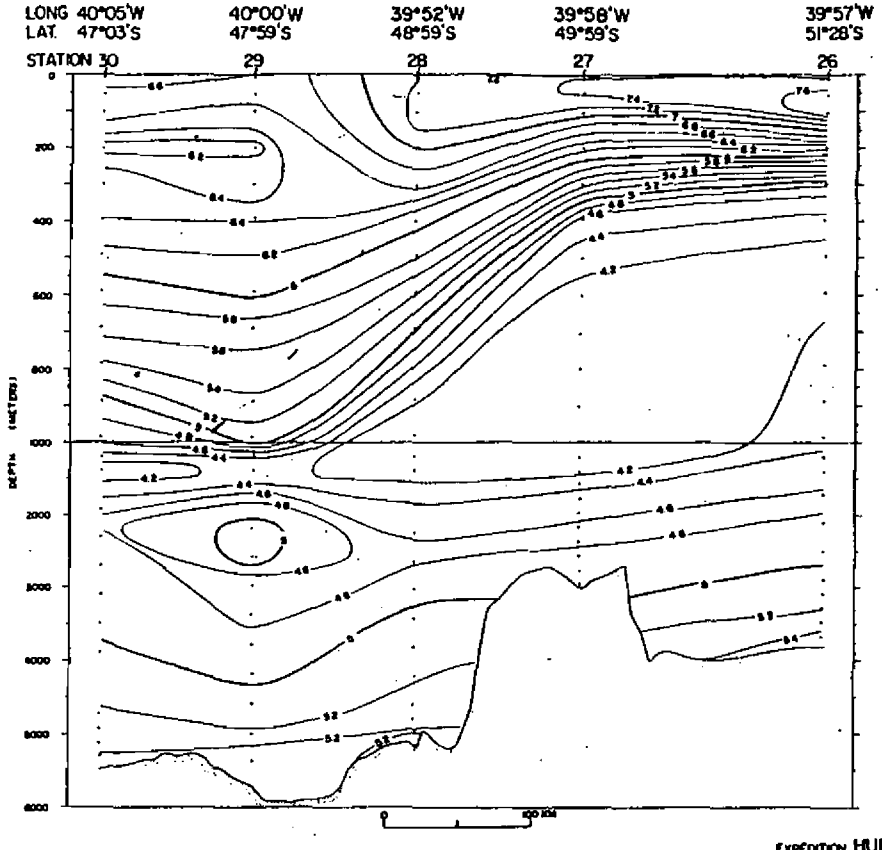


TEMPERATURE (°C)

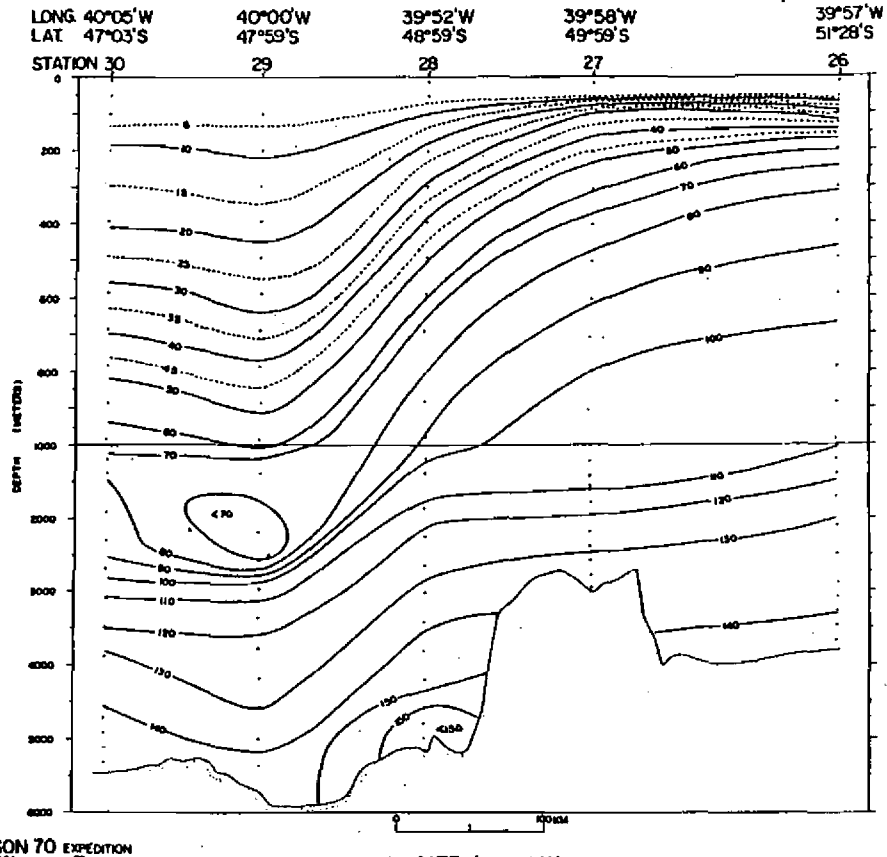


SALINITY (ppt)

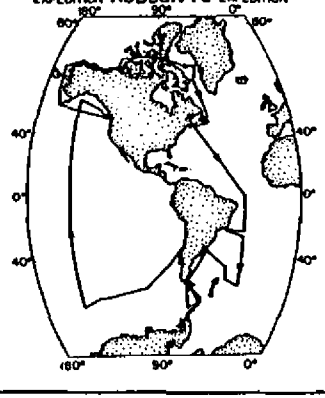


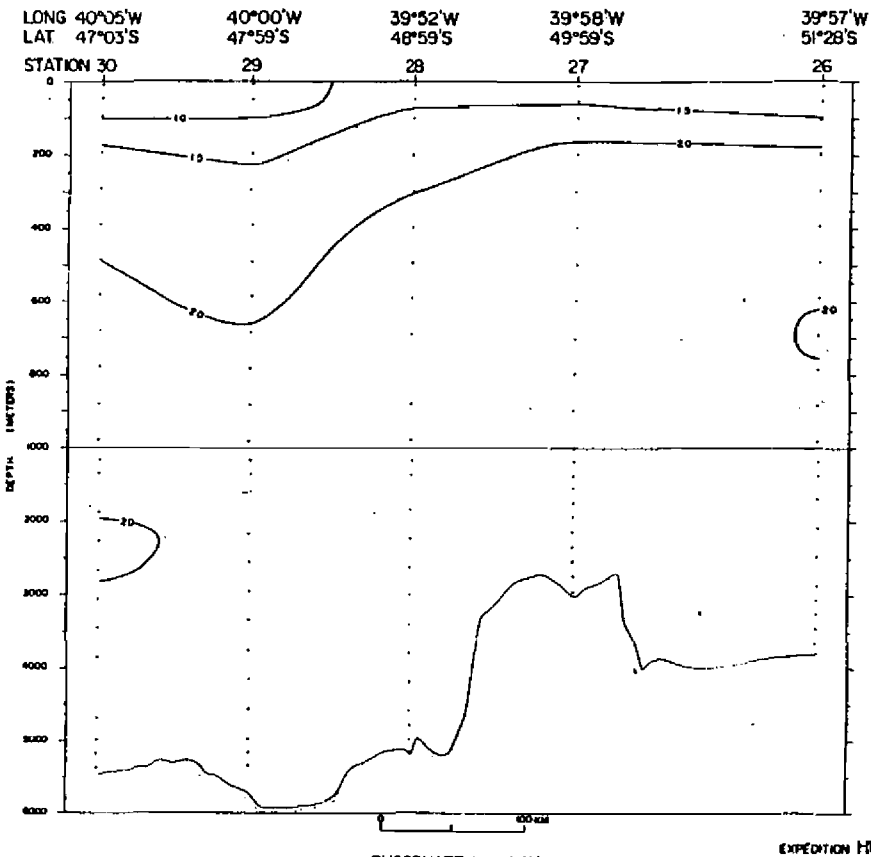


OXYGEN (ml/l)

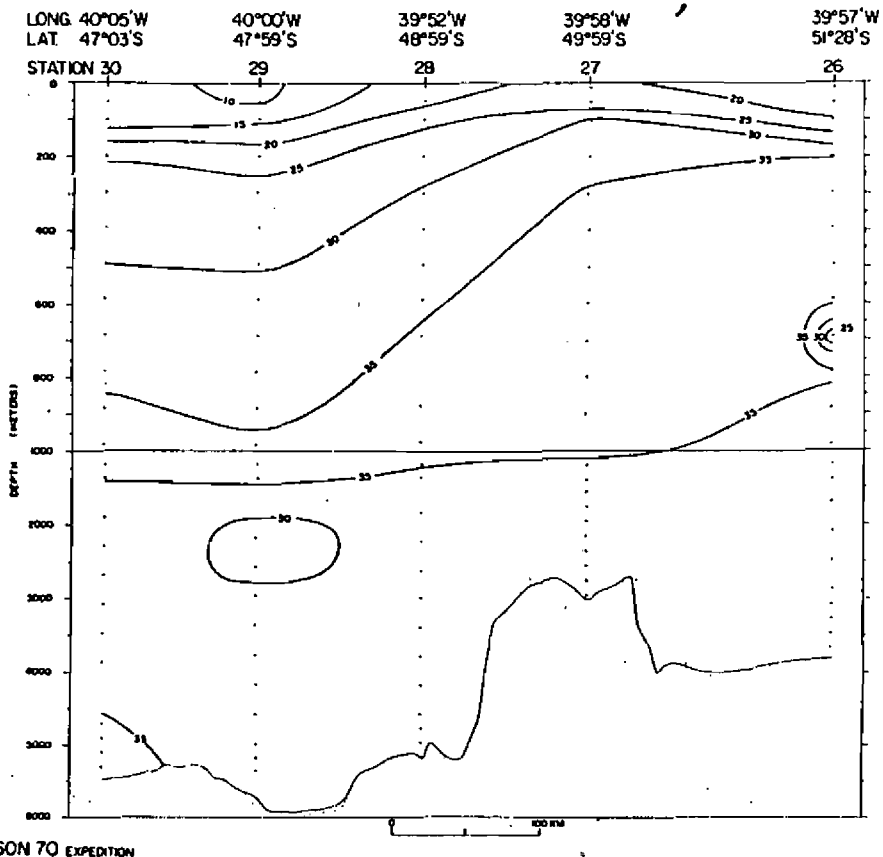


SILICATE (µg-at/l)

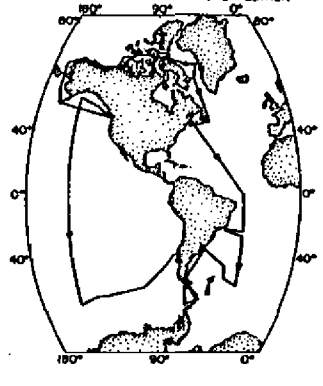


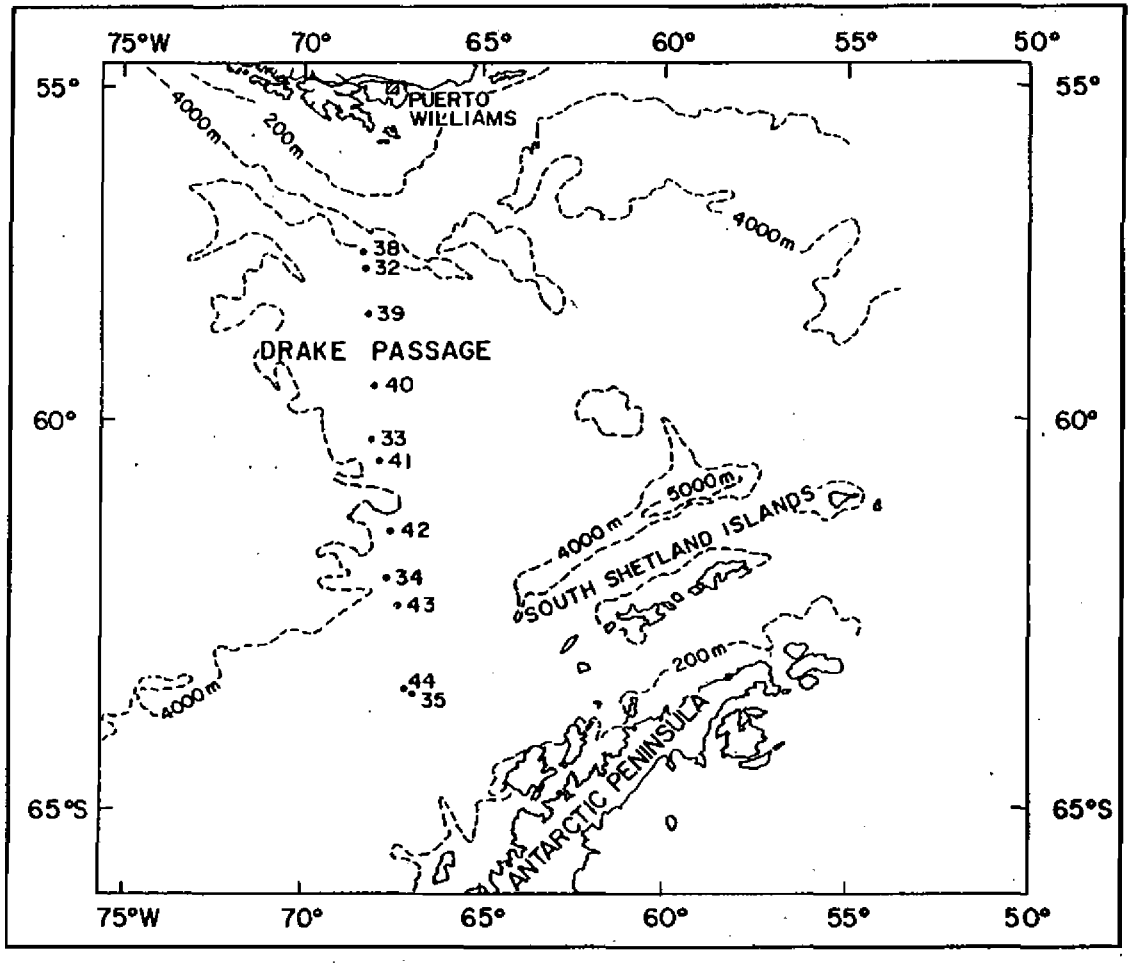


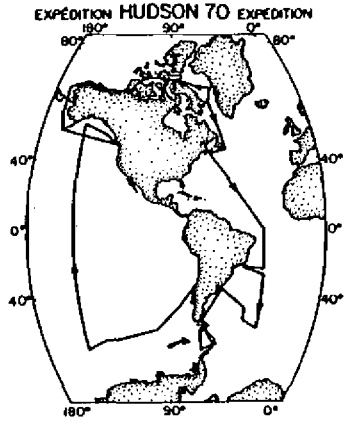
PHOSPHATE (µg-at/l)

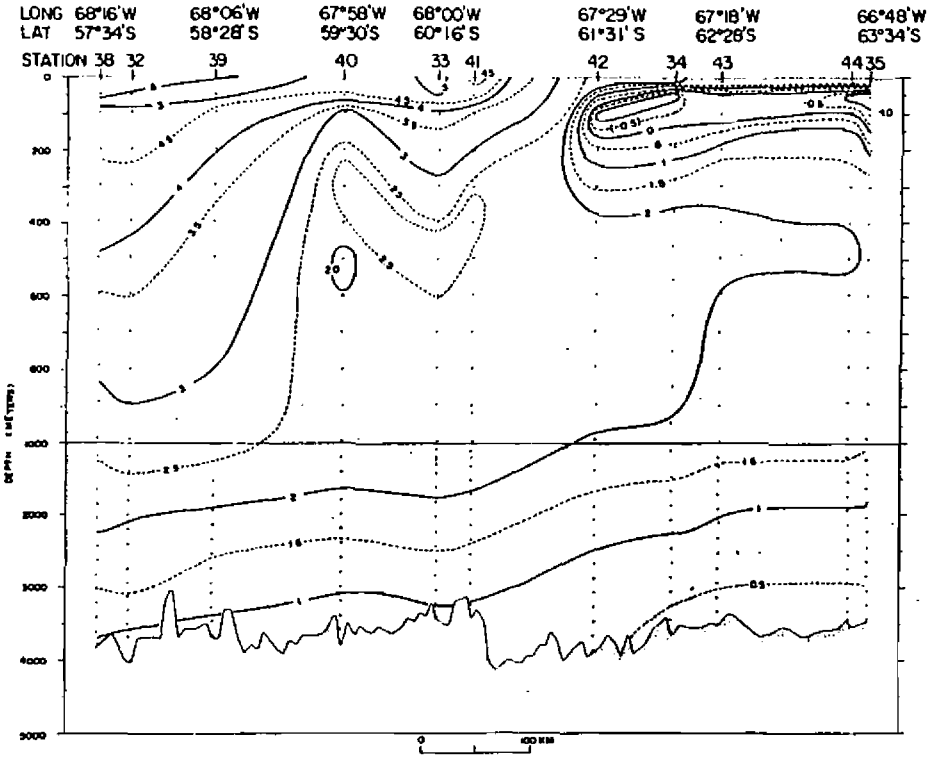


NITRATE (µg-at/l)

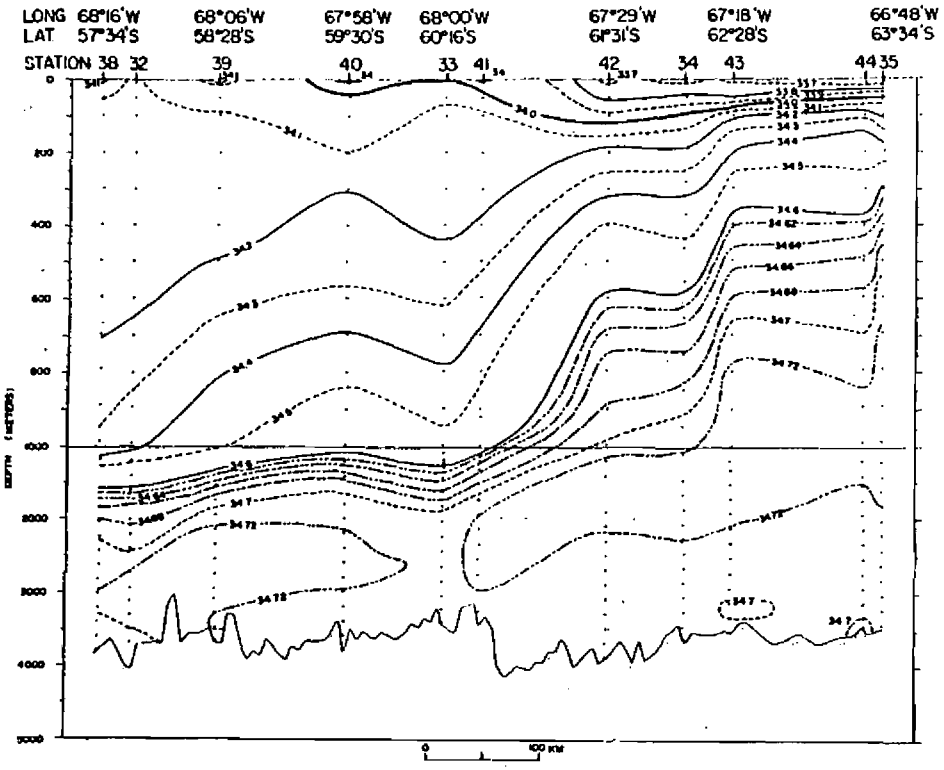



75°W
70°
65°
60°
55°
50°
55°
60°
65°S
PUERTO WILLIAMS
4000m
200m
4000m
38
32
39
DRAKE PASSAGE
40
33
41
42
34
43
44
35
4000m
4000m
5000m
SOUTH SHETLAND ISLANDS
200m
ANTARCTIC PENINSULA

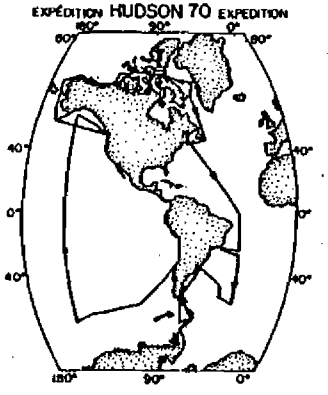

EXPÉDITION HUDSON 70 EXPEDITION
180°
90°
0°
80°
80°
40°
40°
0°
0°
40°
40°
180°
90°
0°

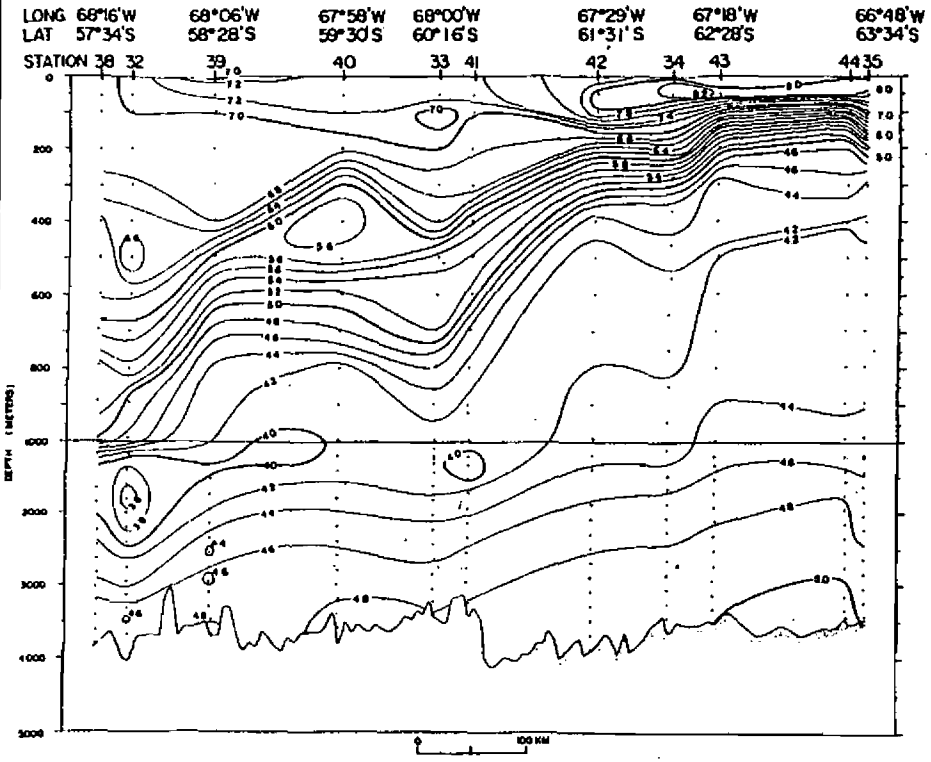


TEMPERATURE (°C)

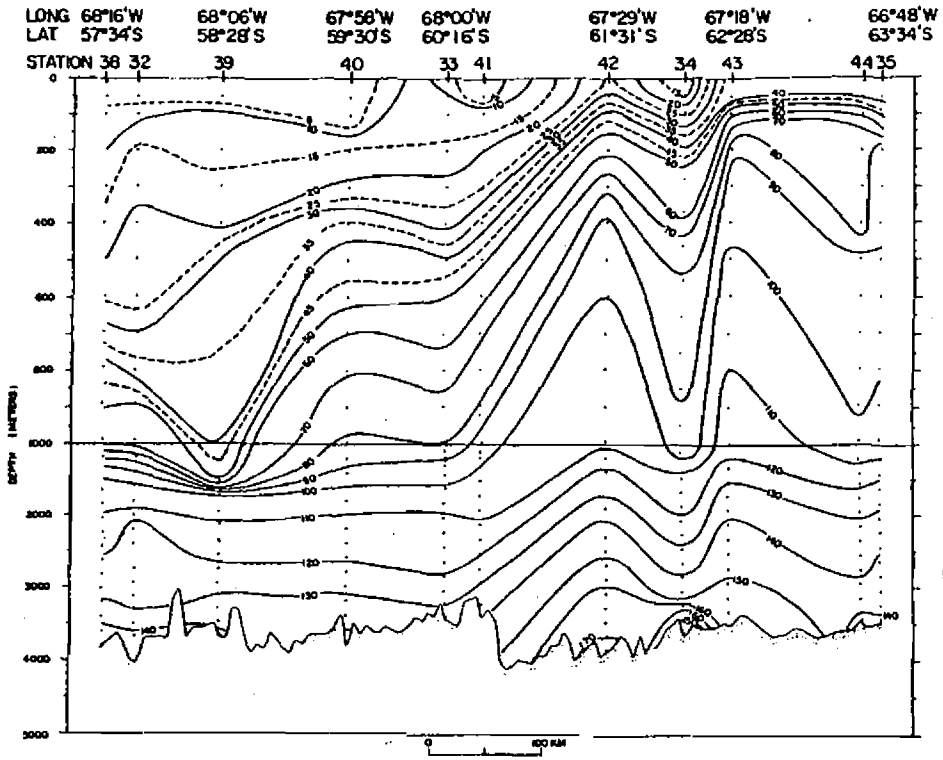


SALINITY (ppt)

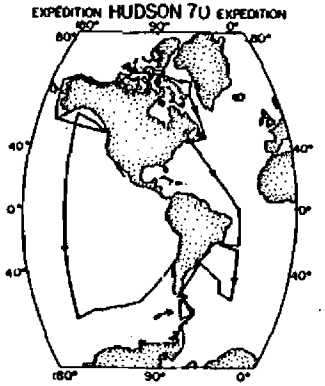


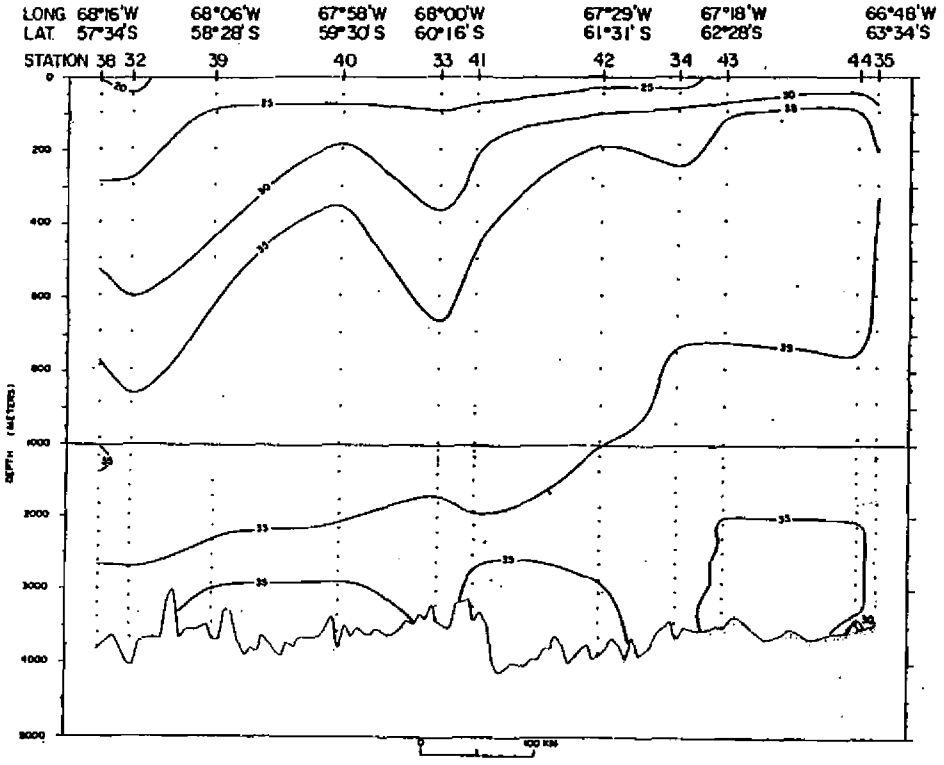


OXYGEN (ml/l)

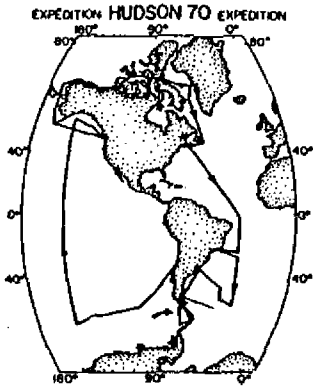


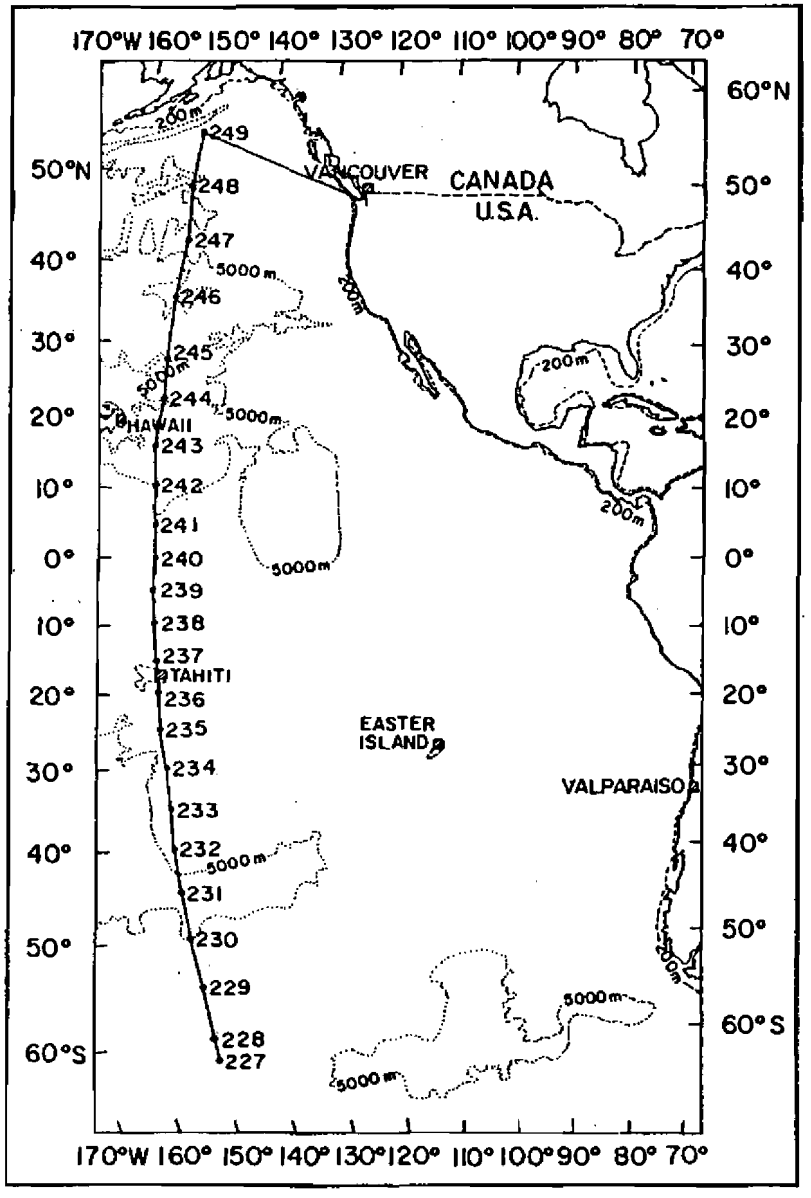
SILICATE (µg-at/l)

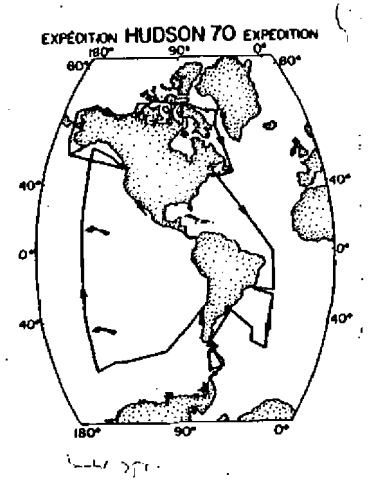


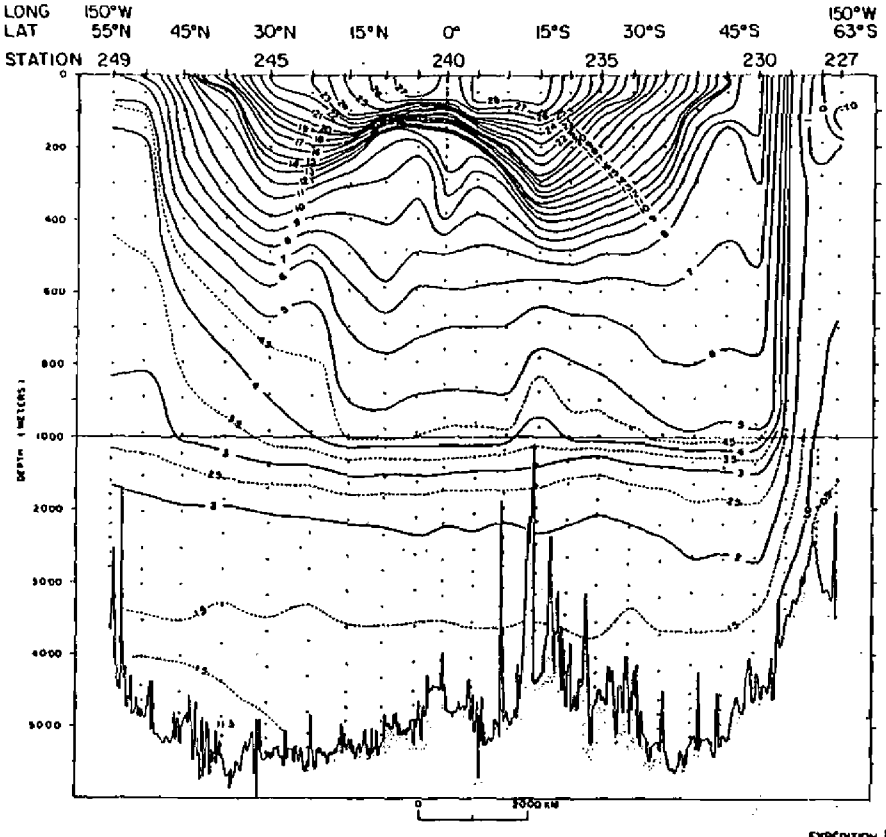


NITRATE (µg-at/l)

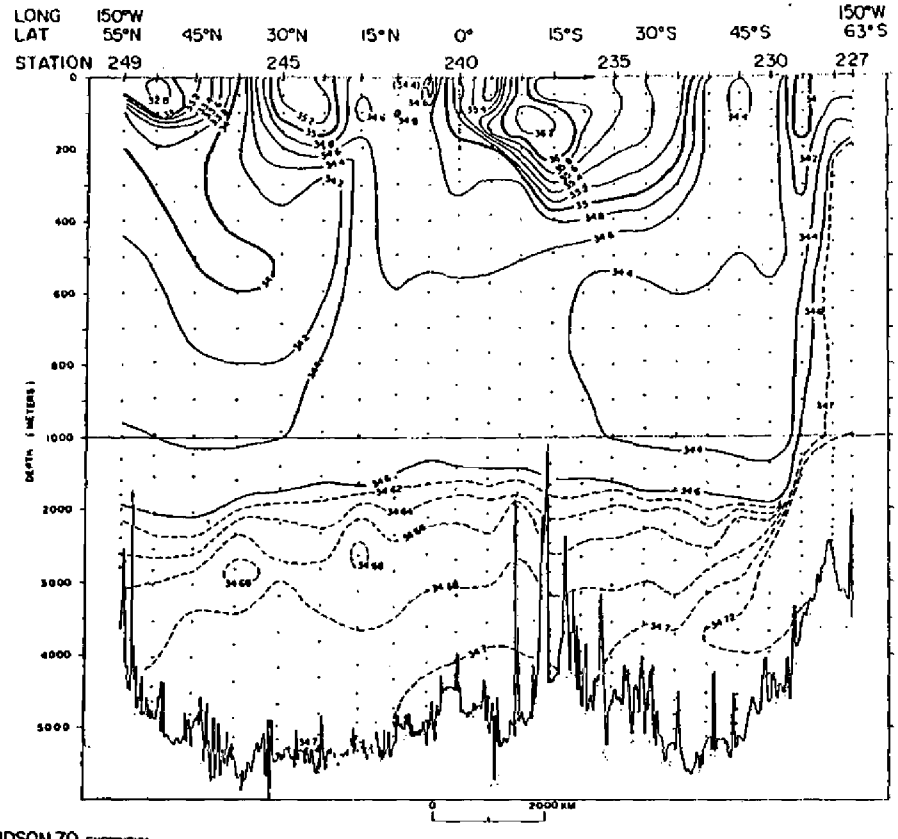



170°W 160° 150° 140° 130° 120° 110° 100° 90° 80° 70°
60°N
50°N
40°
30°
20°
10°
0°
10°
20°
30°
40°
50°
60°S
200m
5000m
249
248
247
246
245
244
243
242
241
240
239
238
237
236
235
234
233
232
231
230
229
228
227
VANCOUVER
CANADA
U.S.A.
HAWAII
TAHITI
EASTER ISLAND
VALPARAISO

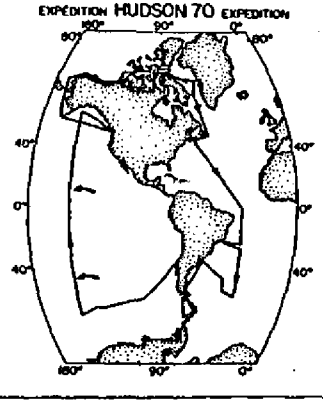

EXPEDITION HUDSON 70 EXPEDITION
180°
90°
0°
60°
40°
0°
40°

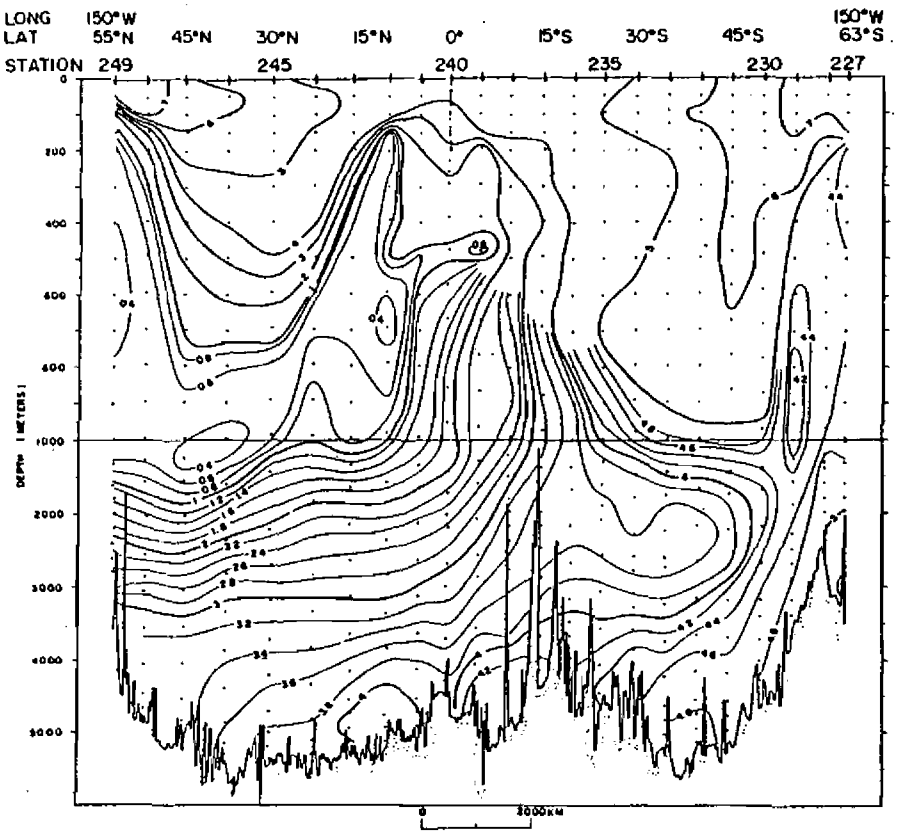


TEMPERATURE (°C)

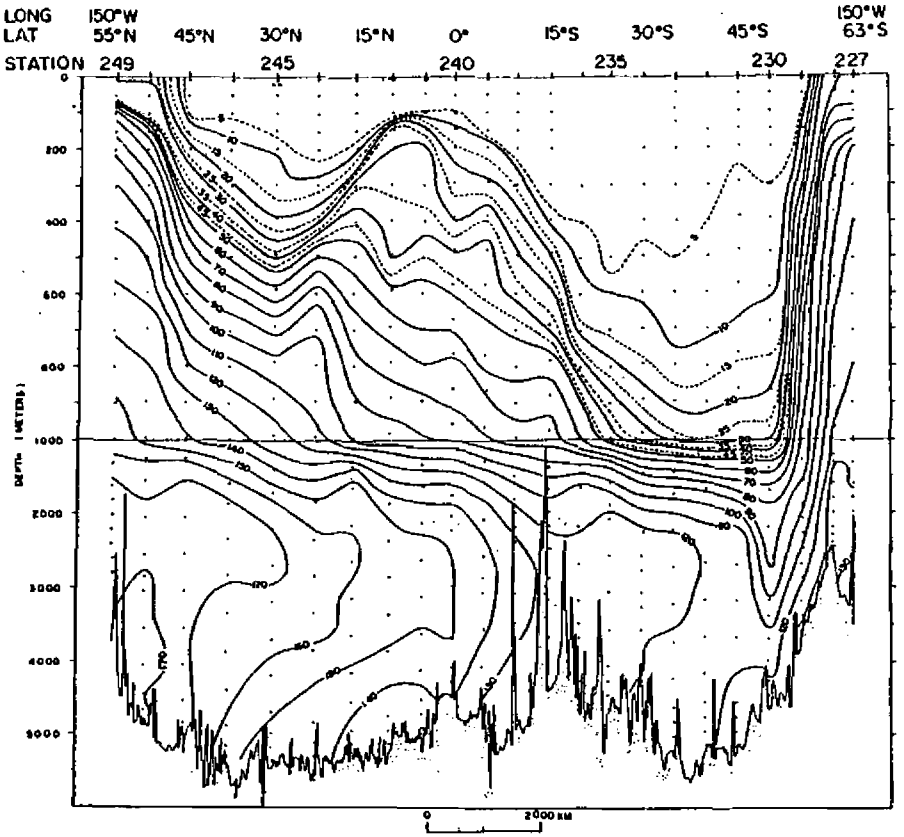


SALINITY (ppt)

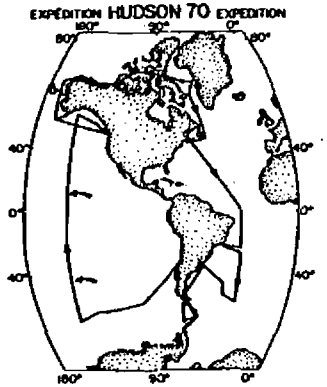


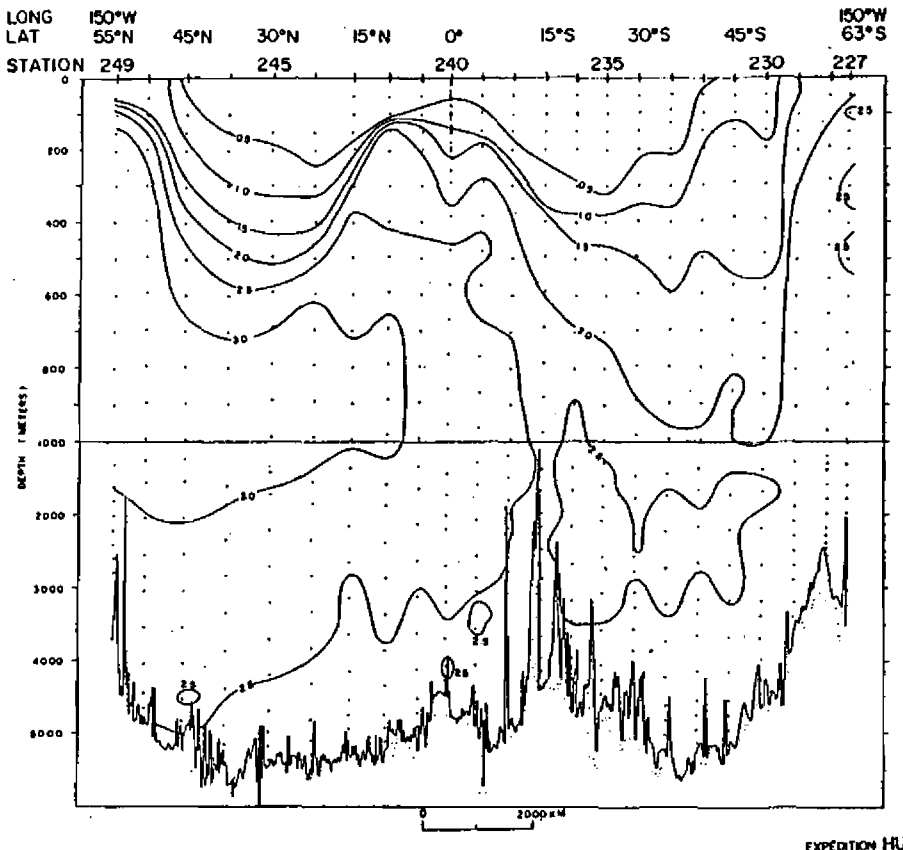


OXYGEN (ml / l)

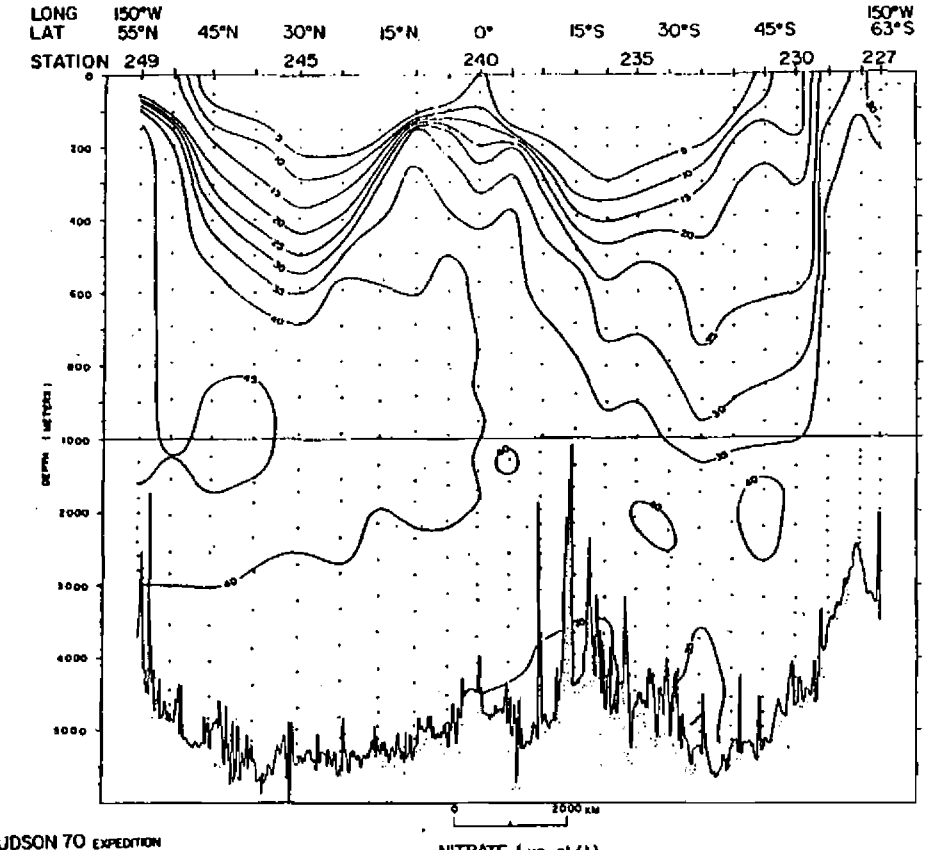


SILICATE (µg-at/l)

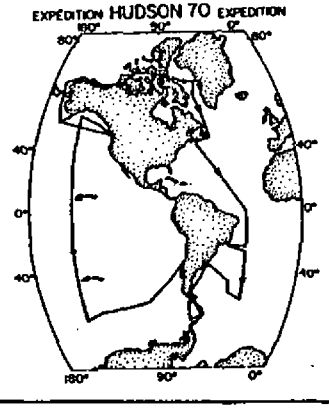


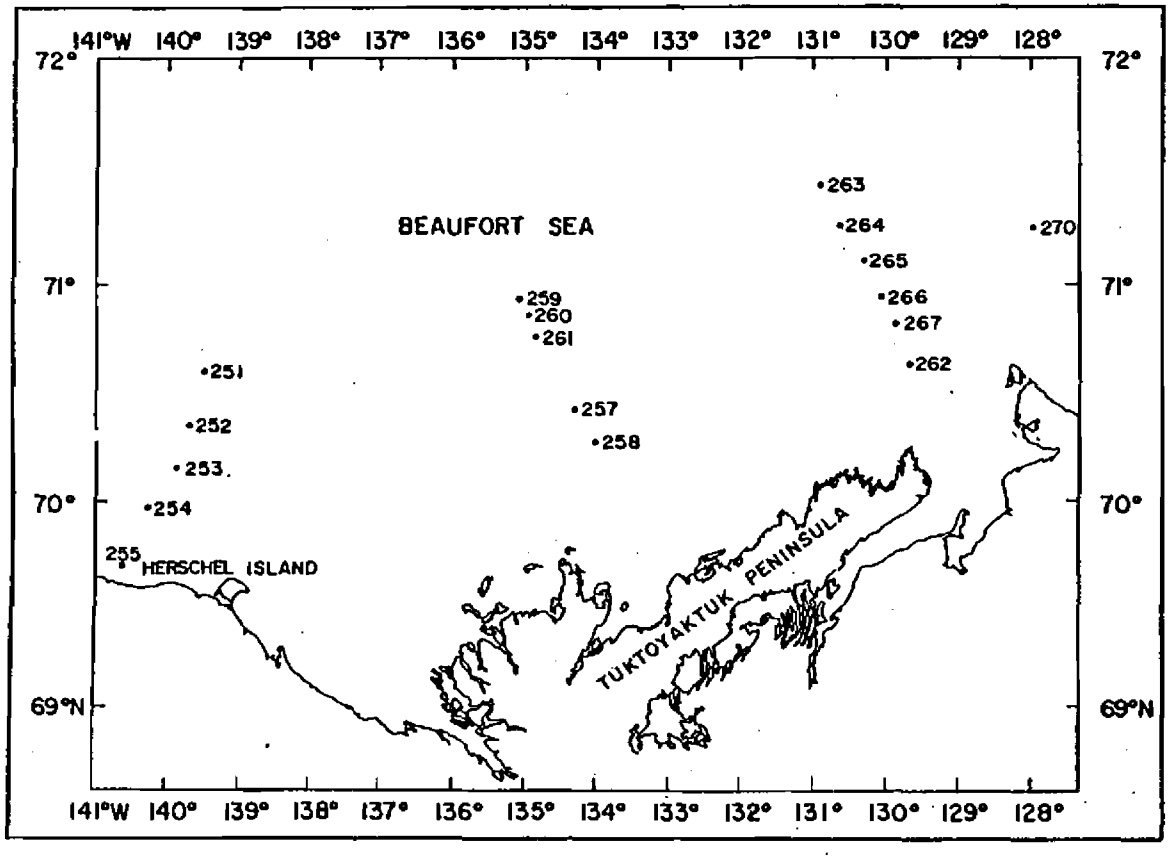


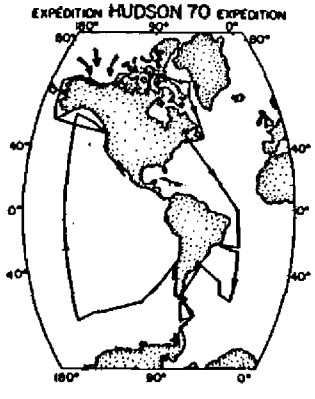
PHOSPHATE (µg-at/l)

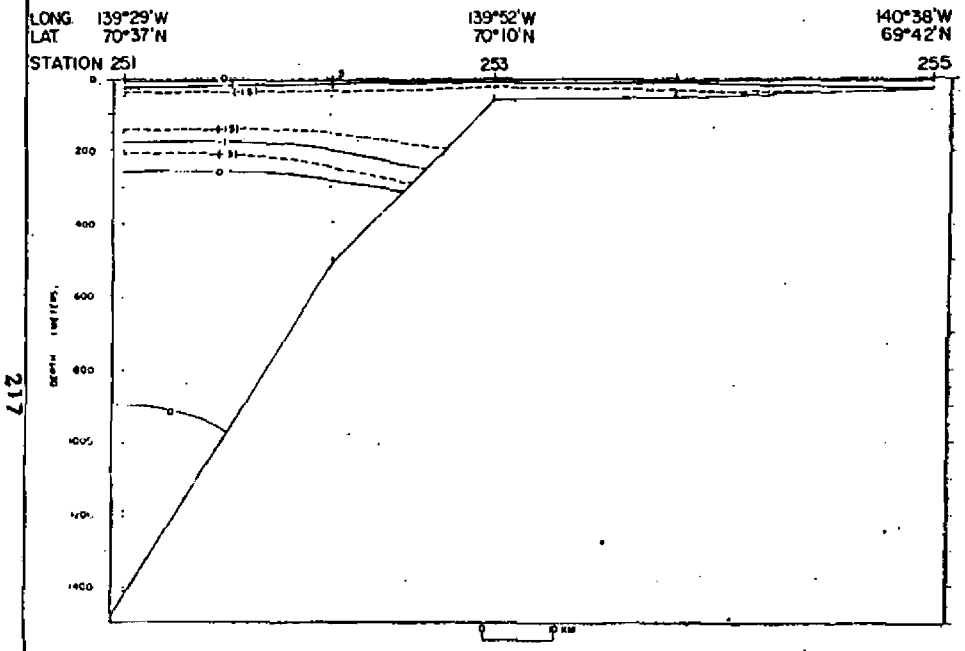


NITRATE (µg-at/l)

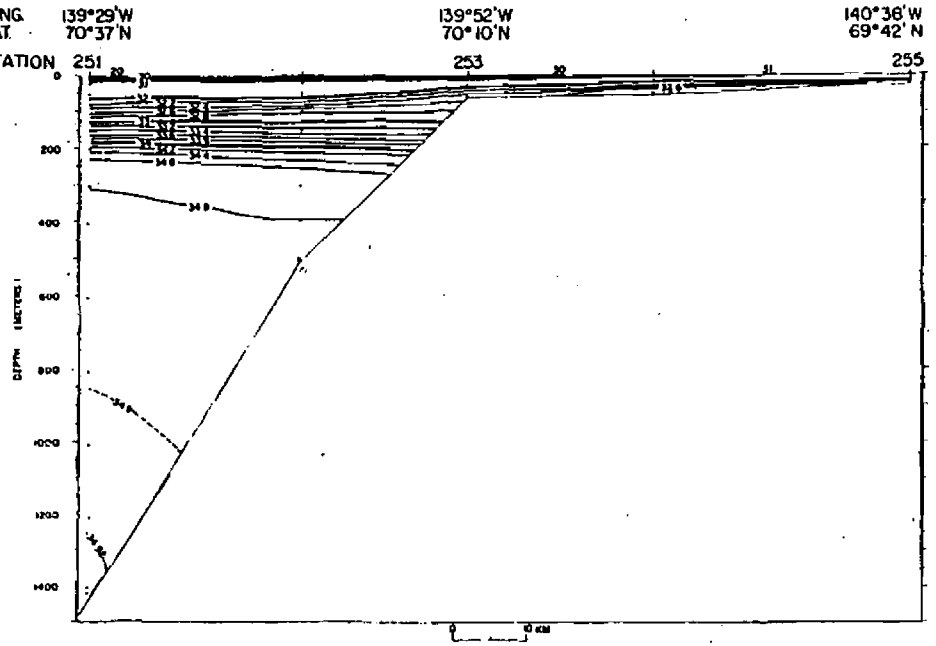



141°W 140° 139° 138° 137° 136° 135° 134° 133° 132° 131° 130° 129° 128°
72°
71°
70°
69°N
BEAUFORT SEA
•251
•252
•253
•254
255
HERSCHEL ISLAND
•257
•258
•259
•260
•261
•262
•263
•264
•265
•266
•267
•270
TUKTOYAKTUK PENINSULA

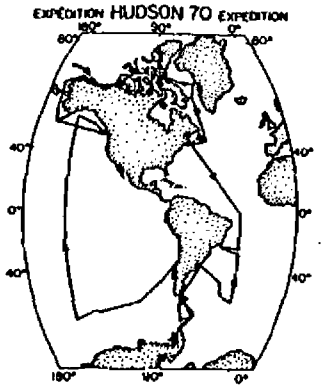

EXPÉDITION HUDSON 70 EXPEDITION

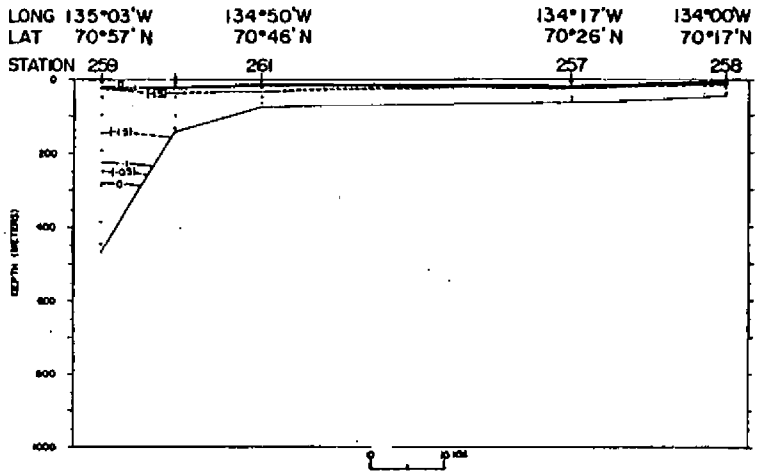


TEMPERATURE (°C)

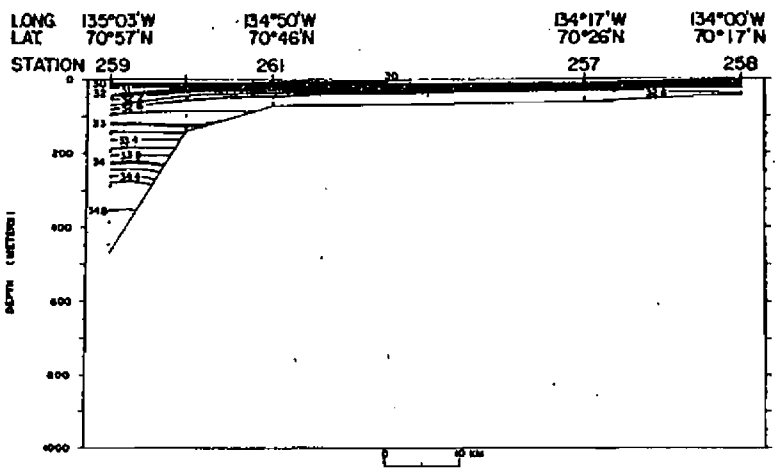


SALINITY (ppt)

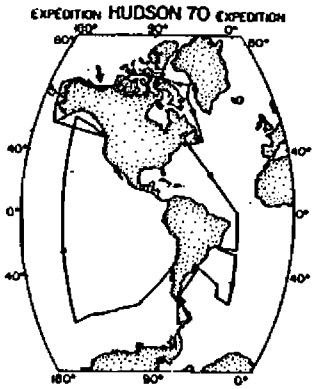


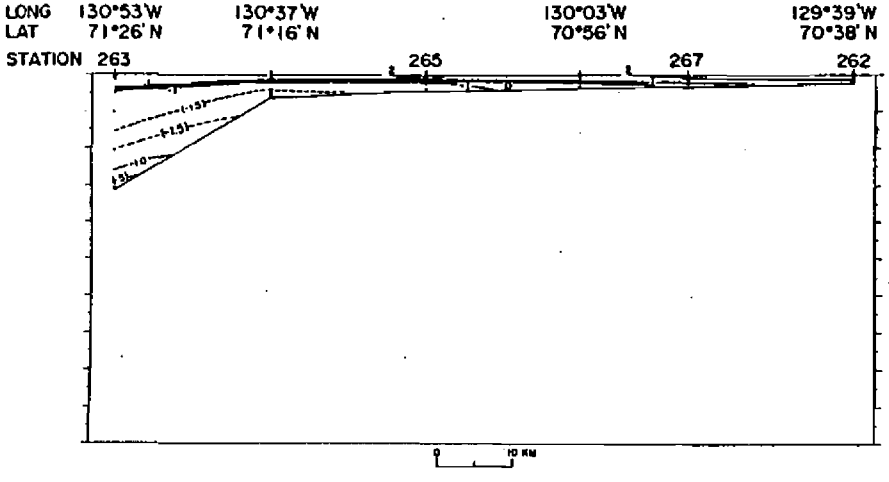


TEMPERATURE (°C)

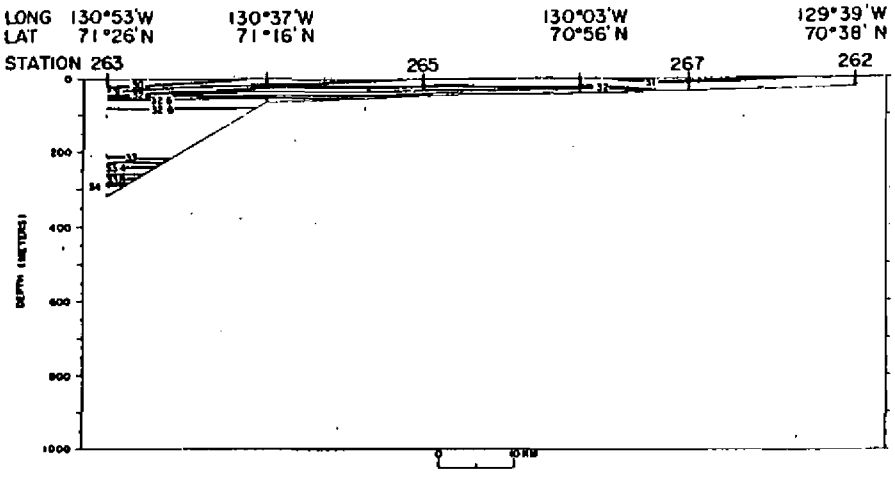


SALINITY (ppt)

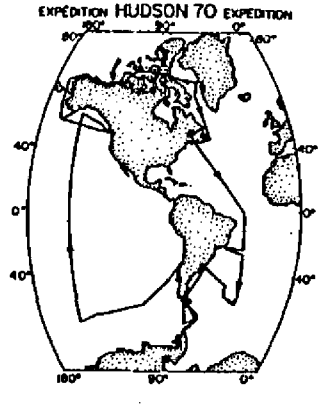


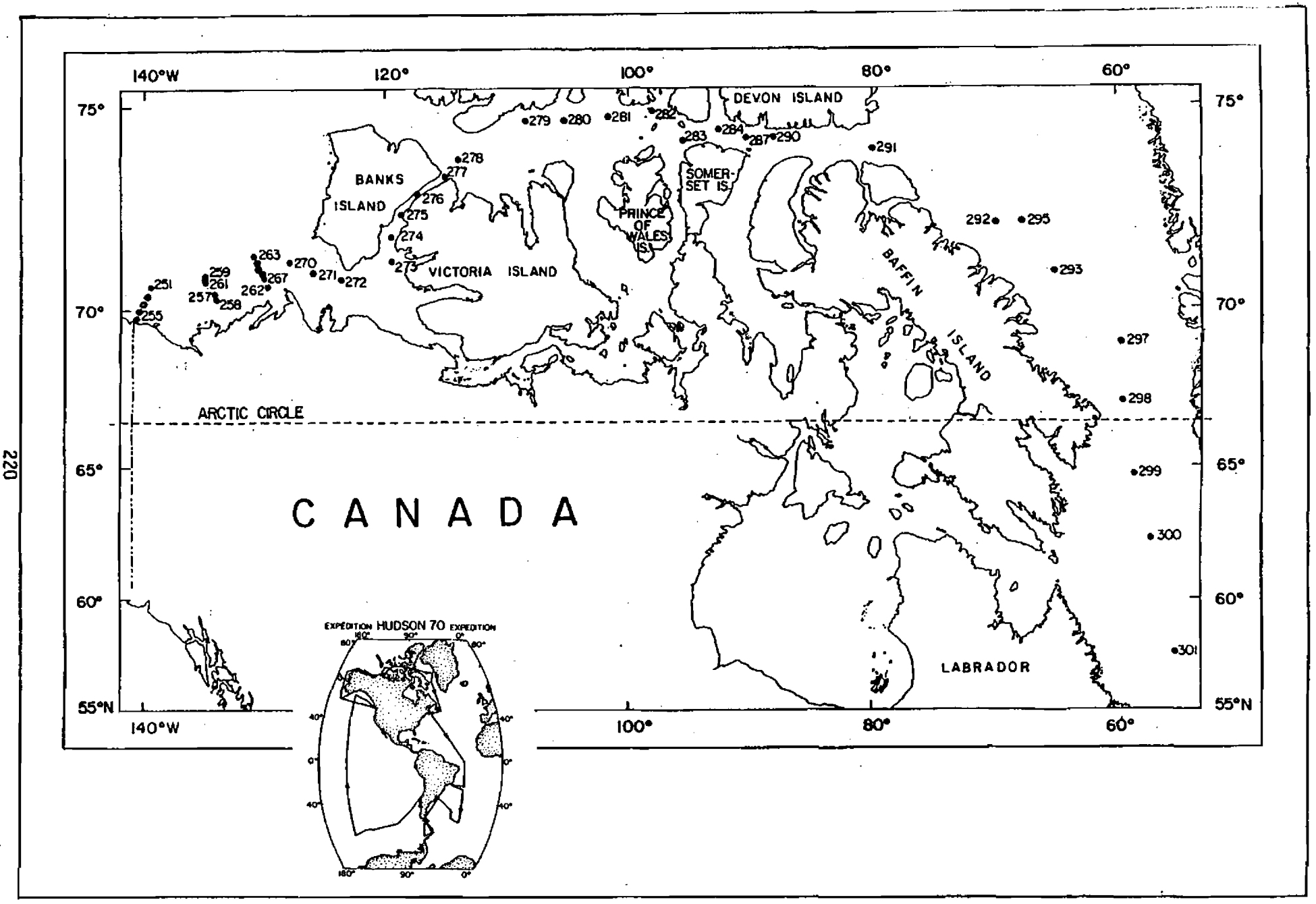


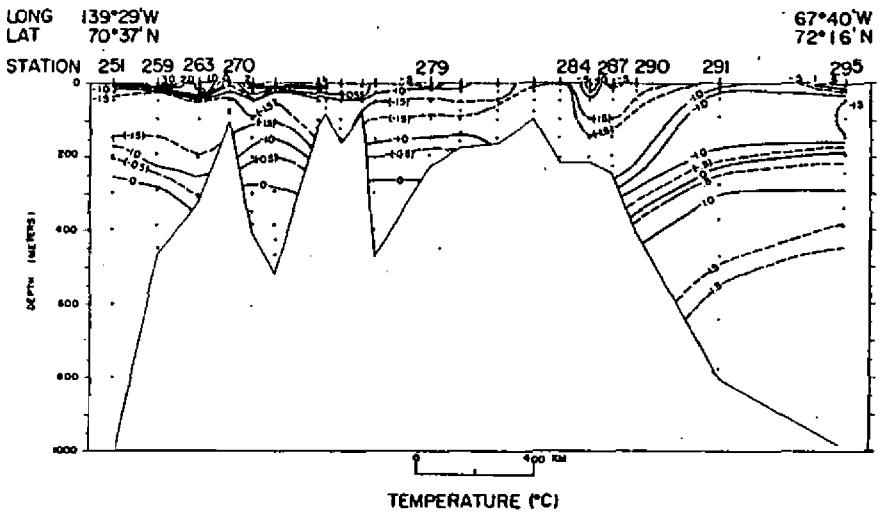
TEMPERATURE (°C)



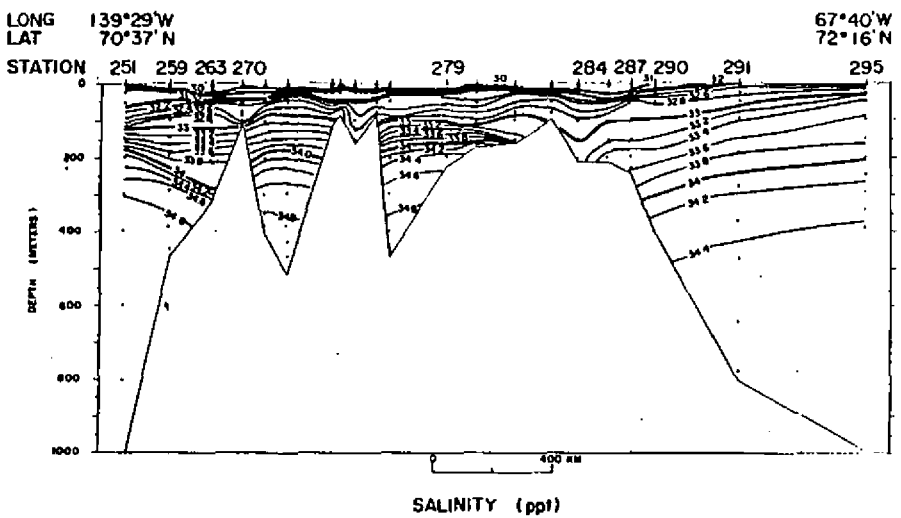
SALINITY (ppt)



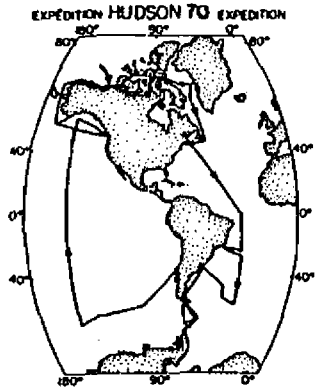

140°W
120°
100°
80°
60°
75°
70°
65°
60°
55°N
DEVON ISLAND
BANKS ISLAND
SOMER-SET IS.
PRINCE OF WALES IS.
VICTORIA ISLAND
BAFFIN ISLAND
ARCTIC CIRCLE
CANADA
LABRADOR
251
255
257
258
259
261
262
263
267
270
271
272
273
274
275
276
277
278
279
280
281
282
283
284
287
290
291
292
293
295
297
298
299
300
301
EXPEDITION HUDSON 70 EXPEDITION

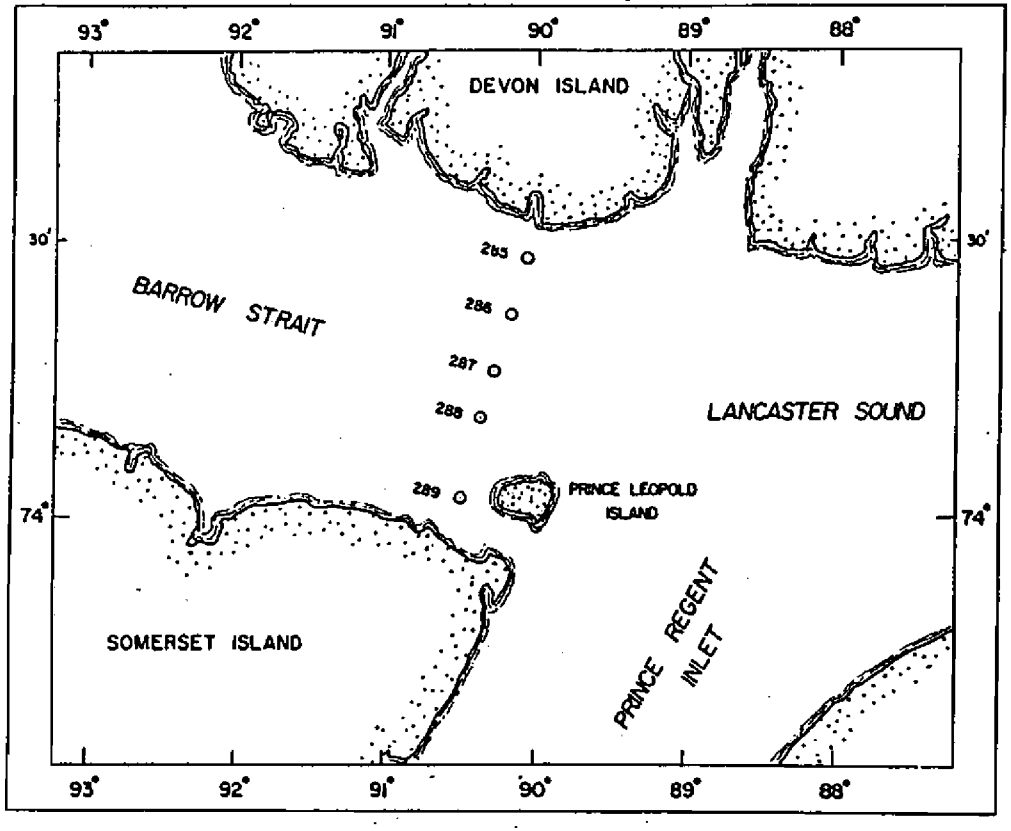


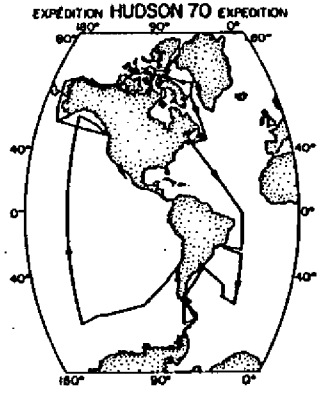
TEMPERATURE (°C)

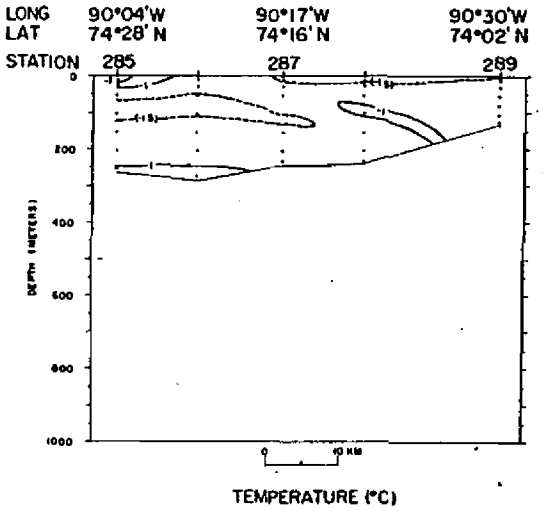


SALINITY (ppt)

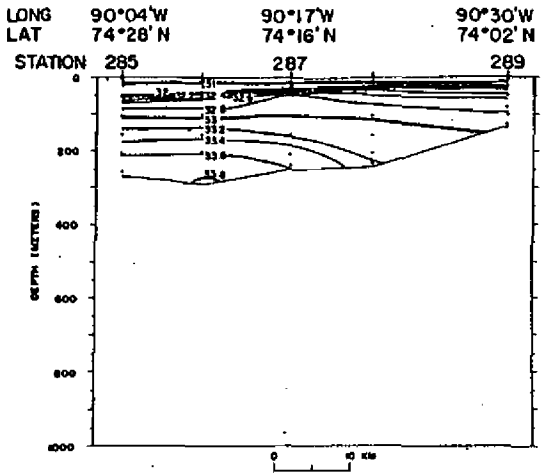



93°
92°
91°
90°
89°
88°
DEVON ISLAND
30'
BARROW STRAIT
285
286
287
288
LANCASTER SOUND
289
PRINCE LEOPOLD ISLAND
74°
SOMERSET ISLAND
PRINCE REGENT INLET

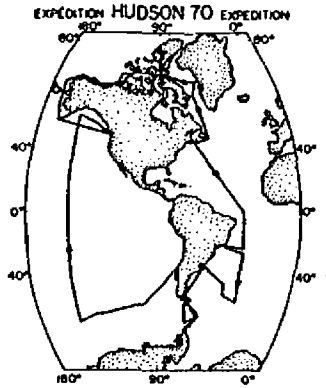

EXPÉDITION HUDSON 70 EXPEDITION

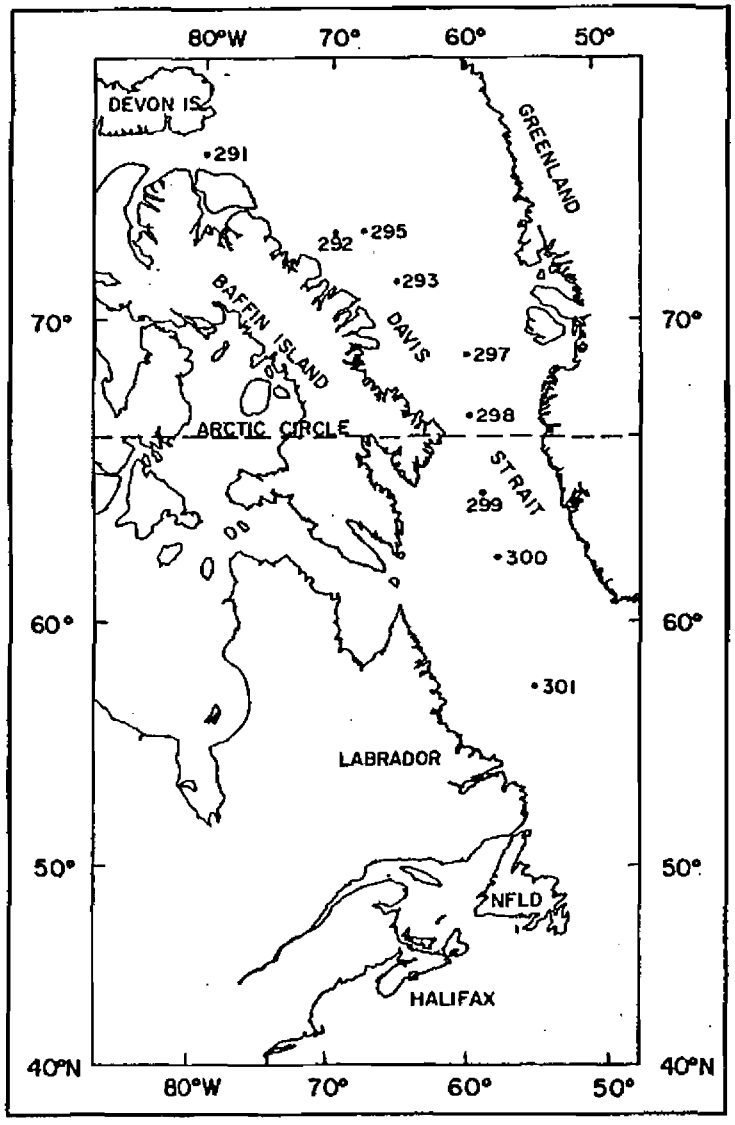


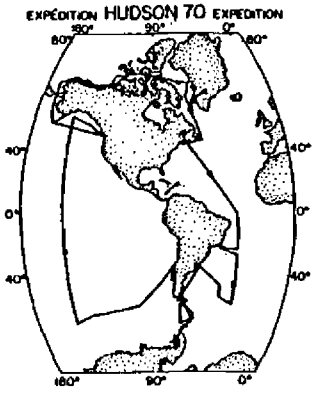
TEMPERATURE (°C)

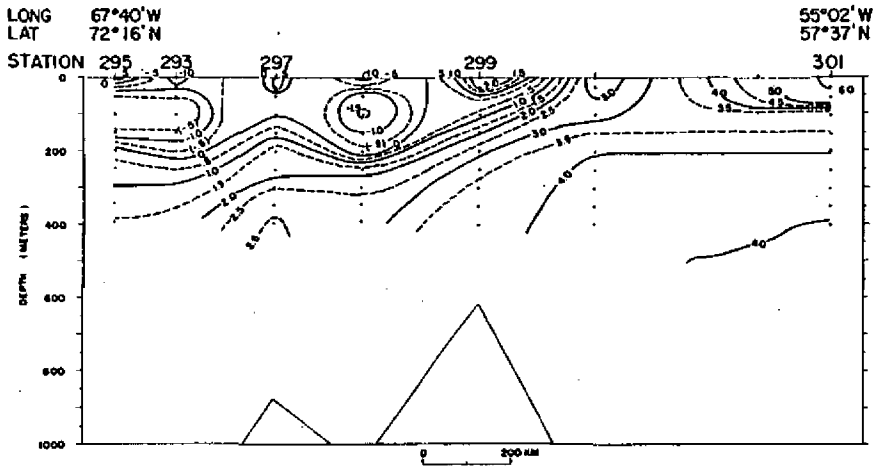


SALINITY (ppt)

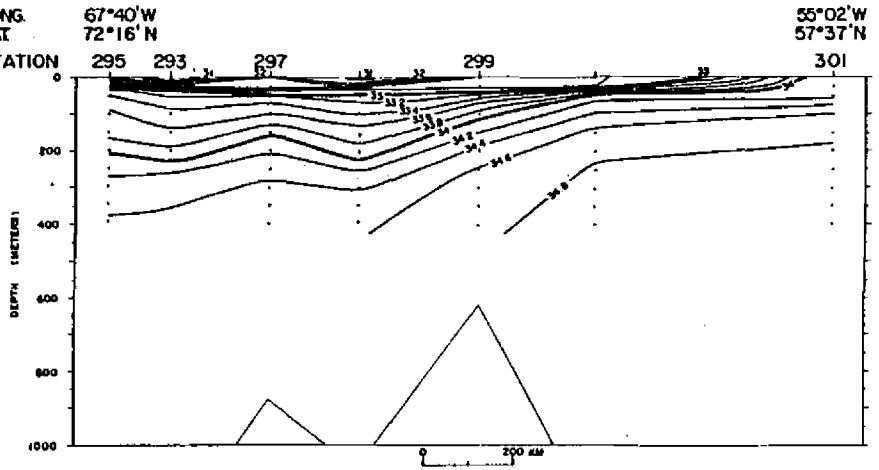



80°W
70°
60°
50°
DEVON IS.
•291
292
•295
•293
GREENLAND
BAFFIN ISLAND
DAVIS
•297
70°
ARCTIC CIRCLE
•298
STRAIT
299
•300
60°
•301
LABRADOR
50°
NFLD
HALIFAX
40°N

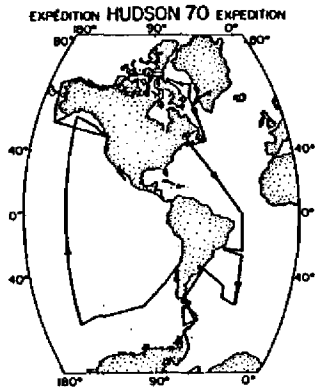

EXPÉDITION HUDSON 70 EXPEDITION



TEMPERATURE (°C)



SALINITY (ppt)



CURRENT METER DATA

CURRENTS

The currents were measured using the film recording Braincon model 316 and 381 current meters. The instruments recorded one exposure every 20 minutes. The film was read manually, and transferred to computer compatible magnetic tape. All graphs were computer produced and plotted on an incremental plotter.

The accuracy of the measurements are (a) current speed ±5 cm/sec for the deeper meters, (b) current direction ±15° which includes the error due to the variation found in the compass swings before and after deployment.

DATA PRESENTATION

For each current meter record, the data are presented on a single page in the form of:

(1) statistical summary and joint distribution table
(2) time series plot, rate and direction
(3) progressive vector plot
(4) stick plot

and for ease of relating the data from the four moorings, the east-west and north-south components of each current meter are displayed together on a separate page, in time series.

STATISTICAL SUMMARY AND JOINT DISTRIBUTION

Statistics - The statistical parameters for each current meter are calculated from the raw data (20 minute sampling interval) and are expressed as U (positive east) and V (positive north). The minimum, maximum, and mean are common measures of the location of a distribution. The standard deviation and variance give an indication of the spread of a distribution. For normal or moderately skewed distributions approximately 68% of the observations will fall within one standard deviation, 95.5% will be within two standard deviations, and better than 99.5% of the observations will lie within three standard deviations from the mean. The trend and intercept are determined by fitting the data to an equation of the form (mt + b) using a linear regression. The trend is simply the slope of the best fit line, the intercept is evaluated for the first sample and time in units of seconds.

Joint Distributions - The joint distribution table describes the percentage occurrence that the data falls into bins defined by bands of speed and direction. In the tables presented here the direction and rate bandwidths are 20° and 5 cm/s. A sample is included in a band if it is equal to or greater than the lower limit, and less than the upper limit. Extreme bands which do not contain any occurrences are dropped, and any bins containing occurrences, but which represent less than 0.1% of the total are reported as 0.0°. Empty bins are left blank. The actual number of occurrences in any given band are reported as subtotals.

TIME SERIES PLOTS

Data for the Rate, Direction, U and V component time series plots were obtained by smoothing the measured data over a three hour period.

The time axis is in units of days with labels every five days and tick marks every 2.5 days. The day number is the G.M.T. day of the year. The vertical scales are in units of cm/s for speed and degrees true for direction.

PROGRESSIVE VECTOR PLOTS

These diagrams are constructed by vectorially adding consecutive data points so as to create the path that a particle would follow if always under the influence of the measured current. The data used for these plots are the same smoothed data used in the time plots. The path is marked every five days by a + sign and the year day number is labelled every ten days. An arrow in the corner of each plot indicates true north and the plot is aligned such that the progressive vector plot and the stick plot have the same orientation.

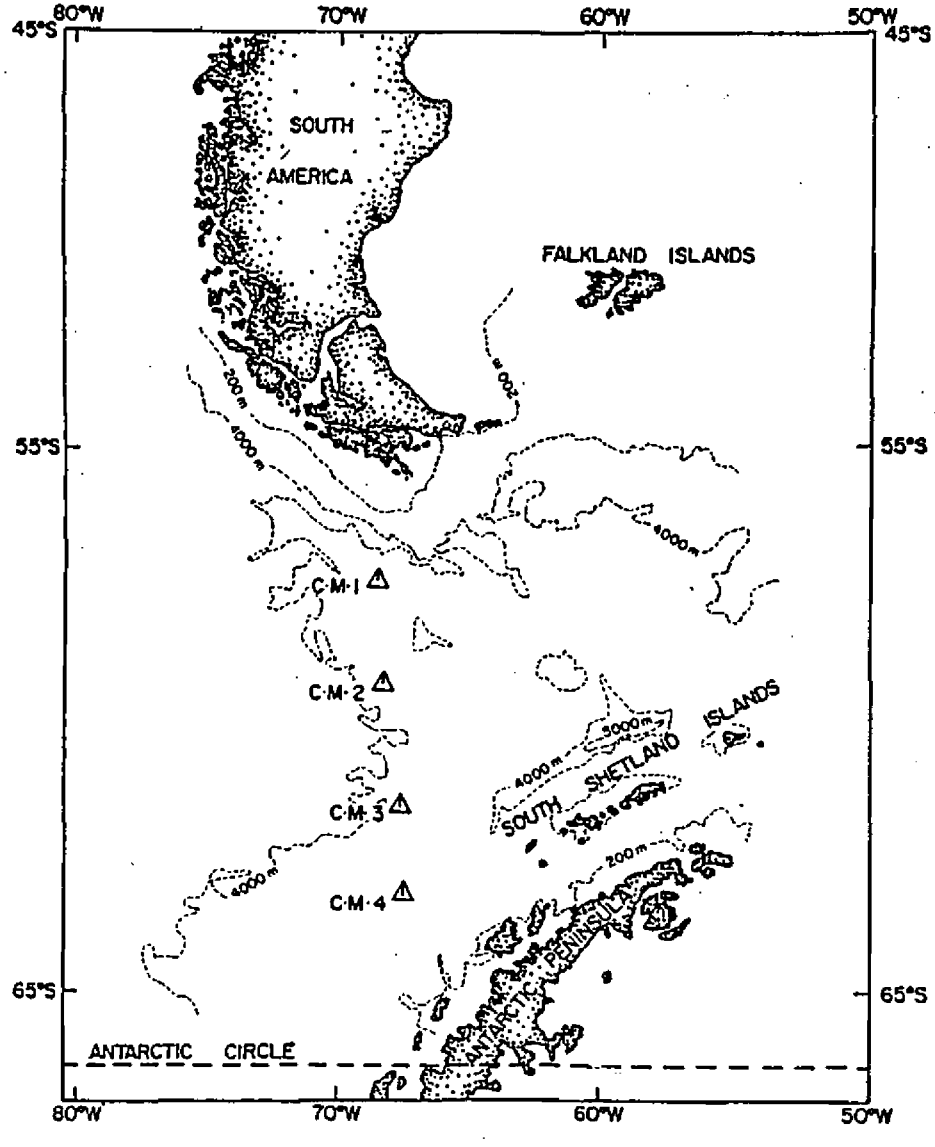
STICK PLOTS

The stick plots were constructed with data that had been smoothed with a filter having a cut-off period of 24 hours and sub-sampled every three hours. The reason for choosing this combination of filter and decimation ratio is purely a visual one. The low frequency motion seemed to be well described and the higher frequencies (tidal and beyond) are removed. Too many data points or sticks make a confused picture whereas too few make the change of velocity hard to follow from one vector to another.

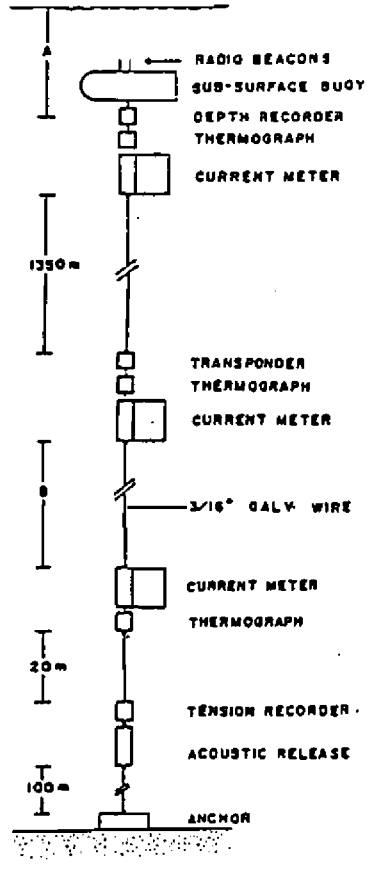
Each stick in the plot is the vector described by the rate and direction data for the time indicated on the horizontal axis at the vector's origin. The time scale is not necessarily the same as that for the rate and direction plots and the amplitude scales may not be the same from one stick plot to another.

HUDSON 70 - DRAKE PASSAGE CURRENT METER INFORMATION (G.M.T. TIME)

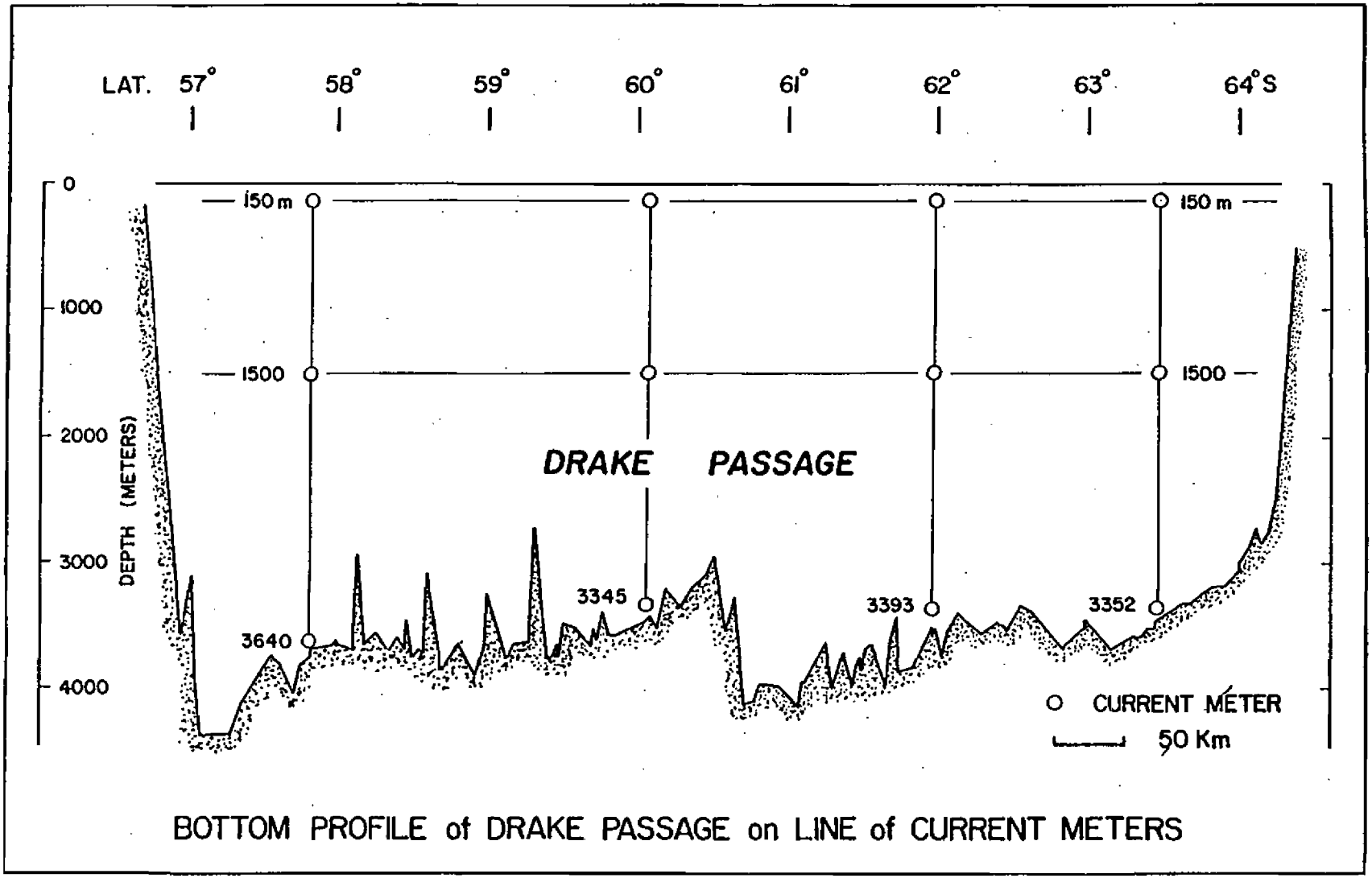
STN. NO.	INSTRUMENT TYPE	DEPTH (M)	POSITION LAT.	POSITION LONG.	SAMPLING INTERVAL	DATA START(HOUR)	DATA START(DAY)	YEAR DAY	DATA DURATION	DATA STOP(HOUR)	DATA STOP(DAY)	YEAR DAY
1	BRAINCON(316)	150	57°49.2S	68°19.6W	20 Min.	19.18	31-01-70	31	10D 15h 20 m	10.38	11-02-70	42
1	BRAINCON(381)	1500	57°49.2S	68°19.6W	20 Min.	17.56	31-01-70	31	10D 17h 40 m	11.36	11-02-70	42
1	BRAINCON(381)	3640	57°49.2S	68°19.6W	20 Min.	19.05	31-01-70	31	10D 17h 0 m	12.05	11-02-70	42
2	BRAINCON(381)	150	60°04.5S	68°04.0W	20 Min.	20.08	01-02-70	32	10D 16h 20 m	12.08	12-02-70	43
2	BRAINCON(381)	1500	60°04.5S	68°04.0W	20 Min.	19.05	01-02-70	32	4D 4h 0 m	23.05	05-02-70	36
2	BRAINCON(381)	3345	60°04.5S	68°04.0W	20 Min.	19.27	01-02-70	32	4D 4h 0 m	23.27	05-02-70	36
3	BRAINCON(381)	150	61°59.0S	67°33.3W	20 Min.	20.29	02-02-70	33	4D 2h 20 m	22.49	06-02-70	37
3	BRAINCON(381)	1500	61°59.0S	67°33.3W	20 Min.	19.04	02-02-70	33	4D 4h 0 m	23.04	06-02-70	37
3	BRAINCON(381)	3393	61°59.0S	67°33.3W	20 Min.	20.06	02-02-70	33	4D 3h 20 m	23.26	06-02-70	37
4	BRAINCON(381)	150	63°28.1S	67°07.0W	20 Min.	19.08	03-02-70	34	4D 1h 40 m	20.48	07-02-70	38
4	BRAINCON(381)	1500	63°28.1S	67°07.0W	20 Min.	19.05	03-02-70	34	4D 2h 0 m	21.05	07-02-70	38
4	BRAINCON(381)	3352	63°28.1S	67°07.0W	20 Min.	17.28	03-02-70	34	4D 0h 20 m	17.48	07-02-70	38



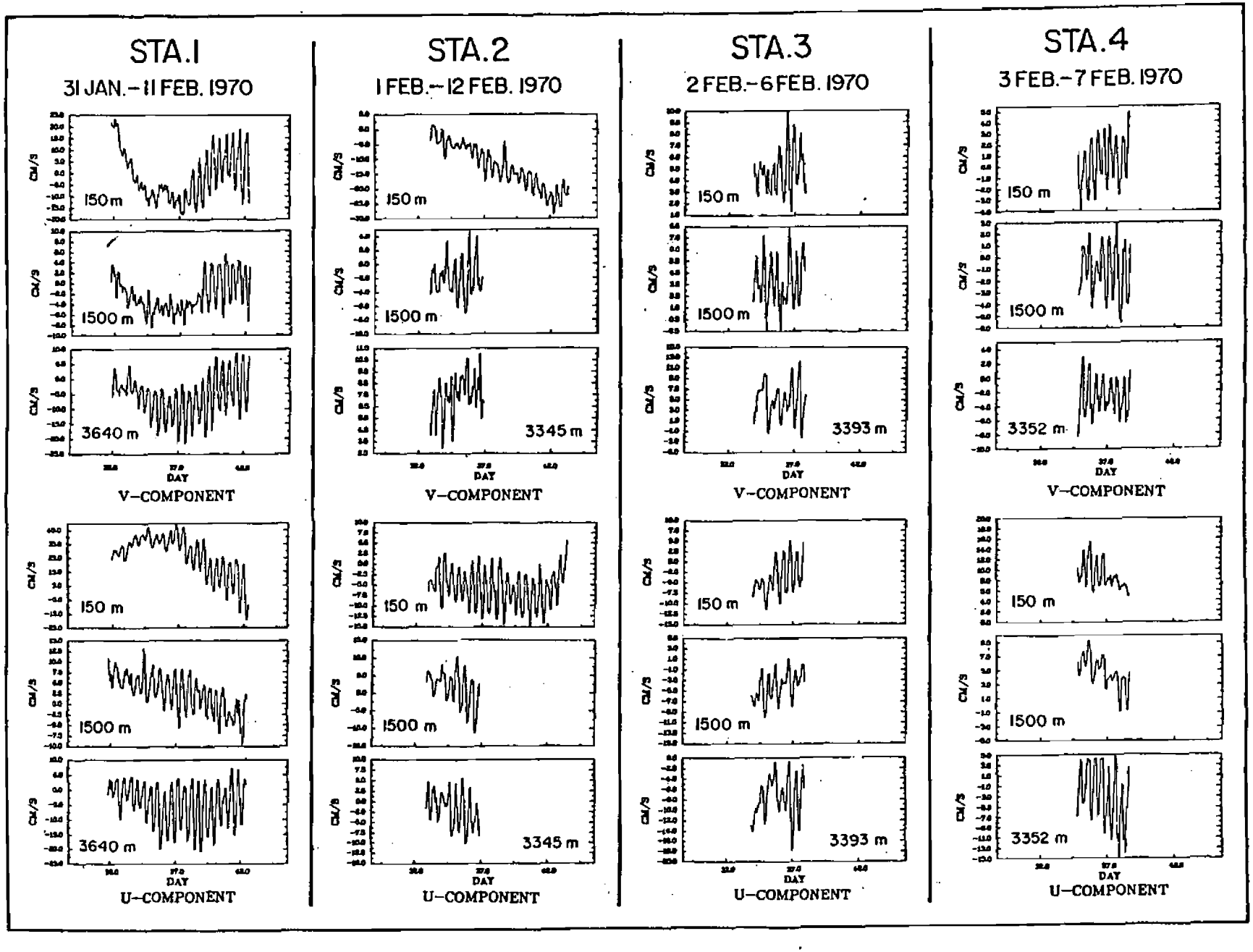
MOORING CONFIGURATION

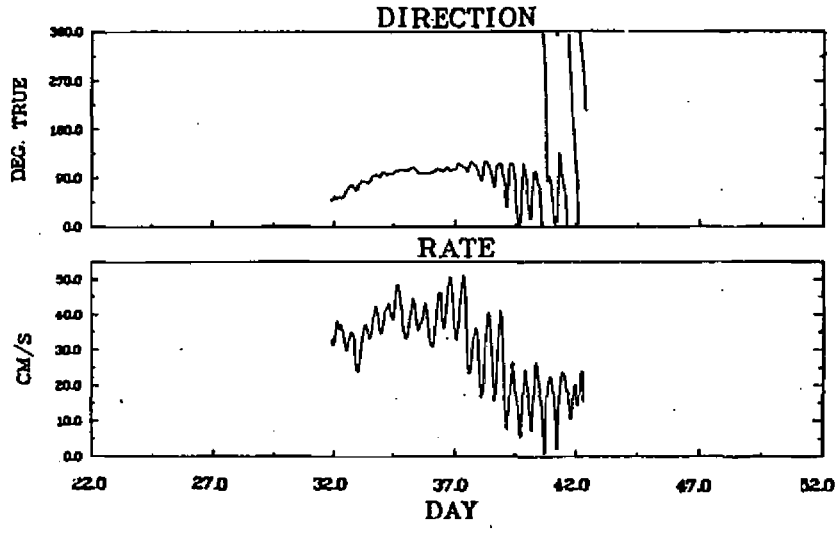


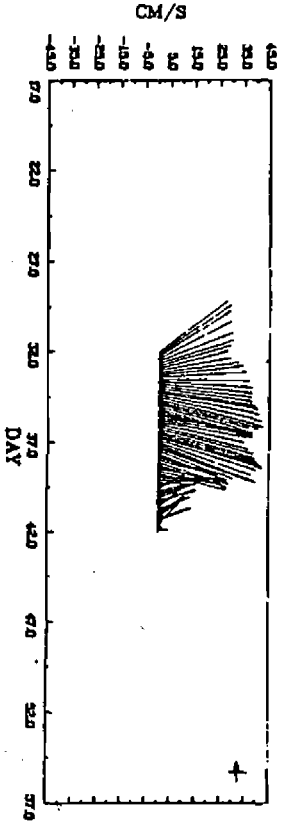
MOORING	LENGTH (meters) A	B
1	162	2137
2	145	1843
3	130	1690
4	132	1850

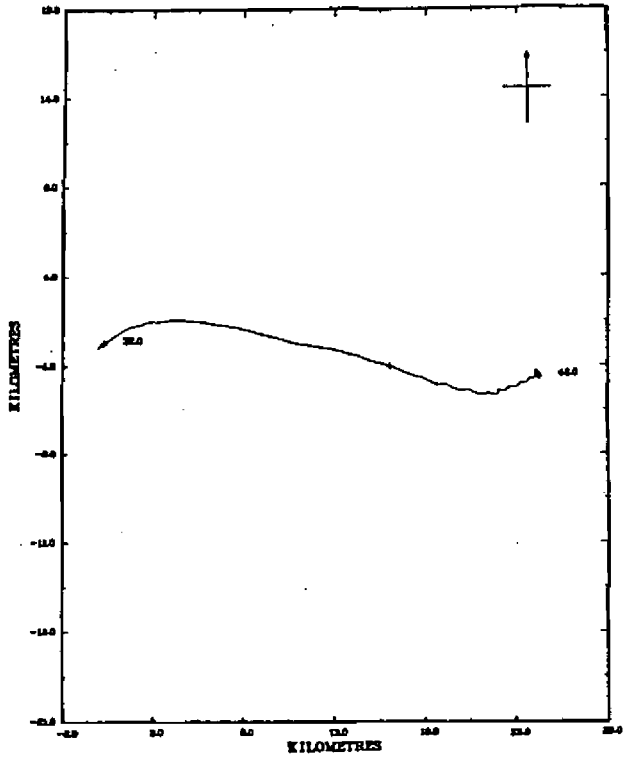


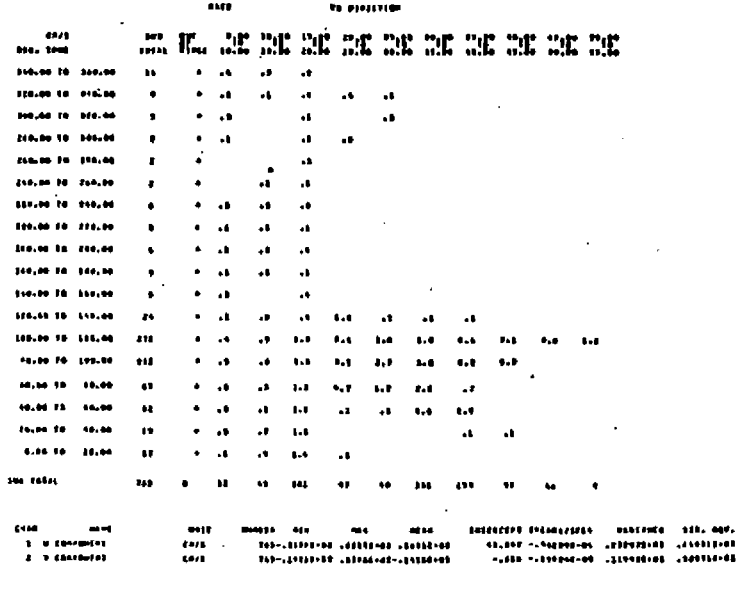
BOTTOM PROFILE of DRAKE PASSAGE on LINE of CURRENT METERS


STA.1
31 JAN.–11 FEB. 1970
150 m
1500 m
3640 m
CM/S
DAY
V–COMPONENT
U–COMPONENT
STA.2
1 FEB.–12 FEB. 1970
3345 m
STA.3
2 FEB.–6 FEB. 1970
3393 m
STA.4
3 FEB.–7 FEB. 1970
3352 m



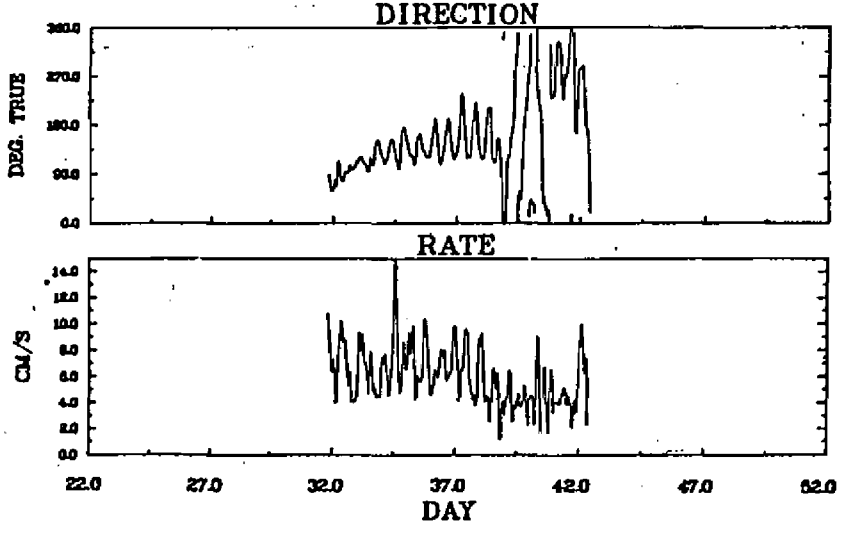


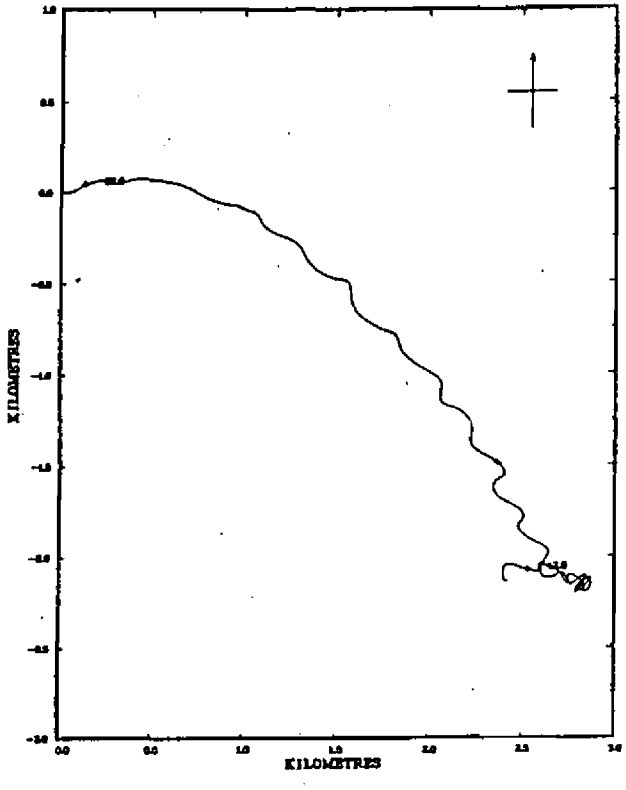


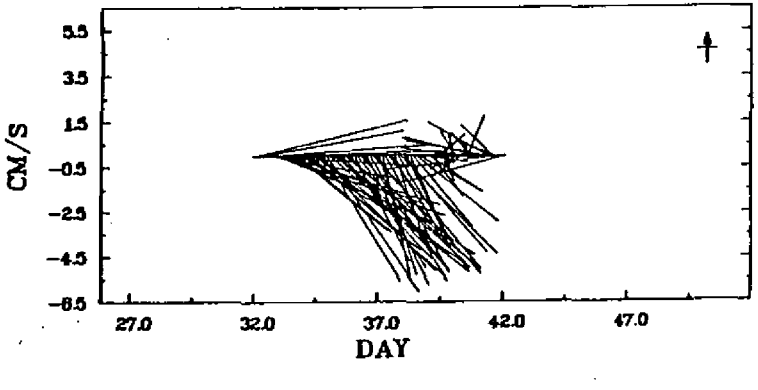


JAN.31-FEB.11 1970

STA.1 150m

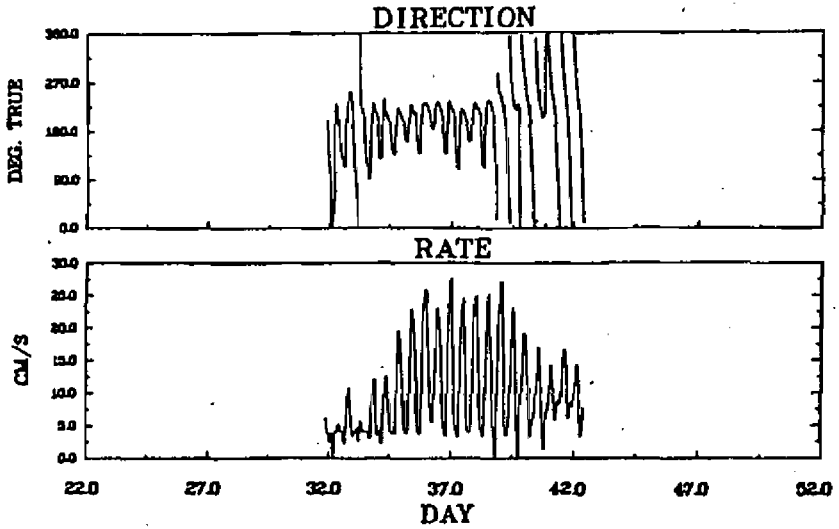


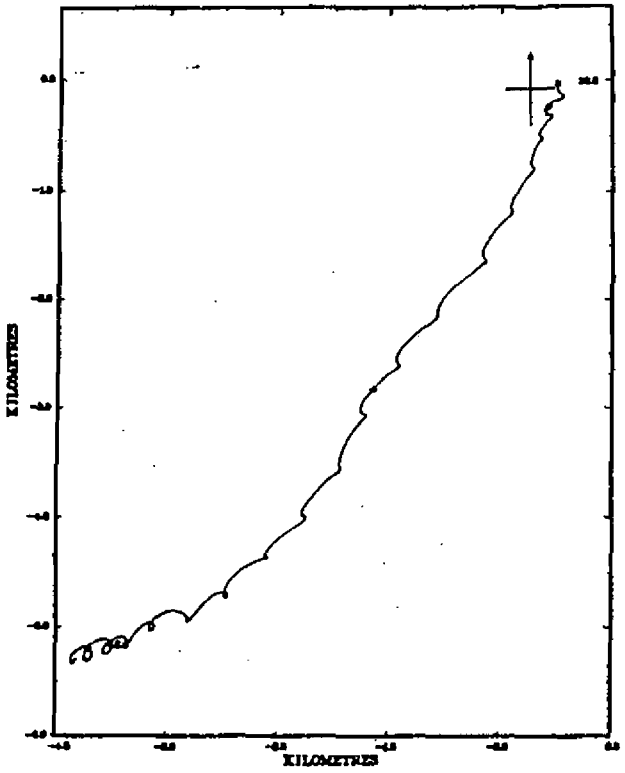


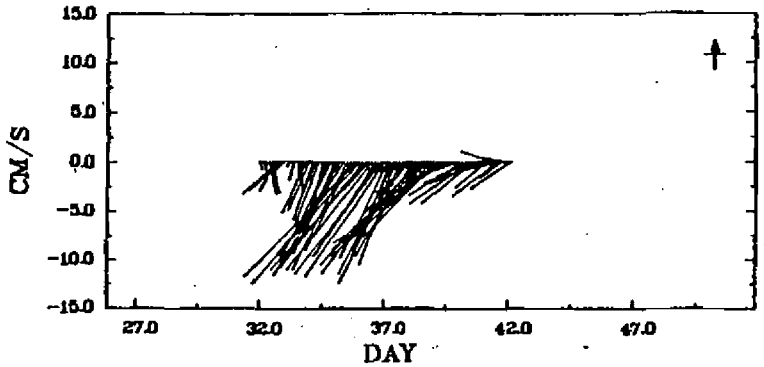


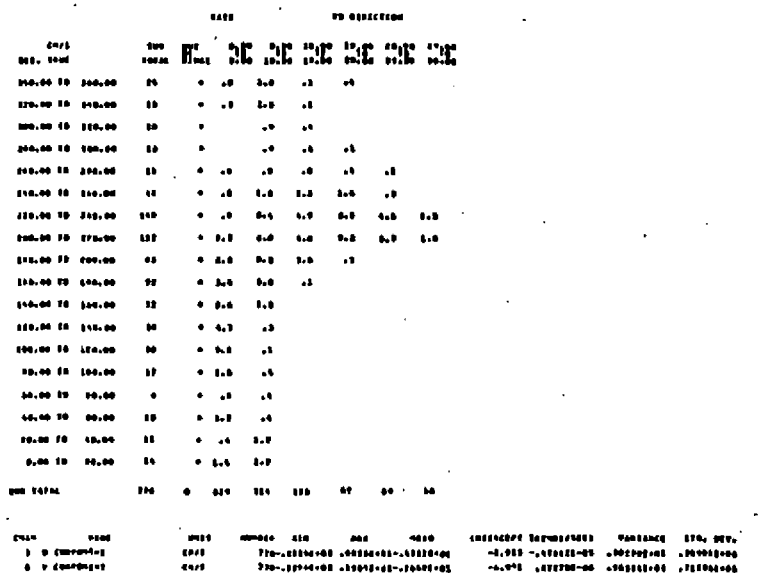
JAN. 31-FEB. 11 1970

STA. 1 1500m



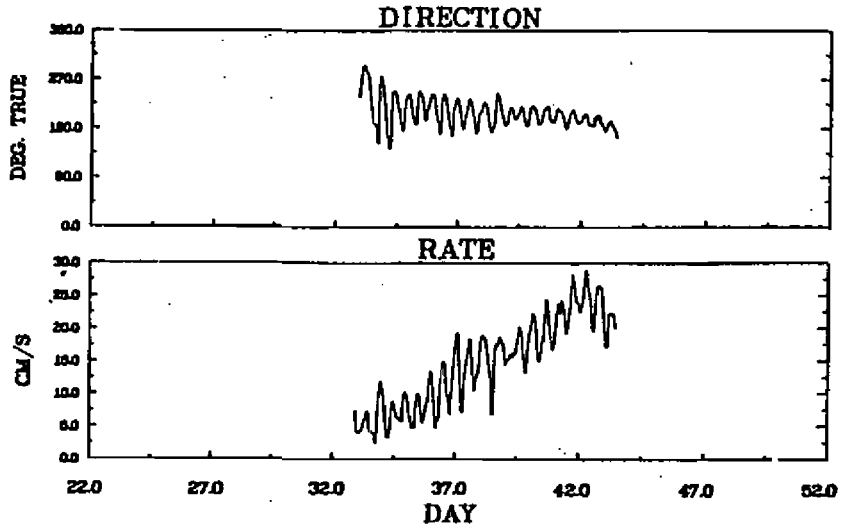


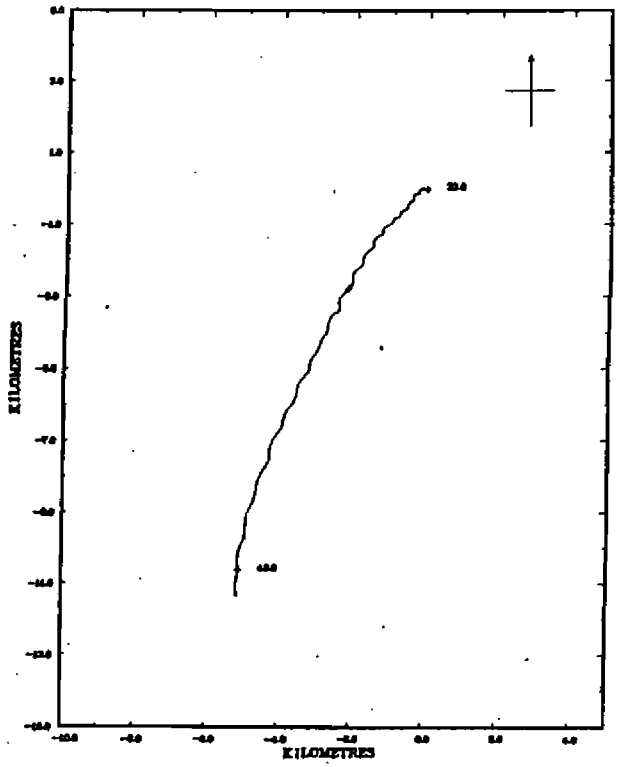


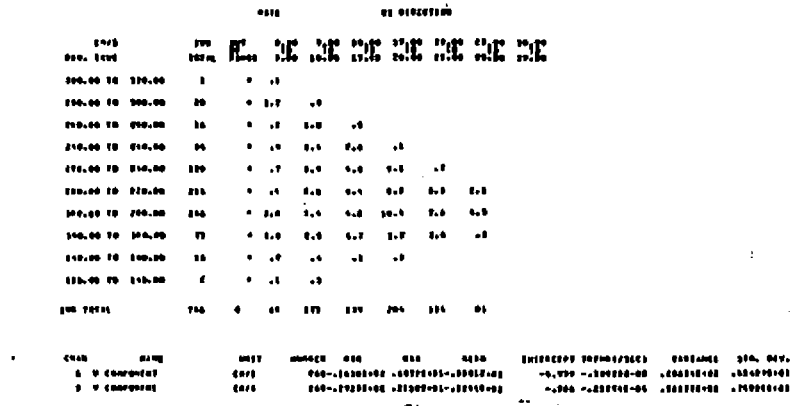


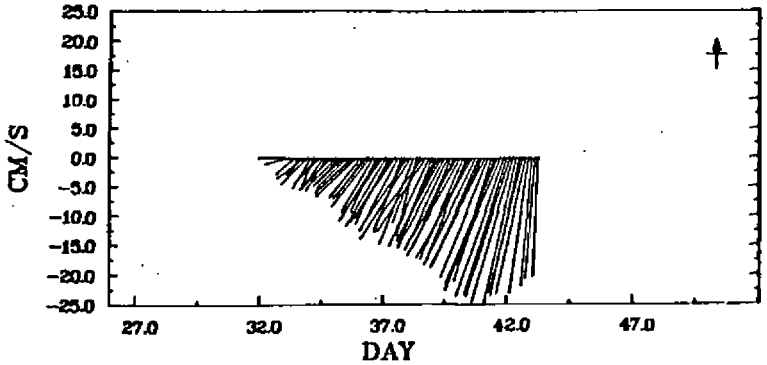
JAN. 31-FEB. 11 1970

STA. 1 3640m



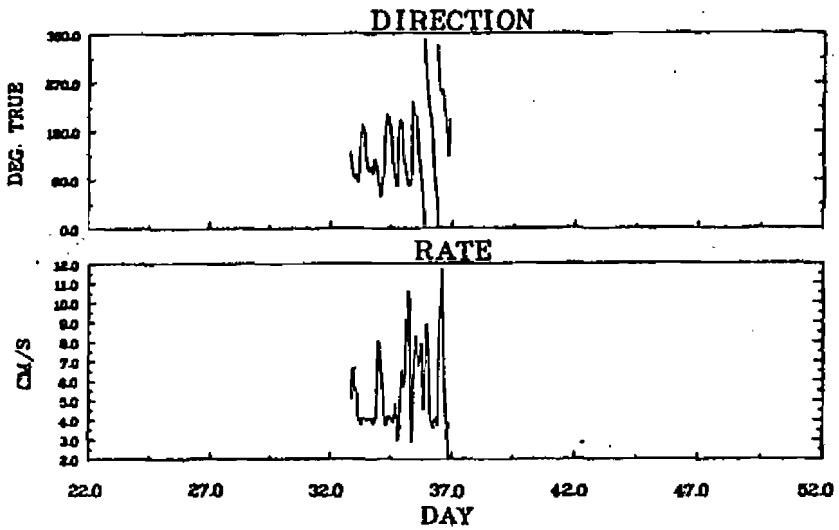


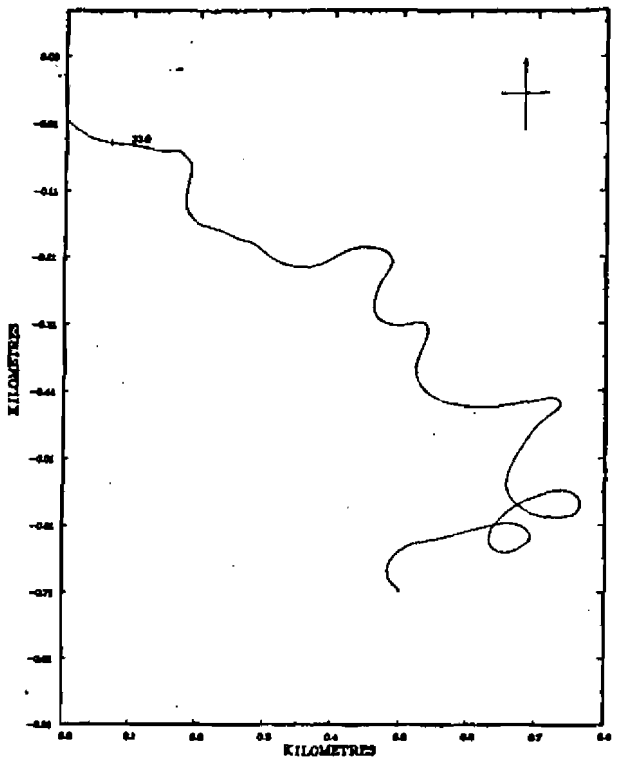


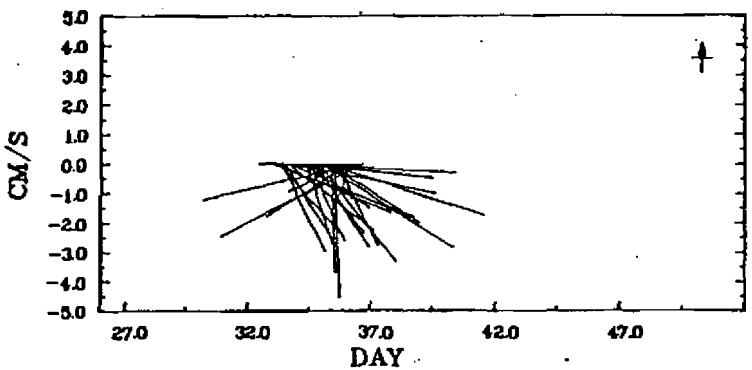


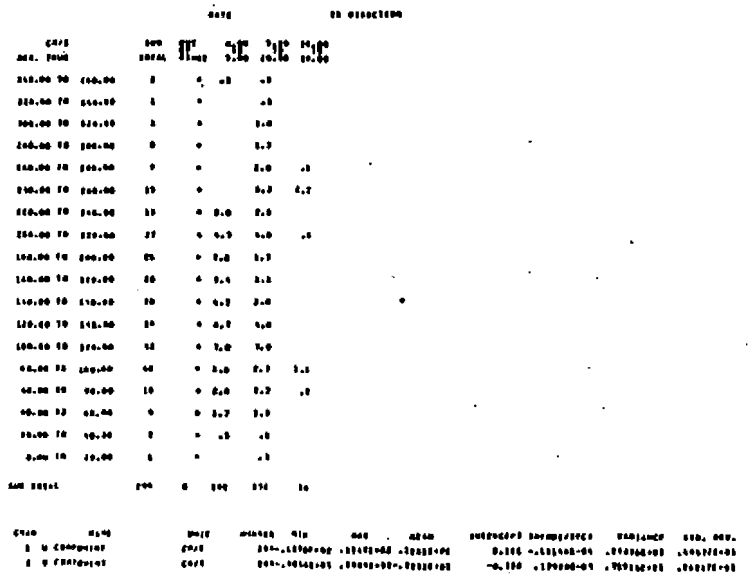
FEB.1-FEB.12 1970

STA.2 150m



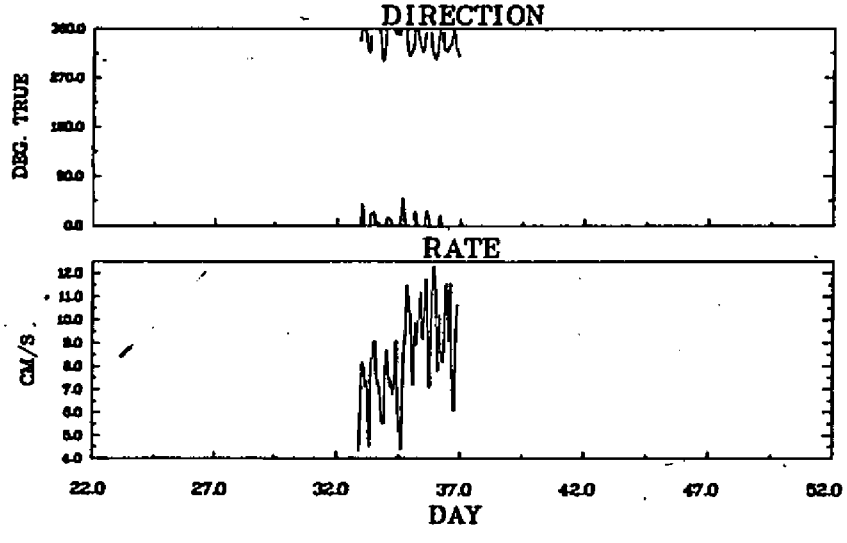


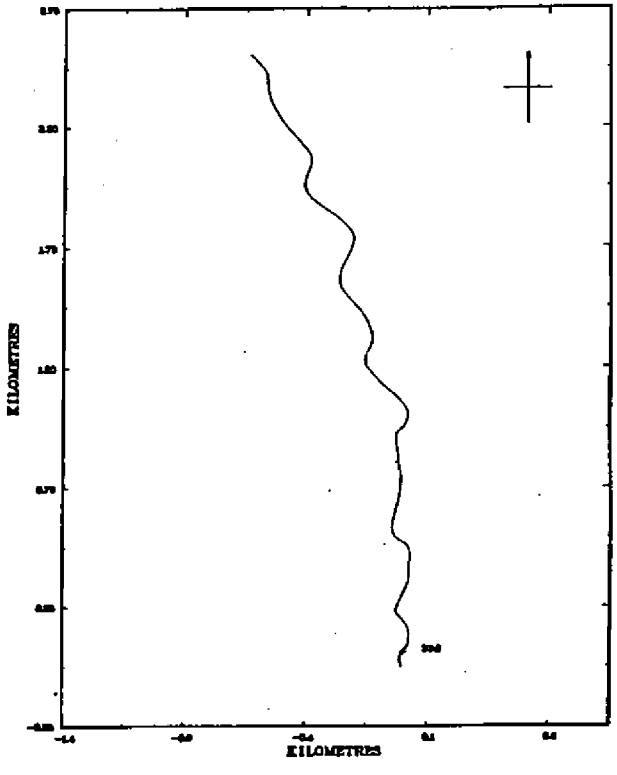


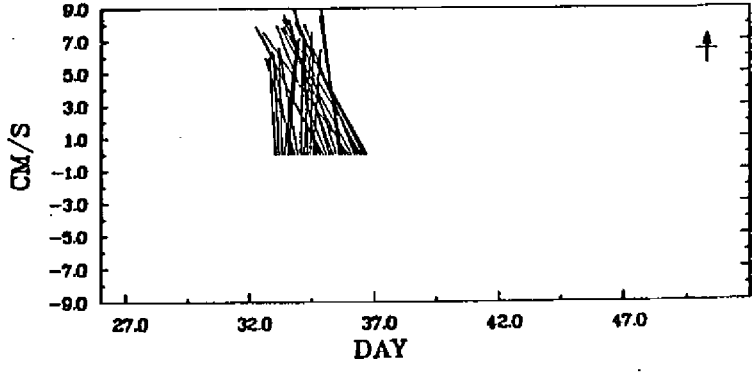


FEB.1-FEB.5 1970

STA.2 1500m

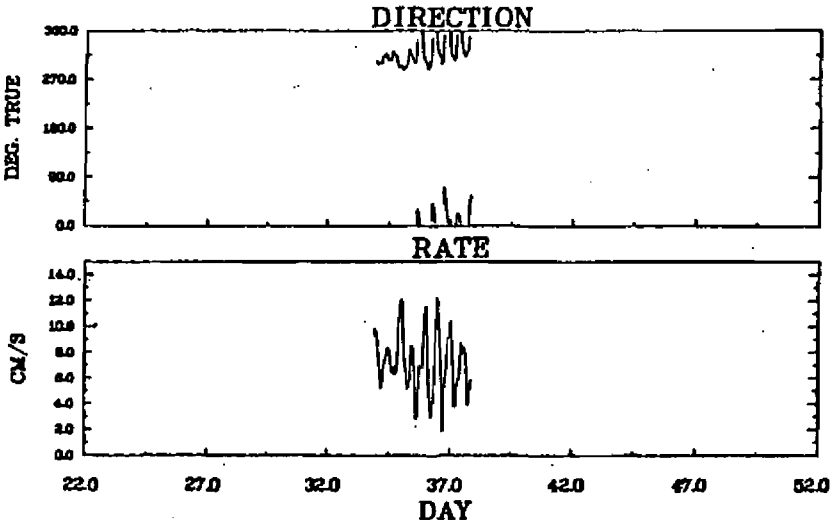


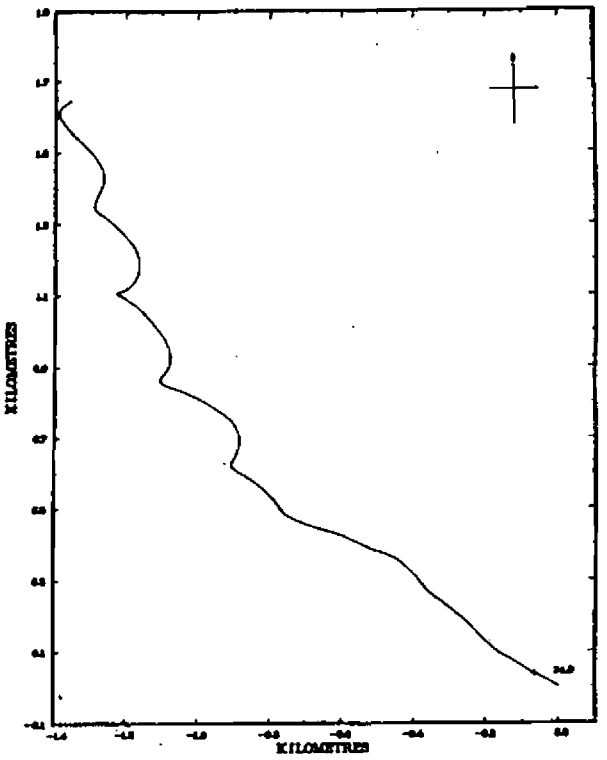


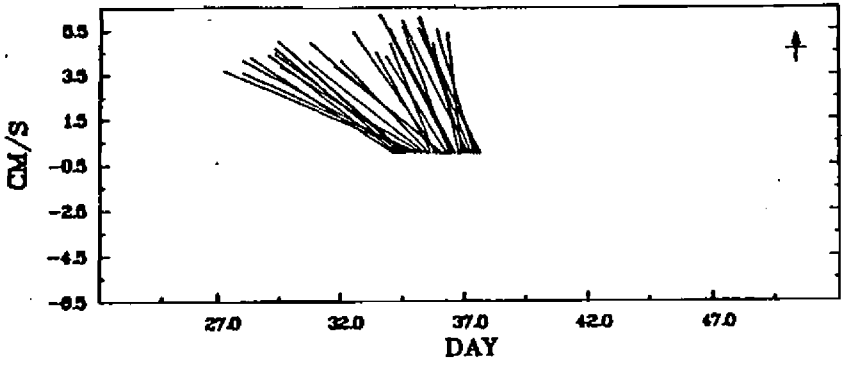


FEB.1-FEB.5 1970

STA.2 3345m

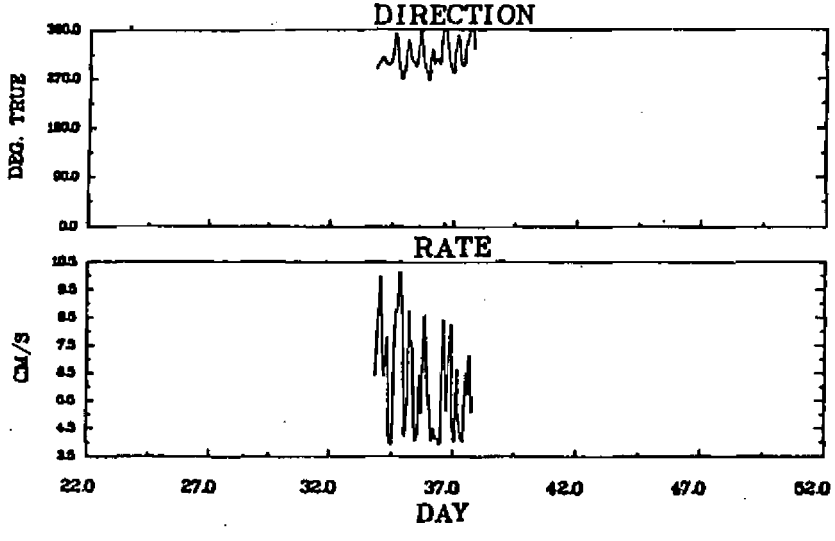


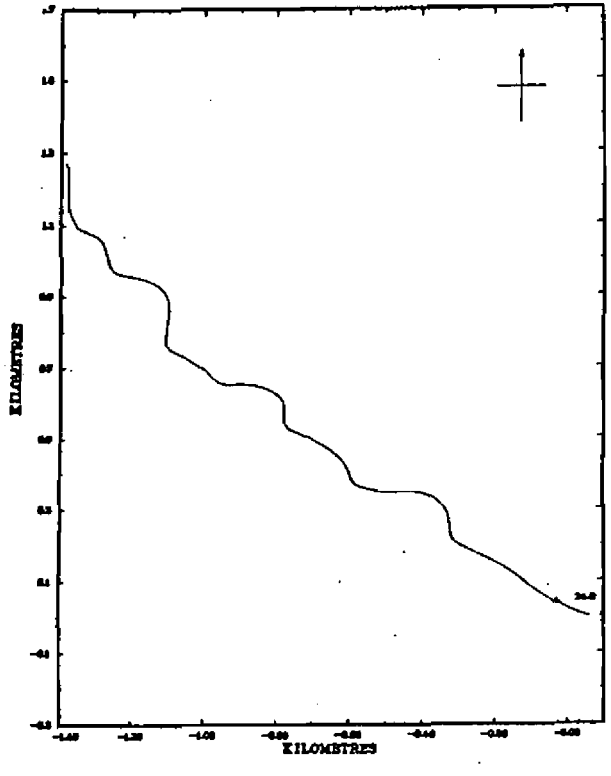


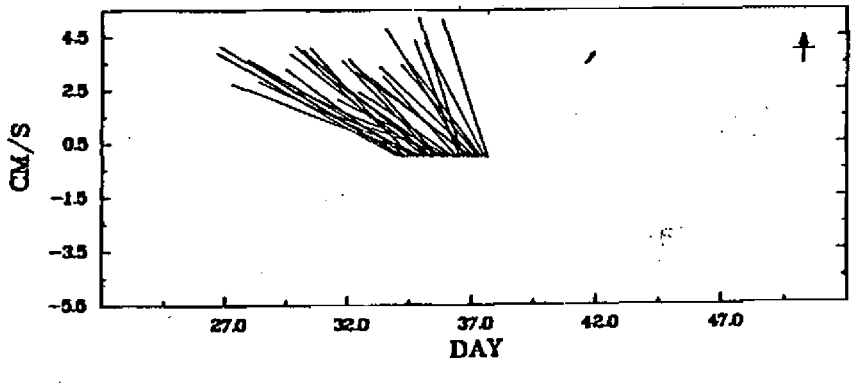


FEB.2-FEB.6 1970

STA.3 150m

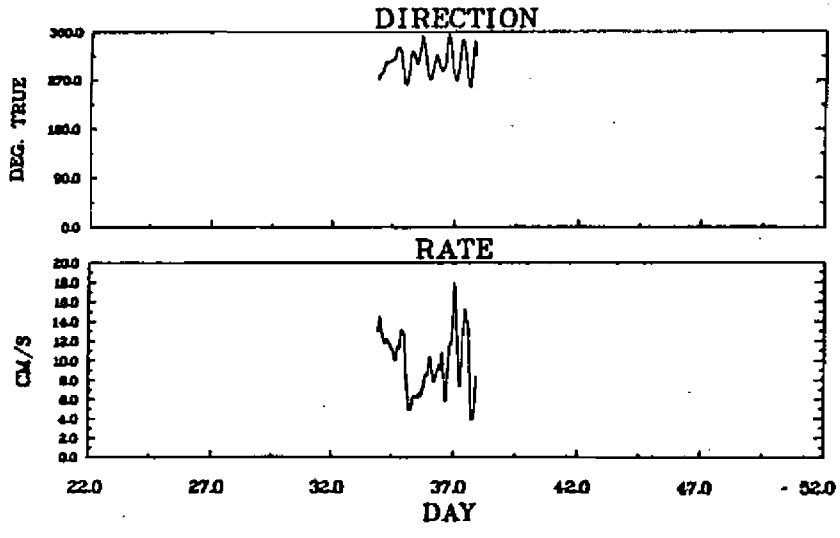


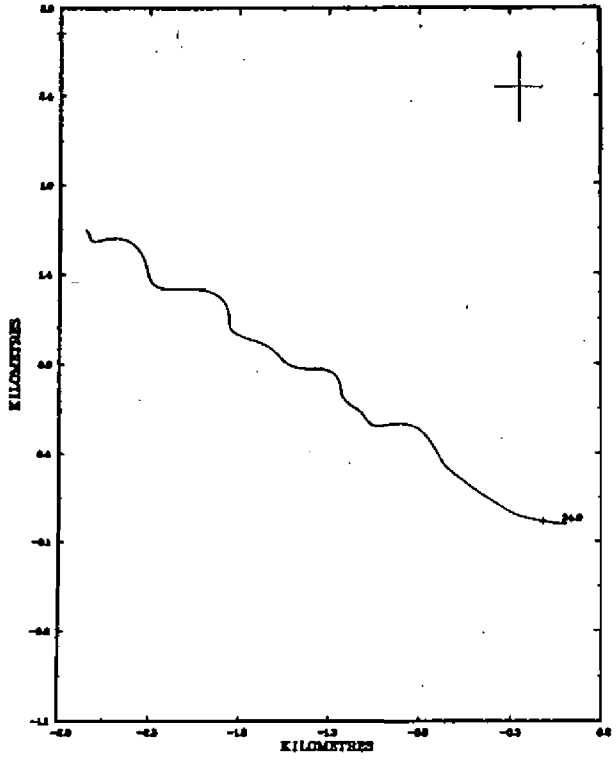


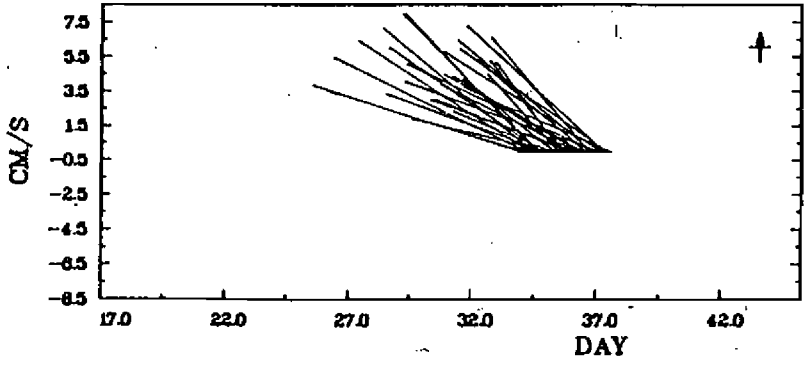


FEB.2-FEB.6 1970

STA.3 1500m

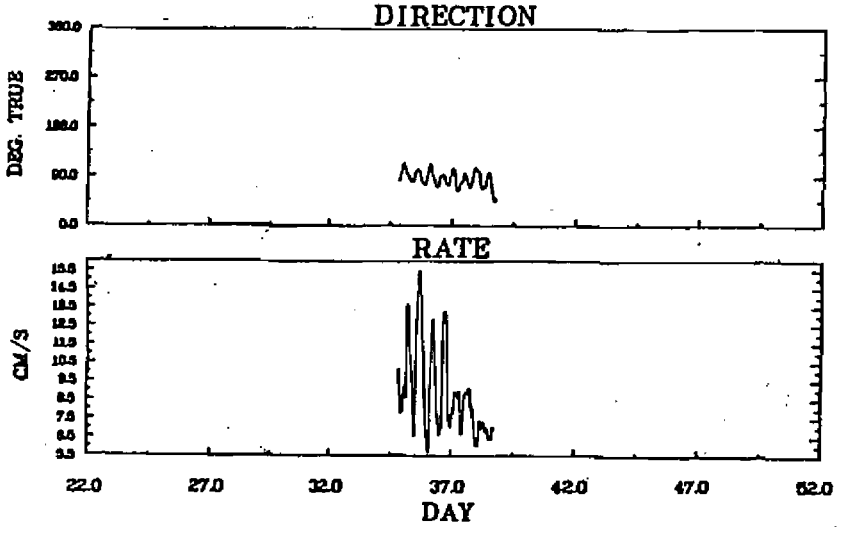


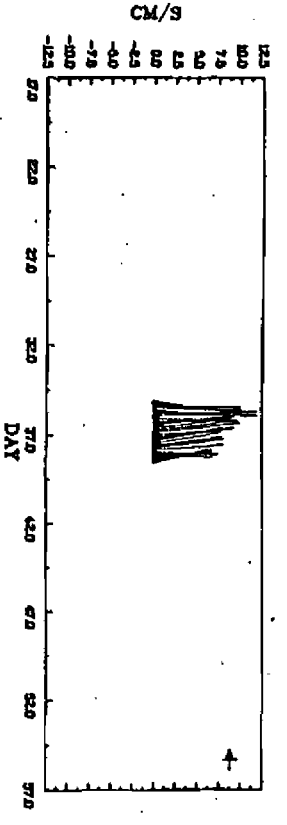


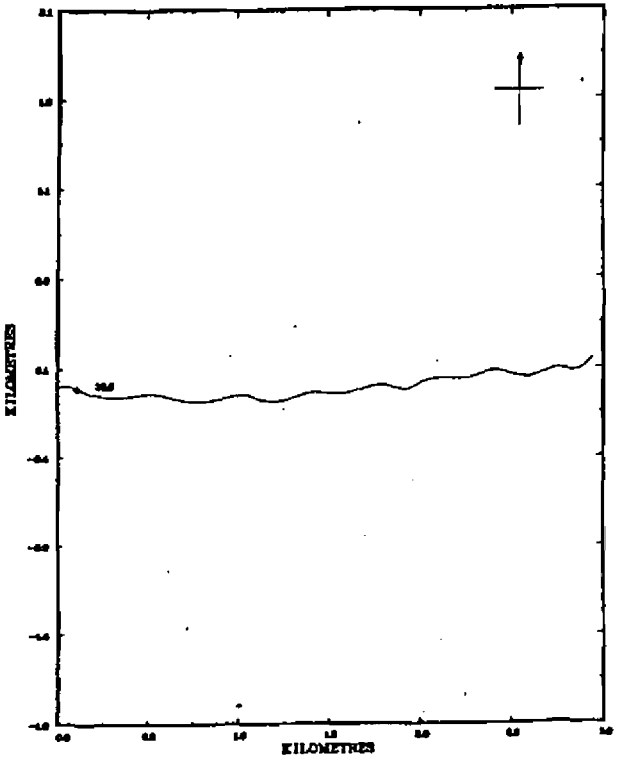


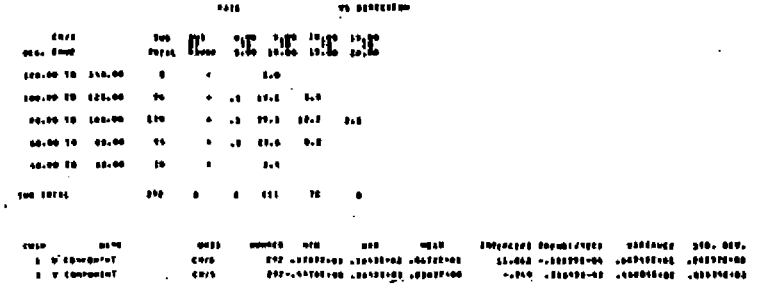
FEB.2-FEB.6 1970

STA.3 3393m



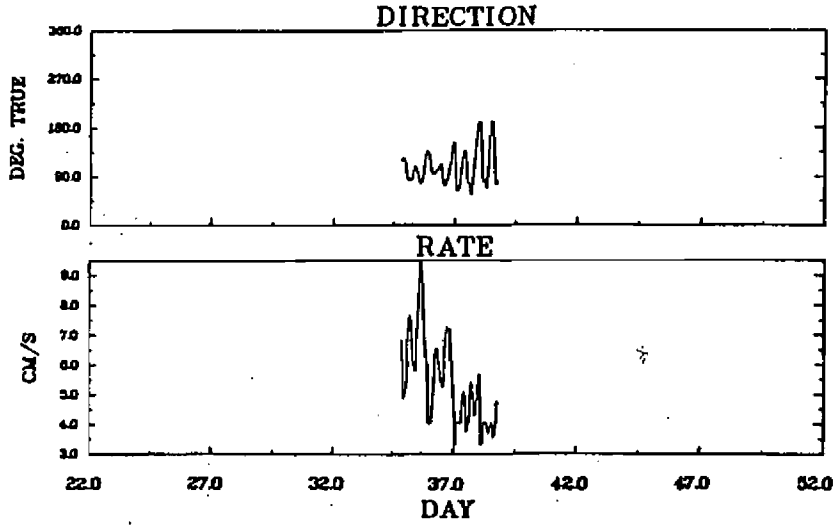


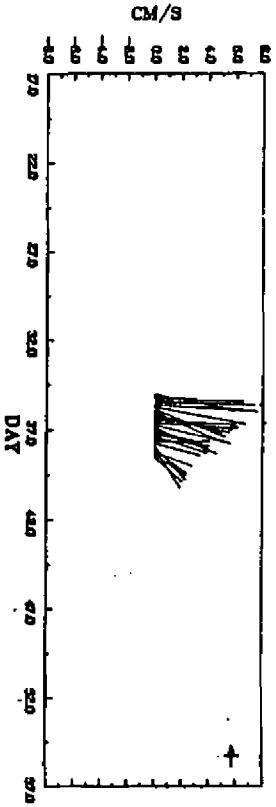


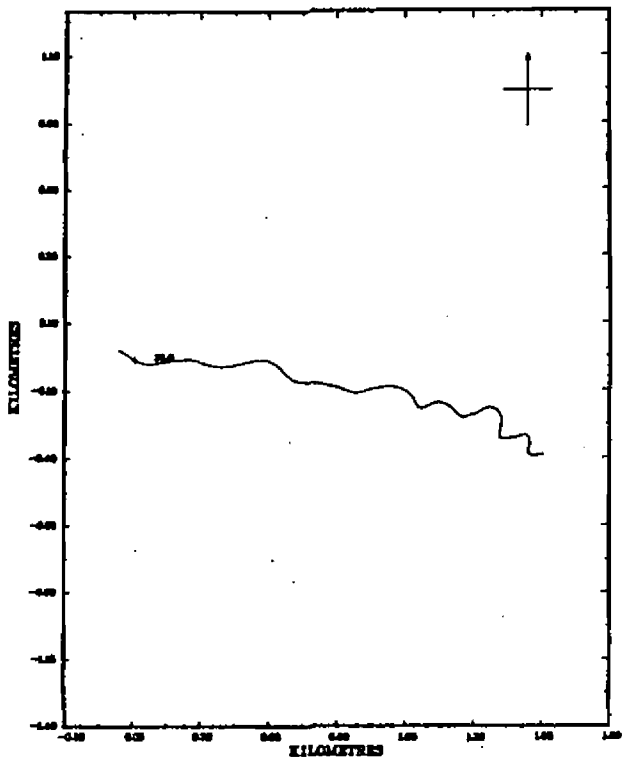


FEB.3-FEB.7 1970

STA.4 150m

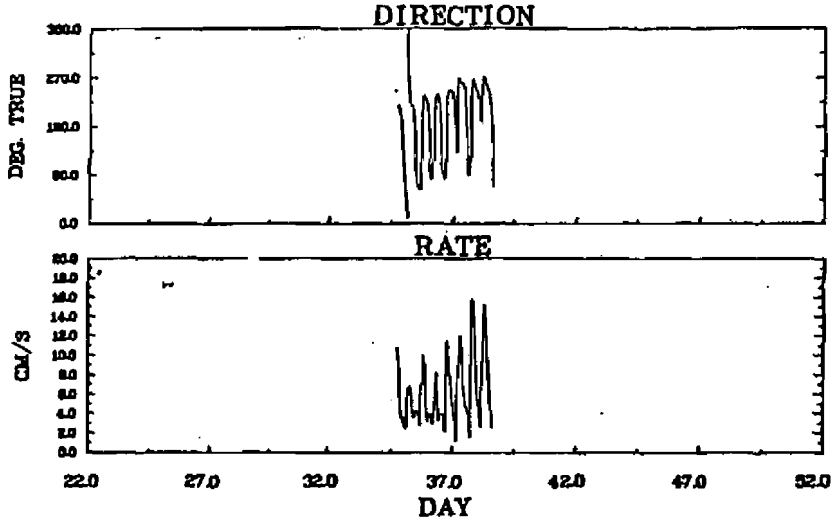


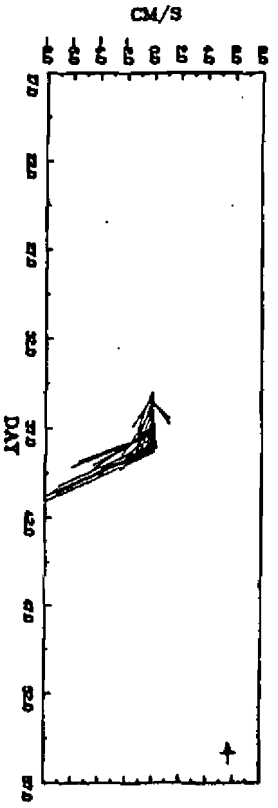


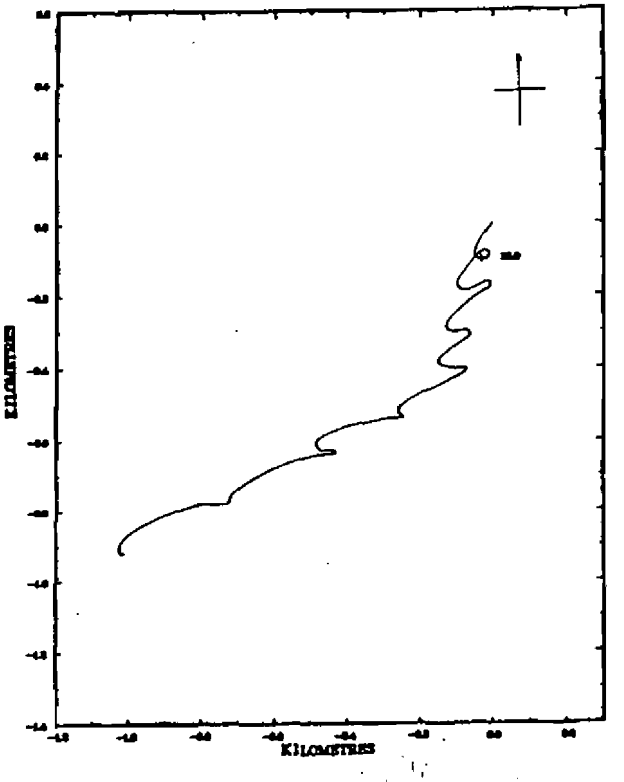


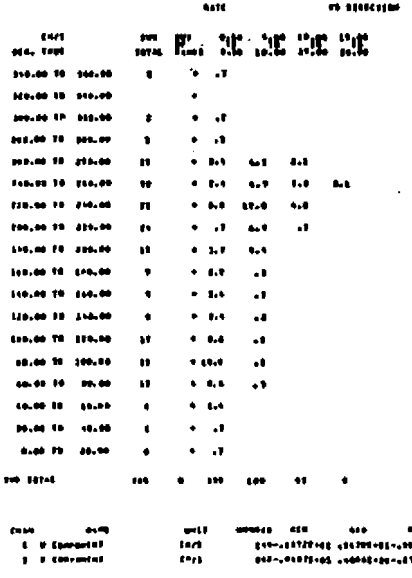
FEB.3-FEB.7 1970

STA.4 1500m





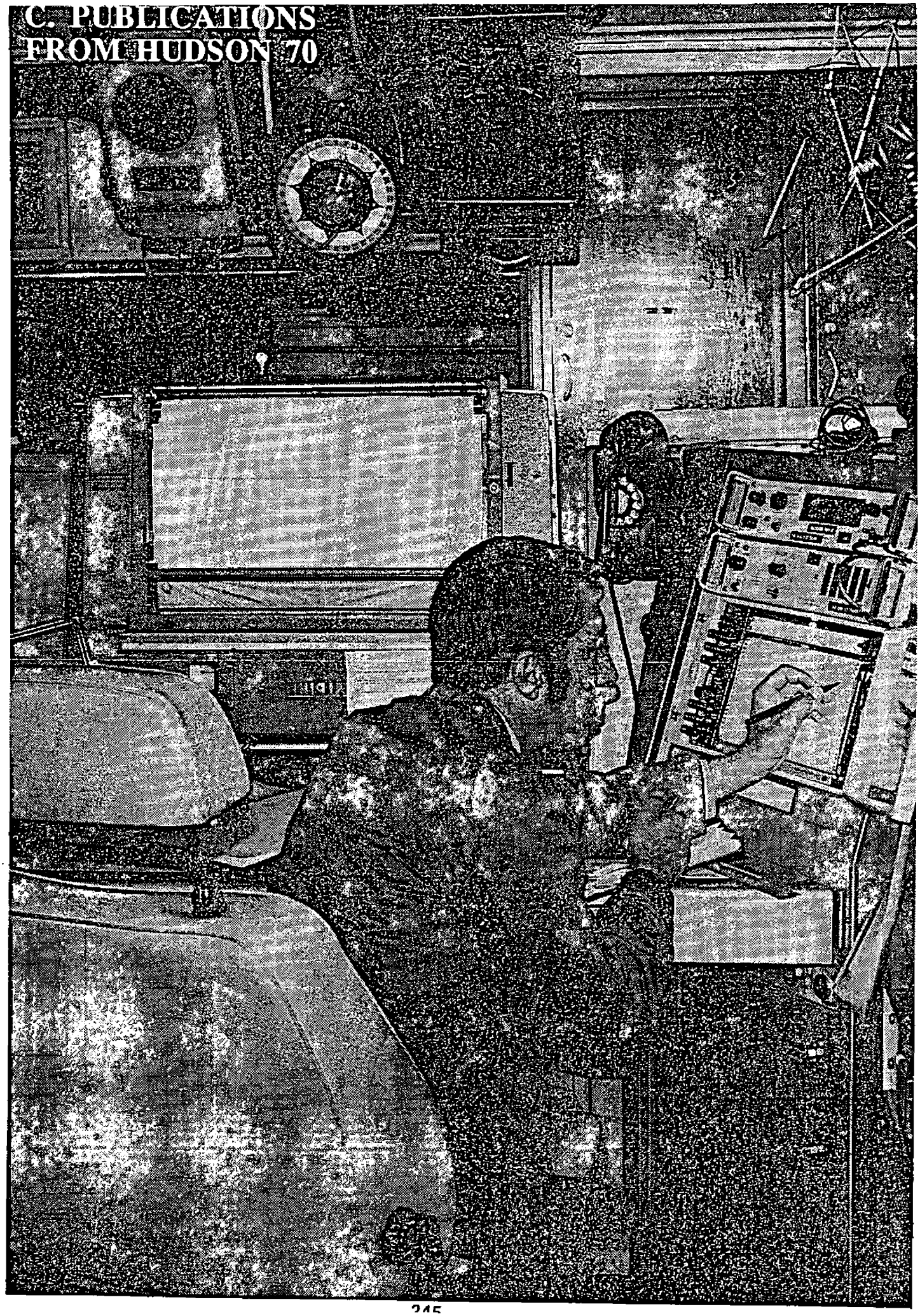




FEB.3-FEB.7 1970

STA.4 3352m

C. PUBLICATIONS FROM HUDSON 70



HUDSON 70 - A BIBLIOGRAPHY OF PUBLISHED PAPERS
(Items included in this volume)

Page

Atkinson, L.P. 1973. Effect of air bubble solution on air-sea gas exchange. Journal of Geophysical Research 78(6): 962-968. 253

Banerji, R.K., C.T. Schafer, and R. Vine. 1971. Environmental relationships and distribution of planktonic foraminifera in the equatorial and northern Pacific waters. Atlantic Oceanographic Laboratory, AOL Report 1971-7. 65p. plus 15p. of appendices and plates. 261

Barrett, D.L., C.E. Keen, K.S. Manchester, and D.I. Ross. 1971. Baffin Bay -- an ocean. Nature 229(5286): 551-553. 345

Brown, R.G.B., F. Cooke, P.K. Kinnear, and E.L. Mills. 1975. Summer seabird distributions in Drake Passage, the Chilean fjords and off southern South America. Ibis 117(3): 339-356. 351

Chase, R.L., and D.L. Tiffin. 1972. Queen Charlotte fault-zone, British Columbia. In: Marine geology and geophysics; section 8, International Geological Congress (24th : 1972 : Montreal) = Geologie et geophysique du milieu marin; section 8, Congres Geologique International (24e : 1972 : Montreal), ed., J.E. Gill. Ottawa: The Congress, 17-27. 371

Cooke, F., and E.L. Mills. 1972. Summer distribution of pelagic birds off the coast of Argentina. Ibis 114(2): 245-251. 383

Coote, A.R., I.W. Duedall, and R.S. Hiltz. 1971. Automatic analysis at sea. In: Advances in automated analysis: Technicon International Congress on Automation (5th : 1970 : New York). Miami: Thurman Associates, v.2: 347-351. 391

Coote, A.R., C.R. Mann, A. Walton, and J.M. Edmond. 1973. Deep-Sea Research 20(6): 579-581. 397

Deevey, G.B. 1974. Pelagic ostracods collected on Hudson 70 between the equator and 55 degrees S in the the Atlantic. Proceedings of the Biological Society of Washington 87(32): 351-380. 401

Duedall, I.W., A.R. Coote, D.F. Knox, and G.F. Connolly. 1971. A dispenser for Winkler's dissolved oxygen reagents. Journal of the Fisheries Research Board of Canada 28(11): 1815-1816. 431

Duedall, I.W., and A.R. Coote. 1972. Oxygen distribution in the Pacific Ocean. Journal of Geophysical Research 77(12): 2201-2203. 433

Duedall, I.W., and A.R. Coote. 1972. Oxygen distribution in the South Atlantic. Journal of Geophysical Research 77(3): 496-498. . . . 437

Foster, L.A. 1972. Current measurements in the Drake Passage. Unpublished M.Sc. thesis, Dalhousie University, Halifax, N.S. 61p. 441

Haworth, R.T. 1971. A geophysical profile in the south-east Pacific. Earth and Planetary Science Letters 11(2): 83-89. 509

Keen, C.E., D.L. Barrett, K.S. Manchester, and D.I. Ross. 1972. Geophysical studies in Baffin Bay and some tectonic implications. Canadian Journal of Earth Sciences 9(3): 239-256. . . . 517

Lalli, C.M., and F.E. Wells, Jr. 1973. Brood protection in an epipelagic thecosomatous pteropod, Spiratella ("Limacina") inflata (d'Orbigny). Bulletin of Marine Science 23(4): 933-941. . . . 537

Lister, C.R.B. 1972. On the thermal balance of a mid-ocean ridge. Geophysical Journal of the Royal Astronomical Society 26(5): 515-535. 549

Mann, C.R. 1971. Hudson '70 and past oceanographic expeditions. In: Canadian Hydrographic Service 10th annual hydrographic conference, 2-4 March 1971, Dartmouth, Nova Scotia: [proceedings]. [Dartmouth, N.S.: The Conference], 160-166. 575

Mann, C.R. 1971. The Hudson-70 cruise: a significant contribution to world oceanography. Science Forum 4(1): 19-22. 585

Mann, C.R., A.R. Coote, and D.M. Garner. 1973. The meridional distribution of silicate in the western Atlantic Ocean. Deep-Sea Research 20(9): 791-801. 591

Manning, R.B. 1971. The postlarva of the stomatopod crustacean, Heterosquilla polydactyla (Von Martens). Proceedings of the Biological Society of Washington 84(33): 265-270. 603

Pelletier, B.R., and J.M. Shearer. 1972. Sea bottom scouring in the Beaufort Sea of the Arctic Ocean. In: Marine geology and geophysics; section 8, International Geological Congress (24th : 1972 : Montreal) = Geologie et geophysique du milieu marin; section 8, Congres Geologique International (24e : 1972 : Montreal), ed., J.E. Gill. Ottawa: the Congress, 251-261. 609

Pickard, G.L. 1971. Some physical oceanographic features of inlets of Chile. Journal of the Fisheries Research Board of Canada 28(8): 1077-1106. 621

Pickard, G.L. 1973. Water structure in Chilean fjords. In: Oceanography of the South Pacific 1972, comp., R. Fraser. Wellington: New Zealand National Commission for UNESCO, 95-104. . . . 651

Ross, D.I. 1972. The Hudson-70 expedition. In: Ocean '72: IEEE International Conference on Engineering in the Ocean Environment (1972 : Newport, RI), Record. New York: Institute of Electrical and Electronic Engineers, 328-332. (IEEE publication 72 CHO 660-1 OCC.) 661

Shearer,J.M., R.F. Macnab, B.R. Pelletier, and T.B. Smith. 1971. Submarine pingos in the Beaufort Sea. Science 174: 816-818. 667

Sheldon, R.W., A. Prakash, and W.H. Sutcliffe, Jr. 1972. The size distribution of particles in the ocean. Limnology and Oceanography 17(3): 327-340. 671

Srivastava, S.P., D.L. Barrett, C.E. Keen, K.S. Manchester, K.G. Shih, D.L. Tiffin, R.L. Chase, A.G. Thomlinson, E.E. Davis, and C.R.B. Lister. 1971. Preliminary analysis of geophysical measurements north of Juan de Fuca Ridge. Canadian Journal of Earth Sciences 8(10): 1265-1281. 687

Vilks, G. 1972. Planktonic foraminifera in the water and sediments of Beaufort Sea, Canadian Arctic. In: Marine geology and geophysics; section 8, International Geological Congress (24th : 1972 : Montreal) = Geologie et geophysique du milieu marin; section 8, Congres Geologique International (24e : 1972 : Montreal), ed., J.E. Gill. Ottawa: the Congress, 135-141. 705

Vilks, G. 1974. The distribution of planktonic foraminifera in the sediments and water of the Northwest Passage and northern Baffin Bay: a tool for paleooceanographic synthesis. In: Offshore geology of eastern Canada, volume 1, Concepts and applications of environmental marine geology, ed., B.R. Pelletier. Ottawa: Geological Survey of Canada, 109-121. (Geological Survey of Canada Paper 74-30 (v.1).) 713

Vilks, G. 1975. Comparison of Globorotalia pachyderma (Ehrenberg) in the water column and sediments of the Canadian Arctic. Journal of Foraminiferal Research 5(4): 313-325. 727

Vilks, G., and D.A. Walker. 1974. Morphology of Orbulina universa d'Orbigny in relation to other spinose planktonic foraminifera. Journal of Foraminiferal Research 4(1): 1-8. 741

von Arx, W.S., D.C. Bowen, J.P. Dean, and R.T. Haworth. 1971. Hudson '70 gravity observations, 62.9 degrees S - 57.5 degrees N along 150 degrees W. Woods Hole Oceanographic Institution Reference No.71-68. 64p. 753

Wagner, F.J.E. 1972. Molluscan fauna as indicators of Late Pleistocene history, southeastern Beaufort Sea. In: Marine geology and geophysics; section 8, International Geological Congress (24th : 1972 : Montreal) = Geologie et geophysique du milieu marin; section 8, Congres Geologique International (24e : 1972 : Montreal), ed., J.E. Gill. Ottawa: the Congress, 142-153. . . 823

Walker, D.A., and G. Vilks. 1973. Spinal ultrastructure of the planktonic foraminifers Hastigerina Thomson and Globigerinella Cushman. Journal of Foraminiferal Research 3(4): 196-198. 835

Wangersky, P.J. 1976. Particulate organic carbon in the Atlantic and Pacific oceans. Deep-Sea Research 23(5): 457-465. 841

Wong, C.S. 1972. Deep zonal water masses in the equatorial Pacific Ocean inferred from anomalous oceanographic properties. Journal of Geophysical Research 77(36): 7196-7202. 851

Zurbrigg, R.E., and W.B. Scott. 1976. Diaphus hudsoni (Pisces: Myctophidae), a new lanternfish from the South Atlantic Ocean. Canadian Journal of Zoology 54(9): 1538-1541. 859

OTHER REPORTS
(Copies not included in this volume)

Bellefontaine, L., J. Pritchard, and B. Reiniger. 1982. Atlas of physical oceanographic data for the South Atlantic Ocean, Drake Passage, Pacific Ocean, and Canadian Arctic - 1970. Canadian Technical Report of Hydrography and Ocean Sciences 14. 45p.

Chase, R.L., A.G. Thomlinson, and W.G. Bertrand. 1972. Catalogue of rock samples collected during phase VII of Hudson - 70 onboard CNAV Endeavour. Bedford Institute of Oceanography, Data Series BI-D-72-3. 126p.

Edmonds, A. 1973. Voyage to the edge of the world. Toronto: McClelland and Stewart Ltd. 254p.

Mann, C.R. 1971. The Hudson 70 expedition. Bedford Institute, Biennial Review 1969/70: 3-9.

Shih, K.G. 1971. Gravity and magnetic data collected in the Northwestern Pacific Ocean and the Bering Sea. Atlantic Oceanographic Laboratory, Data Series BI-D-1971-7. 126p. in various pagings.

Shih, K.G., D.I. Ross, and B.L. Johnston. 1972. Gravity and magnetic data of Baffin Bay collected in 1970, C.S.S. Hudson and C.S.S. Baffin cruises. Bedford Institute of Oceanography, Data Series BI-D-72-5. 247p. in various pagings.

Srivastava, S.P., ed. 1971. Geophysical data collected during Hudson-70, phase VII off British Columbia, Canada. Atlantic Oceanographic Laboratory, AOL Data Series 71-5-D. 295p. in various pagings.

VOL. 78, NO. 6 JOURNAL OF GEOPHYSICAL RESEARCH FEBRUARY 20, 1973

Effect of Air Bubble Solution on Air-Sea Gas Exchange

LARRY P. ATKINSON[1]

Department of Oceanography, Dalhousie University
Halifax, Nova Scotia, Canada

Recent data on ambient wave generated oceanic bubble spectra (Medwin, 1970) permit the calculation of the influence of bubble solution on air-sea gas exchange. Schulkin's formula is used to estimate the depth variation of bubbles, and a square law is used to estimate the increase of bubble volume with wind speed. Calculations indicate that bubble solution can be a very significant factor in gas exchange. Bubble solution enhances gas input and retards degassing of the water column. Preliminary data show a lag time of about 5 hours in the response of the water column to an atmospheric pressure change.

Although there have been few measurements of air-sea gas exchange, nearly all reports on such measurements point out the possible participation of bubbles; *Redfield* [1948] calculated gas exchange coefficients for the Gulf of Maine and felt that the seasonal variation in the gas exchange coefficient could be explained by 'waves, spindrift, and the bubbles.' In his summary of gas exchange measurements in tanks *Kanwisher* [1963] mentions that bubbles must be important in gas exchange, and he stresses the need to know the volume flux of bubbles under various sea conditions. There have been several experimental tank measurements of gas exchange coefficients; there is a revealing difference between these experimental measurements and coefficients measured (often very indirectly) in the ocean. *Schink et al.* [1970] summarized the experimental and oceanic measurements; the higher gas exchange coefficients were attained in natural conditions. The one characteristic definitely missing from experimental measurements is the large breaking wave with resultant bubble production.

Measurements of oceanic gas concentrations have led to speculation and recently to some definite evidence for gas concentration control by bubble solution. *Benson and Parker* [1961, p. 249] felt that, although their N_2/Ar data were near N_2'/Ar', '. . . it is interesting to note that the experimental curve (N_2/Ar) lies above the theoretical curve (N_2'/Ar') at high temperatures where most surface waters are represented. This would be expected if trapping of air bubbles from surface turbulence were significant. . . .' *Bieri* [1971] and *Craig and Weiss* [1971] presented values of up to 10% for the amount of air injected into the water by bubble solution.

The production of bubbles by breaking waves and the presence of bubbles in the upper few meters of the ocean are facts accepted by anyone who has had the opportunity to be at sea. In a stormy sea the position of a breaking wave is marked for minutes by a greenish blue patch of bubble-laden water contrasted against the normal oceanic blue. As the wind speed rises, the sea surface becomes increasingly covered with foam patches until, during hurricane conditions, the sea surface becomes undefinable because of the confusion of breaking waves, bubbles, and spray. Bubbles produced by a breaking wave are carried down the water column by vertical turbulence. Visual observations from the bow port of the R.V. *Atlantis* led *Kanwisher* [1963] to estimate that bubbles penetrated the water column to a depth equal to 2–3 times the wave height. On the average, especially at a higher wind speed and a higher density of breaking waves, the bubble density at a given locality in the water column will remain constant, even though bubbles are constantly passing through the given locality. Under normal circumstances these bubbles will go into solution because of hydrostatic pressure and

[1] Now at Skidaway Institute of Oceanography, Savannah, Georgia 31406.

Copyright © 1973 by the American Geophysical Union.

surface tension. Therefore they represent a source of dissolved gas distributed throughout the water column. This paper demonstrates the magnitude and characteristics of bubble solution of air-sea gas exchange.

SPECTRA AND SOLUTION RATES OF BUBBLES

Because of recent advancements in underwater acoustical research, limited data are available on the size-frequency relationship of bubbles in the surface layer of the ocean; unfortunately, acoustical methods are not reliable at high bubble populations, and no measurements have been made above sea state 2 (wind speed $U = 3$ m/sec). *Medwin* [1965, 1970] used both attenuation and backscattering techniques to measure spectra of bubbles in an isothermal oceanic surface layer during sea state 2. His observations agree qualitatively with results of wind tank experiments by *Glotov et al.* [1962]; a maximum is found at 0.005–0.0150 cm. Medwin's results compare quantitatively with the visual observations of *Blanchard and Woodcock* [1957] (see *Medwin* [1970, Figure 6]). This agreement exists even though the Blanchard and Woodcock observations were in the surf zone and Medwin's were during sea state 2 in the open ocean, when few waves are breaking. *Monahan* [1971] has shown that no breaking waves are present at wind speeds of <3.6 m/sec. If this is true, Medwin's values at a wind speed of about 3 m/sec may be fortuitous, but regardless these values do agree with Blanchard and Woodcock's and will adequately serve as a base for the following calculations. Figure 1 shows a typical oceanic bubble spectrum adapted from *Medwin* [1970, Figure 6]; the maximum frequency at about 0.01 cm is a result of the high solution rates of small bubbles and the high buoyancy of larger bubbles. *Turner* [1961] has shown that bubbles with a radius of <0.0050 cm are stable; although they may appear in a measured spectrum, they are not contributing gas to the water column via bubble solution. The $N(r, U, z)$ refers to the number of bubbles of radius r during wind speed U at depth z. The radius bandwidth dr is 0.0001 cm (1 μm).

DEPTH DEPENDENCE OF BUBBLE SPECTRA

Schulkin [1969] used the following equation as an estimate of the depth dependence of bubble spectra:

$$N(r, U, z) = N(r, U, 1) \cdot (1 - z/L)^{1/2}(1 + z/11)^{1/2} z^{-1/2} \quad (1)$$

where z is the depth in yards and $N(r, U, 1)$ is the bubble density of radius r at the surface (z = yard). For dimensional correctness, $z^{-1/2}$ is understood to mean $(z/1 \text{ yd})^{-1/2}$. According to Schulkin, $(1 - z/L)^{1/2}$ represents the mixing property of the isothermal layer, $z^{-1/2}$ is the natural decay of bubble density with depth, and $(1 + z/11)^{1/2}$ is the contribution of deeper nonsurface bubble sources or bubbles released in air-saturated water by decompression at the crests of internal waves. The actual importance of the decompression process in bubble production is unknown; however, the $(1 + z/11)^{1/2}$ term makes a relatively small contribution to $N(r, U, z)$ and will be retained for completeness. The $z^{-1/2}$ term creates a problem because, as z approaches 0 from 1, $z^{-1/2}$ approaches infinity. This could be avoided by using e^{-z}, but, for the sake of using Schulkin's complete formula, $z^{-1/2}$ will be retained. It must be remembered that the surface refers to 1 meter or 1 yard. For the purposes of the study it is assumed that meters and yards are equivalent. Equation 1 is shown in Figure 2 for a mixed layer depth of 10 and 20 meters. Bubble fre-

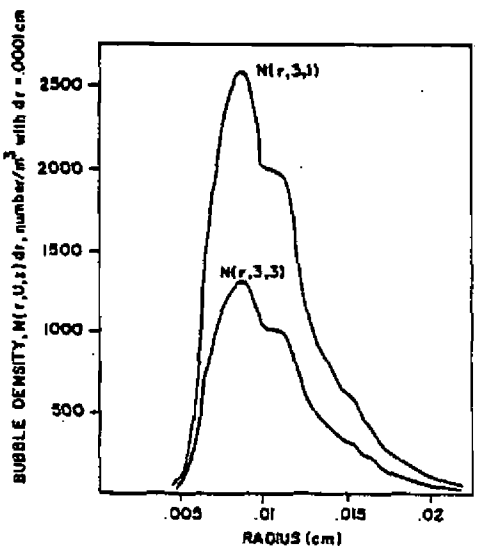


Fig. 1. Medwin's $N(r, 3, 3)$ size frequency bubble spectrum and the calculated surface spectrum.

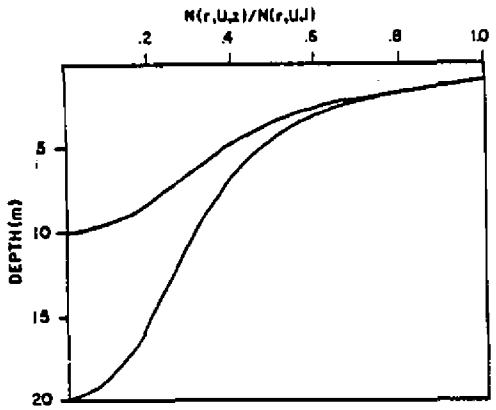


Fig. 2. Bubble frequency versus depth normalized to the surface spectra $N(r, U, 1)$.

quency is expressed as a fraction of the frequency at 1 meter. There is a rapid drop of bubble density in the first 5 meters, then a more gradual decrease to the bottom of the mixed layer.

Calculations of Surface Bubble Spectra

The only data of any use in calculating surface bubble spectra are from *Medwin* [1970, Figure 6]. These data are from sea state 2 ($U = 3$ m/sec) and a depth of 3 meters ($z = 3$ meters). If we use (1) and a mixed layer depth of 10 meters ($L = 10$ meters), Medwin's data are converted to a $U = 3$ surface spectrum by the following calculation:

$$N(r, 3, 1) = N(r, 3, 3) \cdot (1 - z/10)^{-1/2}(1 + z/11)^{-1/2}3^{-1/2}$$

$$\cong 2.0N(r, 3, 3) \qquad (2)$$

The results of this calculation are shown in Figure 1. Changing the mixed layer depth L changes the ratio $N(r, 3, 1)/N(r, 3, 3)$ only slightly. For example, if $L = 20$ meters, $N(r, 3, 1) = 1.8N(r, 3, 3)$, a 10% change.

Wind Dependence of Bubble Spectra

Schulkin [1969] found that sound energy transmitted in the mixed layer is increasingly attenuated with rising wind; he attributed much of the attenuation to bubbles. *Glotov et al.* [1962] felt that the number of bubbles increased exponentially with wind speed during his tank experiments, although other lines of evidence would justify the use of a square extrapolation to estimate the increase of bubble density with wind speed. For example, it is well known that wind stress increases with approximately the square of the wind speed, and *Kanwisher* [1963] and *Downing and Truesdale* [1955] found gas exchange rates to increase with the square of the wind speed. *Blanchard* [1963] found a square law dependence of whitecap coverage on wind speed. More recently, *Monahan* [1971] has demonstrated a dependence on the 3.3 power of the wind.

To calculate the surface bubble spectra for wind speeds other than 3 m/sec, a square law is used to keep the calculation as conservative as possible.

$$N(r, U, 1) = aU^2 \qquad (3)$$

where a is a radius dependent proportionality coefficient. No doubt a is some function of wind speed; at higher wind speeds large bubbles stay in suspension longer as increased turbulence overcomes buoyancy forces. The exact relationship is not known and will have to be ignored in this study. Here a is calculated for each radius at $U = 3$ then used to calculate $N(r, U, 1)$ for various values of U. That is,

$$a = N(r, 3, 1)/3^2$$

$$N(r, U, 1) = N(r, 3, 1)U^2/3^2 \qquad (4)$$

A table was then prepared listing surface bubble spectra versus wind speed.

Solution Rate of Bubbles

Bubble solution rates are quite well known, and the following derivations are from *Wyman et al.* [1952] and *Blanchard and Woodcock* [1957]. According to the general gas law,

$$n = 4\pi r^3 p/3RT \qquad (5)$$

where n is the number of moles of gas in the bubble, R is the gas constant, T is the absolute temperature, r is the bubble radius, and p is the pressure in the bubble. If the surface tension is included, as it should be, the pressure in the bubble will be atmospheric pressure plus hydrostatic pressure plus $2\gamma/r$, the pressure due to surface tension. According to Fick's law of diffusion,

$$dn/dt = -\delta 4\pi r^2(p + 2\gamma/r - p_0) \qquad (6)$$

where $2\gamma/r$, the pressure due to surface tension, is included, p_0 is the partial pressure of air in the bulk water, and δ is a constant defined by $\Delta s/d$, where Δ is the diffusion constant of air in water, s is the solubility of air in water, and d is the shell thickness of water around the bubble across which the diffusion gradient occurs. Differentiating (5) with respect to time and then equating that with (6) and substituting $dV = 4\pi r^2 dr$, we obtain the following equation:

$$dV/dt = -\delta RT 12\pi r^2[r(p - p_0) + 2\gamma]/(3pr + 4\gamma) \quad (7)$$

If we use the values $RT = 2.4 \times 10^4$ cm³ atm/mole, $\gamma = 76 \times 10^{-4}$ atm cm, $\delta = 5 \times 10^{-9}$ mole/cm³ sec atm [*Wyman et al.*, 1952] and let $p = 1 + (z/10)$, (7) reduces to

$$dV/dt = 4.52 \times 10^{-3} r^{-3}[z/10 + 1 - p_0 + 2(76 \times 10^{-6})/r]/[3(z/10 + 1)r + 4(76 \times 10^{-6})] \quad (8)$$

The sign was changed to denote input of gas to the water column. Here p_0 will normally be near 1 atm, and thus it is indicated that the water is saturated.

Source Strength Calculation

The source strength $S(z)$ is the time rate of diffusion of a volume of gas bubbles with a radius between r and $r + dr$ per unit volume of liquid at depth. At each depth, $S(z)$ is

$$S(z) = \int_0^\infty \left(\frac{dV}{dt}\right)_{z,r} N(r, U, z)\, dr \quad (9)$$

To apply this integral to the data derived from Medwin's observations, the following summation is used:

$$S(z) = \sum_{r=0.0046}^{0.02} 5\left(\frac{dV}{dt}\right)_{z,r} N(r, U, z) \quad (10)$$

The surface spectrum was digitized at 0.0005-cm intervals, and so the 5 is placed in (10) to change to a 0.0001-cm interval for summation. The dV/dt is calculated by using (8). Figure 3 shows the results of these calculations for $L = 20$ meters and $U = 10$, 20, 30, and 40 m/sec. Between 0 and 1 meter, $S(z)$ cannot be calculated because, as was mentioned earlier, the depth distribution equation (1) goes to infinity between 1 and 0. Intuitively, I feel that the source strength must be very near 0 at the surface, since the bubble solution rate dV/dt as calculated by equation (8) is near 0 at $z = 0$. Therefore $S(z)$ is extrapolated from $S(1)$ to $S(0) = 0$.

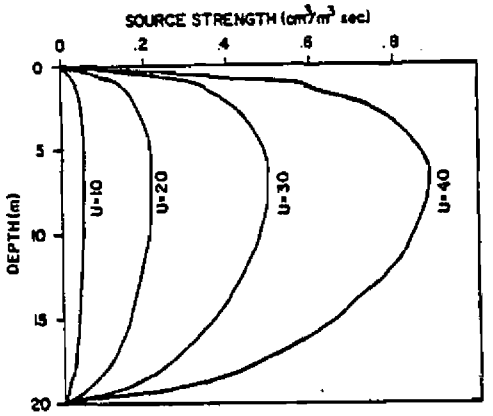


Fig. 3. Source strength versus depth at various wind speeds.

Estimate of Flux Due to Bubble Solution

The source strength at each depth also represents a flux of gas across the air-sea interface. By integrating the source strength (9) with depth, a surface flux can be calculated:

$$\text{Flux} = \int_0^L S(z)\, dz = \int_0^L \int_0^\infty \left(\frac{dV}{dt}\right)_{z,r} N(r, U, z)\, dr\, dz \quad (11)$$

The surface flux is calculated by using the estimate of (10) for the inner integral. The results are in Table 1. Since this flux is only in the area where whitecaps (and thus bubbles) occur, it must be corrected to represent an average flux for each square centimeter of the surface of the sea. The corrected flux is calcu-

TABLE 1. Calculated Flux at Various Wind Speeds for L = 20 Meters

Wind, m/sec	Flux, cm³/cm² sec	Corrected Flux, cm³/cm² sec
10	0.7×10^{-4}	0.017×10^{-4}
20	3.5×10^{-4}	0.9×10^{-4}
30	7.3×10^{-4}	7.3×10^{-4}
40	13.9×10^{-4}	13.9×10^{-4}

lated from *Monahan* [1971, equation 6]. This equation predicts whitecap coverage with wind speed. As was noted by *Blanchard* [1971], *Monahan's* [1971] values probably underestimate the horizontal area where bubbles are present, and thus the correction results in a very conservative estimate. The point is that quite a respectable flux is implied by the mere presence of bubbles in the water column.

Similar implications can be found by using only Medwin's original spectra and minor assumptions concerning the depth distribution.

COMPARISON WITH A STORM REQUIRED FLUX

During the passage of a typical storm the atmospheric pressure may fall and rise 10 to 20 mm Hg or about 1–2%. During the pressure change, gas will transfer from one phase to another at a rate dependent on the partial pressure difference and wind. If we assume a 20-mm Hg pressure drop during 12 hours and a 20-meter mixed layer, a flux of -1.8×10^{-4} cm³ air/cm² sec would be required to maintain equilibrium. Then, as the pressure rises, the flux would be $+1.8 \times 10^{-4}$ cm³ air/cm² sec. If the wind speed is 20 m/sec on the average, the solution of bubbles can contribute approximately 0.9×10^{-4} cm³/cm² sec, or half the flux required to maintain equilibrium. It is clear that the solution of bubbles significantly affects the flux of air in and out of the water column. In fact, bubbles may be a severe impediment to degassing of the water column.

COMPARISON WITH SEASONALLY REQUIRED FLUX

The normal seasonal heating and cooling of the water column causes gas to move across the interface. The flux is dependent on the amount of heating or cooling. In temperate latitudes the mixed water column may vary 20°C. If we assume a 20-meter water column and a normal salinity, the seasonal change would cause a flux of 8.5×10^{-7} cm³/cm² sec. Of course, this is the average for a season, and it could be expected that at times of extreme heating or cooling the required flux could be much higher. *Redfield* [1948] found the annual exchange in the Gulf of Maine to be 1.9×10^{-4} cm³/cm² sec. These values are again much less than the $\sim 10^{-4}$-cm³/cm² sec flux resulting from bubble solution.

ONE-WAY EFFECT AND LAG TIME

Clearly, one of the incongruities in considering the role of bubbles in interfacial mass transfer is the one-way effect. Bubbles and their solution cause a transfer of gas into the water column because, once a bubble enters the main part of the water column, it will never reach the surface. Only bubbles that penetrate just the upper meter or so have any chance of reaching the surface before disappearing because of solution. Thus the effect of bubble solution on gas transfer from air to water is much easier to visualize than that from water to air. In this paper, only the air-water route will be considered. Since the object of this paper is to show that bubbles can indeed affect gas transfer in a substantial way, this limitation is valid. A theoretical development that considers the motion of a bubble in the velocity field of a breaking wave and turbulent mixed layer could lead to new insight into the problem.

If we assume a steadily changing atmospheric pressure, the gas content of the water column should decrease or increase correspondingly. Figure 4 shows how the expected integrated gas content of the mixed water column changes with time in response to changing atmospheric pressure. As atmospheric pressure drops, the total gas in the water column begins to decrease but lags behind the pressure drop. This lag results from the gas input by bubble solution and the mixing characteristics of the water column. As the atmospheric pressure begins to rise again, the water column gas content increases but again lags behind the rise in atmospheric pressure by an amount less than that during degassing. The lag here is caused by the

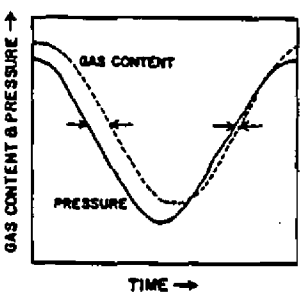


Fig. 4. Variation of mixed-layer gas content with changing pressure. Left center arrows indicate gassing lag, and right center arrows indicate degassing lag. Units are arbitrary.

mixing characteristics of the water column.

Data obtained from the offshore oil rig Sedneth-1 give an indication of the effect of lag time. Figure 5 shows a plot of the difference between the averages of the 0- and 4-meter and the 8- and 12-meter N_2 samples. With a pressure drop of 17 mb the gas content in the 0- to 6-meter interval drops in relation to the 6- to 12-meter interval, and thus it is indicated that the deeper waters of the mixed layer are not in contact with the interface as much as the surface water, as would be expected. The wind during the period started at 25 m/sec, fell to 9 m/sec, and toward the end rose to 16 m/sec. The data show how the water column does not act as a thoroughly mixed bulk water-interface water system but rather the waters of the mixed layer have sporadic depth dependent encounters with the surface. A lag time of approximately 5 hours is indicated.

CONCLUSION

The simple calculations that were made clearly indicate a potential gas flux into the water column resulting from a bubble solution of about 10^{-4} cm³/cm² sec. With even more conservative estimates of bubble populations and lower solution rates because of organic films, the potential flux is still considerable. The one-way effect surely causes higher rates of ingassing relative to degassing. Further theoretical treatment could consider the motions of bubbles in the turbulent mixed layer. This approach would be analogous to particle motion theories with the added complications of buoyancy and depth and radius dependent solution rates. The implications of air bubble solution on the distribution of gases in the mixed layer is discussed by *Atkinson* [1972], and a paper is being prepared on the subject.

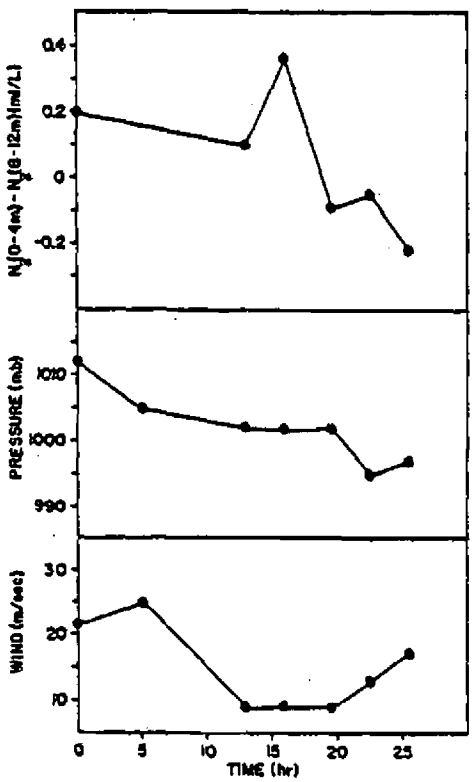


Fig. 5. Change of relative amounts of N_2 in the water column in response to dropping pressure.

Acknowledgments. I wish to acknowledge the discussions with Drs. P. Wangersky, R. Cooke, R. Overstreet, and Mr. T. Yoshinari. This work was part of a Ph.D. thesis submitted to Dalhousie University. Shell Oil Canada. Ltd. is thanked for their cooperation during the use of the offshore oil rig Sedneth-1.

Support was provided by Dalhousie University, National Research Council of Canada, and the Department of Energy, Mines, and Resources.

REFERENCES

Atkinson, L. P., Air bubbles in an oceanic mixed layer: Effect on gas concentrations and air-sea gas exchange, Ph.D. thesis, Dalhousie University, Halifax, Nova Scotia, 1972.

Benson, B. B., and P. M. Parker, Nitrogen/argon and nitrogen isotope ratios in aerobic seawater, *Deep Sea Res., 7,* 237–253, 1961.

Bieri, R. H., Dissolved noble gases in marine waters, *Earth Planet. Sci. Lett., 10,* 329–333, 1971.

Blanchard, D. C., The electrification of the atmosphere by particles from bubbles in the sea, *Progr. Oceanogr., 1,* 71–202, 1963.

Blanchard, D. C., Whitecaps at sea, *J. Atmos. Sci., 28,* 645, 1971.

Blanchard, D. C., and A. H. Woodcock, Bubble formation and modification in the sea and its meteorological significance, *Tellus, 9,* 145–157, 1957.

Craig, H., and R. F. Weiss, Dissolved gas saturation anomalies and excess helium in the ocean, *Earth Planet. Sci. Lett., 10,* 289–296, 1971.

Downing, A. L., and G. A. Truesdale, Some factors affecting the rate of solution of oxygen in water, *J. Appl. Chem., 5,* 570–581, 1955.

Glotov, V. P., P. A. Kolobaev, and G. G. Neuimin, Investigation of the scattering of sound waves by bubbles generated by an artificial wind in seawater and the statistical distribution of bubble sizes, *Sov. Phys. Acoust., 7,* 341–345, 1962.

Kanwisher, J., On the exchange of gases between the atmosphere and the sea, *Deep Sea Res., 10,* 195–207, 1963.

Medwin, H., Design and use of an acoustic spectrometer for the detection of particulate matter and bubbles in the sea, paper presented at 5th International Congress on Acoustics, Liège, Belgium, 1965.

Medwin, H., In situ acoustic measurements of bubble populations in coastal ocean waters, *J. Geophys. Res., 75,* 599–611, 1970.

Monahan, E. C., Oceanic whitecaps, *J. Phys. Oceanol., 1,* 139–144, 1971.

Redfield, A. C., The exchange of oxygen across the sea surface, *J. Mar. Res., 7,* 347–361, 1948.

Schink, D. R., J. J. Sigalove, R. L. Charnell, and N. L. Guinasso, Jr., Use of Rn/Ra ratios to determine air/sea gas exchange and vertical mixing in the ocean, *Rep. Paltr 223,* p. 43, Teledyne Isotop., Palo Alto, Calif., 1970.

Schulkin, M., The propagation of sound in imperfect ocean surface ducts, *Rep. 1013,* p. 128, U.S. Navy Underwater Sound Lab., New London, Conn., 1969.

Turner, W. R., Microbubble persistence in fresh water, *J. Acoust. Soc. Amer., 33,* 1223–1232, 1961.

Wyman, J., P. F. Scholander, G. A. Edwards, and L. Irving, On the stability of gas bubbles in seawater, *J. Mar. Res., 11,* 47–62, 1952.

(Received August 2, 1972;
revised October 31, 1972.)

ATLANTIC OCEANOGRAPHIC LABORATORY

BEDFORD INSTITUTE

DARTMOUTH, NOVA SCOTIA

ENVIRONMENTAL RELATIONSHIPS AND DISTRIBUTION OF PLANKTONIC FORAMINIFERA IN THE EQUATORIAL AND NORTHERN PACIFIC WATERS

by

R.K. BANERJI, C.T. SCHAFER and R. VINE

AOL REPORT 1971-7

JUNE 1971

ABSTRACT

Twenty-nine plankton tows were collected at different water depths in the equatorial and northern Pacific Ocean during the HUDSON 70 cruise. Thirty planktonic foraminiferal species, belonging to eleven genera and three families, have been identified. Absolute and relative abundance of individual species, their size, structural modifications, and coiling directions of the tests are compared with the physical and chemical parameters of the Pacific Water masses. Five major groups of species including warm tropical, warm temperate, cold temperate, cold water and cosmopolitan, were mapped in three different water masses designated here as - Southern, Central and Northern or Subarctic. The abundance ratio of specimens in surface compared to subsurface waters is approximately 5:1. A weak direct relationship exists between water temperature and salinity and the absolute abundance and species diversity of the foraminifera population. There appears to be no simple relationship between size, maturity of forms and various physical factors generally considered to affect the entire faunal assemblage. Kummerform development appears to be an ontogenic feature more or less independent of surrounding physical conditions.

Typical specimens of *Globigerina pachyderma* (Ehrenberg) occur in large numbers in the Northern water mass of the Pacific. Reproduction cycles of several species (e.g. *Globorotalia scitula* (Brady) and *Globorotalia truncatulinoides* (D'Orbigny)) are confirmed indirectly, based on the extreme paucity of specimens in the samples analyzed for this study.

INTRODUCTION

The planktonic foraminifera are free-floating marine protozoans having an external calcareous test. There are more than 30 species known to exist in the present day oceans and these belong to the families Globigerinidae, Globorotaliidae and Hantkeninidae. These protozoans have shown considerable promise as indicators of distinct oceanographic environments (Boltovskoy, 1967) and thus can be used to provide a better understanding of the interrelationships of present day oceanic water masses. In fossilized form, apart from their importance in stratigraphic correlations, planktonic foraminifera can provide useful information concerning ancient water mass and current distribution patterns.

Our present knowledge of planktonic foraminifera dates back to 1826 with the general taxonomic investigations made by D'Orbigny. The geographic distribution of more than 20 species living in present day oceans was established for the first time during the cruise of the HMS *Challenger* from 1872-76 (Brady, 1884). Murray (1897) was the first to recognize the pelagic habit of these organisms, and subsequent investigations by various workers established the importance of planktonic foraminifera in the study of paleoclimatic and paleoecological variations. However, the ultimate key to the understanding of the paleoecological change recorded by these organisms depends upon the careful study of the ecological relationships of living planktonic foraminifera in present oceans.

In recent years, the value of planktonic foraminifera as environmental indicators has increased markedly. Most of these planktonic organisms are sensitive to environmental changes and are often restricted by a few limiting factors which are related to their associated water mass. Temperature, salinity, depth of water, latitudinal variations and inorganic and organic solutes in the surrounding water column are perhaps important. Unfortunately, their direct influence on the physiology of planktonic foraminifera has not been studied experimentally. Hence, the relative importance of these factors on the growth of these protozoans can only be determined by comparing distributional data with other hydrogeological parameters typical of present oceans.

Detailed systematic and quantitative studies of the regional distribution of living planktonic foraminifera have been made by a number of workers mostly in the Atlantic Ocean. However, except for the classic work of Bradshaw (1959) and Parker (1960, 1962) in the north and south Pacific, there have been no detailed investigations in the Pacific Ocean for the last decade. Planktonic foraminifera were collected in the Pacific Ocean between latitude 15°S (near Tahiti) and 55°N (near Vancouver) along longitude 150°W during the HUDSON 70 cruise (figure 1). It is within the scope of this study to identify the species of living planktonic foraminifera that occur in the north and equatorial Pacific, to delimit their geographical distribution and abundance, and to relate the observed distributions to measured physical, chemical, and biological parameters.

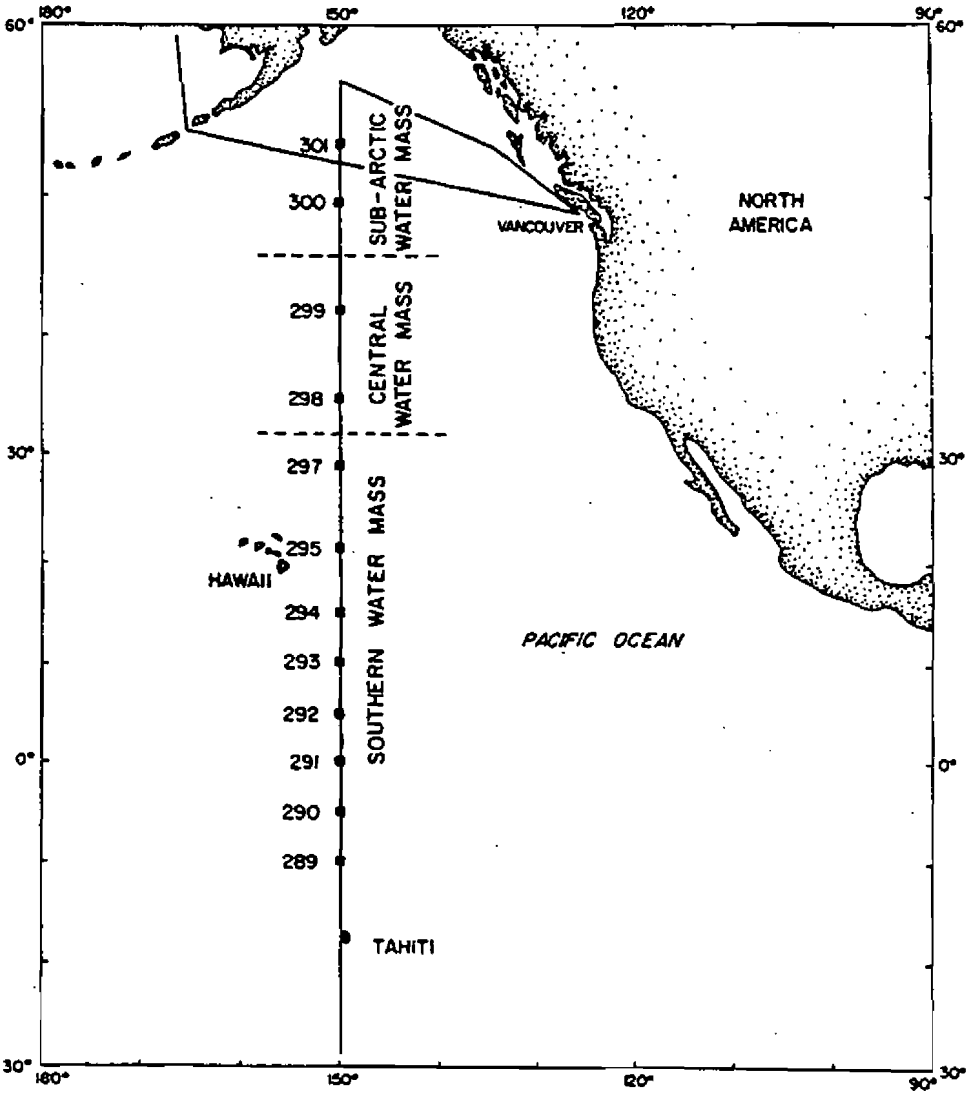


FIGURE 1: Station Locations of Tahiti-Vancouver leg of HUDSON 70 expedition

PREVIOUS WORK

The majority of the publications concerning Pacific planktonic foraminifera appear, to date, to deal mainly with observations on the systematics of various plankton groups occurring in dredged samples and give very little emphasis to environmental relationships.

The first systematic study of living planktonic foraminifera in the Pacific Ocean was conducted by Brady (1884) and Murray (1895). Further reports on the occurrence of planktonic foraminifera were made by Agassiz (1902). Heron-Allen and Earland (1922) studied the plankton samples collected from near New Zealand during the British Antarctic (*Terra Nova*) expedition. Since then, little progress has been made in this field of investigation until the publication of the reports by King and Hida (1957) dealing with variations in the abundance of foraminifera in the equatorial Pacific. In this case, however, no emphasis was placed on the actual distribution of individual species.

Bradshaw's (1959) classic work on the ecology of living planktonic foraminifera in the north and equatorial Pacific Ocean represents a major breakthrough in the long gap of research quiescence. Bradshaw (*op. cit.*) studied the foraminifera from more than 700 plankton samples collected in the north and equatorial Pacific. Twenty-seven species were identified and grouped together into four biogeographic faunas including cold, transitional, central and equatorial. The faunal boundaries coincided with hydrological divisions based on temperature and salinity data. One of the interesting observations made by Bradshaw was that the highest populations of planktonic foraminifera per unit volume of water occurred in the subarctic water mass and at limited localities in the equatorial region. The lowest concentrations were found in the central oceanic areas. He (*op. cit.*) suggested that the abundance was controlled by variations in the distribution of inorganic phosphates.

Parker (1960) extended Bradshaw's study towards the equator and South Pacific by noting the distributional patterns of 16 of the more common planktonic species of foraminifera. She (*op. cit.*) concluded that temperature may be more important than salinity in controlling their distribution. In a later publication (1962) she discussed the systematics of all the planktonic species recorded by her from the South Pacific. Subsequently, the planktonic foraminifera of the Pacific Ocean were largely neglected as later workers began to concentrate their efforts on the fauna of the Atlantic Ocean.

FIELD AND LABORATORY METHODS

Plankton tows were collected with a modified Benthos Multiple Plankton Sampler fitted with 200-micron mesh nets. This type of net is suitable for studying the vertical distribution of planktonic foraminifera because samples can be obtained from specific depth ranges. The device was initially submerged to a depth of 25 metres and towed at a speed of about 1.5 knots for 15 minutes. Two additional tows were made during each cast at 350 and 750 metre depths respectively. The samples collected represent planktonic specimens resident in the 0-200, 200-500 and 500-1000 metre water layers respectively (Table 1). It is assumed, however, that the concentration of planktonic foraminifera is roughly constant in the water layers and that there is no appreciable diurnal change in the faunal population. The volume of water filtered through the nets was monitored using a Tsurumi-Seiki-Kosakusho flow meter attached to one side of the sampler frame. It was integrated with a Benthos Model 1023 acoustic telemeter. The samples were washed from each net and preserved in 10% formalin solution buffered with hexamethylene tetramine.

In the laboratory, the plankton samples were split into a number of fractions depending upon their plankton concentrations. This procedure was used to reduce the final subsample to a convenient size. On the average, half-splitting was found to be satisfactory.

The split sample was sieved through a 63-micron mesh and the retained material then ignited in a low temperature TRACERLAB LTA 600 asher to remove the organic constituents (Vilks, 1970).

After ashing the samples were washed with water and later transferred to a disposable Millipore petri dish. The foraminiferal counts and other morphological observations were made on this petri dish using binocular microscopy. Detailed morphological features were studied using a JEOL Scanning Electron Microscope.

Factor analysis of the faunal data and of other physico-chemical parameters such as latitude, depth, temperature, salinity, oxygen, phosphates and nitrates, etc., was carried out by computer. During the course of the analysis the matrix of correlation between 29 plankton samples with respect to all available parameters was determined. The program used was written by Cameron (1967) and recently modified by R. Cranston (Marine Geology Section - personal communication).

TABLE I

SAMPLING DEPTHS AND GENERAL FAUNAL DETAILS

STA.	DATE	LOCATION		DEPTH OF TOWS (METRES)	VOLUME OF WATER FILTERED (M^3)	SPECIES DIVERSITY (%)	ABSOLUTE ABUNDANCE (1000 M^3)	SPECIMEN TO SPECIES RATIO	PERCENTAGE OF KUMMERFORM
		LAT. N-S	LONG. W						
1	2	3	4	5	6	7	8	9	10
289	MAY 8	10°S	150°W	0 - 190	194.2	50.00	8205	547.00	03.01
				190 - 460	67.5	30.00	0623	69.22	04.76
				460 - 760	295.6	30.00	0231	25.66	08.82
290	MAY 20	5°S	150°W	0 - 200	261.8	53.33	7975	498.44	06.90
				200 - 435	878.3	23.33	0036	05.14	06.66
				765 - 0	730.5	20.00	0057	09.50	04.76
291	MAY 21	0°	150°	0 - 800	2483.1	46.66	5847	417.64	16.61
292	MAY 23	5°N	150°	0 - 800	1638.5	66.66	3187	159.35	12.77
293	MAY 24	10°N	150°W	0 - 190	409.6	53.33	1727	107.94	04.52
				190 - 460	595.4	53.33	1547	96.81	11.95
				460 - 750	532.0	46.66	0599	42.78	07.54
294	MAY 26	15°N	150°W	0 - 170	565.8	63.33	2010	105.79	02.29
				170 - 450	426.5	43.33	0156	012.00	09.09
				450 - 780	553.2	40.00	0481	40.08	06.01
295	MAY 28	22°N	150°W	0 - 180	384.2	63.33	2319	122.05	04.70
				180 - 440	426.5	40.00	0343	28.58	04.11
				440 - 1050	447.6	26.66	0060	07.50	14.29
297	MAY 30	29°N	150°W	0 - 160	506.7	36.66	0273	24.81	05.80
				160 - 475	536.3	40.00	0263	21.91	05.63
				475 - 1030	532.1	36.66	0067	06.91	05.88
298	MAY 31	36°N	150°	0 - 320	777.0	40.00	0112	09.33	09.30
				0 - 900	1554.0	30.00	0244	01.39	08.60
299	JUNE 2	43°N	150°W	0 - 185	443.4	30.00	1342	149.11	12.75
				185 - 850	2010.1	36.66	0746	67.81	14.44
				185 - 0	304.0	30.00	0810	90.00	12.19
300	JUNE 4	49°N	150°W	0 - 1050	3606.4	20.00	1538	256.33	22.19
301	JUNE 5	55°N	157°W	0 - 190	629.2	20.00	0906	151.00	60.48
				100 - 700	2326.8	26.66	0241	030.13	36.80
				100 - 0	312.5	20.00	1439	239.83	43.55

MODIFICATIONS TO BENTHOS MULTIPLE PLANKTON SAMPLER

The net used to collect samples for this study is based on a design produced commercially by Benthos Inc. of North Falmouth, Massachusetts. The sampler consists primarily of a triangular steel frame to which are attached the mouths of three plankton nets. The nets are attached by two points at either end of the frame base (figure 2-A). Because the mouth of the net has been interwoven with 1.7 cm natural rubber tubing it is possible to stretch it into a triangular-shaped opening by attaching a part of its edge to a third point on the triangular frame (figure 2-B,C). Steel rings are used to attach the two lower corners of the nets to the frame; similar rings are used to fasten the upper corner of the nets to the three Benthos 'Pressure Powered Pin' releases. When the device is launched, the first net is held open by the first release pin while the other two nets are folded and held above the first in the upper part of the frame using the two remaining releases (figure 2-C). When the first release pin is activated the upper corner of the first net is closed by the elastic action of the rubber tubing; a ring fastened to the middle of the bottom side of the second net is also released simultaneously thus allowing the second net to open. Activation of the second release pin causes the second net to close and the third net to open. The third release pin holds only the top of the third net so that when it is released the third net is closed and the device may then be retrieved.

In the original Benthos sampler, standard Benthos 'Pressure Powered Pin' releases were used to activate the system. Three releases were mounted on the net frame so that the rings, which are fastened to the nets, could be looped over the outer ends of the respective net pin release shafts (figure 3-E). Calibration curves were supplied by Benthos equating the diameter of shear pins made from various materials to the depth at which these pins could be expected to shear when used in the 'Pressure Powered Pin' systems. The use of various pin diameters, and of pin material, enabled the closing and opening of individual nets at preselected water depths. Thus, it was possible to obtain large samples of plankton from three discrete depths during the same tow.

It was found in this, and in other operations using the 'Pressure Powered Pin' shear release systems, that considerable variation occurred in the release depth when using a shear pin of a given size and material as supplied by Benthos Inc. This made it difficult to predict with precision the actuation depth of the Pressure Powered Pins at sea. A series of tests was conducted to determine the reliability of the release system and how it could be improved. The results showed that there was about a ±20% variation (with respect to calculated figures) between independent shear pins of similar size and material. This situation was improved greatly by using shear pins cut from a single length of aluminum welding wire. It was found that a small piece of welding wire could be sheared in a pressure test tank to obtain an actuation depth and that the remainder of the pin could then be used to release the net at sea. Using this technique an accuracy of about ±2% was obtained. Frequent cleaning and lubrication of the release assemblies also improved their performance.

Additions to the basic sampler system included a Benthos Telemetering Pinger which was linked to various magnetic switches and sensors also mounted

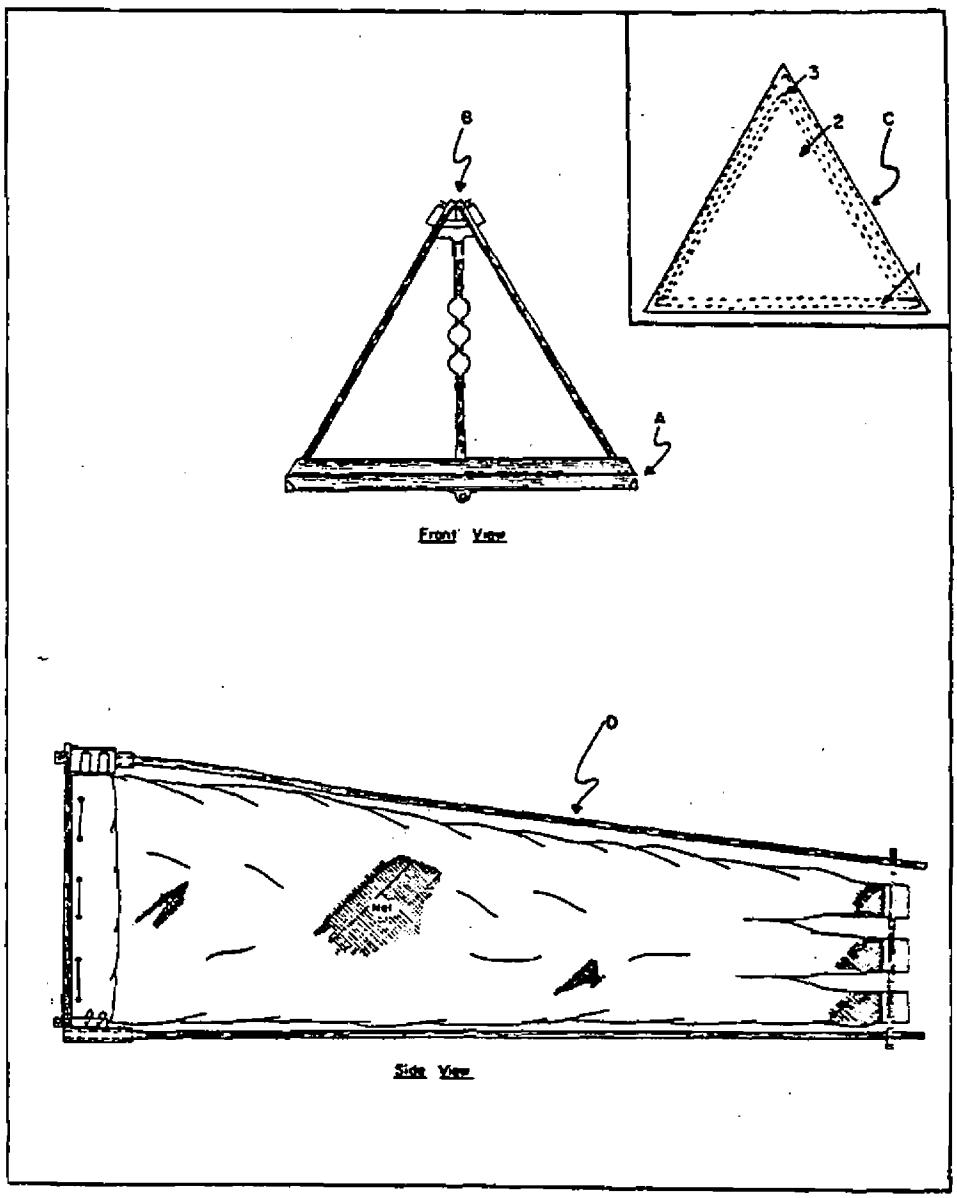


FIGURE 2: Front and side view of modified net frame and diagram showing configuration of nets. In (C) net #1 is closed, #2 is open and #3 is closed and folded above #2.

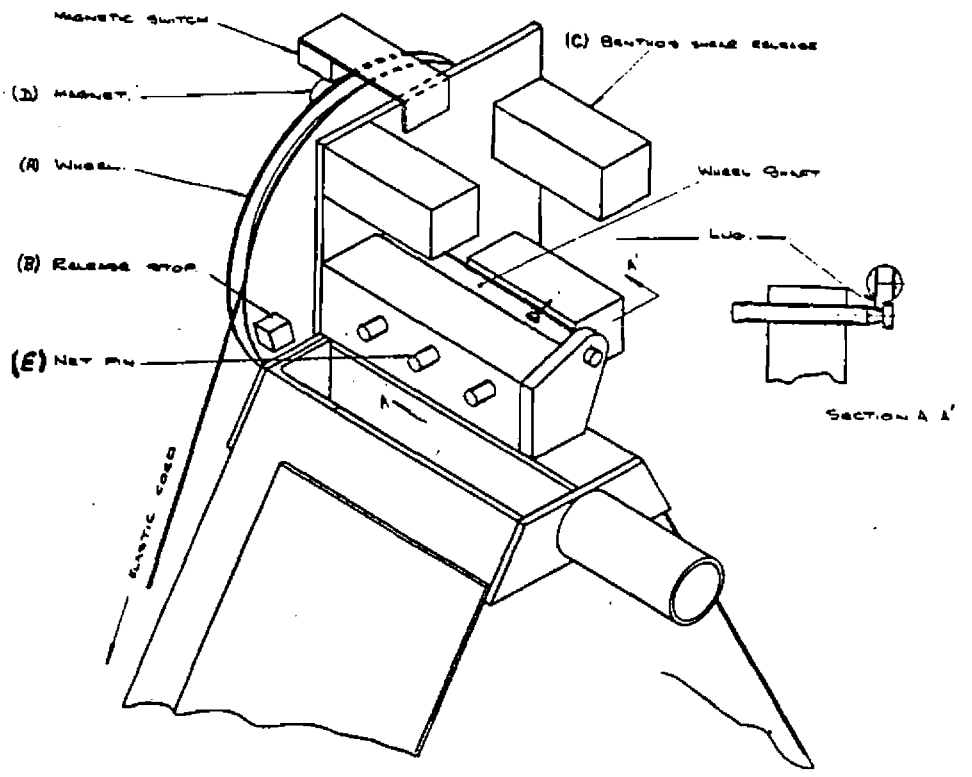


FIGURE 3: Diagram of release linkage used to open and close up three individual plankton nets.

on the triangular part of the net frame. The pinger was used in conjunction with a precision echo-sounder recorder (PESR) so that a continuous record of net depth below the surface, ambient temperature, rate of water flow through the net, and mechanical operation of the 'Pressure Pin' releases could be monitored continuously at the surface (figure 4).

In order to increase the mechanical reliability of the pressure releases a wheel, rotated by an elastic cord and on which was welded three stopping locks, was mounted on the top of the triangular net frame (figure 3-A,B). The first stop rests against the plunger of the first 'Pressure Pin' shear release (figure 3-C). The shaft on which the wheel is mounted contains three small lugs which are aligned with the rods over which the steel net rings are looped. When the first 'Pressure Pin' is actuated, the wheel is rotated by the elastic cord until the second stopping block contacts the plunger of the second 'Pressure Pin' shear release. This rotation causes the first small lug on the wheel to engage and withdraw the rod holding the first two net rings; these rings are connected to the top of net No. 1 and the bottom of net No. 2. Simultaneously, one of the two magnets mounted on the front face of the wheel (figure 3-D) is brought close to a magnetic switch which causes a continuous signal to be transmitted on one channel of the Telemetering Pinger. The signals displayed on the PESR thus give an instant record of this operation (figure 4-R). Actuation of the second 'Pressure Pin' release causes net No. 2 to close and net No. 3 to open; the magnet moves away from the magnetic switch and the continuous signal from the pinger ceases. The third pressure pin closes net No. 3 and a second magnet closes the magnetic switch circuit again, signalling the execution of this last mechanical operation.

A second channel of the Telemetering Pinger is connected to a flow meter mounted in the opening of the net frame. A magnetic switch, mounted next to the revolution counter on the outside of the flow meter, closes briefly after every ten revolutions of the meter impeller. Thus, a short signal is generated on the PESR record and the number of these short signals per centimetre of record is proportional to the flow rate of water passing through the net while the sum of the signals enables calculation of the total volume of water that has been filtered.

Net frame modifications include the addition of two 1-inch diameter tubular sections and a collecting cup clamp which serve to secure the cod end of each net (figure 3-D).

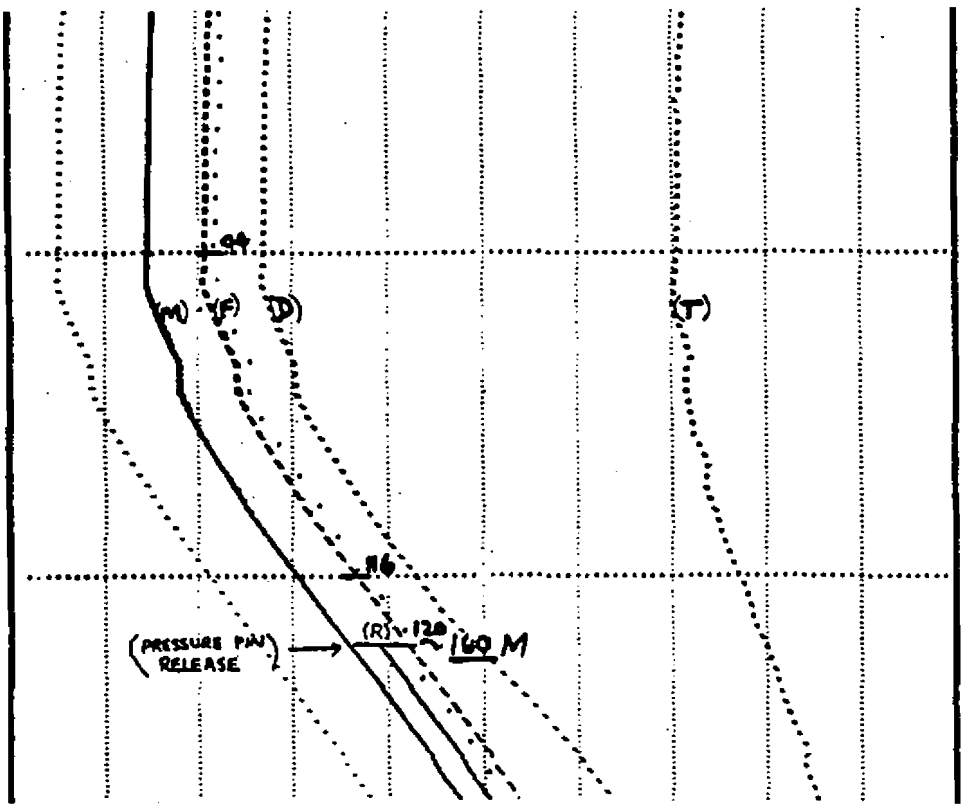


FIGURE 4: Portion of PESR record showing four channels of data that are transmitted continuously; (M) master pulse, (F) flow rate of water through the net, (D) depth of net below the surface, (T) ambient temperature, (R) ON-OFF channel indicating opening and closing of individual nets mounted in the frame.

SPECIFIC OBSERVATIONS

(A) General Aspect of the Planktonic Fauna

All 29 plankton tows in the equatorial and Northern Pacific waters contained foraminifera specimens. In all, 30 species belonging to 11 genera and 3 families have been identified (Table 2); their specific characteristics and their distribution with respect to various hydrological parameters are to be discussed later. In general, the faunal composition is similar to that described by Bradshaw (1959). Most of the species are segregated into restricted horizontal and vertical zones. Based on their associations with certain ranges of water temperature, four groups have been recognized.

(A_1) Warm Water Species Group

This group thrives in the warm water near the equator which is bounded by the 20°C isotherm. Within this group two faunal subgroups can be defined:

(a) Warm Tropical Species Subgroup. This subgroup exists around the equator and to latitude 15°N where the average surface temperature is approximately 25°C. The fauna includes *Candeina nitida* D'Orbigny, *Globigerina calida* Parker, *Globigerinella aequilateralis* (Brady), *Globigerinita glutinata* (Egger), *Globigerinoides conglobatus* (Brady), *Globigerinoides ruber* (D'Orbigny), *Globigerinoides sacculifer* (Brady), *Globigerinoides trilobus* (Reuss), *Globoquadrina conglomerata* (Schwager), *Globoquadrina hexagona* (Natland), *Globorotalia menardii* (D'Orbigny), *Globorotalia tumida* (Brady), *Hastigerina pelagica* (D'Orbigny), *Orbulina universa* D'Orbigny, *Pulleniatina obliquiloculata* (Parker and Jones), and *Sphaeroidinella dehiscens* (Parker and Jones).

(b) Warm Temperate Species Subgroup. This subgroup thrives further north to latitude 30°N and coincides with a surface warm temperature of 20°C. Species common to this subgroup include *Globorotalia inflata* (D'Orbigny), *G. hirsuta* (D'Orbigny) and *Globoquadrina dutertrei* (D'Orbigny). A number of warm tropical forms such as *Globigoinoides ruber* (D'Orbigny), *G. Trilobus* (Reuss), *Globigerinita glutinata* (Egger), *Globigerinella aequilateralis* (Brady) are also present in this subgroup.

(A_2) Cosmopolitan Species Group

Globigerinita glutinata (Egger) is the only true cosmopolitan species present in all the water masses of the northern and equatorial Pacific while *Globorotalia inflata* (D'Orbigny) is present in the subsurface waters at most of the stations.

(A_3) Cold Temperatue Species Group

This group includes forms such as *Globigerina bulloides* D'Orbigny, dextrally coiled *G. pachyderma* (Ehrenberg), *Globoquadrina dutertrei* (D'Orbigny) (large forms), *Globorotalia inflata* (D'Orbigny), along with some cosmopolitan and warm water forms such as *Globigerinita glutinata* (Egger), *Globigerinoides ruber* (D'Orbigny) and *Orbulina universa* D'Orbigny. Members of this group

TABLE 2

LIST OF PLANKTONIC FORAMINIFERAL SPECIES

1. *Candeina nitida* d'Orbigny
2. *Globigerina bulloides* d'Orbigny
3. *Globigerina calida* Parker
4. *Globigerina falconensis* Blow
5. *Globigerina pachyderma* (Ehrenberg)
6. *Globigerina quinqueloba* Natland
7. *Globigerina rubescens* Hofker
8. *Globigerinella adamsi* (Banner and Blow)
9. *Globigerinella aquilateralis* (Brady)
10. *Globigerinita glutinata* (Egger)
11. *Globigerinoides conglobatus* (Brady)
12. *Globigerinoides elongatus* (d'Orbigny)
13. *Globigerinoides ruber* (d'Orbigny)
14. *Globigerinoides sacculifer* (Brady)
15. *Globigerinoides trilobus* (Reuss)
16. *Globoquadrina conglomerata* (Schwager)
17. *Globoquadrina dutertrei* (d'Orbigny)
18. *Globoquadrina hexagona* (Natland)
19. *Globorotalia cavernula* Bé
20. *Globorotalia inflata* (d'Orbigny)
21. *Globorotalia crassaformis* (Galloway and Wissler)
22. *Globorotalia hirsuta* (d'Orbigny)
23. *Globorotalia menardii* (d'Orbigny)
24. *Globorotalia scitula* (Brady)
25. *Globorotalia tumida* (Brady)
26. *Globorotalia truncatulinoides* (d'Orbigny)
27. *Hastigerina pelagica* (d'Orbigny)
28. *Orbulina universa* d'Orbigny
29. *Pulleniatina obliquiloculata* (Parker and Jones)
30. *Sphaeroidinella dehiscens* (Parker and Jones)

thrive in waters from the equator to latitude 43°N, and their northern boundary coincides approximately with the 10°C isotherm.

(A_4) Cold Water Species Group

Globigerina bulloides D'Orbigny, sinistrally coiled *G. pachyderma* (Ehrenberg), *G. quinqueloba* Natland, small forms of *Globoquadrina dutertrei* (D'Orbigny), *Globorotalia cavernula Bé* and the cosmopolitan species *Globigerinita glutinata* (Egger), all of which seem to thrive in waters less than 10°C in the Subarctic regions, comprise this group.

The entire equatorial and northern Pacific regions sampled during this study may be divided into three water masses according to their physical and chemical properties. The water masses from south to north are designated as Southern, Central and Northern or Subarctic Water Masses (figure 1). The boundaries dividing these three water masses coincide approximately with latitude 32°N and latitude 46°N, whereas the northernmost and southernmost boundaries could not be defined due to incomplete coverage. The terms equatorial, northern or southern Pacific as used in this report are, however, purely geographical and relative.

DISTRIBUTION OF PLANKTONIC FORAMINIFERA

(1) Absolute Abundance of Planktonic Foraminifera

The absolute abundance of planktonic foraminifera in a given body of water is generally expressed as the number of individual specimens present per thousand cubic metres of water and this value has been reported by various workers to vary from less than one specimen to 10^8 specimens. This inordinate fluctuation in absolute abundance of planktonic foraminifera is probably due to the physico-chemical complexity of the oceanic water which often manifests itself in the form of local patchiness of foraminifera populations. Sampling methods and laboratory counting procedures employed by various workers can also influence the range of these fluctuations. For example, the clogging of the sampling net restricts the rate of filtration thus causing two counter-effecting errors by lowering the estimate of absolute abundance and by decreasing the effective mesh size thus resulting in an increase in the total catch of specimens. The distributional patterns of planktonic foraminifera obtained from such samples are usually very complicated and not readily amenable to interpretation.

The occurrence of foraminifera in water masses is the result of a complex interaction of various physical, chemical and biological factors of which temperature, salinity and nutrients are the most important. A review of the general hydrographic framework of the Pacific provides a more understandable picture of the distributional patterns. Distributional patterns related to depth of the sea water and latitudes are considered here in context with the observations of the present study.

(1) Variations with Depth

At most stations, three plankton tows were taken at approximately 0-200, 200-500, and 500-1000 metres, designated here as Surface (S), Intermediate (M) and Deep (D) tows, respectively. Broad groupings of faunal abundance at various depths and with respect to different water masses are evident (Table 3).

TABLE 3

ABSOLUTE ABUNDANCE OF PLANKTONIC FORAMINIFERA IN WATER MASSES OF THE NORTHERN AND EQUATORIAL PACIFIC OCEAN

Water Mass	Depth in metres	No. of Specimens per 1000 m^3 Water
Equatorial	Surface to 200	2000 - 8205
	200 - 500	500 - 2000
	500 - 1000	<100
Central	Surface to 200	800 - 1342
	200 - 900	100 - 800
Subarctic	Surface to 200	1000 - 1538
	200 - 700	200 - 1000

Since our data are derived from only one set of samples taken during the summer season, they do not lend themselves to broad generalizations for the entire year. Variations in the period of reproductive cycles of the species may give erroneous impressions as to their dominance. However, in general, it may be stated that in the area studied the abundance of planktonic foraminifera decreases rapidly in the three successive water levels at an approximate abundance ratio of 5:1.

The decrease in the faunal abundance with increasing depth has been observed by various workers studying the different oceanic bodies. Lohman (1920) was perhaps the first to give a quantitative estimation of the variations in the total abundance of specimens with respect to depth in Atlantic waters and his data show a pronounced decrease in specimens at depths greater than 200 metres.

Phleger (1945) analyzed the data collected by Schott (1935) during

the *Meteor* expedition in the equatorial Atlantic Ocean and found that the planktonic foraminifera were predominantly present in the upper 100 metres of water. Phleger (1951) determined a mean number of 10.8, 0.5 and 0.7 specimen per cubic metre of water at 75-100 metres, 325-500 metres, and 650-1000 metres water-depth intervals respectively in the Gulf of Mexico and North Atlantic. Emiliani (1959) inferred the depth habitat of foraminiferal species from dead assemblages by means of oxygen isotope ratios and found that the planktonic foraminifera were restricted to the upper 220 metres of water.

Bradshaw (1959), during his study of the northern Pacific, determined the highest concentrations of planktonic foraminifera occurring between 6-30 metres in most tows and the greatest decrease in number per cubic metre was noticed between 50-100 metres. Our observations in equatorial and northern Pacific show an almost uniform reduction in specimen abundance with increasing depth at most stations (Table 1).

The decrease in the foraminiferal population with depth of water is probably related to the intensity of illumination which, in turn, controls phytoplankton distribution. The intensity of light on the surface of the sea depends primarily upon latitude, season and cloud cover. Its penetration in sea water is also dependent on other factors such as scattering by suspended particles and absorption by dissolved organic compounds and phytoplankton pigments (McLellan, 1965). The limit of photosynthesis, in general, has been determined to be 120 metres in clear tropical waters, 40 metres in shelf waters, and 15 metres in turbid waters in temperate latitudes. It is well known that the phytoplankters are one possible source of food for planktonic foraminifera. Thus the direct dependence on photosynthetic organisms may have a strong controlling effect on the bathymetric distribution of living foraminifera. However, the planktonic foraminifera may avoid the high intensity of illumination in the uppermost level and therefore prefer to inhabit the deeper levels as evident from observations made by Boltovskoy (1969) in tropical Atlantic water.

Variations in the density of water may also influence the horizontal stratification of planktonic foraminifera. Laboratory experiments have shown that some zooplankton can accumulate at the boundaries of pronounced density gradients (Harder, 1968). According to Angel (1968), thermoclines, known to be regions of vertical density differences provide a physical barrier through which certain species do not pass. The density of oceanic waters is dependent upon several factors including temperature, salinity and inorganic and organic solutes present in the water. These may, under certain conditions, tend to promote the stratification and concentration of planktonic foraminifera.

(ii). Variation with Latitude and Species Diversity

Latitudinal variation in the composition of planktonic foraminiferal fauna may most easily be explained by using species diversity data. The species diversity is defined as the number of species found in a sample and is generally expressed as:

$$Ds = \frac{S100}{S_T}$$ where Ds = diversity in per cent

S = number of species observed at each station
S_T = total number of species

The species diversity may be expressed both in actual numbers or in relative percentage of species present in an assemblage.

Thirty planktonic foraminiferal species are identified in our samples from the Pacific. The highest number of species occurring in any one sample was never more than 20 (in equatorial warm tropical waters) and may be as low as 6 (in subarctic waters). The complete check list of the identified species is given in Table 2. Absolute and relative abundance is given in Tables 12 and 13, respectively. The plotting of species diversity with respect to latitudes (figure 5) illustrates a uniform decrease in diversity from the equator to the higher latitudes. Certain unexplainable anomalies have been noted at a few stations. An almost similar relationship exists with respect to the absolute abundance of the total planktonic foraminifera population and latitude (Table 4).

TABLE 4

ABUNDANCE AND SPECIES DIVERSITY VS. LATITUDE IN SURFACE WATERS

Water Mass	Latitudes	Station No.	Absolute Abundance per 1000 m^3	Species Diversity	
				Total No. of Species	Relative Percentage of Species
Equatorial Water	10°S	289	8205	15	50.00
	05°S	290	7975	16	53.33
	00	291*	5897	16	46.66
	05°N	292*	3187	20	66.66
	10°N	293	1727	16	53.33
	15°N	294	2010	19	63.33
	22°N	295	2319	19	63.33
	29°N	297	273	11	36.66
Central Water	36°N	298	112	12	40.00
	43°N	299	1342	09	30.00
Subarctic Water	49°N	300	1538	06	20.00
	55°N	301	906	06	20.00

* Composite samples

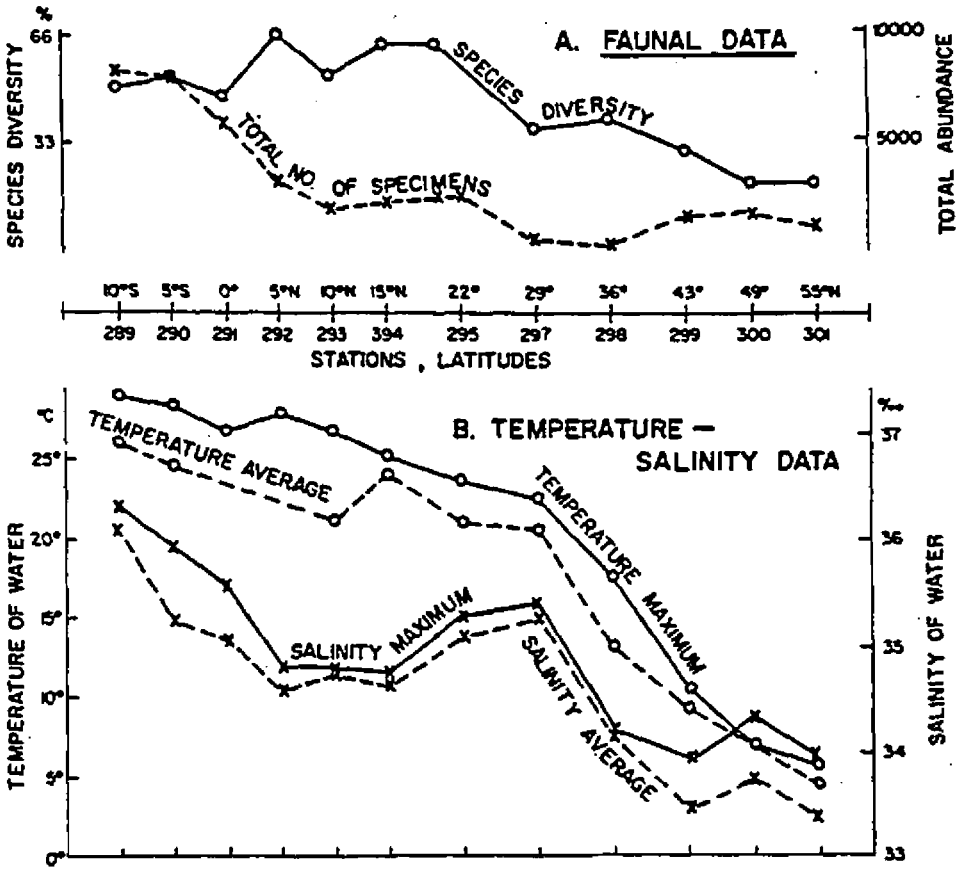


FIGURE 5: Maximum and average temperature-salinity values of surface waters at various stations and the foraminiferal population.

The latitudinal gradients in the diversity of marine organisms have received the wide attention of the ecologists due to their importance in the reconstruction of paloenvironments. Different species groupings that are correlated with water temperature have been mentioned earlier. It is interesting to note that these groupings are also restricted by their respective latitudinal distribution. Previous studies indicate that modern geographic distribution of plankters is related directly or indirectly to the present latitudinal temperature gradient of the earth and may be disturbed only by changes in the oceanic circulation patterns. Our data also show that a simple direct relationship exists between the temperature, salinity and the absolute abundance and species diversity of foraminifera populations (figure 5).

The present study also reveals a strong species gradient with depth in equatorial waters whereas the decrease is insignificant in Subarctic waters and at some stations reverse trends are noticed (Table 5).

TABLE 5

SPECIES DIVERSITY VS. DEPTH OF WATER AND LATITUDE

Latitude	Depth in metres	Species Diversity in Percentage
5°S	0-200	53.33
	200-435	20.00
15°N	0-170	63.33
	170-450	43.33
43°N	0-185	30.00
	185-850	36.66
55°N	0-100	20.00
	100-700	26.66

Fourteen commonly occurring planktonic species are ranked below in terms of their general compatibility with respect to depth of water in the Pacific (e.g., *Globorotalia inflata* (D'Orbigny) is found in equal abundance at all depths, whereas *Globigerinoides trilobus sacculifer* (Brady) appears to prefer living in near-surface waters).

1. *Globigerinoides trilobus sacculifer* (Brady)
2. *Globigerinella aequilateralis* (Brady)
3. *Hastigerina pelagica* (D'Orbigny)
4. *Globigerinoides conglobatus* (Brady)
5. *Globoquadrina conglomerata* (Schwager)
6. *Pulleniatina obliquiloculata* (Parker & Jones)
7. *Globigerinoides ruber* (D'Orbigny)
8. *Globigerinita glutinata* (Egger)
9. *Globigerinoides trilobus trilobus* (Reuss)
10. *Globigerina bulloides* D'Orbigny
11. *Globoquadrina dutertrei* (D'Orbigny)
12. *Globoquadrina hexagona* (Natland)
13. *Globorotalia hirsuta* (D'Orbigny)
14. *Globorotalia inflata* (D'Orbigny)

CORRELATION MATRIX ANALYSIS

The analysis of 29 Pacific plankton samples indicates strong but almost equal effects of temperature and salinity on the absolute abundance and species diversity. The species diversity and specimen abundance correlate inversely with latitude and directly with temperature (maximum and average values) and average salinity. Nutrients (phosphates and nitrates) are comparatively less significant; however, an inverse correlation of second order of importance was noted. Oxygen appears to be an insignificant factor; its presence in minor amounts is essential for organic metabolism. *Globigerinoides trilobus* (Reuss) and *Globigerinoides ruber* (D'Orbigny) in warm water, and *Globigerina pachyderma* (Ehrenberg) in cold water, are the main constituents of the respective faunas and these species account for most of the changes in the total population of planktonic foraminifera.

TABLE 6

TEST SIZE GROUPINGS AND THEIR RELATIVE PERCENTAGE OF OCCURRENCE OF 7 SELECTED PLANKTONIC FORAMINIFERA SPECIES

SIZE GROUPINGS		SPECIES	Globoquadrina conglomerata (Schwager)				Globigerinoides trilobus trilobus (Reuss)				Globigerinoides ruber (D'Orbigny)				Globigerinoides conglobatus (Brady)				Globigerinita glutinata (Egger)				Globigerina bulloides (D'Orbigny)				Globigerina pachyderma (Ehrenberg)			
		DIAM. IN MICRONS	PERCENTAGE OF			NO OF	PERCENTAGE OF			NO OF	PERCENTAGE OF			NO OF	PERCENTAGE OF			NO OF	PERCENTAGE OF			NO OF	PERCENTAGE OF			NO OF	PERCENTAGE OF			NO OF
WATER MASS	LATITUDE	STATIONS	>450 μ	450-300 μ	< 300 μ	SPECIMENS	> 500 μ	500-400 μ	< 400 μ	SPECIMENS	> 280 μ	280-200 μ	< 200 μ	SPECIMENS	> 450 μ	450-300 μ	< 300 μ	SPECIMENS	> 300 μ	300-240 μ	< 240 μ	SPECIMENS	> 280 μ	280-220 μ	< 220 μ	SPECIMENS	> 280 μ	280-220 μ	< 220 μ	SPECIMENS
SOUTHERN	15°S-10°S	289	27.90	51.16	20.93	43	27.94	45.58	26.47	136	21.81	58.30	19.79	298	27.50	51.25	21.25	80	16.21	48.69	35.13	37								
		290	62.50	25.00	12.50	8	36.25	45.00	18.75	80	32.65	40.81	26.53	49	80.00	40.00		5	35.71	50.00	14.28	14								
	0°S-15°N	291	57.40	35.18	07.40	108	45.71	40.00	14.28	70	30.95	48.80	20.23	84	100.00			4	25.00	55.00	20.00	20								
		293	12.50	50.00	37.50	8	14.52	52.99	32.47	117	19.29	54.36	26.31	57	16.66	66.66	16.68	6	08.33	54.16	37.50	24								
	16°-30°N	295	63.63	27.27	09.09	11	72.22	14.81	12.96	54	54.96	35.11	09.92	131	60.71	28.57	10.71	28	11.86	64.40	23.72	59								
		297						100.00		4	16.66	58.37	25.00	24					28.57	57.14	14.28	14								
SUB-ANTARCTIC-CENTRAL	31°-45°N	298							100.00	2		70.00	30.00	10						66.66	33.33	3		33.33	66.66	6				
		299										66.66	33.33	6					22.22	55.55	22.22	9	31.37	47.05	21.56	51	31.25	50.00	18.75	16
	46°-60°N	300																					28.31	47.78	23.89	113	33.69	36.95	29.34	92
		301																					33.33	44.44	22.22	9	14.75	50.27	34.97	183

SIZE RELATIONSHIP

There appears to be no simple relationship between size, maturity of forms and the physical factors generally considered to be of importance to the entire faunal assemblage. In the present study, it has been observed that at relatively great depths, although the planktonic foraminifera are rare, the adults are of average size. In regions of active growth the size distribution may reflect the degree of maturity of the total population. Table 6 shows the observations made on the size relationship of six planktonic species with respect of depths at various latitudes in the Pacific. The three size groupings of these species according to their percentage of distribution do not indicate any simple relationship existing between size development, depth of water and the latitude at which they occur.

Correlation analysis suggests an inverse relationship of size development, in case of *Globigerinoides ruber* (D'Orbigny), with latitude and a positive correlation with factors such as temperature and average salinity. Oxygen and nutrients seem to have very little significance. The importance of these physical factors in the case of *Globigerinoides ruber* (D'Orbigny) may be explained by its primary mode of living in warm-tropical to warm-temperate waters at lower latitudes. *Globoquadrina dutertrei* (D'Orbigny) was observed in Subarctic waters, where it represented one of the dominant species, although it was only about a half as large as those specimens caught in Central water tows. Similarly, *Globorotalia tumida* (Brady), *Globigerinoides trilobus sacculifer* (Brady) and *Globigerinoides trilobus trilobus* (Reuss) appear to be reduced in size towards higher latitude. Studies of more cosmopolitan species such as *Globigerinita glutinata* (Egger) show almost no significant size relationship with respect to variations in physico-chemical parameters and latitude. The relative significance of latitude on size development of certain planktonic species was first noted by Cushman and Harris (1927). They found a decrease in size of *Globorotalia menardii* (D'Orbigny) both northwards and southwards from the Caribbean area. The relative paucity of this well known species in most of our plankton tows does not permit such generalization.

The increase in the thickness of the test wall by further calcification at increased depths may result in significant change in size of individuals as reported by Bé and Lott (1964). They report that the walls of specimens caught in surface waters are generally thin, whereas those from deeper waters may be thick and at times develop a thick calcite crust which is confined to the last whorl of the test. It is observed in the present study that this calcification, in many cases, does not depend on the maturity of the individuals. For example, juvenile specimens of *Globigerina pachyderma* (Ehrenberg) have relatively thicker walls than mature or adult forms. The calcification develops in those species preferring to live a part or all of their life in deeper waters, thus juvenile specimens of *Globigerina pachyderma* (Ehrenberg) with calcified test prefer to live in deeper water than does the adult form. The correlation analysis has not revealed any significant relationship between size variations of other commonly occurring planktonic species and their depth of occurrence.

KUMMERFORMS

Berger (1969) introduced a new terminology 'kummerform' for those foraminiferal tests having the last chamber equal to or smaller in size than the previous one. However, he noted (1970) that this definition does not apply to *Orbulina universa* D'Orbigny, in which the last chamber is always greater than the previous one. Instead, kummerform *Orbulinas* are those with their penultimate chambers not completely enveloped by the last chamber.

The kummerform development has been observed in a number of species obtained from the present plankton tows. More common occurrences are observed in *Globigerina pachyderma* (Ehrenberg), *Globoquadrina dutertrei* (D'Orbigny), *Globigerinoides ruber* (D'Orbigny) and *Globigerinoides trilobus sacculifer* (Brady); less common in *Globigerinoides conglobatus* (Brady) and *Globoquadrina conglomerata* (Schwager) and rare in *Globorotalia hirsuta* (D'Orbigny), *Globigerina bulloides* D'Orbigny),*Globigerina calida* Parker, *Globoquadrina hexagona* (Natland), *Globorotalia tumida* (Brady) and *Orbulina universa* D'Orbigny (figure 6).

The kummerform development in planktonic species varies considerably. In general, an increase in the percentage of kummerform specimens with respect to depth of water is evident (Table 7).

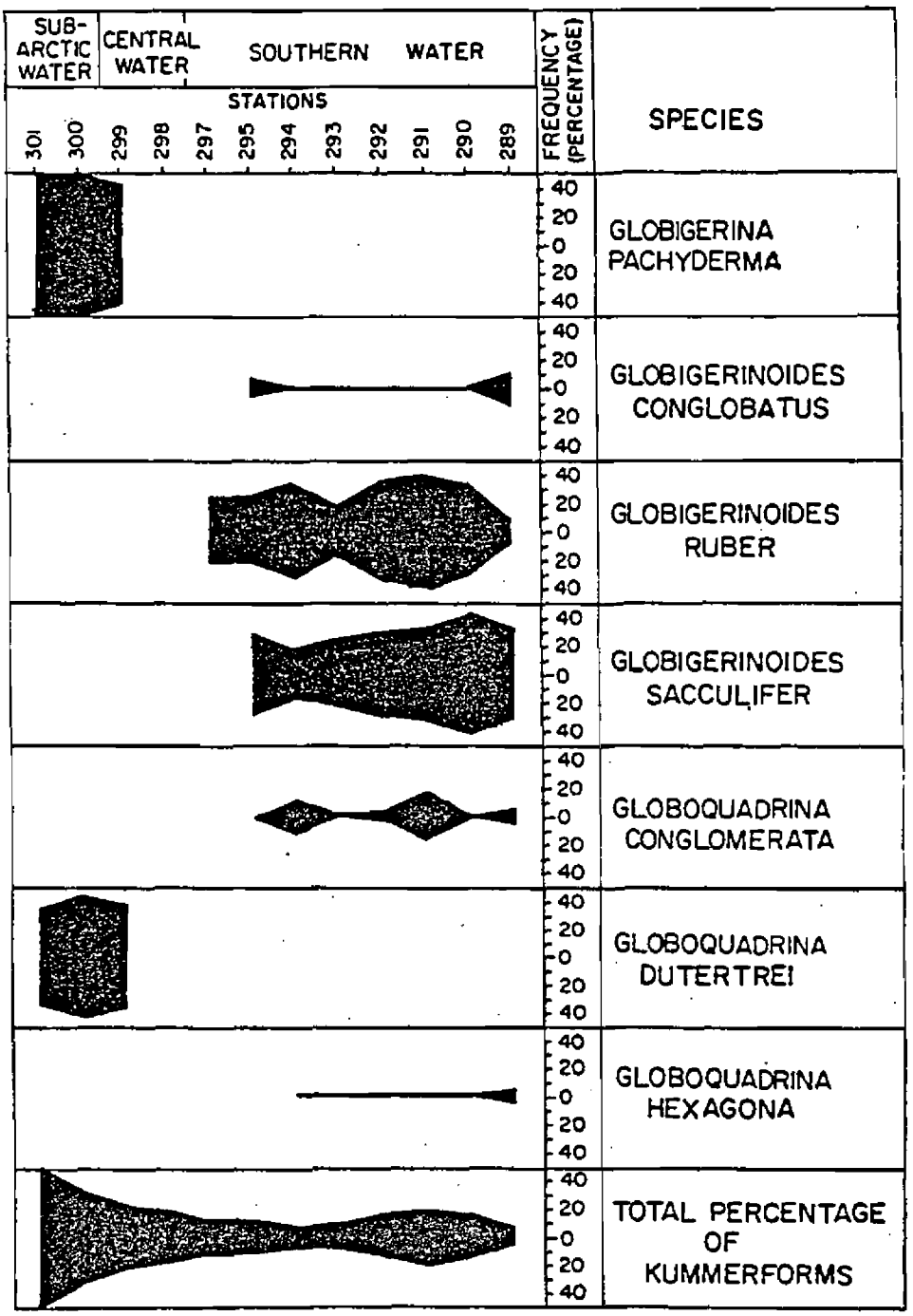


FIGURE 6: Relative abundance of kummerform specimens in surface waters of various plankton stations.

TABLE 7

PERCENTAGE OF KUMMERFORM SPECIMENS
AT VARIOUS LATITUDES AND WATER DEPTHS

Latitude	Stations	Depth of water in metres	Kummerform percentage	Variations with depth (surface water value as 0)
10°S	289	0-190	03.01	
		190-460	04.76	x1.58
		460-760	08.82	x2.93
10°N	293	0-190	04.52	
		190-460	11.95	x2.64
		460-750	07.54	x1.66
15°N	294	0-170	02.29	
		170-450	09.09	x3.96
		450-780	06.01	x2.62
22°N	295	0-180	04.70	
		180-440	04.11	x0.85
		440-1050	14.29	x3.04
29°N	297	0-160	05.80	
		160-475	05.63	x0.97
		475-1030	05.88	x1.01
43°N	299	0-185	12.75	
		185-850	14.44	x1.13
55°N	301	0-190	60.48	
		100-700	36.80	x0.60

It is observed that the increase in the percentage of kummerforms with depth occurs at lower latitude and that this trend decreases towards north. A marked drop in total percentage with increasing depth occurs at latitude 55°N. On the other hand, kummerform development is maximum in Subarctic waters, which is perhaps due to the relatively higher abundance of forms such as *Globigerina pachyderma* (Ehrenberg) and *Globoquadrina dutertrei* (D'Orbigny) in which kummerform development is a common feature.

The correlation analysis of 29 plankton samples indicates that latitude, depth, temperature and average salinity have a significant effect on the development of kummerforms in various species whereas factors such as oxygen and nutrients appear to be unrelated. Latitude appears to be most important of all and has positive correlation with the development of kummerforms whereas temperature and salinity bear an inverse relation. In the case of *Globigerinita glutinata* (Egger) and *Globigerinoides ruber* (D'Orbigny), kummerform development is largely controlled by latitude. It is interesting to note that all these physical factors do not play a uniform role in the development of kummerform specimens in most of the species studied.

Berger (1970) emphasized the importance of kummerforms in ecological studies. He (*op. cit.*) suggested that the kummerforms were the result of environmental stress and that they indicated the termination or drastic slowing down of growth in the specimens concerned. He also noticed that the percentage of kummerforms tend to increase with specimen size, which seems to contradict his statement on the slowing down of growth with the development of kummerform specimens. We have selected a warm water species--*Globigerinoides ruber* (D'Orbigny), a temperate to cold water species *Globoquadrina dutertrei* (D'Orbigny) and a cosmopolitan species *Globigerinita glutinata* (Egger)--to study the relationships between specimen size and kummerform development at various latitudes and water masses.

No significant relationship of the development of kummerforms with the size of individual tests of *Globigerinita glutinata* (Egger) has been noticed in the present study. In the case of *Globoquadrina dutertrei* (D'Orbigny), the kummerform development seems to increase to a significant level for those caught in Subarctic waters, which are generally smaller in size than those thriving in Central waters. Conversely, kummerform development in *Globigerinoides ruber* (D'Orbigny) shows a direct correlation with the size of the individual tests. All these three examples give contradictory results, so that perhaps environment has very little influence in kummerform development. In Banerji's opinion kummerform development is an ontogenic feature, more or less independent of surrounding physical conditions.

The more favourable nutrient conditions available in the Subarctic waters do not reflect the greater development of kummerforms due to environmental stress as emphasized by Berger (*op. cit.*). The correlation analysis has not shown any significant inverse relationship between the average nutrient conditions at each station and kummerform development.

In some specimens, the penultimate chamber has been found to be slightly smaller than the preceding and succeeding chambers (e.g., *Globorotalia tumida* (Brady), *Globoquadrina hexagona* (Natland) and *Globigerina calida* (Parker). This indicates that kummerform development is not restricted to the last chamber alone. Thus if the development of kummerform morphology is the result

of termination or drastic slowing down of growth (according to Berger, 1970), then the normal development can probably continue upon the return of more favourable conditions. It is equally interesting to note that kummerform development has not been noticed consistently in most of the specimens and species recovered from a particular set of samples. Hence environmental conditions cannot be considered as the sole factor for the development of this unusual feature. It is possible that kummerform chamber development reduces the specimen buoyancy enabling it to reside in a deeper, more compatible environment. However, this does not explain the ambiguity in the data (Table 7) in which the lower rate of increase in the percentage of kummerforms at greater depths at some stations is observed.

WATER MASSES AND DISTRIBUTION OF FORAMINIFERA

As stated earlier, three water masses designated as Southern, Central and Northern or Subarctic are recognized in that part of the Pacific Ocean under discussion. Various physical and chemical parameters such as temperature, salinity, oxygen, phosphate and nitrate concentrations of surface water are tabulated in Table 8, and their inter-relations are illustrated in figures 7-12. The distribution of planktonic foraminifera in these water masses is described below.

Southern Water Mass

This water mass includes that part of the equatorial warm-tropical to warm-temperature belt extending from south of the equator to latitude 30°N in the eastern part of the Pacific. It narrows towards the East Indian Archipelago. The stations located within this water mass are 289, 290, 291, 292, 293, 294, 295 and 297. The annual variation of atmospheric temperature is small over most of the region; however, seasonal variations are pronounced in the northern part. The temperature and salinity values of the surface water mass vary from 22°C to 30°C and 34.6 to 36.16‰ respectively, whereas minimum values of 5°C and 34.1‰ are observed at a depth of 1000 metres near latitude 30°N. Phosphate and nitrate concentrations increase with depth and the maximum values are 3.35 and 44.5 µg at/l respectively around 1000 metres depth. The species' diversity varies from 50-66.7% in the surface waters whereas the minimum diversity of 20% was noticed in the subsurface water of station 290 (latitude 05°S).

All of the stations situated within this water mass show a relatively high frequency of typical dominant warm water forms. They are represented by a warm-tropical and warm-temperate species subgroups (as defined on page 13). The warm-tropical species range from the equator up to latitude 15°N where the surface temperature is approximately 25°C. The species thriving in this area in order of their abundance are: *Globigerinoides ruber* (D'Orbigny), *Globigerinoides toilobus trilobus* (Reuss) and *Globoquadrina conglomerata* (Schwager) which are relatively abundant, followed by *Globorotalia tumida* (Brady), *Globoquadrina hexagona* (Natland), *Pulleniatina obliquiloculata* (Parker and Jones), *Globigerinoides trilobus sacculifer* (Brady), *Globigerinita glutinata* (Egger) which are common and finally *Globorotalia menardii*

TABLE 8

PHYSICAL AND CHEMICAL PARAMETERS OF SURFACE WATERS AT VARIOUS LATITUDES

Water Mass	Latitude	Temperature °C		Salinity ‰		Oxygen ml/L		Phosphate µg at/L		Nitrate µg at/L	
		Max	Aver.	Max	Aver.	Max	Aver.	Max	Aver.	Max	Aver.
	10°S	28.92	26.00	36.29	36.07	04.52	04.30	00.59	00.32	06.10	03.40
	05°S	28.34	24.50	35.94	35.27	04.70	03.98	01.77	00.75	24.30	08.00
Southern	00°	26.74	20.57	35.55	35.21	04.56	03.55	01.31	00.80	20.00	11.62
Water	05°N	27.89	21.42	34.80	34.57	04.90	03.58	01.93	01.14	29.20	12.56
	10°N	26.80	21.24	34.80	34.74	04.81	03.33	02.34	01.01	34.70	16.70
	15°N	25.20	24.20	34.74	34.62	04.95	04.89	00.20	00.14	00.20	00.20
	22°N	23.20	21.09	35.25	35.07	04.94	04.98	00.17	00.09	03.00	02.00
	29°N	22.60	20.50	35.42	35.29	05.30	05.18	00.11	00.11	01.90	01.90
Central	36°N	17.60	13.29	34.20	34.11	06.35	05.61	02.33	00.58	16.64	09.50
Water	43°N	10.80	09.48	33.94	33.46	06.84	06.34	01.08	00.70	16.60	07.56
Subarctic	49°N	07.20	04.12	34.35	33.75	07.37	02.81	03.26	02.69	44.70	33.65
Water	55°N	05.90	04.84	33.99	33.40	07.35	04.18	03.16	02.35	46.50	34.40

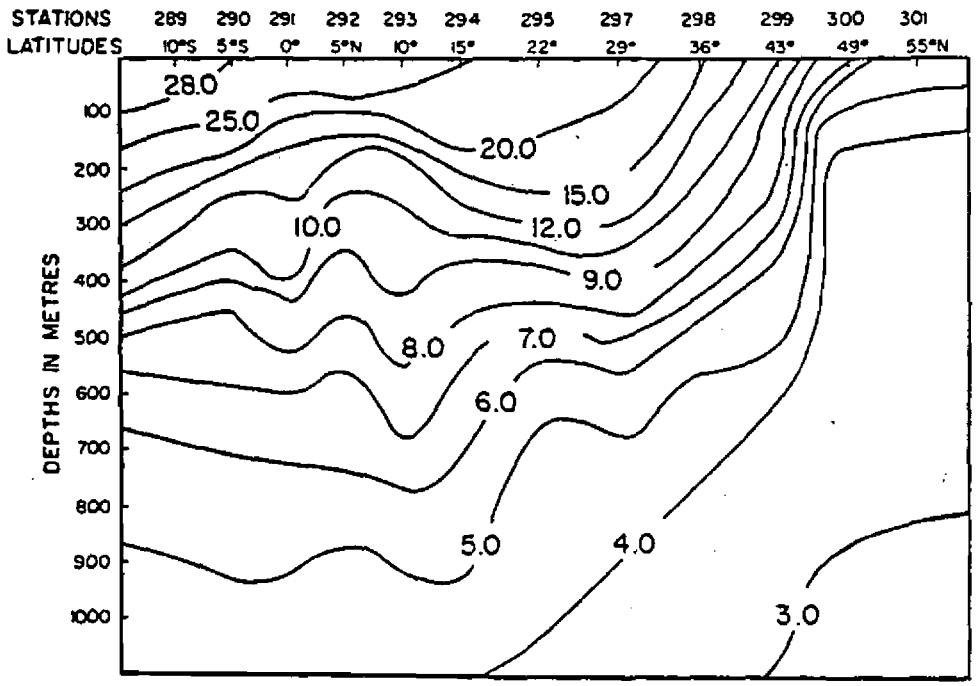


FIGURE 7: Variations in temperature with depth.

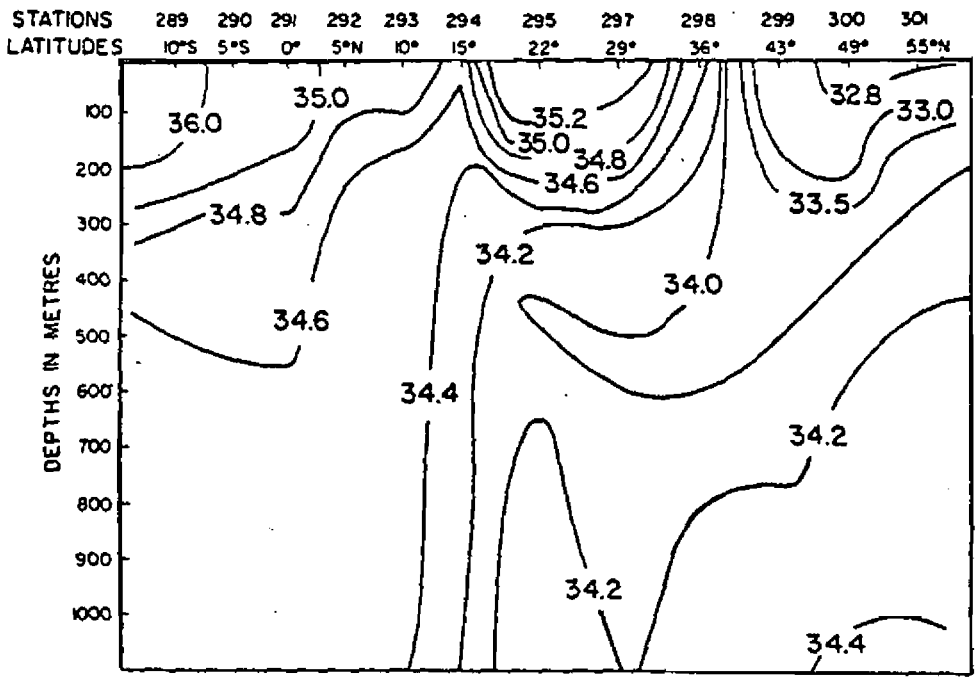


FIGURE 8: Variations in salinity values with depth.

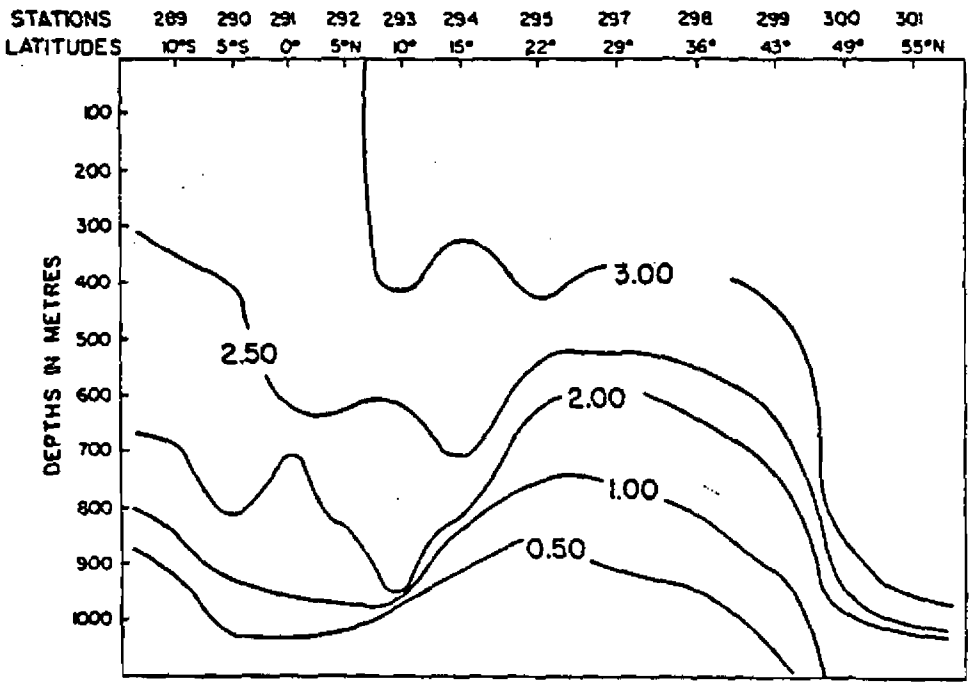


FIGURE 9: Phosphate concentrations vs. depth of water.

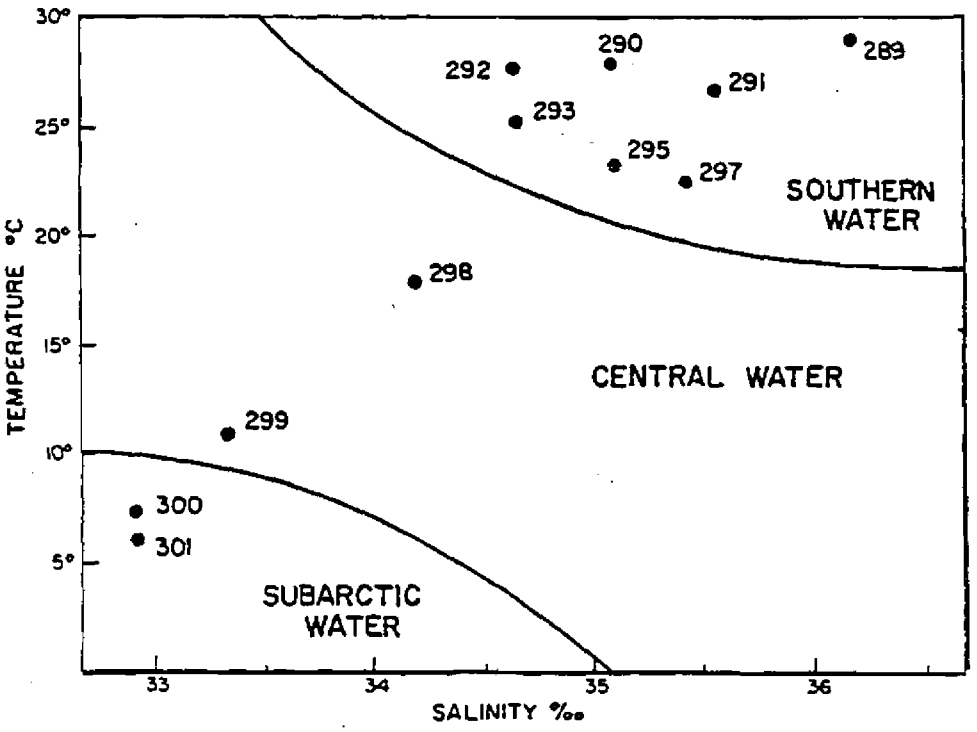


FIGURE 10: Temperature-salinity relations at various stations based on their maximum values.

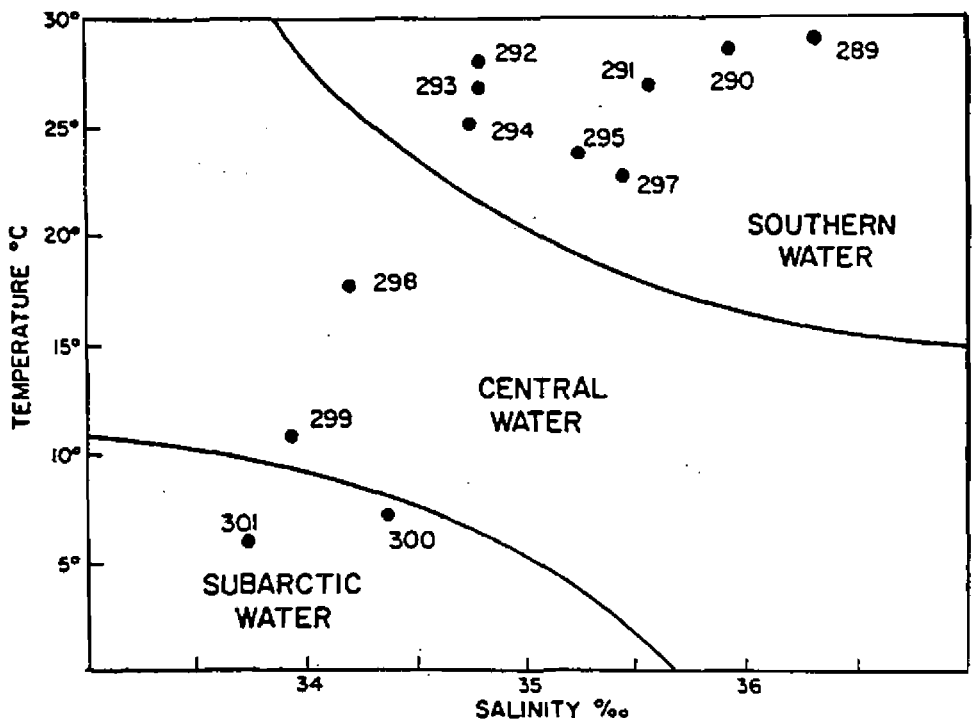


FIGURE 11: Temperature-salinity relations of the surface waters.

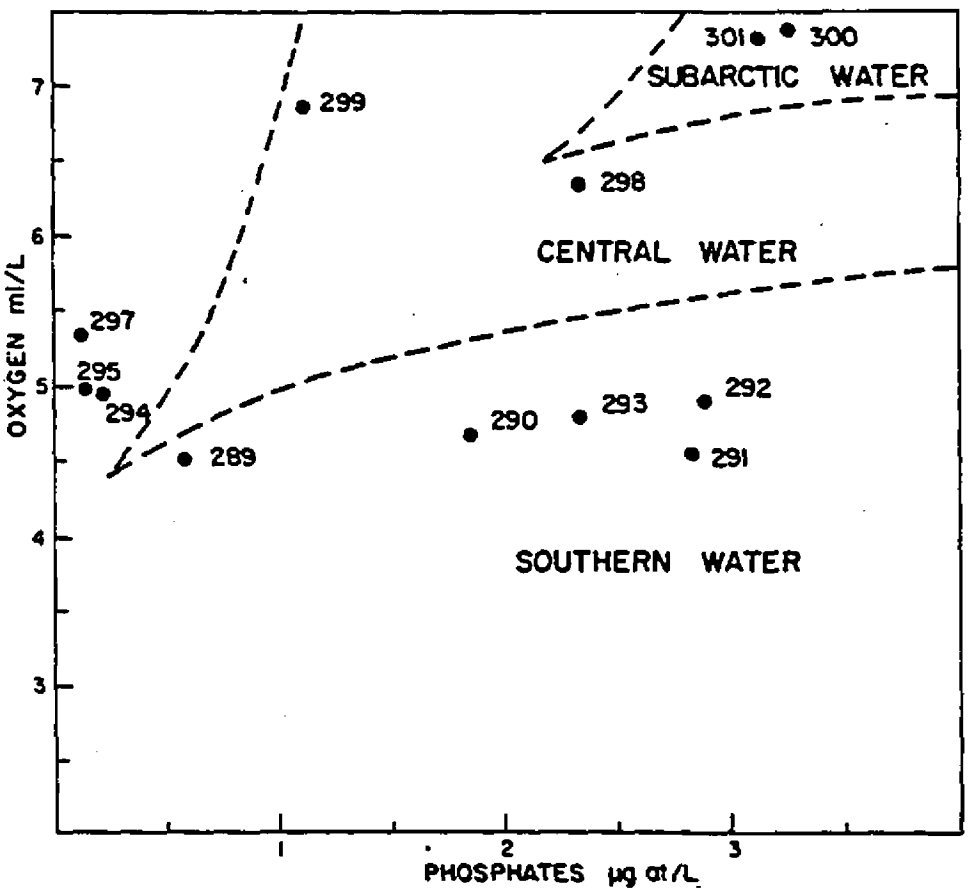


FIGURE 12: Oxygen-phosphate relations of the surface waters.

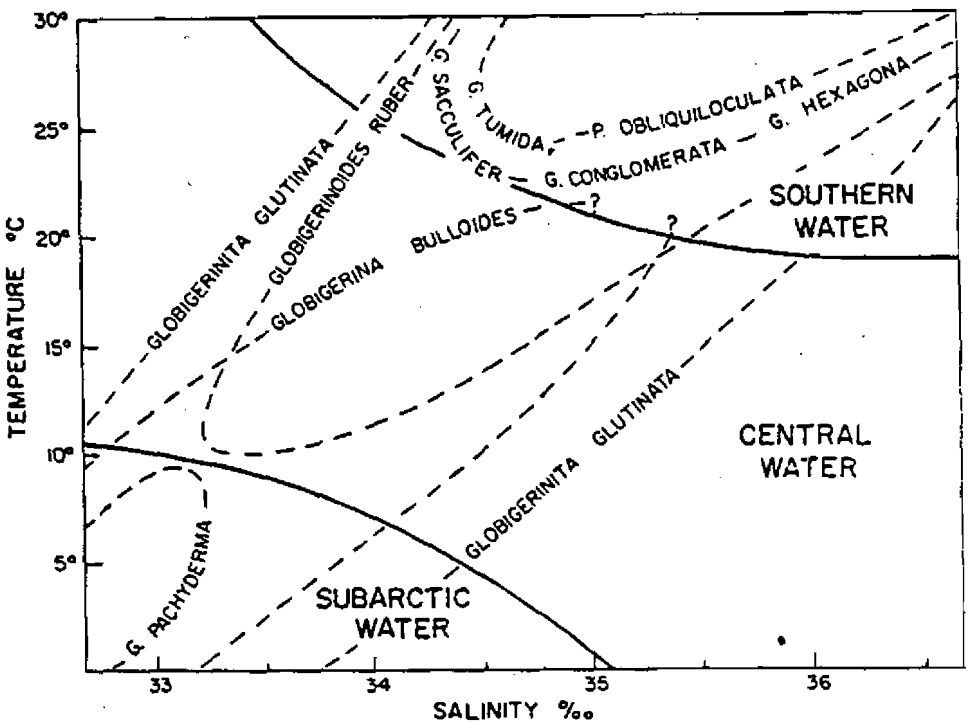


FIGURE 13: Temperature-salinity relations of water inhabited by nine plankton species (based on maximum values of temperature and salinity).

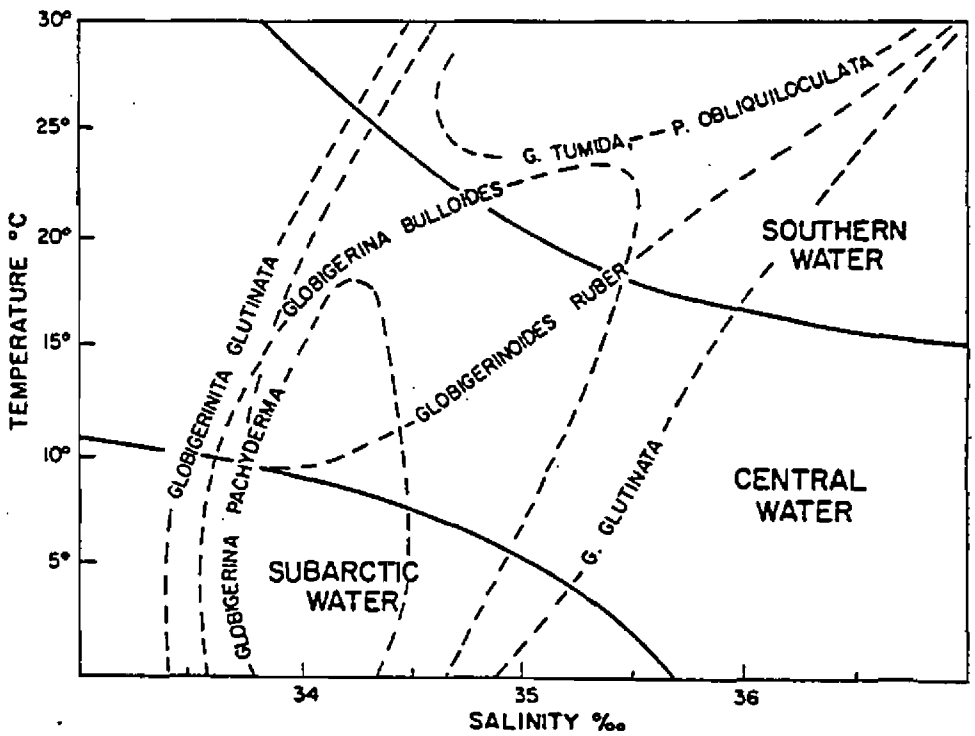


FIGURE 14: Temperature-salinity relations of water inhabited by six planktonic species (based on average values of temperature and salinity of the surface waters).

(D'Orbigny), *Eastigerina pelagica* (D'Orbigny), *Globigerinella aequilateralis* (Brady) and *Globorotalia hirsuta* (D'Orbigny) which are rare and are present only at a few stations. *Candeina nitida* D'Orbigny, *Globigerina calida* Parker, *Globigerina rubescens* Hofker are also rare in the surface waters and very few survive at greater depths. *Globigerinella adamsi* (Banner and Blow) and *Globorotalia scitula* (Brady) are represented by less than 1% of the total planktonic foraminiferal population. *Sphaeroidinella dehiscens* (Parker and Jones) is present in amounts less than 1% in surface water; however, it represents up to 4.5% of the total planktonic foraminiferal population in deeper waters. *Globorotalia truncatulinoides* (D'Orbigny), a well known species in present day seas, is conspicuously rare to absent at most of the stations and it is not recorded from any of the presently studied deep water tows.

Globorotalia inflata (D'Orbigny), which is normally considered as a warm-temperate species, occurs at most of the stations in relatively deeper waters. Among the other warm-temperate species, *Globorotalia hirsuta* (D'Orbigny) also occurs at most of the stations; however, its relative abundance increases at higher latitudes where a maximum value of 5.8% of the total planktonic foraminiferal population was observed in the surface water at station 297 (latitude 29°N). *Globoquadrina dutertrei* (D'Orbigny), a typical temperate-to-cold-water species, was observed between latitudes 15° to 22°N, where its maximum relative abundance was 7.1% at the time of collection.

The cosmopolitan species *Globigerinita glutinata* (Egger) is present at all the stations and at all depths.

Globigerina bulloides D'Orbigny, a cold-to-temperate species appears first in the deeper water at station 295 at latitude 22°N and occurs farther north in the surface waters at station 297 (latitude 29°N).

Plaknton tows taken south of the equator (e.g., stations 289 and 290) are comparatively rich in foraminiferal specimens as compared with those taken to the north. The ratio of total specimens to species number decreases rapidly at stations to the north (Table I).

The decrease in the specimen-to-species ratio reflects a progressively slower rate of reproduction for each individual species. This may be due to the incompatible environmental conditions that prevail towards the north. The high ratio at station 295 is the result of some unknown factor(s). The correlation analysis has not brought out any significant relation between the specimen/species ratio and any known physico-chemical factors. However, a second order positive correlation with average temperature and maximum salinity and a second order inverse correlation with depth of water is evident. *Globigerinella aequilateralis* (Brady), *Globigerinoides trilobus sacculifer* (Brady), *Globigerinoides trilobus trilobus* (Reuss), *Globoquadrina hexagona* (Natland), *Globorotalia tumida* (Brady) and *Pulleniatina obliquiloculata* (Parker and Jones) bring about a significant change in the specimen/species ratio by virtue of their restricted but higher percentage of occurrence at a few stations.

Kummerform development ranged from 2.3 to 6.9% of the total planktonic foraminifera population in the surface waters of the southern area. The maximum value of kummerform percentage was 16.6% at station 291 in a composite sample collected between 0-800 metres.

TABLE 9

ABSOLUTE ABUNDANCE AND RATIO OF SPECIMENS TO SPECIES IN THE SOUTHERN WATER MASS

Latitude	Station No.	Total No. of Specimens	Ratio of Specimens to Species
10°S	289	8205	547.00
05°S	290	7975	498.49
00	291	5849	417.65
05°N	292	3187	139.35
10°N	293	1727	105.79
15°N	294	2010	122.05
22°N	295	2319	24.81
29°N	297	0273	

The Southern water mass is characterized by a high frequency of species of the genus *Globigerinoides* followed by those of *Globoquadrina* and *Globorotalia*. *Globigerina* is rare and is represented by only one or two species at several stations. In general the fauna is sinistrally coiled; however, the ratio of dextrally to sinistrally coiled forms varies to a great extent both geographically and bathymetrically and no general trend can be detected. The correlation analysis has not shown any relationship between coiling direction, relative percentage of species and the various physical and chemical characteristics of this water mass.

Bradshaw (1959) defined limits of the warm water fauna at the boundary of the 20°C isotherm. He recognized two minor faunal groups designated by him as Central water and an Equatorial West-Central water assemblage. The former is characterized by *Globorotalia inflata* (D'Orbigny) and *Globorotalia truncatulinoides* (D'Orbigny) and the latter by *Globoquadrina conglomerata* (Schwager), *Globigerinella sp.*, *Globorotalia tumida* (Brady), *Pulleniatina obliquiloculata* (Parker and Jones) and *Sphaeroidinella dehiscens* (Parker and Jones). The present fauna grouped here as Southern water mass types have greater similarity with Bradshaw's Equatorial West-Central assemblage; however, *Sphaeroidinella dehiscens* (Parker and Jones) is extremely rare. According to Bradshaw *(op. cit.)*, species such as *Globoquadrina hexagona* (Natland), *Globigerinella aequilateralis* (Brady), *Globigerinita glutinata* (Egger), *Globigerinoides conglobatus* (Brady), *Globigerinoides ruber* (D'Orbigny), *Globigerinoides trilobus sacculifer* (Brady), *Globorotalia hirsuta* (D'Orbigny), *Globorotalia menardii* (D'Orbigny) and *Hastigerina rhumbleri* Galloway are common to both the equatorial water masses.

Globorotalia truncatulinoides (D'Orbigny), which is characteristic of Bradshaw's Central water, is extremely rare to absent in most of our samples from Southern waters. The distribution of this species in the Atlantic Ocean has been studied in detail by Bé and Ericson (1963) and according to them, the species occurred abundantly in the central and north Atlantic from late November through April and was rare during the rest of the year. The paucity of this species in Pacific water during May-June (the time of our sampling in the Pacific) is in agreement with the findings of Bé and Ericson (*op. cit.*) in the Atlantic.

Central Water Mass

This water mass lies between the Southern water and Northern or Subarctic water masses and includes a narrow zone which is bounded by latitude 30° and 45°N. Two stations (No. 298 and 299) have been sampled to 900 metres depth. The maximum values of temperature and salinity are 17.6°C and 34.3‰ respectively. Other details concerning the chemistry of the water are given in Table 8.

These two stations were sampled on May 31 and June 2, 1970, and are located in a part of the Northern Pacific, which has a very intricate circulation pattern. Changes in the faunal characters are complicated due to the complexity of the circulation pattern, i.e., the mixing of the Southern warm water with the Northern cold water mass. Hence the samples from this water mass have yielded dominantly warm as well as cold water species. The species' diversity in this area is lower than that of Southern water and varies from 30 to 40% at all depths. The absolute abundance of specimens is significantly lower than that of Southern water and a maximum value of 1342 specimens per 1000 cubic metres of water is recorded from the surface water sample at station 299 (latitude 43°N).

In general, faunal elements of both the Southern and Subarctic waters are intermixed so that the dimensions of the Central water mass vary depending upon the distance from the original faunal province and the degree of mixing. The faunal association is characterized by the first appearance of *Globigerina pachyderma* (Ehrenberg) and the continued increase in the number of *Globigerina bulloides* D'Orbigny, *Globorotalia inflata* (D'Orbigny) and *Globoquadrina dutertrei* (D'Orbigny). Species such as *Globigerinoides ruber* (D'Orbigny), *Hastigerina pelagica* (D'Orbigny), *Orbulina universa* D'Orbigny, all characteristic of Southern water, are persistent although in lower numbers throughout this water mass. Most other warm water species do not thrive here. The mixing of warm water from the south and cold water from the north has a pronounced effect on the distribution of a few of the less tolerant species in samples collected from two stations in the Central water mass. For example, *Globigerinella aequilateralis* (Brady), *Globigerinoides trilobus trilobus* (Reuss), *Globorotalia hirsuta* (D'Orbigny), belonging to a warm water group, occur only at station 298 (latitude 36°N) and are replaced by *Globigerina quinqueloba* Natland and a smaller form of *Globoquadrina dutertrei* (D'Orbigny) at station 299 (latitude 43°N). The latter observations were made on the surface water samples; however, in deeper waters a number of other factors play an important role in the distribution of these species. Most of the species occurring in this water mass have shown a significant correlation between

their distribution and the temperature and salinity of the water. In the case of *Globigerina bulloides* D'Orbigny, salinity is a more important factor and shows an inverse relationship with the relative percentage of occurrence of this species.

The kummerform development in most of the species is very prominent in this water mass as compared with that observed in Southern water. Percentages as high as 14 of the total planktonic foraminifera population have been observed.

There is an interesting observation concerning the general coiling direction of the fauna. The Southern water, as mentioned earlier, and northern Subarctic water masses are characterized by sinistrally (left) coiled forms whereas the Central water contains predominantly dextrally coiled elements (Table 10). The correlation analysis of commonly occurring forms in these water masses with respect to their coiling direction has not shown any significant relationship with the observed physico-chemical parameters. In contrast to the direct correlation of kummerforms with latitude and an inverse correlation with temperature and salinity of water, in other areas, the coiling direction of species in this water mass appears to have an inverse third order correlation with nutrients, and almost no correlation with latitude, temperature and salinity. Thus the change in the coiling direction in the Central water is associated with complex interactions of Southern and Northern water, which perhaps controls significant changes in nutrient concentrations and which may encourage the development of kummerform specimens.

The assemblage of the Central water mass corresponds with that of Bradshaw's 'transition' fauna. According to Bradshaw (*op. cit.*) the species common to this region are *Globigerina bulloides* D'Orbigny, *Globoquadrina dutertrei* (D'Orbigny), *Globigerina quinqueloba* Natland, *Globigerinoides ruber* (D'Orbigny) and *Orbulina universa* D'Orbigny. The northern boundary of this transition region has been arbitrarily defined by him as the northern limit of the distribution of *Orbulina universa* D'Orbigny and large specimens of *Globoquadrina dutertrei* (D'Orbigny), whereas the southern boundary is marked by the appearance of warm water species referred to by him as equatorial species (e.g. *Globigerinoides trilobus sacculifer* (Brady) and *Globorotalia menardii* (D'Orbigny)). The boundaries are somewhat similar to the Central water province as proposed here; however, both larger and smaller forms of *Globoquadrina dutertrei* (D'Orbigny) flourish in this water mass.

Sverdrup *et al.* (1942) have defined an area between latitudes 48°N and 23°N where the southward flowing Subarctic water converges with the equatorial water. Seasonal changes in the upper layers of the water in this area produce relatively complex conditions at certain localities thus encouraging the development of size variations in certain species.

Northern or Subarctic Water Mass

This is the northernmost water mass of the Pacific and is separated from Arctic waters by the Bering Strait. The boundary separating it from the Central water mass runs approximately along latitude 45°N. There are only two stations in this water mass (300 and 301) which were sampled on June 4 and 5 respectively. The maximum temperature and salinity of the water was

TABLE 10

COILING DIRECTION OF THE PLANKTONIC FORAMINIFERA

Water Mass	Latitude	Station No.	Depth (m)	Coiling Direction in percentage	
				Dextral (right)	Sinistral (left)
	10 S	289	0-190	41.61	58.38
			460-760	48.48	55.52
	05 S	290	0-200	27.75	72.25
			200-435	33.33	66.66
	00	291	0-800	24.32	75.68
	0 5	292	0-800	18.19	81.81
Southern	10 N	293	0-190	41.32	58.67
			460-750	37.57	62.42
Water	15 N	294	0-170	32.73	67.27
	22 N	295	0-180	43.22	56.78
			440-1050	35.71	64.29
	29 N	297	0-320	48.43	51.57
			160-475	46.55	53.45
Central	36 N	298	0-320	63.15	36.85
			0-900	51.06	48.94
Water	43 N	299	0-185	55.55	44.45
			185-850	65.68	34.32
			185-0	58.67	41.33
Subarctic	49 N	300	0-1050	32.03	67.97
Water	55 N	301	0-190	12.23	87.77
			100-700	23.22	76.78
			100-0	17.77	82.23

7.2°C and 34.35‰. Phosphate and nitrate concentrations are in general higher here than in Southern and Central waters.

The most interesting feature of the associated fauna is the low but uniform value of 20% species diversity which characterizes most of the plankton samples and the relatively higher specimen-to-species ratios compared to other areas. This indicates that very few species are compatible with the general physical conditions of this water mass. Relatively high values of phosphates probably result in a higher rate of reproduction and a larger standing crop. The correlation analysis has, however, shown a second order of significance for phosphates and nitrates, compared to temperature and salinity, with respect to absolute and relative abundance of the observed specimens.

There are about six species thriving in this water mass including (in order of abundance): left coiled *Globigerina pachyderma* (Ehrenberg), *Globigerinita glutinata* (Egger), *Globigerina quinqueloba* Natland, *Globoquadrina dutertrei* (D'Orbigny), *Globigerina bulloides* D'Orbigny and *Globorotalia inflata* (D'Oribgny). *Globorotalia cavernula* Be´ has been recorded in amounts up to 3% of the total fauna from the subsurface sample at station 301 (latitude 55°N).

The specimens of *Globigerina pachyderma* (Ehrenberg) living in this water mass have a typical quadrate-shaped test with a thicker and sugary-textured wall compared with those recorded from Central waters. The change in coiling direction from right in Central water to left in Subarctic water is a significant factor in delineating the boundary between these two water masses. *Globoquadrina dutertrei* (D'Orbigny) is represented by minute to medium-sized tests having smooth semitransparent walls with a smaller umbilical opening, and umbilical teeth which are characteristic of Central and Southern waters. *Globorotalia inflata* (D'Orbigny), *Globigerina quinqueloba* (Brady) and *Globigerina bulloides* D'Orbigny all show considerable reduction in size, whereas *Globigerinita glutinata* (Egger) remains almost unchanged.

The faunal constituents and other features of this water mass have much in common with the cold water (Subarctic) fauna of Bradshaw (1959). The species recognized in the cold water zone from various parts of the world belong to several series of integrating forms which are very difficult to analyze separately. These intergrading forms have been raised to the status of new species by various workers thus creating more confusion regarding the species concepts of recent planktonic foraminifera, for example, *Globigerina pachyderma* (Ehrenberg) - *Globigerina incompta* Cifelli (new species) - *Globoquadrina dutertrei* (D'Orbigny), and *Globigerina quinqueloba* Natland - *Globigerina quinqueloba egelida* Cifelli (new subspecies). *Globigerina pachyderma* (Ehrenberg) has shown considerable variation in its morphological characters. According to Cifelli (1969), the characteristic *Globigerina pachyderma* (Ehrenberg) has never been definitely identified in recent living faunas. However, our observations of a rich typical '*pachyderma*' assemblage from the Northern water mass of the Pacific refutes this statement.

SUMMARY

Foraminiferal reproduction and distribution in a particular water mass is probably related to various physical, chemical and biological factors affecting the surrounding waters. Each species must be capable of withstanding the maximum variation in environmental conditions in order to survive and reproduce. With a higher range of tolerance of individual species towards these factors, there is ample opportunity for them to attain a wide geographic distribution in different water masses and at varying depths. Thus in any ecological study, the effective tolerance of these species must be properly recorded in terms of their relative abundance and morphological adaptations. However, it should be noted that the tolerance range for reproduction is generally more limited than that required for the later growth of an individual test. Hence, the presence of adult and mature forms alone in any water mass will not reveal the optimum ecological regime. Their association with juvenile and reproductive forms would be helpful in establishing the characteristics of a preferred environment.

Factors which affect the general distribution of planktonic foraminifera may be classified under several headings including water depth, light penetration and intensity, temperature, salinity, density of water, phosphate, nitrate, oxygen carbon dioxide, calcium and magnesium concentration in sea water, and food supply. Most of these factors are, however, interdependent and inter-related to each other and are generally modified by changes in water circulation, atmospheric conditions and geographic location of water masses. Factors such as depth, temperature, salinity, oxygen and nutrient concentrations are easily measurable parameters which have a close bearing on the variation of other physical and chemical factors in a water column. We must introduce some of our correlation analysis findings here.

Depth of Water

As noted earlier, the abundance of planktonic foraminifera decreases sharply with increasing water depth. However, depth itself (hydrostatic pressure) seems to have very little direct influence on the control of plankton distribution. If there is not much of a significant change in factors such as temperature, illumination, salinity, etc., with respect to increasing depth, foraminifera continue to live down to great depths. They may, however, modify certain morphological characters to counter the effects of increasing viscosity. These modifications may include a thickening of the test wall by further calcification and compression of the test, as evidenced by decreasing diameter/thickness ratios of the test, and by closing of the pores. A sharp decrease in illumination with increasing depth has a significant but indirect effect by controlling the distribution of various phytoplankters that serve as a food supply for the foraminifera. The correlation analysis has shown a comparatively lower order of significance for the relationship between water depths and the distribution of planktonic foraminifera.

Temperature of Water

The temperature of water is perhaps the most important factor having a direct effect on the metabolism and reproductive cycles of the organisms. The rate of change of temprature with depth is not constant in all regions from the equator to the poles. Conversely, the temperature decreases with increasing latitudes and is accordingly modified by seasonal variations. Significant seasonal variations occur in the surface layers usually down to a depth of about 200 metres and it is here that the foraminiferal concentration is the highest. The temperature decreases uniformly below this level down to 1000 metres and to 2°C at the bottom. Temperature has, accordingly, a significant relationship to factors such as wind, water circulation, density and viscosity of water. It has also an indirect relationship to the distribution of foraminifera through its influence on the growth and reproduction of photosynthetic mirco-organisms which are a main source of food for the foraminifera.

Temperature seems to be responsible for bringing about significant changes in the absolute and relative abundance of specimens, species diversity and kummerform development in most of the planktonic species studied. As stated previously, the temperature causes a significant change in the viscosity of water which has a direct relation to the resistance to sinking experienced by planktonic foraminifera. In less viscous (warm) waters, the usual modifications in the structure of the test include the development of radial spines and projections which are invariably absent in forms living in the more viscous (cold and deep) waters. Highly ornamented and large-size tests are usually common in warm waters.

Salinity of the Water

This is another important factor for all marine organisms and is closely associated with temperature regarding its effect on the distribution of planktonic foraminifera. In most instances the variations in the foraminiferal associations are observed to be due largely to the cumulative effects of salinity and temperature (figures 13, 14); the variations in the salinity of water both vertically and laterally is somewhat similar to that of the temperature. The influence of salinity on the distribution of planktonic foraminifera is equally as important as temperature, since these organisms are stenohaline and therefore restricted in their distribution to relatively stable offshore areas.

Phosphates and Nitrates

The concentration of phosphates and nitrates in sea water are taken generally as an index of productivity potential and are considered as nutrient factors. These factors are greatly modified by the surface water circulation and the upwelling of water and have a direct correlation with depth of water and an inverse correlation with temperature and oxygen content of water. The high rate of productivity of individual species (as indicated by the higher values of specimen-to-species ratio), is generally observed in cold waters which have a relatively high nutrient content.

Other factors such as oxygen, carbon dioxide silica content and the pH of the water may play an important role in distribution of marine organism in sea water. For example, calcium and magnesium are necessary for the building of calcareous tests and other test-surface modifications.

An attempt has been made to study the relative influence of the major physical and chemical parameters on the general faunal distribution and composition as well as on the various morphological variations in the case of a few well known species, such as *Globigerinoides ruber* (D'Orbigny), *G. conglobatus* (Brady), (warm water species), *Globigerina pachyderma* (Ehrenberg) (cold water species) and *Globigerinita glutinata* (Egger) (cosmopolitan species). The following nine groupings of all the recorded physical, chemical and biological factors may be ranked in order of decreasing importance on the basis of a factor analysis (Cameron, 1967) which accounts for about 99% of the total variance of the distribution of these four species in three water masses of the Pacific Ocean.

1. Latitude, temperature, salinity (average), species diversity, size variations in case of the more latitudinally and bathymetrically restricted species.

2. Absolute and relative abundance of foraminiferal species.

3. Size variations in the case of more cosmopolitan species (*Globigerinita glutinata* (Egger)).

4. Phosphate and nitrate concentration of sea water.

5. Percentage of kummerform specimens.

6. Specimen-to-species ratios.

7. Oxygen content of water.

8. Depth of water.

9. General coiling direction of entire foraminiferal assemblage (calculated on the basis of 12 of the more common species).

DISTRIBUTION AND ECOLOGY OF INDIVIDUAL SPECIES

The distribution of 30 planktonic species of foraminifera identified from the equatorial and northern Pacific and the relative influence of various physical and chemical factors such as latitude, depth, temperature, salinity, and oxygen, phosphate and nitrate concentration in associated waters on the foraminiferal distribution are discussed here. Instead of a complete synonymy, only the original reference to each species is noted. Illustrations of a few interesting specimens are given in plates I-VI.

Family *GLOBIGERINIDAE*

Subfamily *GLOBIGERININAE*

Genus *GLOBIGERINA* D'Orbigny 1826

Globigerina bulloides D'Orbigny

Globigerina bulloides D'ORBIGNY, 1826, Ann. Sci. Nat., Ser. I, V. 7, p. 277.

This species is common in Central and Subarctic waters where it has been shown to represent up to 47% of the total living planktonic foraminiferal population in the surface waters at latitude 43°N. However, it is considerably reduced in its frequency of occurrence towards the north and is replaced eventually by the cold water species *Globigerina pachyderma* (Ehrenberg).

G. bulloides is encountered primarily in surface waters and decreases directly in abundance with depth of water. It first appears in the surface water at latitude 29°N coinciding with the 22°C isotherm and continues to be present at all the stations to the north. At deeper levels it appears farther south at latitude 22°N where it comprises about 7% of the total foraminifera population. Bradshaw (1959) also noticed the occasional low frequencies of occurrences of this species near the equator. According to Parker (1962) it occurred at all latitudes but was more common south of latitude 35°S in bottom sediments.

The correlation analysis shows a direct relationship between its distribution and latitude, oxygen, phosphate, and nitrate concentrations of the water and a strong inverse correlation of its abundance to depth of water. This species has very little similarity in distribution with any of the commonly occurring planktonic species in Pacific waters because temperature and salinity do not appear to play a very significant role in determining its distribution.

Globigerina calida Parker

Globigerina calida PARKER, 1962, Micropaleontology, v. 8, n. 2, pp. 221-222, pl. 1, figures 9-13, 15.

This species is somewhat similar in morphology to *Globigerina bulloides* D'Orbigny; however, it differs in having a more or less planispiral test in the adult with an interiomarginal aperture and radially elongated last chamber. It is mainly a warm-tropical water planktonic species and occurs at all stations from 10°S to 10°N latitude and to almost all water depths considered here. Its relative abundance varies from 0.6% to as much as 26.6% thus indicating a more or less patchy distribution in this narrow zone of southern water. The distribution of *G. calida* does not show any significant relationship with studied physical and chemical parameters except an inverse relationship of second order of importance with latitude. Perhaps the distribution of this species is largely controlled by the availability of associated warm water

phytoplankters which may serve as its chief source of food. In the South Pacific, Parker (1962) noted its presence north of latitude 35°S, thus reflecting its wider distribution there compared to the northern Pacific.

Globigerina falconensis Blow

Globigerina falconensis BLOW, 1959, Bull. Am. Paleontology, v. 29, n. 178, p. 177, pl. 9, figures 40-41.

This species also resembles closely *Globigerina bulloides* D'Orbigny. However, it differs in having a smaller test, a more lobulate periphery, a low arched aperture and a broad lip. It occurs in surface waters only at station 295 (latitude 22°N) where it represents about 5% of the total foraminifera population, thus inhabiting the cooler edge of subtropical waters. In subsurface levels, it is recorded at station 289 (latitude 10°S) and in a composite sample at station 292 (latitude 05°N). According to Bé (1969) *Globigerina bulloides* D'Orbigny grades morphologically and zoographically into *G. falconensis* Blow. Cifelli and Smith (1970) treat *G. falconensis* Blow as a subspecies of *G. bulloides* D'Orbigny. Bradshaw's (*op. cit.*) record of *G. bulloides* from near the equator perhaps belongs to *G. falconensis* Blow. Since this form does not occur in close association with *G. bulloides* D'Orbigny in any of the samples collected during this study, we feel that these two taxa belong to ecologically distinct regions and are not taxonomically related.

Globigerina pachyderma (Ehrenberg)

Aristerospira pachyderma EHRENBERG, 1861, K. Preuss, Akad. Wiss. Berlin, Monatsber, pp. 276, 277, 303.

The tests of this species are widely variable in shape, size, texture and wall characters, thus resulting in a series of intergrading forms which have been described individually as either distinct species, or placed under the synonymy of *G. pachyderma* by various workers. Brady's (1881) original form - *Globigerina bulloides* D'Orbigny var. *borelis* - later considered by Brady (1884) as a junior synonym of *G. pachyderma* has been chosen as the lectotype of *G. pachyderma* by Banner and Blow (1960). Cifelli (1961) erected a new species *Globigerina incompta* from the North Atlantic, which was put under the synonymy of *G. pachyderma* (Ehrenberg) by Parker (1962). Cifelli and Smith in their later work (1970) ruled out the possibility of any gradation between these two species occurring in the North Atlantic and considered *G. incompta* as a separate species.

Family *GLOBIGERINIDAE*

Subfamily *GLOBIGERININAE*

Genus *GLOBIGERINA* D'Orbigny 1826

Globigerina bulloides D'Orbigny

Globigerina bulloides D'ORBIGNY, 1826, Ann. Sci. Nat., Ser. 1, V. 7, p. 277.

This species is common in Central and Subarctic waters where it has been shown to represent up to 47% of the total living planktonic foraminiferal population in the surface waters at latitude 43°N. However, it is considerably reduced in its frequency of occurrence towards the north and is replaced eventually by the cold water species *Globigerina pachyderma* (Ehrenberg).

G. bulloides is encountered primarily in surface waters and decreases directly in abundance with depth of water. It first appears in the surface water at latitude 29°N coinciding with the 22°C isotherm and continues to be present at all the stations to the north. At deeper levels it appears farther south at latitude 22°N where it comprises about 7% of the total foraminifera population. Bradshaw (1959) also noticed the occasional low frequencies of occurrences of this species near the equator. According to Parker (1962) it occurred at all latitudes but was more common south of latitude 35°S in bottom sediments.

The correlation analysis shows a direct relationship between its distribution and latitude, oxygen, phosphate, and nitrate concentrations of the water and a strong inverse correlation of its abundance to depth of water. This species has very little similarity in distribution with any of the commonly occurring planktonic species in Pacific waters because temperature and salinity do not appear to play a very significant role in determining its distribution.

Globigerina calida Parker

Globigerina calida PARKER, 1962, Micropaleontology, v. 8, n. 2, pp. 221-222, pl. 1, figures 9-13, 15.

This species is somewhat similar in morphology to *Globigerina bulloides* D'Orbigny; however, it differs in having a more or less planispiral test in the adult with an interiomarginal aperture and radially elongated last chamber. It is mainly a warm-tropical water planktonic species and occurs at all stations from 10°S to 10°N latitude and to almost all water depths considered here. Its relative abundance varies from 0.6% to as much as 26.6% thus indicating a more or less patchy distribution in this narrow zone of southern water. The distribution of *G. calida* does not show any significant relationship with studied physical and chemical parameters except an inverse relationship of second order of importance with latitude. Perhaps the distribution of this species is largely controlled by the availability of associated warm water

phytoplankters which may serve as its chief source of food. In the South Pacific, Parker (1962) noted its presence north of latitude 35°S, thus reflecting its wider distribution there compared to the northern Pacific.

Globigerina falconensis Blow

Globigerina falconensis BLOW, 1959, Bull. Am. Paleontology, v. 29, n. 178, p. 177, pl. 9, figures 40-41.

This species also resembles closely *Globigerina bulloides* D'Orbigny. However, it differs in having a smaller test, a more lobulate periphery, a low arched aperture and a broad lip. It occurs in surface waters only at station 295 (latitude 22°N) where it represents about 5% of the total foraminifera population, thus inhabiting the cooler edge of subtropical waters. In subsurface levels, it is recorded at station 289 (latitude 10°S) and in a composite sample at station 292 (latitude 05°N). According to Bé (1969) *Globigerina bulloides* D'Orbigny grades morphologically and zoographically into *G. falconensis* Blow. Cifelli and Smith (1970) treat *G. falconensis* Blow as a subspecies of *G. bulloides* D'Orbigny. Bradshaw's (*op. cit.*) record of *G. bulloides* from near the equator perhaps belongs to *G. falconensis* Blow. Since this form does not occur in close association with *G. bulloides* D'Orbigny in any of the samples collected during this study, we feel that these two taxa belong to ecologically distinct regions and are not taxonomically related.

Globigerina pachyderma (Ehrenberg)

Aristerospira pachyderma EHRENBERG, 1861, K. Preuss, Akad. Wiss. Berlin, Monatsber, pp. 276, 277, 303.

The tests of this species are widely variable in shape, size, texture and wall characters, thus resulting in a series of intergrading forms which have been described individually as either distinct species, or placed under the synonymy of *G. pachyderma* by various workers. Brady's (1881) original form - *Globigerina bulloides* D'Orbigny var. *borelis* - later considered by Brady (1884) as a junior synonym of *G. pachyderma* has been chosen as the lectotype of *G. pachyderma* by Banner and Blow (1960). Cifelli (1961) erected a new species *Globigerina incompta* from the North Atlantic, which was put under the synonymy of *G. pachyderma* (Ehrenberg) by Parker (1962). Cifelli and Smith in their later work (1970) ruled out the possibility of any gradation between these two species occurring in the North Atlantic and considered *G. incompta* as a separate species.

The forms occurring in the Subarctic and Central waters of the northern Pacific are similar to those described by Ehrenberg (1861) and differ considerably in shape, development of chambers, and thickness and texture of the test wall with those occurring in the North Atlantic (as described by Cifelli, 1970). No true representative of *G. incompta* Cifelli is recorded from Pacific waters.

Globigerina pachyderma occurs in surface waters north of latitude 36°N, up to a maximum relative abundance of 71% of the total foraminiferal population at station 301 (latitude 55°N). In the deeper tows, it first appears around latitude 29°N where it represents 5% of the total population. The juvenile forms of this species have a characteristic sugary wall texture, are more compact, and have a slit-like aperture. These features are partly obscured in the more adult and larger forms. The development of kummerform specimens is most common in this species and as many as 81% of the specimens in the surface water at station 301 (latitude 55°N) are kummerforms. At this station, an interesting relationship is observed regarding depth of water in contrast to all other species at most of the stations. Be' (1960) on the other hand noted a reduction of the final chamber size of specimens collected at depths greater than 200 metres in Atlantic waters.

The specimens recovered from stations 297, 298 and 299 (latitude 29° to 43°N) are mostly dextrally coiled whereas farther north they are predominantly sinistral. The change from dextral to sinistral coiling occurs somewhere between latitude 44° to 48°N where surface water isotherms vary from 7°C to 10°C. The coiling direction and relative development of kummerforms in *Globigerina pachyderma* (Ehrenberg) recovered from the Subarctic water of the northern Pacific is shown in table II.

The forms occurring in the Subarctic and Central waters of the northern Pacific are similar to those described by Ehrenberg (1861) and differ considerably in shape, development of chambers, and thickness and texture of the test wall with those occurring in the North Atlantic (as described by Cifelli, 1970). No true representative of *G. incompta* Cifelli is recorded from Pacific waters.

Globigerina pachyderma occurs in surface waters north of latitude 36°N, up to a maximum relative abundance of 71% of the total foraminiferal population at station 301 (latitude 55°N). In the deeper tows, it first appears around latitude 29°N where it represents 5% of the total population. The juvenile forms of this species have a characteristic sugary wall texture, are more compact, and have a slit-like aperture. These features are partly obscured in the more adult and larger forms. The development of kummerform specimens is most common in this species and as many as 81% of the specimens in the surface water at station 301 (latitude 55°N) are kummerforms. At this station, an interesting relationship is observed regarding depth of water in contrast to all other species at most of the stations. Bé (1960) on the other hand noted a reduction of the final chamber size of specimens collected at depths greater than 200 metres in Atlantic waters.

The specimens recovered from stations 297, 298 and 299 (latitude 29° to 43°N) are mostly dextrally coiled whereas farther north they are predominantly sinistral. The change from dextral to sinistral coiling occurs somewhere between latitude 44° to 48°N where surface water isotherms vary from 7°C to 10°C. The coiling direction and relative development of kummerforms in *Globigerina pachyderma* (Ehrenberg) recovered from the Subarctic water of the northern Pacific is shown in table II.

TABLE II

DEVELOPMENT OF KUMMERFORMS AND COILING DIRECTION IN *GLOBIGERINA PACHYDERMA* (EHRENBERG)

Latitude	Station	Depth of water in metres	Percentages			
			Specimens	Kummerform	Dextral	Sinistral
29°N	297	0-320	absent	-	-	-
		160-475	02.82	?	100.00	-
		475-1030	05.88	?	100.00	-
36°N	298	0-320	04.65	50.00	50.00	50.00
43°N	299	0-185	12.08	55.55	83.33	16.67
		185-850	19.25	50.00	91.66	08.34
49°N	300	0-1050	22.94	67.39	09.52	90.48
55°N	301	0-190	71.32	80.88	01.47	98.53
		100-700	45.72	70.73	04.06	95.94

According to Parker (1962) specimens of *G. pachyderma* are mostly dextral in the vicinity of latitude 25°S and become sinistral south of latitude 46°S in the South Pacific.

The correlation analysis shows that the distribution of *G. pachyderma* correlates directly with latitude, and inversely with temperature and average salinity. In terms of its geographic distribution, it is similar to *Globoquadrina dutertrei* (D'Orbigny).

Globigerina quinqueloba Natland

Globigerina quinqueloba NATLAND, 1938, Calif. Univ. Scripps Inst. Ocean., Bull. Tech. Ser., v. 4, n. 5, p. 149, pl. 6, figure 7.

We agree with Parker (1962) in retaining the species under *Globigerina* instead of *Globigerinita* as recommended by Loeblich and Tappan (1957). This species occurs in the surface water mostly in association with *Globigerina pachyderma* (Ehrenberg) and *G. bulloides* D'Orbigny in cold Subarctic water. However, in deeper waters in the vicinity of the equator, rare occurrences of this species are noted. Maximum abundance is observed in the deeper water

at station 299 (latitude 43°N) where it comprises about 10% of the total foraminiferal population. It is interesting to note that the forms living in the vicinity of the equator are dextrally coiled whereas farther north they are predominantly sinistral. There is no significant variation in the size and shape of the specimens in these two water masses.

The distribution of *G. quinqueloba* Natland in Pacific waters is largely controlled by temperature and salinity. Nutrients and depth of water seem to be the least significant factors.

Globigerina rubescens Hofker

Globigerina rubescens HOFKER, 1956, Copenhagen Univ. Zool. Mus., Spolia, c. 15, p. 239, pl. 35, figures 18-21.

This species is sporadic in occurrence at most of the stations south of latitude 36°N in shallow to medium depths. The maximum abundance of 9% of the total population was noted in the subsurface water (190-460 metres) of station 389 (latitude 10°S). No record of its occurrence in water deeper than 50 metres has thus far been recorded in the present study. The specimens are generally small in size and never exceed more than 240 microns in diameter. The species is distinguished by its simple structure and its high arched and proportionately large aperture.

Genus *GLOBIGERINOIDES* Cushman 1927

Globigerinoides conglobatus (Brady)

Globigerina conglobata BRADY, 1879, Quart. Jour. Mus. Sci. n. sev., v. 19, p. 286.

This warm-tropical water species is well represented in all depths of the Southern water up to latitude 22°N with a varying relative abundance ranging from 1 to 14% of the total population in the surface water. The observed maximum diameter of this form was 560 microns, and the average was 350 microns. Specimens up to 1 mm diameter have been recorded by Parker (1962) from South Pacific waters where it occurs in sediments north of latitude 35°S. The juveniles of this species differ from the adult in having a relatively large aperture and in the shape and arrangement of their last chamber which is similar to *Globigerina bulloides* D'Orbigny. A bulla-like chamber generally appears in adult tests.

The correlation analysis shows that the distribution of this species is related directly to temperature and salinity and is inversely correlated with phosphate and nitrate concentration of the surrounding water, depth and

latitude. Its distribution is almost similar to that of *Globigerinoides ruber* (D'Orbigny).

Globigerinoides elongatus (D'Orbigny)

Globigerina elongata D'ORBIGNY, 1826, Ann. Sci. Nat. Paris, Ser. 1, tome 7, p. 277.

This minute species seems to be a variant of *Globigerinoides ruber* (D'Orbigny) and differs only in having a more compressed test and small primary aperture. Specimens showing this feature are observed only in the surface water of station 293 (latitude 10°N) where they represent about 2% of the total population. There was no other record of its occurrence in the present study.

Globigerinoides ruber (D'Orbigny)

Globigerina rubra D'ORBIGNY, 1839, In de la Sagra, Hist. Phys. Pol. Nat. Cuba, Foraminiferes, v. 8, p. 82, pl. 4, figures 12-14.

This is a widely distributed species in warm-tropical to warm-temperate waters of Southern and Central water masses and was recorded at almost all depths during the course of the present study. Its greatest relative abundance occurs near the equator (44% in the shallow water and an average of 20% of the total foraminiferal population at greater depths). However, its numbers are reduced northward to 5% at station 299 (latitude 43°N). The morphology of this species varies greatly in terms of size, shape of the individual chambers, aperture, and in its wall characters. Kummerform development in this species is very common in those specimens living near the equator and is rare in Central water forms. Parker (1962) divided this species into three groups based on morphological characters. Most of the variations as noted by her occur in our samples but these groupings are considered here as phenotypic variants rather than subspecies. In the South Pacific Parker (*op. cit.*) recorded this species mostly north of latitude 30°S.

The correlation analysis shows a direct correlation of the abundance of this species with temperature and salinity and inverse correlation with latitude, water depth and phosphate and nitrate concentrations of the associated waters (see Hecht, 1970). Latitude and salinity appear to be important factors in determining its relative abundance. Coiling direction is closely related to the size and other morphological variations in the test. Latitude plays a more significant role in the development of kummerforms in *G. ruber*.

Globigerinoides trilobus trilobus

Globigerina triloba REUSS, 1850, Denkr. K. Akad. Wiss. Wien., v. I, p. 374, pl. 47, figure 11.

This subspecies is similar in the basic morphological construction of its test to *Globigerinoides ruber* (D'Orbigny); however, there is only one supplementary aperture per chamber on the dorsal side of this species in contrast to the two apertures in the case of *Globigerinoides ruber* (D'Orbigny). The growth of the last chamber to a sac-like structure gives rise to *Globigerinoides trilobus sacculifer* (Brady). The typical *G. trilobus trilobus*, having a large semicircular last chamber, occurs predominantly at all depths in warm-tropical to warm-temperate regions in Southern water, and rarely in Central water. A relative abundance of up to 50% is recorded in the surface water at station 294 (latitude 15°N). Forms attain a maximum diameter of 720 microns and an average of 520 microns. The specimens may be coiled in either direction, but are more frequently observed in the sinistral form.

A number of micropaleontologists consider *Globigerinoides trilobus trilobus* and *G. trilobus sacculifer* as one species having two intergrading variants. However, the development of a sac-like feature in *G. trilobus sacculifer* is so characteristic and persistent that, along with its relatively more restricted distribution in Pacific waters (compared with *G. trilobus trilobus*), the separation of these forms into two subspecies seems to be justified.

G. trilobus trilobus (Reuss) appears to be sensitive to most of the physical and chemical parameters of the environment as revealed by the correlation analysis. Factors such as temperature and salinity have a direct correlation with the distribution of this subspecies in Pacific waters, whereas latitude and phosphate and nitrate concentrations of the surrounding water show an inverse correlation.

Globigerinoides trilobus sacculifer (Brady)

Globigerina sacculifera BRADY, 1877, Geol. Mag., new ser., dec. 2, v. 4, n. 12, p. 535.

This is a large sized, well known and easily identifiable form having a well developed sac-like last chamber. It commonly occurs in the warm-tropical Southern water and is found as far north as latitude 22°N. It has a more restricted distribution both in area and in frequency than *Globigerinoides trilobus trilobus* (Reuss) and generally favours surface waters. Maximum relative abundance has been recorded as 5% with an average of about 1% of the total population. Like *G. trilobus trilobus* (Reuss), the specimens of *G. trilobus sacculifer* are usually sinistrally coiled but dextral forms occur frequently. Its maximum diameter is generally more than one and one-half times that of *G. trilobus trilobus* (Reuss), perhaps because of the elongation of the

last chamber into a sac-like feature; however, kummerform development is common.

Genus GLOBOQUADRINA Finaly, 1947

Globoquadrina conglomerata (Schwager)

Globigerina conglomerata SCHWAGER, 1966, *Novara* Exped., 1857-59, Geol. Theil. Bd. 2 Abt. 2, p. 255, pl. 7, figure 113.

This is a warm water species occurring mostly in the surface water of warm-tropical seas to a latitude of 22°N with a maximum relative abundance of up to about 5% of the total population. The species shows a great range of variation; however, its large umbilical-extra-umbilical aperature and pitted walls are characteristic. Temperature seems to play a more significant role in determining its distribution than other environmental factors, whereas latitude and salinity appear to be important in determining the size variations in the tests. According to Parker (1962) this species is found north of latitude 40°S and occurs rarely south of latitude 25°S in the South Pacific.

Globoquadrina dutertrei (D'Orbigny)

Globigerina dutertrei D'ORBIGNY, 1829, in de la Sagra, Hist. Phys. Pol. Nat. Cuba, 'Foraminiferes', v. 8, p. 84, pl. 4, figures 19-21.

This warm-temperate to colder Subarctic water species occurs sparsely at a number of stations. There is a significant amount of morphological variation among specimens collected in transitional waters. Generally, high-spired large-sized forms with a typical cancellate wall and having six to seven chambers in the last whorl are common in warm-temperate waters, especially between latitude 10°N to 36°N where they comprise less than 2% of the total population in surface waters and a maximum of 7% in the deeper waters at station 295 near latitude 22°N. The cold-water forms have a small, rounded test with smooth walls and umbilical teeth which are not prominent. These types are found north of latitude 36°N to at least latitude 55°N and comprise up to 9% of the total population in the surface waters and up to a maximum of 11% in the subsurface waters at station 299 (latitude 43°N). The maximum and average diameters of the specimens collected in the warm water are 720 and 440 microns and from the cold water are 400 and 260 microns respectively. Because of these morphological and geographical variations there has been considerable disagreement over the true ecology of *G. dutertrei*. Bé (1959) included this species in his 'cold preference group' whereas Boltovskoy (1962, 1966) associated it with the warm water species group.

Our correlation analysis indicates a strong direct relationship with latitude and nutrient concentration of the associated waters, and an inverse relationship with temperature and salinity. This analysis also points out an

inverse relationship of second order correlation with size development of this species but most other factors remain constant. Thus this species belongs to two different environmental regions and each is represented by a distinct morphotype.

In South Pacific sediments, *G. Dutertrei* is found north of latitude 45°S (Parker, 1962). Bradshaw (1959) recorded this species in almost all water masses of the Northern Pacific.

Globoquadrina hexagona (Natland)

Globigerina hexagona NATLAND, 1938, Bull. Scripps Inst. Oceanog. Tech. Ser., v. 4, n. 5, p. 149, pl. 7, figure 1.

This species also shows wide variations in morphological characters. The majority of specimens collected appear to thrive in equatorial surface waters up to latitude 22°N. However, in deeper waters *G. hexagona* has been recorded as far north as latitude 43°N. Perhaps there are several phenotypic variants of this species, each inhabiting different ecological regimes. The tropical warm-water forms collected from surface waters have a large well developed test with highly pitted walls and a highly lobulate periphery. Specimens collected from deeper waters, farther to the north, are small, rounded and highly compressed with more or less smooth walls. The warm water forms attain a maximum diameter of more than 360 microns whereas the deeper water and cold water forms average only 300 microns in diameter.

Bradshaw (1959) observed the highest frequency of occurrence of this species around the 'equatorial west central region' of the Pacific with scattered occurrences in the transitional water of the Peru and California currents. It has also been observed in sediments of the South Pacific north of latitude 45°S (Parker, 1962).

The correlation analysis has not shown any significant relationship between the distribution of *G. hexagona* and the other measured environmental parameters.

Genus PULLENIATINA Cushman 1927

Pulleniatina obliquiloculata (Parker and Jones)

Pullenia obliquiloculata PARKER AND JONES, 1862, Philos. Trans., v. 155, p. 368, pl. 19, figure 4.

This species occurs in surface warm-tropical water up to latitude 15°N and rarely in deeper waters. The maximum frequency of occurrence of about 4% of the total population is recorded from station 290 (latitude 5°N). There is

considerable variation in the aperture characters and texture of the wall of this species especially between juveniles and adult forms. According to Bradshaw (1959) *P. obliquiloculata* is most common in tropical regions and maximum abundance is noted south of Hawaii which is in agreement with our present observations. In the South Pacific, Parker (1962) records this species north of latitude 35°S.

The correlation analysis does not show any significant relationship between the distribution of this species and any of the measured physical and chemical parameters.

Subfamily SPHAEROIDINELLINAE

Genus SPHAEROIDINELLA Cushman 1927

Sphaeroidinella dehiscens (Parker and Jones)

Sphaeroidina dehiscens PARKER AND JONES, 1863, Roy. Soc. Lond. Philos. Trans., v. 155, p. 369, pl. 19, figure 5.

This species is extremely rare in our samples and so far it has been recorded from only one station (294, latitude 5°N) in the surface water and at two stations (293, latitude 10°N, and 297, latitude 29°N) in the deeper tows. It never increases in its relative abundance to more than 2% of the total population. According to Bradshaw (1959) *S. dehiscens* is most abundant in the centre of the equatorial Pacific region. It is found north of latitude 40°S in the South Pacific sediments (Parker, 1962).

Subfamily ORBULININAE Schultze

GENUS ORBULINA D'Oribgny 1809

Orbulina universa D'Orbigny

Orbulina universa D'ORBIGNY, 1839, in de la Sagra, Hist. Phys. Pol. Nat. Cuba, 'Foraminiferes', v. 8, p. 3, pl. 1, figure 1.

This well known semicosmopolitan species occurs in most of our samples from Southern and Central water. Because the forms are extremely fragile and delicate many are destroyed during processing of the samples and, consequently, it has not been observed consistently in all the plankton tows. The distribution varies from 0.3% of the total population in the surface waters of station 289 (latitude 10°S) to a maximum of 7% at station 298 (latitude 36°N). It is recorded in one of the deeper tows in Subarctic water at station 301 (latitude 55°N); however, its relative abundance is low (0.7%). The deeper

water forms have both thicker and more opaque walls. According to Bradshaw (1959), *O. universa* is widely distributed in the tropical and temperate regions of the northern Pacific, whereas in the South Pacific Parker (1962) has noted its occurrence north of latitude 50°S although she was not able to establish a definite southern boundary because of the absence of sufficient samples.

Genus CANDEINA D'Orbigny, 1839

Candeina nitida D'Orbigny

Candeina nitida D'ORBIGNY, 1839, In de la Sagra, Hist. Phys. Pol. Nat. Cuba, 'Foraminiferes', p. 108, pl. 2, figures 27, 28.

This is a small species whose sporadic occurrences at a few stations have been noted during the present study. It is present at only two stations (389, latitude 10°S, and 295, latitude 22°N) where it represents less than 1% of the total population in surface waters. Bradshaw (1959) recorded *C. nitida* from tropical and warm-temperate regions of the Northern Pacific, whereas its occurrence in South Pacific sediments is limited to areas north of latitude 30°S (Parker, 1962). Because of its extreme paucity and patchy distribution, no true relationship of its abundance can be established with respect to the other measured parameters.

Subfamily CATAPSYDRACINAE Bolli, Loeblich and Tappan

Genus GLOBIGERINITA Brönnimann, 1951

Globigerinita glutinata (Egger)

Globigerina glutinata EGGER, 1893, Abhandle. K. bay. Akad. Wiss. Munchen, Cl. II, v. 18, p. 271, pl. 13, figure 19-21.

This small cosmopolitan species was observed at varying depths at almost all the stations. Its relative abundance varies from about 3% near latitude 15°N to as much as 20% of the total population in the surface waters near latitude 29°N. Its relative abundance is more or less constant to about 1000 metres depth. The specimens retain essentially their basic morphological characters in all the water masses and at all depths. However, the development of bulla and a supplementary aperture seems to be more common in forms collected from surface waters. The deeper water forms are generally small, rounded and without a supplementary aperture. Because it is a true cosmopolitan species, the various measured physical and chemical parameters seem to have little influence in the control of its distribution in the various water masses surveyed.

Family HANTKENINIDAE Cushman

Subfamily HASTIGERININAE Bolli, Loeblich and Tappan

Genus GLOBIGERINELLA Cushman, 1927

Globigerinella adamsi (Banner and Blow)

Hastigerina (Bolliella) adamsi BANNER AND BLOW, 1959, Palaeontology, v. 2, pt. 1, p. 13, test figure 4a-d.

This species is extremely rare in our samples and represents less than 0.2% of the total population at stations near the equator. Its extreme paucity does not permit definite correlation of its occurrence with various measured environmental parameters.

Globigerinella aequilateralis (Brady)

Globigerina aequilateralis BRADY, 1879, Quart. Jour. Micro. Sci. new ser., v. 19, p. 285.

This well known and widely distributed species occurs in all the shallow-water tows and in a few deep-water tows from warm-tropical to warm-temperate regions in Southern water, and rarely in Central water. The relative abundance never reaches more than 5% of the total population in the surface waters; however, in a deeper tow at station 289 (latitude 10°S), it constitutes about 12% of the total population. Generally, this species ranges in diameter between 300 and 400 microns. However, a specimen of about 960 microns diameter has been observed in the composite sample collected at station 292 (latitude 0.5°N).

The juvenile specimens have their aperture situated laterally toward the umbo so that these forms are, on the whole, asymmetrical. In the adult stage, the addition of new chambers causes the aperture to move to the periphery of the test and thus it acquires its true symmetrical shape. According to Bradshaw (1959) this species is found in tropical and warm-temperate regions of the northern Pacific and Parker (1962) has reported its occurrence north of latitude 45°S in sediments from the southern Pacific.

Genus HASTIGERINA Thomson, 1876

Hastigerina pelagica (D'Orbigny)

Nonionina pelagica D'ORBIGNY, 1829, Voy. Amér. Mérid., 'Foraminiferes', v. 5, pt. 5, p. 27, pl. 3, figures 13-14.

This species occurs generally in association with *Globigerinella aequilateralis* (Brady); however, it seems to have a more restricted range. It has not been recorded south of the equator or north of latitude 29°N. Between these latitudes it has an average relative abundance of 3% in the surface waters, but the greatest numbers of specimens were noted in the subsurface waters of station 297 (latitude 29°N). The forms are, in general, medium sized, and range in diameter up to 360 microns. Several specimens have a maximum diameter of over 900 microns. In the South Pacific, this species is found in bottom sediments north of latitude 30°S and in plankton samples as far south as latitude 50°S (Parker, 1962). Bradshaw (1959) observed it south of latitude 40°N in the northern Pacific.

Family GLOBOROTALIIDAE Cushman, 1927

Subfamily GLOBOROTALIINAE Cushman, 1927

Genus GLOBOROTALIA Cushman, 1927

Globorotalia cavernula Bé

Globorotalia cavernula BE, 1967, Contrib. Found. Foram. Res., v. 18, pt. 3, pp. 128-131, pl. 10, figures 1-6.

This species was first recognized in the Atlantic and Pacific sectors of the Antarctic Ocean. It is extremely rare in the present plankton tows and is recorded only from the subsurface levels of station 201 (latitude 55°N), where it represents about 3% of the total population. The specimens average about 280 microns in diameter with an average maximum diameter of 300 microns. Most of the specimens are dextrally coiled whereas the general assemblage in Subarctic waters are sinistrally coiled.

Globorotalia crassaformis (Galloway and Wissler)

Globigerina crassaformis GALLOWAY AND WISSLER, 1927, Jour. Pal., V. 1, p. 41, pl. 7, figure 12.

A few sporadic occurrences of this species, not exceeding 0.1% of the total planktonic foraminifera population, are noticed in two surface tows collected near the equator. The species is very similar to *Globorotalia hirsuta* (D'Orbigny) except in the degree of umbilical convexity. Because *Globorotalia hirsuta* (D'Orbigny) shows variations in the diameter/thickness ratio of its tests (collected from different depths) it is possible that *G. crassaformis* and *G. hirsuta* are perhaps two phenotypic variants of the same species. However, because of the paucity of specimens showing the features of a typical '*crassaformis*' in our samples, this taxonomic relationship could not be established beyond doubt.

Globorotalia inflata (D'Orbigny)

Globigerina inflata D'ORBIGNY, 1839, in Barker-Webb and Berthelot, Hist. Nat. Iles Canaries, v. 2, Foraminifères, p. 134, pl. 2, figures 7-9.

This species shows considerable variations in morphological characters which are described in detail by Parker (1962). In our samples this species has been recorded at almost all the stations and at varying depths. However, it has not been observed in the surface water south of latitude 22°N. The highest frequency of its occurrence in surface waters is from the Central water (up to 9% at station 299, latitude 43°N). Conversely, this species comprises about 15% of the total population in the subsurface water at station 294 (latitude 15°N). In the South Pacific, *G. hirsuta* occurs north of latitude 45°S (Parker, 1962). Bradshaw (1959) recorded its occurrence throughout the tropical and warm-temperate regions. The correlation analysis suggests that temperature may be the most significant factor controlling the distribution of this species.

Globorotalia menardii (D'Orbigny)

Rotalia menardii D'ORBIGNY, 1826, Ann. Sci. Nat., v. 7, p. 273, n. 26, Modeles, n. 10.

This warm water species occurs at most of the stations in the Southern water mass. It is more common at intermediate depths (down to 500 metres) and is extremely rare in deeper waters. Highest frequency is observed in subsurface waters (200-500 metres) at station 297 (latitude 29°N), where it represents about 35% of the total population. This high concentration probably

reflects its patchy habit and no other studied environmental parameters seem to be related. On the average, a relative abundance of less than 2% is recorded in the surface waters.

The specimens of *G. menardii* show considerable variation in broad morphological characters such as size, shape, diameter/thickness ratios, umbilical opening, and shape of the test chamber. These variations are pronounced in forms collected from the different oceans of the world. Specimens of *G. menardii* from the present-day sea show considerable differences compared with those collected from the Late Tertiary sequence of Trinidad (Bolli, 1957) and South India (Banerji, 1970, a,b,). It may be possible that the Tertiary '*menardii*' assemblage has evolved into a series of new subspecies in the different oceanic water masses of present day seas. However, further detailed study is required on a world-wide basis in order to establish this link.

Globorotalia scitula (Brady)

Pulvinulina scitula BRADY, 1882, Roy. Soc. Edinburg Proc., v. II (1880-82), n. III, p. 716.

This species has thus far been recorded from the surface waters at station 290 (latitude 5°S) where it represents only 0.8% of the total population. Bradshaw (1959) has reported its wide distribution throughout the North Pacific. Perhaps the distribution of *G. scitula* is similar to *Globorotalia truncatulinoides* (D'Orbigny) which shows a seasonal variation in distribution and consequently does not occur in large numbers during the summer months.

Globorotalia truncatulinoides (D'Orbigny)

Rotalina truncatulinoides D'ORBIGNY, 1839, in Barker-Webb and Berthelot, Hist. Nat. Iles Canaries, 'Foraminiferes', v. 2, pt. 2, p. 132, pl. 2, figures 25-27.

This species is extremely rare in our Pacific plankton samples and occurs only in the surface waters up to a maximum relative abundance of about 2% of the total population (station 298, latitude 36°N) in the Central water. As observed by Bé and Ericson (1963) the maximum abundance of this species appears from late November through April in the central North Atlantic. Perhaps this seasonal variation in abundance occurs also in Pacific waters, and if so, it would account for the rare occurrence of this species in our samples. Because of its extreme paucity, no detailed morphological and/or ecological comparison could be made.

Globorotalia tumida (Brady)

Pulvinulina menardii (D'Orbigny) var. *tumida* BRADY, 1877, Geol. Mag., new ser., dec. 2, v. 4, no. 12, p. 535.

This species is fairly common in plankton tows from surface to intermediate depths near the equator. It occurs as far north as latitude 15°N in Southern waters and highest concentrations of about 13% of the total population are observed in the subsurface water at station 290 (latitude 5°S). The specimens show considerable variation in morphology and perhaps more than one phenotype can be recognized. On the average, *G. tumida* ranges in diameter from 400-800 microns, and a few specimens reach a maximum of more than 1 mm. The specimens are, in most cases, sinistrally coiled. The distribution of *G. tumida* appears to be largely controlled by factors such as temperature and salinity. In South Pacific sediments, it is found north of latitude 22°S (Parker, 1962).

CONCLUSIONS

1. Five groups of species have been distinguished in the equatorial and northern Pacific. These groups include a warm-tropical (equator to 15°N), warm-temperate (up to 30°N), cold-temperate (up to 43°N), cold water (north of 43°N), and a cosmopolitan group. Factors such as temperature and nutrients appear to be most important in controlling the geographical limits of these groups.

2. In general, the population density of planktonic foraminifera in Pacific waters decreases rapidly with increasing depth. The abundance ratio of specimens in surface compared with subsurface waters during the period of this investigation was approximately 5:1. The decrease in the foraminiferal population with depth of water is probably closely related to the degree of light penetration in sea water which, in turn, controls phyotplankton distribution. The latter represent a major source of food for the foraminifera.

3. There is a uniform decrease in species diversity from the equator to the higher latitudes in this part of the Pacific. A simple direct relationship seems to exist between the temperature and salinity of water and the absolute abundance and species diversity of foraminifera populations in the Pacific.

4. An examination of the bathymetric distribution of species indicates that forms such as *Globigerinoides trilobus sacculifer* (Brady) and *Globigerinella aequilateralis* (Brady) are restricted to near-surface waters whereas forms such as *Globorotalia hirsuta* (D'Orbigny) and *G. inflata* (D'Orbigny) are found at all the levels that were sampled and show no specific preference for surface waters.

5. In terms of ecological relationships *Globigerinoides ruber* (D'Orbigny) and *G. trilobus trilobus* (Reuss) in warm water, and *Globigerina pachyderma* (Ehrenberg) in cold water, are the main constituents of the respective faunas.

6. There appears to be no simple relationship between size, maturity of forms and various physical factors generally considered to affect the entire faunal assemblage. Correlation analysis, however, suggests some inverse relationship between the size of *Globigerinoides ruber* (D'Orbigny) and latitude. Several other species are reduced in size towards higher latitudes.

7. Calcification of test walls develops in those specimens that live a part, or all of their life in deeper waters. This calcification, in many cases, does not depend on the maturity of the individuals.

8. In general, an increase in the percentage of kummerform specimens with respect to depth of water is evident at lower latitudes. Kummerform development is maximum in Subarctic waters because of the relatively higher abundance of forms such as *Globigerina pachyderma* (Ehrenberg) and *Globoquadrina dutertrei* (D'Orbigny) in which kummerform development is a common feature. Kummerform development may be an ontogenic feature, more or less independent of surrounding physical conditions.

9. The ratio of total number of specimens-to-species decreases rapidly at different stations from south to north in warm-tropical to temperate waters. This decrease may reflect a progressively lower rate of reproduction for each individual species because of the incompatible environmental conditions for most species that are encountered towards the north.

10. Large numbers of typical *Globigerina pachyderma* (Ehrenberg) have been noted in the Northern water mass of the Pacific. This observation is not in agreement with the work of Cifelli (1969) who noted that the characteristic *Globigerina pachyderma* has never definitely been identified in recent living planktonic assemblages.

11. *Globigerina falconensis* Blow does not occur in close association with *G. bulloides* D'Orbigny in any of the samples collected during this study and therefore these two taxa are considered to belong to ecologically distinct regions and are not taxonomically related.

12. The extreme paucity of several species sampled for this investigation (e.g. *Globorotalia scitula* and *G. truncatulinoides*) suggests that their reproduction period is confined to the cooler seasons which is in agreement with the observations of other researchers working in the Atlantic.

ACKNOWLEDGEMENTS

The authors wish to express their appreciation to the scientists and ship's personnel of the Bedford Institute who contributed to the success of this research project. We are especially indebted to Dr. W. Cameron, Chief Scientist on the Tahiti-Vancouver leg of HUDSON 70, and to those members of the Metrology and Chemistry sections of Atlantic Oceanographic Laboratory who contributed their time, equipment and relevant data. Messrs. D. Buckley and R. Cranston were very helpful during the preparation of computer data and programs for the correlation and factor analyses. Drs. F. Wagner and M.A. Rashid and Mr. D. Clark gave valuable assistance throughout the preparation of this manuscript. Mr. D. Walker photographed the scanning electron-micrographs shown in the plates.

This study was supported by the Marine Geology Section, Atlantic Oceanographic Laboratory, Department of Energy, Mines and Resources. Sincere appreciation is due to the authorities of the Columbo Plan of the Canadian International Development Agency, Government of Canada, and to the Oil and Natural Gas Commission, Government of India, for arranging Dr. Banerji's visit to the Bedford Institute during 1970-1971.

REFERENCES

AGASSIZ, A. 1902. Report on the scientific results of the expedition to the tropical Pacific. I. Preliminary report and list of stations: Mus. Comp. Zool., Mem. 26, no. 1, pp. 1-114.

ANGEL, M.V. 1968. The thermocline as an ecological boundary: Sarsia, vol. 34, pp. 299-312.

BANERJI, R.K. 1970a. Conflicting stratigraphic ranges observed in the Miocene planktonic foraminifera from the Cauvery Basin, South India: Proceed. Indian Science Congress Assoc., Kharagpur, India.

BANERJI, R.K. 1970b. Foraminiferal biostratigraphy of Meso-Cenozoic sequence of the Cauvery Basin, South India: Jour. Geol. Society of India, vol. 11, no. 4, pp. 348-357, figures 1-2.

BANNER, F.T., and W.H. BLOW. 1970. Some primary types of species belonging to the Superfamily Globigerinaceae. Contrib. Cushman Found. Foram. Res., vol. 11, pt. 1, pp. 1-14, pl. 1-8.

BE, A.W.H. 1959. Ecology of Recent planktonic formainifera. Pt. 1 - Areal distribution in the western North Atlantic: Micropaleontology, vol. 5, no. 1, pp. 77-100, pl. 1-2.

BE, A.W.H. 1960a. Ecology of Recent planktonic foraminifera. Pt. 2 - Bathymetry and seasonal distributions in the Sargasso Sea off Bermuda: Micropaleontology, vol. 6, pp. 370-392.

BE, A.W.H. 1960b. Some observations on Arctic planktonic foraminifera: Contrib. Cushman Found. Foram. Res., vol. 11, no. 2, pp. 64-68.

BE, A.W.H., and D.B. ERICSON. 1963. Aspects of calcification in planktonic foraminifera (Sarcodina): Ann. N.Y. Acad. Sci., vol. 109, pp. 65-81.

BE, A.W.H., and L. LOTT. 1964. Shell growth and structure of planktonic foraminifera: Science, vol. 145, pp. 823-824.

BE., A.W.H. 1969. Planktonic Foraminifera: Antarctic Map Folio Series, Am. Geog. Soc., pp. 9-12.

BERGER, W.H. 1969. Kummerform foraminifera as clues to oceanic environments: Abstract, Bull. Am. Assoc. Petr. Geol., vol. 53, p. 706.

BERGER, W.H. 1970. Planktonic foraminifera: Differential production and expatriation of Baja California: Limnology Oceanogr., vol. 15, no. 2, pp. 183-204.

BOLLI, H.M. 1957. Planktonic foraminifera from the Oligocene-Miocene Cipero and Lengua formations of Trinidad: U.S. Nat. Mus., Bull. 215, pp. 97-124.

BOLTOVSKOY, E. 1967. Foraminifera as hydrological indicators: Proc. 1st Intern. Conf. Plank. Microfossils, vol. 2, pp. 1-14.

BOLTOVSKOY, E. 1969. Distribution of planktonic foraminifer as indicators of water masses in the western part of the tropical Atlantic: Proc. Symp. Oceanogr. & Fish. Resources of the Tropical Atlantic, UNESCO, Paris, pp. 45-55.

BRADSHAW, J.S. 1959. Ecology of living planktonic foraminifera of the North and Equatorial Pacific Ocean: Contrib. Cushman Found. Foram. Res., vol. 10, pt. 2, pp. 25-64.

BRADY, H.B. 1881. On some Arctic foraminifera from soundings obtained on the Austro-Hungarian North Polar Expedition of 1872-1874: Ann. Mag. Nat. Hist. ser. 5, vol. 8, no. 48.

BRADY, H.B. 1884 Report on the foraminifera dredged by HMS *Challenger* during the years 1873-1876: Rept. Voy. *Challenger*, Zool., vol. 9, 814 pp.

CAMERON, E.M. 1967. A computer program for factor analysis of geochemical and other data: Geol. Surv. Canada, paper 67-34, pp. 1-42.

CIFELLI, R. 1961. *Globigerina incompta*, a new species of pelagic foraminifera from the North Atlantic: Contrib. Cushman Found. Foram. Res., vol. 12, pt. 3, pp. 83-86, pl. 4.

CIFELLI, R., and R.K. SMITH. 1969. Problems in the distribution of Recent planktonic foraminifera and their relationships with water mass boundaries in the North Atlantic: Proc. 1st Intern. Conf. Plank. Microfossils, vol. 2, pp. 68-81, figures 1-7.

CIFELLI, R., and R.K. SMITH. 1970. Distribution of planktonic foraminifera in the vicinity of the North Atlantic current: Smithsonian Contrib. to Paleobiology, no. 4, pp. 1-52.

CUSHMAN, J.A., and R.W. HARRIS. 1927. The significance of relative measurements in the study of foraminifera: Contrib. Cushman Lab. Foram. Res., vol. 2, pt. 4, pp. 92-94.

EHRENBERG, C.G. 1861. Elemente des tiefen Meeresgrundes im Mexikanischen Golfstrome bei Florida; Uber die Tiefgrund-Verhaltinisse des Oceans am Eingange der Davisstrasse und bei Island: K. Pruss Akad. Wiss. Berlin, Monatsber.

EMILIANI, C. 1954. Depth habitat of some species of pelagic foraminifera as indicated by oxygen isotope ratios. Am. Jour. Sci., vol. 252, pp. 149-158.

HARDER, W. 1968. Reactions of planktonic organisms to water stratification: Limnol. Oceanogr. vol. 13, pp. 156-168.

HERON-ALLEN, E., and A. EARLAND. 1922. Foraminifera: British Antarctic (*Terra Nova*) Exped., vol. 6, no. 2, pp. 25-268.

KING, J.E., and T.S. HIDA. 1957. Zooplankton abundance in the central Pacific, Part 2: U.S. Fish and Wildlife Service Fish. Bull. 118, pp. 365-395.

LOHMAN, H. 1920. Die Bevolkerung des Ozeans mit Plankton nach den Ergebnissen der Zentrifugenfange wahrend der Ausreise des *Deutschland* 1911: Arch. Biontologies, vol. 4, no. 3, pp. 1-617.

MURRAY, J. 1895. Summary of the scientific results obtained at the sounding, dredging and trawling stations of HMS *Challenger: Challenger* Repts. Summary, pt. 1 and 2, pp. 1-1608.

MURRAY, J. 1897. On the distribution of the pelagic foraminifera at the surface and on the floor of the ocean: Nat. Sci. vol. 11, pp. 17-27.

ORBIGNY, A. D'. 1826. Tableau methodique de la classe des cephalopodes: Ann. Sci. Nat., vol. 7, pp. 245-314, pl. 10-17.

PARKER, F.L. 1960. Living planktonic foraminifera from the Equatorial and Southeast Pacific: Sci. Rept. Tohoku Univ. 2nd ser., spec. vol. 4, pp. 609-620.

PARKER, F.L. 1962. Planktonic foraminiferal species in Pacific sediments: Micropaleontology, vol. 8, no. 2, pp. 219-254, 10 pl.

PHLEGER, F.B. 1945. Vertical distribution of pelagic foraminifera: Am. Jour. Sci., vol. 243, pp. 377-383.

PHLEGER, F.B. 1951. Ecology of foraminifera, northwest Gulf of Mexico. Pt. 1, Foraminifera distribution: Geol. Soc. Am., Mem., vol. 46, pp. 1-88.

SCHOTT, W. 1935. Die Foraminiferen in dem aquatorialen Teil des Atlantischen Ozeans: Wiss. Ergeb. Deutsch Atlantische Exped. *Meteor* 1925-1927, Bd. 2, pt. 3, sect. B, pp. 43-134.

SVERDRUP, H.V., M.W. JOHNSON, and R.H. FLEMING. 1942. *The Oceans, their Physics, Chemistry and general Biology.* Prentice Hall, Englewoodcliffs, N.J., 1087 pp.

APPENDIX I

TABLES OF ABSOLUTE AND RELATIVE PER CENT OF PLANKTONIC FORAMINIFERA SPECIES

TABLE 12

ABSOLUTE ABUNDANCE OF PLANKTONIC FORAMINIFERA IN THE PACIFIC OCEAN

ABSOLUTE ABUNDANCE OF PLANKTONIC FORAMINIFERA	WATER MASS	LATITUDES	STATIONS	DEPTH OF TOWS IN METRES	Candeina nitida D'ORBIGNY	Globigerina bulloides D'ORBIGNY	Globigerina calida PARKER	Globigerina falconensis BLOW	Globigerina pachyderma (EHRENBERG)	Globigerina quinqueloba NATLAND	Globigerina rubescens HOFKER	Globigerinella adamsi (BANNER AND BLOW)	Globigerinella aequilateralis (BRADY)	Globigerinita glutinata (EGGER)	Globigerinoides conglobatus (BRADY)	Globigerinoides elongatus (D'ORBIGNY)	Globigerinoides ruber (D'ORBIGNY)	Globigerinoides sacculifer (BRADY)	Globigerinoides trilobus (REUSS)	Globoquadrina conglomerata (SCHWAGER)	Globoquadrina dutertrei (D'ORBIGNY)	Globoquadrina hexagona (NATLAND)	Globorotalia cavernula BE	Globorotalia inflata (D'ORBIGNY)	Globorotalia crassaformis (GALLOWAY AND WISSLER)	Globorotalia hirsuta (D'ORBIGNY)	Globorotalia menardii (D'ORBIGNY)	Globorotalia scitula (BRADY)	Globorotalia humida (BRADY)	Globorotalia truncatulinoides (D'ORBIGNY)	Hastigerina pelagica (D'ORBIGNY)	Orbulina universa D'ORBIGNY	Pulleniatina obliquiloculata (PARKER AND JONES)	Sphaeroidinella dehiscens (PARKER AND JONES)	All others
	SOUTHERN	10°S	289	0 - 190	082		051						329	474	947		3675	041	1503	453		474				021				010		062			062
				190 - 460			030				059				059		178		089					030		089	030								059
				460 - 760	007		014	014					027	034			081		014					020											020
		5°S	290	0 - 200			183				336		122	428	153		1711	428	2689	244						183	031	55	024				367		306
				200 - 435			009										005		005					005			002		005						005
				765 - 0			003										008		025	011				005											005
		0°	291	0 - 800			341					012		148	026		572	103	553	2180		109					013		785		064	026	785		142
		5°N	292	0 - 800	029		024	068		049	107	4	056	283	112		065	102	776	449		107				010	010		054		068	027	156		051
		10°	293	0 - 190			181						068	151	024	042	371	029	644	054		024					034		015	005	015		039		073
				190 - 460			037						027	081	064		279	013	302	077		252		020		084	010		201		020		027		050
				460 - 750						004				128	008		090	075	154	030	023	045		011					015			004	004		008
		15°N	294	0 - 170									053	053	067		074	191	1004	057	032	060		085		011	011		004		131	071	046	018	042
				170 - 450										005	009		019		033	005	005	019		023		014			005		005	005			009
				450 - 700						007				040			173	025	098	007	025	036		033		004								022	011
		22°N	295	0 - 180	005			135			167		062	385	146		723	026	281	057	026	114		036		036	021				047	026			026
				180 -440						014	005		014	028			023		005		014	042				169	005				019				005
				440 -1050		004				004				013			018				004			009		004									004
		29°N	297	0 - 160		016							012	055			110		016					020		016	016			004	008				
				160 -475		007			007				007	015			022					011				056	093				030	007		004	004
				475 -1030		004			004				004	004			008		004					015			008				004				012
	CENTRAL	36°N	298	0 -320		018			005		005		005	000			036		008					008		003				003		008			005
				0 -900																															
		43°N	299	0 - 185		640			162	081				081			063				117			126								045			027
				085 -850		219			143	080				072							080	008		040	004	016						076			012
				185 - 0																															
	SUB-ARCTIC	49°N	300	0 -1050		469			353	246				202										146											
				0 - 190		038			647	079				066							051			025											
		55°N	301	100 - 0		096			870	045				249							077			102											
				100 -700		022			110	008				048							015		007	029								002			

TABLE 13

RELATIVE ABUNDANCE OF PLANKTONIC FORAMINIFERA IN THE PACIFIC OCEAN

RELATIVE ABUNDANCE OF PLANKTONIC FORAMINIFERA			Candeina nitida D'Orbigny	Globigerina bulloides D'Orbigny	Globigerina calida Parker	Globigerina falconensis Blow	Globigerina pachyderma (Ehrenberg)	Globigerina quinqueloba Natland	Globigerina rubescens Hofker	Globigerinella adamsi (Banner and Blow)	Globigerinella aequilateralis (Brady)	Globigerinita glutinata (Egger)	Globigerinoides conglobatus (Brady)	Globigerinoides elongatus (D'Orbigny)	Globigerinoides ruber (D'Orbigny)	Globigerinoides sacculifer (Brady)	Globigerinoides trilobus (Reuss)	Globoquadrina conglomerata (Schwager)	Globoquadrina dutertrei (D'Orbigny)	Globoquadrina hexagona (Natland)	Globorotalia cavernula Be	Globorotalia inflata (D'Orbigny)	Globorotalia crassaformis (Galloway and Wissler)	Globorotalia hirsuta (D'Orbigny)	Globorotalia menardii (D'Orbigny)	Globorotalia scitula (Brady)	Globorotalia humida (Brady)	Globorotalia truncatulinoides (D'Orbigny)	Hastigerina pelagica (D'Orbigny)	Orbulina universa D'Orbigny	Pulleniatina obliquiloculata (Parker and Jones)	Sphaeroidinella dehiscens (Parker and Jones)	All others
LATITUDE	STATION	DEPTH OF WATER																															
10°S	289	0-190	01 00		00 83						04 01	05.77	11 54		44.79	00.50	18.32	05.52			05.57								00.13		00.25	00.75		00.96
		190-460			04.76				09.52				09.52		28.57		14.29						04.76		14.29	04.76							09.52
		460-760	02.94		05.88	05.88					11.76	14.71			35.30		05.88						08.82										08.82
5°S	290	0-200			02.30				04.21		01.53	05.36	01.91		21.46	05.36	33.71	03.06							02.30	00.38	00.76	09.20				04.60		03.85
		200-765			26.65										13.33		13.33						13.33			06.66		13.33						13.36
		765-0			04.76										14.29		42.85	19.05					09.52										09.52
0°	291	0-800			05.83					00.20		02.53	02.44		09.79	01.76	09.46	37.29			01.87					00.22		15.42		01.10	00.44	13.42		00.22
5°N	292	0-800	00.92		00.76	02.14			01.53	03.37	00.16	01.76	08.88	03.52	18.97	03.21	24.33	15.45			03.37				00.31	00.31		01.68		02.14	00.83	04.90		01.45
		0-190			10.45							03.59	08.76	01.41	02.54	21.47	01.69	37.29	03.11		01.41					01.98			00.85	00.28	00.85		02.56		01.75
10°N	293	190-460			02.59							01.74	05.22	04.13		18.04	00.87	19.57	05.00		16.30		01.30		05.43	00.65		13.04		01.30		01.74		03.27
		460-750							00.63				21.18	01.26		15.09	12.58	25.79	05.03	03.77	07.75		01.89					02.52			00.63	00.63		01.04
		0-170										02.64	02.64	03.52		03.70	09.50	50.00	02.82	01.58	02.99				00.53	00.53		00.18		06.51	03.52	02.89	00.88	05.68
15°N	294	170-450											05.03	06.06		12.12		21.21	03.03	03.03	12.12							05.03		05.03	05.03				06.06
		450-760							01.50				08.27			36.09	05.26	20.30	01.50	05.26	07.52		06.77		00.75								04.51	02.26
		0-180	00.22			05.83				17.17		02.69	16.59	06.28		31.17	01.21	17.11	02.47	01.12	04.93		01.57		01.57	00.90				02.02	01.12			01.02
22°N	295	180-440						04.11	01.37			04.11	08.22			05.65		01.37		04.11	12.33				49.32	01.37				05.78	02.87		01.41	01.33
		440-1050		07.14				07.14					21.43			28.57				07.14				14.29			07.14							07.09
		0-160		05.80								04.35	20.29			10.58		05.80					07.25		05.80	05.80			01.45	02.90				
29°N	297	160-475		02.82			02.82					02.82	05.63			09.45					04.23				21.13	35.21				11.27	02.87		01.41	01.33
		475-1030		05.88			05.88					05.88	05.88			11.76		05.88					23.53			11.76				05.88				17.66
36°N	298	0-320		16.26			04.65		04.65			04.65	06.98			52.56		06.98					06.98		02.33				02.33		06.98			04.62
		0-900		06.80			00.80		02.40				00.80			03.20				00.80	7.68				07.92				00.80		04.00			00.80
		0-185		47.65			12.08	06.04					06.04			04.70				08.72			09.40								03.36			02.00
43°N	299	185-850		29.41			19.25	10.70					09.63							10.70	01.07		05.35	00.53	02.14						10.16			01.05
		185-0		25.20			21.16	16.26					07.32							11.38			15.45		00.81						01.62			00.81
49°N	300	0-1050		30.50			22.94	15.99					13.10							07.92			09.50											
		0-190		04.19			71.32	08.74					07.37							05.59			02.79											
55°N	301	100-0		06.66			80.44	05.11					17.33							05.33			07.11											
		100-700		08.92			45.72	05.34					20.07							06.32		02.97	11.89											

EXPLANATION OF PLATES

PLATE I

Figure

1, 2 — *Candeina nitida* d'Orbigny, 1, dorsal view; 2, ventral view. Sample No. 295, X177.

3, 4 — *Globigerina pachyderma* (Ehrenberg), both ventral views of kummerforms. Sample No. 301, X245.

5, 6, 7 — *Globigerina pachyderma* (Ehrenberg), 5, ventral view; 6, lateral view; 7, dorsal view. Sample No. 300, X272.

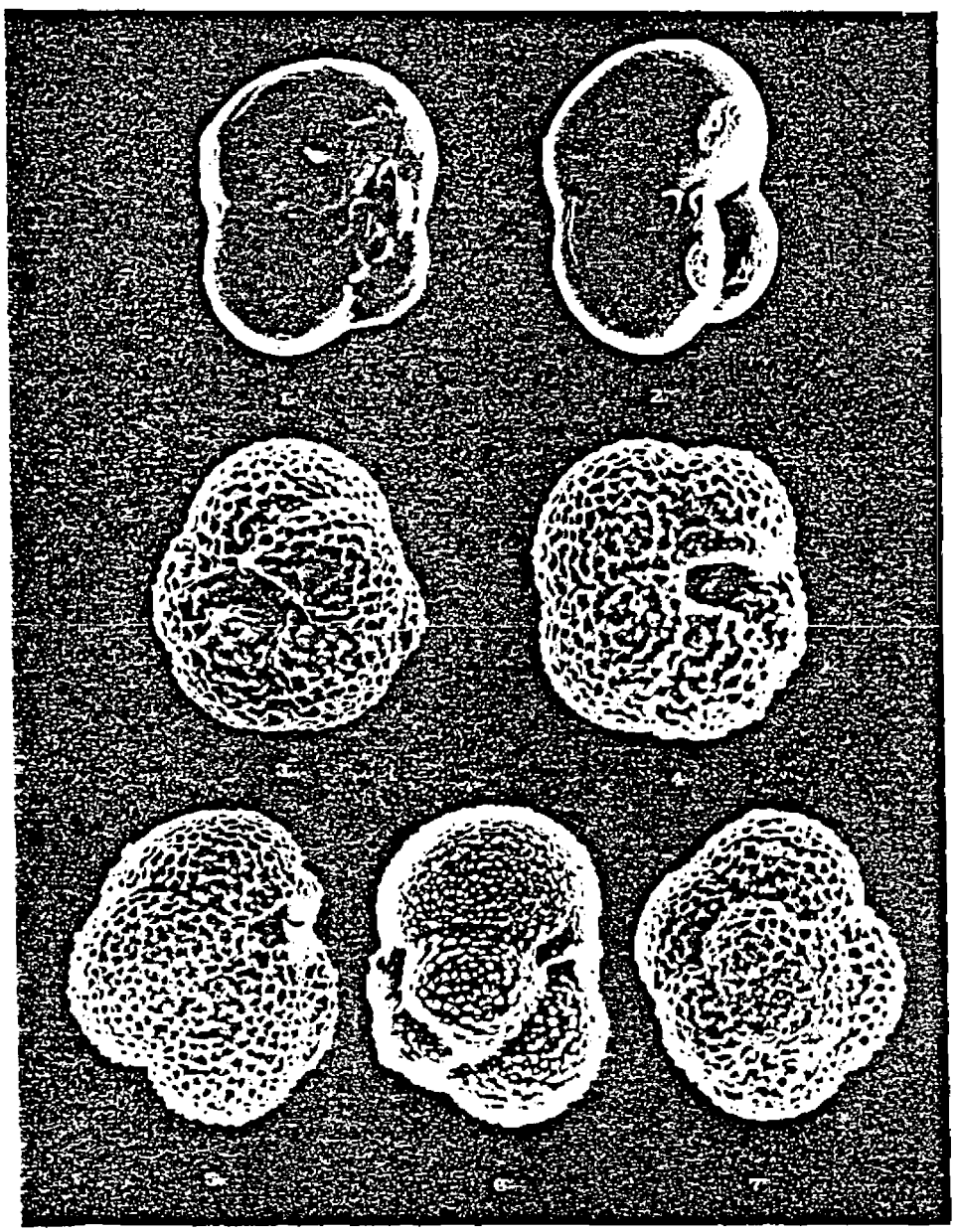


PLATE II

Figure	
1, 2	*Globigerina pachyderma* (Ehrenberg), 1, side view, showing highly pitted walls; 2, dorsal view. Sample No. 300, X245.
3	*Globigerina rubescens* Hofker, ventral view showing broad crescent shape aperture and almost hexagonal pores. Sample No. 290, X204.
4, 5	*Globigerinella aequilateralis* (Brady), 4, dorsal view, 5, showing the aperture; these two specimens show different wall structures. Sample Nos. 293, 297, X136.
6, 7	*Globigerinoides conglobatus* (Brady), 6, side view, 7, apertural view. Sample No. 294, X156.

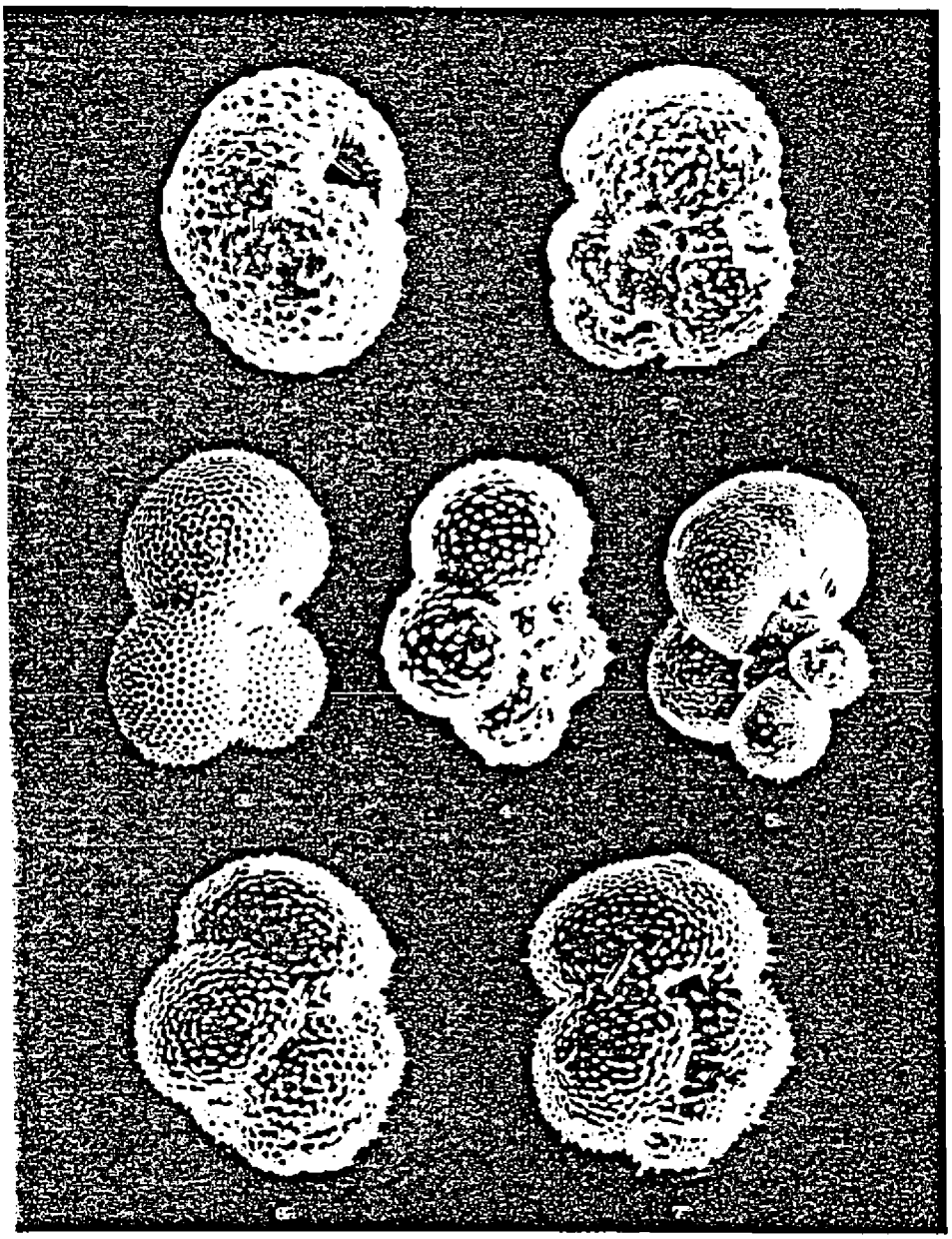


PLATE III

Figure

1, 2 *Globigerinoides conglobatus* (Brady), showing different views of the apertural side, coarse pitting of the walls and spines. Sample No. 290, X136.

3, 4, 5 *Globigerinoides conglobatus* (Brady) 3, dorsal view showing two supplementary apertures; 4, 5, specimens having different wall ornamentation with blunt spines. Sample No. 295, X136.

6, 7 *Globigerinoides ruber* (d'Orbigny), 6, ventral views showing typical circular aperture; 7, dorsal view with supplementary aperture. Sample No. 293, X156.

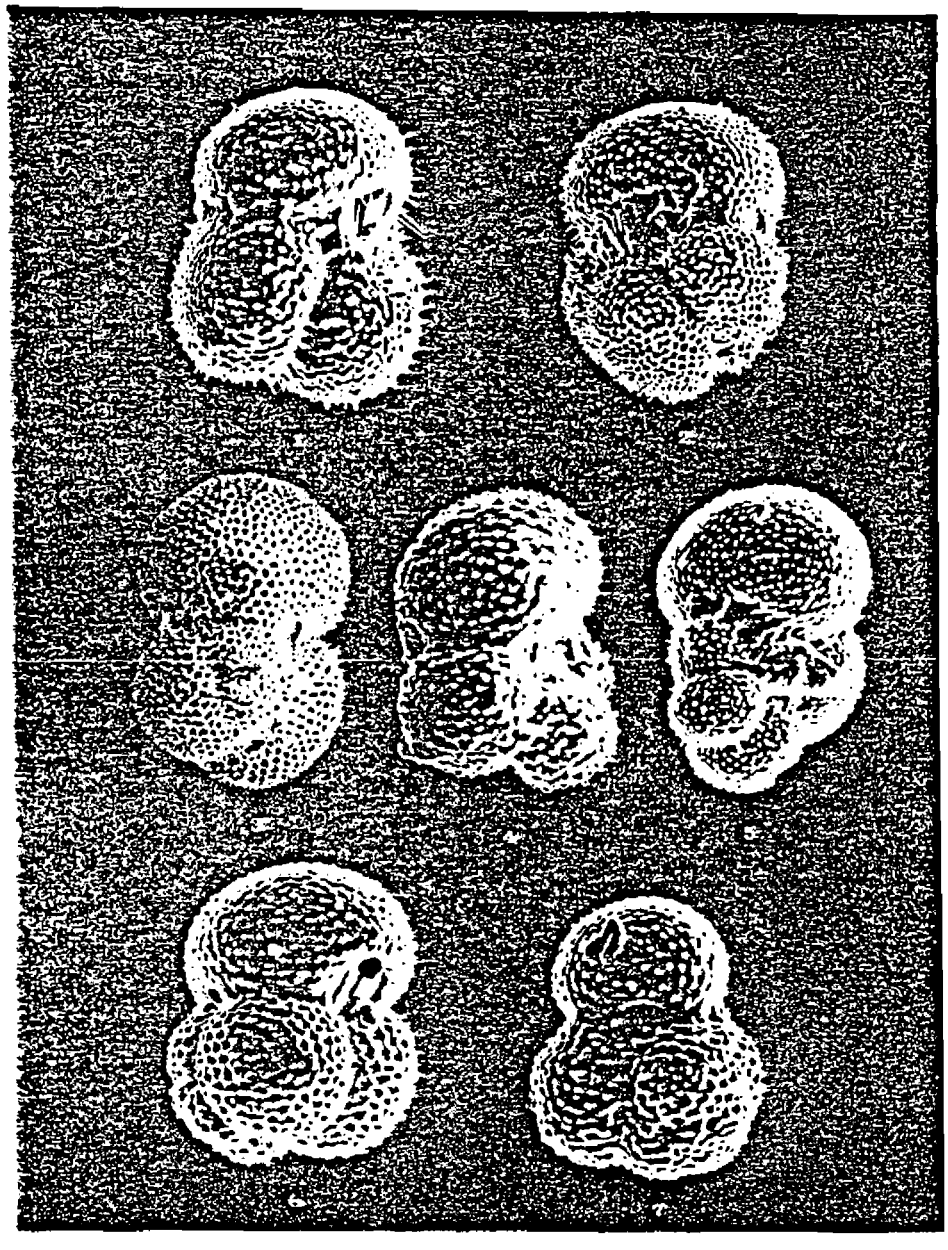


PLATE IV

Figure

1, 2 — *Globigerinoides sacculifer* (Brady), both dorsal sides showing different types of sac development in the last chamber and surface features. Sample No. 289, X61.

3 — *Globigerinoides trilobus* (Reuss), showing big last supplementary aperture and almost spineless surface with circular to semi-exagonal pores. Sample No. 293, X61.

4, 5, 6 — *Globigerinoides trilobus* (Reuss), 4, 6, ventral view; 5, side view; showing highly pitted coarse surface with typical hexagonal pores and small broken spines. Sample No. 294, X61.

7, 8, 9 — *Globoquadrina conglomerata* (Schwager), 7, 9, dorsal view; 8, apertural view, highly pitted walls except almost smooth on the ventral side of the last chamber. Sample No. 290, X102.

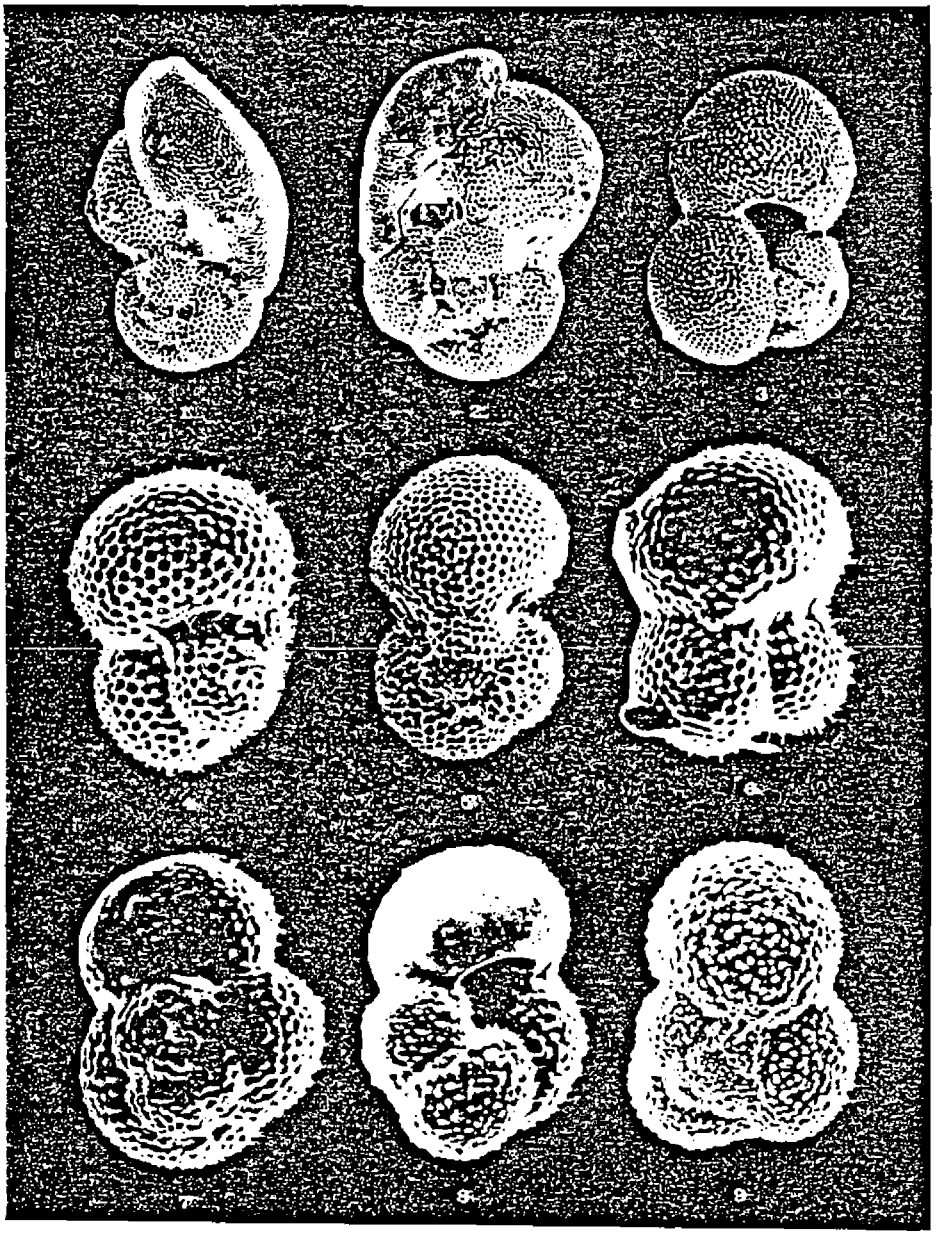


PLATE V

Figure

1, 2, 3 *Globoquadrina dutertrei* (d'Orbigny), 1, apertural view of a kummerform showing highly irregular deeply incised pitted surface, broad umbilical opening. Sample No. 293; 2, specimen having ventral bulla, an unusual features, note the difference in surface feature. Sample No. 294; 3, tilted side view showing less pitted walls with fine pores. Sample No. 295, X177.

4, 5, 8 *Globoquadrina hexagona* (Natland), 4, side view; 5, ventral view; 8, dorsal view; showing highly coarse typical *Globoquadrina* type of surface features, last chamber compressed to bulbous. Sample No. 293, X218.

6, 7 *Globorotalia cavernula* Bé, 6, dorsal view; 7, apertural view showing long slit aperture; surface smooth having fine pores. Sample No. 301, X156.

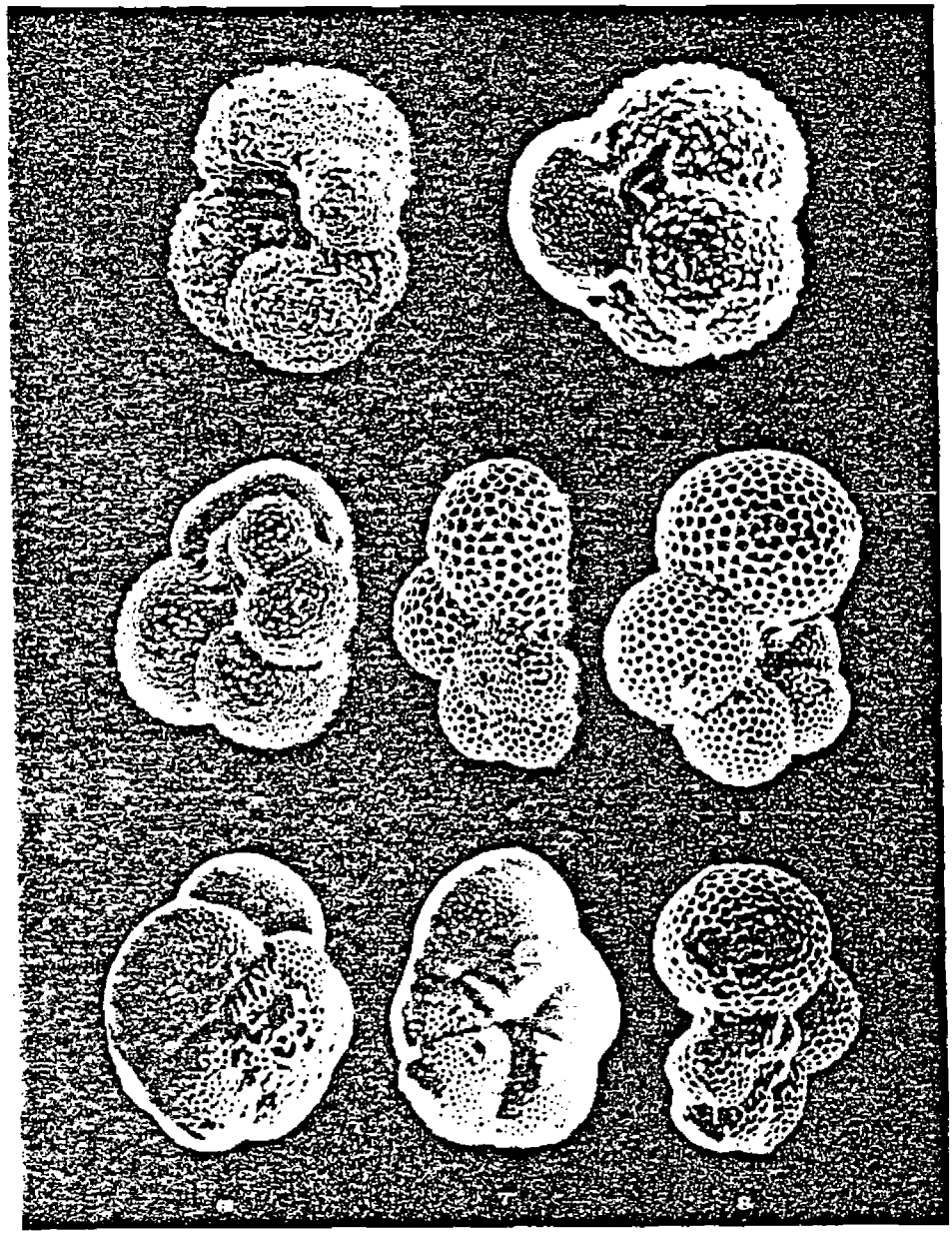


PLATE VI

Figure

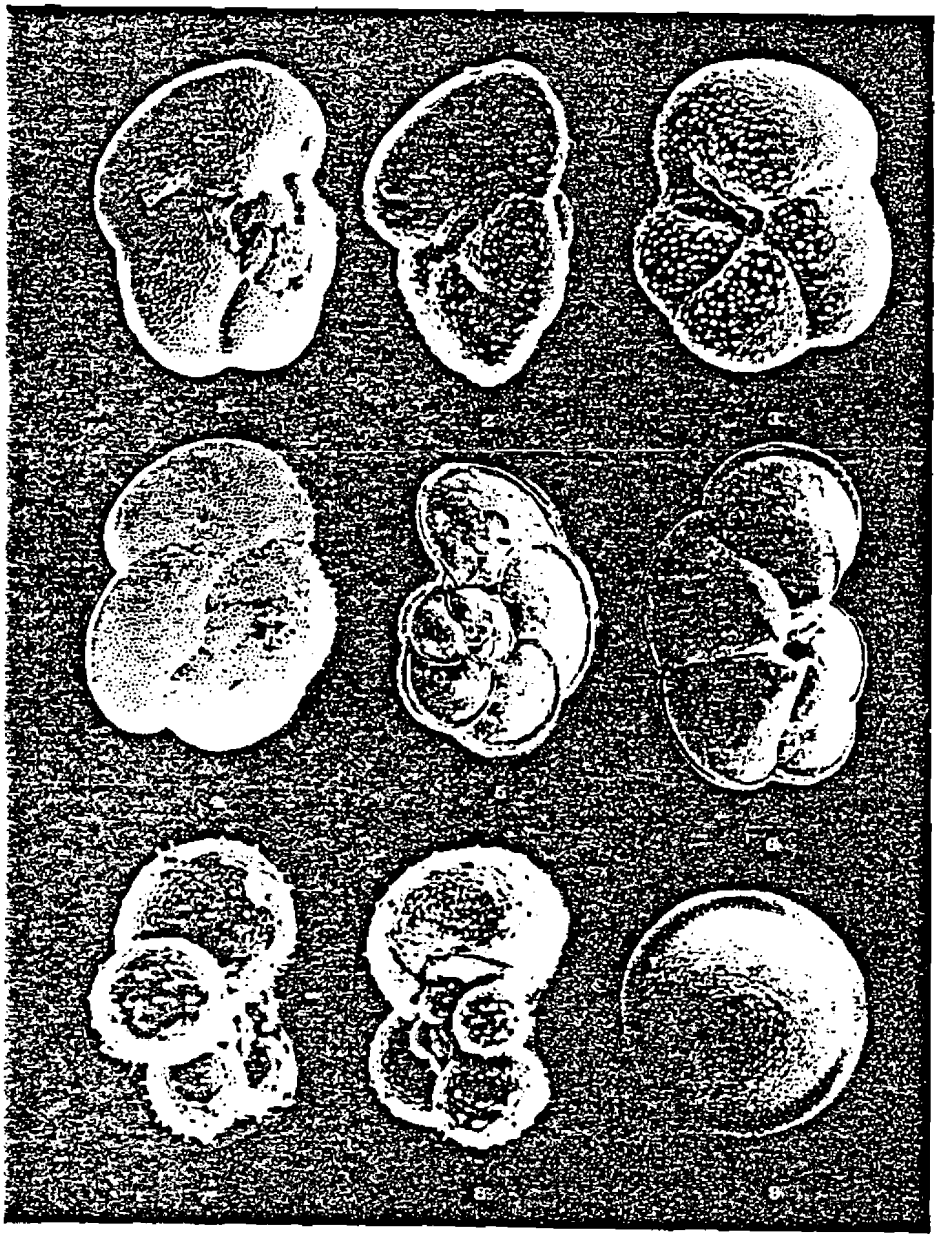
1, 2, 3 *Globorotalia hirsuta* (d'Orbigny), 1, dorsal view; 2, side view showing aperture with lip; 3 ventral view; note the fine pores on the surface. Sample No. 297, X150.

4 *Globorotalia hirsuta* (d'Orbigny), dorsal view, showing larger size pores on the earlier chambers. Sample No. 290, X136.

5, 6 *Globorotalia menardii* (d'Orbigny), 5, dorsal view, Sample No. 290, X61; 6, ventral view, Sample No. 295, X136.

7, 8 *Hastigerina pelagica* (d'Orbigny), 6, tilted dorsal view, 7, showing aperture. Sample No. 294, X183.

9 *Orbulina universa* d'Orbigny, showing surface feature. Sample No. 294, X82.



(*Reprinted from Nature, Vol.* 229, *No.* 5286, *pp.* 551–553, *February* 19, 1971)

Baffin Bay—an Ocean

RECENT theories of the opening of the Atlantic Ocean and the Labrador Sea and of the relationship of the assumed motions to the history of Baffin Bay lead to contradictory opinions about the nature of the crust beneath the bay. The fit of the continents[1] and the similarities of the rock types and their ages along the opposing coastlines of Greenland and Northern Canada[2,3] suggest that the two have separated by continental drift. Geophysical studies in the Labrador Sea (unpublished work of X. Le Pichon, R. D. Hyndman and G. Pautot) imply that Baffin Bay was formed by seafloor spreading and therefore that oceanic crust should lie beneath it. Conversely, from an interpretation of the geology along the coastlines, the present configuration of the bay has been attributed to the extension of continental material and subsequent faulting along its margins[4]. The latter hypothesis is supported by a study of

surface waves[3] which showed that the Lg phase is transmitted across the area. This surface wave is generally associated only with continental crustal structure. The lack of any positive evidence which could be used to resolve this controversy prompted us to conduct the experiment described here.

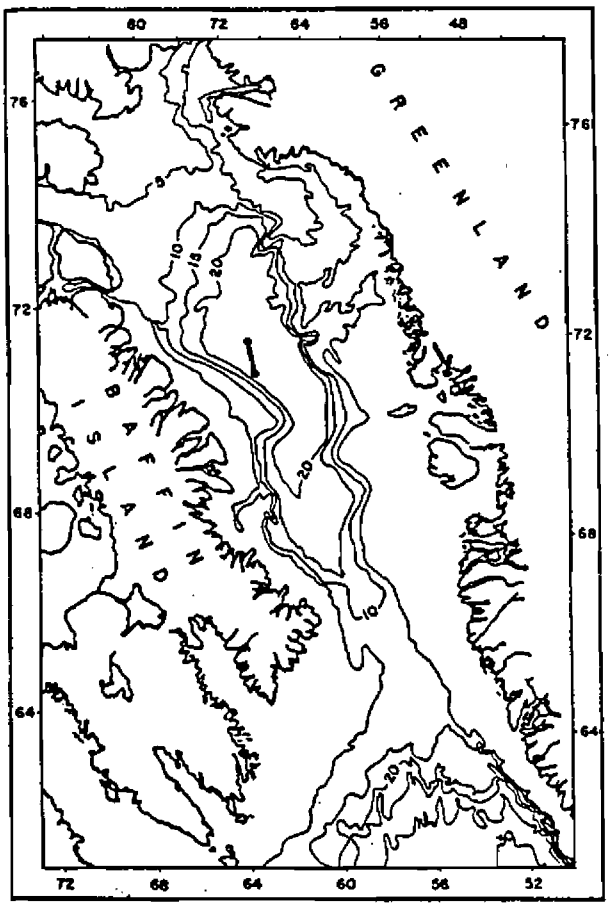


Fig. 1 Location of the refraction line (the heavy black line). The bathymetry contours are in hundreds of metres.

A two-ship seismic refraction line was performed in the deep region of Baffin Bay in October 1970 (Fig. 1). CSS Hudson acted as the recording ship and USCGC Edisto as the shooting ship. The line was reversed ; however, the second shot line did not coincide exactly with the first due to

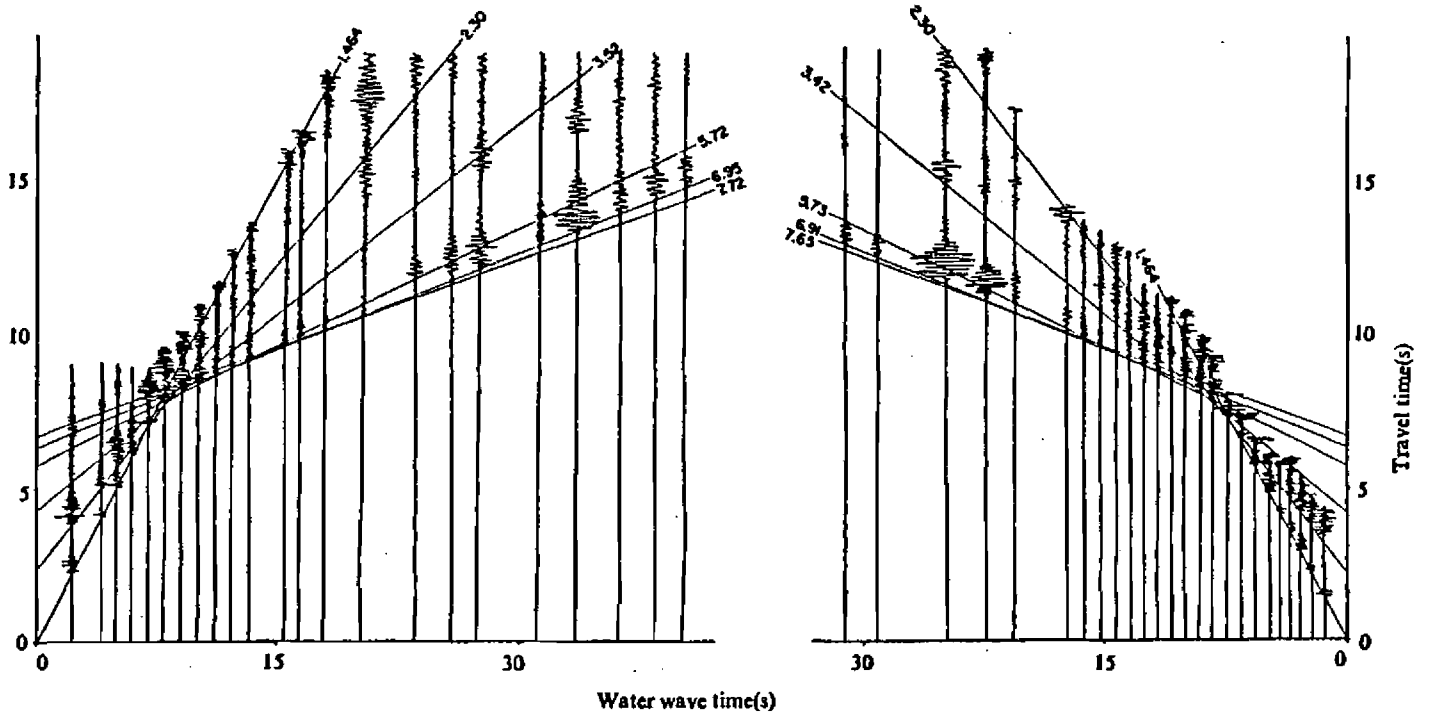


Fig. 2 The record stations. Velocities are in km/s. The right-hand figure shows recordings at the southern station and the left-hand figure shows recordings at the northern station.

ice conditions at the two ends of the proposed line. The two resulting shot lines did not diverge by more than 18 km. Also, Hudson drifted about 12 km and 6 km respectively at the southern and northern receiving stations during the listening periods. The positions of the shot lines were determined by LORAN navigation and the location of the receiving stations by satellite fixes. The explosive charges were fuse fired and the charge sizes ranged from 30 to 500 pounds (13 to 230 kg).

Corrections were applied to remove variations in the travel times due to bottom topography along the shot lines and beneath the receiving stations. The constant water depth to which all travel times have been corrected is 2.30 km. Shot to receiver ranges were obtained from the direct water wave arrivals using a velocity of 1.464 km/s for sound in seawater. This value was calculated from previous measurements of temperature and salinity in central Baffin Bay[6]. Recordings of all shots were appropriately arranged and are presented as record sections in Fig. 2.

Five crustal velocities are shown on each record section. The velocities of 7.7 km/s and 6.9 km/s are well established, the former by first arrivals and the latter by good second arrivals. The 5.7 km/s velocity is defined by first arrivals over a small distance interval—this is best seen on recordings at the northern station. The values of the two lower velocities, 2.3 and 3.5 km/s, have been assumed; however, their values are not critical to the results reported here.

True velocities and the layer thicknesses were calculated and these are shown in Table 1. The velocities, 5.7, 6.9 and 7.7 km/s, are similar to those measured for layers 2 and 3 and the M discontinuity respectively in the ocean basins[7], and we shall use this terminology in the following discussion. The total depth to the M discontinuity from the sea surface is

Table 1 Layer Thicknesses and Velocities

Layer	Velocity (km/s)	Thickness (km) Southern station	Northern station
Water	1.464	2.3	2.3
Unconsolidated sediment	2.30	2.1	2.0
Sediment	3.47	2.0	2.3
Layer 2	5.72	2.0	2.1
Layer 3	6.93	1.9	2.1
Mantle	7.68	—	—

The positions of the southern and northern stations were 71° 39′ N, 65° 55′ W and 72° 18′ N, 66° 13′ W respectively. These are median positions taken during the time that Hudson was on station.

11 km including 4 km of sediment. This depth and the layer velocities bear no similarity to continental crustal values but are closely related to those obtained in oceanic areas. There are, however, several differences. The unusually thick sedimentary cover is substantiated by reflexion profiling results, and in view of the landlocked nature of Baffin Bay a thick sequence of sediments is not unreasonable. The thickness of layer 2 is similar to that measured in the deep ocean basins but the thickness of layer 3 is appreciably less. If the deep central portion of Baffin Bay was formed by seafloor spreading, the lesser thickness of basaltic crustal rocks could be attributed to a different rate of outpouring of crustal material or to a different spreading rate than is at present observed at active ridges.

The velocity of the mantle rocks, 7.7 km/s, is slightly lower than that normally found in the ocean basins. It is not, however, significantly less than the mean measured beneath the Eastern North Atlantic basin[7], 7.85 km/s with a standard deviation of 0.18 km/s. Also, the mantle velocity may be lower because the M discontinuity is shallower and the pressure less at the base of the crust here than in most other oceanic regions. Therefore, it would be unrealistic, though perhaps tempting, to attribute the low mantle velocity to "anomalous mantle" material often associated by some workers with mid-ocean ridges[8].

In conclusion, both the thickness of the crust and the measured velocities show that the central deep portion of Baffin Bay is oceanic and that it cannot be attributed to extended and faulted continental material.

We thank the masters, officers, crew and the scientific parties of CSS Hudson and USCGC Edisto for their help. This work was part of the Hudson-70 expedition organized by the Atlantic Oceanographic Laboratory of Bedford Institute as a Canadian contribution to the International Decade of Ocean Exploration.

D. L. Barrett
C. E. Keen
K. S. Manchester
D. I. Ross

Atlantic Oceanographic Laboratory,
Bedford Institute,
Dartmouth, Nova Scotia

Received December 2, 1970.

[1] Bullard, E. C., Everett, J. E., and Smith, A. G., *Phil. Trans. Roy. Soc.*, A, 258, 41 (1965).
[2] Rosenkrantz, A., and Pulvertaft, T. C. R., *Amer. Assoc. Petrol. Geol. Mem.*, 12, 883 (1969).

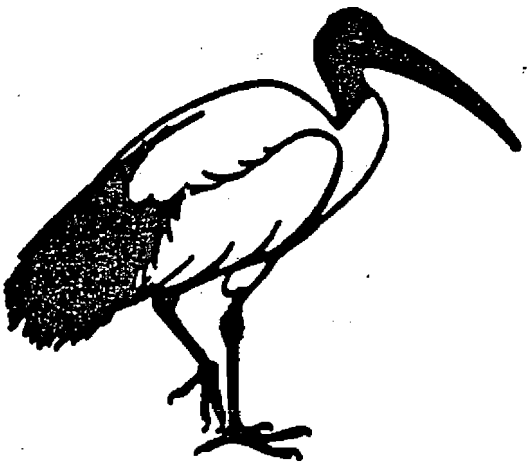
[3] Wilson, J. T., *Phil. Trans. Roy. Soc.*, A, 258, 145 (1965).
[4] Kerr, J. W., *Earth Planet. Sci. Lett.*, 2, 283 (1967).
[5] Oliver, J., Ewing, M., and Press, F., *Bull. Geol. Soc. Amer.*, 66, 1063 (1955).
[6] Baffin Bay 1963 CODC Data Record Series No. 7 (1967).
[7] Raitt, R. W., *The Sea*, 3 (edit. by Hill, M. N.), 82 (1963).
[8] Talwani, M., Le Pichon, X., and Ewing, M., *J. Geophys. Res.*, 70, 341 (1965).

Printed in Great Britain by Flarepath Printers Limited, Watling Street, Colney Street, St. Albans, Herts.

Dick Brown

THE IBIS

JOURNAL OF THE BRITISH ORNITHOLOGISTS' UNION



Edited by
LORD MEDWAY

NUMBER 3 July 1975 VOLUME 117
£3.05

Published for
THE BRITISH ORNITHOLOGISTS' UNION
by
ACADEMIC PRESS

SUMMER SEABIRD DISTRIBUTIONS IN DRAKE PASSAGE, THE CHILEAN FJORDS AND OFF SOUTHERN SOUTH AMERICA

R. G. B. Brown, Fred Cooke, P. K. Kinnear & Eric L. Mills

Received 17 November 1973

From December 1969 to April 1970 and in March and April 1972 we carried out regular seabird watches in the course of several crossings of Drake Passage and the Patagonian Shelf, and during a detailed oceanographic exploration of the Chilean fjords. Brown, Cooke and Mills were on one of the South American and Antarctic legs of the Canadian HUDSON '70 oceanographic expedition around the Americas. Kinnear was on passage to and from a British Antarctic Survey station on the Argentine Islands. Details of our itineraries are given in Appendix 1 (see also Figures 1–3).

Our observations confirm and add to what is known of seabird distributions in the area. We have tried to interpret some of them in oceanographic terms; the fact that we were able to use data collected on an oceanographic cruise has had obvious advantages. These interpretations are tentative, since so little is known of the birds' feeding habits or even of their pelagic distributions, and since the oceanographic data are often sparse. The great mobility of seabirds, and their need to compromise between the pelagic areas where they feed and the land where they breed, do not make them ideal oceanographic subjects. But they are part of the marine environment, and it seems worth making the attempt.

SPECIES DISTRIBUTIONS

The Patagonian Shelf and the Antarctic Peninsula have the best, and the Chilean fjords the worst coverage in the literature. Seabird breeding distributions have been described by Cawkell & Hamilton (1961), Humphrey *et al.* (1971), Johnson (1965, 1972), Murphy (1936) and Watson *et al.* (1971). Watson *et al.* (1971), Dabbene (1921–26), Escalante (1971) and Ozawa (1967) reviewed pelagic distributions; it has been useful to compare our observations with those of Jehl (1973a), Lathbury (1972 and unpubl.) and Tickell & Woods (1972), published since Watson *et al.* (1971), and with Holgersen (1957). Our observations generally agree with the literature, and in the summaries we have principally stressed points of difference. Our detailed observations will be deposited with the Royal Naval Bird Watching Society and with the Canadian Wildlife Service.

Cooke & Mills (1972) have presented their observations on the Patagonian Shelf separately, but these have been reworked here to incorporate Kinnear's data.

Penguins (See Tables 1 and 2)

Our penguin sightings were all close to known breeding areas: *Spheniscus magellanicus* in the Chilean fjords, the Falklands and off Argentina; *Eudyptes crestatus* and *chrysolophus* in the Falklands, and *E. crestatus* in Tierra del Fuego as well; *Pygoscelis antarctica* and *P. adeliae* in the vicinity of the Antarctic Peninsula, and *P. papua* there and also in the Falklands.

Wandering Albatross *Diomedea exulans* (Tables 1 and 2)

Royal Albatross *Diomedea epomophora* (Tables 1 and 2)

'Great' albatrosses were commonest near the Falklands, in Drake Passage north of the Antarctic Convergence, off the Chilean coast north of 48° S, and south of the Rio de la Plata. We did not consistently attempt to separate the two species. Undoubted young *exulans* (Serventy, Serventy & Warham 1971, Tickell 1968) occurred over the whole of this range, as did birds with white bodies and black upper wings (subadult *exulans*, or *epomophora sanfordi* of any age) and white birds with

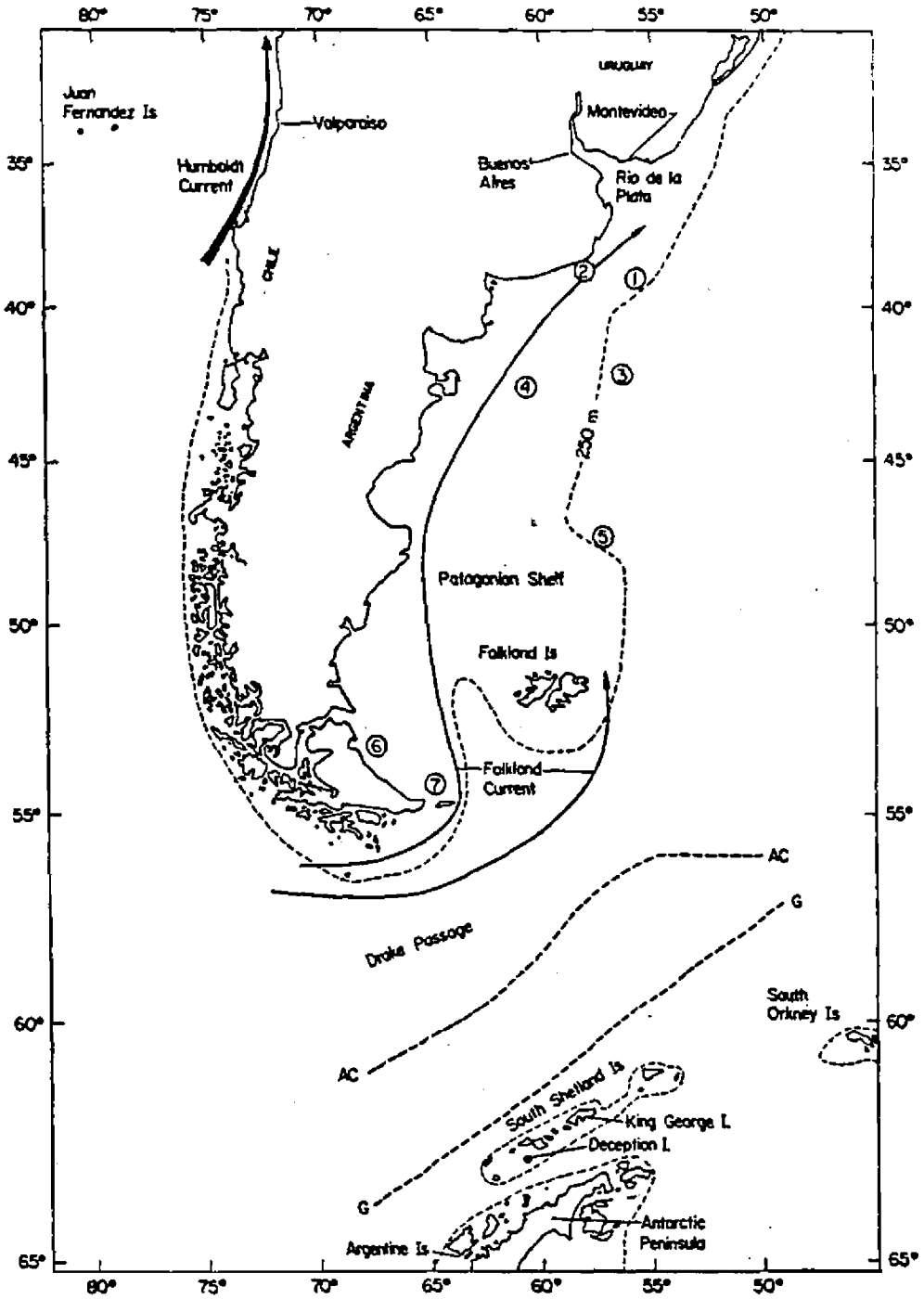


FIGURE 1. Drake Passage and southern South America. G indicates the northern limit of the Graham Land Area plankton fauna (Mackintosh 1934) and AC the Antarctic Convergence. Numbers in circles refer to the seabird concentrations listed in Table 3.

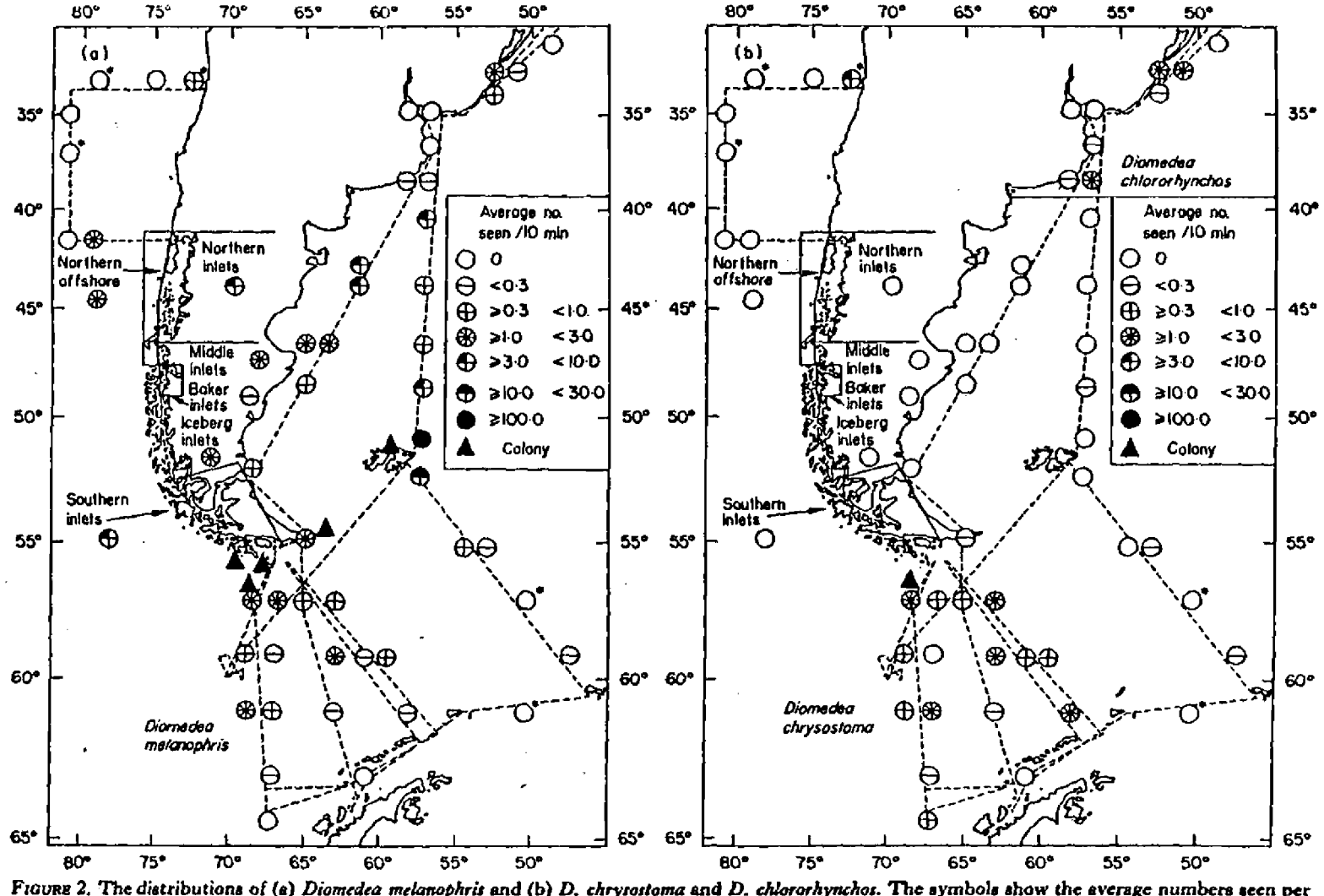


FIGURE 2. The distributions of (a) *Diomedea melanophris* and (b) *D. chrysostoma* and *D. chlororhynchos*. The symbols show the average numbers seen per 10-minute watch from the moving ship, for each 2° S × 2° W block in which observations were made; in the Chilean fjords the averages refer to the subdivisions listed in Appendix 2. * indicates averages based on a total of 30–50 minutes' observation; the rest are based on at least an hour. (– – –) ships' tracks.

TABLE 1

Relative abundance of seabirds at different surface temperatures in Drake Passage and off southern South America, based on the average numbers seen per 10-minute transect from the moving ship

Zone	Antarctic				Subantarctic										Subtropical								
Surface temperature °C	0	1	2	3	4	5	6	7	8	9	11	12	13	14	15	16	17	18	19	20	21	22	23
Pygoscelis adeliae	+	+																					
Sterna vittata	2	1																					
Fulmarus glacialoides	4	1																					
Daption capense	5	3	1		1																		
Pygoscelis papua	+	+			+																		
Pygoscelis antarctica	+	+	+			+																	
Phoebetria palpebrata	1	1	1		1																		
Fregetta tropica	3	2	1	2	1	1	1																
Oceanites oceanicus	4	3	2	3	2	2	2	3	2	1		1	3	2		1	1						1
Macronectes sp.	2	2	1		1	2	2	3	3	4	2	1		2		1	2		1	1	1		
Catharacta skua	1	1						1	1	1				1					1		1		
Larus dominicanus	1	1								1	1								2	1	1		2
Diomedea chrysostoma		2	2	3	1	2	2	1		2				1	2								
Pachyptila sp.	3	2	1		1	1	2	2	1	3	3												
Halobaena caerulea		1	1			2	1	4	2		2												

Pelecanoides sp.		1	1	3		1	1	1	2	1	3	3			1								
Diomedea melanophris		2	2	2		2	2	2	5	3	4	2	4	3	3		2	3	2			1	3	
Diomedea exulans + *epomophora*		1	1			1	2	3	3	3	1	1	3		2		3	1		2	1			
Puffinus griseus		1	1				1	1	1	4	3	1	3		1		2	3	1		1			
Procellaria aequinoctalis		1	1				1	1	1	2		1	4	3	2		2	4	3		1	2	2	
Eudyptes crestatus										+	+	+												
Spheniscus magellanicus										+	+	+			+			+						
Fregetta grallaria									1	1	1	1			1									
Stercorarius parasiticus										1		1	1		3			1	1		3			
Puffinus gravis (A)									4	3	5	2	5	4	3			5	4		3	3	1	2	2
Sterna hirundinacea												3													
Pterodroma incerta (A)				1			1	1	1		3	1	5		3			3	2				1	1
Calonectris diomedea (A)													2					2	1		2	4	1	2	2
Puffinus puffinus (A)															1						4			1	1
Diomedea chlororhynchos (A)																					3	2	2	1	1
Puffinus creatopus (P)															1		3	1	3		2				
Pterodroma externa (P)															1		2	4	4	5	6				
Pterodroma longirostris (P)															1		1			2	3				
No. observations—all areas	24	80	41	6		14	60	47	27	42	19	37	12	3	38		10	58	30	3	66	23	18	9	51
(A) only															34			53	22		55	23	18	9	51
(P) only															4		10	5	8	3	11				

Key: 1 = <0·3 4 = >3·0 <10·0 + = present, not counted
2 = >0·3 <1·0 5 = >10·0 <30·0
3 = >1·0 <3·0 6 = >30·0 <100·0
A blank indicates that the species was not recorded at the temperature in question

Notes: Temperatures are those noted at the time of observation, except for most of Kinnear's cruises, where the monthly averages in Anon (1971a) and Mackintosh (1946) have been used.
No observations were made at 10 °C.
(A) indicates species seen only in the Atlantic, and (P) only in the Pacific. For these, the averages are based only on the number of Atlantic or Pacific observations for the temperature in question.

black only on the primaries (adult *exulans*, or *epomophora epomophora* of any age). The very white birds seemed particularly common from Cape Horn south to 58° S.

Black-browed Albatross *Diomedea melanophris* (Fig. 2; Tables 1 and 2)
Grey-headed Albatross *Diomedea chrysostoma* (Fig. 2; Tables 1 and 2)
Yellow-nosed Albatross *Diomedea chlororhynchos* (Fig. 2; Table 1)
Light-mantled Sooty Albatross *Phoebetria palpebrata* (Table 1)

Diomedea melanophris was the commonest albatross, especially in the Falklands and the Chilean fjords, but was scarce south of the Antarctic Convergence and north of 48° S in the Pacific. *D. chrysostoma* was commonest between Cape Horn and the Antarctic Convergence, but absent north of 54° S, apart from a small flock off Valparaiso in April 1970.

In the South Atlantic *D. chlororhynchos* breeds only in the Tristan da Cunha group. Ozawa put the western edge of its summer pelagic range at *c.* 30° W, and to judge from the literature it is rare off eastern South America. Surprisingly, we saw *c.* 50 birds in a seabird concentration southwest of the Rio de la Plata on 23 January 1970 (Table 3). There were none in this general area on 4 January, and our only record for this earlier period was a single doubtful sighting at 34° 03′ S 52° 50′ W on 31 December. In April 1972 we only saw them between 33°–28° S.

Phoebetria palpebrata was scarce, and mainly seen south of the Antarctic Convergence.

Giant Petrel *Macronectes giganteus* and *M. halli* (Table 1).

Common from the Antarctic Peninsula up to 36° S in the Atlantic and 33° S in the Pacific. Almost all were in the dark plumage phase, but there were a few white-phase birds close to the Antarctic Peninsula. We did not attempt to separate the species (Bourne & Warham 1966); however, about 15% of the dark-phase birds in the Chilean fjords had the whiteish head typical of adult *giganteus*, while the rest had the all-dark plumage typical of immatures of either species.

Cape Pigeon *Daption capense* (Table 1)
Southern Fulmar *Fulmarus glacialoides* (Table 1)
Snow Petrel *Pagadroma nivea*
Antarctic Petrel *Thalassoica antarctica*

All four species were Antarctic birds. Both *Daption capense* and *Fulmarus glacialoides* were common only south of the Antarctic Convergence, though a few *F. glacialoides* were seen in the Chilean fjords in March 1970 and 1972. Numbers were greatest close to the Antarctic Peninsula, though Kinnear's observations in the Argentine Is indicated that in summer they were commoner about 20 miles offshore to the west than in the immediate offshore zone. Our only pelagic *Pagodroma nivea* and *Thalassoica antarctica* sightings were of single birds, respectively at 64° 14′ S 61° 53′ W on 6 March 1972 and at 63° 32′ S 66° 38′ W on 4 February 1970. By contrast Lathbury found both species rather commoner in early 1970.

Prions *Pachyptila* spp. (Table 1)
Blue Petrel *Halobaena caerulea* (Table 1)

Pachyptila desolata, *turtur* and *belcheri* all occur in our area, though *belcheri* is the commonest (Harper 1972, Johnson 1972). We could not separate the species at sea, and sometimes also found it difficult to distinguish *Pachyptila* spp. from *Halobaena caerulea*.

Prions were locally common north of the Falklands in April 1972 (Table 3), but were otherwise absent north of 55° S; small numbers were seen all across Drake Passage. *Halobaena caerulea* was abundant north of the Falklands between 46° 30′ S–48° 30′ S on 6 January 1970, and was seen fairly regularly between Cape Horn and the Antarctic Convergence, but was scarce farther south.

Our only Chilean record was at 50° 24′ S on 14 March when a single bird, of one or other of these genera, was seen in the ship's lights at night.

Shoemaker *Procellaria aequinoctalis* (Tables 1 and 2)

Commonest on the Patagonian Shelf down to 45° S, but scarce in the deeper water north of the Falklands; also common along the Chilean coast north of 48° S. They were virtually absent south of 55° S.

Pink-footed Shearwater *Puffinus creatopus* (Tables 1 and 2)

There were three birds off the Chilean coast at 47° 34′ S, but the species was otherwise only seen north of 42° S in the Pacific.

Cory's Shearwater *Calonectris diomedea* (Table 1)
Manx Shearwater *Puffinus puffinus* (Table 1)
Little Shearwater *Puffinus assimilis*

Calonectris diomedea was the commonest of these shearwaters in the Atlantic in January 1970, especially just south of the Rio de la Plata and with scattered sightings down to 40° S; this appears to be an extension of the known winter range of this species (see Cooke & Mills 1972). *Puffinus puffinus* has a similar distribution, though it ranged down to 50° S. *P. puffinus* was not seen in April 1972, and the only *C. diomedea* were three birds at 32° 38′ S 51° 39′ W.

We saw a total of *c.* 25 *P. assimilis* on 4 January 1970, between 39° 20′ S–40° 10′ S 56° 25′ W. They were identified by their flight: fast, almost auk-like wingbeats interspersed with glides, unlike the flight of *P. puffinus*, the other black-and-white shearwater in the area. Surface temperatures were fairly cool (12°–16 °C), which suggests *assimilis* rather than the similar warm-water *P. lherminieri* (see Post 1967). Jehl saw a small flock off Chiloe I. in June 1970 and suggests that they may breed in that part of the Chilean coast. Our only Pacific record is doubtful: two fairly small dark-and-white shearwaters seen in the ship's lights deep in the fjords at 42° S.

Greater Shearwater *Puffinus gravis* (Table 1)

Abundant in almost all the sea-bird concentrations off the Argentine coast (Table 3). Small numbers were seen in the Falklands, and our southernmost record was a bird in Lemaire Strait on 8 March 1970. We saw none north of 33° S in April 1972. However in late December 1969 birds were seen in ones and twos from just north of the Equator to the Rio de la Plata; these were all heading south, and were presumably migrant stragglers.

Sooty Shearwater *Puffinus griseus* (Tables 1 and 2)

Common in the Chilean fjords, and seen as far north as Valparaiso. Also common along the north coast of the Falklands in March 1972, and in two sea-bird concentrations off the Argentine coast (Table 3), but otherwise scarce in the Atlantic and in Drake Passage; there were only occasional sightings north of 40° S and south of 57° S.

Juan Fernandez Petrel *Pterodroma externa* (Table 1)

Stejneger's Petrel *Pterodroma longirostris* (= *P. leucoptera masafuerae*) (Table 1)

Numbers of both species progressively increased as we approached the Juan Fernandez Is, where both breed on Masafuera; surprisingly, the largest concentration of *Pterodroma externa* was just northeast of Masatierra at sunset on 4 April. All the *externa* seen had the brownish-grey upper plumage characteristic of the Juan Fernandez breeding population (Palmer 1962). *P. longirostris* was scarcer; it was identified by its small size, dark grey head and M-shaped wing pattern (King 1967). The similar, paler *Pterodroma cookii* was not seen but could have been overlooked.

Kermadec Petrel *Pterodroma neglecta*

The species breeds on Masatierra, Juan Fernandez; our only definite record was a dark-phase bird there on 4 April, though there were two doubtful sightings farther south in the Pacific. Both Murphy and Johnson noted that the Masatierra breeding population is declining, apparently through human interference, and it is disturbing that we should have seen so few. Not only were we there during their breeding season but, as Johnson (1965) described, the species is partly diurnal; the birds begin to leave their nests on the cliffs around the settlement as early as 15.00–16.00 hrs. We were anchored off the settlement until well past this time, yet saw none.

Schlegel's Petrel *Pterodroma incerta* (Table 1)

White-headed Petrel *Pterodroma lessoni*

Great-winged Petrel *Pterodroma macroptera*

Soft-plumaged Petrel *Pterodroma mollis*

Pterodroma incerta was the only common gadfly petrel in the Atlantic; it was present in several seabird concentrations on the Patagonian Shelf (Table 3), though absent from those closest to the Argentine coast. There were a few in March in Drake Passage, but our only sighting south of the Antarctic Convergence was *c.* 5 birds at 60° 29′ S 63° 44′ W on 7 March 1972.

We saw three *P. lessoni* on 6 January 1970 at 47° 40′ S 57° 00′ W. *P. mollis* is regularly reported off the Argentine coast and farther east; surprisingly, our only record was of six birds which followed the ship on 18 February 1970 at 59° 32′ S 58° 03′ W, well south of the Antarctic Convergence. To judge from Watson *et al.* (1971) our three *macroptera* sightings were unusually far west; there were two birds at 39° 21′ S 56° 20′ W on 4 January 1970, and single birds at 59° 38′ S 68° 54′ W and in Cockburn Channel in March 1972. Johnson did not record the species; the Cockburn Channel bird seems to be the first record for Chile.

Wilson's Storm-Petrel *Oceanites oceanicus* (Table 1)

White-bellied Storm-Petrel *Fregetta grallaria* (Table 1)

Black-bellied Storm-Petrel *Fregetta tropica* (Table 1)

Grey-backed Storm-Petrel *Garrodia nereis*

Fregetta tropica was the most southerly storm-petrel; it was fairly common in Drake Passage, especially close to the Antarctic Peninsula, but was seldom seen north of the Convergence. *Oceanites oceanicus* was common there and near its colonies in the Cape Horn area, and was also locally common off the Chilean coast farther north. It was scarce in the Atlantic north of 42° S in December–January, but in April 1972 there were scattered birds up to just south of the Equator, presumably migrating to the North Atlantic (Roberts 1940). *F. grallaria* was seen in small numbers north of the Falklands, and also close to their colony on Masatierra, Juan Fernandez. *Garrodia nereis* breed commonly in the Falklands, but our only definite sighting was a bird at 48° 01′ S 57° 06′ W on 5 April 1972.

Diving petrels *Pelecanoides* spp. (Tables 1 and 2)

Diving petrels were commonest at the northern and southern ends of the Chilean fjords and in the seabird concentration in Lemaire Strait (Table 3). They were seldom seen far from the coasts of South America or the Falklands. *P. magellani* is the common species of the Chilean fjords (Murphy 1936, Bourne 1968), and we have three positive identifications of it in the Southern Inlets. Murphy stated that *P. urinatrix coppingeri* nests in the fjords between 47°–50° S, but we saw no diving petrels at all in that area. Our Falklands birds were probably *P. urinatrix berard*, which is common among these islands.

Bigua Cormorant *Phalacrocorax olivaceus*

Rock Shag *Phalacrocorax magellanicus* (Table 2)

Red-footed Shag *Phalacrocorax gaimardi* (Table 2)

Phalacrocorax olivaceus and *P. magellanicus* were seen in small numbers all through the Chilean fjords, and *P. magellanicus* in the Falklands as well. We have no definite records of *P. gaimardi* south of the southern end of Estero Elefantes (46° 19′ S) in the Chilean fjords; it was locally common

there, in Canal Chacao (42° S) and off Valparaiso. Jehl only saw it north of 42° S in June 1970, and suggests a northward movement in winter; but this is inconclusive, since he did not visit Estero Elefantes.

King Shag *Phalacrocorax albiventer* (Fig. 3; Table 2)
Blue-eyed Shag *Phalacrocorax atriceps* (Fig. 3; Table 2)

We saw *Phalacrocorax atriceps* at Deception I. and in the Argentine Is, and *P. albiventer* in the Falklands. The species-pair was seen all through the Chilean fjords. Behn *et al.* (1955) stated that *P. atriceps* is the only one of the pair found in western Magellan Strait and farther north, and is the dominant species in the fjords south of the Strait; *P. albiventer* is dominant only in eastern Magellan Strait. Humphrey *et al.* (1970) stated that *P. albiventer* is the dominant species south of the Strait. We identified the species by the extent of white on the cheeks (see Murphy 1936: 880); Figure 3 shows the distribution of *P. atriceps* in terms of the percentage present in sample counts of identified birds of both species. It confirms that *P. albiventer* is dominant south of the Strait, but also shows that it extends much farther west than has previously been reported.

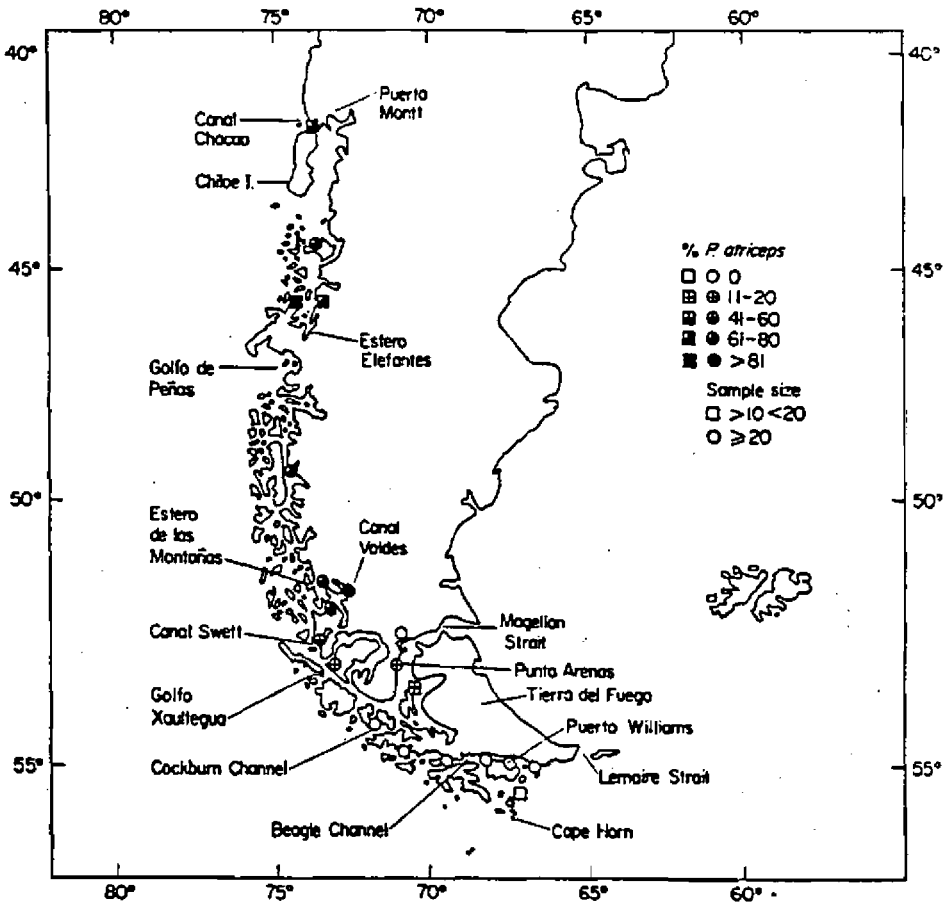


FIGURE 3. The percentage of *Phalacrocorax atriceps* in identified samples of *P. atriceps* + *P. albiventer* in the Chilean fjords.

The boundary between the two species is quite sharp. There were only three *P. atriceps* in a sample of 61 identified birds (4·8%) in Golfo Xaultegua at the western end of the Strait (53° 08′ S 73° 09′ W), but 51 in a sample of 98 (52·4%) in Canal Swett (52° 42′ S 73° 26′ W), only 20 miles away by water, and 84 in a sample of 105 (80·0%) in Estero de las Montañas (51° 59′ S 73° 18′ W). Similarly, in May 1970 Jehl found *P. atriceps* scarce in the fjords south of 50° 36′ S.

Behn *et al.* (1955) suggested that *P. Atriceps* is the species of the wet zone on the western slope of the Andes, and *P. albiventer* of the drier pampas to the east. However Figure 3 shows that *P. albiventer* is dominant in many western areas. It also shows *P. atriceps* dominant in Canal Valdes (52° 02′ S 72° 57′ W), a fjord which extends through the Andes onto the pampas. The controlling factor is more likely to be oceanographic. Pickard (1971; see also Figure 4) shows that the water of the Southern Inlets in the Magellan Strait area is oceanographically distinct from that in the rest of

TABLE 2

*Relative abundance of seabirds in different parts of the Chilean fjords. For species marked * the table shows the average number per 10-minute transect. This is inappropriate for the less conspicuous species, marked †; for these, the table shows the average number of sightings per hour's observation, irrespective of how many birds were seen at each sighting. Species are arranged in the groupings discussed in the text*

		Southern Inlets	Middle Inlets	Iceberg Inlets	Baker Inlets	Northern Inlets	Northern Offshore
	No. transects	100	24	15	10	50	13
	Hours observation	26·3	9·5	4·0	3·5	14·5	4·3
(i)	**Diomedea exulans* + *epomophora*	0·13	0	0	0	0·24[3]	1·54
	**Puffinus griseus*[3]	8·29	0·71	0	0·10	0·66	17·15
	**Pelecanoides* sp.	1·88[1]	0·46	0·17	0	4·22	2·77
(ii)	†*Sphenisicus magellanicus*	0·99	1·16	0·25	0·28	1·03	0·23
	**Diomedea melanophris*[3]	8·43	2·75	1·00	0·20	4·86[3]	1·54
	†*Phalacrocorax magellanicus*	0·34	1·16	0	0	0·21	0·23
	**Phalacrocorax atriceps* + *albiventer*	13·56	10·71	4·73	0·20	22·70	0·08
	**Larus dominicanus*	2.44	6·83	2·00	0	2·31	0·15
(iii)	**Catharacta skua*	1·05	1·42	0·73	0	0·20	0·08
	**Sterna hirundinacea*	8·42	3·04	0	0	0·04	0·31
(iv)	**Procellaria aequinoctalis*	0·06	0	0	0	1·88	0·46
	**Puffinus creatopus*	0	0	0	0	0	4·08
	**Phalacrocorax gaimardi*	0	0	0	0	0·42	0
	**Larus maculipennis*	0	0.29	0	0	1·70	0

Notes: [1] Based on 101 transects.
[3] Based on 52 transects.
[3] Large numbers of Sooty Shearwaters and Black-browed Albatrosses were seen but not counted in Beagle Channel on 13–14 March 1972; the Southern Inlets averages for these species are therefore underestimates of the true density in that area.

the Chilean fjords; the boundary, like that between these shags, lies close to Canal Swett. We suggest that *P. albiventer* is the species of this cold, relatively highly saline water-type; presumably the key is some prey also associated with the water-type.

Holgersen (1957 and pers. comm.) sailed through Magellan Strait in November-December 1947. Like ourselves he used Murphy's (1936) diagrams of the shags' cheek patterns to identify them, but was unable to make a single positive identification of *P. albiventer*. The great majority of birds which he saw at close range in Punta Arenas harbour were undoubtedly *P. atriceps;* by contrast we counted only seven in an identified sample of 36 (19·4%) there in February 1970. There may therefore have been a recent extension in the range of *P. albiventer*, perhaps linked to a westerly extension of the Magellan Strait water-type.

Northern (Red-necked) Phalarope *Lobipes lobatus*

Two or three birds were seen at close range at the western end of Magellan Strait on 8 March 1970; Johnson recorded the species as a rare straggler to Chile, but the bill shape left no doubt of the identification. Another phalarope (possibly *Phalaropus fulicarius*) was seen in Cockburn Channel on 13 March 1972.

Pomarine Jaeger (Skua) *Stercorarius pomarinus*
Parasitic Jaeger (Arctic Skua) *Stercorarius parasiticus* (Table 1)
Long-tailed Jaeger (Skua) *Stercorarius longicaudus*
Skua (Great Skua) *Catharacta skua* (Table 2)

Stercorarius parasiticus was regularly seen on the Patagonian Shelf in January 1970, but was scarce south of Magellan Strait; there were two in Beagle Channel on 27 January, and a few off eastern Tierra del Fuego on 21 February (Table 3). There were a few *S. pomarinus* in the seabird concentration on 23 January (Table 3), and three *S. longicaudus* next day at 49° 20′ S 65° 28′ W. By contrast the southernmost record of any jaeger in the Atlantic in April 1972 was a *S. pomarinus* at 19° 17′ S 38° 48′ W. The only jaegers seen in the Pacific north of Beagle Channel were three *S. parasiticus* near Puerto Montt in late March 1970.

Catharacta skua was common along coasts south of the Antarctic Convergence, in the Falklands and in the Chilean fjords north to 43° S, with a few sightings farther north. It was unusual to see them far from land. No attempt was made to differentiate the species (or subspecies) *C.* (*s.*) *maccormicki.*

Dominican Gull *Larus dominicanus* (Tables 1 and 2)
Brown-Headed Gull *Larus maculipennis* (Table 2)
Grey-headed Gull *Larus cirrocephalus*
Franklin's Gull *Larus pipixcan*
Scoresby's Gull *Gabianus scoresbii*

Larus dominicanus was scarce in Chile north of 44° S, but was otherwise common close to land throughout our area. *L. maculipennis* was seen in the Rio de la Plata estuary, in the Falklands and locally in the Northern Inlets, but farther south in Chile was seen only in Punta Arenas and Puerto Natales harbours. *L. cirrocephalus* was seen only in the Rio de la Plata and *Gabianus scoresbii* only in the Falklands and the Southern Inlets. There were a few *L. pipixcan* just south of Puerto Montt in late March 1970, but the main concentration was a flock of over a thousand, all in full breeding plumage, in Canal Chacao on 31 March.

South American Tern *Sterna hirundinacea* (Table 2)
Antarctic Tern *Sterna vittata*
Arctic Tern *Sterna paradisaea*

Most terns in the Chilean fjords appeared, from their size, to be *Sterna hirundinacea;* these were commonest in the Southern Inlets and in a seabird concentration off Tierra del Fuego (Table 3). They were seldom seen at any distance from land.

Birds which we identified as *S. vittata* were quite common along coasts south of the Antarctic Convergence. The only *S. paradisaea*, identified with reasonable certainty by their smaller size when compared to *S. hirundinacea*, were a few in the fjords at 47° 30′ S on 19 March 1970.

Sheathbill *Chionis alba*

Seen only on coasts south of the Antarctic Convergence, apart from some birds in the Falklands in March 1972.

Off Valparaiso we also saw several of the species associated with the Humboldt Current upwelling: *Pelecanoides garnoti*, *Pelecanus thagus*, *Sula variegata*, *Phalacrocorax bougainvillii*, *Larus modestus* and *Larosterna inca*. We did not see *Adamastor cinereus*, though Dabbene, Watson *et al.* and Tickell and Woods all note regular sightings off the Argentine coast. Nor did we see *Diomedea cauta*, *Pterodroma brevirostris* or *P. cookii*, all reported by Jehl or Lathbury in Chilean waters in 1970. In contrast to Jehl's observations in mid-May 1970 we found *Diomedea chrysostoma*, *Phoebetria palpebrata*, *Macronectes giganteus* (white-phase), *Daption capense*, *Fulmarus glacialoides* and *Pachyptila* spp. all either very scarce or absent along the Chilean coast in March 1970 and 1972. We were clearly too early for the northward migration of these species.

SEABIRD DISTRIBUTIONS AND OCEANOGRAPHY

The summary of distributions in the last section was primarily geographical. The aim of this section is to discuss these distributions in terms of the oceanographic factors which might be controlling them.

PELAGIC DISTRIBUTIONS

Murphy (1936) and Watson *et al.* (1971) divided the survey area into three zones. The *Antarctic* zone lies south of the Antarctic Convergence; its summer surface temperatures range between −1·0° and +3·5 °C, and salinities between 33–34‰. The *Subantarctic* extends north from this to the Subtropical Convergence (*c.* 30° S) in the Atlantic, and to an ill-defined boundary south of Juan Fernandez in the Pacific; temperatures are between 4°–19 °C and salinity is *c.* 34‰. The *Subtropical* zone extends up to the Tropical Convergence (*c.* 15° S) in the Atlantic; the eastern limit in the Pacific is at the Humboldt Current (Fig. 1). Temperatures are between 19°–23 °C and salinity is *c.* 36‰.

Table 1 shows the relative abundance of seabirds in summer at various surface temperatures in Drake Passage and off southern South America (but excluding the Chilean fjords). Many seabirds are clearly specific in their zone preferences at this time of year. Indeed many of them either spend the whole year in the temperature zone (e.g., penguins, diving petrels and shags: Jehl 1973 a, Szijj 1967) or wholly or partly migrate to the corresponding zone in the Northern Hemisphere (*Puffinus gravis* and *griseus:* e.g. Palmer 1962). Others to some extent abandon the Antarctic part of their breeding range and spread into the Subantarctic and even into the Subtropics (*Diomedea chrysostoma, Phoebetria palpebrata, Daption capense, Fulmarus glacialoides:* Jehl 1973a, Szijj 1967, Watson *et al.* 1971). *Oceanites oceanicus* is the species whose summer and winter habitats differ most widely; it breeds in areas where the water is colder than 10 °C, yet most of the population winters where it is warmer than 15 °C, usually close to areas of upwelling (Bourne 1963, Roberts 1940). It is to be hoped that, as observations accumulate, it will be possible to examine such seasonal similarities and differences in pelagic habitat in greater detail.

Temperature and salinity are convenient indices of the niches occupied by the plankton and other organisms on which the birds feed. The biogeography is best known for the Antarctic and Subantarctic zones (Mackintosh 1934, 1960, Marr 1962). In our survey area the Antarctic has two subdivisions (Fig. 1). Macroplankton is generally scarce in the Graham Land Area, but there are very large local surface swarms of 'krill' *Euphausia superba* and of salps. In the Northern Zone, between this and the Antarctic Convergence, *E. superba* is replaced by other *Euphausia* species and macroplankton is generally more abundant though without large swarms of any species. The *Euphausia* species change again north of the Convergence, but average densities are low; there are instead large swarms of 'lobster-krill', the pelagic immature stages of the decapods *Munida subrugosa* and *gregaria*, found up to 41°30'S on the west coast of South America, and to 35°S on the east (Matthews 1932, Rayner 1935). There are comparable changes in other plankton species.

Antarctic and Subantarctic seabirds feed on plankton and on the fish and squid higher up the food web (e.g. Bierman & Voous 1950, Murphy 1936, Tickell 1964). Their diets are too poorly known for one to attempt any detailed correlations of birds and prey species. But such birds as *Pygoscelis antarctica, Daption capense* and *Fulmarus glacialoides*, commonest in summer in the area of the Antarctic Peninsula, would appear to be part of the Graham Land Area fauna. In our area *Diomedea melanophris* seems to be a Subantarctic species whose distribution extends south of the Convergence into the Northern Zone (Fig. 2a). By contrast *D. chrysostoma* (Fig. 2b) is practically confined to the Northern Zone and the waters between it and the colony south of Cape Horn. This pattern suggests that the Northern Zone may be an important feeding area for South American *D. chrysostoma* in summer; if the Subantarctic zone was important one would expect to see them commonly, like *D. melanophris*, north as well as south of Cape Horn. The foods of these two albatrosses are known to differ (Tickell 1964), but it is not yet possible to link them with the plankton species which act as biogeographic indicators of the zones.

On a much smaller scale it is interesting to look at the local sea-bird concentrations on the Patagonian Shelf (Fig. 1, Table 3) in oceanographic terms. Those immediately south of the Rio de la Plata (nos. 1 and 2) have been reported, for example, in October (Murphy 1936), November and March (Holgersen 1957) and January and April (Tickell & Woods 1972), in all of which months *Puffinus gravis* was a dominant species, just as in our own January and February sightings. Birds concentrate in the area during the winter too, but the species change. *Daption capense* and *Diomedea melanophris* are dominant in July (Jehl 1973b), and the banding returns suggest that *D. melanophris* occurs there all winter (Sladen, Wood & Monaghan 1968, Tickell 1967). We found sharp changes in surface temperature there, probably marking the boundary between warm coastal water and the cold Falkland Current; such boundaries tend to concentrate both plankton and the birds which feed on it (e.g. Ashmole & Ashmole 1967). Concentration 1 was at the edge of the continental shelf, where one would expect nutrients to be upwelled into the surface layers, leading to a high production of phytoplankton and therefore zooplankton.

TABLE 3

Sea-bird concentrations on the Patagonian Shelf. Species of minor importance are in parentheses

No.	Date	Position	Species
1.	4 Jan. 1970	39° 50′ S 56° 25′ W	*Puffinus gravis*, *Pterodroma incerta* (also *Calonectris diomedea*, *Procellaria aequinoctalis*).
2.	23 Jan. 1970	38° 44′ S 57° 40′ W	*Puffinus gravis* and *puffinus*, *Calonectris diomedea*, *Diomedea chlororhynchos*, *Stercorarius parasiticus* (also *S. pomarinus*).
3.	5 Jan. 1970	42° 51′ S 56° 39′ W	*Puffinus gravis*, *Pterodroma incerta*, *Diomedea exulans* + *epomophora*, *Oceanites oceanicus*.
4.	24 Jan. 1970	44° 20′ S 61° 40′ W	*Puffinus gravis* and *griseus*, *Procellaria aequinoctalis*, *Diomedea melanophris*, *Spheniscus magellanicus*.
5.	5 Apr. 1972	48° 00′ S 57° 00′ W	*Puffinus gravis* (also *Pterodroma incerta*, *Pachyptila* sp., *Diomedea melanophris*).
6.	21 Feb. 1970	53° 10′ S 67° 50′ W	*Puffinus gravis*, *Spheniscus magellanicus*, *Sterna hirundinacea*, *Stercorarius parasiticus*.
7.	8 Mar. 1972	54° 49′ S 64° 57′ W	*Puffinus griseus*, *Pelecanoides* sp., *Diomedea exulans* + *epomophora*, *Diomedea melanophris* (also *Sterna* sp., *Macronectes* sp.)

The other concentrations are harder to interpret. No. 4 was in an area where Aragno (1968) found relatively high levels of nutrients, probably due to upwelling at the western edge of the Falkland Current. His data suggested that productivity may be even higher farther east, and Cooke & Mills (1972) speculated that large numbers of seabirds may eventually be found between 42°–45° S, 57°–60° W. Concentration 3, independently observed by Kinnear, seems to meet this prediction, as do two April concentrations of *Puffinus gravis*, reported in much the same area by Tickell & Woods (1972). Concentration 5, at the edge of the continental shelf, may well be at another area of upwelling. Concentrations 6 and 7, east of Tierra del Fuego, are in what is probably a regular feeding area for seabirds; Humphrey *et al.* (1970) noted an observation of a small *Puffinus gravis* concentration near no. 6 in January 1966. Dr W. R. P. Bourne (pers. comm.) points out that upwelling is to be expected where, as in this case, shallow waters lie in the lee of the prevailing winds and currents.

THE CHILEAN FJORDS

It is difficult to examine the birds' preferred temperatures and salinities in any detail out at sea, since these factors change gradually and only within a relatively narrow range.

This was not so in the Chilean fjords, where surface temperatures ranged between 2·9°–15·7 °C and salinities between 0·4–33·6‰ and where there were often abrupt changes within very short distances (Anon 1971b). Following Pickard (1972; see also Appendix 2) the fjords can be subdivided on oceanographic grounds into six water bodies, each with its characteristic temperature-salinity relationship (Fig. 4), and the birds' abundance varies between these subdivisions (Table 2). It is informative to examine the birds' distributions against this background. For example, *Diomedea melanophris* is commonest at the northern and southern ends of the fjords, and scarcest in the middle (Fig. 2a); what is at first sight an odd distribution pattern becomes much less puzzling once one takes into account the oceanographic variations within the fjord system.

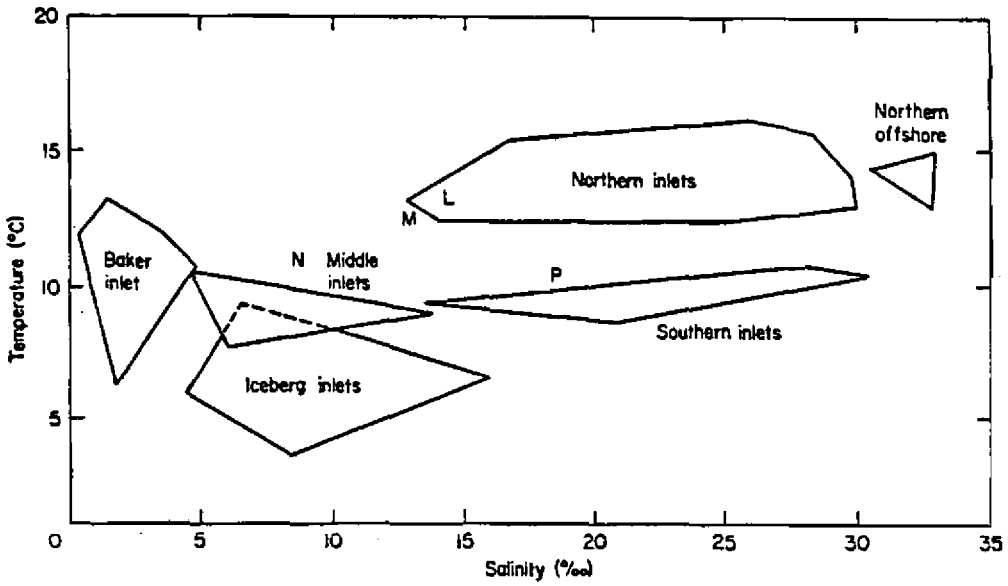


FIGURE 4. Surface temperatures and salinity characteristics of the water types in the Chilean fjords, adapted from Pickard (1971): see also Appendix 2. The envelopes enclose the range of temperature-salinity relationships for each water type.

Table 2 suggests that the commoner species in the fjords can be grouped as follows:

(i) *Diomedea exulans* + *epomophora*, *Pelecanoides* spp. and *Puffinus griseus* were commonest in the Southern Inlets and Northern Offshore, and the first two in the Northern Inlets as well. Their preference would appear to be for conditions associated with high-salinity waters; temperature is less important, at least within the range shown in the fjords.

(ii) *Diomedea melanophris*, *Spheniscus magellanicus*, *Phalacrocorax magellanicus* and *atriceps* + *albiventer* and *Larus dominicanus* were similar, but with a broader salinity preference, since they were also fairly common in Middle Inlets and in some cases Iceberg Inlets as well. The comparative preferences of *P. atriceps* and *P. albiventer* have already been described.

(iii) By contrast *Catharacta skua* and *Sterna hirundinacea* had broad salinity preferences, but were scarce in the warmer Northern Inlets and Offshore. Conditions associated with low temperatures seem to be important here. On the face of it this seems anomalous for the tern, which breeds in warmer waters along the Argentine coast (Murphy 1936).

(iv) *Puffinus creatopus*, *Procellaria aequinoctalis*, *Phalacrocorax gaimardi* and *Larus maculipennis* were commonest in the warm, highly saline waters of the Northern

Inlets and Offshore. Again, temperature seems the key factor; they were absent from the cold but equally saline Southern Inlets. *L. maculipennis* was in fact seen in colder waters, but only as a scavenger in harbours.

TABLE 4

Oceanographic parameters of the Chilean fjords. Averages for small crustaceans refer to cm³ per sample, and for other animals to the number of individuals caught; averages ≥ 5 are given to the nearest whole number. Fish and/or crustacean traces on an echo-sounder ('echo-index') were rated on an arbitrary 0–3 scale

Averages:	Southern Inlets	Middle Inlets	Iceberg Inlets	Baker Inlets	Northern Inlets	Northern Offshore
(i) *Isaacs-Kidd midwater trawl (averages/½-hour tow):*						
no. tows	3	4	3	5	8	4
Munida sp.	183	26	9	3·0	0·1	252
range	49–467	0–90	1–16	0–11	0–1	0–1000
Other large crustaceans[1]	44	10	46	24	25	0·3
range	1–87	0–38	7–117	6–58	0–102	0–1·4
Small fish[2]	16	15	30	10	19	27
	0–25	0–37	2·9–48	0–23	0–63	0–68
Small crustaceans	759	803	588	154	800	173
range	42–1462	29–1260	356–1009	32–422	100–1300	17–378
(ii) *1-m net, vertical haul (averages/haul):*						
no. hauls	11	9	3	11	27	—
Small crustaceans	27	119	56	12	100	
range	7–71	0–154	0–83	0–47	12–317	
(iii) *Echo-index:*						
no. readings	5	8	5	10	12	—
average	1·2	1·6	1·3	1·8	2·1	
range	0–2	0–3	1–3	0–3	0–3	
(iv) *Secchi disc (m) from Anon (1971b):*						
no. readings	18	17	4	18	29	—
average	6·0	4·9	3·0	1·6	6·8	
range	1·0–9·0	0·5–8·5	0·2–4·0	0·5–5·5	1·0–12·5	

Notes: [1] Mainly euphausids.
[2] Mainly myctophids and engraulids.

As with the pelagic distributions, these preferences probably reflect the distributions of prey associated with these water bodies. The biological data from the fjord cruise have not been published, and so no information is available on qualitative variations in fish and plankton species in the fjords. However, Table 4 shows some quantitative indices of the abundance of potential prey species. These are not completely satisfactory, since they vary not only with the species but also with the method of capture. They also vary widely within subdivisions, partly because *Munida* and fish occur in localized schools, and partly because the tows are too few to adjust for time of day and therefore the degree of vertical migration. But there are some possible correlations between the presence of birds and of potential prey. For example, *Munida* are probably an important food for *Puffinus griseus*, which feed extensively on crustaceans in the fjords (e.g., Palmer 1962). Tables 2 and 4 show that both the birds and *Munida* were commonest in the Southern Inlets and Northern Offshore; however this must remain speculative, in view of the variability of the tows. Again, diving petrels feed on small crustaceans (Murphy 1936) and they were common in the Northern Inlets where small crustaceans were also abundant. On the other hand, crustaceans were just as abundant in the Middle Inlets, where these birds were scarce.

On the other hand there are some clear correlations between the absence of birds and of food. All species were scarcest in the Baker and Iceberg Inlets (Table 2). On almost every index the Baker Inlets were the most barren part of the fjords, so this is not surprising. The Iceberg Inlets seem, on several indices, to be quite productive of potential prey; the limiting factor there may be silt. The Secchi disc figures are nearly as low as in the Baker inlets, and since most of the birds are divers, they might well find feeding difficult under such conditions.

The relative abundance of *Phalacrocorax atriceps* and *P. albiventer* in the Iceberg Inlets at first sight goes against this suggestion, but there is reason to regard them as a special case. We sometimes saw local concentrations of 25–100 birds or more in areas of the Middle and Iceberg Inlets where they did not appear to be breeding or roosting. In the most striking example over a hundred shags (and as many *Sterna hirundinacea*) were flocking at the boundary line between clear and silty water, close to the glacier face in Seno Glacier (52° 43′ S). Dunbar (1951) and Hartley & Fisher (1963) described similar concentrations by Arctic sea-birds; the silty 'brown zone' is an upwelling of highly saline water which carries plankton to the surface, and that in Seno Glacier was presumably upwelling food in the same way. Here and at two other faces where the birds were flocking we found fairly sharp changes in surface temperature and salinity between oceanographic stations; changes of 0·7 °C and 1·0‰ per mile in two cases, and 0·1 °C and 1·0‰ in the third. Continuous sampling between stations would probably have shown more abrupt changes than these figures suggest. Four more shag concentrations (three of them in glacier inlets, though not at the actual face) occurred where temperature and/or salinity was changing at over 0·5 °C or ‰ per mile; two others were in narrow channels connecting bodies of water of differing salinity. In all of these cases the relatively unstable physical properties of the water suggest some kind of upwelling which might concentrate prey at the surface where the birds could exploit it despite the siltiness of the water. On the other hand, five other local shag concentrations were in fjords where there was very little change in temperature and salinity. Two of these were glacier inlets; more detailed sampling might have given a different picture. Obviously the shags are not totally dependent on upwelling areas for their food supply, but they certainly seem to exploit them where these exist.

CONCLUSIONS

The discussions in the last section refer only to sea-bird distributions around southern South America. It would be premature to generalize from them over the whole of the species' range, since in some cases it appears that different factors may operate in different areas. For example, we only rarely saw *Diomedea melanophris* south of the Antarctic Convergence; Holgersen (1957) and Tickell & Woods (1972) confirmed this. But they are commonly seen south of the Convergence near South Georgia (Watson *et al.* 1971). They are also common down to 68° S in February in the New Zealand sector (Fowler 1973, van Oordt & Kruijt 1953); these birds seem to be of the New Zealand subspecies *D. melanophris impavida*, which evidently has an Antarctic as well as a Subantarctic pelagic range.

One might expect subspecies to have different food preferences. It is much harder to understand such anomalies in cases such as *Puffinus griseus*, whose South American and New Zealand populations cannot at present be separated subspecifically (Murphy 1964). We rarely saw these birds south of the Antarctic Convergence; nor did Holgersen (1957), Tickell & Woods (1972), van Oordt & Kruijt (1953) or Bierman & Voous (1950) in an arc of the Southern Ocean extending from 100° W to 80° E. On the other hand, Watson *et al.* (1971) showed that they are common south of the Convergence down to 65° S in the New Zealand sector, and van Oordt & Kruijt (1953) saw very large numbers

close to the Antarctic Continent, *c.* 63° S, 120°–160° E, in February 1952. *Puffinus griseus* is not always found south of the Convergence in this sector (e.g., Fowler 1973), and Murphy (1964) suggested that van Oordt & Kruijt's birds may have been on passage across an ecologically unfavourable zone. But on the face of it, the species seems to have different ecological requirements in different parts of its range.

It is possible that more sophisticated taxonomic techniques may reveal differences between the two *Puffinus griseus* populations. The anomaly may also be due to inadequacies in oceanographic as much as in ornithological knowledge. There is a parallel in the North Atlantic, where many seabirds and marine organisms are confined to Arctic waters in the west, but extend well down into the warmer Boreal zone in the east (Dunbar 1954, Salomonsen 1972). The North Atlantic anomaly obviously has an oceanographic basis, if a mysterious one, and something analogous may explain the discrepancies in the distributions of *Puffinus griseus* and *Diomedea melanophris*. But much more work remains to be done before it will be safe to generalize about the pelagic ecology of seabirds.

ACKNOWLEDGMENTS

We would like to thank the captains and crews of RRS 'Bransfield', MV 'Forrest', RRS 'John Biscoe', CSS 'Hudson' and MV 'Perla Dan' for their cooperation. We are also grateful to Dr B. McK. Bary, Dr W. R. P. Bourne, Dave Clark, Dr J. R. Jehl Jr, Roderick Maclean, Neil Macpherson, Dr G. L. Pickard, Dr R. Pocklington, Dr S. Pond, Dr C. E. Tull and Dr G. E. Watson for help and advice of various kinds. Cooke and Mills were supported by grants from the National Research Council of Canada, the School of Graduate Studies, Queen's University, and the Faculty of Graduate Studies, Dalhousie University. Kinnear held an appointment with the British Antarctic Survey.

SUMMARY

The paper summarizes observations on the pelagic distributions of sea-birds in Drake Passage and off southern South America, collected by ship-borne observers between December 1969 and April 1970, and in March and April 1972. The birds' distributions have been related to sea surface temperatures and, in the case of the Chilean fjords, to water types defined in terms of temperature and salinity; a partial attempt has been made to relate them to the distribution of the macroplankton.

The boundary between the ranges of *Phalacrocorax albiventer* and *P. atriceps* in the Chilean fjords is much farther west than previously reported, and there is some evidence that it has moved westwards within the last 20 years. It is suggested that its position is determined by oceanographic rather than climatic factors.

A sighting of *Pterodroma macroptera* in Cockburn Channel is the first record of this species for Chile. Exceptionally southerly records of *Lobipes lobatus* in Magellan Strait, and *Pterodroma mollis* south of the Antarctic Convergence are also described. An apparent decline in the numbers of *Pterodroma neglecta* at Masatierra, Juan Fernandez, is noted.

REFERENCES

ANON 1971a. Monatskarten für den Sudatlantischen Ozean (Dritte Auflage). Deutsches Hydrographisches Institut, Hamburg.

ANON 1971b. Chile 70 cruise. Institute of Oceanography, University of British Columbia: Data Report 31.

ARAGNO, F. J. (ed.) 1968. Datos y resultados de las campanas pesqueria 'Pesqueria III' (20 de febrero al 20 marzo de 1967). Mar del Plata, Argentina: Publicaciones del Projecto de Desarrollo Pesquero (serie Informes Tecnicos) Mn. 10/111.

ASHMOLE, N. P. & ASHMOLE, M. 1967. Comparative feeding ecology of sea-birds of a tropical ocean island. Bull. Peabody Mus. nat. Hist. 24: 1–131.

BEHN, F., GOODALL, J. D., JOHNSTON, A. W. & PHILIPPI B., R.A. 1955. The geographic distribution of the Blue-eyed Shags, *Phalacrocorax albiventer* and *Phalacrocorax atriceps*. Auk 72: 6–13.

BIERMAN, W. H. & VOOUS, K. H. 1950. Birds observed and collected during the whaling expeditions of the 'Willem Barendsz' in the Antarctic, 1946–47 and 1947–1948. Ardea 37 (special number): 1–123.

BOURNE, W. R. P. 1963. A review of oceanic studies of the biology of seabirds. Proc. 13 int. orn. Congr.: 831–854.

BOURNE, W. R. P. 1968, Notes on the diving petrels, Bull. Br. Orn. Cl. 88: 77–85.

BOURNE, W. R. P. & WARHAM, J. 1966. Geographical variation in the Giant Petrels of the genus *Macronectes*. Ardea 54: 45–67.

CAWKELL, E. M. & HAMILTON, J. E. 1961. The birds of the Falkland Islands. Ibis 103a.: 1–27.

COOKE, F. & MILLS, E. L. 1972. Summer distribution of pelagic birds off the coast of Argentina. Ibis 114: 245–251.

DABBENE, R. 1921–26. Los petreles y los albatros del Atlantico Austral. Hornero 2: 157–179, 241–254; 3: 1–33, 125–158, 227–238, 311–348.
DUNBAR, M. J. 1951. Eastern Arctic Waters. Bull. Fish. Res. Bd Can. 88. Ottawa.
ESCALANTE, R. 1970. Aves marino del Rio de la Plata y aguas vecinas del Oceano Atlantico. Montevideo: Barreiro y Ramos S.A.
FOWLER, J. A. 1973. A transect diagram for oceanic birds recorded between McMurdo Sound, Antarctica, and New Zealand, February–March 1973. Notornis 20: 314–317.
HARPER, P. C. 1972. The field identification and distribution of the Thin-billed Prion *Pachyptila belcheri* and the Antarctic Prion *P. desolata*. Notornis 19: 140–175.
HARTLEY, C. H. & FISHER, J. 1936. The marine foods of birds in an inland fjord region in West Spitsbergen. J. Anim. Ecol. 5: 370–389.
HOLGERSEN, H. 1957. Ornithology of the 'Brategg' Expedition. Scientific Results of the 'Brategg' Expedition 1947–48, no. 4. Bergen.
HUMPHREY, P. S., BRIDGE, D., REYNOLDS, P. W. & PETERSON, R. T. 1970. Preliminary Smithsonian Manual. Birds of Isla Grande (Tierra del Fuego). Washington, D.C.: Smithsonian Institution.
JEHL, J. R. 1973a. The distribution of marine birds in Chilean waters in winter. Auk 90: 114–135.
JEHL, J. R. 1973b. Winter populations of marine birds on the Argentine coast: R/V 'Hero' cruise 72–3b. Antarctic Jlt. U.S. 8: 32–33.
JOHNSON, A. W. 1965. The birds of Chile and adjacent regions of Argentina, Bolivia and Peru, vol. 1. Buenos Aires: Platt Establicimentos Graficos S.A.
JOHNSON, A. W. 1972. Supplement to the birds of Chile and adjacent regions of Argentina, Bolivia and Peru. Buenos Aires: Platt Establicimentos Graficos S.A.
KING, W. B. 1967. Preliminary identification manual. Sea-birds of the tropical Pacific Ocean. Washington D.C.: Smithsonian Institution.
LATHBURY, SIR G. 1972. HMS 'Endurance'—passage to the Antarctic—October 1969–May 1970. Observation of seabirds. Sea Swallow 22: 10–15.
LATHBURY, SIR G. (unpubl.). An account of the sea-birds seen during the visit of HMS 'Endurance' to South America and the Antarctic, October 1969 to May 1970. MS in the Alexander Library, Edward Grey Institute, Oxford.
MACKINTOSH, N. S. 1934. Distribution of the macroplankton in the Atlantic sector of the Antarctic. 'Discovery' Rep. 9: 65–160.
MACKINTOSH, N. S. 1946. The Antarctic Convergence and the distribution of surface temperatures in Antarctic waters. 'Discovery' Rep. 23: 177–212.
MACKINTOSH, N. S. 1960. The pattern of distribution of the Antarctic fauna. Proc. Roy. Soc. London Ser. B 152: 624–631.
MARR, J. W. S. 1962. The natural history and geography of the Antarctic krill (*Euphausia superba* Dana). 'Discovery' Rep. 32: 33–464.
MATTHEWS, J. H. 1932. Lobster-krill: anomuran Crustacea that are the food of whales. 'Discovery' Rep. 5: 467–484.
MURPHY, R. C. 1936. Oceanic birds of South America. New York: Am. Mus. nat. Hist.
MURPHY, R. C. 1964. Systematics and distribution of Antarctic petrels. *In* Carrick, R., Holdgate, M. and Prevost, J. (eds) Biologie Antarctique, Premier Symposium, Biologie Antarctique. Paris 1962: Hermann.
OZAWA, K. 1967. Distribution of seabirds in austral summer season in the Southern Ocean. Antarctic Rec. 29: 1–36.
PALMER, R. S. (ed.) 1962. Handbook of North American Birds, vol. 1. Yale University Press.
PICKARD, G. L. 1971. Some physical oceanographic features of inlets in Chile. J. Fish. Res. Bd. Can. 28: 1077–1106.
POST, P. W. 1967. Manx, Audubon's and Little Shearwaters in the northwestern North Atlantic. Bird-Banding 38: 278–305.
RAYNER, G. W. 1935. The Falkland species of the crustacean genus *Munida*. 'Discovery' Rep. 10: 209–246.
ROBERTS, B. B. 1940. The life cycle of Wilson's Petrel *Oceanites oceanicus* (Kuhl). Brit. Graham Land Exped. 1934–37, Sci. Reps 1: 141–194.
SALOMONSEN, F. 1972. Zoogeographical and ecological problems in Arctic birds. Proc. 15 int. Orn. Congr.: 25–77.
SERVENTY, D. L., SERVENTY, V. & WARHAM, J. 1971. The handbook of Australian seabirds. Sydney: A. H. & A. W. Reed.
SLADEN, W. J. L., WOOD, R. C. & MONAGHAN, E. P. 1968. The USARP Bird Banding Program, 1958–1965. In Austin, O. L. (ed.) Antarctic bird studies. Am. Geophys. Union Antarctic Research Series 12: 1–55.
SZIJJ, L. J. 1967. Notes on the winter distribution of birds in the western Antarctic and adjacent Pacific waters. Auk 84: 366–378.
TICKELL, W. L. N. 1964. Feeding preferences of the albatrosses *Diomedea melanophris* and *D. chrysostoma* at South Georgia. *In* Carrick, R., Holdgate, M. W. and Prevost, J. (eds) Biologie Antarctique, Premier Symposium, Biologie Antarctique. Paris 1962: 383–387.
TICKELL, W. L. N. 1967. Movements of Black-browed and Grey-headed Albatrosses in the South Atlantic. Emu 66: 357–367.
TICKELL, W. L. N. 1968. Biology of the great albatrosses. *In* Austin, O. L. (ed.), Antarctic bird studies. Am. Geophys. Union Antarctic Research Series 12: 1–55.

TICKELL, W. L. N. & WOODS, R. W. 1972. Ornithological observations at sea in the South Atlantic Ocean. 1954–64. Bull. Br. Antarct. Surv. 31: 63–84.

VAN OORDT, G. J. & KRUIJT, J. P. 1953. On the pelagic distribution of some Procellariforms in the Atlantic and Southern Oceans. Ibis 95: 615–637.

WATSON, G. E., ANGLE, J. P., HARPER, P. C., BRIDGE, M. A., SCHLATTER, R. P., TICKELL, W. L. N., BOYD, J. C. & BOYD, M. M. 1971. Birds of the Antarctic and Subantarctic. Am. Geogr. Soc. Antarctic Map Folio 14.

APPENDIX 1

Itineraries: (see also Figures 1–3; ships' tracks are shown on Figure 2).

1969–70:	
21 December	crossed the Equator (PKK)
1–2 January	at Montevideo
8–12 January	in the Falkland Islands
16 January	at Signy, South Orkneys
17–18 January	near the Antarctic Peninsula and South Shetlands
22 January	leave Buenos Aires (FC and ELM)
26–29 January	in Magellan Strait, Cockburn and Beagle Channels
3–7, 14–17 February	near the Antarctic Peninsula and South Shetlands
9, 19–20 February	at Puerto Williams
21 February	to Punta Arenas via Lemaire Strait
1–8 March	Punta Arenas to Southern Inlets (RGBB)
9–19 March	in Middle, Iceberg and Baker Inlets
20–28 March	in Northern Inlets
29–30 March	at Puerto Montt
4 April	at Masatierra, Juan Fernandez
6 April	arrive Vulparaiso
1972	
6 March	leave Argentine Islands via Gerlache Strait (PKK)
8 March	in Lemaire Strait
10–11 March	at Punta Arenas
12–14 March	in Magellan Strait, Cockburn and Beagle Channels
15–20 March	aircraft beacon work in Drake Passage, *c.* 59° S 69° W
22 March	arrive Falkland Islands
25–29 March	by ship along the north coast of the Falklands
5 April	leave Falkland Islands
9–11 April	at Montivideo
20 April	crossed the Equator

APPENDIX 2

PHYSICAL OCEANOGRAPHY OF THE CHILEAN FJORDS

Water bodies can be defined in terms of their temperature-salinity and temperature-oxygen relationships, measured at depths where these factors are more stable than in the more readily modifiable surface layers. Pickard (1971; see also Anon 1971b) used these relationships to divide the Chilean fjords into the Southern, Middle and Northern Inlets. Within the Middle Inlets he separated off those with ice in the water (Iceberg Inlets), and suggested one could do the same with the fjord system centering on Canal Baker (Baker Inlets).

Figure 4 shows a modified version of his surface temperature-salinity plot for these areas. The modifications are as follows:

(i) We have followed his suggestion and plotted Baker Inlets separately. With these, we have included observations made near Pickard's stations L, M and N, geographically adjacent to the Baker system proper. Although these stations are markedly more saline on the surface than the rest of the Baker Inlets, the differences disappear at greater depths.

(ii) Pickard's ocean stations B, C and D, off the Golfo de Peñas and the Northern Inlets, are fairly similar oceanographically, and rather unlike the adjacent fjords. We have plotted them separately as the Northern Offshore area, and added observations farther north off Canal Chacao, out to about 75° 20′ W.

(iii) Pickard's station P is geographically part of the Middle Inlets and we have included it with that area, even though the station is oceanographically atypical.

(iv) Southern Inlets are as defined by Pichard, but we have added seabird observations made in the fjords south of Magellan Strait, where in fact no oceanographic work was carried out.

R. G. B. Brown, Canadian Wildlife Service, Marine Ecology Laboratory, Bedford Institute for Oceanography, Dartmouth, Nova Scotia, Canada

Fred Cooke, Department of Biology, Queens' University, Kingston, Ontario, Canada

P. K. Kinnear, 2 Mounthooly Street, Lerwick, Shetland, ZE1 OBJ.

Eric L. Mills, Department of Oceanography, Dalhousie University, Halifax, Nova Scotia, Canada

Queen Charlotte Fault-Zone, British Columbia

R. L. CHASE and
D. L. TIFFIN,
Canada

ABSTRACT

The Queen Charlotte fault, west of British Columbia and Alaska, is a seismically active transform fault along the continental margin between the North American and Pacific lithospheric plates. Six continuous seismic profiles across the fault between latitudes 52°N and 55°N show that both continental rise and continental shelf are virtually absent. The insular mountains, up to 1100 m high, are separated from deep sea floor at 3 km depth by an 18- to 25-km-wide continental slope. The latter is tripartite, having steep upper and lower slopes with gradients of the order of 20°, probably fault scarps, and a central part with a gentle reverse gradient, sometimes broken by ridges and sediment-filled troughs. The oceanic basement, overlain by hemipelagic and turbiditic sediments as thin as 1.3 km, extends to the base of the continental slope and dips gently toward the continent to form the Queen Charlotte trough. The trough is 30 km wide and up to 800 m deep and is partly filled with flat-lying sediment. Faulting extends from the interior of the Queen Charlotte Islands to at least 20 km seaward from base of the continental slope, and possibly farther, to the western margin of the trough. Dredging indicates that ice-transported boulders blanket the upper continental slope. No in-situ crystalline outcrops were sampled. The oldest dated sediment recovered from the continental slope is Lower Pliocene. The Queen Charlotte Islands appear to have protected the adjoining seafloor from the accumulation of large quantities of sedimentary material during the Pleistocene.

WILSON (1965) proposed the term "transform fault" for strike-slip faults joining linear belts of crustal extension (oceanic ridges) to other such belts or to belts of crustal consumption (trenches, arcs). He deduced that the fault system along the continental margin north of Vancouver Island and west of the Queen Charlotte Islands (St. Amand, 1957) should be a dextral transform fault joining the northern end of Juan de Fuca ridge to the Alaska-Aleutian trench-arc system, and named the feature the Queen Charlotte Islands fault. First-motion studies of earthquakes by Hodgson and Milne (1951) and Tobin and Sykes (1968) confirmed the dextral nature of the fault.

As an active transform fault coincident with a continental margin, the Queen Charlotte fault is, to our knowledge, unique. Although lacking in deep- and intermediate-focus earthquakes, and showing less activity than many other parts of the circum-Pacific seismic zone (Tobin and Sykes, 1968), the Queen Charlotte Fault zone is nevertheless one of the most active earthquake zones in Canada. Movement on the fault can result in severe damage to insular and coastal communities of British Columbia and Alaska.

Sutherland-Brown (1968) described the geology of the Queen Charlotte Islands immediately east of the fault zone, and reconnaissance studies of the

Authors' addresses are given at the back of this book.

oceanic area to the west have been reported by Atwater and Menard (1970), Dehlinger *et al.* (1971), Hayes (1970), Srivastava *et al.* (1971), and others. The geology of the fault zone itself between 51° and 55°N has not been investigated. The objectives of this project, of which this is the initial report, are to delineate the fault zone along the continental margin and sea floor, to study the geological formations exposed along the fault and to determine, if possible, the effects of the fault on the morphology of the margin and the role it has played in the tectonic history of the region.

The study was initiated in 1970 with two continuous seismic profiles (Profiles E and F, Fig. 1) obtained during the Hudson 70 Expedition (Srivastava *et al.*, 1971). In 1971, five additional continuous seismic profiles were run and six dredge samples taken at sites within the fault zone. Locations of seismic profiles and dredge sites are shown in Figure 1. Interpretative tracings of the profiles are reproduced as Figures 2 to 8. Six profiles (A to F, Fig. 1) cross the Queen Charlotte fault-zone. The seventh (G) crosses the continental slope just east of the fault-zone. Vertical exaggeration of the profiles varies from 4.6 to 10. The vertical scale is in seconds of two-way travel time, which may be converted to water depths in fathoms (1 fathom = 6 feet) by multiplication by the factor 400, or in kilometers by factor 0.75. An estimate of thickness of sediment can be made by assuming a velocity of sound in unconsolidated sediments of 2 km/second. Each vertical scale-division is then 1 kilometer. The horizontal scale below each profile is approximate because of slight variations of ship's speed during recording. The nomographs of angles allow estimation of apparent slopes on the sea floor.

We shall discuss the profiles from south to north. Profile G (Figure 2), which runs from near the shelf break, across the upper part of the continental slope, illustrates the topography of the continental margin near the southern end of the Queen Charlotte fault in the area. According to theories of plate tectonics, the southern terminus of the Queen Charlotte fault should be the northern end of

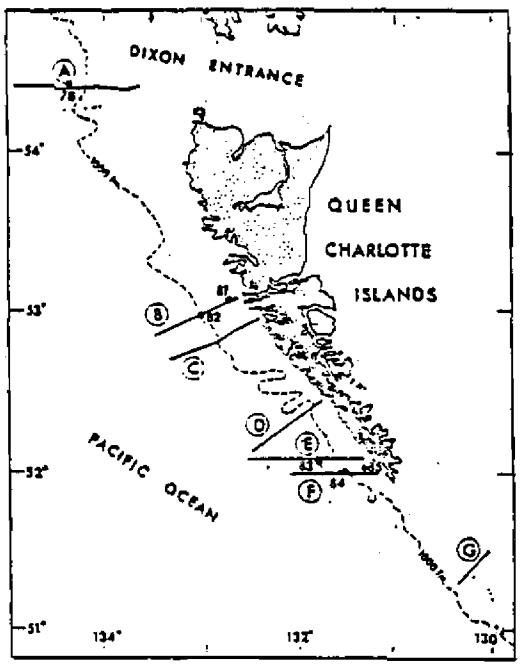


FIGURE 1 — Location of continuous seismic profiles and bottom sample sites. All profiles except profile G cross the Queen Charlotte fault-zone.

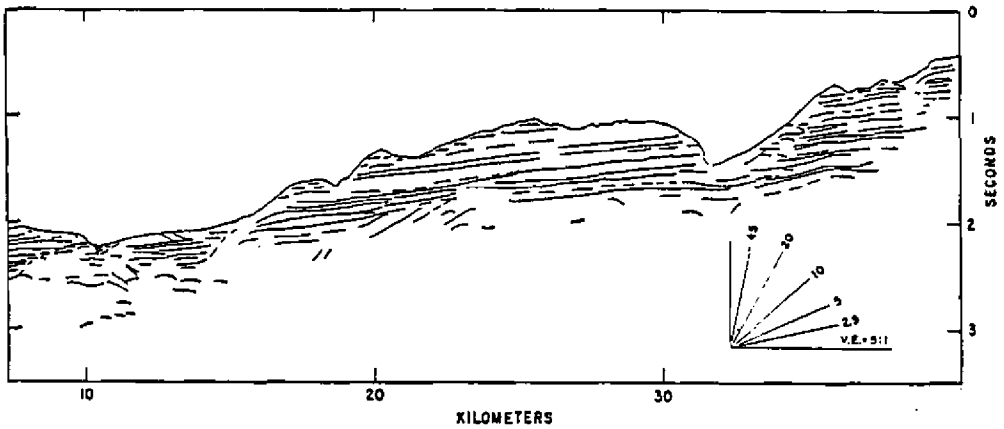


FIGURE 2 — Profile G, a line-drawing interpretation of a seismic reflection profile on the continental slope off Queen Charlotte Sound. See Figure 1 for location. The vertical scale is in seconds of two-way travel time. A nomograph allows estimation of angles on the sea floor. V.E. = vertical exaggeration. This profile does not extend to the base of the continental slope. The Queen Charlotte fault zone lies to the west of the end of the profile. The valley at 31 km is a canyon cutting downslope and crossed obliquely by the ship's track.

the oceanic ridge which lies off northwestern United States and southeastern British Columbia, segments of which include the Gorda, Juan de Fuca and Explorer ridges. The ridge approaches the North American continent and meets it at a triple plate junction (see Figure 9) in the area of the Dellwood Knolls near 50°50'N, 130°30'W (Srivastava, *et al.*, 1971). The location of the fault zone between the southern end of the Queen Charlotte Islands and the northern end of Vancouver Island is not apparent from the distribution of earthquake epicentres (Tobin and Sykes, 1968), which are scattered over a broad band in this area, nor is the topography sufficiently distinctive to allow precise positioning of the fault trace. The sea floor over much of this southern area has been described as having fracture-zone topography (McManus, 1967). The adjacent shelf is as much as 120 km wide in Queen Charlotte Sound, the embayment between Vancouver Island and the Queen Charlotte Islands. Both shelf and upper slope are cut by numerous deep valleys, one of which is shown in Figure 2. The average gradient of the slope is less than 5°. A thick sequence of almost undisturbed sedimentary strata is present on the slope, overlying a more deformed deeper layer. No evidence of displacement attributable to faulting is apparent in the upper layers of sediments. The present Queen Charlotte fault must therefore lie west of mid-slope in this area.

By contrast, west of the Queen Charlotte Islands, earthquake epicentres show that the fault lies along the margin of the continent. The topography also suggests fault control. The shelf is narrow, in places virtually non-existent, and the continental slope is steep. Insular mountains rise as high as 1100 m within two km of the shoreline (see Plate I, Sutherland-Brown, 1968), and show truncated spurs with triangular facets toward the sea.

Profiles B, C, D, E and F (Figures 3 to 7) indicate the character of the margin west of the Queen Charlotte Islands. The continental shelf is only about 5 km wide or less. The continental slope varies in width from 18 to 25 km, with an average gradient as high as one in nine (6.5°). From mountain summit to base of slope, the gradient is similar, the shelf being no more than a notch. Although

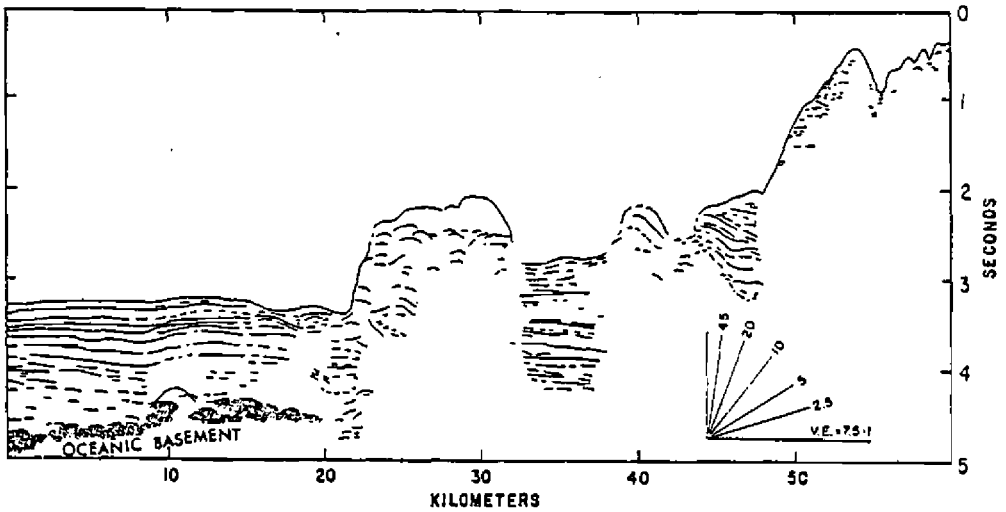


FIGURE 3 — Profile F. West of Queen Charlotte Islands the continental shelf is extremely narrow and the slope is steep. The slope in the south is rugged, with horst- and graben-like features. Seismic basement under oceanic sediments is elevated at the base of the slope. Profiles E and F are from Srivastava *et al.* (1971).

steep, this gradient is not as great as that of the continental slope west of the Scott Islands, south of the supposed southern end of the fault, where the average gradient is as high as 15° (Tiffin, *et al.*, in prep.).

The slope is characteristically composed of three parts: an upper virtually unbroken steep slope, a middle plateau area, flat — or broken by ridges and troughs — and a lower steep slope, which terminates abruptly at the deep ocean floor. The upper slope, with relief up to 1.8 km, has a gradient of as much as 20°. The topography of the middle sector varies considerably. In the northern profiles it is subdued, becoming more rugged to the south in profiles (E) and (F). In the latter profile it is broken into three horst-like features separated by two grabens. The lower slope, an escarpment up to 1.5 km high, has slopes as great as 23°. Acoustic reflectors beneath the upper slope indicate that sedimentary strata underlying this sector are in places faulted and folded. Lack of penetration in profiles D and E may be due to the presence of crystalline rocks at or near the sea floor. Recent closely spaced faulting is evident on the uppermost slope of profiles B and possibly F. The grabens and synclines beneath the central sector of the continental slope are partially of wholly filled with strata up to 1.7 seconds thick; their increasing deformation with depth indicates that deformation proceeded with sedimentation. The horsts and grabens and folding of underlying strata are most suitably explained by strike-slip movements with vertical (dip-slip) components along several parallel or subparallel steeply dipping faults which form part of the Queen Charlotte fault zone. The lower slope is underlain by sedimentary strata and is almost certainly a fault-scarp (profiles B, E and F). Elsewhere (Profiles C, D), similar scarps may be buried by sediments filling the Queen Charlotte trough.

The ocean floor west of the Queen Charlotte Islands, 2700 to 3000 m deep, lies only 30 km from the summits of the insular mountains. Several peculiarities are aparent in the profiles from this area. Most noticeable is the complete lack of continental rise. Instead, the ocean floor dips slightly toward the continent to form the Queen Charlotte trough, a shallow depression at the base of the slope

(Profiles B, C, D and E). The trough at one time may have been up to 800 m deep and 30 km wide. It is now partly filled with flat-lying sediments.

A typically oceanic sequence underlies the Queen Charlotte trough and the sea floor to the west. The lowest reflector is the oceanic basement, overlain by up to 1.8 sec. (1.8 km) of sedimentary strata. The age of the basement here may be inferred from the map of magnetic anomalies of Atwater and Menard (1970) to be approximately 5 m.y. in the south, increasing to 12 m.y. in the north. The average rate of deposition at the point of deepest burial of the basement has been 36 cm/10^3 years. However, because the sequence overlying the basement comprises three distinct units, undoubtedly different rates of accumulation apply. The lowest unit exhibits the lack of strong internal reflectors characteristic of slowly accumulating hemipelagic or pelagic sediments, and probably accumulated when the terrain was not subjected to deposition from turbidity currents generated on or near the continental margin. Such a condition could have arisen if a deep trench existed at the bottom of the continental slope, or if the ocean floor at time of deposition formed the seaward flank of an oceanic ridge. The latter condition is more likely, although the former is possible (Atwater, 1970). Overlying the transparent layer is a well-stratified sequence. To the west, similar strata form the levees of Moresby Channel (Srivastava *et al.*, 1971). Hence this unit is likely composed of terrigenous turbidites which accumulated rapidly in the Plio-Pleistocene. The third unit of flat-lying strata is infilling the Queen Charlotte trough, and may be a deposit from turbidity currents generated on the slope off the Queen Charlotte Islands.

Beneath the flat-lying sediments in the trough, the underlying units and oceanic basement dip landward and extend to the base of the continental slope where they disappear abruptly. The trough ends in the south near the southern tip of the Queen Charlotte Islands (Mammerickx and Taylor, 1971), just south of profile F. The latter profile shows that the oceanic basement in that region is elevated at the base of the slope under the area normally occupied by the trough. The northern end of the bathymetric expression of the trough occurs at about latitude 53°30'N (Chart 3000, Canadian Hydrographic Service). However, the trough probably extends north as a buried feature: Profile A, off Dixon Entrance shows an area of disturbance 24 km in width where the trough should be, just west of the base of a large hill forming the lower slope.

The most northerly profile (A, Fig. 8) shows a smooth shelf underlain by a reflector of 0.4 to 0.5 sec., under which folded strata occur. East of this profile, records not reproduced here indicate that westerly dipping strata are truncated by the shelf. The profile gives no indication of recent movement on the outer shelf. The slope in the profile has a gradient of 2.5°, considerably gentler than that to the south. Irregular topography of the upper slope appears to have resulted from slumping, but internal deformation and differential uplift may have contributed to its formation.

The smooth mid-slope ends abruptly at a hill or seamount on the base of the slope which has a relief of 1600 m above the flat ocean floor and slopes of greater than 20° on its sides. Penetration of about 1 second into sediments under mid-slope shows they are monoclinal, generally conforming to the slope angle at the top, but increasingly deformed by folding and perhaps faulting at depth. Strata dipping toward the slope on its east side show that it is most probably cored with upfolded sediments originating from below the mid-slope sequence apparent in the profile. Dredging on the east flank of the seamount recovered a fractured, semi-consolidated, green-grey mudstone containing an undiagnostic microfauna.

Oceanic basement, not seen in the profile, must be deeper than the 2.2 seconds

of penetration achieved in the sediments west of the seamount. Assuming a depth of sediment of 2.2 km and an age of basement of 12 m.y. (Atwater and Menard, 1970), the minimum average rate of sedimentation since formation of the basement is 19 cm/10^3 years.

Sampling along the continental slope showed the presence of a veneer of Pleistocene cobbles and boulders on the sea floor, these being the only crystalline rocks recovered. Six dredge hauls yielded sedimentary material (Fig. 1). The oldest sedimentary rock recovered was Lower Pliocene argillaceous limestone from the middle slope at site 84. The depositional environment was upper bathyal (B. E. B. Cameron, pers. comm.), indicating that no significant change in depth has occurred since deposition. Quaternary mud was recovered at sites 81, 82, 83 and 85, and barren limestone with chert inclusions at site 82. The latter resembles early Pliocene limestone from Tofino Basin, west of Vancouver Islands (B. E. B. Cameron, pers. comm.).

LOCATION AND EXTENT OF QUEEN CHARLOTTE FAULT ZONE

The geometry of plate tectonics indicates that the relative strike-slip movement of the American and Pacific plates in the Queen Charlotte area should be of the order of 5 cm per year. Does accommodation to this displacement take place on one of many faults? Atwater (1970) postulated that adjustment might be spread through a zone hundreds of km wide virtually encompassing the North American Cordillera. Sutherland-Brown (1968), on the basis of topographic evidence derived from hydrographic charts, placed the fault as a single trace on the middle slope, generally conforming to the base of the steep upper section (Fig. 4, 5, 6) and following an alignment of a series of depressions (the synclinal basins or grabens of profiles A to F). He also noted two other major faults, both trending northwesterly: the Rennell-Louscoone fault, 25 km northeast of the Queen Charlotte fault through the Queen Charlotte Islands, and the Sandspit fault, 60 km northeast, partly under Hecate Strait and partly through the eastern Queen Charlotte Islands. Right-lateral movement of at least tens of kilometers is indicated on the Rennell-Louscoone fault, and significant horizontal movement, but of unknown sense and magnitude, on the Sandspit fault. The profiles contain evidence that the fault zone extends west of Sutherland-Brown's postulated fault-line into the deep ocean floor. In profile B, faulting extends some 15 km seaward from the base of the slope, and in A, 20 km. The southern profiles show less unequivocal evidence for faulting on the sea floor. However, the pattern of linear magnetic anomalies which characterizes the Northeast Pacific dies out at approximately the western margin of the Queen Charlotte trough (Srivastava *et al.*, 1971), a phenomenon best explained by strike-slip faulting in the basement beneath the trough, which would result in interruptions of the original horizontal continuity of the basement and hence of the anomalies.

ORIGIN OF FEATURES ON THE CONTINENTAL SLOPE

The steepness of the lower continental slope, 20° or more in places (profiles B and F), suuggests that it is a fault scarp. Flat-lying oceanic sediments abut it with little disturbance or disappear under it with no evidence of faulting (e.g. Profile F).

Sutherland-Brown (1968) suggested large-scale slumping as one explanation of the line of depressions halfway down the continental slope. This seems plausible to explain the form of the slope in profiles C and D, where the reversed gradient of the seafloor in the central sector is sub-parallel to strata below, and the mass

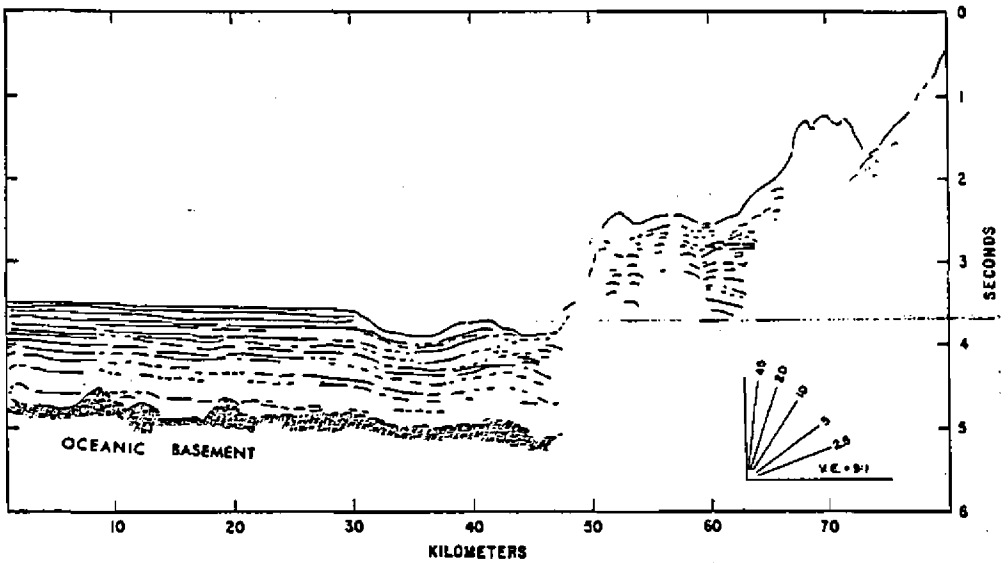


FIGURE 4 — Profile E. Profiles B to F show characteristic division of slope into a steep upper section, a mid-slope plateau and a steep lower section. Seismic basement disappears beneath the lower slope.

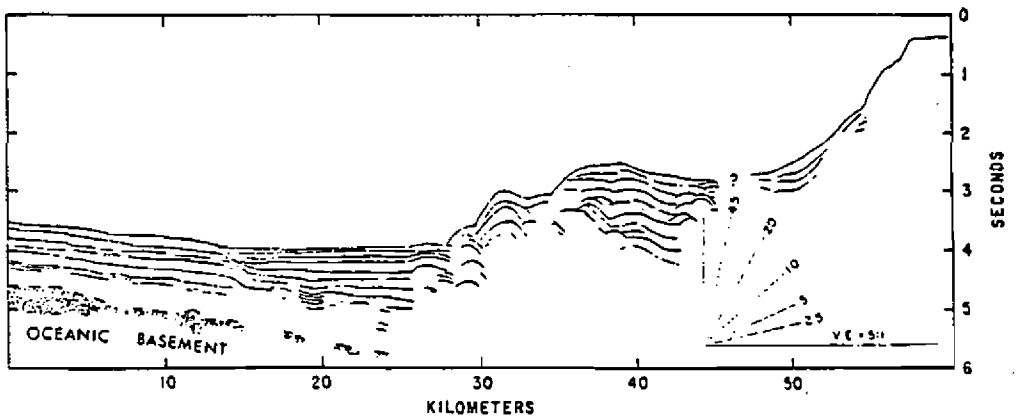


FIGURE 5 — Profile D. The mid-slope plateau in some areas has a reverse gradient. Sutherland-Brown (1968) draws the Queen Charlotte fault trace through the depression on the plateau. The sediment-filled trough is apparent at the base of the slope.

of deformed strata to the west could form the "toe" of the slope. A slump block up to 30 km wide and of the order of many tens of kilometers long would be required to form the configuration observed. Such a process seems a less likely explanation of the western horst of profile F, although the features to the east on the same profile could be related to slumping. It is doubtful that the seamount in profile A is a slump feature; it may be part of a sedimentary fan deformed by movements in underlying crystalline basement.

ORIGIN OF THE QUEEN CHARLOTTE TROUGH

The Queen Charlotte trough extends, both as a bathymetric and a sub-surface feature, over a distance of 250 km at the foot of the continental slope. We put

forward three possible origins for the trough. First, the trough is a remnant of a former trench formed when the Pacific plate was being subducted beneath the North American plate. It is difficult to see how a trench could retain its form while being subjected to strike-slip faulting parallel to its length, and the interruption of linear magnetic anomalies at the western margin of the present trough is best explained by strike-slip faults under the trough. However, seismic evidence (Molnar and Sykes, 1969) indicates that the Puerto Rico trench, ten times as deep, is subjected to movements predominantly parallel to its length.

Second, a small compressional component of stress exists at present across the Queen Charlotte fault, causing some underthrusting of the Pacific plate be-

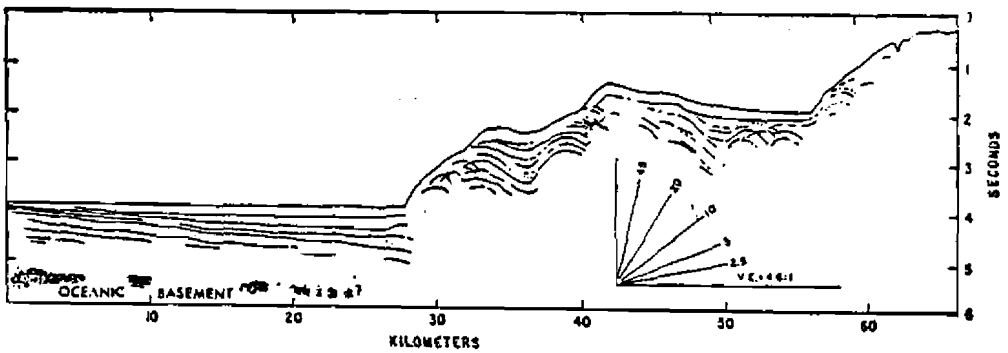


FIGURE 6 — Profile C. Both oceanic seismic basement and overlying sediments dip toward the continent and appear to continue under the slope.

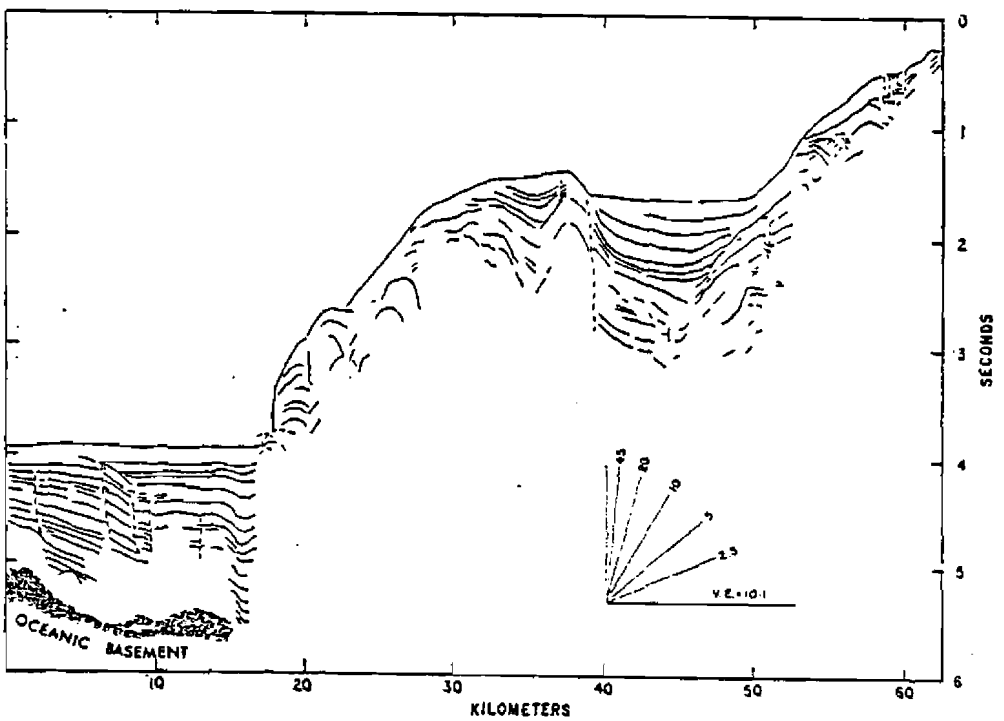


FIGURE 7 — Profile B. Faulting in sediments under the buried trough is apparent here. Deep sediments are slightly folded before disappearing under the slope.

neath the American plate. This would cause downwarping of the Pacific plate to produce the trough, and uplift of the overriding plate, perhaps evidenced by the existence of the insular mountains of the Queen Charlotte Islands. Data on first-motions of earthquakes in the region are as yet too few to confirm or refute this hypothesis.

Third, the trough is caused by downwarping of the margin of the Pacific plate as a result of the accumulation of sediments on the continental slope, the basement of which is somehow welded to the Pacific plate, breaking intermittently during motion along the fault. Negative gravity anomalies beneath the slope (Srivastava *et al.*, 1971; Couch, 1969) suggest that thick sediment accumulations

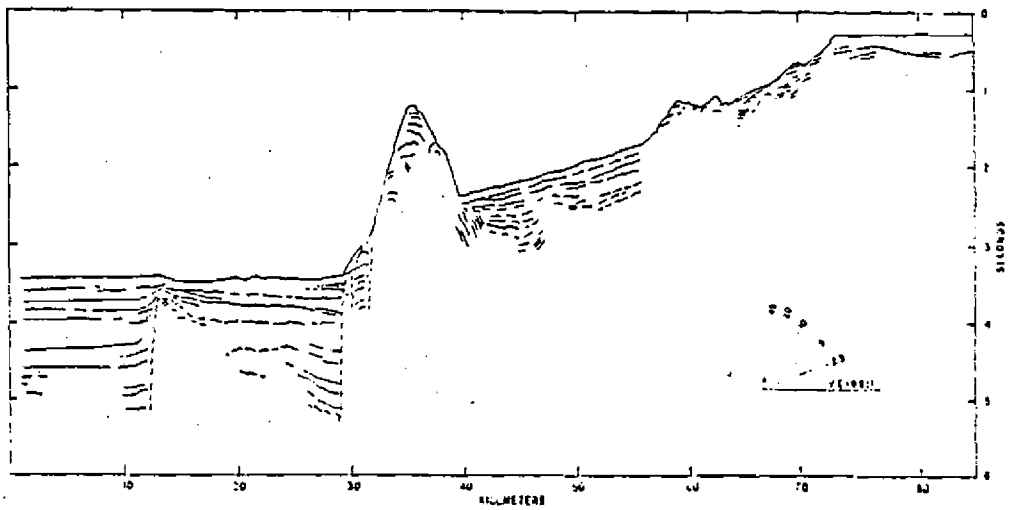


FIGURE 8 — Profile A. The continental margin west of Dixon Entrance is atypical of that farther south. The slope is more regular, and the gradient gentler. The 1650-m hill or seamount at the base of the slope is probably almost circular in plan.

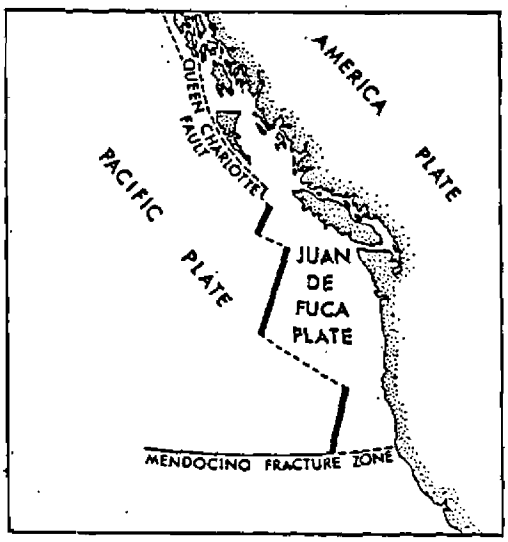


FIGURE 9 — Schematic illustration of crustal plates in the Northeast Pacific area. A triple junction must occur near 50°50'N, 130°30'W if the Queen Charlotte fault continues south along the continental margin. In southeast Alaska, the fault may bifurcate, with the western leg joining the Fairweather fault system, the eastern leg connecting to the Denali fault. The boundary between the American and Juan de Fuca plates is not defined.

may occur under the slope. Transmission of stress across the fault surfaces remains a problem.

More information is required before the origin of the trough can be explained unequivocally.

OCEAN-FLOOR SEDIMENTATION WEST OF QUEEN CHARLOTTE ISLANDS

Large quantities of sedimentary material, presumed to be mainly detritus from glaciers terminating in Queen Charlotte Sound, are found in basins at the foot of the slope off northern Vancouver Island (Tiffin, *et al.*, in prep.), fans at the foot of the slope north of the Dellwood area, and over the deep-sea areas to the west, carried and distributed there by deep sea channels such as Moresby and Scott channels (Mammerickx and Taylor, 1971). Such fans and channels are absent west of the Queen Charlotte Islands, and sedimentary cover is relatively thin despite the proximity of the continent. It is thought that the Queen Charlotte Islands formed a barrier which prevented deposition of sediment in the area immediately southwest during the Pleistocene. However, if the paleomagnetic ages quoted by Atwater and Menard (1970) for the ocean floor west of Queen Charlotte trough are correct, a minimum rate of sedimentation of 18 cm/thousand years has obtained since the formation of the basement. High rates of sediment accumulation appear to be general for the ocean floor in the area. Rates of accumulation in the basins to the south must be considerably greater. If the rate of displacement on the Queen Charlotte fault has been 5 cm/yr, sediments deposited during Pleistocene time across the fault at the base of the continental slope west of Queen Charlotte Sound should now have been moved 25 to 50 km northwestward. This displacement would bring them against the base of the slope west of the Queen Charlotte Islands. They may now form the isolated hills and ridges indicated by bathymetric charts in the area off the southern tip of the Queen Charlotte Islands (Mammerickx and Taylor, 1971), and associated with minor gravity lows and lack of magnetic expression. Further seismic information over these features will aid in verifying this interpretation.

SUMMARY

The continental margin west of the Queen Charlotte Islands differs from most other continental margins by possessing neither a continental rise nor a deep oceanic trench. Instead, crust of typical deep oceanic type extends right to the foot of the continental slope. The lack of a continental rise evidences the youth of the continental margin, also indicated by the age of the magnetic anomalies in the ocean to the west. The lack of trench indicates that little or no subduction has taken place at the margin, at least in the past few million years. Deformation associated with the Queen Charlotte fault zone extends from the western margin of the Queen Charlotte trough to the continental shelf and possibly in places into the Queen Charlotte Islands themselves. The fault zone under the continental slope, which at depth must lie in crystalline rocks, is veneered by sedimentary material folded and faulted with variable intensity. No crystalline rocks were recovered from the fault-zone except glacially transported boulders, a layer of which appears to blanket the upper continental slope where crystalline outcrops are most likely to occur. The oldest sedimentary rocks recovered are of Lower Pliocene age. Whereas in the north the Queen Charlotte fault-zone is coincident with the continental margin, south of the Islands it is to the west of the margin, and may terminate in the area of the Dellwood Knolls (51°N, 130°30'W). The

Queen Charlotte Islands appear to have shielded the adjacent ocean floor at the foot of the continental slope from the accumulation of large quantities of sedimentary material during the Pleistocene.

ACKNOWLEDGMENTS

The authors thank the Masters, scientific parties and crews of the Canadian Scientific Ships *Hudson* and *Parizeau*, who were responsible for collecting the data on which this study is based, and B. E. B. Cameron, of the Geological Survey of Canada, for prompt examination and identification of the microfaunas of the dredged samples.

The work was supported by grants from the Defense Research Board and National Research Council of Canada, and from the following oil companies: Imperial Oil Limited, Gulf Oil Canada Limited and Chevron Standard Limited, all of Calgary, Alberta.

REFERENCES

Atwater, T., 1970. Implications of plate tectonics for the Cenozoic tectonic evolution of Western North America. Geol. Soc. Am. Bull. 81, p. 3513-3536.

Atwater, T. and Menard, H. W., 1970. Magnetic lineations in the northeast Pacific. Earth and Planet. Sci. Lett., 7, p. 445-450.

Couch, R. W., 1969. Gravity and structures of the crust and subcrust west of Washington and British Columbia. Ph.D. dissertation, Oregon State Univ., Corvallis.

Dehlinger, P., Couch, R. W., McManus, D. A., and Gemperle, M., 1971. Northeast Pacific Structure. *In* Maxwell, A. E. (*Editor*), The Sea, 4, pt. 2, p. 133-189.

Hayes, J. D. (*Editor*), 1970. Geological investigations of the North Pacific. Geol. Soc. Am., Mem. 126, p. 323

Hodgson, J. H., and Milne, W. G., 1951. Direction of faulting in certain earthquakes of the North Pacific. Bull. Seis. Soc. Am., 41, p. 221.

Mammerickx, J., and Taylor, I. L., 1971. Bathymetry of the Pioneer Survey area north of 45°N Latitude. Geol. Data Cent., Scripps Inst. of Oceanogr., Spec. Chart Number 1.

McManus, D. A., 1967. Physiography of Cobb and Gorda Rise, Northeast Pacific Ocean. Bull. Geol. Soc. Am., 78, p. 527-546.

Molnar, P., and Sykes, L. R., 1969. Tectonics of the Caribbean and Middle America regions from focal mechanism and seismicity. Geol. Soc. Am. Bull., 80, p. 1639-1684.

Srivastava, S. P., Chase, R. L., Davis, E. E., Keen, C. E., Lister. C. R. B., Manchester, K. S., Shih, K. G., Thomlinson, A. G., and Tiffin, D. L. 1971. Preliminary analysis of geophysical measurements north of Juan de Fuca Ridge. Can. J. Earth Sci.

St. Amand, P., 1957. Geological and geophysical synthesis of the tectonics of portions of British Columbia, the Yukon Territory, and Alaska. Bull. Geol. Soc. Am., 68, p. 1343.

Sutherland-Brown, A., 1968. Geology of the Queen Charlotte Islands, British Columbia. B.C. Dept. Mines and Petr. Res., Bull. 54, p. 225.

Tiffin, D. L., Cameron, B. E. B., and Murray, J. W., (In Prep.). Tectonics and depositional history of the Continental Margin off Vancouver Island, British Columbia.

Tobin, D. G., and Sykes, L. R., 1968. Seismicity and tectonics of the northeast Pacific Ocean. J. Geophys. Res. 73, p. 3821-3845.

Wilson, J. T., 1965. Transform faults, oceanic ridges, and magnetic anomalies southwest of Vancouver Island. Science, 150, p. 482-485.

[*From* IBIS, 114 (1972): 245–251]

SUMMER DISTRIBUTION OF PELAGIC BIRDS OFF THE COAST OF ARGENTINA

FRED COOKE & ERIC L. MILLS

Received on 10 January 1971

In 1969–70 the Canadian Government Research Vessel CSS 'Hudson' made an oceanographic cruise around the Americas. On several stages of the journey bird watches were carried out on a regular basis. This paper reports on the birds seen between the mouth of the Rio de la Plata (37° 36′ S, 56° 54′ W) and the eastern entrance of the Straits of Magellan (52° 24′ S, 67° 12′ W) from 23 until 26 January 1970 and on the birds seen east of Tierra del Fuego on 21 February 1970 (Fig. 1).

Summer observations for this area of the South Atlantic Ocean are scarce in the literature. Captain Cook on his first voyage, 1768–71, passed close to the mouth of the

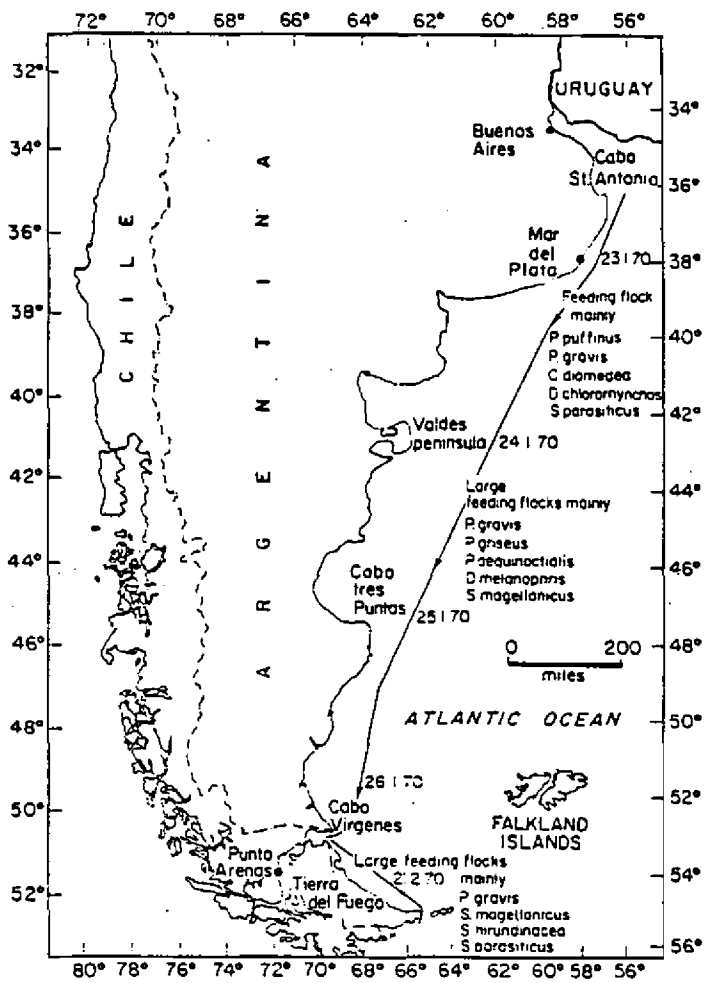


FIGURE 1. Track of CSS 'Hudson' off coast of Argentina, with main sea-bird concentrations January–February 1970

Rio de la Plata in summer and landed on Tierra del Fuego (Lysaght 1959). Many species of sea-birds were collected off Argentina by his naturalists, Joseph Banks and Daniel Solander. Murphy (1936) gives an extensive account of R. H. Beck's travels in this area in the austral spring of 1914 and 1915. The Norwegian 'Brategg' Expedition of 1947–48 sailed south from Montevideo to the Straits of Magellan en route to Antarctica (Holgersen 1957) and recorded shearwaters and albatrosses south of the Rio de la Plata in November 1947. Olrog (1958) made a voyage from the Rio de la Plata south to 60° S from December 1952 to April 1953. Ozawa (1967) records the summer distributions determined on cruises of a Japanese research vessel and a whaler between 1964 and 1967. Sea-birds of the Rio de la Plata area have recently been considered in detail by Escalante (1970). Many of the older records in the area of the Falkland Current were summarised in chart form by Dabbene (1921–26).

METHODS OF OBSERVATION AND ANALYSIS

Our method of recording was to divide the day into five 3-hour periods, 09.00–11.59, 12.00–14.59, 15.00–17.59, 18.00–20.59 and 21.00–24.00 GMT. These are recorded as time periods A–E respectively in Table 1. During these periods we attempted to watch for at least three-quarters of an hour within each interval. The length of observations varied considerably due to other duties on the ship and so the records have been standardised by tabulating the number of birds seen per hour.

Sightings were made from the house top deck which was approximately 12 m above the sea surface. 8 × 35 and 9 × 50 binoculars were used and all birds seen were identified as accurately as viewing conditions would allow. Many factors can bias data collected in this way and these should be taken into account in interpreting the observations. For instance albatrosses can be seen at much greater distances than storm-petrels. Some birds such as Cape Pigeons *Daption capensis* are positively attracted to ships at sea whereas others such as prions may actively avoid contact. Species such as Giant Petrels *Macronectes giganteus* may follow ships for hours on end, thus making accurate counts difficult. Birds may be differently affected by changing weather conditions, or may be active at different times of day.

In the table all species observed are recorded, together with the approximate latitude, longitude and distances from land at the mid-point of the three-hour period. Sea temperature, wind direction and wind speed are also included.

DISCUSSION OF RESULTS

Two large and important feeding areas were found south from the Rio de la Plata. The first, a few kilometres off the coast south of Mar del Plata, was recorded by Murphy (1936) in describing the travels and collections of R. H. Beck, who in October 1914 found "an extraordinary intermingling of species from opposite ends of the Atlantic Ocean". As might be expected, the species assemblage we recorded from the high summer differed from that reported by Murphy and contained two warm water species (Yellow-nosed Albatross *Diomedea chlororhynchos* and Cory's Shearwater *Calonectris diomedea*) not seen by Beck. It also lacked some southerly species such as Magellanic Penguin *Spheniscus magellanicus*, Royal Albatross *Diomedea epomophora*, Black-browed Albatross *D. melanophris*, Cape Pigeon, Sooty Shearwater *Puffinus griseus* and Wilson's Petrel *Oceanites oceanicus*.

The second feeding area was situated some 200 km east of the Valdés Peninsula. The total number of birds observed per hour was greater than at the more northerly feeding area. Great Shearwaters *Puffinus gravis* and Sooty Shearwaters, White-chinned Petrels *Procellaria aequinoctialis* and Black-browed Albatrosses predominated, and several family groups of Magellanic Penguins were noted.

TABLE 1

Species of sea-birds observed off the coast of Argentina, 23–26 January 1970

(A–E indicate the time periods 09.00–11.59, 12.00–14.59, 15.00–17.59, 18.00–20.59, 21.00–24.00 GMT. The figure in a time period for each species is number of birds per hour.)

Date	23 January 1970					24 January 1970					25 January 1970					26 January 1970		
Time	A	B	C	D	E	A	B	C	D	E	A	B	C	D	E	A	B	Total
Eudyptes crestatus																	0·5	1
Spheniscus magellanicus									0·9	26·4	6·7	12·8	4·0	3·3	2·5	0·8	0·5	79
Penguin sp.																	1·0	2
Diomedea exulans or *D. epomophora*				0·6				1·3	1·8		3·9				0·6	0·8		12
Diomedea melanophris					0·6	4·8	11·5	10·7	54·6	14·7	15·5	11·2	14·7	3·3	2·5	0·8	3·5	197
Diomedea chlororhynchos	1·4	2·2	21·3	1·2														69
Diomedea sp.			0·4	0·6	0·6		0·5	0·4			1·0				1·3		0·5	9
Macronectes giganteus	0·7	0·4	0·4		0·6	4·2	1·9	2·2	0·9	3·1	2·9	3·2	2·7	1·1	2·5	1·6	1·0	46
Pachyptila sp.																16·3	19·0	58
Procellaria aequinoctialis			0·4	0·61	2·3	8·5	21·6	15·5	122·2	19·0	2·9	6·4	4·0		1·3	0·8	0·5	283
Calonectris diomedea	57·9	6·9	0·4															184
Puffinus gravis			31·1	29·0	12·6	21·2	45·2	44·9	588·9	82·8	13·6	10·4	6·7	44·7	11·4	0·8	0·5	1251
Puffinus griseus					0·6		9·1	7·1	94·4	20·2		0·8					1·0	174
Puffinus puffinus			64·0	1·8	0·6										4·4			182
Storm petrel sp.						0·5												1
Pelecanoides sp.																27·6	2·5	30
Stercorarius parasiticus		1·45	32·6		3·4	0·5		0·4	1·8		5·8	0·8		1·1	47·5	0·8		185
Jaeger sp.	0·3	0·7	41·6				0·5	0·4				0·8		9·8	29·7			73
Stercorarius skua				0·61				0·4						1·1	1·3			5
Larus dominicanus	0·3	6·9	11·2														0·5	51
Sterna hirundinacea																	2·0	4
No. hours per session	2·83	2·75	2·60	1·62	1·75	1·88	2·08	2·25	1·08	1·63	1·03	1·25	0·75	0·92	1·58	1·23	2·00	
No. species per session	5	5	8	6	7	6	6	8	8	6	7	7	5	6	10	9	10	5
No. individuals per session	172	51	543	56	37	75	188	188	935	271	54	58	24	59	166	62	66	3005
No. individuals per hour	60·8	18·5	203·4	34·6	21·1	39·9	90·4	83·6	865·7	166·3	52·4	46·4	32·0	64·1	105·1	50·4	33	
Latitude S	37·7	38·1	38·8	39·2	39·8	42·2	42·9	43·6	44·2	44·7	47·0	47·5	48·2	48·8	49·4	51·0	52·4	
Longitude W	57·0	57·2	57·8	58·2	58·7	60·2	60·6	61·2	61·6	62·2	63·7	64·3	65·1	65·6	65·7	66·9	67·2	
Kilometres from shore	11	19	32	60	112	250	210	200	200	250	145	105	56	72	145	80	16	
Sea temp. at surface (°C)	20·9	20·7	20·3	19·9	19·5	17·7	17·3	16·8	16·4	16·2	14·8	15·0	15·8	15·9	15·1	12·7	12·1	
Wind direction	200				90	60		110		160	300		220		320		260	
Wind speed in knots	6				6	25		20		20	15		5		13		15	

Both feeding areas are closely linked to the oceanography of continental shelf waters east of Argentina. Thomsen (1962) and Mandelli & Orlando (1966) state that subantarctic water of the Falkland Current (Corriente de Malvinas) characteristically has temperatures of 4°–14°C and salinities between 33·7 and 34·15‰. This water typically occurs on the outer part of the continental shelf, usually to a depth of about 200 m, and occasionally extends much closer to shore, coming in close contact with warmer and less saline water (" coastal water ") of uncertain origin.

Water hugging the coast from the Valdés Peninsula to north of Mar del Plata has salinities from 33·7–33·8‰ (characteristic of Falkland Current water) but elevated temperatures in the range 18°–20°C (charts in Aragno 1968). At the surface this water mass is separated from cold, dense saline offshore water of the Falkland Current by a tongue of lower salinity (33·5–33·6‰) extending northeast up the middle of the continental shelf. This is underlain by cold, dense water of the Falkland Current, extending landward over the continental shelf to a depth of less than 50 m (see sections of salinity and sigma-t in Aragno 1968).

Only prolonged northerly or westerly winds (characteristic of this area in summer) are necessary to cause coastal upwelling of the bottom water, which could be rapidly warmed without much salinity change. Thus the " coastal water " we encountered off Mar del Plata probably originated from deeper Falkland Current water by upwelling and warming. Its relatively high phosphate levels (0·6–0·9 μg At/l) compared to the less saline surface water to seaward (0·1 μg At/l) indicate that biological productivity will be enhanced there, accounting for both the established fishery and large number of birds just off Mar del Plata.

Farther south, east of the Valdés Peninsula, our records of large numbers of birds coincide with the 14° C isotherm and relatively high levels of nitrate (3–11 μg At/l), phosphate (0·4–1·0 μg At/l) and chlorophyll a (1·0–1·7 mg/m^3) (Aragno 1968) compared to other points on the ship's track. Thus, although the Valdés Peninsula is a noted sea-bird colony, we saw outstanding aggregations of sea-birds only along the nutrient-rich landward edge of the Falkland Current. Although the sections and horizontal distributions shown by Aragno (1968) do not extend much east of this area, they suggest an area of even higher productivity east of our points of observation and large numbers of birds will probably be found there eventually, between approximately 42°–45° S and 57°–60° W.

A third and even more extensive feeding area was observed on 21 February as the ' Hudson ' was steaming northwest along the east coast of Tierra del Fuego. This was located approximately at 52° 54′ S, 67° 30′ W. The predominant birds in this area were Great Shearwaters, Magellanic and Rockhopper Penguins *Eudyptes crestatus*, South American Terns *Sterna hirundinacea*, Parasitic Jaegers *Stercorarius parasiticus* and King Cormorants *Phalacrocorax albiventer*. We do not have any oceanographic information available which could help explain the presence of so many birds in this area, but it seems likely that coastal upwelling was the physical process responsible for the presence of food.

Two obvious discontinuities occurred in the transect. The first was around latitude 39° S, marking our first contact with the landward edge of unmodified water of the Falkland Current. North of this latitude Yellow-nosed Albatross and Cory's Shearwater predominated; southward Black-browed Albatrosses, Greater, Sooty and Manx Shearwaters *Puffinus puffinus*, White-chinned Petrels and Magellanic Penguins were found. The second discontinuity occurred around latitude 50° S and was marked by the appearance of prions *Pachyptila* sp. and diving petrels *Pelecanoides* sp. It is not clear whether their occurrence is related to some oceanographic feature or if we recorded only the northward extreme of range from breeding colonies in the Falkland Islands. South American Terns appeared at this latitude also and it seems likely that their presence was related to the proximity of the Argentine mainland, roughly 90 km to the west of our track.

From our data there is no evidence for a general increase in the abundance of sea-birds as one travels south; however, of the three feeding areas described above the most northerly one had fewest birds and the most southerly the greatest number. Proximity to land clearly influences the distribution of the Kelp Gull *Larus dominicanus* and the South American Tern which on this and other sections of the cruise were not observed further than 40 km from shore. The absence of Manx Shearwaters and paucity of jaegers on 24 January when the ship was more than 160 km from land could be attributed to the distance from land or our proximity to offshore water of the Falkland Current.

Also significant in this transect is the absence of many species which might have been expected in the South Atlantic at this season. Cape Pigeon, Southern Fulmar *Fulmarus glacialoides*, Soft-plumaged Petrel *Pterodroma mollis*, Schlegel's Petrel *Pterodroma incerta* and Pediunker *Adamaster cinereus* were not observed during this phase of the cruise. Their absence is hard to understand, since one might expect that some non-breeding adults would stay in the winter range of these antarctic or subantarctic pelagic species. Holgersen (1957) noted similar absences during the ' Brategg ' Expedition so they must be a regular feature of the southern summer off Argentina.

The distribution of some of the tubenoses is worthy of special comment.

The Black-browed Albatross was the common albatross south of 39° S in or near the edge of the Falkland Current waters. In contrast the Yellow-nosed Albatross was seen only in the warmer water north of 39° S. The lack of overlap in range between these two species was striking on our transect and is in contrast to the intermingling between the Black-browed and Grey-headed Albatross *Diomedea chrysostoma* which we observed in the Drake Passage.

Since Cory's Shearwater is not mentioned in Olrog's ' Las aves Argentinas ', which covers the South Atlantic between latitudes 35° S and 68° S and longitudes 25° W and 74° W, and is considered occasional or uncertain by Escalante (1970), a more detailed description of this sight record should be given. 184 individuals were seen and many of these came close to the ship giving us excellent opportunities of observing the salient field marks. The shape was that of a typical shearwater, slightly larger than the Great Shearwater. The upper parts were grey-brown, the under-parts and under-wings white. The dark upper part of the head gradually merged into the white throat and chin. Most birds had no rump mark but occasional birds had a pale line at the base of the tail. Some birds also had whitish flecks on the upper surface of the wings. Bill apparently dark, legs pinkish. Flight similar to but more ponderous than that of the Great Shearwater.

This species was replaced by the Great Shearwater south of latitude 39° S, when the ship was very close to or in Falkland Current waters. Only one Cory's Shearwater was seen south of the first sighting of the Great Shearwater. Wynne-Edwards (1935) points out that in the North Atlantic the northern limit of the Cory's Shearwater more or less coincides with the southern limit of the Great Shearwater during the northern hemisphere summer, and off southern New England Cory's Shearwater, common over warmer water in the edge of the Gulf Stream, is replaced by the Great Shearwater over colder shelf waters (Mills, pers. obs.). Captain D. Stam has recorded the species north of Montevideo as far west as 33° S, 49·5° W (Bourne 1970). Our sightings represent, therefore, an extension of the known winter range of this species, which also includes waters off the southern tip of Africa (Van Oort & Kruijt 1953, Bourne 1955, 1970).

The Great Shearwater was much the commonest bird on this section of the cruise. It was seen from 38° 48′ S to 53° 12′ S, but was not recorded in the Drake Passage. Three birds were seen in Chilean waters west of the entrance of the Straits of Magellan, southwest of Punta Dungeness, although Johnson (1965) does not list the species for Chile. Why so many birds of this species should be present in the breeding season so far (*c.* 4,800 km) from the major nesting grounds in the Tristan da Cunha Archipelago is a

puzzle. R. W. Woods (1970) notes that it is one of the most numerous species on the route between Montevideo and the Falkland Islands in the southern summer.

The Manx Shearwater was found in large flocks off Mar del Plata and encountered again in groups of ones and twos at around latitude 49° 24′ S, which is ten degrees of latitude farther south than its southern limit as described in the A.O.U. Checklist (1957).

ACKNOWLEDGMENTS

Our presence on part of ' Hudson 70 ', the round-the-Americas cruise of CSS ' Hudson ', was supported by grants from the National Research Council of Canada, School of Graduate Studies, Queen's University, and Faculty of Graduate Studies, Dalhousie University. We are grateful to Dr W. R. P. Bourne for his helpful comments on an early draft of this paper.

SUMMARY

Eighteen species of sea-birds were observed from CSS ' Hudson ' in the South Atlantic between the Rio de la Plata and Tierra del Fuego in late January and late February 1970. Major feeding areas were noted off Mar del Plata, the Valdés Peninsula and Tierra del Fuego, Argentina, the first two in rich modified or unmodified water of the subantarctic Falkland Current, associated with upwelling. The southernmost area had most birds, the northernmost fewest. A temperate-latitude assemblage including Yellow-nosed Albatross and Cory's Shearwater occurred off Mar del Plata in warmed water of subantarctic (Falkland Current) origin. South of 39° S these two species were replaced by Black-browed Albatross and Great Shearwater in cold offshore water of the Falkland Current. Off the Valdés Peninsula Black-browed Albatross, Great and Sooty Shearwaters, White-chinned Petrels and family groups of Magellanic Penguins occurred near the edge of highly-productive water of the Falkland Current. The largest feeding area, east of Tierra del Fuego, had Magellanic and Rockhopper Penguins, Great Shearwaters, King Cormorants, South American Terns and jaegers, but no oceanographic information is available. At 50° S prions and diving petrels appeared for the first time, marking a possible oceanographic discontinuity or proximity to colonies on the Falkland Islands. Several common species of the South Atlantic were not seen on the transect including Cape Pigeon, Southern Fulmar, Soft-plumaged Petrel, Schlegel's Petrel and Pediunker. Kelp Gull, South American Tern, Manx Shearwater and jaegers were rare or absent far from land. New southern limits for the western South Atlantic Ocean were established for Cory's and Manx Shearwaters, and the Great Shearwater was observed for the first time in Chilean waters.

REFERENCES

A.O.U. CHECKLIST, 5th ed. 1957. Baltimore, Maryland: American Ornithologists Union.

ARAGNO, F. J. (Ed.) 1968. Datos y resultados de las campañas pesqueria " Pesqueria III " (20 de febrero al 20 de marzo de 1967). Mar del Plata, Argentina: Publicaciones del Projecto de Desarrollo Pesquero (Serie Informes Técnicos) No. 10/111.

BOURNE, W. R. P. 1955. On the status and appearance of the races of Cory's Shearwater *Procellaria diomedea*. Ibis 97 : 145–149.

BOURNE, W. R. P. 1970. Observations of seabirds. Sea Swallow 20 : 47–54.

DABBENE, R. 1921–26. Los petreles y los albatros del Atlántico austral. El Hornero 2 : 157–179, 241–254; 3 : 1–33, 125–158, 227–238, 311–348.

DE SCHAUENSEE, R. M. 1966. The species of birds of South America with their distribution. Narberth, Penn.: Livingston Publishing Co.

ESCALANTE, R. 1970. Aves marinas del Rio de la Plata y aguas vecinas del Océano Atlántico. Montevideo: Barreiro y Ramos S. A.

HOLGERSEN, H. 1957. Ornithology of the " Brategg " Expedition. Scientific Results of the " Brategg " Expedition 1947–48, No. 4. Bergen.

JOHNSON, A. W. 1965. The birds of Chile and adjacent regions of Argentina, Bolivia and Peru. Vol. 1. Buenos Aires: Platt Establicimientos Gráficos S. A.

LYSAGHT, A. 1959. Some eighteenth century bird paintings in the library of Sir Joseph Banks (1743–1820). Bull. Br. Mus. nat. Hist. (Hist. ser.) 1 (6) : 251–371.

MANDELLI, E. F. & ORLANDO, A. M. 1966. La produccion orgánica primaria y las caracteristicas físico-químicas de la Corriente de Malvinas. Boletin del Servicio de Hidrografía Naval (Buenos Aires) 3 : 185–196.

MURPHY, R. C. 1936. Oceanic birds of South America. New York: Am. Mus. nat. Hist.

OLROG, C. C. 1958. Observaciones sobre la avifauna antarctica y del alta mar desde el Rio de la Plata hasta los 60° de latitud sur. Acta zool. Lilloana 15 : 19–30.

OLROG, C. C. 1959. Las aves Argentinas. Tucuman: Universidad Nacional de Tucuman, Instituto " Miguel Lillo ".

OZAWA, K. 1967. Distribution of sea birds in austral summer season in the Southern Ocean. Antarctic Rec. 29 : 1–36.

THOMSEN, H. 1962. Masas de agua caracteristicas del océano Atlántico (parte sudoeste). Pub. H. 632, Serv. Hidrog. Naval, Buenos Aires.
VAN OORDT, G. J. & KRUIJT, J. P. 1953. On the pelagic distribution of some Procellariiformes in the Atlantic and Southern Oceans. Ibis 95 : 615–637.
WOODS, R. W. 1970. Great Shearwater *Puffinus gravis* breeding in the Falkland Islands. Ibis 112 : 259–260.
WYNNE-EDWARDS, V. C. 1935. On the habits and distribution of the birds of the North Atlantic. Proc. Boston Soc. nat. Hist. 40 : 233–340.

Dr Fred Cooke, Dept. of Biology, Queen's University, Kingston, Ontario, Canada

Dr Eric L. Mills, Dept. of Oceanography, Dalhousie University, Halifax, Nova Scotia, Canada

Automatic Analysis at Sea

ARTHUR R. COOTE, IVER W. DUEDALL and RAYMOND S. HILTZ

Recently, the Canadian Government Oceanographic Research Ship HUDSON completed an extensive eleven month cruise after circumnavigating the Americas. During the Atlantic, Antarctic and Pacific portions of this cruise, and in the Chilean Fjords, simultaneous determinations of silicate, phosphate and nitrate were made using a Technicon® AutoAnalyzer.® For a 7-month period the equipment and methods were employed continuously. Measurements of analytical precision were obtained and from comparisons of our results with marine nutrient standards (5) the accuracy of the methods has been assessed.

Instruments and Methods

Automatic analysis is being used at sea increasingly and many methods for the determination of a variety of constituents are available (2-6). Fig. 1 shows the flow diagram for the simultaneous determination of 3 nutrients: silicate, phosphate and nitrate. The distinguishing features are the large industrial sampler, a pump II and 50 mm flowcells.

Silicate Method

Details of the method are described in Technicon #1-116. The method makes use of the reduction of the silicomolybdate complex to molybdenum blue with stannous chloride. Tartaric acid is used to suppress the phosphate complex. Measurement is made at a wave length of 820 mμ in 50 mm flowcells using a range expander setting of 1. The detection range of the method is 0-180 μg at Si/l.

Phosphate Method

The method used was improvised at sea, after the intended method #I 36-69W was discovered to be extremely sensitive to silicate. The change was effected by converting the ascorbic acid line of that method (#I 36-69W) to stannous chloride (0.5 ml stock diluted to 200 ml with 10% HCl). Measurement was made at a wave length of 660 mμ in a 50 mm flowcell using a range expander setting of 2. The detection range of the method is 0-4 μg at PO_4/l.

Nitrate plus Nitrite

Details of the method are described in Technicon #43-69W. The method is based on the reduction of nitrate to nitrite in a copperized cadmium column followed by diazotization and coupling to form an azo dye. The measurement is carried out at a wave length of 520 mμ in a 50 mm flowcell using a range expander setting of 1. The detection range of the method is 0-50 μg at NO_3/l.

CSK Marine Nutrient Standards

Under the joint sponsorship of the Science Council of Japan and the Intergovernmental Oceanographic Commission, UNESCO, standards for marine nutrient analysis have been prepared by Sugawara (1) at the Sagami Chemical Research Center. These standards are prepared from purified materials using carefully selected techniques including final sterilization of the samples. They were used as received and required a minimum of handling. Their concentrations are known (1) with a precision of 2.6% (S.D.) or less for phosphate and 0.5% (S.D.) or less for silicate.

Sampling and Storage of Samples

Samples for nutrients were drawn from Teflon-coated Knudsen bottles used on the oceanographic casts. Typically, three casts were required at deep stations. The nutrient samples were the last to be drawn. Twenty-five ml of sea water were drawn into plastic test tubes and a few drops of chloroform were added prior to storage in a refrigerator until needed.

Plastic test tubes, made from B & D syringe barrels, were used after the discovery that silicate was dissolving from the Kimax test tubes. These plastic tubes were more of a problem to clean than glass tubes.

It was found that cleaning after each use with chromic acid was satisfactory. Iodine solution, available from the oxygen reagents, was used for

Presented at the Technicon International Congress, November 2-4, 1970, in New York, New York, by Arthur R. Coote, M.Sc., Atlantic Oceanographic Laboratory, Iver W. Duedall, M.Sc., Marine Ecology Laboratory, Raymond S. Hiltz, Atlantic Oceanographic Laboratory, Bedford Institute, Dartmouth, Nova Scotia, Canada. A Bedford Institute – Contribution No. 217.

Litho in U.S.A.

sterilizing the larger plastic bottles which contained synthetic sea water.

Standardization Procedure and Data Handling

Calibrations, using composite standards, were made before and after each main sample run. Low, medium and high standards were prepared by diluting aliquots of stock solutions with synthetic sea water or sea water of low nutrient content, such as Sargasso sea water.

Blanks containing the synthetic sea water were interspersed with regular samples at intervals of 10 or 15 samples. This provided sufficient indication of baseline drift.

Peak heights and baseline values were read from the charts and the nutrient concentrations were calculated according to the method given by Strickland and Parsons (6) for the logarithmic unit.

$$\text{Logarithmic unit} = \log \frac{100R - 100 + b}{100R - 100 + n}$$

where R = range expansion setting used, b = baseline in %T and n = peak height in %T. (%T = Percent Transmittance.) Changes in the calibration, before and after, were linearly interpolated among the intervening samples. Composite standards contained the following ratios of Si to P to N: the low range, 4:1:8; the medium range, 40:2:16; and the high range, 120:4:28.

Results and Discussion

A number of difficulties were encountered with the methods and are mentioned here as they may continue to prove pitfalls for the inexperienced. While these problems might be considered minor when ashore it should always be kept in mind that even the most minor problems can have very serious consequences when they occur aboard ship. The more important of these difficulties were: (a) production of gas within the Cd-Cu reduction column; (b) fouling of synthetic sea water by mold-like growths; (c) dissolution of silicate from the walls of the Kimax glass test tubes; (d) interference from silicate in the phosphate method #I 36-69W that was used initially.

Gas bubbles appeared in an older Cd-Cu reduction column, presumably due to the production of hydrogen. While this did not visibly interfere with photometer output the disruption of the column was a nuisance. Fresh columns did not give this trouble. After an initial breaking-in period of 8 hours, the nitrate reduction columns lasted for weeks.

The growth of molds in the synthetic sea water wash solution stored in bottles and in some of the tubing lines is an important continuing problem, especially in tropical regions. Replacement of certain tubing lines, such as the tartaric acid line, and sterilization of bottles and tubes with either

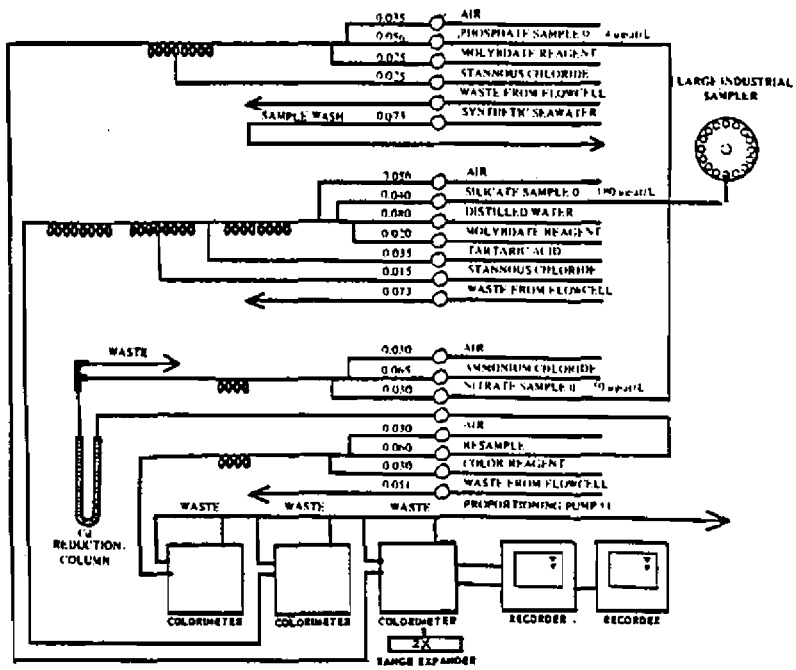


Figure 1

chromic acid or iodine is required frequently. Sea water, low in nutrients, such as that from the Sargasso, is most suitable for blanks and wash. The preparation of sea water for blanks by the method of Kuenzler *et al* (7) should be useful. Our experience does not include a full test of this method but certainly nominally low nutrient synthetic sea water produces growths, perhaps from nutrient absorbed into the plastic or from reagents. Mold can be removed by filtering the sea water.

Sea water stored in Kimax glass test tubes picked up appreciable silicate from the glass. Storage of 25 ml of sea water in a glass test tube for 48 hours resulted in an increase of 20 μg at/l of silicate. Plastic tubes were used after this was discovered. For the most exact work, it may be necessary to store the silicate samples in plastic containers and to store phosphate and nitrate samples in glass containers.

The phosphate method, #I 36-69W, suffered seriously from silicate interference. This feature of the method has been explained by Grasshoff (3) as resulting from omission of the antimony from the ascorbic acid reducing solution. However, at the time of the departure of the CSS HUDSON, we were unaware of this. A satisfactory phosphate determination was improvised using stannous chloride as reductant in place of the ascorbic acid.

Precision and Accuracy of Silicate and Phosphate Data

Statistical data of several types have been obtained: (a) relative or self-consistent data provided by the standards run before and after each set of samples; (b) data obtained from duplicates taken from the same Knudsen bottles; (c) data from the duplication of overlapping casts; and (d) data derived from comparisons with CSK marine nutrient standards.

Table I shows the precisions derived from standardizations. These data show the basic reliability of the method: for silicate this ranges from 9% coefficient of variation at the 4 μg at/l level to 0.5% at 120 μg at/l; and for phosphate the range is 2.6% at the 1 μg at/l level to 0.9% at the 4 μg at/l level. Table II lists the precisions obtained with duplicates taken from individual Knudsen bottles. The values of 0.8% for silicate at greater than 100 μg at/l and 1.5% for phosphate at 1-2 μg at/l show only a slight drop-off from those of Table I.

Table III illustrates the agreement found between the same samples run about 12 hours apart. A slight fall-off in precision, perhaps due to storage, is evident.

Table IV contains data obtained by running CSK (1) marine silicate and phosphate as samples. The agreement is good for silicate, about -0.6%, but in the case of phosphate it is poorer, about 6%

Table I. Estimates of Precision Derived from Standardizations.

Silicate				Phosphate			
Concentration μg at Si/l	n*	Std. Dev. μg at/l	Coeff. Varn. %	Concentration μg at P/l	n	Std. Dev. μg at P/l	Coeff. Varn. %
4	74×(3)	0.31	9	1	44×(3)	0.026	2.6
40	74×(3)	0.37	0.9	2	44×(3)	0.018	0.9
120	57×(3)	0.56	0.5	4	44×(3)	0.036	0.9

*n = number of replicate determinations

Table II. Estimates of Precision Derived from Duplicate Samples on Each Oceanographic Cast.

Silicate				Phosphate			
Concentration μg at Si/l	n*	Std. Dev. μg at/l	Coeff. Varn. %	Concentration μg at P/l	n*	Std. Dev. μg at/l	Coeff. Varn. %
25-50	28×(2)	0.61	1.6				
50-100	11×(2)	0.66	0.9	1-2	47×(2)	0.021	1.5
> 100	20×(2)	0.84	0.8				

*n = number of replicate determinations

Table III. Precision Derived from Redetermining Samples After a 12-Hour Time Lapse.

Nom. Depth (metres)	Silicate µg at Si/l Run #1	Run #2	Δ_{2-1}	Phosphate µg at P/l Run #1	Run #2	Δ_{1-2}
0	–	–	–	–	–	–
10	–	–	–	–	–	–
50	1.15	0.94	0.21	–	–	–
100	1.08	1.01	0.07	–	–	–
200	1.60	1.4	0.20	–	–	–
300	2.50	2.4	0.10	0.24	0.23	0.01
400	4.02	4.00	0.02	0.48	0.49	-0.01
500	6.29	6.20	0.09	0.75	0.71	0.04
600	11.7	11.6	0.10	1.15	1.14	0.01
700	17.3	16.9	0.40	1.44	1.44	0
800	22.8	22.5	0.30	1.58	1.56	0.02
A900	29.4	29.3	0.10	1.75	1.73	0.02
B900	29.1	29.3	-0.20	1.75	1.73	0.02
1000	38.5	38.3	0.20	1.82	1.81	0.01
1200	53.5	53.7	-0.20	1.95	1.94	0.01
1600	55.5	55.3	0.20	1.56	1.55	0.01

Table IV. Results of Comparisons Made With CSK Standards for Silicate and Phosphate.

Silicate µg at/l				Phosphate µg at/l			
Reputed	Found	Δ_{F-R}	%	Reputed	Found	Δ_{F-R}	%
10.0	10.1	+0.1	+1	0.496	0.49	-0.006	- 1
10.0	10.1	+0.1	+1	0.496	0.50	+0.004	+ 1
10.0	9.86	-0.14	-1	0.496	0.46	-0.036	- 7
10.0	9.52	-0.48	-5	0.496	0.45	-0.046	- 9
25.0	25.3	+0.3	+1	0.996	1.04	+0.044	+ 5
25.0	25.3	+0.3	+1	0.996	0.90	-0.096	-10
50.0	51.8	+1.8	+4	0.996	0.93	-0.066	- 7
100.0	102.1	+2.1	+2	0.996	0.87	-0.126	-13
100.0	102.1	+2.1	+2	0.996	0.89	-0.106	-11
				1.992	1.70	-0.292	-15
			Av = +0.6	1.992	1.92	-0.072	- 4
				1.992	1.89	-0.102	- 5
				1.992	1.82	-0.172	- 9
				1.992	1.82	-0.172	- 9
				2.988	2.92	-0.068	- 2
				2.988	2.93	-0.058	- 2
				2.988	2.94	-0.048	- 2
				2.988	2.92	-0.068	- 2
				2.988	2.74	-0.248	- 8
				2.988	2.74	-0.248	- 8
CSK nitrate standards were not available for use during the cruise.						Av =	- 6
						Std. Dev. =	4

below the reputed value. This difference in performance appears to be real and may indicate either some small hidden flaw in the method for phosphate which was not optimized or a problem of contamination. This has not been investigated.

Fig. 2 is presented to illustrate further the overall reproducibility. Solid dots and triangles show the data obtained from two casts which overlapped. In addition to the factors influencing precision, already mentioned, it shows the agree-

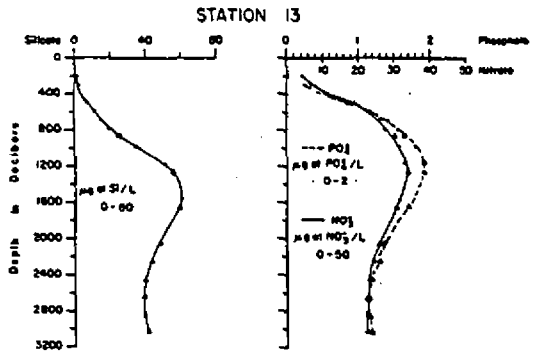


Figure 2

ment between samples taken from casts made several hours apart in time and several miles apart in space.

Fig. 3 is a silicate section along 30° W longitude compiled from data which are still preliminary. It is presented to illustrate how nutrient distributions may follow the general pattern of oceanic circulation. The main features of this distribution are the high silicate concentrations in the Antarctic bottom water which descends from the surface south of the Antarctic convergence. At mid-depths the presence of North Atlantic Deep water containing a silicate minimum is indicated. Above this is the Antarctic Intermediate water containing a silicate maximum. These broad features of the circulation in the South Atlantic have been known (8) and are further substantiated in this work. It is hoped that a closer examination of the silicate and other nutrient distributions may expose more details of the circulation.

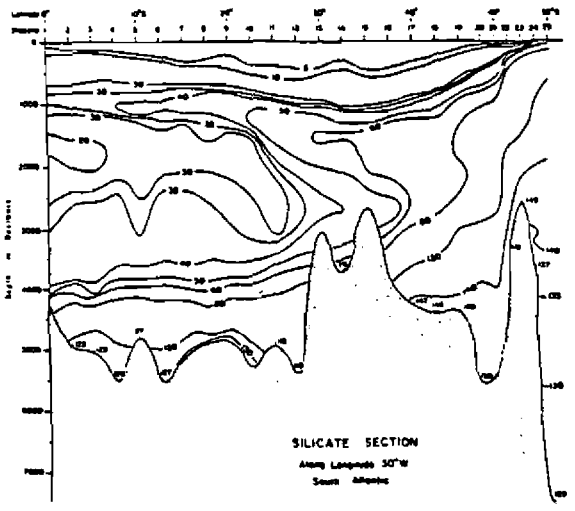


Figure 3

The special nature of many of the problems associated with the performance of chemical analyses in sea-going laboratories has been discussed by several (2,9) investigators. Not the least of all the problems arises from the ship's motion and its effect on equipment and the analyst. A second problem, or set of problems, results from the isolation of the ship from the usual sources of supply and maintenance. Breakdowns that on land would be considered minor often lead to the complete failure of a program at sea. In addition, space on board ship is severely restricted. However, equipment such as the Technicon AutoAnalyzer, which was originally intended for clinical use, has demonstrated its ability to satisfy most of these requirements. The AutoAnalyzer is able to work long hours, week after week, and makes possible the routine determination of many chemical constituents with a precision heretofore almost unattainable at sea. In doing so it raises the problem of data handling which will probably require further automation. But that is another problem.

References

1. Sugawara, K., On the preparation of CSK standards for marine nutrient analysis, Chemistry Working Group, Sub-Committee for CSK, Sagami Chemical Research Center, Japan, 1969.
2. Grasshoff, K., Automatic determination of fluoride, phosphate and silicate in sea water, Automation in Analytical Chemistry, Technicon International Symposium, London, 1965, pp. 304-307.
3. Grasshoff, K., A simultaneous multiple channel system for nutrient analysis in sea water with analog and digital data record, automation in analytical chemistry, Technicon International Congress, Chicago, 1969, pp. 133-145.
4. Brewer, P. G., and Riley, J.P., The automatic determination of silicate-silicon in natural waters with special reference to sea water, *Anal. Chim. Acta, 35*: 514-519, 1966.
5. Armstrong, F. A. J., Stearns, C. R., and Strickland, J. D. H., The measurement of upwelling and subsequent biological processes by means of the Technicon Auto-Analyzer and associated equipment, *Deep Sea Res., 15*: 381-389, 1967.
6. Strickland, J. D. H., and Parsons, T. R., *A Practical Handbook of Sea Water Analysis*, Bulletin 167, Fisheries Research of Canada.
7. Kuenzler, E. J., Guillard, R. R. L., and Corwin, N., Phosphate-free sea water for reagent blanks in chemical analysis, *Deep Sea Res., 10*:749, 1963.
8. Deacon, G. E. R., The hydrology of the southern ocean, *Discovery Reports, 15*:1-124, 1937.
9. Andersen, N. R., Automated nutrient analysis in oceanography, *Oceanology, 5(9)*:26-28, 1970.

Deep-Sea Research, 1973, Vol. 20, pp. 579 to 581. Pergamon Press. Printed in Great Britain.

SHORTER CONTRIBUTION

A correction to CIRCE silicate values for the South Atlantic; comparison with HUDSON-70 silicates

A. R. COOTE.* C. R. MANN,* A. WALTON* and J. M. EDMOND†

(*Received* 3 *October* 1972; *in revised form* 7 *December* 1972; *accepted* 14 *December* 1972)

Abstract—A re-examination of the AutoAnalyzer silicate method used on the HUDSON-70 Expedition and of the calculations of silicate values for the Atlantic section of the CIRCE Expedition has shown that the silicate values reported by CIRCE for the South Atlantic were about 50% too low, due to a calculation error involving the standard. While re-examining the AutoAnalyzer procedures, differences of up to 10% in silicate content were found between sodium metasilicate and sodium fluorosilicate solutions that had been prepared in synthetic sea water. The sodium fluorosilicate solutions agreed with CSK International Standards, as had sodium metasilicate solutions prepared in real sea water during the Pacific leg of HUDSON-70.

SOME TIME ago it was found that silicate concentrations for the South Atlantic, as measured on the HUDSON-70 Expedition, disagreed with results obtained during leg 9 of the CIRCE Expedition (EDMOND and ANDERSON, 1971), abroad R. V. *Argo*. Where the two cruise tracks intersected in the vicinity of HUDSON-70 Sta. 3 and *Argo* Sta. 246, at about 5°S and 30°W, the HUDSON-70 silicate values were a factor of 2 higher than the CIRCE data reported by Edmond and Anderson. Both sets of data did, however, show extrema (maxima and minima) at the same depth, which could be related to the water mass structure of the South Atlantic. To resolve the difference, a re-examination of the procedures used on both expeditions, by AutoAnalyzer on HUDSON-70 (COOTE, DUEDALL and HILTZ, 1970) and by manual method on the CIRCE Expedition (EDMOND and ANDERSON, 1971), was therefore undertaken. Library samples of pre-weighed sodium metasilicate had been retained from HUDSON-70 and were re-examined by comparison with several classes of silicate standards prepared in-house. A number of CSK International Standards (SUGAWARA, 1969) were also examined. The AutoAnalyzer methods used to make these comparisons have been described by COOTE, DUEDALL and HILTZ (1970).

Table 1 contains some of the results obtained while re-examining the HUDSON-70 procedures. Table 2 shows all the silicate values we obtained for CSK International Standards (SUGAWARA, 1969) during the Pacific leg of HUDSON-70 and during the intercomparison tests. In Fig. 1, corrected CIRCE and uncorrected HUDSON silicate data are plotted as a function of potential temperature and are in good agreement after correction. The results of Table 1 indicate that variations in the nature of the standards may introduce as much as 10% uncertainty in the accuracy of the results. However, where accuracy has been tested using CSK International Standards (SUGAWARA, 1969) (Table 2), the agreement has been excellent.

On the basis of the results presented in Tables 1 and 2, it was evident that the HUDSON-70 results were not in error by 50%. The original data for the CIRCE Expedition was then re-examined and it was found that for CIRCE legs 8 and 9 in the South Atlantic (EDMOND and ANDERSON, 1971), the silicates had been incorrectly calculated on the basis of an erroneously assumed value for the amount of sodium fluorosilicate used to prepare the silicate standards; the strength of the standard had been changed between the Pacific and Atlantic portions of the expedition. Thus, a correction factor of 2·05 must be applied to the silicate values obtained for the South Atlantic by EDMOND and ANDERSON (1971).

*Atlantic Oceanographic Laboratory, Marine Sciences Directorate, Department of the Environment, Canada.

†Massachusetts Institute of Technology, Cambridge, Massachusetts, U.S.A.

Table 1. *Comparison of in-house silicate solutions.*

Reputed silicate concentrations of in-house calibration standards	4·0 μg atoms Si/l.	40·0 μg atoms Si/l.	100·0 μg atoms Si/l.	*Relative percentage silicate**
Measured silicate concentrations of solution I (sodium metasilicate)	3·3 3·2	36·4 36·2	89·6 89·4	90
Measured silicate concentrations of solution II (fused quartz)	3·6 3·4	37·8 38·2	95·4 95·3	95
Measured silicate concentrations of CSK standards			99·8 99·7	100

*Percentage of silicate relative to sodium fluorosilicate standard, solution III used to calibrate the AutoAnalyzer in September, 1971: diluted with synthetic sea water (STRICKLAND and PARSONS, 1968).

The HUDSON-70 Atlantic silicates were calibrated using sodium metasilicate prepared in synthetic sea water, and may be subject to a correction of up to 10%. However, there is sufficient uncertainty in the experimental significance of the data that this correction will not be made until we are fully convinced of its validity and usefulness. As already mentioned, the small differences that exist between corrected CIRCE data and HUDSON data near 5°S, 30°W (Fig. 1) seems reasonable for such an intercomparison involving silicates and may, in large part, be real. Our data do, however, indicate the desirability of using sodium fluorosilicate, prepared in-house, as a secondary standard and that the primary standardization be based on CSK or some similar set of standards.

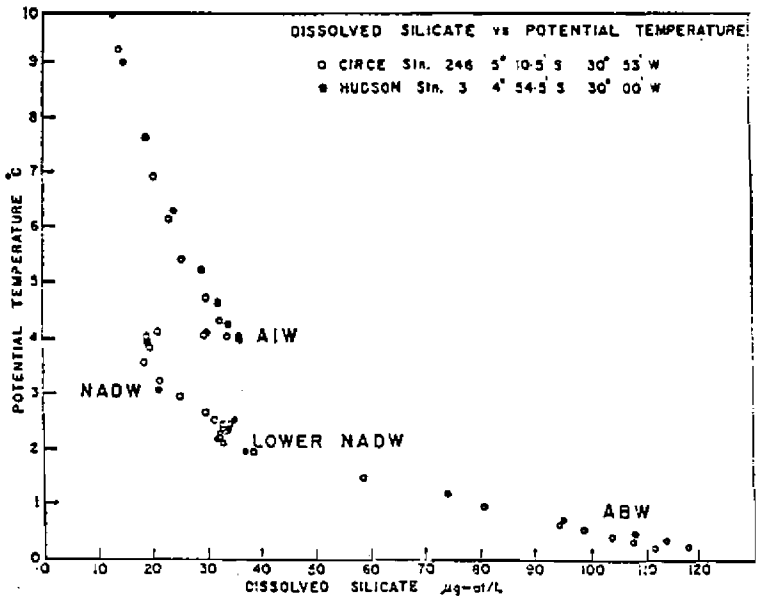


Fig. 1. Dissolved silicate versus potential temperature for CIRCE Sta. 246 and HUDSON Sta. 3 in the Equatorial Atlantic. The dissolved silicates from CIRCE have been multiplied by 2·05. AIW=Antarctic Intermediate Water, NADW=North Atlantic Deep Water, ABW=Antarctic Bottom Water.

Table 2. Comparison of CSK International Standard solutions.

Reputed concentrations of CSK standards	µg atoms Si/l.							
	0	5·0	10·0	25·0	50·0	100·0	150·0	200·0
Concentrations found during Pacific leg of HUDSON-70*	0·5		9·94 9·99 9·87 9·49	25·2 24·8	51·5 51·4	102·3 102·1		
Concentrations found during tests, September, 1971†		5·2 5·2	10·0 10·0		50·0 49·9	99·8 99·7	149·9 150·2	201·0 200·8

*Calibrated using sodium metasilicate during HUDSON-70: diluted with filtered Sargasso Sea water.

†Calibrated using sodium fluorosilicate: diluted with synthetic sea water.

Acknowledgements—The assistance of Mr. IVER DUEDALL and Mr. RAY HILTZ in carrying out silicate measurements during HUDSON-70 and at Bedford Institute of Oceanography is gratefully acknowledged. We also thank Dr. C. S. WONG for obtaining the CSK Standards that were used during HUDSON-70.

REFERENCES

COOTE A. R., I. W. DUEDALL and R. S. HILTZ (1970) Automatic analysis at sea. In: *Advances in Automated Analysis*, Vol. 2, *Industrial Analysis*, Technicon International Congress, Thurman Assoc. Publ., pp. 347–351.

EDMOND J. M. and G. C. ANDERSON (1971) On the structure of the North Atlantic Deep Water. *Deep-Sea Res.*, **18**, 127–134.

STRICKLAND J. D. H. and T. R. PARSONS (1968) A practical handbook of seawater analysis. *Bull. Fish. Res. Bd Can.*, **167**, 311 pp.

SUGAWARA K. (1969) On the preparation of CSK standards for marine nutrient analysis. Scientific Committee on Oceanographic Research. ICSU Intergovernmental Oceanographic Commission, UNESCO. Chemistry Working Group Sub-Committee for CSK. National Committee on Oceanographic Research. Science Council of Japan, Tokyo. 56 pp.

Vol. 87, No. 32, pp. 351–380 22 October 1974

PROCEEDINGS
OF THE
BIOLOGICAL SOCIETY OF WASHINGTON

PELAGIC OSTRACODS COLLECTED ON HUDSON 70 BETWEEN THE EQUATOR AND 55°S IN THE ATLANTIC

By Georgiana B. Deevey
Florida State Museum, University of Florida, Gainesville, Florida 32611

Zooplankton samples were collected in the South Atlantic on the first two legs of the CSS HUDSON 70 Expedition. Between the equator and 55°S, samples were obtained routinely along the 30°W Longitude parallel (Fig. 1). The first leg of the expedition left Halifax in mid-November 1969 and arrived at Rio de Janeiro in mid-December. The second leg left Rio on December 20th, proceeded down the 30°W Longitude parallel to 55°S, then passed northeast of South Georgia and up the 40°W Longitude parallel to 47°S, crossed the Argentine Basin to the Rio Plata and arrived in Buenos Aires in mid-January, 1970. Between the equator and 25°S, zooplankton samples were collected for the micropaleontology program by vertical tows, 200–0 m, with a ½ meter net of No. 8 mesh. South of 27°30′S, hauls were made with ¾ m nets of No. 6 mesh to varying depths with up to 4,000 m of cable out, and the 200–0 m vertical tows were also obtained.

Some 70 species of pelagic ostracods were recorded, of which two belong to the family Cypridinidae and the rest to the family Halocyprididae. Since many species of ostracods are bathypelagic, only 33 species were found in the 200–0 m tows collected between the equator and 25°S. Eight species (*Conchoecia acuminata, C. allotherium, C. atlantica, C. concentrica, C. echinata, C. inermis, C. incisa* and *C. stigmatica*) were not noted south of 16°S. Six more species (*C. ctenophora, C. echinulata, C. microprocera, C. macrocheira, C. parthenoda*

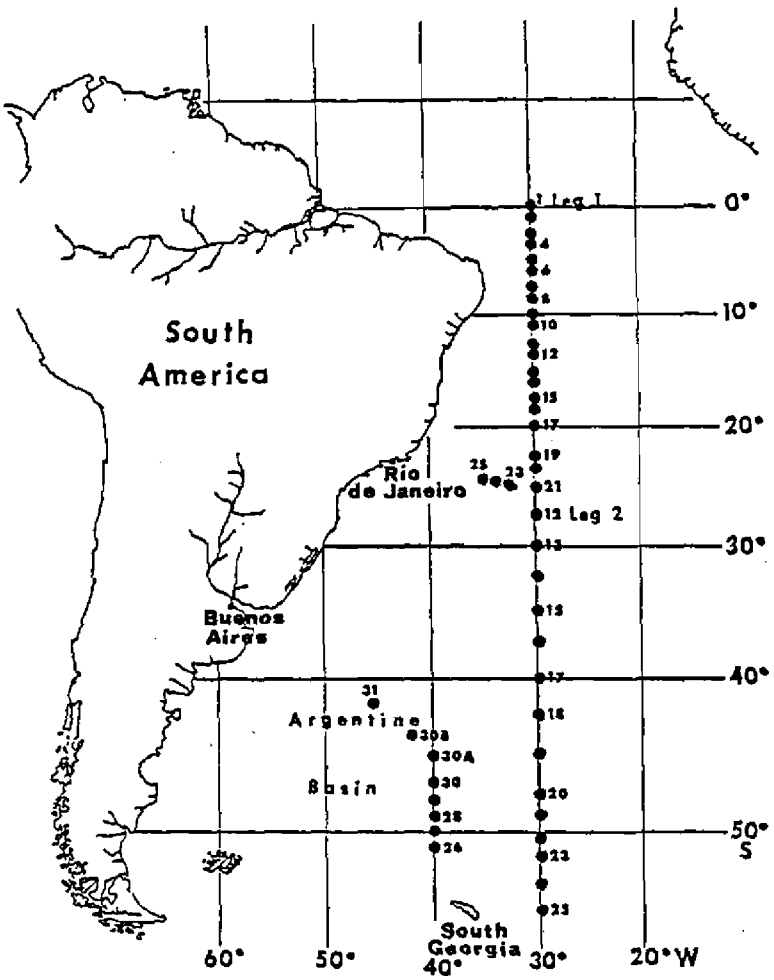


FIG. 1. Map of zooplankton station locations for Legs 1 and 2 of HUDSON 70.

and *C. pseudoparthenoda*) did not occur south of 30°S. Between 30°S and 40°S, 42 species were recorded, half of which were not noted south of the subtropical convergence. Between the subtropical and subantartic convergences, around 42°S–49°S, 27 species were present in the samples, although 9 of these were not found south of 45°S. South of the subantarctic convergence 18 species occurred between 50°S and 55°S. Two

TABLE 1. Station data, Leg 1, Halifax to Rio de Janeiro. 200–0 m vertical tows.

Station	Date	Latitude	Longitude	Time of day	No. species
1	XI/30/69	0°02′N	29°58.3′W	10.40 AM	12
2	XI/30	0°51′S	30°W	9.00 PM	21
3	XII/1	2°29′S	30°W	10.20 AM	18
4	XII/1	3°32′S	30°07′W	10.00 PM	16
5	XII/2	4°55′S	30°W	10.20 AM	16
6	XII/2	6°04′S	30°W	10.15 PM	18
7	XII/3	7°27′S	30°03′W	10.20 AM	14
8	XII/3	8°30.8′S	30°W	10.20 PM	14
9	XII/4	9°59′S	30°W	10.30 AM	11
10	XII/4	10°59′S	29°59′W	10.00 PM	16
11	XII/5	12°26′S	30°07′W	10.00 AM	10
12	XII/5	13°29′S	30°W	10.30 PM	16
13	XII/6	14°55′S	30°07′W	10.30 AM	7
14	XII/6	15°47′S	29°59′W	10.15 PM	13
15	XII/7	17°32′S	30°W	1.30 PM	8
16	XII/7	18°19.5′S	30°04′W	10.50 PM	11
17	XII/8	20°S	30°W	8.15 AM	10
18	XII/8	20°02.6′S	30°31.3′W	Midnight	17
19	XII/9	22°30.2′S	29°58′W	2.15 PM	9
20	XII/9	23°21′S	29°55′W	9.45 PM	19
21	XII/10	25°S	30°W	8.30 AM	14
22	XII/10	24°52.5′S	30°08′W	8.15 PM	15
23	XII/11	24°37′S	32°30.6′W	8.15 AM	12
24	XII/11	24°17.3′S	32°44′W	9.00 PM	16
25	XII/12	24°13.4′S	35°W	7.15 AM	15

species, *C. isocheira* and *C. belgicae*, were found only south of the subantarctic convergence. The total number of species recorded therefore decreased markedly between the subtropical and subantarctic convergences. HUDSON 70 specimens extend the southward ranges in the Atlantic for 27 species, some by only a few degrees. The northward range was extended for two species, *C. belgicae* and *C. major* (= *C. plactolycos major*). *C. plactolycos* (= *C. plactolycos plactolycos*), described from the Indian Ocean, is now known from the Atlantic. A few species, such as *C. elegans* and *C. skogsbergi*, increased in size farther south. Larger forms began

TABLE 2. Station data, Leg 2, Rio de Janeiro to Buenos Aires.

Station	Date	Latitude	Longitude	Total M of cable	No. species
12	XII/23/69	27°31.6′S	30°07′W	450	18
13	XII/24	30°00′S	29°59′W	1400	32
14	XII/25	30°25.05′S	30°10.5′W	1500	30
15	XII/26	35°00′S	30°04.7′W	1800	36
16	XII/27	37°28′S	29°59.2′W	2500	30
17	XII/28	39°55′S	29°53′W	2500	30
18	XII/29	42°30′S	29°57.5′W	2500	24
19	XII/30	45°07.3′S	29°59′W	2500	15
20	XII/31	47°35′S	29°53.4′W	2500	9
21	I/1/70	49°03.4′S	29°48.7′W	2500	14
22	I/2	50°33.3′S	29°35.4′W	2500	12
23	I/3	52°04′S	30°04′W	2500	7
24	I/4	53°27′S	29°59.5′W	2500	6
25	I/5	54°55′S	29°23′W	2500	11
26	I/8	51°28′S	39°57′W	3000	14
27	I/8	49°59′S	39°58′W	1000	9
28	I/9	48°59′S	39°52.4′W	500	6
29	I/10	47°59′S	39°59.6′W	400	7
30	I/10	47°03′S	40°04.6′W	3000	13
30A	I/11	45°10.6′S	41°10.8′W	4000	16
30B	I/12	44°12.4′S	42°46′W	4000	25
31	I/13	41°46.5′S	46°26.4′W	2500	31

to appear in the region of the subtropical convergence, but the increase in size was gradual; two distinct size ranges for a species were not noted.

The station data for Legs 1 and 2 are given in Tables 1 and 2. Table 2 shows the decrease in numbers of species/station south of the subtropical convergence, and the increase in numbers of species as the ship proceeded north over the Argentine Basin. Table 3 lists the species of ostracods, together with the stations from which they were recorded and their overall latitudinal distribution. All specimens have been deposited in the Florida State Museum.

I am indebted to Gordon Riley, Director of the Institute of Oceanography at Dalhousie University, for arranging for my travel between Halifax and South America, to C. R. Mann

TABLE 3. The species of ostracods, their station records and latitudinal distribution.

Species	Stations	Latitudinal distribution
Gigantocypris müllerl	Leg 2: 16, 18, 19, 22, 24, 30A	37°28′S–53°27′S
Macrocypridina castanea	Leg 2: 13, 15	30°S–35°S
Fellia cornuta dispar	Leg 2: 13–19, 30B	30°S–45°S
Halocypria globosa	Leg 1: 18, 20–25; Leg 2: 12–16, 18, 30A, 31	20°S–45°S
Halocypris brevirostris	Leg 1: 2–25; Leg 2: 12–19, 21, 31	0°–49°S
Archiconchoecia cucullata	Leg 2: 13–17, 22, 30B	30°S–50°33′S
A. striata	Leg 1: 2–4, 6–8, 10–25; Leg 2: 12–16, 31	0°–41°45′S
Conchoecia acuminata	Leg 1: 3–6	2°26′S–6°S
C. acuticosta	Leg 2: 14–19, 30B, 31	32°25′S–45°S
C. aequiseta	Leg 2: 13–16, 31	30°S–42°S
C. allotherium	Leg 1: 2–14	0°51′S–15°42′S
C. amblyopostha	Leg 2: 13–17, 30, 31	30°S–47°S
C. ametra	Leg 2: 13–17, 30B, 31	30°S–44°S
C. atlantica	Leg 1: 2, 3, 5–7	0°51′S–7°27′S
C. belgicae	Leg 2: 25, 26	51°28′S–55°S
C. bispinosa	Leg 1: 2, 4, 6, 8, 10, 12, 14, 16, 18, 20, 22, 24, 25; Leg 2: 12–17, 31	0°–42°S
C. borealis antipoda	Leg 2: 15, 17–28, 30–31	35°S–55°S
C. brachyaskos	Leg 2: 16–18, 21–23, 25–27, 30A–31	37°28′S–55°S
C. chuni	Leg 2: 14–22, 25, 27–31	32°25′S–55°S
C. concentrica	Leg 1: 2	0°51′S
C. ctenophora	Leg 2: 13	30°S
C. curta	Leg 1: 1–12, 14, 16–18, 20, 21, 23–25; Leg 2: 12–15	0°–35°S

TABLE 3. Continued.

Species	Stations	Latitudinal distribution
C. daphnoides	Leg 1: 5, 20; Leg 2: 12–17, 31	5°S–42°S
C. dichotoma	Leg 2: 18	42°30'S
C. echinata	Leg 1: 1–6, 10, 18	0°–20°S
C. echinulata	Leg 1: 10, 14, 20, 22, 24, 25; Leg 2: 12, 13	11°S–30°S
C. edentata	Leg 1: 20; Leg 2: 17, 18, 25	23°19'S–55°S
C. elegans	Leg 1: 1–9, 15, 17, 20–25; Leg 2: 13–23, 25–31	0°–55°S
C. gaussae	Leg 2: 14, 26	32°25'S–51°28'S
C. glandulosa	Leg 2: 30B	44°S
C. haddoni	Leg 2: 15–19, 21, 26, 30–31	35°S–51°28'S
C. hettacra	Leg 2: 21–30B	49°S–55°S
C. hirsuta	Leg 2: 15, 30B, 31	35°S–44°S
C. hyalophyllum	Leg 1: 6; Leg 2: 12–18, 31	6°S–42°30'S
C. imbricata	Leg 1: 16, 24; Leg 2: 12–17	18°S–40°S
C. incisa	Leg 1: 4	3°40'S
C. inermis	Leg 1: 12	13°30'S
C. isocheira	Leg 2: 21, 22, 24–26	49°S–55°S
C. kyrtophora	Leg 2: 17	40°S
C. lophura	Leg 2: 13–17, 19, 30B, 31	30°S–45°S
C. loricata loricata	Leg 2: 15	35°S
C. macrocheira	Leg 1: 2; Leg 2: 12	0°–27°32'S
C. macromma	Leg 2: 30B	44°S
C. magna	Leg 1: 1–14, 16–18, 20–25; Leg 2: 12–18, 31	0°–42°S
C. major (= C. plactolycos major)	Leg 2: 21, 23–26, 30, 30B	44°S–55°S

TABLE 3. Continued.

Species	Stations	Latitudinal distribution
C. mamillata	Leg 2: 13–16, 30B, 31	30°S–44°S
C. microprocera	Leg 1: 2, 3, 9, 10, 12, 15, 17, 18, 20–25	0°–25°S
C. nasotuberculata	Leg 1: 2–4, 6, 8, 10, 14, 24; Leg 2: 13, 14, 17, 18, 31	0°–42°30'S
C. oblonga	Leg 1: 1–14, 16–25; Leg 2: 12–16, 31	0°–42°S
C. obtusata antarctica	Leg 2: 7–22, 26–31	40°S–51°28'S
C. parthenoda	Leg 1: 1–3, 9–15, 17, 19–25; Leg 2: 12, 13	0°–30°S
C. parvidentata	Leg 2: 15–20, 29–31	35°S–48°S
C. plactolycos	Leg 2: 30B, 31	42°S–44°S
C. plinthina	Leg 2: 18	42°30'S
C. porrecta	Leg 1: 1–6, 8, 10–25; Leg 2: 12, 13, 15, 16	0°–37°28'S
C. procera	Leg 1: 1–14, 16, 18–25; Leg 2: 12–15, 17	0°–40°S
C. pseudoparthenoda	Leg : 1–3, 5–7, 10; Leg 2: 12, 13	0°–30°S
C. rotundata	Leg 1: 2–9, 12, 15, 17–25; Leg 2: 12–15	0°–35°S
C. secernenda	Leg 1: 8, 12; Leg 2: 12	8°31'S–27°30'S
C. serrulata	Leg 2: 17–22, 26–31	40°S–51°30'S
C. skogsbergi	Leg 2: 13–27, 30–31	30°S–55°S
C. spinifera	Leg 1: 2, 12, 18, 20, 22; Leg 2: 13–17, 31	0°–42°S
C. spinirostris	Leg 1: 1–25; Leg 2: 12–17, 31	0°–42°S
C. stigmatica	Leg 1: 1, 3, 5, 7–9	0°–10°S
C. subarcuata	Leg 1: 8, 10, 12, 14, 18, 25; Leg 2: 13–16	8°31'S–37°28'S
C. symmetrica	Leg 2: 15–23, 25–27, 30–31	35°S–55°S
C. teretivalvata	Leg 1: 5; Leg 2: 13–21, 29–31	5°S–49°S
C. valdiviae	Leg 2: 14, 15, 17, 18, 30A–31	32°25'S–45°S

and R. J. Conover of the Bedford Institute of Oceanography for inviting me to participate on Leg 2 of HUDSON 70, and to G. Vilks for permission to examine the ostracods in the 200–0 m vertical tows. This work was partially supported by grants GB-15575 and GA-36512 from the National Science Foundation.

THE SPECIES OF OSTRACODS

Suborder CYPRIDINIFORMES Skogsberg

Family CYPRIDINIDAE Dana

Gigantocypris muelleri Skogsberg. One gravid female, 19.9 mm long, and 7 juvenile specimens were taken in hauls with 2,500 m of cable out, between 37°30'S and 53°30'S.

Distribution: 63°38'N–62°S in the Atlantic.

Macrocypridina castanea (Brady) s. str. One female 5.9 mm long and a female 6.2 mm long were found at 30°S and 35°S. Poulsen (1962) designated the Indo-Pacific form as *M. castanea rotunda*.

Distribution: 56°N–35°S in the Atlantic.

Suborder HALOCYPRIFORMES Skogsberg

Family HALOCYPRIDIDAE Dana

Subfamily ARCHICONCHOECINAE Poulsen

Archiconchoecia cucullata (Brady). A number of specimens were taken in tows with 750–4000 m of cable out, between 30°S and 50°30'S.

Distribution: 52°N–50°30'S in the Atlantic; Indian Ocean. These specimens extend the southward range.

A. striata Müller. This tiny species was common in the 200–0 m hauls taken between the equator and 25°S and was present to 37°30'S, 30°W and at about 42°S in the Argentine Basin; it did not occur south of the subtropical convergence.

Distribution: 36°N–42°S in Atlantic; Indian and Pacific Oceans and Mediterranean. These specimens extend the southward range.

Subfamily HALOCYPRINAE Poulsen

Halocypria globosa Claus. *H. globosa* occurred from 20°S–42°S, 30°W, and in the Argentine Basin between 42°S and 45°S. Females were caught at shallow depths, but males (Fig. 2h) were taken only in samples collected with 750–2500 m of cable out.

Distribution: 64°N–37°S in the Atlantic; Pacific and Indian Oceans. These specimens extend the range south to 45°S.

Halocypris brevirostris (Dana). This species was present in all 200–0 m tows obtained between the equator and 25°S, and was found down to 49°S, extending the southward range in the Atlantic. Between the

equator and 32°30'S, adult specimens were 1.15–1.25 mm long. Females up to 1.45 mm long appeared at 35°S; between 37°30'S and 42°30'S females were 1.5–1.6 mm long.

Distribution: 60°N–49°S in the Atlantic; Pacific and Indian Oceans.

Fellia cornuta dispar (Müller). Müller (1906a) described two subspecies of *F. cornuta*, the typical form, *F. cornuta typica* (1906a) = *F. cornuta cornuta* (1912), which has a sharp horn on each side of the shoulder vaults (Fig. 2a), and *F. cornuta dispar* for some southern hemisphere males which lacked these projections and had rounded shoulder vaults. Both Müller and Poulsen (1969a) recorded only males as lacking the sharp horns. Müller's specimens were found south of 29°S in the Atlantic and Indian Oceans, and Poulsen's south of 30°S in the Pacific off New Zealand. The typical horned form has been recorded from around 20°N–38°S in the Atlantic, around the equator in the Indian Ocean and Indo-Pacific regions, and from around 30°N–45°S in the Pacific. Both males and females, lacking the sharp lateral processes, were found between 30°S and 45°S, in hauls with 1100–2500 m of cable out; no typical forms were taken. Juvenile specimens 1.30–1.45 mm long (Fig. 2f) had small lateral points on the shoulder vaults, not as large and curved as in the typical form (Fig. 2a). Specimens 2.0–2.1 mm long had either no points or very tiny points (Fig. 2g). Mature males 2.9–3.1 mm long (Fig. 2d, e) and females 3.00–3.35 mm long (Fig. 2b, c) had completely rounded shoulder vaults. This subspecies can therefore be distinguished from the typical form in the juvenile stages.

Distribution: 29°S–45°S in the Atlantic; south of 29°S in Pacific and Indian Oceans.

Subfamily Conchoecinae Poulsen

Most Halocyprids belong to the genus *Conchoecia*, for which over 90 species have been described. Müller's (1906a) system of grouping species together into more or less natural groups of related forms will be followed here.

Spinifera Group Müller

C. spinifera Müller. This species was recorded from the equator to 40°S, 30°W and at about 42°S in the Argentine Basin, extending the recorded southward range. It did not occur south of the subtropical convergence.

Distribution: 52°N–42°S in the Atlantic; Indian and Pacific Oceans.

C. oblonga (Claus). Müller (1906a) distinguished two forms of this species, Form A in which the right asymmetrical gland opens at the postero-ventral corner, and Form B in which the gland opens just anterior to this location. In the Canary Island region Angel (1969) found Form A at shallower depths than Form B. The two forms were not distinguished in the HUDSON 70 material. *C. oblonga* was found from the equator to 37°S and at about 42°S in the Argentine Basin, extending its southward range.

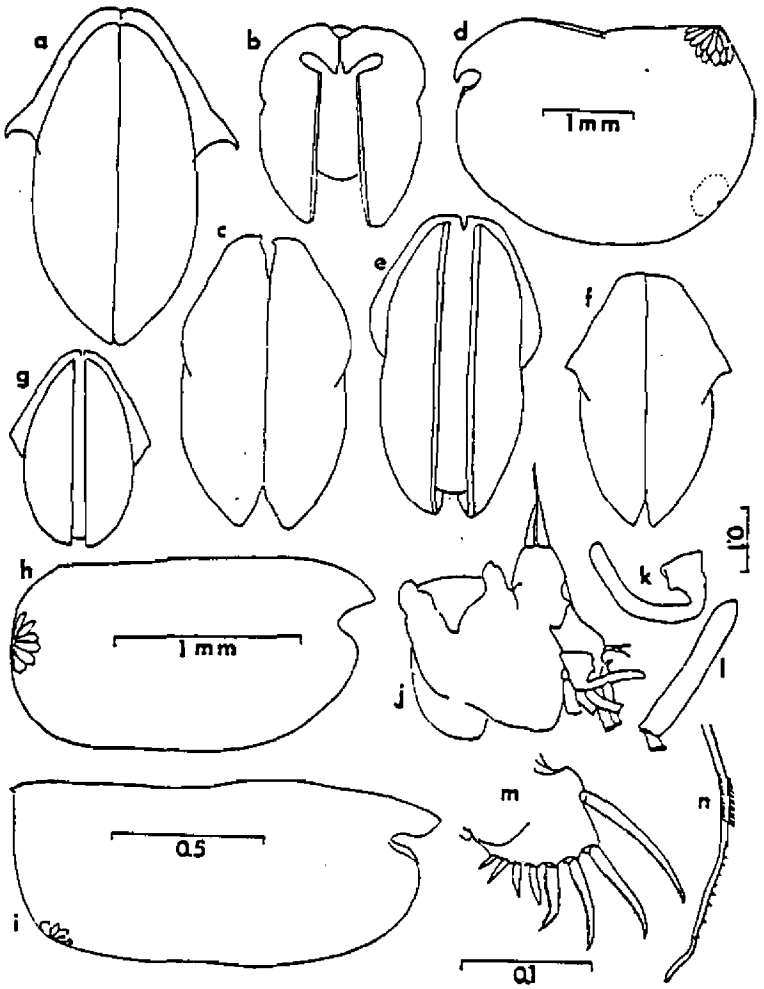


FIG. 2. a, Ventral view of female *Fellia cornuta cornuta* from the Caribbean Sea; b and c, Anterior and dorsal views of female *F. cornuta dispar*; d and e, Lateral and ventral views of male *F. cornuta dispar*; f, Dorsal view of 1.3 mm juvenile; g, Ventral view of 2.0 mm juvenile; h, Lateral view of *Halocypria globosa* male; i, Lateral view of *Conchoecia allotherium* male; j, Endopodite of left second antenna of *C. allotherium* male; k, Right clasper; l, Capitulum of frontal organ; m, Furca; n, Distal part of proximal secondary seta of male first antenna. Scale on b for a–e and g, on h for f and h, on i for i, on right margin for l and m, at bottom for j, k, and n. Scales in mm.

Distribution: 48°N–42°S in Atlantic; Indian and Pacific Oceans.

C. allotherium Müller. Males of this species were taken in two of the 200–0 m tows from 0°51'S and 15°42'S. This species is similar in size and shape to *C. oblonga* Form A (Fig. 2i); also the 4th claw on the furca is curved as in *C. oblonga* (Fig. 2m), and Müller was unable to differentiate the females of the two species. The male is distinguished by a double row of spinules near the tip of the proximal secondary seta (Fig. 2n) of the first antenna, and the frontal organ is bare of spinules (Fig. 2l).

Distribution: 18°N–35°S in Atlantic; 10°N–10°S in Indian Ocean.

C. aequiseta Müller and *C. hirsuta* Müller. Females of these two species are indistinguishable, and males are differentiated only on the basis of long hairs on the distal bristle of the first endopodite joint of the second antenna in *C. hirsuta*. This bristle is bare in *C. aequiseta* males and in females and juveniles of both species. Females and juveniles identified as *C. aequiseta* were found between 30°S and 37°30'S, 30°W; a *C. aequiseta* male was taken at 42°S in the Argentine Basin. *C. hirsuta* males were present in samples from 35°S, 30°W and from 42°S–44°S in the Argentine Basin, so both forms occur south to the region of the subtropical convergence.

Distribution: For *C. aequiseta* 32°N–31°S and for *C. hirsuta* 29°N–35°S in the Atlantic; Indian Ocean. The HUDSON 70 males extend the southward range to 42°S and 44°S, respectively.

C. echinata Müller. This species occurred from the equator to 20°S.

Distribution: 37°N–29°S in Atlantic; Pacific and Indian Oceans.

C. inermis Müller. A single specimen was taken at 13°30'S in a 200–0 m night haul, extending slightly the known southward range.

Distribution: 43°N–13°30'S in Atlantic; Indian Ocean.

C. mamillata Müller. This species was taken in hauls with 1100–4000 m of cable out from 30°S–37°30'S, 30°W, and from 42°S–44°S in the Argentine Basin.

Distribution: 48°N–56°S in the Atlantic; Indian and Pacific Oceans.

Elegans Group Müller

C. elegans Sars. This was one of the commonest species, and occurred from the equator to 55°S. Between the equator and 25°S, males and females were 1.2–1.3 mm long; between 30°S and 40°S larger specimens up to 1.60–1.65 mm long were found; south of 45°S females were 1.5–1.8 mm long and males 1.75–1.85 mm in length.

Distribution: 80°N–55°S in Atlantic; Indian and Pacific Oceans.

Procera Group Müller

C. microprocera Angel. *C. microprocera* was taken at 14 stations between the equator and 25°S in the 200–0 m vertical tows.

Distribution: 32°N–25°S in Atlantic.

C. procera Müller. This species occurred from the equator to 40°S and was not found south of the subtropical convergence.

Distribution: 32°N–40°S in the Atlantic; Mediterranean and Indian Ocean.

C. brachyaskos Müller. *C. brachyaskos* was recorded from 37°30′S to 55°S, 30°W and from 42°S–45°S in the Argentine Basin, from hauls with 1000–4000 m of cable out. Females (Fig. 3a) were 1.5–1.6 mm and males (Fig. 3b) 1.4–1.5 mm long. Although larger than the specimens recorded from the Sargasso Sea (Deevey, 1968), the frontal organs (Fig. 3c, d) and male claspers (Fig. 3f, g) were similar. Also the armature (Fig. 3e) of the male first antenna had no more teeth or spinules than that of the smaller males.

Distribution: 32°N–56°30′S in the Atlantic; Indian and Pacific Oceans.

Acuminata Group Müller

C. acuminata (Claus). This species was taken in only 4 of the 200–0 m tows collected between 2°26′S and 6°S.

Distribution: 46°N–37°S in the Atlantic; Pacific and Indian Oceans.

Obtusata Group Müller

C. obtusata Sars var. *antarctica* Müller. *C. obtusata* is a bipolar species. *C. obtusata antarctica* was found from 40°S to 50°30′S, 30°W and from 42°S to 51°30′S in the Argentine Basin, in hauls with 100–200 m of cable out, as well as the deeper tows. The length range for males (Fig. 3j) was 1.25–1.35 mm and for females (Fig. 3i) 1.65–1.85 mm. The antarctic form differs from the arctic form primarily in the shape of the frontal organs (Fig. 3n, o) and the right male clasper (Fig. 3m) and usually in the shape of the posterior end of the shell. The capitulum of the frontal organs of both males and females is sharply pointed, and the right male clasper is bent at a more acute angle than in the arctic forms. The armature of the principal seta of the male first antenna (Fig. 3p) is apparently similar.

Distribution: 23°S–68°S in Atlantic; 26°S–68°S in the Pacific. *C. obtusata obtusata* occurs chiefly north of 60°N in the Atlantic and Arctic Ocean and at 58°N in the Skager Rak and Cattegat.

Rotundata Group Müller

This group is greatly in need of taxonomic revision. Müller originally included 7 species in this group, which differs from all others in the position of the asymmetrical glands: *C. macromma, C. pusilla major, C. pusilla minor, C. glandulosa, C. kyrtophora, C. nasotuberculata, C. rotundata* and *C. isocheira. C. rotundata* has since been separated into 3 species (Iles, 1953): *C. rotundata, C. skogsbergi* Iles and *C. tereti-valvata* Iles, and Rudyakov (1962) has described *C. abyssalis* from the Pacific. Eleven species were found in the HUDSON 70 samples, in-

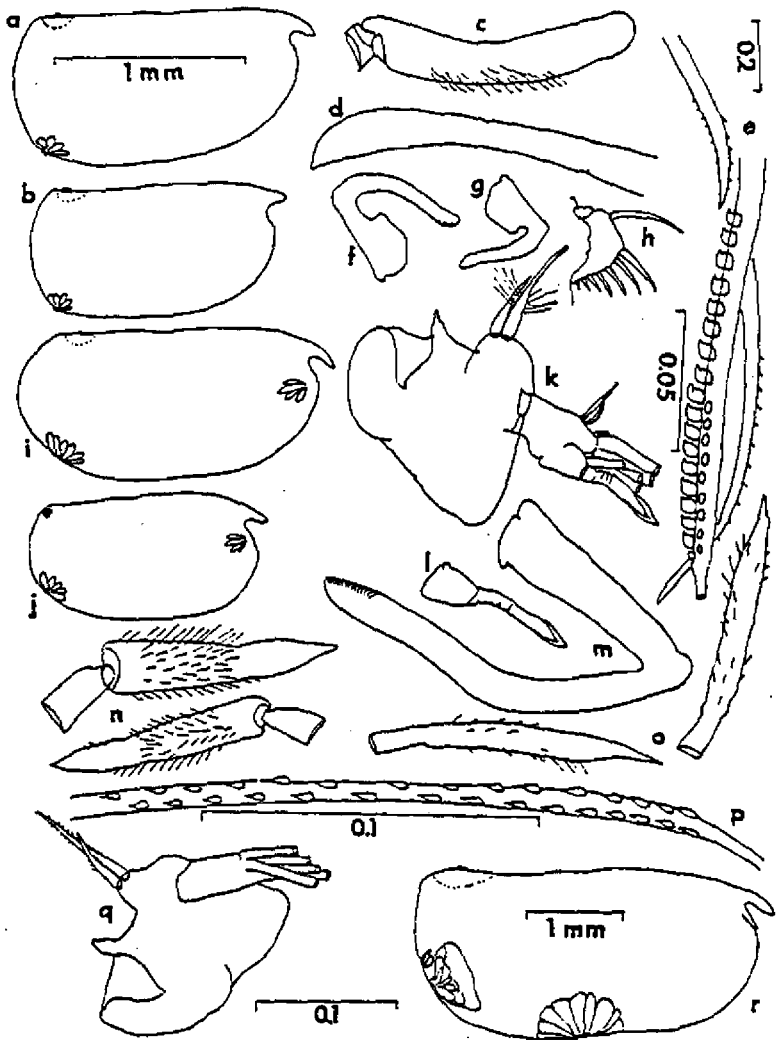


FIG. 3. a and b, Lateral views of female and male *Conchoecia brachyaskos*; c and d, Capitulum of frontal organs of male and female; e, Armature of male first antenna; f and g, Right and left male claspers; h, Female furca; i and j, Lateral views of female and male *C. obtusata antarctica*; k, Endopodite of male left second antenna; l and m, Left and right male claspers; n, Capitulum of frontal organs of two males; o, Capitulum of frontal organs of two females; p, Armature of principal seta of male first antenna; q, Endopodite of female second antenna; r, Lateral view of female *C. gaussae*. Scale on a for a, b, i and j, at upper right for h, beside e for e, below p for p, at bottom center for c, d, f, g, k–o and q, on r for r. Scales in mm.

cluding two new forms, which, due to insufficient material, will not be described in this report. Of the known species, only *C. abyssalis* and *C. pusilla* were not recorded.

C. teretivalvata Iles (Figure 4). This species was recorded from 5°S in the 200–0 m tows and from 30°S–49°S, 30°W and from 42°S–48°S in the Argentine Basin. As in the case of *C. skogsbergi*, smaller and larger forms were present, and the larger forms may eventually prove to be a different species, but males of both sizes had the large penis (Fig. 4l) shaped as figured by Müller (1894, Pl. 6, Fig. 20). Females and males, 0.85–0.90 mm long (Fig. 4b, g, h), occurred down to 42°30′S and at 42°S in the Argentine Basin. Larger specimens 1.0–1.1 mm long (Fig. 4a, j) were found from 40°S–49°S, between the subtropical and subantarctic convergences. Smaller males had 9–10 pairs of teeth on the principal seta of the first antenna, and larger males 10–11 pairs of teeth (Fig. 4e). Larger and smaller males had claspers of similar shape (Fig. 4c, d, i).

Distribution: Mediterranean; warmer Atlantic to 29°S in Benguela Current. These specimens extend the range southward.

C. rotundata Müller. This species, as described from the Sargasso Sea (Deevey, 1968), occurred from the equator to 35°S. The length range for females was 0.87–0.95 mm and for males 0.80–0.85 mm (Fig. 5h).

Distribution: 32°N–35°S in Atlantic; tropical Pacific.

C. skogsbergi Iles. *C. skogsbergi* was recorded from 30°S–55°S, 30°W and from 42°S–47°S in the Argentine Basin, from all stations where samples were collected with 1000 or more meters of cable out. Smaller specimens, females 1.10–1.25 mm long and males 1.05–1.20 mm long, such as those described from the Sargasso Sea (Deevey, 1968) were found from 30°S–35°S where larger specimens 1.35–1.50 mm long were also present. South of 35°S females were 1.4–1.7 mm long and males 1.35–1.75 mm long (Fig. 5b). Males 1.7 mm long had 14 pairs of teeth on the principal seta of the first antenna, whereas males 1.25 mm long had 13 pairs of teeth.

Distribution: 32°N–65°S in the Atlantic.

C. nasotuberculata Müller. This species (Fig. 5a) was found from the equator to 42°30′S, just south of the subtropical convergence.

Distribution: 18°N–40°S; Indian Ocean and Mediterranean. These specimens extend the range slightly south.

C. kyrtophora Müller. This is not the species described (Deevey, 1968) as *C. kyrtophora* from the Sargasso Sea. One female 0.93 mm long (Fig. 5g) and one male 0.95 mm long were collected at 40°S in a haul with 2500 m of cable out. This species is closely related to *C. nasotuberculata*, but the female is distinguished by lacking the lateral bumps on the shell that are characteristic of female *C. nasotuberculata*.

Distribution: 14°N–35°S in Atlantic; Indian Ocean. These specimens extend the range 5° south.

C. macromma Müller. Two females 1.40 (Fig. 5c, d) and 1.27 mm long and one male 1.50 mm long were collected at 44°12.4′S, 42°46′W

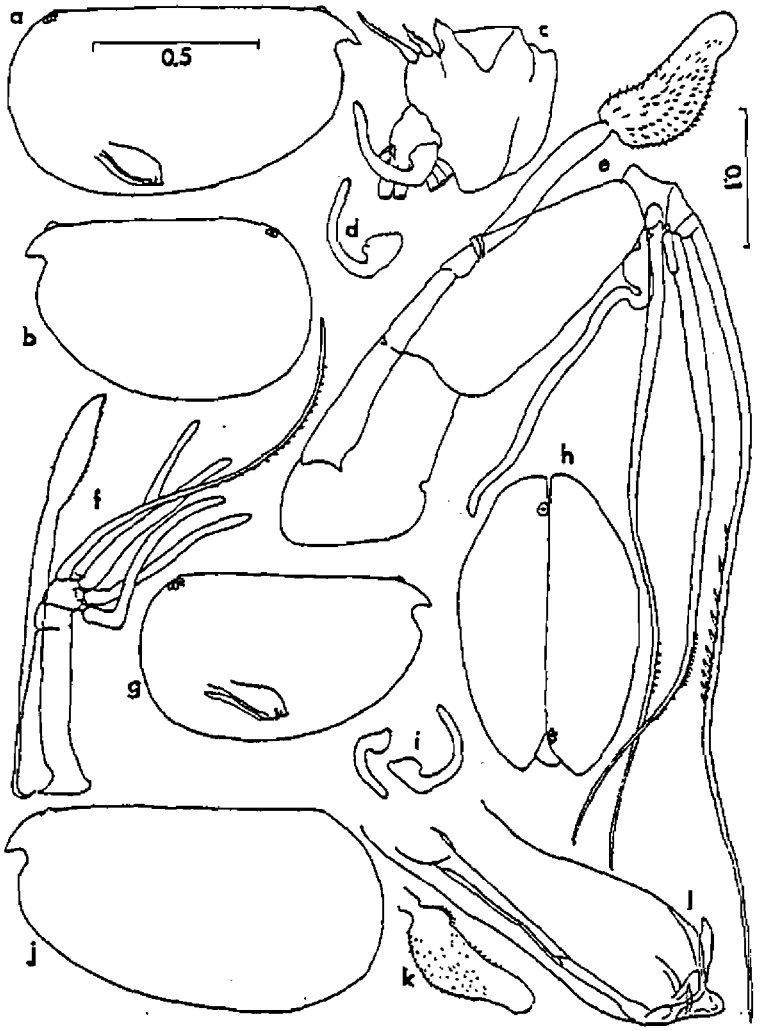


FIG. 4. *Conchoecia tereticalvata*. a, A 1.10 mm male; b, 0.92 mm female; c, Endopodite of right second antenna of 1.07 mm male; d, Right clasper of 1.05 mm male; e, Frontal organ and first antenna of 1.05 mm male; f, Frontal organ and first antenna of 0.92 mm female; g and h, Lateral and dorsal views of 0.85 mm male; i, Left and right claspers of 0.9 mm male; j, 1.1 mm female; k, Capitulum of frontal organ of 0.9 mm male; l, Penis of 1.0 mm male. Scale on a for a, b, g, h and j, at upper right for c–f, i, k and l. Scales in mm.

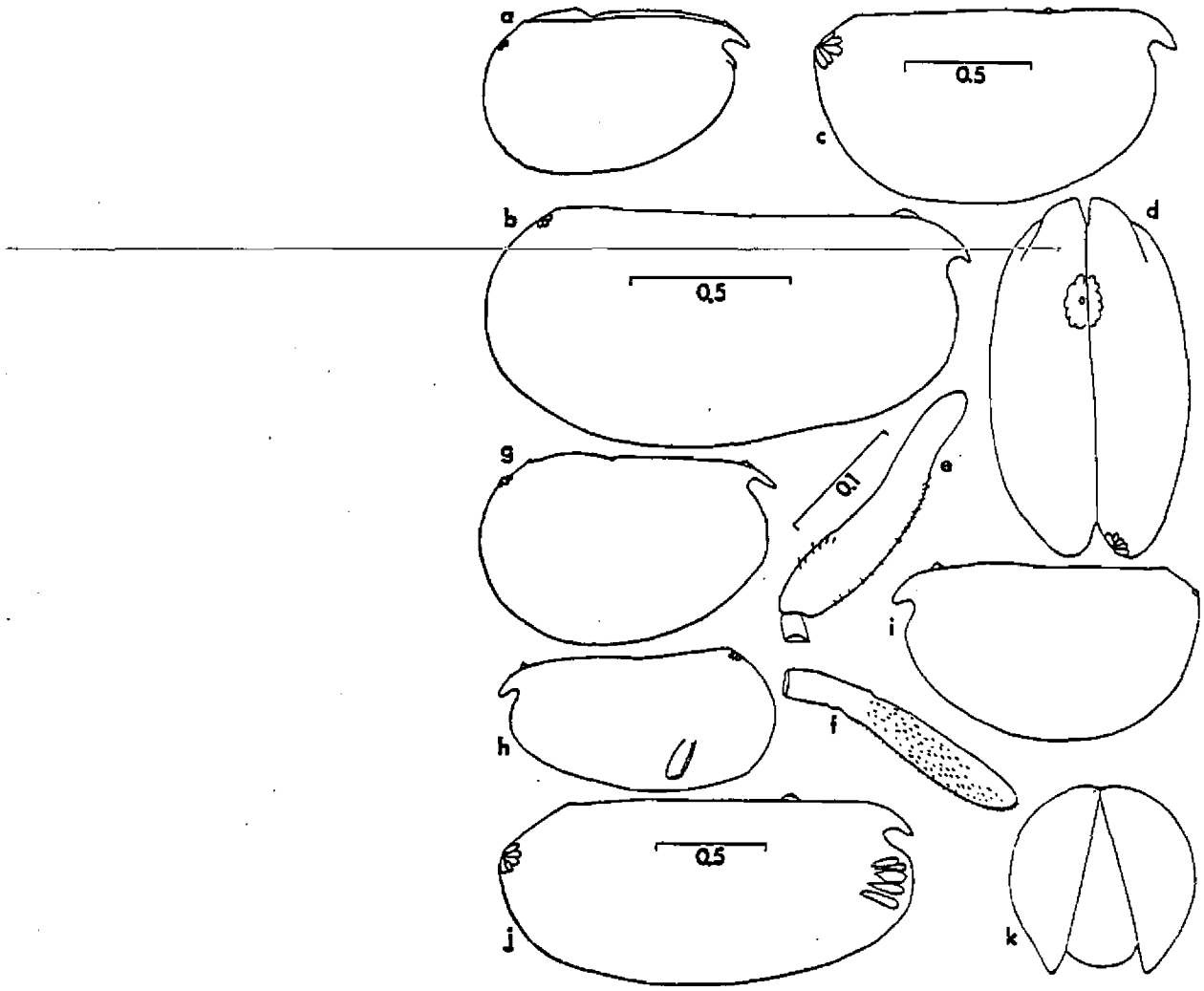


FIG. 5. a, Lateral view of 0.85 mm female *Conchoecia nasotuberculata*; b, 1.6 mm male *C. skogsbergi*; c and d, Lateral and dorsal views of 1.4 mm female *C. macromma*; e and f, Capitulum of frontal organs of male and female *C. macromma*; g, Lateral view of 0.93 mm female *C. kyrtophora*; h, 0.85 mm male *C. rotundata*; i, 0.93 mm female *C. isocheira*; j and k, Lateral and posterior views of 1.95 mm female *C. glandulosa*. Scale on b for a, b, g–i, on c for c and d, in center for e and f, on j for j and k. Scales in mm.

in a haul with 4000 m of cable out. Although these specimens are larger than those described by Müller from 24°N–3°S in the Atlantic, the position of the asymmetrical glands, the frontal organs (Fig. 5e, f), and the structure of the first and second antennae agree with his figures. Iles (1953) listed one female from a 750–1000 m haul at 25°S in the Benguela Current, but did not give its size or any corroboratory data.

Distribution: 24°N–25°S in the Atlantic; Indian Ocean. These specimens extend the range to 44°S.

C. glandulosa Müller. One female 1.95 mm long (Fig. 5j, k) was caught at 44°S in the Argentine Basin in a haul with 4000 m of cable out.

Distribution: 32°N–64°S in the Atlantic; Pacific and Indian Oceans.

C. isocheira Müller. *C. isocheira* (Fig. 5i) occurred from 49°S–53°S, in hauls with a minimum of 500 m of cable out. The length range for females was 0.95–1.05 mm and for males 0.84–1.00 mm.

Distribution: 53°S–71°S in the Atlantic, Indian and Pacific Antarctic. The HUDSON 70 specimens extend the range a few degrees to the north.

Curta Group Müller

C. curta Lubbock. This species was found from the equator to 35°S, and did not occur south of the subtropical convergence.

Distribution: 48°N–37°S in the Atlantic; Indian and Pacific Oceans and Mediteranean.

C. echinulata (Claus). *C. echinulata* was present from 11°S–30°S.

Distribution: 34°N–37°S in Atlantic; Indian Ocean.

C. stigmatica Müller. Juvenile specimens of this species were noted from the equator to 10°S in the 200–0 m tows.

Distribution: 0°39'N–31°S in Atlantic; Indian and Pacific Oceans.

C. acuticosta Müller. This species occurred from 32°30'S–45°S, 30°W and from 42°S–44°S in the Argentine Basin, primarily in hauls with 1000–4000 m of cable out.

Distribution: 27°N–36°S in the Atlantic; Indian and Pacific Oceans. These specimens extend the range to 45°S.

Bispinosa Group Müller

C. haddoni Brady and Norman. *C. haddoni* was present from 35°S to 51°30'S, 30°W, and from 42°S–47°S in the Argentine Basin, in hauls with 1000–4000 m of cable out. The length range noted for females was 2.8–3.1 mm and for males 2.30–2.55 mm. Müller noted that the southern forms were larger than those from the North Atlantic, where Angel (1970) recorded length ranges of 2.15–2.53 mm for females and 1.75–2.00 mm for males.

Distribution: 60°N–51°30'S in Atlantic; Indian Ocean.

C. bispinosa Claus. *C. bispinosa* was found from the equator to 40°S, 30°W and at 42°S in the Argentine Basin. Ramirez and Moguilevsky (1971) identified all their specimens, collected between 36° and 38°S, as *C. secernenda*, but their smaller males around 2.1 mm long were

evidently *C. bispinosa*, since they noted 29 pairs of teeth on the principal seta of the male first antenna. Apparently, as in the case of *C. haddoni*, specimens of *C. bispinosa* are larger in the South Atlantic than in the North, HUDSON 70 females were 1.85–2.20 mm long and males 1.90–2.00 mm long. Angel (1970) recorded length ranges of 1.8–2.1 mm for females and 1.65–1.88 mm for males from around 29°N–33°N in the eastern North Atlantic. Females from the Sargasso Sea were 1.80–1.95 mm long and males 1.65–1.80 mm long (Deevey, 1968).

Distribution: 43°N–42°S in the Atlantic.

C. secernenda Vavra. This species was caught only in several 200–0 m tows between 8°30'S and 27°30'S, 30°W, and apparently is not as abundant in the South Atlantic as in the North. Judging by their large size (females 2.6 mm and males 2.3 mm mean length) Poulsen's (1969b) specimens identified as *C. bispinosa* from the Gulf of Guinea are presumably *C. secernenda*; he did not state the number of teeth on the principal seta of the male first antenna, but believes *C. secernenda* and *C. bispinosa* to be synonymous.

Distribution: 37°N–38°S in the Atlantic.

C. atlantica (Lubbock). *C. atlantica* was found only between 0°51'S and 7°27'S, 30°W.

Distribution: 40°N–37°S in the Atlantic; Indian and Pacific Oceans.

Gaussae Group Skogsberg

Skogsberg (1920) included *C. gaussae* and *C. incisa* in this group, both of which Müller (1906a) had put in the *Bispinosa* Group. In this report *C. edentata*, which Müller assigned to the *Acuminata* Group, is also included. These three species differ from all others in having large compound glands on the mid-ventral margin of both shells, as well as the usual asymmetrical glands. Poulsen (1969b) has provisionally included *C. congolensis* Poulsen in this group, although it lacks the glands on the ventral margin.

C. edentata Müller. Three females, 1.65, 1.73, 1.73 mm long, and two juvenile specimens 1.40 and 1.45 mm long were collected between 23°S and 55°S. Müller described this species from a 1.7 mm male and an immature female. Barney (1921) recorded 4 specimens from a 0–1000 m haul at about 72°S in the Pacific Antarctic, and Iles (1953) a single female from a 250–500 m tow at 23°S in the Benguela Current. Rudyakov (1962) gave a supplementary description of a 1.83 mm female and 2 males, 1.43–1.45 mm long.

Distribution: 0°39'N–56°S in the Atlantic; 55°S–62°S in the Indian Ocean; 72°S and 44°N–50°N in the Pacific.

C. incisa Müller. A single female, 2.37 mm long, was caught in a 200–0 m tow at 3°40'S, 30°W. Müller (1906a) described this species from a 2.15 mm male and a 2.5 mm female from the Indian Ocean. Poulsen (1969b) has since recorded 3 females, 2.5–2.6 mm long, from a station near the equator in the Gulf of Guinea. Angel (1969) noted this species from the Canary Island region.

Distribution: 29°N–3°40'S in the Atlantic; 2°S–26°S in the Indian Ocean.

C. gaussae Müller. One female, 3.45 mm long, was caught at 32°30'S in a haul with 750 m of cable out, and another female, 3.85 mm long (Fig. 3r), was taken at 51°30'S in a tow with 3000 m of cable out. Müller (1908) described the species from a single male, 3.1 mm long, from 35°11'S, 2°43'E. Skogsberg (1920) described the female from a 3.6 mm specimen from 50°S in the Atlantic. A subspecies, *C. gaussae curilensis*, has been described from the Kuril Kamchatka region from two females 4.08–4.18 mm long (Rudyakov, 1962). The only other recorded specimens are two 4.0 mm females and a 3.3 mm male from 2°S–6°35'S in the Gulf of Guinea (Poulsen, 1969b).

Distribution: 2°S–51°30'S in the Atlantic; 46°31'N, 154°22'E in the Pacific

Loricata Group Müller

C. loricata loricata (Claus). A single male, 1.8 mm long, was found at 35°S in a haul with 1800 m of cable out.

Distribution: 46°N–37°S in the Atlantic; Indian Ocean and Mediterranean.

C. ctenophora Müller. One female, 2.7 mm long, was taken at 30°S in a haul with 1400 m of cable out.

Distribution: 18°N–35°S in the Atlantic; near equator in Indian and Pacific Oceans.

Serrulata Group Skogsberg

C. concentrica Müller. A single female, 1.55 mm long, was found at 0°51'S.

Distribution: 38°N–3°S in the Atlantic; Malay Archipelago and Indian Ocean.

C. serrulata Claus. This species occurred from 40°S–51°30'S, in hauls with 100 or more meters of cable out. It was most numerous between 47°S and 49°S, over the convergence in subantarctic waters in the Argentine Basin. The length range for females was 1.40–1.65 mm and for males 1.25–1.35 mm.

Distribution: 10°S–58°S in the Atlantic; to 59°S in the Indian Ocean and to 68°S in the Pacific.

Magna Group Müller

C. magna Claus. *C. magna* occurred from the equator to 42°30'S, and was present in almost all 200–0 m tows. Females had a length range of 1.7–2.0 mm and males of 1.6–1.9 mm.

Distribution: 52°N–55°S in the Atlantic; Indian and Pacific Oceans and Mediterranean.

C. lophura Müller. This species, easily recognized by the large group of gland cells on the ventral margin at the postero-ventral corner of the

shell, was found from 30°S–45°S, in hauls with 750–2500 m of cable out.

Distribution: 46°N–48°S in the Atlantic; Pacific and Indian Oceans and Mediterranean.

C. parvidentata Müller. *C. parvidentata* occurred from 35°S–48°S, to the region of the subantarctic convergence. Females had a length range of 2.55–2.85 mm and males of 2.15–2.50 mm.

Distribution: 31°N–48°S in Atlantic; Indian Ocean.

C. hyalophyllum Claus. This species was recorded from 6°S in a 200–0 m tow and from 27°30′S–42°30′S. Females were 1.65–1.80 mm long and males 1.55–1.70 mm long.

Distribution: 52°N–48°S in the Atlantic; Indian Ocean.

C. macrocheira Müller. *C. macrocheira* was noted on only two occasions, at 0°51′S and at 27°30′S, in hauls with 200–450 m of cable out.

Distribution: 60°N–34°S in the Atlantic; Indian and Pacific Oceans.

C. subarcuata Claus. This species was recorded from 8°31′S–37°30′S, and did not occur south of the subtropical convergence.

Distribution: 59°N–56°S in the Atlantic; Indian and Pacific Oceans.

C. parthenoda Müller. *C. parthenoda* was found from the equator to 30°S. The two specimens described as *C. parthenoda* by Ramirez and Moguilevsky (1971, p. 657, Pls. 12–13) may represent *C. magna*; at least in the case of the male the size is too great and the left asymmetrical gland is not placed far enough forward on the dorsal margin.

Distribution: 37°N–30°S in the Atlantic; Indian and Pacific Oceans.

C. pseudoparthenoda Angel. This species occurred from the equator to 30°S in 200–0 m tows. The male specimen figured as *C. parthenoda* from Barbados (Deevey, 1970) is now recognized as *C. pseudoparthenoda*. Also, in all probability Poulsen's (1969b) description and figures of his male *C. parthenoda* represent *C. pseudoparthenoda*.

Distribution: 14°N–30°S in the Atlantic.

C. spinirostris Claus. *C. spinirostris* was recorded from the equator to 40°S, 30°W and to 42°S in the Argentine Basin, and was not found south of the subtropical convergence.

Distribution: 45°N–24°S in the Atlantic; Pacific and Mediterranean. These specimens extend the range to 42°S.

C. porrecta Claus. This species was found from the equator to 37°30′S, and also did not occur south of the subtropical convergence. Because of their size, the specimens identified by Poulsen (1969b) as *C. spinirostris* must be *C. porrecta*; Poulsen does not separate these two species.

Distribution: 41°N–2°N in the Atlantic; Mediterranean. These specimens extend the range to 37°30′S.

Mollis Group Müller

C. amblypostha Müller (Figure 6). This species occurred from 30°S–40°S, 30°W and from 42°S–47°S in the Argentine Basin, in hauls with 1100–3000 m of cable out. Poulsen (1969b) recorded this species from 1°S–17°S in the Gulf of Guinea, from 670–800 m depths. Müller (1906a)

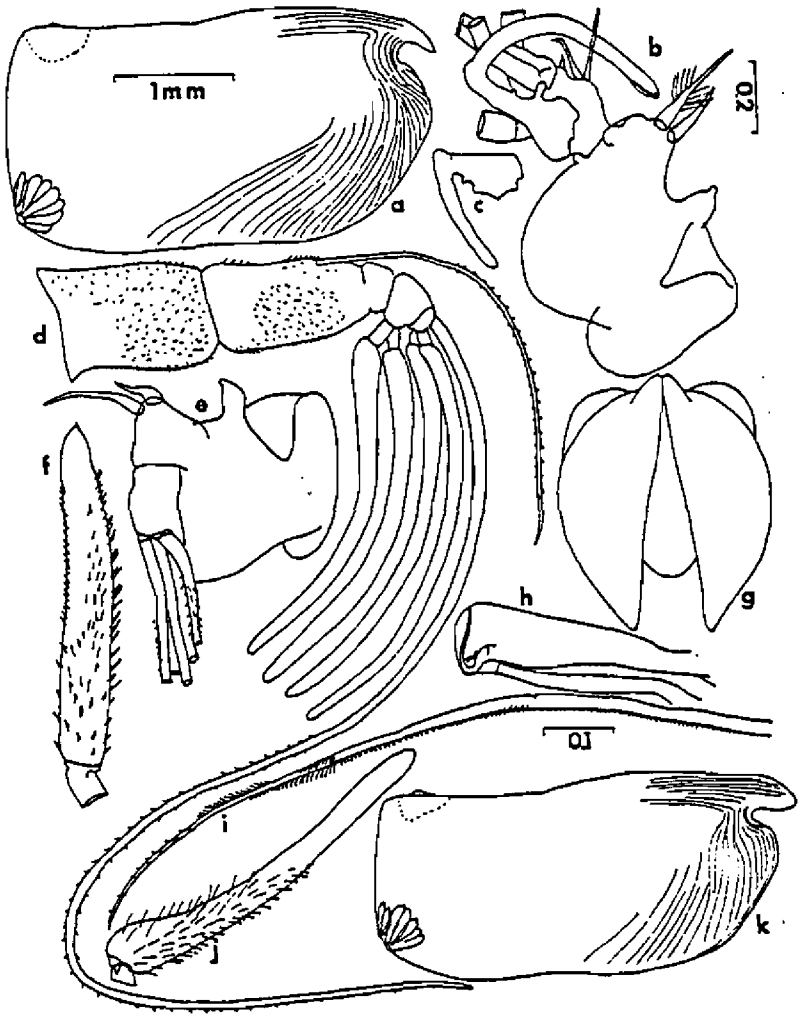


FIG. 6. *Conchoecia amblypostha*. a, Lateral view of female; b, Endopodite of male right second antenna; c, Left clasper; d, Female first antenna; e, Endopodite of female second antenna; f, Capitulum of female frontal organ; g, Posterior view of female; h, Male penis; i, Armature of distal secondary seta of male first antenna; j, Capitulum of male frontal organ; k, Lateral view of male. Scale on a for a, g, k, below i for b–f, i, j, at upper right for h. Scales in mm.

was unable to differentiate the females (Fig. 6a, g) from those of *C. mollis*, but males are distinguished by the armature of the first antenna, particularly the distal secondary seta (Fig. 6i) and the shape of the penis (Fig. 6h). No *C. mollis* males were noted. Females had a length range of 3.30–3.75 mm and males of 3.2–3.5 mm. The female frontal organ (Fig. 6f), first and second antennae (Fig. 6d, e) are indeed similar in structure and spination to those of female *C. mollis*. The male claspers (Fig. 6b, c) are also similar in the two species, but the male *C. mollis* lacks the long hairs on the "b" bristle of the endopodite of the second antenna that are present in male *C. amblypostha*.

Distribution: 1°S–37°31′S in the Atlantic; Indian Ocean. These specimens extend the range to 47°S.

C. dichotoma Müller. A single immature female, 2.04 mm long, was taken at 42°30′S in a haul with 2500 m of cable out. Poulsen (1969b) recorded 3 specimens from 0°50′S.

Distribution: 0°50′S–35°S in the Atlantic. This specimen extends the range to 42°30′S.

C. plactolycos Müller (Figure 7). Müller described two subspecies of *C. plactolycos*: *C. plactolycos typica* (1906a) = *C. plactolycos plactolycos* (1912) and *C. plactolycos major* (1906a, 1908). Specimens of both of these forms were collected in the HUDSON 70 samples and are easily distinguishable, so that each form should be raised to the rank of species. According to rule, *C. plactolycos plactolycos* thus becomes *C. plactolycos* Müller and *C. plactolycos major* is named *C. major* Müller. Müller described *C. plactolycos* from a single male 2.3 mm long from 29°S in the Indian Ocean. One male, 2.5 mm long, was taken at 44°12.4′S, 42°46′W in a haul with 4000 m of cable out. This specimen (Fig. 7c, d, g–k) agrees with Müller's description in the shape of the shell, location of the glands, shape of the frontal organ and clasping organs and the armature of the first antenna (Müller, 1906a, p. 114, Pl. 25, Figs. 14–20). *C. plactolycos* is closely similar to *C. major*, but is smaller in size and the sculpturing of the shell is difficult to discern. The principal seta of the male first antenna has 33 pairs of short fat teeth (Fig. 7i) as against 43 pairs for the *C. major* male (Fig. 8i) and the distal secondary seta is not armed (Fig. 7d) as in the larger form. The medial glands on the posterior margin are much more visible in the *C. plactolycos* male (Fig. 7k). A single female, 2.7 mm long (Fig. 7a, b), taken at 41°44.6′S, 46°33′W, resembles the male in shape and sculpturing. The female differs from that of *C. major* in having fewer spinules on the basal segments of the first antenna (Figs. 7f and 8d) and in lacking spinules on the anterior side of the principal seta. Unfortunately, the distal part of the capitulum of the frontal organ was broken off (Fig. 7e).

Distribution: 42°S–44°S in the Atlantic; 29°S in the Indian Ocean.

C. major (= *C. plactolycos major*) Müller (Figure 8). *C. major* was recorded from 49°S–55°S, 30°W and from 44°S–47°S in the Argentine

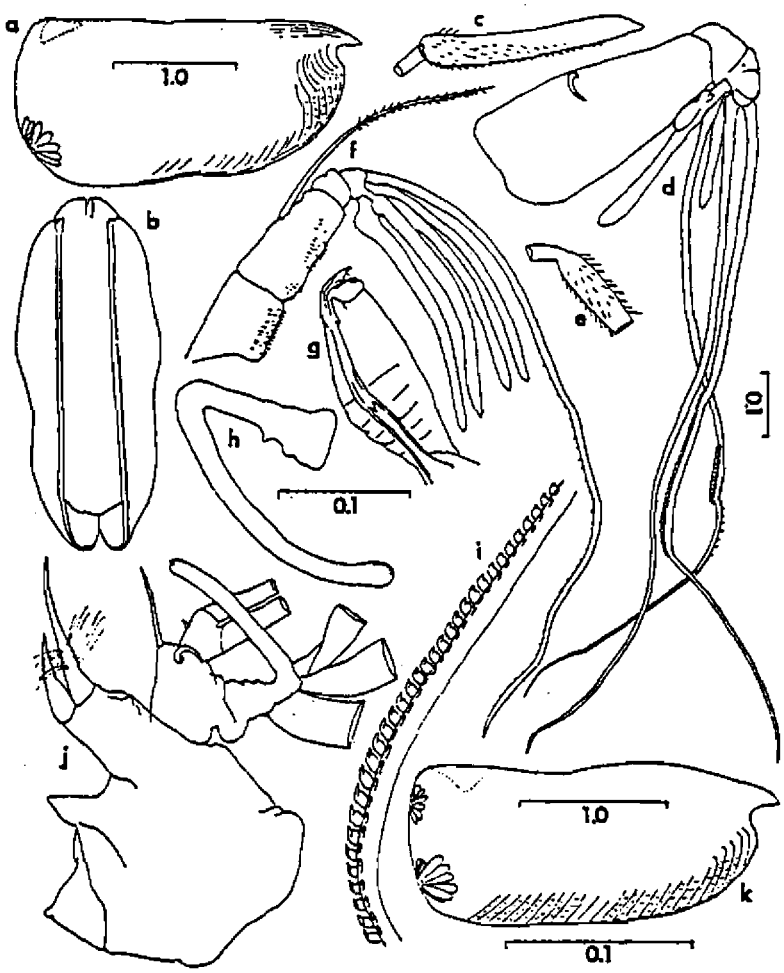


FIG. 7. *Conchoecia plactolycos* (= *C. plactolycos plactolycos*). a and b, Lateral and ventral view of female; c, Capitulum of male frontal organ; d, Male first antenna; e, Proximal part of capitulum of female frontal organ; f, Female first antenna; g, Male penis; h, Male right clasper; i, Armature of principal seta of male first antenna; j, Endopodite of male left second antenna; k, lateral view of male. Scale on a for a and b, on k for k, in center for j and h, at bottom right for i, on right margin for c–g. Scales in mm.

Basin in hauls with 2500–4000 m of cable out. The length range for females was 3.1–3.6 mm and for males 2.97–3.30 mm. Apparently this is the first record of this species since Müller (1906a, 1908) described it from 56°S in the Atlantic and 62°S–65°S in the Indian Ocean. The

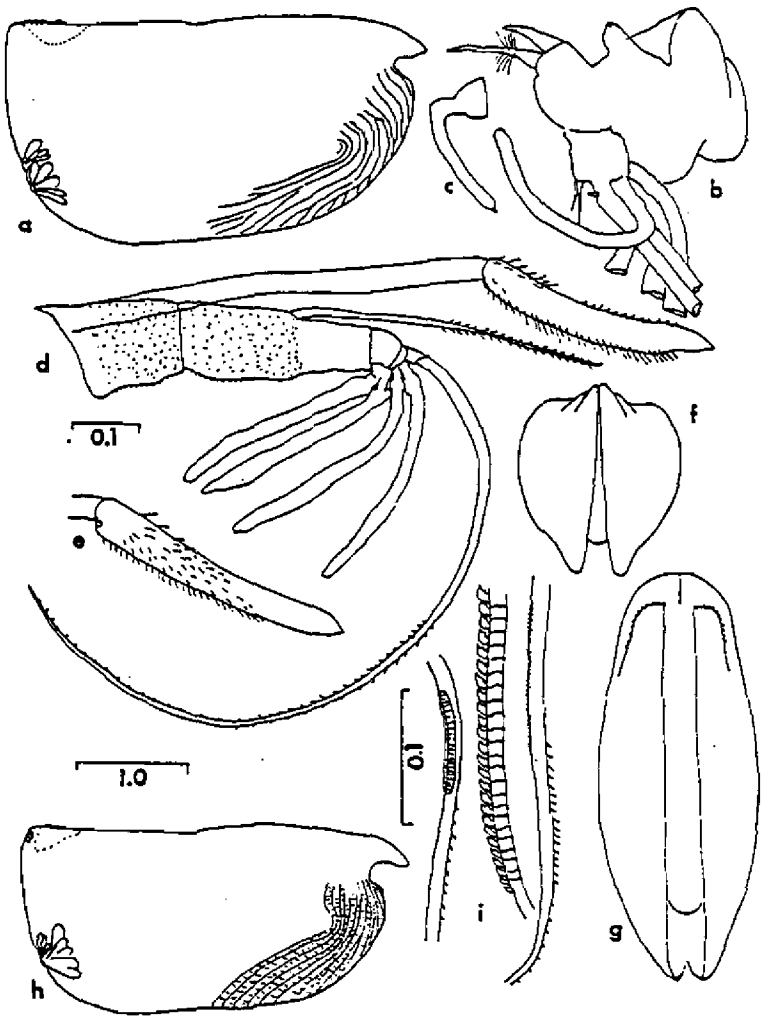


FIG. 8. *Conchoecia major* (= *C. plactolycos major*). a, Lateral view of female; b, Endopodite of male right second antenna; c, Male left clasper; d, Frontal organ and first antenna of female; e, Capitulum of male frontal organ; f, g and h, Posterior, ventral and lateral views of male; i, Armature of male first antenna. Scale above h for a, f–h, beside i for i, at left center for b–e. Scales in mm.

sculpturing on the shell (indicated in Fig. 8a, h) is much more definite than in *C. plactolycos*; other differences have been noted above.

Distribution: 56°S in Atlantic; Indian Ocean. These specimens extend the range north to 44°S.

C. borealis Sars var. *antipoda* Müller. *C. borealis antipoda* occurred from 35°S–55°S, 30°W and from 42°S–51°28′S in the Argentine Basin, in hauls with 1000–4000 m of cable out. The length range for males was 2.80–3.05 mm and for females 3.05–3.35 mm. The antarctic form is larger than the arctic form for which Skogsberg (1920) gave measurements of 2.1–2.3 mm for males and 2.4–2.9 mm for females. The female has more sharp-edged shoulder vaults (Fig. 9a, b) than the male (Fig. 9c, h). The male appears to differ from male *C. borealis* Sars, as figured by Skogsberg (1920, Fig. 135-4), in having fewer teeth on the principal seta (Fig. 9e); 40–45 pairs of teeth were noted, whereas Skogsberg described 50–55 pairs of teeth on the principal seta of males from Lofoten. The clasping organs and frontal organ (Fig. 9d, f, g) are similar to those of the arctic form.

Distribution: 1°S–65°S in the Atlantic and Antarctic Oceans.

Imbricata Group Müller

C. imbricata (Brady). This species was recorded at 18°S, 24°S and from 27°30′S–40°S, and was not found south of the subtropical convergence.

Distribution: 63°N–55°S in the Atlantic; Pacific and Indian Oceans.

C. ametra Müller. *C. ametra* was taken from 30°S–40°S, 30°W and from 42°S–44°S in the Argentine Basin, in hauls with 1100–4000 m of cable out. A length range of 3.75–4.10 mm was noted for males and of 4.5–4.8 mm for females.

Distribution: 60°N–37°S in the Atlantic; Indian and Pacific Oceans. These specimens extend the range south to 44°S.

C. plinthina Müller. A single juvenile specimen, 4.1 mm long, was found at 42°30′S in a haul with 2500 m of cable out. This is the largest species of this group.

Distribution: 48°N–31°S in the Atlantic; Indian and Pacific Oceans. This specimen extends the range to 42°30′S.

C. symmetrica Müller. *C. symmetrica* occurred from 35°S–55°S, 30°W and from 42°S–47°S in the Argentine Basin, in hauls with 1000–4000 m of cable out. The length range for females was 4.1–4.5 mm and for males 3.7–4.0 mm.

Distribution: 0–55°S in the Atlantic; Indian Ocean and Pacific Antarctic.

Alata Group Müller

C. hettacra Müller. *C. hettacra* (Fig. 9i–k) occurred from 49°S–55°S, 30°W and from 42°S–51°30′S in the Argentine Basin, at shallow depths, since it was taken in the 200 and 100 m tows. The length range for females was 2.25–2.45 mm and for males 1.80–1.95 mm.

Distribution: 47°S–57°S in the Atlantic, so these specimens extend the range north to 42°S; 43°S–70°S in the Indian Ocean.

C. valdiviae Müller. This species occurred from 32°30′S–42°30′S,

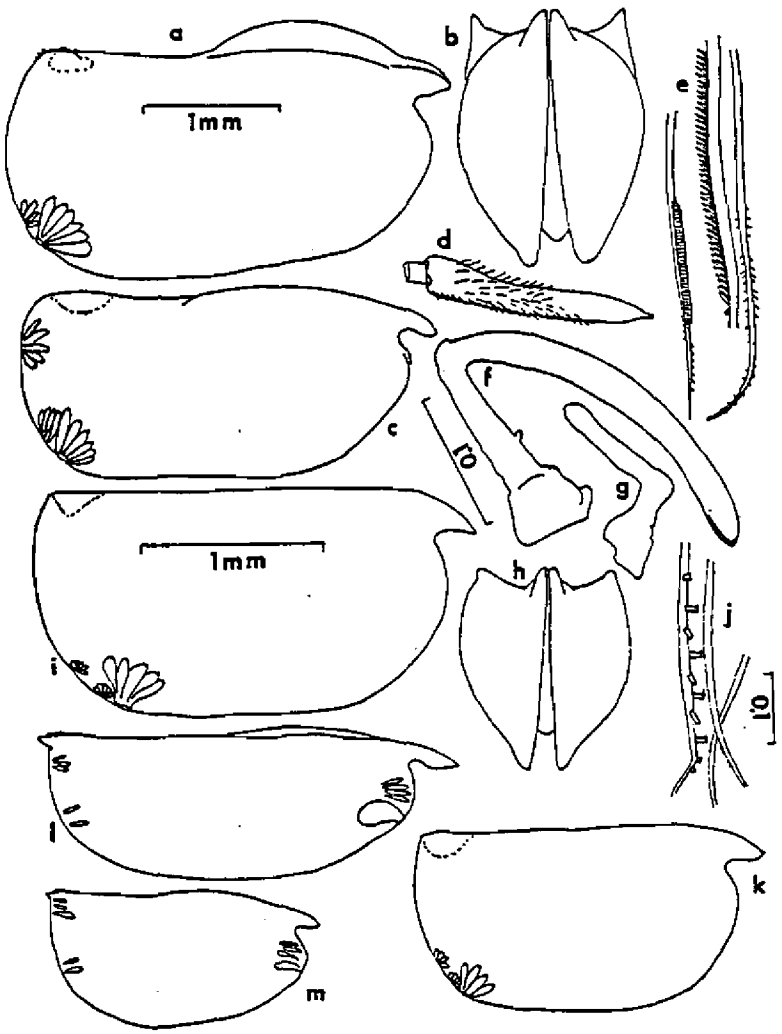


FIG. 9. a and b, Lateral and posterior views of female *Conchoecia borealis antipoda*; c, Lateral view of male; d, Capitulum of male frontal organ; e, Armature of male first antenna; f and g, Right and left male claspers; h, Posterior view of male; i, Lateral view of female *C. hettacra*; j, Armature of *C. hettacra* male first antenna; k, Lateral view of male; l and m, Lateral views of female and male *C. chuni*. Scale on a for a–c and h, beside f for f and g, on lower right margin for d, e, and j, on i for i, k–m. Scales in mm.

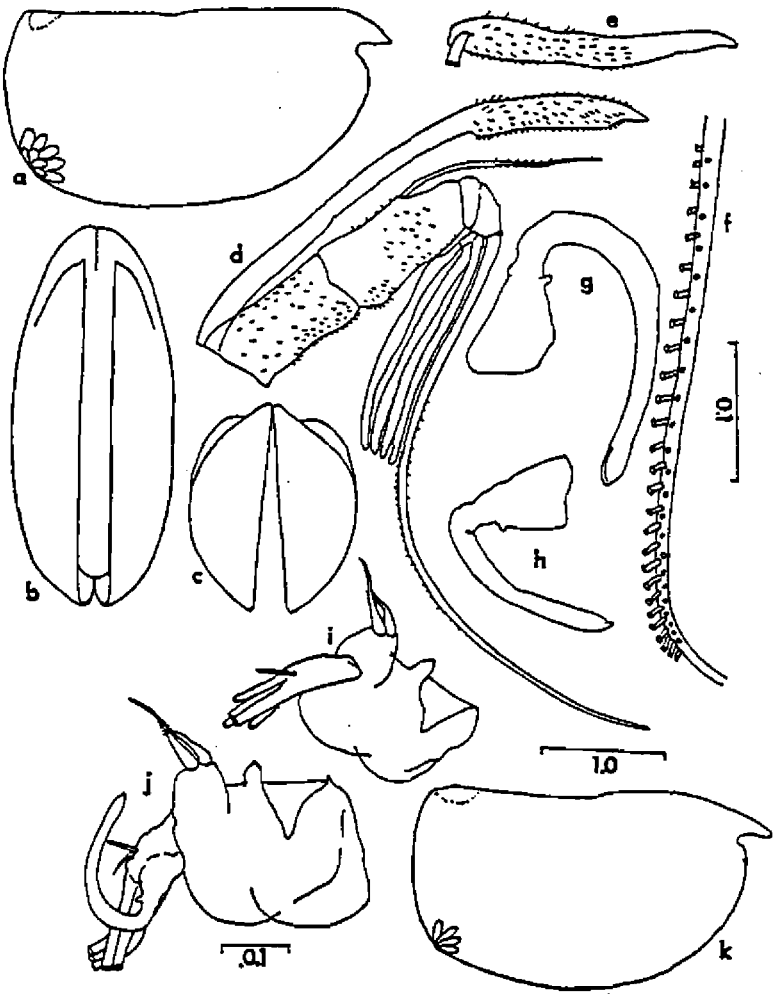


FIG. 10. *Conchoecia belgicae.* a, b and c, Lateral, ventral and posterior views of female; d, Female frontal organ and first antenna; e, Capitulum of male frontal organ; f, Armature of principal seta of male first antenna; g and h, Right and left male claspers; i, Endopodite of female second antenna; j, Endopodite of male right second antenna; k, Lateral view of male. Scale above k for a–c and k, at bottom for d, e, i, j, on right margin for f–h. Scales in mm.

30°W and from 42°S–45°S in the Argentine Basin. *C. valdiviae* is exceptionally large and bulky, deep red in color when alive. Most specimens were immature, but one female was 5.35 mm long and one male 5.0 mm in length.

Distribution: 28°N in the Gulf of Mexico (Kornicker, 1968) to 47°S in the Atlantic; to 58°S in the Indian Ocean.

C. belgicae Müller (Figure 10). One 2.8 mm male was obtained at 51°30'S, 40°W, in a haul with 600 m of cable out, and one female 2.9 mm long was taken at 55°S in a haul with 1100 m of cable out. These specimens agree with Müller's (1906b) and Skogsberg's (1920) descriptions and figures. Müller's "Belgica" females were 2.4–2.7 mm long and his males 2.4–2.6 mm long, but speciemns from the Gausstation (66°2.9'S, 89°38'E) were larger: females 2.6–3.0 mm long and males 2.6–2.8 mm in length. Figure 10 illustrates the shape of the male and female shells and the structure of the first and second antennae. According to Skogsberg, the male first antenna has 27–30 pairs of teeth, similar in shape to those of the *C. hettacra* male (Fig. 9j). The HUDSON 70 specimen had 26 teeth in lateral view, the two rows unevenly paired (Fig. 10f).

Distribution: Müller described this species from 70°S–71°S in the Pacific Antarctic, and obtained it later from 65°S–66°S in the Indian Antarctic. Skogsberg's specimens were from about 66°S in the Atlantic. Barney (1921) reported it abundant at a number of stations in the Ross Sea and McMurdo Sound and also at two stations north of New Zealand. The HUDSON 70 specimens extend the range in the Atlantic north to 51°30'S.

Daphnoides Group Müller

C. daphnoides (Claus). *C. daphnoides* was recorded from about 5°S and 23°S to 40°S, 30°W, and at 42°S in the Argentine Basin, and therefore was not found south of the subtropical convergence. Males ranged in length from 2.8–3.1 mm and females from 4.8–5.6 mm.

Distribution: 60°N–37°S in the Atlantic; Indian and Pacific Oceans. These specimens extend the range to 42°S.

C. chuni Müller. *C. chuni* (Fig. 9l, m) was taken from 32°30'S–55°S, 30°W, and from 42°S–50°S in the Argentine Basin, in shallow as well as deeper hauls. The length range for males was 1.40–1.55 mm and for females 2.0–2.4 mm.

Distribution: 26°S–53°S in the Atlantic; 2°S–44°S in the Indian Ocean, and to 64°S in the Pacific. These specimens extend the range slightly to 55°S.

Literature Cited

Angel, M. V. 1969. Planktonic ostracods from the Canary Island region; their depth distributions, diurnal migrations, and community organization. J. Mar. Biol. Assoc. U. K., 49:515–553.

———. 1970. The redescription of *Conchoecia bispinosa* Claus, *C. haddoni* Brady & Norman and *C. secernenda* Vavra from the North Atlantic. Crustaceana, 18:147–166.

BARNEY, R. W. 1921. Crustacea. Part V. Ostracoda. Brit. Antarctic (Terra Nova) Exped., 1910, Zool. Nat. Hist. Rep., 3(7):175–189.

DEEVEY, G. B. 1968. Pelagic ostracods of the Sargasso Sea off Bermuda. Peabody Mus. Nat. Hist., Yale, Bull. 26, 125 p., 65 figs.

———. 1970. Pelagic ostracods (Myodocopa Halocyprididae) from the North Atlantic off Barbados. Proc. Biol. Soc. Washington, 82:799–824.

ILES, E. J. 1953. A preliminary report on the Ostracoda of the Benguela Current. Discovery Rep. 26:259–280.

KORNICKER, L. S. 1968. Bathyal Myodocopid Ostracoda from the northeastern Gulf of Mexico. Proc. Biol. Soc. Washington, 81: 439–472.

MÜLLER, G. W. 1894. Die Ostracoden des Golfes von Neapel. Fauna und Flora des Golfes von Neapel, Monogr. 21:1–404, 40 Pls.

———. 1906a. Ostracoda. Wissensch. Ergeb. d. Deutschen Tiefsee-Expedition auf dem Dampfer "Valdivia" 1898–1899, 8:1–154, Pls. 5–35.

———. 1906b. Ostracoden. Expedition Antartique Belge. Resultats du Voyage du S. Y. Belgica en 1897–1898–1899. Rapp. Scient., Zool., 7 p., 1 Pl.

———. 1908. Die Ostracoden der Deutschen Südpolar-Expedition 1901–1903. Deutsche Südpolar-Expedition 1901–1903, X, Zool. II: 53–181, Pls. 4–19.

———. 1912. Ostracoda. Das Tierreich, Lief. 31, 434 p., Berlin.

POULSEN, E. M. 1962. Ostracoda-Myodocopa Part I Cypridiniformes-Cypridinidae. Dana-Report No. 57, 414 p., 181 figs.

———. 1969a. Ostracoda-Myodocopa Part IIIA Halocypriformes-Thaumatocypridae and Halocypridae. Dana-Report No. 75, 100 p., 40 figs.

———. 1969b. Ostracoda-Myodocopa from the eastern tropical Atlantic. Vidensk. Meddr. Dansk Naturh. Foren. 132:129–197.

RAMÍREZ, F. C., AND A. MOGUILEVSKY. 1971. Ostracodos planctionicos hallados en aguas oceanicas frente a la Provincia de Buenos Aires (Resultados de la XLI Comissae Oceanografica Costa Sul). Physis, 30(81):637–666.

RUDYAKOV, YU. A. 1962. Ostracoda Myodocopa (family Halocypridae) from the N. W. Pacific Ocean. Trudy Inst. Okeanol., 58:172–201. 14 figs.

SKOGSBERG, T. 1920. Studies on marine ostracods Part I (Cypridinids, Halocyprids and Polycopids). Zool. Bidr. Uppsala, Suppl. I, 784 p., 153 figs.

A Dispenser for Winkler's Dissolved Oxygen Reagents[1]

I. W. DUEDALL

Fisheries Research Board of Canada
Marine Ecology Laboratory, Bedford Institute, Dartmouth, N.S.

A. R. COOTE, D. F. KNOX, AND G. F. CONNOLLY

Department of the Environment
Marine Sciences Branch
Atlantic Oceanographic Laboratory, Bedford Institute, Dartmouth, N.S.

DUEDALL, I. W., A. R. COOTE, D. F. KNOX, AND G. F. CONNOLLY. 1971. A dispenser for Winkler's dissolved oxygen reagents. J. Fish. Res. Bd. Canada 28: 1815–1816.

A new dispenser for delivering Winkler's oxygen reagents simultaneously is described.

DUEDALL, I. W., A. R. COOTE, D. F. KNOX, AND G. F. CONNOLLY. 1971. A dispenser for Winkler's dissolved oxygen reagents. J. Fish. Res. Bd. Canada 28: 1815–1816.

Les auteurs décrivent un nouveau dispensateur à distribution simultanée des réactifs du dosage de l'oxygène suivant la méthode de Winkler.

Received July 12, 1971

DURING the *Hudson'70* Expedition, a specially designed dispenser (Fig. 1) for the oxygen pickling reagents was used in Carpenter's (1965) modification of the Winkler dissolved oxygen method. Participants of the Expedition commented on the usefulness of this dispenser; this note outlines the design features. The main feature, which was originally suggested to us by K. Grasshoff, is that the required amounts of the two pickling reagents ($MnCl_2$ and NaI–NaOH) are added simultaneously from two syringes when the dispenser crank is turned one revolution. In our procedure, a water sample is first drawn into an iodine flask and the sample is immediately brought into contact with the syringe needles of the dispenser. The flask is then raised so the needle tips are situated near the bottom of the flask. The oxygen reagents are dispensed, the iodine flask is stoppered and shaken, and the sample is analysed according to Carpenter's technique.

The dispenser (Fig. 2) consists of two 30-ml B-D®[2] plastic syringes in which the syringe barrels are fastened to an anodized aluminum stationary plate and the syringe plungers are fastened to a sliding plate; the two plates are connected by a threaded pipe having 9 threads per inch. The syringe size was chosen so that all 25 oxygen samples from one oceanographic bottle cast could be pickled

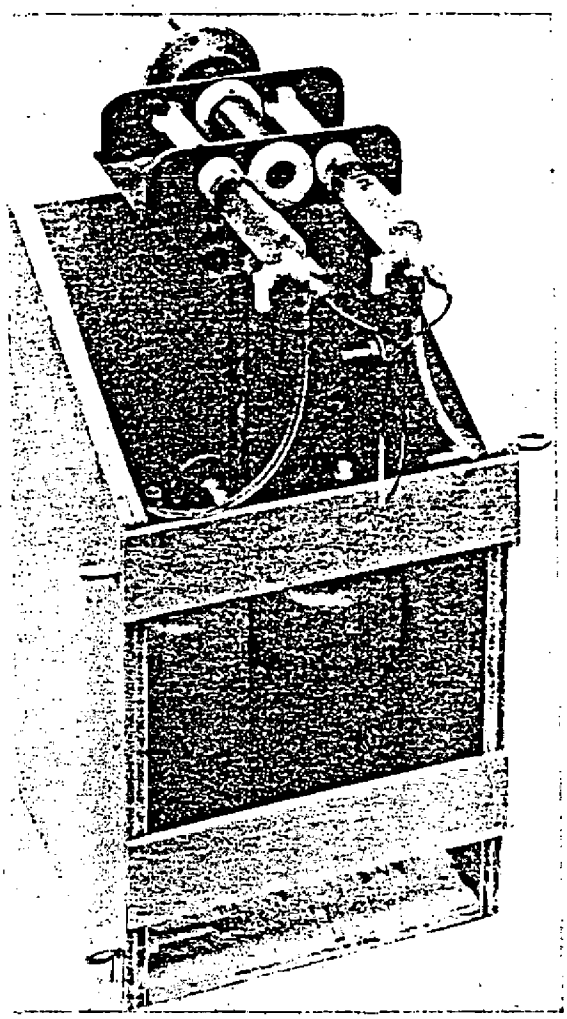


FIG. 1. The reagent dispenser.

[1]B.I. Contribution 275.
[2]Becton, Dickson and Co., Rutherford, N.J.
[3]Bard-Parker Co., Rutherford, N.J.

Printed in Canada (J2234)

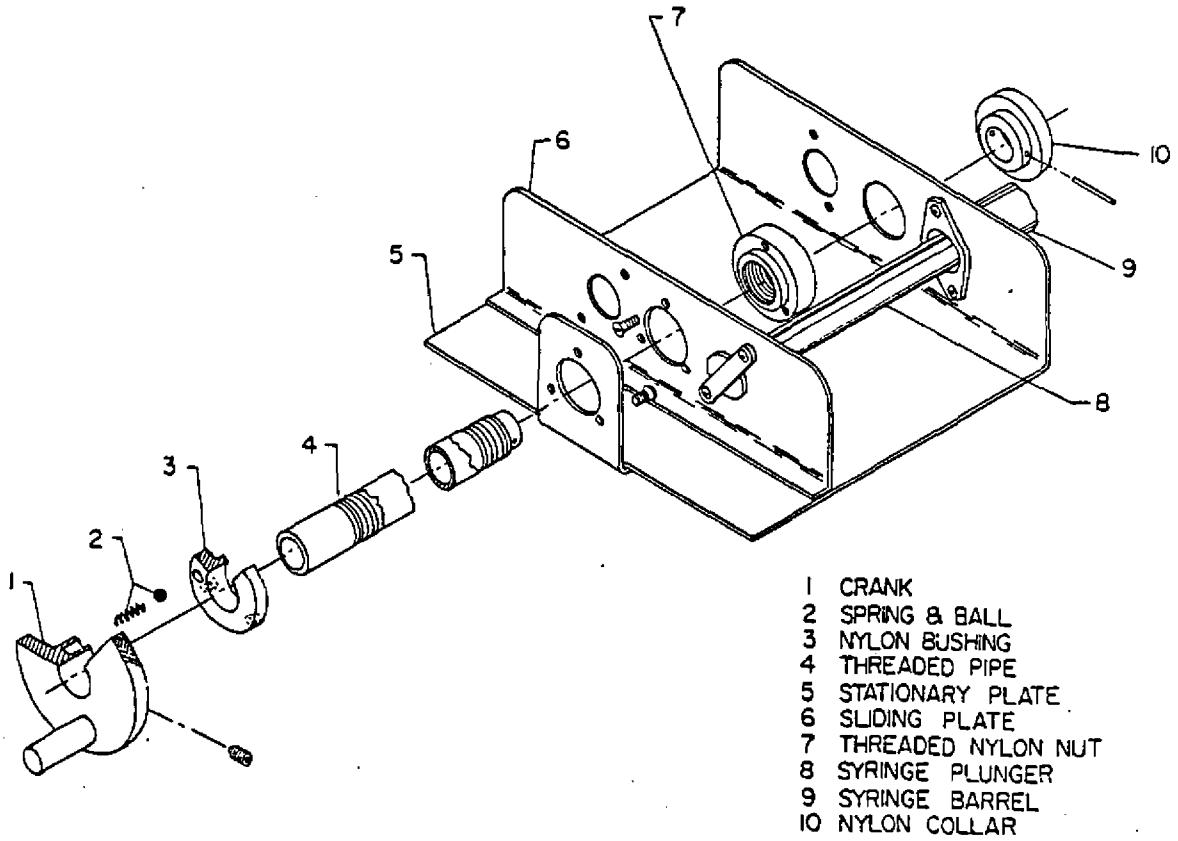


FIG. 2. An "exploded" view of the dispenser.

from a single filling. One revolution of the crank delivers 0.97 ml of each reagent with a repeatability of ±.003 ml. A spring and ball was fixed in the crank and a small hemispherical depression was ground in the nylon bushing so the operator could accurately sense one revolution of the crank. B-P® three-way valves (No. 3406) were fitted on the tops of the syringes to allow convenient refilling from reagent reservoirs.

CARPENTER, J. H. 1965. The Chesapeake Bay Institute technique for the Winkler dissolved oxygen method. Limnol. Oceanogr. 10: 141–143.

Oxygen Distribution in the Pacific Ocean[1]

IVER W. DUEDALL

Fisheries Research Board of Canada, Marine Ecology Laboratory
Bedford Institute, Dartmouth, Nova Scotia

ARTHUR R. COOTE

Atlantic Oceanographic Laboratory, Bedford Institute, Dartmouth, Nova Scotia

A Pacific Ocean oxygen section based on data collected during the *Hudson 70* expedition is presented. The section is on the 150°W meridian and extends from 63°S to 55°N. The oxygen features described are consistent with features reported by Reid (1965). Also shown in the section is evidence for the recently reported bottom current that flows east around Hawaii (Edmond, Chung, and Sclater, 1971).

We report a new oxygen section for the Pacific Ocean. The section is along the 150°W meridian from 63°S to 55°N and was prepared from data collected during the *Hudson 70* expedition (Bedford Institute cruise 69-050). Dissolved oxygen was one of the most useful water-mass indicators measured because its vertical distribution varies considerably and also because it is relatively easy to measure. It can be related to other chemical parameters (e.g., total carbon dioxide, nutrients, and particulate carbon) whose concentrations were also determined by us and by others who participated in the expedition. The present arguments about the origin and maintenance of the oceanic oxygen-minimum zone [*Craig*, 1971; *Menzel*, 1970; *Suess and Goldberg*, 1971] and the apparent need by those planning Geosecs to have more data about the distribution of properties has prompted us to report this data now. The distribution of silicate, nitrate, and phosphate will be reported later.

Figure 1 shows the cruise track and the station positions occupied from April to June 1970. The first station (227) was at 63°S. From 60°S to 10°N the stations were spaced 5° apart and from 10°N to 55°N the station spacing was 6°–7°. At each station about 25 oxygen samples were withdrawn from teflon-coated Knudsen water bottles and then analyzed for dissolved oxygen by a modification of the Winkler method [*Carpenter*, 1965]. Between the surface and 1000 meters the bottles were spaced 100 meters apart, and between 1000 meters and the ocean bottom the spacing ranged from 200 to 400 meters. The sampling technique and details of the Winkler method are described elsewhere [*Duedall and Coote*, 1972]. However, it is worth while pointing out that the precision of our oxygen values at the 95% confidence level is ±0.06 ml/l. It is based on 85 sets of duplicate samples withdrawn from Knudsen bottles at intervals during the course of the expedition, and deposited into separate 55-ml iodine flasks. These flasks varied about 5% in their calibrated volumes.

The oxygen section is shown in Figure 2. It was prepared from vertical profiles of oxygen by contouring the oxygen concentrations at 0.2-ml/l intervals. The main oceanographic features shown in this 150°W section are similar to those in the oxygen section reported by *Reid* [1965] for 160°W, and also in the section reported by *Smetanin* [1962] for 160°W from 69°S to 44°S and for 174°–176°W from about 38°S to 52°N. The main features shown here are the Antarctic intermediate water, the South Pacific deep water, and the Pacific intermediate water.

The Antarctic intermediate water is characterized by a gradual sloping tongue of oxygen-rich water situated at about 700 meters, which

[1] Bedford Institute Contribution.

Copyright © 1972 by the American Geophysical Union.

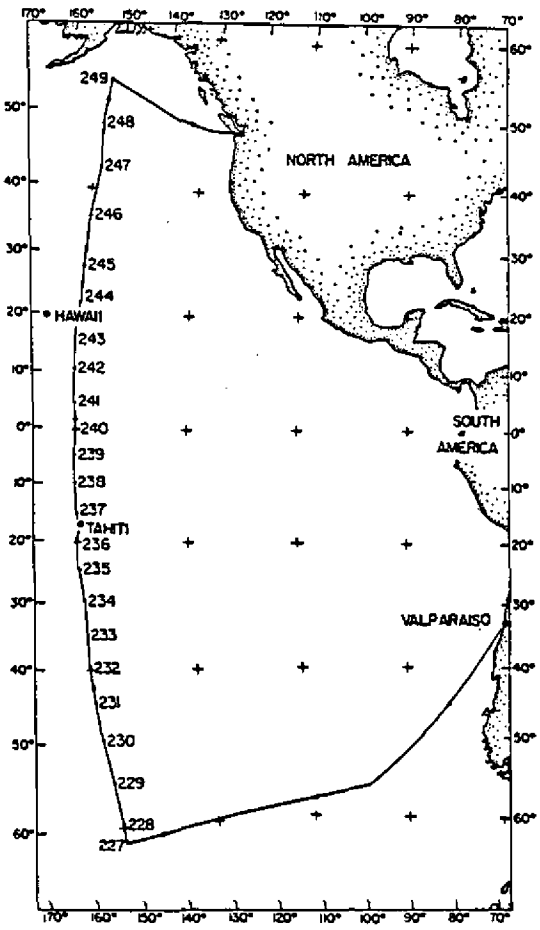


Fig. 1. Location map (polyconic projection) shows the positions of oceanographic stations 227–249 taken during the *Hudson 70* expedition.

extends to about 20°S. This water is analogous to the Antarctic intermediate of the South Atlantic, and it is formed in the south polar-front zone somewhere between 50°S and 55°S, where cold oxygen-rich Antarctic surface water meets warm and slightly more salty subantarctic surface water. The polar-front zone is complicated and is believed to be a region of convergence, although *Gordon* [1971] pointed out that divergence can also occur in this region.

The South Pacific deep water is characterized as a thick trough situated between 1500 and 3500 meters, which is low but fairly constant in oxygen content. In the center of this trough is the deep-oxygen minimum. *Craig* [1971] recently calculated the position of this minimum by means of an advection-diffusion model. This South Pacific deep-oxygen minimum appears analogous to a lens of low-oxygen water observable in the South Atlantic [*Duedall and Coote*, 1972, Figure 2], except that in the South Atlantic the oxygen minimum is not as thick or as deep as it is in the South Pacific. Also the oxygen values in the core of the South Atlantic deep-oxygen minimum are about 0.6 ml/l higher than the values found in the core of the oxygen minimum of the South Pacific deep water [*Reid*, 1965]. The apparent similarity between the deep-oxygen minimums of the South Atlantic and South Pacific suggests that they are formed and maintained by similar processes. However, the South Pacific shows strong east-west gradients in water properties while in the South Atlantic the mid-depth properties are nearly unchanged to the coast [*Reid*, 1965].

The North Pacific intermediate water, which *Reid* [1965] has described so comprehensively, has an intense oxygen minimum where the values in the core range from 0.4 ml/l to 1 ml/l. This oxygen minimum is a dominant feature of the intermediate water because it extends from about 8°S to at least 55°N, and it ranges in depth from 500 meters to 1200 meters (Figure 2). A near-surface oxygen maximum situated between 20°N and 30°N (Figure 2) is also mentioned by Reid as being a significant feature of the intermediate water as well as the North Pacific salinity minimum whose core is situated close to the core of the oxygen minimum. It can be seen in Figure 2 that four zones exist where the oxygen minimum is intensively developed: an equatorial zone, 5°S–5°N; a subequatorial zone, 8°N–12°N; a subtropical zone, 32°N–45°N; and a subarctic zone, 52°N–55°N. It is apparent from Reid's work that the presence of these minimums is a reflection of the North Pacific circulation system where oxygen decreases downstream from its aeration source and replenishment is primarily by vertical diffusion. The equatorial minimum is situated at 500 meters and is the least developed with oxygen values of about 1 ml/l. According to Reid it 'is centered on the boundary between the westward-flowing equatorial current and the south equatorial counter current east of 130°W.' The subequatorial minimum, whose oxygen values drop to about 0.4 ml/l, is situated in a cyclonic gyre formed by part of the north equatorial current and part of the north equatorial counter current [*Reid*,

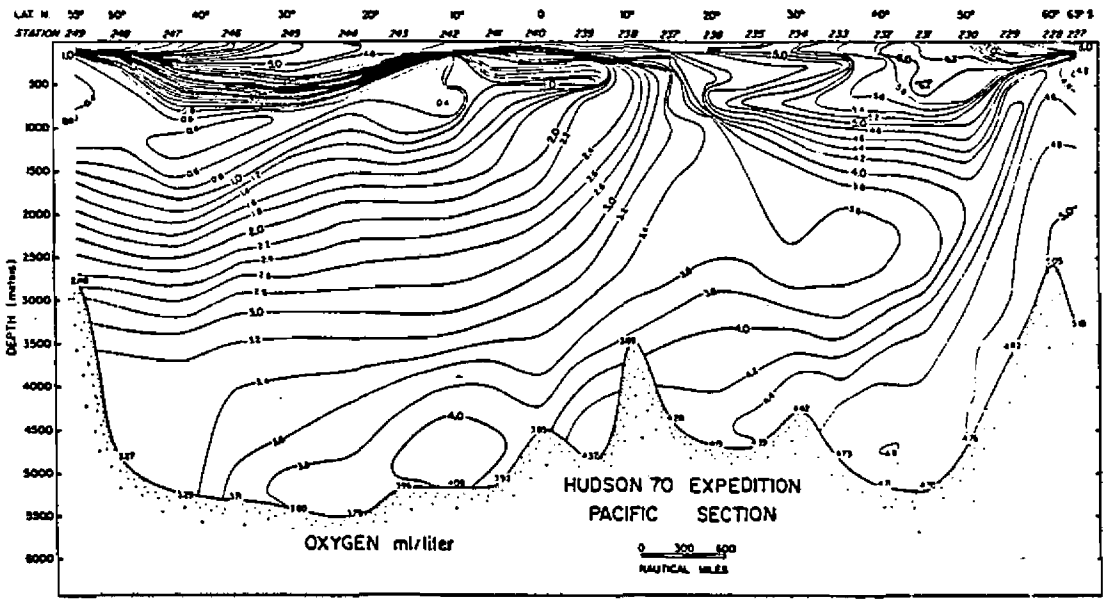


Fig. 2. Oxygen section (150°W) of the Pacific Ocean.

1965]. The subequatorial minimum, whose oxygen values are also about 0.4 ml/l, is situated downstream on the eastern side of the subtropical gyre (anticyclonic). The subarctic minimum whose oxygen values are also about 0.4 ml/l is situated in the subarctic gyre (cyclonic) which extends into the Gulf of Alaska. The above described oxygen-minimum features and gyres are clearly shown in Reid's work [*Reid*, 1965, Figures 18, 20, 23, and 25].

At 5000 meters at stations 243, 244, and 245, the oxygen profiles show slight maximums that are systematic and unexplainable on the basis of the precision of our method. These maximums are probably associated with the newly reported bottom current that branches off from the western boundary current and flows as a narrow current between the mid-Pacific mountains and the Line Islands and then around the Hawaiian Islands ridge [*Edmond et al.*, 1971]. Edmond et al. were not able to detect, using available data, the current further east of 154°W; however, it is apparent from Figure 2 that the bottom flow is detectable to at least 150°W.

Acknowledgments. We thank Carl Cunningham and Elaine Garland for their assistance in drawing the section. We also thank John Edmond for alerting us to his paper in which the bottom current around the Hawaiian Island ridge is described.

REFERENCES

Carpenter, J. H., The Chesapeake Bay Institute technique for the Winkler dissolved oxygen method, *Limnol. Oceanogr., 10*, 141–143, 1965.

Craig, H., The deep metabolism: Oxygen consumption in abyssal ocean water, *J. Geophys. Res., 76*, 5078–5086, 1971.

Duedall, I. W., and A. R. Coote, Oxygen distribution in the South Atlantic, *J. Geophys. Res., 77*, 496–498, 1972.

Edmond, J. M., Y. Chung, and J. G. Sclater, Pacific bottom water: Penetration east around Hawaii, *J. Geophys. Res., 76*, 8089–8097, 1971.

Gordon, A. L., Antarctic polar front zone, in *Antarctic Oceanology I, Antarctic Res. Ser.*, vol. 15, edited by J. L. Reid, 343 pp., AGU, Washington, D.C., 1971.

Menzel, D. W., The role of an in situ decomposition of organic matter on the concentration of non-conservative properties in the sea, *Deep Sea Res., 17*, 751–764, 1970.

Reid, J. L., *Intermediate Waters of the Pacific Ocean*, 85 pp., Johns Hopkins Press, Baltimore, Md., 1965.

Smetanin, D. A., Certain features of meridional distribution of chemical characteristics of water in the Pacific Ocean, *Chemistry of Sea Water*, edited by S. V. Bruevich, 197 pp., translated from Russian, Israel Program for Scientific Translations, Jerusalem, 1968.

Suess, H. E., and E. Goldberg, Comments on paper by H. Craig, Abyssal carbon and radiocarbon in the Pacific, *J. Geophys. Res., 76*, 5131–5132, 1971.

(Received December 23, 1971;
revised January 12, 1972.)

Oxygen Distribution in the South Atlantic[1]

IVER W. DUEDALL

Fisheries Research Board of Canada, Marine Ecology Laboratory
Bedford Institute, Dartmouth, Nova Scotia

ARTHUR R. COOTE

Atlantic Oceanographic Laboratory, Bedford Institute, Dartmouth, Nova Scotia

A new section for dissolved oxygen in the South Atlantic is presented. It has been prepared from data collected during the *Hudson 70* expedition. The section, along the 30°W meridian from the equator to 55°S, confirms that the main oxygen features along this line have remained essentially constant over the last 40 years.

Dissolved oxygen was routinely measured during the *Hudson 70* expedition (Bedford Institute cruise 69-050) because of its relationship to the nutrient and organic carbon cycles in the ocean and its usefulness as a water mass tracer. The oxygen section we are reporting is based on data collected during the South Atlantic phase of the expedition. The data reported are probably relevant to recent questions dealing with oxygen consumption in the deep ocean [*Craig*, 1971]. Also it is timely that we report this section and our techniques since they may be of use to the Geosecs planning group.

The cruise track (Figure 1) of this phase of *Hudson 70* consisted of a north to south transect along the 30° meridian beginning at the equator and extending to 55°S. Twenty-five stations were occupied along this line. The station intervals were 2½° for stations 1 to 20 and 1½° for stations 20 to 25; the last 5 stations were situated in the zone of the antarctic convergence. At each station about 25 samples were analyzed for dissolved oxygen by means of the Winkler method [*Carpenter*, 1965]. Knudsen bottles (teflon lined) were used to collect the water samples. In the depth interval between 0 and 1000 meters the bottles were spaced about 100 meters apart, and in the interval between 1000 meters and the ocean bottom, the spacing was usually 200 meters. Each oxygen sample was carefully withdrawn into a 55-ml iodine flask from a Knudsen bottle within moments after the bottle arrived at the surface; the sample was immediately pickled using a specially designed dispenser that added both oxygen reagents simultaneously [*Duedall et al.*, 1971]. The over-all precision of our technique at the 95% confidence level, based on 85 independent duplicate samples collected throughout the entire expedition, was ±0.06 ml/l.

Figure 2 shows the oxygen section prepared from these data. The section was contoured at 0.2 ml/l oxygen intervals from the vertical profiles for oxygen. Using this interval, the loss of detail in the transcription of the vertical profile data was minimal. The main features of the South Atlantic oxygen distribution, as originally described by *Deacon* [1933], are clearly shown in the section (Figure 2). First, there is the North Atlantic Deep Water, which extends south to nearly 40°S, and is the largest water mass shown. It is characterized by the large mass of water that is nearly homogeneous with respect to oxygen (values range from 5.8 to 6.2 ml/l). Second, there is the Antarctic Bottom Water whose oxygen content ranges from about 4.8 to about 5.8 ml/l. Third, there is the Antarctic Intermediate Water that originates to the antarctic convergence and is shown in Figure 2 as a tongue of high-oxygen water extending to about 28°S, which is sandwiched between the subsurface oxygen minimum and the mid-depth oxygen minimum. The subsurface equatorial

[1] Bedford Institute Contribution 267.

Copyright © 1972 by the American Geophysical Union.

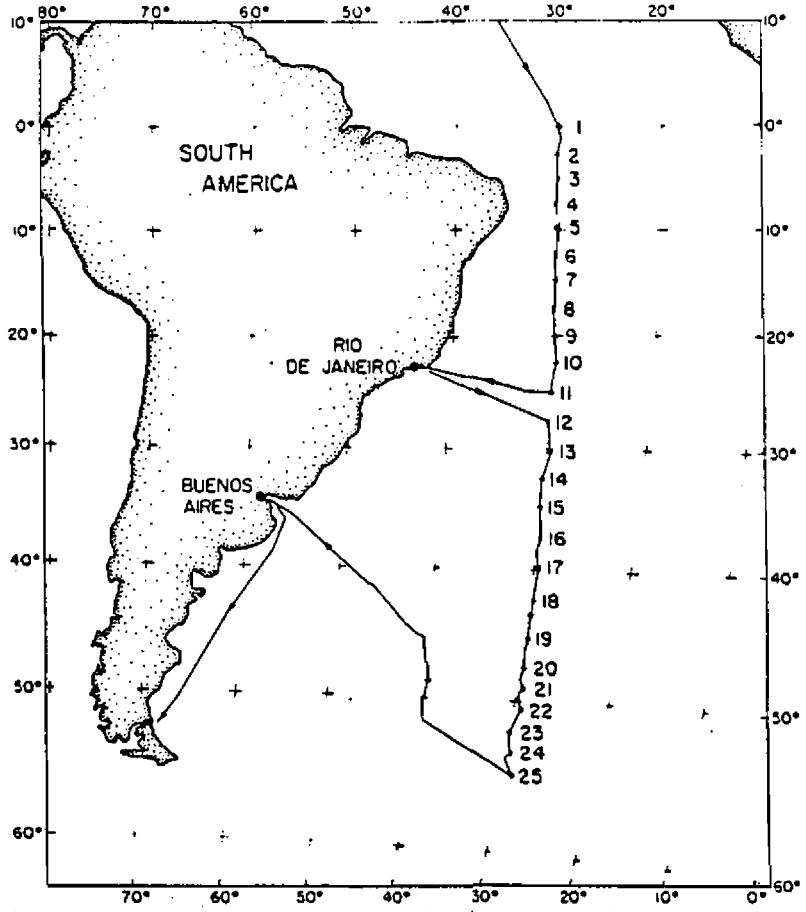


Fig. 1. Location map (polyconic projection) showing the positions of the first 25 oceanographic stations taken during the *Hudson 70* expedition.

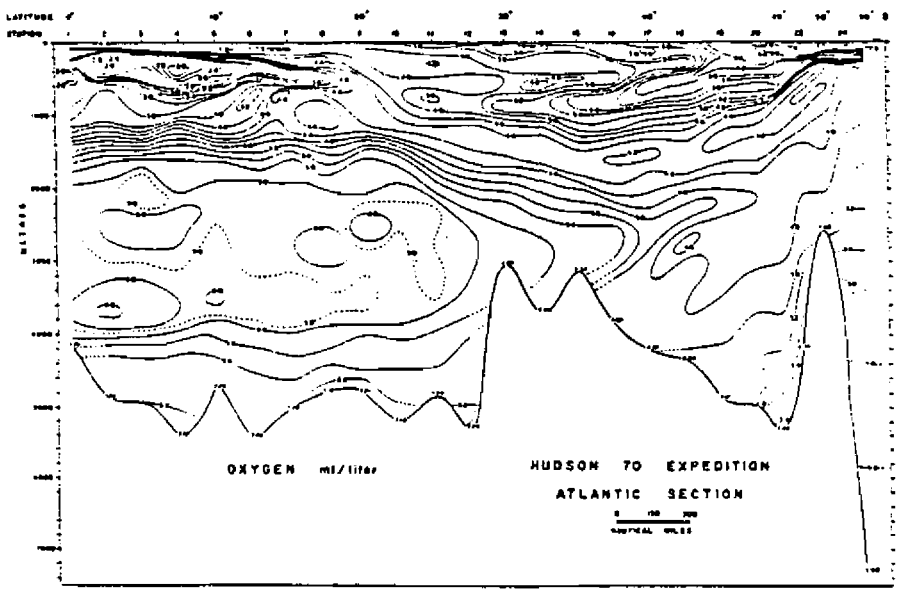


Fig. 2. Oxygen section of the South Atlantic.

water, which in Figure 2 is seen to have a core of very low oxygen values (about 30% of saturation), probably originates off the west coast of Africa where biological processes cause oxygen to be depleted [*Menzel and Ryther*, 1968; *Hart*, 1960].

Descriptions of the above mentioned water masses and others have appeared several times in the literature since the publication of Deacon's work on the South Atlantic. Our oxygen values are about 0.3 to 0.5 ml/l higher than those shown in Deacon's oxygen section. However, it is claimed [*Gordon*, 1967; Gordon, personal communication] that the *Discovery*'s oxygen data was about 0.5 ml/l low because of a systematic error. Accepting this, the section shown in Figure 2 is similar to that reported by Deacon, and confirms the statement that the basic features of the oxygen distribution along this line in the South Atlantic have essentially not changed within the last 40 years, a finding that most oceanographers would expect.

Acknowledgment. We thank C. C. Cunningham for his assistance in drawing the oxygen section.

REFERENCES

Carpenter, J. H., The Chesapeake Bay Institute technique for the Winkler dissolved oxygen method, *Limnol. Oceanogr., 10*, 141, 1965.

Craig, H., The deep metabolism: Oxygen consumption in abyssal ocean water, *J. Geophys. Res., 76*, 5078, 1971.

Deacon, G. E. R., A general account of the hydrology of the South Atlantic Ocean, *Discovery Reports, 7*, 171, 1933.

Duedall, I. W., A. R. Coote, D. F. Knox, and G. F. Connolly, A dispenser for Winkler's dissolved oxygen reagents. *J. Fish. Res. Bd. Can.*, in press, 1971.

Gordon, A. L., Structure of the antarctic waters, *Antarctic Map Folio Ser.*, Folio 6, Amer. Geogr. Soc., New York, 1967.

Hart, T. J., and R. I. Currie, The Benguela Current, *Discovery Rep., 31*, 127, 1960.

Menzel, D. W., and J. H. Ryther, Organic carbon and the oxygen minimum in the South Atlantic Ocean, *Deep Sea Res., 15*, 327, 1968.

(Received October 12, 1971.)

CURRENT MEASUREMENTS IN THE DRAKE PASSAGE

by

LESLIE ALEXANDER FOSTER

Submitted in partial fulfillment

of the requirements for the Degree of

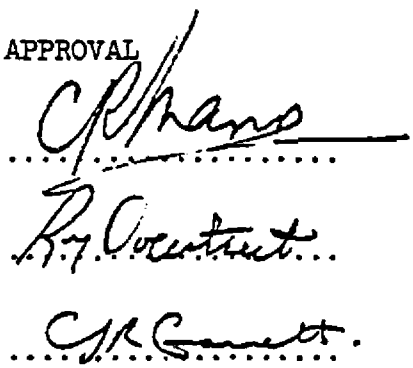
MASTER OF SCIENCE

at

Dalhousie University

March 1, 1972

APPROVAL



DALHOUSIE UNIVERSITY

Date March 1, 1972

Author Leslie Alexander Foster

Title Current Measurements in the Drake Passage

Department or School Oceanography

Degree MSc Convocation - May Year 1972

Permission is herewith granted to Dalhousie University to circulate and to have copied, at its discretion, the above title upon the request of individuals or institution.

Leslie A. Foster
Signature of Author

EXTENSIVE QUOTATION OR FURTHER REPRODUCTION OF THIS MATERIAL FOR COMMERCIAL PURPOSES BY PERSONS OR AGENCIES OTHER THAN DALHOUSIE UNIVERSITY MAY NOT BE MADE WITHOUT THE EXPRESS PERMISSION OF THE AUTHOR.

TABLE OF CONTENTS

ABSTRACT ii

ACKNOWLEDGEMENTS iii

LIST OF TABLES iv

LIST OF FIGURES iv

1. INTRODUCTION

1.1 The Southern Ocean 1
1.2 Data Collection 3

2. CURRENT MEASUREMENTS

2.1 Introduction 8
2.2 Data Reduction 9
2.3 Frequency Analysis 11
2.4 Daily Means 12

3. HYDROGRAPHIC DATA

3.1 Introduction 15
3.2 Water Masses 16
3.3 Current Meter Results 18

4. TRANSPORT

4.1 Introduction 20
4.2 Geostrophic Currents 20
4.3 Drake Passage Transport 22
4.4 Comparison With Past Results 25

5. CONCLUSION 26

BIBLIOGRAPHY 28

APPENDIX I Depth Recorders and Thermographs 32

APPENDIX II Experimental Errors 34

FIGURES 36

ABSTRACT

As part of the Hudson '70 Expedition, an array of 12 current meters was moored in the Drake Passage near longitude 68° W for 10 days in February, 1970. A hydrographic section was run across the passage at the beginning and end of the mooring period. The geostrophic currents using assumed levels of no motion gave results similar to past studies. The current meter records indicated that a minimum velocity is found in the middle of the water column and they also showed the presence of a semi-diurnal tidal component.

The best compromise between the current meter data and the hydrographic data is a variable level of no motion with a net transport of 5 sverdrups toward the west, but because of lack of current meter data at the convergence zone, an unambiguous transport figure could not be determined.

ACKNOWLEDGEMENTS

I would like to thank Dr. C. R. Mann of the Bedford Institute for the permission to undertake this study using the data he collected in the Antarctic and for the supervision he gave to me during the project. I would also like to thank Dr. D. J. Lawrence and Mr. R. R. Lively of the Bedford Institute for the assistance in the reduction of the current meter records and also to the staff of the Ocean Circulation Division for their assistance. Financial assistance was supplied by Dalhousie University and the National Research Council.

LIST OF TABLES

Table 1. Past Studies in the Drake Passage 4

Table 2. Station Positions.....5

Table 3. Current Meter Summary 13

LIST OF FIGURES

Figure 1. Location Map 36

Figure 2. Mooring Configuration 37

Figure 3. Progressive Vector - Rate Direction Diagrams 38

Figure 4. Current Meter Power Spectra 41

Figure 5. Daily Average Currents 46

Figure 6. Temperature Cross Section 49

Figure 7. Salinity Cross Section 50

Figure 8. Sigma-T Cross Section 51

Figure 9. Oxygen Cross Section 52

Figure 10. Core Layers 53

Figure 11. Potential Temperature-Salinity 54

Figure 12. Potential Temperature-Oxygen 55

Figure 13. Geostrophic Velocity- Horizontal Reference Level 56

Figure 14. Geostrophic Velocity- Variable Reference Level 57

Figure 15. Current Meter Velocities (contoured) 58

Figure 16. Velocity Shears 59

Figure 17. Depth Recorder Plots 60

Figure 18. Thermograph Records 61

CHAPTER 1

INTRODUCTION

1.1 The Southern Ocean

The circulation of the world ocean is intimately tied to that of the Southern or Antarctic Ocean. In its unique position, it encompasses a part of every ocean, the Atlantic, Pacific and Indian and its properties are felt in each. Three important features of the physical oceanography of the Southern Ocean are the Antarctic Circumpolar Current, the Antarctic Convergence and the Antarctic Bottom Water.

The first significant expedition to the Antarctic region was the Discovery (Clowes 1933, Deacon 1937). Other major expeditions have been the Ob (Kort 1959) and the Eltanin (Gordon 1967b). Since the Drake Passage is the narrowest part of the system, various transport calculations have been made there. Until 1971, all estimates of the transport in the Antarctic Circumpolar Current depended on hydrographic data alone through the use of the geostrophic assumption. Depending on the "level of no motion" assumed, the transport varied from 0 to 218 sverdrups (1 sverdrup = 10^6 m^3/sec) eastward through the Drake Passage (Gordon 1967a). Reid and Nowlin (1971) reported on the transport through the Drake Passage using bottom current meter data of up to 4 days duration and arrived at 237 sv directed toward the east. South of Australia, Callahan (1971) found an easterly transport of 233 sv using bottom current meter data of 1 to 2 days duration. Bottom current patterns have been deduced from the potential temperature distribution and bottom photographs (Gordon 1966).

The Antarctic Circumpolar Current is different from other major current systems for three reasons: it is not impeded by land barriers (except the 1000 km constriction at the Drake Passage), the waters are weakly stratified (a seasonal thermocline is not present), and the permanent wind field is zonal and westerly (Ichiye 1970). Over most of the region of the Circumpolar Current, the depths are greater than 3000 m but to the east of the Drake Passage in the Sandwich Arc, depths of less than 1000 m are found. There are also a series of ridges across the Drake Passage near 59° W which rise to 1700 m (Reid and Nowlin 1971).

Various theoretical studies have been made of the Antarctic Circumpolar Current (Munk and Palmen 1951, Hidaka and Tsuchiya 1953, Stommel 1957, Ichiye 1970, Gill and Bryan 1971). A detailed survey of the various theories was made by McKee (1966). The zonal transports obtained by Munk and Palmen and Hidaka and Tsuchiya are orders of magnitude higher than assumed unless very large values of lateral eddy viscosity are used. Stommel closed off the Drake Passage. Kamenkovich (as reviewed by McKee (1966)) discussed the influence of bottom relief on the Antarctic Circumpolar Current. Ichiye determined the transport by means of the zonally averaged hydrodynamic equations and found values of transport through the Drake Passage corresponding to those obtained by Reid and Nowlin (1971). Gill and Bryan's numerical model showed that a "shallow gap" Drake Passage gave rise to a greater zonal transport than a "deep gap" model.

At the centre of the Circumpolar Current is the Antarctic Convergence or Polar Front. Well known as a region of high productivity, its exact nature is not well understood, and in fact there is a controversy over whether or not it is a region of convergence or divergence or both (Gordon 1967b). Its position varies as much as 4° of latitude even in

the narrow Drake Passage (Gordon 1967b).

The formation of the Antarctic Bottom Water is thought to be mainly in the Weddell Sea and its properties have been traced well into the Atlantic (Warren 1971). There are several theories of its formation (Gordon 1971a).

Direct current measurements are rare in the Southern Ocean and more are needed to detail the above features. Ledenev (1961) reported on surface currents in the Drake Passage and southern Pacific using a GEK. Capurro (1967, 1968) used parachute drogues and Swallow Floats to make deep measurements but no transport calculations were made. Reid and Nowlin (1971) and Callahan (1971) have been mentioned previously. A summary of past investigations into the transport through the Drake Passage is shown in Table 1 (after Gordon 1967a).

One of the objectives of the Hudson '70 Expedition from the Bedford Institute was to measure the currents in the Drake Passage with an array of self recording current meters and run a hydrographic section in order to estimate the volume transport.

1.2 Data Collection

To measure these currents, an array of 12 moored current meters was laid and other hydrographic data collected in the first two weeks of February 1970. The area of survey and station positions are shown in Figure 1 and the positions detailed in Table 2. From January 31, 1970 to February 4, 1970, the 4 current meter moorings were laid and hydrographic stations 32 - 35 completed. From February 11 to 15, the moorings were recovered, stations 38 to 44 and Bathysonde stations 29 to 35 completed.

AUTHOR	DATA	SEASON	REFERENCE LEVEL	METHOD	TRANSPORT (sv)
Clowes (1933)	Discovery	Summer	3500 m	Deep Isobaric Surface	110 (above 3500 m)
Sverdrup (1942)	Composite	Composite	3000 m	Deep Isobaric Surface	90
Kort (1959)	Ob	Winter	3000 m Bottom	Deep Isobaric Surface Bottom	134 165
Ostapoff (1960)	Discovery	Summer	Variable	Defant's method with Equivalent Barotropic Assumption	nil
Ostapoff (1961)	Discovery	Summer	Variable 2000 m 3000 m	Defant-Eq. Bar. Ass. Deep Isobaric Surface Deep Isobaric Surface	nil 33 85
	Ob	Winter	Variable 2000 m 3000 m	Defant-Eq. Bar. Ass. Deep Isobaric Surface Deep Isobaric Surface	9 34 86
Eskin (1962)	Composite	Summer Winter	3500 m 3500 m	Deep Isobaric Surface Deep Isobaric Surface	150 123
Gordon (1967a)	Ob	Winter	Variable	T-S relation with Eq. Bar. Ass.	218
Reid & Nowlin (1971)	Thomas Washington	Summer	Variable Bottom Currents	Deepest common depth Moored current meters	114 237

TABLE 1 Summary of past investigations into Drake Passage transport (after Gordon 1967a)

STATION	LATITUDE	LONGITUDE	DATE
(Bathysonde)			
29	56° 41.1's	68° 27.5'W	10 Feb. 1970
30	57 02.1	68 25.4	10 Feb.
31	58 01.4	68 17.6	11 Feb.
32	58 58.5	68 03.4	12 Feb.
33	60 01.6	67 54.6	12 Feb.
34	61 02.2	67 43.3	13 Feb.
35	61 58.3	67 35.2	13 Feb.
36	62 59.6	67 13.5	14 Feb.
37	63 59.6	66 57.4	14 Feb.
38	64 20.0	66 58.0	14 Feb.
(Bottle)			
32	57 48.6	68 18.5	31 Jan.
33	60 16.3	67 59.6	2 Feb.
34	62 07.2	67 33.0	3 Feb.
35	63 34.1	66 47.6	4 Feb.
38	57 33.5	68 15.7	11 Feb.
39	58 28.3	68 06.2	11 Feb.
40	59 29.7	67 57.7	12 Feb.
41	60 32.1	67 45.6	12 Feb.
42	61 31.0	67 29.0	13 Feb.
43	62 28.2	67 17.8	14 Feb.
44	63 30.6	67 06.2	14 Feb.
46	60 53.6	57 46.0	17 Feb.
47	60 23.3	56 42.6	18 Feb.
(Mooring)			
1	57 49.2	68 19.6	1-11 Feb.
2	60 04.5	68 04.0	2-12 Feb.
3	61 59.0	67 33.3	3-13 Feb.
4	63 28.1	67 07.0	4-14 Feb.

TABLE 2 Station Positions

21 Sippicon Expendable Bathythermographs (XBT) were launched to a depth of 750 m at frequent intervals along the section line.

Each hydrographic station consisted of Knudsen Bottles with reversing thermometers (protected and unprotected), the bottom bottle being lowered to within 10 m of the sea floor with the aid of a pinger. The salinities were measured on board ship using an Autolab Inductive Salinometer and the oxygen content was measured by the Winkler method. The temperature data from the bottle casts were corrected using the most recent thermometer calibrations. Continuous bottom soundings were obtained with an EDO Echo Sounder in conjunction with a Gifft Precision Depth Recorder and navigation control was by means of the United States Navy Navigational Satellite System (ITT receiver on line with PDP-8L computer).

Each current meter mooring consisted of a subsurface float, 3 Braincon Histogram Current Meters set for 150 m and 1500 m from the surface and 120 m from the sea floor, a Braincon Model 562 Depth Recorder near the top current meter, 3 Braincon Model 146 Thermographs at the same depths as the current meters and an acoustic release above the anchor. Of the total of 12 current meters used, 11 were Braincon Model 381 and the other a Braincon Model 316. The general mooring configuration is shown in figure 2.

The data recovery was excellent--all moorings came up on command, all current meters, depth recorders and 10 of the 12 Thermographs gave usable data. The weather was good for this phase with the exception of a strong south easterly storm in the middle of the recording period.

The length of the time series collected (10 days) would not allow a complete tidal analysis, but the data could be used to demonstrate

the variability of the flow, to estimate the transport and offer a comparison with the geostrophic calculations.

CHAPTER 2

CURRENT MEASUREMENTS

2.1 Introduction

There are various methods of measuring ocean currents; Swallow Floats, parachute drogues, Transport Floats (Volkmann 1962) and moored current meters. Of these methods, moored current meters enable one to examine higher frequency components and take longer time series at a particular location. The main problem with moored current meters, other than the laying and recovery and instrument malfunction is that of mooring motion. In the experiment reported here, the meters recorded tilts of the mooring line and the top recorder had a depth recorder just above it. The problems of mooring motion are discussed in Appendix II.

The Braincon Histogram Current Meter (Model 381 or 316) measures speed with a savonius rotor and direction with a large tail fin which orients the entire instrument case relative to a magnetic compass--the instrument case being free to rotate on a tension rod to which the mooring line is attached. The information is recorded in analogue form on 16 mm film--each film frame being held steady while a time exposure is built up of current speed (number of revolutions of the rotor), direction, tilt and tilt direction. To establish a time reference for each film frame, a luminous wristwatch is incorporated into the recording mechanism such that a time exposure of the watch face is recorded on each frame. The film is then advanced in the next minute, making a total of 20 minutes for each data frame. Therefore, over a recording interval, one can find the

average speed, the most frequent direction of the current, the angle and direction of tilt and the time.

2.2 Data Reduction

Each film frame is read on a film reader and the data transferred to magnetic tape. The readings consist of the arc length proportional to the number of revolutions of the savonius rotor, the mid point of the direction arc and the tilt angle and direction. The resulting magnetic tape is then edited to correct obvious reading errors and the starting and ending times are established with the aid of the mooring logs in conjunction with the times recorded on the film. A frame count is made to ensure that no readings have been added or deleted. Magnetic compass readings are converted to true directions using compass calibrations done at the Bedford Institute. A problem developed here since some calibrations were not done until a year after immersion of the meters and also because the calibrations were done at the Bedford Institute while the recordings were made in Antarctica. This point will be discussed in Appendix II on experimental errors. The angular length of the speed arc is converted to current speed with the aid of a calibration curve supplied by the manufacturer. The final tape then produced contains the speed and true direction for each 20 minute interval--this tape forming the basis for further analysis. For numerical analysis of the data, the readings were resolved into two components, the major component at 085° and the minor at 355°, these directions being perpendicular and parallel to the section line respectively.

For display purposes, the data are presented in two formats--rate-direction and progressive vector for all meters (figure 3). A summary

of the data obtained is shown in Table 3.

All the rate-direction plots show what appears to be a semi-diurnal component, this being more evident in the shallow and deep meters. Also, it can be seen that the highest speeds occurred at the shallow and deep locations, while the intermediate depths had speeds the order of 5 cm/s, the threshold of the instrument. The variability of flow is indicated by the number of changes that took place over the recording interval. At meter 4-3332 (station 4, depth 3332 m), the currents began weakly but became constant in direction after about February 8. Meter 1-3649 has a very definite semi-diurnal component and what appears to be a 10-day component while meter 4-1482 shows a complete direction change during the 10 days of recording. Meter 1-162 started out with a strong current which died towards the end of the recording period while 2-145 did the reverse.

A progressive vector diagram is generated by the vector addition of each current reading and represents the path a small water element would follow provided the current was uniform over an area of the ocean at least as large as that covered by the diagram. Although this may be an unreasonable assumption, this type of diagram is an excellent way of revealing any rotational motion or change in the mean current and gives a quick general summary of current variability and trend. These diagrams (figure 3) show that there is a strong eastward flow at the north and south ends of the Drake Passage near the surface while at the same depth in the center of the passage a convergence is seen with the southward flow increasing in strength and the northward veering in direction from north-west to north-east. Except for meter 2-3338 which showed northerly flow, the current at the deep locations was generally to the west. At the intermediate depths, the flow was generally south-east at the northern

stations, northwest at station 3 and the previously mentioned reversal at mooring 4.

On most records, a significant change took place on or about February 8. At meters 1-162, 1-1512 and 2-3338 the current slowed down while at meters 2-145 and 4-3332 it speeded up around this time. The reversal at meter 3-1480 occurred the same day. It is possible that this event is related to a storm which passed through the area on February 7, on which date winds of 70 knots from 140° were logged by the ship (the position of the ship was about 300 nautical miles east of mooring 3).

2.3 Frequency Analysis

In order to separate the M_2 and S_2 tidal components, record lengths of 15 days or more are required. Since these records were all less than 15 days in length, a power spectrum analysis was run in order to determine the dominant frequency components. Following this procedure, a finite Fourier Analysis was run in order to estimate the amplitude of the dominant components.

A Power Spectrum Analysis (Munk, Snodgrass and Tucker 1959 and Blackman and Tukey 1959) gives an estimate of the power contained in each frequency band. For each component current, the data were normalized so that the average was zero, the lagged products calculated and the sine and cosine transformations taken. The resulting energy was smoothed by Hamming. For the longer records, the spectra were estimated over 112 frequency bands, each bandwidth being .013 cycles/hour. For the shorter records the corresponding figures were 56 frequency bands with a bandwidth of .027 cycles/hour. The spectra for all records are shown in figure 4

with the 95% confidence limits noted. It can be seen that there is only one significant peak in each record, its magnitude being greater at the shallow and deep meters. This dominant peak on all records occurs at a period of 12.4 hours indicating that the dominant period is of tidal nature rather than inertial which in this region ranges from 13.4 to 14.5 hours. It must be stated again though, that the records were not long enough to do a more detailed analysis.

To estimate the amplitude of the tidal currents near a period of 12.4 hours, the method of Finite Fourier Analysis was used. In this method, one fits the time series to a sum of sinusoids of varying amplitude and phase, each sinusoid being a harmonic of the length of the record. Since the records were of varying length, it was decided to shorten each such that one of the harmonics was of period 12.4 hours. At the most, this involved truncating 8 hours off the longest records. The resulting amplitudes of the harmonics near 12.4 hours are shown in Table 3. As was expected, the greatest tidal currents occurred at the shallow and deep locations.

2.4 Daily Means

To estimate the volume transport through the Drake Passage, a daily mean current was determined in order to tie in with the hydrographic data (Chapter 3). With longer record lengths than these, all the tidal components can be computed and subtracted from the record giving a residual current of which the daily mean is taken. With shorter records, the data can be smoothed by taking a running mean with length at least twice as long as the dominant period--in this case 12.4 hours and calculating the daily

METER	DURATION (days)	PEAK SPEED (cm/s)	MEAN SPEED (cm/s)		SEMI-DIURNAL TIDAL AMPLITUDE (cm/s)	
			MAJOR	MINOR	MAJOR	MINOR
1-162	10.3	53.5	27.5	4.0	8.1	4.9
1-1512	10.3	15.4	1.7	2.3	2.5	0.7
1-3649	10.3	30.4	-6.1	4.1	8.2	5.4
2-145	10.5	51.5	-13.3	17.4	7.2	3.5
2-1495	4.3	11.3	0.7	1.5	3.2	1.2
2-3338	10.5	12.4	-1.5	-4.1	2.5	0.9
3-130	10.7	23.7	-1.2	-5.6	3.4	0.6
3-1480	10.7	9.8	-2.2	-2.1	2.0	0.6
3-3370	6.3	21.6	-6.2	-4.7	5.4	2.1
4-132	4.3	27.8	11.5	2.9	3.8	0.2
4-1482	10.3	10.8	-0.7	1.0	1.4	0.6
4-3332	10.3	27.8	-6.9	1.0	3.3	1.0

TABLE 3 Current Meter Summary
(Positive directions are east and south respectively)

mean of the smoothed record. The latter procedure was followed with the present data and the daily mean of the smoothed record was calculated as was the daily mean of the unfiltered record. Since the dominant period was so near 12 hours, there was virtually no difference between the two approache Also, in smoothing the data with a 24.8 hour running mean, a complete day's record is lost. Therefore, the daily mean was calculated by simply taking the mean of the unfiltered data and the results can be seen in section in figure 5b for the major and minor components. In figure 5a, the same data can be seen in horizontal plan. In examining figure 5, it can be seen that eastward flow is found at the north and south ends of the passage near the surface with westerly flow elsewhere. In figure 5a, the convergence zone is seen clearly at the 150 m depth.

Before a transport value can be calculated, the hydrographic data will be presented and the various water masses discussed.

CHAPTER 3

HYDROGRAPHIC DATA

3.1 Introduction

As outlined in Chapter 1, the following hydrographic data were collected: 11 bottle stations to within 10 m of the sea floor, 21 XBT's to 750 m, 10 Bathysondes to 2500 m and continuous bottom soundings. Unfortunately, the Bathysonde data had some unresolved discrepancies in them as compared to the bottle data and as a result were not used. The XBT's were used to complete the temperature cross sections. The bottom soundings, obtained using an assumed sound velocity of 1463 m/s were corrected for the calculated sound velocity from the nearest hydrographic station. In general, the corrections amounted to an addition of about 60 m to a recorded depth of 3500 m and correspondingly smaller amounts for shallower soundings. The data collected are presented in cross sections of temperature, salinity, sigma-t, and oxygen for stations 38-44 since they were done consecutively in a four-day period (figures 6-9). Also shown are the cores of the various water masses (figure 10) and the Potential Temperature - Salinity and Oxygen diagrams for all stations (figures 11 and 12). From the examination of these figures, one can identify the various water masses present and with the aid of the progressive vector diagrams from the current meters (figure 3) and the daily means (figure 5), the motion of each mass can be deduced and compared to the assumed motion obtained from previous studies of the circulation.

3.2 Water Masses

As in previous studies of the Antarctic waters (Sverdrup 1942, Deacon 1963, Kort 1959, Miditun and Natvig 1957, Gordon 1967b, 1971b) a clear separation of the various water masses is apparent from figures 6-12. Proceeding north from the Antarctic, the sea surface temperature increases slowly from 1.6°C until at latitude 61°S, the gradient increases sharply to 4°C and then increases slowly again. The area of 61°S is significant on all section diagrams--the vertical gradients of temperature, salinity, sigma-t and oxygen are all large south of this point in the first 250 m. At 61°S the isolines experience their steepest northward slope--this then is the Antarctic Convergence or Polar Front. That it is a convergent region is shown in the diagram of the daily mean current (figure 5a).

South of the convergence and above 250 m is the Antarctic Surface Water. It is cold (-1°C to +1°C), fresh (salinity 33.7 o/oo to 34.1 o/oo) and is strongly stratified with the density increasing from 27.0 o/oo to 27.6 o/oo. The oxygen values found here are the highest in the section (6-8 ml/l). On the Potential Temperature - Salinity and Oxygen diagrams, this mass is labelled--note how it stands out from waters at the same depth north of the convergence (figures 11 and 12). The Core Layer of the Antarctic Surface Water is the temperature minimum (Gordon 1967b) which can be traced to just north of the convergence (figure 10). The properties of this water mass are determined by ice melting in the summer, making it fresh, and by cooling in the winter (Gordon 1967b).

Below 3000 m and south of the convergence is some Antarctic

Bottom Water with temperature below 0.5°C, density 27.86 o/oo and oxygen 5 ml/l. Since it is felt that most Antarctic Bottom Water is produced in the Weddell Sea (Gordon 1971b), its presence here is a good indication of a westerly bottom current as is indicated by the current meters and postulated by Gordon (1966).

Between the Antarctic Surface Water and the Antarctic Bottom Water is the largest mass in the section diagrams--the Circumpolar Deep Water. With temperature varying from 0.5°C to 2°C, it is found beneath 250 m in the south and 2000 m in the north of the section. It is characterized on its upper boundary by a temperature maximum layer below the Antarctic Surface Water and an oxygen minimum throughout the section (Gordon 1967b). Its core is a salinity maximum. The salinity and sigma-t values of this mass are nearly 34.7 o/oo and 27.8 o/oo respectively. On the Potential Temperature - Salinity and Oxygen diagrams (figures 11 and 12) this mass is common to waters north and south of the convergence. It is believed to move in a generally southward direction in the Atlantic bringing waters from the northern ocean to the Antarctic. Upon reaching the Antarctic, part of the water mass is converted at the sea-air interface to form Antarctic Surface Water while the remainder mixes with the shelf water to form Antarctic Bottom Water. The Circumpolar Deep Water is generally thought to circulate in an easterly direction as the Antarctic Circumpolar Current (Gordon 1971a).

North of the Antarctic Convergence is the Sub-Antarctic Surface Water with higher temperatures and density of about 26.9 o/oo to 27.1 o/oo. It is generally southward moving and meets the Antarctic Surface Water at the convergence. The resulting mixture having a higher density sinks and moves northward as the Sub-Antarctic Intermediate Water. This mass

is separated from the Circumpolar Deep Water beneath it by a tongue of high oxygen (5-6 ml/l) obtained from the Antarctic Surface Water as well as a salinity minimum core.

On the Potential Temperature - Salinity and Oxygen diagrams (figures 11 and 12), the stations north and south of the convergence are plotted with closed and open circles respectively. It can be seen how the water masses are different on either side of the convergence and above the Circumpolar Deep Water but unite to form a common mass at the Circumpolar Deep Water.

The data presented here is similar to both the Discovery (Deacon 1937) and the Ob (Kort 1959) cross sections--what do the current meters indicate about the general motion of the water masses?

3.3 Current Meter Results

In figure 10 are shown the different water masses as defined by their core layers. In attempting to use the bottom current meters to estimate the mean motion, some difficulties may ensue since it can be seen that meters 1-3649 and 2-3338 are near topographic lows.

With this qualification in mind, meters 1-1512, 1-3649, 2-1495, 2-3338, 3-1480 and 4-1482 are in the Circumpolar Deep Water as defined by the oxygen minimum. At meters 1-1512 and 2-1495, the motion is south-east as postulated for the CDW however 3-1480 is northwest while 4-1482 has the reversal from south-east to south-west. The peak speeds of these currents are about 10 cm/s. The bottom meters, 1-3649 and 2-3338 show south-west and north motion respectively.

The meters in the Antarctic Bottom Water, 3-3370 and 4-3332 show the west motion as postulated by Gordon (1966) with peak speeds of 22 and 28 cm/s respectively.

Meter 1-162 has the highest speeds (peak 53.5 cm/s) and is predominately eastward while 2-145 is south-west with a peak of 51.5 cm/s. These meters are in the Sub-Antarctic Surface or Intermediate Water. The salinity minimum layer separating these masses is very close to meter 1-162.

At the other side of the convergence, meter 3-130 is definitely in the Antarctic Surface Water and has a northerly motion with a peak speed of 23.7 cm/s while 4-132 indicates easterly motion with a peak of 27.8 cm/s. It should be noted that the southward flow to the convergence was stronger than the northward and as the southward increased in strength, the northward diverted from north-west to north-east.

CHAPTER 4

TRANSPORT

4.1 Introduction

The purpose of this chapter is to combine the hydrographic and current meter data in order to estimate the volume transport through the Drake Passage. Using the available data, the transport may be calculated by various means: the geostrophic method using an assumed level of no motion, the current meter data alone or the geostrophic method using the current meters as reference.

4.2 Geostrophic Currents

The dynamic method of computing ocean currents (Neumann and Pierson 1966) or the geostrophic method makes use of the basic assumption that in a steady state, the horizontal pressure gradient and coriolis force are in equilibrium and friction is not considered. From the distribution of the density the relative pressure gradients can be computed. The surface relative to which current velocities are computed is called the reference surface and in order to obtain an absolute velocity of the current, it is necessary to know the velocity at this reference surface, either by direct measurement or by inferring a surface of zero-velocity called a "level of no motion". A first assumption is that at great depths, the velocity is zero. In the Antarctic, where the water is

weakly stratified and no permanent thermocline is present, estimates of levels of no motion have varied from a horizontal one at 2000, 3000, or 3500 m (Sverdrup 1942, Ostapoff 1961, Miditun and Natvig 1957) to a variable-depth reference (Ostapoff 1960, 1961, Gordon 1967a).

The variable level of no motion used by Ostapoff (1960, 1961) is a result of the Equivalent Barotropic Assumption of Neumann (1960). First applied to the Gulf Stream, the assumption is that a stratified upper layer is moving upon a more uniform lower layer. In practice, Ostapoff assumed Defant's (1961) level of no motion in the South Atlantic of 2500 m to be correct for the northern Drake Passage. He then calculated the mean density of the upper layer to that depth. At successive stations to the south he then determined the depth of the upper layer which had the same mean density. Since the water became denser to the south, the depth of constant mean density reached closer to the surface. This variable depth was then used as the "level of no motion".

Gordon (1967a) used the Equivalent Barotropic Assumption for his level of no motion but the starting point was different. From the analysis of the hydrographic data (Gordon 1966), he deduced that all the currents in the northern Drake Passage were easterly with no zero reference layer and that the only westward flow occurred in the southern part of the passage beneath 1800 m. As a result, his level of no motion began at 1800 m in the south Drake Passage and with the aid of the Equivalent Barotropic Assumption was extrapolated to a total depth of 9000 m in the north. It should be noted that this reference level intercepted the sea floor at latitude 59°S.

The resulting transport figures for these reference levels are given in Table 1.

4.3 Drake Passage Transport

The first approach taken was to assume a horizontal level of no motion in order to compare the data taken by the Hudson with that of the Discovery and the Ob. A depth of 3000 m was adopted and the results are shown in figure 13. It can be seen that the net transport was to the east (72 sv) with a small westerly flow above the reference level between stations 40 and 41 and below the reference level elsewhere. This transport resembles other results in the same area (Table 1). The greatest eastward flow occurred in the region of the convergence with a peak surface speed of 23.7 cm/s. The westward flow between stations 40 and 41 and low vertical shear is a characteristic of the Southern Ocean (Reid and Nowlin 1971, Miditun and Natvig 1957, and Callahan 1971) and has been noted in sections at 68°W, 90°W and 132°W. Reid and Nowlin give as the origin of the westward flow, above the reference level, the deflecting nature of the ridge located to the east of the Drake Passage while Callahan attributes it to counterflow over the Indian-Antarctic Ridge. Thus in many respects, the geostrophic flow pattern using these data and the 3000 m reference level resembles previous results.

The next approach was to use the Equivalent Barotropic Assumption in the manner of Ostapoff (1960, 1961). The mean density to 2500 m in the northern Drake Passage (station 38) was 27.464 o/oo. Using this

value, the depth to which the mean density was 27.464 o/oo was calculated for the other stations and the reference level was taken as the mean of adjacent stations. The resulting level of no motion was:

Station Pair	Level
38-39	2329 m
39-40	1780 m
40-41	1445 m
41-42	1036 m
42-43	466 m
43-44	309 m

The results are shown in figure 14. The net transport is 5 sv toward the west and compares with Ostapoff's value of zero for the Discovery and Ob sections. The major difference occurred between stations 40 and 41 where the transport was toward the west above the reference level whereas Ostapoff found all the westward transport below the reference level.

The current meter data alone were used to estimate the volume transport by contouring the velocity sections perpendicular to the passage for February 5, 10, and the overall mean current and calculating the volume transport. The results can be seen in figure 15. All the current meters were operating on February 5, but by the 10th, three of them had stopped--for these three, extrapolations from previous days records were used and the values are shown in parenthesis. From figure 15, it can be seen that a significant change took place in the transport between February 5 and 10. On February 5, the eastward flow was pronounced at the northern end of the passage near the surface with a peak speed of 39.6 cm/s while by the 10th, this speed had decreased to 7.7 cm/s. Similarly,

at mooring 2 near the surface, the daily mean increased from 10.3 to 21.6 cm/s to the west. At the southern end of the passage, the flow to the east also decreased between February 5 and 10. On both days, the net transport was toward the west, 4 sv and 62 sv respectively. For the overall mean of the current meters, the transport was 15 sv toward the west. These results are, of course, limited by the fact that some meters only operated for a few days, no current meter data were available at the location of the highest geostrophic velocity (station pairs 39-40 and 41-42) and constant velocity shears were assumed both vertically and horizontally between current meter locations.

It was hoped that the means of the current meter data could be used in conjunction with the hydrographic data in order to assign a reference velocity to the geostrophic calculations. In figure 16 is seen a comparison of the vertical shears as measured by the current meters as near as possible to the same day as the running of the hydrographic station pair, the mean vertical current meter shear and the geostrophic shear. In one case, (mooring 4), the geostrophic currents as calculated by the Bathysonde data is also shown since station pair 43-44 did not straddle the mooring location. Below 2000 m at mooring 1, the current as measured by the mean of the current meters and geostrophic current match extremely well. The very low geostrophic currents at mooring 2 is matched by both current meter results below 1500 m. At mooring 3, the geostrophic and current meter results would match at depth if the zero of geostrophic velocity was located at about 400 m. At mooring 4, there does not seem to be any reasonable compromise that would match the geostrophic and current meter results, except a zero level at the surface.

It was not possible to tie in the high surface speeds at moorings 1 and 2 with the hydrographic data. It appears then from these data that the most suitable reference level would be a variable one starting at about 2000 m in the north and rising up to near surface in the south as was done by Ostapoff (1960, 1961) and is shown in figure 14 with a net transport of 5 sv toward the west.

4.4 Comparison with past results

In summary, the following transport figures were found:

Method	Net Transport
3000 m horizontal reference level	72 sv (east)
Variable reference level	5 sv (west)
Current Meter Mean (5 Feb.)	4 sv (west)
Current Meter Mean (10 Feb.)	62 sv (west)
Current Meter Mean (Overall)	15 sv (west)

The value of transport with the horizontal reference level is similar to that found by Sverdrup (1942) and Ostapoff (1960, 1961). It is somewhat less than that of the Russian authors (see Table 1). With the variable reference level, which gives the best compromise with the current meter data, the results are similar to those of Ostapoff (1960, 1961). A high westerly transport as seen by the mean of the current meters on February 10 has not been reported previously.

CHAPTER 5

CONCLUSION

Several important results have come from this study. In the first case, the hydrographic sections were similar to others taken in the same area for many years. This fact demonstrates that the water properties are relatively constant as has been reported by Bowen and Stommel (1971). The 10 days of current meter data demonstrated the variability of the flow and showed that an eastward flow is found only at the north and south ends of the passage and that this flow is time dependent. Also, a minimum velocity was seen in the middle of the water column. The Antarctic Convergence Zone was clearly indicated with the southern motion overriding the northern and the records also showed that tidal motions occur at all depths in the passage. An event was seen in almost all current meter records occurring on the same day at all depths. It is speculated that it may have been the result of a severe south-easterly storm in the area--unfortunately, the weather records are scanty--but if the wind did affect the currents down to 3500 m, estimates of volume transport using the current meter data will be in doubt. Until longer records are obtained in the area, the true representativeness of these data cannot be determined. Webster (1968) shows the effect of using a 9-day record and a 2-month record from the same area. While the 9-day record indicated southerly flow, the 2-month record showed a net westerly motion.

In conclusion, it is not possible to give an unambiguous

transport figure for the Drake Passage because of the short length of the current meter records and also because no current measurements were made at the convergence itself.

BIBLIOGRAPHY

BLACKMAN, R. B. and J. W. TUKEY (1958) The Measurement of Power Spectra. Dover Publications, Inc., N.Y. 190 pp.

BOWEN, J. L. and H. STOMMEL (1971) How variable is the Antarctic Circumpolar Current? Research in the Antarctic, Pub. No. 93, Am. Assoc. Adv. Sci., Washington, D. C.

CALLAHAN, J. E. (1971) Velocity structure and flux of the Antarctic Circumpolar Current south of Australia, J. Geophys. Res. 76 (24), 5859-5864

CAPURRO, L. R. A. (1967) Medicion de correintes superficiales y profundas en el Pasaje Drake. Publnes. Serv. Hidrogr. Nav., B. Aires, H 641, 57 pp.

CAPURRO, L. R. A. (1968) Velocity measurements in the Southern Ocean. Main Review Paper, Section 1: Surface and Upper Layers. Symposium on Antarctic Oceanography, Santiago, Chile, 13-16 Sept., 1966, Scott Polar Res. Inst., 58-66, Cambridge, England.

CLOWES, A. J. (1933) Influence of the Pacific on the circulation in the southwest Atlantic Ocean. Nature, London, 131, 189-191

DEACON, G. E. R. (1937) The hydrology of the Southern Ocean, Discovery Rept., 15, 1-124.

DEACON, G. E. R. (1963) The Southern Ocean, in The Sea, vol. 2, ed. M. N. Hill, 281-296, Interscience, N. Y.

DEFANT, A. (1961) Physical Oceanography, vol. 1, 729 pp. Pergamon Press, London

ESKIN, L. I. (1959) Contribution to the study of the water and thermal balance of Drake Passage, Inform. Biull. sov. antark. Eksped., 12, 29-32. (Eng. transl., Sov. Antarc. Exped. Inf. Bull., 2, 52-55, Elsevier, Amsterdam, 1964)

GILL, A. E. and K. BRYAN (1971) Effects of geometry on the circulation of a three-dimensional southern-hemisphere ocean model. Deep-Sea Res. 18 (7) 685-721

GORDON, A. L. (1966) Potential temperature, oxygen and circulation of bottom water in the Southern Ocean. Deep-Sea Res. 13 (6), 1125-1138

GORDON, A. L. (1967a) Geostrophic transport through the Drake Passage. Science, 156 (3783), 1732-1734

GORDON, A. L. (1967b) Structure of Antarctic Waters between 20°W and 170°W. Antarctic Map Folio Ser., Am. Geogr. Soc., Folio 6, 9 pp., 14 plates

GORDON, A. L. (1971a) Recent physical oceanographic studies of Antarctic water., Research in the Antarctic, Pub. No. 93, Am. Assoc. Adv. Sci., Washington, D. C.

GORDON, A. L. (1971b) Oceanography of Antarctic waters, in Antarctic Research Series 15, Antarctic Oceanology I, ed. J. L. Reid, Am. Geophys. Union, Washington, D. C.

HIDAKA, K. and M. TSUCHIYA (1953) On the Antarctic Circumpolar Current. J. Mar. Res. 12, 214-222

ICHIYE, T. (1970) Contributions to dynamics of the Antarctic Circumpolar Current (A. C. C.) (I. Zonal Transport) J. Ocean. Soc. Jap. 26 (6), 340-353

KORT, V. G. (1959) New data on the transport of Antarctic waters. Inform. Biull. sov. antark. Eksped., 9, 31-34 (Eng. transl., Sov. Antarc. Exped. Inf. Bull., 1, 358-361, Elsevier, Amsterdam, 1964)

KORT, V. G. (1962) The Antarctic Ocean, Sci. Am., 207 (3), 113-126

LEDENEV, V. G. (1961) Contribution to the study of surface currents in the seas of the Pacific sector of the Antarctic. Inform. Biull. sov. antark. Eksped., 27, 18-24 (Eng. translation Sov. Antarc. Exped. Inf. Bull., 3, 257-262, Elsevier, Amsterdam, 1965)

MCKEE, W. D. (1966) The Theories of the Antarctic Circumpolar Current. Survey Paper No. 1, Horace Lamb Centre for Ocean. Res., Flinders Univ. of S. Aust.

MIDITUN, L. and J. NATVIG (1957) The waters of the Pacific Antarctic Ocean. Sci. Res. "Brategg" Exped. 1947-1948, No. 3, 130 pp.

MUNK, W. H. and E. PALMEN (1951) Notes on the dynamics of the Antarctic Circumpolar Current. Tellus 3, 53-55

MUNK, W. H., F. E. SNODGRASS and M. J. TUCKER (1959) Spectra of low-frequency ocean waves, Bull Scripps Inst. Ocean. 7 (4), 283-362

NEUMANN, G. (1960) On the dynamical structure of the Gulf Stream as an Equivalent-Barotropic flow, J. Geophys. Res., 65 (1), 239-247

NEUMANN, G. and W. J. PIERSON, jr. (1966) Principles of Physical Oceanography. 545 pp., Prentice-Hall Englewood Cliffs, N.J.

OSTAPOFF, F. (1960) On the mass transport through the Drake Passage. J. Geophys. Res., 65 (9), 2861-2868

OSTAPOFF, F. (1961) A contribution to the problem of the Drake Passage circulation. Deep-Sea Res., 8, 111-120

REID, J. L. and W. D. NOWLIN, jr. (1971) Transport of water through the Drake Passage. Deep-Sea Res., 18 (1), 51-64

STOMMEL, H. (1957) A survey of ocean current theory. Deep-Sea Res., 4, 149-184

SVERDRUP, H. U., M. W. JOHNSON and R. H. FLEMING (1942) The Oceans. 1087 pp., Prentice-Hall, New York

VOLKMANN, G. H. (1962) Deep current observations in the western North Atlantic. Deep-Sea Res. 9, 493-500

WARREN, B. A. (1971) Antarctic deep water contribution to the World Ocean., Research in the Antarctic, Pub. No. 93, Am. Assoc. Adv. Sci., Washington, D. C.

WEBSTER, F. (1968) On the representativeness of direct deep-sea current measurements. Prog. in Ocean. 5, 3-15.

APPENDIX I

DEPTH RECORDERS AND THERMOGRAPHS

As was stated in Chapter 1, each mooring had a depth recorder near the top current meter and a thermograph adjacent to each current meter.

The Depth Recorders were Braincon Type 562--pressure is sensed by a Bourdon Tube and the motion of the tube is coupled to a pointer on pressure sensitive paper. The records were read every hour and the mean level of the instrument found. Differences from the mean level were then plotted against time as shown in figure 17. It can be seen that the greatest variation in depth occurred at Mooring 1 with a maximum excursion of 14.4 m above and 32.8 m below the mean level. The motion of this depth recorder correlated with the current meter at Mooring 1 (figure 3a). By comparing these two figures, it can be seen that as the current speed increased, the depth recorder went down, and as the currents decreased toward the end of the record, the depth recorder motion resembled the motion at the other moorings with excursions of only 3-4 m.

The temperature recorders were Braincon Type 146 Recording Thermographs which utilize a time exposure of a mercury in glass thermometer on a 70 mm film. The film is exposed by a phosphorescent light source placed under the thermometer; the light passing through the thermometer onto the film producing a bar graph on the film. A stepping mechanism advances the film every 20 minutes. The time series for each thermograph is shown in figure 18 for the 10 instruments that worked. Most of the records indicate the same temperature as would be expected from the hydrographic casts (figure 6). The major exceptions were Thermographs 2-145 and 3-130. At Thermograph

2-145, the temperature is around 3°C but on the last day of recording, the temperature dropped to 1.5°C. According to the temperature section (figure 6), the 3°C isotherm passed through this location with a cell of 2° water at about 400 m. At Thermograph 3-130, located just south of the convergence zone, the temperature record gives an indication of the intense thermal structure in this region.

APPENDIX II

EXPERIMENTAL ERRORS

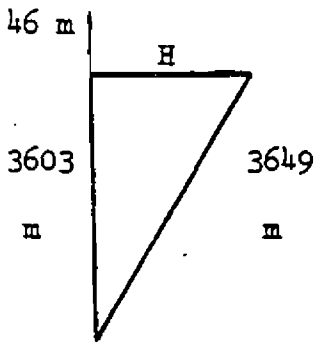
The experimental errors in the current meter data can be divided into 3 categories: instrument error, compass calibrations and mooring motion.

According to the manufacturer's specifications the instrument error on the speed readings is ±3% full scale. In the case of the shallow meters this error is ±8 cm/s; for the deeper meters, ±4 cm/s. In direction, the error is ±4°; in tilt and tilt direction, ±3° and ±10° respectively. The tilt and tilt direction readings are used as a correction to the speed readings, but all tilts recorded in these data were less than 7°, and with this small value, negligible corrections were made to the speed.

The compass calibrations were done by swinging the instrument through one complete revolution clockwise and counter-clockwise and recording the indicated compass reading for each 10° of the arc. By taking the mean of the two compass readings for the same true direction and deducting the magnetic variation (Halifax 23°W), a compass error for each 10° of arc was determined. Two of the meters were calibrated in this manner in December 1969 and in February and June 1971. The difference in calibration was about 5°. The result seemed to indicate that the calibration of the meters did not change appreciably in a period of 14 to 18 months. However, all meters were swung in February 1971 and again in August 1971 and some significant calibration differences were found, the greatest being 20°, with most being in the region of 10° difference. In general, an experimental error of ±15° was assigned to the direction readings.

The mooring motion was best indicated by the motion of the depth

recorders (figure 18) since the tilt of the current meters was small. The only significant motion of the depth recorder occurred at Mooring 1, with a maximum excursion 47 m. At this meter site (1-162), the direction recorded by the current meter was constant (figure 3) which seems to indicate that this meter was moving back and forth rather than circularly. An estimate of the change in speed can be estimated by calculating the maximum horizontal displacement and dividing by the time of the movement (6 hours).



From the Pythagorean Theorem, H = 578 m and the effect on the speed would be $5.78 \times 10^4/6 \times 3600 = 2.7$ cm/s. Since the speed recorded at the time of maximum mooring motion was 50 cm/s an effect on the speed of about 5% would be expected.

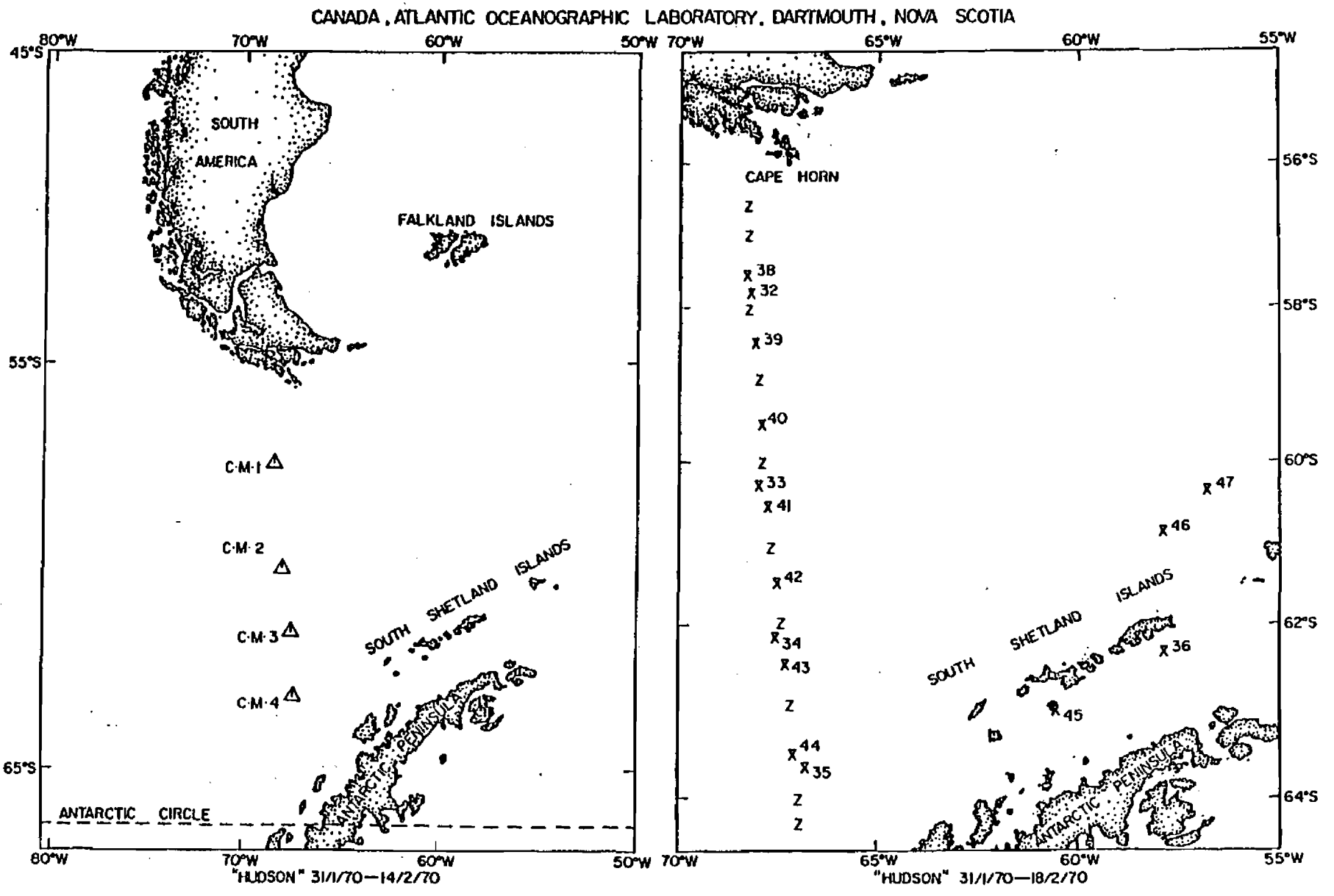
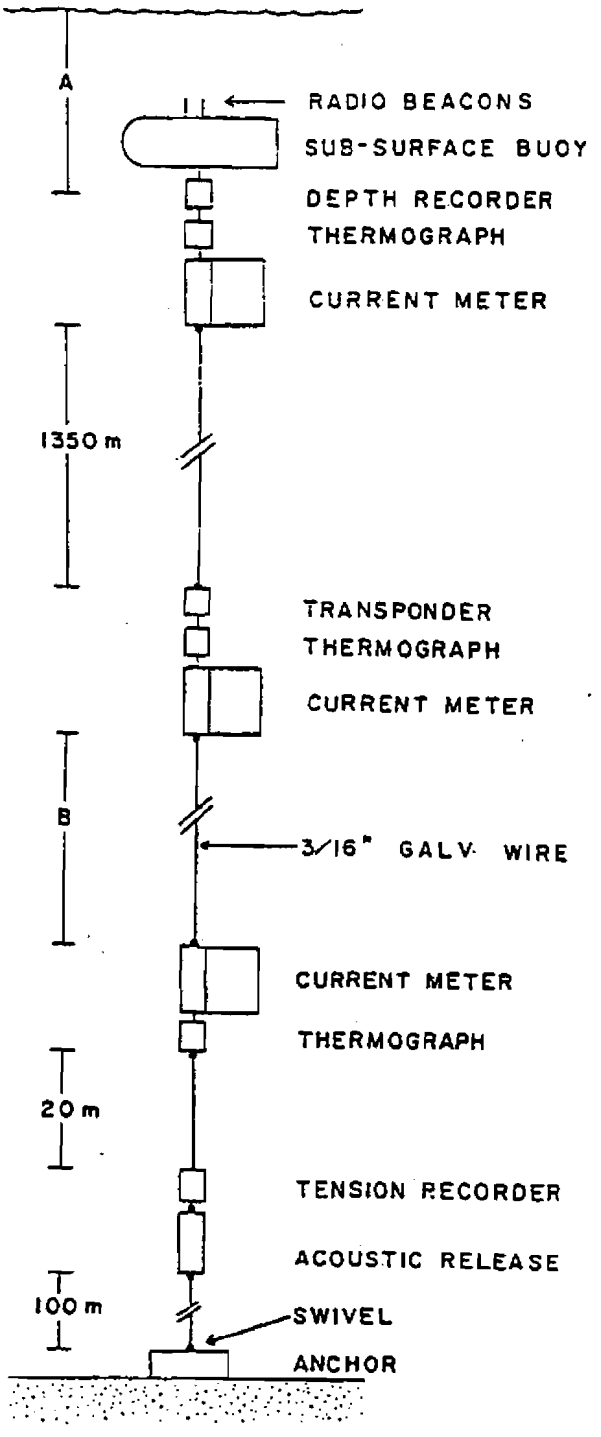


Figure 1 Location Map
CM = Current Meter Mooring, Z = Bathysonde Station
X = Bottle Station

MOORING CONFIGURATION



MOORING	LENGTH (meters) A	B
1	162	2137
2	145	1843
3	130	1890
4	132	1850

Figure 2

Figure 3 Progressive Vector and Rate Direction Diagrams

For each current meter, the progressive vector (upper) and rate direction (lower) diagram is shown on the following pages. The beginning of the progressive vector diagram is indicated by "0" and each successive 24 hour period is marked with a "+". Each meter is numbered as in text--"Meter 1-162" refers to Mooring 1, Depth 162 m.

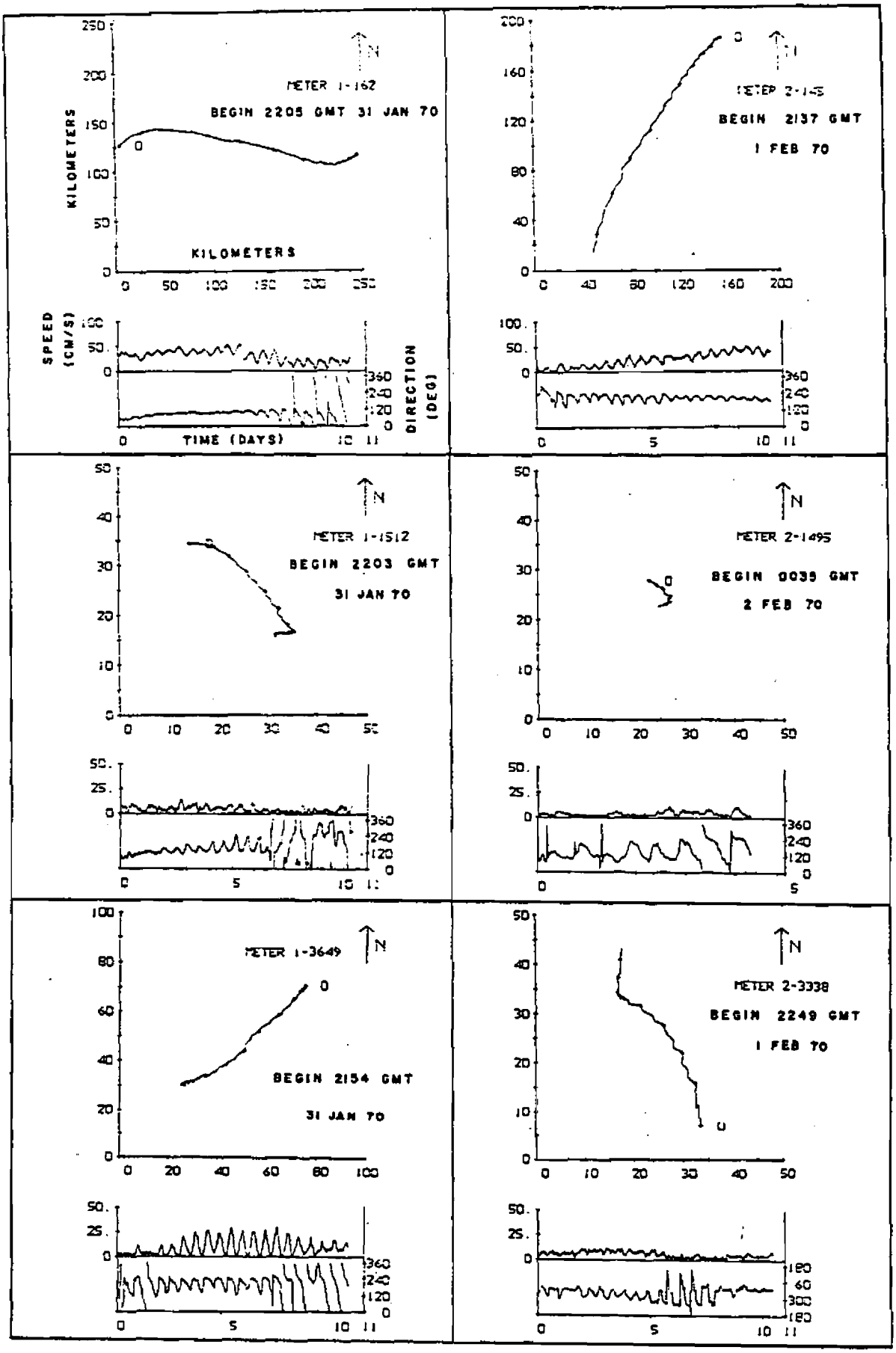

METER 1-162
BEGIN 2205 GMT 31 JAN 70
KILOMETERS
KILOMETERS
SPEED (CM/S)
DIRECTION (DEG)
TIME (DAYS)
METER 2-145
BEGIN 2137 GMT
1 FEB 70
METER 1-1512
BEGIN 2203 GMT
31 JAN 70
METER 2-1495
BEGIN 0035 GMT
2 FEB 70
METER 1-3649
BEGIN 2154 GMT
31 JAN 70
METER 2-3338
BEGIN 2249 GMT
1 FEB 70

Figure 3a

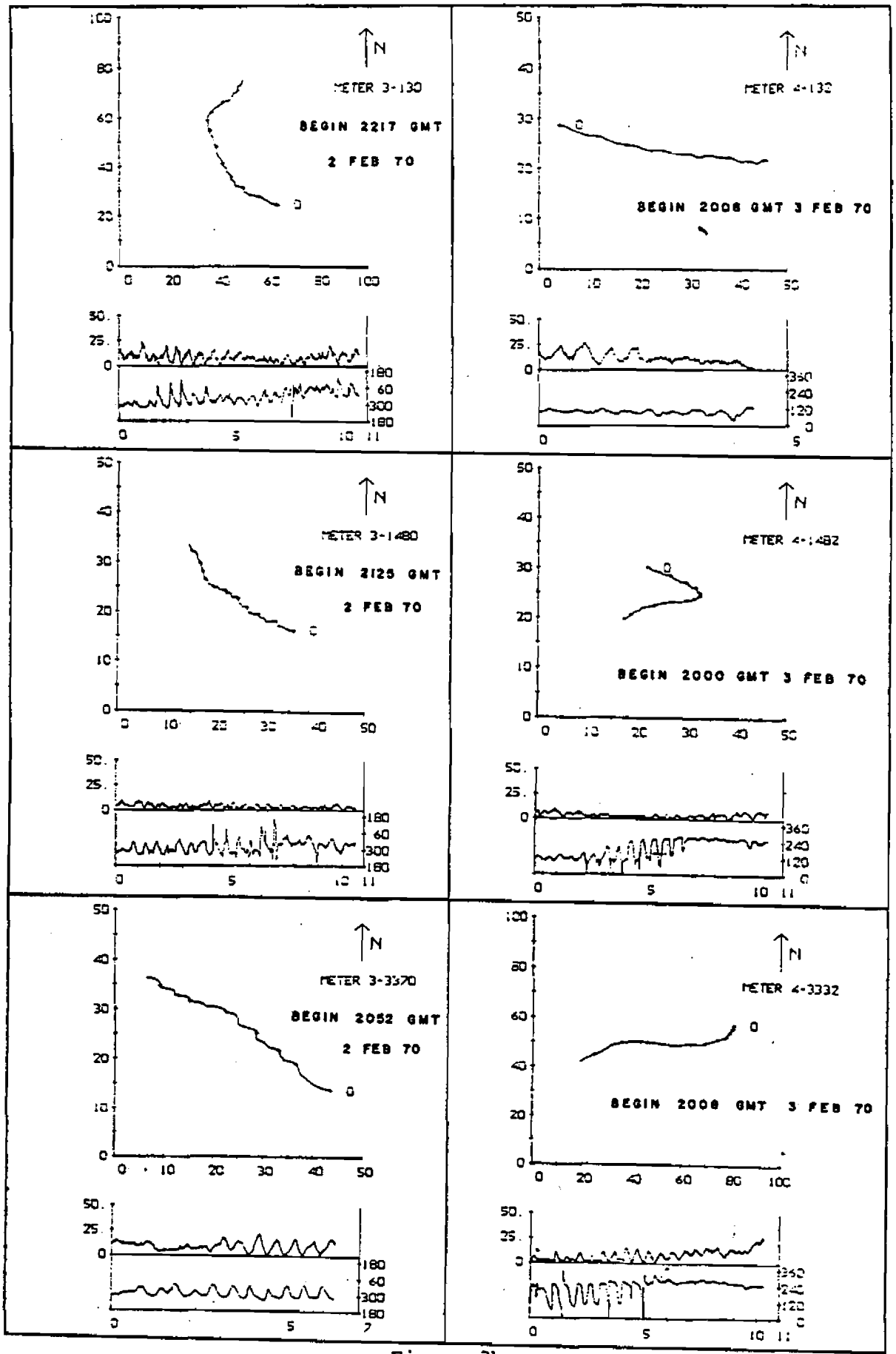

METER 3-130
BEGIN 2217 GMT
2 FEB 70
METER 4-130
BEGIN 2008 GMT 3 FEB 70
METER 3-1480
BEGIN 2125 GMT
2 FEB 70
METER 4-1482
BEGIN 2000 GMT 3 FEB 70
METER 3-3370
BEGIN 2052 GMT
2 FEB 70
METER 4-3332
BEGIN 2008 GMT 3 FEB 70
N

Figure 3b

Figure 4 Current Meter Power Spectra

The following diagrams show the Power Spectra for each component of each current meter. The significant peak on all diagrams near a period of 10 hours is at 12.4 hours.

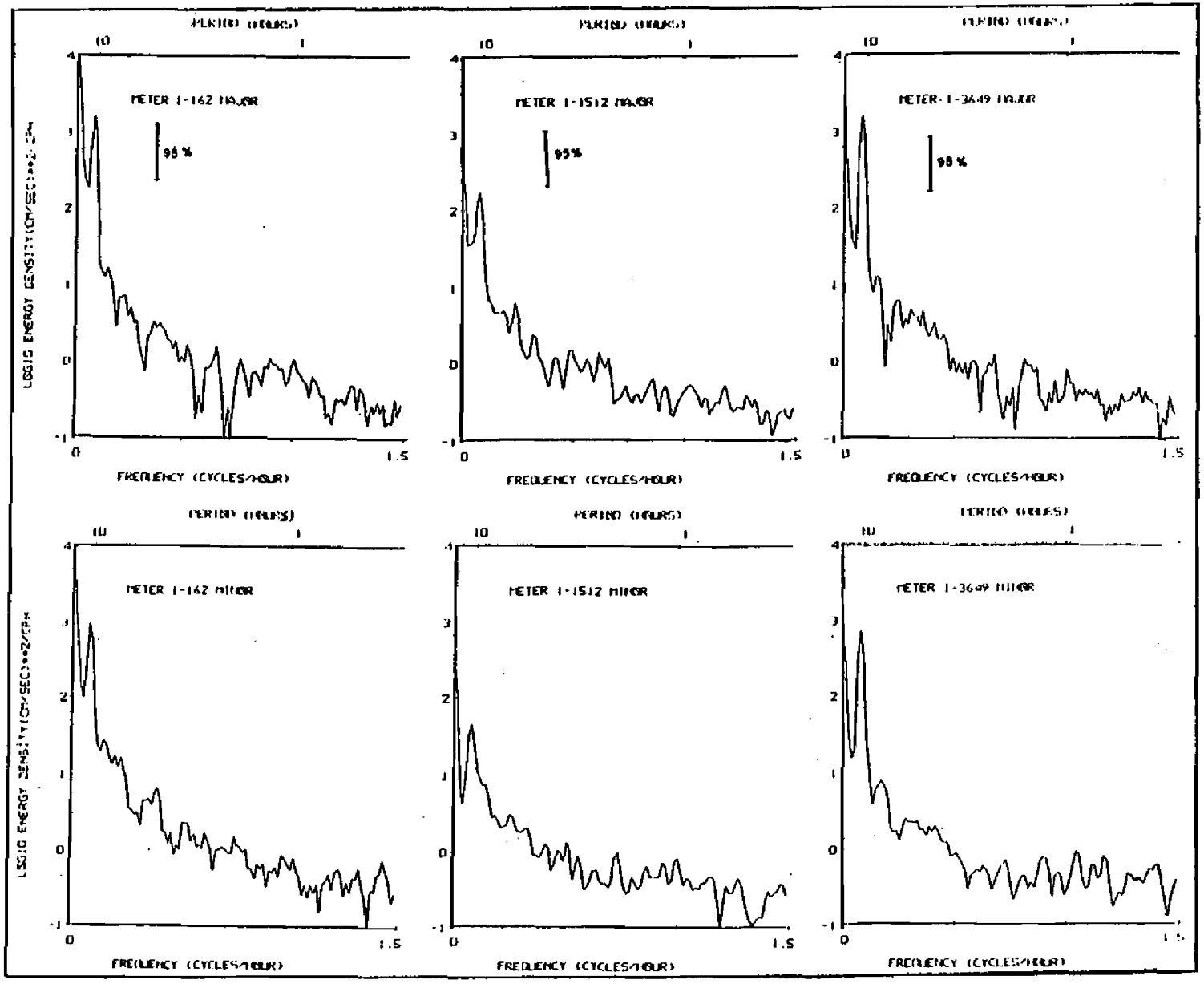


Figure 4a Current Meter Power Spectra--Mooring 1

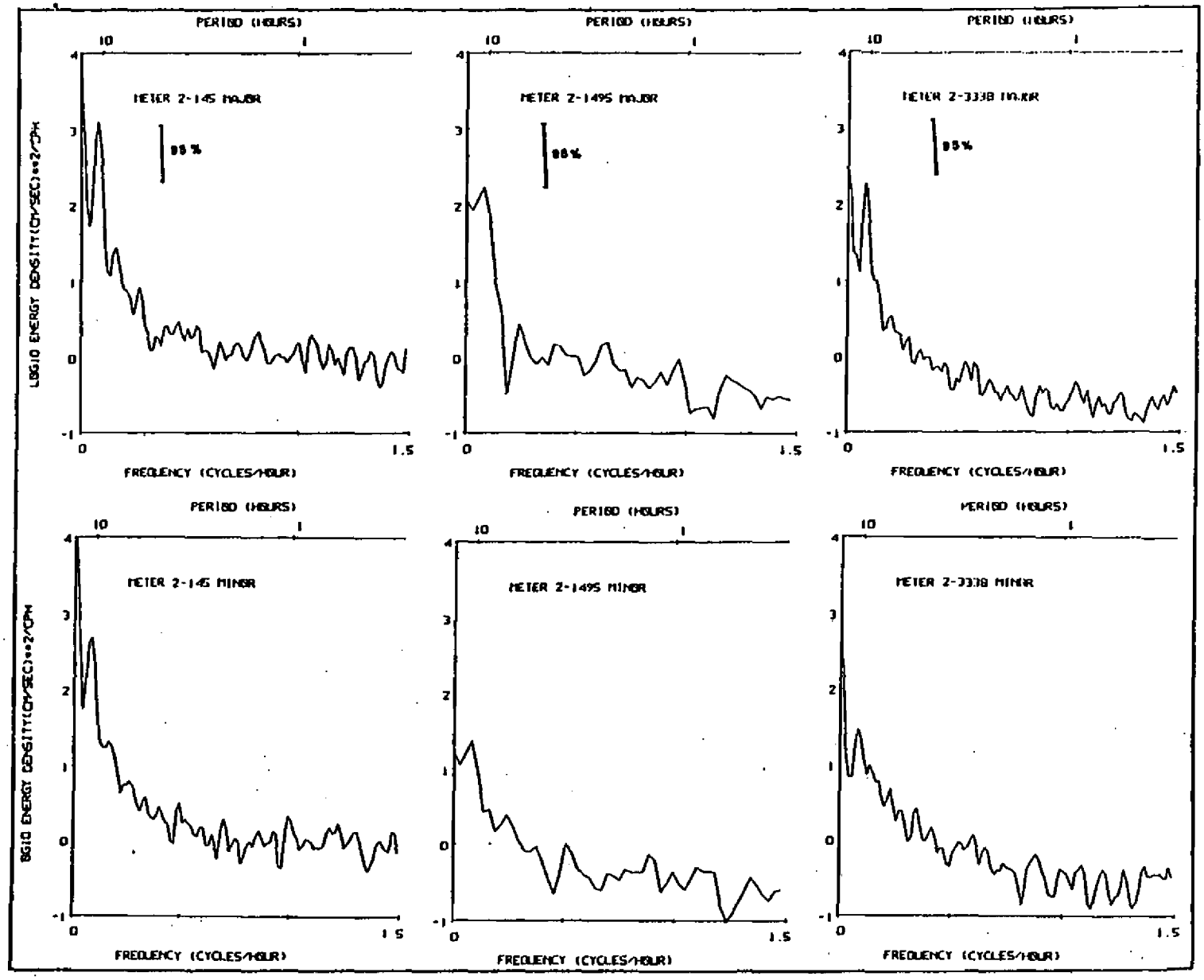


Figure 4b Current Meter Power Spectra--Mooring 2

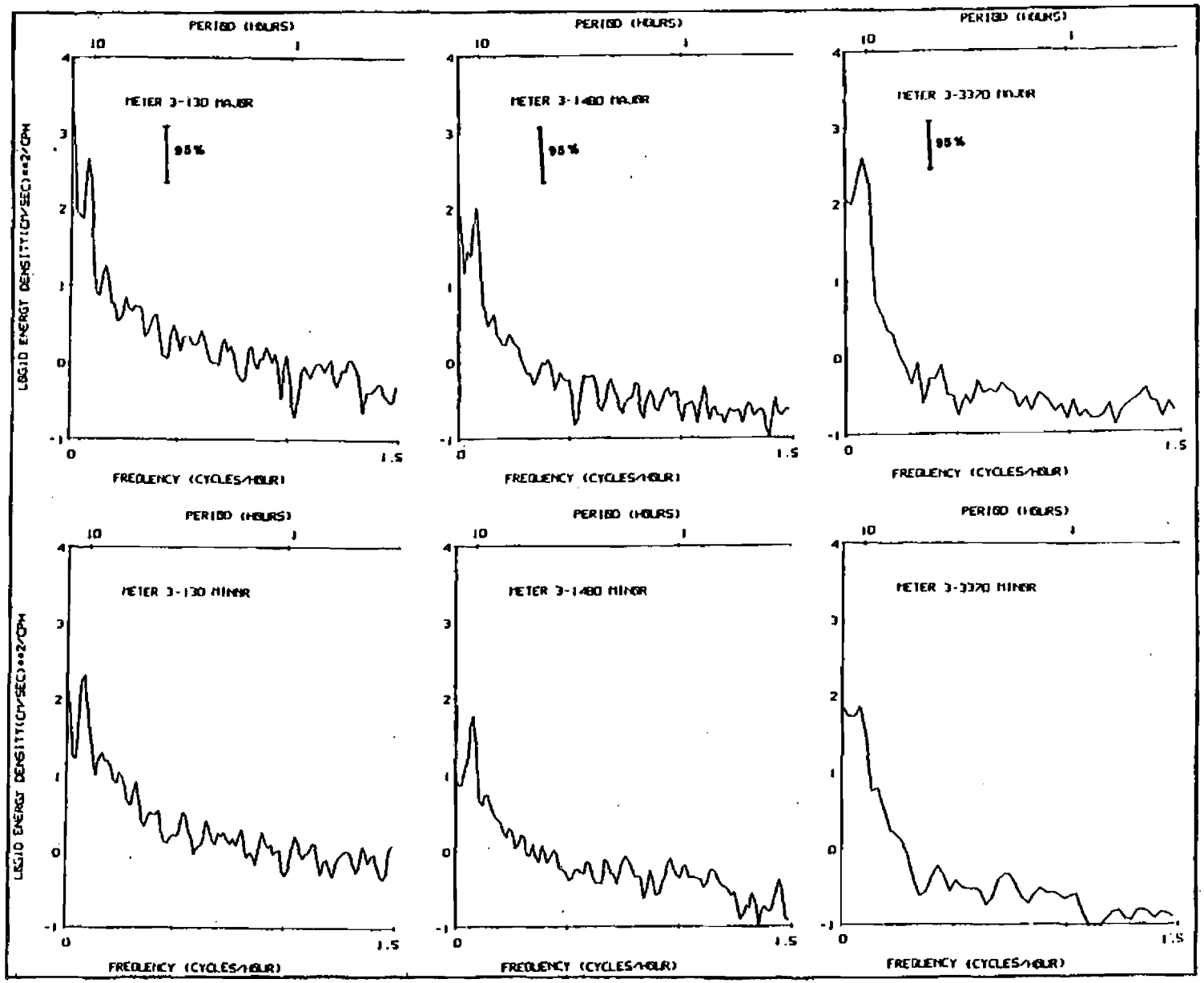


Figure 4c Current Meter Power Spectra--Mooring 3

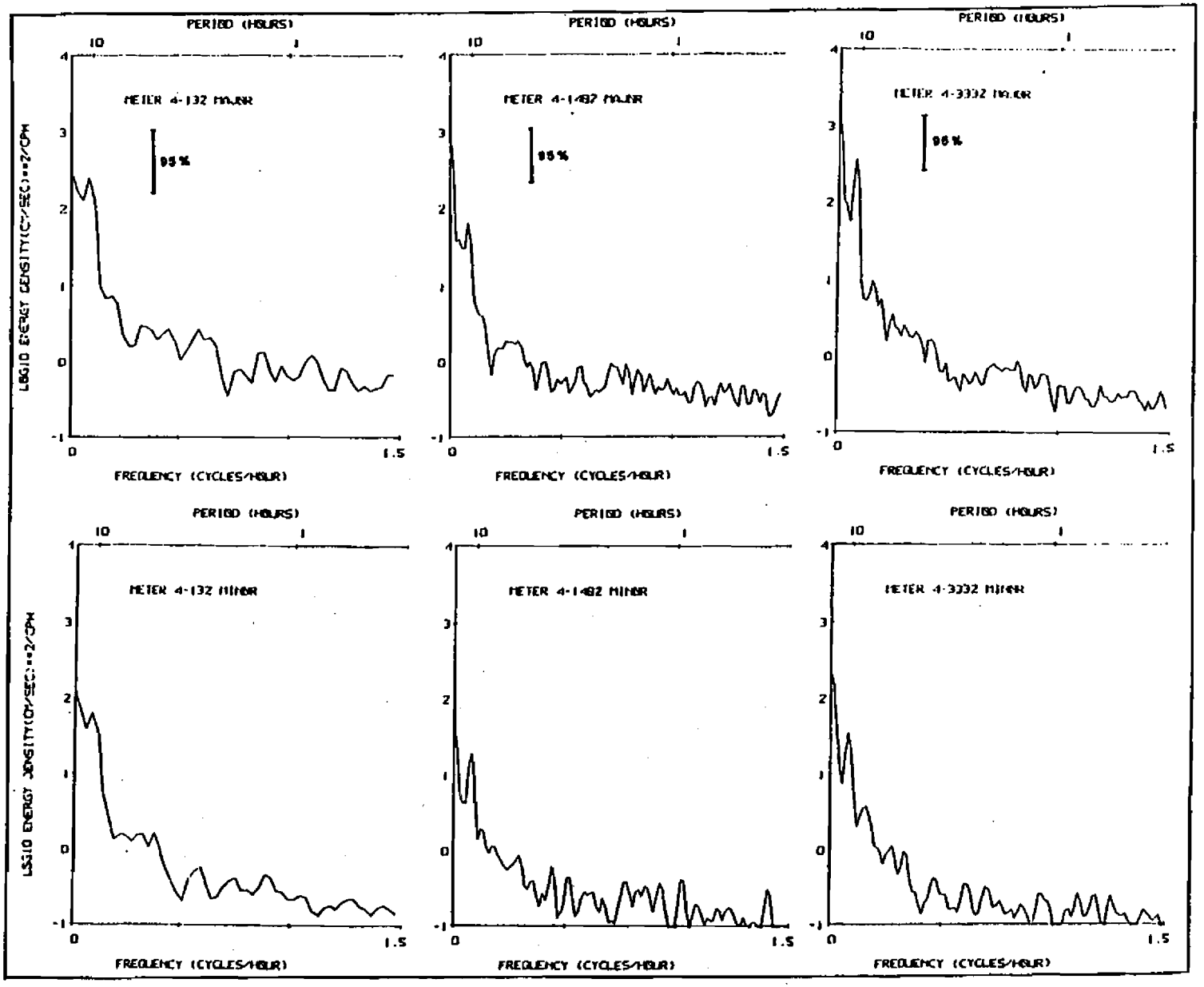


Figure 4d Current Meter Power Spectra--Mooring 4

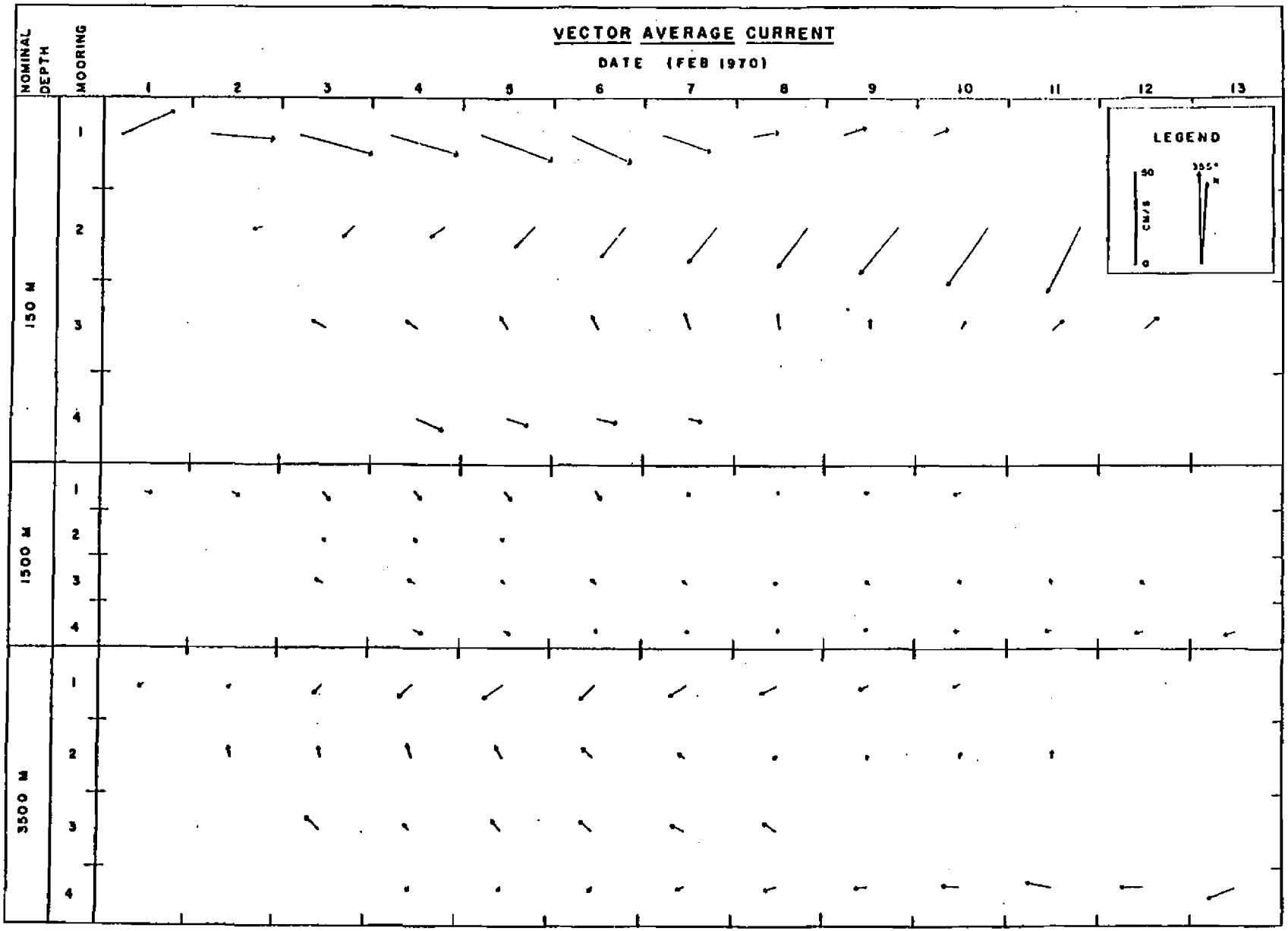

VECTOR AVERAGE CURRENT
DATE (FEB 1970)
NOMINAL DEPTH
MOORING
1
2
3
4
5
6
7
8
9
10
11
12
13
150 M
1500 M
3500 M
LEGEND
50
CM/S
0

Figure 5a

DAILY AVERAGE CURRENT (cm/s)

Each frame represents the Drake Passage cross section from north to south with the daily average component current in cm/s marked at each current meter site. A blank indicates that the current meter was not operating. The major component is along the line 085° - 265° with the current to the east positive. The minor component is along the line 175° - 355° with current to the south positive. Each section has been contoured with negative (west and north) current stippled.

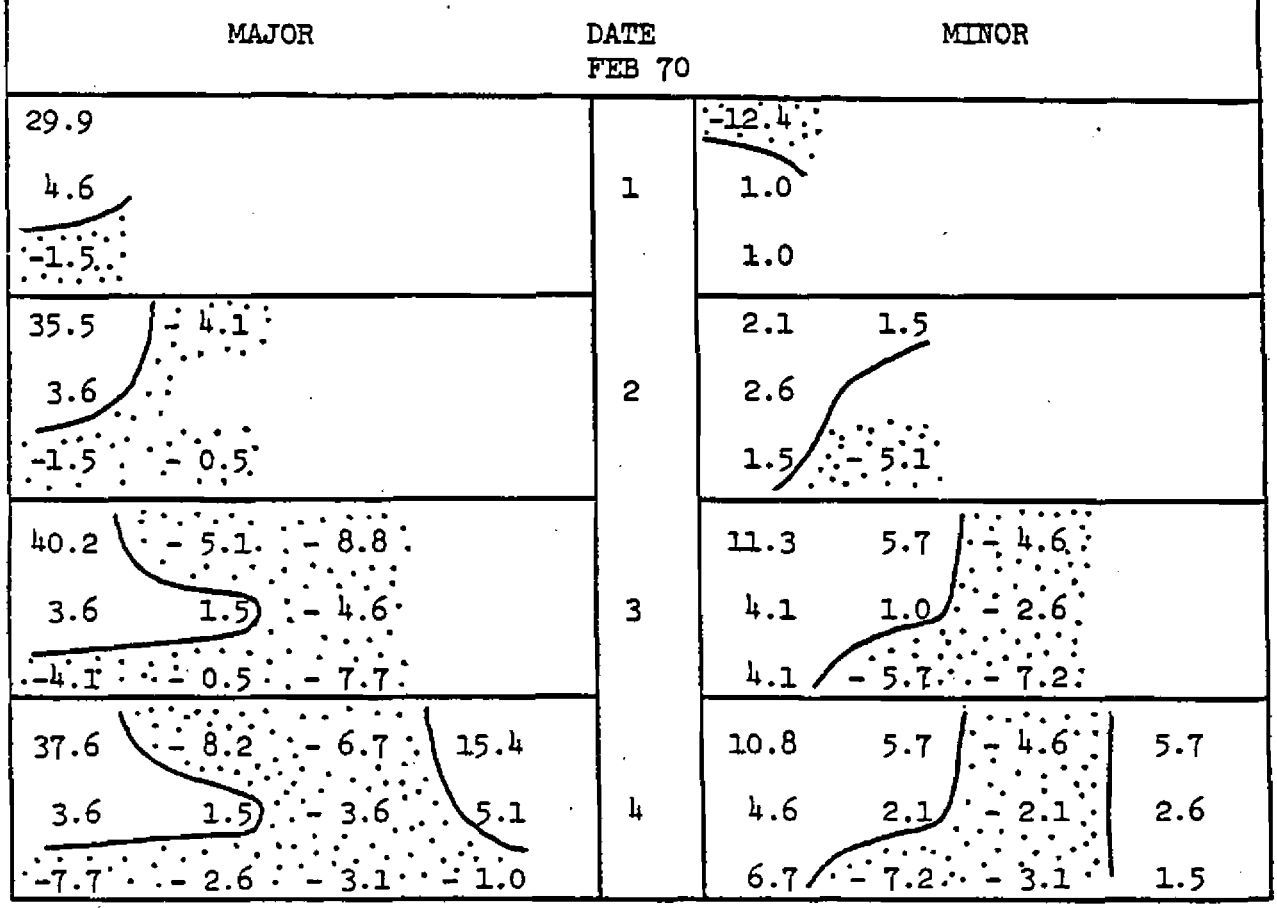


Figure 5b

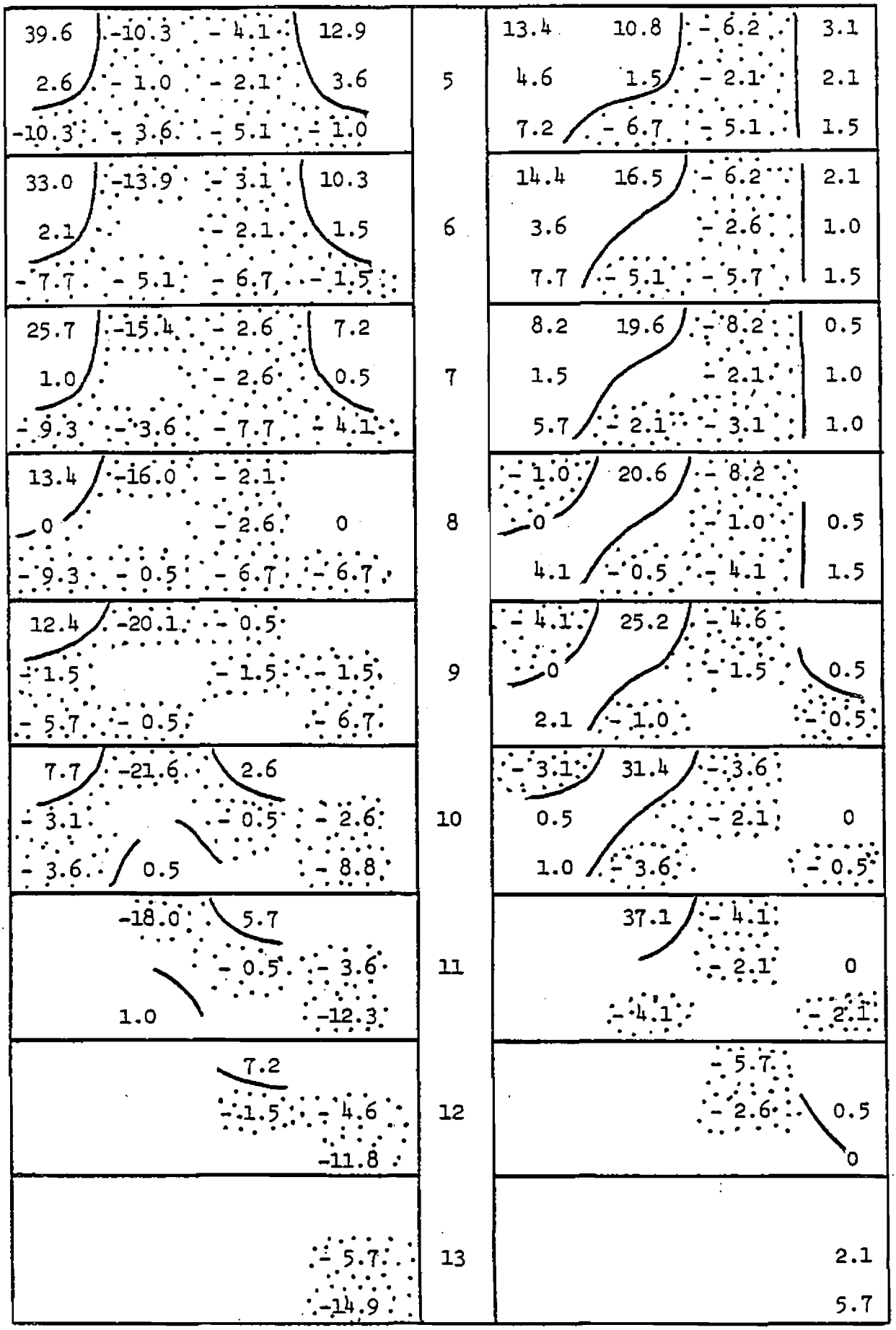


Figure 5b (continued)

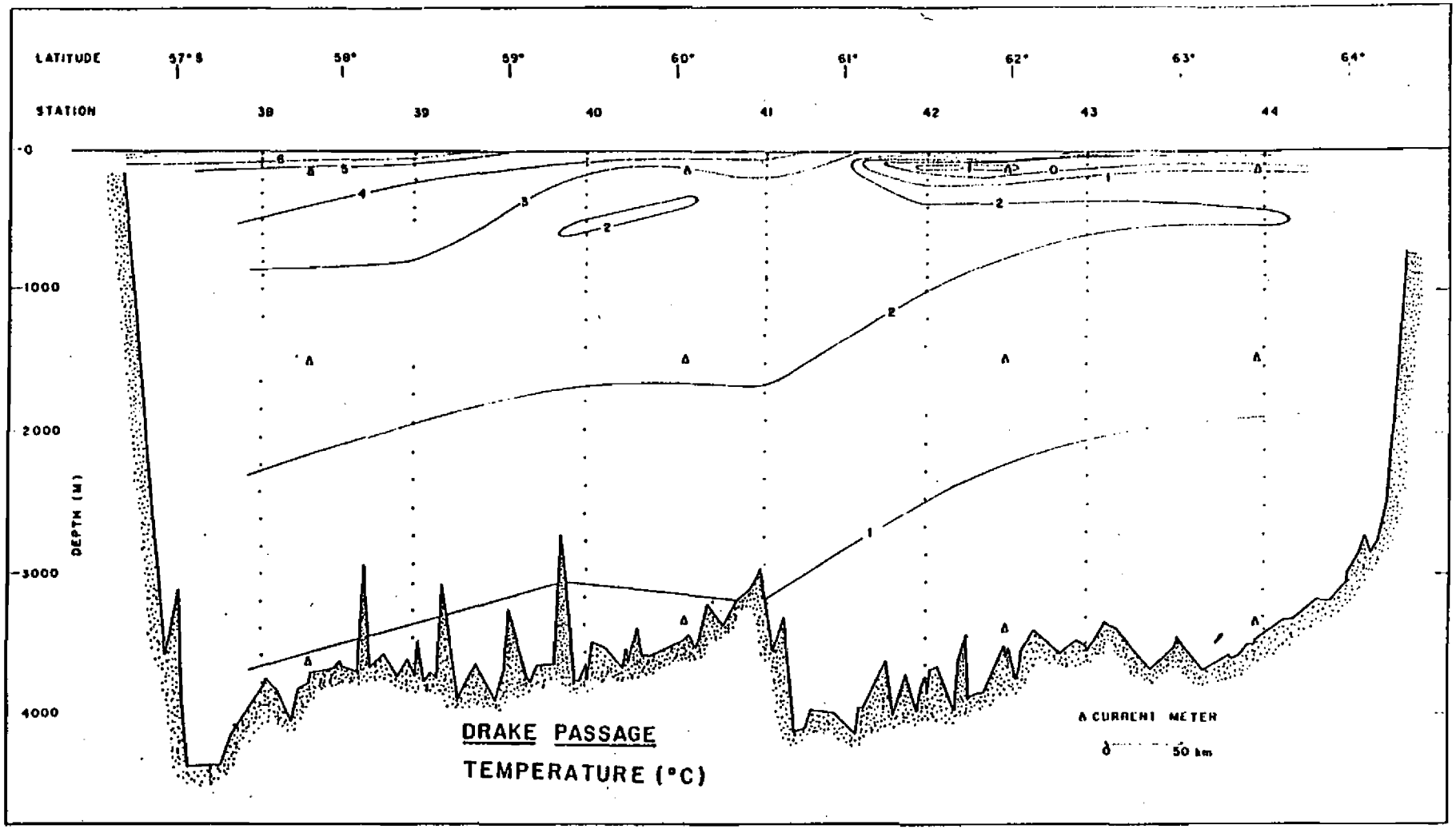

LATITUDE
57° S
58°
59°
60°
61°
62°
63°
64°
STATION
38
39
40
41
42
43
44
0
1000
2000
3000
4000
DEPTH (M)
DRAKE PASSAGE
TEMPERATURE (°C)
CURRENT METER
50 km

Figure 6

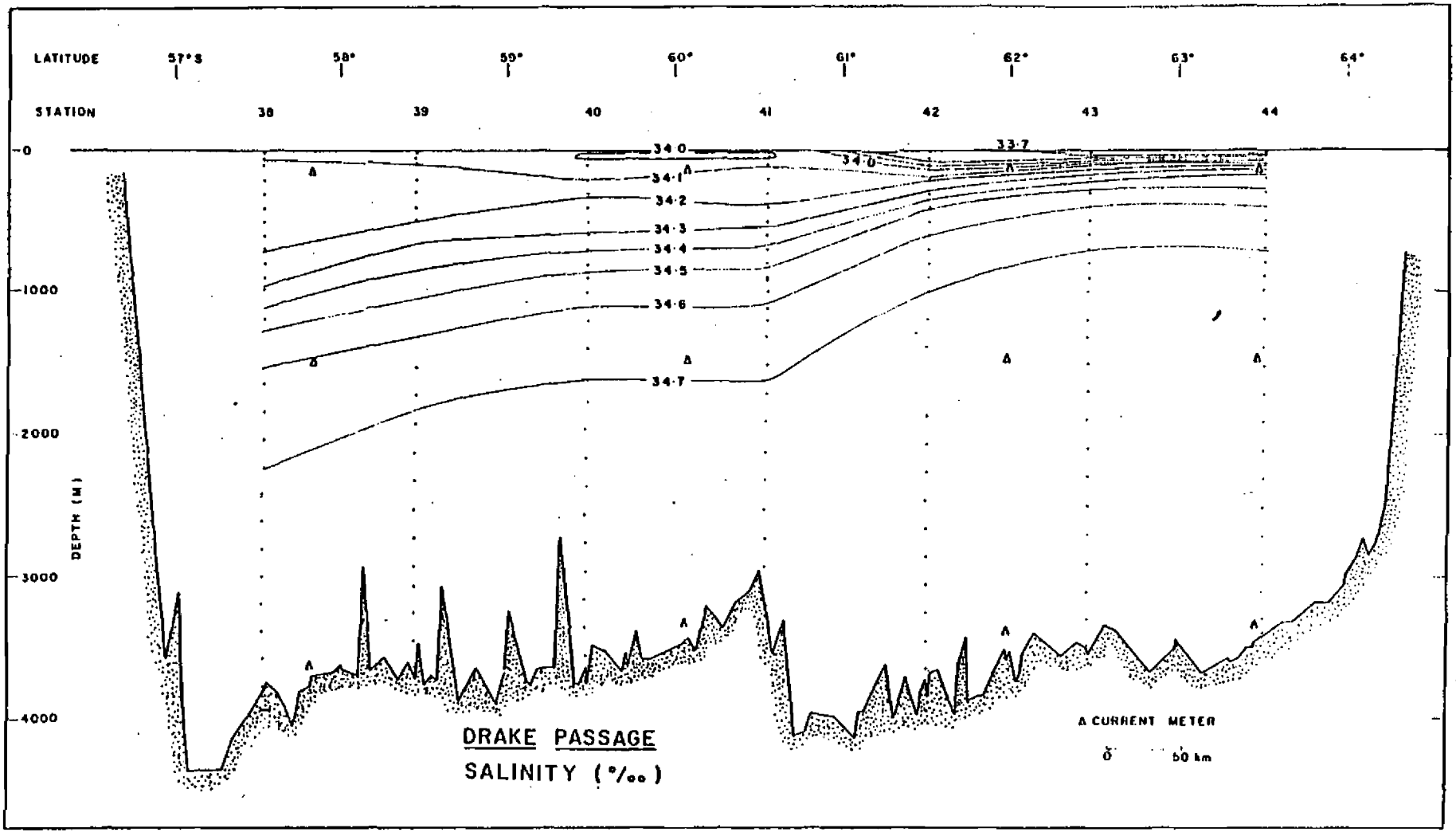

LATITUDE
57°S
58°
59°
60°
61°
62°
63°
64°
STATION
38
39
40
41
42
43
44
0
1000
2000
3000
4000
DEPTH (M)
34·0
34·1
34·2
34·3
34·4
34·5
34·6
34·7
33·7
DRAKE PASSAGE
SALINITY (‰)
A CURRENT METER
50 km

Figure 7

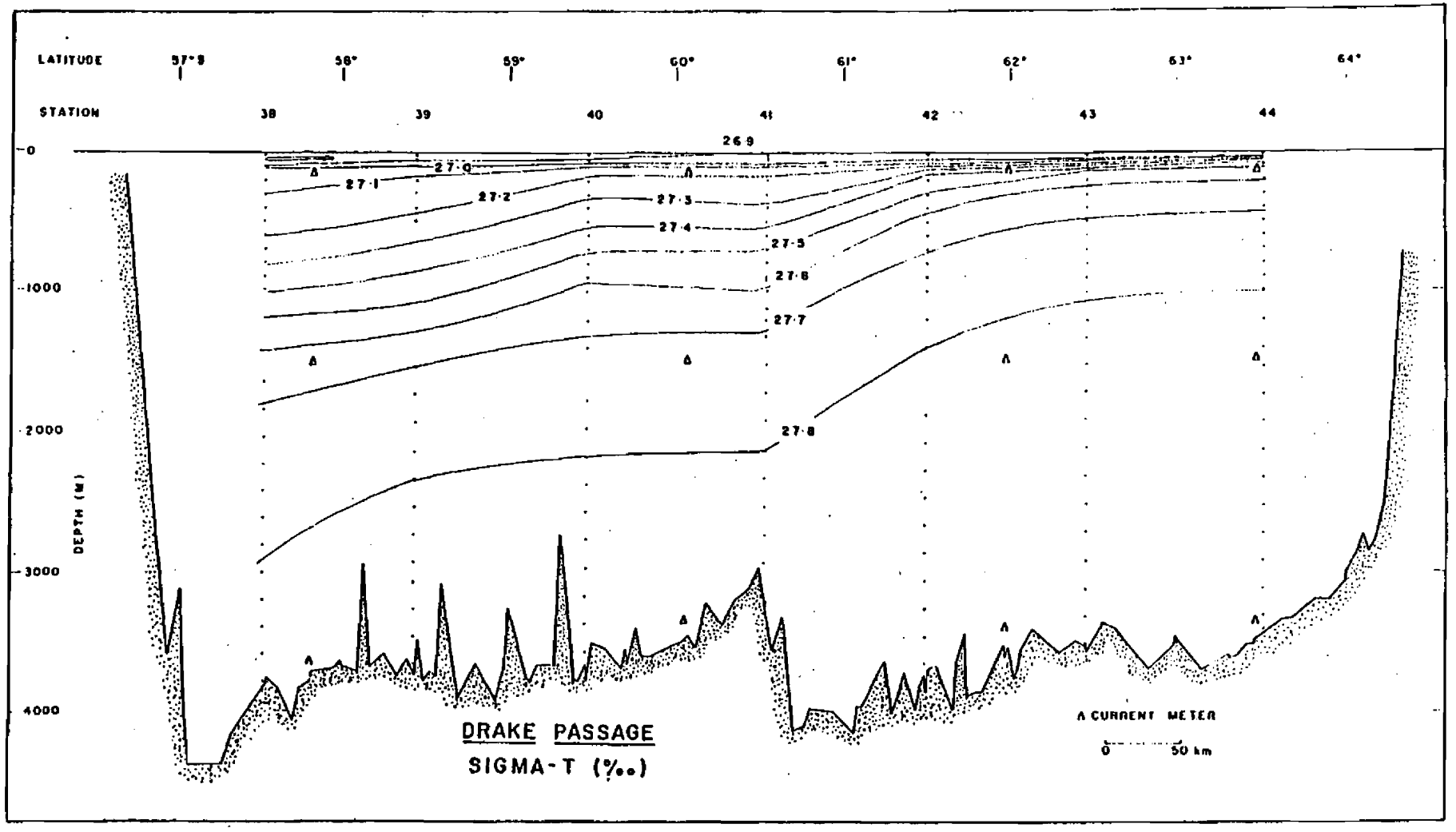

LATITUDE
57°S
58°
59°
60°
61°
62°
63°
64°
STATION
38
39
40
41
42
43
44
26.9
27.0
27.1
27.2
27.3
27.4
27.5
27.6
27.7
27.8
0
1000
2000
3000
4000
DEPTH (M)
DRAKE PASSAGE
SIGMA-T (‰)
A CURRENT METER
0
50 km

Figure 8

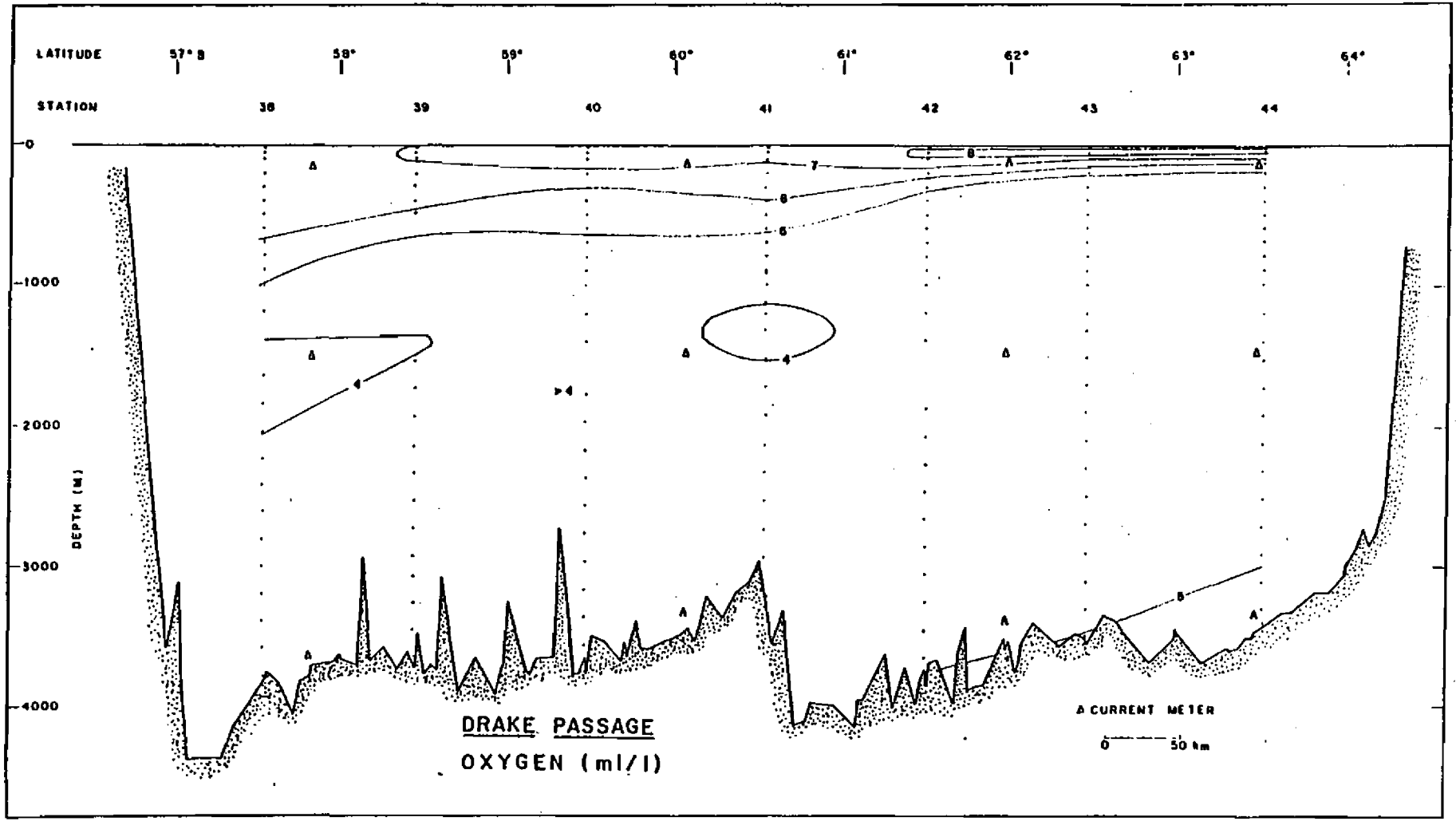

LATITUDE
57° S
58°
59°
60°
61°
62°
63°
64°
STATION
38
39
40
41
42
43
44
0
-1000
-2000
-3000
-4000
DEPTH (M)
DRAKE PASSAGE
OXYGEN (ml/l)
A CURRENT METER
0
50 km

Figure 9

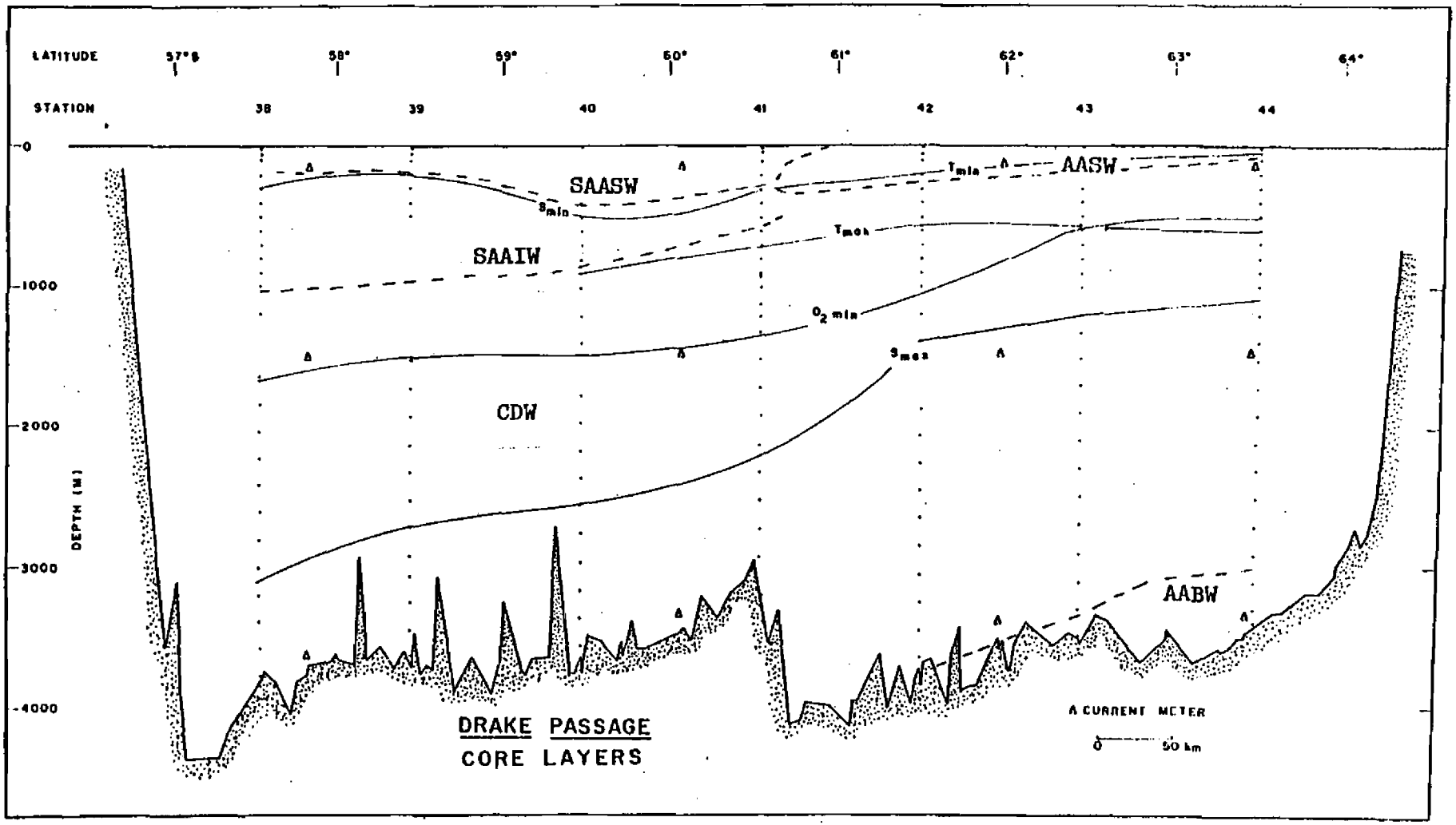


Figure 10 SAASW-Sub-Antarctic Surface Water, SAAIW-Sub-Antarctic Intermediate Water, CDW-Circumpolar Deep Water, AASW-Antarctic Surface Water, AABW-Antarctic Bottom Water

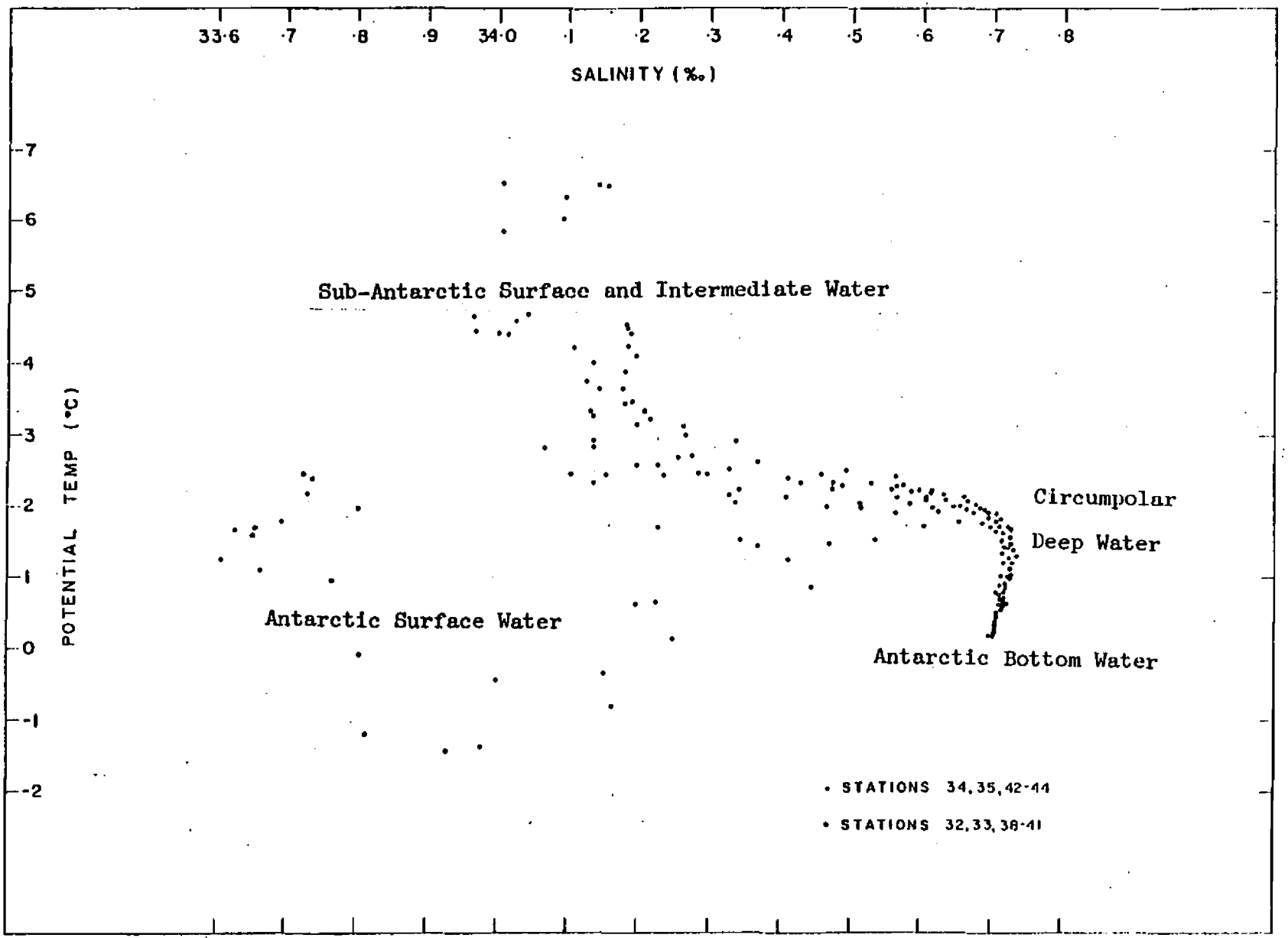


Figure 11 Potential Temperature vs. Salinity

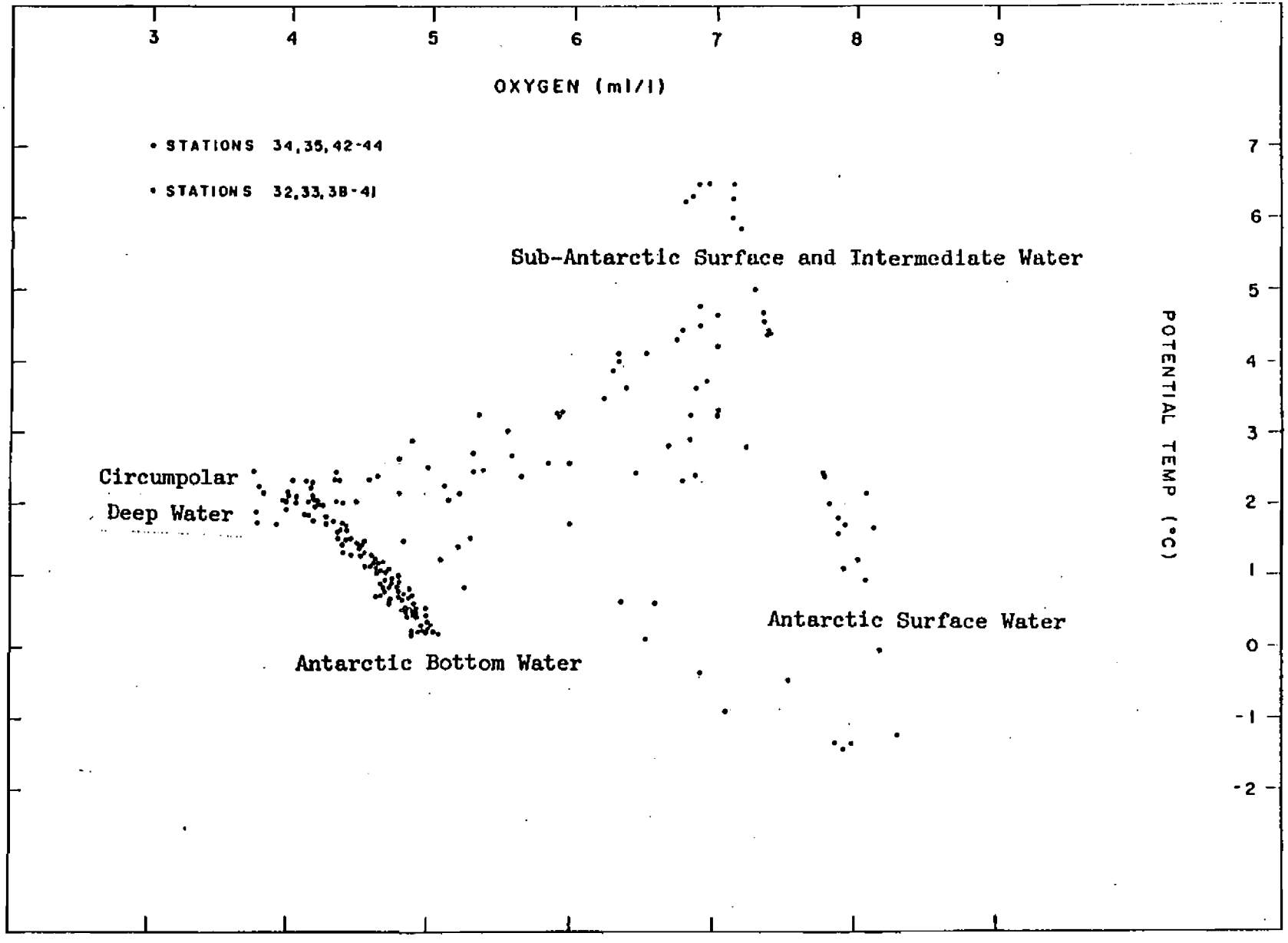


Figure 12 Potential Temperature vs. Oxygen

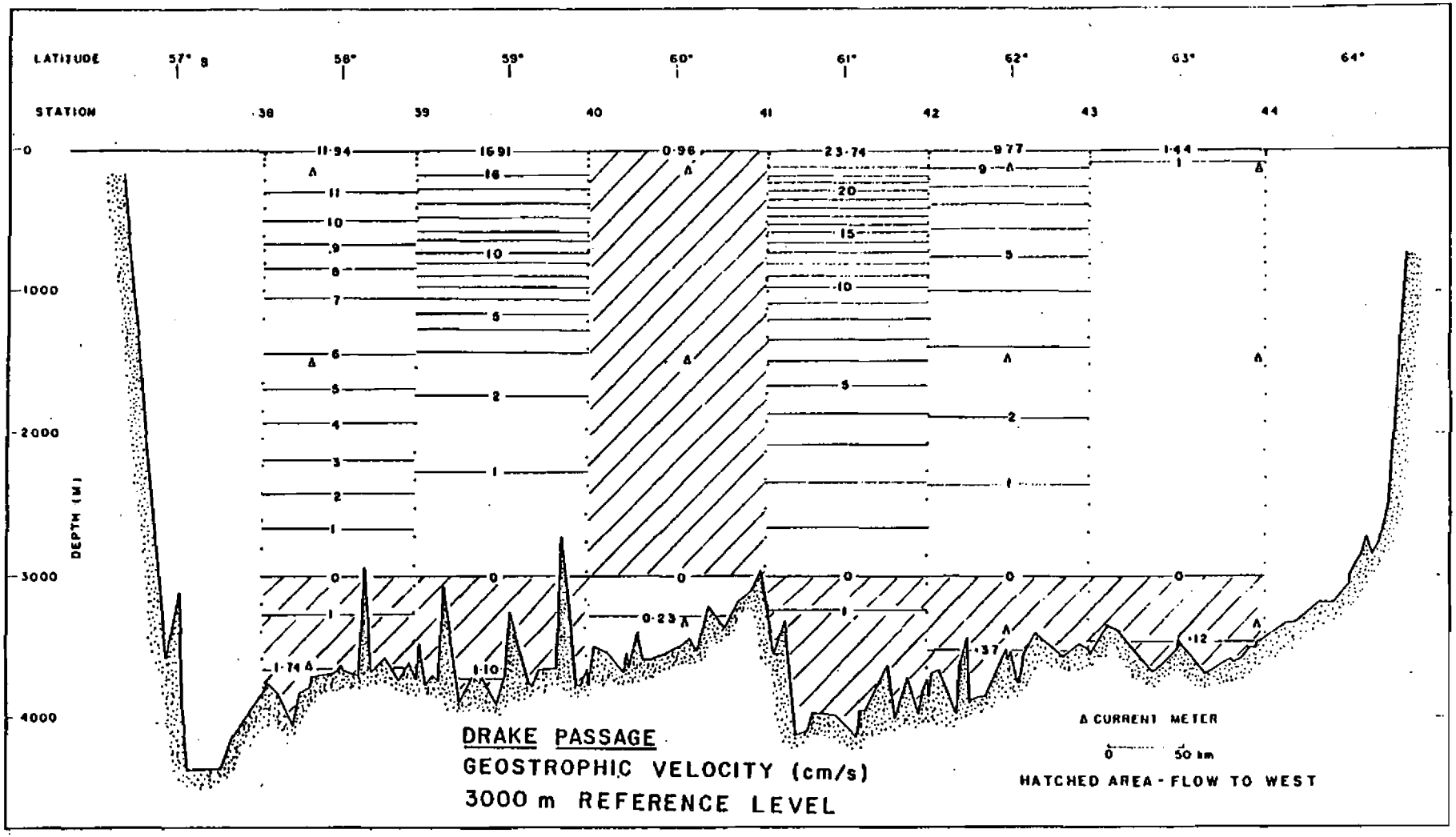

LATITUDE
57° S
58°
59°
60°
61°
62°
63°
64°
STATION
38
39
40
41
42
43
44
DEPTH (M)
0
1000
2000
3000
4000
11·94
16·91
0·96
23·74
9·77
1·44
1·74
1·10
0·23
·37
·12
DRAKE PASSAGE
GEOSTROPHIC VELOCITY (cm/s)
3000 m REFERENCE LEVEL
A CURRENT METER
0
50 km
HATCHED AREA - FLOW TO WEST

Figure 13

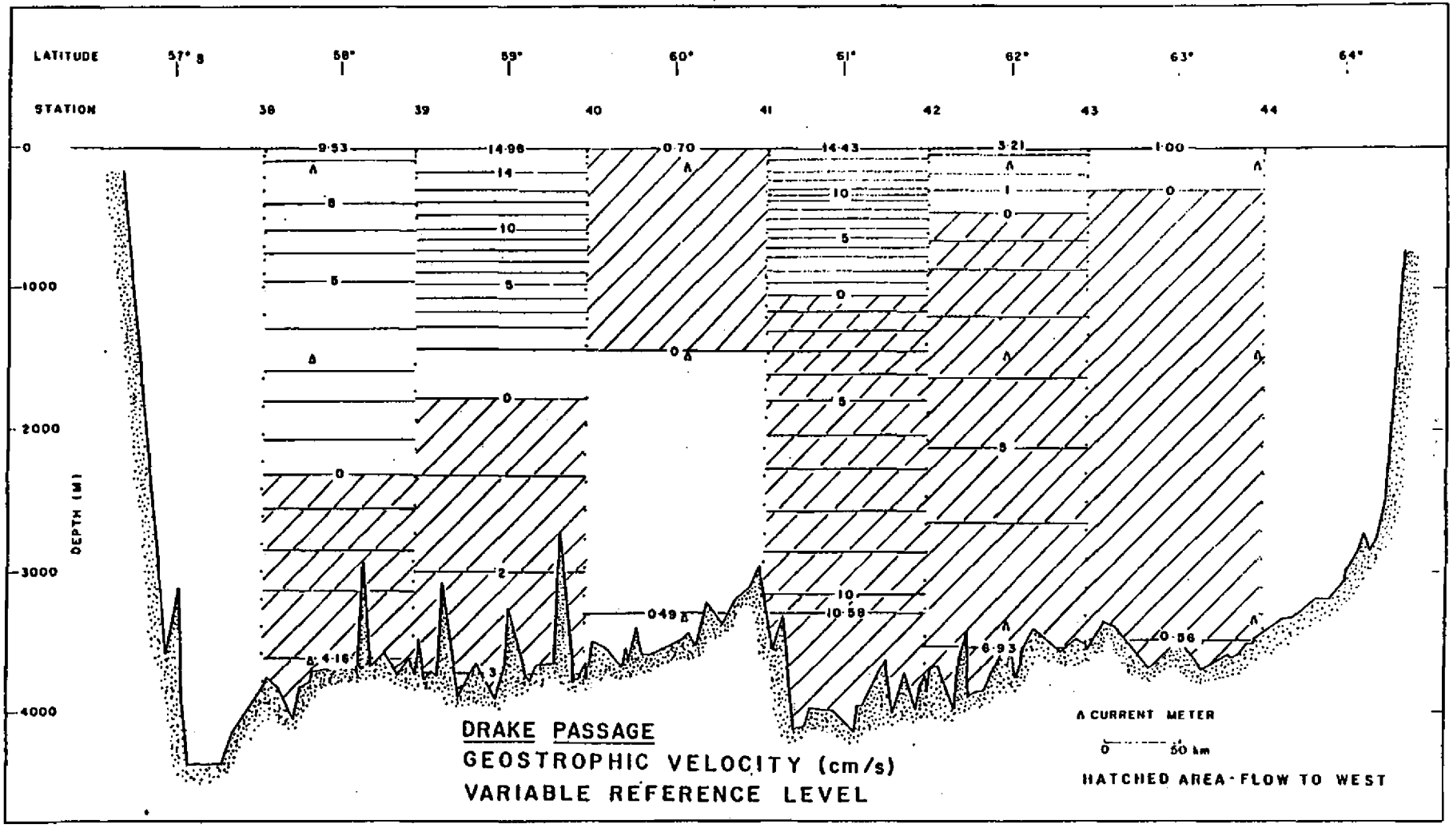

LATITUDE
57° S
58°
59°
60°
61°
62°
63°
64°
STATION
38
39
40
41
42
43
44
0
1000
2000
3000
4000
DEPTH (M)
9·93
14·98
0·70
14·43
3·21
1·00
14
8
10
5
5
5
0
0
0
5
5
0
0
2
0·49
10
10·58
4·16
6·93
0·56
A CURRENT METER
0
50 km
HATCHED AREA - FLOW TO WEST
DRAKE PASSAGE
GEOSTROPHIC VELOCITY (cm/s)
VARIABLE REFERENCE LEVEL

Figure 14

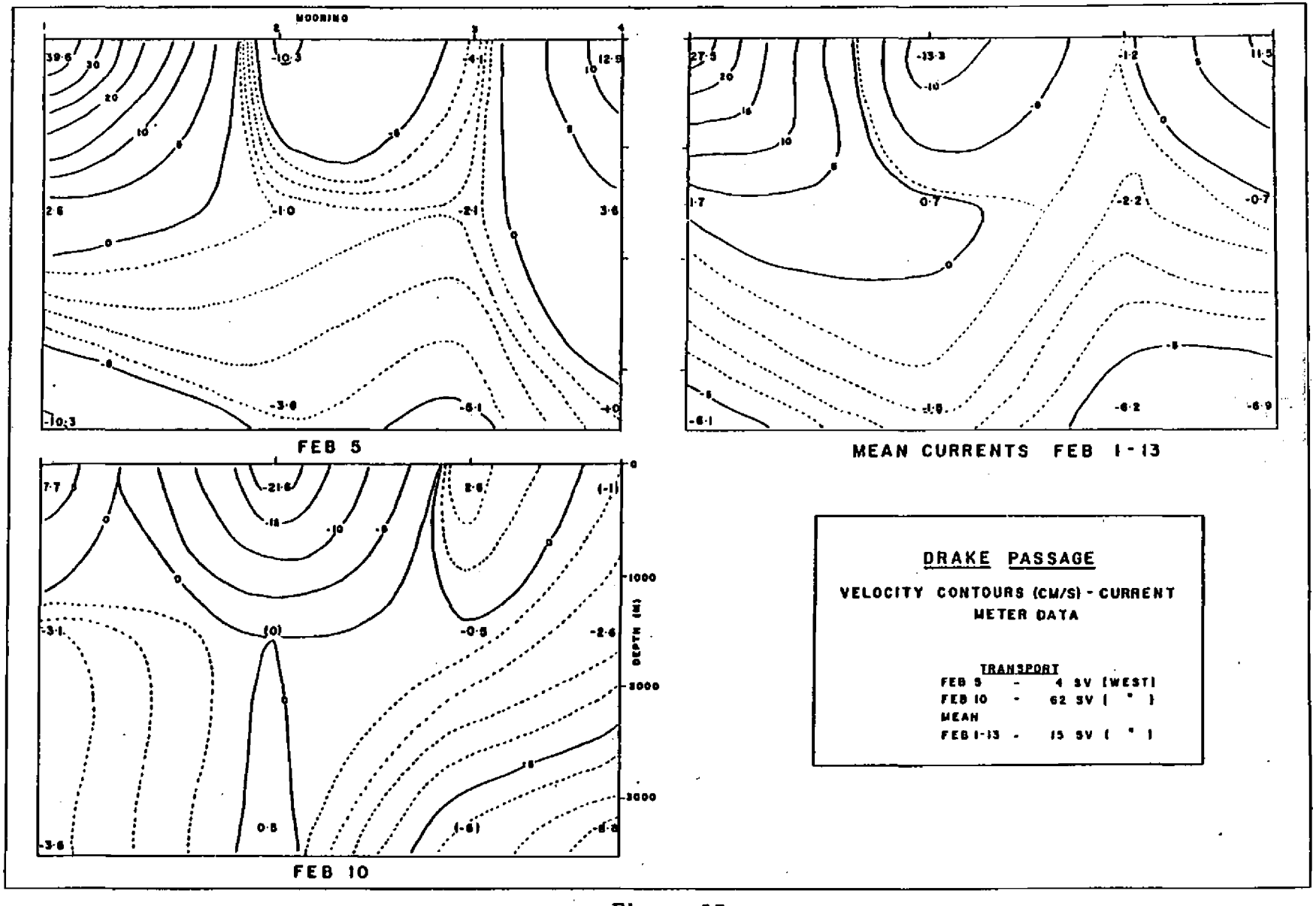

MOORING
FEB 5
MEAN CURRENTS FEB 1-13
FEB 10
DEPTH (M)
1000
2000
3000
DRAKE PASSAGE
VELOCITY CONTOURS (CM/S) - CURRENT METER DATA
TRANSPORT
FEB 5 - 4 SV (WEST)
FEB 10 - 62 SV (")
MEAN
FEB 1-13 - 15 SV (")

Figure 15

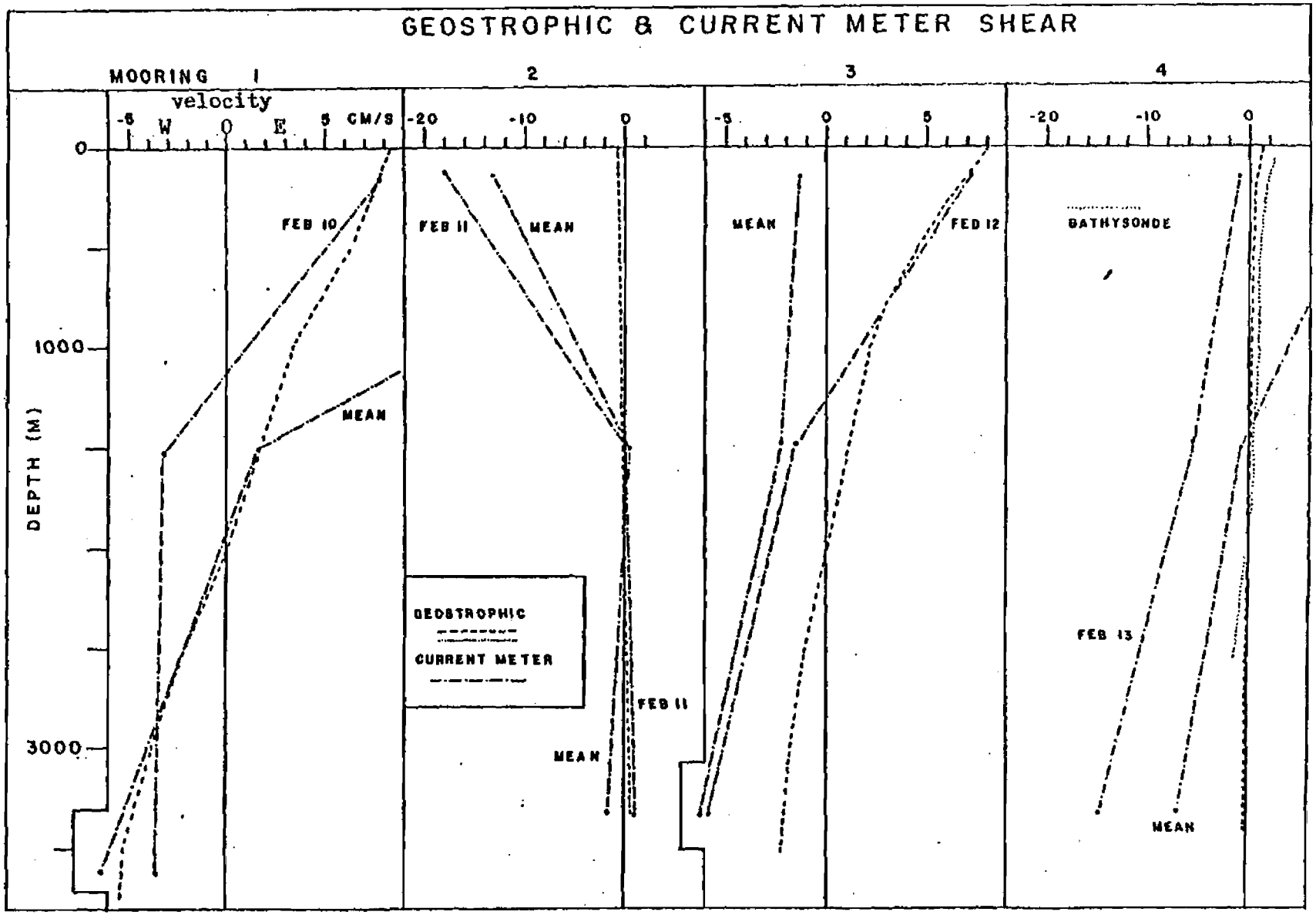

GEOSTROPHIC & CURRENT METER SHEAR
MOORING 1
2
3
4
velocity
-5 W 0 E 5 CM/S
-20 -10 0
-5 0 5
-20 -10 0
0
1000
3000
DEPTH (M)
FEB 10
MEAN
FEB 11
MEAN
MEAN
FEB 12
BATHYSONDE
FEB 13
MEAN
FEB 11
MEAN
GEOSTROPHIC
CURRENT METER

Figure 16

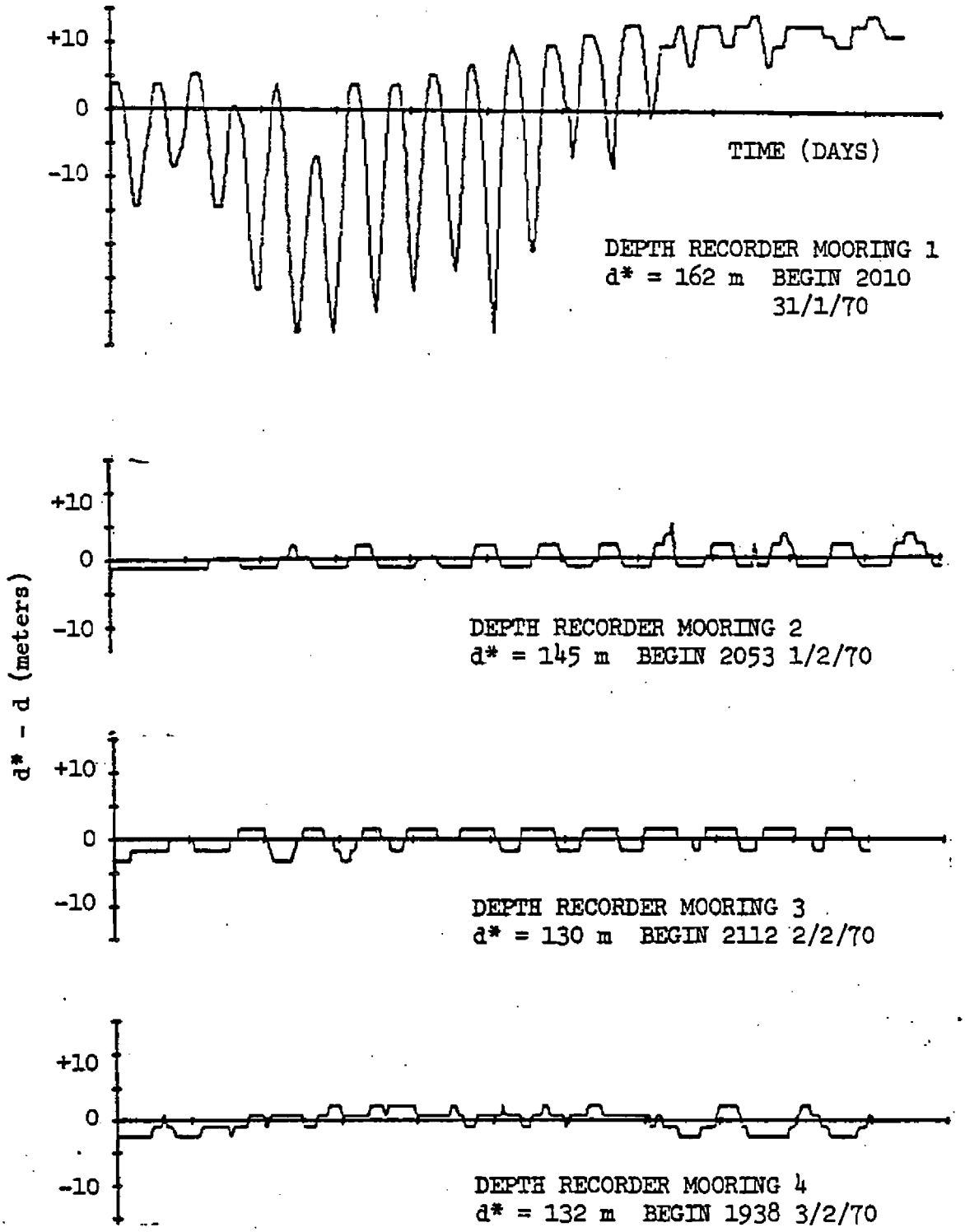


Figure 17 Depth Recorder Plots
d* = Mean depth of recorder
d = Depth of recorder

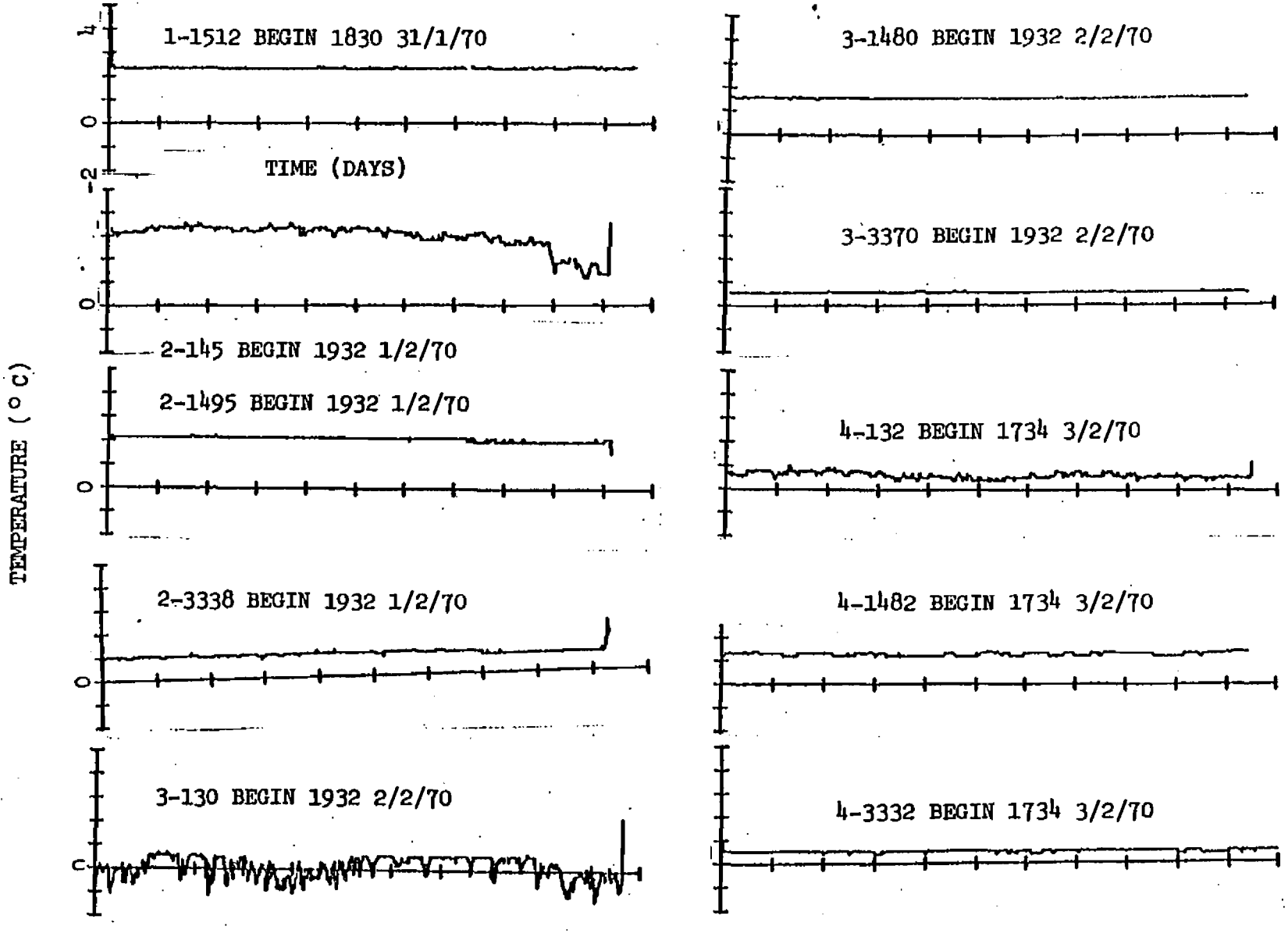


Figure 18 Thermograph Records

EARTH AND PLANETARY SCIENCE LETTERS 11 (1971) 83–89. NORTH-HOLLAND PUBLISHING COMPANY

A GEOPHYSICAL PROFILE IN THE SOUTH-EAST PACIFIC

R. T. HAWORTH*
Atlantic Oceanographic Laboratory,
Bedford Institute, Canada

Received 14 December 1970
Revised version received 12 March 1971

A crossing of the South-east Pacific has revealed features at 54½°S, 95°W named Hudson Peak and Deep which appear to be related to regional changes in the tectonic and/or oceanographic conditions. The features lie at the centre of a depression extending for 1500 km, each half of the depression representing a different physiographic province. The regional variations in topography may be explained if Hudson Peak and Deep lie in a region of progressive subsidence. It is suggested that the features are part of a fracture zone. Magnetic and gravity data examined qualitatively show that the feature is magnetically quiet with suggestion of a mass deficiency beneath Hudson Deep. Away from the Peak and Deep, magnetic anomalies with peak-to-peak amplitudes of up to 600 gammas occur.

1. Introduction

The track of Canadian Scientific Ship *Hudson* from Valparaiso to 63°S 150°W, part of the *Hudson* '70 scientific expedition, crossed a little known area of the South Pacific where features of geophysical interest were found.

Fig. 1 shows the track of C.S.S. *Hudson* between Valparaiso and Tahiti. At 54°38'S, 95°12'W a depth of 6103 m was recorded, the greatest depth of the entire Pacific track. Sixty km before this, at 54°19'S, 94°33'W a peak with a depth of 2920 m had been crossed. For ease of reference to the profiles, the names Hudson Peak and Hudson Deep will be used in this paper to describe the features. Although from Peak to Deep the average slope is 3°, and the recovery from depth is of the same order, individual slopes over the feature are much greater.

The history of geological and geophysical exploration of the Pacific up to 1962 is described by Menard [1]. This book provides an excellent summary of our knowledge of the Pacific Ocean basin at the beginning of the last decade. The discoveries since its publication emphasize the rapidity of advances in geophysics during that interval. Menard had few tracks available from which to produce a bathymetric chart of the South-east Pacific Basin (or Pacific-Antarctic Basin [1] or Bellingshausen Sea [2]). The Russian bathymetric chart [3] differs from that of Menard even with regard to the position of what is now known as the Eltanin Fracture Zone, one of the most prominent features in the area. Much of this discrepancy can be attributed to the poor quality and scarcity of position fixes in the pre-satellite navigation days. On both of the previously mentioned charts little topographic detail is given in the South-east Pacific Basin. The area is featureless on the Russian chart except for a shoal of 3951 m at 57°S, 99°W in a regional depth of 5000 m.

The work carried out aboard U.S.N.S. *Eltanin* after the mid sixties led to a considerable increase in knowledge of the area, although this is somewhat fragmentary. Sykes [4] determined that earthquake epicentres in the South Pacific were associated with the Eltanin Fracture Zone originally recognized by Menard [5]. Coverage with seismic reflection profiles has enabled Ewing et al. [6] to describe the sediment distribution in the South Pacific. Northrop et al. [7] have proposed a relation between seismic slip rate and sea floor spreading rate using data only from this area.

* B.I. Contribution no. 216.

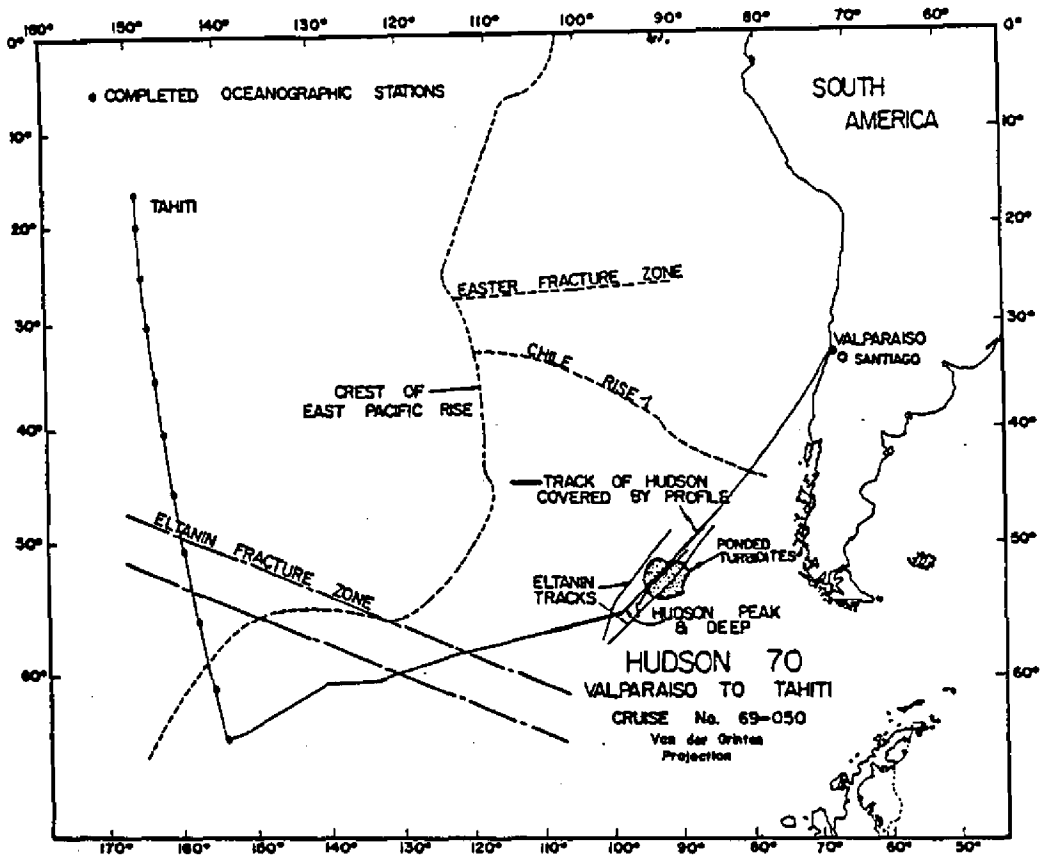


Fig. 1. Track of chart C.S.S. *Hudson* in the South Pacific. The thicker line shows the track of *Hudson* covered by the data profile.

Pitman et al. [8] and Heirtzler et al. [9] have used the *Eltanin* and *Vema* magnetic data to demonstrate proposed sea floor spreading in the South-east Pacific. New bathymetric data allowed Heezen and Tharp [10] to include some detail in the south east portion of their physiographic map of the Pacific. As a result of this and further information, the South-east Pacific is no longer an unexplored waste. The exploration is, however, so relatively sparse that the data gathered by C.S.S. *Hudson* in previously traversed areas is essential to a more accurate regional interpretation of the structure of that region.

2. Instrumentation

The U.S. Navy satellite navigation system was used to provide the principal navigation information. An ITT 4007AB receiver was interfaced with a PDP 8/L computer to provide for automatic acquisition and majority voting of the received data. As an example of the frequency of fixes, 46 good satellite fixes were obtained during the 58 hr covered by the data profiles presented here. The eight fixes shown on fig. 2 are purely representative positions along the track and should not be implied to be the only ones used during that interval.

The magnetic field was measured with a Barringer Research OM 104 proton precession magnetometer, the gravity field with an Askania and a vibrating string sea gravimeter, and the depth of water with the Bedford Institute precision sounding system. Magnetic and gravity observations were digitally recorded once per minute together with day, time, ships head and log information.

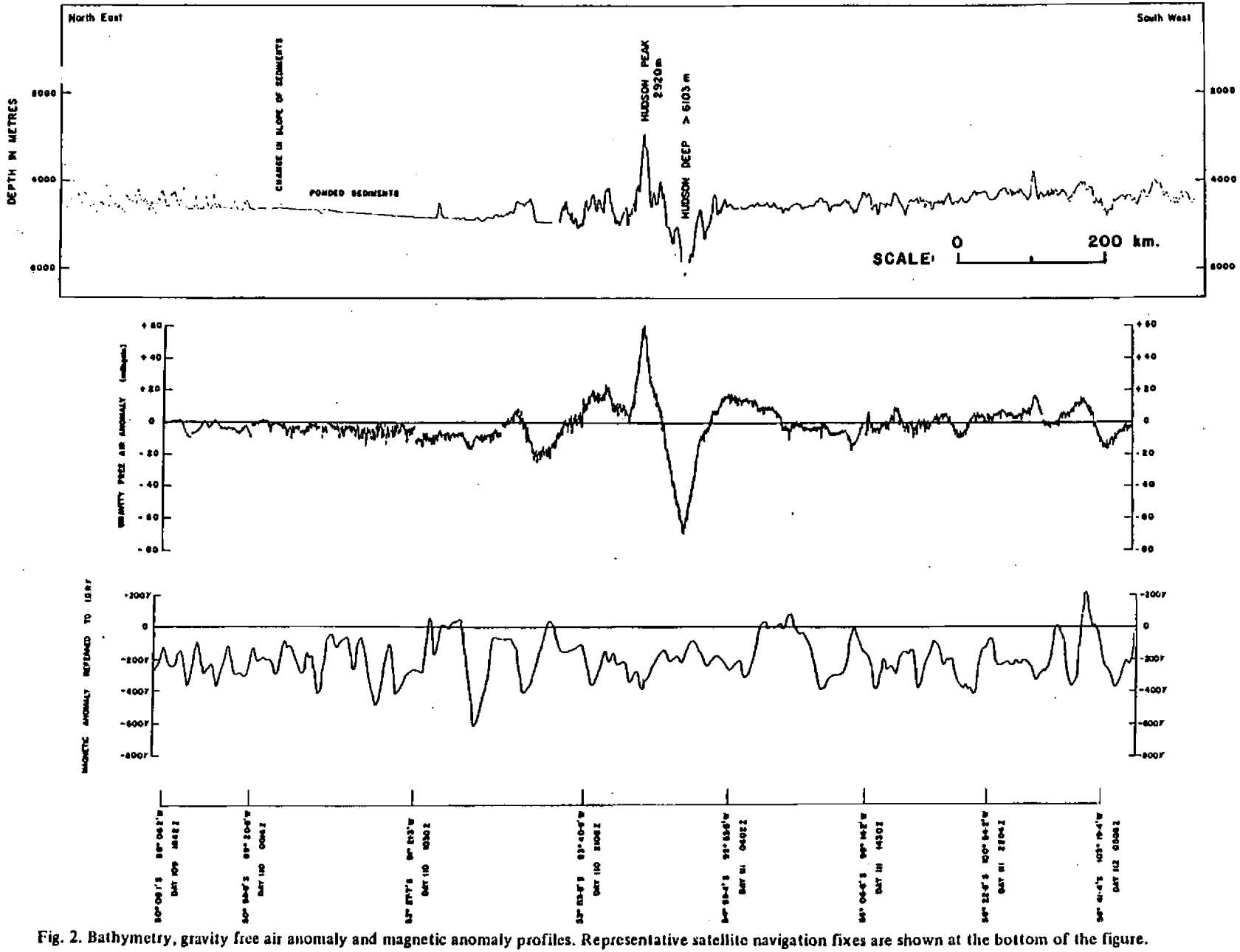


Fig. 2. Bathymetry, gravity free air anomaly and magnetic anomaly profiles. Representative satellite navigation fixes are shown at the bottom of the figure.

3. Data profiles

3.1. *Bathymetry*

In the bathymetric profile of the traverse from north east to south west (left to right in fig. 2) several distinct physiographic features and provinces can be seen. The profile begins in the north east with irregular topography having an amplitude of approximately 750 m and a wavelength of approximately 10 km. This amplitude is gradually reduced as the gullies become more sediment filled. However, the submerged topography may remain constant in amplitude and wavelength with the entire formation dipping to the south west beneath the sediment. This is suggested since the sedimentary basins generally increase in extent between progressively deeper peaks. The sediment completely submerges the topography on this profile at 51°S, 89°20'W and thereafter the profile is smooth with deviations of only a few metres about a mean slope. There is however a distinct change in the slope at approximately 51°15'S, 89°40'W. To the north east of this point the sediments on average have an approximately horizontal surface while to the south west there is a steady slope of 4 min of arc for 200 km. This down slope of the sedimentary surface is terminated at 52°39'S, 91°38'W by a single peak. Thereafter there is only one large sedimentary basin prior to Hudson Peak and Deep. This basin, centred at 53°33'S, 93°05'W, has an upper surface which is 70 m shallower than an extrapolation of the surface of the major basin, and has a slope of approximately 2 min. To the south west there is only a single trace of these undisturbed sediments before encountering Hudson Peak and Deep. Due to an error in programming of the echo sounder while over Hudson Deep, the greatest confirmed depth of 6103 m was measured on the slope up out of the Deep. The maximum possible depth was 6575 m (3600 fathoms). Emerging from Hudson Deep, there is a return to the irregular topography found to the north east of the sedimentary basins. However, in this region it seems that the dominant wavelength is shorter with smaller amplitude divergences from the mean slope, and there is no evidence of undisturbed sediments.

The sedimentary fill to the north east is noted by Ewing et al. [6] to be turbiditic with Antarctica suggested as the source of the sediments. There appears, however, to be some inconsistency in the evidence available regarding this origin. Ewing et al. [6], with reference to Ewing et al. [10], suggest that the dip of the sequence is simply a depositional slope. This may be so for the large Bellingshausen Basin south of 60°S which dips down to the north [11]. However, the sedimentary basin crossed by *Hudson* dips down to the south west suggesting, from the same assumptions, that the sediment was deposited from the north east. In order to explain this, Ewing et al. put forward the evidence of Gordon [12] to show that the currents sweep northwards to the west of the basin and southwards to the east with suggested deposition in between. Gordon's interpretation is based on potential temperature measurements and he cites the bottom photographs of Hollister and Heezen [2] as strong support for that interpretation. Although the agreement between Gordon and Hollister and Heezen is generally good, the two proposed current systems are different in the vicinity of Hudson Peak and Deep. Hollister and Heezen's interpretation of the current pattern is much simpler in this region with little suggestion of strong northward turbidity currents to the west of the sedimentary basin. With either of the suggested current patterns we would expect to find sedimentary basins to the south west of Hudson Peak and Deep. Since these are not found, either the proposed current systems have to be modified or Hudson Peak and Deep separate provinces with different tectonic histories.

The current pattern in the South-east Pacific is considerably influenced by the offset of the East Pacific Rise along the Eltanin Fracture Zone. In a similar way we might expect modification of the current pattern by Hudson Peak and Deep if they form part of an extensive feature. Such an extension is suggested by the apparent absence of sediment in Hudson Deep. If the Peak were an isolated feature, sediment would have filled the Deep. However, as part of a Ridge and Trench, a sufficient physical barrier could be presented to prevent sediment transport and deposition in the vicinity of Hudson Peak and Deep. This extended feature would then be qualified physiographically for the term "fracture zone" [13]. An examination has been made of bathymetric data from *Eltanin* [14] to substantiate this proposition. Despite positional uncertainties of the Eltanin data due to infrequent celestial fixes, it appears that Hudson Peak correlates with a shallower peak to the

north west and a deeper peak to the south east as part of a ridge. Hudson Deep also correlates with a possible trench on a trend paralleling that of the ridge.

Convergence of the regional topographic slopes under Hudson Peak and Deep provides some evidence for a history of tectonic activity. The change in slope of the sedimentary surface seen by *Hudson* at 51°15'S, 89°40'W can be traced to the *Eltanin* profiles and shown to extend for over 300 km in a north west–south east direction. The extent of the slope change suggests that it is not merely an anomaly in the "depositional slope". It would rather suggest extensive tilting after deposition. Ewing et al. [6] suggest however that the area has been tectonically inactive for a long time in view of the smoothness of the sedimentary surface. By accepting the suggestion that tilting occurred after deposition, we would expect the sub-bottom topography to show an increase in slope coinciding with the slope break of the sedimentary surface. Seismic profiling evidence for this would imply that *Hudson*'s geophysical profile extends across an area of progressive subsidence with Hudson Peak and Deep at its centre.

Menard and Atwater [15] account for fracture zone topography in terms of sea floor spreading. The scarp relief along a fracture of the mid-ocean ridge is related to the ridge offset and the period of spreading. The regional topographic trends either side of Hudson Peak and Deep converge either (a) at a point beneath the sediments to the north east of Hudson Peak, or (b) at Hudson Peak and Deep which then separate two physiographic provinces with these two provinces differing in elevation at the point of convergence by 750 m.

Only deep seismic reflection profiler information can decide between these alternatives. If (b) is found to be correct, it is possible that Hudson Peak and Deep are part of a fracture zone of the East Pacific Rise.

Without speculation, we can only infer that Hudson Peak and Deep are roughly at the convergence of two regional topographic trends each extending for approximately 700 km. The critical (but circumspect) step to take is to associate the convergence of the regional trends with the presence of Hudson Peak and Deep. Having taken this step, however, the tectonic significance of the feature is amplified.

3.2. *Gravity field*

The gravity free-air anomaly over the region referred to the 1930 International Gravity Formula is shown as the central profile in fig. 2.

The most striking feature of the profile is the 130 mgal amplitude free-air anomaly across the 3200 m bathymetric expression of Hudson Peak and Deep. Assuming that the latter are part of a linear feature which *Hudson*'s tracks crossed perpendicularly, the Bouguer correction would be 224 mgal (assuming a rock density of 2.67 g cm^{-3}). A simple two dimensional Bouguer anomaly profile over the feature suggests that there is a 20 mgal negative anomaly coinciding with Hudson Deep. However, the profile is extremely noisy and only a three dimensional terrain corrected Bouguer anomaly profile (for which there seems to be too little data) would confirm this.

The only other large features on the profile are associated with topographic expression. The two peaks north east of Hudson Peak are reflected in the free-air anomaly profile as are the topographic variations to the south west. The amplitudes of anomalies to the north east are much less than those to the south west as a result of the sedimentary fill. The smaller the density contrast, the less apparent will significant anomalies be. The level of the noise (due to rough seas) on the profile over the sedimentary basin tends to obscure low amplitude anomalies but some detail can be seen.

Further gravity data in the vicinity seem to be required before proceeding with a quantitative analysis of the region. The only other known gravity data within 1000 km were collected by the Japanese [16]. Although the precise location of these measurements is not known to this author, it seems that the measurements will be sufficiently contiguous with the *Hudson* data to assist in a regional structural interpretation.

3.3. *Magnetic field*

The magnetic anomaly over the region referred to the International Geomagnetic Reference Field [17] is shown as the bottom profile of fig. 2. From the generally negative anomalies it appears that the IGRF does not accurately represent the regional variations in this locality.

The magnetic signature contains no anomalies of amplitude over 600 gamma. The greatest magnetic anomaly may be correlated with a 10 mgal negative gravity anomaly which seems to be associated with a small sedimentary basin at 52°57'S, 92°06'W. The most notable feature is the absence of even moderate anomalies over Hudson Peak and Deep. There is also no regional elevation or depression of the magnetic field. This absence of anomalies is reminiscent of traverses of the Cayman Trough [18].

There may be some significance in the difference between the wavelength of the anomalies to the north east and south west of Hudson Peak and Deep. The anomalies appear to have a shorter wavelength over the major sedimentary basin. The extent of this difference is difficult to ascertain, especially in view of the change in direction of the track at 56°07'S, 98°14'W.

Two of the *Eltanin* tracks in the vicinity have magnetic measurements along them. There is no immediately apparent correlation between either of these profiles and the other, or the *Hudson* magnetic profile. If Hudson Peak and Deep are part of a fracture zone, magnetic trends would not continue across the fracture, and thus any regional trend would be obscured. If such a trend could be found it would indeed be valuable in determining the tectonic significance of the topographic features encountered.

It is possible that the proposed fracture zone might be associated with the bend in the magnetic anomaly pattern as summarized by Pitman et al. [8] from *Eltanin* data across the East Pacific Rise between 40°S and 60°S. A similar association could also be proposed with the Shackleton Fracture Zone of Barker [19]. However, both of these are extremely tenuous connections involving a 1000 km extrapolation of indeterminate features through unsurveyed areas.

4. Summary

Hudson Peak and Deep appear to be in a position where sedimentation is interrupted and/or there is a boundary between provinces with differing tectonic histories. Either of these suggestions leads to the conclusion that Hudson Peak and Deep are part of a more extensive feature suggestive of fracture zone topography. Bathymetric data from other cruises tend to support this. Gravity and magnetic data can be examined only qualitatively but show that Hudson Peak and Deep are magnetically quiet with a possible mass deficiency beneath Hudson Deep.

Acknowledgements

The cooperation of the officers, crew and scientists involved in *Hudson* '70 is gratefully acknowledged. My thanks go especially to Dr. W.S.von Arx who was such a stimulating companion with whom to work on this phase of the cruise. The loan of his vibrating string sea gravimeter is also acknowledged. The comments of J.Brooke, B.D.Loncarevic, R.F.Macnab, D.I.Ross, J.M.Woodside and the reviewers were helpful in preparation of this manuscript.

References

[1] H.W.Menard, Marine Geology of the Pacific (McGraw-Hill, 1964) 271 pp.
[2] C.D.Hollister and B.C.Heezen, The floor of the Bellingshausen Sea, in: Deep-Sea Photography, Johns Hopkins Oceanographic Study No. 3, J.B.Hersey ed. (1967) 177.
[3] Bathymetric Chart of the Pacific, Institute of Oceanology, Academy of Sciences of the U.S.S.R. (1963).
[4] L.R.Sykes, Seismicity of the South Pacific Ocean, J. Geophys. Res. 68, 21 (1963) 5999.
[5] H.W.Menard, The East Pacific Rise, Science 132 (1960) 1737.
[6] M.Ewing, R.Houtz and J.Ewing, South Pacific sediment distribution, J. Geophys. Res. 74, 10 (1969) 2477.
[7] J.Northrop, M.F.Morrison and F.K.Duennebier, Seismic slip rate versus sea-floor spreading rate of the Eastern Pacific Rise and Pacific Antarctic Ridge, J. Geophys. Res. 75, 17 (1970) 3285.
[8] W.C.Pitman III, E.M.Herron and J.R.Heirtzler, Magnetic anomalies in the Pacific and sea-floor spreading, J. Geophys. Res. 73, 6 (1968) 2069.
[9] J.R.Heirtzler, G.O.Dickson, E.M.Herron, W.C.Pitman III and X.Le Pichon, Marine magnetic anomalies, geomagnetic field reversals, and motions of the ocean floor and continents, J. Geophys. Res. 73, 6 (1968) 2119.
[10] B.C.Heezen and M.Tharp, Pacific ocean floor, National Geographic Magazine (October, 1969).
[11] M.Ewing, J.Ewing, R.Houtz and R.Leyden, Sediment distribution in the Bellingshausen Sea, Proc. Symp. Antarctic Oceanog., Santiago, Chile (1966).

[12] A.L.Gordon, Potential temperature, oxygen and circulation of bottom water in the Southern Ocean, Deep Sea Res. 13 (1966) 1125.
[13] Undersea Features: Official Name Decisions Gazeteer No. 111 (U.S.Board on Geographic Names, 1969) 142 pp.
[14] J.R.Heirtzler, D.E.Hayes, E.M.Herton and W.C.Pitman III, Preliminary report of volume 20, U.S.N.S. *Eltanin* cruises 16–21, Technical report no. 3-CU-3-69 from Lamont-Doherty Geological Observatory of Columbia University (June, 1969).
[15] H.W.Menard and T.Atwater, Origin of fracture zone topography, Nature 222 (1969) 1037.
[16] Bureau Gravimetrique International, bulletin d'information no. 22 (March, 1970).
[17] E.B.Fabiano and N.W.Peddie, Grid values of total magnetic density, IGRF–1965, unpublished manuscript of the Coast and Geodetic Survey, E.S.S.A. (1969).
[18] C.Bowin, Geophysical study of the Cayman Trough, J. Geophys. Res. 73, 16 (1968) 5159.
[19] P.F.Barker, Plate tectonics of the Scotia Sea region, Nature 228 (1970) 1293.

Geophysical Studies in Baffin Bay and some Tectonic Implications

C. E. KEEN, D. L. BARRETT, K. S. MANCHESTER, AND D. I. ROSS

Manuscript received July 30, 1971
Revision accepted for publication December 7, 1971

A recent seismic refraction experiment in the deep central region of Baffin Bay showed that it is underlain by oceanic crust. This paper describes the results of gravity, magnetic, and seismic reflection profiling measurements in the bay. There is no definitive evidence for a buried ridge or for magnetic lineations in the center of the area. The magnetic and gravity anomaly fields have been used to define the boundary between the oceanic and continental crust around the bay and therefore the extent of oceanic crust presumed to have been formed by sea-floor spreading. Some of the characteristics of the seismic reflection lines across the continental margins, perhaps typical of this area, are also discussed. The results have been used to reconstruct the history of opening of Baffin Bay in conjuction with geophysical measurements in the Labrador Sea to the south and over the Alpha Ridge in the Arctic Ocean to the north. An attempt has been made to reconcile the geometry of opening with continental geology. Two phases of spreading are suggested. The first involves openings, in both the Labrador Sea and in Baffin Bay, about a pole in the Canadian Arctic Islands. The second, most recent stage of opening, requires that the Nares Strait was once a transform fault, perhaps connecting a Baffin Bay spreading center to the Alpha Ridge to the north.

Une étude de réfraction sismique dans les pronfondeurs du centre de la Baie de Baffin a montrée l'existence de croûte océanique. Cet article donne les résultats de profils gravimétriques, magnétiques, et sismiques dans la baie. Il n'y a pas d'évidence de ride enfouie ou de linéations magnétiques dans le centre de la région. Les anomalies magnétiques et gravimétriques ont servi à déterminer la limite entre la croûte continentale et la croûte océanique autour de la baie, et de là, la partie de la croûte présumée par étalement du fond océanique. Quelques caractères des profils sismiques des marges continentales, particuliers à la région, sont aussi discutés. Les résultats ont servi à reconstituer l'histoire de l'ouverture de la Baie de Baffin en relation avec les mesures géophysiques dans la Mer du Labrador au sud, et au-dessus de la Rive Alpha de l'Artique, au Nord. Un essai de corrélation est tenté entre cette ouverture et la géologie continentale. On suggère l'existence de deux phases d'étalement. La première implique l'ouverture de la Mer du Labrador et de la Baie de Baffin suivant un pôle situé dans les îles de l'Artique canadien. La seconde, plus récente, demande l'existence d'une faille transformante au niveau du détroit de Nares, reliant probablement l'étalement de la Baie de Baffin à la rive Alpha au Nord.

Introduction

Baffin Bay provides an important geographic link between two large oceanic areas, the Arctic Ocean to the north and the Labrador Sea to the south. Reconstructions of plate motions in both regions must be reconciled with the continental geology surrounding the bay and with geophysical measurements defining its structure and history. Past attempts to explain its origin and subsequent evolution have been limited by a lack of geophysical measurements within the area; the evidence being substantially confined to the geology of the surrounding land masses and to some knowledge of the opening of the Labrador Sea to the south. Continental geology is of limited usefulness in defining Cenozoic and Mesozoic plate motions because, with a few important exceptions, Pre-Cambrian and Lower Paleozoic rocks are exposed along most of the surrounding coastline. Previous geophysical studies of the region have been inconclusive. No definite evidence of a buried median ridge or of magnetic lineations indicative of sea floor spreading have been found from the measurements (Keen *et al.* 1970, Barrett 1966). The fact that Baffin Bay is a sea of intermediate depth, reaching 2000 m in its central region, has led some investigators to suggest that the area may not be underlain by oceanic crust. An additional complexity is the substantial number of shallow focus earthquakes in the area; the activity on Baffin Island and the northern portion of the bay being significantly greater than elsewhere in the eastern Arctic (Whitham *et al.* 1970) or in the Labrador Sea. All epicenters, on which data has been published, some of the

[1]Marine Geophysics Division, Bedford Institute, Dartmouth, Nova Scotia B.I. Contribution No. 279.

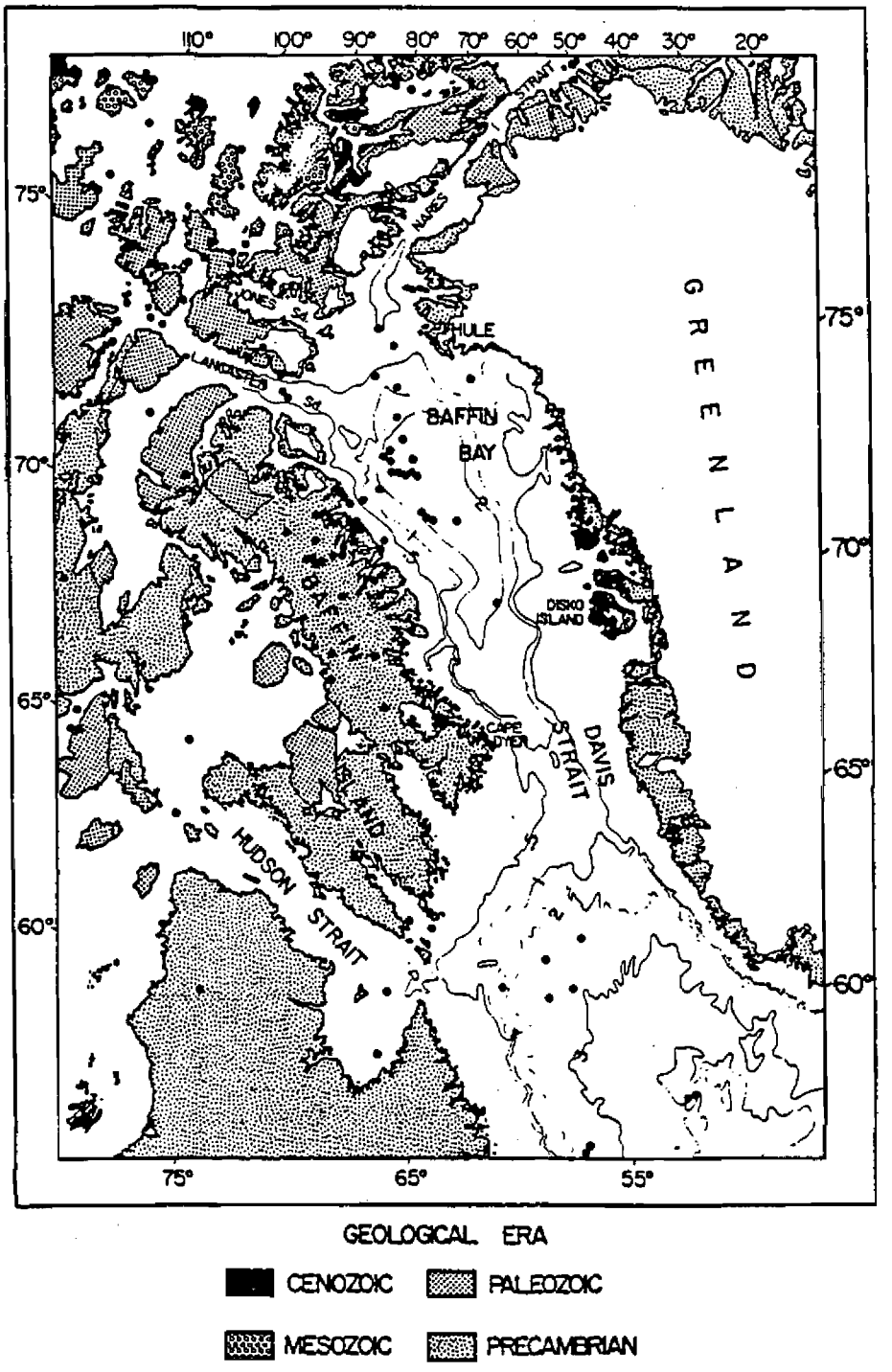


FIG. 1. A map of the Baffin Bay area showing in simplified form the geology and bathymetry. The bathymetric contours are in kilometers. The black dots are earthquake epicenters obtained from a variety of sources, particularly from USC Geol. Surv. data and the Dominion Observatory Seismological bulletins. All earthquakes on which material was published between 1920 and 1969 are shown.

important geological features, and the bathymetry are shown in Fig. 1.

Most investigators have argued that Baffin Bay was formed by sea-floor spreading away from a northern continuation of the Labrador Sea mid-ocean ridge (Wilson 1963, Vogt and Ostenso 1970, Le Pichon *et al.* 1971). This explanation has been criticized because the geology of the Canadian Arctic Islands and of the land bordering Nares Strait has been interpreted to imply that large horizontal displacements could not have occurred there since Paleozoic times (Kerr 1967, Fortier and Morley 1956). It is difficult to open Baffin Bay without invoking several hundred kilometers of horizontal motion along Nares Strait or substantial crustal extension between the Arctic Islands. An alternative suggestion was made by Kerr (1967) who postulated that Baffin Bay is a fault bounded continental depression and that Nares Strait is a submerged rift valley. Le Pichon *et al.* (1971) attempted to reconcile sea-floor spreading in the Labrador Sea and Baffin Bay regions with continental geology. They suggest that the Labrador Sea opened in two phases; the first, 60 to 80 m.y. ago, about a pole at 80° N, 90° W and the second, 40 to 60 m.y. ago, about a pole in western Hudson Bay. These motions do not require lateral movement along Nares Strait and the first phase of opening is supported by geophysical measurements in the Labrador Sea. There is little evidence, however, to support the geometry of the second phase of opening.

The purpose of this paper is to describe the results of a geophysical survey in the Baffin Bay region during 1970 and to relate the results to possible plate motions. Three ships, C.S.S. Hudson, C.S.S. Baffin, and U.S.C.G.S. Edisto were involved in the collection of bathymetric, gravity, magnetic, and seismic reflection and refraction data. Use has been made of earlier, unpublished data by members of Bedford Institute when relevant. The latter were collected during cruises of Canadian Icebreakers to the eastern Arctic from 1963 to 1966 and are limited mainly to bathymetric and magnetic measurements.

The Measurements

Fig. 2a shows all the ship's tracks along which geophysical data have been collected either by the Bedford Institute or by Dalhousie University and Fig. 2b, the ship's tracks corresponding to the Bedford Institute's 1970 studies. The reversed refraction line, shown as a heavy black line in Fig. 2b, was carried out using two ships, the Hudson and the Edisto. The former was the recording ship and the latter, the shooting ship. Conventional two-ship techniques, already described by Barrett *et al.* (1971) were used. Magnetic measurements, including data collected on earlier cruises were made using proton precession magnetometers. The magnetic anomalies were obtained using IGRF regional field and no corrections have been applied to remove diurnal variations which can reach 300 γ in the area. The gravity data were collected with a Graf-Askania gravimeter mounted on a gyro-stabilized platform. Gravity and magnetic measurements were made from the Hudson and the Baffin.

The main components of the seismic reflection system are a 120 m hydrophone streamer and a Bolt model 1500 air gun with a 300 in^3 (0.005 m^3) chamber and a wave shaper to eliminate bubble pulsing. The air gun was fired every 16 seconds at a peak pressure of about 1700 p.s.i. (12×10^5 kg/m^2). The incoming signals were recorded on an Alpine precision depth recorder and on magnetic tape in analogue form. Expendable sonobuoys were used in conjunction with the reflection system to provide sediment velocities. Few of the sonobuoys functioned satisfactorily in Baffin Bay and little useful information was obtained. It is probable that the transmitter aerials were inefficient due to the formation of ice over the exposed parts of the buoys. All seismic reflection measurements were carried out from Hudson.

The primary method of navigation during 1970 was by satellite fixes which are accurate to 2 km or less. Dead reckoning was used to interpolate between fixes. The earlier surveys were performed using LORAN-A, celestial navigation, and radar fixes on land.

Results

The main discovery, upon which discussions of all other results are based, is that the crust beneath the deep central region of Baffin Bay is oceanic. This was determined from the two-ship refraction line, the results of which have been described in an earlier paper by Barrett *et al.*

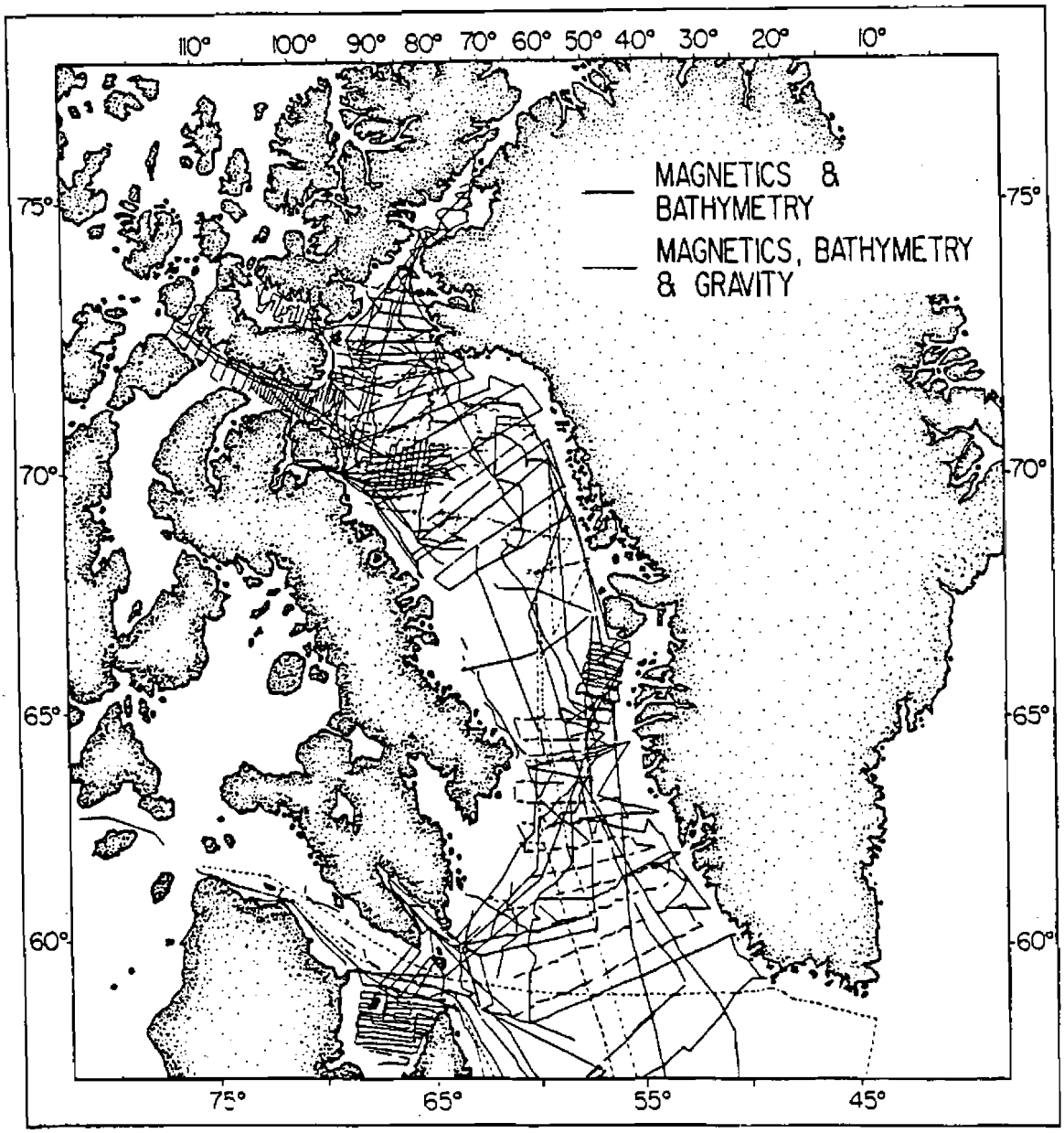


FIG. 2a. Ships' tracks along which geophysical data have been collected by the Atlantic Oceanographic Laboratory and Dalhousie University.

(1971). The time-distance plot is reproduced in Fig. 3 and the layer velocities and thicknesses, in Table 1. The time-distance plot shows that the velocities of the upper layers are uncertain; the 2.3 and 3.5 km/s velocities having been assumed for the purposes of the calculations. However, the other layers have been adequately defined and the depth to the M. discontinuity, 10 km, is unlikely to be in error by more than 20% because of these assumed velocities. This would not affect the main conclusion.

The gravity and magnetic data are presented in Figs. 4 and 5 respectively. The magnetic data shown were collected during some of the earlier cruises and the anomaly map does not include all tracks along which measurements have been

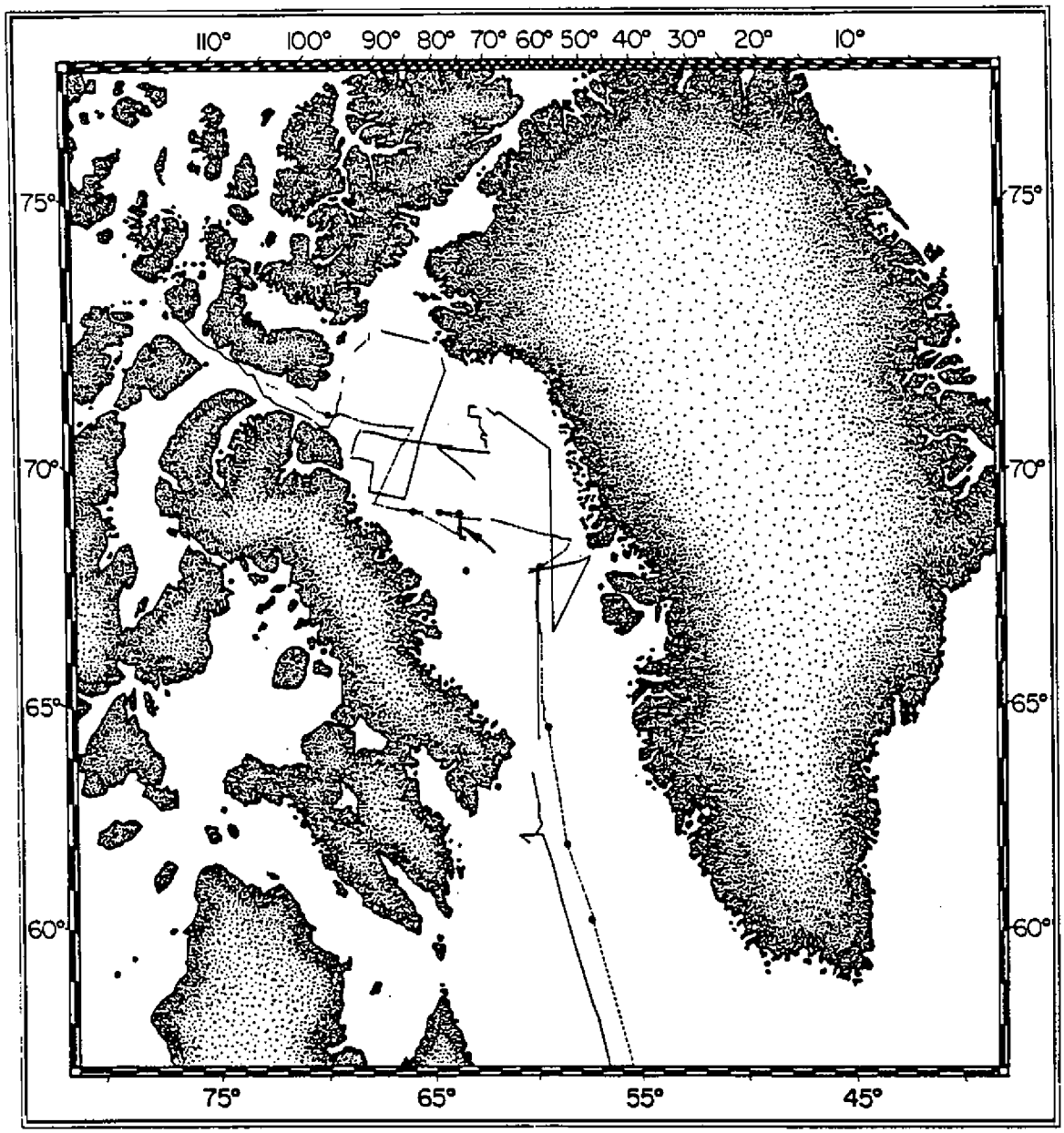


FIG. 2b. Ships' tracks during 1970. The solid lines are Baffin's tracks and the dashed lines, Hudson's tracks. The heavy solid line indicated by the arrow is the position of the refraction line. The dots are positions at which cores or bottle stations, not discussed in this paper, were obtained.

made. It is, however, representative of the main features of the area. The free-air, gravity anomaly map includes all data obtained by the Bedford Institute within the area shown in Fig. 4.

In the central, deeper regions of the Bay the magnetic anomalies exhibit low amplitudes, seldom exceeding 300 γ and long wavelengths, typically 30 km. On the eastern and western shelves, however, the anomalies are characteristically large, often more than 1000 γ and have shorter wavelengths. The gravity anomalies show large positive values where the tracks cross the continental margins, indicated by the dashed lines in Fig. 4. Models of the crustal structure

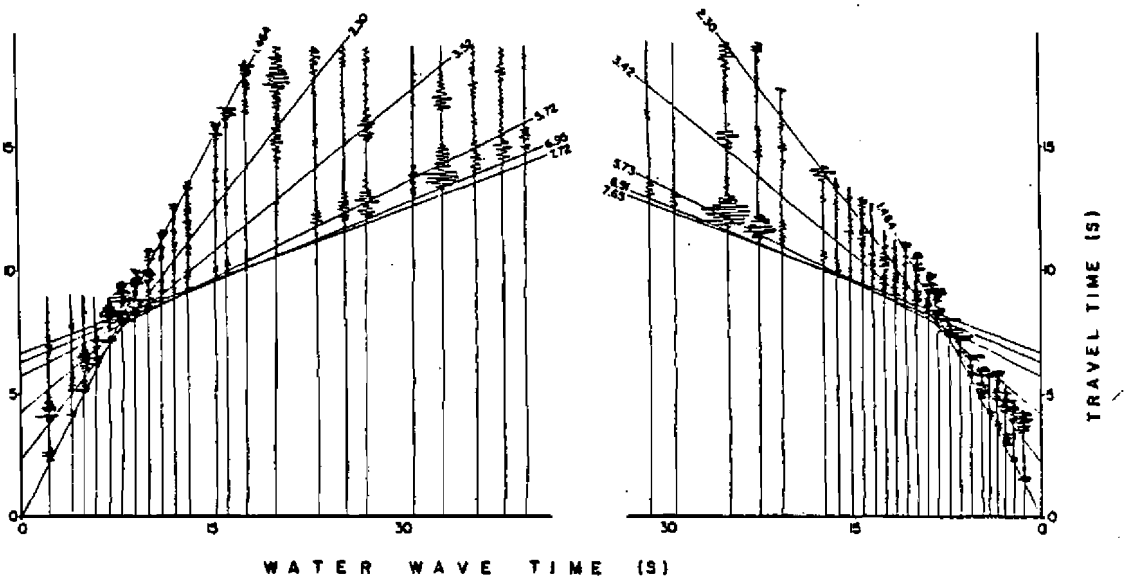


FIG. 3. The time-distance plots presented as record stations. Velocities are in km/s. The right-hand plot shows recordings at the southern station and the left-hand plot, recordings at the northern station.

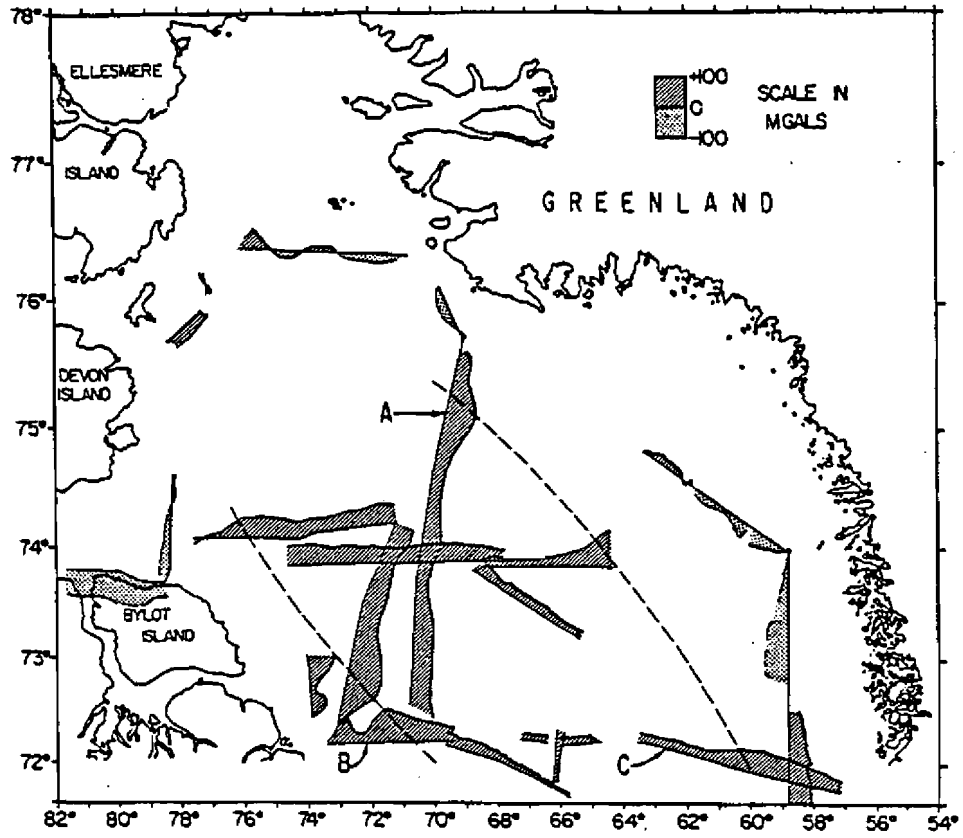


FIG. 4. Free-air gravity anomaly map showing data collected by the Hudson and the Baffin in 1970. The lines along which models of the crustal structure have been constructed are indicated by arrows and a letter. The dashed lines show the position of the 'shelf-edge' anomalies.

TABLE 1. Layer thicknesses and velocities

Layer	Velocity km/s	Thickness in km	
		Southern station	Northern station
Water	1.464	2.3	2.3
Unconsolidated sediment	2.30	2.1	2.0
Sediment?	3.47	2.0	2.3
Layer 2	5.72	2.0	2.1
Layer 3	6.93	1.9	2.1
Mantle	7.68	–	–

NOTE: The positions of the southern and northern stations are 71°39′ N, 65°55′ W and 72°18′ N, 66°13′ W respectively. These are median positions taken over the time that the HUDSON was on station.

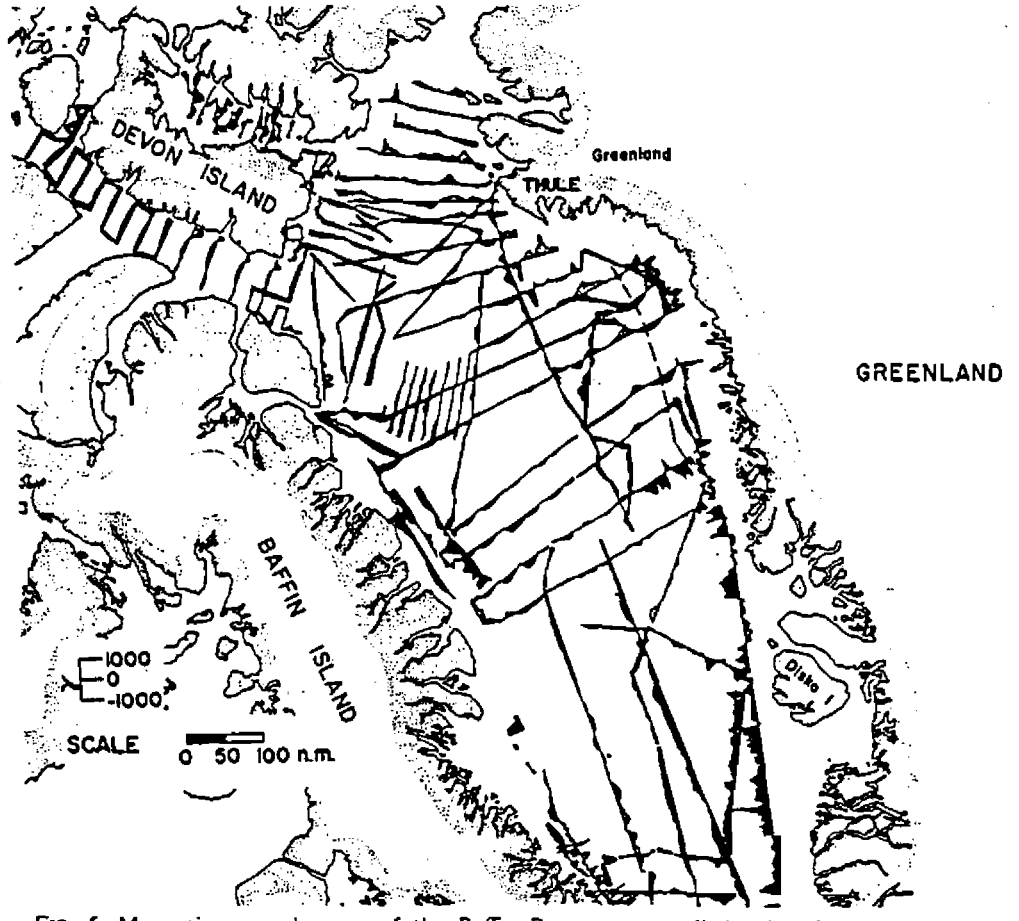


FIG. 5. Magnetic anomaly map of the Baffin Bay area compiled using data from earlier cruises. The dashed line along the west Greenland shelf shows the position of the wide negative anomaly discussed in the text. Shaded anomalies are positive, black are negative.

have been obtained which satisfy the gravity measurements along some of these profiles and confirm that these anomalies are associated with the transition from continental to oceanic crust. The models are described in more detail later. The area occupied by oceanic crust, determined from the gravity results, is also the region of low magnetic relief and it appears that the edge of the oceanic region may also be reflected in the change from low to high intensity magnetic

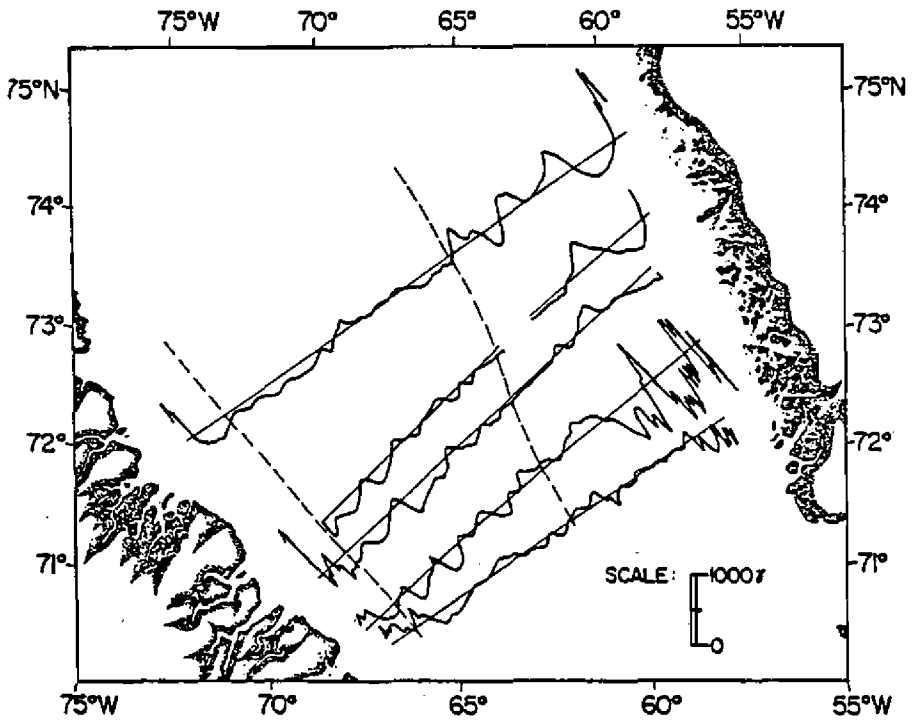


FIG. 6. Magnetic anomalies along five tracks across central Baffin Bay. The dashed lines correspond to the gravity 'shelf-edge' anomalies of Fig. 4.

anomalies. These characteristics of the gravity and magnetic fields are similar to those observed at other, better documented, continental margins and oceanic areas, the northwestern Atlantic for example (Emery *et al.* 1970). However, there is no evidence for a quiet magnetic zone paralleling the margin of the bay nor is there a 'slope anomaly', both of which are conspicuous features of the Atlantic margin. The apparent absence of these may be related to different times of opening in the two areas but it would be unrealistic to speculate further without more data, particularly seismic reflection profiles defining the topography of the magnetic basement in central Baffin Bay.

The high frequency, high intensity, magnetic anomalies along the shelves may in some areas be attributed to occurrences of basalt, perhaps related to the Tertiary basalts observed on land in the Disko Island area of west Greenland and at Cape Dyer on Baffin Island. The seaward extent of the Disko basalts has been mapped by Park *et al.* (1971) who showed that they continue well to the north of any outcrops on land. The large magnetic anomalies along the Baffin Island shelf have not been so well defined. As discussed later, there is some evidence that they are also caused by basic intrusions.

There is a broad magnetic low trending north-northwest along the Greenland shelf. Its axis is shown by the dashed line in Fig. 5. This feature appears to be truncated to the south by the northern boundary of the Disko basalts. Barrett and Manchester (1969) have calculated the depth to magnetic basement along a profile across the low and have shown that the basement has the form of a graben or basin, 2.5 km deep. A graben trending west-northwest and filled with about 2 km of Proterozoic and Paleozoic sediment occurs on land in the Thule area (Dawes 1971, Henderson 1971). The age of the sediments filling the graben beneath the Greenland shelf is not known but the geology of the Thule area suggests that the initial formation of the feature may have occurred during the Pre-Cambrian. The gravity profiles across this part of the Greenland shelf exhibit large negative values reaching a minimum of about −80 mgal in the area occupied by the magnetic low. Along the north-south track, the gravity values rise sharply in the south to a maximum of 80 mgal (Fig. 4). The point at which the transition occurs

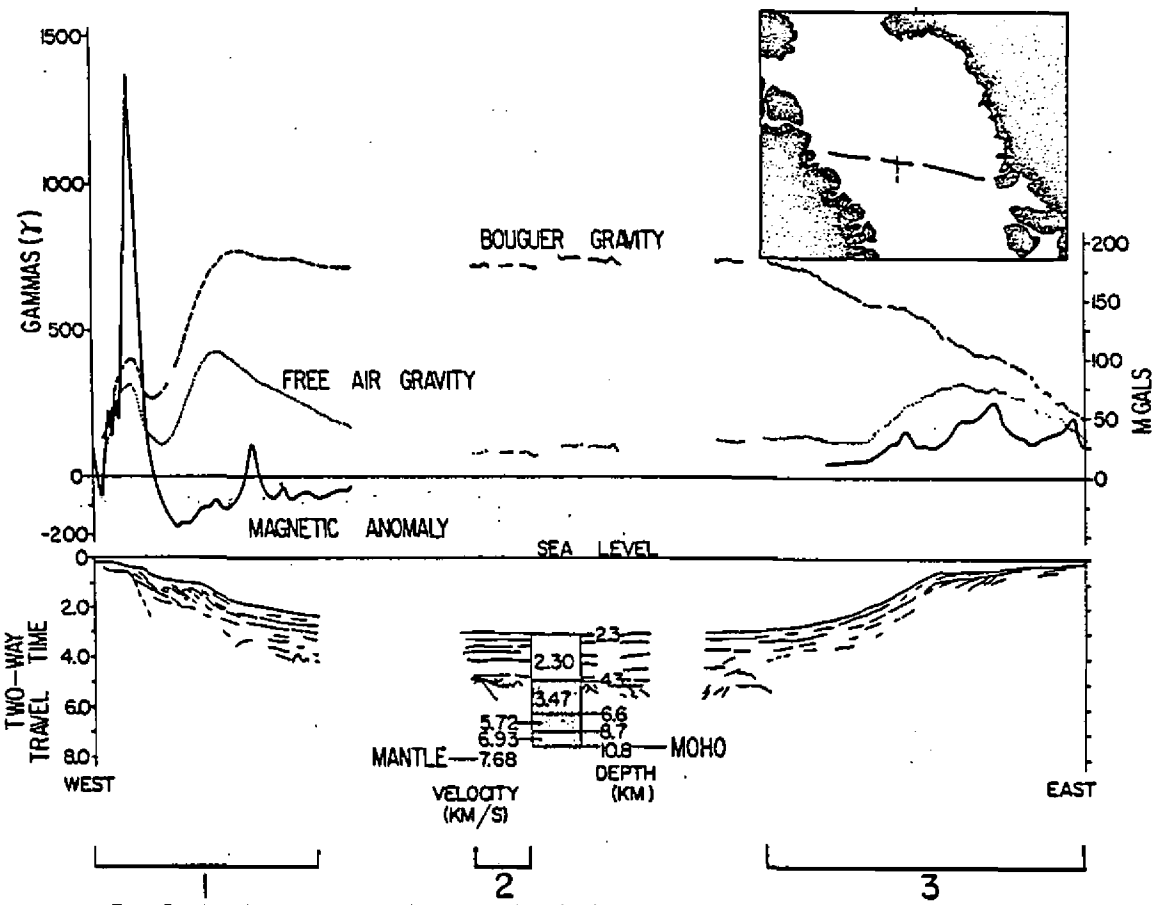


FIG. 7. Gravity and magnetic anomalies, bathymetry, and a line drawing of the seismic reflection results along a track across Baffin Bay. The position of the line is shown on the index map in the upper right-hand corner of the diagram. The dashed line is the position of the seismic refraction experiment, the results of which have been superimposed upon the seismic reflection data. The travel time scale is in seconds. A density of 2.67 g/cm^3 was used to calculate the Bouguer anomaly. The numbered square brackets indicate the sections of the original records which are presented in Fig. 8.

corresponds to the apparent termination of the graben by the Disko basalts. Henderson (1972) has estimated that there is up to 8 km of basalt filling the southern end of this feature. An approximate calculation, based upon two dimensional slabs, shows that an abrupt change from 8 km of sediment to 8 km of basalt along the track is consistent with the observed gravity anomaly.

Figure 6 shows the magnetic anomalies along five tracks across the bay. This indicates the magnetic characteristics of the central area more clearly than Fig. 5. An attempt was made to examine these profiles for evidence of magnetic lineations in the oceanic area. Some correlation among the profiles is possible, particularly between the anomalies at the western end of the three central lines. However, there does not appear to be any definitive evidence of magnetic lineations. A more detailed magnetic survey may, however, reveal their presence.

The gravity, magnetic, and seismic reflection results along an east-west traverse across the Bay are presented in Fig. 7. The results of the refraction experiment are also shown. The reflection profile indicates that there is a thick sequence (about 2 seconds two-way time) of flat-lying sediment in the deep region. This may be underlain by a rough reflector corresponding to the boundary between the 2.3 and 3.5 km/s layers which have been assumed in order to satisfy the refraction measurements. The nature of this horizon is more evident in Fig. 8 which shows portions of the original reflection records.

The reflector is weak and discontinuous and its reality must be viewed with scepticism until more precise measurements are available. A short sonobuoy refraction line was also obtained in the central area and a velocity of 2.3 km/s was measured. This is the same as the velocity assumed for the upper part of the sedimentary column in the refraction measurements described earlier. The magnetic and gravity anomalies in the central area show little variation. If a buried median ridge exists, it must be isostatically compensated, possibly by the remnant of a low density body due to high temperature within the upper mantle. This has been suggested by Le Pichon *et al.* (1971) to explain the lack of positive gravity values over the Labrador Sea ridge.

The important problem of the occurrence of a ridge in the center of the bay remains unanswered. The composition of the material lying directly beneath the flat-lying sediment, for which we have assumed a velocity of 3.5 km/s, and whose upper surface corresponds to a rough reflector is not known. It is tempting to associate this layer with layer 2. However, the rough reflector occurs intermittently across all of the deeper, central portion of the traverse and does not appear to reflect a topographic high. Also, it is a much weaker reflector than that which is usually correlated with the sediment-basalt interface.

The occurrence of large positive anomalies in the gravity and magnetic fields on the Baffin Island shelf (Fig. 7) appears to be caused by a horst, one side of which is well defined on the reflection record (20 km, profile 1, Fig. 8). The shelf in this area may have experienced a rather complicated depositional and tectonic history. Bathymetrically, it takes the form of a series of terraces, separated by regions in which the water depth changes rapidly. The sediments beneath the central terrace appear to be highly disturbed and the reflection profile (30 to 60 km, profile 1, Fig. 8) suggests that this may be caused by large scale slumping within the disturbed zone. The slumping may be related to the relatively high earthquake activity within the area. Beneath the distributed zone the reflectors are continuous and terminate against the horst. Their continuity implies that the step-like nature of the shelf is not tectonically controlled although the evidence is incomplete because reflections from the basement rocks were not observed. On the seaward side of the disturbed zone the sediments dip gently toward the deeper water and this part of the shelf appears to be prograding.

The Greenland shelf is simpler, at least along the traverse shown in Fig. 7 and Fig. 8. The reflection profile suggests that the shelf is prograding. There is also a prominent unconformity between the uppermost sediments and those beneath; the latter beds exhibiting greater dips. The upper part of the sediment column on the shelf and slope is disturbed and this may be attributed to slumping although these structures bear little resemblance to the disturbed sediment on the Baffin Island shelf. Unfortunately the traverse did not extend sufficiently far to the east to allow detection of the northern extension of the Disko basalts.

Results along the track which trends east-west and begins at the entrance to the Lancaster Sound are shown in Figs. 9 and 10. No magnetic data were collected along this track. On the western part of the line the sediments are gently folded. This area corresponds to negative free-air gravity values. Gravity lows are apparently characteristic of the Lancaster Sound area (Fig. 4). To the east, the sediments are relatively undeformed and the dips of the horizons may result from a prograding shelf. The transition from deformed to undeformed sediment does not correspond to the bathymetric expression of the continental margin; the increase in water depth occurs about 100 km to the east of the change. The flat nature of the sea floor and the apparent truncation of some of the sedimentary layers indicates that the area may have been subjected to glacial scouring. The gravity anomaly as well as the change in sedimentary characteristics suggests that the true boundary between continental and oceanic crustal structure occurs to the west of the increase in water depth. The eastern part of the line which is underlain by undeformed sediment corresponds to a region of high free-air gravity values, 60 to 80 mgal. This change from negative to positive gravity values is probably caused by a decrease of the total crustal thickness to the east.

A short sonobuoy refraction line was obtained in the area shown in Fig. 9. The velocity of the deformed sediment obtained from this line is 3 km/s or less in the top kilometer of the

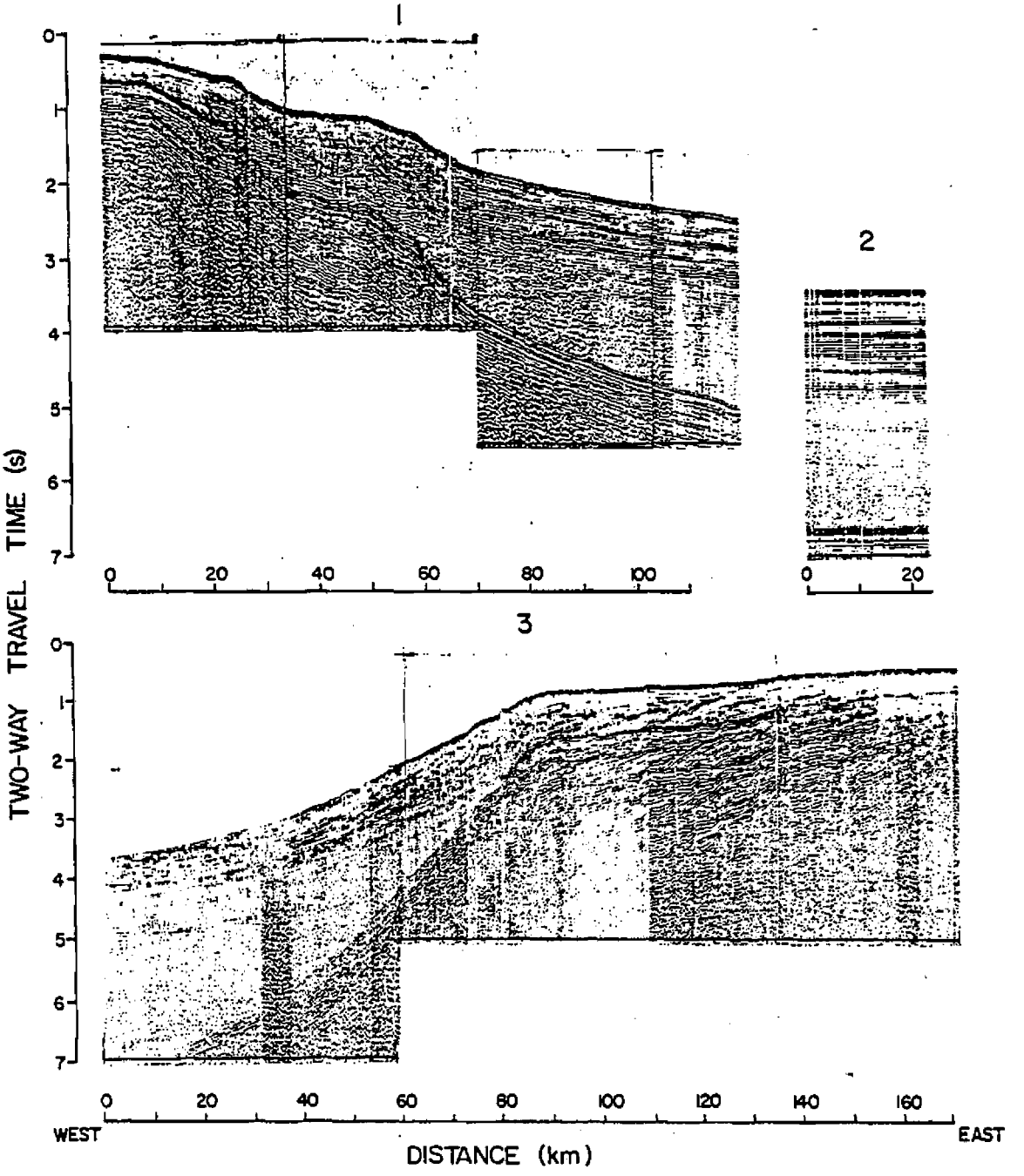


FIG. 8. Sections of the original seismic reflection records along the track shown in Fig. 7. The numbers indicate the positions of these sections along the track as described below Fig. 7.

section. Although there is no direct relationship between age and seismic velocity, it is unlikely that these sediments are older than the Mesozoic Era. Older rocks are usually associated with higher compressional velocities, especially if deformation has occurred. A more detailed account of the Lancaster Sound area is given by Keen *et al* (1972).

Crustal Models

Before discussing these results in relation to possible plate motion it is important to establish, as accurately as possible, the extent of oceanic crust in the centre of Baffin Bay. We have postulated that the transition from continental to oceanic structure is reflected by gravity "shelf-edge" anomalies and, in some areas, by a change

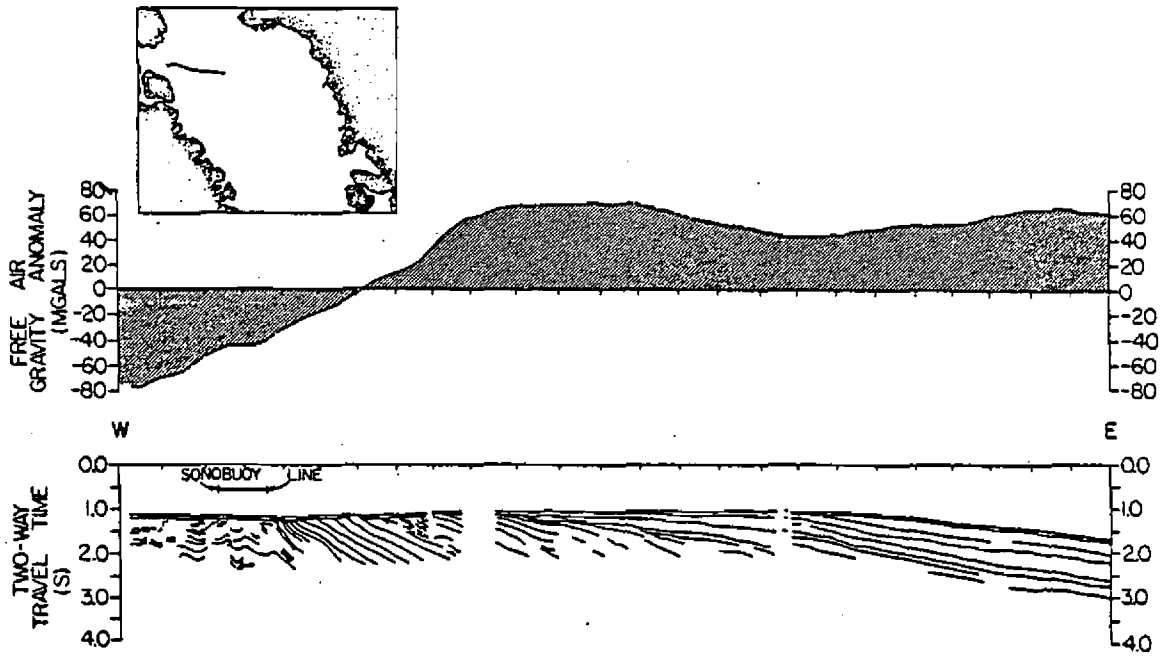


FIG. 9. The free-air gravity anomaly and a line drawing of the seismic reflection record along a track from the entrance of Lancaster Sound to the east as shown by the index map. The location of a short sonobuoy refraction line is also indicated. The ticks along the horizontal scale are hour marks, or at intervals of approximately 11 km.

from low to high magnetic anomalies. In order to justify this claim, crustal models which satisfied the gravity observations were constructed along several of the lines (lines A, B, and C of Fig. 4). The models and the corresponding observed and calculated gravity anomalies along lines B and C are shown in Fig. 11. The models were obtained using the results of the refraction experiment to define the crustal structure in the deep central part of the Bay. Densities were selected on the basis of the seismic velocities for the oceanic parts of the models using the velocity-density relationships of Nafe and Drake (Talwani *et al.* 1959) and Woollard (1962). The models were calculated using a standard computer program for two dimensional bodies.

It would be unrealistic to suppose that these models are detailed representations of the crust. More seismic refraction control is necessary, especially beneath the continental area before final sections can be presented. They do, however, show that the "edge" anomalies are associated with a changing crustal thickness from values associated with continental structure to those associated with oceanic areas. It is difficult to conceive of another mode of crustal variations which would produce the observed gravity measurements. The inferred slope of the M discontinuity near the continental margins is similar to that observed along the Atlantic margin (Keen and Loncarevic 1966). The rather more complicated form of the gravity variations along line B is caused by the presence of a high density body which resembles a dike intruded into the surrounding material. There is also a magnetic anomaly of 1400 γ associated with this feature (Fig. 7). Thus, both the gravity and magnetic anomalies suggest that the body is a basic intrusive. The gravity anomaly map (Fig. 4) shows that it may extend some 80 km. at least, along the Baffin Island shelf. Perhaps this linear intrusive is similar in origin to dikes along the western margin of the Atlantic; the Triassic basalts in Nova Scotia for example. These dikes have been associated with the initial stage of spreading; uplift and rifting of the continents (Vogt 1970).

Discussion

We have shown that a large portion of Baffin Bay is underlain by oceanic crust, the transition from oceanic to continental structure having been defined by the gravity and magnetic measurements. There is no conclusive evidence for

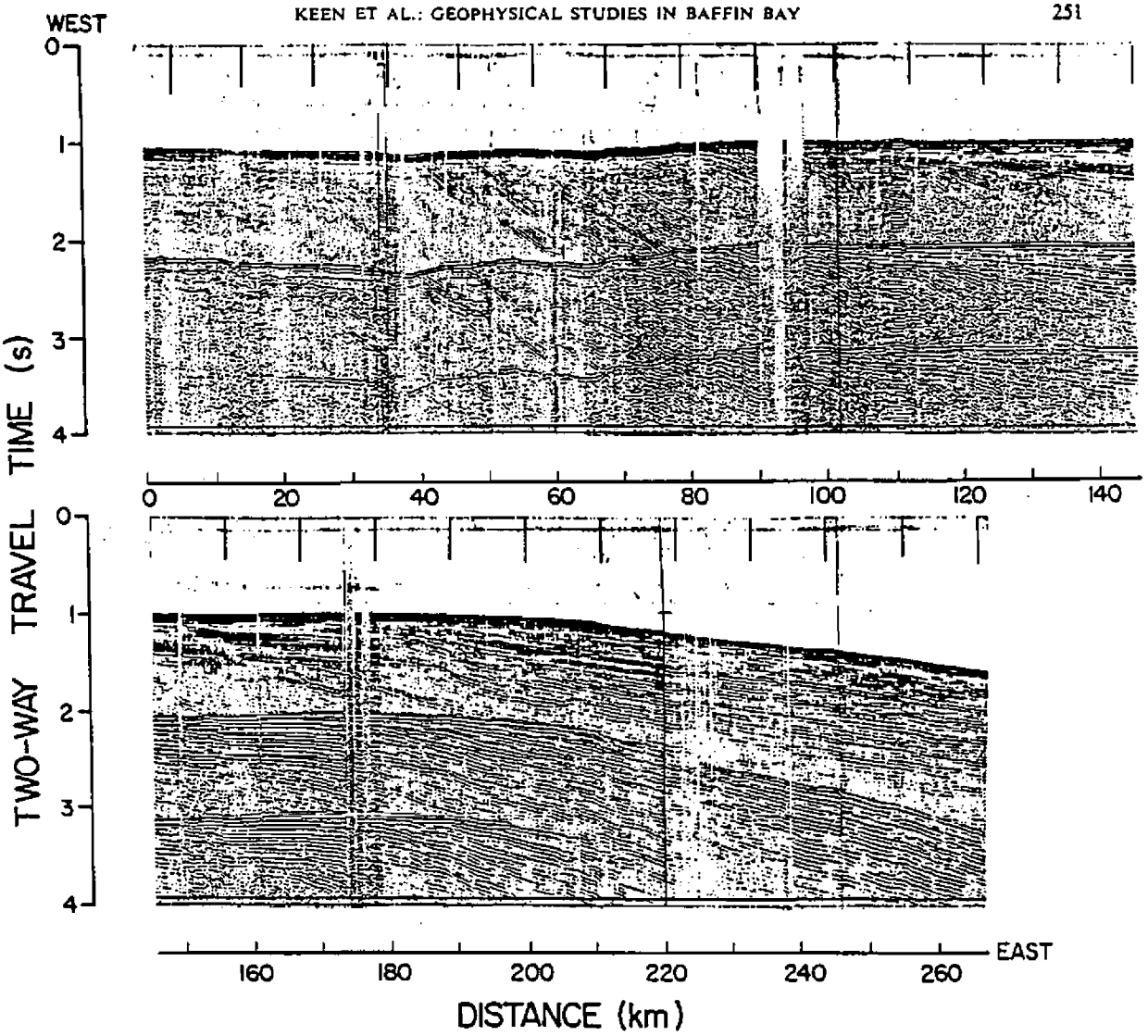


FIG. 10. The original seismic reflection record along the track shown in Fig. 9.

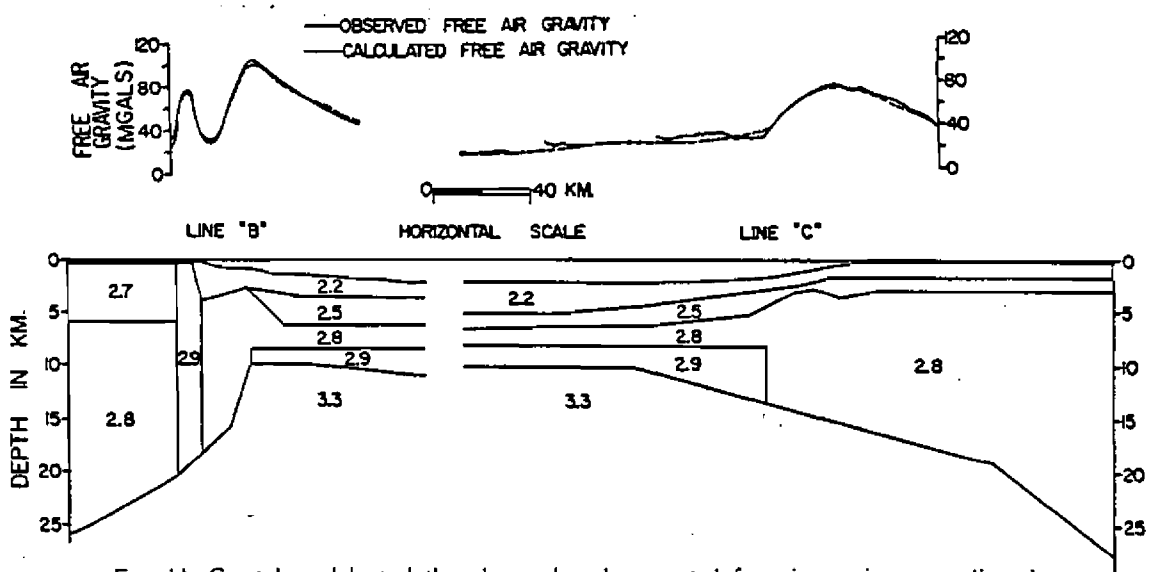


FIG. 11. Crustal models and the observed and computed free-air gravity anomalies along lines B and C whose positions are shown in Fig. 4. The numbers on the models are densities in g/cm^3.

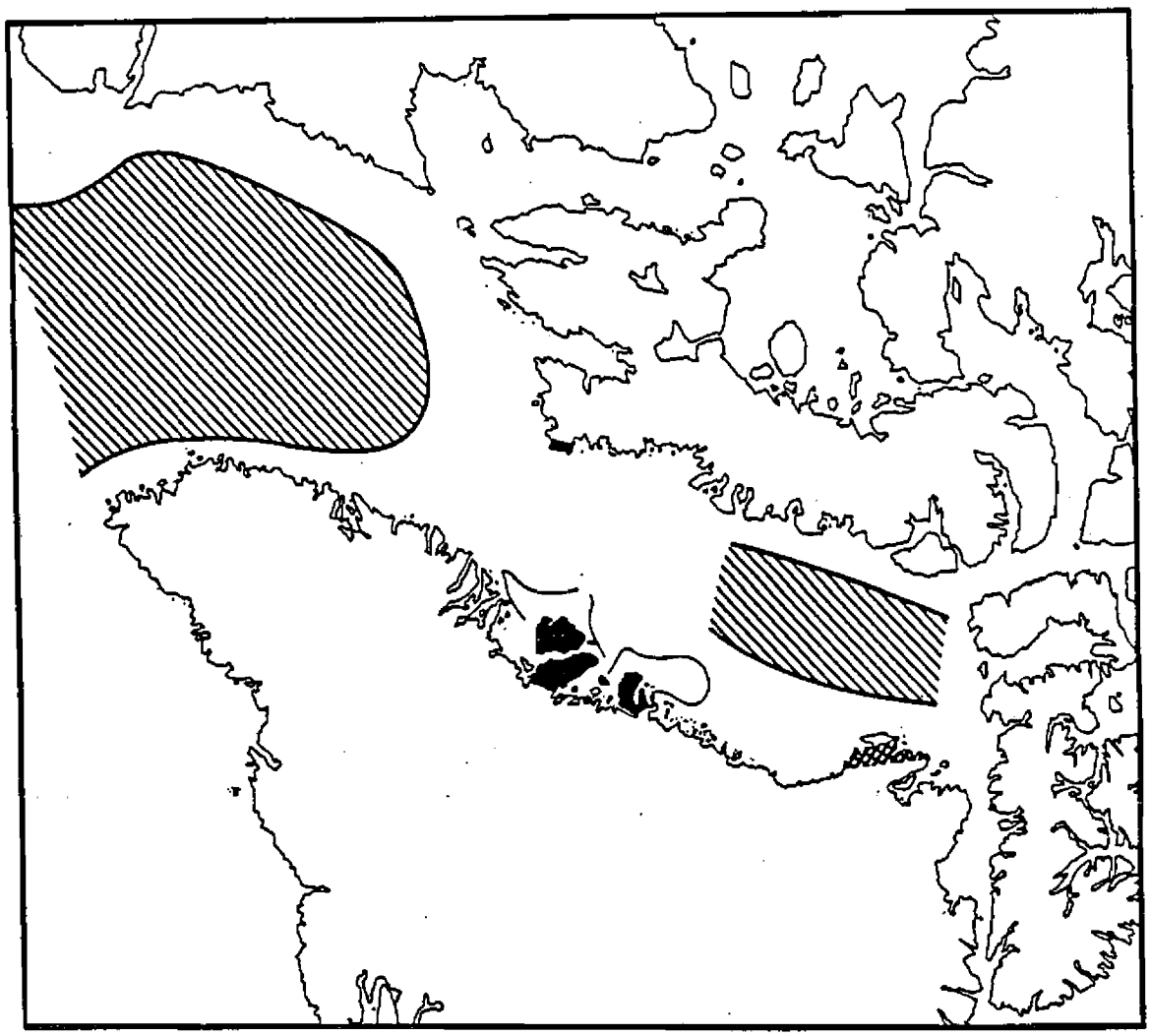


FIG. 12a. A map of the Labrador Sea-Baffin Bay area at present. An oblique Mercator Projection has been used about a pole at 19° N, 173° E. The areas occupied by diagonal lines show the approximate extent of oceanic crust in the Labrador Sea and Baffin Bay. The black areas on land indicate the location of Tertiary basalts and their seaward extension on the Greenland side by the solid black lines. The cross hatched area in northern Greenland represents the location of the graben in the Thule area.

a buried ridge beneath the bay nor have magnetic lineations or fracture zones, conventional measures of directions and rates of plate motions, been delineated. However, if the assumption is made that the bay was formed by sea-floor spreading in conjunction with the opening of the Labrador Sea, a preliminary attempt to define the geometry of the opening can be made. Any reconstruction must also be consistent with the known continental geology.

We postulate that there have been two poles about which opening has occurred. The two stages of motion are illustrated in Fig. 12. Oblique Mercator projections have been used so that the map's pole positions are the poles about which rotation has occurred and motion takes place along lines of latitude (MacKenzie and Parker 1967). In Baffin Bay we have attempted to close the area occupied by oceanic crust and in the Labrador Sea we have assumed that the 1000 km contours should match prior to sea-floor spreading. The 1000 km contour was chosen, rather arbitrarily, because of our ignorance of the continent-ocean transition in

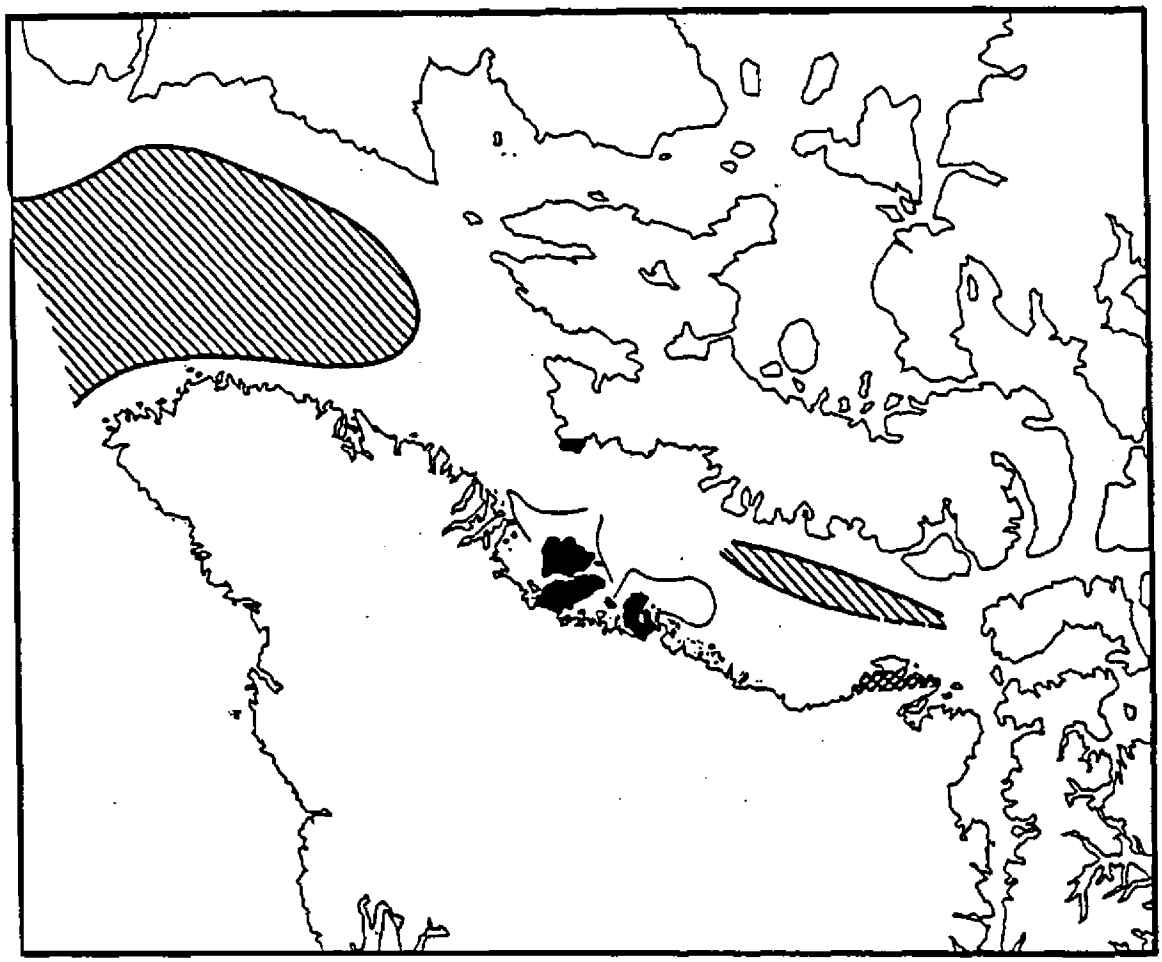


FIG. 12b. The relative positions of the continents before the most recent phase of spreading about the pole at 19° N, 173° E. The projection and markings are those of Fig. 12a.

this area. This contour is the same as that used by Bullard *et al.* (1965) in their fit of the Atlantic.

The extent of oceanic crust in northern Baffin Bay can most easily be explained by allowing for some strike-slip motion along Nares Strait. We suggest that the Nares Strait is a dormant transform fault, perhaps connecting an inactive Baffin Bay ridge to the Alpha ridge in the Arctic Ocean. Although many geologists have argued that there cannot have been substantial horizontal displacement along Nares Strait, others believe that a displacement of 150 to 200 km is consistent with the geology of the area (P. Dawes, personal communication, 1971). The present configuration of Greenland and North America is shown in Fig. 12a, projected about a pole at 19° N, 173° E so that Nares Strait becomes a line of latitude. The positions of the continents before rotation about this pole (Fig. 12b) was obtained by allowing a displacement of 150 km along Nares Strait. This rotation accounts for a large proportion of the oceanic crust in Baffin Bay.

Evidence for the second, earlier phase, of spreading, comes mainly from geophysical studies in the Labrador Sea (Le Pichon *et al.* 1971, Laughton 1971). A pole at 80° N, 90° W was suggested for the period 60 to 80 m.y. ago. In order to account for the folding and faulting which occurred in the northern Arctic Islands in early Tertiary time (Thorsteinsson and Tozer 1970) we have moved the pole to the southwest (77° N, 100° W) so that compressional features lie to the north, tensional features to the south. This change, however, has little effect upon

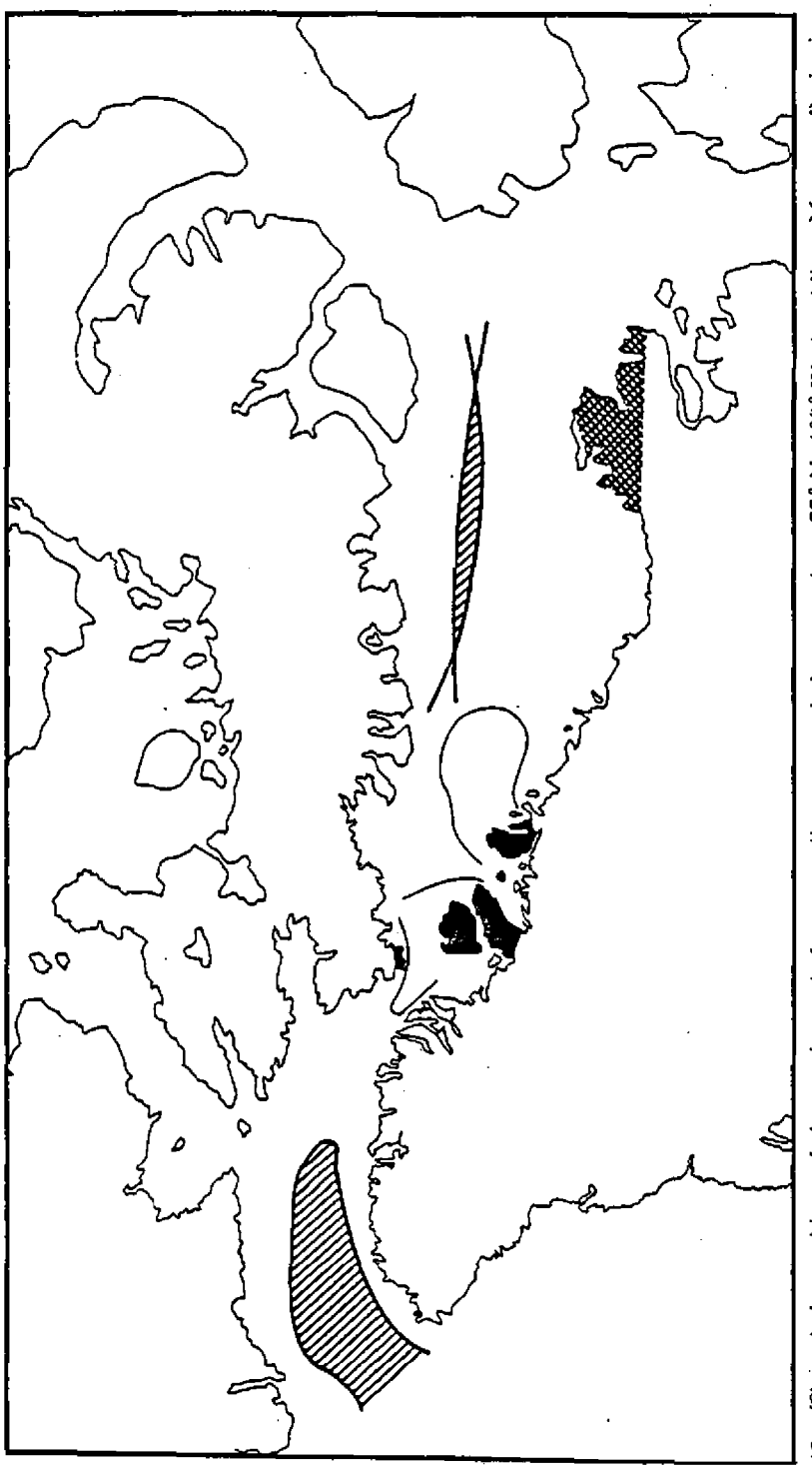


FIG. 12c. The relative positions of the continents before spreading occurred about a pole at 77° N, 100° W. An oblique Mercator Projection about this pole has been used. The markings are those of Fig. 12a.

motions in the Labrador Sea. North America and Greenland were rotated about this pole until no oceanic crust remained in Baffin Bay (Fig. 12c). The small misfit which occurs because of the assumed continental-oceanic crustal boundaries may be rectified when more data are available. Fig. 12c shows the positions of Greenland and North America before these two phases of motion occurred. The map has been projected about the pole at 77° N, 100° W.

Although the reconstruction based upon rotation about these two poles may well be modified by further studies in the area, a number of interesting features can be seen. The Tertiary basalts occurring on opposite sides of the Davis Strait do not appear to overlap at the end of the first phase of opening. Their seaward extent on the western side is, however, not well known. According to Laughton (1971) this phase terminated about 60 m.y. ago which accords well with the ages of the basalts, about 57 to 59 m.y. This suggests that they might be associated with a change of the direction of spreading at this time. The closing of Davis Strait is consistent with the ideas advanced by Clarke and Upton (1971) who believe that it was formed by an excessive outpouring of lava during sea-floor spreading and is essentially oceanic in origin.

The most recent phase of spreading in Baffin Bay, involving lateral displacement along Nares Strait, may have occurred in conjunction with spreading both in the Labrador Sea and the Arctic Ocean. Ages for spreading about the Alpha Ridge, 40 to 60 m.y. ago, and for the latest stage of opening in the Labrador Sea, 47 to 60 m.y. ago, are similar (Vogt and Ostenso 1970, Laughton 1971) and the postulated directions of motion are consistent with the proposed Baffin Bay pole of rotation. This suggests that there may have been a continuous active ridge system from the Labrador Sea through the Arctic Ocean.

The graben in the Thule area of west Greenland, which appears to continue to the south beneath the Greenland shelf may have once been joined to Jones Sound (Fig. 12c) whose topography suggests that normal faulting has occurred along its boundaries. However, further studies are necessary to confirm this hypothesis.

There should be no recent earthquake activity which can be directly related to the motions proposed here since spreading has ceased. However, the earthquakes in northern and central Baffin Bay trend down the centre of the Bay. This is particularly apparent only in the large earthquakes, over magnitude 5.0, as plotted by Whitham *et al.* (1970). Perhaps stresses caused by subsidence of the central area are being released along an old zone of weakness which may mark the position of a former active ridge crest.

Finally, the Labrador Sea cannot be completely closed without invoking substantial overlap of the continents in northern Baffin Bay. This may be explained by allowing more complex motions to occur for which there is now no evidence. Alternatively, some of the Labrador Sea may have been formed during an earlier stage of opening of the North Atlantic. Features such as Frobisher Bay and Cumberland Sound near southern Baffin Island and Hudson Strait resemble grabens and may represent the northerly continuation of a pre-Tertiary opening of this area.

The results presented in this paper have allowed us to speculate on the evolution of the Baffin area. Some of the assumptions implicit in the discussion of plate motions are admittedly crude. For example, deformation within the Canadian Arctic Islands during the Tertiary has not been quantitatively related to the postulated motions. The extent of oceanic crust across Davis Strait has not been adequately mapped. The amount of lateral displacement along Nares Strait which was adopted was rather arbitrarily chosen to produce the 'best fit' of the continental margins. There are several experiments which should be conducted in order to confirm or refute some of the suggestions presented in this paper. The nature of the Davis Strait and Nares Strait regions, the possible existence of magnetic lineations, and of a ridge in central Baffin Bay are among the more outstanding problems remaining.

Acknowledgments

We are very grateful to the Masters, Officers and Crew of C.S.S. Baffin, U.S.C.G.S. Edisto, and C.S.S. Hudson for their help and cooperation during the experiments. We thank all our colleagues, in particular T. B. Smith and J. Woodside who helped collect the data. Many

profitable discussions were held with members of Dalhousie University who also worked in the Baffin Bay area during 1970 and with G. Henderson of the Greenland Geological Survey.

BARRETT, D. L. 1966. Lancaster Sound shipborne magnetometer survey. Can. J. Earth Sci., 3, pp. 223–235.

BARRETT, D. L., KEEN, C. E., MANCHESTER, K. S., and Ross, D. I. 1971. Central part of Baffin Bay is oceanic. Nature, 229, pp. 551–552.

BARRETT, D. L. and MANCHESTER, K. S. 1969. Crustal structure in the Baffin Bay and Davis Strait region from magnetometer surveys (Abstr.). Trans. Amer. Geophys. Union, 50, p. 135.

BULLARD, E. C., EVERETT, J. E., and SMITH, A. G. 1965. The fit of the continents around the Atlantic. *In* A Symposium on Continental Drift. Phil. Trans. Roy. Soc. Lond. A, 258, pp. 41–51.

CLARKE, D. B. and UPTON, B. G. J. 1971. Tertiary basalts of Baffin Island: Field relations and tectonic setting. Can. J. Earth Sci., 8, pp. 248–258.

DAWES, P. R. 1971. The North Greenland fold belt and environs. Bull. Geol. Soc. Denmark, 20, pp. 197-239.

EMERY, K. O., UCHUPI, E., PHILLIPS, J. D., BOWIN, C. O., BUNCE, E. T., and KNOTT, S. T. 1970. Continental rise off eastern North America. Am. Assoc. Pet. Geol. Bull., 54, pp. 44–108.

FORTIER, Y. O. and MORLEY, L. W. 1956. Geological unity of the Arctic Islands. Trans. Roy. Soc. Can., Ser. 3, 50, pp. 3–12.

HENDERSON, G. 1972. The geological setting of the West Greenland basin in the Baffin Bay region. *In* Proc. of Earth Sci. Symp. on Offshore Eastern Canada. (P. J. Hood, *Ed.*). Geol. Surv. Can. Paper 71-23 (in press).

KEEN, C. E. and LONCAREVIC, B. D. 1956. Crustal structure on the eastern seabord of Canada: Studies on the continental margin. Can. J. Earth Sci., 3, pp. 65–76.

KEEN, M. J., LONCAREVIC, B. D., and EWING, G. N. 1970. Continental margin of eastern Canada: Georges Bank to Kane Basin. *In* The Sea, Part II. (A. E. Maxwell, *Ed.*). Interscience Publications, New York, 4, pp. 251–291.

KEEN, M. J., JOHNSON, J., and PARK, I. 1972. Geophysical and geological studies in Eastern and Northern Baffin Bay and Lancaster Sound. (Submitted to Can. J. Earth Sci., November 1971).

KERR, J. E. 1967. A submerged continental remnant beneath the Labrador Sea. Earth and Planet. Sci. Lett., 2, pp. 283–289.

LAUGHTON, A. S. 1971. The southern Labrador Sea – A key to the Mesozoic and early Tertiary evolution of the North Atlantic. (Submitted to Nature, May 1971).

LEPICHON, X., HYNDMAN, R. D., and PAUTOT, G. 1971. A geophysical study of the opening of the Labrador Sea. J. Geophys. Res., 76, pp. 4724–4743.

MCKENZIE, D. P. and PARKER, R. L. 1967. The north Pacific: An example of tectonics on a sphere. Nature, 216, pp. 1276–1280.

PARK, I., CLARKE, D. B., JOHNSON, J., and KEEN, M. J. 1971. Seaward extension of the West Greenland Tertiary volcanic province. Earth and Planet. Sci. Lett., 10, pp. 235–238.

TALWANI, M., SUTTON, G. H., and WORZELL, J. L. 1959. A crustal section across the Puerto Rican trench. J. Geophys. Res., 64, pp. 1545–1555.

THORSTEINSSON, R. and TOZER, E. T. 1970. Geology of the Arctic Archipelago. *In* Geology and Economic Minerals of Canada. (R. J. W. Douglas, *Ed.*), pp. 549–590.

VOGT, P. R. 1970. Magnetized basement outcrops on the southeast Greenland continental shelf. Nature, 226, pp. 743–744.

VOGT, P. R. and OSTENSO, N. A. 1970. Magnetic and gravity profiles across the Alpha Cordillera and their relation to Arctic sea floor spreading. J. Geophys. Res., 75, pp. 4925–4927.

WHITHAM, K., MILNE, W. G., and SMITH, W. E. T. 1970. The new seismic zoning map for Canada: 1970 Edition. The Canadian Underwriter, June 15.

WILSON, J. T. 1963. Continental drift. Scientific American, 208, pp. 86–100.

WOOLLARD, G. 1962. The relation of gravity anomalies to surface elevation, crustal structure and geology. Wisc. Univ. Geophys. and Polar Res. Centre Research Rep., Ser. No., 62-9.

BROOD PROTECTION IN AN EPIPELAGIC THECOSOMATOUS PTEROPOD, *SPIRATELLA* ("*LIMACINA*") *INFLATA* (D'ORBIGNY)

CAROL M. LALLI AND FRED E. WELLS, JR.

BROOD PROTECTION IN AN EPIPELAGIC THECOSOMATOUS PTEROPOD, *SPIRATELLA* ("*LIMACINA*") *INFLATA* (D'ORBIGNY)

CAROL M. LALLI AND FRED E. WELLS, JR.

Reprinted from BULLETIN OF MARINE SCIENCE
Vol. 23, No. 4, December, 1973
pp. 933-941
Made in United States of America

BROOD PROTECTION IN AN EPIPELAGIC THECOSOMATOUS PTEROPOD, *SPIRATELLA* ("*LIMACINA*") *INFLATA* (D'ORBIGNY)

CAROL M. LALLI AND FRED E. WELLS, JR.
Marine Sciences Centre, McGill University, Montreal, Quebec, Canada

ABSTRACT

Brood protection is described for the first time in *Spiratella inflata*, an epipelagic thecosomatous pteropod common in tropical and subtropical waters. Adults larger than 1.1 mm in shell diameter brood embryos and early veligers in their mantle cavities, where the young are attached to the mantle lining. Veligers are released into the sea when they measure 0.066 to 0.068 mm in shell diameter, and they attain a size of approximately 0.40 mm before metamorphosis to the adult form is completed. This type of development is compared with that of other thecosomes and with the general developmental patterns of opisthobranchs.

INTRODUCTION

Little is known of the biology of the thecosomatous pteropods, whose shells form the pteropod oozes found on some areas of the ocean floor. However, these pelagic opisthobranch molluscs are generally regarded as protandrous hermaphrodites, laying floating egg masses and having a free-swimming veliger stage. The only known exceptions to this type of development are certain bathypelagic or mesopelagic species, in which spawn and free-swimming larval stages may be suppressed. Viviparity or ovoviviparity has been reported in *Spiratella helicoides* (Jeffreys) (Bonnevie, 1913; Tesch, 1946), *Clio chaptalii* (Souleyet) (Tesch, 1946, 1948), *Clio recurva* (Childern) (van der Spoel, 1970), and has been suggested to be the mode of development in *Clio campylura* (Tesch) (Tesch, 1948). We now report that a common epipelagic thecosome, *Spiratella inflata*, retains embryos within the mantle cavity and releases free-swimming veliger larvae.

MATERIALS AND METHODS

Three plankton tows were made twice monthly, from June 1971 through May 1972, at a station 3 miles west of the Bellairs Research Institute in St. James, Barbados, West Indies (13° 11' N, 59° 41' W). Oblique hauls from 300 m to the surface were taken with an open meter-net of No. 20 nylon equipped with a flowmeter. Collections were immediately preserved in 10 per cent formalin buffered with hexamethyl tetramine. Living specimens of *Spiratella inflata* were obtained from similar tows, which were diluted in buckets of sea water immediately after collection. These diluted collections were examined under a dissecting microscope in the shore lab-

oratory, and live adults were transferred by pipette to small glass containers of fresh sea water which were examined periodically for free-swimming veligers.

Either subsamples or entire preserved plankton tows were sorted for thecosomes. Counts were made of the numbers of individuals of each thecosome species present. At least 200 individuals of *S. inflata* were randomly selected from each month's collections for measurement; an ocular micrometer was used to measure the maximum width of the largest shell whorl. Numbers of *S. inflata* with young contained in the mantle cavity were recorded.

Whole mounts of *S. inflata* decalcified in Bouin's fixative were prepared for detailed microscopical examination. Specimens were stained in eosin and 70 per cent alcohol, dehydrated in an alcohol series, cleared in toluene, and mounted in Permount on a microscope slide. Paraffin serial sections 10μ thick were prepared of 46 specimens ranging in shell diameter from 0.95 to 1.28 mm; seven of these specimens were brooding females. All sections were stained with Ehrlich's hematoxylin and eosin. In addition, unstained embryos dissected from Bouin-fixed females and pieces of the mantle cavity lining with attached embryos were examined with phase microscopy.

Results

The original observations of veligers being brooded in the mantle cavity of an adult *Spiratella inflata* were made (by CML) during Phase II of the Hudson 70 Expedition (sponsored by the Bedford Institute of Oceanography, Marine Sciences Branch of the Canada Department of Energy, Mines and Resources). Feeding experiments were conducted on shipboard in the South Atlantic, with various thecosome species being presented as live potential prey to gymnosomatous pteropods. During the course of one experiment, an unidentified gymnosome larva captured and began to ingest an individual of *S. inflata* measuring 1.5 mm in shell diameter. Immediately after being captured, the *Spiratella* released approximately 30 live shelled veligers from its mantle cavity. The parent was eaten by the gymnosome, but the veligers continued to swim freely in a small container of sea water for 3 days before they died. Later work on *S. inflata* collected from waters off Barbados confirmed the original observation and permitted a more complete description of brooding and larval development.

In 12 consecutive months of collections at Barbados, *S. inflata* was consistently the most numerous thecosome species, averaging 3033 individuals/1000 m^3 of water and reaching a maximum abundance of 6292/1000 m^3 during August. Three other species of *Spiratella* were present at much lower average densities: *S. trochiformis* (D'Orbigny), 357 individuals/1000 m^3; *S. bulimoides* (D'Orb.), 113; and *S. lesueuri* (D'Orb.), 19.

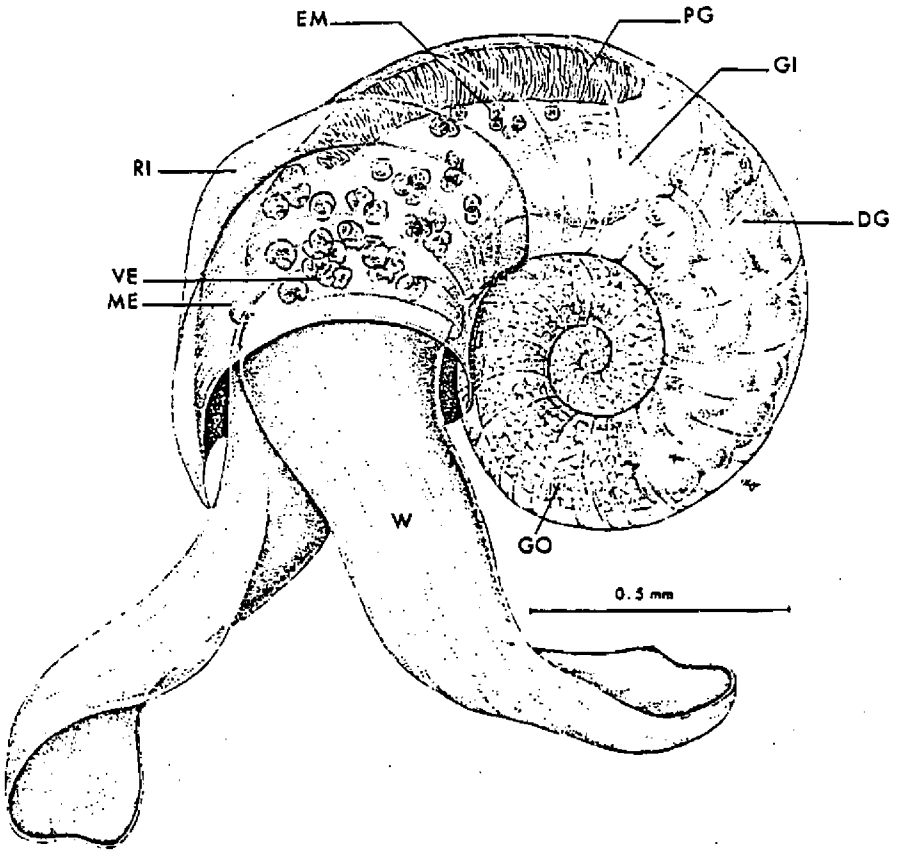


FIGURE 1. Lateral view of a *Spiratella inflata* brooding embryos in the mantle cavity. DG, digestive gland; EM, early embryonic stages; GI, gizzard; GO, gonad; ME, edge of mantle; PG, pallial gland; RI, rib of shell; VE, shelled veligers; W, wing.

Specimens containing embryos and/or veligers in the mantle cavity constituted only a small percentage of the total population of *S. inflata*. Only the largest individuals of *S. inflata*, measuring 1.1 to 1.3 mm in diameter, may harbour young, and these individuals consistently accounted for 5 per cent or less of the total population. Further, not all individuals within this size-range contained young. The shells of 33 brooding specimens were crushed and the young removed. These adults had an average of 44.8 embryos and/or veligers in the mantle cavity, with one specimen containing 67 shelled veligers. Brooding adults and free-swimming veligers of *S. inflata* were collected throughout the 1-year sampling period, indicating that reproduction is continuous in this area.

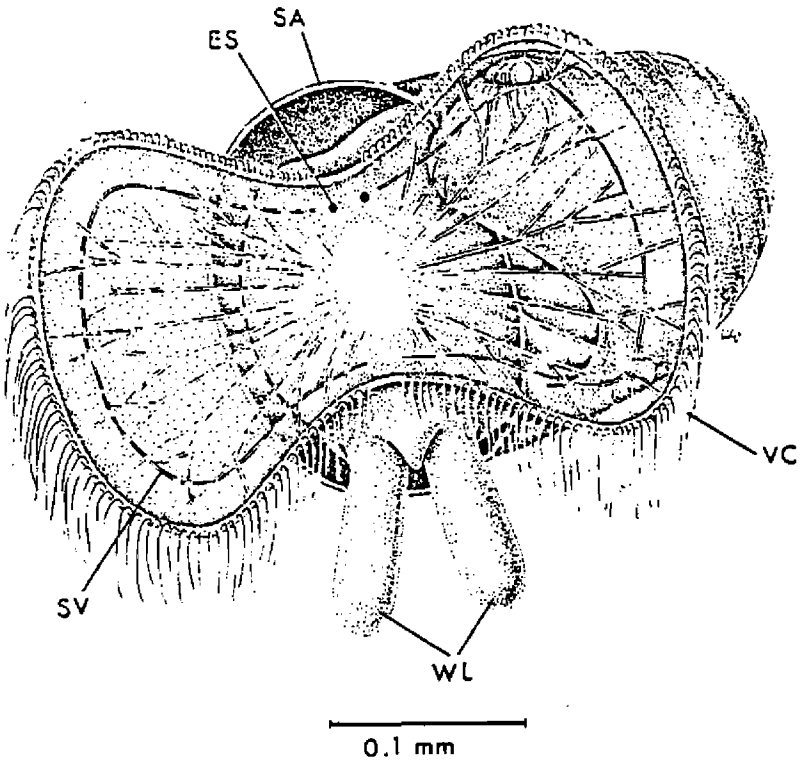


FIGURE 2. Free-swimming veliger of *Spiratella inflata* just prior to completion of metamorphosis. ES, eyespot; SA, inflated aperture of shell; SV, subvelar ridge; VC, preoral cilia of velum; WL, wing lappets.

Development begins within the reproductive tract; embryos in early stages of development could be seen in the tract near the common genital pore, which opens into the posterior mantle cavity. Older embryos in various stages of development were found in the mantle cavities of brooding individuals of *S. inflata* (Fig. 1), where they adhered to the mantle lining. Gastrulae were the youngest stages found in the mantle cavity and were positioned farthest from the shell aperture and nearest the genital pore. We were unable to detect any evidence of an egg capsule around eggs or embryos, or a mucous egg mass, nor were we able to find an albumen or mucous gland in the reproductive tract of any of the sectioned specimens. Shelled veligers were present in the anterior area of the mantle cavity, under the most inflated portion of the adult shell. The veligers apparently detach from the mantle lining just prior to leaving the parent, as they were observed swimming freely in the mantle cavity at that time.

Free-swimming veligers, examined immediately after release from the parent, had a smooth sinistral shell of one whorl measuring 0.066 to 0.068 mm in greatest diameter. They had a bilobed velum, eyespots, and a small ciliated foot provided with a transparent operculum. Later veligers (Fig. 2), collected live from plankton tows in the South Atlantic, measured 0.30 mm in diameter and had two shell whorls, an inflated body whorl, and wing lappets developing from the foot area. The lappets eventually become the swimming wings. We assume that metamorphosis proceeds as described by Lebour (1932) for *Spiratella retroversa* (Fleming), with gradual loss of the velum and concomitant growth of the wings. In Barbados specimens, metamorphosis was complete at 0.40 mm shell diameter.

As the species name implies, *Spiratella inflata* is characterized chiefly by the marked inflation of the body whorl and aperture of the shell. This shell inflation serves to distinguish even late veligers (Fig. 2), but becomes more evident in postveligers. When individuals attain a shell diameter of 0.9 mm, a thickened shell area, or rib, begins to develop along the axis of the last whorl (Fig. 1, RI) and eventually projects from the outer lip as a rostrum (see also Tesch, 1913, 1946). We believe that the characteristic shell structure is related to brood protection in this species, with the inflated body whorl and expanded mantle cavity providing space for the brooding of young and the thickened rib strengthening the shell over this area.

Discussion

Spiratella inflata has an extensive geographic range, occurring predominantly in tropical and subtropical surface waters of all the oceans. In many areas of its range, as off Barbados, *S. inflata* coexists with two or three other epipelagic species of *Spiratella*: *S. bulimoides*, *S. lesueuri*, and *S. trochiformis* (Tesch, 1946; Moore, 1949; Wormelle, 1962; Fager & McGowan, 1963; Chen & Bé, 1964; Myers, 1968; Lewis & Fish, 1969; Deevey, 1971). Little is known of the biology of these species and nothing of the ecological factors which permit their coexistence. We believe that a description of development and of the veliger of *S. inflata* may prove helpful in taxonomic separation of the young stages of these coexisting congeneric species.

Type of development is variable within the genus *Spiratella* and is best known in the epipelagic, cold water species, *S. retroversa* (Lebour, 1932) and *S. helicina* (Phipps) (Massy, 1920; Paranjape, 1968). In both species, the spawn consists of floating egg masses from which free-swimming veligers hatch. Lebour (1932) reported that *S. retroversa* embryos were shell-less when released from egg masses in the laboratory. The shell and bilobed velum developed when the free-swimming young were 0.05 mm in diameter, wing rudiments developed at 0.32 mm, and metamorphosis was almost complete at 0.37 mm. Paranjape (1968) reported that newly hatched

veligers of *S. helicina* were shelled and measured 0.075 mm in diameter. His study terminated at 30 days after hatching, when the veligers measured 0.20 mm; wing development had not begun at this time, and maximum size of the veligers is unknown. In comparison, shelled veligers of *S. inflata* measured 0.066 to 0.068 mm in diameter when released from the parent, and they attained a size of approximately 0.40 mm when metamorphosis was completed. Morton (1954) studied reproduction in *S. bulimoides* and assumed that development was of the same type as in *S. retroversa* and *S. helicina*, although egg masses and veligers were not collected in plankton tows and remain undescribed. To our knowledge, nothing is known of reproduction and development of *S. trochiformis* and *S. lesueuri*. The two remaining species of the genus, the epipelagic *S. inflata* and the bathypelagic *S. helicoides*, retain eggs and developmental stages within the adult. Thus, it is clear that the type of development varies within the genus *Spiratella* and is not correlated with known ecological factors.

Although both *S. inflata* and *S. helicoides* release living young, it would not be correct to assign them to the same developmental type. According to Tesch (1946), *S. helicoides* is viviparous, with encapsulated eggs and embryos being retained within the mucous gland of the reproductive tract until development is complete; young released into the mantle cavity are miniature adults with fully developed wings and no trace of a velum. Similarly, embryos of *Clio recurva* remain in the lumen of an accessory sexual gland where they apparently develop into miniature adults with wings (van der Spoel, 1970). Development of the embryos of *S. helicoides* and *C. recurva* is apparently sustained by nutrients derived from the egg and reproductive tract. In contrast, our results indicate that females of *S. inflata* have no albumen or mucous accessory glands and that embryos without capsules are expelled from the reproductive tract in very early stages of development, adhere to the mantle lining, and develop into shelled veligers within the mantle cavity. The veligers are eventually released into the sea and metamorphosis to the adult occurs during a free-swimming stage. The method by which embryos of *S. inflata* are nourished outside the reproductive tract is unknown; further work is being done on this aspect of development, as well as on the anatomical modifications of the reproductive system.

Because most of the embryonic development proceeds outside of the reproductive tract, the retention of young by *S. inflata* must be regarded as brood protection rather than ovoviviparity or viviparity. It seems likely that brood protection, rather than viviparity, is also the case in the bathypelagic species, *Clio chaptalii* and *C. campylura*. Tesch (1946, 1948) reported finding encapsulated embryos in the mantle cavities of both species, but none in the reproductive ducts or glands.

Thompson (1967) recently reviewed developmental processes in opisthobranchs, excluding thecosomatous and gymnosomatous pteropods, and

established three distinct developmental types: (1) species with planktotrophic larvae; (2) species with lecithotrophic larvae; and (3) species with direct development. The species of all categories spawn egg masses, and thus it is clear that thecosomes with brood protection or viviparity cannot be properly placed within any of these groups. The only other opisthobranchs reported to have brood protection or viviparity are the gymnosomatous pteropod, *Hydromyles globulosa* (Rang) (Meisenheimer, 1905), and possibly the interstitial opisthobranch, *Pluscula cuica* Marcus (Marcus, 1953). Thus, retention of eggs and larvae is unusual in opisthobranchs and seems to be restricted to those species occupying unusual molluscan habitats.

Retention of young is also rare in other molluscan taxa, although brood protection seems to be more common in bivalves, whereas suppression of developmental stages is more often achieved in gastropods through ovoviviparity or viviparity (Fretter & Graham, 1964). These authors have suggested that the different mechanisms of embryo retention in these two classes are related to the inability of most gastropods to use the mantle cavity as a brood pouch. In this regard, it is interesting to note that *Spiratella inflata* and *S. helicoides* have larger mantle cavities than those species of *Spiratella* which lay eggs in floating egg masses.

Acknowledgments

C. M. Lalli wishes to thank the Bedford Institute of Oceanography, Dartmouth, Nova Scotia, for permission to participate on the Hudson 70 Expedition, and the Faculty of Graduate Studies and Research of McGill University for travel and research funds used during this cruise. We also wish to thank the personnel at the Bellairs Research Institute of McGill University, Barbados, for their cooperation in obtaining plankton collections and for use of laboratory facilities. Part of this research was supported by National Research Council of Canada Grant No. A5248 to C. M. Lalli.

Sumario

Protección de la Cría en un Pterópodo Thecosomato Epipelágico, *Spiratella* ("*Limacina*") *inflata* (D'Orbigny)

Por primera vez se reporta la protección de la cría por un thecosomato epipelágico, *Spiratella inflata.* Los adultos con conchas de diámetros mayores de 1.1 mm pueden criar embriones y primeras velígeras en sus cavidades del manto, donde los jóvenes se adhieren al forro del manto. Adultos en cría y velígeras nadando libremente fueron colectados durante todos los meses del año, lo que indica que la reproducción es contínua frente a Barbados. Las velígeras tienen una concha siniestra lisa de una vuelta que mide de 0.066 a 0.068 mm de diámetro al ser liberada y alcanza un diámetro de 0.4 mm antes de que la metamorfosis al estado adulto sea completa.

El tipo de desarrollo encontrado en *S. inflata* es comparado con el de

otros thecosomatos y con el patrón de desarrollo general de otros opistobranchios.

REFERENCES

BONNEVIE, K.
1913. Pteropoda. Rep. 'Michael Sars' N. Atl. Deep Sea Exped., *3*(1): 1-85.

CHEN, C. AND A. W. H. BÉ
1964. Seasonal distributions of euthecosomatous pteropods in the surface waters of five stations in the western North Atlantic. Bull. mar. Sci. Gulf Caribb., *14*(2): 185-220.

DEEVEY, G. B.
1971. The annual cycle in quantity and composition of the zooplankton of the Sargasso Sea off Bermuda. I. The upper 500 m. Limnol. Oceanogr., *16*(2): 219-240.

FAGER, E. W. AND J. A. MCGOWAN
1963. Zooplankton species groups in the North Pacific. Science, N. Y., *140* (3566): 453-460.

FRETTER, V. AND A. GRAHAM
1964. Reproduction. Pp. 127-164 *in* Wilbur, K. M., and C. M. Yonge (Eds.), Physiology of Mollusca. Volume 1. Academic Press, New York.

LEBOUR, M. V.
1932. *Limacina retroversa* in Plymouth waters. J. mar. biol. Ass. U.K., *18* (1): 123-129.

LEWIS, J. B. AND A. G. FISH
1969. Seasonal variation of the zooplankton fauna of surface waters entering the Caribbean Sea at Barbados. Caribb. J. Sci., *9*(1 & 2): 1-24.

MARCUS, E.
1953. Three Brazilian sand Opisthobranchia. Bolm Fac. Filos. Ciênc Univ. S Paulo (Zool.), *18:* 165-203.

MASSY, A. L.
1920. Mollusca. III. Eupteropoda (Pteropoda Thecosomata) and Pterota (Pteropoda Gymnosomata). Br. Antarct. Terra Nova Exped. 1910, Nat. Hist. Rep. Zool., *2:* 203-232.

MEISENHEIMER, J.
1905. Pteropoda. Wiss. Ergebn. dt. Tiefsee-Exped. 'Valdivia,' *9:* 1-314.

MOORE, H. B.
1949. The zooplankton of the upper waters of the Bermuda area of the North Atlantic. Bull. Bingham oceanogr. Coll., *12:* 1-97.

MORTON, J. E.
1954. The pelagic Mollusca of the Benguela Current. Part I. First survey, R.R.S. 'William Scoresby,' March 1950, with an account of the reproductive system and sexual succession of *Limacina bulimoides*. 'Discovery' Rep., *27:* 163-199.

MYERS, T. D.
1968. Horizontal and vertical distribution of thecosomatous pteropods off Cape Hatteras. Unpublished Ph.D. dissertation, Duke University, 224 pp.

PARANJAPE, M. A.
1968. The egg mass and veligers of *Limacina helicina* Phipps. Veliger, *10* (4): 322-326.

SPOEL, S. VAN DER
1970. The pelagic Mollusca from the "Atlantide" and "Galathea" Expeditions collected in the East Atlantic. Atlantide Rep., *11:* 99-139.

TESCH, J. J.
1913. Pteropoda. Das Tierreich, *36:* 1-154.
1946. The thecosomatous pteropods. I. The Atlantic. Dana Rep., *28:* 1-82.
1948. The thecosomatous pteropods. II. The Indo-Pacific. Dana Rep., *30:* 1-45.

THOMPSON, T. E.
1967. Direct development in a nudibranch, *Cadlina laevis*, with a discussion of developmental processes in Opisthobranchia. J. mar. biol. Ass. U. K., *47*(1): 1-22.

WORMELLE, R. L.
1962. A survey of the standing crop of plankton of the Florida Current. VI. A study of the distribution of the pteropods of the Florida Current. Bull. mar. Sci. Gulf Caribb., *12*(1): 95-136.

On the Thermal Balance of a Mid-Ocean Ridge

Geophys. J. R. astr. Soc. (1972) 26, 515–535.

On the Thermal Balance of a Mid-Ocean Ridge

C. R. B. Lister

(Received 1971 June 18)

Summary

The northernmost expressions of the East Pacific Rise spreading centre, the Juan de Fuca Ridge and Explorer Trough, have unusual heat-flow distributions. Crestal values are only moderately high, but flank areas that are models of undisturbed sedimentation have mean heat flows near 7 HFU (290 mW m^{-2}). The values in these areas retain considerable scatter, but the detailed distribution is close to the opposite of that expected from conductive heat-flow refraction. The high mean values confirm that sea-floor spreading occurs by the upwelling of hot (magma temperature) material. The low crestal measurements and the non-refractive scatter in the flank areas strongly suggest that hydrothermal circulation is the dominant heat transfer process in fresh crestal material. Much of the heat loss from the new lithospheric material must occur through open circulation near the ridge crest and is never reflected in measurements of surface conduction.

1. Introduction

The investigation of the heat-flow anomaly at mid-ocean ridges has been an important aim of marine heat-flow measurement since the earliest studies were made (Bullard & Day 1961). A substantial body of data is now available, and has been summarized by several authors (Lee & Uyeda 1965; Langseth, Le Pichon & Ewing 1966; Le Pichon & Langseth 1969). Although the mean heat flow near ridge crests is usually higher than the global average, it is not dramatically so, and the scatter in the measurements is such as to compromise the validity of these means, both statistically and physically. The overall results are not in agreement with the generation of new oceanic crust at the ridges from material at a reasonable temperature (McKenzie 1967), and the recent reinforcement of the sea-floor spreading hypothesis by evidence from other fields (Vine & Matthews 1963; Peterson *et al.* 1970) requires that the disagreement between the heat flow and the other data be resolved.

It has been pointed out before (Lister 1970a; Sclater *et al.* 1970) that some environmental control is essential for any measurement whose scatter is sufficient to arouse suspicion of physical cause for the variation. In this study, standard surveying techniques were carefully applied to the area of interest to obtain enough topographic data at least for the *topological* situation of each heat-flow measurement to be estimated. The influence of thermal refraction cannot be separated from other causes of variation unless the sign and approximate magnitude of the expected correction are known *individually* for each station. This information has been obtained for almost all of the measurements quoted here, together with data that set an upper limit on the possible magnitude of recent surface disturbances. This last is important because of the suggestion by Sclater, Mudie & Harrison (1970) that the low heat-flow

values often measured in valleys are caused by recent slumps of sediment from nearby hills or ridges. The assumption that the heat flow is governed solely by conduction in the crustal materials can therefore be tested directly without making alternative assumptions about the thermal regime at depth. Only when this test has been made can the overall thermal balance of a ridge crest be discussed.

The region of the North-east Pacific off the coast of North America is dominated tectonically by two long active transform faults and the most northerly expressions of the East Pacific Rise spreading axis. The San Andreas Fault, running from the Gulf of California to Cape Mendocino, is a right-lateral transform fault joining the equatorial East Pacific Rise to the ridge segments off the coasts of Oregon and Washington (see Fig. 1). The magnetic survey of Raff & Mason (1961) suggests that there are three segments of active spreading: the Gorda Ridge, the Juan de Fuca Ridge, and Explorer Trough (Vine 1966). They are joined by the Blanco Fracture Zone, and an ill-defined fault zone between the Juan de Fuca Ridge and Explorer Trough. The system ends in another long active transform fault, the Queen Charlotte Fault, and this extends toward the Alaskan end of the Aleutian Trench, completing the source-to-sink pattern (Atwater 1970).

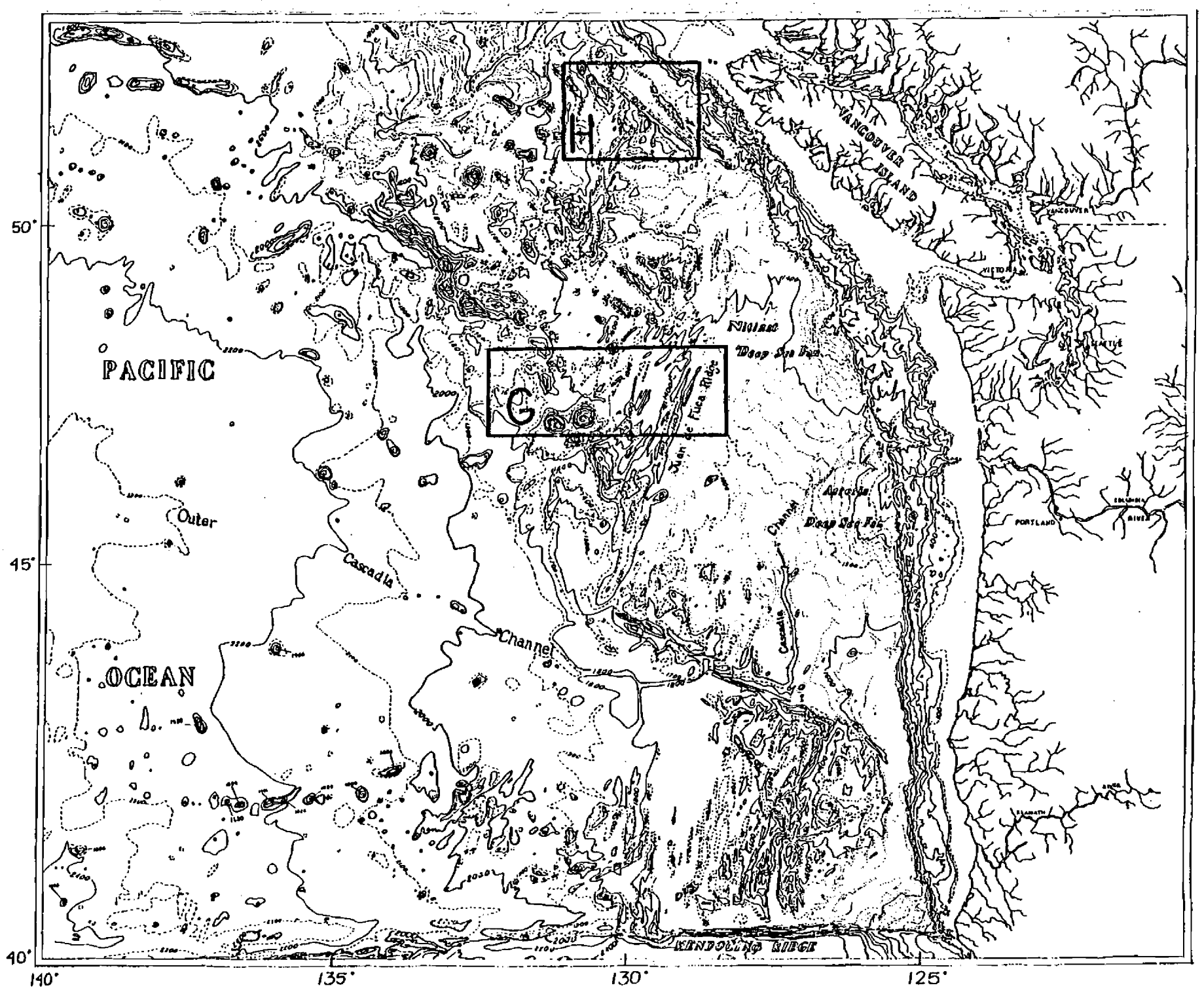
Of the three spreading segments, the Juan de Fuca Ridge is the longest and the best defined physiographically. On the western side it has all the characteristics of a mid-ocean ridge: mountainous topography rising gradually to a crest at the centre of magnetic symmetry. The eastern side, however, appears dramatically different on the map, because the ridge has been inundated by the sediment fill of Cascadia Basin. Heavy continental sediment runoff through the Fraser and Columbia River systems has been ponded near the coast by the Juan de Fuca Ridge and by high topography on the Blanco Fracture Zone. Thus the Juan de Fuca Ridge is a unique example of a classic 'mid-ocean' ridge which has been inundated by terrigenous sediments almost to the crest on one side, but is sufficiently far from the continental margin to be structurally integral.

Freedom from structural interference is not a characteristic of Explorer Trough, however, for it is a small feature amid complex topography and structure just off the continental rise, north-west of Vancouver Island. The magnetic anomalies associated with it are poorly defined (Vine 1966), and interpretation is further complcated by the fact that it is a trough not a ridge. However, the lack of sediments in the topographic lows, relative to the surrounding ocean floor, confirms the magnetic and now thermal evidence that rifting of the crust has taken place recently (see Fig. 9). The feature is thus interesting as a spreading centre that has not, as yet, developed into a full-scale ridge, and will be useful for structural comparisons in the future.

This paper presents field results from two studies: one on the Juan de Fuca Ridge and one in the Explorer Trough region. The principal investigation is a transect across the Juan de Fuca Ridge at 47° N, and is shown on the location map (Fig. 1) as rectangle 'G'. Data for this area have been accumulated over several years from short cruises of RV *Thomas G. Thompson*, and include a substantial body of bathymetric surveying. The smaller study is within rectangle 'H', and consists of a heat-flow profile across the north-eastern extremity of Explorer Trough. This was completed on Phase *VII of Hudson* 70, a circumnavigation of the Americas by C.S.S. *Hudson*. No detailed surveying was carried out in this area, but the topographic features are large enough in scale to be delineated adequately by the bathymetric data of the *Pioneer* survey (cf. Fig. 1, Raff & Mason 1961).

2. Experimental techniques

Heat-flow measurements were made by examples of both generic types of marine apparatus. The corer-outrigger instrument has been described in Lister (1970a), and consists essentially of a 450 × 8 cm gravity corer equipped with a digital bridge



1. Bathymetric map of the ocean floor off Oregon, Washington, and British Columbia, after Mammerickx & Taylor (1971). Contour intervals: full lines 200 fm, dashed lines 100 fm

recorder and three thermistor outriggers. Sediment conductivities were estimated by oven-drying samples from the cores and using the water content versus conductivity nomograph of Ratcliffe (1960). The probe instrument uses the same digital recorder but a sensor arrangement modified to measure thermal conductivity *in situ* over the whole length of the probe. Geothermal gradient and conductivity are measured sequentially in 30 min on the ocean floor, and the probe dimensions have been made small to permit this (200 × 1 cm). The instrument and the interpretation techniques have been fully described in Lister (1970b). The corrections for initial-disturbance decay and the conductivity values were obtained by graphical methods from a large-scale analogue printout of the digital data. The technique has the advantage of permitting a selection of the data points to be computed, avoiding any disturbances experienced by the instrument and the occasional digitisation errors.

The cores obtained by the corer-outrigger apparatus were split and examined stratigraphically in addition to being used for the water content/ conductivity determinations. Total carbonate assays were made on selected parts of some to assist in distinguishing biogenic from terrigenic material, since the carbonate is exclusively of biogenic origin. The carbonate fraction of the cores was also used to obtain radiometric ages for samples from the uppermost 70 cm by measurement of the carbon-14 decay activity in derived methane (A. W. Fairhall*). Three normal cores were dated to establish the sedimentation rate and pattern, and the technique was then used to examine two disturbed cores that could have included slump or slump-exposed material.

The general distribution of sediment on the ocean floor in the areas was examined by acoustic reflection sounding. The systems used on the Juan da Fuca Ridge transect emitted short pulses of medium-frequency (150–300 Hz) sound that have a favourable penetration/resolution ratio in deep-ocean sediments. The early profiles were made with several models of a repulsion-type moving coil electromagnetic transducer energized with 11000 J, but the survey east of the ridge crest was made with an attraction-type electromagnetic transducer pulsed by 250 J. The same, somewhat noisy, 15 m line hydrophone was used throughout, and the signal was processed by automatic gain controlled amplifiers equipped with 12 db/octave variable filters. Full-wave variable density recording was used, but the attraction-transducer records were enhanced by a delay-line pulse shape correlator manually set to match the outgoing pulse. The ultimate resolution of both systems was about 10 ms (7·5 m) but the interpretability of the correlated records is better because of the symmetrical printed pulse free of multiples. Except in the flat-lying sediment fill of Cascadia Basion, resolution is limited by the roughness of the bottom rather than by the acoustic system.

The sediment distribution in the Explorer Trough region was estimated by reference to 40 cu in airgun profiles provided by R. L. Chase (University of British Columbia). In particular, the principal heat-flow profile was arranged along airgun profile UBC 70–16–14, that crosses the troughs about 15 km south-west of Paul Revere Ridge. Resolution on this profile was about 60 ms (45 m), as can be judged from Fig. 9.

A bathymetric background is necessary to identify the lateral extent of features observed on transect profiles. In the Explorer Trough region, it was obtained from a map contoured from previous survey data at 9 km line spacing (Mammerick & Taylor 1971). The features in this area appear to have diametral dimensions of about 15 km (Fig. 8), and are therefore adequately delineated. No significant discrepancies were observed between the contour map and echo-soundings on the cruise.

The topography on the western flank of the Juan de Fuca Ridge is, however, far more complex and of finer scale. No adequate map of the area was available at the time the investigation was started, and even the 9-km line spacing of the Pioneer Survey (Mammerick & Taylor 1971) cannot resolve the topographic structure. A bathymetric

*Professor, Chemistry & Geophysics, University of Washington

survey was therefore conducted as part of the investigation, to identify topographic trends near the transect line. Navigation was by Loran-A radiolocation which is good to ±2 km over most of the area, deteriorating steadily with increasing distance from the coast. Line crossings were used to improve the topological accuracy of the contour map by ensuring that track lines were plotted at the correct relative positions. A standard 12 kHz, 50° beam, echo-sounder gave the depth information, presented on the 1-s sweep of a precision dry-paper recorder. Two-way travel times were used in compiling the maps, to emphasize that sound velocity corrections were not made.

The concentration of stations near 47° N 132° W is in an ultra-detailed survey area, where navigation was assisted by taut-moored radar reflector buoys. Only the outlines of the detailed map have been transferred onto the figure used in this paper (Fig. 3). The survey was intended to establish the resolution limits and characteristic response of standard echo-sounding systems. The information has been valuable in interpreting the more widely-spaced lines employed in later stages of the study.

Heat-flow stations can be affected by small-scale local topography as well as by the large-scale features observable on surface echo-sounding records (Sclater *et al.* 1970). One method of obtaining information about the local irregularities to be expected in an area is photography from a camera drifting near the bottom. The method is severely limited by the loss of visual acuity in bottom water at ranges of more than 10 m, but can produce valuable information about local slope angles, sediment distribution, and bottom currents. An Edgerton stereo camera cycling every 16 s was drifted at 5–8 m above bottom in several places on the western flank of the Juan de Fuca Ridge. On some stations a narrow-band green interference filter was used to enhance the contrast of distant objects. On the Explorer Trough investigation a different technique was tried for the first time, and gave valuable information about the nature of the floor of the main trough. A slow frame-rate cine camera, synchronized to a pulsed Thallium Iodide arc light, was substituted for the stereo camera. The film gives almost continuous coverage of a considerable (c. 150 m) section of ocean floor.

3. Transect of the Juan de Fuca Ridge

A consolidated track chart of the investigations is presented in Fig. 2 to indicate the extent of bottom coverage. The background for the heat-flow results in Fig. 3 is bathymetry derived from these tracks and from the more general data available in earlier studies. The heat-flow measurements are listed by station in Table 1, except for one measurement from *Vema* 20 (Paul J. Grim, private communication), whose relationship to the topography on the map is not known with precision. The first fifteen entries in Table 1 have been listed in more detail in Lister (1970a), but the remainder are new. Gradient linearity and the quality of the conductivity measurements were taken into account in establishing the error bands for the heat-flow measurements.

The distribution of long gravity core samples of the sediment is shown in Fig. 2. There are wide variations in the apprearance and layering of the sediments because both biogenic and terrigenic materials are deposited on the Juan de Fuca Ridge, sometimes in almost equal proportion. However, most cores exhibit a characteristic dark surface layer that probably represents postglacial deposition, since carbon-14 radiometric ages below it are greater than 15 000 years (A. W. Fairhall, private communication). Two important disturbed cores (measurements TT31–3 and TT31–9, Table 1) were dated radiometrically at more than one depth to make sure that recent slumping can be ruled out. One, discussed at length in Lister (1970a), is normal except for the loss of the top section on board ship. The other has older sediment in the top 20 cm than deeper within it, and dares confirm that a buried dark layer a 25 cm corresponds to normal surface material. It is probable that the corer caused

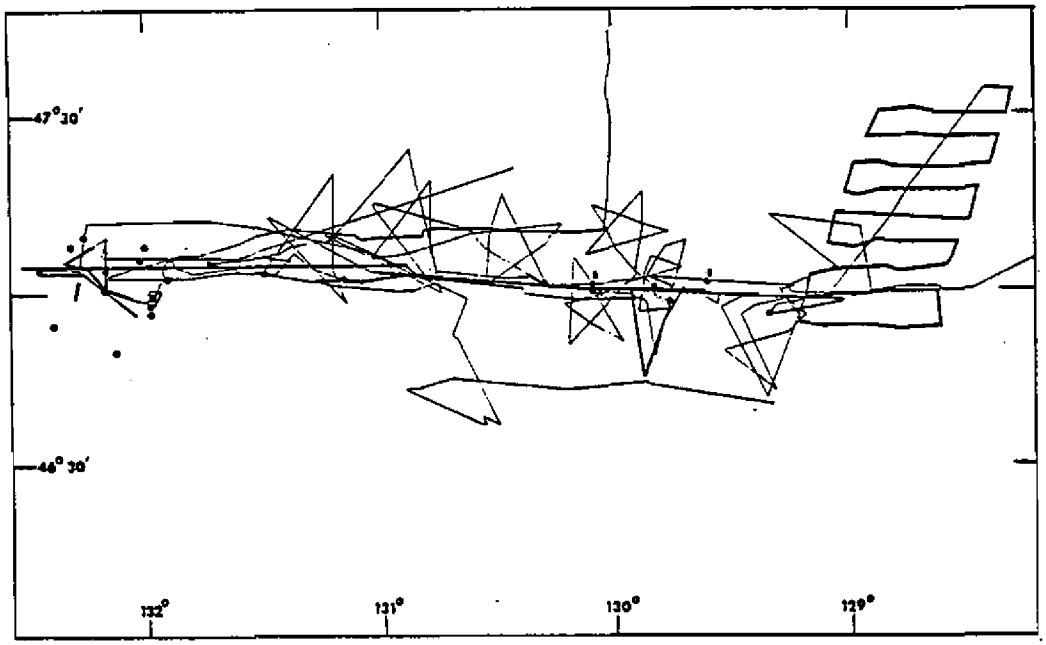


FIG. 2. Consolidated track chart of the Juan de Fuca Ridge investigations (not including the detailed survey area near 47° N 132° W). Core samples are shown by filled circles; superscript *B* means box core of surface material only.

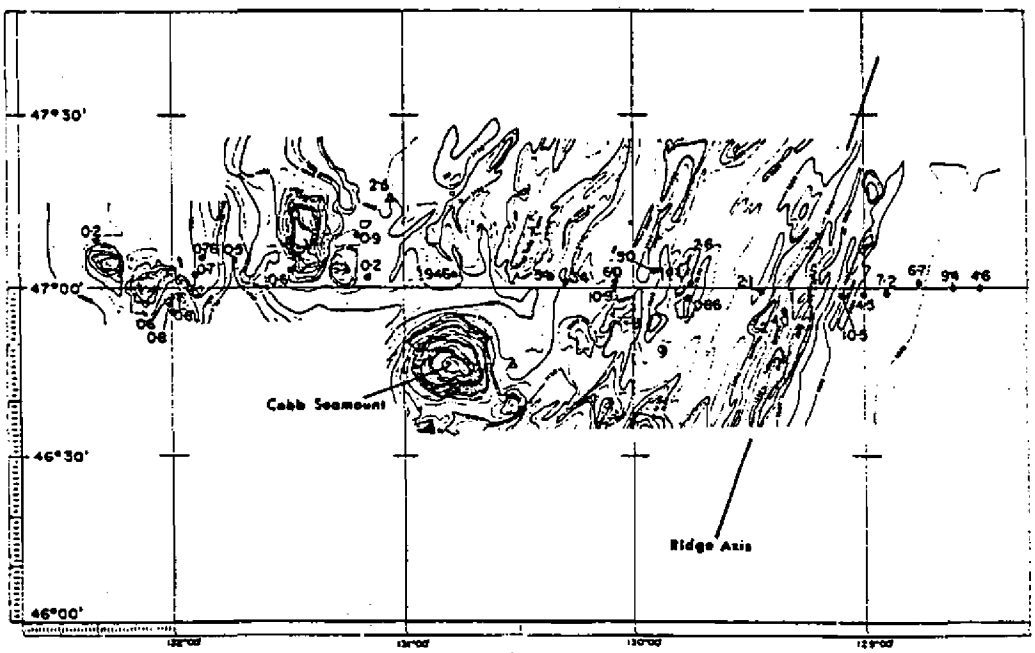


FIG. 3. Bathymetry and heat-flow data across the Juan de Fuca Ridge (axis shown). Map corresponds to area G in Fig. 1. Contour interval is in milliseconds of two-way travel time (×0·4 to convert to uncorrected fathoms). Heat-flow values are in microcalories per square centimetre per second (HFU).

Table 1

Heat-flow measurements: Juan de Fuca Transect

Station	Latitude (N)	Longitude (W)	Depth (sec, 2-way)	Conductivity ($\times 10^{-3}$ cal cg)	Heat flow ($\times 10^{-6}$ cal cm^{-2}–s^{-1})	Error band (±)	Heat flow (mW m^{-2})
TT3–1	46° 59·5′	131° 48·8′	4·24	2·0†	>0·6		25
TT3–2	46° 58·0′	131° 57·3′	4·29	1·9	0·8	0·06	34
TT3–3	46° 55·8′	131° 57·0′	4·32	1·89	0·9	0·1	38
TT3–8	47° 05·0′	131° 53·5′	4·31	1·93	0·7	0·06	29
TT17–1	46° 38·0′	134° 16·0′	5·15	2·13	0·2	0·06	8
TT17–5	47° 08·4′	132° 19·6′	4·34	2·08	0·2	0·06	8
TT31–1	47° 09·0′	131° 12·0′	4·09	1·86	0·9	0·04	38
TT31–2	47° 03·0′	131° 30·0′	3·96	1·96	0·6	0·03	25
TT31–3	46° 55·0′	129° 21·0′	3·40	2·04	4·0	0·10	168
TT31–4	46° 59·5′	129° 27·0′	3·61	2·14*	2·1	0·10	88
TT31–6	46° 58·0′	129° 46·0′	3·78	2·09	0·86	0·04	36
TT31–9	47° 00·0′	130° 06·0′	3·61	1·89	10·9	0·20	456
TT31–11	47° 02·0′	131° 10·0′	4·11	1·95	0·2	0·02	8
TT31–12	47° 10·0′	131° 44·0′	4·42	1·87	0·5	0·03	21
TT31–13	47° 05·0′	131° 52·5′	4·16	2·18*	0·76	0·04	32
TT40–5	47° 02·0′	130° 47·0′	3·75	1·93	9·46	0·20	396
TT40–6	47° 02·0′	130° 21·5′	3·71	2·17*	3·4	0·20	142
TT40–7	47° 01·0′	130° 17·5′	3·82	1·81	3·4	0·20	142
TT40–9	47° 01·0′	130° 05·0′	3·52	2·38*†	6·0	0·50	251
TT40–12	47° 01·0′	129° 45·0′	3·65	2·15*	2·6	0·30	109
TT40–15	47° 03·0′	129° 55·0′	3·57	2·15*	5·0	0·10	210
TT40–19	46° 58·5′	129° 06·0′	3·51	2·20	10·5	0·20	440
TT40–20	46° 59·0′	129° 00·5′	3·56	2·08*	4·5	0·30	189
TT40–22	46° 59·0′	128° 54·5′	3·56	2·21*	7·2	0·30	302
TT40–23	47° 01·0′	128° 46·0′	3·59	2·18*	6·7	0·30	281
TT40–24	47° 00·0′	128° 37·0′	3·65	2·06*	9·4	0·90	394
TT40–25	47° 00·0′	128° 30·0′	3·65	2·89*†	4·5	+0·60 −0·10	189

* *In situ* heated probe measurement (Lister 1970b)

† Assumed

‡ Partial penetration: lowest sensor

the disturbance by touching the sediment before penetrating fully, but even if a local slump has occurred here, the gradient is unlikely to have been affected. The therma time constant of 25 cm of sediment of normal diffusivity ($0{\cdot}0025\ cm^2\ s^{-1}$) is only 0·01 yr, and it is only 1 yr for the whole 200 cm sediment column at this station.

The most striking feature of the heat-flow distribution west of the ridge crest is the zone of sustained high values, between 45 and 75 km (Fig. 3). An acoustic reflection profile across the western boundary of this zone is shown in Fig. 4, where the measured heat flow changes by a factor of 50 over a distance of 25 km. The high value is on a ridge, and the low value is in a valley, which is the reverse of what would be expected from simple heat-flow refraction. The core from the valley station does show evidence of turbidite deposition in the past, but it also has the dark-coloured surface layer indicative of slow deposition in the post-glacial environment. Total sediment thickness is 50 m in a valley 6 km wide: the steady-state refraction correction due to the sediment fill is negligible, and the time constant of the whole layer is 300 yr. There is no evidence of sediment disturbance in the last 13 000 yr, and the good constancy of the heat flow between the long and short probe intervals rules out any significant water temperature change.

The oceanic basement in the middle of the high heat-flow area is remarkably smooth on a small scale, so that the acoustic profiler was able to resolve 30–50 m of sediment draped over the abyssal hills. A section of profile near the two values of 3·4 HFU (Fig. 3) is reproduced in Fig. 5. Notable is the hard basement echo indicative of the absence of surface roughess greater than 10 m. In contrast to this, a section of the same acoustic profile, taken under identical recording conditions, but east of the high heat-flow zone, shows diffuse basement echoes except for short segments of valley floor (Fig. 6). The wider valley contains 25 m of sediment, but the narrower one, leading down to a ponded basin, contains 70 m. This latter valley is probably connected to the Vancouver Island turbidite source, but the 25 m cover is consistent with reasonable quasi-pelagic sedimentation rates and the 1 My magnetic spreading age of the ocean floor at this point (Vine 1966). The basement roughness on the hills is here greater than 25 m, so that bare rock may be expected to outcrop on the hills although they are no larger than those in the high heat-flow zone further west. The gross topographic relief of 0·2 km over a wavelength of 10 km can generate a refractive deviation of only 6 per cent, and the lowest measurement in the area (0·86) is in any case on the floor of a narrow valley (see Fig. 3).

East of the ridge crest, the heat-flow measurements are high, much more consistently than on the western side. The scatter is still considerable, but no longer

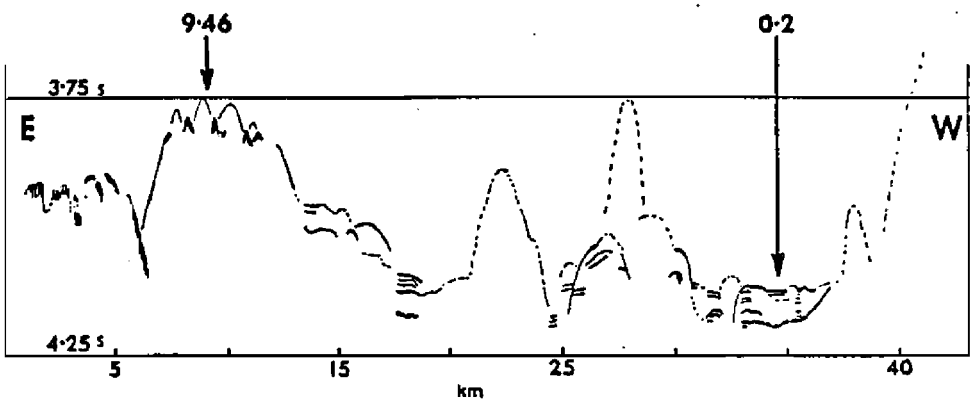


FIG. 4. Tracing of a seismic reflection profile between 130° 40′ W and 131° 15° W, at the western edge of the high heat-flow zone. Vertical exaggeration 30 : 1.

over an order of magnitude: the highest measurement is only 47 per cent above the 6 station mean of 7·15 HFU. Some, but not all, of the variation can be accounted for by the basement relief under the sediments, and the effect of the high turbidite sedimentation rates. The five innermost measurements fall on the acoustic reflection profile shown in Fig. 7. The value of 10·5, 12 km from the ridge crest, was taken at the extreme edge of a small sedimented valley, within 100 m of the outcropping rock slope that itself is 100 m high. The situation of the measurement is akin to a mixture of the cases treated by Lachenbruch (1968) and Von Herzen & Uyeda (1963). On the one hand the measurement is within one scale height of what may be a 45° slope, and on the other, it is in a sediment-filled trough that may not be too far from elliptical in cross-section. While the solutions referred to may not be added, a rough idea of the effect of the actual topography may be obtained by multiplying the corrections: the observed flow should be $\times 1{\cdot}17$ because of the slope and $\times 0{\cdot}9$ because of the trough, or only about 5 per cent too high. At the known spreading rate of the ridge (Vine 1966), the valley should be about 0·4 My old, and unless the 40 m of sediment were deposited recently, the sedimentation correction is only 3–5 per cent (Fig. 9 in Von Herzen & Uyeda 1963). Thus the expected net correction for this station is nearly zero, in so far as it can be estimated.

Another station that is notably out of line is the first on the abyssal plain proper, 4·5 HFU at 18 km from the crest. This is in a substantial sediment-filled trough, where both the refractive and sedimentation corrections are significant. A minimum sedimentation correction results if all 200 m of sediment has been deposited when the valley was formed: +7 per cent. A reasonable maximum corresponds to sedimentation 0·1 cm yr^{-1} for the last 200 000 years, or +15 per cent. The ellipsoidal trough solution, which should be a good approximation for a centrally located measurement, gives a further +10 per cent. Thus the measurement should be raised to between 5·2 and 6 HFU, not enough to be in line with a decreasing trend from the ridge crest, but at least changed in the right direction.

The last major out-of-line value is the 9·4 HFU at the extreme left of Fig. 7. There is some rise in the basement near the measurement, at least 100 m in 5 km, but it is less pronounced than the buried hill under the nearby 6·7 HFU value. In the case of a thin high-resistivity layer overlying topography on a medium of lower resistivity, the Jeffreys (1938) approximation must be modified to a surface thermal resistivity model. This shows that the effect of buried topography is *enhanced* by the ratio of the thermal resistivities minus one, provided the slopes are gentle enough for the basic Jeffreys approximation to be valid. Even with the $\times 1{\cdot}5$ enhancement, the correction to the measurement (on the sinusoidal ridge approximation) is only −5 per cent for the visible basement relief; it could be higher if basement deepened suddenly beyond where the profile terminates (cf. Fig. 2). There is some evidence that this may be the case, but basement returns on that section of Fig. 7 are not clear enough to be sure.

The prominent basement ridge under the measurement of 6·7 HFU (Fig. 7) should be taken into account. As it is flat topped, the inclined plane solutions of Lachenbruch (1968) may be used, and show that the −7 per cent correction is less than would be the case for a sinusoidal ridge of similar height. The enhancement factor is applied to the slope height in this case.

4. Explorer trough study

The pertinent measurements made from the *Hudson* are listed in Table 2. They are distributed over the ocean floor on, or south-west of, the prominent fault line associated with the upwarping of the Paul Revere Ridge (Fig. 8). This feature is capped by sediment layers that dip toward the north-east and outcrop on the south-west slope (R. L. Chase, private communication). It is therefore a piece of normal ocean floor

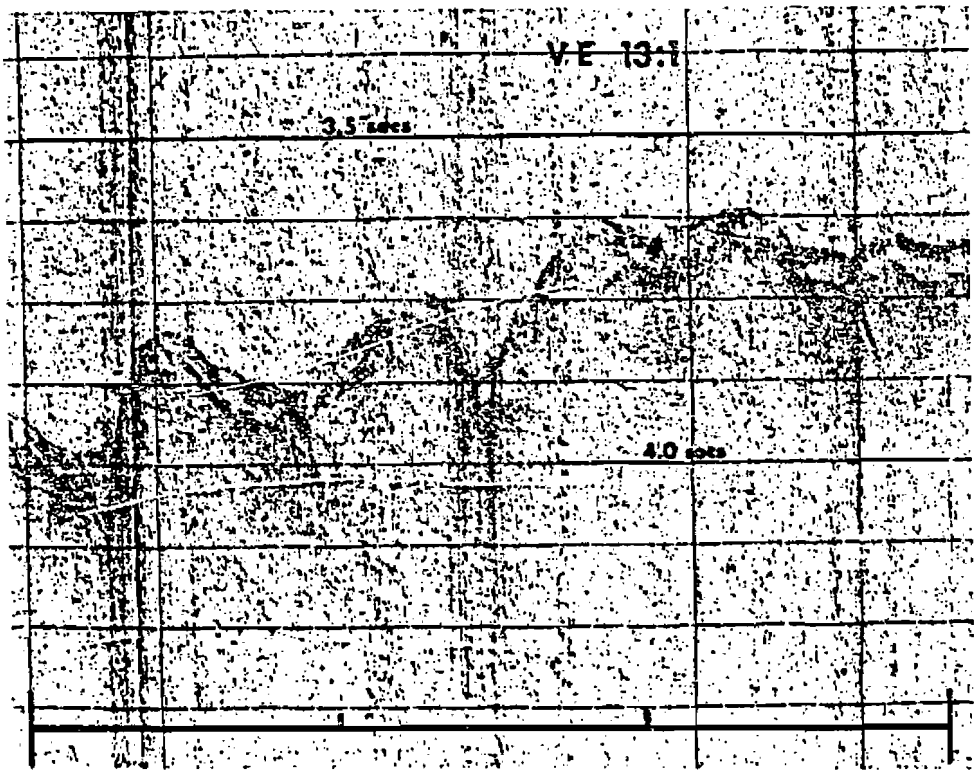


FIG. 5. Reflection profile of evenly sedimented basement within the high heat-flow zone, near 47° N and between 130° 23′ W and 130° 09′ W. Horizontal scale is 15 km long with 5-km divisions.

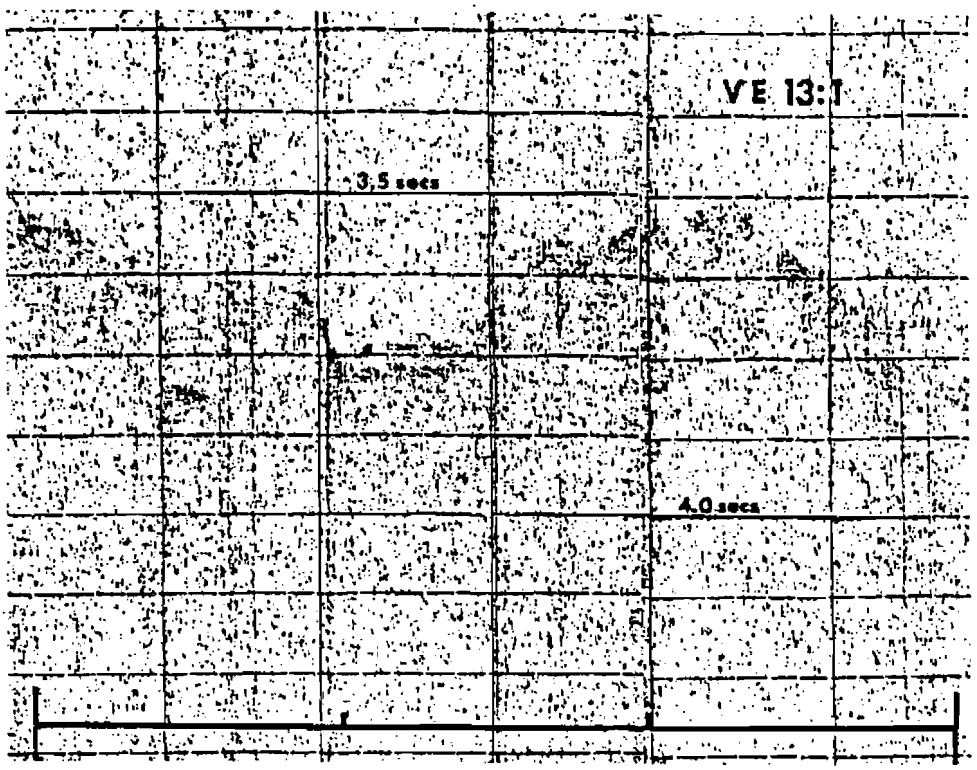


FIG. 6. Reflection profile near 47° N, from 139° 51′ W to 129° 37′ W, an area of moderate heat flow near the ridge crest. Horizontal scale is 15 km long with 5-km divisions. To the left of the 3·5-s identifier, a small peak reaching 3·35 s does not register on this record, due to strong scattering of the sound.

facing p.522

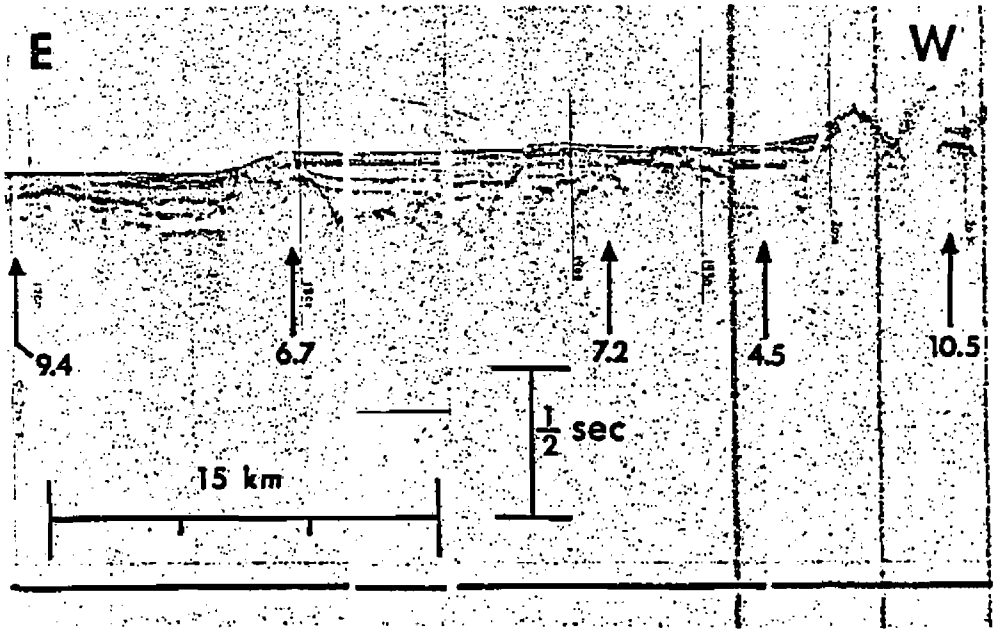


FIG. 7. Reflection profile east of the ridge crest near 47° N, with heatflow values (in HFU) superimposed. Vertical exaggeration 15 : 1.

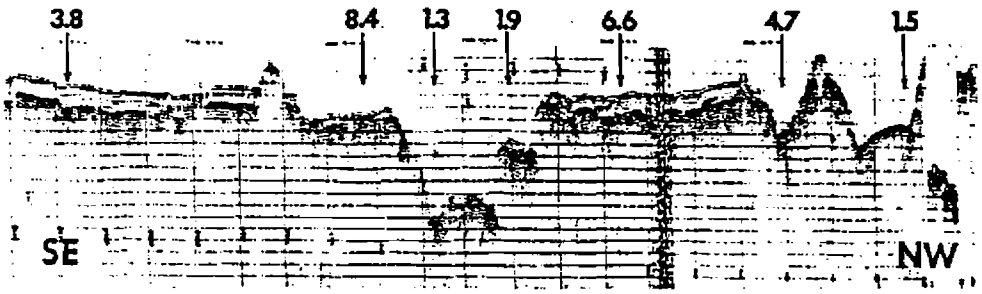


FIG. 9. The heat-flow measurements near the Explorer troughs projected onto UBC airgun profile 70–16–14. Profile by courtesy of Dr R. L. Chase, University of British Columbia. The vertical scale is from 2·5 to 5 s in 20 divisions, and the profile is 77 km long, so that the vertical exaggeration is 10 : 1.

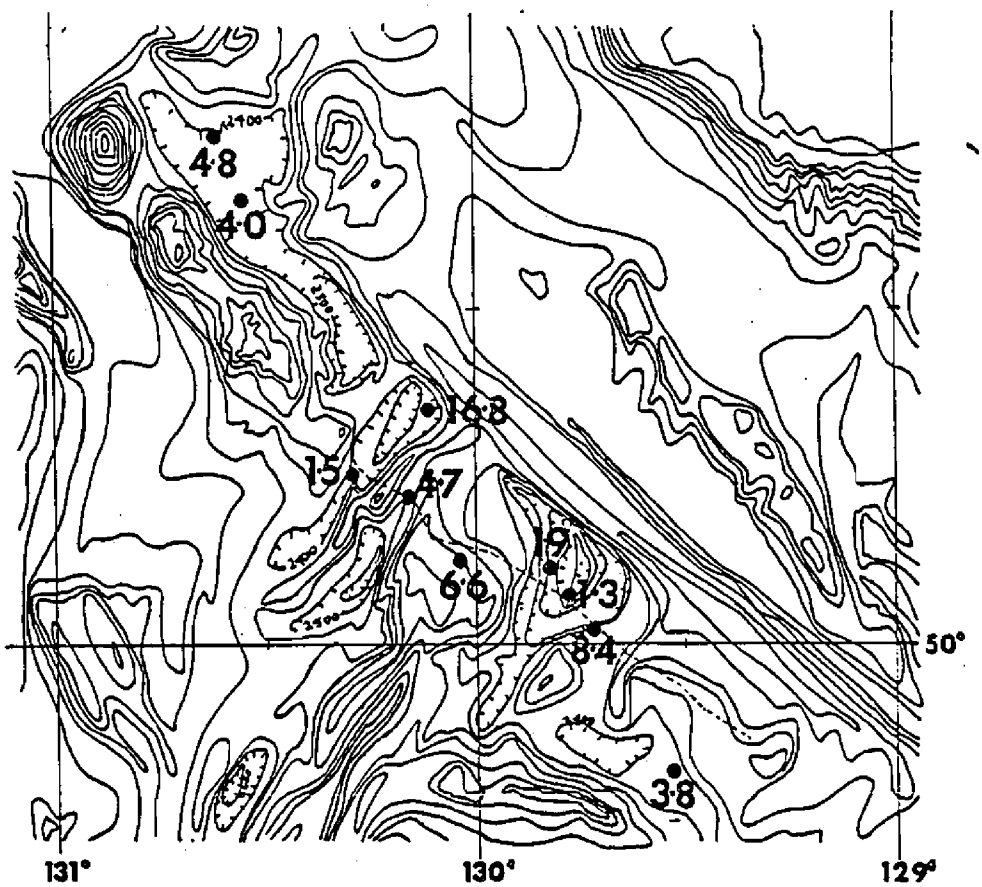


FIG. 8. Bathymetry and heat-flow data near Explorer Trough. The map is area H of Fig. 1 shown in more detail: contour interval 100 m. Paul Revere Ridge is the strong NW–SE lineation across the middle right of the area. UBC profile 70–16–14 is the faint dashed line running across the troughs almost parallel to the P.R. ridge.

that has been upwarped, rather than a linear volcanic pile, and represents a clear boundary to the spreading centre. The first seven measurements form a profile across the two troughs that abut the upwarped scarp, and were sited as close as possible to airgun reflection profile UBC–70–16–14 (R. L. Chase, private communication).

The measurements have been projected onto the profile in Fig. 9, and it is striking that the floors of the troughs are almost bare of sediment although the surrounding topography is well covered: in the case of south-easterly trough, to the very brim. The measurement in the north-westerly trough obtained only partial penetration with the 2-m probe, and a cine camera station was run nearby to determine the structure of the smooth, acoustically-hard floor. It is indeed quite flat, and consists of sediments interrupted every few metres by outcropping, though sediment-covered, boulders. A lava flow covered by 1 m of sediment would fit the appearance precisely. The relative absence of sediments strongly suggests that the floors of *both* troughs were formed recently, and the distribution of heat-flow measurements is therefore extraordinary. All the measurements on the sedimented basement near the troughs are high, but those in the troughs themselves are not, even though the bench in the middle of Fig. 9 is sediment-covered. The trend is exactly opposite to what would be expected from refraction through the topography, and so refraction corrections have not been made.

Table 2

Heat-flow measurement: Explorer Trough area

Station	Latitude (N)	Longitude (W)	Depth (sec, 2-way)	Conductivity ($\times 10^{-3}$ cal cg)	Heat flow ($\times 10^{-6}$ cal $cm^{-2}-s^{-1}$)	Error band (±)	Heat flow (mW m^{-2})
H70–4	49° 58·60′	129° 32·60′	2·78	2·19	3·8	0·04	159
H70–5	50° 01·57′	129° 43·04′	3·13	2·08	8·4	0·30	352
H70–6	50° 04·36′	129° 46·36′	4·36	1·94	1·3	0·10	54
H70–7	50° 07·70′	129° 49·80′	3·70	1·92	1·9	0·20	80
H70–8	50° 07·50′	130° 01·80′	2·79	2·19	6·6	0·20	276
H70–9	50° 13·20′	130° 09·20′	3·22	2·34	4·7	0·10	197
H70–10	50° 15·26′	130° 17·84′	3·25	1·71‡	1·5	0·30	63
H70–11	50° 21·00′	130° 06·60′	3·53	2·43	16·8	0·40	704
H70–12	50° 45·90′	130° 36·60′	3·28	2·27	4·8	0·10	201
H70–13	50° 39·50′	130° 33·00′	3·27	2·06	4·0	0·06	168

All these measurements were made with the *in situ* conductivity probe.

‡ Incomplete penetration: lowest sensor value.

The remaining three measurements are essentially on the Paul Revere fault line (Fig. 8). One, at the end of the north-westerly trough, is in a small shallow sediment pond at the base of the ridge slope. It is unusually high, even for this area. The other two are in a larger and deeper sediment pond to the north-west. This straddles a possible final spreading rift leading to the Queen Charlotte Fault proper, which essentially follows the continental margin off the Queen Charlotte Islands (Fig. 1). In view of the exceedingly high value farther down the Paul Revere Fault, the two measurements of 4 and 4·8 HFU do not confirm that this trough is the site of further spreading, but neither do they rule it out.

5. Discussion

The heat-flow measurements of this study differ from previous results (cf: Le Pichon & Langseth 1969) primarily in the presence of numerous zones of high values. Near Explorer Trough, both the plateaus have high heat flow (Fig. 9) and so does the fault line associated with the Paul Revere Ridge (Fig. 8). The more extensive transect of the Juan de Fuca Ridge establishes two major high zones: the sedimented flank east of the crest, mean 7·1 HFU, and between 50 and 130 km west of the crest, mean 6·4 HFU (Fig. 3). It is notable that all the areas where the heat flow is high have an even sediment cover thicker than local basement roughess (Figs 5, 6, 7 & 9), though this *by itself* is not sufficient to ensure a high measured heat flow (Fig. 4).

If an even sediment cover is necessary to measure consistently high heat flow, one must test the possibility that local sediment ponds separated by outcropping rocks can result in substantially depressed heat flow in those ponds. Von Herzen & Uyeda (1963) have shown that an isolated circular pond depresses the heat flow most, and if the conductivity contrast were as high as 3 and the basin were hemispherical, a measurement in it would be 0·4 of the true value. If the rock topography between basins is elevated, the depression is reduced, and the interference between neighbouring basins also reduces the effect. The 0·4 factor therefore represents a maximum for any reasonable configuration of lightly sedimented ocean floor, and cannot be expected to apply on an average basis to randomly located measurements. If the extreme correction factor were applied to all the inner western flank values (mean 2·4) it would bring them up to the same level as the others—yet all the heat-flow measurements can hardly have been made in deep local sediment pockets. The heat-flow contrast shown in Fig. 4 is orders of magnitude larger than the 2·5 : 1 expected, and moreover the *high* value is on the ridge where outcropping rocks may be common, not in the valley. The explanation cannot be applied at all to the measurements in the Explorer Troughs themselves: the local ponds would have effects smaller than the gross topographic effects of opposite sign. Therefore, while local refraction is likely to have some depressant effect on heat-flow measurements in rough topography, it cannot explain the gross contrasts observed in this study.

The next question that arises is whether even the highest values are high enough to be consistent with a conductively cooled sea-floor spreading model fed by material at observed lava temperatures (1400 °C). The simplest spreading model has been analytically solved by McKenzie (1967), but an even simpler model is adequate for use here: cooling of a half-space from uniform initial temperature, neglecting lateral conduction entirely. The solution is given in Carslaw & Jaeger (1959, p. 59) and the surface gradient is $T_0/\sqrt{(\pi\kappa t)}$, where T_0 is the initial temperature, referred to surface zero, κ is the diffusivity of the rock material, and t is time. The time axis can be translated into spreading distance, and although the solution is clearly inapplicable close to the ridge crest, where lateral heat flow is important, the approximation is good once the spreading distance substantially exceeds the penetration depth of conductive cooling $2\sqrt{(\kappa t)}$, at which depth $T = 0{\cdot}84T_0$. The Juan de Fuca spreading velocity is 3 cm yr^{-1} (Vine 1966) and if a diffusivity of 0·007 $cm^2\ s^{-1}$ may be assumed

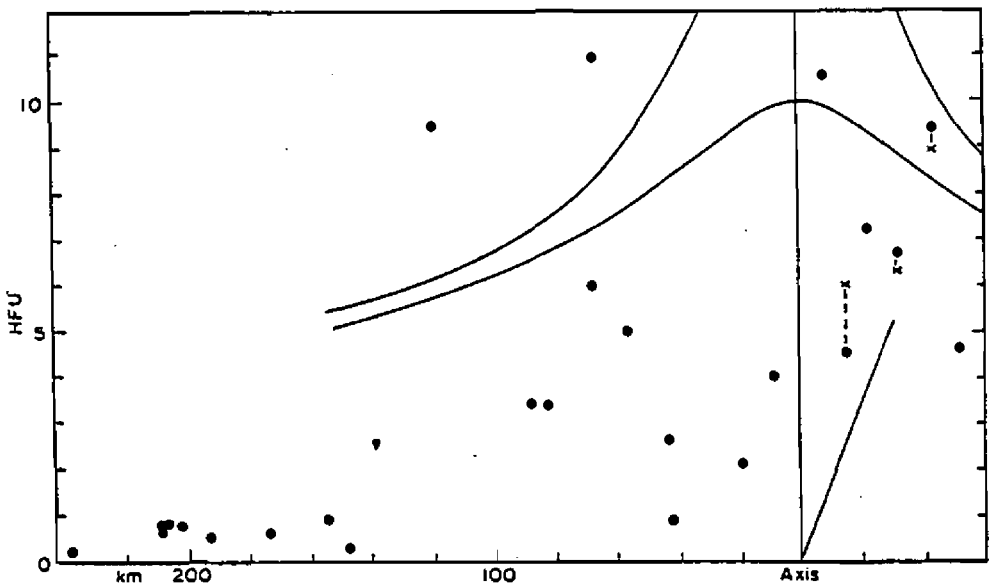


FIG. 10. Heat flow in HFU, versus distance from the crest of the Juan de Fuca Ridge. Filled circles: raw measurements from this study; inverted triangle: measurement from previous study projected onto profile; crosses: values corrected for sedimentation and refraction. The angled line from the crest origin shows the angle of the ridge crest relative to the profile. The solid curves are half-space conductive solutions for constant initial temperature (upper) and an initial linear gradient to magma temperatures. Spreading times have been corrected for the angle of the profile to the spreading direction.

for the rocks, the spreading distance is three times the penetration depth at a distance of 30 km from the ridge crest. The reason this is considered adequate is apparent from Fig. 10, where the upper curve is the heat flow predicted by the cooling model: it comes on scale at 30 km. All the heat-flow values of the ridge crest study are also plotted in Fig. 10 by their distance from the ridge crest along the 47th parallel. Only the highest values west of the ridge crest are above the conductive cooling curve; the mean in the high heat-flow zone, at 6·4, is not too different from the mean of the cooling curve in that region, 7·5. However, none of the measured values less than 50 km from the crest reach the curve, and the discrepancy increases as the ridge crest is approached.

The lower curve in Fig. 10 has been obtained from another simplistic model. In this case it is assumed that a linear gradient corresponding to a surface heat flow of 10 HFU is somehow established by cooling of the rocks as they are emplaced. With the figures used ($K = 0{\cdot}007$ cal cm^{-1} s^{-1} °C^{-1}, $T_0 = 1400$ °C), the penetration of this cooling is 10 km. The model was chosen because it gives a monotonically decreasing surface heat flow and a simple form for it: $q_0 \operatorname{erf} d/2\sqrt{(\kappa t)}$, where q_0 is the initial heat flow and d is the penetration depth. The solution was obtained from Carslaw & Jaeger (1959, p. 59), and it again ignores lateral conduction, but in this case it is a good approximation throughout. It is apparent from Fig. 10 that this model cannot be distinguished from purely conductive cooling in the western flank area of high heat flow, but it comes much closer to agreeing with the values on the eastern flank. The negligible effect of drastically different crestal conditions on the flank heat flow is important: not only do flank measurements give no insight into dyke injection or other ridge spreading mechanisms, but the explanation for depressed flank heat-flow values must be sought in locally operating mechanisms of non-conductive heat loss. A comparison between the theoretical and measured heat flow at 3 My on this

ridge flank, 7 HFU, and the normalized means for the East Pacific Rise, 2·6 HFU, and the Mid-Atlantic Ridge, 1·9 HFU (Le Pichon & Langseth 1969) shows that there is something to be explained.

At some distance from the ridge crest in any convecting model the upper boundary reaches a state that corresponds closely to a lithospheric layer cooling slowly by conduction. The total heat output between the crest and such a point on the flank must be equal to the heat lost by the lithospheric material in cooling from its initial state. If the temperature distribution at this flank point is similar to that of a half-space cooling from an initial uniform temperature, the total heat output can be obtained simply by integrating the surface heat flux of the one-dimensional model through time. This is only a fair approximation for the more imaginative convective models, but, since the real situation is complicated by processes of partial melting, magma percolation and differentiation, a more elaborate calculation is hardly justified. The interestingly simple result is that the mean heat flow between the ridge axis and a point on the flank is just twice the heat flow at that point computed from the one-dimensional cooling model. For example, in Fig. 10 the mean heat for flow the 100 km (full-width) central zone is nearly 16 HFU, and, so long as volcanic activity is confined to this zone, and cooling is conductive, the result is not affected by the detailed spreading model. In fact, the real heat loss should be substantially greater than this, since a proportion of the uppermost 10 km of material comes up molten, and the latent heat of freezing must be added to the integrated specific heat. The addition could be considerable: the latent heat of melting for dry Forsterite can be estimated from the Clausius–Clapeyron equation and data in Clark (1966); it is 800 cal cm^{-3}.

The thermal balance of the ridge crest zone is thus incompatible with the conductive cooling of material upwelling at a reasonable magmatizing temperature, and the observed level of the heat-flow measurements. The presence of high values in rough agreement with the conductively expected heat flow on the western flank suggests that the discrepancy is caused by failure of the assumption of conductive cooling at the crest rather than a more general failure in the sea-floor spreading hypothesis. It is then not necessary to postulate unusual local heat sources for an area of oceanic

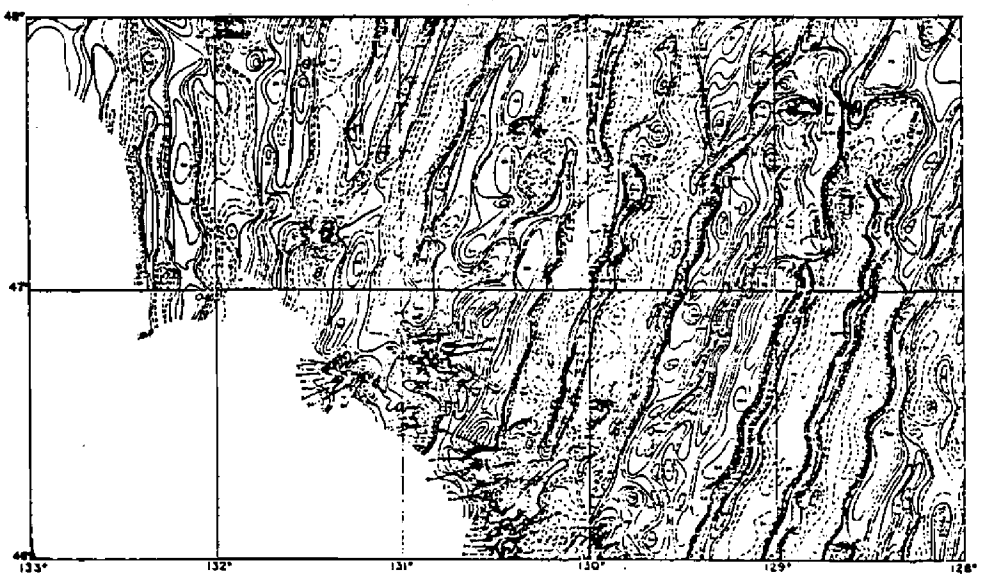


FIG. 11. A portion of the Raff & Mason (1961) magnetic survey, with an addition near 47° N 132° W, reproduced to cover the same area as Fig. 3. Positive anomalies are contoured as full lines, negative as dashed lines; contour interval 100γ.

crust that is a classic example of undisturbed sedimentation (Fig. 5). It may be argued that the abrupt decrease in heat flow beyond 131° W (Fig. 3) is not in agreement with this idea, but a consideration of the magnetic evidence makes it even more plausible. Fig. 11 is a reproduction of a portion of the Raff & Mason (1961) magnetic anomaly map corresponding to the area of this investigation (Fig. 3). The abrupt decrease in heat flow to more usual flank values occurs west of 131° W. This is the point at which the long anomaly trends begin to diverge from parallelism with the ridge crest: at 131° 30′ W the broad negative lineation is almost NS in strike, and the three positive lineations immediately east of it at the northern edge of the map have been compressed into a broad positive band at 47° N. The special conditions of ocean floor-spreading that produced the smooth basement of the high heat-flow zone cannot be expected to extend into the disturbed region probably indicative of the birth of the Juan de Fuca spreading epoch. Note that the well surveyed and sampled area near 47° N 132° W lies on true NS lineations of an earlier spreading era, so that the well established low heat flow could be due to a greater age of the lithosphere there.

6. Hydro-thermal convection

Once it is established that a substantial part of the surface heat loss at the ridge crest is non-conductive, no great imagination is needed to select the most likely mechanism: hydrothermal circulation in the oceanic crust. Iceland is a part of the Mid-Atlantic Ridge, and it is laced with hot springs and geysers. Other tectonically active regions of the world contain large-scale geothermal areas: New Zealand, Italy, California, to name a few. The mechanisms involved in these areas have been discussed at length by Elder (1965) and others; the important question is whether a hypothesis of hydrothermal circulation can help to explain other aspects of the ridge heat-flow observations beside the gross heat loss. The purpose of the following discussion is to show that it *does* explain both the valley effect in rough topography and the relatively uniform heat flow observed where basement topography has been buried by sediments.

If hydrothermal circulation is to occur, the convective driving forces must exceed the viscous drag of water percolation through the rock. Although both the thermal expansion and the fluidity of water will be decreased somewhat by the high ambient pore pressure beneath the ocean, the principal unknown is the permeability to be expected of the oceanic crustal rocks. Borehole tests in the New Zealand geothermal area (Elder 1965) suggest bulk permeabilities of 0·01 Darcy ($0{\cdot}987\times10^{-8}$ cm^2), but it is possible that the rarity of major geothermal areas is due more to lack of permeability than to lack of heat sources in other regions. If the oceanic basaltic layer is assumed to have a permeability k of 10^{-4} Darcy, an effective circulation depth h of 7 km, a diffusivity κ_m of 7×10^{-3} cm^2 s^{-1}, and a temperature difference ΔT of 1400 °C, while the percolating water has a thermal expansion coefficient α of 8×10^{-4}/°C and kinematic viscosity ν of $1{\cdot}5\times10^{-3}$ cm^2 s^{-1}, corresponding to water at 200° C (Elder 1965); then the Rayleigh stability number $\mathscr{R} = k\alpha g\Delta T h/\kappa_m\nu$ is approximately 80. It has been shown (Lapwood 1948) that convection can occur for Rayleigh numbers greater than 40 if the pattern is forced by uneven heating from below. Very conservative values have been assumed for the permeability and for the expansion and fluidity of water, since the latter increase with temperature in the range (<300 °C) where measurements have been made (Elder 1965). Therefore convective overturn of the pore water in the crustal layer near a ridge crest is highly likely, since the requirement of uneven heating is almost certainly met.

On the flanks of a ridge, both the thermal drive and the forcing effect of uneven heating must decrease as the lithosphere becomes older, and eventually convection will cease. The situation is complicated by the unknown effect of weathering and hydrous alteration of the rock on its permeability, and the natural variability in the

large-scale structure of the crust. The case where convection ceases as soon as cooling has penetrated to 10 km has been treated above, and the lower heat-flow curve of Fig. 10 describes the subsequent conductive cooling. The heat flow predicted by this curve is greater than the mean of most ridge flank values until the lithosphere is about 30 My old (Le Pichon & Langseth 1969), but although the *means* are thereafter in rough agreement, there is still more scatter in the measurements than can be expected from conductive refraction. Only in the older ocean basins does the heat flow reach the uniformity purely conductive flow should have (cf. Reitzel 1963). This is, perhaps, to be expected: low permeability regions will cease to convect while comparatively young, but where the permeability is high, say 0·01 Darcy as in geothermal areas, the flow can continue until the thermal drive drops below 140 °C over 10 km, a gradient corresponding to less than normal basin heat flow in the absence of convection.

At the ridge crest the hydrothermal circulation must be open, since an essentially infinite reservoir of fluid abuts the free surface of the crest. The free boundary should slightly reduce the Rayleigh number required for the onset of flow, but its most

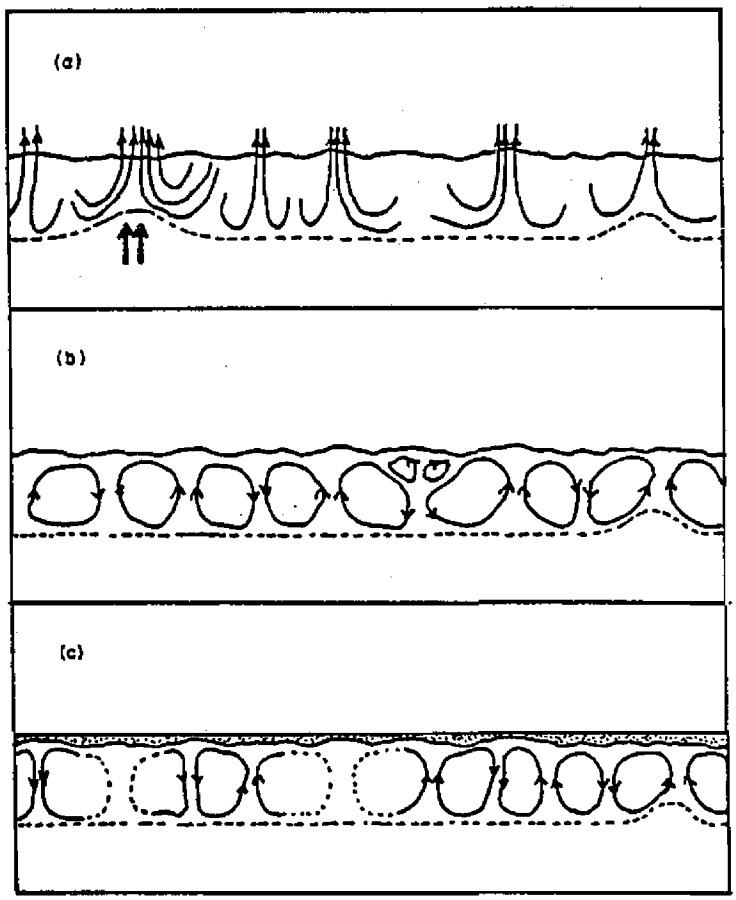


FIG. 12. (a) Pattern of convection to be expected near a ridge crest, where the permeable layer is open to the ocean. (b) Convective pattern forced by topography in an area of permeable crust bounded by a thin impermeable blanket of sediment. (c) The case of permeable crust with a rough boundary, buried by flat-lying sediments. The varying thermal resistance of the sediment blanket overpowers the direct effect of the topography.

important effect is on the thermal gradient at the boundary. Elder (1965) presents the results of one experiment on convection in a permeable layer heated along an infinite strip of width $2l$ below it. The heat output of the system is sharply concentrated over a band of width $0{\cdot}8l$, outside of which there is almost no heat output at all. The importance of this can be gauged when the effect of topography on the convective pattern is considered. Ridges and seamounts in the permeable material will act as chimneys for the hot flow, while valleys, representing the deepest penetration of cold bulk seawater, are natural sites for the ingoing return flow. The type of circulation to be expected is shown in Fig. 12(a) for two-dimensional topography, and in a perfect, or uniform percolation, system, zero heat flow should observed in the down-draught zones.

The plausibility of a circulation system for removing the initial heat of the fresh crust can be tested by a basic thermal output calculation. Suppose that at a ridge spreading at 3 cm yr^{-1} (one side), the top 10 km of lithosphere is cooled an average of 700° C, releasing 700 cal cm^{-3}. The continuous thermal output of 100 m of crest is $1{\cdot}4 \times 10^6$ cal s^{-1} (or 6 MW), and if the circulation mechanism results in a hot spring at about 50 °C, it must run at 28 l. s^{-1}, equivalent to a 20-cm diameter pipe discharging at 1 m s^{-1}. This would be a large spring, but by no means exceptional, and it could surface anywhere over the central 1km of the ridge crest. If the heat were dispersed into a cross-ridge flow of 1 cm s^{-1}, and 100 m thick, the temperature rise of the ocean water would be about 0·014 °C. Since the thermal gradient in the near-bottom water observed on lowering the heat probe is commonly 0·01 °C/30 m, it would not be easy to detect the heating in the topographically disturbed flow near a ridge crest. Only a careful areal study of absolute temperature at a fixed depth, on the lines of Chung *et al.* (1969), would be able to test for the overall thermal output of the ridge crest.

The second test of the hydrothermal circulation hypothesis is the distribution of measured heat flow over topography bounded by an impermeable layer, such as the high heat-flow region on the western flank of the Juan de Fuca Ridge. There are two reasons why this area can be considered bounded by an impermeable layer of sediment: the mean heat flow is close to what it should be for conductive cooling (Fig. 10), and the pelagic sediment, besides being of low inherent permeability (Appendix), can can readily plug the discrete vents of the hard rock structure at the interface. If the heat flow in the region were purely conductive, the even sediment cover over gently undulating basement (Fig. 5) would require the measurements to have a low scatter, and to be higher in the valleys and on the flanks of the ridges or hills than on the crests. Although the sample in Fig. 3 is a small one, the tendency is clear: the highest values are on top of hills or ridges, and lower values are observed on the flanks or in valleys. The high value of 10·9 HFU at 130°06′W, discussed at length in Lister (1970a), is a striking case.

It is situated on the brow of a hill, a place where conductive refraction would generate a minimum of surface heat flux, yet the measurement is nearly twice as high as one made nearby in a small valley or hollow. The values measured near Explorer Trough (Fig. 9) are an even more telling example of heat-flow correlation with topography opposite to that expected from conductive refraction. As the area is complicated by an apparent split in the spreading centre, and thus has an ill-defined recent history, it would be premature to attempt a detailed interpretation. The effect of an undulating impermeable boundary on hydrothemal convection in a permeable layer is illustrated diagrammatically in Fig 12(b). Valleys or surface depressions tend to depress the isotherms beneath them and therefore are places of preferential separation for the cold columns. By elimination, hills and ridges will become the sites for the hot rising columns, and should thus show the highest conductive heat flow through the impermeable sediment blanket. The forcing effect of the topography can be visualised by considering the stability of a cooled boundary layer on an inclined plane: the denser boundary layer will tend to slide down the plane until separation

occurs. The ability of the surface topography to control the cell geometry will depend on the ratio between the inverse wavenumber of the most pronounced topography and the cell size, and the relative effect of variations in the lower boundary of the permeable layer. If the permeability decreases gradually with depth, only large variations in the height of the lower boundary will affect the convection pattern, but such large variations could occur. Variations in the permeability of the crustal material are also likely to distort the cells, so high heat flow should by no means be 100 per cent correlated with the tops of hills or ridges. The evidence certainly suggests a positive correlation between high heat flow and topographic elevations, as opposed to the negative correlation that would be expected from conductive refraction.

The third test of the convection hypothesis is the prediction of the heat-flow variation on a flat sediment plain overlying topography on the basement. The contrast in thermal conductivity between moderately compacted sediment and basaltic rock is about 1 : 2·5, so that, in the absence of convection, the isotherms in the basement will be distorted by −1·5 times the topography, provided that the Jeffreys (1938) approximation is valid. The coldest areas of the upper boundary of the permeable material are now the highest topographically, and the sense of any convective flow should be reversed from its original configuration before the sediments were laid down (Fig. 12(c)). The geometrical effect aiding the motion and separation of a cold boundary layer is no longer operative, and the forcing effect of the buried topography is probably somewhat weaker than that of similar topography coated with an impermeable skin (see second test, above).

Now, the hottest water is in contact with the thickest sediment blanket, and the coolest water occurs where the sediment blanket is thinnest. Whether the highest heat flow will be observed over basement lows or highs depends on whether the temperature difference between the hot and cold columns of the cell is greater or less than the basal temperature difference between the sediment colums for a uniform heat flow equal to the regional average. In general, when the sediment thickness is much less than 0·4 times the convection penetration into the crust, and the Nusseldt number is not too high, the highest heat flows should be observed over troughs in the basement. If convection is vigorous, and the temperature difference across the cell is a small fraction of that required for equal conductive flow, it is possible for the heat flow to be quite uniform even over rough buried basement. Conversely, if the basement relief is too low to force the cell pattern, and the Nusseldt number is low, there will be 'hot spots' over the rising columns, uncorrelated with the topography.

The four Cascadia Plain stations in Fig. 7, and the one further east (Fig. 10), bear out the prediction in a general way. The mean heat flow for the region is in fair agreement with the lower cooling curve in Fig. 10: this corresponds to strong initial convection cooling the crest to considerable depth, followed by a resumption of conductive flow. Surface sealing and a reduction in the vigour of convection would produce similar results to true bulk conduction, and there are enough variable parameters to produce a range of models with reasonable mean heat flows. The chief discrepancy from prediction is the low value at the edge of the plain. It is within 3 km of outcropping basement, and it is not too implausible to suggest that the low value is due to forcing of an eddy under the plain by vigorous open cells near the ridge crest. The odd high (9·4 HFU) value over no particular basement disturbance corresponds well with the idea of an upwelling hot spot over a cell not correlated with topography.

7. Conclusions

The unusual heat-flow distribution across the Juan de Fuca Ridge at 47° N, and, to a lesser extent, the heat-flow distribution near Explorer Trough, can be interpreted to agree with a simple model of sea-floor spreading. The crucial requirement is that

the rock material at the ridge crest be immediately cooled to a depth of 5–10 km by open hydrothermal circulation. If the permeable crustal layer is subsequently sealed off by sedimentation, then the measured heat flow increases to values compatible with conductive cooling models. On the western flank of the Juan de Fuca Ridge, an area of unusually smooth basement appears to have been adequately sealed off by hemipelagic sedimentation; on the eastern side the encroaching turbidities have completely buried the basement topography. In both these areas, the mean heat flow is near 7 HFU, and is consistent with either conductive flow after cooling by hydrothermal circulation, or continued circulation beneath an impermeable boundary. The *distribution* of the measured values over the topography is more consistent in all areas with continued hydrothermal circulation, forced in part by the topography, than with conductive refraction. The continuation of hydrothermal flow in inadequately sealed areas is also necessary to explain the low values commonly found on ridge flanks (cf. Le Pichon & Langseth 1969).

The hypothesis can be further tested by examining the relationship between measured heat flow and topography in areas where topological information is complete for large-scale features, and the distribution of sediments is known. Eventually, the ridge crest hot springs should be found (and possibly tapped for geothermal energy), but it has been shown that the hot water will be hard to detect in an open ocean with significant bottom current flow. The principal value of the data presented in this paper is to confirm the long-held suspicion that the thermal balance of a ridge crest is dominated by circulatory cooling rather than by conductive processes.

Acknowledgments

This paper summarizes the work of several years, supported by Grants GA–577, GA–1640 and GA–27947 of the National Science Foundation, and Contract Nonr–477(37), Project NR 083012 of the Office of Naval Research, both of the United States of America. The work off C.S.S. *Hudson* was possible through the generosity of the Department of Energy, Mines, and Resources of Canada, at the Bedford Institute of Oceanography, and through a travel grant made by the Department of Oceanography, University of Washington. I wish to thank Dr R. L. Chase, of the University of British Columbia, for making available one of his seismic profiles, Dr A. W. Fairhall, of the University of Washington, for running carbon–14 dates on critical core samples, and Mr E. E. Davis for his invaluable assistance, both on the *Hudson* and subsequently with the data reduction.

Geophysics Group and Department of Oceanography,
University of Washington, WB-10,
Seattle,
Washington 98105

References

Atwater, T., 1970. Implications of plate tectonics for the Cenozoic tectonic evolution of western North America, *Bull. geol. Soc. Am.*, **81**, 3513.

Bullard, E. C. & Day, A., 1961. The flow of heat through the floor of the Atlantic Ocean, *Geophys. J. R. astr. Soc.*, **4**, 282.

Carslaw, H. S. & Jaeger, J. C., 1959. *Conduction of Heat in Solids*, Oxford University Press.

Chung, Y., Bell, M. L., Sclater, J. G. & Corry, C., 1969. *Temperature data from the Pacific abyssal water*, Scripps Institute of Oceanography, University of Calfornia, La Jolla, Data Report, 69, 17.

Clark, S. P. (Editor), 1966. *Handbook of Physical Constants*, Geological Society of America, New York.

Elder, J. W., 1965. Physical processes in geothermal areas, *Am. geophys. Un. Mon.*, **8**, 211.

Hamilton, E. L., 1964. Consolidation characteristics and related properties of sediments from experimental Mohole (Guadalupe site), *J. geophys. Res.*, **69**, 4257.

Jeffreys, H., 1938. The disturbance of the temperature gradient in the Earth's crust by inequalities of height, *Mon. Not.. R. astr. Soc., Geophys. Suppl.*, **4**, 309.

Lachenbruch, A. H., 1968. Rapid estimation of the topographic disturbance to superficial thermal gradients, *Rev. Geophys.*, **6**, 365.

Langseth, M. G., Le Pichon, X. & Ewing, M., 1966. Crustal structure of the mid-ocean ridges, 5, Heat flow through the Atlantic Ocean floor and convection currents, *J. geophys. Res.*, **71**, 5321.

Lapwood, E. R., 1948. Convection of a fluid in a porous medium, *Proc. Camb. phil. Soc.*, **44**, 508.

Lee, W. H. K. & Uyeda, S., 1965. Review of heat-flow data, in *Terrestrial Heat Flow*, Geophysical Monograph, **8**, 87.

Le Pichon, X. & Langseth, M. G., 1969. Heat flow from the mid-ocean ridges and sea-floor spreading, *Tectonophysics*, **8**, 319.

Lister, C. R. B., 1970a. Heat flow west of the Juan de Fuca Ridge, *J. geophys. Res.*, **75**, 2648.

Lister, C. R. B., 1970b. Measurement of *in situ* sediment conductivity by means of a Bullard-type probe, *Geophys. J. R. astr. Soc.*, **19**, 521.

Mammerickx, J. & Taylor, I. L., 1971. *Bathymetry of the Pioneer survey area, north of 45° Latitude, Special chart No.* 1, Scripps Institue, of Oceanography, University of California, La Jolla.

McKenzie, D. P., 1967. Some remarks on heat flow and gravity anomalies, *J. geophys. Res.*, **72**, 6261.

Peterson, M. N. A. *et al.*, 1970. Initial reports of the deep-sea drilling project, U.S. Government Printing Office, Washington, D.C., **2**.

Raff, A. D. & Mason, R. G., 1961. Magnetic survey off the west coast of North America, 40°N to 52°N latitude, *Bull. geol. Soc. Am.*, **72**, 1267.

Ratcliffe, E. H , 1960. The thermal conductivities of ocean sediments, *J. geophys. Res.*, **65**, 1535.

Reitzel, J. S., 1963. A region of uniform heat flow in the North Atlantic, *J. geophys. Res.*, **68**, 5191.

Sclater, J. G., Mudie, J. D. and Harrison, C. G. A., 1970. Detailed geophysical studies on the Hawaiian Arch near 24°25'N, 157°40°W: a closely spaced suite of heat-flow stations, *J. geophys. Res.*, **75**, 333.

Vine, F. J. & Matthews, D. H., 1963. Magnetic anomalies over oceanic ridges, *Nature*, **199**, 947.

Vine, F. J., 1966. Spreading of the ocean floor: new evidence, *Science*, **154**, 1405.

Von Herzen, R. P. & Uyeda, S., 1963. Heat flow through the eastern Pacific Ocean floor, *J. geophys. Res.*, **68**, 4219.

Appendix I

The permeability k of a representative sample of deep-sea sediment has been estimated from the transient loading curve of Mohole Phase I, sample EM8–10, published by Hamilton (1964). Axial loading was applied to a circular disk of sediment by a pair of porous plugs, and the pore fluid was squeezed out into these plugs. During the ' primary consolidation ' phase (9 min), the rate of shrinkage of the sample should be controlled by the permeability of the sediment, the permeability of the interface between sediment and plug, and the permeability of the plug itself. It will

be assumed that the permeability of the plug is much higher than that of the sediment, that the interface resistance is negligible compared to the bulk sediment resistance after the first few seconds of loading, and also that the dimensional changes are small enough to be ignored in setting up the flow equations. Since the total primary consolidation in the case considered is 4 per cent, a simple constant-dimension treatment is adequate.

The actual equilibrium response of the sediment fabric to loading is non-linear (Fig. 13(a), points), and varies from sample to sample. The effect of this can be estimated by considering the transient response for two cases: the fully linear compaction OP, and the sudden compaction model OYP where the sediment fabric shows no strength until the final level of compaction is reached. The first case corresponds to a diffusion equation solution, while the second results in a sharp state transition boundary that moves away from the free surface at a steadily decreasing rate.

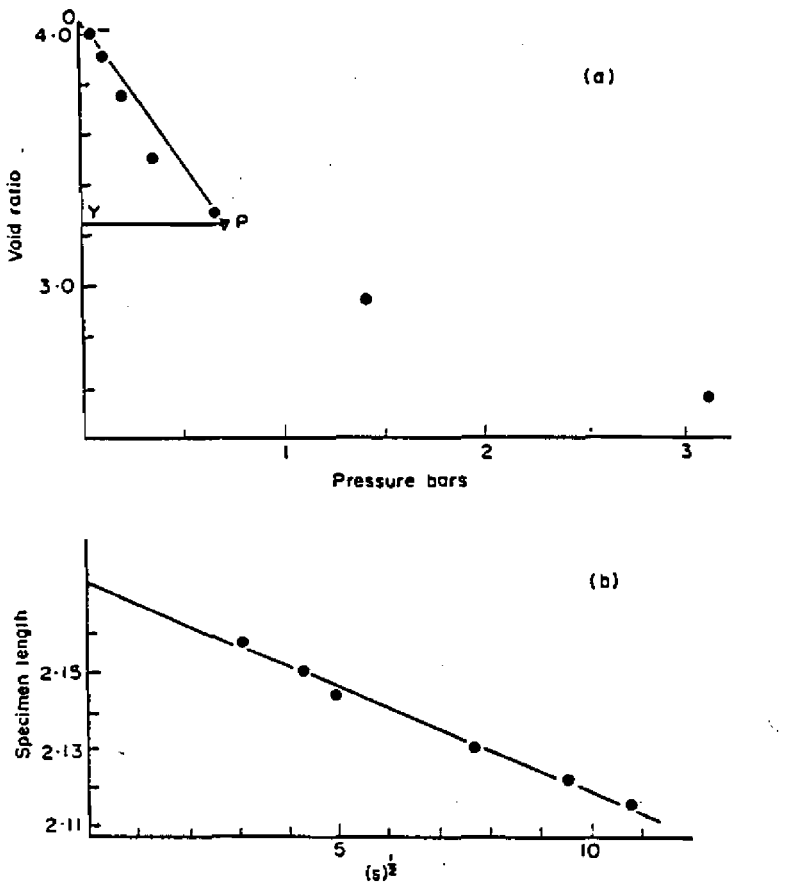


FIG. 13. (a) Steady-state compaction of Mohole sample EM–10 versus increasing pressure, after Hamilton (1964). (b) Transient primary compaction of the same sample with an applied pressure of 0·7 bars, plotted against square root of time. Replotted from Hamilton (1964, Fig. 9).

The linear model

If a compression state Θ is defined by $\Theta = (V_0 - V)/(V_0 - V_p) = (V_0 - V)/\Delta V$, where V_0 = initial volume, V_p = final volume, V is the actual volume, and ΔV is the final volume change, then the pore pressure at any point $P = P_0(1-\Theta)$, where P_0 is the loading pressure. Since it is the volume change that provides the flow, a one-dimensional diffusion equation $d\Theta/dt = [kP_0/\rho v \Delta V]\, d^2\Theta/dx^2$ results for the axial loading case, where x is axial distance, ρ is density and v is kinematic viscosity of the pore fluid. If the sample is long enough, the initial compaction will follow the solution for the semi-infinite solid $1-\Theta = \text{erf}\,[x/2(\kappa' t)^{\frac{1}{2}}]$, where $\kappa' = kP_0/\rho v \Delta V$, *at both ends*, so that $dy/dt = [2(d\Theta/dx)_{x=0}]\, P_0 k/\rho v$ and the displacement

$$y = -(4k\, P_0 t^{\frac{1}{2}})/(\rho v \sqrt{(\pi\kappa')}) = -(4/\sqrt{\pi})\, [kP_0 \Delta V/\rho v]^{\frac{1}{2}}\, t^{\frac{1}{2}}$$

The moving transition model

In this model the compacted boundary layer has a linear pressure gradient across it P_0/x, and the velocity of the sharp transition is given by $dx/dt = (k/\rho v)\,(P_0/x)\,(1/\Delta V)$ since the flow is provided by collapse of more material. The single boundary solution for this is $x = \sqrt{((2kP_0 t)/(\rho v \Delta V))}$ and therefore $y = 2\Delta V x = 2[\sqrt{((2kP_0 \Delta V)/\rho v)}]\, t^{\frac{1}{2}}$.

It is interesting that the two models both give a $y \propto t^{\frac{1}{2}}$ curve for the transient displacement in the compaction machine, and the value of k that would be calculated for the extreme non-linear model is $2/\pi$ of that for the linear model. The actual compaction data have been picked off Fig. 9 in Hamilton (1964), and are plotted in Fig. 13(b). The points lie close to a $y/t^{\frac{1}{2}}$ compaction line of 0·0054 cm $s^{-\frac{1}{2}}$, and using the values $P_0 = 0{\cdot}7$ bars, $\Delta V = 0{\cdot}042$, $\rho v = 0{\cdot}01$ poise, the values of k that result are

$$k_{\text{linear}} = 1{\cdot}95 \times 10^{-12}\ \text{cm}^2$$

$$k_{\text{transition}} = 1{\cdot}24 \times 10^{-12}\ \text{cm}^2.$$

The points in Fig. 13(a) represent *equilibrium* rather than *primary* compaction, but there is no reason to suspect that the primary compaction response would be more non-linear than the equilibrium response. Since the k calculated for the extreme OYP path differs little from k_{linear}, it is safe to take the latter as a good approximation to the steady-state permeability of the sample, some 2×10^{-12} cm^2 or 2×10^{-4} Darcy. Note that this value is for a sediment sample consisting of 60 per cent water by weight: closer packed material may have up to 10 times less permeability.



CANADIAN HYDROGRAPHIC SERVICE

TENTH ANNUAL CANADIAN HYDROGRAPHIC CONFERENCE

2-4 MARCH 1971

HOLIDAY INN

DARTMOUTH, NOVA SCOTIA

9
35
71

HUDSON '70 AND PAST OCEANOGRAPHIC EXPEDITIONS

by

C. R. Mann

When the HUDSON returned from her voyage around the Americas, everyone felt that it had been a great cruise, had produced a lot of results and compared well with past expeditions. I thought it would be interesting tonight to talk about four of the great oceanographic cruises of the past, with HUDSON '70 being the fourth one, instead of talking about HUDSON '70 alone.

The first major oceanographic expedition was the CHALLENGER expedition in 1872-76, and so it is natural to select this expedition as the first to discuss. It was an English expedition mainly biological in content that circumnavigated the globe in four years. At the time, nothing was known about the deep oceans and the CHALLENGER was charged with the job of going and finding out all about them. The second expedition I chose is the MICHAEL SARS expedition run by the Norwegians. I chose this because I think it is the first international expedition that was even run. It was not a large expedition, and covered only the North Atlantic, but it in part resulted from the formation of an international body called the International Commission for the Exploration of the Seas in 1902, and was jointly arranged by English and Norwegian scientists. In 1947 the ALBATROSS expedition was run by Sweden. I selected this expedition because it was the expedition in which the first extensive coring of the sediments of the world oceans was done. I was also drawn to the Swedish expedition because it was the first deep sea expedition of the Swedes and HUDSON '70 was our first deep sea expedition. Finally we come to HUDSON '70. I will try to keep some sort of a theme going through the discussion of the expeditions. I am going to emphasize the origins of the expeditions, and the equipments that were used on them.

Let us go back to the time just before the CHALLENGER expedition in 1872. Before CHALLENGER there had been many expeditions but they had been mainly voyages of discovery. The scientists who were sent on them were interested in such things as the transit of Venus, which Cook went to look at, and not too many were interested in the oceans. The first dredging of the ocean bottoms was started around 1750 by the Italians. It was shallow water dredging and was continued on the continental shelves by the Europeans. By the early 1800's flora and fauna had been found on the continental shelves but the general belief was that life didn't exist in the abyssal parts of the ocean. By 1864 a substantial list of species in the continental shelves had been catalogued by a Norwegian scientist, Michael Sars, who listed 92 species that lived between 400 and 600 meters. In 1858, the first transatlantic cable was layed. In 1860, it broke and on cable recovered from a depth of 2000 meters was found coral. At shallower depths molluscs and worms were found adhering to the cable. This was one of the first evidences that there was life in the deeper parts of the oceans. In the early 1800's then a very intensive study was developing of the biological life of the oceans.

Hydrography was also beginning to develop. The earliest hydrographic soundings appeared on charts in 1585. The first contours that were drawn on maps were drawn by hydrographers not geographers, and they were contours of the sea floor. Soundings had been taken for quite a few hundred years but the first abyssal soundings of the deep oceans didn't start to appear until the 1800's. The first extensive abyssal soundings were made on an Antarctic expedition lead by James Ross in 1839-43, because in the early 1800's the hydrographer had acquired the technique of abyssal sounding. Measurement of temperatures in the deep oceans had also developed. Early attempts had been to insulate the thermometers and to provide enough lag so that when they were drawn up to the surface the temperature didn't change too much. In 1860 Six's maximum and minimum thermometer was adapted for use in the oceans by Wyville Thomson. This allowed temperature measurements to be made in the abyssal oceans.

We find, you see, that around 1860 hydrographers have acquired the ability to do deep sea soundings, that there is great interest in biology of the oceans and there is evidence that there is life in the abyss, and that thermometers have been developed which will allow temperature to be measured in the deep ocean. These developments set the stage for the CHALLENGER expedition.

The expedition was developed from the work of a few men of whom Wyville Thomson was one of the main figures. Thomson was an English naturalist. In the 1860's he became interested in the biology of the oceans, and together with the Hydrographer from the Navy, organized two cruises, one on LIGHTNING and one on PORCUPINE in 1867 and 1868. They dredged down to 4000 meters and found many unknown life forms. This created a great deal of interest and the result was that the British decided to send out an expedition to find out all about the oceans. The CHALLENGER was the ship selected; she wasn't a small ship, she was 2306 tons, auxiliary steamed with twin propellors. Wyville Thomson was given the task of heading the expedition. CHALLENGER sailed in December 1872 and returned in May 1876 after having crossed all the major oceans several times.

Let us look at the work they did and the techniques they used. Sounding was done by line. The lines they used for soundings on the CHALLENGER were one inch hemp lines with three or four 50 kilogram weights attached. There were 100 fathom marks on the line and they could sound the deep oceans with an accuracy of 100 feet. They didn't wish to drag all the weights up so these were held on a tube that extended below the weights and plunged about 18 inches into the bottom. When the line was pulled up the weights fell off and an 18 inch core of the bottom was brought up. With this equipment they sounded the depth of the ocean and also took the first cores. They were not so interested in geology at that time, what they were interested in was the biological composition of the cores. As a result of the expedition, it was first determined that the oozes found over the ocean floors were composed of skeletons of small animals.

Temperatures were measured with a development of Six's maximum and minimum thermometer. They found, on the CHALLENGER expedition, that the ocean was layered. Before it had been believed that the ocean had a constant temperature from top to bottom. Water samples were taken with water bottles that were attached to the sounding line along with the thermometers. The interesting thing about the water bottle was that using one inch hemp lines they couldn't send messengers down the line to trip it as we do today and the bottle was devised to close automatically when they commenced hauling in the sounding line.

The major work on the CHALLENGER was the biological work, which was done with large trawls. Fish from great depths were caught with these trawls that were put down and dragged near to the bottom. A trawl coming aboard was not much different than a trawl coming up these days. There was the inevitable bucket and sample jars that we have today to collect specimens. Townets, as they were called then were used for catching fish or plankton at the shallow depths. The word plankton wasn't coined in those days. It means wanderer and didn't come into use until 20 or 30 years after the expedition. The net looks very much like nets today except that it didn't have a little cup at the end. The sailors on CHALLENGER had to be good seamen. All this gear had to be put on hemp lines, the trawls were managed with three inch lines, and they had to stream 6,000 meters of line so the men must really have been very good at rigging. They built accumulators to reduce sudden strains with strips of rubber which were one inch diameter and three feet long. Up to 80 of these were used in a configuration that could carry a load up to 2½ tons.

The results of the CHALLENGER expedition were the first discoveries in deep sea biology, the first chemical analysis of the oceans, the first knowledge of the extent and composition of the deep sea oozes, the first description of the oceans layers and one of the first bathymetric charts made of the ocean. There just cannot be another CHALLENGER expedition, because the members of the expedition had a whole ocean about which nothing was known and one just doesn't have this any more.

Let's jump ahead now. There were 50 volumes published as a result of CHALLENGER's voyage, mainly by John Murray, a biologist, who was interested in deep sea oozes. When he attended a conference in 1909, at the International Commission for the Exploration of the Seas, Murray thought that somebody ought to go out in the North Atlantic and should confirm some of the CHALLENGER findings and continue with its work. There were still unanswered questions. One of them at that time was "Did fish live at mid-depth?" The CHALLENGER trawls were brought up through the whole water column and strained all the water as they came up and there was no knowing where the fish had come from. Around this time the Norwegians had developed techniques for closing nets, were very active, and Murray approached the Norwegians with an offer to put up the money for an expedition if they would provide a ship. The Norwegians agreed to provide the MICHAEL SARS. She was not like the CHALLENGER; the CHALLENGER was a navy ship which was specially fitted out for her expedition. The MICHAEL SARS was built in 1900 by the Norwegians especially for the purpose of research in connection with the Norwegian Fisheries.

MICHAEL SARS sailed from Norway in 1910 to England. She went down to the Strait of Gibralter across the Atlantic to Newfoundland then back to Norway. The soundings on the chart showing her track are all the soundings there were in the North Atlantic at that time greater than 1000 fathoms. There were 1873 soundings altogether. The chart also shows the deeps. The beginnings of the mid-Atlantic Ridge appear in the bathymetry. Of course the chart doesn't look anything like our charts of today. But remember that each number on that chart meant one lowering of several miles of line.

By the time of the MICHAEL SARS expedition, sounding equipment had improved immensley and was done with a wire line on a specially designed high speed winch. Reversing thermometers had been developed, which meant that ocean temperatures could be measured much more accurately, and Nansen invented the reversing water bottle. What must have made this possible was the advent of steel wires, instead of hemp lines, so a messenger could be slipped down them and the bottle closed. Now we find that we have better thermometers, better sounding machines, and better sampling techniques for temperature and salinity. What was perhaps more important was that nets have been developed that could be closed at mid depths so that the scientists could examine the biology at mid-water depths. They had also developed current meters. Here one sees some similarity between the MICHAEL SARS expedition and the HUDSON '70 expedition. As part of their work the ship stopped in the Straits of Gibralter for a few days and the current meters were used to obtain some of the first measurements of currents through the Strait. The MICHAEL SARS set off on her expedition with improved equipment with her main task being to study the mid-water fish with equipment which hadn't been available on the CHALLENGER. The result of that expedition was that a great deal more was learned about the plankton, the fish, the temperatures, and salinities of the ocean.

We jump ahead to just after World War II and we come to the ALBATROSS expedition. During the war the Swedes had developed an Oceanographic Institute but could not undertake investigations on the high seas, so they developed equipment. Most important they developed deep sea coring techniques, which together with echo sounding machines that had been developed prior to the War, made coring of the ocean floors to 70 feet into the sediments a feasible operation. This meant for the geologists that they could now examine the sediments in the deep oceans. They had to go all over the oceans to do it and this formed the basis for the ALBATROSS expedition. The expedition was funded privately in Sweden with individuals contributing sums up to $200,000. A large shipping consortium loaned their training ship for the cruise and outfitted it. The ship was the ALBATROSS. There was no governmental or other funds provided. The ALBATROSS went around the world in 1947-48 and brought back many samples of cores which were subsequently worked on by many laboratories around the world as well as in Sweden. The scientific team also undertook measurements in physical oceanography and chemistry and studied the equatorial current system.

Next we have the HUDSON '70 expedition. Like its predecessors the HUDSON expedition had its origins in the development of improved and new equipment. It was comprised of individual programs at various places around the Americas. The original program was a series of studies in different areas. In the Antarctic where I wished to work, in the Chilean Fjords where the University of British Columbia wished to work, off the west coast of Vancouver Island where the geophysicists wished to work, in the MacKenzie Delta Area for the geologists, and again for the geophysicists in Baffin Bay. This was the original program. We discussed this program in 1967 without doing much and then decided we would get serious about it. A preliminary program was drawn up which Dr. Ford took to Ottawa as at this time we had to start to think about support for the expedition. Dr. Ford asked other leading scientists how they felt about Canada running an expedition such as this. Their reaction was very favourable and so we continued to go ahead. When it was realized that we were going to go, more people became interested and programs developed for the transits between the major areas in which we wanted to work. The transit down the South Atlantic became the most popular part of the cruise. HUDSON left Halifax in November 1969 and ran a major program down the South Atlantic; it was mainly a program for the biologists and chemists who wanted to study aspects of marine biology and chemistry on an ocean wide basis. The line down the South Atlantic was a very attractive line to run because there are great movements of water from south to the north and changes occuring as the waters move. The ship went to Buenos Aires and then worked in the Drake Passage where we measured the currents, and did a biological program for Dalhousie. We also made some measurements of the turbidity of the deep water for Woods Hole using a new light meter. The interesting thing about these three programs is that none of them were possible 10 years ago. Sleds used to collect bottom fauna were developed in the last 10 years to study bottom fauna on a world wide basis. Ten years ago we couldn't put current meters in the deep ocean, but we have developed a technique of doing so, and can now measure currents in places like the Drake Passage. The measurements of the turbidity of the ocean were made because recently a large layer of sediment was discovered in the deep ocean suspended in the water near the bottom. The question is how far over the ocean do these large layers of sediment laying just above the bottom extend. Again this particular piece of work is interesting because this is the way many of the oceanographers are beginning to operate these days. They have to study an ocean, and they hop from one ship to another and with their equipment. In this case they brought their equipment to Halifax, put it on our ship and we took it with us to South America where they joined us, did their work and then flew home. The equipment was carried to Vancouver and it eventually found its way back to its home to Woods Hole. From Drake Passage the HUDSON went to the Chilean Fjords and then she ran a line up the Atlantic passing Tahiti. She worked off the coast of Vancouver for

four weeks doing geophysics and then went into the MacKenzie area for the geology program. This was continued through to Resolute. Baffin Bay was more geophysics and then home. There were many other new equipments used by the geophysicists, geologists, chemists and hydrographers on board. Satellite navigation deserves mention because without it, the accurate positioning required for buoy laying and geophysical mapping would not have been possible. The HUDSON returned home in October, 1970. We were given a fine welcome with a fire boat and speeches. All of us on board were rather abashed at this but maybe it's not a bad thing to have a little bit of pomp and ceremony after a ship has sailed such a long distance. We were welcomed home by the Minister of Energy, Mines and Resources, Mr. Greene. When we planned this expedition I was late in getting the final manuscript describing the expedition ready for Dr. Ford to take to Ottawa, and I was getting a little worried (this is in August 1968) that if we didn't get this thing off the ground in a couple of months we wouldn't make the next year's starting date. Dr. Ford took it to Ottawa. I don't know how he wangled things but anyway he ended up with Mr. Greene and Mr. Greene said go on and do it. Bill came back and we sort of gulped and started. Mr. Greene supported the expedition and in a sense he was the patron of it. I feel that this should be recognized and also Dr. Ford's work in sponsoring the expedition and obtaining the necessary support.

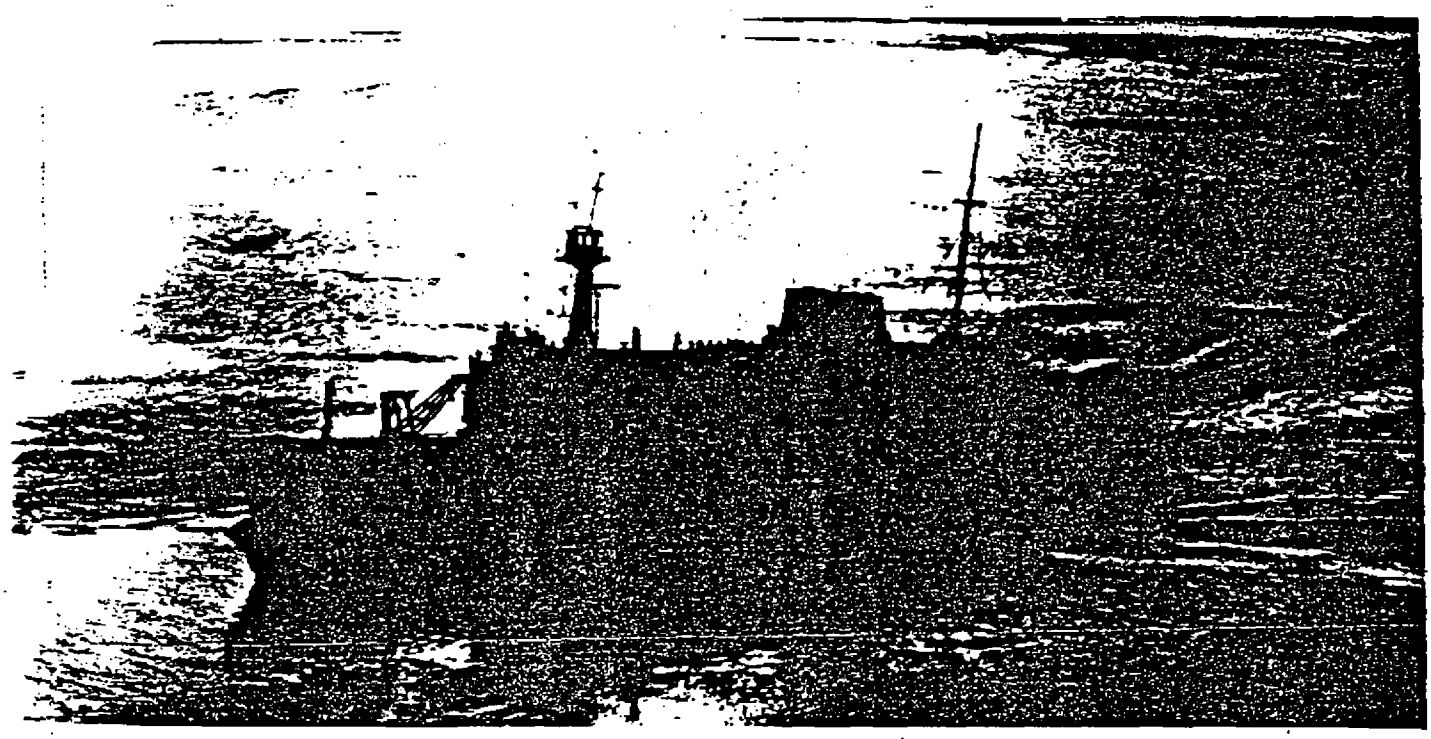
All these expeditions have another side to them other than the primary scientific task. The CHALLENGER was charged with the task of observing the lands and the peoples, particularly of all the islands she visited. The ALBATROSS was charged with being an ambassador of Sweden and calling at various Swedish outposts. HUDSON called at Buenos Aires partly because we had an interest in designing and selling a research ship to the Argentinians.

I see according to me it's quarter after 8 in Ottawa, and quarter after 9 here, so I don't think I am going to summarize. Let me just leave it at this and you can draw your own conclusions about these expeditions and where HUDSON '70 fits in. THANK YOU.

The HUDSON 70 cruise:
a significant contribution
to world oceanography

The Hudson-70 cruise: a significant contribution to world oceanography

C. R. Mann



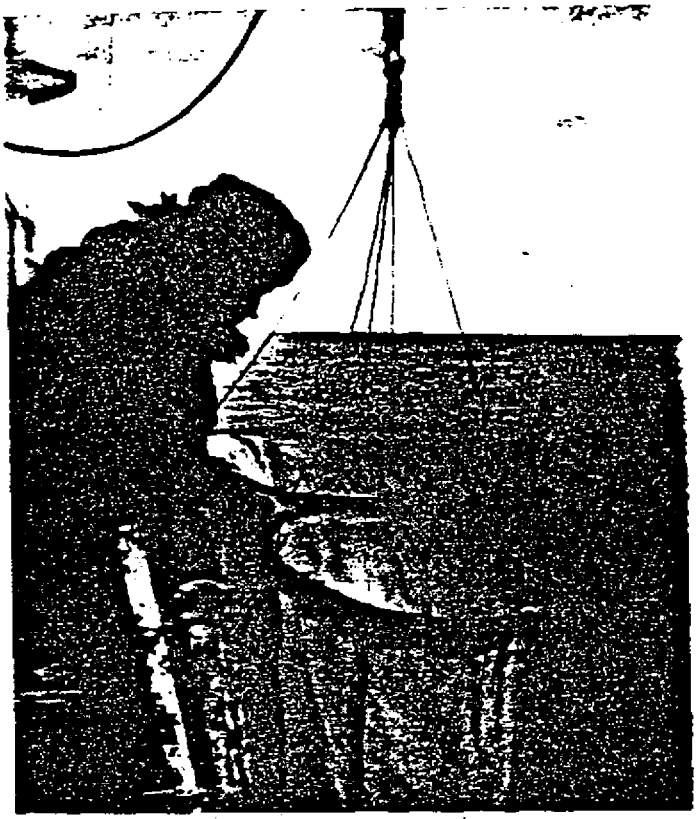
From November 1969 to October 1970 Canada's largest research vessel, the 4700-ton CSS *Hudson*, sailed on an oceanographic expedition around the Americas, carrying Canadian marine scientists to four oceans: the South Atlantic, the Antarctic, the Pacific and the Arctic. All who took part felt a sense of achievement and it seems timely to review the work of the expedition and its motivations.

The expedition had its origins in the great expansion in Canadian marine science from 1950 to 1970, and the establishment of laboratories devoted exclusively to study of the marine environment in universities and government departments across Canada. During this period substantial programs in marine geology and geophysics, physical oceanography and chemistry emerged to complement an already active program in marine biology fostered by the Fisheries Research Board. The major laboratory, the Bedford Institute, was opened in 1961 under the Department of Mines and Technical Surveys (now Energy, Mines and Resources) and houses an almost complete marine science community. Ships specifically designed for marine science were constructed; the largest of these, the CSS *Hudson*, was commissioned in 1961 and is manned by the Atlantic Oceanographic Laboratory at Bedford.

By 1967 a great deal of exploratory geophysics and geology had been done along the eastern seaboard and Arctic using the *Hudson*, and it was considered that the ship should be employed on the western continental shelf and in the Beaufort Sea to explore these areas with the sophisticated geophysical system that had been assembled aboard her.

At the same time the physical oceanographers, chemists and biologists had developed equipment that allowed a new insight into the currents, chemistry and biological life of the oceans, and it became necessary to

DR MANN, a physical oceanographer, is head of the ocean circulation section of the Atlantic Oceanographic Laboratory at the Bedford Institute, Dartmouth, NS. He co-ordinated the scientific projects for the entire Hudson-70 cruise, and was on board the *Hudson* for a total of 4½ months, first in the Atlantic and Antarctic, then again in the Arctic.

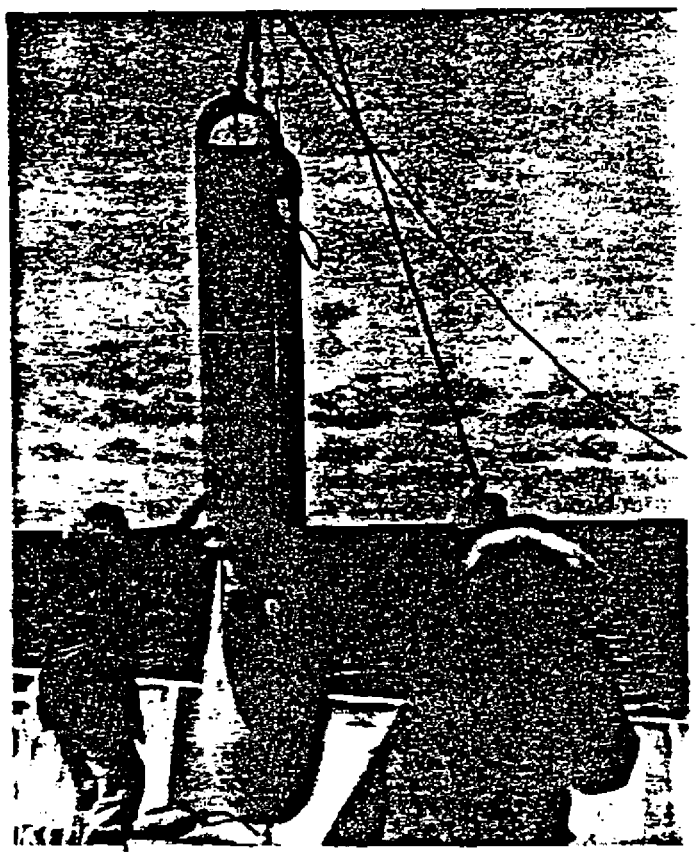


employ these techniques on an ocean-wide scale to obtain an understanding of the complete system. The geophysical and geological work in the western Arctic and on the western continental shelf and slope, together with ocean-scale experiments in the other disciplines, were the basis for the Hudson-70 expedition.

The first plan for the expedition was drawn up in January 1968 when it became clear that the scientific program could best be accomplished by sending the *Hudson* on a voyage around both North and South America. The track of the ship would give north-to-south transects of the Atlantic and Pacific oceans and would bring her back to her home port in Halifax through the Arctic following a period on the west coast. The passage around South America would also allow an opportunity for the National Museum of Natural Sciences to collect biological specimens in the untouched islands at Tierra del Fuego and for a group from the University of British Columbia to extend their studies of fjords to the Chilean fjord system. Additional impetus came at this time from an announcement by the Intergovernmental Oceanographic Commission of Unesco of an International Oceanographic Decade from 1970 to 1980 during which member countries would support an accelerated program of ocean exploration.

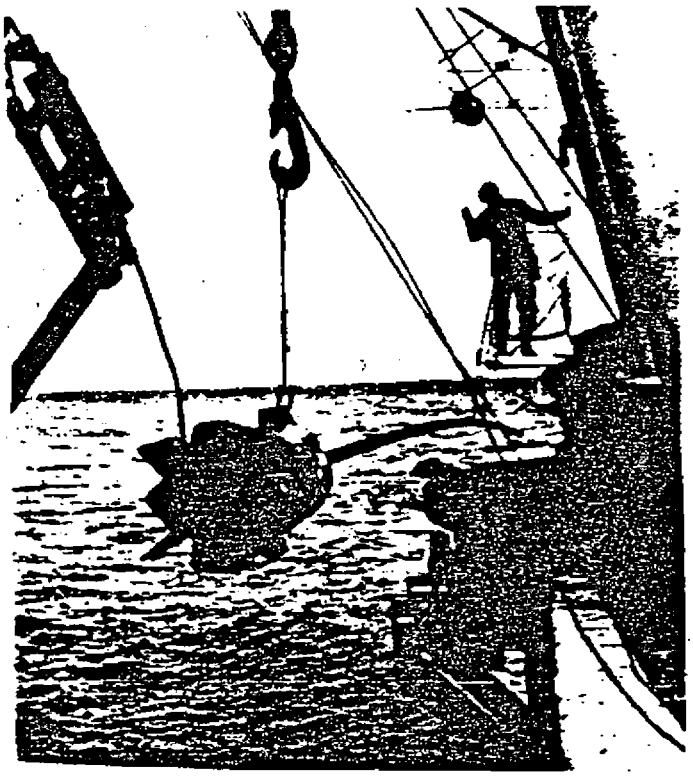
By August 1968 a detailed scientific program was drawn up that was subsequently approved by the minister for energy, mines and resources, the Hon. J. J. Greene, in November. The direction and timing of the voyage were dictated by the seasons as it was necessary to be in the Antarctic regions in January and February, the southern summer, and in the Arctic in September in order to traverse the Northwest Passage. This could only be done, still allowing time for the scientific program, by circumnavigating the Americas clockwise, leaving Halifax in November and arriving back in October of the following year. The sailing date was set for late 1969 to allow time for preparation and assembly of equipment, and on 19 November 1969 the *Hudson* left Halifax on her eleven-month voyage.

The scientific team assembled for the early part of the voyage, through the South Atlantic, was mainly composed of biologists and chemists. Their interest in the South Atlantic stemmed from the large scale movement, north and south, of masses of water that interleave at depth to form layers of different temperatures and salinity, and come together at the surface to create oceanographic boundaries across which abrupt changes in temperature occur. The layers and boundaries make up the ocean climate where life exists.



As the ship sailed south, biologists collected small planktonic organisms used as food by mid-water fish, traced the distribution of different species in the water masses, and at the same time made measurements of the production of particulate organic matter in the surface zone, on which the production of marine life is ultimately dependent. At the other end of the size scale, a physicist recorded sound transmissions from whales to study the possibility that large animals in the ocean may use the sound reflected from plankton to

locate their food. Collections were made of the mid-water fish, which seem to form layers over all the oceans, and an estimate of their abundance was made by acoustic physicists, who have recently developed improved acoustic techniques with which to map the layers and measure the size and concentration of the fish in them. Other biologists used the ship as a floating laboratory to conduct feeding experiments with plankton and to study the process of photosynthesis.



The latter experiment caused some amusement shipboard – and a healthy suntan – as the experimental work had to be done during four hours at noon, in the tropics, from one of the *Hudson*'s lifeboats tethered to the ship by several hundred yards of line. The biologists' program was complemented by chemists who determined the nutrient concentration in the water masses and studied the role of particulate organic carbon in the biological cycle. This comprehensive program was tied together by a group of physical oceanographers studying the small-scale structure of the water masses and at the same time providing the chemists and biologists with a description of the physical environment.

Following the work in the South Atlantic most of the scientific party left the ship at Buenos Aires, and she was joined by additional physical oceanographers and a new biological team. The new party took the ship south to the Drake Passage between Cape Horn and Antarctica. On the way one of the ship's launches was left at a Chilean naval base on Isla Nawarino, just north of Cape Horn, with a party of biologists



who spent three weeks collecting around the shores of the southern islands of Tierra del Fuego. The *Hudson* proceeded south to set four buoys carrying current meters between Cape Horn and Anvers Island, to measure the ocean currents carrying water from the Pacific to the Atlantic through the Drake Passage (see 'A Canadian finger on the ocean's pulse,' SF 15, June 1970). The physicists had spent two years prior to the voyage designing the buoy system specifically for this measurement and it was with some jubilation that all the meters and their records were recovered, as mooring a buoy in water two miles deep is a hazardous business with the possibility of total loss of the equipment. While the current meters were in position, the South Shetland Islands were visited to collect samples of mud in the bays as part of a biological study of the distribution of deep sea fauna and their possible emergence in the shallow polar regions. The concentrations of trace elements in the deep adjacent waters were determined as part of a program to assess their concentration throughout world oceans.

From Drake Passage the *Hudson* moved into the Chilean fjord system that extends over 1000 miles north along the coast. The current systems, chemistry and biological life in fjords depend markedly on runoff from the surrounding country, the presence of glaciers, and temperatures and salinities of the ocean at their mouth. The Chilean system is largely unexplored, and has physical surroundings different from west coast Canadian fjords, so the Canadian party onboard, with six Chilean scientists who joined the ship, garnered a

590

great deal of new information. Passage through the fjords proved to be the most difficult part of the voyage for the *Hudson* because of strong currents and winds blowing down from the surrounding mountains, which could rise to 50 knots in minutes and threaten to set the ship ashore in the narrow waterways.

The *Hudson*'s next task was to steam the length of the Pacific from Antarctica to Alaska. The 150 W meridian of longitude was chosen for the transect to allow a south-to-north gravity profile as free as possible of local changes due to topographic features such as island arcs. The gravity measurements are to be used to estimate the shape of the geoid (sea level) in the Pacific for comparison with estimates by satellite. The motivation for this work stems from the possibility of measuring changes in mean sea level by microwave altimeters mounted on satellites and using the information to monitor changes in ocean currents. Many of the biologists and chemists from the Atlantic rejoined the ship to continue their work in the Pacific and to obtain comparative measurements in both oceans.

Vancouver was reached six months after the ship left Halifax. Here the laboratories were stripped and refurbished with gear for the geophysical and geological program that was to be the major work as the ship rounded Canada. Four weeks were spent working between Vancouver Island and the Queen Charlottes with CNAV *Endeavour*. Gravity, magnetics, seismic profiling and heat flow measurements were made over the continental shelf and slope to study continental drift and the resulting geological formations on the west side of a continent.

From Vancouver the *Hudson* headed north through the Bering Strait to the Beaufort Sea to explore the geology of the western Arctic in a multi-ship operation with CSS *Baffin*, CSS *Richardson*, and CSS *Parizeau*, from the Energy, Mines and Resources fleet. The emphasis in the *Hudson*'s program was on the collection of sediment samples, gravity and magnetic data, reflection profiles, and oblique echo sounder profiles to show ice scouring, all directed at studies of the structure and recent geology of the sediments and crust. The southern Beaufort Sea was of particular interest to the geologists since it appears to be a submerging coastline whereas the coastline in the north and east Arctic is emerging. An environmental program was carried on along with the geological one and an extensive sampling of foraminifera (a widely-dispersed group of marine protozoa) in the ocean water was obtained in the western Arctic and later through to Baffin Bay. Part of this unique collection will be retained by the National Museum to form a basis for the description of species living in Canadian waters, and part used to collate the species distribution with the ocean environment in which they live. Comparison with the distributions of foraminifera preserved in sediment then gives a picture of the oceans as they existed in the past

If the west-to-east passage through the Arctic was not the most difficult, it was the most exciting. The ship left the Beaufort Sea late in the season when the ice was closing into the coast, passed through the Prince of Wales Strait, and then through the heavy ice in Viscount Melville Sound in convoy with the *Baffin* and the DOT icebreaker *John A. Macdonald*. Resolute was reached on September 29. The transit of the Northwest Passage assured completion of the circumnavigation, the first time it has been accomplished by any ship.

A brief geophysical survey in Baffin Bay completed the scientific work. Here the United States Coast Guard Cutter *Edisto* with a party from Bedford aboard joined the *Hudson* to run a seismic refraction profile to determine whether the crust beneath the Bay was oceanic or continental in character. With this last experiment completed, the *Hudson* turned south to steam home and arrive in Halifax on 16 October 1970, eleven months after setting out on her historic voyage.

Looking back, the expedition was far more successful than might reasonably have been expected at the outset. This was due to good fortune with the weather (only three days were lost through storms), to the efforts of the 122 scientific staff who at one time or other sailed on the ship during her passage through four oceans, and, not the least, to the efforts of a dedicated crew. The expedition provided an opportunity for marine scientists across Canada to join together in a common venture and extend their investigations to relatively inaccessible areas of the oceans at a time when assessment of the marine environment on a global scale is becoming of increasing importance.

The institutions represented were the Atlantic Oceanographic Laboratory (EMR), Marine Ecology Laboratory (FRB), Geological Survey of Canada (EMR), Defense Research Establishment Atlantic (DRB), National Research Council, National Museum of Natural Sciences, Royal Ontario Museum, Canadian Wildlife Service, Dalhousie University, The University of British Columbia, and McGill, Queen's and Trent Universities. And from the United States, Woods Hole Oceanographic Institution, Scripps Institute of Oceanography, and the University of Washington. At several places scientists from the United Kingdom, Brazil, Argentina and Chile joined the ship to work with their Canadian counterparts on investigations of common interest, giving the expedition an international content. The impact of the wealth of material collected is impossible to assess as several years of processing and interpretation lie ahead, but there is little doubt that Hudson-70 will rank with the major expeditions of the past 50 years, and that it has resulted in a significant contribution to the exploration of the oceans and the floors beneath.

Deep-Sea Research, 1973, Vol. 20, pp. 791 to 801. Pergamon Press. Printed in Great Britain.

The meridional distribution of silicate in the western Atlantic Ocean

C. R. MANN,* A. R. COOTE* and D. M. GARNER†

(*Received* 12 *September* 1972; *in revised form* 14 *April* 1973; *accepted* 20 *April* 1973)

Abstract—Meridional sections of silicate, salinity, and potential temperature have been constructed that run through the western basins of the Atlantic Ocean. A comparison of these distributions shows that extrema (maxima or minima) in vertical plots of silicate versus depth can be traced back to sources of water masses that are rich or poor in silicate. The dominant features are a silicate maximum at intermediate depths (~1000 metres) that is associated with the northerly movement of Antarctic Intermediate Water; and an increase in silicate towards the bottom, in the deepest water, which is associated with the northerly movement of Antarctic Bottom Water. Both these waters are rich in silicate. In the northernmost basins (the Labrador and Newfoundland basins) a decrease in silicate towards the bottom is caused by the overflow of Norwegian Sea Water, of low silicate content, through the Denmark Strait.

INTRODUCTION

IN THIS paper we present meridional sections of silicate, potential temperature, and salinity for the Western Atlantic. The sections have been constructed from data obtained at the stations shown in Fig. 1. The data to the east of Greenland are from C.S.S. *Hudson* cruise BI 0267, in 1967, and the data to the southeast of Newfoundland from C.S.S. *Baffin* cruises, B-4 in 1964, and BI 0566 in 1966.‡ The data between 0° and 20°N are from *Atlantis II* in 1964 (METCALF, 1969). Silicate was determined on board ship by the method of GRASSHOFF (1964) on these four cruises. The data in the South Atlantic were obtained on C.S.S. *Hudson* during the *Hudson* 70 expedition using an Auto-Analyser. The technique used in this case has been described by COOTE, DUEDALL and HILTZ (1970).

There are gaps in the data in the North American Basin and in the Newfoundland Basin which we could have filled with data from a variety of ships. However, a section we constructed, using all available data, was so patchy in appearance that we were uncertain as to whether the patchiness was real or due to differences in measurement techniques. As a result, we have restricted the data to the above set, which we believe to be internally consistent.

The sections have been examined to determine whether extrema (maxima or minima) in vertical profiles of silicate can be traced to sources of water masses, along with associated features in temperature and salinity. This should be possible if advection is the dominant process determining the silicate distribution, and not biochemical processes. Silicate can then be used to trace the movement of water masses,

*Atlantic Oceanographic Laboratory, Bedford Institute of Oceanography, Dartmouth, Nova Scotia, Canada.
†Present address: Dept. of Physics, University of Auckland, Auckland, New Zealand.
‡Available from the Canadian Oceanographic Data Centre.

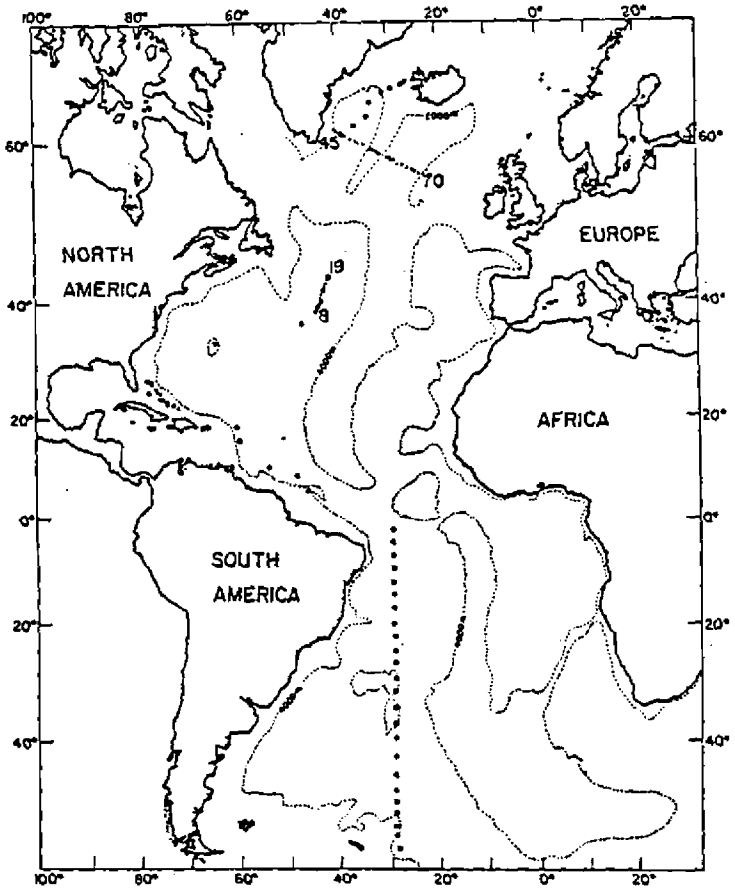


Fig. 1. Positions of stations used in this report. The large dots are the positions of the stations used in the meridional sections. The small dots, Stas. 8–19, and 45–70, refer to sections across the Southeast Newfoundland Ridge and the Reykjanes Ridge.

as has been suggested by several authors (COOPER, 1952; RICHARDS, 1958; METCALF, 1969; EDMOND and ANDERSON, 1971; STEFÁNSSON and ATKINSON, 1971).

BOTTOM WATER

The first feature of interest in the section of silicates (Fig. 2) is the maximum at the bottom, which extends from the Antarctic to 40°N, the northernmost part of the North Atlantic Basin. The pattern of the isopleths of silicate below 3000 meters is very similar to the pattern of the isotherms and isohalines (Figs. 3 and 4). Another way of examining this correspondence is to plot vertical profiles. These show (Figs. 5, 6 and 7) that the rapid increase in silicate towards the bottom, corresponds closely to the decreases in temperature and salinity that mark the transition from the deep water of the North Atlantic moving south, to the Antarctic Bottom Water moving north. In other words, the silicate maximum at the bottom is associated with a minimum in potential temperature and salinity, which identify the Antarctic Bottom Water.

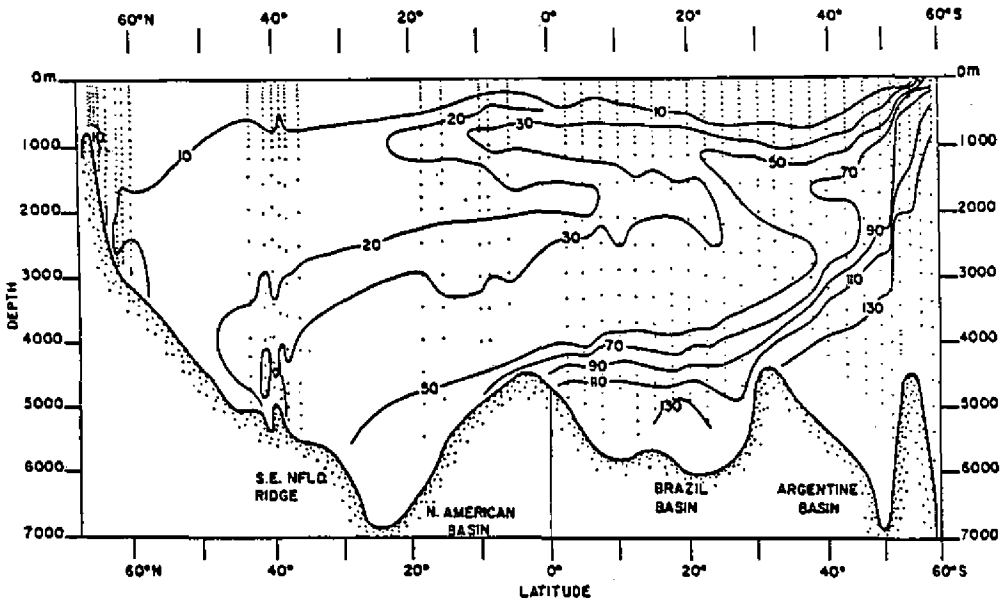


Fig. 2. Meridional distribution of silicate in the Western Atlantic.

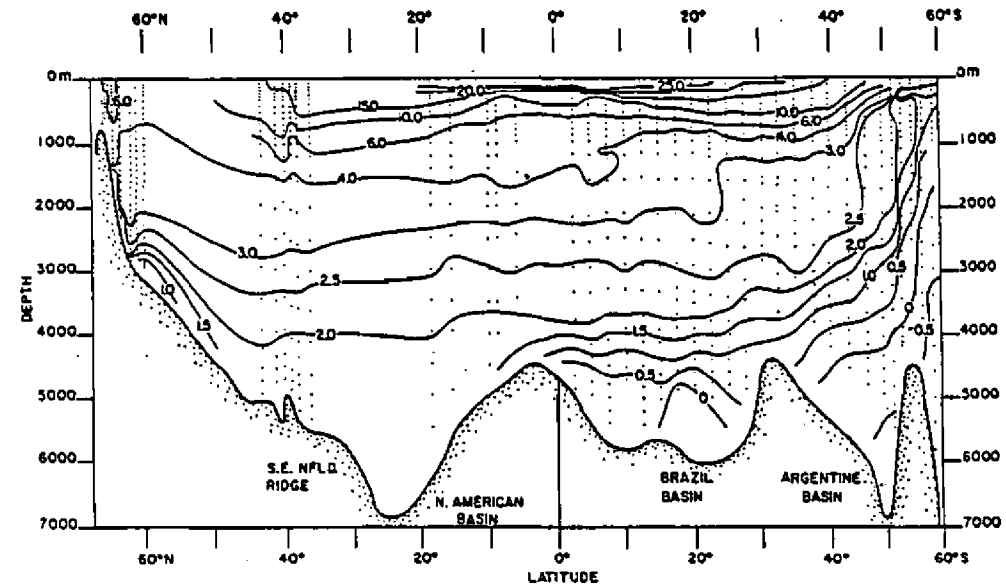


Fig. 3. Meridional distribution of potential temperature in the Western Atlantic.

The three features can be traced back to the southern Argentine Basin, where the Antarctic Bottom Water enters the Atlantic's western basins.

The bottom water first enters the Argentine Basin where the coldest water has a potential temperature of −0·5°C and a silicate content that may rise above 140 μg atoms/l. The water then flows north to enter the Brazil Basin, but its northerly passage is blocked by the Rio Grande Rise, at 30°S, with a sill depth of approximately

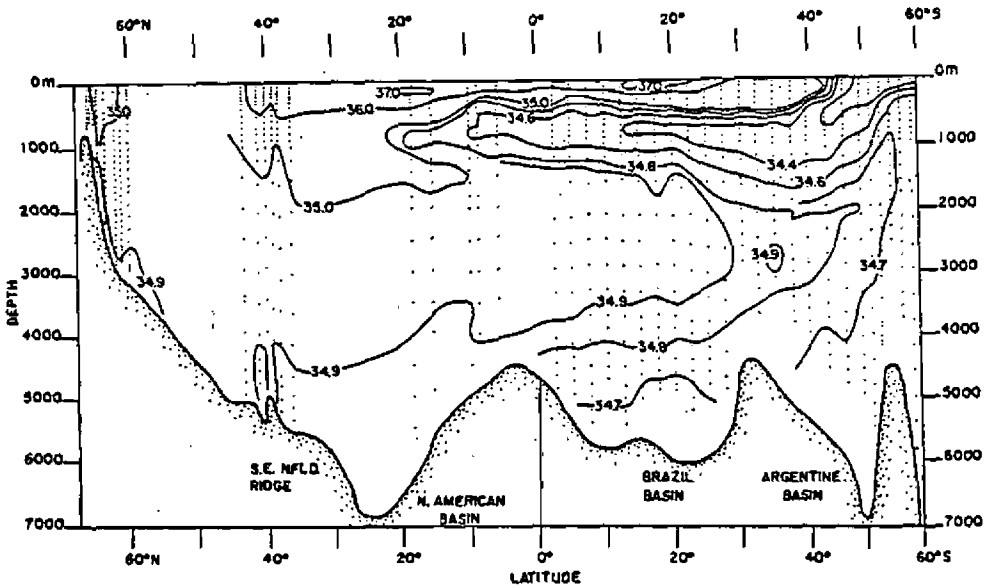


Fig. 4. Meridional distribution of salinity in the Western Atlantic.

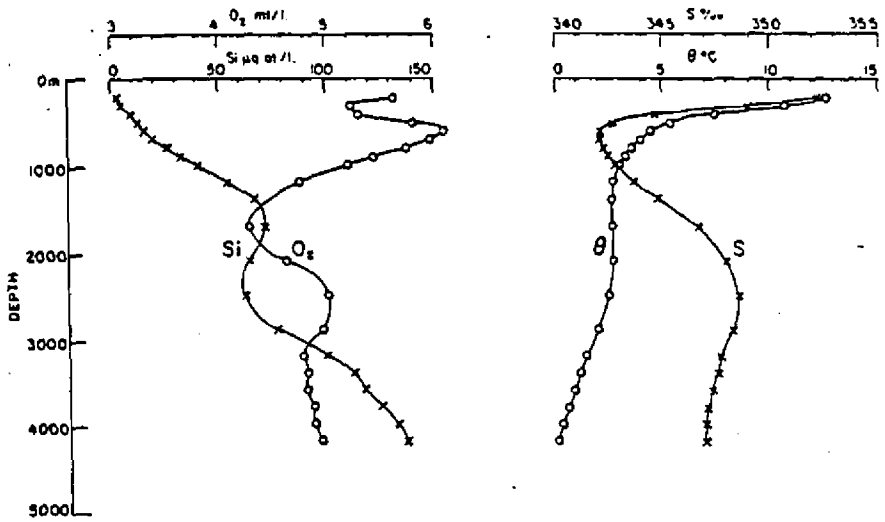


Fig. 5. Vertical profiles of dissolved silicate, oxygen, salinity, and potential temperature at 29°53'W, 39°55'S.

4400 meters. As a result, the bottom of the Brazil Basin is flooded with water of higher potential temperature ($\theta \sim 0°C$) and lower silicate content (~ 130 μg atoms/l.) than the Argentine Basin. The northerly flow of bottom water is again impeded at the Equator, where the sill depth between the Brazil Basin and the North American Basin is 4500 meters. Water with a potential temperature near 1°C, and silicate near 80 μg atoms/l. can flow over the sill into the North American Basin (METCALF and STALCUP, 1969) but does not penetrate very far north, according to Worthington and

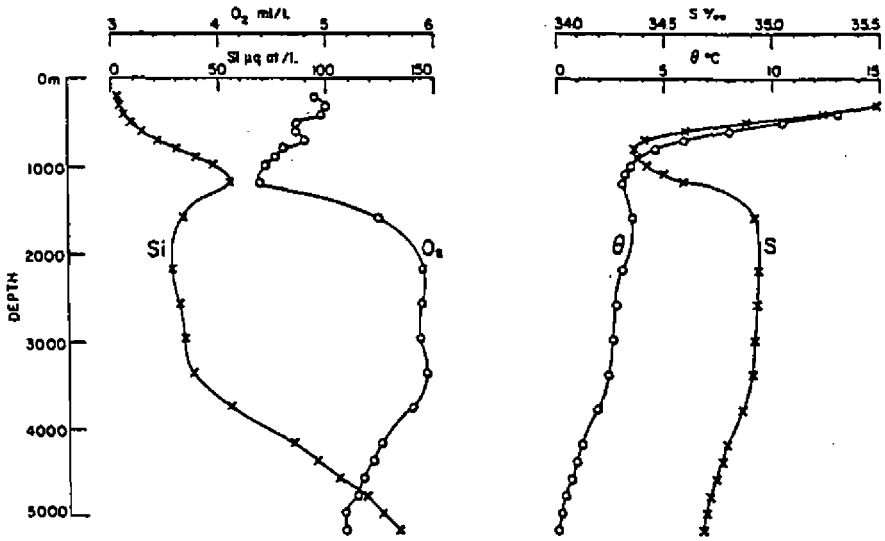


Fig. 6. Vertical profiles of dissolved silicate, oxygen, salinity, and potential temperature at 29°58′W, 22°30′S.

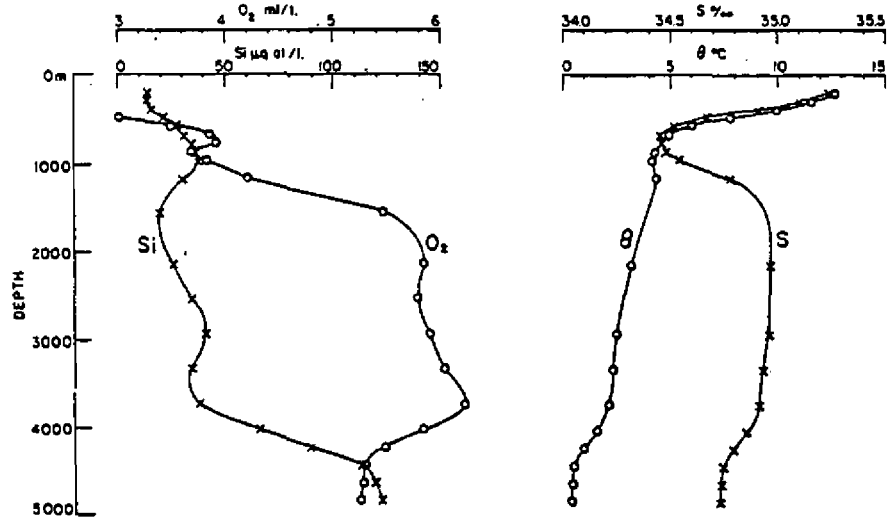


Fig. 7. Vertical profiles of dissolved silicate, oxygen, salinity, and potential temperature at 30°43′W, 2°29′S.

Wright's charts of salinity on potential temperature surfaces (WORTHINGTON and WRIGHT, 1970). These charts show that the temperature of the bottom water in the North American basin increases from south to north, and that the major part of the basin is covered with bottom water with a potential temperature of 1·7–1·8°C. If this water has come from the Argentine Basin, it should have a silicate content of about 50 µg atoms/l. In the northern part of the basin silicate in the bottom water is somewhat lower, 25–40 µg atoms/l. The lower values could be due to mixing with bottom

water from the north that is low in silicate. METCALF's (1969) chart of silicate on the 2°C potential temperature surface in the North Atlantic suggests this.

In the Newfoundland and Labrador basins, north of 40°N, silicate concentrations decrease toward the bottom. Near the Denmark Strait, the decrease is clearly caused by the overflow of Norwegian Sea Water, which floods the bottom of the Labrador Basin (LEE and ELLETT, 1967) with water of very low silicate content. In the Denmark Strait, the overflow has a silicate content of 7–8 μg atoms/l. (STEFÁNSSON, 1968). It flows south along the foot of the East Greenland Continental Slope as bottom water, with a salinity of less than 34·9‰ and silicate less than 9 μg atoms/l. The overflow can be traced in a series of sections run by *Hudson* in 1967. One of these, Stas. 45–70 in Fig. 1, is shown in Fig. 8. In this section, the water from the Denmark Strait overflow is found at the bottom, between Stas. 45 and 51. Further south, in the vicinity of the Southeast Newfoundland Ridge, the overflow water is only barely distinguishable in *T*/*S* diagrams but still appears to exert an influence on the silicate distribution at the bottom. We have run several sections across the Ridge (Fig. 9 is an example) and have found considerable spatial variations in the silicate in the bottom water. These variations are, apparently, caused by water from the North American Basin moving

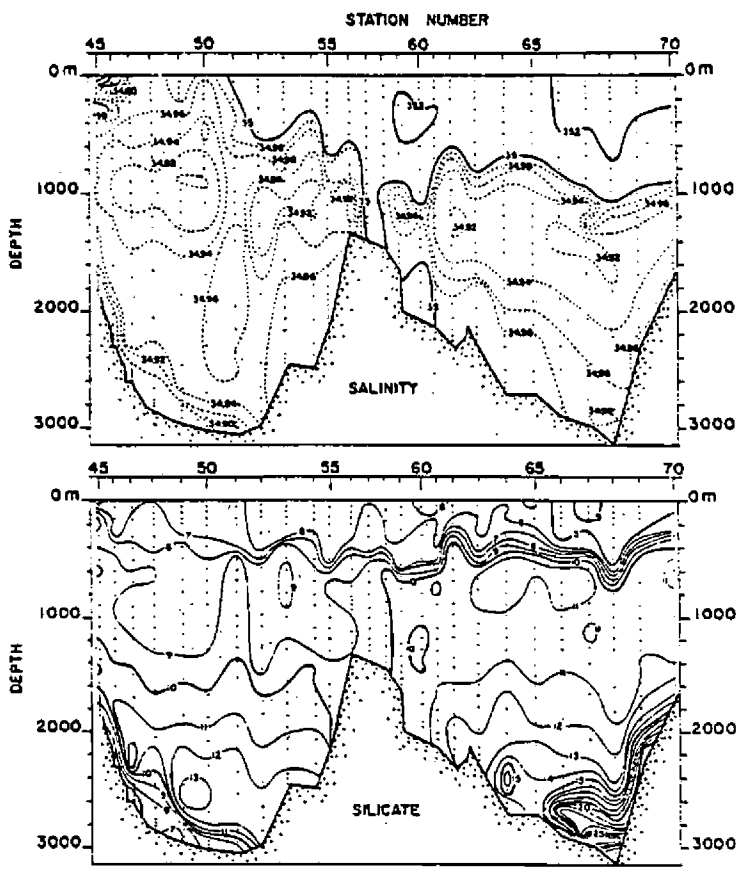


Fig. 8. Section of salinity and silicate running east from Greenland across the Labrador Basin, the Reykjanes Ridge, and the north part of the West European Basin.

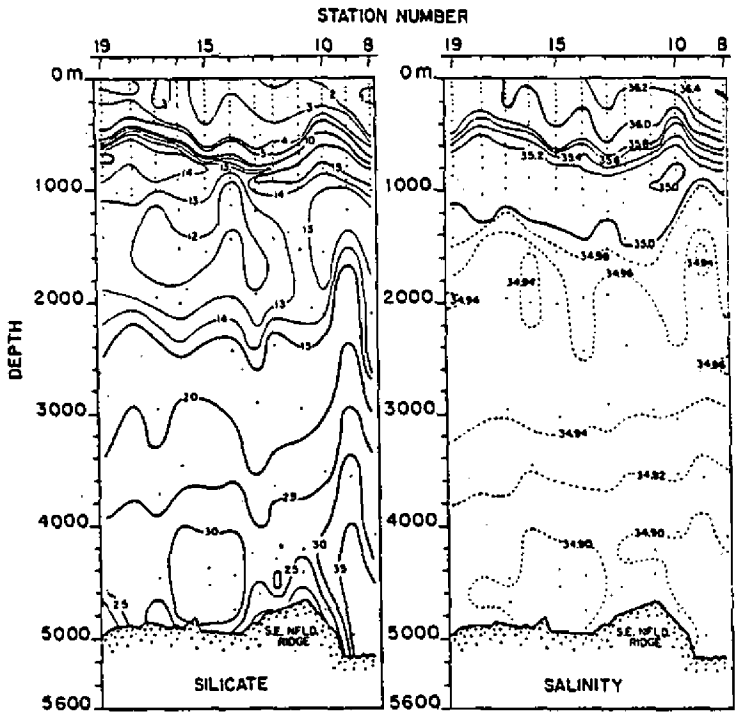


Fig. 9. Section of salinity and silicate across the Southeast Newfoundland Ridge.

north across the Southeast Newfoundland Ridge and intermingling with the deep and bottom water from the north. Just south of the ridge, the near-bottom water of the North American Basin has a salinity below 34·9‰ and a silicate content above 30 μg atoms/l. Our interpretation of Fig. 9 is that this water has moved north across the ridge to override the remnants of the Denmark Strait overflow, whose silicate content and salinity have risen to about 18 μg atoms/l. and above 34·9‰, respectively, by vertical mixing (WORTHINGTON and WRIGHT, 1970, plates 3–15).

Before leaving the examination of silicate in the bottom waters, there are two features in Fig. 8 that are noteworthy. Firstly, the overflow between Iceland and Scotland passes through this section flowing along the east side of the Reykjanes Ridge at a depth of 2000 meters. It can be identified by the core of salinity greater than 35‰. There is not, however, any silicate feature associated with this salinity core. Secondly, a core of silicate greater than 25 μg atoms/l. lies at the bottom of the West European Basin at a depth of 2900 meters. The oxygen content and salinity of the water in this core are slightly lower than in the surrounding water, which indicates that this feature results from the spreading of Antarctic Bottom Water through the eastern basins. We have constructed a section through these basins which supports this explanation. However, most of the data for the eastern basins in the South Atlantic are from a *Discovery II* section run in 1933 (CLOWES, 1938) in which the silicate data is 30–40 μg atoms/l. lower than more recent measurements made in the same area.

DEEP WATER

The deep waters of the North Atlantic flow south at depths between 1500 and 4000 meters and give rise to a tongue of high salinity water that extends to 50°S where it rises nearly to the surface (Fig. 4). The southerly flow results in a broad maximum in profiles of salinity versus depth. A broad silicate minimum coincides with the salinity maximum (Figs. 5, 6 and 7), and the silicate distribution (Fig. 2) has a southerly-directed tongue-like structure in the deep water, as does the salinity distribution. In the equatorial region, the maximum in salinity occurs at 1500 to 2000 meters depth, and identifies the upper deep water that originates as the Mediterranean outflow. The minimum values of silicate are found at the same depth, and result in the tongue of water with silicate less than 30 μg atoms/l. extending from 20°N to 20°S latitude. The silicate minimum is evidently created because the North Atlantic Deep Water has a much lower silicate content than the Antarctic Intermediate Water that lies above it, or the Antarctic Bottom Water that lies below it. The North Atlantic Deep Water is composed of waters from the Norwegian Sea, the Labrador Sea, and the Mediterranean Sea, all of which have a low silicate content. Water from the Norwegian Sea enters the Atlantic as overflows that have a silicate content less than 10 μg atoms/l., as previously described. Water from the Labrador Sea has a silicate content of about 10 μg atoms/l., (MCGILL and CORWIN, 1965), as does water from the Mediterranean Sea (SCHINK, 1967). Antarctic Intermediate Water and Antarctic Bottom Water have much higher silicate concentrations, 70 μg atoms/l. and 140 μg atoms/l., respectively, where these water masses move into the western basins of the Atlantic from the south (Fig. 2).

Profiles of silicate versus depth near the Equator exhibit a weak, secondary, silicate maximum between 2500 and 3000 meters depth and a weak, coincident, oxygen minimum, Figs. 6 and 7. The feature has been observed by EDMOND and ANDERSON (1971),* who considered that this secondary maximum in the deep water might be induced by the low silicate content of the Denmark Strait overflow, which forms the lower part of the North Atlantic Deep Water. If the feature is induced by the Denmark Strait overflow, then it should become more pronounced in the stations to the north, but it does not appear at all in a section from Cape Lookout to Bermuda reported by STEFÁNSSON and ATKINSON (1971).

An examination of the charts of salinity on potential temperature surfaces published by WORTHINGTON and WRIGHT (1970) suggests another reason for this silicate maximum. The maximum occurs at a potential temperature between 2·4°C and 2·6°C, and at a depth between 2500 and 3000 meters, just above the crest of the Mid-Atlantic Ridge in southern equatorial regions. Worthington and Wright's charts suggest that there could be a westerly advection of water across the crest of the Mid-Atlantic Ridge in Equatorial regions, and that the properties of water on 2·4°C to 2·6°C surfaces are more influenced by this flow than surfaces above or below. During the CIRCE Expedition in 1968, water with a potential temperature of 2·4°C in the eastern basin, at 7°47'S, 6°09'W (R.V. *Argo* Sta. 223), was found to have a silicate content of 42 μg atoms/l., and an oxygen content of 5·5 ml/l. These are similar θ/Si and θ/O_2 values

*We note here that the silicate values reported by EDMOND and ANDERSON are from the CIRCE Expedition, in 1968. These are in error, and should be multiplied by a factor of 2 (COOTE, MANN, WALTON and EDMOND, 1973).

for this potential temperature to those found by the *Hudson* 70 Expedition in the western basin at similar latitudes (Fig. 7), and lend some weight to the alternative explanation for the secondary silicate maximum; that the weak maximum in the deep waters is caused by westerly advection or lateral mixing The decrease in silicate above the maximum can be ascribed to the influence of the Mediterranean outflow. Whichever explanation is correct, tracing of this feature will obviously provide some insight into the movement of water between 2500 and 3000 meters in the Equatorial Atlantic.

INTERMEDIATE WATER

At intermediate depths of 1000 to 1500 meters the major feature in the silicate distribution is the tongue of high silicate that stretches north from 50°S, the Antarctic Convergence, to 20°N. The silicate tongue lies below the tongue of low salinity that identifies the Antarctic Intermediate Water. A similar tongue of high silicate in the eastern South Atlantic has been reported by CLOWES (1938). The maximum concentration of silicate, in vertical profiles through the tongue, occurs at the same depth as a weak minimum in potential temperature and an oxygen minimum (Figs. 5–7). All three extrema trace back to the Antarctic Convergence, where they rise towards the surface (Fig. 10). Through most of the South Atlantic, the depth of these maxima and minima coincides with the depth of the 27·6 potential density surface.

These features suggest that advection is the dominant process that creates this intermediate silicate maximum. Advection of cold water from the area of the convergence is the only way the temperature minimum can be created, and this advection

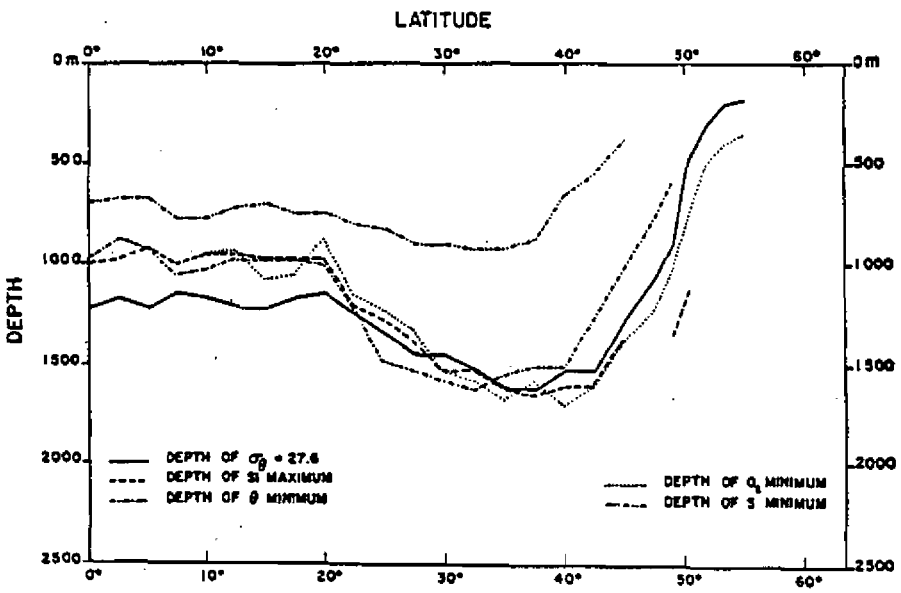


Fig. 10. Depth of the intermediate silicate maximum, the oxygen minimum, the potential temperature minimum, the salinity minimum, and the 27·6 potential density surface, in the South Atlantic.

must also result in a transport of silicate-rich water from the convergence. The coincidence of the temperature minimum and silicate maximum with the 27·6 potential density surface is also a feature that is to be expected if the water sinks and flows north into the South Atlantic, since the northerly moving water will tend to flow along surfaces of constant potential density. As GRILL (1970) has pointed out, intermediate maxima can be created by a balance between vertical mixing, vertical advection, and solution or synthesis of biogenous silica. But there does not seem to be any reason why a maximum, generated by purely vertical processes, should occur along the same potential density surface, but at different depths, in the South Atlantic.

In equatorial regions, north of 20°S, the silicate maximum and temperature minimum no longer coincide with the 27·6 potential density surface, but appear higher in the water column at a potential density of about 27·4. The reason for this could be erosion of the extrema from below by the low silicate and higher temperature water of the Mediterranean outflow, which would move the extrema to a shallower depth. The change in depth occurs reasonably abruptly at 20°S. We have no explanation for this, except to note that there is also an abrupt change in the slope of the isopycnal surfaces at this latitude, which means that the meridional section crosses the northern part of the South Atlantic gyre.

There is some evidence that the intermediate silicate maximum could be traced into the Gulf Stream and as far north as the Newfoundland Banks. A silicate maximum of about 16 μg atoms/l. occurs in a section across the Gulf Stream from Cape Lookout to Bermuda reported by STEFÁNSSON and ATKINSON (1971). A similar maximum has been consistently observed in sections we have run across the Gulf Stream in the vicinity of the Newfoundland Banks. For example, the Gulf Stream in the section in Fig. 9 lies between Stas. 8 and 10, and a contrary running branch of the Gulf Stream between Stas. 10 and 12 (MANN, 1967). The maximum in silicate in both Stefánsson and Atkinson's section, and sections near the Banks, occurs at a potential density about 27·4. This is close to the potential density (27·43–27·45) at which the maximum occurs in the northern part of the South Atlantic, so there is some reason to believe that the maximum in the northern sections results from advection of Antarctic Intermediate Water into the Gulf Stream System.

CONCLUSION

In studying the silicate distribution in the western basins we have been able to trace the major maxima and minima back to sources of water masses which are identifiable by the wealth or poverty in their silicate content, as well as by their salinity or temperature characteristics. We also find that the small-scale features in the silicate distribution observed near the bottom over the Southeast Newfoundland Ridge are related to features in the salinity distribution. These features lead us to conclude that advection is the dominant process that determines the silicate distribution in the western basins, even at intermediate depths. This conclusion is consistent with the findings of MENZEL and RYTHER (1968) in the South Atlantic, based on a study of the organic carbon and the oxygen minimum.

It is evident that the silicate distribution is dominated by the northerly flow of Antarctic Bottom Water and Intermediate Water. As far north as the Newfoundland Basin, the silicate content of the near-bottom water seems to be determined by an

influx of water with an Antarctic component. The intermediate silicate maximum associated with the Gulf Stream system in the same general area may also trace back to the Antarctic through the influence of the Antarctic Intermediate Water.

REFERENCES

CLOWES A. J. (1938) Phosphate and silicate in the Southern Ocean. *Discovery Rep.*, **19**, 1–20.

COOPER L. H. N. (1952) Factors affecting the distribution of silicate in the North Atlantic Ocean and the formation of the North Atlantic Deep Water. *J. mar. biol. Ass. U.K.*, **30**(3), 511–526.

COOTE A. R., I. W. DUEDALL and R. S. HILTZ (1970) Automatic chemical analysis at sea. *Advances in Automated Analysis*, Thurman Associates Publishers, **2**, 347–352.

COOTE A. R., C. R. MANN, A. WALTON and J. M. EDMOND (1973) A correction to CIRCE silicate values for the South Atlantic; comparison with *Hudson*-70 silicates. *Deep-Sea Res.*, **20**, 579–581.

EDMOND J. M. and G. C. ANDERSON (1971) On the structure of the North Atlantic Deep Water. *Deep-Sea Res.*, **18**, 127–131.

GRASSHOFF K. (1964) On the determination of silica in sea water. *Deep-Sea Res.*, **11**, 597–604.

GRILL E. V. (1970) A mathematical model for the marine dissolved silicate cycle. *Deep-Sea Res.*, **17**, 245–266.

LEE A. J. and D. J. ELLETT (1967) On the water masses of the northwest Atlantic Ocean. *Deep-Sea Res.*, **14**, 183–190.

MANN C. R. (1967) The termination of the Gulf Stream and the beginning of the North Atlantic Current. *Deep-Sea Res.*, **14**, 337–339.

MCGILL D. A. and N. CORWIN (1965) The distribution of nutrients in the Labrador Sea, summer 1964. *U.S. Cst Guard oceanogr. Rep.*, **10**, 25–33.

MENZEL D. W. and J. H. RYTHER (1968) Organic carbon and the oxygen minimum in the South Atlantic Ocean. *Deep-Sea Res.*, **15**, 327–337.

METCALF W. G. (1969) Dissolved silicate in the deep North Atlantic. *Deep-Sea Res., Suppl.*, **16**, 139–145.

METCALF W. G. and M. C. STALCUP (1969) Current meter and hydrographic station data from *Crawford* cruise no. 165, in the tropical Atlantic Ocean, February–April 1968. Woods Hole Oceanographic Institution, Reference No. 69–72. (Unpublished manuscript.)

RICHARDS F. A. (1958) Dissolved silicate and related properties of some western North Atlantic and Caribbean Waters. *J. mar. Res.*, **17**, 449–465.

SCHINK D. R. (1967) Budget for dissolved silica in the Mediterranean Sea. *Geochim. cosmochim. Acta*, **31**, 987–999.

STEFÁNSSON U. (1968) Dissolved nutrients, oxygen, and water masses in the northern Irminger Sea. *Deep-Sea Res.*, **15**, 541–575.

STEFÁNSSON U. and L. P. ATKINSON (1971) Relationship of potential temperature and silicate in the deep waters between Cape Lookout, North Carolina and Bermuda. *J. mar. Res.*, **29**, 306–318.

WORTHINGTON L. V. and W. R. WRIGHT (1970) North Atlantic Ocean atlas of potential temperature and salinity in the deep water. *Atlas Ser. Woods Hole oceanogr. Instn*, **2**, 24 pp., 58 pls.

Vol. 84, No. 33, pp. 265–270 4 November 1971

PROCEEDINGS
OF THE
BIOLOGICAL SOCIETY OF WASHINGTON

THE POSTLARVA OF THE STOMATOPOD CRUSTACEAN *HETEROSQUILLA POLYDACTYLA* (VON MARTENS)

By Raymond B. Manning
Smithsonian Institution, Washington, D.C. 20560

The postlarva of stomatopod crustaceans, the single transitional stage between the free-swimming larvae and the benthic adults, is rare in collections in comparison with either larvae or adults. Consequently, postlarvae are very poorly known and their identification with adults has often proved difficult. Recent studies on young stomatopods, including work by Alikunhi (1967) on various species, Bigelow (1931) on *Pseudosquilla*, Manning (1962) on *Alima*, Manning (1969a) on *Pseudosquillopsis*, and Michel and Manning (in press) on *Chorisquilla* have demonstrated that postlarvae often exhibit enough adult characters to allow their identification with certainty. Although postlarvae have been identified for several species in different genera, these stages apparently are not known for members of the lysiosquillid genus *Heterosquilla* which now includes 12 species in two subgenera.

In 1970, E. L. Bousfield, National Museum of Natural Sciences, Ottawa, a participant in the Hudson 70 Oceanographical Expedition to Cape Horn, collected 10 specimens of a lysiosquillid at Navarino Island, Chile. These specimens proved to be the postlarvae of *Heterosquilla polydactyla* (Von Martens), the only lysiosquillid known to occur in that area (Manning, 1969). Adults of this species have been taken at several localities between Valparaiso, Chile, and Golfo Nuevo, Argentina; other authors recently reporting this species include Schmitt (1940) and Bahamonde (1957, 1968).

I thank E. L. Bousfield for allowing me to work with these

specimens and for depositing some of them in the collection of the Division of Crustacea, National Museum of Natural History, Smithsonian Institution, and W. Duane Hope for reviewing the manuscript. The illustrations were made by my wife Lilly. Studies on larval and postlarval stomatopods have been supported through the Research Awards Program of the Smithsonian Institution.

Heterosquilla (*Heterosquilla*) *polydactyla* (Von Martens)

Figure 1

Heterosquilla (*Heterosquilla*) *polydactyla*.—Holthuis, 1967, p. 11 [complete synonymy].—Manning, 1969, p. 45, figure 8 [older references].
Heterosquilla polydactyla.—Bahamonde, 1968, p. 112, figures 3, 4.

Material: 10 postlarvae, total length 19–21.5 mm; Banco de Las Tacas, eastern Navarino Island, Chile; 55°05′ S, 67°04.5′ W; fine sand beach; E. L. Bousfield, Station F12; 5 February 1970.

Description: Eye of moderate size, cornea trilobed (appearing bilobed in dorsal view, inner lobe bilobed dorsoventrally), outer lobe the largest; eyes not extending to end of antennular peduncle. Ocular scales erect, completely fused along midline. Antennular peduncle half or slightly less than half carapace length; dorsal processes of antennular somite visible lateral to rostral plate as small, triangular projections; antennular flagella about half again as long as stalk, dorsomesial branch comprising 25-28 articles, stouter, shorter ventrolateral branch comprising 8 articles. Antennal scale suboval, about half as long as carapace; antennal peduncle not extending beyond eye; antennal flagellum about 1.3 times as long as scale, comprising about 15 articles; antennal papillae not visible. Rostral plate triangular, longer than broad, apex acute but rounded, deflexed mesially; plate completely covering ocular scales and bases of eyes. Carapace smooth, unarmed; gastric grooves distinct; lateral plates strongly narrowing anteriorly. Raptorial claw slender, dactylus armed with 14–17 teeth; propodus subequal to carapace in length, outer edge of opposable margin completely pectinate, inner edge of opposable margin with 4 movable spines; carpus of claw with sharp, dorsal ridge terminating in slender tooth; merus more than half again as long as ischium; basal segment of claw with prominent, ventrally projecting spine. Mandibular palp and 5 epipods present. Thoracic somites smooth dorsally; lateral margins of sixth and seventh somites subtruncate; ventral surface of sixth, seventh and eighth somites with ventral projection laterally, mesial to base of each walking leg; seventh and eighth thoracic somites with median ventral spine, sharper on seventh somite. Posterior margin of basal segment of each walking leg with inner and outer spines, projecting ventrally, sharpest on anterior two legs. Abdomen smooth, depressed, anterior 5 somites unarmed; articulated anterolateral plates present; sixth somite with strong posterolateral spines, lacking ventral spine in front of

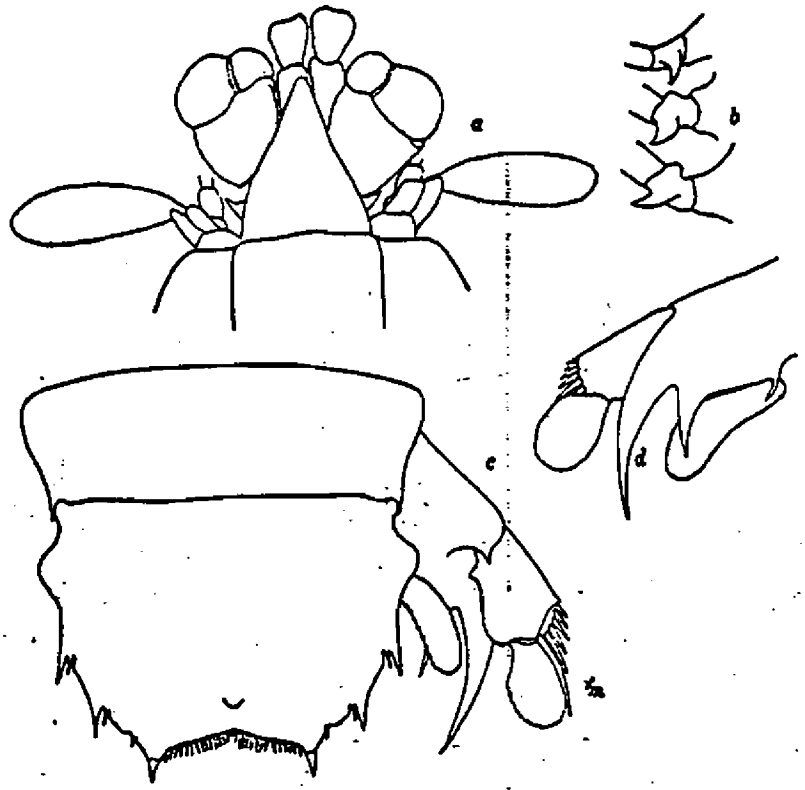


FIG. 1. Postlarva of *Heterosquilla polydactyla* (Von Martens): *a*, anterior portion of body; *b*, basal segments of walking legs; *c*, sixth abdominal somite, telson, and uropod; *d*, uropod, ventral view. (Setae omitted in all).

articulation of each uropod. Telson flattened, broader than long, with 3 pairs of marginal teeth, submedians with movable apices; lateral margins with broad, rounded lobe anteriorly; 14–15 slender submedian, 2 intermediate, and 1 lateral denticles present; dorsal surface of telson with low, inconspicuous longitudinal median boss, visible in some specimens, boss terminating in low, rounded median projection; submedian projections absent. Uropod flattened, basal segment with dorsal spine at articulation of exopod; proximal segment of exopod longer than distal, with 6–7 movable spines on outer margin, distalmost not extending to apex of distal segment; endopod slender, curved; basal prolongation of uropod consisting of 2 curved spines, outer larger, with smaller spine on inner margin at articulation of endopod. Color faded in most specimens, but one ornamented with scattered dark chromatophores on body, arranged in bands on thoracic and abdominal somites.

Measurements: Measurements, in mm, of selected specimens are as follows:

Total length	19.5	20	20	20.5	21
Carapace length	3.8	3.8	3.8	3.9	3.8
Cornea width	1.1	1.1	1.0	1.1	1.1
Rostral plate length	1.8	1.6	1.6	1.6	1.8
Rostral plate width	1.4	1.4	1.4	1.4	1.5
Fifth abdominal somite width	4.5	4.5	4.4	4.4	4.3
Telson length	3.1	3.1	3.0	3.0	2.9
Telson width	4.0	3.8	3.8	3.9	3.8
Teeth on claw	16	15	17	14	15
Uropod spines	7	6	7	6	7
Submedian denticles	14	14	15	15	14–15

Discussion: These specimens are readily identifiable as the postlarvae of *Heterosquilla polydactyla*: the long, triangular rostral plate and the large number of teeth on the dactylus of the claw are diagnostic for the species. Although identifiable with *H. polydactyla*, these specimens show several differences from the adults, a function of their immaturity. The eyes are of the postlarval type, trilobed rather than bilobed as in the adult; as pointed out by Manning (1969a), the secondary subdivision of one lobe of the eye is characteristic of the postlarvae of *Pseudosquillopsis*; it may help in recognizing postlarvae of *Heterosquilla* as well. The postlarvae lack the antennal papillae of adults; apparently they develop at some subsequent stage. Several features of the postlarva are absent or modified in the adult: the strong ventrally projecting ischial spine and the ventrally projecting thoracic spines found in the postlarvae are absent in the adult (the median ventral spine on the eighth thoracic somite of the postlarva is present as a low rounded keel in adults), and adults have but one rather than two basal spines on the walking legs. Lastly, the median and submedian bosses of the telson, well developed in adults, are represented by at most a low median boss terminating in a rounded posterior projection.

The characteristically banded color pattern of the adult is visible on one of the 10 specimens studied; presumably it first appears at this stage.

Usually it is possible to sex postlarvae, for the buds of the male copulatory tubes are visible at the bases of the last pair of walking legs. In these specimens the male copulatory tubes (if present) cannot be seen. The tubes may be obscured by the spines on the thoracic sterna and at the bases of the walking legs.

According to information supplied by E. L. Bousfield, the beach on which these specimens were collected had a very gentle slope; the substratum was fine to very fine dark sand of sedimentary rock and shell

origin. The collections were made at mid-water level at low tide. The animals were living in burrows in the sand, and those collected had left their burrows and had been trapped or blown away by drying winds. Associated organisms included small phoxocephalid and haustoriid amphipods and a large serolanid isopod. The surface temperature of the water was 9.5°C.

Distribution: Southern portion of South America, where it has been reported from scattered localities between Maullin Island (near Chiloe Island), Chile, to Chubut Province, Argentina.

Literature Cited

Alikunhi, K. H. 1967. An account of the post-larval development, moulting, and growth of the common stomatopods of the Madras coast, pp. 824–939, figures 1–194, plates 1–3. *In* Proceedings of the Symposium on Crustacea, Marine Biological Association of India, Part II: iv + 945 pp.

Bahamonde N., Nibaldo. 1957. Sobre la distribución geográfica de *Lysiosquilla polydactyla* Von Martens, 1881 (Crustacea, Stomatopoda). Invest. Zool. Chil. 3(5–7): 119–121, figures 1–3.

———. 1968. Bosquejo taxonomico sobre los estomatopodos de Chile (*Crustacea, Stomatopoda*). Rev. Univ., Univ. Cat. Chile, no. 31: 107–120, figures 1–8.

Bigelow, R. P. 1931. Stomatopoda of the southern and eastern Pacific Ocean and the Hawaiian Islands. Bull. Mus. Comp. Zool. Harvard, 72 (4): 105–191, figures 1–10, plates 1–2.

Holthuis, L. B. 1967. Fam. Lysiosquillidae et Bathysquillidae. Stomatopoda I. *In*: Gruner, H.-E., and L. B. Holthuis, eds., Crustaceorum Catalogus, ed. a, pars 1: 1–28.

Manning, Raymond B. 1962. *Alima hyalina* Leach, the pelagic larva of the stomatopod crustacean *Squilla alba* Bigelow. Bull. Mar. Sci. Gulf & Carib., 12 (3): 496–507, figures 1–4.

———. 1969. Stomatopod Crustacea of the western Atlantic. Stud. trop. Oceanogr., Miami, 8: vii + 380 pp, figures 1–91.

———. 1969a. The postlarvae and juvenile stages of two species of *Pseudosquillopsis* (Crustacea, Stomatopoda) from the eastern Pacific region. Proc. Biol. Soc. Washington, 82: 525–537, figures 1–4.

Michel, A., and Raymond B. Manning. In press. The pelagic larvae of *Chorisquilla tuberculata* (Borradaile, 1907) (Stomatopoda). Crustaceana.

Schmitt, Waldo L. 1940. The stomatopods of the west coast of America based on collections made by the Allan Hancock Expeditions, 1933–38. Allan Hancock Pacific Exped., 5 (4): 120–225, figures 1–33.

Sea Bottom Scouring in the Beaufort Sea of the Arctic Ocean

B. R. PELLETIER and
J. M. SHEARER,
Canada

ABSTRACT

Marine geological investigations undertaken during the summers of 1970 and 1971 in the Beaufort Sea with echo-sounding and side-scan sonar equipment have shown the sea bottom to be composed mainly of linear scratches of varying width, depth and length. Churning and scouring by ice islands and pressures ridges as they scrape the bottom are thought to be the origin of these features. In many areas, generally in depths of water between 10 and 30 m, the bottom is marked by systems of parallel scours. This is thought to be a result of one or more pressure ridges moving as a solid unit with the Arctic pack ice.

The frequency of occurrence of scouring along the ship's track is similar and at a maximum (15 to 20 scours/km) for all depth ranges between 10 and 50 m. Below 50 m the frequency of occurrence decreases, with no scours observed at depths >75m. The above data are difficult to reconcile with observations made from submarines of the actual depth distribution of pressure ridge keels. This disparity is thought to be due to the cumulative nature of scouring on the bottom. Depending upon the rate of sedimentation at any given point, deep scours (maximum observed relief about 10 m) which may be the result of scouring in earlier post-glacial times (lower sea level) may still possess some topographic expression. Unless these relict scours are recognized, anomalously high results would be obtained for the present amount of scouring at various depths.

INTRODUCTION

PHYSIOGRAPHIC IRREGULARITIES occurring on the sea-floor of the Alaskan and Beaufort shelves were described by Carsola (1954). These features were also observed during bathymetric investigations of the Beaufort Sea (Fig. 1) in 1970 by several vessels of the Marine Sciences Branch of the Canadian Department of Energy, Mines and Resources, namely the Canadian Scientific Ships *Richardson*, *Parizeau*, *Baffin* and *Hudson*. One type of these irregular features was tentatively ascribed to the action of scouring by ice. Concurrently with bathymetric surveying, the Atlantic Oceanographic Laboratory of the Bedford Institute in Dartmouth, Nova Scotia, and the Geological Survey of Canada, Ottawa, carried out side-scan sonar investigations in the Beaufort Sea from the CSS *Richardson* and the CSS *Hudson* which revealed the three-dimensional nature of these ice-formed scours (Figs. 2 to 4). A distance of about 1,000 kms was traversed using an Edgerton Germerhausen and Greer side-scan sonar unit, consisting of a towed fish (transducer frequency 100 KHz.) and a recorder. The survey covered the entire width of the continental shelf along 14 lines which extended in a

Authors' addresses are given at the back of this book.

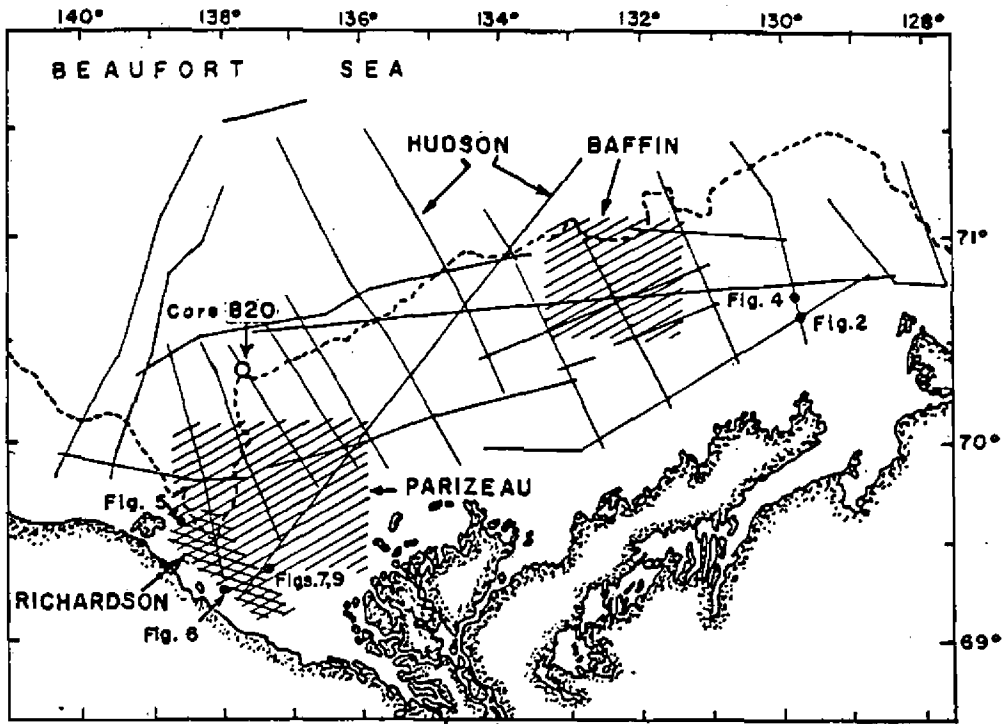


FIGURE 1 — General diagram of Beaufort Sea area. Hachured zones represent detailed work carried out in 1970 by the Canadian Scientific Ships *Baffin*, *Hudson*, *Parizeau* and *Richardson*. General location, where applicable, of subsequent Figures is shown. Solid lines indicate geophysical surveys carried out by CSS *Hudson*, and broken line indicates the 100-m isobath.

direction perpendicular to the shoreline. Additionally, several smaller transects of the inner shelf were carried out in the vicinity of Mackenzie Bay and the adjacent area to the east.

NATURE OF BOTTOM-SCOUR FEATURES

Bottom-scour features, or ice scours, occurring on the shelf of the Beaufort Sea range in relief up to 10 m. Their widths vary from a few metres to several tens of metres, and their lengths are as great as 8 km. Commonly they occur as single features, but families or groups of parallel scours are found that are thought to be due to the action of larger pressure ridges of ice which are characterized by many protruding keels along their length, and which have moved over the floor of the ocean as a single mass. Numerous occurrences of cross-cutting relationships are displayed on the records, indicating that several periods of ice-scouring have occurred (Fig. 2).

At present not enough survey coverage exists to establish the statistical occurrence of scours of a given relief for various depths of water. However, when considering scours of differing relief from the entire survey area it was found that the frequency of scours per kilometre of survey line was somewhat constant (at 15 to 20/km) to water depths around 50 m (Fig. 5). In deeper water, the frequency of occurrence of these features was considerably less. 75 m is the maximum depth at which scouring was recorded. Weeks *et al.* (1971), using ob-

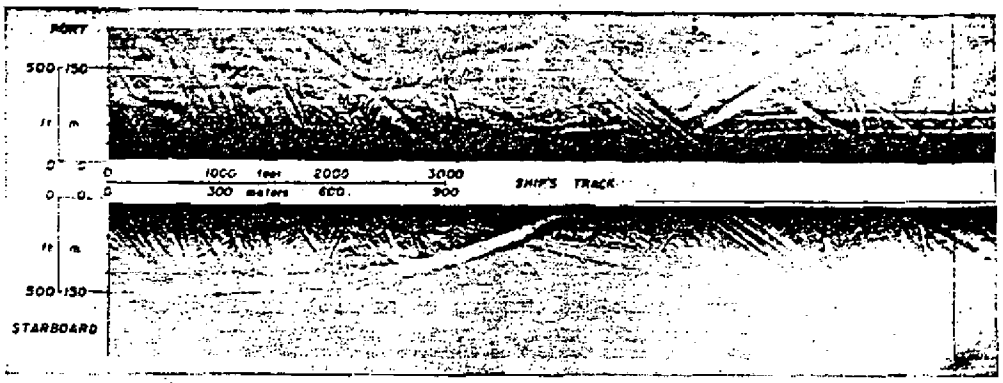


FIGURE 2 — Side-scan sonar photo reproduction of sea bottom. Resolution of scours to 1.5 m is possible. Bottom with respect to ice scouring is considered saturated. Notice on right side of Figure two scours of different generations which in turn have a different relationship with a third cross-cutting scour.

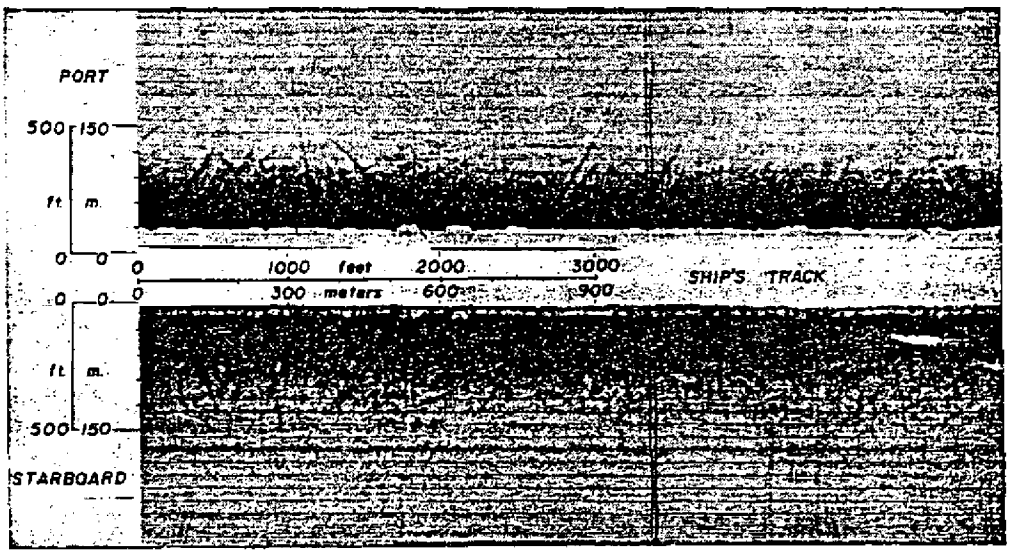


FIGURE 3 — Side-scan record of bottom in about 30 m of water. Bottom close to saturation. At around 600-m mark (2000 feet) two scours possessing around 10 m of relief can be noticed.

servations by means of submarines beneath the ice and from aircraft flying over the surface, have estimated that subsea ice thicknesses to 10 m are common, with a rapid decrease in frequency of occurrence for thicknesses of 20 to 30 m. The disparity between the observations by Weeks *et al.* (1971) and the data from the echo-sounder is considerable. One means of accounting for the apparent scouring at depths greater than 10 m involves preservation of the scours from one year to the next until a so-called "saturation" value is reached. This value is defined as the number of scours of a given width that can exist within a finite distance (in our case 15 to 20/km) such that when subsequent scouring occurs older scours are overrun. At shallow depths this saturation number is

probably obtained very quickly, whereas with increasing depths of water it will probably take considerably longer.

Two important factors in estimating this saturation value from echo-sounding and side-scan records are: (1) the orientation of the survey line with respect to the mean direction of the ice scour — an oblique traverse will give an apparently greater width for each scour and an apparently lower number of scours per unit of distance; and (2) the average slope of the sea bottom. For a given distribution of pressure-ridge keel thicknesses, the apparent frequency of occurrence of scours over a unit distance will be higher in areas of greater bottom slope, because more pieces will run aground in a shorter distance. Also, areas of steeper slopes are likely to have scours of greater relief (Martin McDonald, General Dynamics, personal communication) because the necessary frictional resistance to stop the advance of a given mass is obtained in a shorter distance than in an area of more gentle slope. Ramifications to this situation will arise when the substrate is not uniform.

VERTICAL AND HORIZONTAL DISTRIBUTION OF SCOURS

As indicated above, scouring on the present bottom is common to depths of 50 m. Of significance is the fact that buried scours were observed to have much the same frequency distribution as those on the surface (Figs. 6, 7). When the section is shallower than 50 m, scouring is prevalent throughout, but where the section is deeper than 50 m, the scouring is considerably less frequent with commonly occurring undissected horizontal beds. The similarity of the present frequency distribution to that observed in the sedimentary record has a number of important implications and three main independent variables must be investigated: rate of sea-level change, rate of sedimentation and rate of scouring.

(a) *Rate of sea-level change*: The post-glacial sea-level history of the Beaufort Sea area is unknown, but farther west, in the Chukchi Sea, Creager and McManus (1967) have evidence, from dating of cores, of lower sea levels in post-glacial Wisconsin times which seem to approximate the general world-wide lowering of sea level (Shepard and Curray, 1967; Milliman and Emery, 1968). Shearer (1971) reported evidence on the existence of buried shorelines that are thought to indicate lower sea levels, although no independent estimates of time exist. If we assume that sea levels in this area can be approximated by a general world-wide submergence curve, then relative rates of sea-level rise can be calculated. Based on these presumed rates of sea-level rise the total amount of time that any given point on the sea bottom lies between the sea level datum and the 50-m isobath for given increments of time in the past can be calculated. If it is assumed that little scouring takes place at depths down to 10 m (shore-fast ice zone and zone of reworking by-waves), thus it is in the depth interval from 10 to 50 m below any given datum where scouring to any significant degree will take place.

Table 1 is a tabulation of the time of transgression at given points below the present datum and the corresponding time during which significant scouring occurred at these various levels.

Table 1 shows that shallower depths (<50 m) have had more exposure to scouring effects. This is the result of the much faster rate of sea-level rise in earlier (post-glacial) times.

Another major implication of this sea-level curve is that a point now at 50 m depth was not even submerged until about 12,800 years ago, which provides at least a maximum age of any existing scours. As shown in Table 1, scouring at 50 m did not take place until further submergence of approximately 10 m, so that the maximum dates can be further reduced to around 11,800 years.

TABLE 1

Sea Level Datum	Approximate Time of Transgression (Shepard and Curray, 1967)	Bottom Depth (d)	Scouring of Bottom (d) when Datum at		Time available for scouring at point (d)
−100 m	17400 yrs. B.P.	−100 m	−90 to −50m	3700 yrs.	(16500-12800)
− 90	16500	− 90	−80 to −40	3800	(15600-11800)
− 80	15600	− 80	−70 to −30	4500	⋮
− 70	14900	− 70	−60 to −20	5000	⋮
− 60	13900	− 60	−50 to −10	5900	⋮
− 50	12800	− 50	−40 to 0	11800	⋮
− 40	11800	− 40	−30 to 0	10400	etc.
− 30	10400	− 30	−20 to 0	8900	⋮
− 20	8900	− 20	−10 to 0	6900	⋮
− 10	6900	− 10	little preserved		
0	0	0	scour		

Examination of the two remaining variables in the context of the deduced variation in rates of sea-level rise is necessary.

(b) *Rates of sedimentation*: During the classical Wisconsin maximum the Mackenzie Bay area of the Beaufort Sea is thought to have been filled with a large ice tongue (Shearer, 1972). In early post-glacial times large amounts of meltwater running into Mackenzie Bay are thought to have transported tremendous amounts of debris into the glacially scoured canyon (Fig. 8), forming a large outwash delta graded to a lower sea level (≅ minus 60 to 70 m) (Shearer, 1971, 1972). Subsequent to retreat of the glaciers, the amount of sediment brought into the Mackenzie Canyon must have diminished considerably, and a regime of deposition of recent clays ensued. These sediments are clearly visible in Figure 6, and possess a unique stratigraphy consisting of well-bedded sediments overlain by 10 to 12 m of highly scoured sediments. A radiocarbon date (GSC-1511) was obtained from Core 820 taken on the HUDSON 70 expedition (see Fig. 1). This core was taken in about 350 m of water on the northeast side of Mackenzie Canyon, and is thought to be representative of the post-outwash regime existing in the Mackenzie Bay — Beaufort Sea area. A date of 3530 yrs. ± 240 was obtained on shell material from about 4 m down the core, giving an approximate rate of sedimentation of 1 m/1000 years. In Figure 6, where the scoured section of the record is 10 to 12 m thick, an age for the base of the scoured unit (around 45 m depth) would be around 10,000 to 12,000 years. In this case, the estimated age of the initiation of frequent scouring coincides closely with the previously estimated level of longer time exposure to scouring processes as deduced from the rate of sea-level rise.

On examination of the *C.S.S. Parizeau's* echo-sounding records from the Beaufort Shelf east of the Mackenzie Canyon, it is apparent that a large variation in the thickness of the recent mud unit exists from one point to another. This fact implies that the rates of sedimentation vary a great deal within short distances, which in turn causes difficulty in choosing a reliable sedimentation rate in order to work out the age of individual scours. Where the recent mud cover is thin, the rate of sediment accumulation must be considerably less than 1 m/1000 years and in other areas, such as north of Pelly Island (Fig. 8) where over 30 m

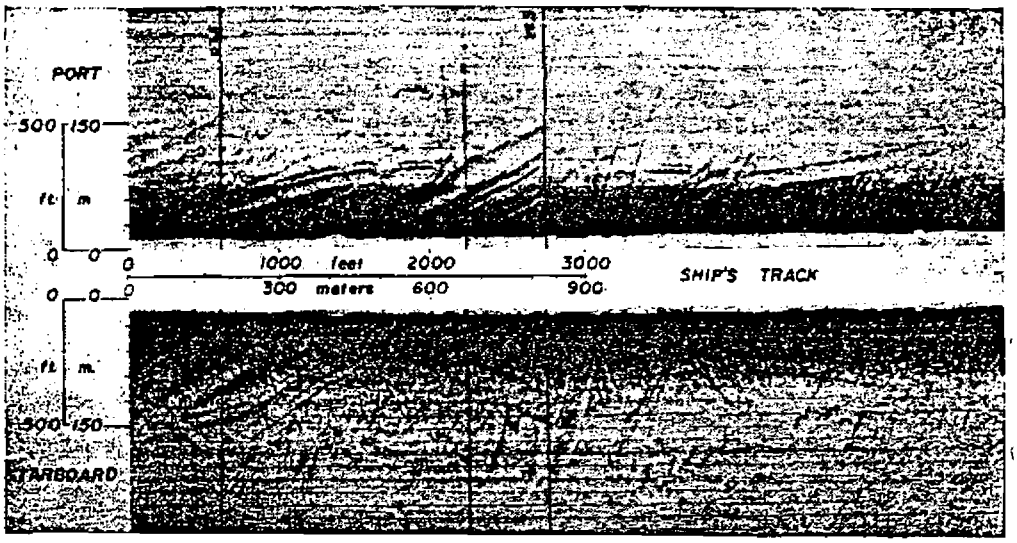


FIGURE 4 — Bottom scours from an area very close to Figure 3. Note scour running parallel to ship's track on port side of record. Faint cross talk of this scour is visible on starboard channel.

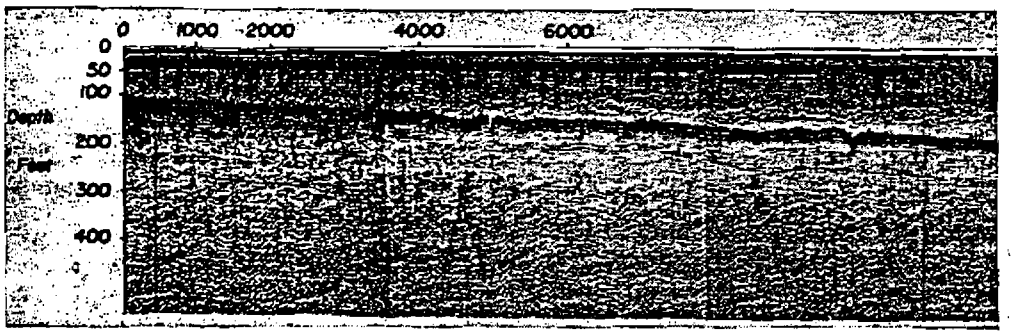


FIGURE 5 — Shallow seismic profile running from the west side of Mackenzie Bay eastward into the canyon. Note that frequency of bottom scouring diminishes considerably as one progresses into deeper water.

of scoured sediment exist, a much higher rate of around 3 m/1000 years must exist.

In the above discussion, it has been assumed that all sedimentary units were deposited in the marine environment. In some cases, where old river channels existed, it is possible to have had fluvial sediments deposited prior to transgression of the sea, thus giving apparently no evidence of scouring. This is not the main reason for the vertical discontinuity in scouring, because in most areas a lateral discontinuity between a bedded unit and a time-equivalent scoured sediment exists (Fig. 7).

(c) *Rate of Scouring*: There is no unanimity in answer to the questions of ice cover in the Arctic Ocean in Wisconsin and post-Wisconsin times. Ewing and

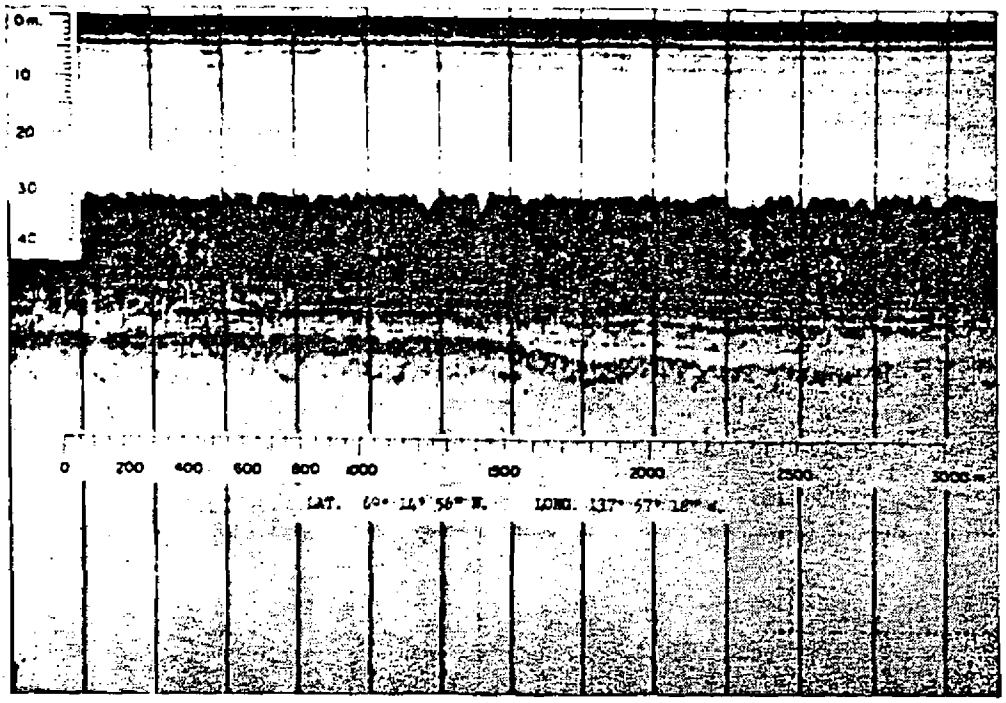


FIGURE 6 — Record showing internal structure of post-delta muds. Top 10 to 12 m of sediments possesses little or no bedding, presumably because of scouring factor. Base of scoured zone lies at around 45 m.

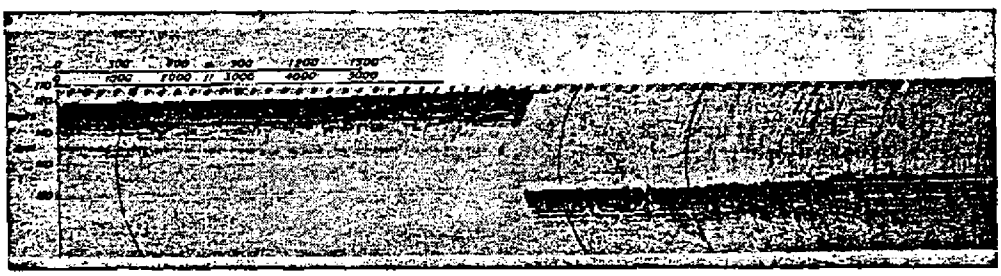


FIGURE 7 — Frequency of scouring not quite as high as seen in Figure 6. Right-hand side of record possesses little evidence of bedding, indicating high frequency of scouring. At point C scour is buried to point where surface expression is almost absent.

Donn (1956, 1958) propose the necessity of an ice-free ocean in pre-glacial times, providing a source area for the continental glaciers which followed. During glacial times and in early post-glacial times the Arctic seas were ice-covered. Olausson and Jonasson (1969) propose that the lack of a halocline in glacial times (very little surface run-off) favoured complete water mass mixing, the prevention of pack ice formation, and hence an ice-free Arctic Ocean. A time of 11,000 yrs. B.P. is given as that time when the transition from an ice-free to an ice-covered ocean took place. Clark (1971) proposed that the Arctic Ocean has been ice-covered since the Middle Pliocene and apparently finds no inconsistencies from data based on core studies.

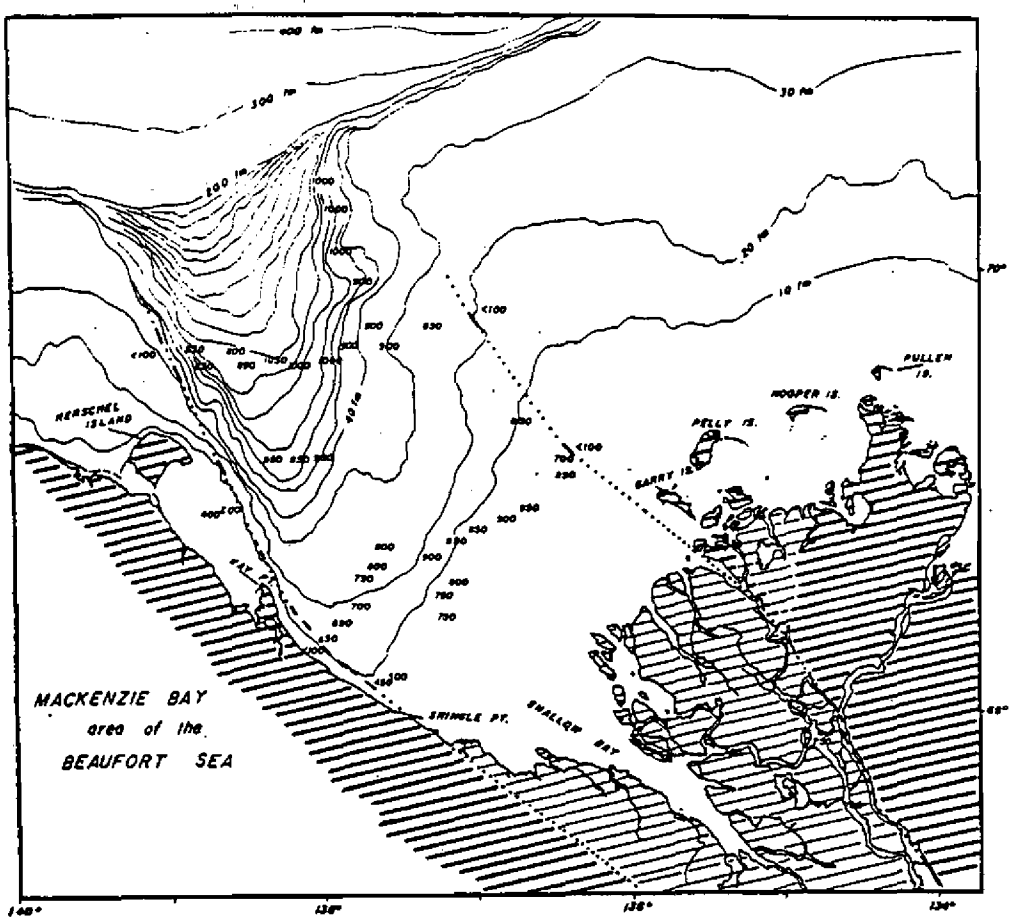


FIGURE 8 — Solid black lines and dots are the known and assumed edges, respectively, of the buried ice scour channel. Small figures are depths in metres to base of scour channel, with those figures outside channel representing thickness of sediment deposited in post-canyon scour times. Reproduced from Figure 1 of Shearer (1972).

The authors are not in a position to debate, at present, the merits of each of these papers. It cannot be ignored that a change in the frequency of scouring is thought to have occurred around 10,000 to 12,000 years ago. This of course coincides with the theory of ice cover presented by Olausson and Jonasson (1969). At this point it is not known whether the changes in rates of sea-level rise and sedimentation were enough to give the contrast observed in the sedimentary record (Fig. 6) or whether a change in ice cover providing many more floating pieces was also necessary.

ORIENTATION OF THE ICE SCOURS

To obtain a general orientation of the ice scours it is necessary to examine the side-scan records and measure the angle between the trend of the scour and the heading of the ship. However, the horizontal scale along the ship's course is not equal to the hori-

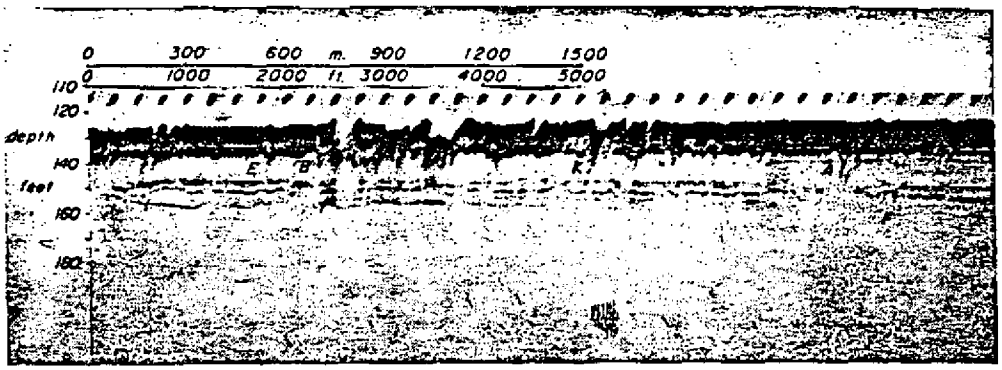


FIGURE 9 — Buried scoured layer visible, with recent scour of about 4 to 5 m (15 feet) cutting into older scour at point B. Points A, E and K are buried scours possessing modified relief on the surface.

zontal scale perpendicular to the course, which necessitates the computation of a correction factor in order to arrive at the correct azimuth for the scour features. A graph was drawn correlating the original scour angle θ with the corrected scour angles θ_1 based on the tan θ of the original angle multiplied by a factor (in this case 1/1.64) such that the scales are made equal and then reconverted from the new tan θ_1, to θ_1. This new θ_1 was then added to the ship's course, whence the true north bearing.

An examination of the records revealed that the pattern of scour trends was fairly uniform from one survey line to the next, although variations along the lines were common. To obtain a quantitative evaluation of these trends one survey line extending across the continental shelf and another shorter line extending parallel to the coast and about 20 km offshore were selected as representative samples of the area. Between consecutive Fix numbers (fiducial lines on the records), the bearing of every scour was measured and recorded in 10°-class intervals. A summation of the number of scours within each class (18 classes in all from 0° to 180°) for each of the two lines was made and plotted in the form of a rose diagram (Fig. 10). Two dominant directions, one for each sample line (125° and 95° respectively) are apparent.

The assumption is made that the ice was pushed toward shore, probably at some oblique angle, so that a vector property may be assigned to a graphical plot showing the direction of scouring. This direction corresponds generally to the direction of prevailing westerly and northwesterly winds in the wintertime (Pilot of Arctic Canada, Vol. III, climatological table for Herschel Island). Therefore it appears likely that Arctic sea ice is driven onshore by winds and currents to form pressure ridges and produce scouring by the attendant deeper keels of such ridging. The discrepancy in the primary directions of scour between the two lines covered could be due to the fact that the scouring frequency was not weighted properly. In a few cases, between two consecutive Fixes, a large number of parallel scours were noted. If these scours were formed by a number of ridges all frozen into the Arctic pack ice, then they could represent in fact only one pass of a scouring ice mass and not as many as indicated if each scour is taken as independent from its adjacent one.

The age of any given scour can be calculated if the rate of sedimentation and the amount of infilling since scour formation are known. As seen in Figure 9, often a much greater thickness of sediment than just the original relief of the scour covers it, without completely obliterating the original morphology (up to four times the original relief). At point K in Figure 9, 4 to 5 m of sediment have been deposited since scour formation in a scour with an original relief of only 2 to 3 m. Using a rate of sedimentation of 1 m/1000 years, this scour became filled in 2000 to 3000 years, but still possessed some surface expression 4000 to 5000 years after its formation. With normal echo-sounding records which give little or no penetration below the bottom, it is impossible to even guess the age of any given scour because of the relationship between the amount of infilling and relief.

It would seem that much of the present surface is composed of scours formed a long time ago (6000 years) and are in this sense relict. Theoretically for a scour with 3 to 4 m of original relief, it might take up to 12 or 16 m of

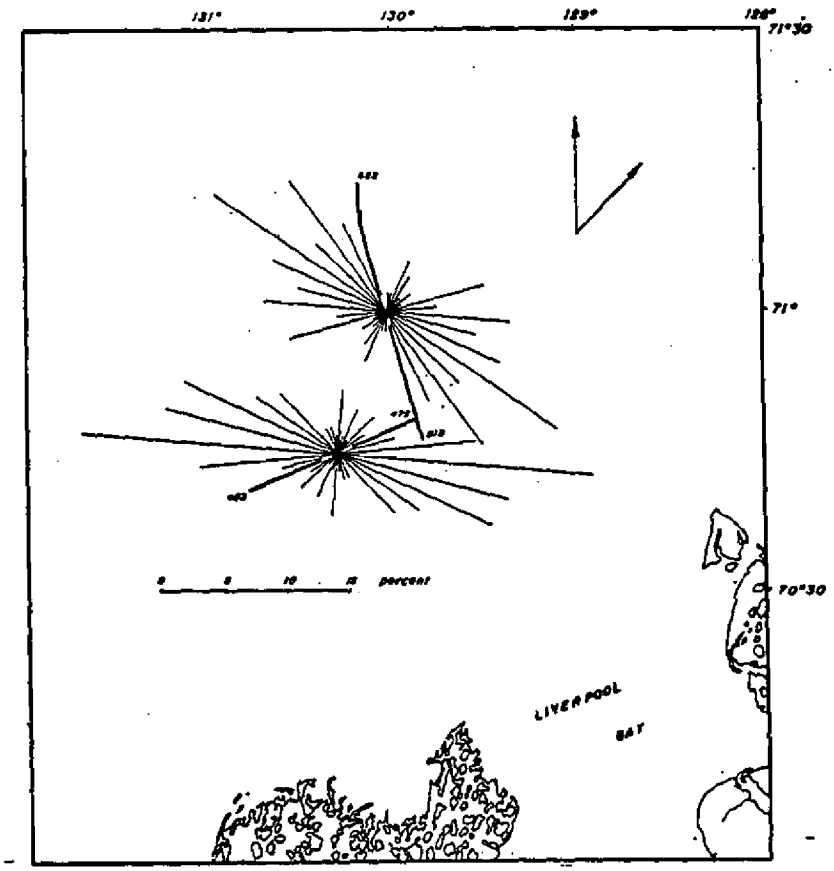


FIGURE 10 — Rose diagram summating frequency of direction in 10°-class intervals for two lines; one perpendicular and the other parallel to the long axis of the continental shelf.

sediment to completely bury the scour. Using a sedimentation rate of 1 m/1000 years the age of such a scour (>12,000 y.) would imply its formation when the sea-level datum was lower. The inclusion of this scour in working out the frequency of bottom scours versus given depths (using present datum) would give erroneously high results. Depending on the locale (rate of sedimentation at that point), scours of similar relief may have vastly different ages (younger in Mackenzie canyon area and older farther east on the Beaufort shelf proper where the rates of sedimentation are generally much less).

CONCLUSIONS

Frequent ice scouring of the sea bottom of the Beaufort Sea has occurred to water depths of 50 m. The frequency of occurrence is much greater than that observed in the ice masses themselves, which can be reconciled by the cumulative nature of scouring on the bottom. Exceptionally, some scouring has been observed in water depths to 75 m. The rates of sea-level change, rates of sedimentation, and rates of scouring seem to vary with time in a way such as to apparently concentrate scouring at depths less than 50 m. An age determination on individual scours is impossible as the amount of infilling and the sedimentation rate are not sufficiently well known. The general direction of onshore movement of ice-producing scours seems to be in the 95° to 125° true north sector.

ACKNOWLEDGMENTS

The authors thank Captain D. W. Butler, master of CSS *Hudson*, Captain V. Dale Johnson, master of CSS *Richardson*, and their ships' companies for unstinting assistance in carrying out this survey in difficult waters. We also thank Anthony Harding of Hunting Geology and Geophysics, London, U.K., for his technical assistance on the side-scan sonar aboard ship, and our critical readers, John Hnatiuk of Gulf Oil Canada, and G. Vilks and A. C. Grant of the Bedford Institute, Dartmouth, N.S. Jan Sklenar is to be commended for his patience in tabulating and calculating the scour properties.

REFERENCES

Carsola, A. J., 1954. Micro-relief on the Arctic sea floor. Bull. Am. Assoc. Pet. Geol. 38, p. 1587-1601.

Clark, David L., 1971. Arctic Ocean ice cover and its late Cenozoic history. Bull. Geol. Soc. Am. 82, p. 3313-3324.

Creager, J. S., and McManus, D. A., 1967. Geology of the floor of the Bering and Chukchi Seas — American Studies. *In* Hopkins, D. M. *(Editor)*, The Bering Land Bridge, p. 7-31.

Ewing, M., and Donn, W. L., 1956. A theory of Ice Ages. Science, 123, p. 1061-1066.

———, 1958. A theory of Ice Ages, II. Science, 127, p. 1159-1162.

Milliman, J. D., and Emery, R. O., 1968. Sea levels during the past 35,000 years. Science 162, p. 1121-1123.

Olausson, Eric, and Jonasson, Ulf C., 1969. The Arctic Ocean during the Würm and early Flandrian. Geol. Fören. Stockh. Förh., 91, p. 185-200.

Shearer, J. M., 1971. Preliminary interpretation of shallow seismic reflection profiles from the west side of Mackenzie Bay, Beaufort Sea. *In* Report of Activities. November 1970 to March 1971, Geol. Sur. Can. Pap. 71-1B, p. 131-138.

———, 1972 (In Press). Geological structure of the Mackenzie Canyon area of the Beaufort Sea. *In* Report of Activities, April to October 1971, Geol. Surv. Can., Pap. 72-1A.

Shepard, F. P., and Curray, J. R., 1967. Carbon 14 determination of sea level changes in stable areas. Prog. in Oceanog. 4, p. 283-291.

Weeks, W. F., Kovacs, A., Hibler, W. D., and Breslau, L., 1971. Sea ice pressure ridges: formation, properties and distribution. Fourth Minefield Conference.

Some Physical Oceanographic Features of Inlets of Chile

G. L. PICKARD

Institute of Oceanography
University of British Columbia, Vancouver, B.C.

PICKARD, G. L. 1971. Some physical oceanographic features of inlets of Chile. J. Fish. Res. Bd. Canada 28: 1077–1106.

The first systematic study of physical oceanographic characteristics of the fjord inlets of Chile was carried out by the Institute of Oceanography of the University of British Columbia during March 1970 as Phase V of the *Hudson* 70 Round-the-Americas Expedition of the Bedford Institute, Canada Department of Energy, Mines and Resources.

Observations were made of temperature, salinity, and dissolved oxygen at 175 stations in 32 inlets and in the passages outside them, and soundings were made along 3500 km of track. The sounding data are presented as longitudinal sections, and water properties are summarized in temperature–salinity and temperature–dissolved oxygen correlation plots and characteristic diagrams; comparisons are made with observations for the British Columbia and Alaska inlets reported by Pickard in 1961 (18: 907–999) and 1967 (24: 1475–1506) in the Journal of the Fisheries Research Board of Canada. Observations were also made of nutrients in some Chilean inlets; these will be reported at a later date.

In mean and extreme values, the dimensions of the inlets in Chile are similar to those in British Columbia/Alaska; only two shallow sills were recorded. More inlets had glaciers contributing melt water directly to them and more had icebergs present than is the case in the northeast Pacific inlets. Vertical salinity profiles in Chile were similar to those in British Columbia/Alaska, but the thinner surface layer was of higher salinity, except in the inlets having icebergs, and the deepwater salinities were 1–2‰ higher in Chile. Temperatures were 2–5 degrees C higher in Chile except in the iceberg inlets where surface values were lower than those in Alaska. Several of the iceberg inlets in Chile had much more complicated temperature/depth profiles than in Alaska, with as many as seven maxima and minima below the surface. The glacial silt in the inlet waters was more conspicuous and extensive in Chile than in British Columbia/Alaska. Dissolved oxygen values in Chile were much the same as in British Columbia/Alaska with higher values in the iceberg inlets in Chile than in Alaska, and there was little evidence of very low values characteristic of stagnant basins. The lack of low dissolved oxygen values suggests free exchange with outside waters and the inlet deepwater characteristics indicate that the effective sill depths between inlets and the ocean are only 100–150 m deep. At least four distinct major regions are evident from water properties among the inlets of Chile.

PICKARD, G. L. 1971. Some physical oceanographic features of inlets of Chile. J. Fish. Res. Bd. Canada 28: 1077–1106.

La première étude systématique de l'océanographie physique des fjords du Chili fut accomplie par l'Institut d'Océanographie de l'Université de Colombie Britannique en mars 1970. Ce projet était la cinquième phase de l'expédition *Hudson* 70 autour des Amériques organisée par l'Institut Bedford du Ministère de l'Energie, des Mines et des Ressources du Canada.

Nous avons mesuré la température, la salinité et l'oxygène dissous à 175 stations dans 32 fjords et dans les passages extérieurs, et nous avons fait 3500 km. de sondages. Les sondages sont présentés sous forme de diagrammes de température–salinité et de température–oxygène. Ces observations sont comparées à celles faites dans les fjords de Colombie Britannique et d'Alaska, déjà publiées par Pickard en 1961 (18: 907–999) et 1967 (24: 1475–1506) dans le *Journal of the Fisheries Research Board of Canada*. Des mesures des concentrations de sels nutritifs dans quelques-uns des fjords du Chili seront publiées plus tard.

Les dimensions des fjords du Chili ressemblent à celles des fjords de Colombie Britannique et d'Alaska; seulement deux de ces fjords ont un seuil peu profond. On trouve toutefois au Chili plus de fjords où des glaciers contribuent directement de l'eau de fonte et des icebergs qu'en Colombie Britannique/Alaska. Les profils verticaux de salinité de l'eau des fjords chiliens ressemblent à ceux de Colombie Britannique/Alaska, mais la couche de surface y est plus

Printed in Canada (J2105)

salée (sauf où flottent des icebergs) et la salinité des eaux profondes est plus haute au Chili de 1–2‰. Les eaux au Chili sont plus chaudes de 2–5 C. qu'en Colombie Britannique/ Alaska, sauf dans les fjords à icebergs où les eaux de surface sont plus froides. Plusieurs des fjords à icebergs du Chili ont des profils verticaux de température plus complexes qu'en Alaska, avec jusqu'à sept maxima et minima sous la surface. La vase des glaciers ("poudre de roche") dans les eaux des fjords est plus évidente et plus répandue au Chili qu'en Colombie Britannique/ Alaska. La concentration en oxygène dissous est à peu près la même au Chili, mais dans les fjords à icebergs du Chili les concentrations sont plus élevées, et on ne trouve pas les concentrations très basses qui caractérisent les bassins stagnants. L'absence de basses concentrations d'oxygène suggère que l'eau des fjords se mêle sans encontres aux eaux des passages extérieurs; les caractéristiques des eaux des fjords indiquent de plus que les seuils qui les séparent de l'océan n'ont que de 100–150 m. de profondeur. On distingue, d'après les caractéristiques générales de ces eaux, quatre régions océanographiques principales le long de la partie sud de la côte du Chili, découpée de fjords.

Received March 31, 1971

THE southern thousand miles of the coast of Chile contains one of the major fjord regions of the world, but until the present work in 1970 there had been no systematic oceanographic study of the waters of this region.

Members of the Institute of Oceanography of the University of British Columbia had studied the inlets of British Columbia and Alaska on the west coast of North America for many years (Pickard 1961, 1963, 1967) and had for some time desired to study those on the west coast of South America. The opportunity to do so arose as a part of the Round-the-Americas expedition by the C.S.S. *Hudson* (*Hudson* 70 Expedition by the Bedford Institute, Marine Sciences Branch of the Canada Department of Energy, Mines and Resources). The study of the Chilean fjord inlets was included as Phase V of that cruise, from March 4 to 30, 1970. The Institute of Oceanography designation is the "Chile 70" cruise.

The object of the study was to learn as much as possible about the oceanography of the region to add to the available knowledge of fjord regions and to compare with other fjord regions, particularly that of the northeast Pacific (British Columbia and Alaska). As the time available was limited, it was decided to observe the distribution of water characteristics in as many fjords as possible distributed along the entire coast, taking stations at intervals of 8–16 km (5–10 nautical miles). In the absence of any previous work, the selection was somewhat arbitrary but with emphasis on the longer fjords. Because of our interest in estuarine regions, preference was given to fjords in the mainland coast that might be expected to experience significant river runoff, rather than to those in the large islands separated from the mainland by the narrow waterways that form an "inland passage" along the coast.

One of the difficulties in planning the Chile 70 cruise was that although the inland passage was well enough surveyed to allow the passage of deep-sea vessels, many of the fjords were not surveyed at all. The intention was to have the sounding launches precede the ship in the unsurveyed waters. Unfortunately, equipment problems made it impractical to use the launches and it was considered imprudent to work with the ship itself in the unsurveyed areas. Data were obtained in some of these from a ship's lifeboat, using a hand winch, but it was not possible to transfer the echo sounders from the launches to the lifeboat and therefore soundings were not obtained in the regions studied from the lifeboat.

The primary purpose of this paper is to present a broad summary of the observed oceanographic characteristics of the Chilean fjords, as these have not previously been described. Some comparisons with the fjord characteristics of North America are also presented, but discussion of many of the details of the features observed in Chile is left until later.

Water samples were obtained using Copenhagen reversing water bottles and temperatures were measured with Richter and Wiese reversing thermometers and temperature profiles with a 270 m bathythermograph. The salinity was determined with an AutoLab Inductive Salinometer (range 0–40‰) and the dissolved oxygen content by a modified Winkler titration, using reagents as recommended by Carritt and Carpenter (1966). (Nutrients were determined at some stations using a Technicon AutoAnalyser — these results will be reported later by I. W. Duedall.) In addition, temperature and salinity profiles were obtained with a Bissett-Berman model 9060 Selfcontained Salinity, Temperature, Depth (STD) Recorder (0–500 m depth range) using the 30–40‰ or 0–40‰ salinity range as appropriate.

In the inlets and inside passages, 175 stations were occupied for reversing water-bottle casts and 148 STD and 150 bathythermograph casts were made; in addition four stations were occupied for bottle, STD, and bathythermograph casts at stations in the Pacific Ocean off entrances to the inside passages. Meteorological observations were made at each station and Secchi disc measurements made at stations occupied in daylight.

The Chilean charts were used for navigation, and positions were determined by radar fixes on shore marks. Continuous echo soundings were made throughout the cruise.

General Characteristics of the Region

Topography

Figure 1 shows on the right the location of the fjord inlet region of Chile on the Pacific coast of South America, and on the left is shown the Pacific coast of North America rotated through 180° to facilitate comparison with the southern fjord coast in terms of latitude. Figure 2 shows the Chilean region on a larger scale, with the studied inlets named and locations given for other oceanographic stations and for climatological stations referred to later.

The fjord inlet region (Fig. 2) extends from near Puerto Montt at 41.4°S to Tierra del Fuego at about 55°S, south of the Estrecho de Magallanes. The region is generally rugged, with relief of 500–2000 m in the immediate neighbourhood of the inlets, the central part of the area having the greatest relief. The mainland coast is separated from the Pacific Ocean by a large number of islands and narrow passages, the majority of these being unsounded.

In the northern third of the region, from about 41.4°S to 46.5°S, most of the mountains close to the inlets are covered with trees to 1500 m elevation or more, but south of 47°S the tree line descends until in the Estrecho de Magallanes region it is at some 500 m or less above sea level. Very conspicuous features, both visually and in their effect on the coastal waters, are the many glaciers south of 46°S. Some descend from large ice fields in the mountains to sea level in the inlets; others are just small caps on rounded mountains at elevations of 500–1000 m. The areas of light-coloured rock surrounding the small cap glaciers suggest that the latter are decreasing in size. In several of the inlets ice was encountered during this cruise with bergy bits up to about 5 m in length. These will be referred to as "iceberg inlets."

Longitudinal profiles of the inlets traversed by the C.S.S. *Hudson* (Fig. 3 and 4) were prepared from the continuous sounding records made during the Chile 70 cruise and from the Chilean charts. These profiles are only first approximations because the midchannel course followed by the ship does not necessarily follow the line of maximum depth. In addition, there were some places where the soundings obtained during the runs in and out of an inlet were significantly different. Such differences could be due to the irregular character of the bottom in many areas and to the fact that navigation by

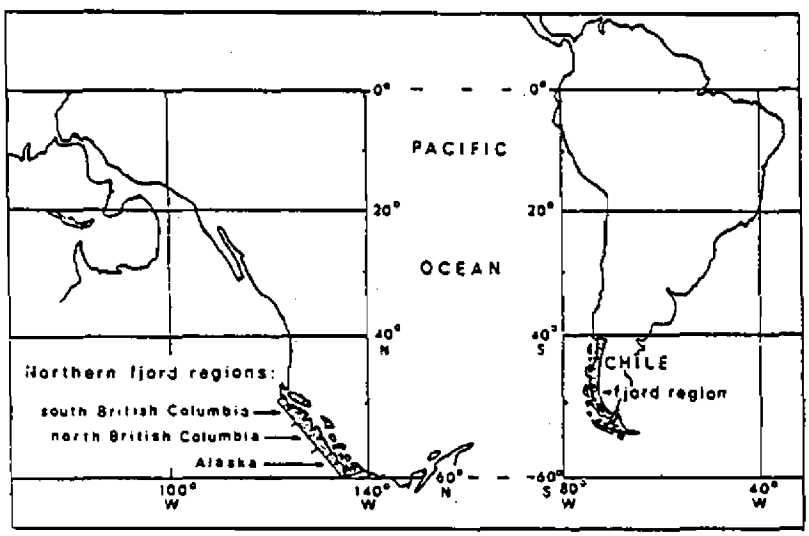


FIG. 1. Right, location of fjord inlet region of Chile; left, location of fjord inlet region of British Columbia/Alaska rotated 180° to show relative latitudes.

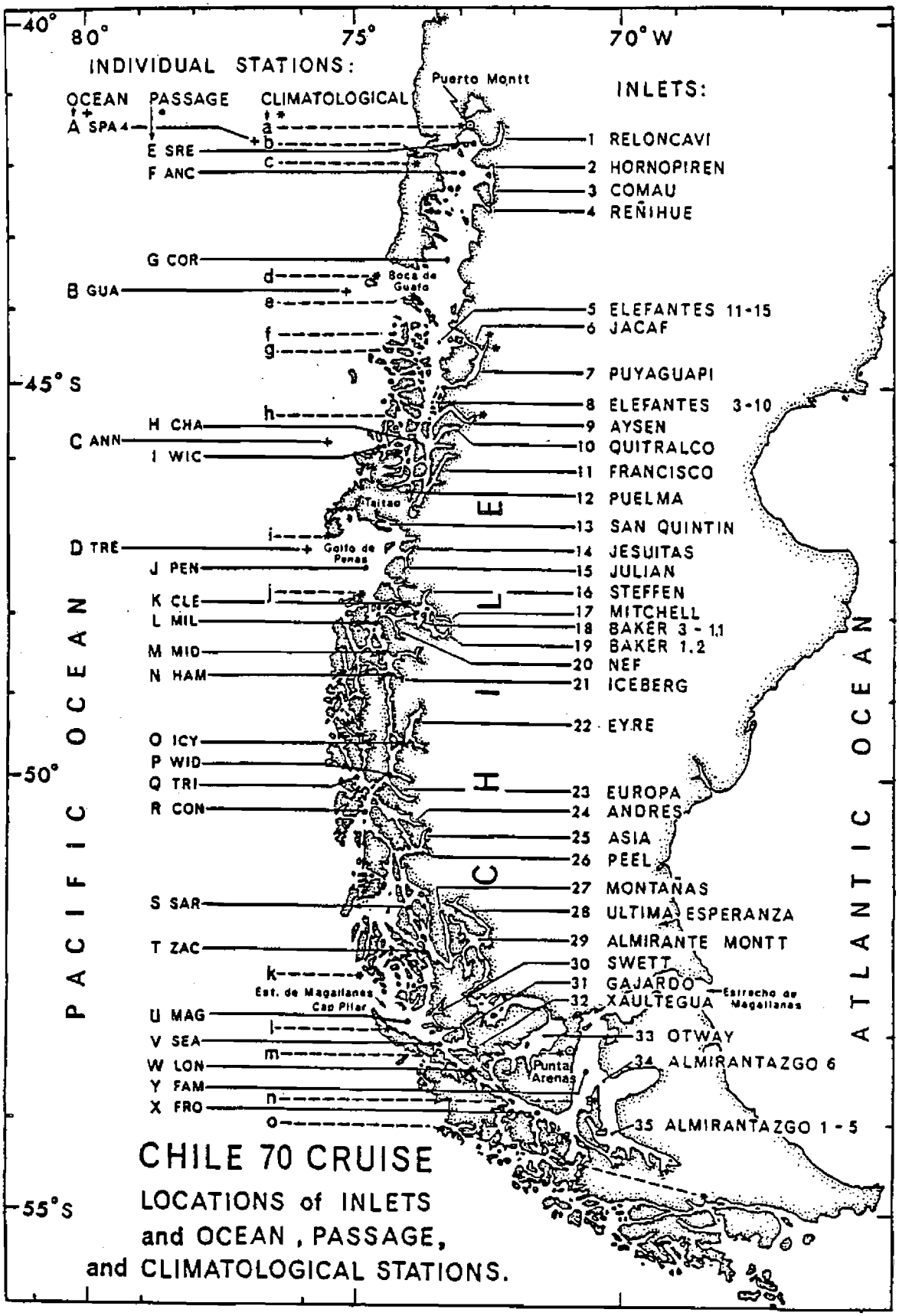

40°
80°
75°
70° W
INDIVIDUAL STATIONS:
OCEAN
PASSAGE
CLIMATOLOGICAL
A SPA
E SRE
F ANC
G COR
B GUA
H CHA
C ANN
I WIC
D TRE
J PEN
K CLE
L MIL
M MID
N HAM
O ICY
P WID
Q TRI
R CON
S SAR
T ZAC
U MAG
V SEA
W LON
Y FAM
X FRO
a
b
c
d
e
f
g
h
i
j
k
l
m
n
o
Puerto Montt
Boca de Guafo
Golfo de Penas
Taitao
Est. de Magallanes
Cap Pilar
Punta Arenas
Estrecho de Magallanes
INLETS:
1 RELONCAVI
2 HORNOPIREN
3 COMAU
4 REÑIHUE
5 ELEFANTES 11-15
6 JACAF
7 PUYAGUAPI
8 ELEFANTES 3-10
9 AYSEN
10 QUITRALCO
11 FRANCISCO
12 PUELMA
13 SAN QUINTIN
14 JESUITAS
15 JULIAN
16 STEFFEN
17 MITCHELL
18 BAKER 3 - 1.1
19 BAKER 1.2
20 NEF
21 ICEBERG
22 EYRE
23 EUROPA
24 ANDRES
25 ASIA
26 PEEL
27 MONTAÑAS
28 ULTIMA ESPERANZA
29 ALMIRANTE MONTT
30 SWETT
31 GAJARDO
32 XAULTEGUA
33 OTWAY
34 ALMIRANTAZGO 6
35 ALMIRANTAZGO 1 - 5
PACIFIC OCEAN
ATLANTIC OCEAN
CHILE
45° S
50°
55° S
CHILE 70 CRUISE
LOCATIONS of INLETS
and OCEAN, PASSAGE,
and CLIMATOLOGICAL STATIONS.

FIG. 2 Locations of inlets and of ocean and passage stations studied in Chile 70 cruise, and of climatological stations used for reference. (See Tables 1–3 for keys to station-identifying letters.)

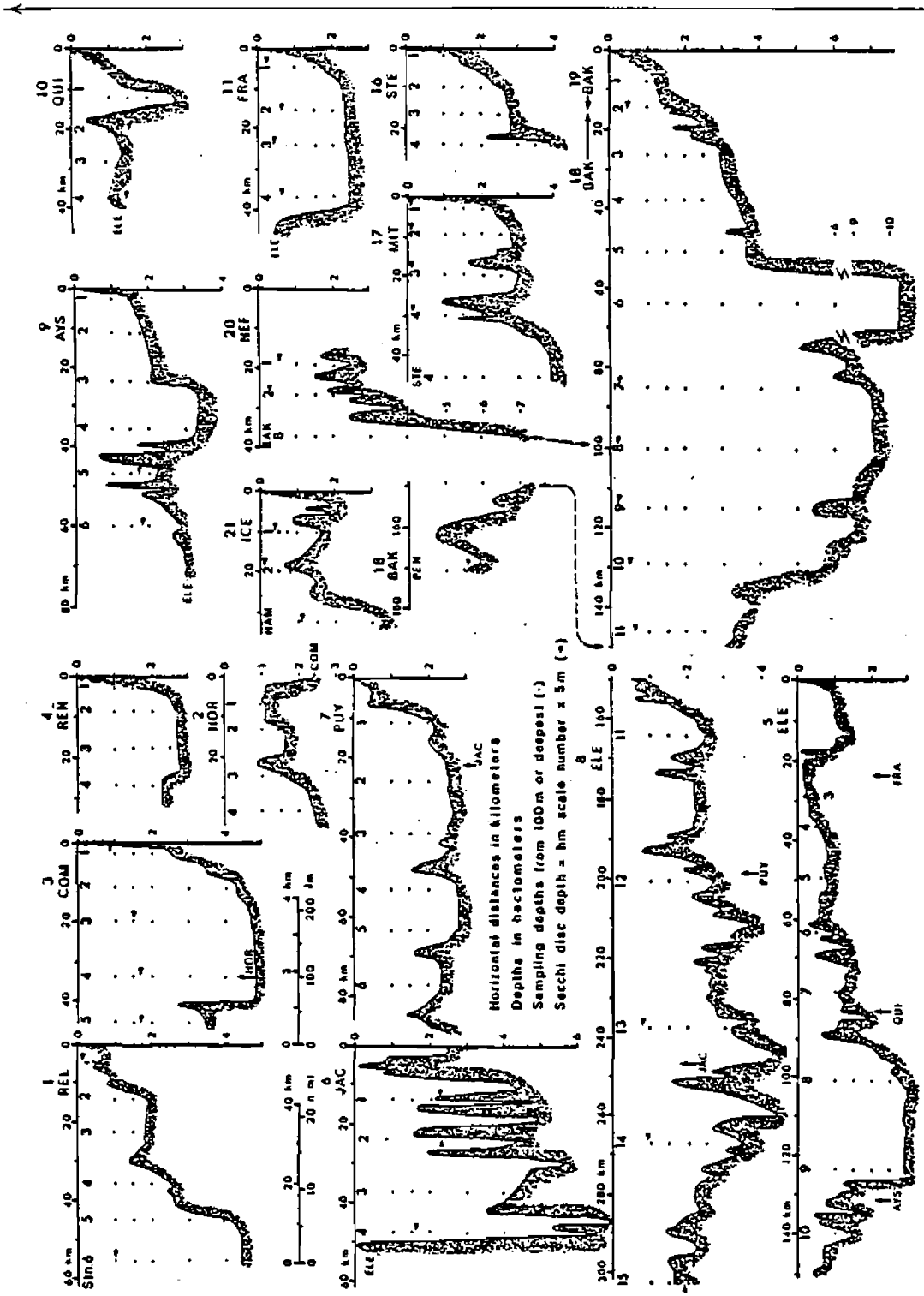


FIG. 3. Longitudinal sections along inlets studied in Chile 70 cruise, numbers 1–21 in northern part of coast.

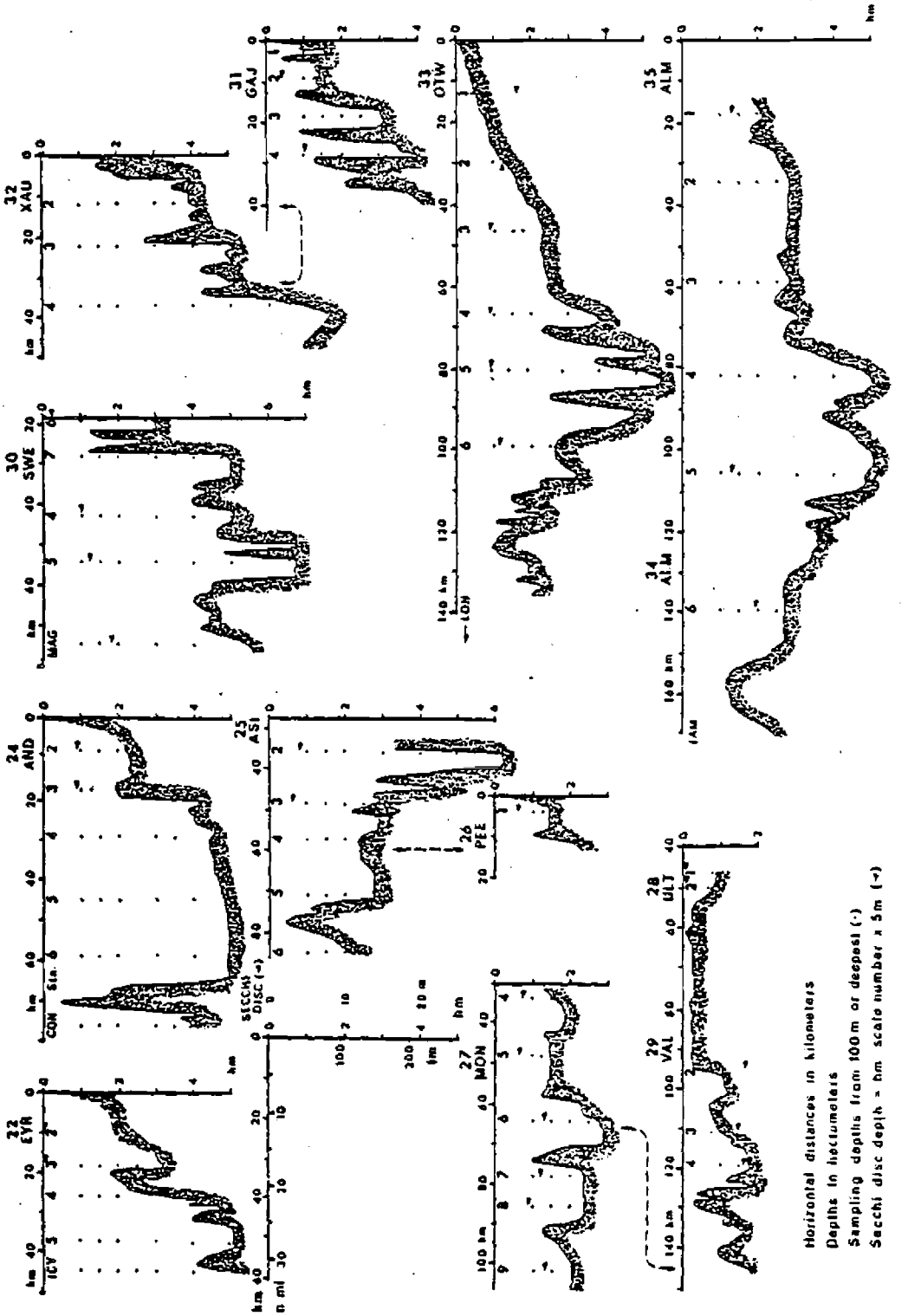


FIG. 4. Longitudinal sections along inlets studied in Chile 70 cruise, numbers 22–35 in southern part of coast.

radar fixes on the shoreline is not accurate enough for good sounding runs over the prevailing rugged bottom topography. In preparing the longitudinal sections, shallow soundings (suggesting sills) that appeared on the ship's records have been ignored unless supported by soundings on the Chilean charts and by significant differences in the water characteristics below the apparent sill depth on either side. No attempt has been made to correct for tidal height in preparing the profiles. The range of spring tides for most of the coast is only about 2 m, with higher values up to about 6 m only in the Golfo Reloncavi area near Puerto Montt in the north.

In Table 1 are given the names and dimensions of the inlets studied; the depths have been rounded off to the nearest 5 m because of the limitations of the data. The "outer sill depth" is that of the shallowest sill in the outer one-third of the inlet length. It should be noted that these sills are between the inlets and the inside passages or straits; none of the inlets studied opens directly to the Pacific Ocean. Generally there are depths between the inside passages and the ocean that are shallower than much of the passages themselves. The deepest connections to the Pacific are probably through the Boca del Guafo (43.5°S) and Golfo de Penas (47.5°S) with depths of about 150 m; the connections further south appear from the charts to have least depths of less than 100 m.

As in the northeast Pacific fjord region, several designations are used for the bodies of water without any apparent oceanographic consistency. The most common are "canal" (= canal, channel, passage), "estero" (= bay, cove, channel, estuary, strait), "estuario" (= estuary), and "seno" (= bay). For convenience, the bodies of water studied will be referred to in general as inlets (because not all of them are fjords), and the names mentioned above (e.g., canal, estero, etc.) will be omitted when referring to specific inlets.

In Table 1 and Fig. 2 the inlets are listed from north to south by name and also by an identifying number starting with 1 at the north. On the figures showing water properties, an inlet will generally be identified by its number as this is more compact and will more readily indicate to most readers the inlet's position along the coast than would its proper name. Two identifying numbers are used for three inlets (Elefantes 5 and 8, Baker 18 and 19, and Almirantazgo 34 and 35) as the water properties showed significant differences between sections of these inlets, usually due to the presence of a sill. Station positions along each inlet are numbered starting with 1 at the inland end. The stations in the Pacific off the fjord coast and those in the passages are identified by letters in Fig. 2 and in diagrams of water properties. The positions of these stations are given in Table 2.

Anticipating the oceanographic results to be presented, it is convenient to divide the region into three main areas, the northern from Puerto Montt (41.4°S) to the Peninsula de Taitao (46.5°S), the middle from there to the Cap Pilar (western) entrance to the Estrecho de Magallanes (about 52.7°S), and the southern from there to Seno Almirantazgo (54.5°S). In the middle region, the water characteristics suggest a further subdivision into the north middle (about 47–48.5°S around Canal Baker, 18 and 19), the iceberg inlets (48.5–51°S), and the south middle.

Climate

The southern part of Chile is very sparsely populated and there are not many climatological stations along the inlet coast (see Fig. 2 where climatological stations are indicated by lower case letters). In particular there is a big gap between 48° and 52.5°S. However, a general summary of the climate has been assembled from the paper by Reed (1929), from tables in the USNOO Sailing Directions (Anon. 1952), and from data supplied by Sr H. Sievers, Head, Centro Nacional de Datos Oceanograficos, Chile. The stations used are listed in Table 3 and the locations shown on Fig. 2.

The monthly mean air temperature has a maximum in January or February and a minimum in July or August (Fig. 5). The annual mean air temperature decreases roughly linearly from 10 C in the north to 5 C in the south (Fig. 6), with an annual range of monthly mean temperature of 6 C in the north to 9 C in the south.

The rainfall from 42°S to 53°S averages about 2700 mm per year, with a maximum of 5090 mm per year at the Pacific entrance to the Estrecho de Magallanes (Fig. 6). These data are for the outer coast — the values for the inlets themselves among the coastal mountains could be higher. An indication of the local variability is given by comparing the annual rainfalls at two pairs of stations: Guafo (*d*) with 1040 mm and Melinka (*e*) with 3170 mm, which are 80 km apart, and Rio Cisnes (*g*) with 590 mm and Puerto Puyuhuapi (*f*) with 3870 mm, which are only 20 km apart. The rainfall at the southern and more easterly stations of Punta Arenas (*m*), Bahia Harris (*n*), and Ushuaia (*o*) is considerably less at about 600 mm but these stations are in the rain shadow of the mountains to their west.

The rainfall has a maximum in winter (May-August) in the northern area (e.g., Fig. 5, station *c*)

TABLE 1. Salient dimensions of inlets studied in Chile 70 cruise. Depths taken from Chilean charts or soundings, or both, by C.S.S. *Hudson*, all rounded to nearest 5 m, no correction for tide height.

No.	Abbreviation	Name	Length (*km*)	Mean width (*km*)	Mean midinlet depth (*m*)	Max depth (*m*)	Outer sill depth (*m*)	Glacier[a]	Ice in water[b]	Notes
1	REL	Estero Reloncavi	56	2.7	225	450	None			
2	HOR	Canal Hornopiren	37	2.2	160	250	None	V. small		
3	COM	Estero Comau	41	4.5	420	480	270			
4	REN	Estero Reñihue	28	5.1	245	280	230			
5,8	ELE	Estero Elefantes	300	11.5	185	440	150			c
6	JAC	Canal Jacaf	52	3.8	340	690	25			
7	PUY	Canal Puyuguapi	100	4.2	220	280	140	Possible		
9	AYS	Seno Aysen	70	4.2	225	335	70			
10	QUI	Estero Quitralco	39	3.4	125	275	100			
11	FRA	Estuario Francisco	44	2.7	200	240	40			
12	PUE	Estero Puelma	89	2.0	...	>150	...			d
13	SQU	Bahia San Quintin	32	8.2	30	60	None			
14	JES	Seno Jesuitas	19	2.2	...	>200	...	Yes		d
15	JUL	Estero Julian	22	0.8	...	>200	...	?		d
16	STE	Estero Steffen	24	3.4	240	285	220	Yes		
17	MIT	Estero Mitchell	45	2.3	265	390	140			
18,19	BAK	Canal Baker	160	3.1	470	1050	75	Yes	Some	e
20	NEF	Estero Nef	37	1.3	275	370	240			f
21	ICE	Seno Iceberg	26	1.9	125	160	70	Yes	Yes	
22	EYR	Seno Eyre	46	4.6	310	510	410	Yes	Yes	
23	EUR	Seno Europa	56	3.0	...	>200	...	Yes	Yes	d
24	AND	Canal & Estero Andres	70	4.4	365	500	50			
25	ASI	Estero Asia	85	3.2	265	620	45	Yes	Yes	g
26	PEE	Estero Peel	9	2.9	140	150	105	Yes	Yes	h
27	MON	Estero de las Montañas	102	3.3	225	290	100	Yes		i
28	ULT	E. Ultima Esperanza	56	...	...	>80	10	Possible		d
29	VAL	Golfo Almirante Montt	35	5.9	75	180	30			j
30	SWE	Canal Swett	59	2.8	445	670	410	Yes		k
31	GAJ	Canal Gajardo	41	1.7	200	400	130	Yes		
32	XAU	Golfo Xaultegua	46	4.6	465	760	430	Small		
33	OTW	Seno Otway	124	15.0	215	540	90			
34,35	ALM	Seno Almirantazgo	163	13.7	300	500	110	Yes		l
Mean values etc:										
Chile		32 inlets	66	6.1	265	410	145	14	6	
British Columbia		44 "	47	2.3	310	385	125	6	None	
Alaska		16 "	117	9.5	350	480	155	8	4	

[a]From Anon. (1968) and observation during cruise.
[b]Observed in March 1970.
[c]Inlet 5 is Canal Moraleda, stations ELE 11–15, and inlet 8 is Estero Elefantes, stations ELE 3–10, the former being geographically a continuation of the latter.
[d]Insufficient soundings available.
[e]Inlet 19 is Estero Steele, stations BAK 1 and 2, and inlet 18 is Canal and Seno Baker, stations BAK 3–11, the latter being a continuation of the former.
[f]Nef — soundings for outer 22 km.
[g]Comprising Estero Asia and outer part of Estero Peel; soundings for outer 50 km.
[h]Side arm from junction of Asia and outer part of Peel.
[i]Comprising Seno Union and Canal de las Montañas, soundings for outer 60 km.
[j]Comprising Canal Valdes and Golfo Almirante Montt.
[k]Comprising Bahia Beaufort, Seno Glacier, and Canal Swett; soundings for outer 40 km.
[l]Inlet 34 station ALM 6, inlet 35 is stations ALM 1–5, the two forming Seno Almirantazgo.

TABLE 2. Ocean and passage station positions, Chile 70 cruise.

Identifying letter	Abbreviation	Location	Lat S	Long W	Depth (*m*)
		Ocean stations			
A	SPA4	W of Canal Chacao	41°40.0′	77°00.0′	2950
B	GUA	W of Isla Guafo	43 45.5	75 11.7	990
C	ANN	W of Bahia Anna Pink	45 45.0	75 40.2	970
D	TRE	W of Cabo Tres Montes	47 00.4	75 47.5	1960
		Passage stations			
E	SRE	Seno Reloncavi	41 43.1	72 45.2	350
F	ANC	Golfo de Ancud	42 04.2	73 09.0	340
G	COR	Golfo Corcovado	43 18.4	73 17.6	225
H	CHA	Canal Chacabuco	45 44.6	73 59.2	135
I	WIC	Boca Wickham	45 00.0	74 30.6	240
J	PEN	Golfo de Penas	47 34.5	74 54.1	190
K	CLE	Canal Martinez	47 47.8	74 16.6	275
L	MIL	Canal Messier	48 00.8	74 41.4	1000
M	MID	" "	48 25.6	74 32.6	1280
N	HAM	" "	48 32.0	74 26.7	350
O	ICY	Canal Icy	49 38.5	74 14.1	500
P	WID	Canal Wide	49 59.4	74 26.2	1080
Q	TRI	Canal Trinidad	50 01.7	74 55.2	300
R	CON	Canal Concepcion	50 20.4	74 49.5	405
S	SAR	Canal Sarmiento	51 36.6	73 59.8	930
T	ZAC	Canal Smyth	52 01.5	73 46.2	380
U	MAG	Estrecho de Magallanes (W)	52 54.1	73 56.1	550
V	SEA	Paso Largo	53 07.8	73 25.0	1130
W	LON	Paso Largo	53 20.8	73 02.2	820
X	FRO	Paso Froward	53 51.0	71 38.0	300
Y	FAM	Estrecho de Magallanes (E)	53 29.2	70 37.2	410

TABLE 3. Climatological stations in southern Chile: positions and sources of data.

Identifying letter	Station name	Lat S	Long W	Sources of data*
a	Puerto Montt	41°21′	72°56′	CNDOC
b	Puerto Corona	41 47	73 52	CNDOC
c	Ancud	41 52	73 49	CNDOC
d	Isla Guafo	43 34	74 45	USNOO
e	Melinka	43 54	73 45	Reed
f	Puerto Puyuhuapi	44 20	72 28	CNDOC
g	Rio Cisnes	44 32	72 24	CNDOC
h	Puerto Aysen	45 24	72 42	CNDOC
i	Cabo Raper	46 50	75 35	CNDOC
j	San Pedro	47 43	74 55	CNDOC
k	Los Evangelistas	52 24	75 06	USNOO
l	Bahia Felix	52 58	74 05	Reed
m	Punta Arenas	53 10	70 54	USNOO
n	Bahia Harris	53 50	70 24	Reed
o	Ushuaia	54 50	68 20	USNOO

*Sources: CNDOC, Centro Nacional de Datos Oceanograficos, Chile; USNOO, Anon. (1952); Reed, 1929 paper.

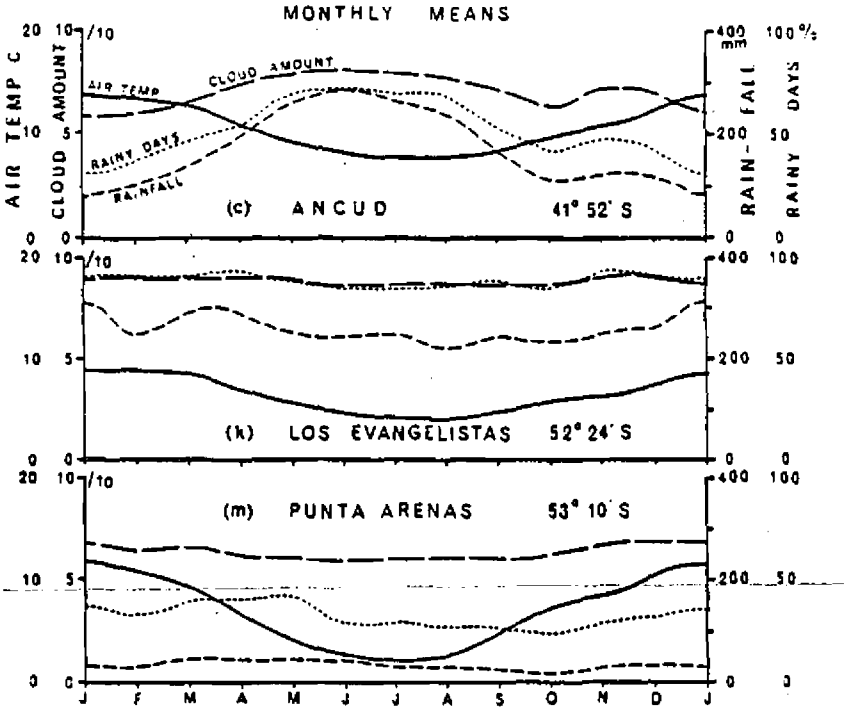


FIG. 5. Annual variation of monthly mean air temperature, rainfall, rainy day frequency, and cloud amount at selected stations in fjord inlet coast of Chile.

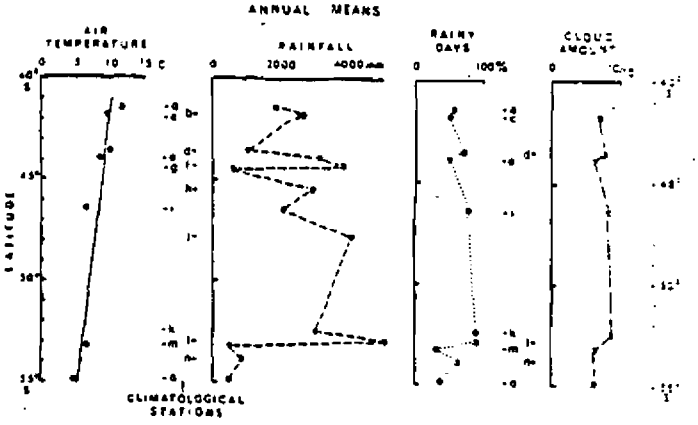


FIG. 6. Variation with latitude of annual mean air temperature, rainfall, rainy day frequency, and cloud amount for fjord inlet coast of Chile. (See Table 3 for station key.)

but south of about 47°S it is fairly evenly distributed through the year (e.g., Fig. 5, station *k*). In the middle part of the coast there is rain on 80–90% of days of the year, in the north and south on 30–50% of days (Fig. 6). The cloud cover averages $\frac{8}{10}$–$\frac{9}{10}$ in the middle coast and $\frac{6}{10}$–$\frac{7}{10}$ elsewhere (Fig. 6).

The general impression from accounts of the climate of the fjord region is of an inhospitable region typified by a paragraph in the USNOO Sailing Directions referring to one of the channels: "The navigation is perfectly easy in moderately fine weather: the real difficulty of it consists in the

almost perpetual rain, thick weather, and strong gales, with very heavy williwaws, which come down the steep mountain sides with a force which must be felt to be believed." If this is a correct assessment, we were fortunate in having better than average weather during the Chile 70 cruise, with rain on only 40% of the days, mean cloud cover of 5.5/10, and frequency of wind speeds as follows: calm or light airs 34%; 1–10 mph 23%; 11–20 mph 29%; 21–30 mph 8%; 31–60 mph 6%.

Results

Temperature, Salinity, and Oxygen

The values for water temperature, salinity, and dissolved oxygen are presented in this paper in graphical form rather than in numerical tabulation. In diagrams of publishable size the former method is less precise than the latter but is more compact and better adapted for displaying comparisons within the area of study and with regions elsewhere. The lower precision is considered not significant in view of the probability that seasonal and year-to-year variations in water properties may be expected to be considerably larger than the precision of measurement by the techniques used. The measured values are tabulated in a data report (Anon. MS 1971) of the Institute of Oceanography, University of British Columbia. The data are also deposited with the Centro Nacional de Datos Oceanograficos de Chile, Cascilla 324, Valparaiso, Chile and with the Instituto Central de Fisica, University of Concepción, Chile.

Temperature–Salinity and Temperature–Oxygen Correlations

It was found that although there were significant horizontal variations in water properties, particularly salinity, in some inlets in the upper 20 m of water, the major systematic variations were in the vertical direction in the upper 200 m. For the first description, therefore, water characteristics are displayed as temperature–salinity (T–S) and temperature–oxygen ($T–O_2$) correlation plots for selected depths of 0, 20, 50, 100, and 200 m in Fig. 7–11. Some information on water properties at greater depths is given later. In reducing the data for presentation on these plots, the mean value of the water property at each depth in each inlet was calculated and the range of values also noted (maximum minus minimum value). On the figures, the mean value of temperature–salinity or temperature–oxygen for each inlet is indicated by the number of the inlet as given in Table 1. To indicate the significance of the separation of the points, a "reduced mean range" of properties is shown on each figure. This range was obtained by first calculating the mean of the ranges for all inlets at that depth, then extracting those values more than three times the first mean, and calculating the mean of the remainder ("reduced mean"). The reduced mean range and the extracted values are given on each figure. Note that the reduced mean ranges are generally small compared with the differences in mean values between inlets, and that geographic variations of mean properties are evident. The northern inlets (1–12) are in the short-dash envelope, the north middle ones (14–20) in the dot-dash envelope, the southern group (30–35) are within the full-line envelope, and the inlets with glacier ice in the water are indicated by triangles and connected by a long-dash line.

In Fig. 7–11 are also shown values for T–S and $T–O_2$ correlations for one of the ocean stations (Guafo, B) and for the selection of passage stations for which T–S and $T–O_2$ diagrams are given in Fig. 14.

Salinity–Depth Profiles

In all the inlets visited, the surface salinity at the inlet head was less than at the mouth and, with a few minor exceptions mentioned in the next paragraph, the salinity increased with depth. Both of these are characteristics of estuarine regions. Most of the salinity increase occurred in the upper 20 or 30 m; in some instances there was an isohaline layer of a few meters depth from the surface. Table 4 summarizes some of the characteristics, i.e., the surface and deep salinity, the salinity–depth profile type in the upper layer (Fig. 12), the isohaline layer depth and the depths at which the salinity reached 50 and 90% of the deepwater salinity (to indicate the distribution of fresh water with depth).

The locations where there were decreases of salinity with increasing depth were at one station each in Comau (3) and Reñihue (4) in the north, and at four in Almirantazgo (35) in the south. The change of salinity was only 0.01–0.07‰, in all instances in the vicinity of 100 m depth. The STD traces confirmed these minor localized salinity inversions, which were compensated by temperature changes so that the water remained stable. Larger inversions of 0.03–0.12‰ were noted at three passage stations (F, I, and R) between 100 and 200 m, whereas the ocean stations showed a salinity maximum at 200–300 m with a decrease of 0.01–0.11‰ to a minimum at 500–600 m.

About 20% of the inlet stations showed a surface salinity higher than that at the first subsurface depth sampled (usually 2 or 5 m). During the early part of the cruise this phenomenon was correlated

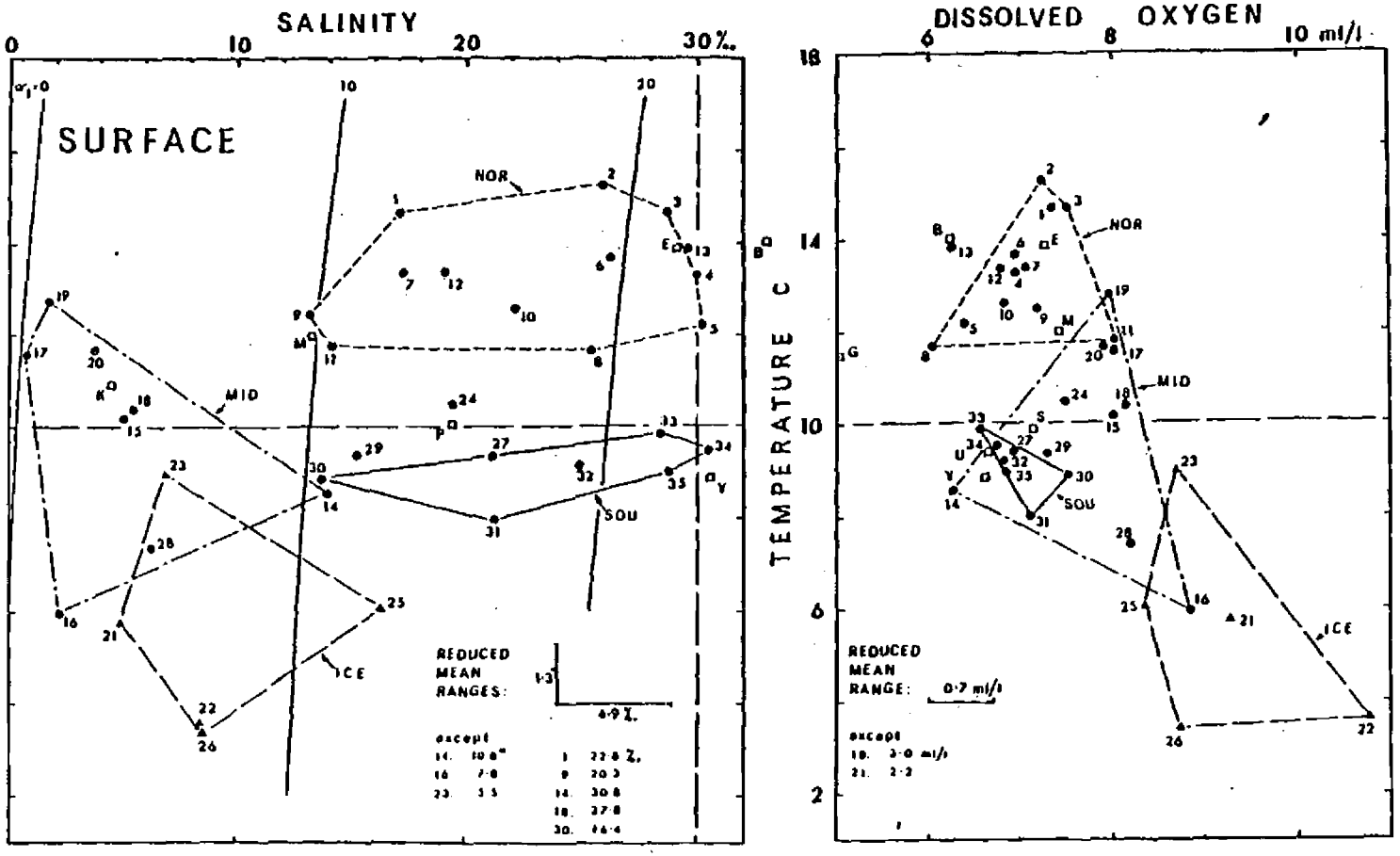


FIG. 7. Temperature–salinity and temperature–dissolved oxygen correlation plots for Chile inlets, Chile 70 cruise, surface values.

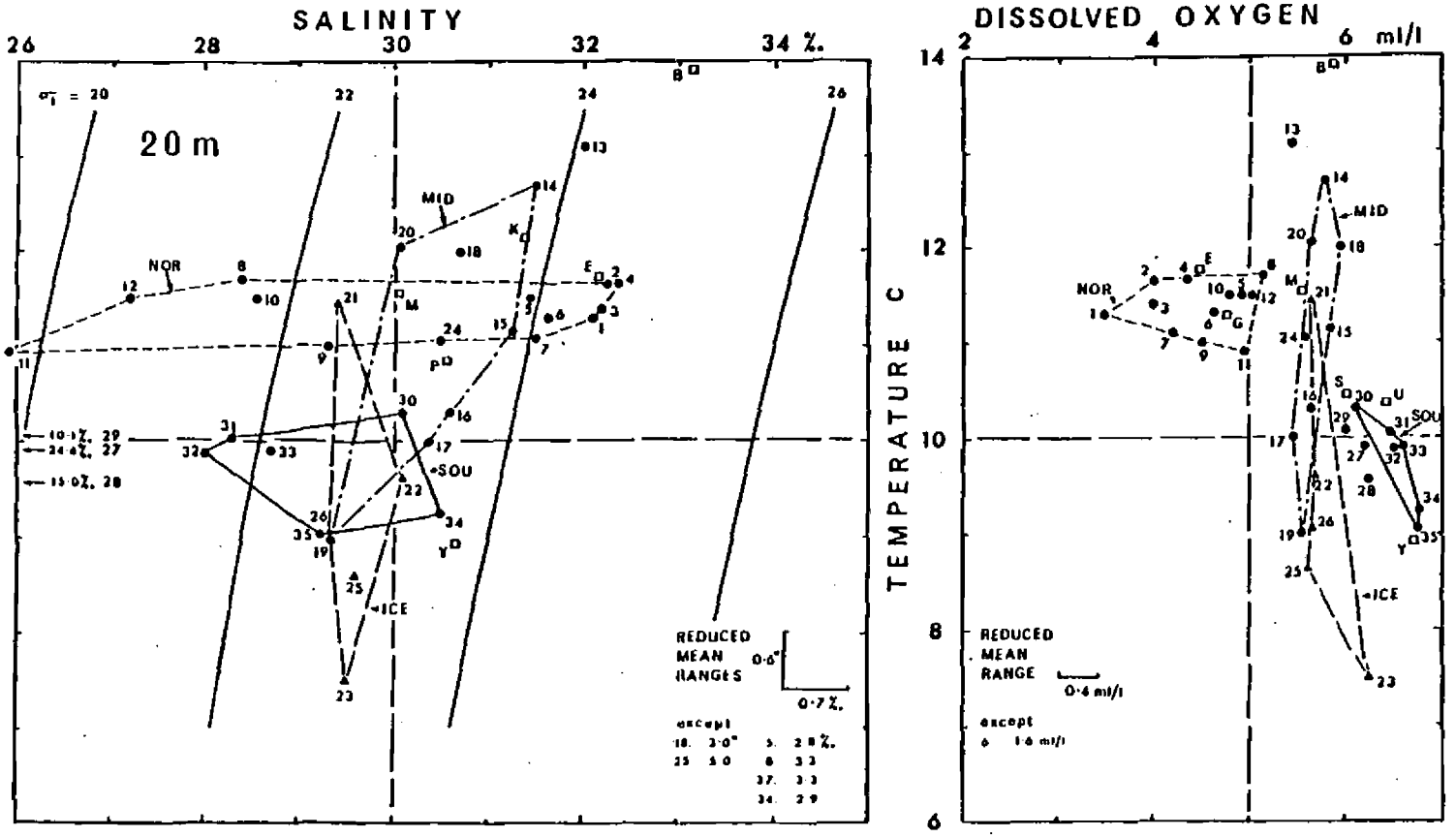


FIG. 8. Temperature-salinity and temperature-dissolved oxygen correlation plots for Chile inlets, Chile 70 cruise, 20 m depth.

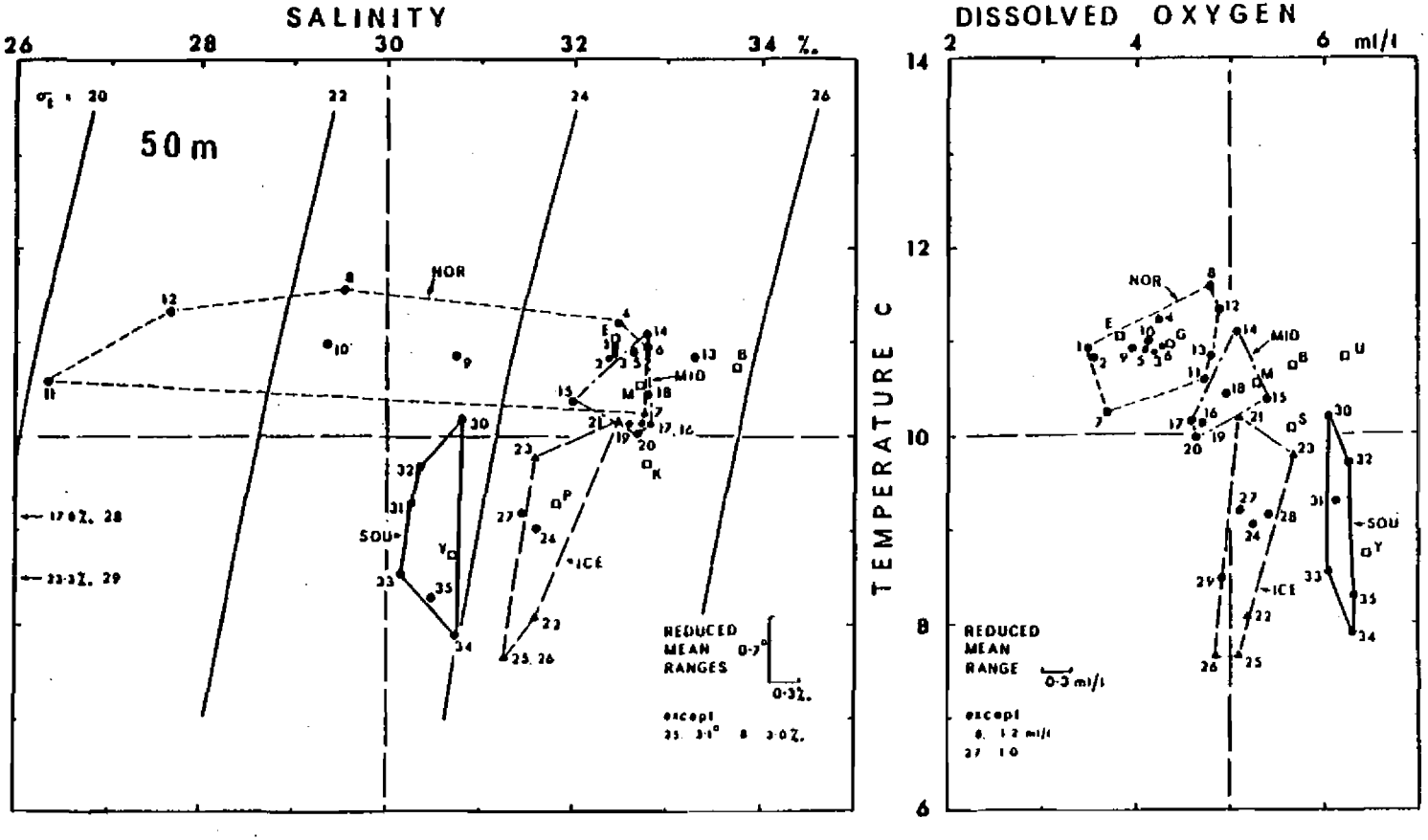


FIG. 9. Temperature-salinity and temperature-dissolved oxygen correlation plots for Chile inlets, Chile 70 cruise, 50 m depth.

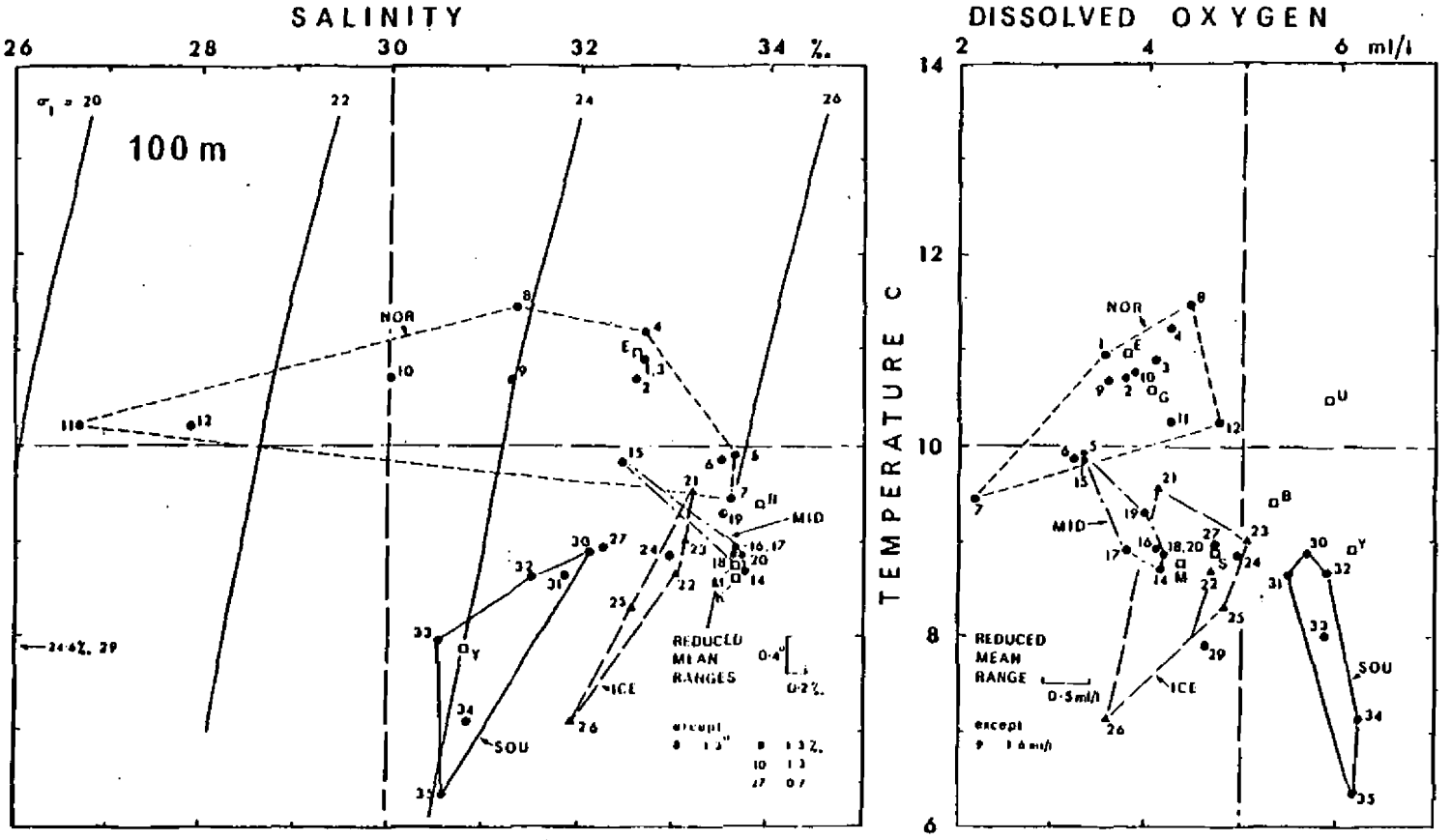


FIG. 10. Temperature-salinity and temperature-dissolved oxygen correlation plots for Chile inlets, Chile 70 cruise, 100 m depth.

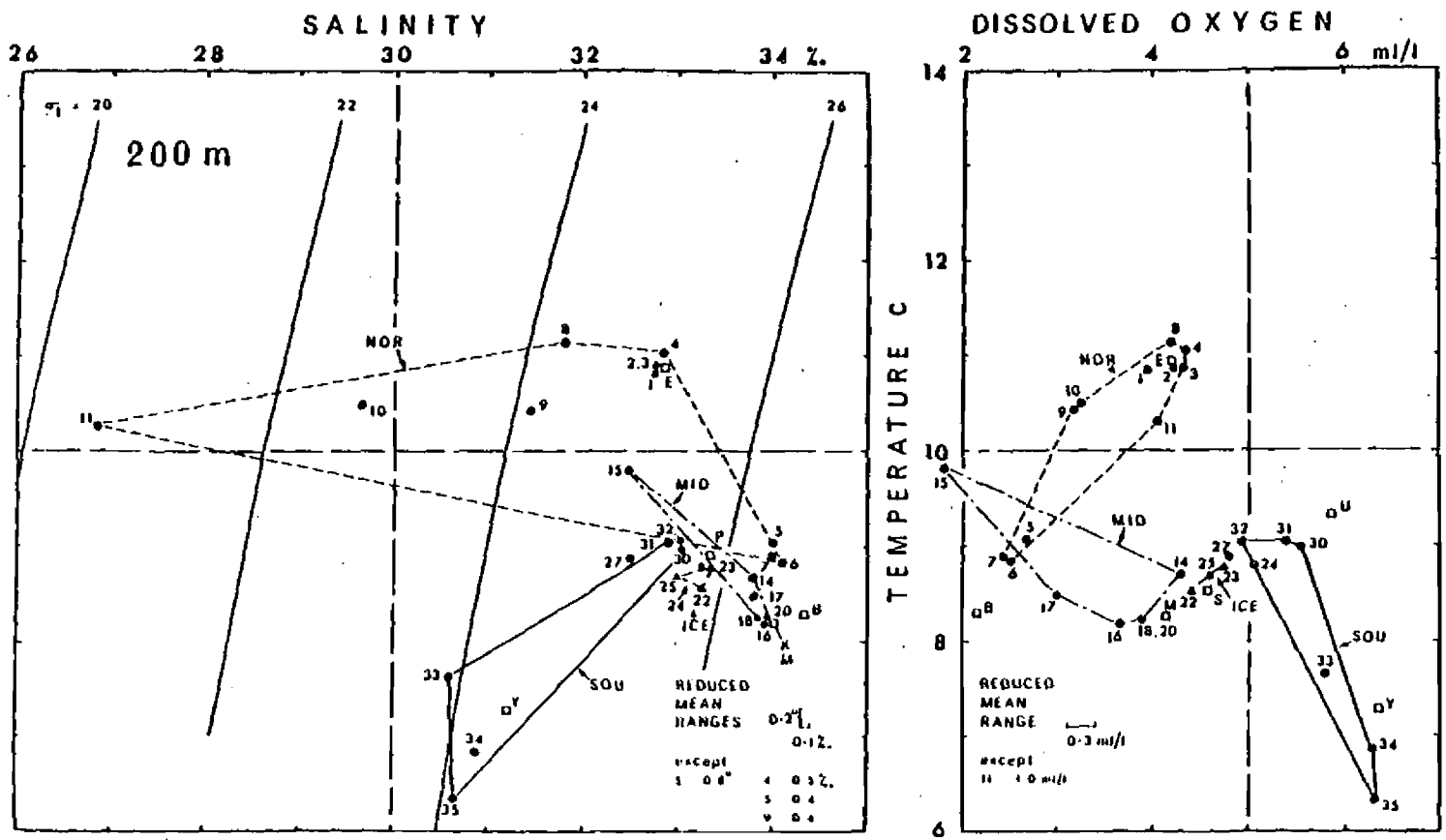


FIG. 11. Temperature-salinity and temperature-dissolved oxygen correlation plots for Chile inlets, Chile 70 cruise, 200 m depth.

TABLE 4. Surface and deep salinity values and salinity profile characteristics in inlets of Chile (Chile 70 cruise data).

		Salinity (‰)			Salinity–depth profile							
		Surface			Type			Depth of surface layer near inlet head (*m*)	Dimensions (*m*) 50%		90%	
	Inlet	Mo[a]	Hd[a]	Deep	Mo	Mi	Hd[a]		Mo	Hd	Mo	Hd
1	REL	26	4	32.8	2	2	1*b*	2	0	3	6	9
2	HOR	29	21	32.8	2	–	2	None	0	0	0	1
3	COM	30	28	32.9	2	2	2	None	0	0	0	<1
4	REN	31	28	32.9	2	–	2	None	0	0	0	<1
5	ELE.11–15	30	–	34.2	1*c*	–	–	–	0	–	10	–
6	JAC	29	24	34.2	1*c*	–	1*c*	7	0	6	23	14
7	PUY	22	16	34.0	2	2	1*b*	2.5	0	0.5	18	18
8	ELE 3–10	28	22	32.1	1*c*	1*c*	1*b*	7	0	0	8	7
9	AYS	24	4	31.4	2	2	2	None	0	1.5	13	12
10	QUI	27	20	29.7	1*c*	1*b*	2	2	0	0	0	4
11	FRA	18	7	26.9	1*b*	–	1*b*	1	0	2	10	12
12	PUE	–	20	27.9	–	1*c*	2	None	–	0	–	7
13	SQU	30	30	32.9	1*c*	–	2	None	0	0	0	0
14	JES	31	0	33.8	1*c*	–	1*b*	1	0	2	0	9
15	JUL	–	5	32.5	–	–	2	None	–	3	–	9
16	STE	1	4	33.9	1*b*	–	1*b*	3	4	4	20	20
17	MIT	1	<1	33.9	1*b*	–	1*b*	5	6	6	20	22
18,19	BAK	9	2	34.0	1*b*	1*b*	1*a*	3	2	4	11	25
20	NEF	3	–	33.9	1*b*	1*b*	–	–	3	–	23	–
21	ICE	3	–	33.3	2	2	–	–	3	–	22	–
22	EYR	10	6	33.4	2	1*b*	1*b*	8	2	6	19	22
23	EUR	10	<5	33.3	2	2	–	None	1	–	22	–
24	AND	21	<18	33.3	2	2	2	None	0	0	13	15
25	ASI	16	20	33.1	2	1*b*	2	None	0	0.5	22	25
26	PEE	–	9	31.9	–	–	1*b*	1	–	1	–	21
27	MON	23	<20	32.5	1*b*	1*b*	–	–	0	–	26	–
28	ULT	7	–	17.9	1*a*	1*a*	–	4	4	–	6	–
29	VAL	17	14	25.0	1*b*	–	1*b*	12	0	0	41	20
30	SWE	23	<7	33.2	1*b*	2	–	–	0	3	20	20
31	GAJ	24	20	33.1	1*b*	–	1*b*	10	0	0	28	28
32	XAU	28	22	33.2	1*c*	–	2	None	0	0	35	40
33	OTW	29	28	30.6	1*c*	1*c*	1*c*	45	0	0	0	10
34,35	ALM	30	28	30.8	1*c*	1*c*	1*c*	30	0	0	0	29

[a]Mo = mouth, Mi = middle, Hd = head of inlet.

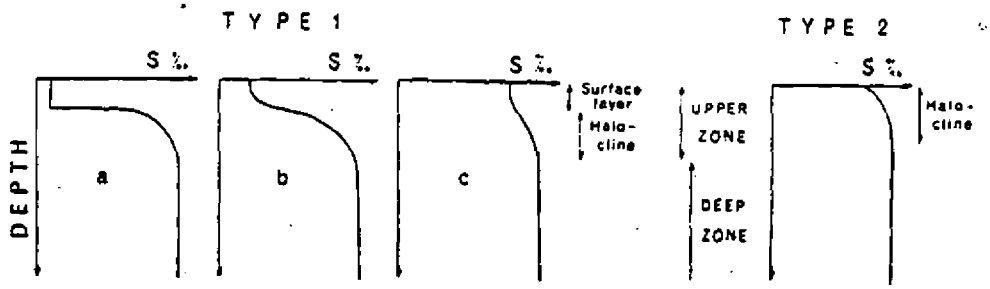


FIG. 12. Typical salinity–depth profile types in estuarine regions.

with strong wind conditions and was assumed to be real and due to evaporation at the surface. Later it was learned that the discharge for an evaporator, newly fitted for this cruise, occurred intermittently on the starboard side aft of where the water samples were taken and this must be assumed to be the cause for the high surface salinity values. The correlation with high wind conditions was probably real because the *Hudson* normally lies stern to wind on station and when the wind was strong enough and the surface layer density relatively high, some of the high salinity water discharged from the evaporator might not sink immediately and could contaminate the surface layer where the surface sample was taken.

Temperature–Depth Profiles

In contrast to the salinity–depth profiles, which generally showed an increase of salinity with depth, because salinity is the chief determinant of density in these waters, the temperature–depth profiles showed considerable variety in form. The basic one was of decrease of temperature with increase of depth but in many instances there were marked maxima and minima. The inlets having inflow of water from glaciers frequently had temperature–depth profiles with several maxima and minima.

Table 5 summarizes the information on temperature–depth profile types. These have been divided into two basic types: A, in which the temperature decreases monotonically with depth increase; and B, with one or more temperature maxima or minima. These have been divided into subtypes shown schematically in Fig. 13. For this purpose an extremum at the surface or bottom (e.g., in type A profiles) has not been counted as a maximum or minimum. The BT or STD records were used to determine the profile type; in the case of the B.3 type, this was the only way, as the maxima or minima were often so closely spaced that they would not be located when using a practical number of water bottles.

Table 5 has been arranged with the inlets in north to south order to show the tendency for types of profiles to group in geographical regions of the coast. The depth in meters of the upper isothermal layer in type A.2 profiles is shown in parentheses in the A.2 column of the table, and the maximum total number of maxima and minima in B.3 profile inlets is shown in parentheses in the B.3 column.

In identifying the temperature profile types on the BT or STD record, small scale maxima or minima (fine structure) of vertical dimensions less than 5 m were ignored. With this proviso it was found that in almost all instances the temperature–depth profiles in an inlet were of one type.

Temperature–depth profile types for the ocean and passage stations are shown by letters in Table 5 alongside the nearest inlet, and the information on possible glacier water contribution and ice occurrence has been repeated for convenience.

Dissolved Oxygen–Depth Profiles

The general trend in the dissolved oxygen–depth profiles was a decrease with depth from the surface. At the ocean stations there was a very pronounced subsurface minimum and a less pronounced deeper maximum; at the passage and inlet stations there were, in some instances, less pronounced maxima and minima in the profiles. The four basic types of oxygen–depth profile are shown schematically in Fig. 14, and Table 6 indicates the type of profile found at ocean, passage, and inlet stations.

At the ocean stations the oxygen–depth profiles (Type D) were characteristic of the south Pacific eastern boundary region and were significantly different from those for the passage and inlet stations. The major characteristic at the four ocean stations was a marked minimum of 2.0–3.9 ml/liter at 170–270 m depth, increasing to a maximum of 5.8–6.1 ml/liter at 550–600 m depth. A subsidiary minimum occurred at 30–50 m depth and a subsidiary maximum of 5.8–6.0 ml/liter at 80–100 m in some instances.

At the passage stations the surface values were generally slightly higher (5.5–7.5 ml/liter) than at the ocean stations (5.8–6.3 ml/liter) and below the surface the dissolved oxygen generally decreased, with most of the decrease in the upper 50 m. Most of the passage stations (type B) showed a slight oxygen minimum at 150–200 m where the value was 0.1–0.3 ml/liter less than that of the deeper water, and some of the passage stations (type C) in the middle region also showed a small oxygen maximum at 100 m or at 300–400 m. The deepwater oxygen values were generally 3.5–4.5 ml/liter in the northern and north middle region (stations E–P), 5.0–5.5 ml/liter in the south middle region (stations Q–T), and 5.5–6.5 ml/liter in the southern region (stations U–Y).

In the inlets the oxygen–depth profiles were similar to those at the passage stations, with surface values of 5.5–8.5 ml/liter and the main decrease extending over a greater depth to 50–200 m. Most of the inlets in the northern and southern regions had a minimum at 75–200 m (type B) where the values were 0.1–1.0 ml/liter lower than in the deeper water, whereas in the middle region the oxygen content generally decreased continuously to a uniform value in the deep water (type A). As in the passage stations, the deepwater values increased

TABLE 5. Types of temperature-depth profiles in Chile inlets, Chile 70 cruise. (Inlets by number, ocean and passage stations by letter.)

Temp profile type (see Fig. 13)						Glacial water inflow	Ice in water
A.1	A.2	B.1	B.2	B.3			
1 E	A(50)[a]						
2 F						V. small	
3							
4 G							
5	B(30)						
6							
	7(5)					Possible	
8							
9			9				
10	H(100)						
			11 I				
12	C(50)						
13							
J	D(55)	14				Yes	
				15(3)[b]		?	
				16(3)		Yes	
			17				
		18 K				Yes	Little
			19				
	L M(25)	20 N					
				21(3)	O(3)	Yes	Yes
	Q(20)			22(7)	P(4)	Yes	Much
				23(4)	R(4)	Yes	Yes
				24(3)			
				25(4)		Yes	Yes
		S		26(3)		Yes	Yes
		27 T				Yes	
				28(3)		Possible	
		29					
		V	30	30(5)	U(3)	Yes	
		W		31(4)		Yes	
				32(4)		Small	
X	33(3)						
Y	34(20)						
	35(20)					Yes	

[a]Depth in meters of upper mixed (isothermal) layer in type A.2 profiles.
[b]Number of maxima and minima, not counting top and bottom extrema, in type B.3 profiles.

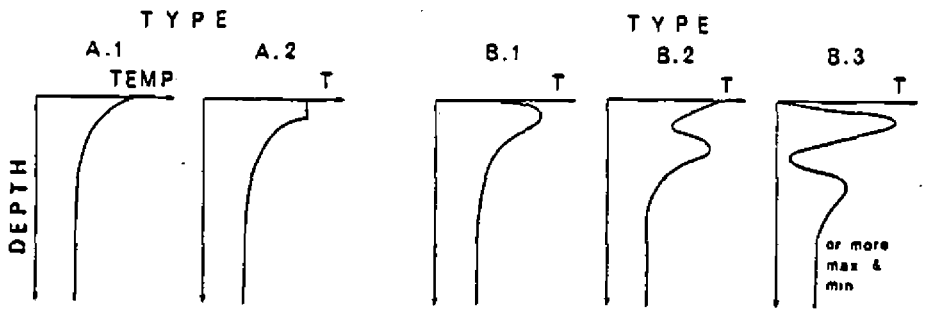


FIG. 13. Typical temperature-depth profile types in Chile inlets, Chile 70 cruise.

southward from 3 to 4 ml/liter in the northern and north middle regions, to 4.5–5.0 ml/liter in the south middle and 5.5–6.5 ml/liter in the southern region.

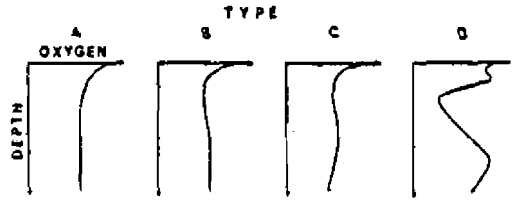


FIG. 14. Typical dissolved oxygen–depth profile types in Chile inlets, Chile 70 cruise.

TABLE 6. Types of dissolved oxygen–depth profiles in Chile inlets, Chile 70 cruise. (Inlets by number, ocean and passage stations by letter.)

Oxygen profile type (see Fig. 14)			
A	B	C	D
	1 E		A
	2 F		
		3	
G	4		
5		5	B
	6		
	7		
8	8		
	9	9	
10 H		10	
11	I	11	
		12	C
13			
14 J			D
15			
16			
17			
18 K		18	
19		19	
20 L	N	M	
21	O		
22	22	P,Q	
23		R	
24		24	
25		25	
26		S	
27	27 T		
28			
29			
	30 U		
31	W		
	32		
33	33	X	
	34 Y		
	35		

WATER PROPERTIES AT DEPTHS GREATER THAN 200 M

The depth of 200 m was selected as the maximum for the general display and comparison of water properties because there was information to this depth for more than 65% of the inlet stations (90% of the inlets). Values for 300 m or more were available for only 25% of the stations (only 40% of the inlets) and for 400 m or more for only 18% of the stations (only 23% of the inlets). In Table 7 are shown the changes in water properties beyond 200 m as the differences between the values at 400 and 200 m and between 600 and 200 m.

SECCHI DISC DEPTHS

Secchi disc depths were determined only at daylight stations, about 50% of the total, and as a result the distribution was rather irregular. However, they do show a broad trend, with the lowest average values in the north middle and iceberg inlet region and the highest in the north as follows:

	Inlets		Passage stations same regions	
	Mean & no. observations (*m*)	Range of values (*m*)	Mean & no. observations (*m*)	Range of values (*m*)
1 Reloncavi to 12 Puelma	6.3 (25)	0.5–11.5	7.8 (7)	3.5–12.5
14 Jesuitas to 26 Peel	2.1 (21)	0.1–7	1.9 (5)	0.8–8
27 Montanas to 35 Almirantazgo	5.0 (29)	0.5–9.5	7.1 (4)	6.5–9

The low values in the middle region (inlets 14–26) appeared to be due chiefly to very large amounts of glacial silt in the water.

Ocean stations B, C, and D were taken at night and no secchi depths were measured; at ocean station A off the north of the inlet region the secchi depth was 11 m. At seven ocean stations west and north of the inlets, in transit to Valparaiso after the inlet section of the cruise, the secchi depths were from 6 to 17 m, averaging 12 m.

Discussion

GEOGRAPHICAL DISTRIBUTION OF WATER PROPERTIES

The T–S correlation plots suggest groupings among the inlets. The data for the inlets in the northern region (inlets 1–12 in Fig. 7–11) form one group on the plots, whereas those for the

TABLE 7. Properties of deep water in inlets of Chile expressed as change in property from 200 to 400 m or from 200 to 600 m depth.

		Temp (C)		Salinity (‰)		Dissolved O^2 (*ml/liter*)		No. stations	
		200–400 m	200–600 m	200–400 m	200–600 m	200–400 m	200–600 m	200–400 m	200–600 m
				Ocean stations					
A	SPA4	−2.29	−3.21	+0.07	+0.05	+0.85	+1.73	1	1
B	GUA	−2.24	−3.29	−0.08	−0.11	+2.38	+3.48	1	1
C	ANN	−2.21	−3.07	−0.05	−0.07	+2.31	+3.26	1	1
D	TRE	−1.92	−2.55	+0.02	+0.01	+1.84	+1.94	1	1
				Passage stations					
L	MIL	−0.25	−0.40	+0.07	+0.11	0	−0.30	1	1
M	MID	−0.23	−0.40	+0.07	+0.11	−0.11	−0.40	1	1
O	ICY	+0.04		+0.12		+0.30		1	0
P	WID	−0.10	−0.23	+0.07	+0.09	−0.13	−0.25	1	1
Q	TRI	−0.14	−0.09	+0.10	+0.12	+0.10	+0.09	1	1
S	SAR	−0.23	−0.28	+0.10	+0.11	+0.24	+0.16	1	1
U	MAG	−0.98		+0.11		+0.12		1	0
V	SEA	−0.61	−0.66	+0.23	+0.23	+0.14	+0.19	1	1
W	LON	−0.43	−0.45	+0.23	+0.25	−0.08	0	1	1
Y	FAM	−0.16		+0.12		+0.08		1	0
				Inlets					
1	REL	0		+0.05		+0.25		2	0
3	COM	+0.10		+0.24		−0.56		3	0
5	ELE	0		+0.05		−0.17		1	0
6	JAC	−0.20		+0.03		+0.22		2	0
18	BAK	−0.23	−0.29	+0.07	+0.09	−0.04	−0.15	5	2
22	EYR	+0.05		+0.11		+0.18		1	0
24	AND	+0.03		+0.06		−0.39		2	0
25	ASI	0		+0.05		−0.09		1	0
30	SWE	−0.63		+0.17		+0.32		3	0
32	XAU	−0.41	−0.60	+0.23	+0.23	+0.31	+0.52	2	1
33	OTW	−0.25		+0.06		+0.20		1	0
35	ALM	+0.40		+0.12		−0.05		2	0

southern region (inlets 30–35) form a separate group at lower temperatures and with a much smaller salinity range below the surface (referred to again below). The north middle region inlets overlap the temperature range for the north and south regions at most depths, but have a much smaller salinity range below the surface, and the iceberg inlets form a separate group at most depths.

The temperature of the upper waters in the northern group of inlets is 3–5 degrees C higher than in the southern group and the average temperature difference in the surface water of the ocean outside the north and the south entrances to the passages and inlets is about 4.5 degrees C (Sverdrup et al. 1946, charts II and III, and USSR Ministerstvo Oborny 1953, charts 17 and 18). These differences correspond closely to the mean air temperature difference of 5 degrees C between the north and south (Fig. 6), suggesting that climatic conditions control the temperature in the upper waters. Below the surface layer the temperature difference between north and south decreases to only 2 degrees C at 20 m and less than 3 degrees C at 100 m and deeper. The properties of the subsurface waters (below about 20 m) in the inlets are probably determined more by those in the passages outside them (and these by the ocean water characteristics outside) than by the local climate. This suggestion is supported by the fact that the inlets that had glacier ice in them form a subgroup of the middle region with generally lower temperatures at the surface, and possibly at 5 m, but

the direct effect of the ice in reducing the surface temperature does not appear to extend much below 20 m depth.

The larger salinity range for the northern group of inlets than for the southern is because the former includes, toward the head of Elefantes (8), several inlets that are remote from the ocean source of water and are separated from it by relatively shallow sills.

On the T–O_2 plots, the northern and southern inlet group data points and the iceberg inlet (subgroup) data points form separate groups at all depths except 5 m (not shown here), whereas the remaining middle group inlets have properties intermediate between those for the northern and southern group. The separation on the T–O_2 plots is more marked than on the T-S plots: at all depths from 50 m and deeper, the northern, north middle, and southern inlet T–O_2 points fall into distinct groups with some overlap at 200 m due to Estero Julian (15), which has the lowest oxygen content of the inlets studied. The gradient of temperature from north to south contributes to this separation, as it does in the T-S plots, but the ranges of oxygen content emphasize the distinction between groups more than do the ranges of salinity.

Characteristic Diagrams

Although the T-S and T–O_2 correlation plots display the value of these water properties at set depths over the whole inlet region, they do not describe the water mass properties as a function of depth at specific locations. To investigate the relations between the water masses in the inlets, those in the passages, and those in the ocean, T-S and T–O_2 characteristic curves were drawn from the mean values for each inlet. These curves are too numerous to present independently here and become confusing when plotted together. Therefore, selected T-S and T–O_2 curves for the ocean and passage stations are shown in Fig. 15*a* and 16*a* and for the inlets in Fig. 15*b* and 16*b*.

T-S Diagrams

In Fig. 15*a*, six T-S curves have been chosen to represent the 4 ocean and 21 passage stations, and in Fig. 15*b* nine curves represent the 35 inlets. The group of stations or inlets represented by each curve is indicated on each figure. Curve B is taken to represent the ocean source water outside the passages and inlets. It is realized that the ocean water off the coast is likely to vary in properties with time as is evident from the differences between the T-S (and T–O_2) curves, even for the close-in stations B, C, and D, taken within a period of 1 week during this cruise. However, stations taken in 1967 from the U.S.N.S. *Eltanin* (Anon. 1969) in the vicinity of the present ocean station B (Guafo) show very similar T-S (and T–O_2) characteristics to those observed in 1970. It is particularly regretted that time did not permit taking ocean stations off the southern part of the coast (south of 47°S).

All the inlet water T-S curves are on the low salinity side of the ocean water curve and the differences in salinity between the inlet and ocean waters decrease with increasing depth, suggesting that the deep water of the inlets at the time of this survey had resided there long enough to suffer dilution by downward diffusion of fresh water from the river runoff and ice melt in the upper layers. The high salinity represented by curve 7 on Fig. 15*b* may indicate a recent inflow of ocean water to these three inlets, the mouth of Elefantes (5) and Jacaf (6) and Puyaguapi (7), which open in to it, as these three are close to the ocean.

There is no identity of deepwater properties in the passages with those in the ocean outside (Fig. 15*a*), and the limiting depth of exchange is therefore not immediately apparent. However, if one assumes that exchange between ocean and passages is predominantly along isopycnal surfaces, then the maximum density water in the passages (e.g., station M) must come from depths of less than 200 m in the ocean, probably 100–150 m, indicating the effective sill depths. This depth range is consistent with what can be determined from the charts.

A conspicuous feature of the passage station T-S curves is the considerable difference between the two for stations X and Y, the most easterly in the Estrecho de Magallanes, and all the remainder. (A corresponding difference in deepwater characteristics between inlets 33, 34, and 35, and the remaining inlets is evident.) Depths on the charts indicate a sill depth to the west of passage station X of more than 100 m but the differences in T-S (and T–O_2) curves between the neighbouring passage stations (W and X) on either side of the sill suggest a shallower depth. It is suggested that the source water for inlets 33, 34, and 35 (Otway and Almirantazgo) comes from the Atlantic through the eastern entrance to the Estrecho de Magallanes, whereas that for all the other inlets comes from the Pacific, or that the water in the eastern part of the Estrecho de Magallanes is sufficiently isolated by the sills at west and east that it can retain characteristics permanently modified by local conditions.

The progressive change in T-S curves along the northern region, indicated by those for inlets 2, 7, 9, and 11, emphasizes the effect of increasing distance from the ocean toward the head of Elefantes (8).

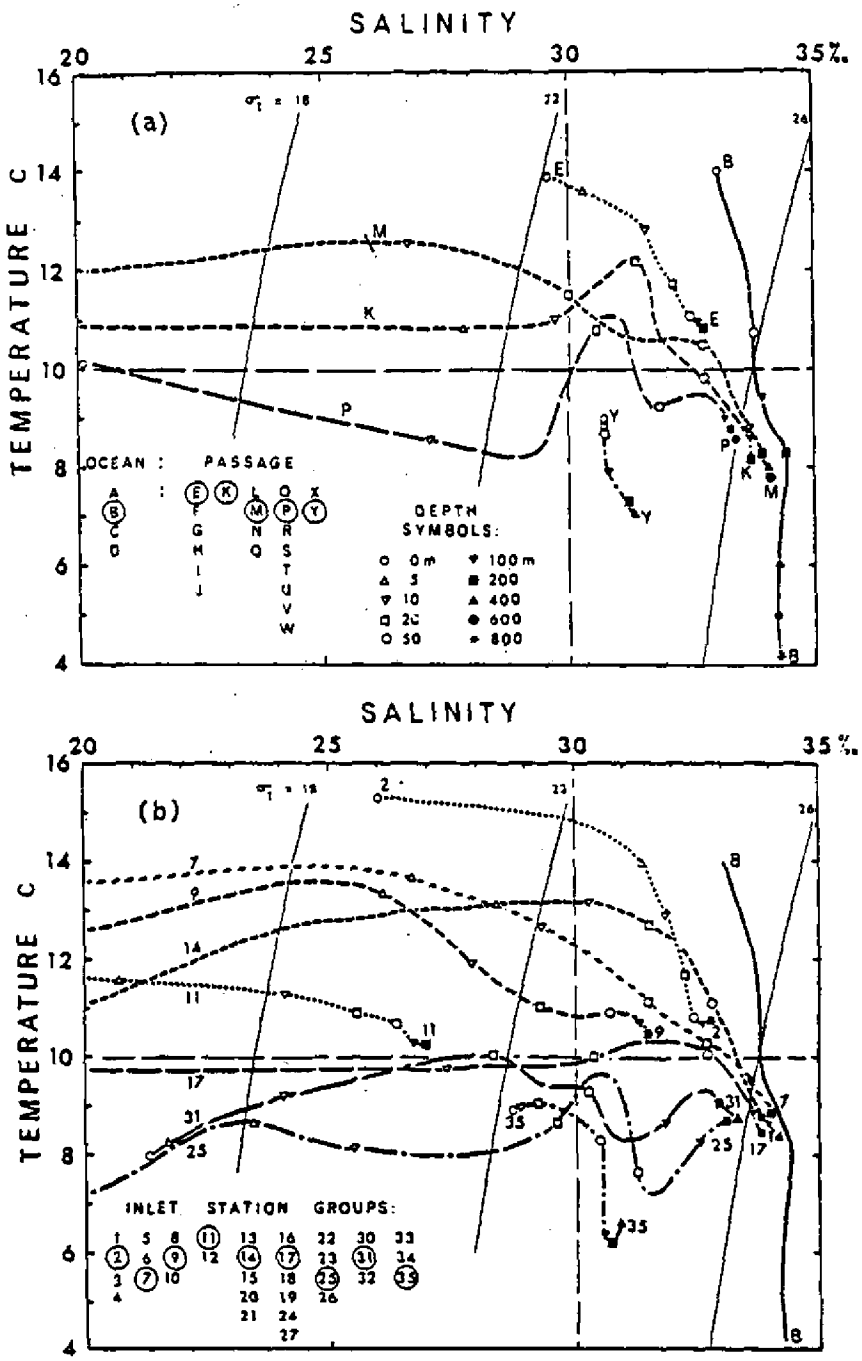


FIG. 15. Selected temperature–salinity diagrams to represent (*a*) ocean and passage stations, and (*b*) inlet stations, Chile 70 cruise. The group of stations or inlets best represented by each curve is shown on the figures with the type station circled.

Another dividing sill in the middle region is at the Angostura Inglesa between passage stations N and O (exemplified in Fig. 15*a* by curves for stations M and P).

T-O_2 Diagrams

It was more difficult to select typical T-O_2 curves than T-S curves, probably because some trend and possible separation is affected by the fact that the latter two properties determine density, which, as a rule, is arranged in an orderly fashion by gravity, but dissolved oxygen content does not significantly affect density. Figure 16*a* shows the T-O_2 curves selected to characterize the ocean and passage waters. For the inlets, the best that could be done was to draw envelopes of T-O_2 curves for groups of inlets (Fig. 16*b*). These groups were suggested by geographical position, and by the relation of inlets to passage stations.

A sequence of inlet and passage station characteristics, similar to the geographical sequence demonstrated by the T-S and T-O_2 correlation plots for constant depths, is again evident. The T-O_2 characteristic curves in the passages (except X, Y) show some similarity to ocean water characteristics above the oxygen minimum, which is a feature of the Pacific waters off South America and is at about 200 m depth close to the coast of southern Chile.

Deeper Water Properties

At the ocean stations the water temperature continued to decrease below 200 m (Table 7) because the main thermocline continued to below 800 m here, but the salinity changes were small and variable in sign because the salinity reached a weak maximum at about 250 m (from bottle casts and STD records). The oxygen content increased below 200 m because the oxygen minimum occurred at about 150–200 m. In the passages, the salinity increased with depth, the differences being larger than in the ocean, which is consistent with the passage water coming from well above the salinity maximum outside, i.e., from depths of less than about 200 m.

In the inlets the salinity increased with depth beyond 200 m. The temperature generally decreased with depth with the larger decreases being in the southern group (e.g., 30 and 32) at the west end of the Estrecho de Magallanes. These observations in the passages and inlets are consistent with the observed property distributions in the ocean, but the relatively large increase in oxygen content with depth in the southern inlets appears inconsistent with the water coming from depths of less than 200 m outside where the oxygen generally decreased to this depth. However, at some ocean stations (e.g., Guafo, B) there was a subsidiary oxygen minimum at 30 m and a maximum at 75–100 m. This gave rise to an increase in oxygen content with depth in the upper layer, which is probably the source of the inlet waters and could explain the increase with depth found inside if it is typical of the ocean water off the southern coast.

Comparison between the Inlets of Chile and those of British Columbia and Alaska

Geographic features

If the northeast Pacific inlets (British Columbia and Alaska) are combined as a group, then their mean length and width are almost the same as those studied in Chile, but, as seen in Table 1, the Chile inlets fall between the British Columbia and Alaska ones as separate groups. In depths the three regions are similar in mean values.

In Table 1, 14 inlets each in Chile and in the northeast Pacific are listed as having glaciers that definitely or probably contribute melt water. This number is believed to be the total in the northeast Pacific but maps and charts indicate that there are probably twice as many in Chile as the 14 studied during this cruise. Also, there are undoubtedly others than the six studied in Chile that have glacier ice in their waters. The indirect and direct influence of glaciers on the oceanography of the inlets is greater in Chile than in the northeast Pacific.

Water properties

The data obtained on water characteristics during the Chile 70 cruise are compared, by means of T-S and T-O_2 envelope diagrams, with data obtained by the University of British Columbia in the inlets of British Columbia and Alaska. In a previous paper, Pickard (1967, fig. 17) compared the waters of the latter two regions by means of such diagrams, which showed the envelopes of the points representing the combinations of mean values of these properties along inlets. It was shown that the waters of the southern British Columbia inlets, which are the lowest latitude group in the fjord coast of the northeast Pacific, were generally warmer and less saline than those of northern British Columbia, whereas the properties in the Alaska inlets overlapped the latter group but extended to slightly lower temperatures and higher salinities. The inlets with glacier ice in the water (occurring only in Alaska) formed a separate class with intermediate salinities but distinguished from the others by generally lower temperatures.

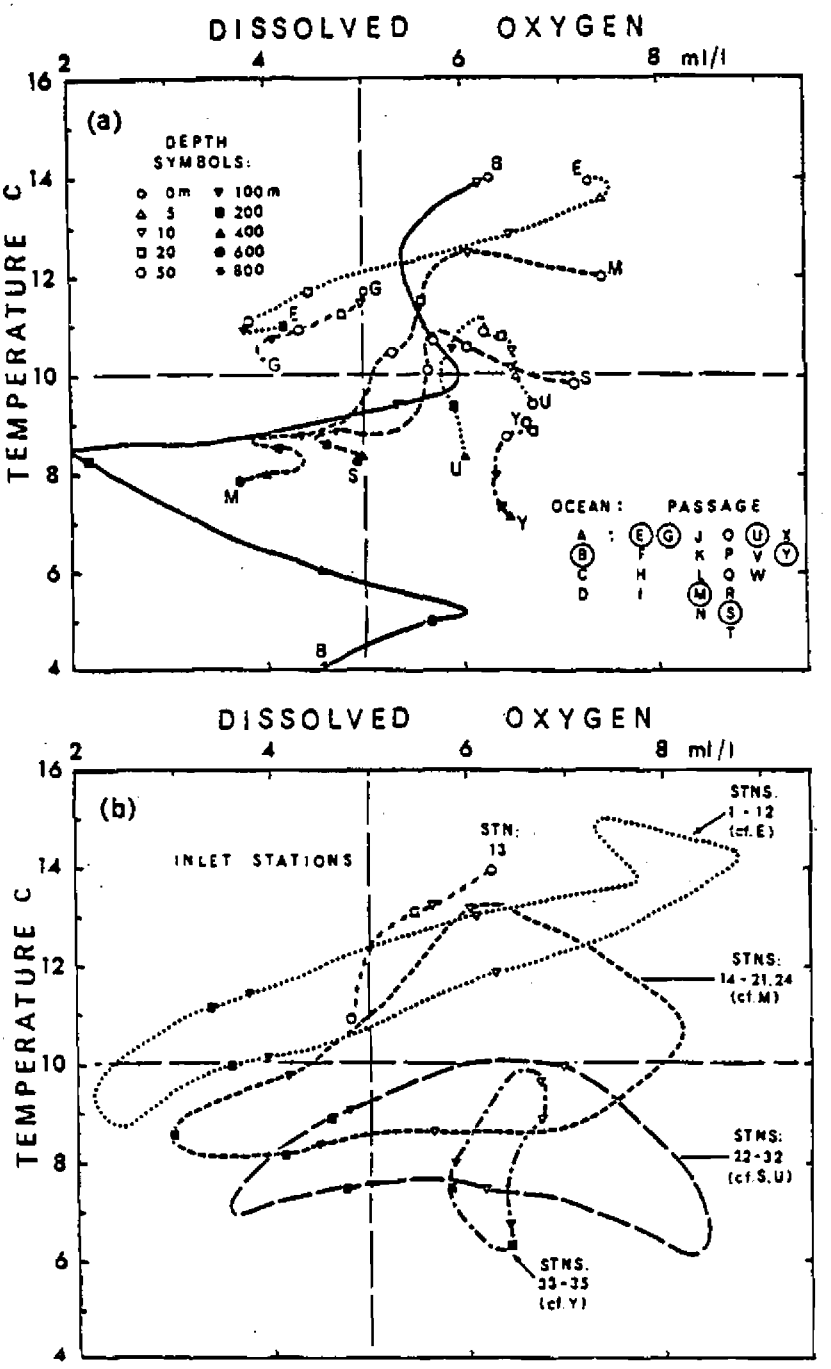


FIG. 16. (*a*) Selected temperature–dissolved oxygen curves to represent ocean and passage stations, and (*b*) envelopes of temperature–dissolved oxygen curves for groups of inlets with an indication of average depth at 10, 100, and 200 m, Chile 70 cruise.

For comparison with the Chile inlets, T-S and T-O_2 envelope diagrams are shown for the surface, 20-, 50-, 100-, and 200-m depths in Fig. 17–19. Note that in Fig. 17 the ranges of temperature, salinity, and oxygen are different from those in the other two figures. The northern British Columbia group, which is similar to the Alaska group, has been omitted to simplify these diagrams and the British Columbia data have been brought up to date to 1969. When the Chile and the British Columbia/Alaska regions are being compared, it should be remembered that, as these are in opposite hemispheres, the northern Chile and southern British Columbia inlets are the lower latitude groups, whereas the southern Chile and Alaska groups are the higher latitude ones (Fig. 1). In addition, the latitude ranges for the southern and northern hemisphere groups are not the same, the Chile inlets being generally about 6° lower in latitude than the British Columbia/Alaska ones (see Fig. 18). The southern British Columbia inlets, group A, are smaller ones in the extreme south and have shallow sills, which account for the lower salinities and higher temperatures in this group.

When the envelopes are being compared, it should also be noted that although the Chile data are from a single cruise in the early fall, the British Columbia/Alaska data are from as many as 10 cruises per inlet from 1951 to 1969, although only summer data have been used for the present diagrams. Therefore, if some of the British Columbia/Alaska data envelopes are larger than Chile ones, this may be attributable to year-to-year variations introducing additional scatter.

In Fig. 17, for the surface (or near-surface values for oxygen in some British Columbia inlets where surface values were not available) the temperature scale covers 3–20 C, salinity from 0 to 35‰, and oxygen from 5 to 11 ml/liter. In temperature, the most obvious feature is that the southern British Columbia group covers a larger range than the northern Chile group, although the latter extends over a larger latitude range (5.5° of latitude compared with 3°), but this may simply be a result of there being more data for British Columbia. The mid-Chile group with a latitude range of only 1.5° covers a larger temperature range than does the more extensive northern Chile group, but has a lower mean temperature for a lower latitude than the southern British Columbia group. The southern Chile group has a small temperature range and a lower mean value than for the Alaska inlets, although the former are at 4° lower latitude on the average. The Chile iceberg inlets are colder at the surface than the Alaska ones.

In salinity at the surface, the lower latitude inlets in both hemispheres have a full range of values from near zero to 30‰, whereas the higher latitude group values are in the upper half of this range, except for the Chile iceberg inlets, which are much less saline than the Alaska ones. The latter is taken as a significant difference between the two regions, as the Alaska data were collected at a comparable time of year during or just after the maximum river runoff.

In oxygen values at the surface, the Chile and British Columbia/Alaska inlets have about the same mean values, but the Chile iceberg inlets have

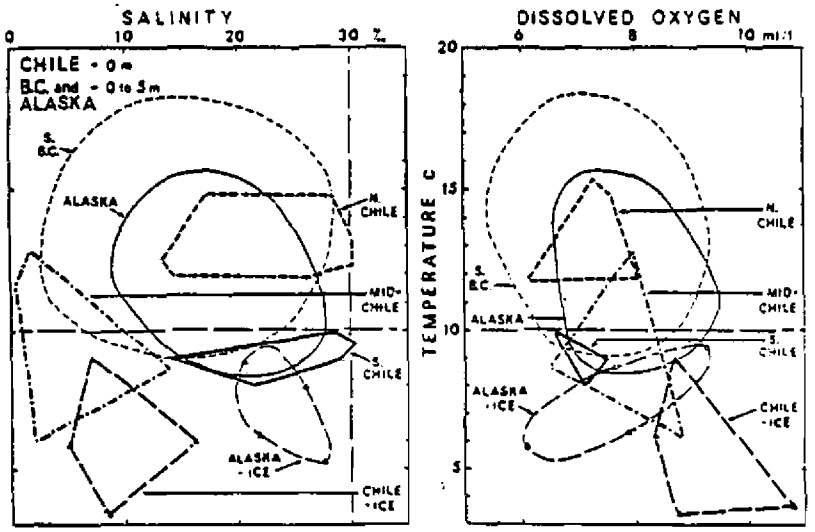


FIG. 17. Envelopes of temperature–salinity and temperature–dissolved oxygen characteristics for Chile and for British Columbia/Alaska inlets, surface or near surface values. ("ICE" denotes inlets with icebergs.)

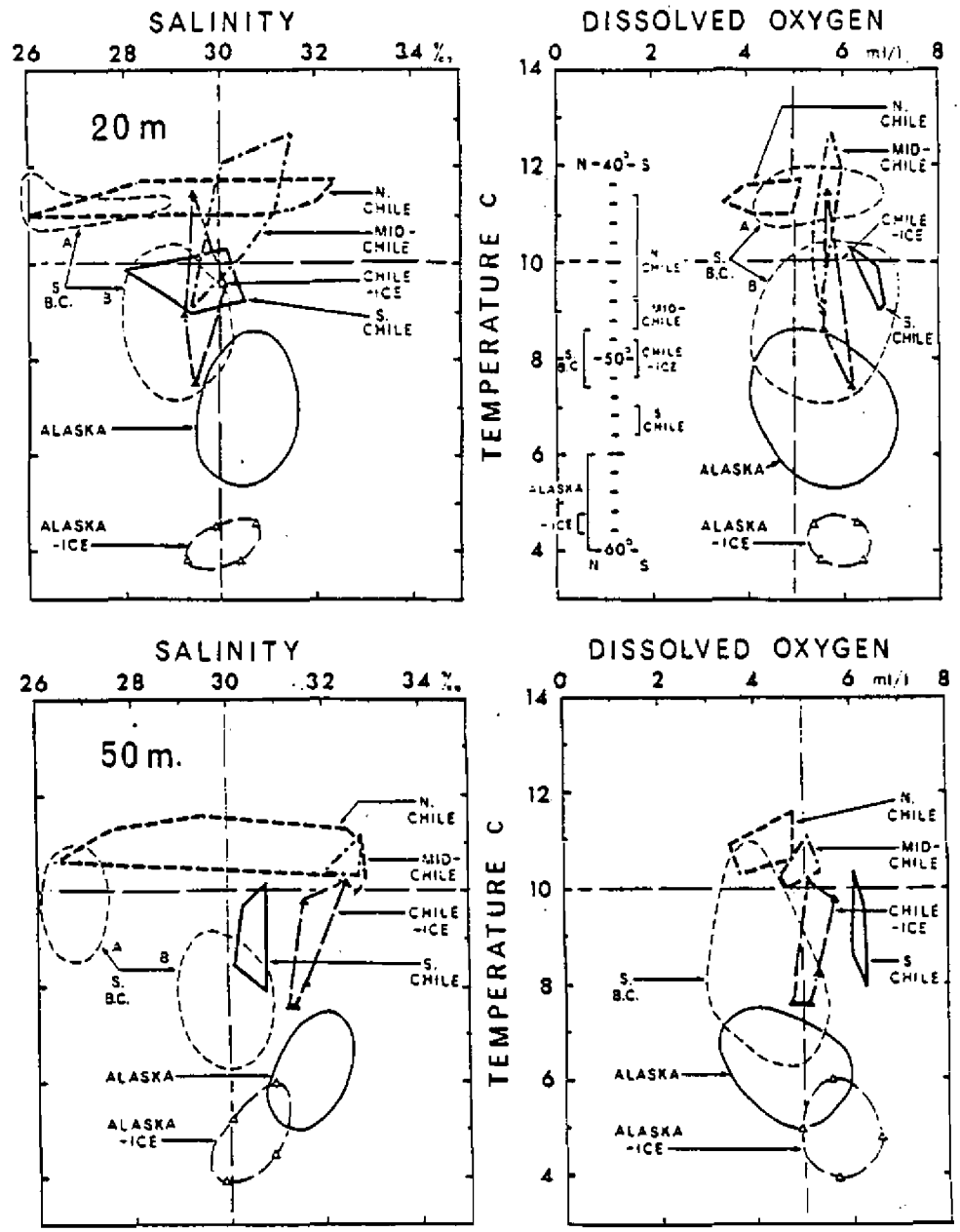


FIG. 18. Envelopes of temperature–salinity and temperature–dissolved oxygen characteristics for Chile and for British Columbia/Alaska inlets, 20 and 50 m depth. ("ICE" denotes inlets with icebergs.)

higher values than the Alaska ones. (The suggestion has been made that the higher silt content of the water in these inlets than in Alaska might influence the measurement by the Winkler method, but no specific reasons are suggested.)

For the subsurface levels, I will first compare the water properties individually, referring to Fig. 18 and 19, in which the temperature range is reduced to 3–14 C, salinity to 26–35‰, and oxygen changed to 0–8 ml/liter. The temperatures of the northern and mid-Chile inlets are highest, the temperatures in the southern British Columbia inlets (at 48–52°N) are similar to those in the southern Chile ones (at 52–54°S), and the temperatures in the Alaska

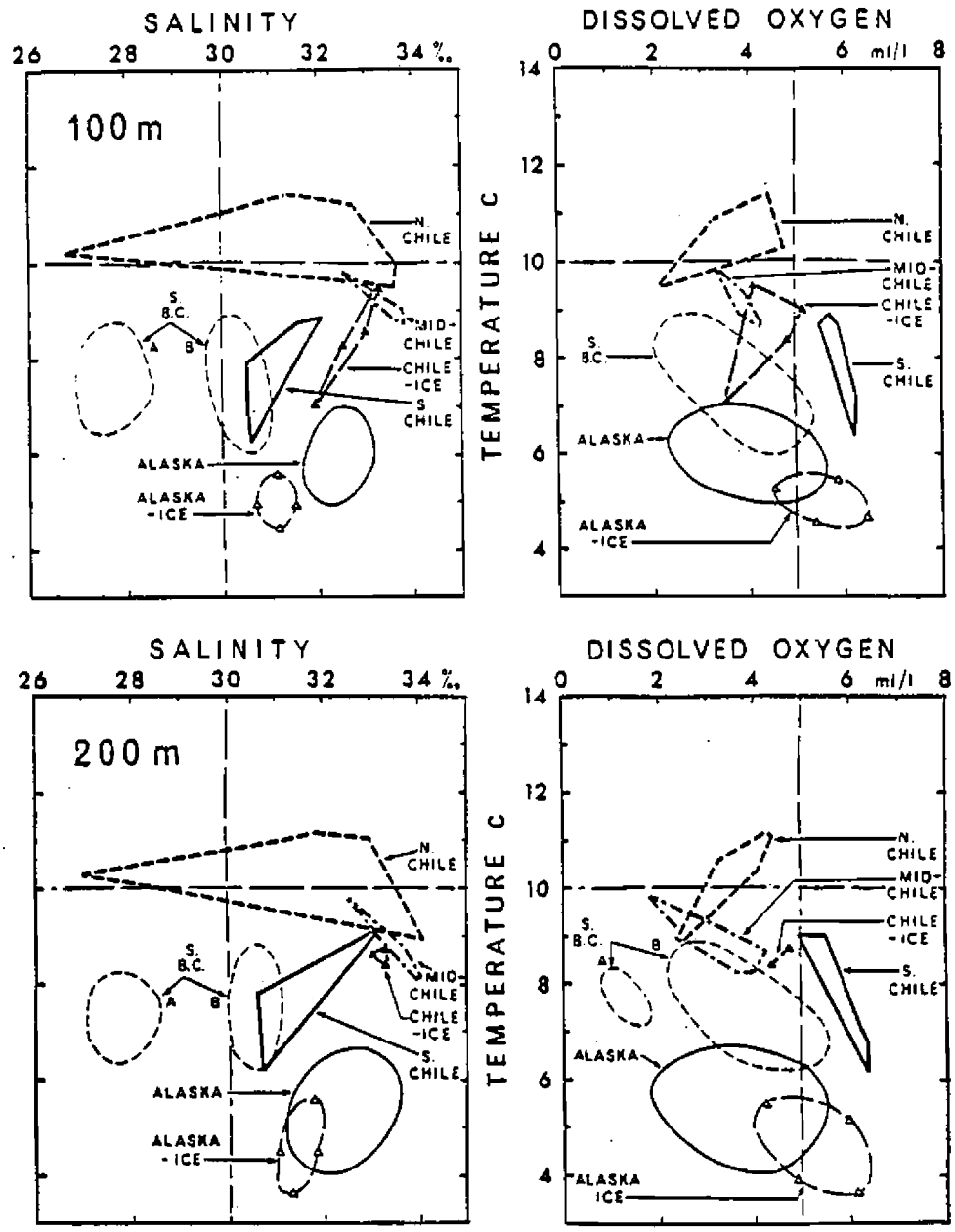


FIG. 19. Envelopes of temperature–salinity and temperature–dissolved oxygen characteristics for Chile and for British Columbia/Alaska inlets, 100 and 200 m depth. ("ICE" denotes inlets with icebergs.)

inlets are lower than these by 2–3 degrees C. In contrast to the surface situation the Chile iceberg inlets at 48–51°S are warmer by 4–5 degrees C than the Alaska ones at 57–59°N. Below 20 m depth the ranges of temperature for the groups compared above are substantially the same, except that above 200 m the Chile iceberg inlets show a larger range of temperatures than the Alaska ones.

The salinities below the surface for the northern Chile group (one-third of the total) extend over a range of 6.5‰, encompassing the values for all the other Chile inlets and almost all the northeast Pacific ones. This large salinity range is chiefly due to the low values in the inlets 10, 11, and 12

toward the head of the long Elefantes system (inlets 5 and 8). In contrast, the mid-Chile group, which has more direct and deeper connection with the Pacific, has a salinity range of 2.5‰, or less.

The oxygen content below the surface has the same overall range of values in Chile as in British Columbia/Alaska to 100 m depth; below this, a few of the British Columbia inlets have lower values (to less than 1 ml/liter) than observed anywhere in Chile. A tendency for oxygen values to increase with latitude in Chile is the other feature of this region.

Now I use the characteristic diagrams for their main purpose, to display the combinations of properties that occur. At the surface, the T-S combinations are so diverse that the envelopes overlap for most of the regions, both north and south of the equator. The exceptions are the iceberg inlet envelopes, both for T-S and T-O_2, which are distinct from the other groups and distinct between Chile and Alaska, and the southern Chile envelopes, which are at the lower end of the temperature range of the Chile noniceberg inlets.

At 20 m there is some overlap between the T-S envelopes for the four Chile inlet groups, but deeper than this they are substantially distinct. For T-O_2 the envelopes for the contiguous mid-Chile and iceberg groups overlap at 20 m but are distinct at most greater depths. The T-S envelopes for the Chile inlets are separate from those for British Columbia/Alaska because both the temperature and salinity values are generally higher in Chile, and the T-O_2 envelopes are separated chiefly because of the higher temperatures in Chile. The temperature and salinity differences between the Chile inlets and the British Columbia/Alaska ones below the surface are in the same directions as the values in the ocean outside to about 200 m (Fig. 20). There is no apparent correlation in dissolved oxygen content for which the range of values in the two inlet regions is much the same, although the ocean water outside Chile has lower oxygen values in the upper 200 m than that outside British Columbia/Alaska.

Secchi disc depths in the inlets in Chile and in the northeast Pacific have the same range of values from a fraction of a meter near sources of glacier runoff to 10 m or more in the outer passages. A notable exception was that in Baker (18) secchi depths of only 1 m (due to glacial silt) were observed up to 80 km from the melt-water inflow, whereas in the northeast Pacific such low values are not found more than 15–20 km from the inflow. The Baker system was also a region of much lower plankton concentration than elsewhere and of few birds (field observations during Chile 70 by B. McK. Bary and R. B. Brown respectively).

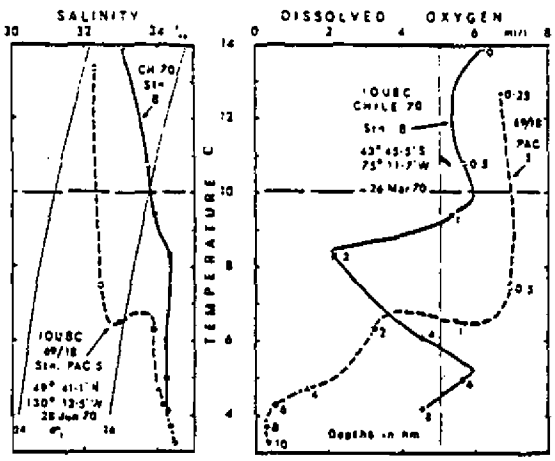


FIG. 20. Temperature–salinity and temperature–dissolved oxygen curves for typical ocean stations off Chile and off British Columbia.

Conclusions

The Chile 70 cruise included 32 inlets of 15–300 km length, averaging 66 km, in the mainland and Tierra del Fuego coasts of southern Chile. From the charts it is estimated that there are at least another 35 inlets of 15 km or more length in these coasts and 50 or so of 15 km or more length in the islands west of the mainland coast. This count does not include passages that open at both ends to the sea. Of the unstudied inlets, the largest (Skyring) approaches 100 km length, 10 are of 40–50 km length, and the rest are shorter. Although the studied inlets comprise only about one-half of the total in the mainland coast, they do include the majority of the longer ones and I venture to suggest that they provide a representative picture of the inlet characteristics of the mainland coast of Chile.

As determined during the Chile 70 cruise, this picture is of a typical fjord or deep estuary coast, with a basic two-layer water system of a shallow low-salinity layer over more saline deep water, the upper-layer low salinity being due largely to river runoff. The direct effects of the glaciers in contributing rock flour and icebergs to the water are more extensive in Chile than in British Columbia/Alaska, and complicated temperature structures in glacier and iceberg inlets are a feature of the Chile coast. From charts and maps, it is estimated that as many as 15 more Chile inlets than the 15 studied may have significant glacier water runoff and possibly 5 of these may have glacier ice in addition to the 6 studied.

Stagnant basins are uncommon and this may well be another feature of the Chile inlets. The absence of shallow sills is the main reason for this

in the inlets studied. A potentially interesting region, which was not practical to study during Chile 70, is the deep basin in the west end of Skyring Water (northwest of Otway, inlet 33) where there are depths of 600 m or more. The sill depth from Otway is about 10 m but there is a narrow and shallow connection at the west to Gajardo (31) with reported strong currents that might bring in saline water to refresh the deeper layers.

In the islands off the mainland coast the majority of the inlets appear to have direct connection to the ocean waters outside, and this, together with the small watersheds and small stored runoff areas, suggests that these bodies would generally have higher salinity water, close to oceanic values, and lack the low salinity surface layer characteristic of the estuarine structure of the inside inlets.

Suggestions for future studies of the physical oceanography of the inlets in Chile include: (1) observing at different times of the year in selected typical inlets to determine the variations in water properties through the year; (2) devoting particular attention in this respect to the glacier inlets to determine the reasons for their complex temperature structure; (3) comparing the seasonal variations in the inlets with glacier water runoff only, such as Steffen (16), with those having icebergs as well, although the latter will present serious difficulties unless a vessel strengthened against ice is available; (4) extending observations to the unexplored mainland inlets as opportunity offers: (5) gathering information on river runoff and precipitation, particularly in the middle coast region, to relate to the freshwater distribution in the inlets as indicated by the salinity decrease below that of the ocean source water; (6) examining a selection of the inlets in the islands to see if they have any unanticipated characteristics.

Acknowledgments

I express my thanks to many organizations and individuals who made this study possible: to the Director, Atlantic Oceanographic Laboratory, Marine Sciences Branch, Canada Department of Energy, Mines and Resources, for making time available to the University of British Columbia for this investigation in Chile during the *Hudson* 70 Expedition; to the Chilean Government for permitting us to make these detailed oceanographic investigations in their inshore territorial waters and for their assistance in making arrangements for the cruise through Capitan R. Herrara, Director, Instituto Hidrografico, Armada de Chile and Sr H. Sievers, Head, Centro Nacional de Datos Oceanograficos de Chile; to the Chilean scientists who took part in the cruise and assisted in the physical oceanographic observations (Prof H. Inostroza, Drs L. Chuecas and F. Rey, Srs R. Montaner, B. Uccelletti, and N. Silva); to Drs W. V. Burt and G. S. Pond of Oregon State University for their assistance during the cruise; to Mr I. W. Duedall of the Marine Ecology Laboratory, Fisheries Research Board of Canada, for making available facilities for determining dissolved oxygen and nutrients and taking part in the field work; to Mr P. Wadhams (A.O.L.) for computing on board; to Mr J. Pilote (A.O.L.) for all the hydrographic sounding; to Dr B. McK. Bary (U.B.C.) as Assistant Chief Scientist; and particularly to Mr M. P. Storm of this Institute for preparing the field equipment, being responsible for the salinity determinations, and for assembling the data report. Especially, I thank Captain D. W. Butler, Master, C.S.S. *Hudson*, and his officers and crew for their generous assistance in all phases of the field work and for their skill in handling the ship and boats, particularly in confined and incompletely surveyed waters. The support of the National Research Council through Grant A.5091 is gratefully acknowledged.

ANON. 1952. Sailing directions for South America, Vol. 2, 3. 5th ed. Publ. H.O. 24, U.S. Naval Oceanographic Office, Washington, D.C. 380 p.

1968. Mapa geologico de Chile. Instituto de investigaciones geologicas, Chile.

1969. Physical and chemical data from the SCORPIO Expedition in the south Pacific Ocean, U.S.N.S. Eltanin Cruises 28 and 29, 12 March–31 July 1967. Scripps Institution of Oceanography, Woods Hole Oceanographic Institution and Massachusetts Institute of Technology, S.I.O. Ref. 69-15.

MS 1971. Chile 70 Cruise, 1970. Inst. Oceanogr. Univ. British Columbia Data Rep. 31: 49, fig. 1.

CARRITT, D. E., AND J. H. CARPENTER. 1966. Comparison and evaluation of currently employed modifications of the Winkler method for determining dissolved oxygen in seawater: a NASCO report. J. Mar. Res. 24: 286–318.

PICKARD, G. L. 1961. Oceanographic features of inlets in the British Columbia mainland coast. J. Fish. Res. Bd. Canada 18: 907–999.

1963. Oceanographic characteristics of inlets of Vancouver Island, British Columbia. J. Fish. Res. Bd. Canada 20: 1109–1144.

1967. Some oceanographic characteristics of the larger inlets of southeast Alaska. J. Fish. Res. Bd. Canada 24: 1475–1506.

REED, W. W. 1929. Climatological data for southern South America. U.S. Weather Bur. Dep. Mon. Weather Rev. Suppl. 32: 23 p.

SVERDRUP, H. U., M. W. JOHNSON, AND R. H. FLEMING. 1946. The oceans, their physics, chemistry and general biology. Prentice-Hall Inc., New York, N.Y. 1087 p.

USSR MINISTERSTVO OBORONY. 1953. Morskoi Atlas. Tom II. Fiziko-geograficheskii. Moscow. Izdaniye glavnogo shtaba voennomorshikh sil. 76 charts.

Water Structure in Chilean Fjords

G. L. PICKARD

Institute of Oceanography, University of British Columbia,
Vancouver 8, B.C., Canada

Abstract

In 1970 a physical oceanographic study was made in 32 fjord inlets of the Chilean coast; the results have been summarised in the Journal of the Fisheries Research Board of Canada (Pickard, 1971). The water in the Chilean inlets has an estuarine structure resulting from river run-off much of which is melt water from glaciers. In the inlets studied the density is mainly determined by salinity which decreases in the upper layers as one proceeds up the inlets from the ocean. The deep waters indicate that the outer sill depths on the shelf are 75 to 150 m deep; within the inlets there is little horizontal change in temperature or salinity of the deep waters along the inlets except where there are sills. Inland of these the deep water is less saline and cooler than to seaward.

A major feature of the Chilean inlets is that many of them have glaciers descending to tidewater, and icebergs floating in the water.

The temperature and salinity structures are relatively simple in the northern and southern extremities of the fjord region but in the middle zone the temperature profiles show maxima and minima which are most marked in the inlets with glacier ice in the water. It is suggested that the temperature structure is partly a result of winter cooling giving a primary minimum at 75 to 100 m depth, together with a secondary minimum due to continuing *in situ* cooling below the surface by the icebergs in the water or at the glacier face in the inlet.

INTRODUCTION

The first systematic study of the oceanographic characteristics of the fjord inlets in the south coast of Chile was made in March 1970 during the *Chile 70* cruise of the Institute of Oceanography of the University of British Colombia as Phase V of the Canadian *Hudson 70* Round-the Americas Expedition. The primary purpose of *Chile 70* was to determine some of the physical oceanographic characteristics of the region in order to enlarge our knowledge of fjord estuaries and to compare the Chilean fjords with other geographically similar regions. As time was limited and the area is extensive, occupying over 1000 miles of Chile's coast, it was only possible to carry out a water sampling programme in a selection of inlets, and no current measurements were made.

A general review of the physical oceanographic results of *Chile 70* has been published (Pickard 1971) and some characteristics of the north American inlets have been described in earlier papers (Pickard, 1961, 1963, 1967) which contain further references.

GEOGRAPHICAL CHARACTERISTICS OF THE REGION

The Chilean fjord region (fig. 1) extends from about 41° S to 55° S along the Pacific coast of South America. The mainland (inner) coast has at least 67 inlets of 15 km or more length, with the Andean Cordillera 50–100 km to the east. Off the mainland coast are a large number of islands forming the (outer) Pacific coast, and these have at least 50 inlets of 15 km or more length. During the *Chile 70* cruise, observations were, with one exception, limited to the mainland coast inlets because our interest is chiefly in the estuarine bodies of water, i.e., those which have access to the ocean and have significant river run-off. There is undoubtedly some run-off into the inlets in the large islands but it is assumed to be much less than that into the mainland inlets. During *Chile 70*, samples were taken in 32 of the inlets from Almirantazgo at 54.5° S, in Tierra

Oceanography of the South Pacific 1972, comp. R. Fraser. New Zealand National Commission for UNESCO, Wellington: 1973.

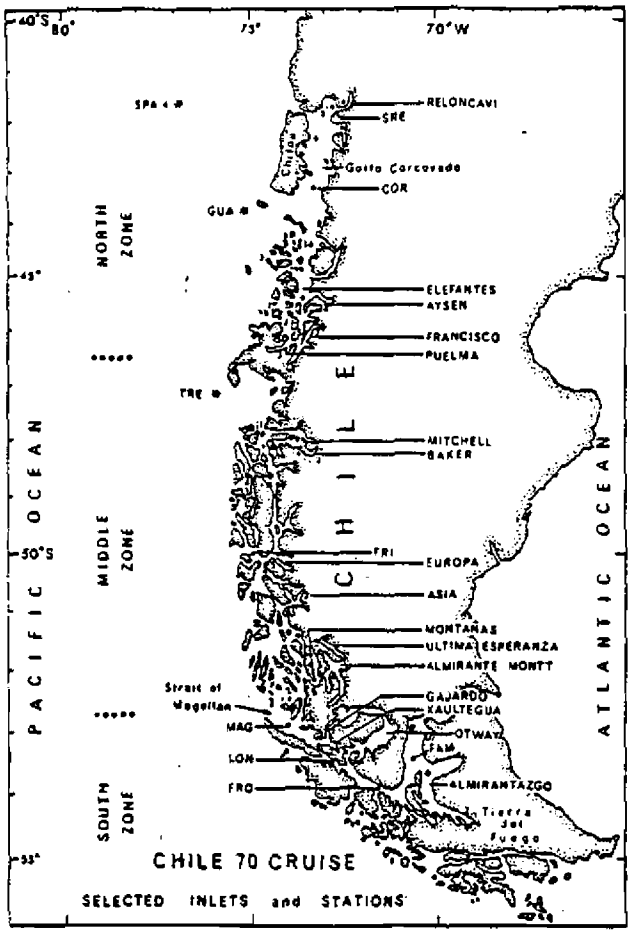


FIG. 1. Coast of southern Chile with inlets and stations referred to in this paper.

del Fuego south of the Strait of Magellan, to Reloncavi at 41.5° S at the northern limit of the fjord coast.

In local topography the north and south American fjord inlet regions are similar, the sides of the inlets being steep above and below sea level, particularly in the middle zone in Chile. The inlets studied had lengths from 9–300 km (average 66 km), average widths from 0.8–15 km and depths to 1050 m (average 265 m). These dimensions are generally similar to those of the inlets in British Columbia/Alaska in the north American Pacific coast. In both regions very shallow sills which could lead to stagnation of water in isolate basins are not common.

In two respects the Chilean region differs from Britis Columbia/Alaska. Firstly, in Chile the Andes for a barrier east of the coast and relatively close to it s that the catchment area for precipitation on land t form the rivers is much smaller than in the nort American region where many large rivers flowing int the inlets drain extensive areas inland of the coa mountain range. Secondly, in Chile there are more ir lets (at least 11) where glaciers extend to water leve and contribute icebergs to the estuarine waters com pared to only 4 in Alaska and none in British Columbia Probably at least 30 in Chile have significant run-o from glaciers which descend to or close to sea level.

The *Chile 70* cruise was carried out in autum (March). Precipitation data show a June maximum o about twice that during March in the north but n marked seasonal variation along the rest of the coast The mean air temperature reaches a maximum in Jan uary everywhere and so river run-off due to snow melt, probably most significant in the middle and south thirds of the coast, may be expected to be a maximum some 2 or 3 months before the *Chile 70* cruise took place. In the north American inlet coast the maxi mum average rate of summer meltwater run-off is typically two or three times the annual average. In the absence of any other systematic oceanographic in formation for the Chilean region, it is assumed tha the run-off of fresh water into the inlets at the time of the *Chile 70* cruise was about one half of the annua maximum and that the accumulation of fresh water in the inlets at the time was probably greater than the annual average.

In oceanographic characteristics the coast may be divided into three main zones, the North, Middle, and South as shown on fig. 1. The oceanographic observations were made at stations in the inlets themselves, in the passages between the mainland coast and the islands, and in the ocean off the coast. As the various topographic terms in the inlet names, such as "canal", "estero", "estuario" do not appear to have any oceanographic consistency, the various inlets will be referred to by their proper name only, e.g., as "Reloncavi", "Baker", etc. The oceanographic station identifiers use the first three letters of the inlet name and a number starting from the inlet head, or simply the first three letters for passage and ocean stations.

WATER STRUCTURE

Conventional water sampling techniques were used with temperatures measured with Richter and Wiese thermometers, salinity with an Autolab Inductive Salinometer, and dissolved oxygen by a modified Winkler procedure. In addition, a Bissett-Berman Model 9060 Self-contained Salinity/Temperature/Depth Recorder was used, and proved an extremely valuable adjunct, both providing completely independent records of temperature and salinity and also facilitating the preparation of water property profiles and T-S diagrams. Both of these features were particularly useful in a region from which no previous records were available.

TEMPERATURE/DEPTH STRUCTURE

The feature to which this paper is particularly directed is the temperature/depth structure of which there are basically two types as shown in fig. 2. Type A shows a monotonic decrease of temperature with depth, with or without a surface mixed isothermal layer, while type B shows a series of temperature maxima and minima below the surface with the surface value being either greater than or less than the deep water value. The more extreme examples of this second type were found in the inlets having considerable quantities of glacier

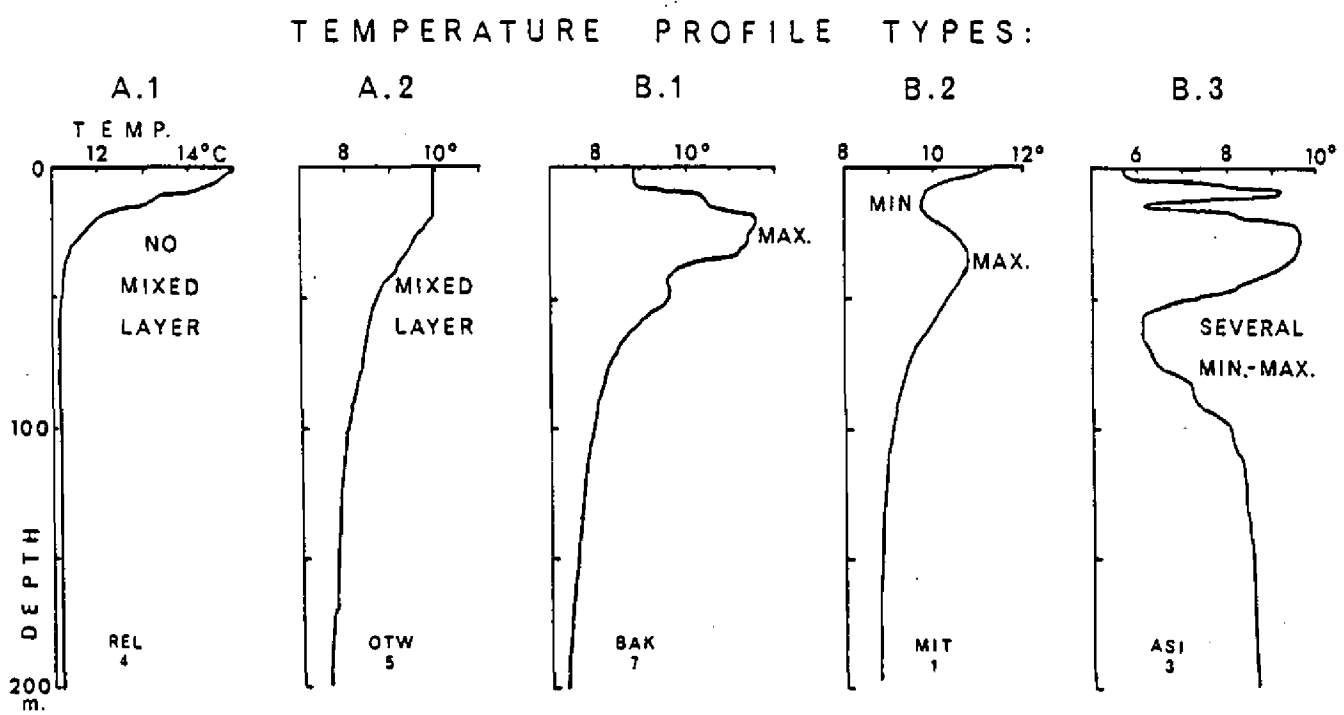


FIG. 2. Examples of temperature/depth profile types in Chilean inlets.

ice in the water toward the inlet head. However, because the density structure and stability in this type of estuary are determined chiefly by the salinity distribution, rather than by temperature, the water structure will be examined through the T-S diagrams so that all three characteristics, temperature, salinity, and density may be considered together.

Note that in all the T-S diagrams (figs 3 to 10) the salinity scale is compressed below 20‰.

SOUTH PACIFIC OCEAN WATER

Nine stations were taken at or beyond the 1000 m isobath off the inlet coast to obtain some information on the ocean waters which are the source of the inlet saline waters. The ocean stations showed characteristics typical of the eastern boundary region. For the stations just off the shelf there was a decrease in salinity of 1.3–2.3‰ between the surface and 200 m and then little change to 800 m (e.g., GUA in fig. 3 and TRE in fig. 5), while for those further off shore the increase was only 0.3–0.5‰ (e.g., SPA 4 in fig. 3). The temperature showed a mixed layer to 60 m and then a clear thermocline down to 4°C at 800 m. The dissolved oxygen showed the usual marked minimum at 200–250 m, the minimum values being 2–3 ml/l compared to 6 ml/l above and below.

INLET WATER CHARACTERISTICS

The salinity distribution was basically an estuarine two-layer one with an upper layer of a few metres depth of lower salinity water over a more saline deep layer. In most of the inlets the salinity reached 90% of the deep water value by 10–20 m depth; in about one-third of the inlets the halocline started at the surface, so that an isohaline upper layer was less common than in the North American inlets. Combined with the higher surface salinity values in Chile, this suggests that the freshwater run-off in Chile is less than in British Columbia/Alaska.

The temperature distribution in the North Zone showed a maximum value at the surface and a decrease with increasing depth, in some cases from an isothermal upper layer (e.g., types A.1 and A.2 in fig. 2). However, in most of the inlets in the Middle and South Zones of the coast maxima and minima occurred in the temperature/depth profile, with the surface value generally being a minimum (types B.1, B.2, and B.3 in fig 2).

The dissolved oxygen profiles showed a decrease from values of 6–11 ml/l at the surface to 2–6 ml/l in the deep water. In general the oxygen content was lower in the north and higher in the south, possibly suggesting more vertical circulation in the south.

T-S DIAGRAMS

In the following description a selection of inlets will be used to typify the water characteristics in the various regions.

Fig. 3 shows the successive modifications of ocean water, starting from an ocean station SPA 4 about 200 km off shore to a station just off the shelf (GUA) and proceeding to the north through the Golfo Corcovado between the mainland and the large island of Chiloe. At passage station COR the bottom water (175 m depth) corresponds to that at about 70 m depth at the ocean station GUA. At passage station SRE the salinity has been reduced to 28‰ while at stations up the inlet Reloncavi (REL 4 and 1) the further decrease in salinity due to river inflow is obvious, although it must be pointed out that in the North Zone, the modification is limited to the upper 20 m. The water structures in the other inlets in this area between 41° and 43° S are similar. Typically of fjord inlets the deep water has only a small range of values of temperature and of salinity along each inlet, provided that there are no isolating sills.

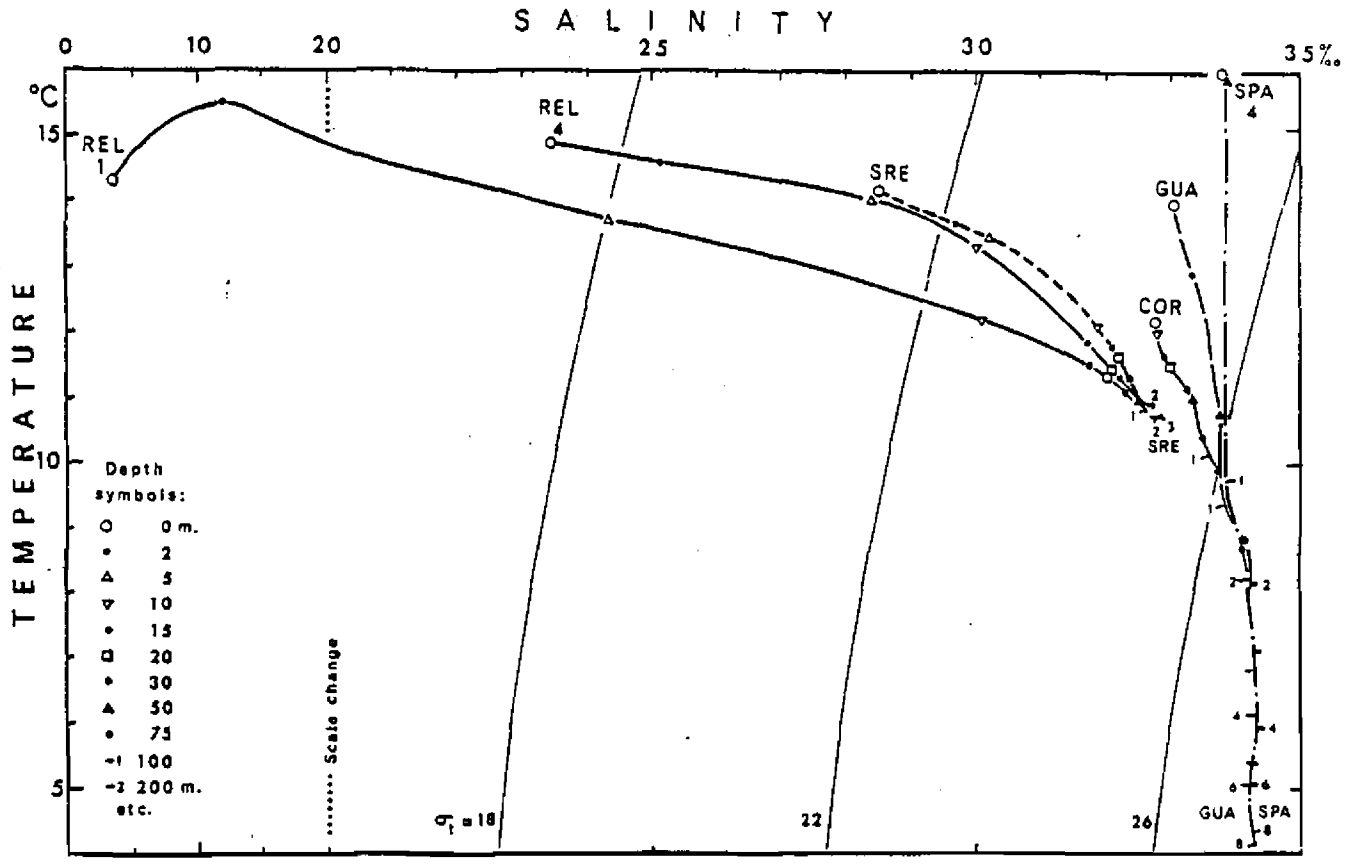


FIG. 3. Temperature/salinity curves for stations in North Zone, northern part.

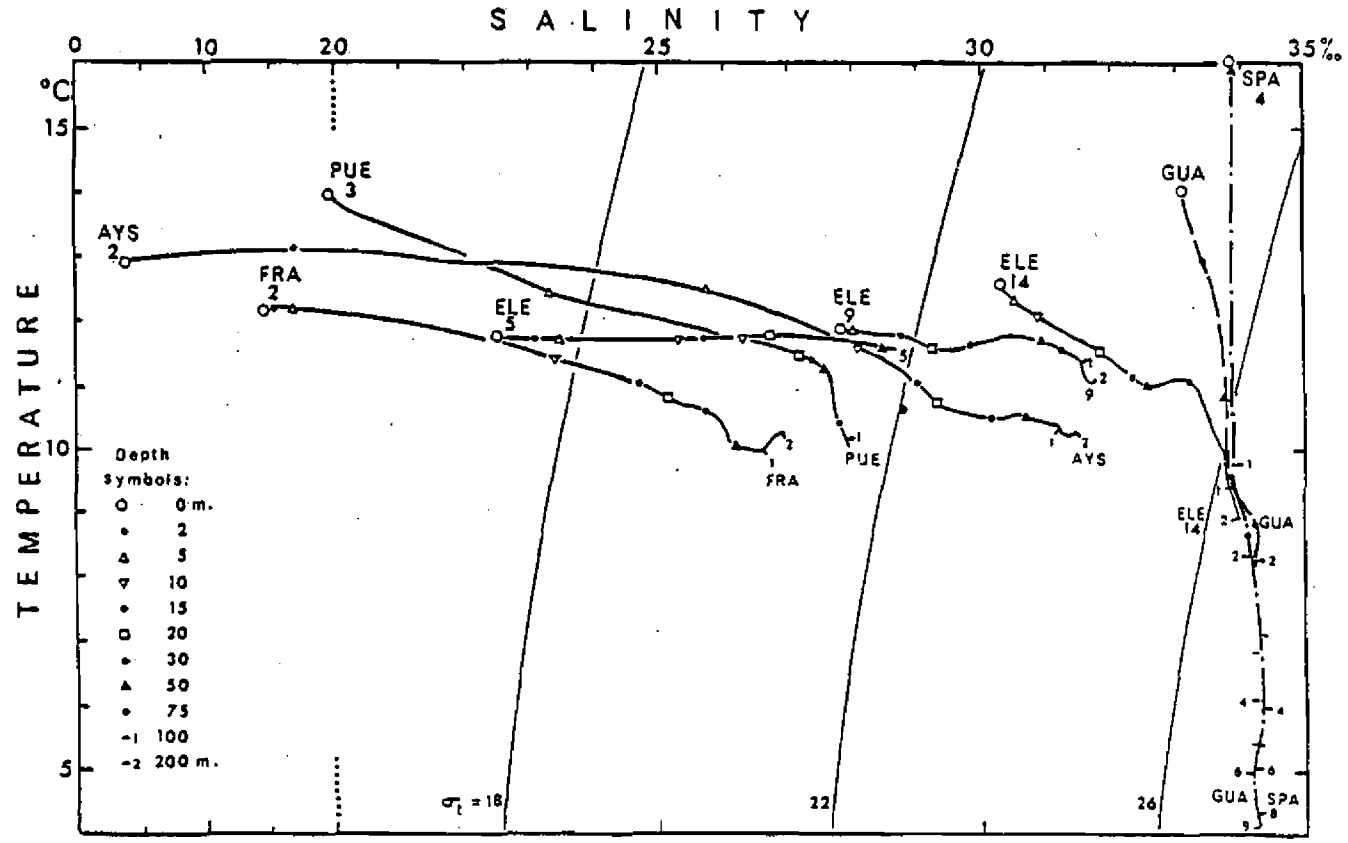


FIG. 4. Temperature/salinity curves for stations in North Zone, southern part.

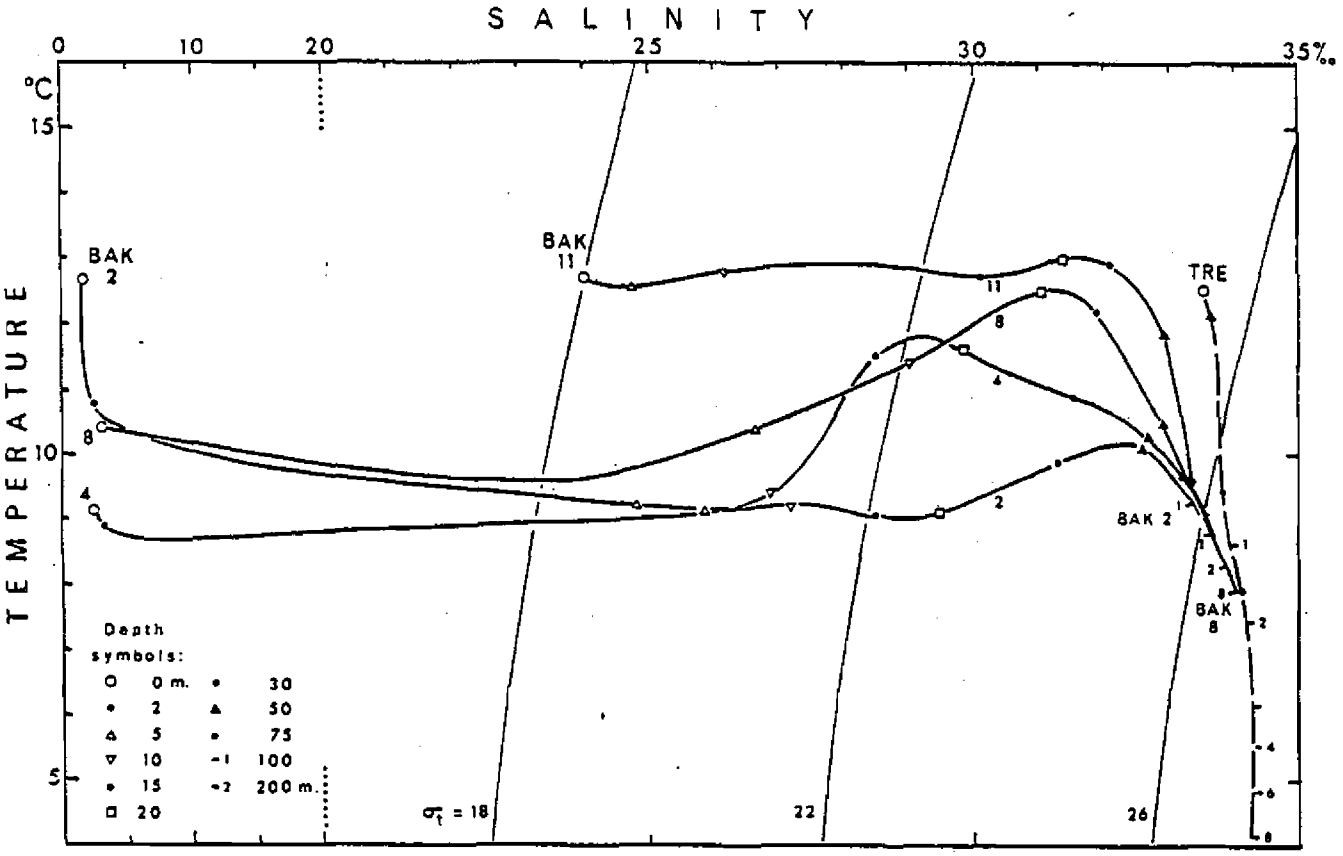


FIG. 5. Temperature/salinity curves for stations in Middle Zone, northern part.

Fig. 4 shows the successive modification from the same ocean stations (SPA 4 and GUA) but in the southerly direction through the narrower inlet system of Elefantes and Francisco, and in several side inlets. The deep water (200 m) at the first inlet station, ELE 14, is almost identical to that at 120–130 m at GUA. Further inland a succession of sills occurs. Across these the deep water salinity decreases from 31.9‰ at ELE 9 to 28.8‰ at ELE 5, and to 27‰ at FRA 2. This progressive decrease in salinity is greater than in the group of inlets to the north. The cause may, in part, be due to greater river run-off but is probably largely due to the isolating effect of the sills. The step-by-step decrease in the successive basins inland is evidence that there must be significant downward mixing of fresh water despite the commonly accepted characteristic that in highly stratified estuaries the mixing process between the upper and deep layers results chiefly in an upward movement of saline water into the upper layer (and thence out of the inlet) with very little downward mixing of fresh water.

The water characteristics in two side inlets, Aysen (AYS) and Puelma (PUE) are also shown to lie on the T-S diagram in positions corresponding to their geographic location along Elefantes. The former has a large river emptying into it while the latter is on the outer coast side with only small streams running into it.

Fig. 5 shows the first stage in the development, in the Baker inlet system, of the characteristic feature of the Middle Zone T-S curves which show a progressive decrease in salinity away from the ocean (station TRE), as in the North Zone, but with mid-depth temperature maxima and minima. Along Baker, in contrast to Elefantes, there are no significant sills and the deep water retains a high salinity along 90% of its length, almost within the precision of measurement. However, the upper 50 m shows significant modifications as seen for inlet station BAK 11 near the mouth through stations 8 and 4 to 2 which is close to the head of the inlet and inland of the main river run-off. The characteristics within the inlet are very low surface salinities and a subsurface temperature maximum at 20–40 m depth.

Fig. 6 shows a more pronounced temperature maximum/minimum structure in Europa, where there was a considerable amount of ice in the water; it also shows T-S curves for the water at the nearest passage station outside (TRI) and for the ocean at station TRE.

Fig. 7 shows the most extreme development of the temperature maximum/minimum structure observed during this cruise. This was in Asia. Station ASI 2 was the innermost station sampled, with station 4 being about mid-inlet and station 6 at the mouth where the inlet connected with the inside passage. Other inlets with icebergs in the Middle Zone, south of Baker, also showed this type of water structure.

The next system south, consisting of Montagnes, Almiralte Montt (station abbreviation VAL), and Ultima Esperanza (fig. 8), showed a return to the pattern observed in the northern inlets without the marked temperature structure observed in the northern part of the middle region. Montagnes has glaciers contributing melt water but, as far as was observed, no ice was discharged into the inlet. Almiralte Montt which is inland of and separated by a shallow sill from Montagnes, and Ultima Esperanza which in turn is inland of

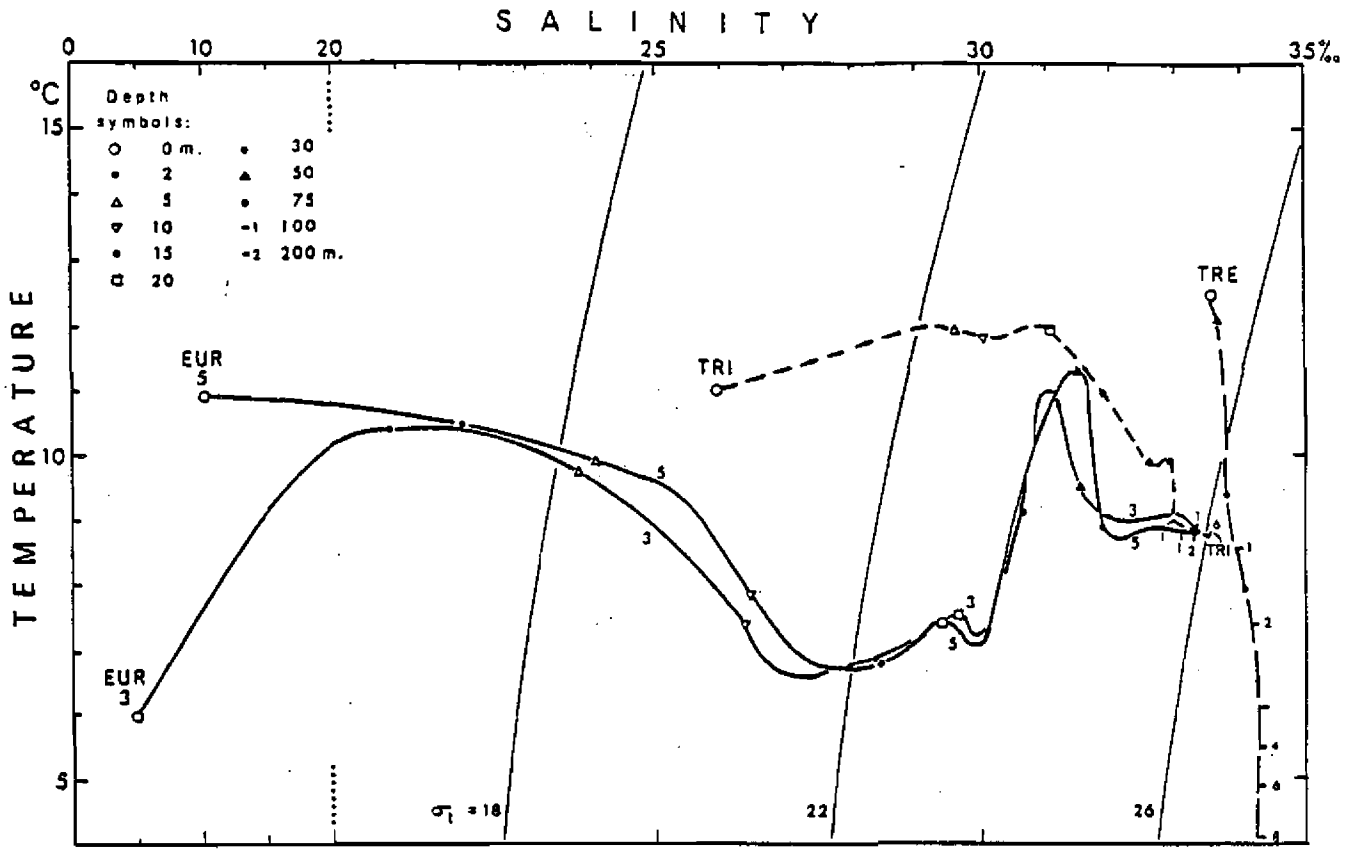


FIG. 6. Temperature/salinity curves for stations in Middle Zone, middle part.

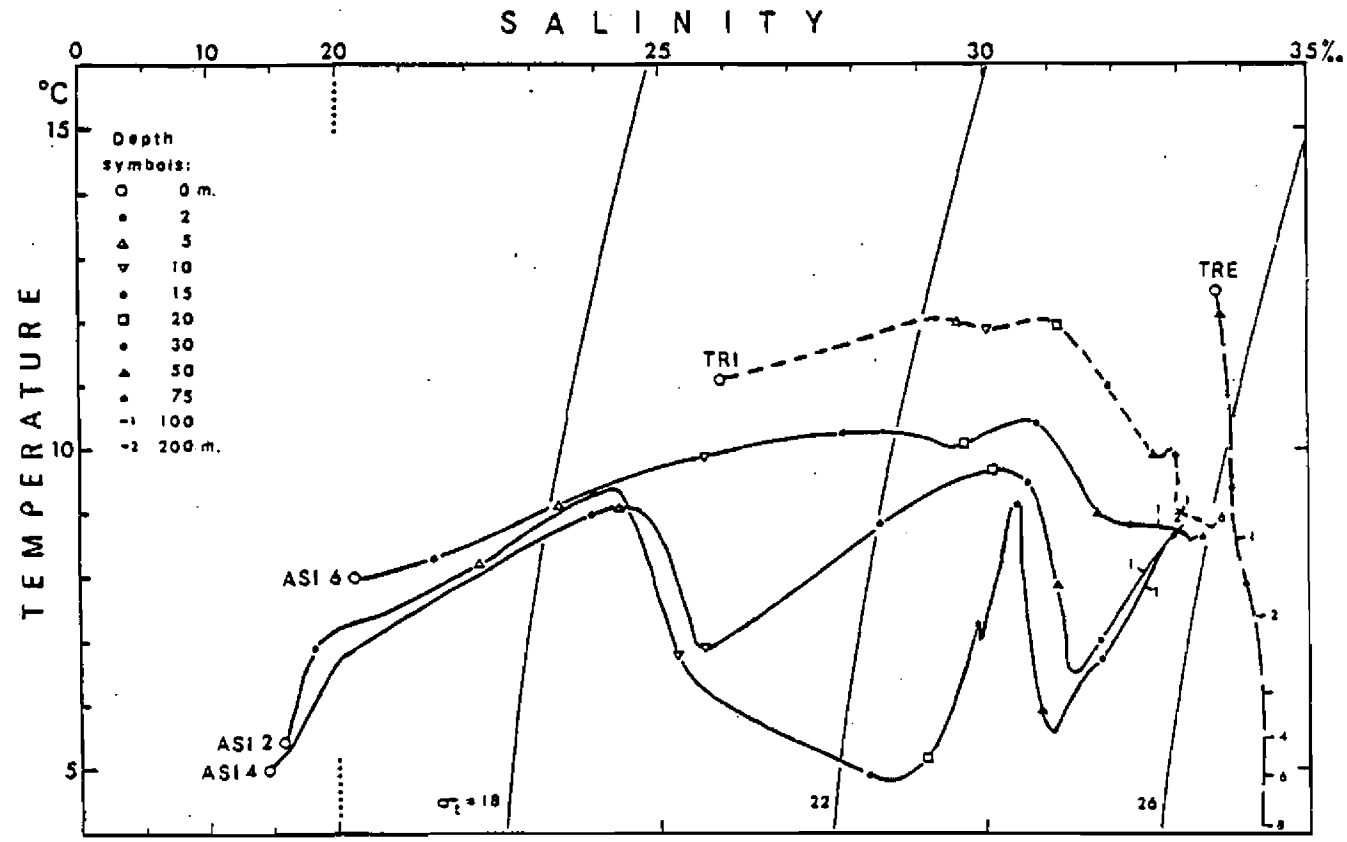


FIG. 7. Temperature/salinity curves for stations in Middle Zone, middle part.

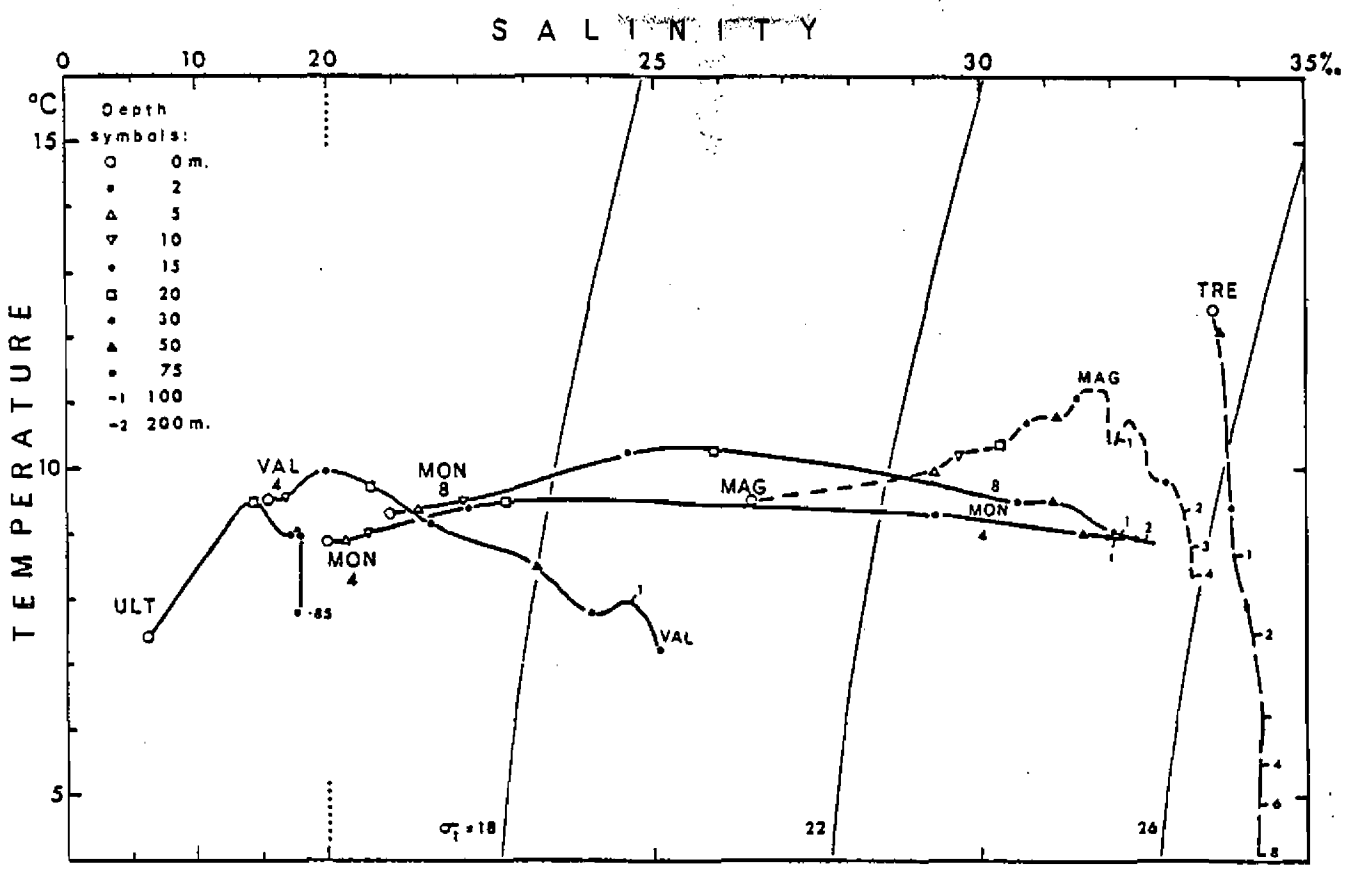


FIG. 8. Temperature/salinity curves for station in Middle Zone, southern part.

Almiralte Montt and separated from it by a shallow sill, show progressive and considerable decreases in salinity but a very limited temperature range. (Time permitted us to proceed only about one-fifth of the way along Ultima Esperanza during this cruise.)

The T-S curve for passage station MAG in the western opening of the Strait of Magellan is presumed to give a better indication of the ocean surface water here, at least below about 100 m depth, than is station TRE to the north.

South of Montagnes there is a group of inlets in the South Zone which appears to receive glacial run-off and a small amount of ice near their heads. Fig. 9 shows the structure at Gajardo station 2 (inner) and 4 (outer), and the station in the Strait of Magellan (MAG) outside. The temperature structure with maxima and minima is evident in Gajardo (which had ice near the head but probably has sills between stations 2 and 4) but is less pronounced than those in figs. 6 and 7.

Finally, fig. 10 shows T-S curves for the most southerly of the inlet stations, Almirantazgo, in Tierra del Fuego south of the Strait of Magellan. Station 2 is near the head and station 6 is near the mouth, a few miles from the eastern part of the strait. The water in the strait at station FAM, just outside Almirantazgo, is clearly different from that further west and is assumed to be of Atlantic origin. A comparison of the T-S curves at passage stations along the Strait of Magellan from west to east indicates that the change in water mass occurs between 73° W (passage station LON) and 71° 40′ W (station FRO which is similar to FAM). It is presumed that there must be a sill (or sills) in this section but the bottom along this reach is very irregular and the soundings on the chart are not sufficient to locate it directly.

DISCUSSION

The simplest structures in the Chilean inlets occurred at the northern and southern extremes. In the most northerly group off the Golfo Corcavado (fig. 1), using Reloncavi as an example (fig. 3), the basic characteristic was a progressive decrease in salinity away from the ocean, particularly in the upper 20 m. Evidently there is a sill between the passage stations COR and SRE; the available charts do not have sufficient soundings at the critical positions to determine its depth directly.

The other feature in this figure is the decrease in temperature from the outer ocean station SPA 4 to the passage station COR. It is suggested that for station COR this is primarily due to the cool run-off from the Elefantes system (fig. 4) while the temperature at GUA (and other shelf stations to the south) is typical of the northward flowing ocean waters close to the coast.

In Almirantazgo (fig. 10) and outside it (FAM) the

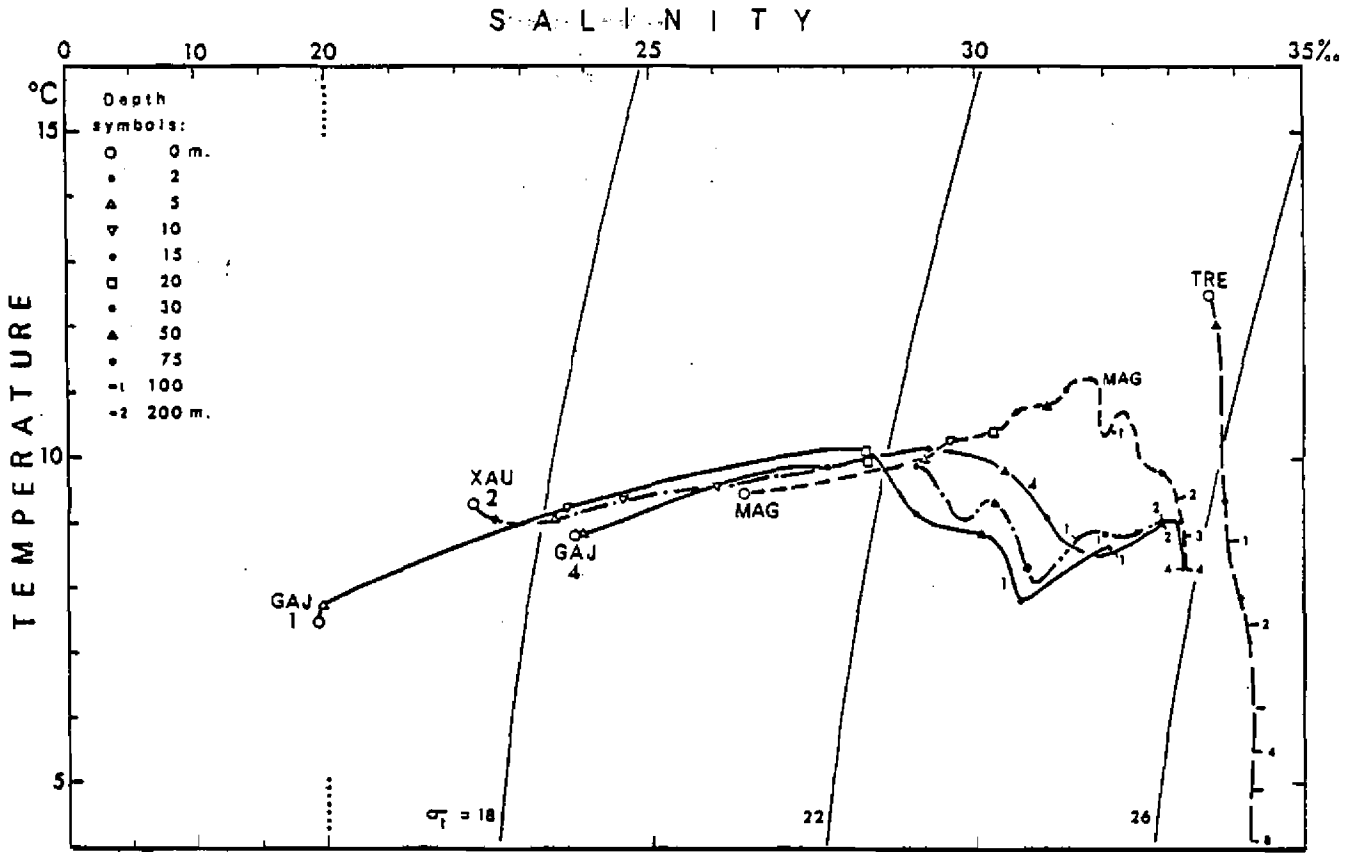


FIG. 9. Temperature/salinity curves for station in South Zone, north-western part.

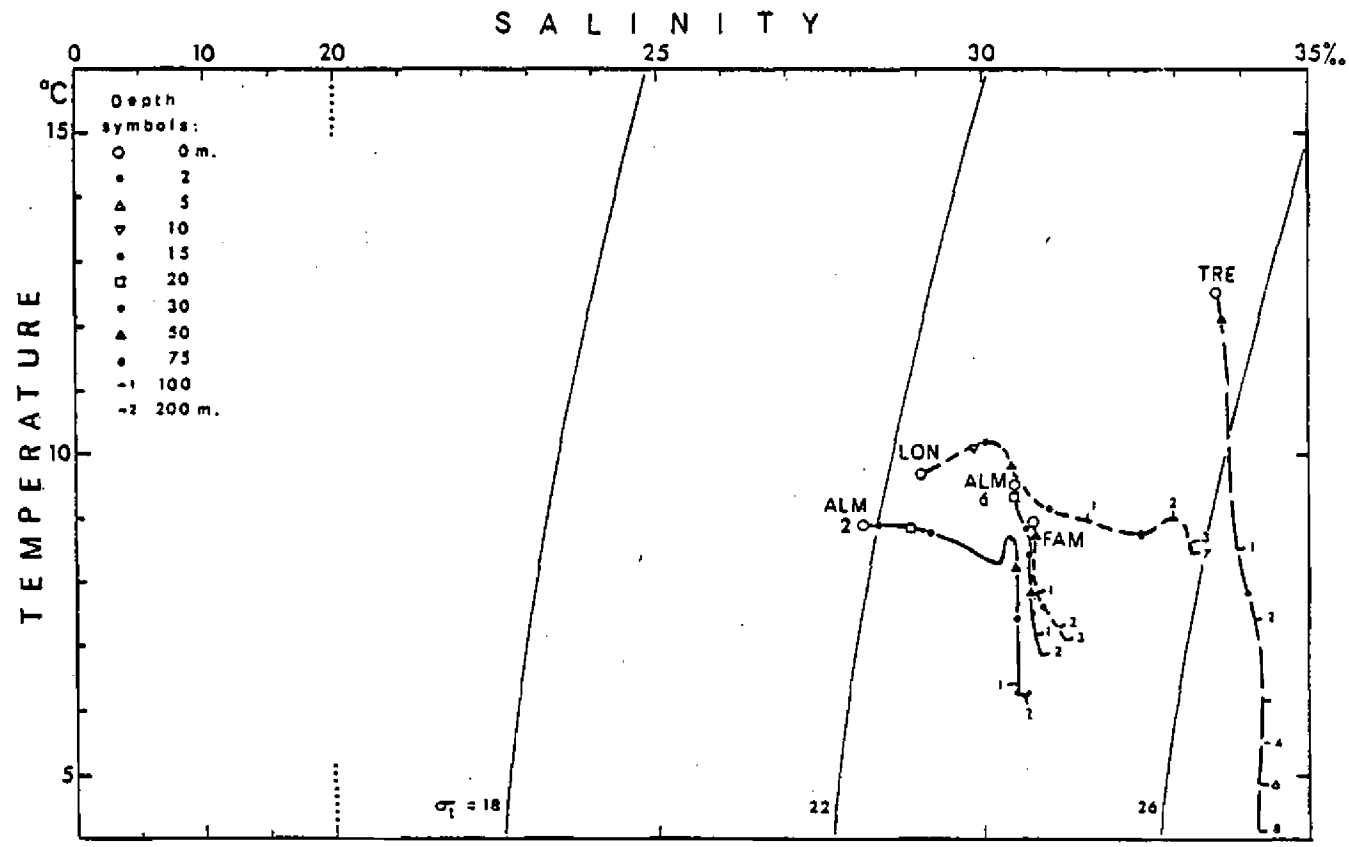


FIG. 10. Temperature/salinity curves for stations in South Zone, south-eastern part.

density was largely determined by temperature, in contrast to most of the other inlets, except at the head (e.g., ALM 2) where there were glaciers evidently yielding fresh water to reduce the upper layer salinity somewhat. Wind mixing may also be a significant factor here as strong winds are common in this region and the outer part of Almirantazgo is wide and exposed.

In fig. 8 the water in Montagnes shows a wide range of salinity but little temperature structure. The slightly lower temperatures at the surface relative to 20 m depth are attributed to glacier water inflow but no ice was seen in the water.

The effect of sills is evident in the Elefantes system (fig. 4) where both the charts and soundings during *Chile 70* indicate sills between ELE 14 and 9, and between ELE 9 and 5. In AYS 2 and FRA 2, the lower basin water temperatures than in Elefantes are taken to be indicative of the mean winter climatic temperatures in this region, only the upper layers warming up in the summer. The side inlet Puelma is to the west of Elefantes and has a smaller watershed to supply river run-off, hence the higher surface salinity.

The Baker system (fig. 5) is very deep and it is evident that there are no shallow sills inside the shelf where the sill depth appears to be about 150 m.

Extensive glaciers and snow fields were visible from the ship in this region and evidence of considerable run-off was evident from the large quantity of glacial silt in the upper waters, even in the passages 100 km or more from the main rivers. This cool fresh water run-off gives rise to the cool low salinity layer to about 30 m depth, particularly from BAK 8 inland. A few pieces of glacier ice were seen near BAK 4 but the low temperature in the upper 10–15 m is attributed chiefly to cool water run-off. The general rise in temperature of this upper layer to seaward is attributed to the net heat input through the water surface during the summer. The relatively high temperature in the upper few meters at BAK 2 (and 1) was probably because this inner end of the inlet is a backwater, the main river run-off occurring to seaward at about BAK 4. The water at BAK 1 and 2 was relatively clear compared to the turbid, silt-laden water seaward from BAK 4.

Referring to fig. 6 the water characteristics at passage Station TRI suggest a shelf sill depth of less than 100 m. Then Europa shows the well-developed temperature maxima-minima structure which appears to be characteristic of iceberg inlets. Here there was some ice at station EUR 4 and a lot at EUR 3 beyond which it was not practical to proceed. There was a major temperature minimum at about 15 m and a small one at 60–80 m with a sharp maximum at 40–50 m.

In fig. 7 are seen in Asia the best developed examples of the T, z structure for iceberg inlets. In this inlet the icebergs were present from station ASI 5 to the head. Here there is a major temperature minimum at 10–15 m again and a second conspicuous minimum at 60–70 m with a sharp maximum at 30 m.

The other inlets which had ice in them during *Chile 70* were Gajardo and Xaultegua (fig. 9) which show a temperature structure with a surface minimum and a single subsurface temperature minimum at about 75 m.

The surface minima (with low salinity) at EUR 3, ASI 2–4, and GAJ 1 and similar inlets were presumably attributable to the ice in the water at the time, and the low value at GAJ 4, where there was no floating ice, could have been due to wind mixing from the 40-knot winds observed on the previous day.

With regard to the subsurface minima I can only speculate. In the British Columbia inlets, which have no ice, a subsurface minimum between 50 and 100 m is common, being most marked in spring and eroding away through the summer. This minimum is attributed to winter cooling by strong winter outflows of continental arctic air which cool and mix the water to about 100 m, followed by a spring warming of the upper layer (whose salinity is then decreased by river run-off) resulting in a subsurface temperature minimum. One explanation of the temperature/depth profiles in the Chilean inlets might be that similar processes occur, followed by an intrusion of warmer water from outside at about 30 m to provide a temperature maximum separating the two temperature minima. This suggestion, however, takes no account of the fact that the marked temperature minima structure is peculiar to the inlets with glacier ice in the water.

A second suggestion is that the deeper temperature minimum (about 75 m) is due to winter cooling but that the shallower minimum (10–15 m) is due to continuing *subsurface* cooling of water of 25–30‰ salinity by the larger icebergs in the water or at the main face of the glacier. The larger bergs projected up to 2 m above the water surface and therefore could have extended to 5–10 m below the surface; the glacier faces could have been deeper but no close-up observations were possible.

CONCLUSIONS

In the main, the water structure in the Chilean fjord inlets is similar to that in the north American ones, the density being determined chiefly by salinity, and a typical estuarine circulation (low salinity water flowing out in an upper lower and higher salinity water flowing in below this) must occur. A feature peculiar to the inlets which have icebergs from glaciers is a temperature/depth profile with two major subsurface minima. A possible explanation is that the deeper minimum is a residual from winter cooling of the whole upper layer to about 100 m while the shallow minimum at about 10–15 m is due to continuing *in situ* cooling by ice reaching to these depths. This must be regarded as speculative, and time series studies would be desirable to provide more substantial evidence for study.

ACKNOWLEDGMENTS

I am indebted to the Atlantic Oceanographic Laboratory of the Bedford Institute for making *c.s.s. Hudson* available for this cruise, to the Chilean authorities for permitting us to work freely in Chilean territorial waters, and to the captain, officers, and crew of *c.s.s. Hudson* and to many north American and Chilean colleagues who took part in the field work during the *Chile 70* cruise.

REFERENCES

PICKARD, G. L. 1961: Oceanographic features of inlets in the British Columbia mainland coast. *J. Fish. Res. Bd. Canada, 18*: 907–999.

——— 1963. Oceanographic characteristics of inlets of Vancouver Island, British Columbia. *J. Fish. Res. Bd. Canada, 20*: 1109–1144.

——— 1967. Some oceanographic characteristics of the larger inlets of south-east Alaska. *J. Fish. Res. Bd. Canada, 24*: 1475–1506.

——— 1971. Some physical oceanographic features of inlets of Chile. *J. Fish. Res. Bd. Canada, 28*: 1077–1106.

OCEAN '72
IEEE INTERNATIONAL CONFERENCE ON

ENGINEERING IN THE OCEAN ENVIRONMENT

RECORD

Held at The Newport Harbor Treadway Inn
Newport, Rhode Island 02840
September 13-15, 1972

THE HUDSON-70 EXPEDITION

D. I. ROSS

Atlantic Geoscience Centre
Bedford Institute of Oceanography

Abstract

HUDSON-70 was a multidisciplinary oceanographic cruise encircling North and South America. The aim of the expedition was to make a significant contribution to the exploration of the world's oceans at the beginning of the International Decade of Ocean Exploration. The program included the total spectrum of oceanographic studies of interest to scientists today covering the fields of the life sciences, physics of the oceans and the earth sciences. Probably one of the main achievements for oceanographic studies was the opportunity to use identical measuring equipment in the two major oceans of the world - the Atlantic and Pacific, and at the same time obtain data in areas where little, if any, information was previously available particularly in the Arctic and Antarctic regions. This paper will review some of the more important scientific results of the cruise.

One of the major projects undertaken by the Bedford Institute in 1969 and 1970 was an oceanographic expedition around North and South America on the CSS HUDSON. The aims of the expedition were to make a significant contribution to the exploration of the world's oceans at the beginning of the International Oceanogrephic Decade and to continue the exploration of the Canadian continental shelf. A preliminary scientific program was drawn up in January 1968 which was then reviewed and revised during the following summer as requests to take part in the expedition were received from many scientists from laboratories across Canada and the United States. By August the major part of the program was finalized and the expedition was given the name HUDSON-70. Following authorization by the Minister of Energy, Mines and Resources, and a year of hectic preparation, the HUDSON sailed south from Halifax on the 19th of November 1969. Eleven months later, October 16, 1970, she arrived back in Halifax having completed her scientific work and become the first ship ever to circumnavigate the Americas.

The first leg of the voyage took the HUDSON down the South Atlantic Ocean to the vicinity of South Georgia with a call at Rio de Janeiro enroute. Acousticians, biologists, chemists, geologists and physical oceanographers made up the scientific party, most of whom sought samples for studies of oceanwide distributions. The long transect of the South Atlantic provided the opportunity to collect on this scale. As the ship proceeded south, plankton hauls were made at different depths from the surface to 1500 m; the acoustic characteristics of the deep scattering layer were mapped and mid-water trawls made to sample the fish in it; sea water samples were collected for chemical analysis; and measurements were made of the size and distribution of particulate matter at the sea surface. Experiments were conducted on the feeding habits of plankton and on the process of photosynthesis, and the sounds emitted by whales were recorded whenever they were sighted. Altogether the ship was very busy with every square foot of laboratory space occupied and a full 12 hours required at each station to make all the collections and observations. Christmas day was celebrated in the middle of the south Atlantic with Christmas dinner, and a station.

From the vicinity of south Georgia, HUDSON sailed to Buenos Aires, then south to work between South America and Antarctica. Four buoys, each carrying three current meters and three temperature recorders were laid across the Drake Passage and recovered after 11 days. Recovery of the current meters, all of which worked except one, was a major achievement as the recorders contribute the first comprehensive set of direct current measurements across this important passage. A set of mud samples for a study of the emergence of benthic feuna in polar regions was collected in the bays of the South Shetland Islands. Sea water samples for trace element analysis were collected in the deep waters of Drake Passage. While HUDSON was laying the current meters and collecting the mud samples a launch party left at Puerto Williams, a Chilean Naval Base, to collect

fresh and salt water invertebrates and intertidal algae in the coastal channels of Tierra del Fuego. Of the collection of invertebrates, about one-third are probably new to science. An unexpected discovery was a primitive species of beach flea which has changed little in 100 million years.

From Puerto Williams the HUDSON sailed to Punta Arenas and then carried a party of Canadian and Chilean scientists to study the physical oceanography, chemistry, and biological life of the Chilean fjords. These fjords whose marine characteristics were unexplored, extend nearly 100 miles along Chile's southern coast. Thirty-three fjords were visited and it was found they could be classified into three groups: northern, middle and southern. The northern group has clear surface water and high productivity; the middle group has less saline and very silty water (due to rock flour from glaciers); and the southern group, opening off the Strait of Magellan, has subsurface water of markedly different characteristics from the others, indicating that it might have its origin in the Atlantic rather than the Pacific. Besides affording the opportunity to study and compare Chilean and west coast Canadian fjords, the expedition provided valuable information that Chilean oceanographers can use to plan further work.

Valparaiso was reached on April 15. Here most of the biologists and chemists who had taken part in the South Atlantic leg of the expedition rejoined the ship to continue their work in the Pacific. Magnetometry and gravity were added to the observations, the latter to calculate the slope of the sea surface from Antarctica to Alaska to provide a base measurement for the determination of ocean currents by satellite observations. The track provided the longest continuous gravity line along any meridian. An unexpected deep trench with adjacent peaks was found in the South Pacific; this indicates that the Pacific has not moved as a single block and that more trenches may be found in future surveys.

As the ship approached Vancouver, the only serious setback of the voyage occurred due to fatigue in a cover plate of one of the main engines. Repairs to engines reduced the time available for the geophysics program off the coast of British Columbia from six to four weeks. Despite the delay, the HUDSON with the CNAV ENDEAVOUR carried out most of the planned two-ship geophysical survey over the continental shelf and slope between Vancouver Island and the Queen Charlottes. The object of the survey, comprised of gravimetry, magnetometry, bathymetry, seismic profiling, heat flow measurements and coring, was to study Continental Drift; the results support the hypothesis that the ocean floor is drifting away from the mainland. In the Explorer Trench a record high heat flow, measured in cooperation with the University of Washington, showed the trench to be an active zone of rifting, explaining some of the earthquake activity on the west coast.

On August 13 the HUDSON left Victoria to work in the Beaufort Sea, travel through the Northwest Passage to Baffin Bay, and return to Halifax. Four weeks were spent in the Beaufort Sea as part of a two-ship program of geology and hydrography with the Bedford Institute's other major ship, the CSS BAFFIN, which had come west through the Panama Canal and gone into the Beaufort Sea two weeks earlier. The team of geologists and geophysicists on the HUDSON obtained an extensive sampling of the sediments on the Beaufort Sea shelf, together with reflection profiles and gravity measurements. The discovery of extensive bands of coarse sands 30 to 60 m below sea level, probably representing relic beaches, and of sediment-filled depressions in the earth's crust will contribute greatly to an understanding of the geological history of the Canadian Arctic. Samples of foraminifera and plankton obtained in the water masses of the Beaufort Sea, and through the Prince of Wales Strait into Baffin Bay form the most comprehensive single collection through the archipelago. A major part of the collection will be retained at the National Museum, Ottawa, as the basis of a description of specimen types and as a national reference. The foraminifera collection is of considerable interest because from it, together with information from cores, much can be learned about the past history of the Arctic Ocean.

The Northwest Passage was traversed between September 22 and September 30. Transcending the rounding of Cape Horn, this was the most exciting part of the voyage, particularly as it had been left so late in the season with the risk of being caught in the ice for the winter. The passage was made through the Prince of Wales Strait, with the HUDSON and the BAFFIN proceeding independently to its northern end where they were met by the ice-breaker, the JOHN A. MACDONALD. The three ships sailed in convoy through heavy ice in Viscount Melville Sound to Resolute where a jubilant party celebrated the west-to-east journey and the virtual success of the rounding of the Americas.

It seemed a fitting end that the final major experiment of the voyage, to determine whether the crust beneath Baffin Bay was continental or oceanic, should be successful. The United States Coastguard

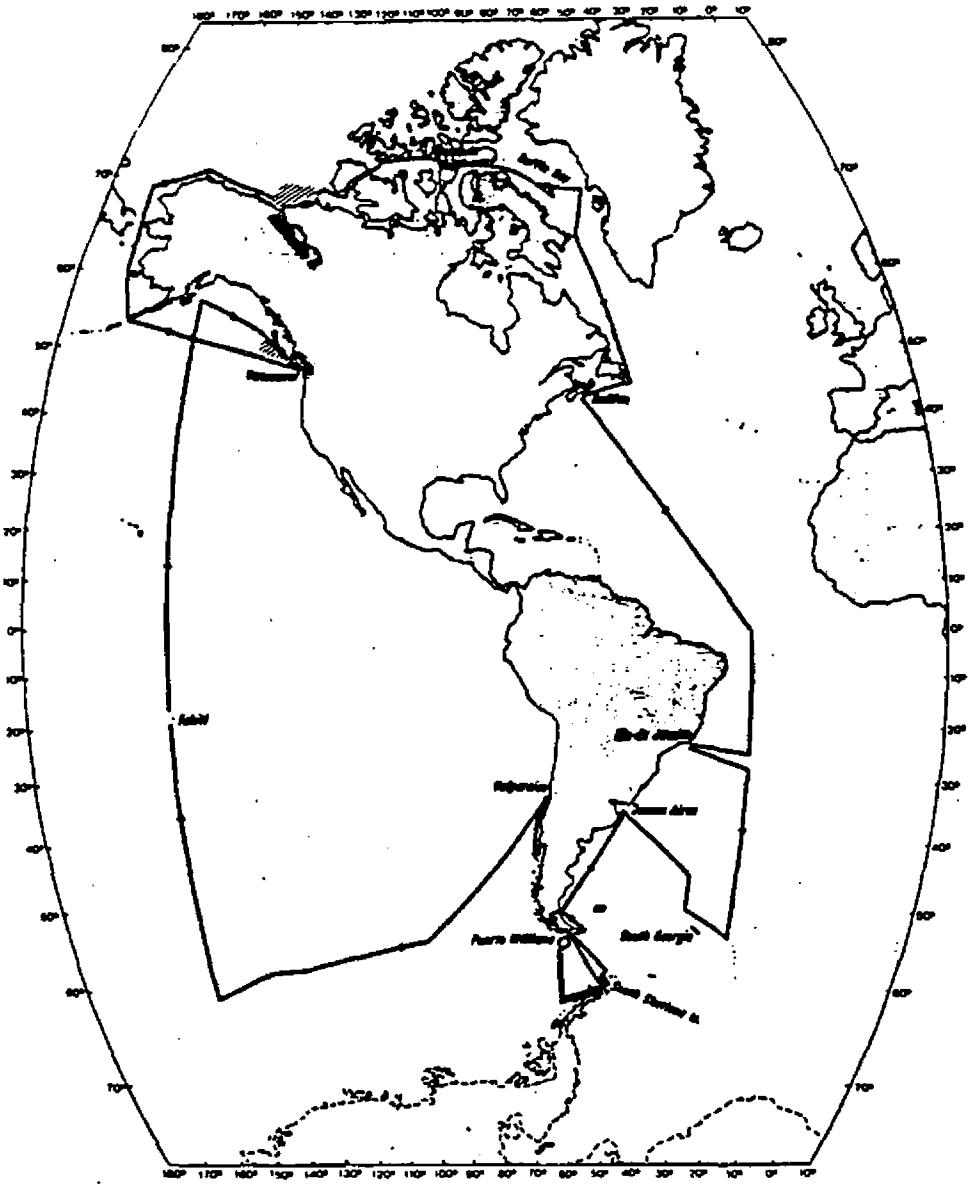
Cutter, the EDISTO, with a party from the Bedford Institute aboard, joined the HUDSON is Baffin Bay to act as shot-ship for a seismic refraction profile of the crust beneath the Bay. This was one of the few experiments where an analysis could be completed quickly on board. The profile proved conclusively that Baffin Bay has an oceanic structure and settled one of the important questions about the geology of the eastern Arctic. From Baffin Bay, the HUDSON sailed for Halifax arriving home on the 16th of October, 1970.

By any measure, this expedition was a success. The HUDSON sailed 55,000 miles, carried 122 scientific staff during the course of her voyage, and generated an impressive statistic of samples and observations. All of the scientific program was completed and most of the scientists collected many more samples than they had set out to obtain. Much of the credit goes to the crew of the ship, to Captain D. Butler, who completed the circumnavigation, and to Captain F. Mauger, who was captain during the west coast survey. HUDSON-70 was a collaborative venture and its success was due in large part to the efforts and cooperation of the Chief Scientists each of whom organized their own part of the program. They are listed below:

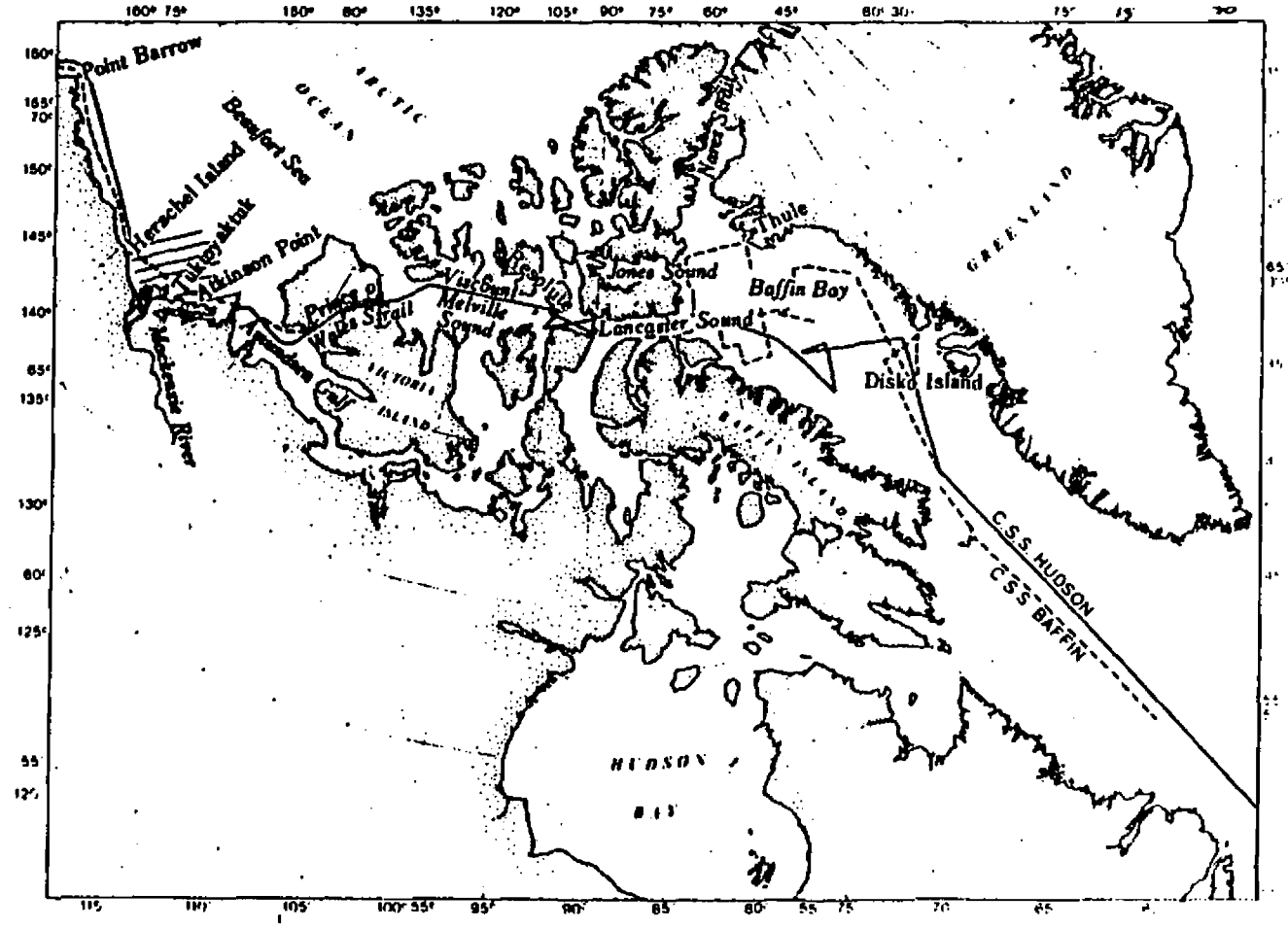
C.R. Mann*	Halifax to Punta Arenas
G.L. Pickard'	Punta Arenas to Valparaiso
R.C. Melanson*	Valparaiso to Tahiti
W.M. Cameron+	Tahiti to Vancouver
C.D. Maunsell*	West Coast Survey
B.R. Pelletier*	Vancouver to Resolute
D.I. Ross*	Resolute to Halifax

*Atlantic Oceanographic Laboratory
'University of British Columbia
+Director, Marine Sciences Branch, Energy, Mines and Resources.

Text reproduced from Bedford Institute Ocean Science Reviews 1969/70 by kind permission of C. R. Mann.



HUDSON's track and main ports of call.



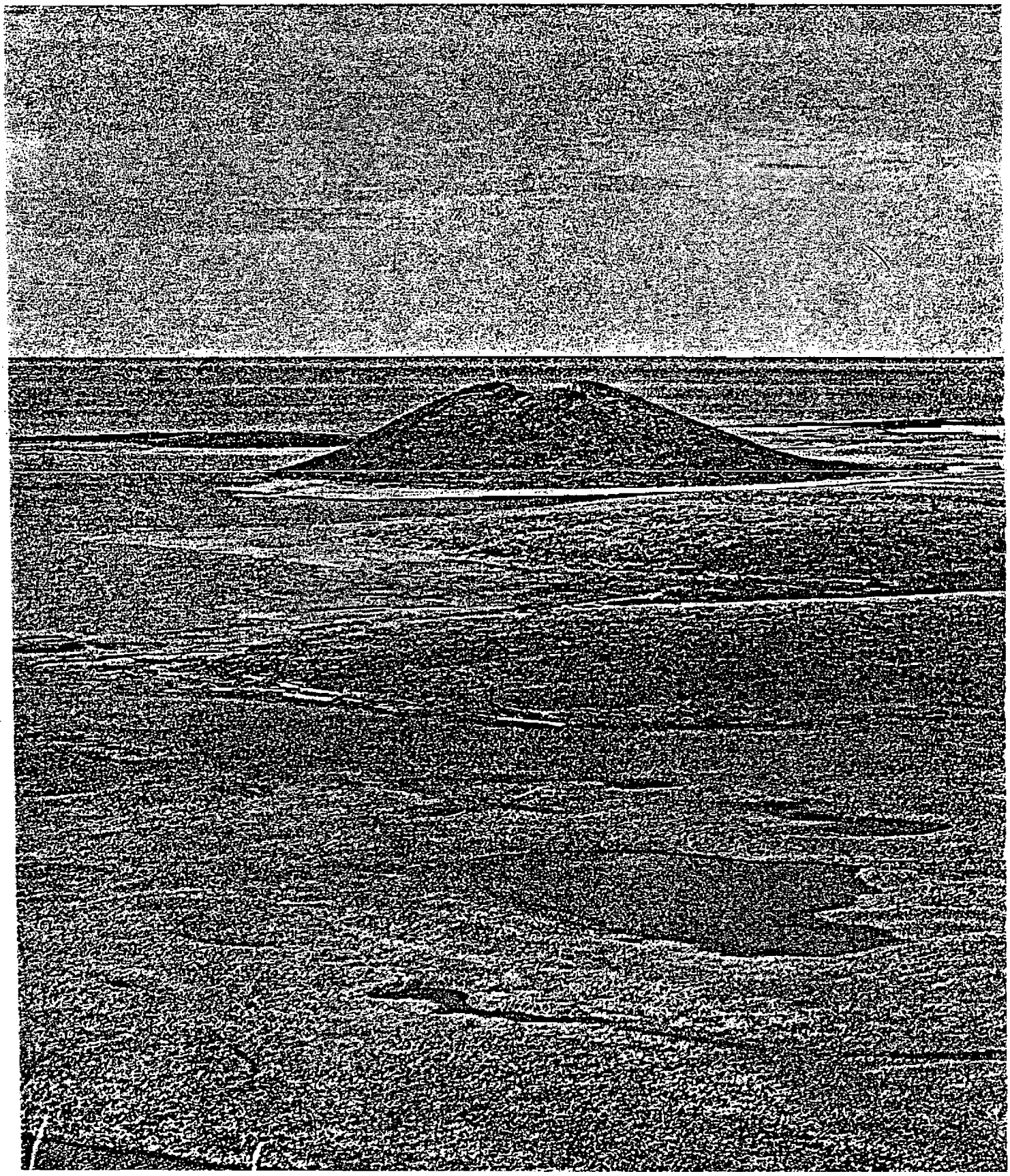
Tracks of the CSS HUDSON and the CSS BAFFIN through the Canadian Arctic.

Reprinted from
19 November 1971, Volume 174, pp. 816-818

SCIENCE

Submarine Pingos in the Beaufort Sea

J. M. Shearer, R. F. Macnab, B. R. Pelletier and T. B. Smith



Submarine Pingos in the Beaufort Sea

Abstract. *Numerous underwater mounds found on the continental shelf of the Beaufort Sea are thought to be pingos (hills that have a central core of ice) which have formed in the marine environment subsequent to oceanic transgression.*

An abrupt shoaling of the ocean floor in the Beaufort Sea was first noticed in 1969 by hydrographers aboard the C.C.G.S. *John A. MacDonald*, a Canadian icebreaker escorting the tanker S.S. *Manhattan* through the Canadian Arctic to Prudhoe Bay, Alaska. The shoal manifested itself as a rapid rise of the sea bottom from 49 to 23 m below sea level, over a horizontal distance of 200 m. This rapid rise was followed immediately by an equally rapid drop to 49 m. On the return voyage from Prudhoe Bay both ships skirted the shoal by passing to the north of its position, and no attempt was made to relocate the feature. For local reference the shoal was christened the "Admiral's Finger."

In response to a lack of detailed bathymetric information on the western Arctic, as typified by this incident, the Canadian Hydrographic Service in 1970 embarked on an extensive mapping program in the Beaufort Sea and adjacent regions. Coincident with this program a major research project was undertaken by the Department of Energy, Mines and Resources, designed to investigate the nature and distribution of marine sediments along the southeastern margin of the Beaufort Sea. During the course of these two projects, bathymetric, gravimetric, and magnetic data, complemented by seismic reflection data, side-looking sonar records, and numerous grab and core samples were mapped on a reconnaissance basis over the whole of the southeastern continental shelf, and in greater detail over selected areas of interest.

One of these areas was chosen with a view to carrying out a detailed survey of the Admiral's Finger and the surrounding area, in order to learn more about the nature and extent of this apparent topographic anomaly. The site of this survey, which was carried out by the C.S.S. *Baffin*, covered 5000 km² at a point located near the edge of the continental shelf, about 120 km northwest of Atkinson Point, Northwest Territories (Fig. 1, inset map). Sounding data were obtained over 9000 km of parallel tracks at an average separation of 0.5 km, and gravity and magnetic data were obtained over 4000 km at an average separation of 1 km.

Unexpectedly, this detailed survey revealed a large number of underwater mounds interrupting an otherwise smooth sea floor (Fig. 1). Each mound bore, in size and shape, a superficial resemblance to the Admiral's Finger. As far as could be inferred from detailed topographic examinations by means of launches, the mounds were generally irregular and asymmetric in form, with one side steeper than the other. The diameters of the bases averaged 400 m, and the elevations, from base to peak, 30 m. In most cases, a shallow (0 to 10 m) moat or depression surrounded the base of the feature.

A total of 78 mounds was located in the survey area, with minimum depths above their summits ranging from 15.4 m to more than 45 m. Their distribution appeared to be random. Several were grouped in clusters, others were paired, and the remainder were scattered singly within the 70-m isobath.

During the same period, similar features were discovered outside the survey area by investigators aboard the C.S.S. *Hudson* and C.S.S. *Parizeau*, who were engaged in hydrographic and scientific activities. Seven were identified on the east side of Mackenzie Canyon (at 69°55′N, 137°10′W) by means of side-scan sonar (Fig. 2). A seismic reflection profile (Fig. 3) was obtained over another feature located at 70°51′N, 131°72′W, just to the east of the survey area described above. These observa-

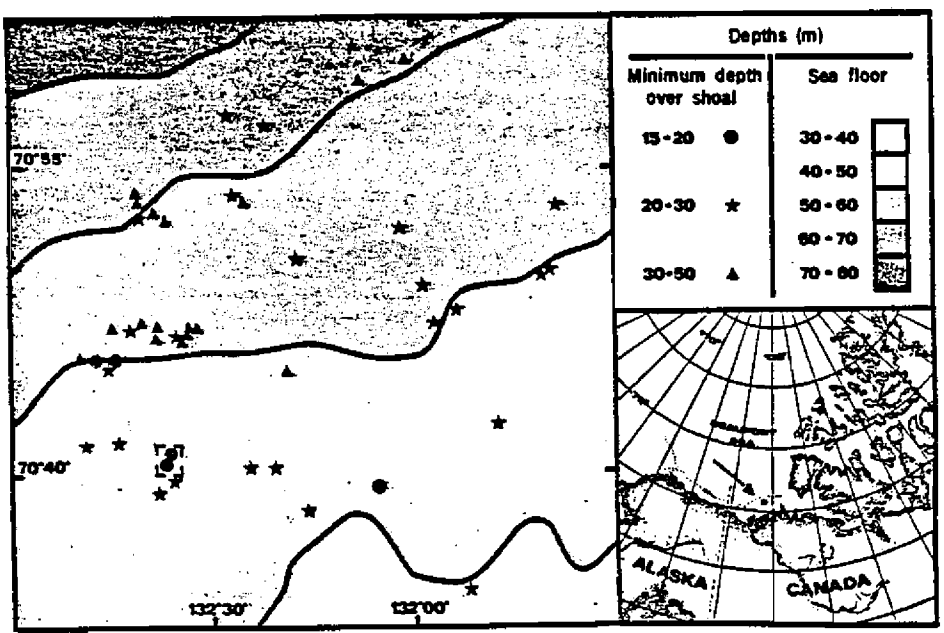


Fig. 1. Distribution and least depths of the underwater mounds mapped in 1970 by hydrographers aboard the C.S.S. *Baffin*. The region shown in this diagram does not represent the full survey area. The shoal located near 70°35′N, 132°15′W is thought to be the one traversed by the S.S. *Manhattan* and C.C.G.S. *John A MacDonald* in 1969. The box at 70°40′N, 132°35′W contains the shallowest features located.

tions indicate that more shoals may exist on the unmapped portions of the continental shelf of the Beaufort Sea, particularly since the seven mounds located by means of side-scan sonar were not detected by the ship's echo-sounder. The implications with respect to deep-draft shipping in the western Arctic are serious, since the features represent a hazard to navigation in ice-infested waters.

No detectable correlations were apparent between these small-scale topographic features and the geophysical observations. The magnetic field, measured to a precision of 1 gamma, displayed no evidence of shallow sub-bottom structure. As expected, the gravity field was dominated by the shelf-edge anomaly, and the shipboard system, measuring to a precision of 1 mgal, gave no indication of perturbations associated with the sea-floor mounds. Sub-bottom reflectors, as viewed in the seismic reflection trace (Fig. 3), show little deviation from the horizontal, which rules out a diapiric or intrusive origin, as earlier suggested in (*1*).

The similarity in the morphology of these submarine features with pingos (hills that have a central core of ice) on the Tuktoyaktuk Peninsula, 120 km to the south (*2–4*), suggests a similar mode of formation. Two modes of origin will be discussed: terrestrial and submarine.

In the first case these offshore features are presumed to represent the submerged portion of a group of pingos all formed originally above sea level. During the last glacial maximum the worldwide sea level is thought to have been some 100 to 125 m below its present level. On emerged areas of the Beaufort Sea outside the ice margin, permafrost probably existed in response to mean annual air temperatures that were below 0°C. A landscape similar to that now present above sea level may have existed, and scattered lakes, in which winter ice did not freeze to the bottom, would have been present with the associated depression of the permafrost layer beneath these insulated areas. Shoaling of these lakes either by infilling or draining (the latter commonly by shoreline retreat) would have caused freezing to the bottom during the winter with the subsequent formation of pingos in a manner similar to that suggested by MacKay (*2*) (discussed more fully below). However,

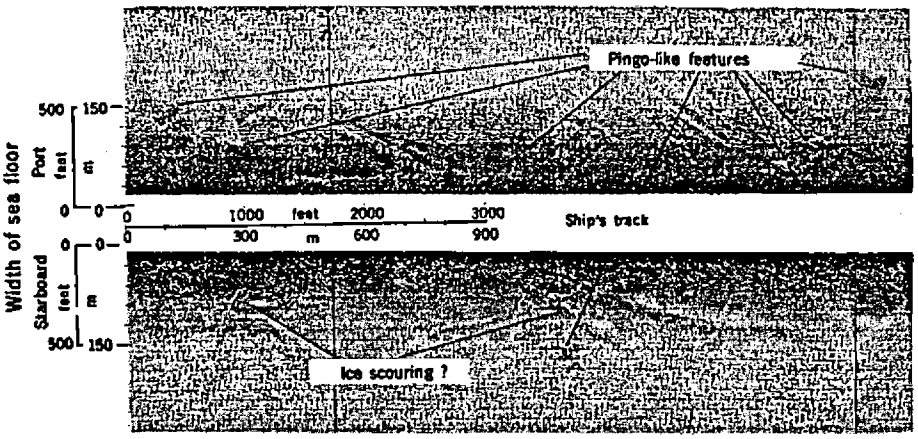


Fig. 2. Photoreproduction of a section of the side-scan sonar record on the east side of Mackenzie Canyon (65°55'N, 137°10'W).

examination of the effect of even moderate wave action at the present shoreline, where leveling is fairly complete and rapid, raises doubts with respect to the possibility that these proposed pingos could have survived the postglacial transgression.

In the second case, these offshore features are presumed to be pingos in the genetic sense, which have formed subsequent to oceanic transgression and in the submarine environment. If the shoaling of the lakes described above did not occur prior to the incursion of the sea, the unfrozen pore water in the interstices of the sediments occupying the permafrost depressions could have remained unaffected by the transgression. Synchronous with this transgression of the sea was the exchange and mixing of the fresh lake water with the seawater. (The mixing of seawater with freshwater in the pore spaces of the sediments underlying the original lake basin is believed to be very slow or non-existent because of the sealing effect of the fine lacustrine sediments and the progressively increasing thicknesses of marine clay.) The thermal regime in the lake bottom was therefore altered from that of an unfrozen freshwater layer to one governed by the temperature of the seawater. In this respect, most temperatures recorded on the sea bottom in the Beaufort Sea in August and September 1970 were below −1°C, many being the lowest temperature possible without freezing (−1.8°C) for the given salinity. If we assume that conditions similar to those of the present existed at the time of transgression, the displacement of fresh water by the colder salt water would have been accompanied by a migration of the 0°C isotherm downward into the sediments beneath the lake basin. Freezing of the interstitial water and the associated upheaval of the overlying material would have resulted, in a manner similar to that occurring on dry land.

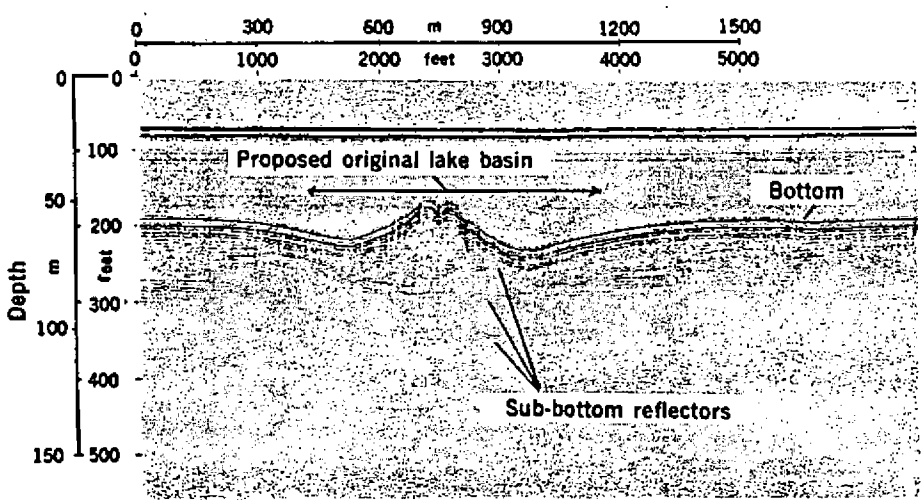


Fig. 3. Seismic reflection trace over one of the pingo-like features.

With the thermal regime established, it is pertinent to mention briefly the pressure relations involved in the formation of a pingo. The two major mechanisms (not mutually exclusive) described in the recent literature are (i) upheaval due to the hydrostatic pressure of expelled pore water (*2*, *3*) and (ii) uplift due to the frost-heave process (*5*). Given the temperature conditions discussed above, the first water to freeze is the pore water just beneath the impermeable lake bottom sediments. As the frost line advances, excess pore water is expelled into the unfrozen material. This surplus water, combined with the sealing effect of the frozen lake bottom, causes a buildup of hydrostatic pressure (*6*) which is sufficient to lift the overlying layer to the heights observed. In a fine-grained soil, this migration and accumulation of pore water may be followed by the formation of ice lenses and by volume expansion (frost heave), which will produce uplift over and above that already caused by hydrostatic pressure. A load of 40 m of water, or any other load influencing equally the overburden and pore-water pressures, will not affect the frost-heave phenomenon which develops in the soil upon freezing. Uplift due to hydrostatic pressure will occur when the pressure exceeds the binding strength of the impermeable frozen layer plus the pressure of the 40-m water load, which is very small (about 4 atm) as compared with the total pressures involved (*6*).

The minimum age of a mature pingo can be estimated by determining the time required for the freezing of the permafrost depression beneath the original lake bed. The size of this depression must first be calculated by assuming that the ice core of the pingo has the shape of a cone with a radius of 200 m and a height of 20 m. If this core is pure or almost pure ice, then the volume of sediment from which the ice was derived will be equal to the volume of the cone divided by the product of the sediment porosity (30 percent) and the ratio of the volume expansion of ice to the total volume of ice ($\simeq 0.1$). If the depression is approximated by a cylinder with a radius of 400 m (the size of the original lake basin), its depth is calculated to be about 60 m. The time needed for the 0°C isotherm to reach this level depends mainly upon the thermal conductivity of the sediment, the surface temperature, and the geothermal heat flow. If we assume reasonable values for these parameters, it would take about 5000 years for the frost line to reach this depth.

In the case of submarine pingos, this reasoning implies that marine transgression must have occurred prior to 5000 years B.P. This date is supported by worldwide curves of postglacial sea level submergence (*7*), which indicate transgression at these depths (30 to 70 m) taking place well before 5000 years B.P.

Note added in proof: Additional pingos have been discovered on the floor of the Beaufort Sea near the site of the survey area of 1970 (*8*).

J. M. SHEARER
Geological Survey of Canada, Ottawa, Ontario

R. F. MACNAB
B. R. PELLETIER, T. B. SMITH
Atlantic Oceanographic Laboratory, Bedford Institute, Dartmouth, Nova Scotia

References and Notes

1. W. C. Gussow, *Bull. Amer. Ass. Petrol. Geol.* 38, 2225 (1954); R. C. Bostrom, *J. Glaciol.* 6, 568 (1967).
2. J. R. Mackay, *Geogr. Bull. Can. No. 18* (1962), p. 21.
3. ———, in *Proceedings of an International Conference on Permafrost* (National Research Council, Washington, D.C., 1966), pp. 71–76.
4. ——— and J. K. Stager, *Geogr. Bull. Can.* 8, 360 (1966).
5. P. J. Williams, *Norwegian Geotech. Inst. Publ. No. 72* (1967), p. 91.
6. In a closed system, 1 atm of pressure is built up for every 0.007°C below the freezing temperature of the medium (0°C for fresh water). When water freezes in this way at −1° to −1.8°C, it develops an internal pressure ranging between 140 and 250 atm.
7. F. P. Shepard, in *Essays in Marine Geology in Honor of K. O. Emery*, T. Clements, Ed. (Univ. of Southern California Press, Los Angeles, 1963), pp. 1–10.
8. S. Huggett, personal communication.
9. We thank the officers and crew of the C.S.S. *Baffin*, C.S.S. *Parizeau*, and C.S.S. *Hudson* for their cooperation in the field. We are also grateful to R. K. Williams for the account of the discovery of the Admiral's Finger, and to A. C. Grant, J. Hnatiuk, A. Judge, J. R. Mackay, V. Rampton, and P. J. Williams for discussions on the geological aspect of this report. Bedford Institute contribution No. 257.

21 June 1971; revised 24 August 1971

COVER

Pingo rising out of the flat landscape near the village of Tuktoyaktuk, Northwest Territories. In size and shape, this pingo is practically identical to those found on the floor of the Beaufort Sea (background). Photograph was taken from the top of another pingo. See page 816. [Roger Belanger, Atlantic Oceanographic Laboratory, Dartmouth, Nova Scotia, Canada]

THE SIZE DISTRIBUTION OF PARTICLES IN THE OCEAN

By R. W. Sheldon, A. Prakash, and W. H. Sutcliffe, Jr.

Reprinted from Limnology and Oceanography
Vol. 17, No. 3, May 1972
pp. 327–340
Made in the United States of America

THE SIZE DISTRIBUTION OF PARTICLES IN THE OCEAN[1]

R. W. Sheldon, A. Prakash, and W. H. Sutcliffe, Jr.
Fisheries Research Board of Canada, Marine Ecology Laboratory,
Bedford Institute, Dartmouth, Nova Scotia

ABSTRACT

Frequency distributions of particle size between sizes of about 1 and 100 μ are given for both surface and deep water of the Atlantic and Pacific Oceans. The form of the size spectra varies predictably both geographically and with depth. A hypothesis is presented to show that, to a first approximation, roughly equal concentrations of material occur at all particle sizes within the range from 1 μ to about 10^6 μ, i.e. from bacteria to whales.

INTRODUCTION

The gross distribution of total suspended particulate matter in the sea is relatively well documented, but very little is known of the distribution of particle size and of its variation areally and with depth. Some attempts have been made to estimate particle size from optical measurements (e.g. Burt 1958), but the prevailing opinion at present seems to be that optical determinations can do little more than indicate that most of the particles in the sea are large relative to the wavelength of light (Jerlov 1968). Size fractionation by means of screens and filters has been tried (e.g. Mullin 1965; Saijo 1964), but the results of the filter fractionations are questionable (Sheldon and Sutcliffe 1969). Microscopic methods have been used, and these probably give reasonably accurate estimates of particle size, but even when semiautomated they are tedious and time consuming. The particle volume data given by Krey (1967) indicate a mean equivalent spherical diameter of about 5–6 μ for particles in the surface waters of the North Atlantic. At a depth of 500 m the mean size was slightly more than 6 μ. Recent work by Gordon (1970) has shown that particles are numerically most abundant at small sizes (<7 μ), and there is no significant change in size distribution with depth.

The development of electronic methods has greatly simplified the process of counting and sizing marine particles (Sheldon and Parsons 1967*a*). In this paper we present results of electronic determinations of particle size for material in suspension in the Atlantic and Pacific Oceans.

We would like to thank Coulter Electronics, Inc., for the loan of a model T Coulter counter. This helped our work in the Pacific considerably. We would also like to thank Duke University for providing ship time on RV *Eastward* and Dr. C. T. Schafer for allowing us to examine his North Pacific zooplankton samples.

MATERIALS AND METHODS

Surface-water samples were collected from the Atlantic, Pacific, and Southern

[1] Bedford Institute Contribution.

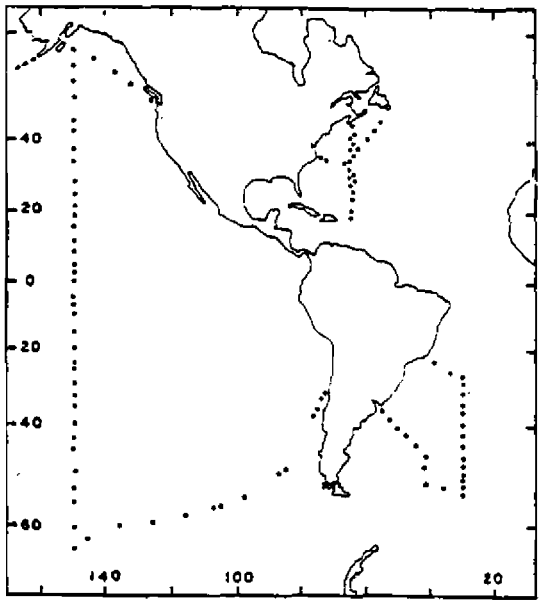


FIG. 1. Location of sample stations.

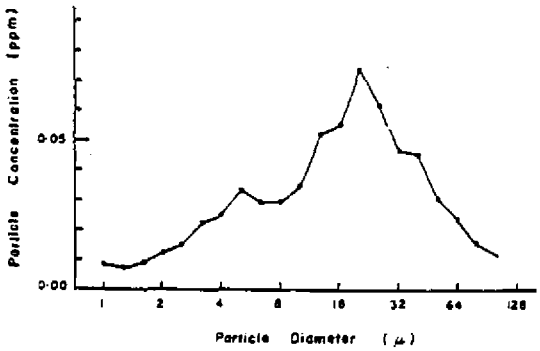


FIG. 2. Size-frequency distribution; to show the notation of the axes and the least number of data points used to define the form of the distribution. Concentration is *by volume*. All the size-frequency distributions in Figs. 3–9 were constructed in this way.

Oceans (Fig. 1). Deep-water samples were taken only from the North Atlantic, the South Pacific, and the Southern Ocean (*see* Figs. 8 and 9). Most of the North Atlantic samples were taken from CSS *Hudson* in winter (January–February) and autumn (October–November) 1968. Some samples were taken from RV *Eastward*, offshore from Cape Hatteras, in November 1969, and some were taken from RV *Panulirus*, near Bermuda, in August 1968. All the South Atlantic and Pacific samples were taken from CSS *Hudson* during the *Hudson* 70 expedition. The South Atlantic samples were taken in December and January 1969–1970 (summer); the south Pacific samples were taken in April and May 1970 (autumn), and the North Pacific samples were taken in May and June 1970 (summer).

All the surface-water samples were taken from CSS *Hudson* either with a bucket or via a continuously pumped seawater sampling loop. The intake for the sampling loop was about 4 m below the waterline, but the sampling depth varied with the movement of the ship. The bucket samples were taken either from the bow with the ship moving slowly ahead or from the stern with the ship underway (usually 12–14 knots). Subsurface samples were taken with Niskin bottles (*Hudson*), with Teflon-lined Nansen bottles (*Panulirus*), or with a 200-liter Gerard-Ewing sampler (*Eastward*). Neither the size distribution nor the concentration of the suspended particulate material was affected by the method of collection. In no sample were we able to detect particle contamination.

Particle size distributions were measured with a Coulter counter (Sheldon and Parsons 1967*a*), usually within 1 hr, but always within 6 hr, of collection. Those samples not processed within about an hour (deep-water samples) were kept cool and dark. Particles with equivalent spherical diameters from 0.63 μ to about 100 μ were considered, but in many samples a smaller size range was measured. The lower limit of measurement depends to some extent on the operating conditions and also on experimental technique. The upper limit depends on the concentration of large particles in the sample (Sheldon et al. 1967).

The results are presented as smoothed size-frequency polygons (Fig. 2). The size increments (abscissa) are logarithmic and follow a series of V, $2V$, $4V$, where V is individual particle volume. These are equivalent to diameter increments of $2^{1/3}$ or $\frac{1}{3}\ \phi$ (Sheldon and Parsons 1967*a*; Sheldon

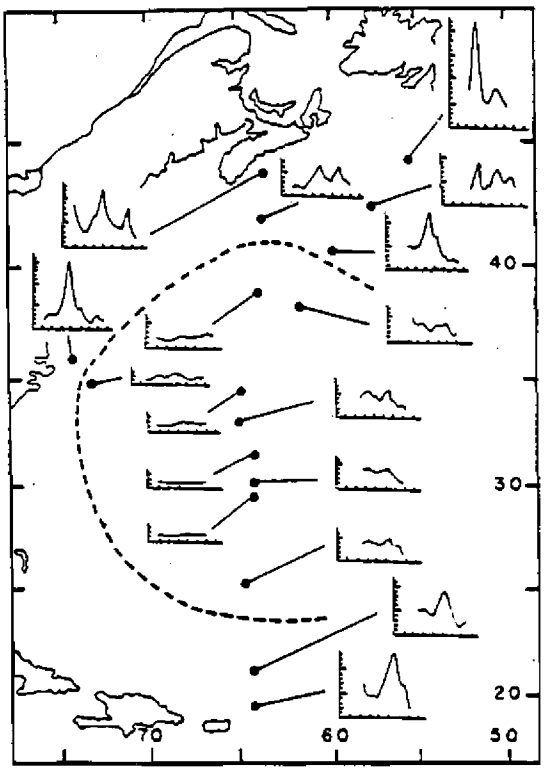


FIG. 3. Distribution of particles in the surface waters of the North Atlantic. The broken line shows the limit of the Sargasso Sea as indicated by the particle spectra.

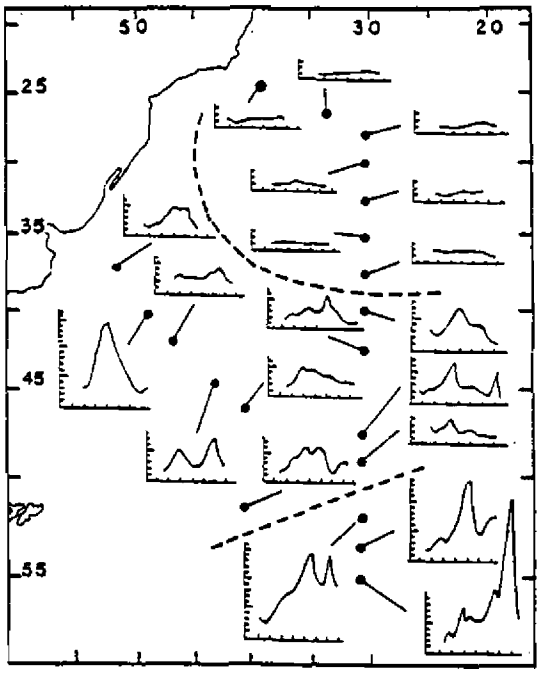


FIG. 4. Distribution of particles in the surface waters of the South Atlantic. The broken line in the north represents the limit of the subtropical water as indicated by the particle spectra. The broken line in the south represents the approximate position of the Antarctic Convergence.

1969). The ordinate represents the concentration of material in one size interval. The unit, part per million by volume, was selected because it is near to the form in which we obtain our raw data; this is equivalent to milligrams per liter if a particle density similar to that of water is assumed. We believe that this form of presentation is the best graphical method for size-frequency distributions of marine particulate material (Sheldon and Parsons 1967*b*).

GEOGRAPHIC DISTRIBUTION

The North Atlantic (Fig. 3)

In the central area, roughly between latitudes of 20° and 40°, particle concentration was low; there were approximately equal amounts of material in each size grade and there was but little variation in the form of the distributions from place to place. There was, however, evidence of seasonal variation in the total amount of particulate material present. The curves on the right-hand side of Fig. 3 (within the Sargasso Sea) are for samples taken in January. They show substantially higher concentrations than the curves on the left-hand side, which are for samples taken in November. Seasonal variation of the order shown (i.e. about a factor of 5) is not unusual for the subtropical North Atlantic (Menzel and Ryther 1960).

In more temperate waters, above about latitude 40°, the total concentration of particulate material was greater and the form of the spectra varied from place to place. The distributions still tended to have similar concentrations in each size grade but superimposed on this average level were definite, and sometimes pronounced, peaks. These peaks probably represented populations either of phytoplankton or of detrital particles.

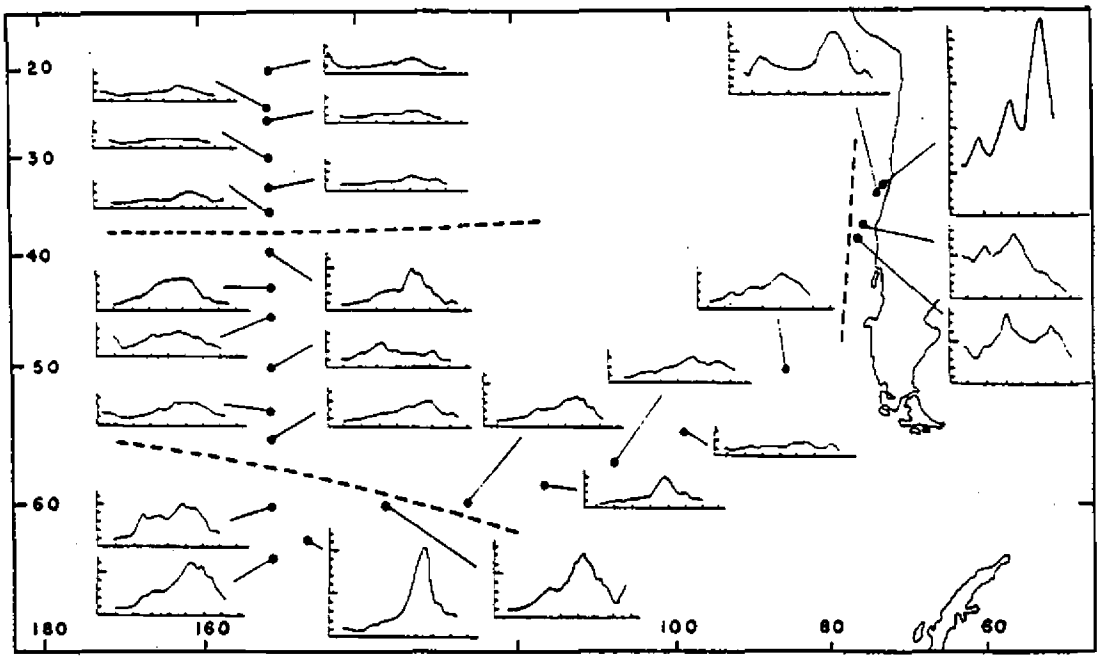


FIG. 5. Distribution of particles in the surface waters of the South Pacific. The broken line in the north represents the limit of the subtropical water as indicated by the particle spectra. The broken line in the south represents the approximate position of the Antarctic Convergence. The Chilean coastal zone is also shown (*see text*).

To the south of about latitude 25° the total concentration was also greater and the spectra showed a definite peak at around 20-μ particle diameter. This may have been caused by the nearness of the West Indian Islands, but the high standing stocks produced by the "island mass effect" tend to occur only close to the land (Doty and Oguri 1956). For instance, particle distributions near to Bermuda were typical of the Sargasso Sea and relatively high concentrations were found only within a few kilometers of the fringing reef. The relatively high concentrations found to the south of the Sargasso Sea were first encountered many kilometers to the north of Puerto Rico, and it is more likely, therefore, that they were in some way associated with the Antilles Current.

The South Atlantic (Fig. 4)

Between about latitudes 25° and 50° the South Atlantic was essentially a mirror image of the North Atlantic. The southern equivalent of the Sargasso Sea was quite clearly defined by the characteristic particle spectra, and the more temperate water to the south of about latitude 35° was also easily recognized.

To the south of about latitude 50°, beyond the Antarctic Convergence, the concentration of particles was high and relatively large particles formed the greatest bulk of material. These were mainly diatoms.

The South Pacific (Fig. 5)

The pattern of occurrence of particle size spectra was essentially similar to that of the South Atlantic, except that in the South Pacific the concentration of particles to the south of the Antarctic Convergence was rather less than we found in the South Atlantic. However, this may have been because the South Pacific samples were taken in the southern autumn. The high concentrations found near the

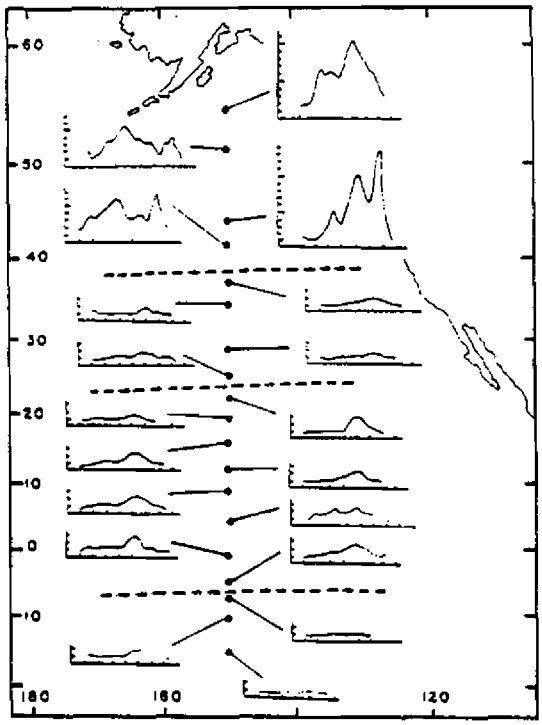


FIG. 6. Distribution of particles in the surface waters of the equatorial and North Pacific. This figure is continuous with Fig. 5 and shows, in ascending order, southern subtropical water, equatorial water, northern subtropical water, and temperate water, as indicated by the particle spectra.

Chilean coast were probably due to an effect of the Humboldt Current.

The Equatorial and North Pacific (Fig. 6)

To the south of about latitude 5°S the particle spectra were similar to those of the Sargasso Sea (*see also* the northern part of Fig. 5). Between about latitudes 5°S and 20°N the concentration of material was not great but it tended to be higher than in the subtropical area, and there was a tendency for a peak to occur at a particle diameter of about 20 μ. In the North Atlantic similar distributions were found to the south of the Sargasso Sea, although in this area the total concentration of particulate material was greater.

In the North Pacific the subtropical water with low particle concentration and particle spectra similar to the Sargasso Sea

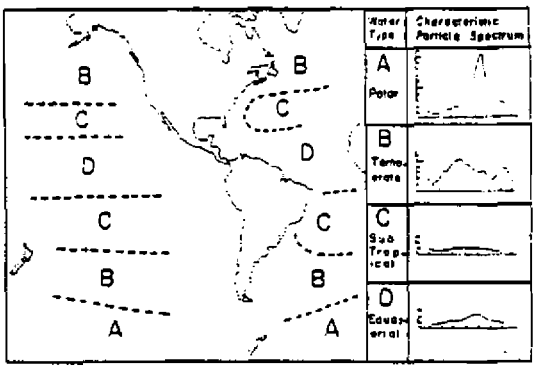


FIG. 7. Geographic pattern of particle size spectra of the surface waters.

could be recognized between about latitudes 20° and 40°. To the north of 40° high concentrations were found with large particles (diatoms) predominating in many of the samples. In other samples smaller particles were most abundant. These were probably small diatoms and flagellates. As these samples were taken during the northern summer this was not unexpected.

Summary (Fig. 7)

There were definite geographic variations in the distribution of particle size spectra, and certain areas of the ocean can be characterized simply by the size-frequency distribution of the suspended particulate material. Perhaps the clearest case is that of the subtropical areas. The roughly equal concentration of material in all size grades, together with the well-known fact of low total concentration, was first noticed in the Sargasso Sea. Subsequently, similar areas were found in the subtropical South Atlantic and in both the North and South Pacific. Particle spectra from temperate waters are also quite characteristic. Not every sample from the equatorial and polar waters was characteristic. Some of the variation could have been seasonal. However, each large area of ocean was sampled during a relatively short period and when taken as a whole the geographic pattern is fairly clear. Figure 7 represents an interpretative summary of the information contained in

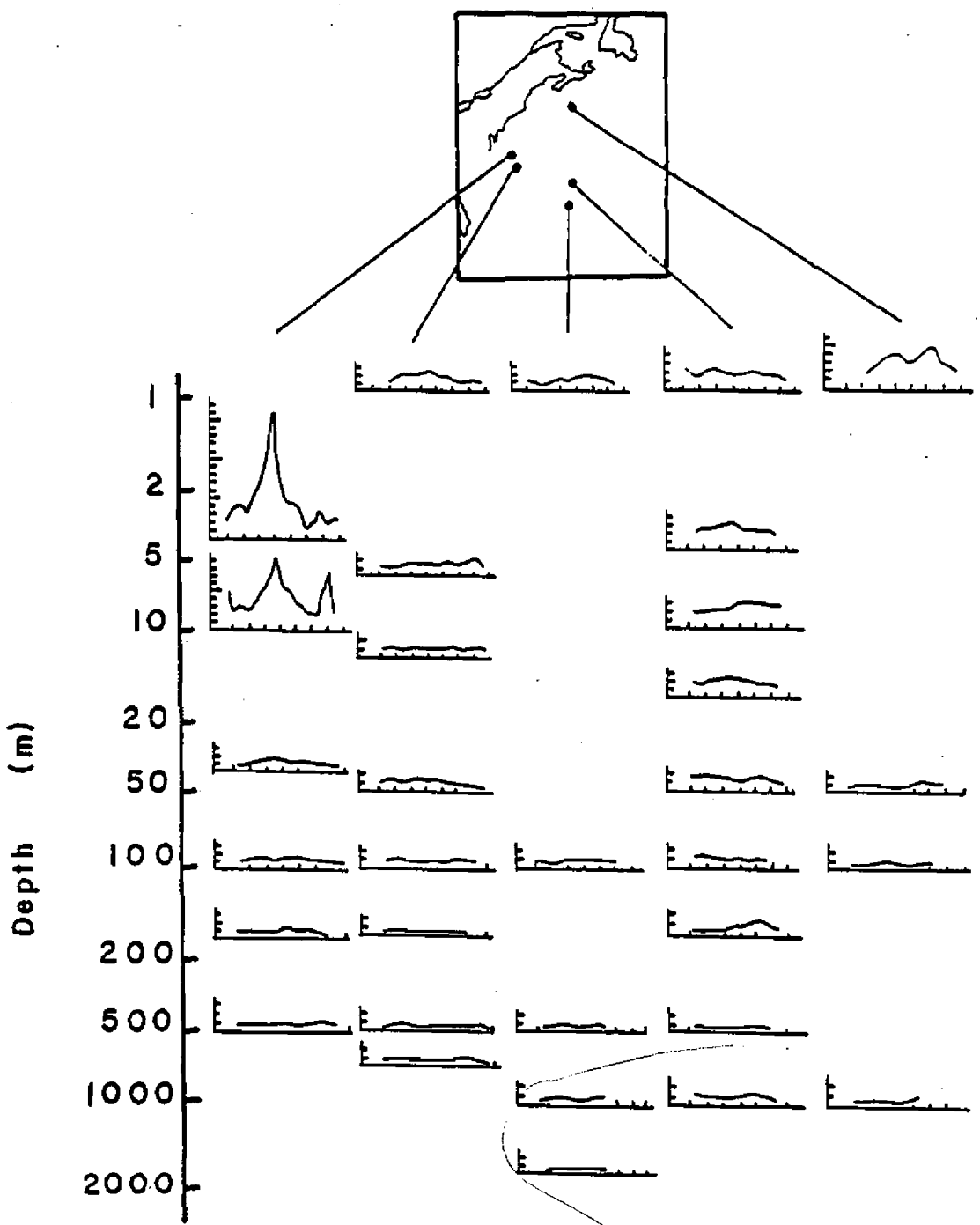


FIG. 8. Size distributions of suspended particulate matter at various depths in the western North Atlantic.

Figs. 3–6. Some parts are speculative; for instance the equatorial area of the Atlantic was defined only by two samples taken to the north of Puerto Rico, but it is clear from the evidence presented in Figs. 3–6 that the geographic pattern outlined in Fig. 7 is probably correct to a first approximation.

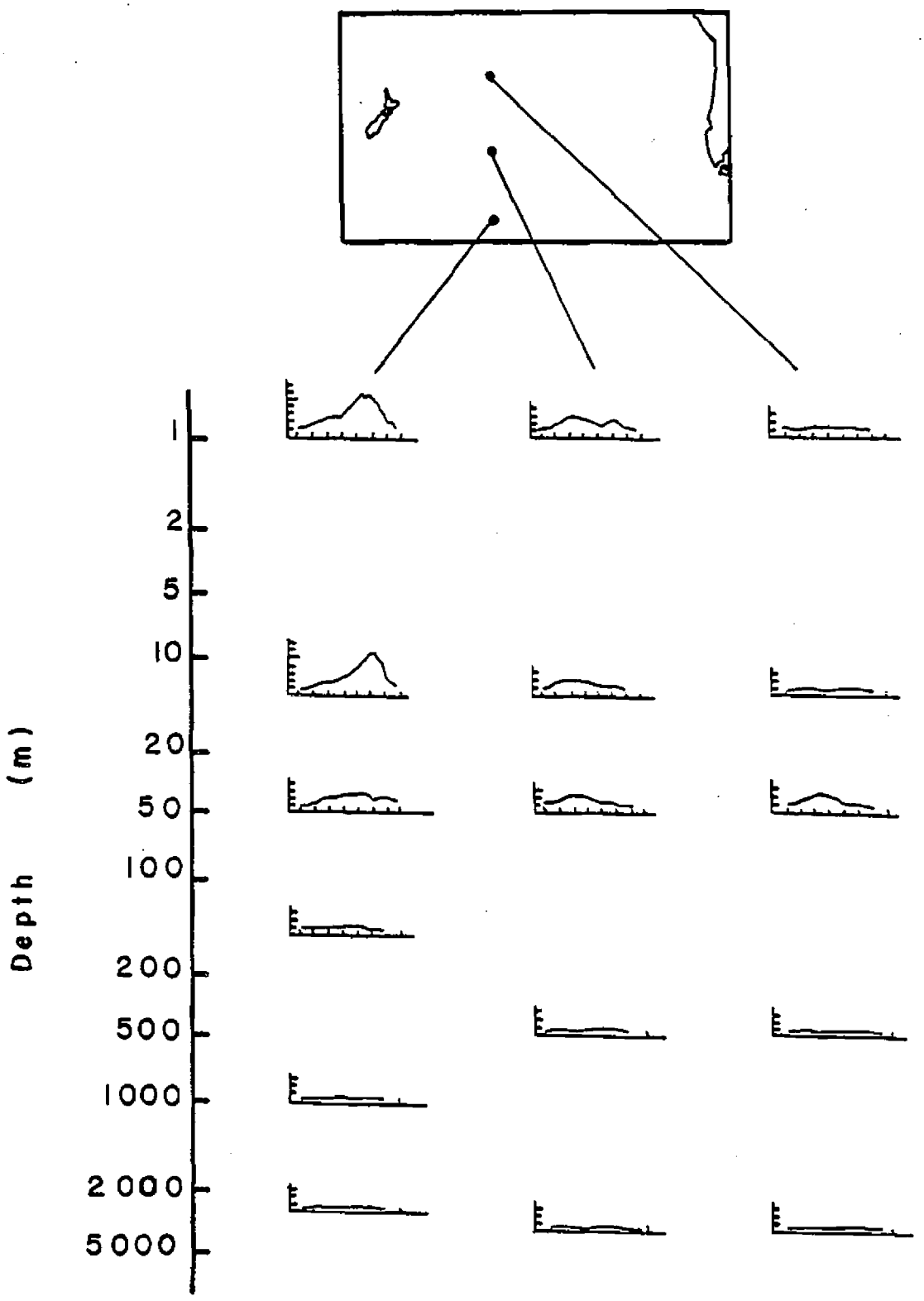


FIG. 9. Size distributions of suspended particulate matter at various depths in the South Pacific.

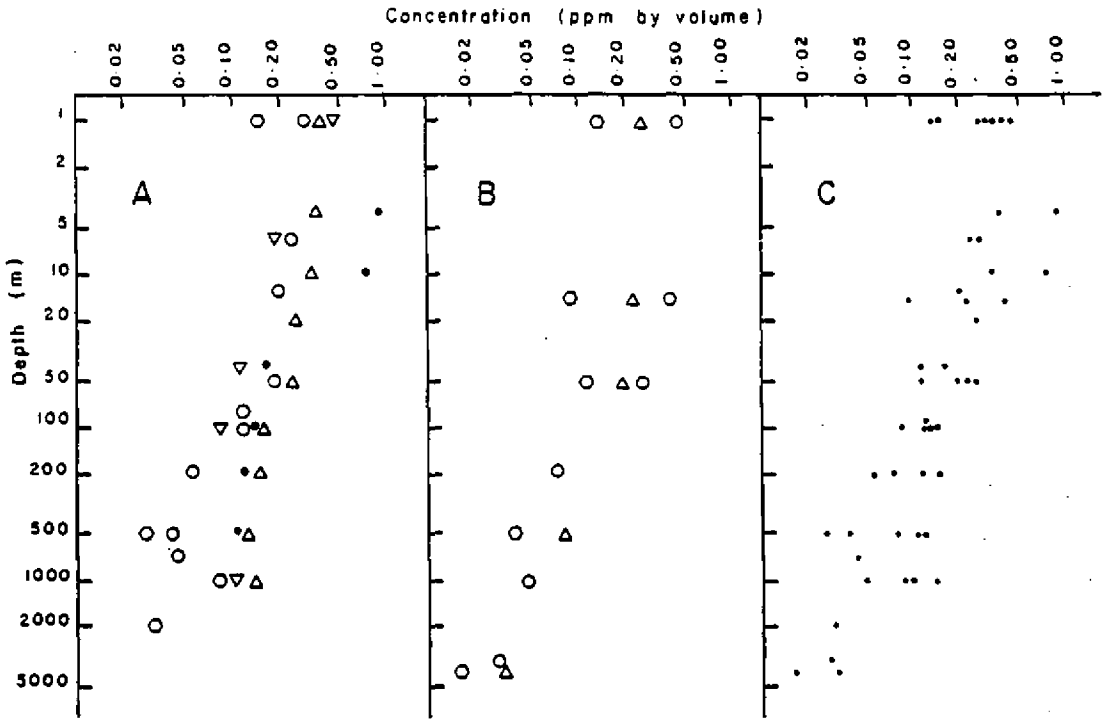


FIG. 10. Total particle concentration vs. depth. Particle size range ca. 1–100 μ.
A. The North Atlantic: ●—36° 25′ N, 74° 43.5′ W, 23–25 November 1969; ○—35° 00′ N, 73° 00′ W, 26–28 November 1969; ▽—41° 40′ N, 64° 03′ W, 29 October 1968; ○—29° 22′ N, 64° 03′ W, 2 November 1968; △—32° 18′ N, 64° 37′ W, 9–15 August 1968. These locations are shown in Fig. 8.
B. The South Pacific: ○—62° 50′ S, 149° 56′ W, 27 April 1970; △—49° 56′ S, 150° 02′ W, 1 May 1970; ○—29° 59′ S, 149° 59′ W, 7 May 1970. These locations are shown in Fig. 9.
C. Data from A and B plotted together.

DEPTH PROFILES

Samples were taken at various depths down to 2,000 m at 5 stations in the North Atlantic (Fig. 8) and to 4,200 m at 3 stations in the South Pacific (Fig. 9). The form of the particle size distributions in the surface waters varied from place to place as described above, but at depth it was remarkably uniform and resembled that of the subtropical surface water except that the total concentration of particulate material was less.

Two basically different kinds of depth profile could therefore be recognized. In the subtropical areas the particle size spectra of the surface waters showed roughly equal amounts of material in each size grade, and at depth the form of the size spectra was similar except that the concentration level was lower. In other areas there was no definite similarity between the form of the spectra at the surface and at depth.

In the deep water the *total* concentration of material was moderately variable (Fig. 10), even though the size distributions were of more or less constant form. The decrease of total concentration with depth is well known, but the depth to concentration relationship appears to be roughly log linear. It should be emphasized that these data are for concentration of particulate matter by volume in the areas we investigated. They are not therefore directly comparable with chemical data, which are given as concentration by weight, nor are they necessarily representative of the world's oceans.

DISCUSSION

Various workers have suggested that the average size of suspended particulate matter decreases with depth, and similar conclusions have been drawn both from light-scattering data and from microscopic observations (e.g. Burt 1958; Sasaki et al. 1962). Our observations, and those of Krey (1967) and Gordon (1970), seem to disagree with this, but much depends on the meaning attached to the term "average particle size." An average value can only be given to a population with finite limits. The precise definition of average is unimportant to this discussion, but it must represent some measure of a central tendency. The size distributions of particulate material in the sea, when expressed in the form we have used, are open ended. There is, therefore, no average size. As there are roughly similar *amounts* of material in logarithmically equal size intervals it follows that in any sample there will be many more small particles than large ones (Sheldon and Parsons 1967*b*). Distributions of particle number will be exponential (Beardsley et al. 1970), and the average size will be near to the smallest observable size.

Therefore, if we measure the *weight* or *volume* of material in suspension there is no average size. But if we *count* the *numbers* of particles the average size will be close to the smallest observable size.

We would suggest that average particle size apparently decreases with depth simply because, as the concentration of material decreases, the chance of finding large particles in any given sample volume also decreases. This would give an apparent increase in the relative numbers of small particles.

It is common practice to give a lower limit of particle size for the analysis of particulate material. This is usually defined in practical terms as the material retained by a specified type of filter. Not much attention has been paid to the upper size limit of the particles in a sample. If we consider a size distribution between the limits of 1 μ and 1 mm, with a constant concentration per size grade of 0.01 ppm (approximately similar to Sargasso Sea surface water), then ⅓ of the total sample will lie in the range 1–10 μ, ⅓ will be 10–100 μ, and ⅓ will be 100 μ–1 mm. However, although the sample is equally divided in terms of bulk, the number of particles per unit volume decreases rapidly as particle size increases. There will be, on average, only one particle of 100-μ diameter in 50 ml of water. A 1-liter sample would probably be representative to include this particle size. But there will be, in this example, only one particle of 1-mm diameter in 50 liter of water. A 1-liter sample would become inadequate at a particle size somewhere between these limits. That is to say, there will be inadequate numbers of particles sampled, yet the concentrations may be significant.

It has been our practice to screen samples at 160 μ. This is not really necessary for determinations of particle concentration by Coulter counter because anomalous concentrations at large particle sizes can be eliminated statistically; but for other kinds of analytical work the chance occurrence of large particles could result in anomalous determinations of particle concentration. In most surface waters 1 liter will give an adequate sample of the particles passing a 160-μ screen.

In deep water the sampling problem could be troublesome. Here the concentrations are about 10 times less than at the surface. According to our hypothesis there will be only one particle of 100-μ diameter in 500 ml of water and only one particle of 1-mm diameter in 0.5 m^3. There is clearly a need to define not only a lower limit but also an upper limit of particle size for analytical work. Sample size will then depend on the upper limit of particle size which is selected.

We measured accurately both particle size and number but we could not determine particle composition. A mineral grain and a flagellate of similar volume would be counted as similar particles. To check the nature of the suspended material we made qualitative microscopic ob-

servations on settled material whenever possible, but the inevitable difficulties associated with shipboard operation meant that not more than about 10–20% of the samples were examined in this way. However, enough samples were examined to show that, as one might expect, the suspended matter was mostly plankton and organic detritus, at least at the larger sizes. Inorganic particles not obviously associated with organisms did occur but they were not common.

Hobbie et al. (1972) have shown that in the western North Atlantic the suspended matter is mostly organic even though rather less than half of the particulate organic carbon is associated with living material (Sutcliffe et al. 1970). This does not mean that there is virtually no inorganic material in suspension. The interpretation that we place on our observations depends to some extent on the viewpoint we adopt. We consider a diatom to be a single organic particle, yet if it were analyzed chemically only a fraction of its living weight would be reported as organic carbon. Analyses are usually given in terms of dry weight, and with the data in this form the skeleton (considered to be inorganic) would make up a substantial part of the total. Therefore, when we say that most of the suspended matter is organic we do not mean that, chemically, inorganic materials are absent, but we do mean that most of the suspended matter in the ocean is associated either with nonliving organic matter or with organisms.

The tendency for roughly similar amounts of particulate material to occur in logarithmically equal size ranges has ecological implications of considerable significance. There is no reason to believe that the size range over which most of our measurements were made is atypical, except in that it was a relatively easy range to measure. Therefore, if the form of the size distributions is such that concentrations are roughly equal between 1 and 100 μ, why should not similar concentrations occur at sizes smaller than 1 μ or greater than 100 μ?

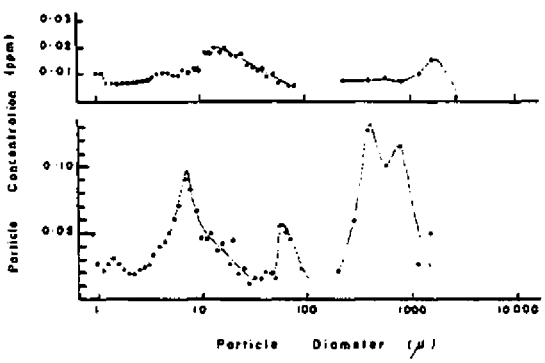


FIG. 11. Complete size spectrum over the size range 1 μ to about 4,000 μ for low and high standing stocks. Upper curve—10° 09′ S, 150° 02′ W, 18 May 1970. Lower curve—35° 00′ S, 73° 00′ W, 28–28 November 1969. Both examples from near surface water.

Particle concentrations at sizes less than 1 μ are difficult to measure accurately but we have made some observations which suggest that in the open ocean, concentrations in the size range 0.5–1 μ are not dissimilar to those in the range 1–100 μ. Quantitative observations in the size range 100–4,000 μ (zooplankton) are easier to make and in Fig. 11 we give examples at different levels of standing stock of size distributions for a range of particle size from 1 μ to about 4,000 μ. The concentrations in the zooplankton size range are similar to the concentrations in the phytoplankton size range (*see also* Harvey 1950; LeBrasseur et al. 1969; Parsons et al. 1969; Sheldon and Parsons 1967*b*).

In Fig. 12 we have attempted a synthesis of published information to establish the relationship between standing stocks of particles over a much wider size range. By considering a size range from bacteria to whales we have covered the whole of the marine food chain, more or less. In the phytoplankton and zooplankton size ranges we have used averages of our own observations. For the larger size ranges we have recalculated published information to make it roughly comparable with our data. These estimates are, of course,

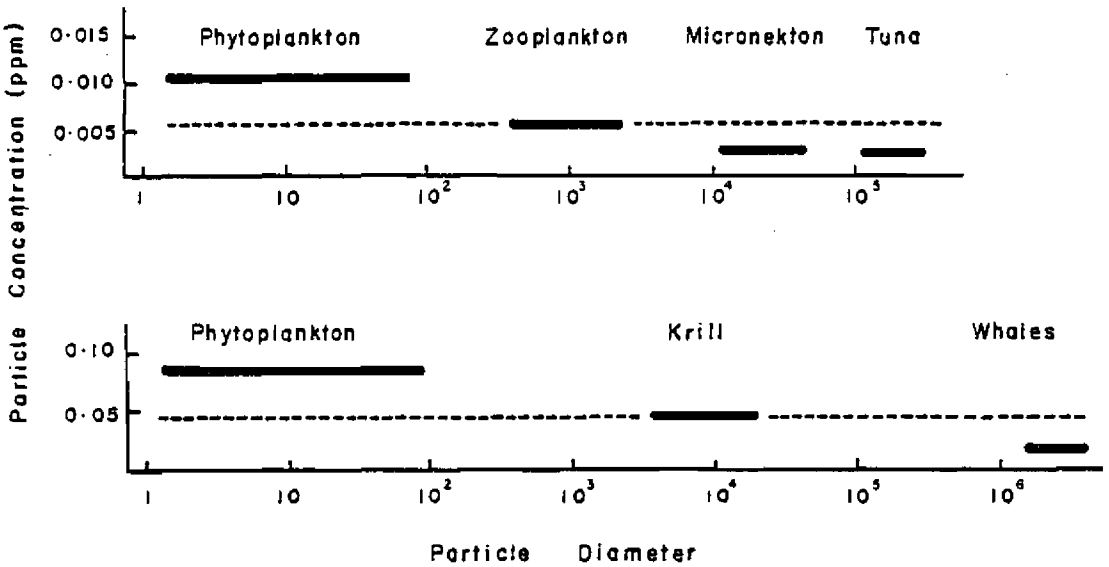


FIG. 12. Estimates of standing stock (thick lines). Above: equatorial Pacific. Below: Antarctic. The thin broken line is an estimate of the true or potential standing stock of living material. Some of the estimates were derived from data of Blackburn (1968), Blackburn et al. (1970), Mackintosh (1970), Mackintosh and Brown (1956), Marr (1962), and Riley (1963).

a first approximation only, but they are not likely to be grossly in error.

The patterns of standing stocks are similar in the two areas considered, but the absolute values differ by about a factor of 10. This is to be expected, although part of the difference may be because observations in the Antarctic were made only during the southern summer.

If we consider only the living material then the concentrations in the phytoplankton size range should be reduced by a factor of at least two (Sutcliffe et al. 1970). The zooplankton concentrations are roughly correct as it is unlikely that many nonliving particles occur in that size range. The estimated concentration of tuna (Riley 1963) probably represents a minimum for particles in its size range. The figure quoted for the concentration of whales in the Antarctic is also likely to be a minimum. The broken lines at constant concentration on Fig. 12 represent our estimates of the probable or potential standing stocks of living particles. It is unlikely that the true situation is as simple as this. Some decrease of standing stock may occur as particle size increases, but the decrease from phytoplankton to whales is probably no more than a factor of two or four, and is certainly less than an order of magnitude.

The food-chain relationships of the ocean are such that, in general, relatively large predators feed on relatively small prey. It follows from this that the pattern of standing stock that we have outlined can only be maintained if the rate of particle production varies inversely with particle size. Figure 13 shows, to a first approximation only, the relationship between rate of production (or doubling time) and particle size. There are many published data on growth, and the points and areas on the figure are only intended to be representative. Single-celled species are represented as points and other species are represented by larger areas. This is because the growth rate (or doubling time) and size of a multicellular organism varies significantly during its lifetime but a single-celled organism is less variable in this respect. The size is given as equivalent spherical diameter to be comparable

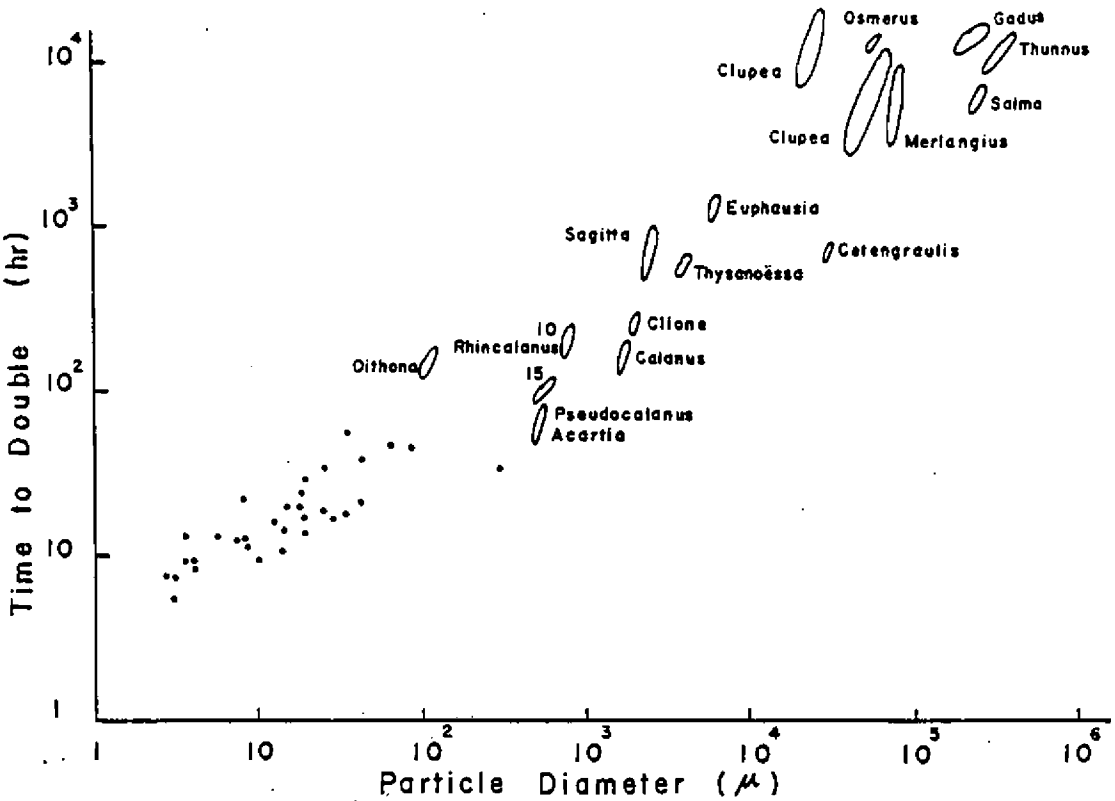


FIG. 13. The relationship between rate of production and particle size. The numbers near to the *Rhincalanus* patches indicate the temperature at which the growth took place. The uppermost of the two *Clupea* areas represents *C. sprattus*. The lower area represents both the Atlantic (*C. harengus*) and Pacific (*C. pallasi*) herring. For other explanations *see text*. Data from Altman and Dittmer (1964), Conover and Lalli (1972), Einarsson (1945), Eppley and Sloan (1966), Ford (1933), Garrod and Gambell (1965), Heinle (1966), Johnson (1970), Lebour (1925), Marshall and Orr (1955), MacLaren (1965, 1969), Mullin and Brooks (1970), Prakash (1967), Smayda (1966), and Williams (1964).

with other data in this paper; the equivalent spherical diameter of a fish varies with its shape but is about a fifth to a third the actual length. For a crustacean the spherical diameter is about half the actual length. Growth rate varies with temperature but this effect is small relative to the scale we use (*see Rhincalanus*, Fig. 13). However, the cool-water species tend to fall on the upper part of Fig. 13, indicating that at any one size, rate of production is highest in warm water.

Although for a balanced system the form of Fig. 12 predicts, qualitatively, the form of Fig. 13, and vice versa, the quantitative relationships seem to depend on subtle interactions between the growth rates and metabolic efficiencies of predators and prey. There is a need for further work to develop a sound theoretical framework, but the validity of our hypothesis can be roughly established from Fig. 13. In two well-known predator-prey links, *Clupea* to *Calanus* and *Calanus* to diatoms, rates of production vary by roughly an order of magnitude for each step. If the ecologic efficiency is about 10% then the standing stocks must be similar.

REFERENCES

ALTMAN, P. L., AND D. S. DITTMER. 1964. Biology data book. Fed. Amer. Soc. Exp. Biol. Washington. 633 p.

BEARDSLEY, G. F., JR., H. PAK, E. CARDER, AND B. LUNGREN. 1970. Light scattering and

suspended particles in the eastern equatorial Pacific Ocean. J. Geophys. Res. **75**: 2837–2845.

BLACKBURN, M. 1968. Micronekton of the eastern tropical Pacific Ocean: family composition, distribution, abundance and relations to tuna. U.S. Fish. Wildl. Serv. Fish. Bull. 67, p. 71–115.

———, R. M. LAURS, R. W. OWEN, AND B. ZEITZSCHEL. 1970. Seasonal changes in standing stocks of phytoplankton, zooplankton and micronekton in the eastern tropical Pacific. Mar. Biol. **7**: 14–31.

BURT, W. V. 1958. Selective transmission of light in tropical Pacific waters. J. Mar. Res. **5**: 51–61.

CONOVER, R. J., AND C. M. LALLI. 1972. Feeding and growth in *Clione limacina* (Phipps), a pteropod mollusc. Exp. Mar. Biol. Ecol. **8**: In press.

DOTY, M. S., AND M. OGURI. 1956. The island mass effect. J. Cons., Cons. Perm. Int. Explor. Mer **22**: 33–37.

EINARSSON, H. 1945. Euphausiacea. 1. Dana Rep. 27, p. 1–185.

EPPLEY, R. W., AND P. R. SLOAN. 1966. Growth rates of marine phytoplankton: correlation with light absorption by cell chlorophyll *a*. Physiol. Plant. **19**: 47–59.

FORD, E. 1933. An account of the herring investigations conducted at Plymouth during the years from 1924–1933. J. Mar. Biol. Ass. U.K. **19**: 305–384.

GARROD, D. J., AND R. GAMBELL. 1965. Whiting of the Irish Sea and the Clyde. Fish. Invest. London Ser. 2 **24**(3): 64 p.

GORDON, D. C. 1970. A microscopic study of organic particles in the North Atlantic Ocean. Deep-Sea Res. **17**: 175–185.

HARVEY, H. W. 1950. On the production of living matter in the sea off Plymouth. J. Mar. Biol. Ass. U.K. **29**: 97–137.

HEINLE, D. R. 1966. Production of a calanoid copepod *Acartia tonsa* in the Patuxent River estuary. Chesapeake Sci. **7**: 59–74.

HOBBIE, J. E., O. HOLM-HANSEN, T. T. PACKARD, L. R. POMEROY, R. W. SHELDON, J. P. THOMAS, AND W. J. WIEBE. 1972. Distribution and activity of microorganisms in ocean water. Limnol. Oceanogr. **17**(4): In press.

JERLOV, N. G. 1968. Optical oceanography. Elsevier. 194 p.

JOHNSON, P. O. 1970. The Wash sprat fishery. Fish. Invest. London Ser. 2 **26**(4): 77 p.

KREY, J. 1967. Detritus in the ocean and adjacent sea, p. 389–394. *In* G. H. Lauff [ed.], Estuaries. Amer. Ass. Advan. Sci. Publ. 83.

LEBOUR, M. V. 1925. The dinoflagellates of northern seas. Mar. Biol. Ass., Plymouth. 250 p.

LEBRASSEUR, R. J., W. E. BARRACLOUGH, O. D. KENNEDY, AND T. R. PARSONS. 1969. Production studies in the Strait of Georgia. Part 3. J. Exp. Mar. Biol. Ecol. **3**: 51–61.

MACKINTOSH, N. A. 1970. Whales and krill in the twentieth century, p. 195–212. *In* M. W. Holdgate [ed.], Antarctic ecology, v. 1. Academic.

———, AND S. G. BROWN. 1956. Preliminary estimates of the southern populations of the larger baleen whales. Norsk-Hvalfangst-Tid. **45**(9): 469–480.

MCLAREN, I. A. 1965. Some relationships between temperature and egg size, body size, development rate and fecundity of the copepod *Pseudocalanus*. Limnol. Oceanogr. **10**: 528–538.

———. 1969. Population and production ecology of zooplankton in Ogac Lake, a landlocked fjord on Baffin Island. J. Fish. Res. Bd. Can. **26**: 1485–1559.

MARR, J. 1962. The natural history and geography of the Antarctic krill. Discovery Rep. **32**: 33–464.

MARSHALL, S. M., AND A. P. ORR. 1955. The biology of a marine copepod *Calanus finmarchicus* (Gunnerus). Oliver and Boyd. 188 p.

MENZEL, D. W., AND J. H. RYTHER. 1960. The annual cycle of primary production in the Sargasso Sea off Bermuda. Deep-Sea Res. **6**: 351–367.

MULLIN, M. M. 1965. Size fractionation of particulate organic carbon in the surface waters of the Indian Ocean. Limnol. Oceanogr. **10**: 459–462.

———, AND E. R. BROOKS. 1970. Growth and metabolism of two planktonic marine copepods as influenced by temperature and type of food, p. 74–95. *In* J. H. Steele [ed.], Marine food chains. Oliver and Boyd.

PARSONS, T. R., R. J. LEBRASSEUR, J. D. FULTON, AND O. D. KENNEDY. 1969. Production studies in the Strait of Georgia. Part 2. J. Exp. Mar. Biol. Ecol. **3**: 39–50.

PRAKASH, A. 1967. Growth and toxicity of a marine dinoflagellate *Gonyaulax tamarensis*. J. Fish. Res. Bd. Can. **24**: 1589–1606.

RILEY, G. A. 1963. Theory of food chain relations in the ocean, p. 438–463. *In* M. N. Hill [ed.], The sea, v. 2. Wiley.

SAIJO, Y. 1964. Size distribution of photosynthesizing phytoplankton in the Indian Ocean. J. Oceanogr. Soc. Jap. **19**: 187–189.

SASAKI, T., N. OKAMI, G. OSHIPA, AND S. WATANABE. 1962. Studies on suspended particles in deep water. Sci. Pap. Inst. Phys. Chem. Res. (Tokyo) **56**: 77–83.

SHELDON, R. W. 1969. A universal grade scale for particulate materials. Proc. Geol. Soc. London 1659, p. 292–295.

———, T. P. T. EVELYN, AND T. R. PARSONS.

1967. On the occurrence and formation of small particles in seawater. Limnol. Oceanogr. 12: 367–375.

———, AND T. R. PARSONS. 1967*a*. A practical manual on the use of the Coulter counter in marine science. Coulter Electronics, Toronto. 66 p.

———, AND ———. 1967*b*. A continuous size spectrum for particulate matter in the sea. J. Fish. Res. Bd. Can. 24: 909–915.

———, AND W. H. SUTCLIFFE, JR. 1969. Retention of marine particles by screens and filters. Limnol. Oceanogr. 14: 441–444.

SMAYDA, T. J. 1966. A quantitative analysis of the phytoplankton of the Gulf of Panama. 3. Bull. Inter-Amer. Trop. Tuna Comm. 11(5): 355–612.

SUTCLIFFE, W. H., JR., R. W. SHELDON, AND A. PRAKASH. 1970. Certain aspects of production and standing stock of particulate matter in the surface waters of the Northwest Atlantic Ocean. J. Fish. Res. Bd. Can. 27: 1917–1926.

WILLIAMS, R. B. 1964. Division rates of salt marsh diatoms in relation to salinity and cell size. Ecology 45: 877–880.

Preliminary Analysis of Geophysical Measurements North of Juan de Fuca Ridge[1]

S. P. SRIVASTAVA, D. L. BARRETT, C. E. KEEN, K. S. MANCHESTER, AND K. G. SHIH
Atlantic Oceanography Laboratory, Bedford Institute, Dartmouth, Nova Scotia

AND

D. L. TIFFIN
Marine Sciences, Department of Energy, Mines and Resources, Vancouver, British Columbia

AND

R. L. CHASE AND A. G. THOMLINSON
Department of Geology, University of British Columbia, Vancouver, British Columbia

AND

E. E. DAVIS AND C. R. B. LISTER
Department of Oceanography, University of Washington, Seattle, Washington 98105

Received May 14, 1971
Revision accepted for publication July 20, 1971

Preliminary analyses of gravity, magnetic, seismic reflection and refraction, dredging, and heat flow measurements off Queen Charlotte Islands and Vancouver Island are presented. Seismic reflection and gravity measurements show the presence of a sedimentary basin at the foot of the continental slope in which the sediments are progressively more intensely deformed from north to south, indicating the interactions between the lithospheric plates. Heat flow values in the northern part of Explorer Ridge, and recovery of fresh basalts with little mineral coating in this region suggest that Explorer Ridge is a presently active spreading segment of East Pacific Rise. Seismic Refraction results in the deep ocean basin west of Queen Charlotte Islands show a marked anisotropic mantle P wave velocity, the direction of maximum velocity being 107° east of north and the maximum change in velocity being about 0.6 km/s.

L'article présente les résultats préliminaires de l'étude de la gravité, du magnétisme, de la réfraction et réflexion sismique, de dragages et de mesures du flux thermique au large des Iles de la Reine Charlotte et de l'Île de Vancouver. La réflexion sismique et les mesures de gravimétrie indiquent la présence d'un bassin sédimentaire au pied du talus continental; la déformation des sédiments y augmente progressivement du Nord vers le Sud, indiquant l'interaction entre des plaques de la lithosphère. Les valeurs du flux thermique dans la partie septentrionale de la Chaîne Explorer et la découverte de basaltes frais, avec altération superficielle minime, suggère que cette chaîne est actuellement un segment actif de l'East Pacific Rise. La réfraction sismique du fond du bassin océanique, à l'Ouest des Iles de la Reine Charlotte, montre une anisotropie marquée de la vitesse des ondes P, la direction de la vitesse maximale étant 107° et la différence entre les vitesses atteignant un maximum de 0.6 km/s.

Introduction

The results presented in this paper describe a variety of geophysical measurements obtained off the west coast of Canada during 1970. The area is important because it provides an opportunity to study the relationship of three plates and their effect upon the continental margin. Atwater (1970) has described the evolution of western North America using the distribution and focal mechanisms of earthquakes, the magnetic anomaly pattern in the Pacific, and the geological history of western North America. Figure 1 shows the present configuration of various plates and their relation to each other off the coasts of British Columbia and the northwestern United States as interpreted by Atwater (1970). According to her, a trench existed offshore from western North America during mid-

[1]Bedford Institute Contribution No. 254.

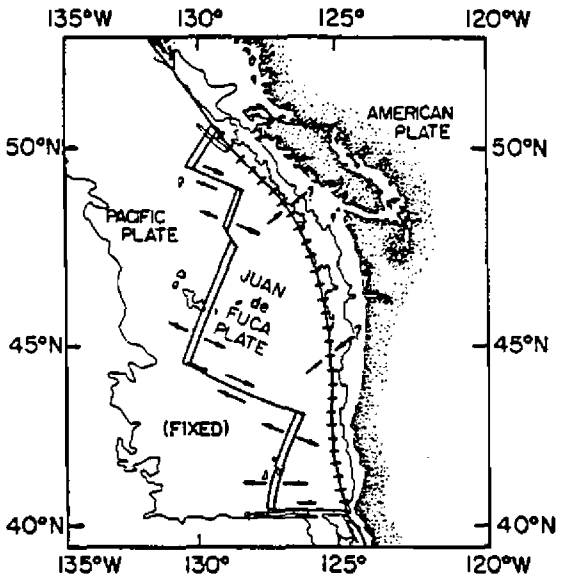


FIG. 1. Present plate configuration and motions near Juan de Fuca ridge (after Atwater 1970).

Tertiary time. The trench lay between the American plate and the Farallon plate (McKenzie and Morgan 1969). The latter lay on the east side of the East Pacific rise; the portion remaining today is called the Juan de Fuca plate (Fig. 1). The trench consumed the Farallon plate at a rate much faster than the rate at which it was formed at the ridge. Eventually, the ridge itself was overrun by the trench and trench activity stopped. There are only two places off North America where ridge segments presently exist; one west of Mexico and in the Gulf of California and the other off the coasts of British Columbia, and the northwestern United States. Thus the East Pacific rise after disappearing at the head of the Gulf of California, is offset by the San Andreas fault (Wilson 1965) and reappears as the Gorda, Juan de Fuca, and Explorer Ridges, called Gorda and Cobb Rises by McManus (1967). Farther to the north the Pacific and American plates are separated by the Queen Charlotte transform fault (Wilson 1965).

To study the interactions of the Pacific and American plates in the north, and Pacific, Juan de Fuca, and American plates in the south, geophysical and geological investigations were made west of Vancouver Island and the Queen Charlotte Islands during the Hudson-70 expedition, an expedition organized by Bedford Institute as a Canadian contribution to the International Decade of Ocean Exploration. These include measurement of the gravity and magnetic fields, bathymetry, seismic reflection and refraction, and heat flow, and bottom photography, dredging, and coring. The present paper briefly summarizes these results. Detailed interpretations will be published subsequently.

Measurements

The investigations were made from two ships, C.S.S. Hudson and C.N.A.V. Endeavour. Except for some reflection profiling, all geophysical measurements were made on board C.S.S. Hudson. Dredging and detonation of charges for the seismic refraction experiment were carried out from C.N.A.V. Endeavour. One core was taken and three camera lowerings were made from C.S.S. Hudson. Figure 2 shows the ship's tracks along which gravity, magnetic, bathymetric, and continuous seismic reflection measurements were made, and locations of the heat flow, camera, and dredge stations. The following sections describe briefly the results from each of the experiments conducted during the cruise. Details are given in a data report by Srivastava *et al.* (1971).

(*i*) *Gravity, Magnetic, and Bathymetric Measurements*

The changes in the acceleration due to gravity were recorded using two gravimeters: a Graf-Askania Gravimeter Model GSS-17 and a D4e vibrating string gravimeter belonging to Woods Hole Oceanographic Institution. Both of these gravimeters were mounted on a common gyro-stabilized platform. Total magnetic field intensity was measured using a proton precession magnetometer (Model OM104 of Barringer Research Corp.). Soundings were obtained using a 12.5 KHZ EDO transducer mounted under the ship's hull on a retractable rod in order to raise and lower it as desired, and recorded on an Alpine Mufax recorder programmed through Gifft transceivers. Primary navigation during the survey was provided by satellite navigation and dead reckoning. Data were collected in analog form on chart recorders as well as in digital form on punched paper tape using the Bedford Institute Data Logging (Biodal) system.

Free air gravity values were calculated using the 1930 International Gravity Formula while

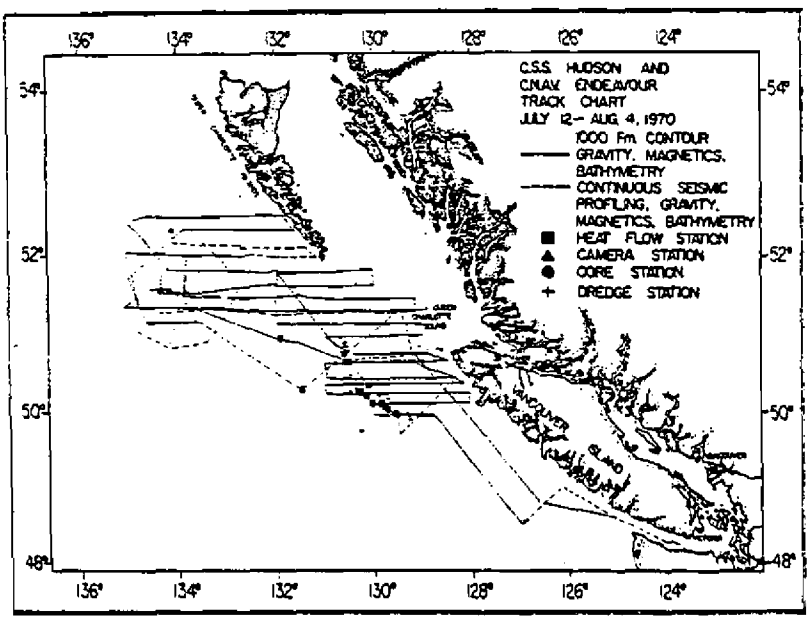


FIG. 2. Map showing the ship's track along which bathymetry, gravity, magnetic, and seismic profiling information was collected. Also shown are the locations of the heat flow, dredge, and camera stations.

magnetic anomalies were computed using the International Geomagnetic Reference Field 1965 (IAGA Comm. 2. 1969) for the regional field. Magnetic data presented here have not been corrected for diurnal variations but station records from Port Hardy (Fig. 2, Lat. 50° 42N, Long. 127° 28W) were checked for magnetic storms and only one minor storm occurred during the time of the survey. For the majority of time, diurnal variations at Port Hardy remained less than 30 to 40 gammas.

To estimate the accuracy of the survey, differences in values for gravity, magnetics, and bathymetry at places where tracks crossed were compiled and plotted as histograms in Fig. 3. The histograms show that for 70% of the times the cross-over remained less than 10 fathoms (ca. 18 m) in bathymetry, less than 4 milligal in gravity and less than 30 gammas in magnetics. The high cross-over values in magnetics can easily be accounted for by the amplitude of diurnal variations in the survey area. Comparisons of large cross-over values as obtained in each of the three measurements with the contoured maps revealed that they corresponded to the areas of the steep gradients and not to positional inaccuracies. The calculated free air gravity and magnetic anomalies were plotted and contoured. Figures 4 and 5 show the contoured anomaly maps.

The free air gravity map (Fig. 4) of the area shows large negative anomalies centered near the base of the slope similar to those observed further south of the present area (Dehlinger *et al.* 1968). Part of this negative free air anomaly can be accounted for by the change in the bathymetry across the continental margin but some of it arises due to the changes in the subsurface structure. A deep sedimentary basin lies at the foot of the slope near the north end of Vancouver Island, as inferred from continuous seismic profiling, Fig. 11. The large negative gravity value of −140 mgal thus corresponds to the thickest part of the sediments in this basin. Another gravity low is observed near the base of Queen Charlotte Fault in the northern part of the map. This low corresponds to the small trough observed in bathymetric map of the area, Fig. 8. The steepness in gravity gradient (15 mgal/km) across the continental margin and the presence of large positive values on the shelf suggest that there may be steep gradient in the depth to Moho in this area. Positive Bouguer anomalies are also observed on Vancouver Island and Queen Charlotte Islands (Stacey and Stephens 1969). The deep ocean

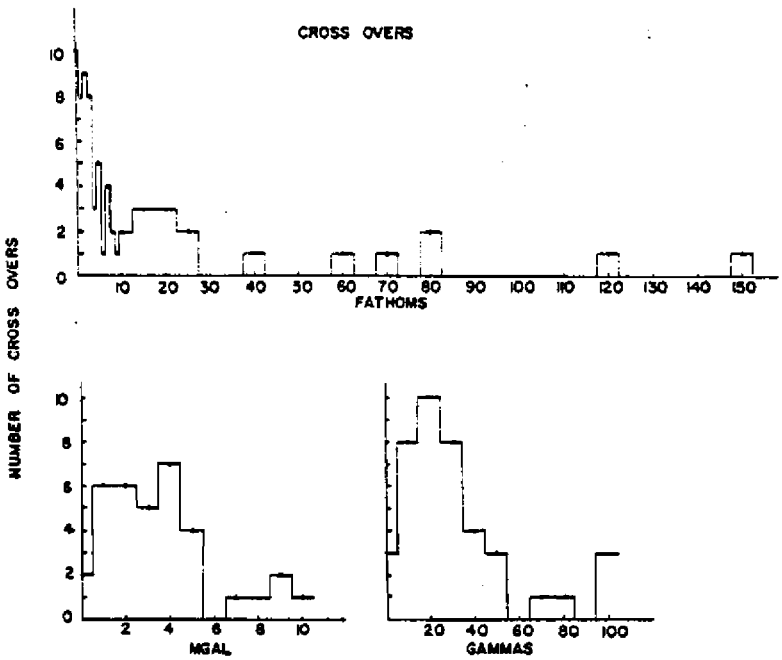


FIG. 3. Histogram of the cross-overs.

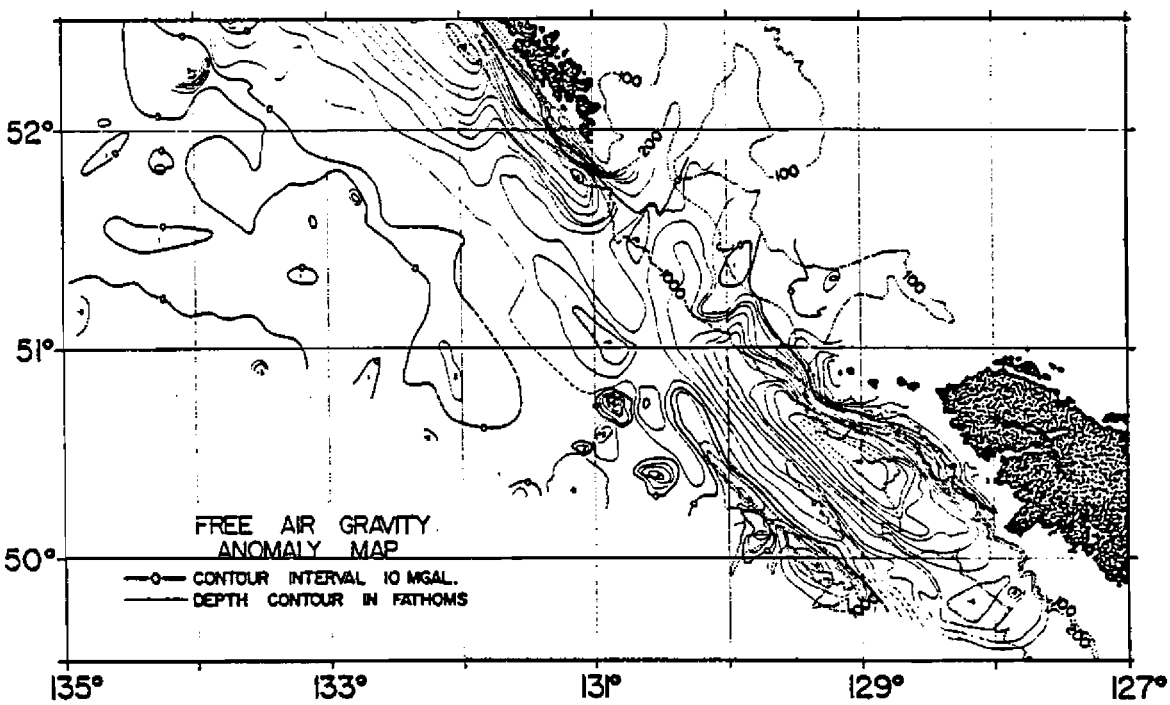


FIG. 4. Free air gravity anomaly map. The values shown in the contour enclosures are the largest or lowest observed values in tens of milligal. Also shown are the major bathymetric features of the area.

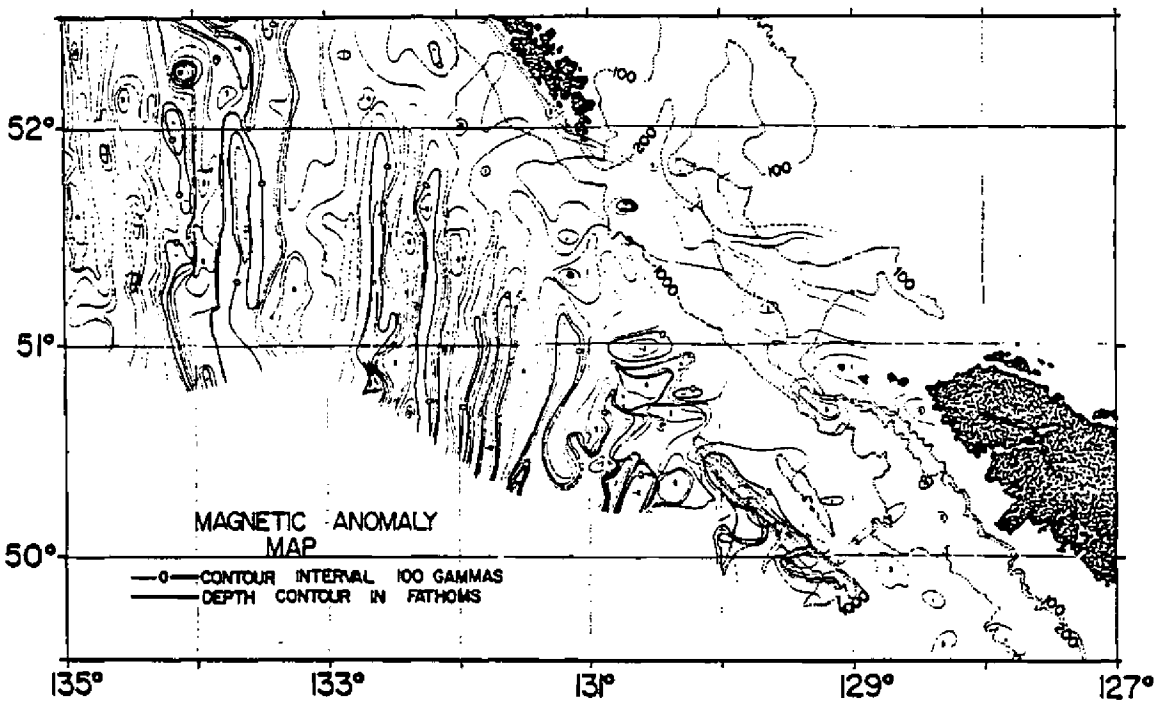


FIG. 5. Magnetic anomaly map. Anomalies are calculated using IGRF as the regional field. The values shown in the contour enclosure are the largest or lowest observed values in hundreds of gammas. Also shown are the major bathymetric features of the area.

basin area west of Queen Charlotte Islands shows primarily zero free air anomaly except for small areas of higher values which are located directed over the seamounts and the small ridges, e.g. Paul Revere Ridge in the southeast corner of the map.

The magnetic anomalies in the area are shown in Fig. 5. Much of this area was surveyed by Raff and Mason (1961) and included in their magnetic anomaly map of the NE Pacific. A comparison of their map with that shown in Fig. 5 shows a systematic difference of 200 gammas between them. This difference is attributed to a difference in the regional field used in establishing anomalies for the area. Raff and Mason (1961) used a second order polynomial fitted to their data as the regional field (Bullard and Mason 1963) whereas the regional field (IGRF) used in Fig. 5 was derived from world wide measurements (IAGA Comm. 2. 1969). Which of the two is a better estimate of the true regional field is difficult to judge at this stage. However, it appears from the present results (Fig. 5) and also from those obtained by Haines *et al.* (1971) using aeromagnetic data that IGRF does not accurately represent the average field over this region because the net anomaly in the area remains largely positive rather than zero.

In order to combine the present anomaly map with Raff and Mason's map we considered the positive 200 gammas contour in Fig. 5 as the zero gamma contour in the Raff and Mason's map. The resultant map is shown in Fig. 6. The positive anomalies are stippled and assigned various ages according to Vine's (1968) calculation. The long straight lines correspond to possible faults or fractures as hypothesized by Vine (1968). The map shows, (*a*) anomaly corresponding to 6 m.y. or number 3 anomaly according to Heirtzler *et al.* (1968) time scale, continuing to the shelf edge off Queen Charlotte Islands, (*b*) a band of positive anomaly lying on the continental shelf between Vancouver Island and Queen Charlotte Islands, (*c*) most of the anomalies from Raff and Mason's map continuing farther to the north, as was also noted by Pitman and Hayes (1968) and Atwater and Menard (1970) from correlations of widely

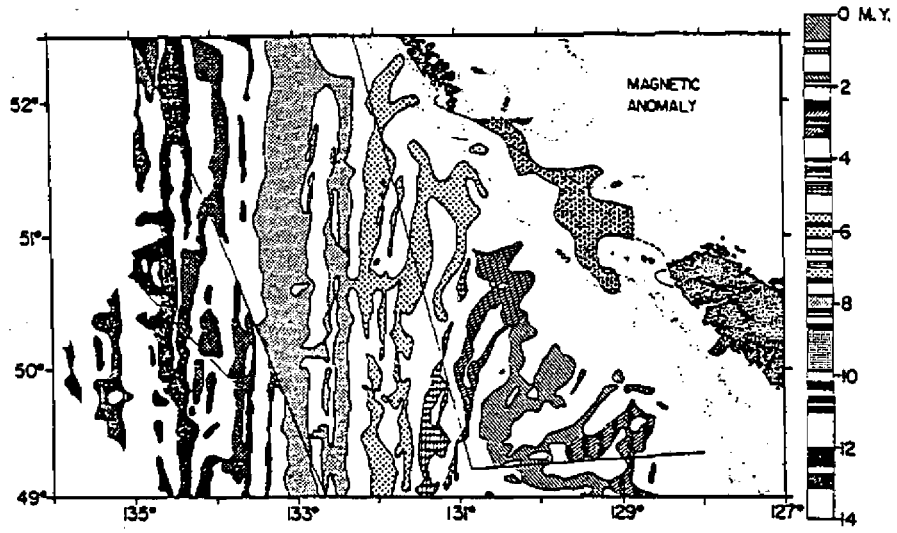


FIG. 6. Magnetic anomalies southwest of Vancouver Island as derived from Raff and Mason's (1961) map and the present data (Fig. 5) after slight adjustment (for detail see text). Areas of positive anomalies are stippled according to Vine's (1968) interpretation. The corresponding ages for the anomalies are shown on the right hand side in million years. Straight lines delineate faults offsetting the anomaly pattern (Vine 1968).

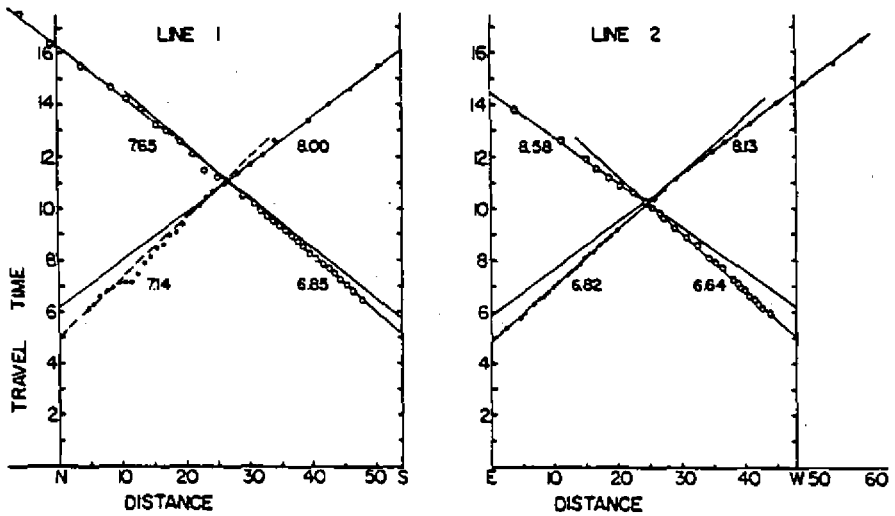


FIG. 7. Travel time curves for NS and EW lines. Both time and distance scales are in seconds.

spaced track data. The anomalies on the slope and shelf are in general positive and in places reach as high as 700 gammas (Fig. 5). They may be associated with the continental margin anomaly. In the southeast sector of the map (Fig. 5) a negative northwest trending anomaly lies over Paul Revere Ridge while in the area of Dellwood Knolls (McManus 1967) north of Paul Revere Ridge the magnetic anomalies are no longer linear.

(ii) Seismic Refraction Measurements

The seismic refraction experiment was designed to measure the anistropy of the mantle P wave velocity. C.S.S. Hudson was used as the receiving ship and C.N.A.V. Endeavour as the shooting ship. Two reversed lines, each about 75 km long were completed, one in the east–west and one in the north–south direction. A circular pattern of shots (radius 75 km) was obtained with Hudson, the listening ship, posi-

tioned at the center of the circle approximately at the intersection of the two reversed lines. The area where the refraction experiment was carried out is shown in Fig. 8. The ships' positions were determined by satellite fixes and by interpolating between fixes using dead reckoning when necessary. Shots were fired at intervals of from 5 to 20 min.

Seismic reflection data and a short (17 Km) sonobuoy refraction line were obtained in the same area. The sonobuoy data provided velocity information on the upper layers which were not well defined by the main experiment. Corrections were applied to the arrival times to remove variations due to bottom topography. The water depth to which all times were corrected is 3 km. Except for two seamounts, topographic variations are few, the topography is smooth, and corrections are accurate to about ±0.02 s. Time–distance plots were constructed for both reversed lines and these are shown in Fig. 7. The velocities were obtained using a value of 1.49 km/s for sound in sea water. This was the mean as measured for the upper 50 m of the water column. However, because of the complexity of velocity distribution with depth in the sea water as obtained from velocimeter measurements, the shot–receiver distance may be in error by as much as the equivalent of 0.2 s in travel time.

Results from the two reversed lines were used to calculate true velocities and layer thicknesses using the slope–intercept method (Ewing 1963). The results are presented in Table 1. Velocities of 6.8 and 8.0 km/s, corresponding to oceanic layer 3 and mantle rocks respectively, are well defined on the time–distance plots. A sediment velocity of 2.3 km/s was assumed for the uppermost layer and its thickness, obtained from seismic reflection measurements in the area taken as the mean. The velocity of layer 2, 4.5 km/s, was obtained from the short sonobuoy refraction line.

The first arrivals obtained from the circular shot line were subjected to a detailed analysis to determine if the mantle rocks are anisotropic with respect to their P wave velocity. About 50 arrival times were used to determine if any systematic variations of velocity with azimuth could be detected. The results show that there is significant anisotropy, the maximum velocity occurring at an azimuth of 107° ±5°. The mean velocity is 8.07 km/s with a maximum change of about 0.6 km/s. The results of the anisotropy experiment are given in detail in a separate paper by Keen and Barrett (1971).

(iii) Seismic Reflection Measurements

Seismic reflection profiling systems were operated on both C.S.S. Hudson and C.N.A.V. Endeavour. The system on Hudson consisted of a 400 ft (122 m) long hydrophone array in the form of 100 ft (30 m) active sections, and a Bolt model 1500 air gun with pulse shaper as source. The 300 in.^{3} (4916 cm^3) gun was fired every 16 s at a peak pressure of about 1700 psi (117215×10^3 dyne/cm^2). Signals were recorded on magnetic tape and graphically on an Alpine wet paper recorder and an EPC dry paper recorder. A slacking winch permitted the hydrophone array to remain almost stationary while signals were being received. The system on Endeavour consisted of a 20 in.^{3} (327.7 cm^3) Bolt Model 600B air gun, fired at 5 to 10 s intervals at a peak pressure of 1600 psi (11032×10^4 dyne/cm^2). The signals were received by a single 100-ft (30 m)-long hydrophone array and recorded on a Gifft wet paper recorder.

TABLE 1. True velocities (V in km/s) and thicknesses (h in km) of the layers calculated from the reversed profiles

Layer description	Northern station		Southern station		Eastern station		Western station	
	V	h	V	h	V	h	V	h
Sediment	2.30*	0.50	2.30*	0.50	2.30*	0.50	2.30*	0.50
Layer 2	4.50	1.94	4.50	2.44	4.50	1.60	4.50	2.17
Layer 3	6.99	8.59	6.99	4.13	6.73	5.22	6.73	5.22
Mantle	7.82		7.82		8.33		8.33	

*Indicates an assumed velocity.

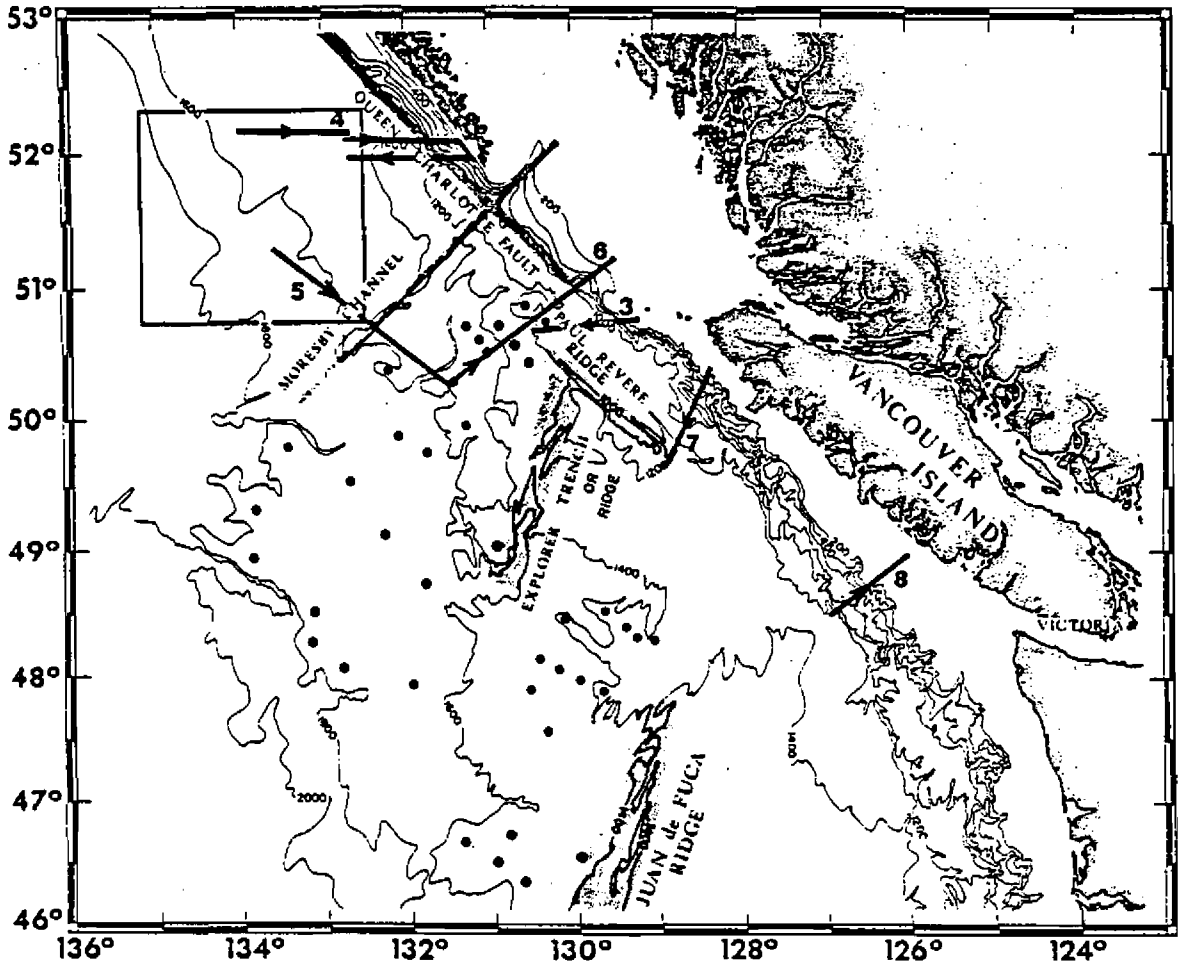


FIG. 8. Map showing the location of continuous seismic profiles in the area. The numbers shown on the track lines correspond to the profile number shown in Figs. 9 to 12. The area where seismic refraction measurements were made is shown as a rectangle in the upper left hand corner. Also shown are the major physiographic features of the area. The dots represent some of the major seamounts. (Bathymetry obtained from Chase *et al.* (1971) map of the North Pacific.)

Figure 8 shows the location of seismic profiles in relation to major tectonic features in the area. Profile 4 crosses the Queen Charlotte Fault while profiles 6 and 3 lie near the junction of this fault, Explorer Ridge[2] and Paul Revere Ridge. Profiles 7 and 8 are southeast of this junction and cross the continental margin. Several profiles were obtained in the oceanic area west of the Queen Charlotte Islands where the refraction experiment was conducted but only one profile, number 5, is shown here. Differences in structural features shown by all profiles are summarized briefly below.

Profile 4: (*Fig. 9*)

The margin along the Queen Charlotte Islands is relatively simple and abrupt in comparison with other areas, with no continental rise. Oceanic basement is traceable to the base of the continental slope only 28 km from the coastline. The south end of what has been called the Queen Charlotte trough or trench (Profile 4*a*, km 60), lies directly at the foot of the slope. The "trough", up to 240 m deep and 6 to 11 km wide, does not everywhere coincide with a

[2]Magnetic anomaly pattern across the Explorer trench shows that it is an active spreading center. Besides, the trench is not continuous: in fact three troughs are present at its NE end. Thus, it is renamed here and called Explorer Ridge.

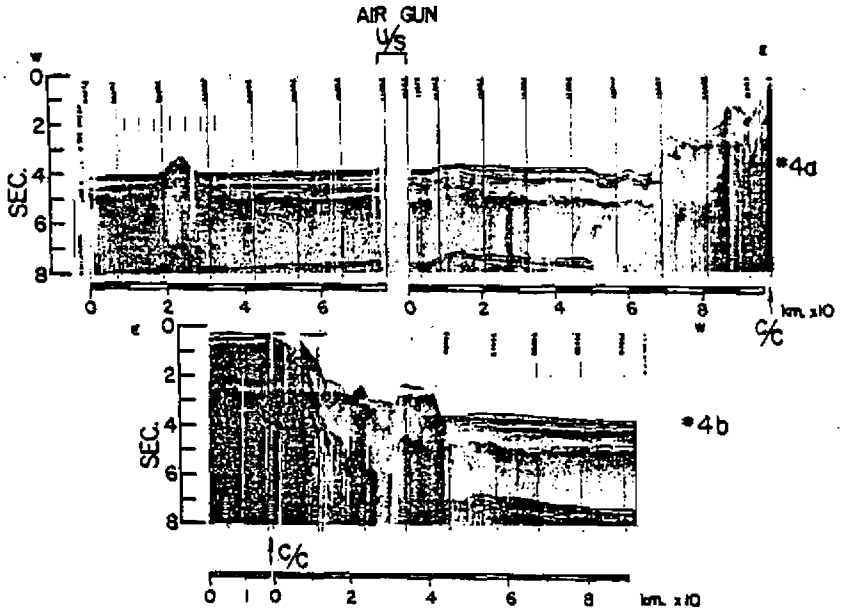


FIG. 9. Profile 4 across the Queen Charlotte Fault and margin. Location of the profile is shown in Fig. 8.

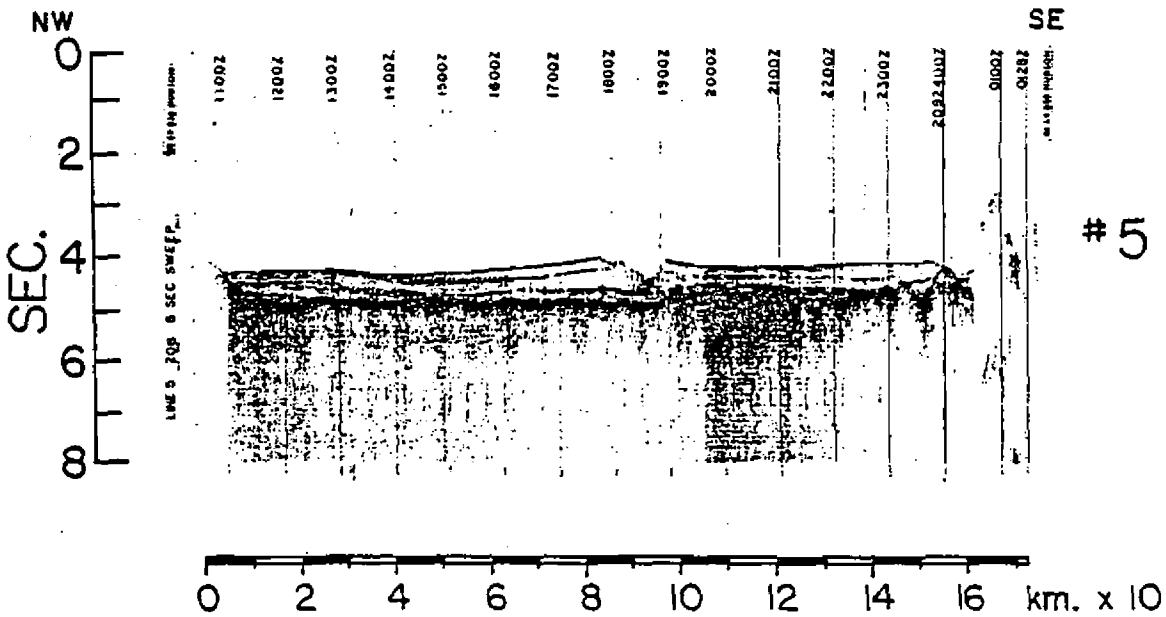


FIG. 10. Profile 5 across Moresby Channel. Location of the profile is shown in Fig. 8.

depression in basement topography, suggesting that it is in part a product of erosion or nondeposition of sediments, though in part also due to basement deformation.

The continental slope west of the Queen Charlotte Islands appears to be a series of vertical fault slices paralleling the continental margin. One fault slice (Profile 4*b*, km 40) appears to be oceanic basement overlain by transparent sediment. Others are capped by sediment up to 1.5 s thick. (The thickness of sediment in seconds refers to two way travel time throughout this paper.) Reflectors in sediment ponds between blocks on the slope dip

landward though this is not very evident from Fig. 9 due to deterioration in reproduction of this profile.

Profile 5: (Fig. 10)

Moresby Channel (Fig. 10, km 90) runs southwest from the continental slope in the area south of Cape St. James to Tufts Abyssal Plain, a distance of several hundred kilometers. A second channel (Fig. 10, km 160), Scott Channel, heads in the same area and runs south of Moresby Channel to join the latter in the vicinity of 50° N, 134° W. Both channels appear on Profile 5, Fig. 10. Moresby Channel is leveed, the northwesterly levee being approximately twice as high as the opposite levee. Reflectors in sediments beneath the channel are disturbed and may indicate some lateral migration of the channel to the southeast. Scott Channel, where cut by Profile 5, lies at the base of a seamount (km 160). Its sides are formed in part by basement outcrop but its bottom is composed of flat-lying sediment. Channel levees comprise a considerable part of the sedimentary column above oceanic basement in this profile.

The ruggedness of the oceanic basement changes across a boundary which coincides approximately with Moresby Channel in Profile 5. In all profiles north of this boundary, oceanic basement is a relatively smooth reflector with a few seamounts. The thickness of sedimentary cover varies from 0.3 to 1 s. In contrast, to the south of the boundary the basement surface is rugged, there are many seamounts, sediment thickness varies considerably but averages much less than in the north, and basement outcrops are common. The difference in sediment thickness may be in part explained by a greater age of the crust to the north, which lies farther from active spreading centers. Difference in basement relief and numbers of seamounts may reflect a change in stress and thermal regimes at the spreading center at which the volcanic layer was formed.

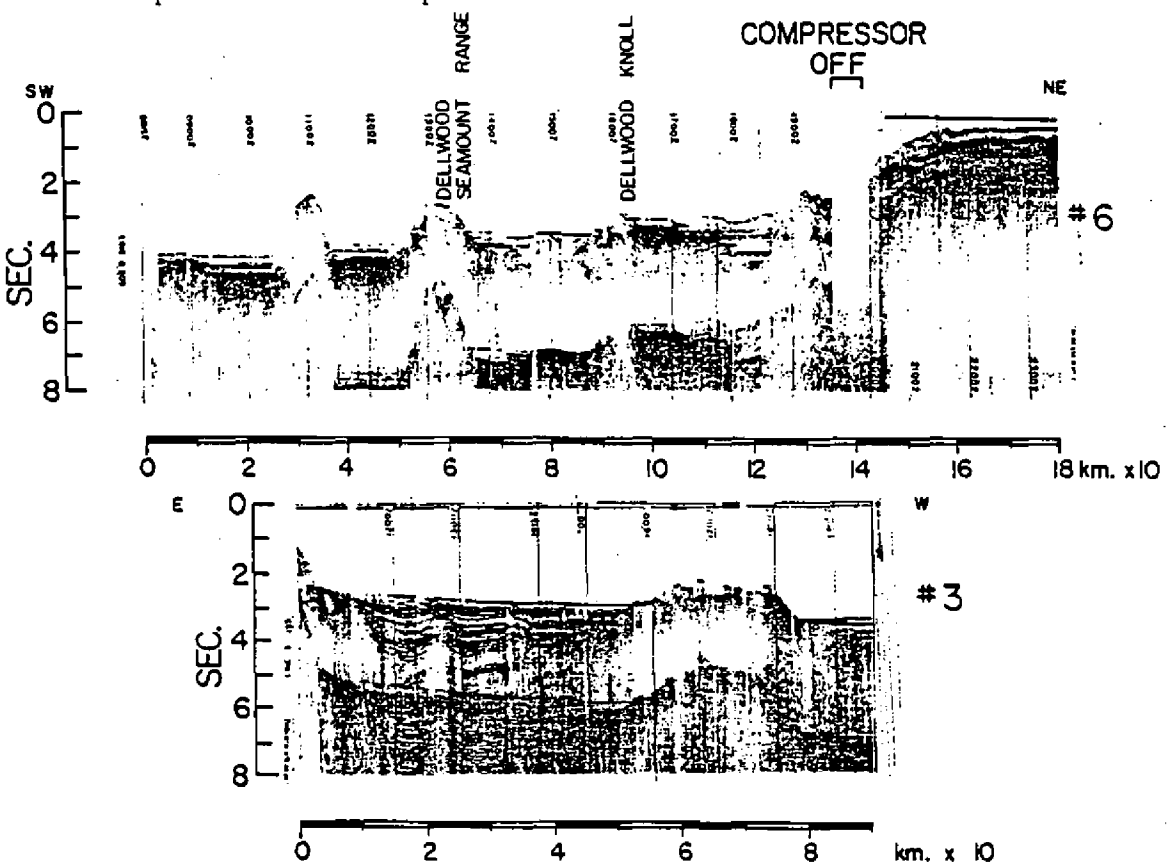


FIG. 11. Profiles 6 (top) and 3 across the continental margin north of Vancouver Island. Locations of the profiles are shown in Fig. 8.

Profiles 6 and 3: (Fig. 11)

The continental margin between Moresby Island and Vancouver Island was described as a 'fracture zone' by McManus (1967). The work of Vine (1968), Morgan (1968), and Atwater (1970) point to its being the location of the triple point between the American, Juan de Fuca, and Pacific plates (Fig. 1). Profiles 6 and 3 cross this region. Profile 6 obliquely crosses the northwest slope of Explorer ridge (km 0–60), which includes two seamount ranges, one unnamed (km 30), and one named Dellwood Range (km 60; McManus 1967). Between Dellwood Range and Dellwood Knolls (km 90; McManus 1967) lies a depression, trending northwest, partly filled with 0.8 s of sediment. On evidence from this reflection profile and other previously obtained by University of British Columbia, from interruption of linear magnetic anomalies, and from indications of shearing in specimens dredged from Paul Revere Ridge (see below), we hypothesize that this depression marks a fracture zone connecting Explorer Ridge to a center of spreading at Dellwood Knolls, and name it here the Revere–Dellwood fracture zone.

Between Dellwood Knolls and the continental slope lies a sedimentary basin filled with at least

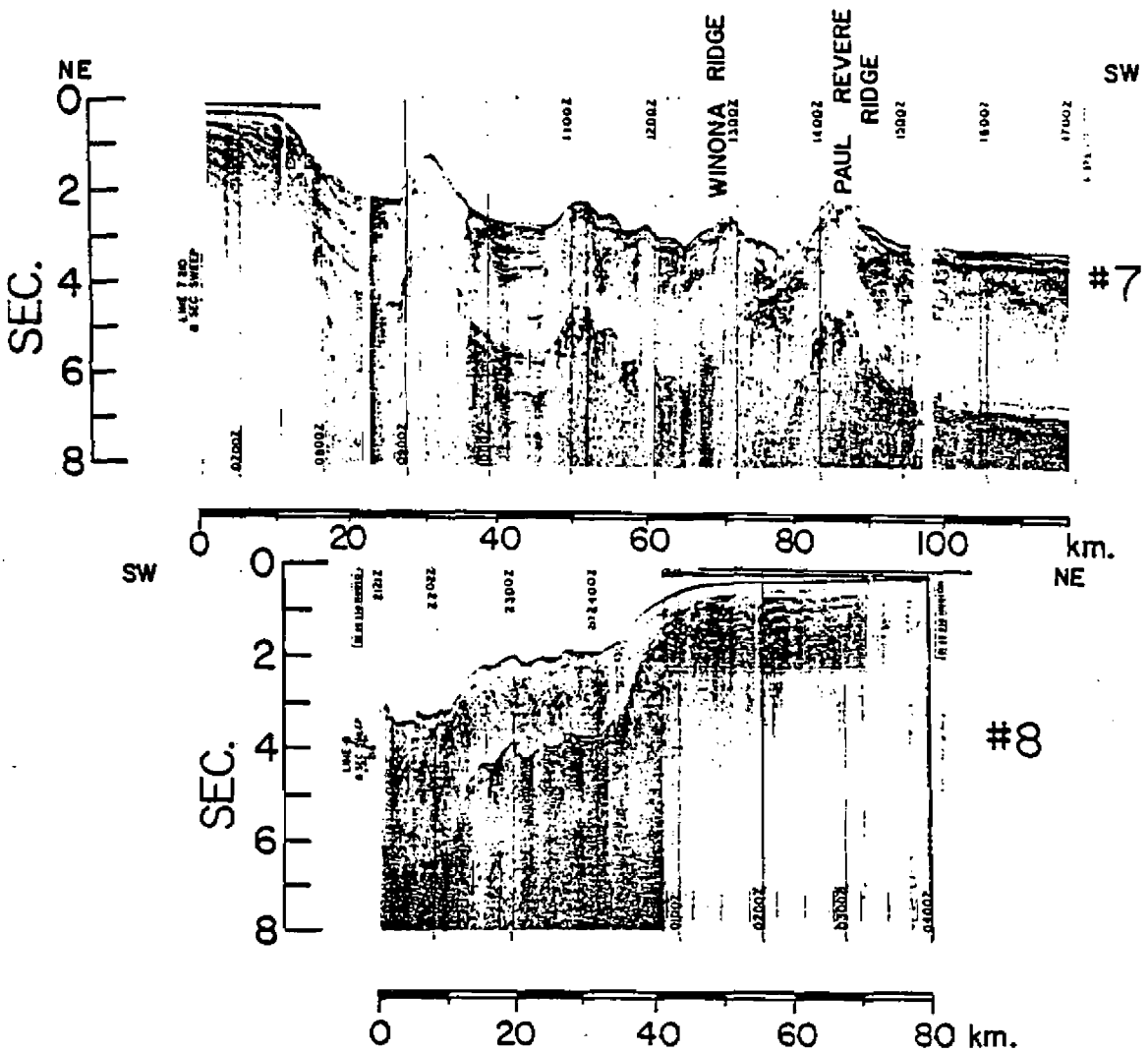


FIG. 12. Profile 7 (top) and 8 across the continental margin off Vancouver Island. Locations of profiles shown in Fig. 8.

2 s of stratified material. The basin widens to the south, and encompasses northwest trending ridges, one of which is Winona ridge (McManus 1967). Hence, we refer herein to the basin as Winona basin. From Profile 6 it appears that strata at the eastern margin of the Winona basin have been folded up and form the lowest part of the continental slope. Profile 3 cuts obliquely across Winona basin between the southern of the two Dellwood Knolls and the continental slope. The basin here consists of a least 2.7 s of gently folded strata whose aggregate thickness increases eastwards from zero at km 60 to a maximum towards the foot of the continental slope. The strata terminate against the flank of the Dellwood Knolls, and may be interbedded with the basalt of which it is composed (see below). All but the uppermost of the Winona sequence is folded in two relatively narrow zones in the center of the basin, the degree of folding increasing downward. The folding could result from differential compaction over inactive ridges in underlying, more competent rock, or localized *en echelon* strike-slip faulting, at depth, while the Winona sequence was being deposited. The width of Winona basin decreases northward from Profile 3 to Profile 6. No similar basin is shown on profiles west of the Queen Charlotte Islands. We assume, therefore, that the basin ends south of Queen Charlotte trough.

Profiles 7 and 8: (Fig. 12)

Shelf strata are truncated on the upper continental slope west of Vancouver Island (Profile 7, km 10), indicating faulting or slumping. Folds and possibly faults in the Winona Basin sequence, here at least 2.5 s thick, form ridges trending northwest. The eastern two (Profile 7, km 30 and km 50) are unnamed; the third is Winona Ridge (km 70). The southwestern margin of the basin is Paul Revere Ridge (km 85, McManus 1967). Strata of the Winona sequence, dipping east off the east flank of Paul Revere Ridge, thicken away from the ridge, indicating that the latter was already a positive feature during their deposition. Basalt, dredged from the west side of the ridge crest near its southern end, may be from the acoustic basement seen dipping under the sediments on the east side of the ridge. A rugged reflector appearing at about 3.75 s near km 110, Profile 7, originates from within the non-sedimentary part of the oceanic crust forming the southeast flank of Explorer Ridge and may be the upper surface of the layer below the volcanics, usually termed layer 3. It may, however, be a reflector within layer 2.

Sedimentary strata on the shelf off southern Vancouver Island (Profile 8) are folded but are not truncated on the upper slope where younger sediments are prograding. Reflectors are, however, truncated by faults beneath a middle slope plateau. Strata at the western end of the profile are also folded and perhaps faulted. A profile by Ewing *et al.* (1968) shows that a thick wedge of undisturbed sediments lies at the base of the slope beyond the end of Profile 8, forming Cascadia abyssal plain.

Heat Flow Measurements

The heat flow measurements were made using a Bullard-type probe modified to measure sediment thermal conductivity *in situ*. The details of this apparatus and the method used are given by Lister (1970). Thirteen heat flow stations were attempted and 12 produced useful results (Fig. 2). Table 2 contains the measured heat flow values at these stations. Two measurements were obtained in the northern part of the area; one on a ridge extending from the continental rise (HF-1) and one in the area where seismic refraction measurements were made (HF-2).

A heat flow value of 1.1 μcal/cm^2-s is normal, but the value in the refraction area at 2.68 μcal/cm^2-s, would be considered somewhat high by most workers. However, the oceanic crust in the region is relatively young and is covered by a substantial accumulation of sediments which have presumably built up steadily since the crust was formed. Measurements in Cascadia basin, (Foster 1962, Talwani *et al.* 1965) another heavily sedimented area, suggest that rapid sedimentation can seal off the oceanic basement for hydro-thermal circulation, and thus result in observed conductive heat flow consistent with reasonable boundary layer cooling models (Oxburgh and Turcotte 1968; McKenzie 1967). The deep sea measurement therefore does not indicate that the crust in the area is necessarily abnormal. The presence or relative absence of hydro-thermal circulation in the upper crustal layers should not have a significant effect on the mantle interface.

The most important part of the heat flow

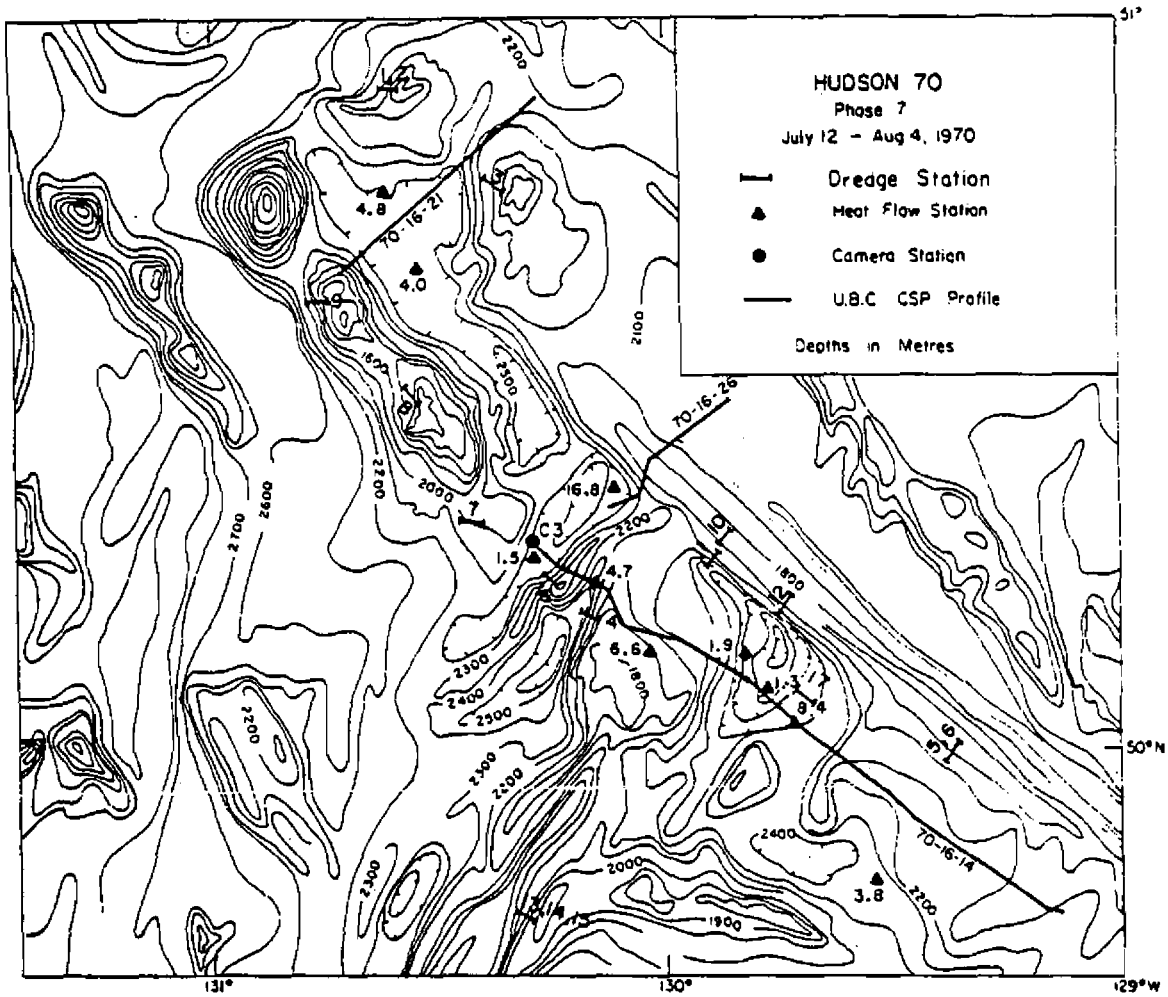


FIG. 13. Bathymetric chart (extract from Mammerickx and Taylor's (1971) chart of the northeast Pacific) showing location of dredge and heat flow stations. The heat flow values are in $\mu cal/cm^2$-s.

TABLE 2. Heat flow measurements

Station	Latitude* N	Longitude* W	Depth† fm	Heat flow $\mu cal/cm^2$-s	Estimated accuracy
HF-1	50° 58.0′	131° 54.7′	1403	1.1	.06
HF-2	51° 34.7′	134° 20.7′	1751	2.7	.05
HF-4	49° 58.6′	129° 32.6′	1111	3.8	.04
HF-5	50° 1.6′	129° 43.0′	1253	8.4	.30
HF-6	50° 4.4′	129° 46.4′	1742	1.3	.08
HF-7	50° 7.7′	129° 49.8′	1480	1.9	.20
HF-8	50° 7.5′	130° 1.8′	1116	6.6	.20
HF-9	50° 13.2′	130° 9.2′	1287	4.7	.07
HF-10	50° 15.3′	130° 17.8′	1300	1.5	.30
HF-11	50° 21.0′	130° 6.6′	1413	16.8	.40
HF-12	50° 45.9′	130° 36.6′	1310	4.8	.10
HF-13	50° 39.5′	130° 33.0′	1308	4.0	.06

*Location by satellite navigation.
†Depth in uncorrected fathoms.

work was a profile across the northern end of the Explorer Ridge and some stations in subsidiary troughs to the north (Fig. 13). The heat flow stations were sited in an attempt to find out whether thermal anomalies confirm Explorer Ridge to be an active spreading center. Seven stations were made across the two trough-like features which terminate at the Paul Revere Ridge. The stations follow University of British Columbia air gun Profile 70-16-14, which was used to locate sediment and index the general structure. Two values in the southeasterly trough are low but the trough is flanked by high heat flows on both sides (8.4 and 6.6 μcal/cm^2-s respectively). A moderately high value (4.7 μcal/cm^2-s) is observed on a ridge near the northwesterly, or main trough but another relatively low value is indicated for the valley itself by a partial penetration station (1.5 μcal/cm^2-s for 60 cm of sediment). The presence of a large seamont immediately beyond the valley terminated the profile, and the important symmetry station for this trough is missing. However, a measurement was made where the northwestern trough abuts the Paul Revere Ridge and a record value of 16.8 μcal/cm^2-s was obtained.

The heat flow evidence thus suggests that *both* troughs are, or have recently been, spreading centers and that the low values obtained in the troughs on the profile are the result of the well known, but not understood, "valley effect" (von Herzen and Uyeda 1963).

Two measurements were made in the subsidiary trough leading northeast from the Revere–Dellwood fracture zone. Owing to navigational problems they are not sited as was intended and, being approximately equal, do not confirm or deny the existence of spreading in this trough. An average heat flow of 4.4 μcal/cm^2-s is rather high, but in view of the other measurement on the same fault line, and dredging of fresh basalt further north of this area (station 2, Fig. 13) it is possible that active spreading is occurring in this region.

Dredging

In the vicinity of Explorer Ridge 17 dredge hauls were attempted, of which 14 were successful, Fig. 13. Preliminary descriptions of the rock recovered are included in Table 3. The dredging method involved lowering a chain-bag dredge from the ship's bow to a slope on the sea floor. When the metered wire length indicated the dredge to be on bottom, the ship moved slowly astern in the upslope direction, paying out enough additional wire to permit dredging with wire angles no greater than 45°.

The objectives in dredging in this area were to obtain outcrop specimens which will permit:

1. Determination of relationships between lithology, magnetic properties, and age of basalts from different magnetic anomalies within the Explorer Ridge area.

2. Resolution of stratigraphic and structural relationships between graywackes, siltstones, and mudstones, and serpentinite on Paul Revere Ridge. All three rock types were recovered in a single earlier dredge haul midway along the ridge. The need to resolve the stratigraphy and structure of Paul Revere Ridge is more pressing because this ridge marks an abrupt northern termination of pronounced magnetic anomalies which characterize the adjacent Explorer Ridge area.

3. Petrography and age-determination of basalts of the Dellwood Range of seamounts and, to the northeast, the Dellwood Knolls, to determine whether or not this portion of the sea floor is spreading.

Basalts dredged from the Explorer Ridge area (sites 4, 7, 15, 16) are vesicular pillow-lavas possessing glassy exteriors which range from fresh to moderately palagonitized and weathered and are thinly encrusted by oxides. In contrast, dredge site 6 and 11 on the Paul Revere Ridge yielded basalts which appear to be older, the glass phase being more deeply weathered and clay-oxide crusts thicker. The relatively young appearance of basalts from Explorer Ridge is consistent with a hypothesis that this is a site of recent sea floor spreading. Paul Revere Ridge seems to be separated from the Dellwood Knolls by a transform fault (the Revere–Dellwood fracture zone) trending northwest along the steep scarp on the west side of Paul Revere Ridge. Included with basalts in dredge haul 11 from this fracture zone are several specimens which appear to be partly serpentinized basic rock, some of which are slickensided. Further evidence of faulting is observed in sedimentary rocks dredged from the crest of Paul Revere Ridge 8 miles (13 km) southeast of site 11. This site (no. 12) includes graywacke, slickensided and contorted interlaminated mudstone, and

TABLE 3. Location and description of dredge stations

Dredge site	° N Lat.	° W Long.	Geographic features	Depth (m) From	Depth (m) To	Description of the dredge hauls
2	50° 53.7′	130° 35.0′	Dellwood Knolls (N.W.)	1900	1500	90% angular fragments of vesicular pillow basalt, many with fresh glassy rind. 10% pebble size glacial erratics of dioritic to granitic composition.
3	50° 46.0′	130° 24.0′	Dellwood Knolls (S.E.)	1900	1500	40% glacial boulders and cobbles, 60% pillow basalt. Generally thin manganese coating but one sample with 2 cm thick crust of manganese oxides.
4	50° 14.1′	130° 13.4′	Explorer Ridge	2500	2000	Fresh, ropey, vesicular basalt with glassy rind.
5	49° 55.7′	129° 20.7′	Paul Revere Ridge (S. slope)	1800	1700	One 13 cm fragment of porous, low density, manganiferous mudstone.
6	49° 58.0′	129° 17.7′	Paul Revere Ridge (crest)	1600	1500	10% glass sponges, infilled with clay and manganese oxide; 25% glacial pebbles and cobbles; 65% basalt with weathered, palagonitized glassy rind.
7	50° 17.9′	130° 24.6′	Dellwood Range (S.E. end)	2000	1900	Mainly vesicular pillow basalt some with glassy rind. No glacial erratics.
8	50° 27.2′	130° 32.5′	S.E. Dellwood Seamount	1475	1300	One large glacial boulder and few glacial pebbles and cobbles; remainder is vesicular, pillow basalt. Many large samples with weathered glassy rind, some with manganese coating about 2 cm thick.
9	50° 36.0′	130° 45.5′	Middle Dellwood Seamount	1800	1500	20% glacial pebbles and cobbles and iron oxide-stained volcanic ash; 75% basalt with manganese oxide coating to 3 cm thick. 5% manganese nodule fragments. Weathered glassy rind on some basalt fragments.
10	50° 14.5′	129° 49.9′	Paul Revere Ridge (crest)	1800	1700	One glacial cobble of intrusive rock.
11	50° 14.5′	129° 54.7′	Paul Revere Ridge (S. slope)	2300	2200	Vesicular olivine basalt, apparently from weathered talus, coated with manganese oxides.
12	Approx. 50° 10.0′	Approx. 129° 45′	Paul Revere Ridge (S. slope)	2200	2000	50% green, partly serpentinized rock (basalt and/or peridotite); 50% graywacke and interbedded mudstone and siltstone, contorted and sheared, containing carbonized plant fragments and lenses of coal up to 8 mm thick.
15	Approx. 49° 46′	Approx. 130° 18′	Explorer Ridge (E. wall)	2100	2000	Pillow basalt with palagonitized glassy rind; one glacial cobble.
16	Approx. 50° 13′	Approx. 130° 14′	Explorer area (N.W. part)	2100	1900	Pillow basalt with glassy rind.
17	Approx. 50° 5.5′	129° 44.5′	Explorer area (N.E. deep)	3200	2400	One angular fragment of fresh, dark green volcanic rock.

NOTE: No. 1, 13, and 14—Dredge unsuccessful.

siltstone containing carbonized plant fragments and thin coal lenses, and serpentinite. Stratigraphic and structural relationships between the sedimentary rocks and the serpentinite remain unresolved, despite attempts to segregate them by dredging over short distances.

Preliminary work on random samples from dredge hauls 2, 3, 7, 8, 9 show that manganese oxide crusts are thicker on basalts from the Dellwood Seamount Range than on basalts from the Dellwood Knolls, indicating that the latter are younger. This possibility is supported by the fact that Dellwood Knolls basalts (particularly those of dredge haul 2) have a fresher appearance than have basalts from the Dellwood seamounts. It is, therefore, tentatively suggested that the sea floor is spreading in the Dellwood Knolls area.

Summary

Seismic refraction results indicate that the crustal structure in the deep ocean west of the Queen Charlotte Islands is similar to that found elsewhere in the Pacific Ocean basin (Raitt 1963; Shor 1962 and Shor *et al.* 1968). The observations show that mantle rocks are anisotropic; the direction of maximum velocity being 107° and the maximum change of velocity about 0.6 km/s. The direction of maximum velocity does not coincide exactly with the presumed east–west direction in which spreading occurred at the time this part of the Pacific plate was formed (Pitman and Hayes 1968). However, the difference is relatively small and may perhaps be attributed to local variations in spreading direction.

The present magnetic measurements overlap Raff and Mason's map and extend northward beyond it. They show a continuation of most of the linear N–S anomalies into the northern area. A constant difference of 200 gammas between Raff and Mason's work and the present data has been attributed to a difference in the regional field used.

Large negative gravity anomalies are observed along the continental slope. The steepness of these anomalies and the presence of positive values on the continental shelf suggest that the Moho dips steeply in this area. Gravity measurements also show lows over areas of thick sediment.

The seismic reflection results show differences in the crustal features between the area west of Vancouver Island and that west of the Queen Charlotte Islands. In the north, transition from continental shelf to oceanic crust characterized by a thin undeformed sedimentary layer takes place across a narrow, steep, intensely faulted continental slope. In the south, the slope broadens, becomes less faulted, and is separated from the typical oceanic crustal sequence by the Winona basin containing up to 2.5 s of sedimentary strata, some of which contain coal. The Winona sequence is deformed into northwest trending ridges.

High heat flow values in the northern part of the Explorer Ridge and recovery of fresh basalts with little or no manganese coating in this region suggest that Explorer Ridge is a presently active spreading center. Another spreading center at Dellwood Knolls is a possibility.

Acknowledgments

We would like to thank our many associates from Atlantic Oceanographic Laboratory, departments of Geophysics and Geology, University of British Columbia who helped us in collecting and reducing the data reported here during phase VII of Hudson-70 expedition. We would like to express our sincere thanks to the masters and crews of C.S.S. Hudson and C.N.A.V. Endeavour without whose help so much could not have been accomplished within such a short cruise. The support before and after the cruise rendered by the Canadian Hydrographic Office, Victoria and the Defence Research Establishment Pacific, Esquimalt is gratefully acknowledged. Scientific assistance and encouragement from Chief Scientist Dr. C. D. Maunsell is gratefully appreciated. The assistance provided by Mr. D. R. Auld of Earth Physics Branch, Department of Energy, Mines and Resources in setting up and maintaining a magnetic monitoring station at Port Hardy for the duration of the survey is gratefully acknowledged.

ATWATER, TANYA. 1970. Implications of plate tectonics for the Cenozoic tectonic evolution of western North America. Geol. Soc. Am. Bull. **81**, pp. 3513–3536.

ATWATER, TANYA and MENARD, H. W. 1970. Magnetic lineations in the northeast Pacific. Earth and Plant. Sci. Lett. 7, pp. 445–458.

BULLARD, E. C. and MASON, R. G. 1963. The magnetic field over the oceans. The Sea, Vol. 3. (*Editor*) M. N. Hill. Interscience Publications, pp. 175–210.

CHASE, T. E., MENARD, H. W., and MAMMERICKX, J. 1971. Bathymetry of the North Pacific. Chart No. 4. Scripps Instit. of Oceanogr. and Inst. of Marine Resources. Univ. of California. Publ.

DEHLINGER, P., COUCH, R. W., and GEMPERLE, M. 1968. Continental and oceanic structure from the Oregon coast westward across the Juan de Fuca Ridge. Can. J. Earth Sci. 5, pp. 1079–1090.

EWING, J. 1963. Elementary theory of seismic refraction and reflection measurements. The Sea, Vol. 3. (*Editor*) M. N. Hill. Interscience Publications. New York. pp. 85–102.

EWING, J., EWING, M., AITKEN, T., and LUDWIG, W. 1968. North Pacific Sediment Layers Measured by seismic profiling. The crust and upper mantle of the Pacific area. A.G.U. monograph No. **12**. pp. 147–173.

FOSTER, T. D. 1962. Heat flow measurements in the northeast Pacific and in the Bering Sea. J. Geophys. Res. **67**, pp. 2991–2993.

HAINES, G. V., HANNAFORD, W., and RIDDIHOUGH, R. P. 1971. Magnetic anomalies over British

Columbia and the adjacent Pacific Ocean. Can. J. Earth Sci. 8, pp. 387–390.

HEIRTZLER, J. R., DICKSON, G. O., HERRON, E. M., PITMAN, W. C. III, and LE PICHON, X. 1968. Marine magnetic anomalies, geomagnetic field reversals and motions of the ocean floor and continents. J. Geophys. Res. 73, pp. 2119–2136.

IAGA Commission 2 working Group 4 (analysis of geomagnetic field). 1969. International Geomagnetic Reference Field 1965. O. J. Geophys. Res. 74, pp. 4407–4408.

KEEN, C. E. and BARRETT, D. L. 1971. A measurement of seismic anisotropy in the northeast Pacific. Can. J. Earth Sci. 8, pp. 1056–1064.

LISTER, C. R. B. 1970. Measurement of in situ sediment conductivity by means of a Bullard type probe. Geophys. J. Roy. Astron. Soc. 19, pp. 521–532.

MAMMERICKX, J. and TAYLOR, I. L. 1971. Bathymetry of the Pioneer survey area. Geological data Center, Scripps. Inst. of Oceanogr. Univ. of California. Special Chart No. 1.

MCKENZIE, D. P. 1967. Some remarks on heat flow and gravity anomalies. J. Geophys. Res. 72, pp. 6261–6274.

MCKENZIE, D. P. and MORGAN, W. J. 1969. Evolution of triple junctions. Nature, 224, pp. 125–133.

MCMANUS, D. A. 1967. Physiography of Cobb and Gorda rises, Northeast Pacific Ocean. Geol. Soc. Am. Bull. 78, pp. 527–546.

MORGAN, W. J. 1968. Rises, trenches, great faults, and crustal blocks. J. Geophys. Res. 73, pp. 1959–1982.

OXBURGH, E. R. and TURCOTTE, D. L. 1968. Mid-ocean ridges and geotherm distribution during mantle convection. J. Geophys. Res. 73, pp. 2643–2661.

PITMAN, W. C. III and HAYES, D. E. 1968. Sea floor spreading in Gulf of Alaska. J. Geoph. Res. 73, pp. 6571–6580.

RAFF, A. D. and MASON, R. G. 1961. Magnetic survey off the west coast of North America. 40° N latitude to 52° N latitude. Geol. Soc. Am. Bull. 72, pp. 1267–1270.

RAITT, R. W. 1963. The crustal rocks. The Sea, Vol. 3. *(Editor)* M. N. Hill. Interscience Publications, New York. pp. 85–102.

SHOR, G. G., JR. 1962. Seismic refraction studies off the coast of Alaska; 1956–1957. Bull. Seismol. Soc. Am. 52, pp. 37–57.

SHOR, G. G., JR., DEHLINGER, P., KIRK, H. H., and FRENCH, W. S. 1968. Seismic refraction studies off Oregon and northern California. J. Geophys. Res. 73, pp. 2175–2194.

SRIVASTAVA, S. P., BARRETT, D. L., BERTRAND, W. G., CHASE, R. C., DAVIS, E. E., KEEN, C. E., MANCHESTER, K. S., LISTER, C. R. B., ROSS, D. I., SHIH, K. G., THOMLINSON, A., and TIFFIN, D. L. 1971. Geophysical data collected during Hudson-70, phase VII off British Columbia. Atl. Oceanogr. Lab. Data Series No. 1971-5-D.

STACEY, R. A. and STEPHENS, L. E. 1969. An interpretation of gravity measurements on the west coast of Canada. Can. J. Earth Sci. 6, pp. 463–474.

TALWANI, M., LE PICHON, X., and HEIRTZLER, J. R. 1965. East Pacific rise, the magnetic pattern and the fracture zones. Science, 150, pp. 1109–1115.

VINE, F. J. 1968. Magnetic anomalies associated with Mid-ocean ridges. The history of the earth's crust. (*Editor*) R. A. Pinney. Princeton University Press. pp. 73–89.

VON HERZEN, R. P. and UYEDA, S. 1963. Heat flow through the eastern Pacific Ocean floor. J. Geophys. Res. 68, pp. 4219–4250.

WILSON, J. T. 1965. Transform faults, oceanic ridges, and magnetic anomalies southwest of Vancouver Island. Science, 150, pp. 482–485.

Planktonic Foraminifera in the Water and Sediments of Beaufort Sea, Canadian Arctic

G. VILKS,
Canada

ABSTRACT

A high biomass of planktonic foraminifera was found in the surface waters of the Beaufort Sea during the summer months. Oceanographic data indicate that subsurface water may be rising along the continental slope, thus causing the high rates of plankton production. Normative sedimentation rates were calculated by using the ratio of planktonic foraminifera in the water column to foraminiferal tests found in the sediment. The distribution of these rates suggests that a local current system is influencing the settling of foraminifera.

INTRODUCTION

BEAUFORT SEA is the southernmost extremity of the Arctic Ocean (Fig. 1) where the 1000-m isobath extends to the south of latitude 71°N. The extensive open water during the summer, in combination with the upwelling of subsurface water along the continental slope, provides an environment where exceptionally high productivity of planktonic foraminifera takes place.

To follow possible chronological changes in the paleoenvironment of the Arctic Ocean, sediment cores have been studied in terms of increasing or decreasing numbers of planktonic foraminifera (see Ericson, *et al.*, 1959, 1964; Hunkins, *et al.*, 1971). The working hypothesis is that relatively high ratios of planktonic tests in the sediment with respect to other detritus supplied at a constant rate indicate higher rates of production in the water column. In the Arctic Ocean the major biomass production takes place within the open leads during the summer. Layers rich in planktonic tests therefore are assumed to indicate relatively milder paleoclimates.

The purpose of this paper is to present a study of a summer biomass of planktonic foraminifera in the Beaufort Sea and its relationship to the preserved tests in the sediment.

Samples for this report were collected from *CSS Hudson* between August 27 and September 22, 1970 (Fig. 2). Plankton samples were taken using a 202-micron net with a 0.5-m square mouth opening. The volume of water filtered was measured with a TSK flowmeter mounted inside the net and level with the frame at the mouth of the net. The net was lowered to 200 m or to the bottom at shallower localities and retrieved at a speed of 30 m per minute. The laboratory treatment of samples is described by Vilks (1970a).

Oceanographic stations were occupied along three traverses (Fig. 3). and at each station standard casts were carried out. Bottom sediments were taken with

Authors' addresses are given at the back of this book.

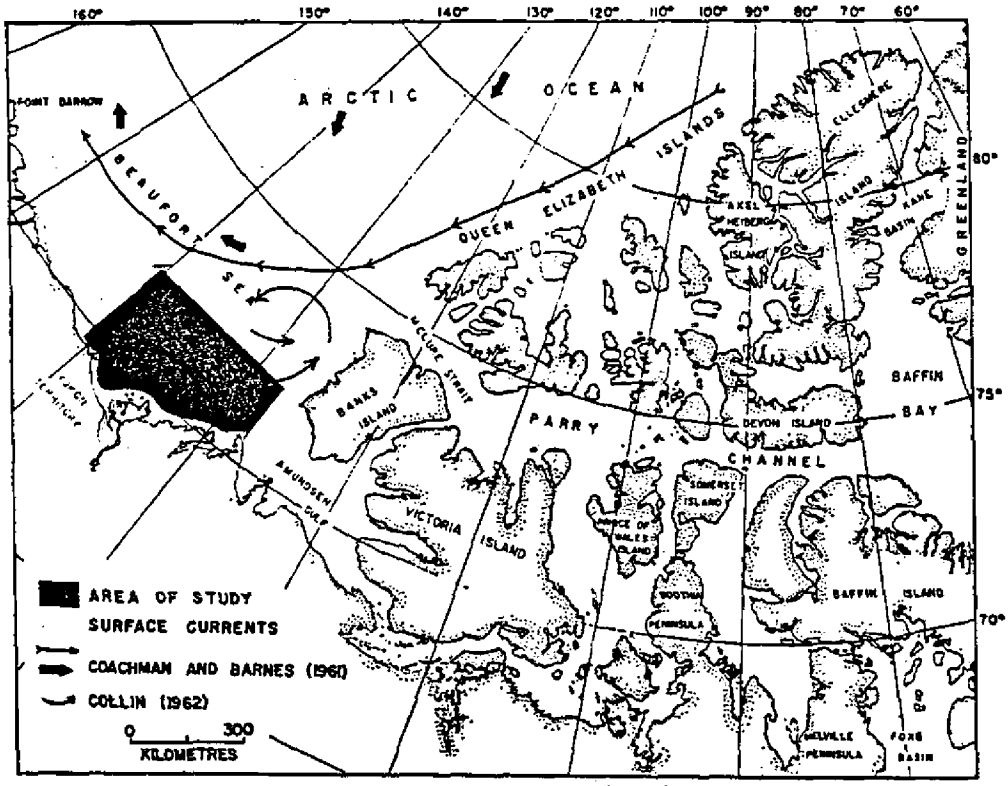


FIGURE 1 — Index map showing area of study and surface currents.

a Van Veen sampler and subsamples were taken from a mixed total sample of sediment for foraminifera analysis.

The author thanks Drs. C. T. Schafer, B. R. Pelletier and D. J. Lawrence for critical review of the manuscript. Dr. F. J. E. Wagner supplied the C^{14} dates.

PHYSICAL ENVIRONMENT

In the Mackenzie River delta area the continental shelf is broad and shallow. The continental slope begins at the 100-m isobath and is relatively steep down to 1000 m (Fig. 2). A prominent feature is the Mackenzie Canyon, which breaks the gentle slope of the continental shelf at the 50-m isobath about 6 km northeast of Herschel Island.

The area may be ice-free to a distance of 200 km from the shore during August and September. However, the polar pack-ice may return any time, although the probability of this happening is low during the peak of the summer. According to Coachman and Barnes (1961) and Worthington (1953), the general direction of surface currents in the Beaufort Sea is clockwise, but according to Collin (1962) an anticlockwise gyre occurs close to the shore (Fig 1).

In the Arctic Ocean the water column consists typically of three layers: (1) the cold and relatively dilute Arctic surface water, (2) the warmer and more saline water of Atlantic origin below 200 m to a depth of about 400 m, and (3) the Arctic bottom water below these two layers. In the Beaufort Sea the Atlantic layer has lost most of its properties.

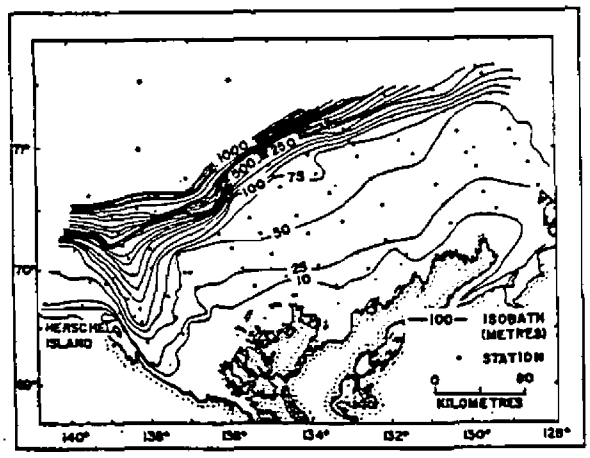


FIGURE 2 — Bottom topography.

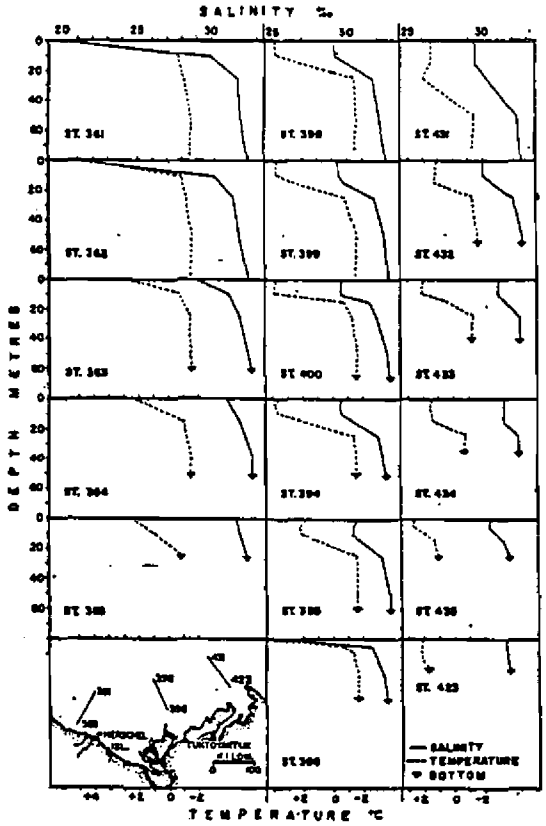


FIGURE 3 — Relationship of salinity and temperature with depth. Dates of survey: stations 361-365 August 30, 365-400 September 6-7, 431-435 September 14, 423 September 12.

Salinity and temperature measurements were taken from *CSS Hudson* along three traverses extending perpendicularly from the shore (Fig. 3). From the surface to a depth of 10 to 20 m there is a relatively warm and dilute surface layer. This surface layer is thinnest at the offshore stations of the eastern traverse, indicating the presence of the melting pack ice. Due to the cooling weather and mixing caused by winds, this very thin surface layer has slightly deteriorated

along the subsequent traverses, except for the shore station of the central traverse. Here the surface water has been diluted by the relatively warm waters entering the sea from the Mackenzie River.

Density-depth profiles (Fig. 4) show that the surface waters of the western traverse are influenced only by the melting pack ice and not by land runoff, which is demonstrated by the landward surfacing of isopycnals. Along the other two traverses there is evidence of the dilution of surface waters by the Mackenzie River, but only at the shoremost stations. On this evidence one may conclude that upon entering the sea the Mackenzie waters are swinging eastward and not extending over the shelf beyond about 50 km.

Below the surface and down to about 120 m the isopycnals slope downward toward the ocean along the three cross sections. The heavier subsurface water is therefore creeping up the continental slope and reaching the surface of the water on the continental shelf, except in those areas influenced by runoff. It is highly suggestive that this is an area of upwelling, but there is also a possibility of a current system developed toward the west along the continental slope.

Most of the sediment to the west of the delta is a very fine clay in which particles larger than 63 microns comprise less than one per cent of the total sample. The continental shelf to the east of the delta contains slightly coarser sediments where the fine fraction is selectively removed by currents and deposited over the edge of the continental slope.

PLANKTONIC FORAMINIFERA

Planktonic foraminifera belonging to the species *Globigerina pachyderma* (Ehrenberg) occur in higher numbers in the water column at the stations over the continental slope and in lower numbers over the shelf and at the offshore stations (Fig. 5). The highest number is 94,765 tests per 1,000 m³ of water filtered, which is comparable to the more productive areas of planktonic foraminifera in the world oceans. The highest productivities of planktonic foraminifera take place in regions of upwelling or mixing, provided that these areas are not extensively influenced by land-runoff. Bradshaw (1959) reported over 100,000 foraminifera per 1,000 m³ of water in the subarctic of the Pacific Ocean and Cifelli (1970) counted up to 80,000 specimens per 1,000 m³ of water filtered in the

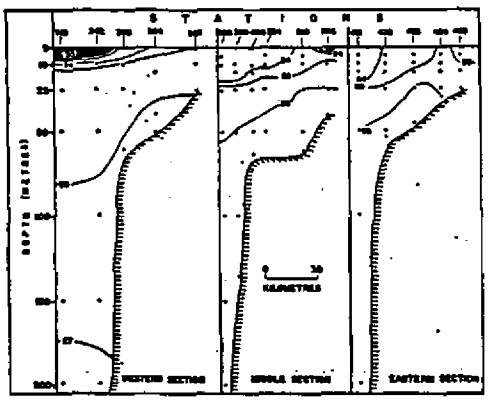


FIGURE 4 — Density relationship with depth.

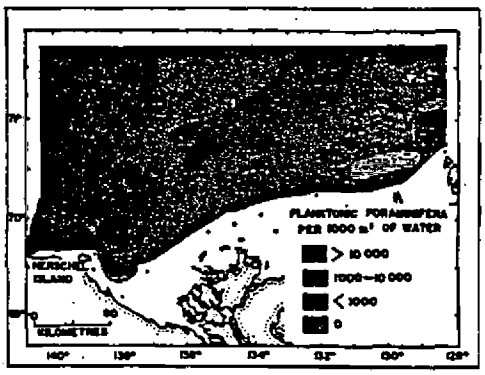


FIGURE 5 — Distribution of planktonic foraminifera in upper 200 metres.

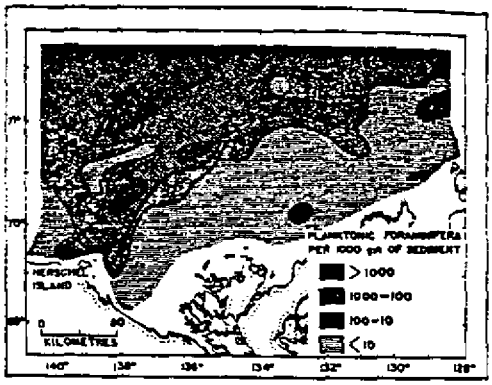


FIGURE 6 — Distribution of planktonic foraminifera in surface sediments.

North Atlantic Drift waters. Bé (1959) reported a mean of 2,400 in Central Atlantic waters, 6,100 in the Gulf Stream system and 796 in the slope waters off Nova Scotia. In the Arctic Ocean, Bé (1960) recorded less than 100 tests per 1,000 m^3 of water and Vilks (1970b) found an average of 309 tests per 1,000 m^3 in McClure Strait. However, in both of these previous studies in the Arctic, plankton tows were taken through openings in the ice.

The number of planktonic foraminifera tests found in a kilogram of sediment at each station is shown in Figure 6. The highest count is 12,257 tests per 1,000 gm of sediment. In comparison to areas nearby, these counts are very low. On the continental shelf off McClure Strait, Vilks (1970b) counted a maximum of 4.9×10^6 tests per kgm of sediment, and most of the area contains more than 10^6 tests per kgm. The high numbers were recorded despite the lower productivity of foraminifera in the water column in these areas. On the continental shelf and slope of the Beaufort Sea the over-all low occurrences of planktonic tests in the sediment may be due to the high rate of deposition of clastic material being supplied by the Mackenzie River. In addition to the possible higher rates of sedimentation, in this area the settling of planktonic tests to the bottom follows a complex pattern; the recorded areas of high standing crops of foraminifera in the water column, in most instances, coincide with low counts of tests in the sediment and vice versa.

In order to explain these anomalies, a simple model of sedimentation has been generated for this area. In this model the ratio of planktonic foraminifera caught in the water column to planktonic tests found in the sediment is used to determine a theoretical rate at which clastic material may be supplied. In developing the model a number of simplifying assumptions must be made: (1) the duration of a generation is one year and samples are taken during the yearly plankton bloom where the standing crop can indicate annual production; (2) planktonic foraminifera play an insignificant role in the food-chain and no solution takes place, therefore, the amount of tests that do not become sediment is negligible; (3) the error in plankton sampling due to variations in population densities is negligible; and (4) only negligible *post mortem* transport of empty tests takes place after reaching the sediment.

In applying this concept, a general formula is developed in which "F" is the number of living planktonic foraminifera caught in a vertical plankton tow and expressed as tests per cm^2 of the bottom and "S" is the number of tests of planktonic foraminifera counted in one gram of dry sediment. If the number of living planktonic foraminifera caught in a column of water is equal to the number that

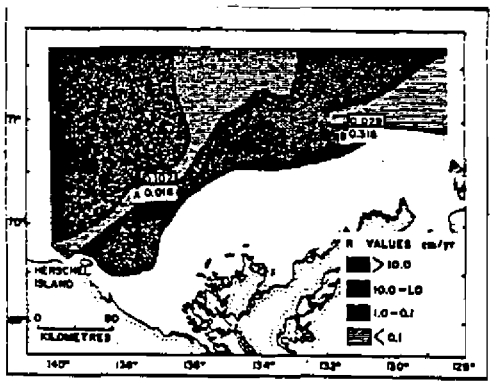


FIGURE 7 — Distribution of R-values. The boxed-in values at localities A and B indicate sedimentation rates determined by C^{14} dating.

fall on the bottom within one year, then F can be expressed as tests/cm²/year. If S is the number of tests per gram of sediment then 1/S is grams of sediment added for each test deposited. It follows that F/S grams of sediment are deposited in an area of one cm² in one year. If ρ is the density of sediment then

$$\frac{F}{S} = \rho R$$

where R is the thickness of F/S grams of total sediment deposited in one year. Therefore, the calculated rate of sedimentation, R, is

$$R = \frac{F}{\rho S} \quad \frac{cm}{yr}$$

At the present state of knowledge pertaining to the life cycles of planktonic foraminifera the model has limited use. Although R gives absolute values, it must be considered in a relative sense as long as F represents a standing crop of foraminifera. In that case it is irrelevant if the assumptions made about the generation length, predation or solution are grossly in error as long as these factors are constant within the area studied and during the time of sampling.

Looking at the plot of R values (see Fig. 7), we realize that the calculated sedimentation rates do not follow a simple model. In this model we would expect high values of R close to the shore and low values seaward, because of the expected lower rates of supply of clastic material at a greater distance from the source. However, the complex relationship of foraminifera tests found in the sediment to that in the water column may be explained best in the area of study by taking into consideration the local current system. In a situation where the tests are not transported laterally during descent, a high value of F in a water column is reflected by a correspondingly high S directly below in the sediment. In these instances the value of R is not influenced by the local high production rates of planktonic foraminifera. On the other hand, if there is an extensive lateral movement during descent, i.e., in areas where there are currents, high R values are obtained in localities corresponding to centres of high productivity, because of a deficit in the number of tests deposited. Similarly, low R values are obtained in localities down-current from these centres, because of the excess of tests deposited. This type of reasoning is illustrated by the comparison of R values and sedimentation rates obtained from C^{14} dates. According to a C^{14} date, the rate of

sedimentation at locality B is 0.029 cm/yr.; at the same locality the R value is 0.316 cm/yr., about ten times too high (see Fig. 7). At locality A a C^{14} date indicates a rate of sedimentation of 0.102 cm/yr., with a corresponding R value 0.016 cm/yr., about five times too low. It can be conceived that at locality B tests have been settling somewhere else, but at locality A tests have been added from a high-productivity zone.

SUMMARY

A high biomass of planktonic foraminifera was found in the Beaufort Sea during the summer months. An upwelling through the canyon and up the continental slope caused the high productivity in these areas. Normative sedimentation rates were calculated by using the ratio of planktonic foraminifera in the water column to foraminiferal tests in the sediment. The results did not provide an unambiguous pattern that could be used to explain the complex relationship of planktonic foraminifera in the water column and the sediment. However, a local current system could be influencing the settling of foraminifera to the bottom. For example, to the northwest of the delta the narrow zone of R values in Figure 7 could be caused by a current toward the southeast. The same current would cause the extremely high R values farther to the west of this area.

REFERENCES

Bé, A. W. H., 1959. Ecology of Recent planktonic foraminifera. Micropaleontology, 5, (1), p. 77-100.

————, 1960. Some observations on the arctic planktonic foraminifera. Contr. Cushman Found. for Foram. Res., XI, pt. 2, p. 64-68.

Bradshaw, J. S., 1959. Ecology of living planktonic foraminifera in the north and equatorial Pacific Ocean. Contr. Cushman Found. Foram. Res., 10, pt. 2, p. 25-64.

Cifelli, R. and Smith, Roberta K., 1970. Distribution of planktonic foraminifera in the vicinity of the North Atlantic current. Smithsonian Contr. Paleobiol. No. 4.

Coachman, L. K., and Barnes, C. A., 1961. The contribution of Bering Sea water to the Arctic Ocean. Arctic, 14, (3), p. 147-161.

Collin, A. E., 1962. Oceanography in the Canadian Arctic. Can. Geograph., 4, p. 120-128.

Ericson, D. B., and Wollin, G., 1959. Micropaleontology and lithology of Arctic sediment cores. *In*: Scientific studies at Fletcher's Ice Island, T-3 (1952-1955). USAF Camb. Res. Cent., Bedford, Mass., Geophys. Res. Pap. No. 63, 1, p. 51-58.

Ericson, D. B., Ewing, M., and Wollin, G., 1964. Sediment cores from the Arctic and Subarctic seas. Science, 144, (3623), p. 1183-1192.

Hunkins, K., Bé, A. W. H., Opdyke, N. D., and Mathiew, G., 1971. The Late Cenozoic history of the Arctic Ocean. *In* Turekian, Karl K., *(Editor)* The Late Cenozoic Glacial Ages, Yaye Univ. Press.

Vilks, G., 1970a. New methods for separation of skeletal material from a plankton sample. Marit. Sediments, 6, (2), p. 72-73.

————, 1970b. Circulation of surface waters in parts of the Canadian Arctic Archipelago based on foraminiferal evidence. Arctic, 23, (2), p. 100-111.

Worthington, L. V., 1953. Oceanographic results of Project Skijump I and Skijump II in the Polar Sea, 1951-1952. Trans. Am. Geophys. Union, 34, (4), p. 543-551.

6 THE DISTRIBUTION OF PLANKTONIC FORAMINIFERA IN THE SEDIMENTS AND WATER OF THE NORTHWEST PASSAGE AND NORTHERN BAFFIN BAY: A TOOL FOR PALEOOCEANOGRAPHIC SYNTHESIS

G. Vilks

The distribution of the various phenotypes of Globorotalia pachyderma *(Ehrenberg) is correlated with oceanographic parameters. Large percentages of small normalform adults were found in the mixed waters of eastern Lancaster Sound. After death 80% of these fragile normalforms are destroyed, leaving the Lancaster Sound sediments almost barren of planktonic foraminifera. The kummerform and quadrate phenotypes that developed under less favourable conditions have thicker test walls and are consequently more readily preserved. It is proposed that the fraction of normalform phenotypes in the sediment cores are useful to interpret paleoenvironments.*

INTRODUCTION

Populations of planktonic foraminifera are abundant in ocean waters and the various calcareous tests preserved in sediments are useful for paleooceanographic reconstructions. In higher-latitude waters planktonic foraminifera are more restricted and, in fact, polar waters are inhabited by only one species, known widely as *Globigerina pachyderma* (Ehrenberg) but also known as *Globorotalia pachyderma* (Ehrenberg). The latter name will be used in this report (Jenkins, 1967).

To reconstruct changes in the Neogene Oceanographic conditions of the Arctic Basin, the preserved tests of *G. pachyderma* in sediment cores have been studied, e.g., Ericson and Wollin, 1959; Ericson *et al.*, 1964; Herman, 1964, 1969, 1971; Clark, 1969, 1971; VanDonk and Mathieu, 1969, and others. Assuming negligible dissolution of tests, it is usually maintained that relatively low numbers of planktonic foraminifera in sediment cores correspond to relatively harsh paleoenvironments (Ericson *et al.*, 1964) or high sedimentation rates (Hunkins *et al.*, 1971). During the winter the ocean surface is covered with a continuous sheet of pack ice that restricts solar radiation upon the surface waters and consequently diminishes primary production and a food source for the zooplankton. During colder periods these conditions prevail throughout the year. During the warmer periods, seasonal opening of leads in the Arctic pack ice, migrating polynya and ice-free marginal areas in the Arctic Basin create conditions wherein the productivity of plankton is increased. Therefore, a sequence of warmer summer seasons is recorded in the sediments by a relatively rich layer of skeletal remains.

This study is intended to provide an improved working hypothesis for paleooceanographic synthesis in marginal zones of the Arctic Basin. This is achieved by a detailed study of the existing relationships between salinity and temperature of the water column and the variants of *G. pachyderma* in the water and sediments of the Northwest Passage and the adjacent waters of Baffin Bay (Fig. 1).

This study is unique in that previous investigations on Arctic planktonic foraminifera have dealt basically with specimens found in the sediments. For example, Phleger (1952) reported the presence of planktonic foraminifera in the sediments at various localities of the Canadian Arctic Archipelago; in comparison to the benthic foraminifera, he found that planktonic tests comprised 20% of the total fauna in Kane Basin, 18% in Kennedy Channel and less than one per cent at various localities in the Northwest Passage and Baffin Bay. Vilks (1969) found planktonic foraminifera in sediments of Hazen Strait (*see* Fig. 11) to a maximum of 282 tests per gram of sediment. A maximum of 4878 tests per gram were found by Vilks (1970a) on the continental shelf off M'Clure Strait. In the same locality (Vilks, 1970a) planktonic foraminifera were found in the water column of 740 tests per 1000 m^3 of water.

Samples for this report were collected from CSS HUDSON during October of 1970. Plankton were collected with vertical tows hauled through the upper 200 m of water and with surface tows to a maximum depth of 5 m. A 202-μ net was used with a 0.5-m square mouth-opening. To measure the volume of water filtered, a TSK flowmeter was mounted level with the frame at the mouth of the net.

All samples were preserved in a 10% formaldehyde-sea water solution buffered with hexamethylene tetramine. To facilitate the finding of the relatively inconspicuous foraminifera in the total plankton yield, each sample was ashed with a TRACERLAB low temperature asher before inspection as described (Vilks, 1970b). This procedure removes all organic material leaving the fragile skeletal material undamaged.

Sediment samples were taken with a Van Veen bottom sampler. In the laboratory, sediments were washed through a 63-μ sieve and the residue inspected for tests of planktonic foraminifera. In addition to the sampling of the plankton and sediments, standard oceanographic bottle casts were taken at every station.

OCEANOGRAPHY

The various channels of the Canadian Arctic Archipelago act as waterways for the southeastwardly moving surface water of the Arctic Ocean (Collin and Dunbar, 1964). These waters are eventually led into Baffin Bay through the Parry Channel System. Because Arctic water is stratified, the bathymetry of these channels is a main factor in determining the type of water that may eventually enter Baffin Bay.

The general bathymetry of the Parry Channel System, Amundsen Gulf and parts of Baffin Bay are shown in Figure 2. The existing physiographic features of the

Offshore Geology of Eastern Canada
Geol. Surv. Can., Paper 74-30, Volume I

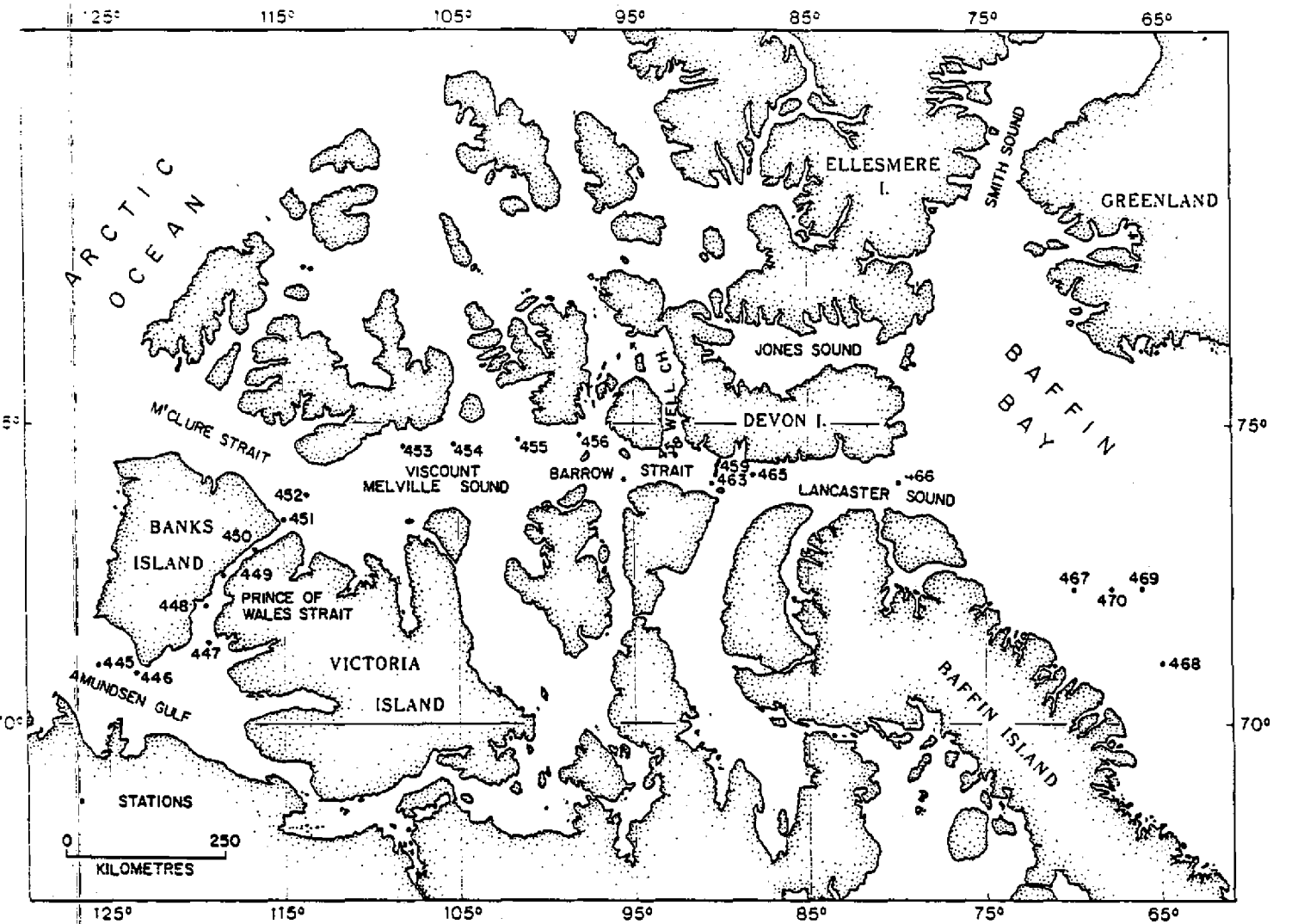


Figure 1. Station locations in the Northwest Passage and Baffin Bay.

channels in the Canadian Arctic Archipelago are attributed to glacial erosion of a fluvial valley system (Fortier and Morley, 1956; Pelletier, 1966; Marlowe, 1968; Vilks, 1969); glaciation is responsible for characteristically straight and steep shore faces, isolated depressions and U-shaped cross sections of the channels. In Amundsen Gulf, M'Clure Strait and Viscount Melville Sound depressions greater than 500 m are found, which are about 50 m deeper than the adjacent continental shelf. Prince of Wales Strait connecting Amundsen Gulf to Viscount Melville Sound is relatively shallow, with a maximum sill depth of 70 m (Canadian Hydrographic Service, 1970, Field Sheet 4335). Another topographic sill occurs in the Parry Channel System at Barrow Strait. This sill has minimum depths of approximately 150 m (CHS Chart 7829). To the east of Barrow Strait the channel depth increases gradually toward Baffin Bay, and at the eastern extremity of Lancaster Sound the water is 800-m deep. This deepening trend continues southeasterly in Baffin Bay proper where, within the limits of the study area, the maximum water depth is slightly in excess of 2000 m.

The relatively deep channel entrance of M'Clure Strait permits a southeasterly migration of the upper 500 m of the Arctic water into Viscount Melville Sound. According to Collin (1962) there is a weak easterly current setting along the north coast of Banks Island, and according to Vilks (1970a) this easterly movement has increased during recent times. Temperature and salinity data collected in Viscount Melville Sound during HUDSON 70 (Fig. 3) indicate the presence of the subsurface Atlantic layer of Arctic water below about 280 m. In Prince of Wales Strait, Bailey (1957) recorded a strong northeasterly movement of the surface water at the north end of the Strait during September, but no appreciable movement at the south end one week later. For Amundsen Gulf (Fig. 4) HUDSON 70 data indicate the presence of the Atlantic layer, which did not migrate into the Prince of Wales Strait due to the shallower depth of the Strait (Fig. 5).

The extent to which the general southeasterly movement of water is diminished at Barrow Strait is not clear. Bailey (1957) indicated that more Arctic water may be entering Lancaster Sound through Wellington Channel than through Barrow Strait, although he also suggested that the relative rates of flow through these channels may be dependent on atmospheric conditions in the Arctic Basin.

During August 1954 the net flow of water through the middle of Lancaster Sound was to the east and

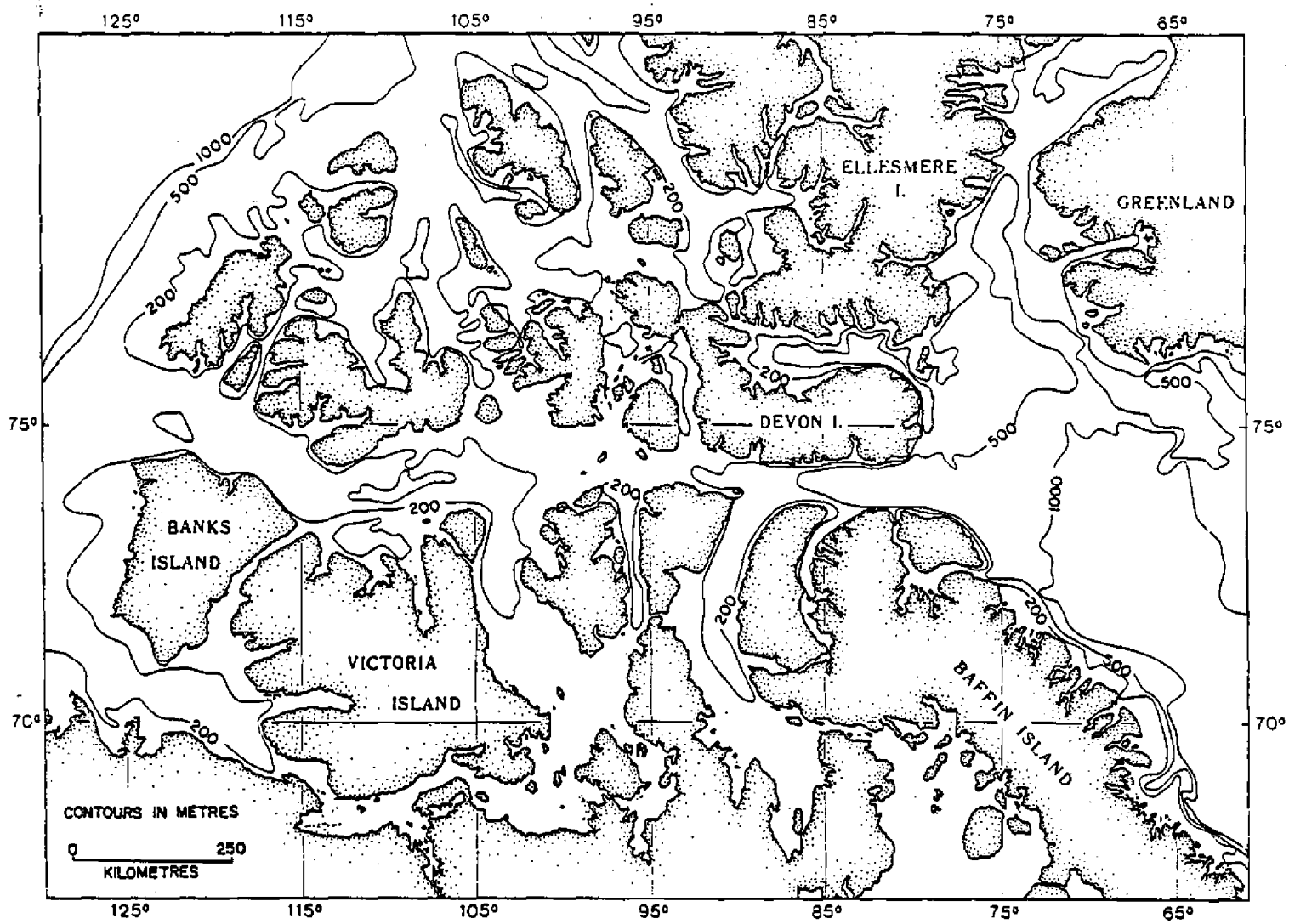


Figure 2. Bathymetry of the Parry Channel system and parts of Baffin Bay.

averaged 22 cm/s from the surface to a depth of 200 m (Bailey, 1957). However, the same section showed a flow towards the west along the coast of Devon Island and, according to the drift pattern of icebergs, this westward flow may extend along the coast as far as Maxwell Bay. The circulation patterns of surface water in Baffin Bay were described by Kiilerish (1939) *vide* Dunbar (1951). Within the area of the present study there is an oblong anticlockwise gyre fed by the westward flowing remnants of the west Greenland current, the southward moving Arctic water from Smith and Jones Sounds, and the outflow from Lancaster Sound.

The basic differences between the water of the Arctic Ocean and Baffin Bay are explained by Bailey (1957). The surface waters of the Arctic Ocean are less saline than those found in the Baffin Bay, but the minimum temperatures are similar; therefore, Baffin Bay surface waters are denser but below about 200 m Arctic waters are denser. This difference and the extent of mixing between the two water masses are shown in Figure 6, a TS diagram based on some of the HUDSON 70 data. Excluding the surface water above 25 m, influenced by local ice conditions, Baffin Bay water below 25 m at Station 470 is denser than the water in both Amundsen Gulf and Viscount Melville Sound. The difference decreases with depth and is almost negligible at 150 m. It is interesting to note that in Lancaster Sound at Station 466 the densities lie between those of the Baffin Bay stations and the two western stations. This indicates that mixing takes place between the Arctic and Baffin Bay waters within the upper 150 m at that locality. Below about 200 m waters at Lancaster Sound and Baffin Bay stations are similar and have lower densities than the Arctic waters of Amundsen Gulf and Viscount Melville Sound.

Figure 7 shows the temperature and salinity relationships with depth at the Baffin Bay station and two of the stations in Lancaster Sound. Both Lancaster Sound stations have nearly isothermal surface water to a depth of about 200 m, with a weak and shallow halocline at Station 462 and a negligible salinity gradient with depth at Station 466. Possibly the water in Lancaster Sound is thoroughly mixed to a depth of about 200 m in late summer shortly before ice formation. The low stability of the surface water in these regions is probably a major factor contributing to the high foraminiferal biomass in the water column encountered in October of 1970.

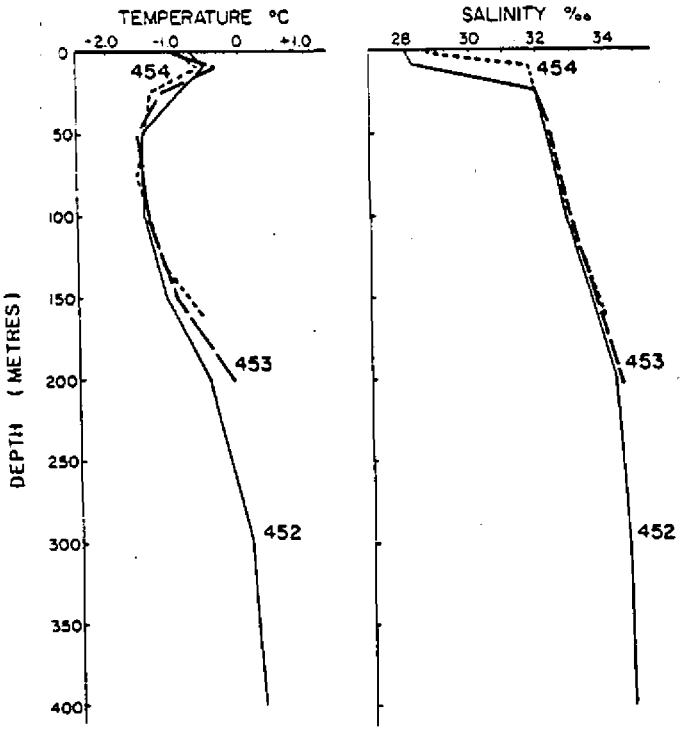


Figure 3. Temperature and salinity relationships with depth at three stations in Viscount Melville Sound.

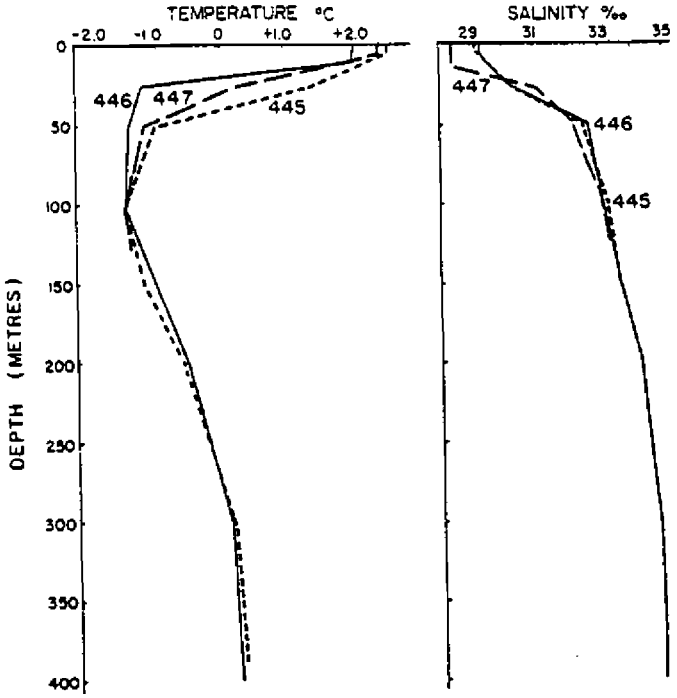


Figure 4. Temperature and salinity relationships with depth at three stations in Amundsen Gulf.

THE ICE COVER

Amundsen Gulf and the Northwest Passage to Lancaster Sound are covered with continuous multiyear ice cemented by younger ice. Lancaster Sound and central Baffin Bay are covered mainly by first-year ice, 1 to 2 m thick and in intermittent motion. At the northern extremity of Baffin Bay there is an area of very dispersed and mobile ice covering two to five-eights of the surface and is known as the North Water (Moira Dunbar, 1954).

Summer ice conditions in the Northwest Passage vary from an occasional ice-free year to an almost solid cover of ice in M'Clure Strait and Viscount Melville Sound. Normally, a zone of open water exists in Viscount Melville Sound by mid-August along the north side, while the remainder of the Strait is covered by a fractured and mobile canopy of ice. In Barrow Strait the ice begins to break up in July but seldom leaves the Strait completely; however, Lancaster Sound is ice free from mid-July to the end of October. In the north end of Baffin Bay the removal of spring ice is facilitated by the presence of the North Water. As temperatures rise, this polynya expands and usually reaches the entrance of Lancaster Sound by June (Dunbar and Dunbar, 1972); by early August the open water extends as far south as latitude 72°N.

Ice returns to the area during October, spreading toward the east and west from Viscount Melville Sound. In Lancaster Sound winter conditions return by the end of October, and in Baffin Bay by the end of November. Thus, in the Northwest Passage summer conditions spread from east to west and the winter conditions vice-versa.

DISTRIBUTION OF PLANKTONIC FORAMINIFERA IN THE WATER COLUMN

It is believed that planktonic foraminifera are endemic to the upper layers of offshore oceanic waters (Loeblich and Tappan, 1964) and that nearshore waters contain less planktonic foraminifera or are barren, depending on local conditions and the extent of terrestrial influence. Areas of upwelling and mixing outside the land influence normally contain higher numbers of planktonic foraminifera.

In the Canadian Arctic Archipelago, decreasing numbers of foraminifera are to be expected in waters closer to the land and away from the unrestricted ocean, in wider and deeper passages and where lateral or vertical mixing take place. This trend is evident in Figure 8, which shows the number of planktonic foraminifera for one cubic metre of water at the various localities examined in the Northwest Passage. The numbers are highest in Amundsen Gulf and Viscount Melville Sound and lowest in Prince of Wales and Barrow Straits. Foraminiferal distribution does not show conclusively in which direction the net movement of water takes place in Prince of Wales Strait, because foraminifera-rich waters could be entering the Strait from both Viscount Melville Sound and Amundsen Gulf. However, a net eastward movement of water through Viscount Melville Sound is reflected in the reduced numbers of foraminifera to the east and away from the Arctic Ocean.

The number of planktonic foraminifera in the water column to the east of Barrow Strait is higher than to the west probably due to the more extensive mixing of the Arctic and Baffin Bay waters and the weak stratification of the upper 200 m (*see* previous notes on oceanography). At the five stations along a traverse across the Lancaster Sound (Stations 459-463 in

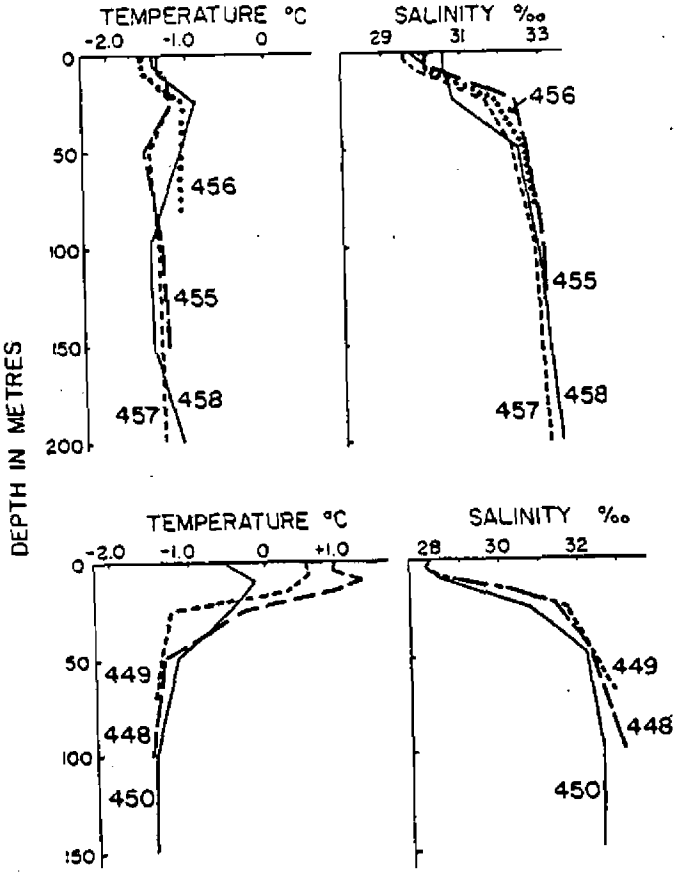


Figure 5. Temperature and salinity relationships with depth at stations 448, 449 and 450 in Prince of Wales Strait and at stations 455, 456, 457 in Barrow Strait.

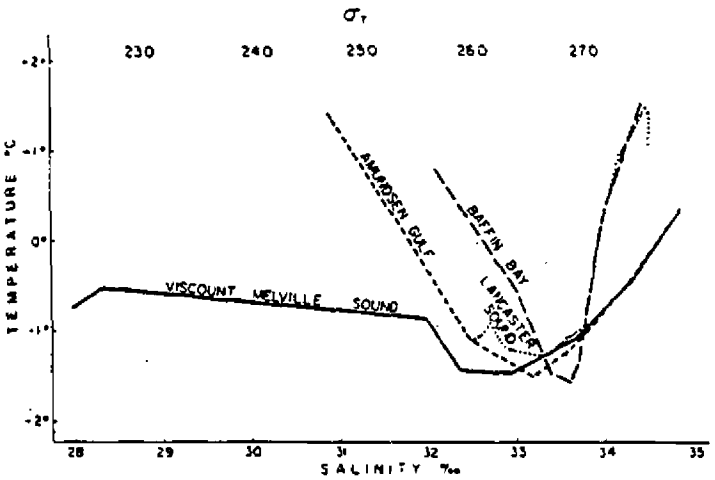


Figure 6. Temperature and salinity relationships of various localities in the Northwest Passage.

Fig. 9) the highest numbers were counted closest to the shore, especially near Devon Island. The higher standing crop of planktonic foraminifera at the margins of the Sound indicate areas where the mixing process is more vigorous.

At Station 466 and close to the entrance of Lancaster Sound in Baffin Bay there are 175 tests per cubic metre. This amount is comparable to the most productive zones of planktonic foraminifera in the world ocean, e.g. Bradshaw, 1959. Stehman (1972) also found higher numbers of planktonic foraminifera at the entrance of Lancaster Sound in comparison to other localities to the south and within Baffin Bay.

INTRASPECIFIC VARIATION

A number of authors have focussed their attention on the various morphological variants of *G. pachyderma* as possible indicators of differences in the environment. Viewing the trochospiral test of a foraminifer from the dorsal side, consecutive chambers can be added either in a clockwise or anticlockwise direction. The first variation is called the right-coiling or dextral and the second the left-coiling or sinistral. Ericson (1959) was the first to recognize dextrally and sinistrally coiled populations of *Globorotalia pachyderma*. He observed that sinistrally coiled *G. pachyderma* dominated the populations to the north of the April 7.2°C surface water isotherm in the North Atlantic and to the south of latitude 50°S in the sub-Antarctic waters.

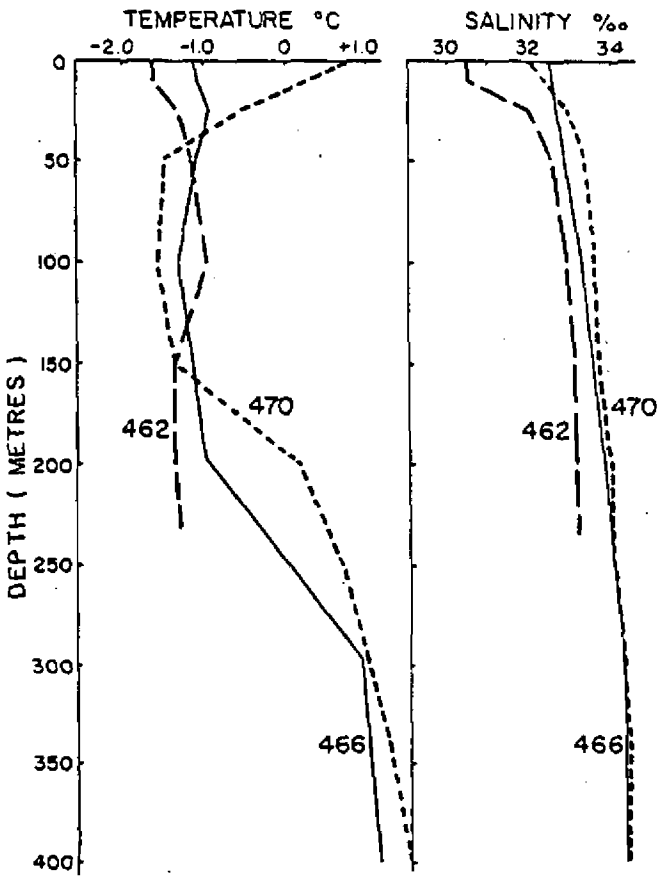


Figure 7. Temperature and salinity relationships with depth in eastern Lancaster Sound and Baffin Bay.

TABLE 1

Per cent dextral *Globorotalia pachyderma* at various localities in the Canadian Arctic Archipelago

Locality	Mean per cent dextral	No. of stations	Coefficient of variation (%)	Range of per cent dextral
Beaufort Sea				
Surface tows	17	46	152	0-100
Vertical tows	11	73	88	0-50
Amundsen Gulf and Prince of Wales Strait	14	7	176	0-67
Viscount Melville Sound and Barrow Strait	5	7	70	0-8
Lancaster Sound	7	7	24	4-9
Baffin Bay	4	4	11	3-4
Bottom sediments				
Beaufort Sea	15	39	157	0-100
M'Clure Strait	6	12	89	1-20

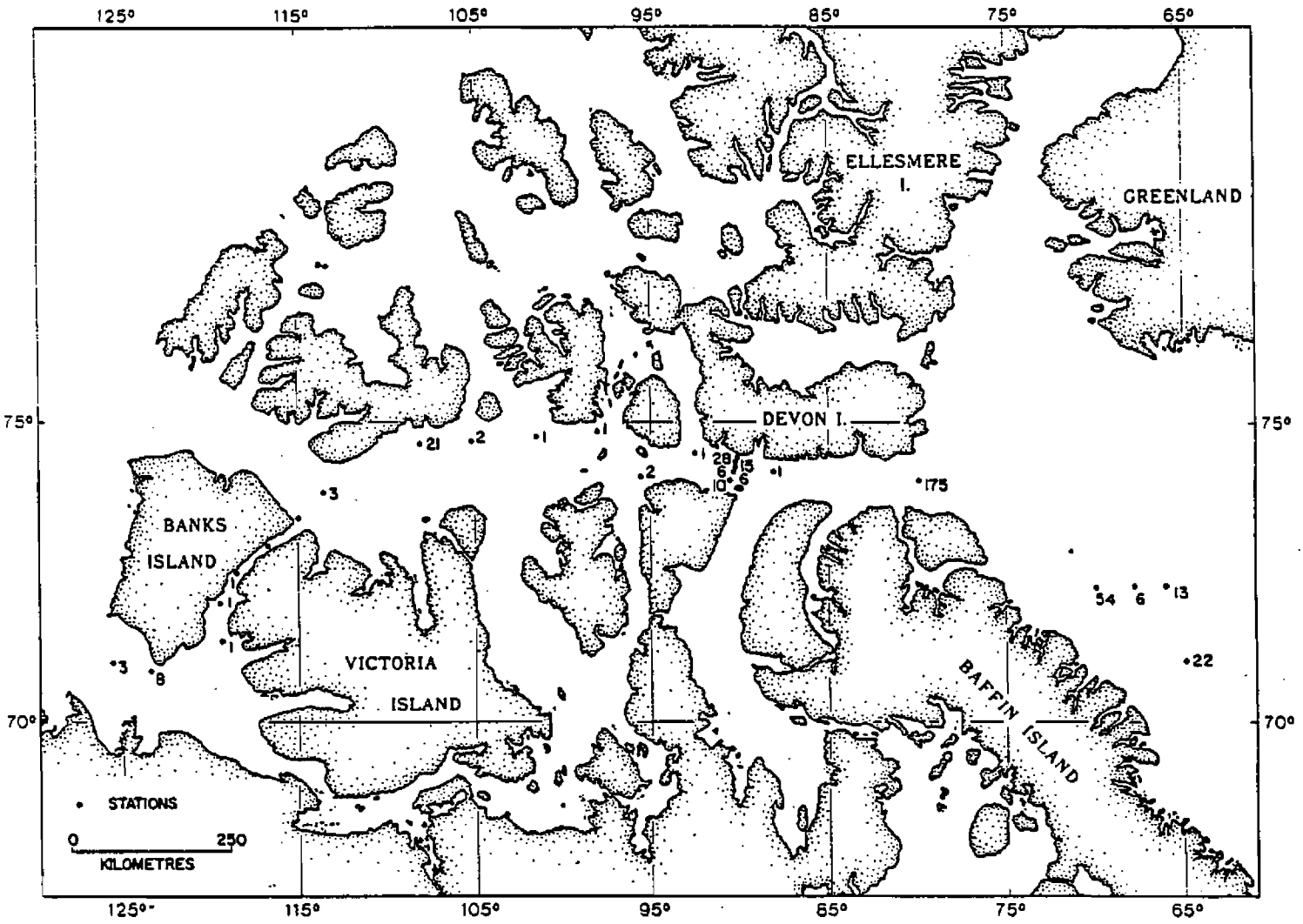


Figure 8. Number of planktonic foraminifera per cubic metre of water at various localities in the Northwest Passage.

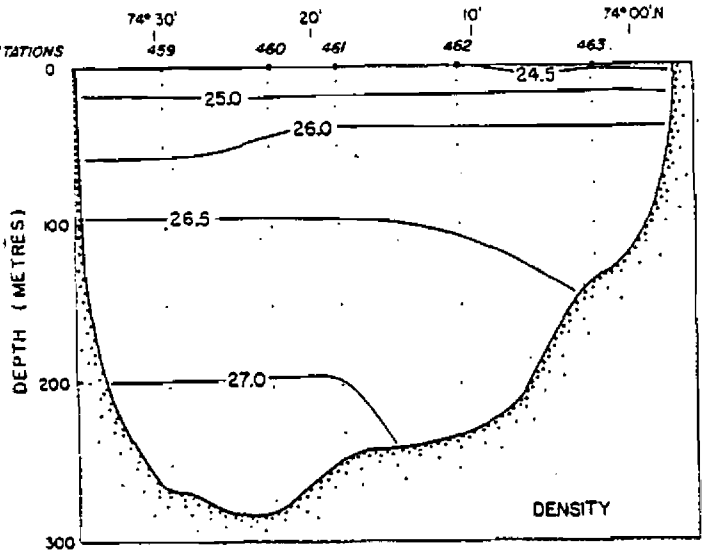
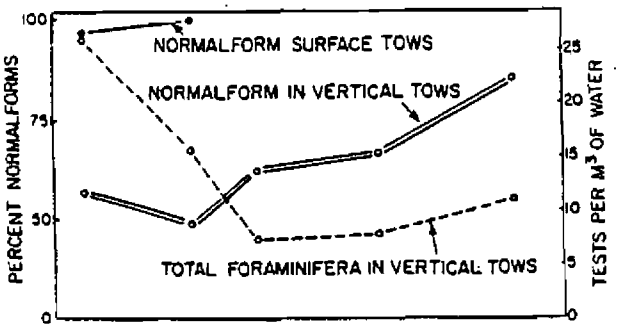
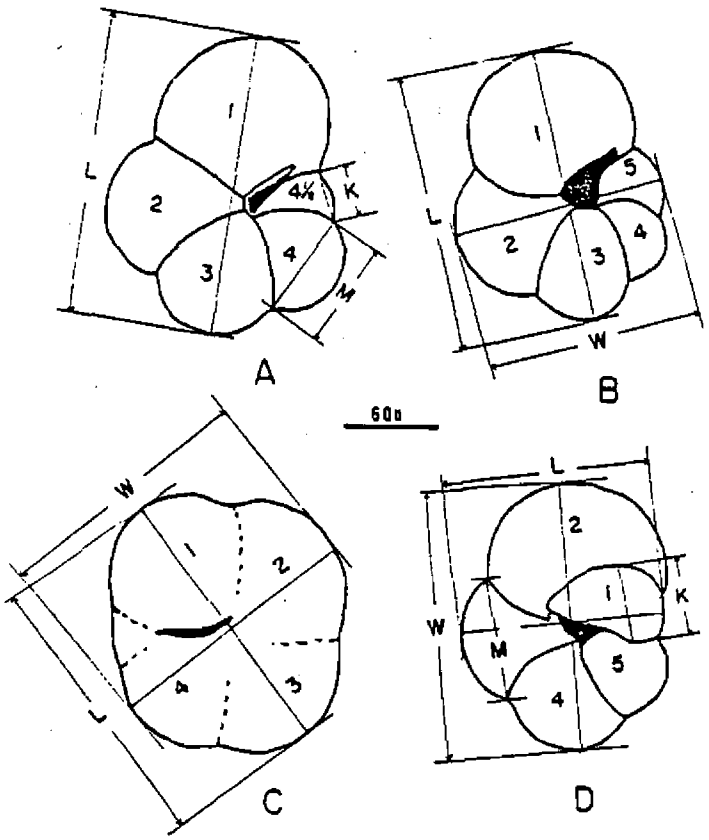


Figure 9.

Relation of density of water with depth along a traverse across the Lancaster Sound following longitude approximately 90°W.



Per cents of normalform *G. pachyderma* in surface and vertical tows along the same traverse. (*see* Figure 10 for definition of normalform *G. pachyderma*.)



General definitions: 1. ultimate chamber
2. penultimate chamber
3. antepenultimate chamber
4. second chamber
5. first chamber

L - distance between the outer margins of ultimate and antepenultimate chambers.

W - distance between the outer margins of the penultimate chamber and the second or first chamber.

Examples:

A. 4½ chambers per last whorl because the distance K is equal or less than ½M.

B. Normalform, because the distance L is larger than W, sinistral, 5 chambers per last whorl.

C. Quadrate, because the distance L is equal to W, dextral, 4 chambers per last whorl.

D. Kummerform, because the distance K is larger or equal than ½ the distance M and distance L is less than W, sinistral, 5 chambers per last whorl.

Figure 10. Illustrated definitions describing test morphology.

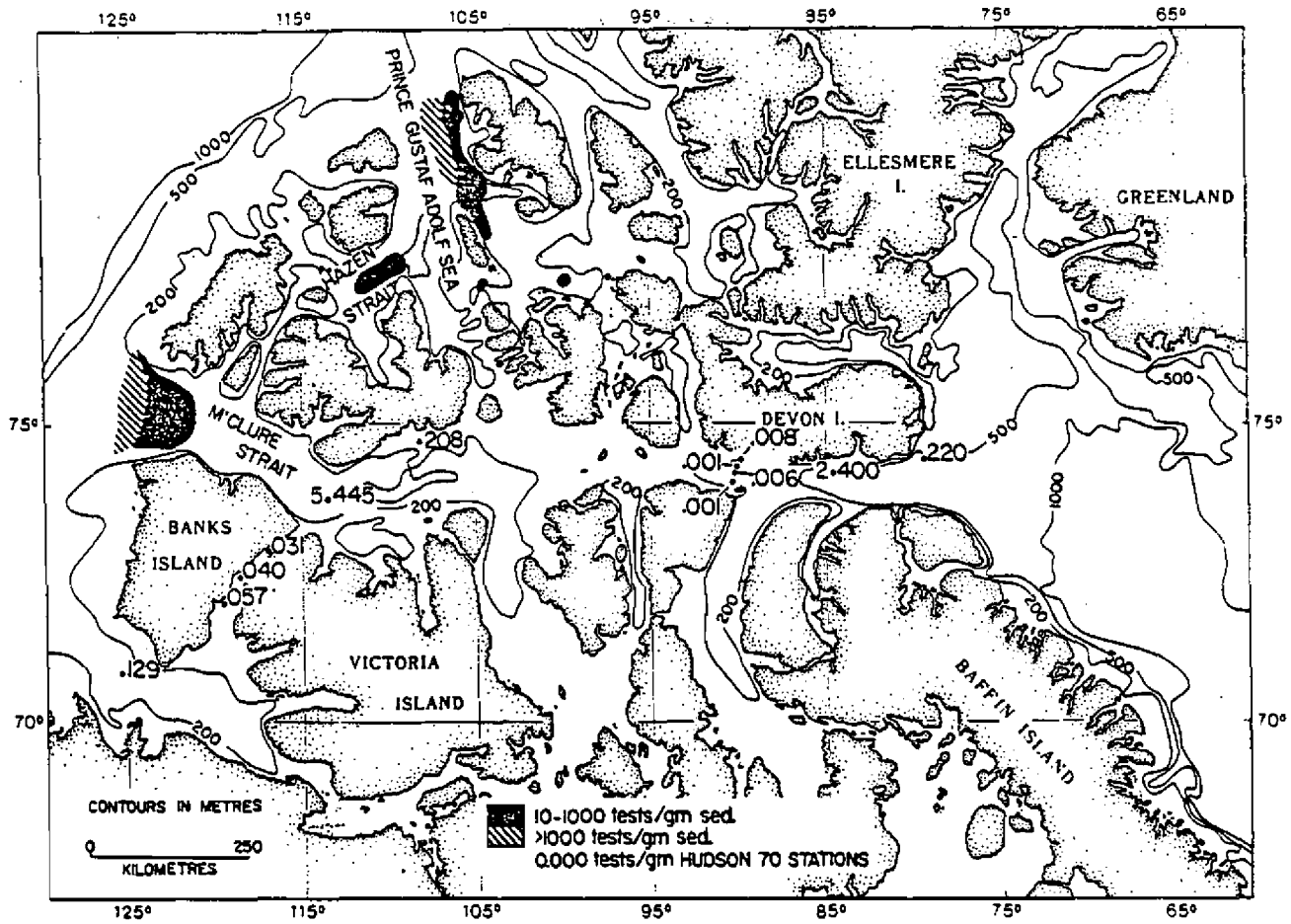


Figure 11. Planktonic foraminifera in sediments of the Northwest Passage and adjacent channels. Samples from Prince Gustaf Adolf Sea were collected by J. Marlowe in 1962; unpublished foraminiferal data were compiled by G. Vilks.

Bandy (1960), suggested that temperature influences the coiling directions of *G. pachyderma*; he demonstrated that 98% of the tests in the Arctic and Antarctic waters are sinistrally coiled and about the same per cent are dextrally coiled in temperate waters. He also demonstrated the geological value of this phenomenon by using the opposite coiling directions to establish the age of the Pleistocene-Recent Boundary in the Quaternary strata of some regions of southern California.

In the Northwest Passage dextral versus sinistral *G. pachyderma* decrease eastward from an average of 14% in Amundsen Gulf and Prince of Wales Strait to 4% in Baffin Bay (*see* Table 1). Another distinctive east-west trend is the lower variability in the coiling ratios eastward, with a coefficient of variation of only 11% in Baffin Bay. Vilks (1973) explained the trend in terms of a warm surface layer in the open water of the Beaufrot Sea, where the dextral forms originate and are carried through the Northwest Passage southeastward by the migrating water masses.

In addition to changes in coiling direction, *G. pachyderma* exhibits a variation in the relative size of the ultimate chamber with respect to the penultimate. Normally, each consecutive chamber grows slightly larger than the previous one; the ratio of the diameters of consecutive chambers is approximately 1.2 (q-ratio of Berger, 1969a). The reduction of the growth rate to a q-ratio of unity or less is associated with a thickening of the test wall, a reduction of aperture and the formation of a quadrate outline of the last whorl.

The reduction of the final chamber may take an extreme form, resulting in a smaller ultimate chamber than the penultimate, or the final chamber may be reduced to a mere lip over the aperture. Both forms have thick test walls suggesting a longer residence time in the water column. The longer time is associated with various environmental stresses and the lack of food is the most effective of these (Berger, 1969b).

To find a possible relation between the various growth stages and the environment studied, three morphotypes were considered: normalform, quadrate and kummerform (Fig. 10). The three groups were separated on the following criteria: *Normalform* - all specimens for which the distance estimated across the test from the ultimate to the antepenultimate chamber is larger than the distance at right angles to this diameter; *Quadrate* - the two diameters are equal, allowing about 10% difference; *Kummerform* - the distance across the test from the ultimate to the antepenultimate chambers is smaller than the distance at approximately right angles to this diameter. The final chamber was not considered a true chamber where it's diameter was less than one-half the diameter of the penultimate chamber. These rare specimens were included with the normalforms.

In the Northwest Passage the percentage of normalforms increases steadily towards the east with significant differences between those of Baffin Bay and of various localities to the west. Baffin Bay and Lancaster Sound foraminifera are also significantly smaller than the specimens found in Viscount Melville Sound and the Beaufort Sea. Berger (1969c) suggested that reproductive rates of planktonic foraminifera are accelerated in fertile areas by individuals maturing at relatively small sizes. Thus, local oceanographic conditions may induce a faster turnover of planktonic foraminifera in the water column resulting in a population of smaller adults and a low fraction of kummerform and quadrate growth stages.

A situation of this type exists during late summer at the mouth of Lancaster Sound and in some areas of northern Baffin Bay. As discussed previously, an extensive mixing of the surface 200 m was taking place at some localities at the time of sampling. Such a condition leads to high plankton turnover at lower latitudes and, thus, the foraminiferal contents at stations 466 and 469 suggest that the plankton in the cold Arctic water may respond to surface mixing in a similar fashion. Thus, smaller normalform foraminifera in the Arctic sediment cores may be interpreted as a local response to higher production rates in the water column. In addition to extensive periods of open water, this situation requires a complete or a partial deterioration of the surface pycnocline - a prominent feature in polar waters. Dissolved nutrients, in general, are not exhausted during the short productive season of Arctic waters (English, 1961) and, thus, mixing is not mandatory for phytoplankton production. However, planktonic foraminifera do not thrive in diluted waters and, therefore, are unable to effectively utilize the high phytoplankton production in the areas where surface water remains diluted either by runoff or meltwater.

COMPARISON OF LIVING AND PRESERVED TESTS OF *GLOBOROTALIA PACHYDERMA*

Up to now the discussion has dealt only with planktonic foraminifera that were caught alive in the water column. Intraspecific variants of *Globorotalia pachyderma* were studied in order to improve the understanding of the life history of this polar planktonic foraminifer and, where possible, explain the distribution of the various forms in terms of oceanographic parameters. The following paragraphs take the study a step further and deal with the problems of preservation of planktonic foraminifera at the sediment-water interface and within the upper few centimeters of the sediments. Assuming that the tests obtained from the sediments were living in surface waters more or less similar to the present, any differences between the forms found in the two types of samples have resulted from *post-mortem* changes. Hence, an insight can be gained into the ultimate fate of foraminiferal tests in the Arctic environment.

The most probable change is the dissolution of the calcareous tests in the water column and/or sediments. Below the surface, sea water is undersaturated with respect to calcium carbonate (Peterson, 1966; Pytkowicz, 1965; Berger, 1967 1970), and foraminiferal tests may go into solution upon descent through the water column. The rate of dissolution sharply increases at the lysocline (Berger, 1968), but the depth of the lysocline may not correspond with the calcium carbonate compensation depth where the rates of dissolution and deposition of calcareous material are equal (Berger, 1968). Below the compensation depth the deep-sea sediments are almost barren of calcareous oozes (Murray and Renard, 1891; Bramlette, 1961). The dissolution of calcareous particles of biogenic origin can be prevented by a protective organic coating (Wangersky, 1969; Berger, 1967).

The "compensation depth" normally occurs at below 3500 to 4000 m (Peterson, 1966) but a 500-m compensation depth has been recorded on the Antarctic Shelf (Kennett, 1966). There is no evidence of a shallow compensation depth existing in the epicontinental seas of the Canadian Arctic. Marlowe and Vilks (1963); Vilks (1964, 1969) found more calcareous specimens preserved in basins deeper than 200 m in Prince Gustaf Adolf Sea and the adjacent channels.

Increased pressure will raise the solubility of calcium carbonate but so will an increase in: (1) the rate at which water is exchanged at the surface of the carbonate particles (Pytkowicz *et al.*, 1967), (2) temperature, and (3) the concentration of CO_2 (Kennett, 1966). Oxygen concentrations appear to be another factor to be considered as Berger and Soutar (1970) reported higher rates of preservation in an anaerobic basin than on the aerobic basin nearby.

It is conceivable that the more fragile species are selectively removed by the process of dissolution (Berger, 1968; Parker and Berger, 1971) and, according to these authors, *Globorotalia pachyderma* is one of the most resistent species.

DISTRIBUTION OF PLANKTONIC FORAMINIFERA IN SEDIMENTS

In addition to the productivity of the surface waters, the total number of planktonic foraminifera found in the sediment is dependent on the resistance of calcareous tests to destruction. In the Northwest Passage the number of planktonic foraminifera is low, in the order of one test per kilogram of sediment (*see* Fig. 11). It is highest in the central depression of Viscount Melville Sound, but the sediments are barren of planktonic foraminifera in the relatively shallow waters of Barrow Strait. On the line of stations across western Lancaster Sound the numbers of planktonic foraminifera were lower than expected relative to the amounts found living in the surface waters. Sediments were not taken by CSS HUDSON to the east of this locality during the fall of 1970 and various other sources were used. In the central part of Lancaster Sound bottom sediments were inspected from core tops collected by Kenting Petroleum Geophysics during the summer of 1972: of eight samples only one contained planktonic foraminifera. At the eastern end of Lancaster Sound close to station 466, Stehman (1972) reported 0.22 tests of planktonic foraminifera per gram of sediment.

To provide a perspective for these numbers, available data from previous studies are included in Figure 11. The amount of planktonic foraminifera found in Hazen Strait by Vilks (1969) is nearly 1000 tests per gram of sediments, but decreases to less than 10 tests per gram in Hecla and Griper Bay. On the continental shelf off M'Clure Strait a maximum of close to 5000 tests per gram of sediment were found by Vilks (1970a). The calcareous sediments of the oceans contain about 10,000 tests per gram of sedi-

ment that are larger than 125μ (Berger, 1971); these numbers are surprisingly high for sediment on a continental shelf.

VARIANTS OF *GLOBOROTALIA PACHYDERMA* FOUND IN SEDIMENTS

In comparison to planktonic foraminifera collected in the water column, the foraminiferal tests found in the sediment contain larger percentages of kummerform and quadrate variants. Using the data of Table 2, it is possible to calculate the per cent loss of normalforms, assuming that at the time of sampling the planktonic foraminiferal population in the water column had reached a steady state of growth and that all kummerform and quadrate variants are preserved in the sediment. The estimated loss is 80% of the total foraminifera in the water column - a figure in agreement with Berger's (1971) estimate of the loss of calcareous skeletons by dissolution.

TABLE 2

Mean per cents of the various growth stages of *Globorotalia pachyderma* collected in the water column and sediment

	N	Q	K	Total no. specimen
Water column	75	18	6	2510
Sediment	38*	44*	18	611

*Significantly different at $p < 0.001$.

It is evident that the mean maximum diameter of specimens collected in the sediment is significantly larger (238μ) in comparison to the mean maximum diameter of specimens collected in the water column (197μ). Also, the larger specimens from the sediments have significantly larger mean numbers of chambers per test (11 in comparison to the mean number of 9 for the living population). These results indicate that in the Arctic environment the preservation is selective towards the larger and older specimen of *Globorotalia pachyderma*.

The normalform and highly productive population with short turnover periods may suffer a much greater destruction than the calculated average and consequently leave very little evidence in the sediments. This factor is responsible for the paucity of foraminiferal tests in the sediments in Lancaster Sound and in northern Baffin Bay, where the waters are dominated by large populations of the small and faster-growing normalforms.

SUMMARY AND CONCLUSIONS

In the epicontinental waters of the Canadian Arctic Archipelago oceanographic conditions, such as the movement and history of the water masses influence the productivity of planktonic foraminifera. The same conditions are also responsible for the preservation of the empty tests in the sediments, where in addition to the local oceanography, the rates of supply of terrestrial material also determine the number of tests found per gram of sediment. The following paragraphs summarize and explain some of the relationships between the numbers and variants of *Globorotalia pachyderma* found in the sediments and water column and the local oceanography.

In the Northwest Passage the water masses migrate to the southeast and, because of the limiting depth at Barrow Strait, only the upper 150 m of the Arctic water enter Lancaster Sound. Here the water from the Arctic Ocean meets the heavier Baffin Bay water and, as a result, various zones of convergence or lateral mixing develop. Lancaster Sound and northern Baffin Bay are also areas of extensive open water during the summer. The mixing and the open water create conditions favourable for the growth of planktonic foraminifera which induce faster rates of maturity resulting in an adult population that consists basically of normalform *Globorotalia pachyderma*. The normalform phenotypes consist of thinner test walls and are more fragile than the kummerform and quadrate variants. These tests are therefore more readily destroyed either by predators or as a result of dissolution. The dissolution is also enhanced by the scouring of the sea floor by migrating water-masses high in dissolved CO_2 (due to low temperatures and a relatively recent contact with the atmosphere). Thus, in Lancaster Sound conditions favourable for high rates of production of planktonic foraminifera may not be favourable for the preservation of empty tests. Therefore, by taking into consideration the local oceanographic setting, it is possible to explain the paucity of planktonic tests in the sediments of Lancaster Sound and Baffin Bay.

In the northwestern entrances of the Canadian Arctic Archipelago such as M'Clure Strait and Prince Gustaf Adolf Sea, conditions are less favourable for the production of planktonic foraminifera. The cover of ice is not entirely removed during the summer season and is usually present in the form of migrating fields of pack ice. The melting ice supplies fresh surface water that mixes slowly with the water below, and thereby maintains a highly stratified surface layer. Under these conditions quadrate and kummerform phenotypes of *G. pachyderma* develop in greater percentages than in the more mixed waters that are characterized by large open areas during summer. These phenotypes are more resistant to destruction than the normalform and are preserved in the sediment in greater numbers. Thus, although the productivity of planktonic foraminifera in the water column of M'Clure Strait is slow, the rates of deposition of empty tests is high, relative to other areas in the Canadian Arctic Archipelago. Here the conditions that are not favourable for growth of planktonic foraminifera are favourable for preservation and produce a layer on the sea floor containing relatively large numbers of tests per gram of sediment.

From the foregoing discussion it is evident that for paleooceanographic synthesis in the Arctic Basin it is necessary to consider the various phenotypes of *Globorotalia pachyderma*, in addition to the relative amounts of tests preserved in the sediment. The following working hypotheses may be useful in interpreting sediment cores collected in the channels of the Canadian Arctic Archipelago.

Numbers of *G. pachyderma*	Per cent normalform	Possible interpretations of the environment
High	High	1. Productive surface water, weak surface pycnocline, large and stationary summer polynya, stagnant bottom conditions.
High	Low	2. Productive surface waters, strong surface pycnocline, extensive open water during summer.
		3. Nonproductive surface waters, limited removal of ice during summer, low sedimentation rates, bottom currents (M'Clure Strait).
Low	High	4. As in (1), but faster sedimentation rates.
		5. As in (3), but stagnant bottom conditions and faster sedimentation rates.
Low	Low	6. As in (2), but higher sedimentation rates (Canadian continental shelf of the Beaufort Sea).
		7. As in (1), but strong bottom currents (Lancaster Sound).

REFERENCES

Bailey, W.B.
1957: Oceanographic features of the Canadian Archipelago; J. Fish. Res. Board Can., v. 14, p. 731-769.

Bandy, O.L.
1960: The geologic significance of coiling ratios in the foraminifer *Globigerina pachyderma* (Ehrenberg); J. Paleontol., v. 34, p. 671-681.

Berger, W.H.
1967: Foraminiferal ooze: solution at depth; Science, v. 156, p. 383-385..

1968: Planktonic foraminifera: selective solution and paleoclimatic interpretation; Deep-Sea Res., v. 15, p. 31-43.

1968a: Planktonic foraminifera: base morphology and ecologic implications; J. Paleontol., v. 43, p. 1369-1383.

1969b: Kummerform foraminifera as clues to oceanic environments; Abstracts, Bull. Am. Assoc. Petrol. Geol., v. 53, p. 706.

1969c: Ecology patterns of living planktonic foraminifera; Deep-Sea Res., v. 16, p. 1-24.

1970: Planktonic foraminifera - selective solution and lysocline; Mar. Geol., v. 8, p. 111.

1971: Sedimentation of planktonic foraminifera; Mar. Geol., v. 11, p. 325-358.

Berger, W.H., and Soutar, A.
1970: Preservation of plankton shells in an anaerobic basin off California; Geol. Soc. Am. Bull., v. 81, p. 275-282.

Bradshaw, J.S.
1959: Ecology of living planktonic foraminifera in the north and equatorial Pacific Ocean; Contrib. Cushman Found. Foram Res., v. 10, p. 25-64.

Bramlette, M.N.
1961: Pelagic sediments; in Oceanography, ed. M. Sears; Am. Assoc. Advance. Sci., Wash., D.C., p. 345-366.

Clark, D.L.
1969: Paleoecology and sedimentation in part of the Arctic Basin; Arctic, v. 22, p. 113-145.

1971: Arctic Ocean ice cover and its Late Cenozoic history; Geol. Soc. Am. Bull., v. 82, p. 3313-3324.

Collin, A.E.
1962: Oceanography in the Canadian Arctic;

Collin, A.E. (cont'd)
Can. Geogr., v. 4, p. 120-128.

Dunbar, Moira
1954: The pattern of ice distribution in Canadian Arctic seas; Trans. Roy. Soc. Can., v. 48, Oceanogr. Sess., p. 9-18.

Dunbar, Moira, and Dunbar, M.J.
1972: The history of the north water; Proceed. Roy. Soc. Edinburg (B), v. 72, p. 232-241.

Dunbar, M.J.
1951: Eastern Arctic waters; Fish. Res. Board Can., Bull. 88, p. 1-131.

English, T.S.
1961: Some biological oceanographic observations in the central north polar sea. Drift Station Alpha, 1957-1958; Arctic Inst. N.A., Res. Paper 13, p. 80.

Ericson, D.B.
1959: Coiling direction of *Globigerina pachyderma*; Science, v. 130, p. 219-220.

Ericson, D.B., Ewing, M., and Wollin, G.
1964: Sediment cores from the Arctic and sub-Arctic Seas; Science, v. 144, p. 1183-1192.

Ericson, D.B., and Wollin, G.
1959: Micropaleontology and lithology of Arctic sediment cores; Geophys. Res. Paper 63, p. 51-58.

Fortier, Y.O., and Morley, L.W.
1956: Geological unity of the Arctic Islands; Trans. Roy. Soc. Can., v. 1, Series 3, p. 3-12.

Herman, Y.
1964: Temperate water planktonic foraminifera; in Quaternary sediments of the Arctic Ocean; Nature, v. 201, p. 386-387.

1969: Arctic Ocean Quaternary microfauna and its relation to paleoclimatology: Paleogeogr., Paleoclimatol., Paleoecol., v. 6, p. 251-276.

1971: Vertical and horizontal distribution of petropods in Quaternary sequences; in Micropaleontology of the Oceans, eds. B.M. Funnell and W.R. Riedel; Cambridge Univ. Press, p. 463-486.

Hunkins, K., Bé, A.W.H., Opdyke, N.D., and Mathieu, B.
1971: The Late Cenozoic history of the Arctic Ocean; in The Late Cenozoic Glacial Ages, ed. Karl K. Turekian; Yale University Press, p. 215-237.

Jenkins, G.D.
1967: Recent distribution, origin, and coiling ratio changes in *Globoratalia pachyderma* (Ehrenberg); Micropaleontology, v. 13, p. 195-203.

Kennett, J.P.
1966: Foraminiferal evidence of a shallow calcium carbonate solution boundary, Ross Sea. Antarctica; Science, v. 163, p. 191-193.

Loeblich, A.R., Jr., and Tappan, H.
1964: Sarcodina, chiefly "Thecamoebians" and foraminiferida; in Treatise on Invertibrate Paleontology, ed. R.C. Moore, Geol. Soc. Am., Part C, Protista 2, v. 1-2.

Marlowe, J.I.
1966: Sedimentology of the Prince Gustaf Adolf Sea area, District of Franklin, Polar Continental Shelf Project; Geol. Surv. Can., Paper 66-29, p. 1-83.

Marlowe, J.I., and Vilks, G.
1963: Marine geology, eastern part of Prince Gustaf Adolf Sea, District of Franklin, Polar Continental Shelf Project; Geol. Surv. Can., Paper 63-22, p. 1-23.

Murray, J., and Renard, A.F.
1891: Deep-sea deposits based on the specimens collected during the voyage of H.M.S. "Challenger" in the years 1872-1876; in Report of the Voyage "Challenger"; Longmans, London, P. 525 (reprinted by Johnson, London, 1965).

Parker, F.L., and Berger, W.H.
1971: Faunal and solution patterns of planktonic foraminifera in surface sediments of South Pacific; Deep-Sea Res., v. 18, p. 73-107.

Pelletier, B.R.
1966: Development of submarine physiography in the Canadian Arctic and its relation to crustal movements; in Continental Drift, ed. G.D. Garland; Roy. Soc. Can., Spec. Publ. 9, p. 77-101.

Peterson, M.N.A.
1966: Calcite: rates of dissolution in a vertical profile in the central Pacific; Science, v. 154, p. 1542-1544.

Phleger, F.B.
1952: Foraminifera distribution in some sediment samples from the Canadian and Greenland Arctic; Contrib. Cushman Found. Foram. Res., v. 3, p. 80-89.

Pytkowicz, R.M.
1965: Calcium carbonate saturation in the ocean; Limnol. Oceanogr., v. 10, p. 220-225.

Pytkowicz, R.M., and Fowler, G.A.
1967: Solubility of foraminifera in seawater at high pressures; Geochem. J., v. 1, p. 169-182.

Stehman, C.F.
1972: Planktonic foraminifera in Baffin Bay, Davis Strait and the Labrador Sea;

Stehman, C.F. (cont'd)
Maritime Sediments, v. 8, p. 13-19.

Van Donk, J., and Mathieu, Y.
1969: Oxygen isotope compositions of foraminifer and water samples from the Arctic Ocean; J. Geophys. Res., v. 74, p. 3396-3407.

Vilks, G.
1964: Foraminiferal study of East Bay, MacKenzie King Island, District of Franklin; Polar Continental Shelf Project; Geol. Surv. Can., Paper 64-53, p. 1-26.

1969: Recent foraminifera in the Canadian Arctic; Micropaleontology, v. 15, p. 35-60.

1970a: Circulation of surface waters in parts of the Canadian Arctic Archipelago based on foraminiferal evidence; Arctic, v. 23, p. 100-111.

Vilks, G. (cont'd)
1970b: New method for separation of skeletal material from plankton sample, Maritime Sediments, v. 6, p. 72-73.

1973: A study of *Globorotalia pachyderma* (Ehrenberg) = *Globigerina pachyderma* (Ehrenberg) in the Canadian Arctic; Unpubl. Ph.D. thesis, Dalhousie University, Halifax, N.S.

Wangersky, P.J.
1969: Distribution of suspended carbonate with depth in the ocean; Limnol. Oceanogr., v. 14, p. 929-933.

Journal of Foraminiferal Research, v. 5, no. 4, p. 313–325, pls. 1–3, October 1975

COMPARISON OF *GLOBOROTALIA PACHYDERMA* (EHRENBERG) IN THE WATER COLUMN AND SEDIMENTS OF THE CANADIAN ARCTIC

GUSTAVS VILKS
Atlantic Geoscience Centre, Geological Survey of Canada,
Bedford Institute of Oceanography, Dartmouth, Nova Scotia

ABSTRACT

Planktonic foraminifera were collected from the water column and sediments of the Beaufort Sea and the Northwest Passage of the Canadian Arctic Archipelago at 175 localities. The mean maximum diameter of specimens collected in the sediment is significantly larger (238 microns) in comparison to specimens collected in the water column (197 microns). The specimens from sediments also have significantly larger mean numbers of chambers per test (11) in comparison to 9 for the living population. These results indicate that in the Arctic environment the preservation is selective towards the larger and older *Globorotalia pachyderma*. The preserved assemblage of variants contains significantly larger percentages of specimens with 4 chambers in the last whorl and in the quadrate growth stage. By comparing the living and fossil assemblages, a minimum average loss of 80 percent is estimated as due to dissolution or destruction by predators. The normalform tests and tests from a highly productive population with short turnover periods may suffer a much greater destruction and consequently leave very little evidence in the sediments.

Surface textures of preserved specimens are not significantly different from the surface textures of encrusted specimens from the water column, indicating that in the Arctic environment the addition of calcite to the test terminates with the death of the individual.

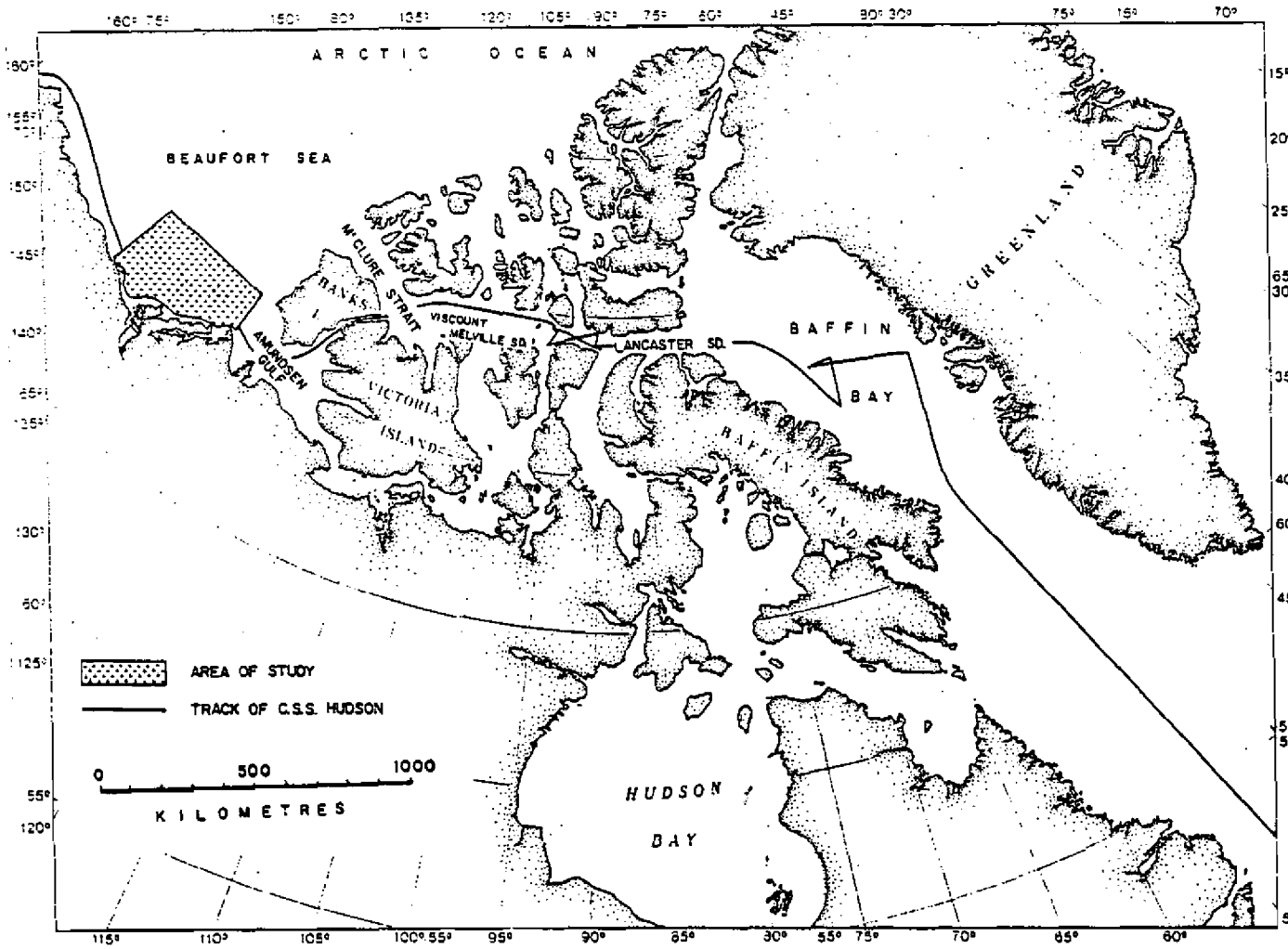
INTRODUCTION

Planktonic foraminifera fossilized in the sediment are often used to reconstruct paleoenvironments of the overlying surface waters. To avoid misinterpretations, it is important to know the extent to which the biocoenoses were altered during preservation of the empty tests. The state of preservation of the fossil foraminiferal assemblages can also be utilized for the identification of bottom paleoenvironments. In situ observations at the sediment-water interface indicate that, in addition to the direct effect of pressure, the solution of calcium carbonate is enhanced by the rate of water being exchanged at the surface of the carbonate particles (Pytkowitz and Fowler, 1967) and by high concentrations of CO_2 (Kennett, 1966). Off California, Berger and Soutar (1970) reported higher rates of preservation in an anaerobic basin than on an aerobic sill nearby. Thus the relative abundance of the more resistant phenotypes of such areas as the Canadian Arctic Archipelago can be used to infer the presence of paleocurrents and zones of convergence where surface waters rich in CO_2 may be scouring the bottom.

In the present paper the corrosive effect of the Arctic aquatic environment on the foraminiferal tests is demonstrated by comparing the morphologies of preserved foraminifera with those collected alive.

DISTRIBUTION

Foraminifera discussed in this report were collected during late summer of 1970 from the water column

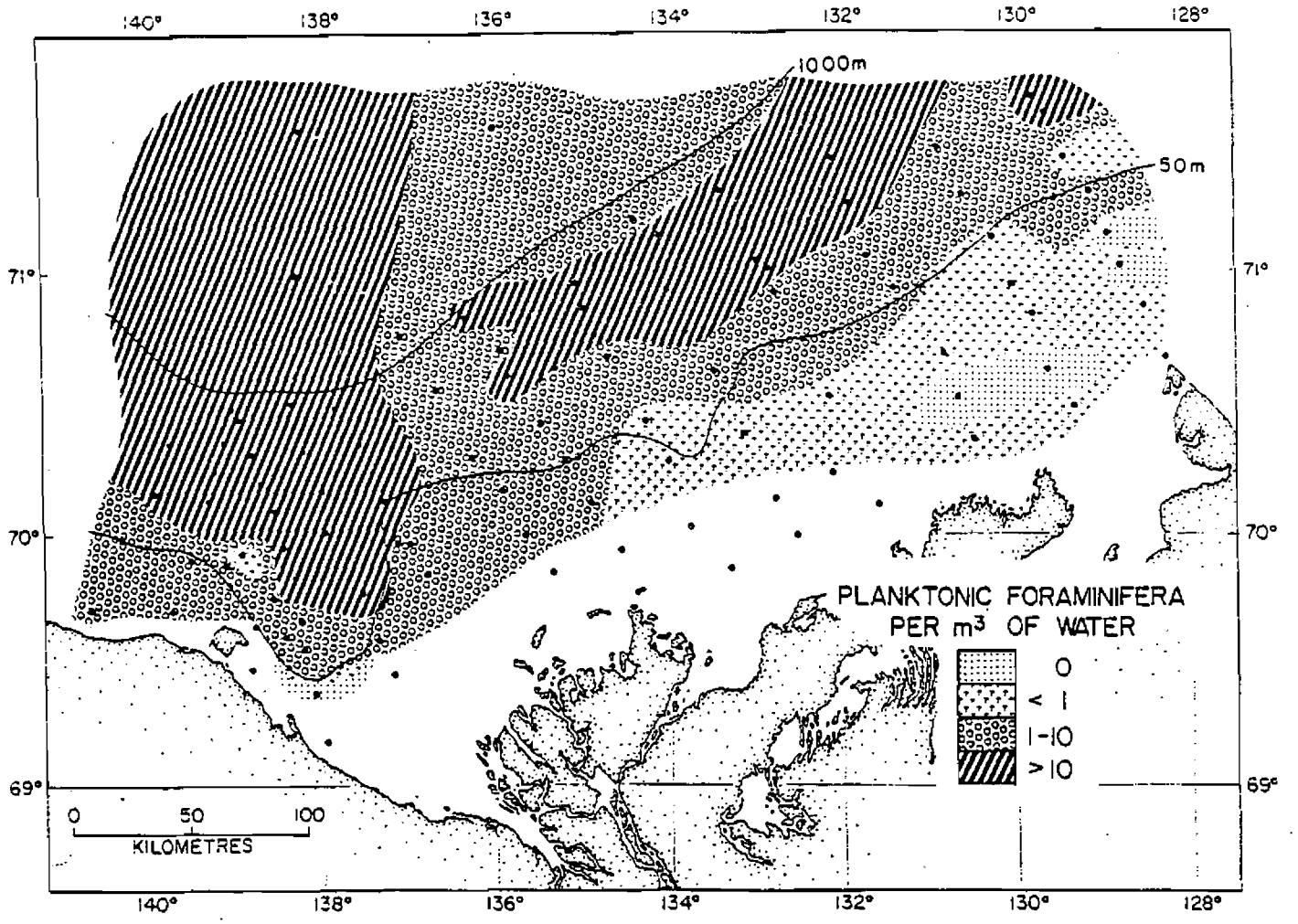


TEXT FIGURE 1

Index map showing the area investigated in the Beaufort Sea and the ship track of C.S.S. HUDSON along which samples were taken during 1970.

and bottom sediments of the southeastern Beaufort Sea and Northwest Passage, the latter including Amundsen Gulf, Viscount Melville Sound and Lancaster Sound (text fig. 1). Conventional sampling methods were used (Vilks, 1973).

In the marginal oceanic environment of the southeastern Beaufort Sea the waters on the continental shelf and slope are modified by the mixing of the waters of the Mackenzie River and the Arctic Ocean. A distributional pattern of planktonic foraminifera should therefore delineate zones comprising relative amounts of the two components, with an inverse relationship between the abundance of planktonic foraminifera and the amount of the river water present. The relative summer distribution of planktonic foraminifera collected in vertical tows in the Beaufort Sea is shown in text figure 2. The hachured pattern represents more than 10 tests of planktonic foraminifera collected for each cubic metre of filtered water, and this high density field extends over the Mackenzie Canyon and the continental slope. From these regions of greater abundances the numbers decrease gradually towards the continental shelf and shore. The data from the few offshore stations also indicate lesser numbers of foraminifera near the edge of the pack ice. In the Northwest Passage foraminiferal numbers decrease with the distance from the Arctic Ocean and Baffin Bay, respectively (text fig. 3). In the eastern end of Lancaster Sound, an exceptionally high number of 175 tests per cubic metre of water was encountered. Here such numbers may re-



TEXT FIGURE 2

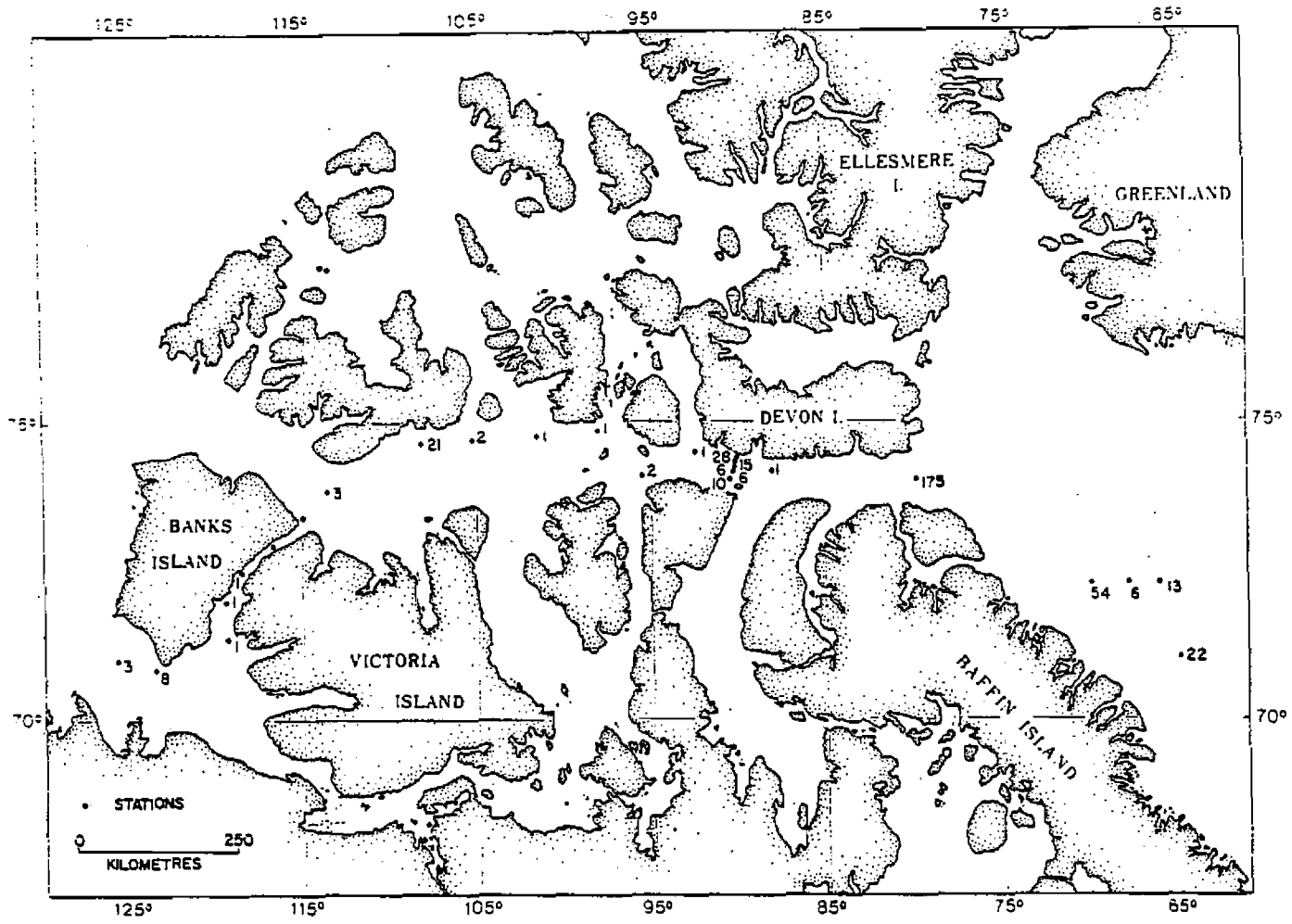
Planktonic foraminifera collected in the water of the Beaufort Sea with vertical tows in the upper 200 metres or to the bottom at shallower localities. Filled in circles indicate station locations including the location of bottom samples.

flect the mixing of waters that enter the area from three different sources, thus resulting in a relatively unstratified water column in the upper 200 metres (Vilks, 1973).

The number of planktonic foraminiferal tests found in the sediment at each station is small (text fig. 4). In the Beaufort Sea the highest number was 12 tests per gram of sediment, and in Viscount Melville Sound of the Northwest Passage the highest number was 5 tests per gram of sediment. To the east of Viscount Melville Sound the sediments were almost barren of plankton tests (text fig. 5) although high numbers were observed in the water column in Lancaster Sound. In contrast to the sparsity of foraminiferal tests in the central and eastern Archipelago, the western entrances contained very high numbers of planktonic foraminifera in the sediment. The areas shown with the hachured pattern of text figure 5 represent counts of more than 1,000 tests per gram of sediment.

COMPARISON OF LIVING AND PRESERVED FORAMINIFERA

The basic morphology of tests found in the sediment and water column was compared as an attempt to elucidate diagenetic processes operating at the sediment-water interface. In this study surface ultrastructure, test maximum diameters, total number of chambers, the number of chambers in the last whorl, and growth stages were considered. The growth stages were estab-



TEXT FIGURE 3

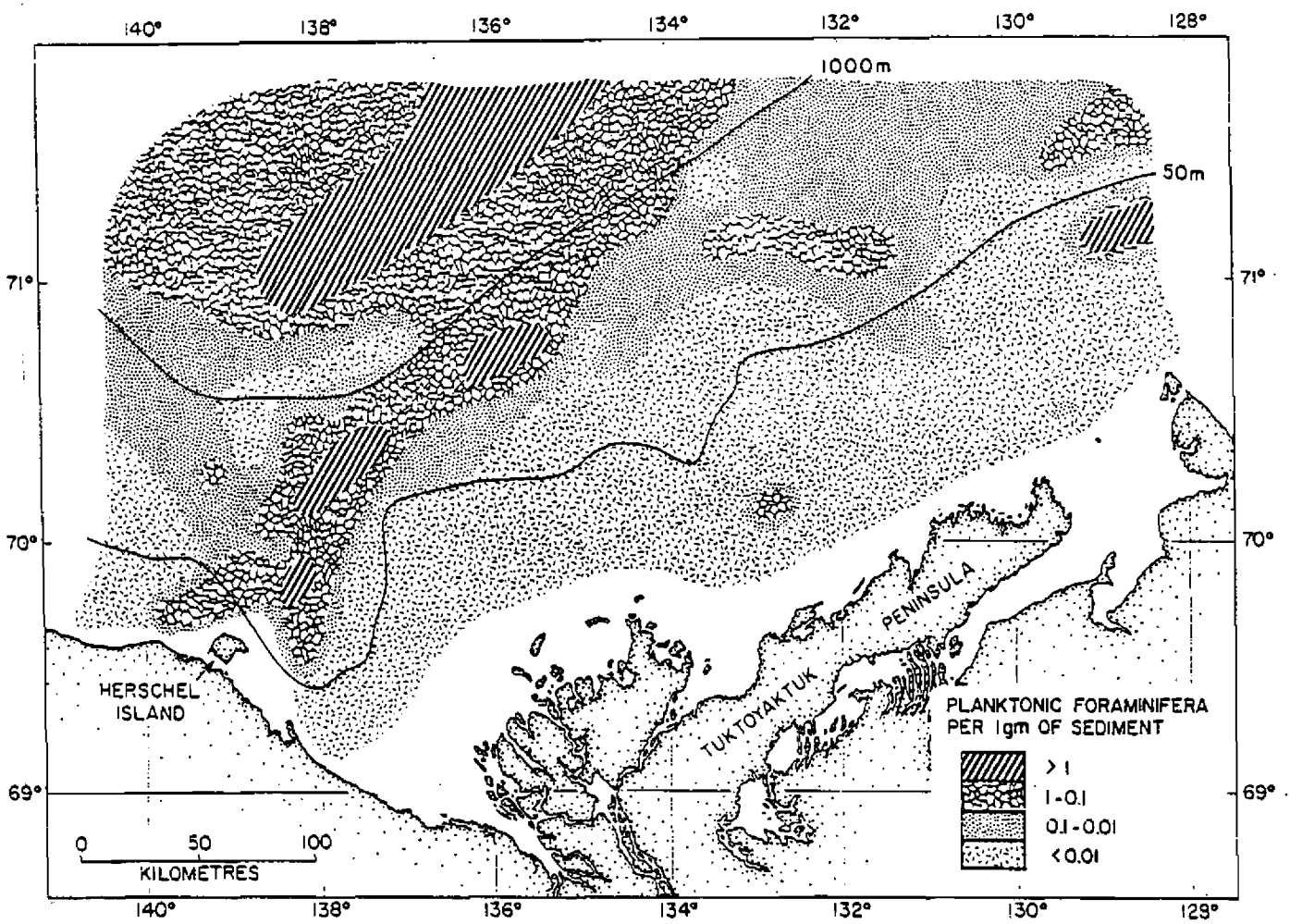
Distribution of planktonic foraminifera in the water columns of the Northwest Passage and northern Baffin Bay. Numbers indicate tests per m³ of water filtered.

lished as follows: Normalform (N)—the distance across the test from the ultimate to the antepenultimate chamber is larger than the distance at right angles to this diameter, Quadrate (Q)—the two diameters are equal, allowing about 10 percent difference, Kummerform (K)—the distance across the test from the ultimate to the antepenultimate chambers is smaller than the distance at approximately right angles to this diameter.

In the water column foraminifera are larger in the Beaufort Sea in comparison to the foraminifera from Lancaster Sound. Maximum diameters and chamber counts of foraminiferal tests collected from the water column are plotted in text figure 6, which shows that the difference in maximum diameters is significant between the two areas, although the number of chambers per test is not significantly different. This would suggest that the populations from the two areas are equally mature. The smaller specimens from Lancaster Sound can be explained on the basis of shorter generations, resulting from the more favorable conditions in the area of mixing waters.

For tests from the sediments the mean maximum diameter is equal from the two areas investigated. Text figure 7 shows the relationship of maximum diameters with the chamber counts of specimens from two samples, one from Beaufort Sea and the other from the Northwest Passage. Neither the mean diameters nor chamber counts are different for tests from the two areas.

The results of the correlation studies relating the maximum diameters and the number of chambers per



TEXT FIGURE 4

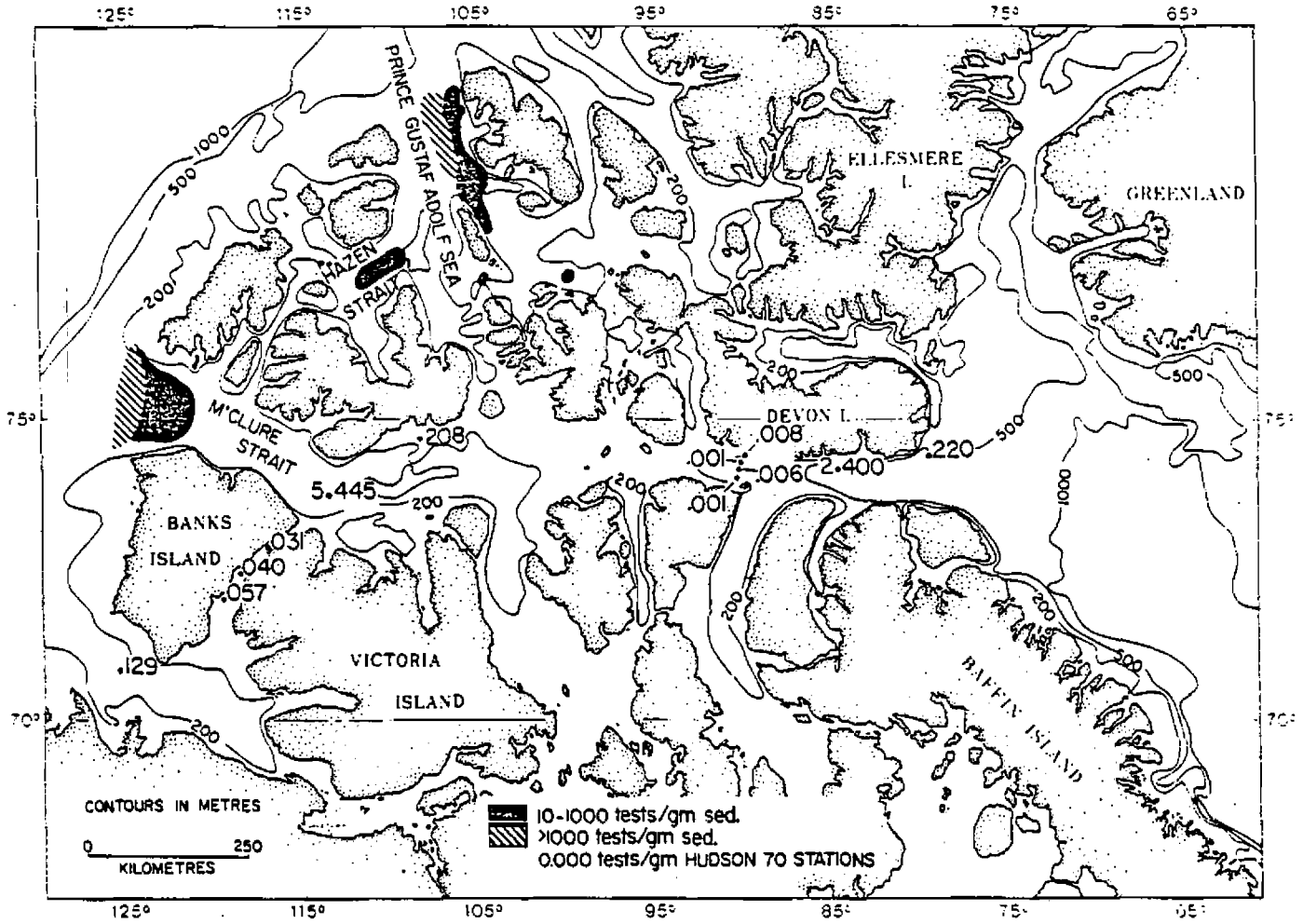
Planktonic foraminifera collected in the sediments of the Beaufort Sea (see text fig. 2 for station locations).

TABLE 1

Correlation between the number of chambers and maximum diameter of *Globorotalia pachyderma* collected in sediments and the water column. (NS = not significantly different, * different at probability P = 0.01, ** at P = 0.001).

Station (water column)	Mean No. of chambers	Mean max. diameter (μ)	Correlation coeff. Linear	Power	Exp.
348 Beaufort Sea	9.6	254	.766	.774	.754
	NS	*			
466 Lancaster Sd. (Sediment)	9.1	155	.763	.766	.762
	**	**			
452 Viscount Melville Sound	11.5	281	.841	.844	.845
	NS	NS			
351 Beaufort Sea	10.0	235	.488	.550	.504

test of foraminifera in the water column and sediments are summarized in table 1. The combined chamber counts from living and preserved specimens were tested for difference with a t-test and, as expected, the specimens found in the sediment contained significantly more chambers in comparison with the specimens from the water column. Because most of the plankton was collected throughout the water column and because conclusive evidence is lacking for *G. pachyderma* maturing at the sediment water interface, this finding indicates that in Arctic sediments juvenile planktonic foraminifera are being preserved in lesser amounts, and that the thicker adult tests are more resistant to postmortem destruction than the juveniles. In the case of *Globorotalia pachyderma* the thicker tests also contain terminal growth stages and therefore it is to be expected that the assemblages in the sediments should contain



TEXT FIGURE 5

Distribution of planktonic foraminifera in the sediments of the Northwest Passage. Numbers indicate tests per gram of sediment.

larger percentages of kummerform and quadrate specimens. In addition, the terminal growth stages tend to reduce the number of chambers in the last whorl, so that larger percentages of four-chambered specimens were found in the sediments as shown in table 2. Therefore, the relatively durable quadrate and kummerform variants dominate the assemblages from the sediment at the expense of the normalform variants which are significantly reduced.

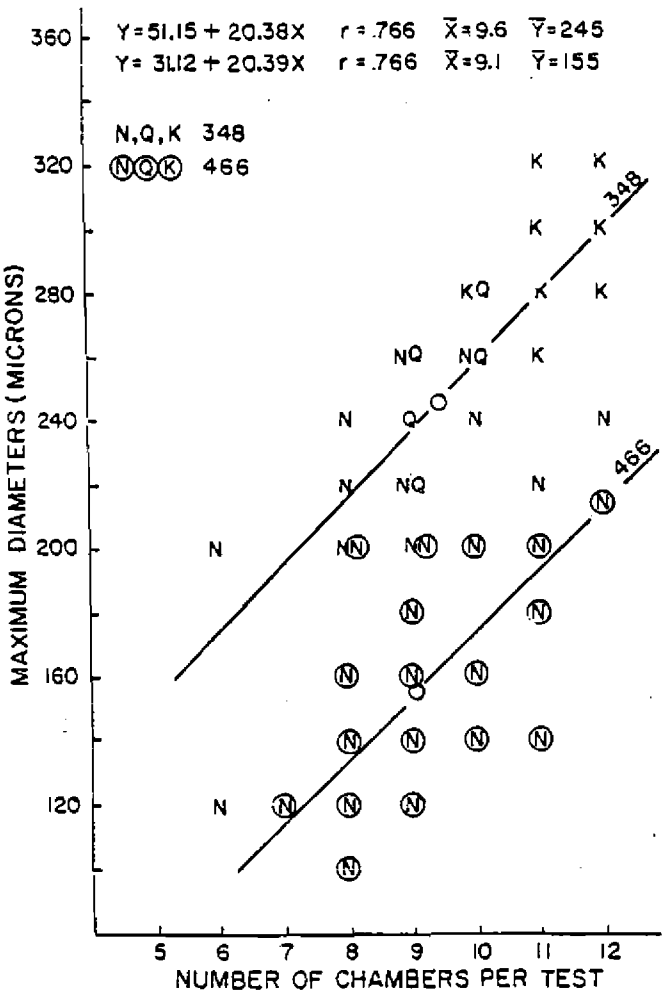
TABLE 2

Mean percentages of the numbers of chambers per last whorl and the growth stages of *Globorotalia pachyderma* collected in the water column and sediment from various places in Beaufort Sea and Northwest Passage. N = normalform, Q = quadrate, K = kummerform. (*Significantly different at probability $P < 0.001$).

	Chambers per last whorl			Growth stage			Total no. specimens
	4	4½	5	N	Q	K	
Water column	58	32	10	75	18	6	2510
Sediment	89*	9*	2	38*	44	18	611

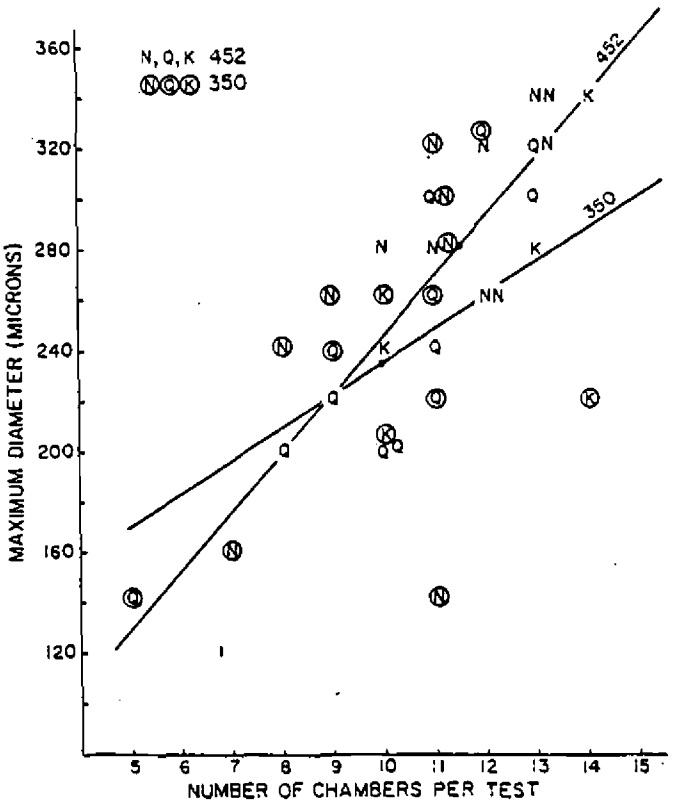
The percentage loss of normalforms can be calculated assuming that at the time of sampling the planktonic foraminiferal population in the water column had reached a steady state with respect to growth and that all kummerform and quadrate variants were preserved in the sediment. On the basis of these assumptions an 80 percent loss of normalform foraminifera was estimated for the Canadian Arctic bottom sediments.

A qualitative survey of surface morphology was attempted in this study, using the scanning electron microscope. The survey was undertaken to seek evidence for vestigial spines, which are useful criteria for separating



TEXT FIGURE 6

Maximum diameters correlated with the number of chambers per test of *Globorotalia pachyderma* collected from the Beaufort Sea (Station 348, lat 70°6.5'N., long 138°31.0'W.) and Lancaster Sound (Station 466, lat 74°01'N., long 70°56'W.). N = normalform, Q = quadrate, K = kummerform. Symbols within circles represent specimens from Lancaster Sound.



TEXT FIGURE 7

Maximum diameters correlated with the number of chambers per test of *Globorotalia pachyderma* collected from the bottom sediments. Beaufort Sea (Station 350, lat 69°50.5'N., long 138°18.0'W.) and Northwest Passage (Station 452, lat 73°48'N., long 113°46.5'W.).

Globigerina quinqueloba and *Globorotalia pachyderma*, and to investigate the process of morphogensis of test surfaces in the Arctic. Altogether, 36 specimens were studied. Plate 1, figures 1 to 3, are scanning electron photomicrographs of three normalform specimens. The specimen shown in plate 1, figure 1, was collected in Baffin Bay, that in plate 1, figure 2, is from Lancaster Sound and that in plate 1, figure 3, is from the Beaufort Sea. The enlarged photomicrographs of plate 1, figures 1 and 2, show a test surface dominated by semirounded protuberances. In plate 1, figure 3, some of these protuberances have already joined and may have acted as centres of deposition for the secondary calcification in a manner similar to that seen in *Globorotalia truncantulinoides* (Bé and Lott, 1964). A more extensive formation of ridges has developed in the three specimens collected from the Beaufort Sea, as shown in plate 2, figures 1 to 3. The enlarged sections of each specimen show a surface morphology dominated by ridges which may be either terraced or laterally smooth and joining around the irregularly spaced pores. These are mature specimens and the example in plate 2, figure 2, contains a terminal growth stage suggesting that the formation of ridges is associated with the age of the individual.

Plate 3, figures 1 to 3, illustrate the surface features of *Globorotalia pachyderma* collected from the bottom sediments. Specimens shown in figures 1 and 2 (plate 3) were collected from a depth of 700 m in the Beaufort Sea. The specimen in plate 3, figure 1, exhibits terraced features similar to those found in the water column. The kummerform specimen in plate 3, figure

2, also shows a crystalline surface texture that was not encountered on the specimens collected in the water column. The specimen shown in plate 3, figure 3, was collected in Viscount Melville Sound from a depth of 500 m, and shows a microcrystalline surface texture.

SUMMARY AND CONCLUSIONS

During the summer planktonic foraminifera were found in reasonably large numbers in Beaufort Sea, but in small numbers in the Northwest Passage except at the eastern extremity where they were exceptionally abundant. In the sediments, planktonic foraminifera are found in small numbers throughout the area of study. In a collection of phenotypes from the water column and the sediments, the following differences and similarities were observed. The mean maximum diameter of specimens collected from the sediment is 238 microns, which is significantly larger than the mean maximum diameter of 197 microns for specimens collected in the water column. The larger specimens from the sediments also have significantly larger mean numbers of chambers per test, with 11 in comparison to 9 for the living population. The fossil assemblages also contain significantly larger percentages of specimens with four chambers in the last whorl. By comparing the living and fossil assemblages, a minimum average loss of 80 percent is estimated as due to dissolution or destruction by predators. The normalform tests and tests from a highly productive population with short turnover periods may suffer a much greater destruction and consequently leave very little evidence in the sediments of the productive surface waters. The scanning electron photomicrographs of the small normalforms collected from the water column, presumably alive, did not show evidence of spines. This suggests that only *G. pachyderma* occupies the high-latitude waters. Surface textures of preserved specimens are not significantly different from those of encrusted specimens obtained from the water column, indicating that in the Arctic environment the addition of calcite to a test terminates with the death of the individual.

The post-mortem dissolution of foraminiferal tests takes place in response to specific environmental factors. In the world ocean at some depth below the surface, sea water is undersaturated with respect to calcium carbonate (Peterson, 1966; Pytkowitz, 1965; Berger, 1967, 1970), and foraminiferal tests may go into solution, to some extent, upon descent through the water column. The rate of dissolution increases sharply at the lysocline (Berger, 1968), but the depth of the lysocline may not correspond with the calcium carbonate compensation depth where the rates of dissolution and deposition of calcareous material are equal (Berger, 1968). Below the compensation depth the deep-sea sediments are almost barren of calcareous oozes (Murray and Renard, 1891; Bramlette, 1961). There is also evidence that the dissolution of calcareous particles of biogenic origin can be prevented by a protective organic coating (Wangersky, 1969; Berger, 1967).

The compensation depth normally occurs below 3500–4000 m (Peterson, 1966) but a 500-metre compensation depth has been recorded on the Antarctic Shelf (Kennett, 1966). There is no evidence of a shallow compensation depth occurring in the epicontinental

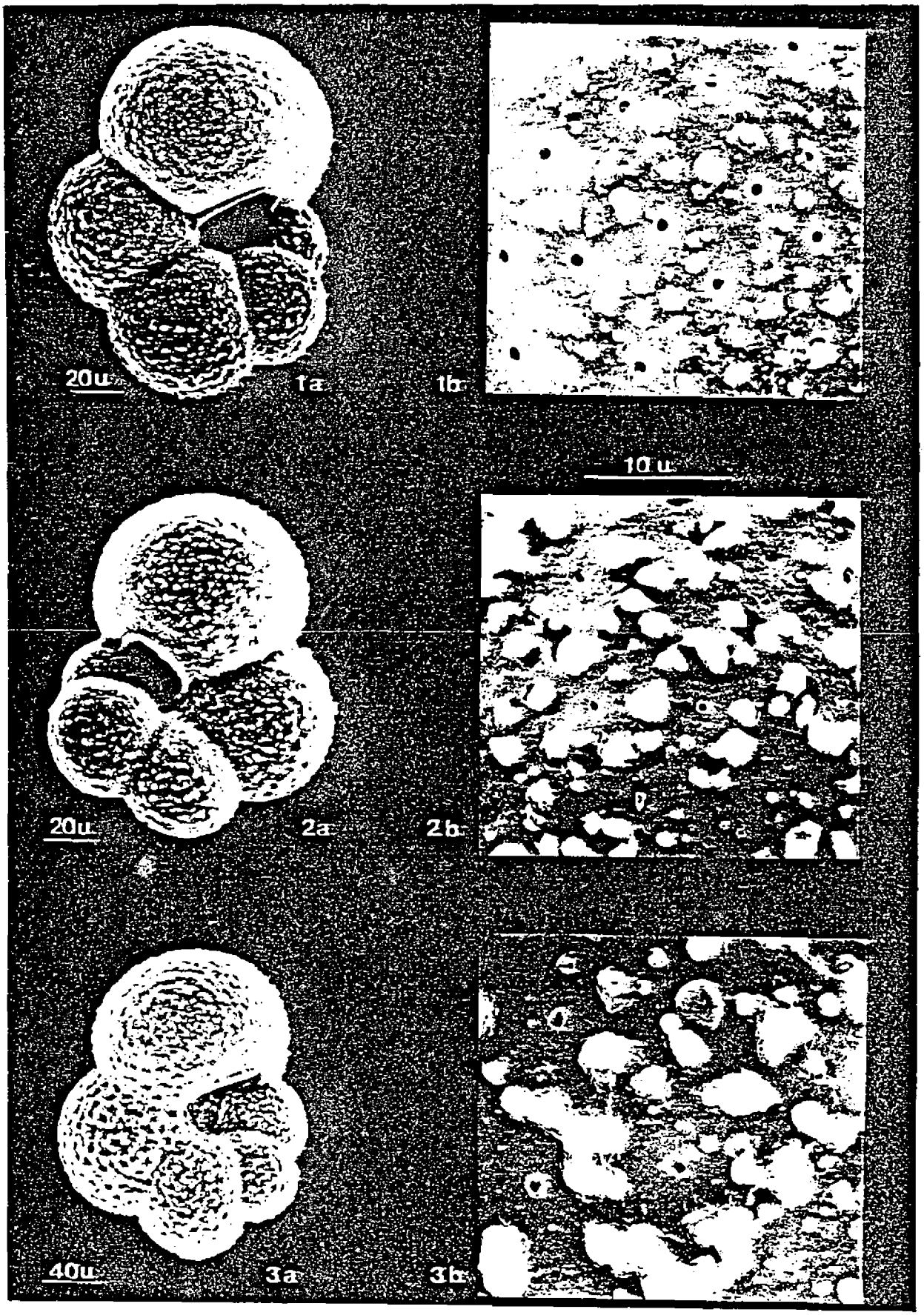
→

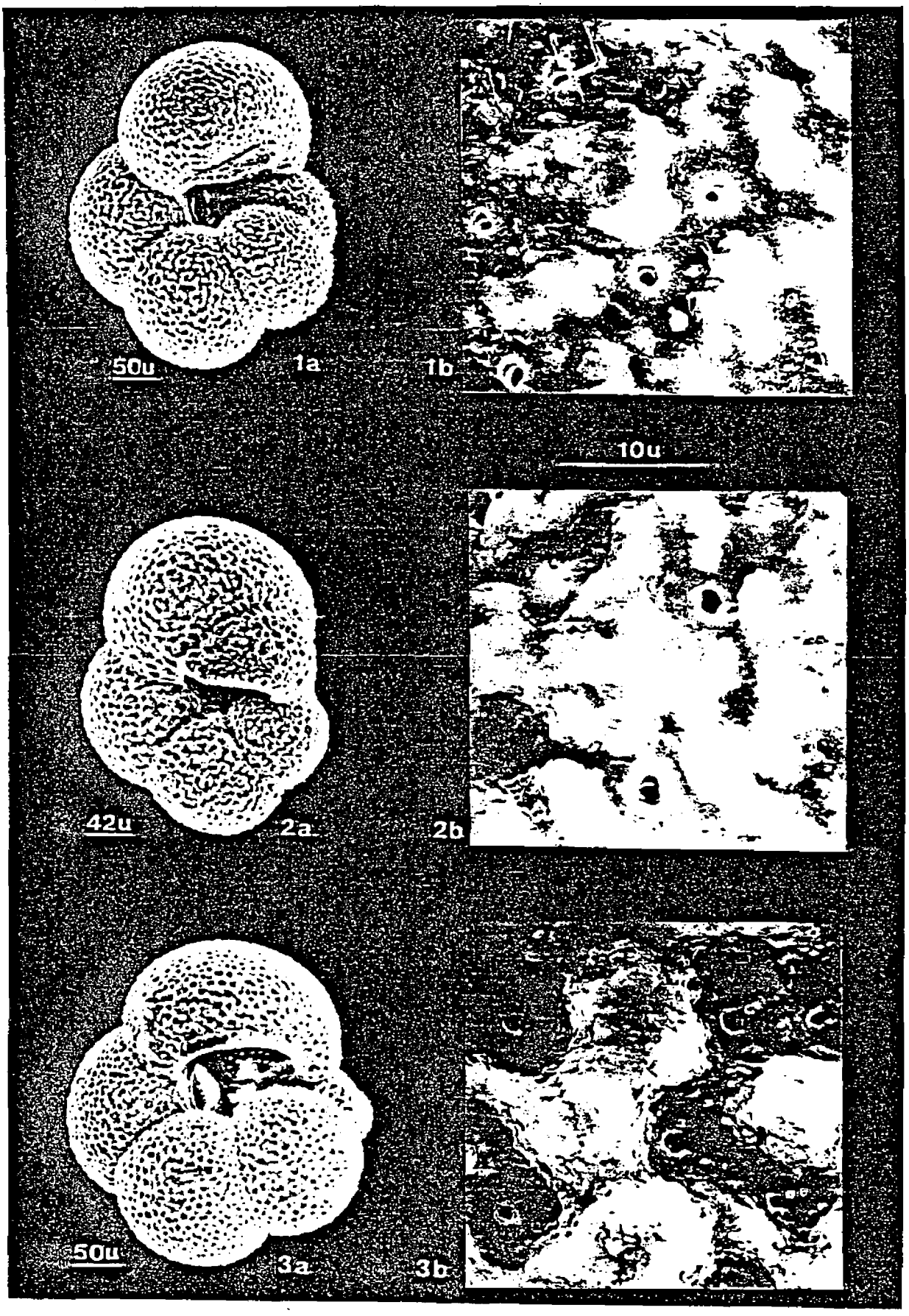
PLATE 1

1a, b *Globorotalia pachyderma*, Station 469, lat 72°18′ N., long 66°02′ W., Baffin Bay. Depth range 0–200 metres, collected Oct. 6, 1970. a. Ventral view, sinistral, 5 chambers per last whorl, normalform, small nonornamental apertural lip. Longest diameter 160 microns, shortest diameter 130 microns. × 500. b. Surface of ultimate chamber. Secondary deposits in the form of punctae containing a few central protuberances that may be bases of vestigial spines. Limited ridge forming has taken place between the punctae. Average maximum pore diameter 1.21 microns. × 3,000.

2a, b *Globorotalia pachyderma*, Station 466, lat 74°01′ N., long 79°56′ W., Lancaster Sound. Depth range 0–200 metres, collected Oct. 1, 1970. a. Ventral view, dextral, 4½ chambers per last whorl, normalform, small and poorly ornamented apertural lip. Longest diameter 138 microns, shortest diameter 110 microns. × 600. b. Surface of ultimate chamber. Secondary deposits in the form of semirounded punctae without central protuberances. Average maximum pore diameter 0.79 microns. × 3,000.

3a, b *Globorotalia pachyderma*, Station 345, lat 70°28′ N., long 138°57′ W., Beaufort Sea. Depth range 0–200 metres, collected Aug. 27, 1970. a. Ventral view, sinistral. 5 chambers per last whorl, normalform, small, ornamented apertural lip. Longest diameter 271 microns, shortest diameter 214 microns. × 280. b. Surface of ultimate chamber. Secondary deposits in the form of semirounded punctae that may be joined by terraced ridges. A number of punctae contain central protuberances. × 3,000.


20u
1a
1b
10 u
20u
2a
2b
40u
3a
3b


50u
1a
1b
10u
42u
2a
2b
50u
3a
3b

seas of the Canadian Arctic. As a rule, in Prince Gustaf Adolf Sea and the adjacent channels, calcareous foraminifera are more abundant at depths greater than 200 m in comparison to shallower localities (Marlowe and Vilks, 1963; Vilks, 1964, 1969).

The evidence of the present study indicates that, in the Arctic archipelago the dissolution of planktonic tests may not be directly associated with the depth of water but rather with the corrosive effect of the mobile bottom waters. In the channels, the presence of bottom currents is normally associated with turbulence in the water column and in areas such as Lancaster Sound the typically stratified Arctic waters are less prevalent due to mixing. Under these conditions the productivity of plankton is enhanced and, as a result, the normalform *G. pachyderma* dominate the population in the upper 200 m of the water. However, these small normalform tests undergo a greater post-mortem destruction in comparison to the larger kummerform and quadrate individuals. Thus an anomalous situation may exist in which the evidence of productive surface waters is destroyed at the sediment-water interface.

The bottom sediments of the western entrances to the Canadian Arctic Archipelago contain considerably greater amounts of planktonic foraminifera in comparison to the sediments of the eastern approaches to the archipelago (text fig. 5). In the west the preservation is enhanced by the larger proportions of kummerform phenotypes produced in the stratified water column, in addition to the less corrosive bottom waters entering the channels from the Arctic Ocean.

ACKNOWLEDGMENTS

The writer wishes to express gratitude to Drs. B. R. Pelletier, C. T. Schafer, and F. J. E. Wagner for a critical review of the manuscript, and Miss B. J. Baker who assisted in making the scanning electron photomicrographs.

REFERENCES

BÉ, ALLAN W. H., and LOTT, LEROY, 1964, Shell growth and structure of planktonic foraminifera: Science, v. 145, no. 3634, p. 823–824.

BERGER, WOLFGANG H., 1967, Foraminiferal ooze: Solution at depth: Science, v. 156, p. 383–385.

———, 1968, Planktonic foraminifera: Selective solution and paleoclimatic interpretation: Deep-Sea Research, v. 15, p. 31–43.

———, 1970, Planktonic foraminifera: Selective solution and lysocline: Marine Geology, v. 8, no. 2, p. 111–138.

BERGER, WOLFGANG H., and SOUTAR, ANDREW, 1970, Preservation of plankton shells in an anaeorobic basin off California: Geol. Soc. America Bull., v. 81, p. 275–282, 3 figs.

BRAMLETTE, M. N., 1961, Pelagic sediments, *in* Sears, M., ed., Oceanography: Washington, D.C., Am. Assoc. Adv. Sci., p. 345–366.

KENNETT, JAMES P., 1966, Foraminiferal evidence of a shallow calcium carbonate solution boundary, Ross Sea, Antarctica: Science, v. 153, no. 3732, p. 191–193.

MARLOWE, J. I., and VILKS, G., 1963, Marine geology, eastern part of Prince Gustaf Adolf Sea, District of Franklin, Polar Continental Shelf Project: Canada Geol. Survey Paper 63-22, p. 1–23.

MURRAY, J., and RENARD, A. F., 1891, Deep-sea deposits based on the specimens collected during the voyage of H.M.S. "Challenger" in the years 1872–1876. Rep. Voyage "Challenger," London, Longmans, p. 525 (Reprinted by Johnson, London, 1965).

PETERSON, M. N. A., 1966, Calcite: rates of dissolution in a vertical profile in the central Pacific: Science, v. 154, no. 3756, p. 1542–1544.

PYTKOWICZ, R. M., 1965, Calcium carbonate saturation in the ocean: Limnology and Oceanography, v. 10, no. 2, p. 220–225.

PYTKOWICZ, R. M., and FOWLER, G. A., 1967, Solubility of

←

PLATE 2

Globorotalia pachyderma, Station 346, lat 70°19′ N., long 138°48′ W., Beaufort Sea. Depth range 0–200.

1a Ventral view, sinistral, 5 chambers per last whorl, normalform, with an irregular and ornamented lip over the aperture. Longest diameter 400 microns, shortest diameter 325 microns. × 200.

1b Surface of ultimate chamber. Secondary deposits forming irregular ridges, which begin to join around the pores. Some of the original bilamellar test surface still exposed. Average maximum diameter of pores 1.57 microns. × 3,000.

2a Ventral view, sinistral, 4 chambers per last whorl kummerform. Longest diameter 325 microns, shortest diameter 242 microns. × 240.

2b Surface of penultimate chamber. The formation of secondary deposits similar to the previous example. Average maximum diameter of pores 1.57 microns. × 3,000.

3a Ventral view, sinistral, 4 chambers per last whorl, normalform. Longest diameter 400 microns, shortest diameter 365 microns. × 200.

3b Surface of ultimate chamber. Secondary deposits forming terraced ridges, which begin to join around the pores. × 3,000.

foraminifera in seawater at high pressures: Geochem. Jour., v. 1, p. 169–182.

VILKS, G., 1964, Foraminiferal study of East Bay, MacKenzie King Island, District of Franklin, Polar Continental Shelf Project: Canada Geol. Survey Paper 64-53, p. 1–26.

———, 1969, Recent foraminifera in the Canadian Arctic: Micropaleontology, v. 15, no. 1, p. 35–60, pls. 1–3.

———, 1973, A study of *Globorotalia pachyderma* (Ehrenberg) = *Globigerina pachyderma* (Ehrenberg) in the Canadian Arctic: Dalhousie Univ., unpub. doctoral thesis.

WANGERSKY, PETER J., 1969, Distribution of suspended carbonate with depth in the ocean: Limnology and Oceanography, v. 14, p. 929–933.

Ms received September 1974
Revised ms accepted November 1974

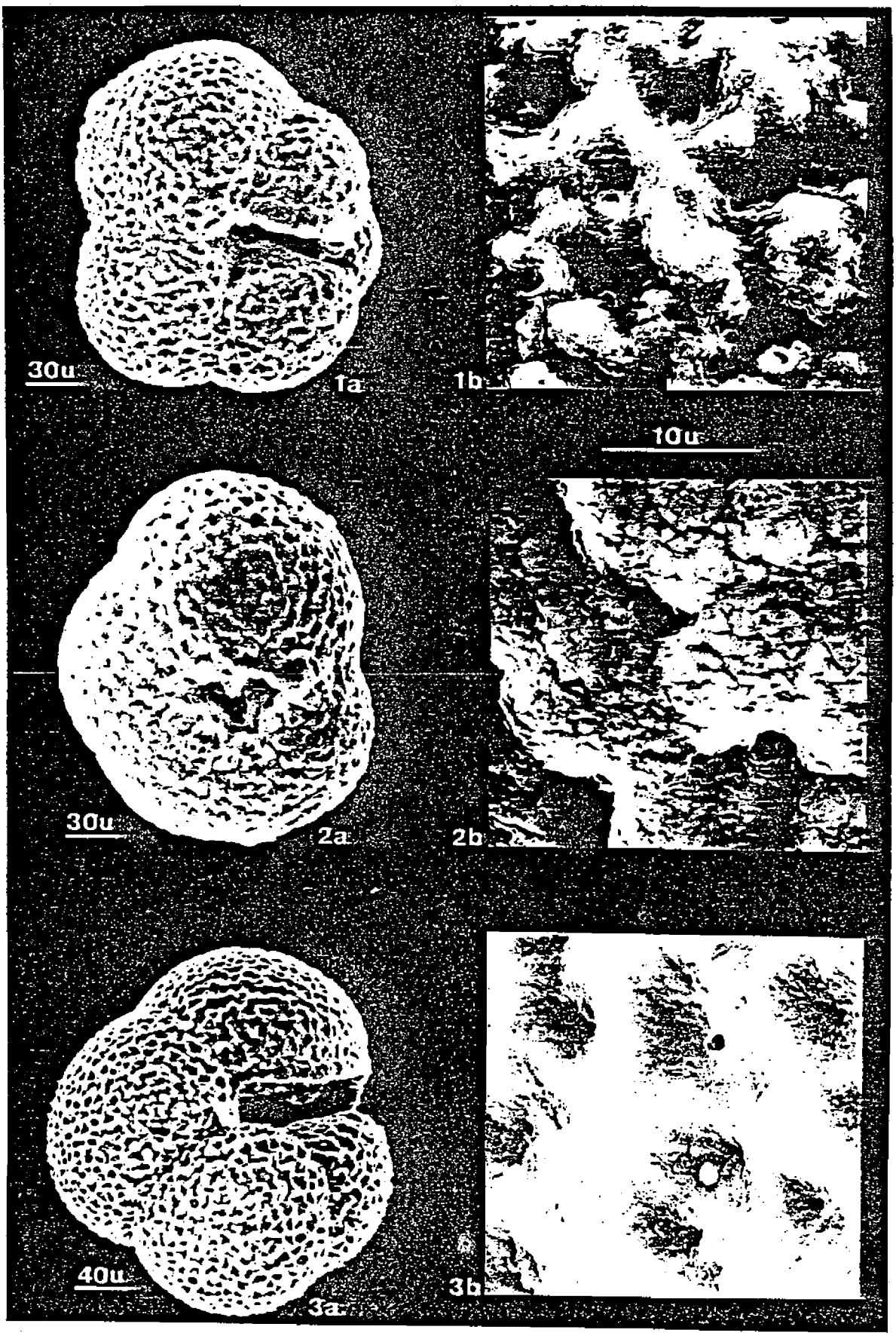
→

PLATE 3

1a, b *Globorotalia pachyderma*, Station 384, lat 70°32′ N., long 136°40′ W., Beaufort Sea. Collected from bottom sediments at 700 metres. a. Ventral view, sinistral, 4 chambers per last whorl, kummerform. Longest diameter 200 microns, shortest diameter 170 microns. × 400. b. Surface of ultimate chamber showing terraced ridges. × 3,000.

2a, b *Globorotalia pachyderma*, Station 384. a. Ventral view, sinistral, 4 chambers per last whorl, normalform. Longest diameter 220 microns, shortest diameter 170 microns. × 400. b. Surface of ultimate chamber showing euhedral crystals. × 3,000.

3a, b *Globorotalia pachyderma*, Station 452, lat 73°48.1′ N., long 113°45.5′ W., Viscount Melville Sound. Collected from bottom sediments at 428 metres. a. Ventral view, sinistral, 4 chambers per last whorl, quadrate. Longest diameter 280 microns, shortest diameter 264 microns. × 300. b. Surface of ultimate chamber showing microcrystalline encrustation. × 3,000.


30u
1a
1b
10u
30u
2a
2b
40u
3a
3b

Journal of Foraminiferal Research, v. 4, no. 1, p. 1–8, pls. 1–3, January 1974

MORPHOLOGY OF *ORBULINA UNIVERSA* D'ORBIGNY IN RELATION TO OTHER SPINOSE PLANKTONIC FORAMINIFERA

GUSTAVS VILKS AND D. A. WALKER
Atlantic Geoscience Centre, Geological Survey of Canada
Bedford Institute of Oceanography, Dartmouth, Nova Scotia, Canada

ABSTRACT

The adult phenotype of the planktonic foraminifer *Orbulina universa* contains two seemingly unrelated forms: the inner trochospiral and the outer spherical. To demonstrate the relationship of this species to other planktonic foraminifera, scanning electron micrographs were studied on specimens collected in surface waters of the Atlantic and Pacific Oceans and the Caribbean Sea.

Most trochospiral forms of *Orbulina* contain supplementary secondary apertures, therefore the species is not related to *Globigerina* d'Orbigny as maintained by several authors. All specimens possess triradiate spines, which are different from any species of the genus *Globigerinoides*, indicating a basic difference between the two genera. *Hastigerina* Thomson and *Globigerinella* Cushman also contain triradiate spines, but these genera are planispiral and therefore different from *O. universa*.

It is suggested that morphology of spines should reflect variations in genetic codes and therefore is useful for the classification of spinose planktonic foraminifera. The micromorphology of *Orbulina universa* is distinct from the other forms of planktonic foraminifera and therefore it is a valid taxon.

INTRODUCTION

Orbulina universa d'Orbigny is ubiquitous in tropical, subtropical and transitional faunal zones of the oceans. The highest abundances occur in the surface waters of strong current systems and regions of upwelling (Bé and Tolderlund, 1971). In addition to its widespread occurrence, *O. universa* is unique among the various living species of planktonic foraminifera in that the adult has formed a globular chamber totally embracing a multichambered test. Thus the adult phenotype contains two seemingly unrelated forms: the inner trochospiral and the outer spherical. Normally the inside test is held in position only by spines without any other contact with the outside test walls, although the dorsal side is usually closer to the spherical wall.

Orbulina universa collected from Recent sands was first described by d'Orbigny in 1839 (*vide* Ellis and Messina, 1942, *et seq.*) and since then the taxonomic status of the genus has been in discussion. On the assumption that the two forms that compose the adult *O. universa* represent the ontogeny of the species, published phylogenetic lineages show that *O. universa* originated from a globigerine forerunner (e.g., Brönnimann, 1951; Blow, 1956). Thus in the scheme of classification, *Orbulina* is included with the globigerinas and by some authors was designated as a type genus for the family *Orbulinidae* which according to Galloway (1933) comprises all planktonic foraminifera, but according to Bolli *et al.* (1957) includes only *Globigerina* and related genera.

TABLE 1

Location of stations, month and year of sampling and depth interval.

Stations	Latitude	Longitude	Date	Depth (m)
69–109VC–1	32°10′N	64°30′W	4/69	0–200
69–303VC–9	32°10′N	64°30′W	7/69	0–200
70–135VC Sfc	41°08.9′N	49°25.1′W	6/70	0–2
69–050VC–57	41°40′S	46°49.9′W	1/70	0–200
69–050VC–91 Sfc	39°59.7′S	150°03.1′W	5/70	0–2
69–050VC–106 Sfc	42°48.2′N	149°52.0′W	6/70	0–2
69–050VC–106	—	—	—	0–200
69–050VC–90 Sfc	44°56.6′S	149°58.8′W	5/70	0–2
69–050VC–3	02°29.3′S	30°05.2′W	12/70	0–200
69–050VC–101 Sfc	10°01.4′N	150°06.8′W	5/70	0–2
70–120VC	37°40.7′N	49°36.1′W	6/70	0–200
68–4–20–9	13°07′N	63°26′W	2/68	0–200
68–4–19–5–1	13°40′N	63°19′W	2/68	0–100
69–025–64	33°00′N	42°30.9′W	6/69	0–200
69–050VC–18	20°07′S	30°28.0′W	12/69	0–200
69–050VC–95 Sfc	19°58.0′S	150°02.6′W	5/70	0–2
69–050VC–92 Sfc	35°00.4′S	150°00.0′W	5/70	0–2
69–050VC–98 Sfc	04°57.4′S	150°10.8′W	5/70	0–2
70–128VC	41°12.1′N	49°27.6′W	6/70	0–200
69–050VC–102 Sfc	16°02.6′N	150°05.4′W	5/70	0–2
69–050VC–50 Sfc	48°59.0′S	39°58.6′W	1/70	0–2
70–104VC	51°73′N	38°98′W	6/70	0–200
69–050VC–97 Sfc	09°46.8′S	150°05.4′W	5/70	0–2
69–050VC–99	00°04.9′S	149°51.4′W	5/70	0–200
69–050VC–104 Sfc	28°51′N	149°57.7′W	5/70	0–2
69–050VC–100	04°46.6′N	150°04.8′W	5/70	0–200

The single origin of *Orbulina* has been disputed by Hofker (1959, 1969), Bandy (1966), and Bandy *et al.* (1969) basically on the grounds that the first appearance of *O. universa* in the Miocene does not take place simultaneously at various localities and because the inner specimen may or may not contain secondary dorsal apertures. By stating that the origin of *O. universa* is polyphyletic and that the living forms may be homeomorphic, these authors question the validity of the name *Orbulina universa* in a taxonomic sense. It has been suggested (Bandy *et al.*, 1969) that *O. universa* originated earlier in the oceans of the lower latitudes from a globigerinoid precursor and is represented in the living population with individuals containing secondary dorsal apertures. The higher latitude *O. universa* originated later from a globigerine precursor without the secondary apertures.

It is possible that this classical approach to the study of fossil forms is insufficient to settle the classification of *O. universa* and it may be necessary to explore new fields and focus on living specimens. Owing to its extensive range in the oceans, detailed study of specimens collected from widely separated areas is necessary. Life cycle studies of laboratory cultures would answer many questions, but technical difficulties in carrying out these experiments have so far prevented many workers from taking this approach. Adshead (1967) was able to observe the development of *Orbulina universa* in a culture containing initially only *Globigerina bulloides*. This is the only published observation of this kind and both Bandy (*op. cit.*) and Hofker (*op. cit.*) use it as evidence for the view that the spherical "*Orbulina*" chamber is a morphological expression of a stage in the life cycle of planktonic foraminifera and may involve several species.

So far a relatively unexplored approach in resolving taxonomic problems of planktonic foraminifera is the comparison of spinal ultrastructures in the various genera. This approach emphasizes skeletal micromorphology in the interpretation of natural relationships between forms, rather than gross morphology of foraminiferal tests (e.g., Lipps, 1966; Reiss, 1968). The presence or absence of spines was used as a criterion to discriminate major taxa by Parker (1962), Bé (1967), and others, but with the advent of the scanning electron microscope, Bé (1969), Bé *et al.*

(1973). Hemleben (1969a, 1969b), Walker and Vilks (1973) introduced a method with which the more questionable relationships could be resolved. Hemleben (1969a, 1969b), and Walker and Vilks (1973) described the various forms of spines that can be found on planktonic foraminifera and Bé (1969), maintained that the similarity of the triradiate spines found on *Hastigerina pelagica* (d'Orbigny) and *Globigerinella aequilateralis* (Bandy) indicate a close affinity of the two forms. Bé *et al.* (1973) also found triradiate spines on both the trochospiral and the spherical tests of *Orbulina universa* collected in the Indian Ocean and concluded that the spherical tests represent one species only. In the present report test morphology and spines of *Orbulina universa* are described in order to demonstrate possible differences with the other species of planktonic foraminifera.

METHODS

The specimens for this study were collected with vertical plankton tows from the upper 200 metres of water during the various cruises of CSS HUDSON (See table 1). Individuals were studied from as widely separated localities as possible in the Atlantic and Pacific Oceans and the Caribbean Sea. Immediately after collection, samples were preserved in a 10% formaldehyde-seawater solution buffered with hexamethylene tetramine. The specimens were examined with a JEOL JSM-2 scanning electron microscope. Prior to the examination, each specimen was exposed to an atmosphere of atomic oxygen for at least 8 hours in a TRACERLAB low-temperature asher (Vilks, 1970). With this treatment it is possible to obtain specimens that are free of organic coating or other impurities. Further preparation for scanning electron microscope examination consisted of placing the specimens onto double-coated adhesive tape ("Sellotape") previously mounted on standard JEOL specimen blocks. The mounted specimens were then dissected with a needle in order to expose the trochospiral internal test. Owing to the fragile nature of the internal test, only about 10% of the dissections were successful and of those all revealed the ventral side. To study the dorsal side the inner specimens were removed to observe the supplementary apertures and spines. All specimens were coated with gold-palladium in an Edwards high-vacuum evaporator.

Altogether, 34 specimens were examined from 25 localities in the tropical, subtropical and transitional faunal zone of the Atlantic and Pacific Oceans and the Caribbean Sea. The summary of these observations is shown in table 2 and representative specimens are illustrated in plates 1–3.

TABLE 2

The distribution and recorded observations of specimens. Blank space indicates that the observation could not be made, 0 indicates the absence of the feature.

Stations	Number of Specimens		Number Possessing Triradiate Spines	Number Possessing Supplementary Apertures
69–109VC–1	1		1	
69–303VC–9	1		1	
70–135VC Sfc	2		2	
69–050VC–91 Sfc	3	(fragments)	3	
——	1		0	1?
——	1	"*Biorbulina*"	1	
69–050VC–106 Sfc	1		1	
——	2	"*O. suturalis*"	0	
69–050VC–90 Sfc	1	"*O. suturalis*"	0	
69–050VC–3	1		1	1
69–050VC–101 Sfc	1		1	1
70–120VC	4		4	4
——	1	"*Biorbulina*"	1	
68–4–20–9	1		1	0
68–4–19–5–1	1		1	1
——	2	(fragments)	2	
69–025–64	1	(fragments)	1	
69–050VC–18	1		1	
69–050VC–95 Sfc	1	(fragment)	1	
69–050VC–92 Sfc	1		1	1?
69–050VC–98 Sfc	1	(fragments)	1	
70–128VC	1		1	1
69–050VC–102 Sfc	4		4	3
Totals	34		30	13

MORPHOLOGY

The inner test is trochospiral and consists of 13–15 spherical chambers (pl. 1, figs. 1–3). The initial whorl contains six chambers, which are devoid of spines. Bé *et al.* (1973) also found the earlier chambers devoid of spines and compared the embryonic stage of *Orbulina universa* to the nonspinose *Globorotalia and Globoquadrina.* The subsequent chambers are spinose and arranged in less open whorls, with four to five chambers per whorl. Preferred coiling direction was not found, and dextral and sinistral specimens occur in close fractions.

The primary aperture is umbilical, open or restricted with nonporous and irregular apertural lip. Along the sutures of the ultimate chamber there are four sup-

ementary apertures, two large and two small. The all supplementary apertures are also present along e sutures of other chambers belonging to the last torl (pl. 1, figs. 1, 2a, 4a, 4b). The surface of the t between spines is smooth (pl. 1, figs. 2b, 3b) but e specimens may have a rough surface texture with ominent spinal shoulders (pl. 2, fig. 2b).

Both the surface texture and the presence of secondy apertures are variable features. Of 13 specimens e did not contain secondary apertures and two were estionable, i.e., the margins were irregular and uld have been broken. The ratio of smooth to irgular surface texture is in the order of ten to one. ie present data did not indicate any latitudinal or termass preferences for the two phenotypes; however, more samples must be studied to establish any ssible relationships.

Only a small fraction of the dissected specimens ntained well-preserved trochospiral tests and approxitely 50% were empty. No correlation was found beeen the state of the trochospiral test and the thickss of the outside shell. The dissolution of the trochoral test takes place initially along the sutures and earlier chambers (pl. 1, figs. 6, 7a), therefore in ny instances the trochospiral tests were found with earlier chambers missing or the late chambers rtly detached.

Spines were present on all specimens including the rtly digested tests. The morphology of the spines complex and is dominated by two basic structures: single cylindrical shafts with circular cross-sections triplanar shafts with triradiate cross-sections. oximally all the spines are circular in cross-section, at varying distances from the base the circular ss-sections give way to triangular, and finally to radiate cross-sections over a short distance. The triliate spines are by far the most common, and the ratio of round to triradiate spines was found to be 1 to 30 (see table 2). The only specimen where triradiate spines were not observed is illustrated in plate 1, figure 7a, and a single spine for this specimen in figure 7b. However, it is possible that the triradiate part of the spines of this specimen have been lost due to poor preservation.

The spines of the trochospiral test penetrate the walls of the spherical chamber and can be distinguished by the low angle of penetration and lack of shoulders (pl. 2, figs. 1b, 2c). These spines are always triradiate. The spines that originate on the wall of the globular chamber are more robust with terraced shoulders (pl. 2, figs. 1b, c). It is not unusual to find two spines on a single shoulder with one spine slightly smaller. The spines of the spherical chambers also become triradiate at some distance from the base (pl. 2, fig. 5b). Normally the spines are broken during the preparation and only rarely can specimens be photographed possessing spines sufficiently long to demonstrate the triradiate shape. Well-preserved spines originating on the globular chamber were found inside the second chamber of a spherical test that would be called *Biorbulina* by Blow (1956) (pl. 2, figs. 5a, b). These spines are round at the base and are surrounded by spinal shoulders and therefore are not penetrating from an inner trochospiral test.

A globular chamber with the trochospiral inner test penetrating the outside wall is shown in plate 2, figures 3a, b, and 4. Bronnimann (1951) erected the species *Orbulina suturalis* to accomodate such forms. *O. suturalis* has been designated by various authors as the ancestor for *Orbulina universa* (e.g., Brönnimann, 1951; Blow, 1956), but is considered by some authors as synonymous to *O. universa* (e.g., Bolli, *et al.*, 1957), or as variants (Bé and Hamlin, 1967). In this study altogether three specimens of *O. suturalis* were investi-

PLATE 1

Figures 1–7 *Orbulina universa* d'Orbigny.

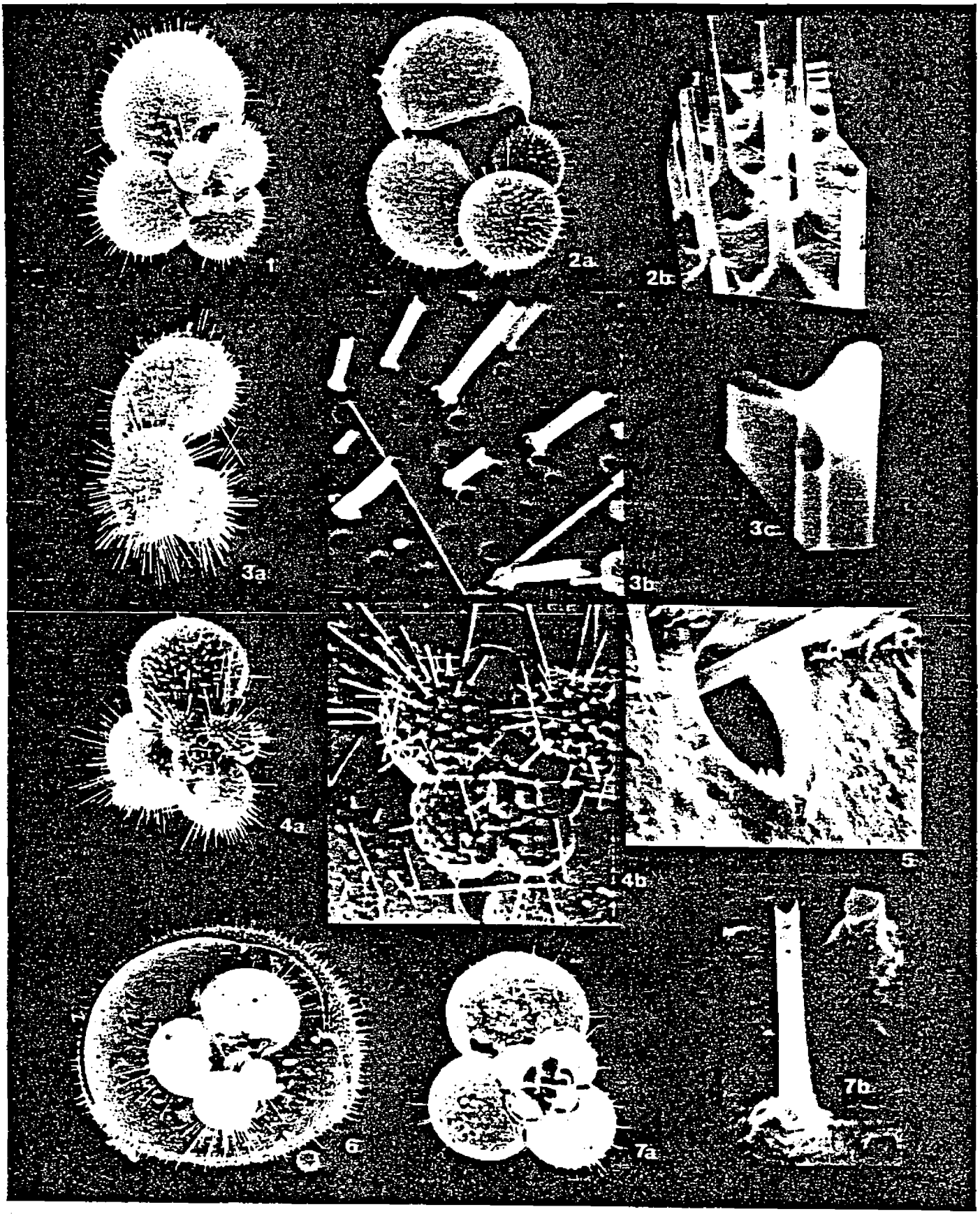
Station 70-120VC, North Atlantic. Dorsal view, showing sutural supplementary apertures, ×180.

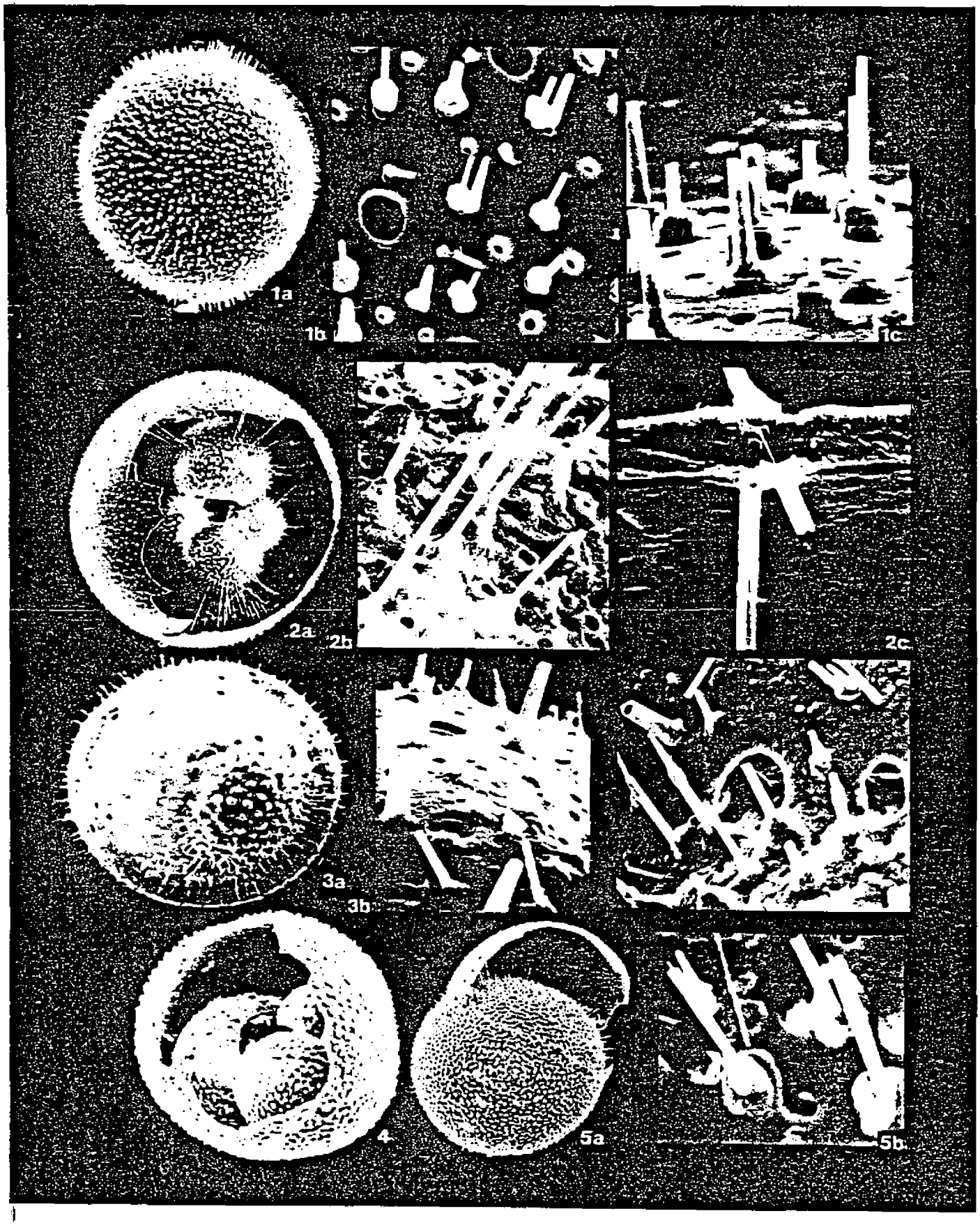
Station 70-120VC. a, ventral view, showing the umbilical primary aperture and a small sutural aperture, ×200: b, surface of penultimate chamber showing triradiate spines, ×3,000.

Station 69-050VC-3, Equatorial Atlantic. a, side view showing a small sutural aperture, ×185; b, surface of penultimate chamber showing triradiate spines, ×2,300; c, tip of a triradiate spine, ×23,200.

Station 69-050VC-102 Sfc, Equatorial Pacific. a, dorsal view showing numerous secondary apertures, ×170; b, section of initial chambers, ×550.

5. *Station 70-128VC*, North Atlantic. Small supplementary aperture along a suture between ultimate and penultimate chambers, ×3,000.
6. *Station 69-050VC-95 Sfc*, Equatorial South Pacific. A dissected spherical test showing partly digested trochospiral test, ×120.
7. *Station 69-050VC-91 Sfc*, South Pacific. a, dorsal view showing partly digested initial chambers, ×120; b, a single spine, ×5,500.


1
2a
2b
3a
3b
3c
4a
4b
5
6
7a
7b


1a
1b
1c
2a
2b
2c
3a
3b
4
5a
5b

gated in detail, two had round spines only and one had no spines (pl. 2, fig. 4). The more robust spines of plate 2, figure 3b are oriented at right angles to the test surface and therefore originate on the outer wall. The fragile spines penetrate the test wall at low angles, originate from the trochospiral specimen inside, and may be relatively long. These penetrating spines are not triradiate, although in the case of the *O. universa* all penetrating spines are triradiate.

The exposed dorsal side of the trochospiral form of *O. suturalis* displayed no evidence of supplementary apertures along the sutures between the trochospiral chambers. However, along the suture delineating the spherical and trochospiral tests there are a number of openings (pl. 2, fig. 3c). These openings are different from the apertures found on the trochospiral test of the *O. universa* in that the distribution and shape of these apertures follow no definite pattern and the marginal lip characteristic of *O. universa* is lacking (see pl. 1, fig. 5).

Comparative Morphology of Other Spinose Planktonic Foraminifera

On the basis of spine ultrastructure we believe that the spinose planktonic foraminifera can be divided into two major groups: 1) those possessing spines with round to triangular cross-sections and 2) spines with triradiate cross-sections. The former group is represented by the genera *Globigerina* and *Globigerinoides* and the second group by *Hastigerina, Globigerinella* and *Orbulina*. In the present day oceans members of the "*Globigerina*" group are represented by 12 species, whereas the "*Hastigerina*" group is represented by only four species (using Bé, 1967, as a source for classification). In addition to being more diverse, the "*Globigerina*" group is also more abundant everywhere and has a wider temperature tolerance range.

Representative specimens of the two groups are shown in plate 3. Figures 1 to 3 illustrate the various features typical of *Globigerina bulloides* d'Orbigny; Figure 1a represents a ventral view of a *G. bulloides* collected in surface waters of the South Atlantic. The test morphology is similar to a typical trochospiral test of *Orbulina universa* as illustrated in plate 1, figure 2a, except that the aperture of *O. universa* is wider along the sutures.

A basic difference, however, exists between the two genera in terms of microstructure. Normally the surface texture of the trochospiral *O. universa* is smooth and the spines do not have extensive spinal shoulders (pl. 1, fig. 3b). The spines of *G. bulloides* invariably develop spinal shoulders (pl. 3, figs. 1b, 3), which grow to form ridges. Thus at low magnifications the surface texture of *G. bulloides* appears to be rough, whereas a surface of the trochospiral *O. universa* is smooth.

The spines of *G. bulloides* have round cross-sections at the proximal end (pl. 3, fig. 3) and remain round to the distal end as demonstrated by a piercing spine tip in plate 3, figure 2. A tip of a spine with three crystalline surfaces is also shown in plate 3, figure 1c.

All species of the genus *Globigerina* lack supplementary dorsal apertures, which is a diagnostic feature for the genus *Globigerinoides*. The last whorl of adult *Globigerinoides ruber* (d'Orbigny) and *Globigerinoides conglobatus* (Brady) have three supplementary apertures per chamber, but *Globigerinoides sacculifer* (Brady) illustrated in plate 3, figure 6 has only one supplementary aperture per chamber. As pointed out above, *Orbulina* has four supplementary dorsal apertures on the ultimate chamber and also frequently on the other chambers on the last whorl. In this respect,

←

PLATE 2

Figure 1–5 *Orbulina universa* d'Orbigny.

1. *Station 69-050VC-91 Sfc*, South Pacific. a, spherical chamber, mag. ×220; b, surface of spherical chamber showing round and triangular spines originating on the outer surface and triradiate spines penetrating at low angle, mag. ×2,200; c, oblique view of the surface showing spines with terraced spinal shoulders, ×3,500.
2. *Station 69-050VC-106 Sfc*, North Pacific. a, dissected spherical chamber showing a ventral view of the trochospiral test, ×185; b, surface of ultimate chamber showing spinal shoulders and triradiate spines, ×2,300; c, fractured edge of spherical chamber showing penetrating triradiate spines, ×7,500.
3. *Station 69-050VC-90 Sfc*, South Pacific. a. *O. suturalis* showing the trochospiral test penetrating the spherical form, ×421; b. oblique view of the spherical test showing round spines penetrating at low angle, ×2,000; c. suture between the spherical and trochospiral test showing marginal apertures, ×2,300.
4. *Station 69-050VC-106*, North Pacific. *O. suturalis* dissected to show the trochospiral test, ×230.
5. *Station 70-120VC*, North Atlantic. a, spherical test with dissected second chamber, ×120; b, surface of spherical test inside the second chamber showing triradiate spines, ×1,700.

Orbulina is different from *Globigerinoides*. The supplementary apertures on the early chambers of these two genera are absent; however, the early chambers in *Globigerinoides* are as spinose as the later chambers, whereas the spinosity is reduced on the early chambers of *O. universa*.

The spines of *Globigerinoides* are triangular to round at the base (pl. 3, fig. 4, 5b) but all spines are round at the distal end (fig. 5c). Pores are regularly spaced and secondary deposition takes place very early in the life cycle, as demonstrated in plate 3, figure 5b, which shows a test surface of the ultimate chamber of a juvenile *G. succulifer* illustrated in figure 5a. The deposition originates around the spine bases and ultimately connects adjacent spines as straight ridges and always at a maximum distance from the pores. Thus a hexagonal pattern of ridges is formed, which is characteristic of the genus *Globigerinoides*.

The surface texture of *Hastigerina* is invariably smooth and the spines are triradiate without a round section at the base, proximally and throughout their length with relatively small spinal shoulders (pl. 3, fig. 7a, b). The chamber arrangement is planispiral with the spines concentrated along the equatorial region of the test. Along the edges, each spine possesses secondary outgrowths at some distance from the base. These outgrowths were termed spinal barbs by Walker and Vilks (1973).

The gross morphology of *Globigerinella* resembles *Hastigerina* and some authors consider *Globigerinella* as a junior synonym to *Hastigerina* (e.g., Bolli *et al.*, 1957). However, in terms of surface texture and spines, the two genera are different. *Globigerinella* may possess all types of spines described in this paper (pl. 3, fig. 8). The triradiate spines are coarser than the cylindrical and triangular spines, but are smaller than those of *Hastigerina*. Proximally the triradiate spines have a circular cross-section with a small shoulder and the triradiate edges are without spinal barbs. The distribution of the various spines is irregular and because of the shoulders the surface texture of *Globigerinella* is not smooth but may be covered with irregular ridges.

DISCUSSION

In terms of the number and shape of apertures and spinal ultrastructure *Orbulina universa* is a unique species. For the determination of the phylogenetic relationships of this species, the resemblance of the juvenile stage to the globigerinids may not be a useful criterion. Juvenile planktonic foraminifera resemble each other (Bé, 1959, text figure 1) and develop specific features only during adolescence and maturity. The young stages of planktonic foraminifera are concentrated in surface waters (Bé, 1960; Bé and Ericson, 1963) where they undergo a period of rapid growth and faster rates of feeding and metabolism than the adults living in the deeper waters. The juveniles therefore occupy a different niche and are adapted to a set of environmental factors that are different from those of the adults. As a result convergence in morphological features of the juvenile stage has taken place, where similar demands by the environment have evoked similar phenotypic responses. It seems that the trochospiral chamber arrangement resembling *Globigerina* is most suitable for the growing cells and in the case of *Orbulina*, it would be difficult to maintain a spherical chamber during this period. It would involve the dissolution of the previous chambers with the increase of size, a feature not common among the foraminiferid protozoans. Thus a trochospiral initial stage of *Orbulina* resembling *Globigerina* does not necessarily imply a close phylogenetic relationship between the two genera.

On the other hand, the popular view that spines of plankton have an important adaptive value for maintaining the organisms in suspension may not be true. Smayda (1970) discussed phytoplankton buoyancy at length and concluded that morphological mechanisms are inadequate for maintaining the cells in suspension. Senescent and dead cells sink faster than viable cells with similar protuberances, therefore physiological mechanisms would appear to be more effective for the maintenance of organisms at the desired levels in the water column. The present authors feel that in the case of planktonic foraminifera, metabolic rates may play an important role in providing the necessary buoyancy. Intensively feeding and rapidly growing individuals are surrounded with an extensive network of anastomosing pseudopodia which provide the necessary microenvironment for flotation. With age and slower metabolic rates the pseudopodia become less active and as a result older foraminifera occupy deeper and denser waters. Freshly caught foraminifera usually sink to the bottom of the container because the pseudopodia are withdrawn due to shock. That the presence of spines may play a secondary role in the adaptation for the planktonic environment is also borne out by the relatively large number of nonspinose planktonic

foraminiferal species. Bé (1967) listed 14 nonspinose species of planktonic foraminifera from a total of 31 species.

Due to a posibly low adaptive value, spines of planktonic foraminifera may be more useful indicators of true relationships between taxa. All spines originate at the primary membrane (Hemleben, 1969a) and therefore the presence or absence of spines reflects a basic difference in the mode of formation of this layer. The building of the test wall takes place in accordance with the genetic code of the taxon and any differences in the structure of the wall indicate genotypic differences between taxa. The presence or absence of spines should therefore indicate a basic nonaffinity between forms. The microstructures of spines should reflect small variations in genetic codes among the spinose forms. On the basis of this conjecture *Globigerina* with the round spines is closer phylogenetically to *Globigerinoides* which possess triangular spines than to *Hastigerina*, *Orbulina* and *Globigerinella* with triradiate spines.

The relationship between *Orbulina suturalis* and *O. universa* can also be established by a close study of spines. The examples of *O. suturalis* inspected for the present study did not show evidence of triradiate spines and only round spines were found. It is therefore suggested that the forms resembling *Orbulina suturalis* Brönnimann (1951) and living in the present day oceans are aberrant *Globigerina bulloides*. The spines of *Biorbulina* are triradiate and although more examples must be studied, it is suggested here that the living form resembling *Biorbulina bilobata* (d'Orbigny) are examples of *Orbulina universa*.

ACKNOWLEDGMENTS

The writers wish to express gratitude to Drs. P. Ascoli, D. E. Buckley, and G. E. Williams for a critical review of the manuscript. Miss B. Baker assisted in the preparation of the scanning electron photomicrographs.

REFERENCES

ADSHEAD, PATRICIA C., 1967, Collection and laboratory maintenance of living planktonic Foraminifera: Micropaleontology, v. 13, no. 1, p. 32–40.

BANDY, O. L., 1966, Restrictions of the "*Orbulina*" datum: Micropaleontology, v. 12, no. 1, p. 79–86, pl. 1.

BANDY, O., VINCENT, EDITH, and WRIGHT, R. C., 1969, Chronologic relationships of Orbulines to the *Globorotalia fohsi* lineage: Rev. Española Micropaleontologia v. 1, no. 2, p. 131–145.

BÉ, ALLAN, W. H., 1959, Ecology of Recent planktonic foraminifera: Micropaleontology, v. 5, no. 1, p. 77–100.

———, 1960, Some observations on the Arctic planktonic Foraminifera: Cushman Found. Foram. Research Contr., v. 11, pt. 2, p. 64–68.

———, 1967, Foraminifera: Fides d'Identification du Zooplancton. Consiel permanent international Pour L'exploration de la mer, Zooplankton Sheet 108, p. 1–8.

———, 1969, Microstructural evidence of the close affinity of *Globigerinella* Cushman to *Hastigerina* Thomson: Internat. Conf. Planktonic Microfossils, 1st. Geneva (1967), Proc., P. Brönnimann and H. H. Renz, eds., v. 1, p. 89–91.

BÉ, ALLAN W. H. and ERICSON, DAVID B., 1963, Aspects of calcification in planktonic Foraminifera (Sarcodina): New York Acad. Sci. Annals, v. 109, art. 1, p. 65–81.

BÉ, ALLAN W. H. and HAMLIN, WILLIAM H., 1967, Ecology of Recent planktonic Foraminifera. Part 3—Distribution in the North Atlantic during the summer of 1962: Micropaleontology, v. 13, no. 1, p. 87–106.

BÉ, ALLAN W. H., HARRISON, STANLEY M., and LOTT, LEROY, 1973, *Orbulina universa* d'Orbigny in the Indian Ocean: Micropaleontology, v. 19, no. 2, p. 150–192.

BÉ, ALLAN W. H. and TOLDERLUND, D. S., 1971, Distribution and ecology of living planktonic Foraminifera in surface waters of the Atlantic and Indian Oceans, *in* Funnell, B. M. and Riedel, W. R. *eds.* Micropaleontology of Oceans: Cambridge, London, Univ. Press, p. 105–148.

BLOW, W. H., 1956, Origin and evolution of the foraminiferal genus *Orbulina* d'Orbigny: Micropaleontology, v. 2, no. 1, p. 57–70, text figs. 1–4.

BOLLI, H., LOEBLICH, A. R., and TAPPAN, H., 1957, Planktonic Foraminiferae Families Hantkeninidae, Orbulinidae, Globorotaliidae and Globotruncanidae, U.S. Natl. Mus. Bull. 215, [Smithsonian Inst., Washington,] p. 3–50, pls. 1–11, text figs. 1–9.

BRÖNNIMANN, P., 1951, The genus *Orbulina* d'Orbigny in the Oligo-Miocene of Trinidad, B.W.I.: Cushman Found. Foram. Research Contr. v. 2, pt. 4, p. 131–138.

ELLIS, B. F., and MESSINA, ANGELINA R., 1942, *et seq.*—*Catalogue of* Foraminifera: [New York:] Am. Mus. Nat. History, Spec. Pub., loose-leaf, illus.

GALLOWAY, F. F., 1933, A manual of Foraminifera: Bloomington, Indiana, Principia Press, p. 483.

HEMLEBEN, CHRISTOPH, 1969a, Ultrastructure Bei Kalkschaligen Foraminiferen: Naturwissenschaften, v. 56, p. 534–538.

———, 1969b, Ultramicroscopic shell and spine structure of some spinose planktonic Foraminfera: Internat. Conf. Planktonic Microfossils, 1st, Geneva (1967), Proc., P. Brönnimann and H. H. Renz eds., v. 2, p. 254–256.

HOFKER, J., 1959, On the splitting of Globigerina: Cushman Found. Foram. Research Contr., v. 10, pt. 1, p. 1–9.

HOFKER, J. SR., 1969, Have the genera *Porticulasphaera*, *Orbulina* (*Candorbulina*) and *Biorbulina* a biologic meaning? Internat. Conf. Planktonic Microfossils, 1st., Geneva (1967), Proc., P. Brönnimann and H. H. Renz eds., v. 2, p. 279–286.

LIPPS, JERE H., 1966, Wall Structure, systematics, and phylogeny studies of Cenozoic planktonic Foraminifera; Jour. Paleontology, v. 40, no. 6, p. 1257–1274.

PARKER, F. L., 1962, Planktonic foraminiferal species in Pacific sediments: Micropaleontology, v. 8, no. 2, p. 219.

Reiss, Z., 1968, Planktonic foraminiferids stratotypes and a reappraisal of Neogene chronostratigraphy in Israel: Israel Jour. Earth Sci., v. 17, iss. N4, p. 153, ref. 46.

SMAYDA, J. THEODORE, 1970, The suspension and sinking of Phytoplankton in the Sea: Oceanog. Marine Biology Ann. Rev., v. 8, p. 353–414, Harold Barnes, *ed.*

VILKS, G., 1970, New method for separation of skeletal material from a plankton sample: Maritime Sediments, v. 6, no. 2, p. 72–73.

WALKER, D. A. and VILKS, G., 1973, Spinal ultrastructure of the planktonic foraminifers *Hastigerina* Thomson and *Globigerinella* Cushman: Jour. Foramin. Research, v. 3, no. 4, p. 196–198.

Ms submitted August 1973

PLATE 3

Figure 1–3 *Globigerina bulloides* d'Orbigny.

1. *Station 69-050VC-50 Sfc*, South Atlantic. a, ventral view ×200; b, surface of penultimate chamber showing spines and ridges, ×1,000; c, tip of a single spine showing crystal surfaces, ×30,000.
2. *Station 70-104VC*, North Atlantic. A round spinal tip penetrating a test wall at low angle, ×10,000.
3. *Station 70-104VC*, Proximal end of spine showing circular cross-section, ×10,000.

Figure 4. *Globigerinoides conglobatus* (Brady).

Station 69-050VC-97 Sfc, Equatorial Pacific. A spine with beveled sides and a tip showing three crystal surfaces, ×10,000.

Figures 5–6 *Globigerinoides sacculifer* (Brady).

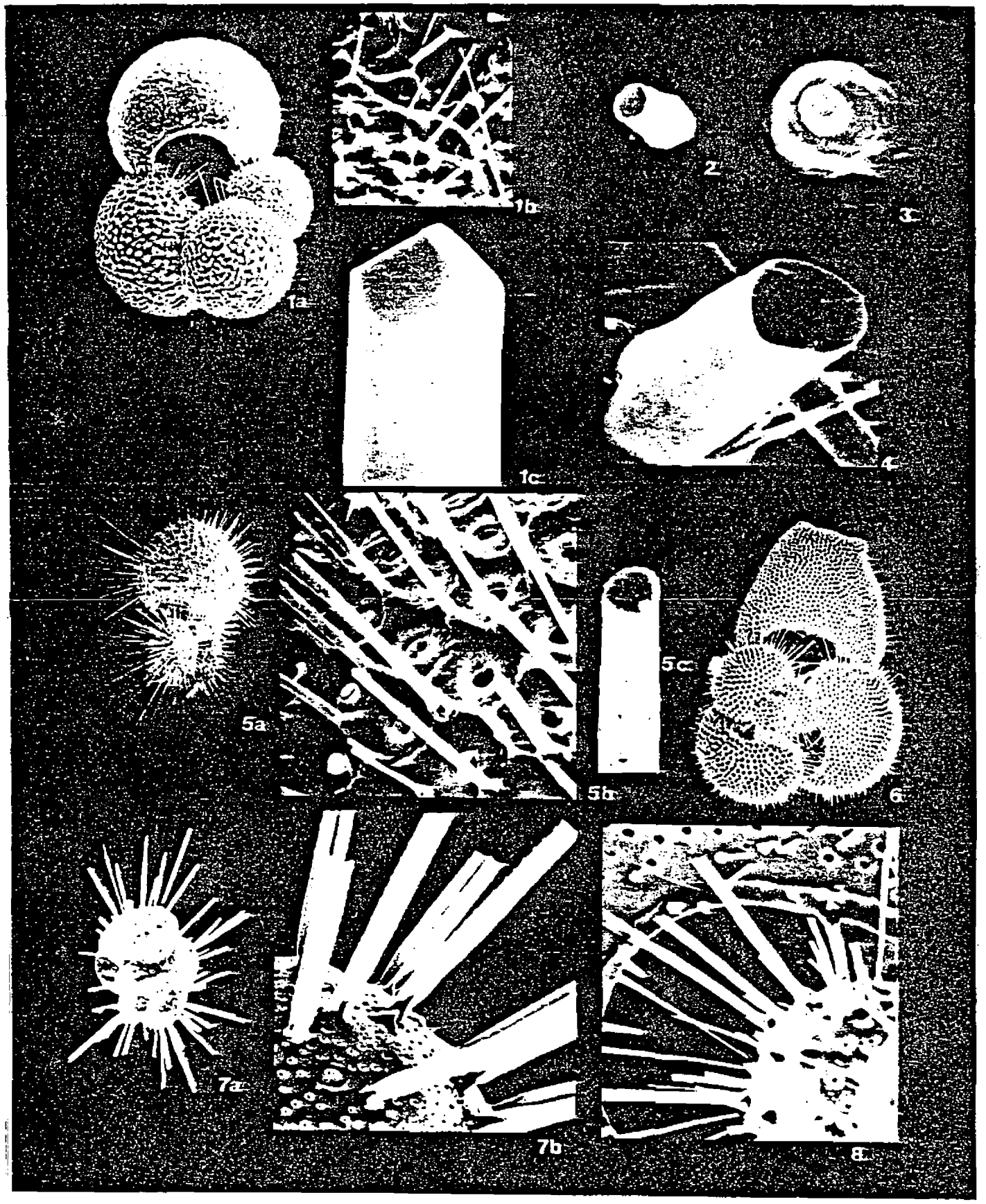
5. *Station 70-120VC*, North Atlantic. a, side view of spinose juvenile, ×180; b, surface of ultimate chamber showing spines and newly formed ridges, ×1,800; c, tip of a spine showing circular cross section, ×10,000.
6. *Station 69-050VC-99*, Equatorial Pacific. Dorsal view showing supplementary apertures, ×140.

Figure 7. *Hastigerina pelagica* (d'Orbigny).

Station 69-050VC-104 Sfc, North Pacific. a, oblique view showing distribution of spines, ×100; b, surface of ultimate chamber showing spines and spinal barbs, ×700.

Figure 8. *Globigerinella aequilateralis* (Brady).

Station 69-050VC-100, Equatorial Pacific. Surface of early chambers and part of aperture showing triradiate, round and triangular spines, ×1,000.


1a
1b
1c
2
3
4
5a
5b
5c
6
7a
7b
8

WOODS HOLE OCEANOGRAPHIC INSTITUTION
Woods Hole, Massachusetts

REFERENCE NO. 71-68

HUDSON '70
GRAVITY OBSERVATIONS
62.9°S - 57.5°N
ALONG 150°W

by

W. S. von Arx, D. C. Bowen, J. P. Dean, R. T. Haworth

November 1971

TECHNICAL REPORT

Supported by the Office of Naval Research under Contract N00014-66-C0241; NR 083-004.

Reproduction in whole or in part is permitted for any purpose of the United States Government. In citing this manuscript in a bibliography, the reference should be followed by the phrase: UNPUBLISHED MANUSCRIPT.

Approved for public release, distribution unlimited.

Approved for Distribution Ferris Webster

Ferris Webster, Chairman
Department of Physical Oceanography

ABSTRACT

To provide geoidal topography over the world oceans, a radar altimeter carried by earth satellite is planned. Ground truth calibration will be provided by a grid comprised of the equatorial belt and meridional traverses along the 30°W and 150°W meridians. Ground truth topography is derived from gravity values measured along these traverses. This report presents the free air gravity values and the computed free air anomalies obtained from 62.9°S to 57.5°N along the 150°W meridian.

INTRODUCTION

Given sufficiently widespread observations of the geopotential topography of the sea surface and knowing the internal distribution of water density, it should then be possible to compute for all depths the geopotential slopes of interior isobaric surfaces and the corresponding values of the global geostrophic transport of mass and heat by the horizontal pressure gradient fields in the ocean.

The necessary measurements of sea-surface slopes can be made with the GEON (Gyro Erected Optical Navigation) system, but it seems possible and more efficient to use an orbiting altimeter.

A satellite altimeter in near-earth polar orbit would provide a coarse-grained topographic map of the sea surface every 12 hours and examine every square degree of the ocean surface about once a week. A time series of such maps would provide evidence of change in the oceans and may reveal unexpected phenomena in the sea for intensive scientific observation.

For purposes of planning and testing, the NASA has altered the payload of the GEOS-C geodetic satellite to accommodate the first oceanographic experiment, i.e., permitting one bay of that satellite to contain a radar altimeter for operation over selected ocean areas where ground truth is available. Direct measurements of ground truth gravity and subsequent determination of geoidal topography has been the concern of a W.H.O.I./ONR project.

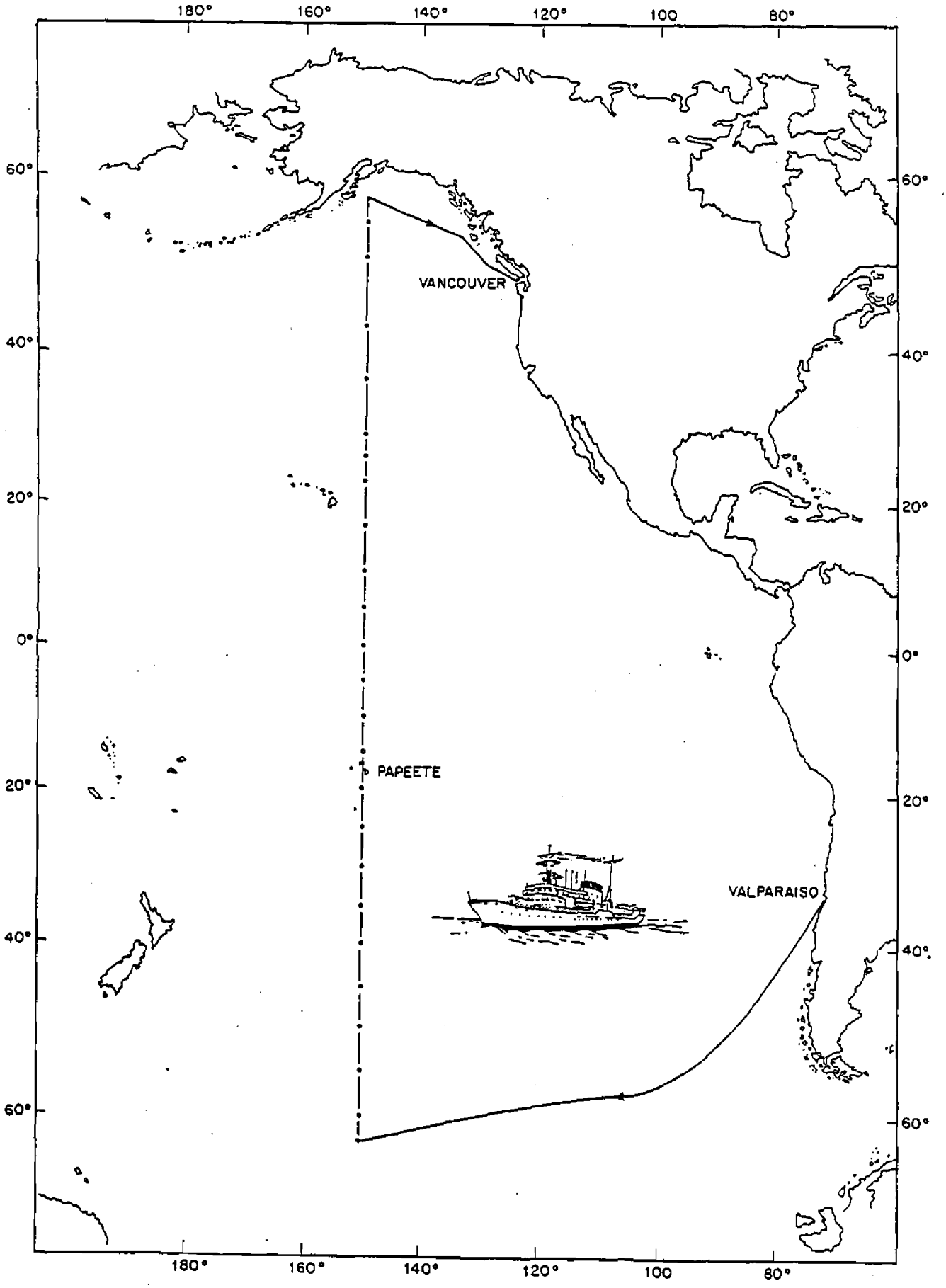


Figure 1. Hudson '70, Phase V & VI

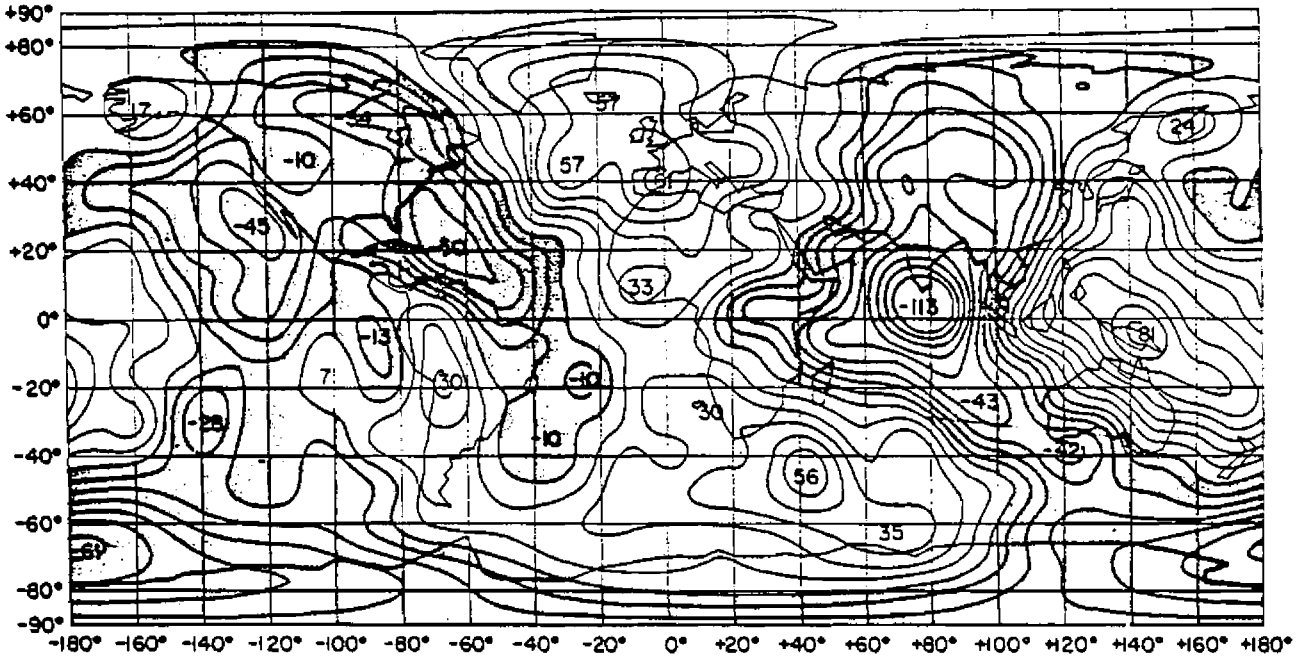


Figure 2. Geoid heights in meters of the new combination solution corresponding to a reference ellipsoid of flattening f = 1/298.255.

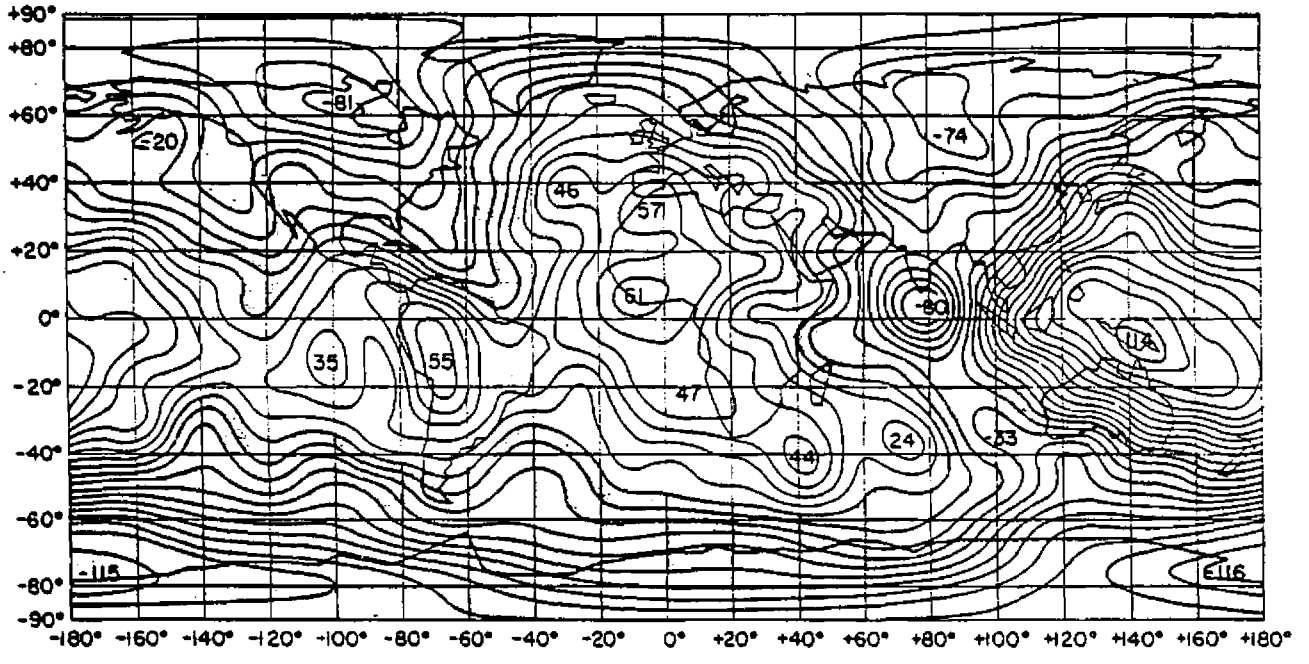


Figure 3. Geoid heights in meters of the new combination solution corresponding to a reference ellipsoid of flattening f = 1/299.67.

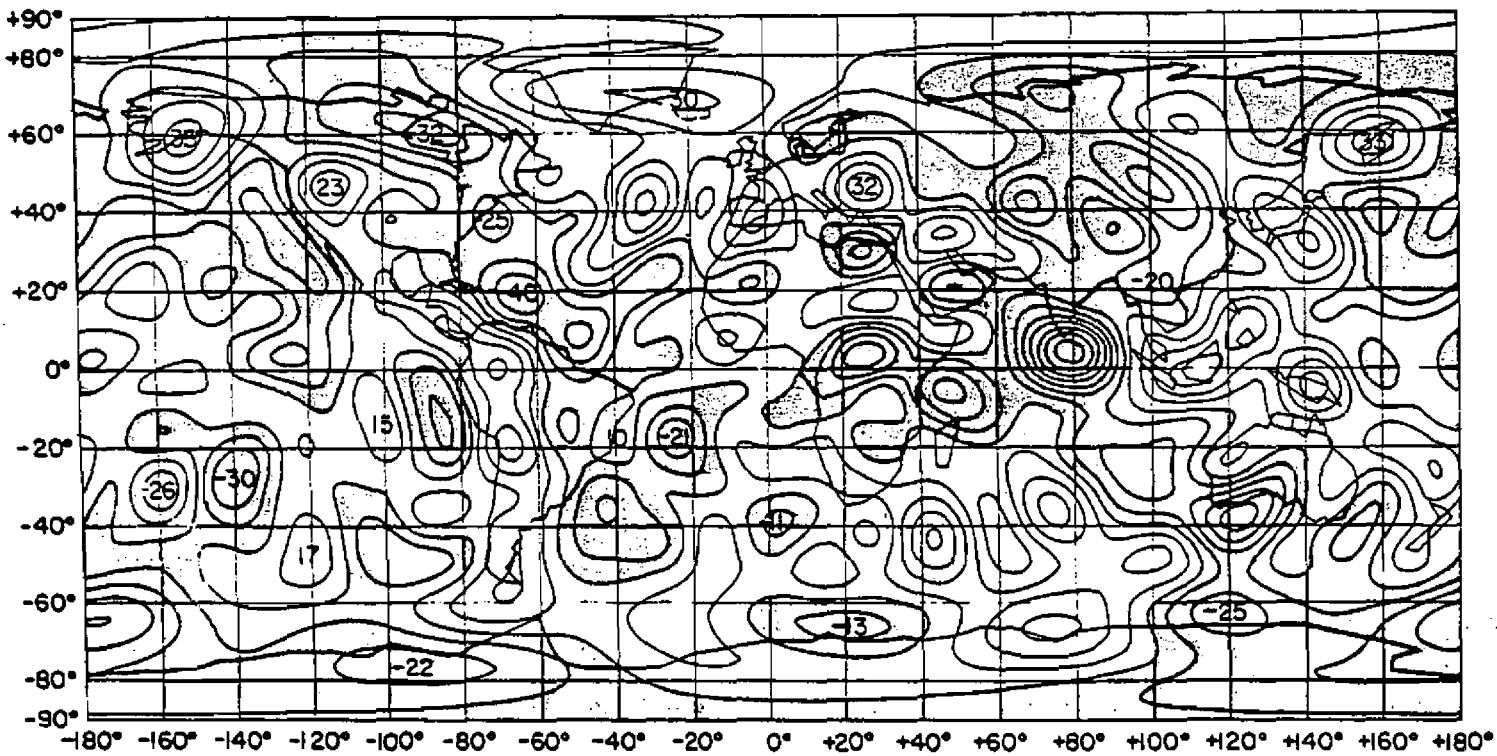


Figure 4. Gravity anomalies with respect to the best fitting ellipsoid f = 1/298.255 from the adopted solution (10-mgal contours).

Through the cooperation of the Canadian Bureau of Energy, Mines and Resources, it was possible in the spring of 1970 to run the CSS Hudson on a gravimetric arc along the 150°W meridian from 62.9°S to 57.5°N latitude. A circumnavigation of the earth on the equator is underway by RV Chain and Atlantis II, and it is planned to run a section along the 30° west meridian from the Weddell Sea to Greenland to complete the ground truth grid.

This report is to present the data obtained during the Hudson '70 cruise of the CSS Hudson, cruise #69-050, phases V and VI. See Figure 1.

These data were obtained with an Ambac Vibrating String Accelerometer (VSA) Gravimeter installed on an Anshultz stable platform.

Drift of the meter was corrected at the rate of -0.1 mgl per day as averaged linearly over the 60-day cruise and shown to be linear from base gravity values measured at three points on the cruise. The Eötvös correction was determined by satellite navigation methods.

Figures 2, 3, and 4 are charts made from satellite track observations providing the low order harmonics of the geoid. These charts are shown for reference through the courtesy of the Smithsonian Astrophysical Observatory.

Table I is the free air gravity values derived from observed values on which Eötvös and gravimeter drift corrections have been made.

Table II is the free air anomaly values with reference to the 1930 International Formula gravity values. (Negative numbers in italics.)

Table III is the free air anomaly values with reference to the 1964 formula adopted by the IAU. (Negative values in italics.)

NOTE 1: Certain values marked (†) were derived from the analog backup record or are interpolations made from the best data available other than the digital data acquisition system.

NOTE 2: One section between 22°N and 43°N has been corrected for a VSA offset. The correction was determined using data taken simultaneously with an Askania gravimeter.

Table I

TABLE I

Gravity at Sea Level along 150°W Longitude
for each Minute of Latitude

φ N	0	1	2	3	4	5	6	7	8	9
00°00'	978.051	.047	.047	.047	.049	.050	.050	.050	.050	.051
10	.051	.051	.052	.053	.053	.052	.052	.053	.053	.054
20	.055	.056	.058	.059	.061	.061	.060	.059	.058	.056
30	.057	.056	.054	.052	.052	.052	.052	.053	.053	.053
40	.052	.052	.051	.054	.055	.055	.056	.056	.057	.057
50	.057	.055	.054	.054	.053	.052	.052	.052	.053	.053
01 00	.052	.052	.051	.051	.051	.050	.051	.051	.050	.049
10	.049	.049	.053	.045	.046	.046	.047	.047	.048	.051
20	.052	.052	.053	.051	.051	.052	.052	.052	.052	.052
30	.052	.053	.053	.053	.054	.055	.057	.058	.058	.058
40	.058	.056	.055	.055	.054	.054	.054	.054	.054	.054
50	.054	.053	.055	.055	.055	.055	.056	.058	.058	.057
02 00	.058	.059	.059	.060	.060	.059	.059	.059	.059	.060
10	.061	.063	.065	.068	.069	.066	.061	.059	.056	.057
20	.056	.056	.056	.056	.056	.056	.055	.056	.056	.056
30	.055	.055	.055	.055	.055	.055	.055	.054	.055	.056
40	.056	.057	.057	.059	.061	.062	.064	.067	.069	.071
50	.074	.075	.076	.077	.078	.075	.073	.068	.061	.057
03 00	.054	.054	.049	.047	.047	.047	.046	.046	.046	.046
10	.045	.047	.048	.048	.049	.050	.051	.052	.052	.053
20	.054	.054	.054	.055	.055	.055	.056	.057	.058	.059
30	.060	.060	.062	.064	.067	.069	.072	.075	.078	.081
40	.082	.084	.085	.086	.086	.085	.085	.086	.085	.085
50	.085	.084	.083	.082	.080	.078	.077	.075	.075	.074
04 00	.074	.074	.075	.074	.074	.076	.076	.076	.076	.077
10	.079	.081	.081	.083	.085	.090	.090	.090	.091	.090
20	.088	.089	.087	.086	.078	.077	.076	.076	.075	.076
30	.075	.076	.076	.078	.078	.082	.084	.087	.088	.091
40	.091	.090	.090	.087	.086	.084	.085	.088	.090	.089
50	.090	.089	.088	.087	.087	.087	.086	.087	.087	.087

05	00	.087	.088	.088	.089	.090	.090	.090	.089	.089	.089
	10	.089	.089	.089	.088	.088	.087	.087	.086	.085	.085
	20	.085	.086	.085	.086	.086	.086	.087	.087	.087	.087
	30	.087	.087	.085	.086	.087	.087	.088	.088	.089	.090
	40	.091	.091	.092	.093	.093	.095	.096	.097	.098	.099
	50	.100	.102	.100	.100	.101	.099	.100	.100	.100	.100
06	00	.100	.100	.101	.101	.101	.101	.101	.101	.101	.101
	10	.100	.100	.100	.100	.101	.101	.101	.100	.100	.100
	20	.100	.099	.099	.100	.100	.101	.102	.103	.106	.109
	30	.111	.111	.110	.109	.109	.109	.109	.109	.110	.112
	40	.112	.113	.114	.114	.116	.116	.117	.118	.119	.119
	50	.120	.121	.122	.123	.123	.123	.123	.123	.123	.116
07	00	.117	.117	.116	.117	.117	.115	.115	.115	.114	.112
	10	.113	.111	.114	.115	.118	.120	.124	.128	.132	.136
	20	.138	.138	.137	.135	.133	.131	.129	.134	.134	.134
	30	.135	.133	.133	.135	.136	.138	.139	.140	.141	.142
	40	.142	.143	.142	.142	.144	.144	.145	.146	.145	.146
	50	.147	.146	.146	.148	.150	.152	.156	.158	.159	.158
08	00	.156	.154	.155	.154	.154	.154	.154	.155	.153	.153
	10	.152	.150	.149	.149	.149	.148	.148	.148	.149	.149
	20	.149	.149	.148	.149	.148	.148	.148	.148	.147	.148
	30	.148	.149	.149	.151	.151	.152	.154	.156	.159	.160
	40	.162	.162	.158	.157	.156	.155	.153	.151	.150	.149
	50	.148	.150	.150	.150	.150	.152	.152	.152	.154	.155
09	00	.157	.157	.159	.160	.161	.161	.162	.163	.164	.164
	10	.165	.166	.167	.169	.171	.173	.176	.179	.183	.184
	20	.186	.187	.188	.189	.188	.188	.188	.188	.188	.187
	30	.187	.188	.188	.188	.189	.189	.189	.187	.187	.187
	40	.188	.188	.188	.189	.189	.190	.190	.190	.190	.189
	50	.187	.186	.186	.186	.186	.187	.188	.189	.190	.190
10	00	.191	.192	.192	.191	.191	.190	.190	.189	.189	.191

TABLE I (Continued)

ϕ N	0	1	2	3	4	5	6	7	8	9
10°00'	978.191	.192	.192	.191	.191	.190	.190	.189	.189	.191
10	.191	.192	.192	.192	.192	.192	.192	.193	.194	.194
20	.196	.197	.198	.199	.201	.201	.202	.203	.203	.205
30	.204	.206	.206	.207	.208	.209	.209	.209	.209	.210
40	.211	.212	.213	.212	.212	.210	.209	.209	.209	.210
50	.210	.212	.213	.214	.215	.216	.215	.215	.216	.216
11 00	.217	.218	.217	.218	.219	.219	.219	.220	.220	.221
10	.222	.224	.225	.225	.226	.227	.227	.228	.229	.231
20	.231	.232	.234	.236	.236	.237	.239	.240	.242	.242
30	.241	.239	.238	.237	.237	.237	.237	.237	.238	.240
40	.241	.242	.242	.242	.242	.244	.245	.247	.248	.249
50	.253	.254	.254	.255	.257	.257	.258	.259	.259	.258
12 00	.258	.259	.260	.261	.260	.261	.262	.262	.263	.264
10	.265	.266	.266	.268	.269	.270	.270	.271	.272	.273
20	.274	.274	.275	.275	.276	.276	.277	.277	.278	.278
30	.279	.281	.283	.284	.285	.286	.287	.288	.288	.289
40	.289	.290	.290	.291	.292	.292	.293	.293	.293	.293
50	.292	.292	.292	.293	.293	.293	.294	.294	.295	.295
13 00	.296	.296	.296	.297	.297	.298	.297	.296	.296	.296
10	.296	.296	.297	.297	.297	.298	.299	.300	.301	.303
20	.303	.304	.306	.307	.308	.309	.309	.311	.312	.313
30	.314	.316	.317	.320	.322	.324	.326	.327	.328	.329
40	.332	.332	.333	.335	.336	.336	.337	.338	.338	.339
50	.340	.339	.338	.336	.334	.330	.326	.323	.322	.320
14 00	.319	.320	.322	.325	.328	.332	.335	.337	.339	.341
10	.343	.344	.346	.348	.347	.347	.348	.347	.347	.346
20	.348	.349	.353	.357	.360	.362	.362	.363	.364	.365
30	.365	.366	.367	.368	.368	.370	.371	.372	.373	.374
40	.380	.380	.380	.380	.380	.380	.379	.379	.380	.379
50	.379	.379	.380	.379	.379	.380	.380	.380	.381	.381

15	00	.382	.383	.382	.383	.384	.384	.384	.385	.386	.388
	10	.388	.389	.391	.392	.393	.395	.396	.396	.397	.397
	20	.398	.399	.399	.399	.399	.400	.401	.401	.402	.403
	30	.404	.405	.406	.406	.408	.409	.409	.411	.412	.413
	40	.414	.415	.416	.417	,419	.418	.421	.422	.424	.425
	50	.425	.428	.429	.430	.431	.432	.433	.434	.432	.432
16	00	.433	.434	.434	.435	.436	.436	.436	.437	.437	.437
	10	.436	.436	.435	.435	.435	.433	.432	.431	.432	.431
	20	.438	.439	.441	.442	.445	.448	.450	.453	.458	.462
	30	.465	.466	.466	.467	.467	.466	.466	.467	.466	.465
	40	.465	.465	.465	.465	.465	.465	.469	.469	.471	.470
	50	.471	.471	.471	.472	.473	.473	.474	.474	.476	.476
17	00	.477	.477	.478	.477	.479	.480	.481	.482	.482	.481
	10	.482	.482	.483	.485	.486	.489	.490	.491	.493	.495
	20	.496	.498	.500	.501	.502	.502	.504	.505	.505	.506
	30	.508	.510	.511	.511	.512	.515	.515	.517	.518	.518
	40	.518	.518	.517	.517	.515	.514	.515	.516	.517	.520
	50	.522	.524	.524	.525	.527	.527	.527	.530	.531	.532
18	00	.534	.534	.535	.537	.537	.538	.538	.539	.540	.540
	10	.542	.543	.544	.544	.546	.546	.547	.548	.549	.550
	20	.552	.553	.554	.556	.554	.557	.557	.558	.555	.557
	30	.556	.557	.558	.559	.561	.561	.563	.563	.564	.564
	40	.565	.567	.567	.567	.569	.569	.569	.570	.571	.572
	50	.572	.573	.568	.568	.569	.569	.570	.571	.572	.573
19	00	.573	.574	.574	.576	.577	.578	.579	.581	.582	.583
	10	.585	.586	.587	.588	.589	.592	.594	.599	.600	.602
	20	.603	.604	.605	.606	.608	.608	.609	.611	.613	.614
	30	.614	.611	.614	.614	.614	.616	.617	.617	.618	.620
	40	.620	.624	.625	.626	.628	.629	.630	.632	.633	.636
	50	.637	.638	.639	.641	.641	.643	.644	.645	.646	.647
20	00	.648	.649	.649	.650	.651	.652	.651	.651	.652	.653

TABLE I (Continued)

φ N	0	1	2	3	4	5	6	7	8	9
20°00'	978.648	.649	.649	.650	.651	.652	.651	.651	.652	.653
10	.653	.654	.655	.656	.657	.657	.659	.659	.659	.659
20	.660	.661	.661	.663	.664	.664	.665	.665	.666	.692
30	.683	.684	.685	.688	.688	.680	.679	.681	.682	.683
40	.683	.683	.685	.686	.687	.688	.689	.690	.690	.690
50	.689	.688	.681	.679	.678	.678	.679	.681	.685	.690
21 00	.694	.700	.700	.697	.696	.696	.696	.698	.700	.703
10	.706	.709	.712	.715	.717	.719	.720	.721	.722	.722
20	.723	.725	.725	.726	.726	.728	.729	.729	.729	.730
30	.731	.733	.734	.737	.739	.743	.741	.741	.742	.746
40	.744	.744	.744	.743	.744	.746	.747	.749	.749	.749
50	.751	.751	.752	.754	.753	.754	.754	.754	.754	.756
22 00	.758	.761	.765	.767	.771	.772	.771	.770	.769	.768
10	.765	.763	.762	.762	.763	.763	.765	.767	.774	.777
20	.780	.784	.785	.788	.791	.793	.793	.794	.794	.795
30	.794	.793	.792	.792	.791	.790	.790	.788	.787	.788
40	.788	.789	.790	.793	.797	.803	.807	.810	.813	.815
50	.816	.816	.817	.818	.818	.820	.820	.820	.822	.822
23 00	.824	.826	.827	.828	.830	.830	.830	.830	.832	.833
10	.833	.835	.837	.837	.837	.838	.841	.843	.844	.845
20	.846	.844	.844	.843	.845	.845	.846	.847	.849	.854
30	.856	.858	.858	.860	.857	.858	.860	.861	.862	.863
40	.865	.866	.867	.867	.867	.869	.869	.870	.871	.872
50	.874	.874	.876	.877	.869	.871	.873	.875	.876	.877
24 00	.878	.878	.882	.883	.884	.886	.888	.888	.889	.891
10	.892	.893	.895	.896	.897	.899	.902	.903	.905	.905
20	.906	.907	.910	.911	.912	.913	.914	.913	.915	.916
30	.916	.917	.918	.919	.919	.920	.920	.922	.923	.924
40	.925	.926	.927	.927	.928	.929	.937	.939	.939	.939
50	.940	.941	.944	.945	.947	.948	.949	.948	.948	.949

25	00	.949	.947	.948	.949	.952	.954	.955	.955	.957	.959
	10	.959	.960	.960	.962	.964	.968	.972	.975	.978	.980
	20	.981	.980	.979	.979	.980	.982	.926	.991	.996	.998
	30	.999	.997	.993	.990	.988	.988	.988	.987	.988	.988
	40	978.988	.989	.991	.992	.991	.992	.993	.994	.997	.***
	50	979.001	.002	.004	.007	.009	.010	.012	.012	.014	.015
26	00	.016	.017	.018	.019	.021	.022	.023	.023	.025	.026
	10	.028	.029	.030	.031	.033	.035	.037	.037	.038	.039
	20	.039	.042	.044	.045	.045	.047	.048	.050	.052	.054
	30	.055	.057	.058	.060	.061	.062	.062	.064	.065	.066
	40	.069	.069	.070	.071	.072	.073	.075	.077	.078	.081
	50	.081	.082	.085	.086	.089	.090	.090	.092	.093	.093
27	00	.096	.097	.098	.100	.101	.103	.104	.104	.104	.106
	10	.105	.106	.107	.108	.108	.110	.112	.112	.112	.112
	20	.113	.115	.116	.117	.118	.120	.121	.121	.122	.124
	30	.125	.125	.126	.128	.133	.134	.134	.135	.136	.138
	40	.139	.140	.142	.143	.144	.146	.148	.150	.151	.151
	50	.152	.154	.155	.157	.160	.161	.162	.162	.165	.166
28	00	.168	.168	.169	.169	.170	.173	.173	.174	.175	.177
	10	.177	.178	.179	.180	.181	.180	.181	.182	.183	.184
	20	.185	.187	.189	.194	.194	.194	.195	.196	.196	.198
	30	.200	.202	.204	.206	.206	.208	.209	.211	.213	.214
	40	.215	.217	.217	.219	.220	.221	.223	.224	.226	.227
	50	.230†	.233†	.236†	.238	.240	.242	.242	.243	.243	.244
29	00	.244	.245	.247	.248	.250	.251	.254	.256	.258	.260
	10	.262	.262	.266	.268	.270	.271	.271	.274	.276	.278
	20	.279	.281	.282	.283	.284	.286	.289	.292	.294	.296
	30	.298	.300	.303	.305	.309	.312	.316	.318	.321	.321
	40	.320	.319	.315	.314	.314	.312	.311	.311	.311	.312
	50	.315	.317	.318	.318	.314	.312	.307	.304	.301	.301
30	00	.299	.299	.303	.306	.314	.320	.328	.334	.342	.345

TABLE I (Continued)

φ N	0	1	2	3	4	5	6	7	8	9
30°00'	979.299	.299	.303	.306	.314	.320	.328	.334	.342	.345
10	.347	.346	.344	.344	.343	.341	.343	.347	.350	.353
20	.354	.354	.353	.353	.352	.351	.350	.350	.350	.349
30	.350	.352	.355	.358	.360	.362	.364	.369	.373	.376
40	.381	.385	.388	.391	.394	.397	.401	.404	.403	.407
50	.408	.411	.413	.413	.416	.416	.417	.418	.418	.419
31 00	.420	.421	.424	.425	.426	.426	.426	.427	.429	.429
10	.429	.430	.430	.433	.434	.433	.434	.434	.436	.436
20	.437	.439	.439	.440	.440	.440	.440	.441	.442	.444
30	.445	.446	.449	.450	.451	.453	.454	.455	.457	.459
40	.461	.462	.464	.465	.467	.468	.469	.469	.471	.471
50	.473	.474	.475	.476	.476	.478	.479	.480	.482	.484
32 00	.486	.487	.489	.490	.491	.493	.494	.495	.496	.497
10	.498	.499	.500	.500	.501	.502	.503	.503	.503	.504
20	.506	.508	.510	.512	.513	.514	.515	.514	.515	.516
30	.517	.518	.518	.519	.520	.521	.522	.524	.525	.524
40	.527	.529	.530	.533	.535	.535	.536	.545	.547	.547
50	.548	.550	.551	.549	.552	.554	.554	.557	.558	.559
33 00	.562	.563	.564	.565	.567	.568	.569	.571	.574	.576
10	.577	.577	.578	.581	.583	.585	.589	.590	.590	.592
20	.593	.593	.583	.585	.588	.588	.590	.591	.592	.594
30	.594	.596	.602	.602	.605	.606	.608	.610	.610	.612
40	.614	.614	.615	.617	.618	.620	.621	.623	.624	.625
50	.626	.627	.630	.630	.630	.632	.632	.634	.634	.632
34 00	.634	.636	.636	.637	.639	.640	.640	.640	.642	.643
10	.645	.647	.656	.658	.659	.661	.661	.659	.660	.661
20	.663	.663	.664	.665	.665	.667	.668	.670	.672	.672
30	.674	.677	.679	.681	.683	.684	.685	.686	.689	.691
40	.691	.692	.693	.694	.697	.697	.698	.701	.701	.703
50	.704	.705	.707	.708	.709	.711	.713	.715	.716	.717

35	00	.719	.719	.722	.723	.725	.726	.727	.728	.729	.732
	10	.734	.736	.738	.740	.741	.742	.742	.745	.747	.748
	20	.750	.752	.754	.755	.757	.758	.758	.760	.761	.762
	30	.762	.763	.765	.766	.768	.775	.776	.778	.780	.780
	40	.782	.784	.784	.785	.787	.788	.790	.792	.795	.797
	50	.799	.800	.802	.803	.804	.806	.808	.811	.812	.813
36	00	.813	.815	.815	.816	.817	.819	.820	.821	.823	.824
	10	.831	.832	.835	.837	.837	.839	.839	.839	.839	.839
	20	.840	.842	.843	.845	.846	.846	.846	.850	.849	.848
	30	.847	.847	.844	.848	.851	.854	.854	.854	.854	.853
	40	.854	.856	.858	.860	.862	.864	.865	.866	.868	.869
	50	.871	.872	.873	.874	.875	.877	.880	.884	.889	.893
37	00	.898	.901	.908	.911	.905	.905	.905	.907	.908	.908
	10	.910	.911	.913	.917	.918	.917	.919	.920	.920	.921
	20	.923	.923	.919	.918	.920	.920	.922	.922	.924	.926
	30	.929	.930	.932	.935	.938	.939	.940	.941	.942	.945
	40	.948	.949	.952	.954	.956	.958	.960	.960	.959	.960
	50	.961	.961	.964	.965	.965	.966	.965	.967	.966	.967
38	00	.972	.973	.973	.972	.973	.972	.970	.970	.969	.969
	10	979.971	.971	.971	.970	.974	.978	.983	.988	.992	.998
	20	980.003	.009	.014	.017	.017	.020	.023	.025	.026	.027
	30	.029	.030	.031	.033	.035	.038	.038	.039	.041	.042
	40	.041	.043	.044	.044	.041	.037	.036	.034	.034	.033
	50	.037	.040	.045	.046	.049	.053	.057	.060	.062	.066
39	00	.068	.074	.077	.079	.082	.084	.083	.083	.080	.079
	10	.077	.074	.069	.069	.070	.071	.074	.075	.077	.081
	20	.085	.088	.094	.095	.098	.099	.100	.104	.106	.108
	30	.110	.113	.116	.119	.120	.119	.118	.117	.115	.116
	40	.116	.119	.122	.124	.127	.128	.129	.130	.132	.132
	50	.132	.132	.132	.134	.134	.133	.132	.132	.132	.132
40	00	.132	.134	.136	.138	.140	.142	.144	.147	.149	.150

TABLE I (Continued)

φ N	0	1	2	3	4	5	6	7	8	9
40°00'	980.132	.134	.136	.138	.140	.142	.144	.147	.149	.150
10	.150	.155	.160	.163	.167	.173	.178	.184	.190	.196
20	.200	.204	.209	.211	.213	.214	.215	.216	.217	.217
30	.218	.220	.221	.222	.224	.225	.226	.226	.226	.227
40	.229	.229	.230	.232	.232	.234	.234	.236	.238	.241
50	.245	.247	.250	.252	.252	.251	.251	.250	.251	.250
41 00	.252	.253	.253	.255	.256	.259	.260	.262	.262	.263
10	.265	.266	.267	.270	.272	.274	.276	.279	.282	.285
20	.286	.289	.291	.292	.292	.292	.292	.294	.294	.294
30	.295	.297	.299	.301	.303	.306	.308	.311	.312	.312
40	.314	.316	.316	.318	.319	.320	.321	.323	.324	.325
50	.323	.324	.325	.326	.327	.330	.331	.333	.335	.336
42 00	.337	.339	.340	.343	.344	.346	.347	.350	.352	.353
10	.354	.356	.358	.360	.361	.360	.361	.363	.364	.365
20	.366	.366	.370	.370	.370	.372	.373	.373	.374	.377
30	.375	.377	.377	.380	.381	.381	.383	.383	.384	.386
40	.387	.388	.388	.391	.392	.395	.397	.401	.403	.403
50	.405	.407	.409	.411	.412	.415	.416	.418	.417	.418
43 00	.421	.423	.423	.426	.429	.431	.434	.435	.437	.438
10	.443	.445	.447	.449	.451	.453	.456	.457	.460	.461
20	.462	.463	.464	.465	.467	.468	.470	.474	.475	.477
30	.479	.480	.481	.482	.484	.486	.487	.487	.488	.488
40	.487	.487	.487	.487	.487	.488	.490	.491	.493	.495
50	.498	.500	.502	.506	.503	.506	.507	.510	.513	.516
44 00	.518	.520	.522	.524	.527	.528	.530	.532	.536	.538
10	.539	.540	.542	.543	.544	.544	.545	.547	.547	.548
20	.549	.551†	.552†	.553†	.554†	.556†	.557†	.558†	.559†	.561†
30	.563†	.564†	.565†	.567†	.568†	.569†	.571†	.572†	.573	.574
40	.576	.577	.579	.582	.583	.586	.588	.589	.592	.593
50	.596	.599	.600	.602	.604	.605	.606	.606	.607	.608

45	00	.610	.612	.613	.615	.616	.618	.619	.621	.622	.623
	10	.624	.626	.628	.629	.631	.633	.634	.638	.639	.640
	20	.642	.643	.644	.646	.647	.649	.650	.652	.653	.654
	30	.655	.656	.656	.658	.658	.661	.662	.663	.664	.666
	40	.667	.670	.669	.671	.673	.674	.676	.678	.679	.682
	50	.682	.685	.686	.688	.690	.691	.693	.697	.699	.701
46	00	.702	.705	.706	.709	.711	.708	.711	.713	.715	.717
	10	.718	.720	.721	.723	.724	.726	.728	.729	.731	.732
	20	.733	.734	.740	.741	.742	.743	.744	.746	.747	.749
	30	.750	.752	.753	.756	.758	.760	.762	.759	.762	.764
	40	.765	.768	.770	.773	.774	.776	.777	.778	.779	.780
	50	.782	.783	.784	.786	.786	.787	.788	.790	.791	.793
47	00	.793	.794	.798	.800	.802	.803	.805	.808	.809	.810
	10	.813	.815	.819	.822	.825	.828	.829	.827	.827	.829
	20	.826	:827	.830	.831	.837	.842	.846	.849	.850	.849
	30	.848	.847	.847	.847	.847	.848	.848	.849	.850	.852
	40	.859	.861	.862	.866	.869	.872	.875	.874	.873	.871
	50	.870	.872	.875	.879	.884	.887	.890	.895	.898	.900
48	00	.904	.906	.909	.911	.913	.912	.913	.912	.912	.911
	10	.911	.911	.910	.909	.911	.913	.916	.916	.918	.918
	20	.919	.920	.922	.923	.926	.927	.930	.931	.933	.936
	30	.939	.942	.944	.945	.947	.949	.950	.951	.952	.953
	40	.954	.956	.958	.959	.961	.963	.965	.967	.968	.969
	50	.970	.974	.975	.977	.978	.980	.982	.984	.986	.987
49	00	980.990	.993	.994	.994	.998	.999	.**1	.**3	.**4	.**6
	10	981.000	.001	.002	.004	.004	.006	.008	.011	.013	.014
	20	.017	.019	.020	.022	.024	.025	.025	.027	.032	.033
	30	.034	.037	.038	.040	.041	.043	.045	.046	.048	.049
	40	.051	.052	.053	.053	.054	.054	.055	.057	.057	.058
	50	.057	.060	.061	.063	.066	.067	.068	.069	.071	.072
50	00	.074	.077	.078	.080	.084	.087	.089	.091	.093	.096

TABLE I (Continued)

φ N	0	1	2	3	4	5	6	7	8	9
50°00'	981.074	.077	.078	.080	.084	.087	.089	.091	.093	.096
10	.098	.100	.101	.101	.103	.105	.106	.108	.111	.113
20	.114	.115	.116	.118	.119	.121	.121	.121	.122	.123
30	.124	.125	.126	.128	.130	.130	.130	.134	.136	.139
40	.139	.140	.139	.139	.140	.141	.143	.144	.145	.147
50	.149	.150	.152	.153	.154	.157	.158	.161	.163	.165
51 00	.166	.170	.173	.176	.178	.180	.183	.183	.184	.186
10	.187	.188	.191	.193	.194	.196	.199	.200	.203	.204
20	.204	.206	.207	.208	.213	.215	.217	.219	.221	.222
30	.223	.225	.227	.228	.230	.230	.232	.234	.235	.225†
40	.227†	.239	.238	.240	.240	.242	.242	.242	.242	.241
50	.240	.242	.246	.250	.256	.261	.267	.273	.281	.285
52 00	.288	.289	.290	.291	.294	.294	.295	.295	.297	.298
10	.297	.298	.296	.297	.297	.297	.300	.302	.303	.305
20	.306	.307	.305	.305	.305	.308	.313	.318	.323	.329
30	.331	.332	.327	.325	.323	.317	.318	.318	.317	.321
40	.324	.328	.331	.338	.345	.359	.374	.387	.403	.417
50	.424	.427	.424	.414	.402	.390	.376	.366	.360	.355
53 00	.350	.347	.348	.346	.347	.348	.349	.349	.351	.353
10	.355	.359	.361	.363	.365	.367	.367	.368	.368	.370
20	.373	.376	.377	.381	.382	.384	.386	.386	.389	.391
30	.393	.396	.400	.402	.404	.406	.409	.409	.412	.413
40	.415	.417	.418	.419	.423	.424	.428	.431	.434	.437
50	.440	.441	.441	.443	.444	.446	.447	.448	.450	.451
54 00	.452	.455	.456	.458	.460	.463	.468	.472	.477	.481
10	.485	.489	.492	.496	.499	.502	.505	.508	.512	.514
20	.520	.523	.526	.530	.535	.539	.547	.554	.558	.552
30	.543	.538	.535	.533	.533	.533	.533	.533	.534	.534
40	.535	.535	.535	.536	.536	.536	.538	.539	.538	.539
50	.539	.539	.537	.536	.536	.535	.535	.537	.537	.535

55	00	.540	.544	.549	.555	.565	.566	.564	.560	.556	.552
	10	.551	.551	.551	.551	.551	.553	.553	.554	.555	.557
	20	.558	.559	.560	.561	.562	.564	.564	.568	.569	.570
	30	.570	.572	.572	.573	.572	.571	.570	.568	.567	.565
	40	.563	.562	.562	.562	.562	.562	.563	.563	.563	.564
	50	.564	.565	.566	.567	.569	.570	.571	.572	.573	.573
56	00	.574	.574	.573	.572	.570	.568	.567	.566	.565	.566
	10	.568	.569	.572	.575	.577	.578	.579	.579	.576	.576
	20	.575	.574	.574	.573	.573	.573	.572	.572	.572	.573
	30	.573	.574	.575	.575	.576	.578	.580	.582	.584	.587
	40	.590	.593	.597	.603	.608	.613	.619	.624	.632	.637
	50	.645	.651	.660	.666	.675	.680	.687	.690	.695	.699
57	00	.703	.709	.715	.719	.724	.727	.736	.738	.744	.748
	10	.750	.750	.751	.752	.754	.757	.761	.765	.769	.774
	20	.780	.782	.784	.789	.794	.795	.794	.796	.798	.801
	30	.806									

TABLE I (Continued)

φ	S	0	1	2	3	4	5	6	7	8	9
00°	00'	978.051	.059	.071	.087	.101	.113	.113	.100	.086	.071
	10	.060	.053	.050	.048	.047	.049	.051	.054	.057	.058
	20	.062	.063	.062	.058	.055	.052	.051	.050	.050	.050
	30	.050	.050	.050	.051	.053	.055	.057	.056	.055	.055
	40	.053	.051	.050	.049	.047	.047	.047	.047	.050	.050
	50	.050	.049	.048	.048	.047	.048	.048	.049	.049	.051
01	00	.052	.052	.052	.051	.050	.049	.048	.048	.049	.054
	10	.052	.052	.052	.053	.052	.052	.053	.053	.053	.053
	20	.054	.054	.055	.054	.053	.053	.055	.055	.054	.054
	30	.052	.052	.052	.053	.054	.053	.054	.056	.056	.056
	40	.057	.057	.058	.059	.059	.060	.059	.060	.059	.060
	50	.059	.059	.055	.056	.056	.056	.057	.056	.055	.055
02	00	.055	.056	.057	.057	.058	.058	.058	.057	.057	.057
	10	.057	.057	.057	.057	.058	.057	.059	.059	.059	.060
	20	.060	.061	.061	.061	.062	.062	.062	.062	.061	.062
	30	.062	.062	.063	.062	.062	.063	.063	.064	.064	.064
	40	.063	.064	.063	.063	.064	.064	.064	.064	.064	.064
	50	.064	.065	.065	.066	.067	.068	.069	.069	.072	.075
03	00	.076	.077	.078	.073	.073	.074	.075	.073	.073	.072
	10	.072	.072	.072	.072	.072	.073	.073	.074	.074	.074
	20	.075	.075	.075	.075	.074	.074	.075	.075	.077	.077
	30	.077	.079	.080	.080	.079	.080	.081	.081	.083	.083
	40	.085	.085	.082	.082	.082	.082	.082	.082	.082	.082
	50	.082	.082	.082	.082	.082	.082	.082	.083	.083	.084
04	00	.084	.085	.085	.085	.086	.086	.087	.088	.088	.088
	10	.089	.088	.089	.090	.089	.089	.090	.089	.088	.087
	20	.087	.087	.086	.085	.084	.084	.084	.083	.083	.083
	30	.083	.081	.081	.080	.081	.082	.083	.084	.086	.085
	40	.083	.082	.080	.080	.080	.081	.084	.084	.084	.084
	50	.085	.086	.085	.086	.085	.085	.084	.084	.084	.084

05	00	.084	.083	.083	.082	.082	.082	.078	.078	.079	.080
	10	.081	.083	.084	.086	.088	.090	.093	.095	.097	.099
	20	.102	.103	.105	.106	.108	.111	.114	.117	.120	.123
	30	.125	.126	.123	.119	.115	.109	.103	.096	.089	.083
	40	.079	.075	.073	.072	.070	.072	.075	.080	.083	.087
	50	.092	.094	.097	.099	.101	.102	.104	.105	.107	.108
06	00	.109	.110	.111	.112	.114	.115	.116	.116	.115	.113
	10	.111	.109	.109	.110	.110	.112	.115	.118	.120	.121
	20	.122	.121	.120	.119	.117	.116	.114	.112	.111	.112
	30	.110	.110	.110	.110	.112	.114	.116	.118	.120	.122
	40	.123	.123	.124	.123	.123	.122	.121	.119	.119	.118
	50	.117	.115	.115	.116	.117	.117	.117	.117	.116	.116
07	00	.116	.116	.116	.115	.116	.115	.115	.114	.113	.113
	10	.114	.113	.113	.114	.113	.113	.114	.114	.114	.115
	20	.116	.117	.118	.121	.123	.125	.126	.127	.127	.127
	30	.126	.125	.127	.127	.127	.127	.128	.128	.129	.129
	40	.130	.130	.130	.130	.131	.131	.132	.131	.131	.131
	50	.131	.131	.131	.132	.132	.133	.133	.133	.133	.134
08	00	.134	.135	.135	.135	.134	.134	.134	.134	.139	.140
	10	.141	.142	.141	.141	.141	.141	.142	.146	.147	.147
	20	.149	.150	.151	.151	.152	.152	.153	.153	.154	.155
	30	.155	.157	.158	.158	.158	.158	.159	.160	.160	.166
	40	.167	.168	.168	.169	.169	.169	.169	.168	.168	.168
	50	.168	.168	.168	.167	.167	.167	.165	.165	.165	.165
09	00	.164	.163	.163	.163	.163	.162	.161	.161	.161	.161
	10	.161	.160	.160	.160	.160	.161	.162	.162	.163	.165
	20	.165	.164	.164	.166	.166	.169	.176	.185	.196	.210
	30	.231	.243	.255	.265	.270	.267	.258	.242	.225	.217
	40	.208	.203	.199	.199	.204	.211	.218	.215†	.212	.209
	50	.208	.207	.207	.209	.209	.208	.206	.204	.202	.201
10	00	.199	.197	.195	.194	.192	.192	.192	.191	.191	.191

TABLE I (Continued)

φ S	0	1	2	3	4	5	6	7	8	9
10°00'	978.199	.197	.195	.194	.192	.192	.192	.191	.191	.191
10	.190	.188	.186	.185	.184	.181	.180	.179	.180	.181
20	.182	.184	.187	.188	.189	.191	.193	.194	.195	.197
30	.200	.202	.204	.207	.209	.209	.211	.213	.213	.213
40	.214	.214	.214	.216	.216	.217	.221	.224	.225	.227
50	.228	.229	.230	.227	.227	.227	.226	.227	.228	.229
11 00	.231	.231	.231	.231	.231	.231	.232	.232	.231	.232
10	.232	.233	.233	.233	.233	.234	.235	.236	.236	.237
20	.238	.240	.243	.244	.246	.247	.249	.250	.251	.251
30	.252	.253	.254	.254	.255	.254	.256	.257	.257	.257
40	.258	.258	.259	.260	.261	.260	.261	.262	.262	.264
50	.264	.263	.265	.265	.266	.267	.267	.268	.268	.269
12 00	.269	.269	.269	.270	.270	.270	.270	.270	.270	.269
10	.269	.269	.269	.271	.272	.273	.274	.278	.280	.280
20	.280	.282	.284	.286	.288	.291	.293	.295	.297	.299
30	.299	.299	.297	.294	.292	.289	.287	.284	.283	.282
40	.282	.280	.280	.280	.279	.279	.278	.278	.278	.277
50	.278	.279	.280	.282	.283	.287	.292	.298	.303	.311
13 00	.314	.314	.309	.305	.299	.293	.288	.283	.279	.277
10	.276	.277	.279	.282	.285	.289	.293	.297	.302	.306
20	.308	.311	.314	.317	.319	.321	.323	.327	.330	.333
30	.339	.346	.354	.359	.364	.367	.369	.373	.378	.379
40	.384	.389	.392	.397	.403	.409	.415	.421	.425	.426
50	.425	.419	.413	.408	.398	.390	.383	.378	.375	.374
14 00	.373	.373	.377	.379	.386	.394	.404	.414	.424	.429
10	.436	.438	.437	.436	.434	.433	.432	.433	.436	.439
20	.440	.440	.440	.445	.452	.460	.462	.462	.460	.454
30	.440	.426	.408	.398	.387	.377	.371†	.365	.361	.356
40	.353	.350	.349	.348	.348	.348	.349	.351	.352	.355
50	.357	.358	.361	.362	.364	.366	.368	.369	.370	.371

15	00	.371	.372	.372	.373	.374	.375	.378	.380	.382	.383
	10	.383	.386	.388	.389	.391	.393	.395	.396	.397	.399
	20	.401	.401	.401	.401	.403	.404	.404	.404	.406	.407
	30	.409	.412	.417	.422	.429	.433	.432	.429	.425	.419
	40	.417	.415	.415	.416	.417	.420	.421	.420	.420	.420
	50	.420	.420	.420	.421	.421	.421	.421	.422	.423	.424
16	00	.425	.426	.428	.429	.429	.430	.431	.432	.433	.431
	10	.432	.433	.433	.432	.432	.433	.434	.436	.435	.436
	20	.437	.437	.436	.443	.443	.443	.443	.443	.444	.444
	30	.443	.443	.444	.444	.446	.449	.451	.452	.453	.455
	40	.458	.461	.462	.462	.464	.463	.461	.460	.460	.461
	50	.461	.462	.463	.464	.465	.466	.468	.469	.471	.471
17	00	.472	.472	.473	.472	.472	.472	.473	.476	.479	.483
	10	.494	.501	.508	.509	.506	.504	.503	.505	.507	.509
	20	.513	.516	.519	.523	.528	.533	.540	.548	.554	.558
	30	.560	.561	.561	.560	.560	.551	.550	.547	.545	.542
	40	.540	.538	.536	.533	.531	.531	.531	.532	.531	.530
	50	.530	.528	.527	.525	.523	.523	.522	.523	.523	.536
18	00	.538	.539	.542	.557	.550	.557	.562	.558	.550	.537
	10	.527	.520	.517	.516	.517	.518	.520	.521	.523	.525
	20	.527	.529	.531	.532	.533	.538	.538	.540	.542	.544
	30	.546	.549	.551	.555	.558	.560	.560	.559	.559	.559
	40	.559	.561	.566	.567	.569	.569	.570	.565	.565	.565
	50	.567	.572	.576	.577	.574	.570	.568	.568	.568	.568
19	00	.570	.573	.577	.580	.583	.590	.591	.591	.588	.587
	10	.584	.583	.583	.584	.585	.586	.588	.591	.596	.604
	20	.609	.614	.617	.618	.615	.611	.608	.605	.605	.604
	30	.605	.604	.606	.607	.607	.609	.611	.615	.618	.622
	40	.625	.626	.625	.625	.624	.622	.622	.620	.620	.620
	50	.620	.620	.620	.621	.621	.622	.623	.625	.626	.627
20	00	.628	.629	.629	.625	.625	.626	.628	.627	.627	.627

TABLE I (Continued)

φ S	0	1	2	3	4	5	6	7	8	9
20°00'	978.628	.629	.629	.625	.625	.626	.628	.627	.627	.627
10	.627	.627	.631	.632	.632	.634	.638	.644	.650	.658
20	.666	.674	.682	.686	.687	.685	.681	.676	.672	.670
30	.669	.669	.672	.675	.676	.676	.675	.675	.675	.675
40	.674	.674	.668	.668	.668	.669	.668	.670	.672	.674
50	.678	.683	.686	.688	.689	.691	.692	.693	.697	.699
21 00	.701	.701	.700	.699	.699	.700	.700	.700	.699	.699
10	.697	.697	.698	.700	.702	.703	.705	.706	.707	.708
20	.710	.713	.717	.722	.726	.728	.727	.725	.724	.722
30	.722	.723	.726	.728	.729	.729	.730	.733	.734	.736
40	.736	.737	.739	.740	.740	.742	.743	.745	.747	.747
50	.747	.750	.752	.754	.755	.755	.754	.755	.754	.753
22 00	.753	.752	.751	.753	.752	.755	.757	.761	.766	.771
10	.774	.775	.774	.769	.766	.764	.762	.762	.762	.764
20	.765	.765	.767	.769	.772	.775	.777	.783	.785	.786
30	.787	.788	.789	.789	.790	.791	.792	.794	.794	.796
40	.797	.797	.796	.796	.795	.795	.795	.793	.794	.796
50	.797	.800	.802	.801	.799	.797	.795	.794	.796	.799
23 00	.804	.807	.810	.812	.812	.812	.815	.819	.827	.834
10	.847	.859	.879	.899	.917	.930	.933	.923	.912	.895
20	.875	.866	.855	.850	.846	.845	.845	.846	.848	.850
30	.851	.852	.853	.853	.853	.853	.853	.854	.856	.856
40	.857	.858	.858	.858	.859	.860	.862	.865	.868	.870
50	.870	.871	.873	.874	.875	.875	.876	.876	.877	.877
24 00	.877	.877	.877	.876	.875	.875	.874	.874	.874	.873
10	.872	.871	.870	.875	.875	.876	.877	.878	.881	.885
20	.890	.894	.900	.907	.911	.913	.915	.916	.918	.920
30	.925	.929	.935	.940	.946	.952	.958	.963	.965	.966
40	.965	.964	.962	.960	.955	.951	.947	.947	.946	.946
50	.947	.948	.950	.950	.950	.951	.952	.953	.955	.957

25	00	.952	.953	.955	.956	.958	.960	.962	.965	.966	.969
	10	.970	.971	.971	.971	.971	.971	.971	.972	.973	.975
	20	.976	.978	.980	.982	.983	.986	.988	.989	.990	.993
	30	978.994	.996	.998	.**1	.**4	.**5	.**7	.*10	.*11	.*13
	40	979.015	.017	.019	.020	.019	.018	.016	.015	.014	.015
	50	.016	.017	.018	.019	.020	.022	.023	.025	.027	.029
26	00	.031	.033	.035	.036	.038	.041	.042	.044	.045	.047
	10	.049	.049	.050	.052	.052	.054	.055	.057	.058	.059
	20	.060	.062	.063	.064	.065	.066	.066	.067	.068	.068
	30	.070	.071	.072	.073	.074	.074	.075	.077	.077	.079
	40	.080	.080	.082	.082	.082	.084	.083	.083	.084	.084
	50	.084	.085	.086	.087	.089	.090	.091	.093	.094	.096
27	00	.098	.098	.098	.101	.102	.103	.103	.105	.110	.113
	10	.116	.118	.120	.123	.125	.127	.134	.135	.137	.137
	20	.138	.140	.140	.141	.142	.143	.145	.146	.147	.148
	30	.150	.151	.151	.151	.153	.155	.156	.158	.158	.162
	40	.164	.166	.169	.170	.172	.173	.176	.177	.177	.175
	50	.174	.172	.174	.177	.180	.184	.189	.196	.202	.208
28	00	.215	.220	.224	.226	.225	.221	.215	.209	.203	.192
	10	.188	.183	.182	.179	.178	.178	.179	.180	.181	.183
	20	.185	.188	.194	.198	.203	.207	.212	.216	.220	.225
	30	.229	.233	.239	.242	.245	.246	.248	.249	.249	.249
	40	.247	.246	.244	.243	.245	.246	.248	.248	.250	.251
	50	.253	.253	.254	.256	.258	.259	.261	.265	.267	.268
29	00	.269	.269	.270	.271	.271	.272	.274	.276	.278	.280
	10	.281	.282	.281	.279	.279	.278	.277	.276	.276	.276
	20	.277	.280	.284	.288	.294	.300	.305	.312	.316	.320
	30	.325	.327	.328	.327	.326	.325	.323	.322	.320	.318
	40	.316	.316	.316	.318	.321	.322	.323	.324	.324	.326
	50	.329	.332	.334	.338	.339	.341	.343	.344	.345	.346
30	00	.348	.348	.349	.351	.353	.356	.358	.361	.362	.364

TABLE I (Continued)

φ	S	0	1	2	3	4	5	6	7	8	9
30°	00'	979.348	.348	.349	.351	.353	.356	.358	.361	.362	.364
	10	.364	.363	.362	.361	.360	.359	.358	.357	.357	.357
	20	.358	.259	.360	.363	.365	.369	.373	.378	.385	.389
	30	.391	.391	.389	.386	.383	.380	.381	.381	.382	.381
	40	.382	.383	.385	.387	.390	.393	.395	.396	.400	.403
	50	.403	.405	.404	.404	.406	.407	.409	.410	.411	.411
31	00	.411	.410	.411	.410	.411	.411	.412	.415	.417	.419
	10	.419	.418	.418	.421	.426	.434	.441	.447	.450	.453
	20	.453	.451	.449	.449	.451	.450	.452	.453	.455	.457
	30	.461	.472	.475	.479	.481	.481	.482	.482	.481	.478
	40	.476	.474	.472	.471	.472	.474	.476	.479	.480	.483
	50	.485	.486	.488	.488	.489	.490	.487	.488	.489	.491
32	00	.494	.497	.500	.501	.502	.502	.502	.502	.502	.501
	10	.501	.499	.501	.501	.504	.506	.507	.510	.510	.512
	20	.514	.516	.518	.520	.521	.522	.524	.525	.528	.528
	30	.531	.533	.535	.536	.540	.541	.543	.545	.547	.550
	40	.552	.555	.558	.559	.561	.562	.563	.564	.565	.564
	50	.563	.561	.561	.561	.562	.563	.564	.566	.569	.573
33	00	.573	.576	.579	.580	.583	.584	.584	.584	.584	.585
	10	.587	.588	.591	.592	.596	.598	.601	.604	.607	.609
	20	.611	.613	.617	.619	.619	.620	.620	.620	.621	.621
	30	.622	.623	.624	.626	.628	.628	.629	.629	.629	.631
	40	.632	.633	.634	.637	.639	.641	.643	.644	.645	.648
	50	.649	.652	.653	.655	.656	.658	.660	.662	.664	.665
34	00	.667	.669	.670	.667	.668	.669	.670	.672	.673	.676
	10	.677	.679	.681	.684	.687	.687	.690	.691	.692	.695
	20	.696	.697	.699	.700	.700	.701	.703	.705	.705	.707
	30	.708	.709	.710	.712	.714	.715	.715	.716	.715	.716
	40	.716	.718	.718	.720	.722	.723	.725	.725	.727	.729
	50	.730	.733	.735	.737	.738	.739	.740	.741	.742	.743

35	00	.743	.745	.746	.747	.750	.752	.753	.754	.756	.761
	10	.759	.762	.763	.764	.765	.767	.767	.769	.771	.771
	20	.773	.775	.775	.777	.779	.779	.780	.782	.783	.784
	30	.786	.787	.792	.793	.795	.796	.799	.800	.805	.809
	40	.811	.813	.813	.813	.812	.811	.810	.812	.812	.813
	50	.816	.816	.818	.819	.820	.823	.825	.826	.826	.827
36	00	.830	.830	.834	.836	.837	.839	.841	.842	.843	.843
	10	.844	.846	.849	.850	.852	.853	.857	.858	.860	.860
	20	.862	.863	.865	.866	.866	.856	.862	.871	.873	.875
	30	.876	.878	.876	.877	.878	.879	.879	.881	.883	.883
	40	.885	.887	.889	.889	.890	.892	.893	.894	.894	.896
	50	.898	.898	.899	.901	.902	.902	.905	.905	.906	.907
37	00	.906	.907	.910	.911	.911	.913	.919	.919	.919	.920
	10	.922	.924	.924	.926	.929	.930	.931	.931	.934	.935
	20	.937	.938	.939	.940	.942	.942	.944	.941	.942	.943
	30	.945	.946	.946	.950	.949	.950	.952	.953	.954	.954
	40	.958	.962	.963	.966	.966	.969	.972	.975	.978	.980
	50	.982	.981	.984	.984	.986	.989	.994	.995	.997	.998
38	00	979.999	.**1	.**2	.**4	.**5	.**7	.**9	.*10	.*13	.*15
	10	980.016	.017	.018	.020	.021	.022	.023	.024	.026	.029
	20	.029	.031	.032	.034	.036	.038	.040	.042	.044	.044
	30	.046	.046	.047	.048	.050	.051	.052	.055	.057	.057
	40	.058	.060	.060	.061	.064	.067	.069	.072	.073	.075
	50	.076	.076	.078	.076	.076	.076	.077	.078	.080	.084†
39	00	.087	.087	.087	.089	.091	.091	.092	.092	.094	.095
	10	.097	.097	.098	.099	.100	.102	.104	.105	.107	.111
	20	.113	.115	.116	.117	.120	.121	.123	.125	.126	.128
	30	.130	.133	.136	.137	.138	.139	.141	.142	.143	.145
	40	.146	.148	.150	.151	.153	.155	.156	.158	.160	.162
	50	.162	.163	.165	.166	.168	.171	.172	.175	.177	.180
40	00	.181	.183	.185	.185	.187	.188	.189	.190	.191	.193

TABLE I (Continued)

φ S	0	1	2	3	4	5	6	7	8	9
40°00'	980.181	.183	.185	.185	.187	.188	.189	.190	.191	.193
10	.194	.195	.197	.196	.197	.199	.200	.202	.202	.203
20	.205	.207	.209	.209	.212	.213	.214	.215	.215	.215
30	.216	.219	.221	.223	.225	.227	.228	.229	.226	.229
40	.231	.233	.234	.235	.236	.238	.240	.242	.243	.245
50	.246	.248	.250	.249	.251	.252	.254	.256	.258	.260
41 00	.262	.264	.267	.269	.270	.270	.272	.271	.272	.272
10	.276	.278	.283	.287	.291	.294	.297	.296	.295	.294
20	.293	.293	.294	.296	.297	.299	.301	.302	.304	.305
30	.306	.309	.309	.310	.312	.313	.317	.318	.321	.323
40	.326	.329	.329	.332	.333	.335	.338	.340	.342	.346
50	.346	.348	.349	.349	.350	.351	.352	.353	.352	.353
42 00	.353	.355	.356	.358	.360	.363	.366	.367	.370	.372
10	.375	.377	.382	.384	.385	.387	.386	.387	.388	.391
20	.392	.395	.396	.400	.400	.402	.403	.404	.406	.408
30	.410	.412	.416	.419	.421	.423	.426	.428	.429	.430
40	.430	.430	.429	.431	.430	.430	.431	.432	.432	.435
50	.437	.440	.440	.441	.443	.445	.446	.447	.447	.447
43 00	.448	.448	.449	.450	.449	.449	.450	.451	.452	.455
10	.458	.459	.461	.463	.465	.469	.471	.473	.477	.478
20	.481	.481	.482	.485	.487	.489	.492	.492	.493	.492
30	.493	.493	.493	.495	.498	.499	.500	.502	.504	.505
40	.508	.508	.509	.510	.510	.512	.513	.515	.514	.516
50	.518	.519	.519	.520	.521	.524	.525	.526	.528	.528
44 00	.529	.531	.531	.533	.535	.537	.538	.540	.543	.541
10	.547	.550	.551	.553	.552	.554	.555	.557	.558	.558
20	.559	.559	.559	.559	.558	.559	.564	.564	.566	.566
30	.568	.569	.571	.574	.575	.579	.581	.582	.584	.588
40	.592	.594	.596	.598	.601	.602	.605	.608	.609	.611
50	.611	.612	.613	.613	.614	.614	.616	.616	.619	.620

45	00	.623	.626	.628	.629	.631	.632	.634	.636	.639	.641
	10	.644	.648	.646	.647	.646	.649	.650	.651	.651	.653
	20	.654	.655	.656	.659	.662	.661	.662	.663	.666	.666
	30	.668	.669	.673	.673	.673	.677	.677	.677	.679	.682
	40	.683	.684	.687	.689	.691	.694	.695	.697	.698	.696
	50	.697	.697	.698	.701	.702	.704	.703	.704	.704	.706
46	00	.711	.711	.713	.715	.716	.717	.719	.723	.725	.731
	10	.733	.735	.738	.741	.740	.740	.741	.742	.743	.746
	20	.748	.749	.753	.755	.756	.758	.759	.760	.762	.763
	30	.765	.767	.768	.770	.771	.774	.776	.778	.779	.780
	40	.781	.782	.783	.783	.783	.784	.784	.782	.780	.780
	50	.779	.779	.781	.782	.784	.785	.789	.790	.793	.794
47	00	.799	.803	.806	.810	.812	.816	.818	.821	.826	.828
	10	.831	.835	.836	.836	.837	.836	.836	.837	.837	.837
	20	.839	.841	.843	.843	.845	.846	.848	.850	.851	.853
	30	.854	.857	.860	.860	.862	.864	.864	.865	.867	.868
	40	.870	.873	.874	.875	.877	.878	.881†	.883†	.888†	.893†
	50	.899†	.903†	.906†	.906†	.905†	.903†	.901†	.900†	.900†	.899†
48	00	.900†	.900†	.900†	.902†	.903†	.903†	.904†	.904†	.904†	.905
	10	.906	.907	.908	.909	.911	.911	.913	.914	.915	.915
	20	.916	.917	.918	.919	.920	.921	.921	.923	.925	.928
	30	.929	.930	.931	.933	.934	.934	.936	.938	.939	.941
	40	.943	.944	.945	.946	.948	.950	.952	.953	.952	.957
	50	.958	.960	.962	.962	.962	.962	.962†	.963†	.963	.963
49	00	980.962	.963	.964	.965	.970	.977	.984	.992	.997	.**3
	10	981.008	.011	.015	.019	.023	.027	.029	.031	.033	.035
	20	.038	.041	.043	.046	.050	.052	.052	.052	.054	.055
	30	.055	.054	.053	.054	.053	.052	.050	.051	.053	.051
	40	.050	.049	.047	.048	.048	.049	.050	.051	.050	.050
	50	.052	.054	.056	.057	.060	.065	.070	.077	.082	.089
50	00	.093	.096	.097	.098	.099	.102	.099	.096	.094	.093

TABLE I (Continued)

φ S	0	1	2	3	4	5	6	7	8	9
50°00'	981.093	.096	.097	.098	.099	.102	.099	.096	.094	.093
10	.092	.091	.090	.086	.087	.088	.091	.095	.097	.100
20	.102	.105	.107	.110	.112	.114	.117	.119	.121	.119
30	.121	.123	.124	.126	.128	.130	.133	.135	.138	.142
40	.144	.146	.149†	.151†	.154†	.155	.157	.158	.159	.160
50	.161	.162	.162	.160	.158	.157	.156	.156	.156	.155
51 00	.156	.157	.159	.161	.163	.165	.167	.169	.172	.176
10	.181	.185	.187	.190	.193	.196	.200	.202	.203	.204
20	.206	.207	.208	.209	.210	.211	.211	.212	.211	.211
30	.211	.212	.213	.214	.215	.216	.217	.219	.221	.222
40	.224	.226	.227	.230	.232	.234	.235	.237	.238	.239
50	.241	.244	.245	.247	.249	.251	.251	.251	.252	.252
52 00	.252	.254	.254	.254	.254	.255	.255	.257	.260	.264
10	.267	.269	.272	.272	.271	.271	.272	.273	.276	.277
20	.281	.281	.282	.282	.282	.280	.280	.280	.281	.283
30	.287	.289	.293	.296	.299	.301	.303	.304	.305	.307
40	.309	.312	.314	.317	.321	.325	.332	.335	.338	.340
50	.339	.337	.336	.337	.338	.340	.341	.343	.346	.348
53 00	.350	.352	.352	.353	.354	.355	.358	.361	.364	.365
10	.366	.367	.366	.367	.367	.365	.366	.366	.366	.367
20	.366	.366	.365	.365	.365	.366	.368	.371	.374	.378
30	.381	.384	.387	.391	.394	.394	.392	.393	.392	.393
40	.394	.397	.399	.401	.403	.405	.408	.410	.413	.415
50	.417	.419	.422	.424	.431	.438	.443	.447	.448	.446
54 00	.441	.436	.433	.433	.434	.436	.437	.439	.441	.441
10	.443	.443	.443	.441	.440	.441	.434	.430	.427	.425
20	.423	.423	.423	.428	.434	.442	.447	.453	.457	.462
30	.466	.469	.468	.468	.468	.470	.471	.474	.480	.484
40	.489	.492	.495	.598	.501	.501	.503	.504	.506	.508
50	.510	.512	.513	.514	.514	.515	.517	.517	.516	.518

55	00	.519	.519	.520	.521	.523	.525	.526	.526	.528	.531
	10	.533	.536	.538	.538	.539	.540	.540	.541	.541	.542
	20	.542	.544	.547	.549	.552	.555	.555	.556	.557	.557
	30	.558	.559	.561	.562	.563	.564	.565	.567	.568	.570
	40	.571	.572	.573	.575	.577	.580	.583	.587	.590	.590
	50	.590	.591	.592	.594	.596	.598	.599	.601	.603	.604
56	00	.606	.607	.608	.610	.611	.612	.615	.616	.618	.619
	10	.624	.623	.624	.625	.627	.628	.629	.629	.630	.632
	20	.633	.634	.635	.636	.637	.639	.640	.642	.643	.647
	30	.648	.647	.647	.645	.644	.644	.645	.645	.646	.648
	40	.649	.648	.647	.647	.646	.649	.652	.656	.662	.668
	50	.672	.673	.671	.673	.673	.674	.674	.674	.676	.679
57	00	.679	.680	.682	.684	.685	.687	.689	.691	.694	.695
	10	.696	.697	.699	.698	.700	.702	.704	.706	.708	.710
	20	.712	.714	.717	.718	.720	.721	.722	.725	.726	.727
	30	.728	.729	.731	.733	.732	.733	.733	.732	.734	.734
	40	.736	.737	.739	.740	.741	.745	.746	.748	.749	.750
	50	.749	.752	.754	.756	.757	.759	.762	.762	.764	.765
58	00	.766	.767	.768	.775	.775	.776	.778	.778	.778	.779
	10	.781	.781	.783	.785	.787	.789	.790	.793	.794	.795
	20	.796	.797	.797	.799	.801	.802	.802	.803	.803	.804
	30	.805	.806	.808	.809	.811	.812	.813	.815	.816	.817
	40	.821	.823	.823	.824	.825	.825	.825	.826	.827	.829
	50	.830	.831	.833	.836	.837	.842	.847	.849	.847	.847
59	00	.847	.847	.847	.849	.850	.849	.851	.853	.857	.861
	10	.863	.866	.867	.868	.868	.870	.871	.875	.876	.873
	20	.874	.877	.879	.881	.883	.885	.889	.889	.889	.888
	30	.889	.889	.890	.896	.897	.898	.900	.902	.900	.898
	40	.897	.899	.898	.901	.900	.899	.900	.900	.904	.907
	50	.911	.915	.919	.921	.922	.921	.920	.921	.921	.924
60	00	.919	.920	.917	.920	.926	.935	.938	.940	.940	.937

TABLE I (Continued)

φ	S	0	1	2	3	4	5	6	7	8	9
60°	00'	981.919	.920	.917	.920	.926	.935	.938	.940	.940	.937
	10	.933	.933	.932	.932	.937	.939	.941	.944	.943	.948
	20	.949	.954	.955	.956	.956	.959	.957	.959	.959	.960
	30	.960	.962	.957	.964	.967	.969	.969	.972	.972	.976
	40	.978	.979	.979	.983	.983	.984	.978	.982	.984	.983
	50	.983	.986	.987	.986	.990	.990	.991	.992	.992	.993
61	00	981.996	.998	.998	.993	.***	.**2	.**3	.**4	.**6	.**5
	10	982.008	.008	.006	.012	.012	.016	.014	.019	.021	.022
	20	.024	.025	.028	.031	.036	.039	.037	.038	.037	.033†
	30	.030†	.027	.026	.023	.028	.031	.034	.037	.040	.045
	40	.048	.049	.051	.049	.056	.057	.060	.062	.064	.066
	50	.069	.069	.072	.071	.073	.073	.072	.071	.070	.069
62	00	.071	.070	.071	.073	.075	.077	.079	.081	.082	.085
	10	.085	.087	.091	.092	.092	.092	.092	.093	.094	.094
	20	.097	.098	.100	.101	.102	.103	.103	.105	.090	.091
	30	.093	.092	.092	.106	.117	.118	.124	.128	.137	.140
	40	.144	.148	.156	.160	.158	.153	.144	.136	.131	.127
	50	.126	.126	.126	.132	.131					

Table II

TABLE II

Free Air Gravity Anomaly at Sea Level along 150°W Longitude
for each Minute of Latitude with reference to
the International Formula (1930) (Negative values in italics)

φ N	0	1	2	3	4	5	6	7	8	9
00°00'	02	*02*	*02*	*02*	*00*	01	01	01	01	02
10	02	02	03	04	04	03	03	04	04	05
20	06	07	09	10	12	12	11	10	09	07
30	08	07	05	02	02	02	02	03	03	03
40	02	02	01	04	05	05	06	06	07	07
50	07	05	04	04	03	02	02	02	02	02
01 00	01	01	00	00	00	*01*	*00*	*00*	*01*	*02*
10	*02*	*02*	02	*06*	*05*	*06*	*05*	*05*	*04*	*01*
20	*00*	*00*	01	*01*	*01*	*00*	*00*	*00*	*00*	*00*
30	*01*	*00*	*00*	*00*	01	02	02	04	05	05
40	05	03	01	01	00	00	00	00	00	00
50	00	*01*	*00*	*00*	*00*	*00*	01	03	03	02
02 00	03	04	03	04	04	03	03	03	03	04
10	05	06	08	11	12	09	04	02	*01*	*00*
20	*02*	*02*	*02*	*02*	*02*	*02*	*03*	*02*	*03*	*03*
30	*04*	*04*	*04*	*04*	*04*	*05*	*05*	*06*	*05*	*04*
40	*04*	*03*	*03*	*02*	*00*	01	03	06	08	10
50	12	13	14	15	16	13	10	05	*02*	*06*
03 00	*09*	*09*	*14*	*17*	*17*	*17*	*18*	*18*	*18*	*19*
10	*20*	*18*	*17*	*17*	*16*	*16*	*15*	*14*	*14*	*13*
20	*12*	*13*	*13*	*12*	*12*	*12*	*12*	*11*	*10*	*09*
30	*08*	*08*	*07*	*05*	*02*	*00*	03	05	08	11
40	12	14	15	15	15	14	14	15	13	13
50	13	12	11	09	07	05	04	02	01	00
04 00	00	00	00	*01*	*01*	01	01	00	00	01
10	03	05	04	06	08	13	12	12	13	12
20	10	10	08	07	*01*	*03*	*04*	*04*	*05*	*05*
30	*06*	*05*	*05*	*03*	*04*	*00*	02	05	05	08
40	08	07	06	03	02	00	00	03	05	04
50	04	03	02	01	00	00	*01*	*00*	*01*	*01*

05	00	01	00	01	00	01	01	00	01	01	02
	10	02	02	02	04	04	05	05	07	08	08
	20	09	08	09	08	09	09	08	09	09	09
	30	09	10	12	11	11	11	10	10	10	09
	40	08	09	08	07	03	06	05	04	04	03
	50	02	01	03	03	02	05	04	04	05	05
06	00	05	06	05	05	06	06	06	07	07	07
	10	08	09	09	09	09	09	09	11	11	11
	20	12	13	13	13	13	12	12	11	08	06
	30	04	04	06	07	07	08	08	08	08	06
	40	06	06	05	05	04	04	04	03	02	03
	50	02	01	01	00	00	01	01	01	02	09
07	00	09	09	10	10	10	12	13	13	14	17
	10	17	19	16	15	13	11	07	04	00	03
	20	05	05	03	01	01	04	06	02	02	02
	30	02	04	05	03	02	01	00	00	01	02
	40	01	02	01	01	02	01	02	03	01	02
	50	02	01	00	02	04	05	09	10	11	10
08	00	07	05	05	04	04	03	03	03	01	00
	10	01	03	05	05	06	07	08	08	07	08
	20	08	09	10	10	11	11	12	12	14	13
	30	14	13	13	12	12	12	10	09	06	06
	40	04	04	09	10	12	13	16	18	20	21
	50	22	21	21	22	22	21	21	22	20	20
09	00	18	19	17	16	16	16	16	15	15	15
	10	15	14	14	12	11	09	07	04	01	00
	20	01	02	03	03	02	01	01	00	00	02
	30	02	02	02	03	02	03	03	06	06	07
	40	06	07	07	07	07	07	07	08	08	10
	50	12	14	14	15	15	15	14	14	13	14
10	00	13	13	13	15	15	17	17	19	19	18

TABLE II (Continued)

φ N	0	1	2	3	4	5	6	7	8	9
10°00'	13	13	13	15	15	17	17	19	19	18
10	19	18	19	19	20	20	21	20	20	20
20	19	18	18	17	16	16	16	15	16	15
30	16	15	15	15	14	14	14	15	15	15
40	14	14	14	15	16	18	20	20	21	20
50	21	20	19	19	18	18	19	20	19	20
11 00	20	19	21	20	20	20	21	21	21	21
10	20	19	18	19	18	18	19	18	18	16
20	17	17	15	14	14	14	12	12	11	11
30	13	15	17	19	19	20	20	21	20	19
40	19	18	19	19	20	19	18	17	16	16
50	13	12	13	12	11	12	11	11	11	13
12 00	14	13	13	13	14	14	13	14	14	13
10	13	12	13	12	11	11	12	11	11	10
20	10	11	10	11	11	11	11	11	11	12
30	11	10	09	08	08	08	07	07	07	07
40	08	07	08	08	07	08	08	08	09	10
50	11	12	12	12	13	13	13	14	13	14
13 00	14	14	15	15	15	15	17	18	19	20
10	20	21	21	21	22	22	21	21	21	19
20	20	20	18	18	18	17	18	17	16	16
30	16	14	14	12	10	09	08	08	07	07
40	05	05	05	04	03	04	04	03	04	04
50	04	05	07	10	12	17	22	25	27	30
14 00	31	31	30	28	25	22	20	18	17	16
10	15	14	13	12	13	14	14	16	16	18
20	17	16	13	10	08	06	07	07	07	06
30	07	07	06	06	07	06	05	05	05	05
40	01	00	01	01	02	03	05	05	05	07
50	08	08	08	10	11	10	11	12	12	12

15	00	12	12	14	13	13	14	15	14	14	13
	10	14	13	12	12	12	10	10	11	11	11
	20	11	11	12	13	13	13	13	14	13	13
	30	13	13	12	13	12	12	13	11	11	11
	40	11	10	10	10	09	11	08	08	07	07
	50	08	05	05	05	05	04	04	04	07	08
16	00	07	07	08	08	08	08	09	09	10	11
	10	12	13	15	16	17	19	21	23	23	25
	20	18	18	17	17	15	12	11	09	05	02
	30	00	01	00	00	01	03	03	03	05	07
	40	08	09	09	10	11	12	09	10	08	10
	50	10	11	12	12	11	12	12	13	12	13
17	00	12	13	13	15	14	14	13	13	14	16
	10	16	17	16	15	15	13	13	13	12	10
	20	10	09	08	08	08	09	07	07	08	08
	30	07	06	06	06	06	04	05	04	04	05
	40	05	06	08	09	12	14	14	14	13	11
	50	10	09	10	10	09	10	10	08	08	08
18	00	07	08	08	07	08	07	08	08	08	09
	10	08	08	08	08	07	08	08	08	08	08
	20	07	07	07	05	08	06	07	07	11	10
	30	12	12	12	11	10	11	10	11	11	12
	40	12	11	12	13	11	12	13	13	13	13
	50	14	14	20	21	21	22	21	21	21	21
19	00	22	22	23	22	22	22	22	21	21	20
	10	19	19	19	19	19	17	16	12	12	11
	20	11	11	11	11	09	10	10	09	08	08
	30	09	14	11	12	13	12	12	13	13	12
	40	13	10	09	09	08	08	08	07	07	05
	50	05	05	05	04	05	04	04	04	04	04
20	00	04	04	05	05	05	05	07	07	07	07

TABLE II (Continued)

φ N	0	1	2	3	4	5	6	7	8	9
20°00'	04	04	05	05	05	05	07	07	07	07
10	08	08	08	08	08	09	08	09	10	11
20	11	11	12	11	11	12	12	13	13	02
30	02	02	02	04	03	06	08	07	07	07
40	08	09	08	08	08	08	08	08	09	10
50	12	14	22	25	27	28	28	27	24	20
21 00	17	12	13	17	19	20	21	20	19	17
10	15	13	11	09	08	07	07	07	07	08
20	08	07	08	08	09	08	08	09	10	10
30	10	09	09	07	06	03	06	07	07	04
40	07	08	09	11	12	11	11	10	11	12
50	11	12	12	11	12	13	14	15	16	15
22 00	14	12	09	08	05	05	07	09	11	14
10	18	21	23	24	24	25	24	23	17	15
20	13	10	10	08	06	05	06	06	08	08
30	10	12	14	15	17	19	20	23	25	25
40	26	26	26	24	22	17	14	12	10	09
50	09	10	10	10	11	10	11	13	12	13
23 00	12	11	11	11	10	11	12	13	12	12
10	14	13	12	13	14	14	12	11	11	11
20	11	15	16	18	17	18	18	18	17	13
30	12	11	13	12	16	16	15	15	15	15
40	14	14	15	16	17	16	17	17	17	17
50	16	18	17	17	26	25	24	23	23	23
24 00	24	25	22	22	22	21	20	21	21	21
10	21	21	20	20	20	19	17	18	17	18
20	18	18	16	16	16	17	17	19	18	18
30	19	19	20	20	21	21	22	21	21	21
40	22	22	22	23	23	23	16	16	17	18
50	18	18	16	16	16	16	16	18	19	19

25	00	20	24	24	24	22	21	21	23	22	21
	10	22	22	23	22	22	19	16	14	12	11
	20	12	14	16	17	17	16	14	10	06	05
	30	05	08	14	18	21	22	23	25	26	27
	40	28	28	27	27	30	30	30	30	28	26
	50	27	27	26	24	23	24	23	24	23	23
26	00	23	24	24	24	23	23	24	25	24	24
	10	23	23	24	24	23	22	21	23	23	23
	20	24	22	22	22	23	22	22	22	21	20
	30	20	19	20	19	19	19	20	20	20	20
	40	18	19	20	20	20	20	19	19	19	17
	50	18	18	17	17	15	15	16	16	16	17
27	00	15	16	16	15	15	14	15	16	17	16
	10	18	19	19	19	20	20	19	20	21	22
	20	23	22	22	22	23	22	22	23	24	23
	30	23	24	24	24	20	20	21	22	22	21
	40	21	22	21	21	21	20	20	19	19	20
	50	21	20	20	19	18	18	18	19	18	18
28	00	17	18	19	20	20	18	20	20	20	19
	10	21	21	21	21	22	24	24	24	25	25
	20	25	24	24	20	21	22	23	23	24	23
	30	23	22	21	20	22	21	21	20	20	20
	40	20	20	21	20	20	21	20	20	19	20
	50	19†	17†	15†	14	13	12	14	14	15	15
29	00	17	17	16	16	16	16	14	14	13	12
	10	11	13	10	09	08	09	10	08	08	08
	20	07	06	07	07	07	07	05	03	02	02
	30	01	00	01	02	05	07	09	10	12	10
	40	08	06	01	02	03	06	09	10	11	12
	50	10	09	09	11	16	19	26	30	34	36
30	00	39	40	37	36	29	24	18	13	06	05

TABLE II (Continued)

φ N	0	1	2	3	4	5	6	7	8	9
30°00'	39	40	37	36	29	24	18	13	06	05
10	04	06	09	11	13	16	16	13	11	10
20	10	11	14	15	17	19	22	23	24	27
30	27	26	25	23	22	22	21	17	15	13
40	09	06	05	03	01	00	03	05	02	05
50	05	06	07	06	07	06	06	05	04	04
31 00	03	03	05	04	04	03	01	01	02	00
10	01	01	03	01	01	04	04	05	05	06
20	06	06	07	07	09	10	11	12	12	11
30	12	12	10	11	11	10	11	11	10	10
40	09	09	09	09	08	09	09	10	10	11
50	10	11	11	11	13	12	12	13	12	12
32 00	11	11	11	11	11	11	11	11	12	12
10	12	13	13	14	15	15	16	17	18	19
20	18	17	17	16	16	17	17	19	20	20
30	21	21	22	23	23	23	24	23	23	26
40	24	24	24	22	22	23	23	16	15	16
50	17	16	17	20	18	18	19	17	18	18
33 00	17	17	17	18	17	17	18	17	16	15
10	15	17	17	15	15	14	12	12	13	13
20	13	14	26	25	24	25	24	25	25	24
30	26	25	21	22	20	21	20	20	21	20
40	20	21	21	21	21	21	21	20	21	21
50	22	22	20	22	23	23	24	23	25	28
34 00	27	27	28	29	28	28	30	31	31	31
10	30	30	22	22	22	21	23	26	27	27
20	26	28	28	29	30	29	30	29	29	30
30	29	28	27	27	26	26	27	27	26	25
40	26	27	27	28	26	27	28	26	28	27
50	27	28	27	28	28	28	27	26	27	27

35	00	27	28	26	27	26	27	27	27	28	26
	10	26	25	25	24	24	25	26	25	24	24
	20	24	23	23	23	23	23	24	24	24	25
	30	26	27	26	26	26	20	21	20	19	21
	40	20	20	22	21	21	21	21	20	19	18
	50	18	18	17	18	18	18	17	17	16	16
36	00	18	17	19	19	20	19	19	20	19	20
	10	14	15	13	12	14	13	15	16	18	19
	20	19	19	19	19	19	21	22	20	22,	24
	30	27	28	33	30	29	27	28	30	31	34
	40	34	34	33	33	31	31	32	32	32	32
	50	32	32	32	33	33	33	31	29	25	23
37	00	19	17	12	10	18	19	21	20	21	22
	10	21	22	21	19	19	22	21	22	23	24
	20	23	24	30	32	32	33	33	34	34	33
	30	31	32	31	30	28	29	30	29	30	29
	40	27	27	26	25	25	24	24	25	28	28
	50	29	30	28	29	30	31	33	33	35	36
38	00	32	33	34	37	37	39	43	44	47	48
	10	48	49	51	53	51	48	44	41	38	34
	20	30	26	22	21	22	21	19	19	19	20
	30	19	19	20	19	19	17	19	19	19	19
	40	22	21	22	23	28	33	35	39	40	43
	50	40	39	35	36	34	32	29	28	27	25
39	00	24	19	18	17	16	16	18	19	24	26
	10	30	34	41	42	43	43	42	42	41	39
	20	36	35	30	31	29	30	30	28	27	27
	30	26	25	23	22	22	25	27	30	33	33
	40	35	33	32	31	30	30	31	31	31	32
	50	34	35	37	36	38	40	43	44	46	47
40	00	49	48	48	47	46	46	45	44	43	44

TABLE II (Continued)

φ N	0	1	2	3	4	5	6	7	8	9
40°00'	49	48	48	47	46	46	45	44	43	44
10	45	42	38	37	34	30	26	22	17	13
20	10	08	04	04	03	04	04	05	05	07
30	07	07	07	07	07	07	08	09	11	11
40	11	12	13	12	14	13	15	14	14	12
50	10	09	08	07	09	11	13	15	16	18
41 00	18	18	20	19	20	18	19	18	20	20
10	20	20	21	19	18	18	17	16	14	13
20	13	12	11	12	13	15	16	16	17	19
30	19	19	18	18	17	16	15	14	14	16
40	15	15	16	16	16	17	17	17	17	18
50	21	22	22	23	23	22	22	22	21	22
42 00	22	22	22	21	21	21	21	20	19	20
10	20	20	19	19	19	22	22	22	22	23
20	23	25	22	24	25	25	25	27	27	26
30	29	29	30	29	29	31	30	32	32	32
40	32	33	34	33	33	32	31	29	28	30
50	29	29	28	28	28	27	27	27	29	30
43 00	28	28	29	28	26	26	24	25	24	25
10	21	21	20	20	19	19	17	18	16	17
20	17	18	18	19	18	19	18	16	16	16
30	15	16	16	17	16	16	16	18	18	20
40	22	24	25	27	28	29	28	29	28	28
50	26	26	25	23	27	26	27	25	23	22
44 00	21	21	20	20	18	19	18	18	15	15
10	15	16	15	16	16	18	18	18	19	20
20	20	20†	20†	21†	21†	21†	21†	22†	22†	22†
30	21†	22†	22†	22†	22†	23†	22†	23†	23	24
40	23	24	23	22	22	21	20	21	19	20
50	18	17	17	17	16	17	17	19	19	20

45	00	19	19	19	19	19	19	19	19	19	20
	10	20	20	19	20	20	19	20	17	18	18
	20	18	18	19	18	19	18	19	18	19	19
	30	20	20	22	21	23	21	22	22	23	22
	40	23	21	24	23	23	23	23	22	23	21
	50	23	21	22	21	21	21	21	18	18	17
46	00	18	16	17	15	15	19	18	17	17	16
	10	17	16	17	16	17	16	16	16	16	16
	20	17	17	13	13	14	14	15	14	15	14
	30	15	14	15	13	13	12	12	16	15	14
	40	15	13	13	11	12	11	12	12	13	13
	50	13	13	14	13	15	15	16	15	16	15
47	00	17	17	15	14	14	14	14	12	13	13
	10	12	11	09	07	06	04	05	08	10	09
	20	14	14	13	13	09	05	03	01	02	04
	30	07	09	11	12	14	14	16	16	17	16
	40	11	10	11	08	07	05	04	06	09	12
	50	15	14	13	10	07	05	04	00	01	02
48	00	04	05	06	07	07	05	04	02	00	02
	10	04	05	08	10	10	09	08	09	09	10
	20	11	11	11	11	10	10	09	09	09	07
	30	06	04	04	04	04	03	04	04	05	05
	40	06	05	05	05	05	04	04	03	04	04
	50	05	02	03	02	03	02	02	01	00	01
49	00	01	02	02	00	03	02	03	04	03	03
	10	04	05	05	05	06	06	05	04	03	04
	20	02	02	02	02	01	02	03	03	01	00
	30	00	01	01	01	01	01	02	01	02	01
	40	02	02	01	00	01	02	03	02	04	04
	50	07	05	06	05	04	04	05	05	05	05
50	00	05	03	04	03	01	01	01	02	02	04

TABLE II (Continued)

φ N	0	1	2	3	4	5	6	7	8	9
50°00'	*05*	*03*	*04*	*03*	*01*	01	01	02	02	04
10	04	05	05	03	04	04	04	04	06	06
20	06	05	05	05	05	05	04	02	02	01
30	01	00	00	00	01	*01*	*02*	01	01	03
40	01	01	*02*	*03*	*04*	*04*	*04*	*04*	*05*	*04*
50	*04*	*04*	*04*	*04*	*05*	*03*	*03*	*02*	*01*	*01*
51 00	*01*	01	03	04	05	05	07	05	05	05
10	05	04	06	06	06	07	08	08	09	09
20	07	08	07	07	10	11	11	12	12	12
30	12	12	13	12	13	11	12	12	12	00†
40	01†	11	09	09	08	09	07	06	04	02
50	*01*	*00*	02	05	09	13	17	22	29	31
52 00	33	32	32	31	33	31	31	29	30	29
10	27	27	23	23	21	20	21	22	21	22
20	21	21	17	16	15	16	20	23	27	31
30	32	31	25	21	18	11	10	09	06	09
40	10	13	14	20	25	38	52	63	78	90
50	96	97	93	81	68	55	39	28	20	14
53 00	07	03	02	*01*	*02*	*02*	*02*	*04*	*03*	*03*
10	*02*	*00*	01	01	02	03	01	01	*01*	*00*
20	01	03	02	05	05	05	06	04	06	06
30	07	09	11	12	12	13	14	13	14	14
40	15	15	15	14	17	16	19	20	22	24
50	25	25	23	24	23	24	24	23	24	23
54 00	23	24	24	25	25	27	30	33	36	39
10	42	44	46	48	50	51	53	55	57	58
20	62	64	65	68	72	74	81	86	87	81
30	71	65	60	57	55	54	52	51	51	49
40	49	47	46	45	44	43	43	43	40	40
50	39	37	34	31	30	27	26	27	25	22

55	00	25	28	32	36	45	44	41	35	30	25
	10	22	21	19	18	17	17	16	15	15	16
	20	15	15	14	14	13	14	13	15	15	16
	30	13	14	12	12	09	07	05	01	*01*	*05*
	40	*08*	*10*	*12*	*13*	*15*	*16*	*16*	*18*	*19*	*20*
	50	*21*	*21*	*23*	*22*	*22*	*22*	*22*	*23*	*23*	*25*
56	00	*25*	*26*	*29*	*31*	*35*	*38*	*40*	*43*	*45*	*46*
	10	*45*	*45*	*44*	*42*	*42*	*42*	*42*	*44*	*48*	*50*
	20	*52*	*54*	*56*	*58*	*59*	*61*	*63*	*65*	*66*	*66*
	30	*68*	*68*	*69*	*70*	*70*	*70*	*69*	*69*	*68*	*66*
	40	*65*	*63*	*60*	*56*	*52*	*49*	*44*	*40*	*34*	*30*
	50	*23*	*19*	*11*	*07*	01	05	10	12	15	18
57	00	21	25	30	33	36	38	45	46	51	53
	10	54	53	52	52	52	54	57	59	62	66
	20	70	71	72	75	79	78	76	77	77	79
	30	83									

TABLE II (Continued)

φ S	0	1	2	3	4	5	6	7	8	9
00°00'	02	10	22	38	52	64	64	51	37	22
10	11	04	01	*01*	*02*	*00*	02	05	08	09
20	13	14	13	09	06	03	02	01	01	01
30	01	01	01	01	03	05	07	06	05	05
40	03	01	00	*01*	*03*	*03*	*03*	*03*	*00*	*00*
50	*00*	*01*	*02*	*02*	*03*	*02*	*02*	*01*	*02*	*00*
01 00	01	01	01	00	*01*	*02*	*03*	*03*	*02*	03
10	01	01	01	02	01	00	01	01	01	01
20	02	02	03	02	01	01	03	03	02	01
30	*01*	*01*	*01*	*00*	01	00	01	03	03	03
40	04	04	04	05	05	06	05	06	05	06
50	05	05	00	01	01	01	02	01	00	00
02 00	00	01	01	01	02	02	02	01	01	01
10	01	00	00	00	01	00	02	02	02	03
20	02	03	03	03	04	04	04	04	02	03
30	03	03	04	03	03	03	03	04	04	04
40	03	04	03	02	03	03	03	03	03	03
50	02	03	03	04	05	06	06	06	09	12
03 00	13	14	15	09	09	10	11	09	09	07
10	07	07	07	07	07	07	07	08	08	08
20	09	08	08	08	07	07	07	07	09	09
30	09	11	11	11	10	11	12	11	13	13
40	15	15	12	11	11	11	11	11	10	10
50	10	10	10	09	09	09	09	10	09	10
04 00	10	11	10	10	11	11	12	12	12	12
10	13	12	12	13	12	12	12	11	10	09
20	09	08	07	06	05	04	04	03	03	02
30	02	00	00	*01*	*01*	*00*	01	02	03	02
40	00	*01*	*04*	*04*	*04*	*03*	*01*	*01*	*01*	*01*
50	*01*	*00*	*01*	*00*	*02*	*02*	*03*	*03*	*04*	*04*

05	00	04	05	06	07	07	08	12	12	11	11
	10	10	08	07	06	04	02	01	02	04	06
	20	08	09	11	12	13	16	19	21	24	27
	30	29	29	26	22	17	11	05	02	10	16
	40	20	25	27	28	30	29	26	21	19	15
	50	10	09	06	04	03	02	00	01	02	03
06	00	04	04	05	06	07	08	09	08	07	05
	10	03	00	00	01	00	02	05	07	09	10
	20	10	09	08	06	04	03	00	02	03	03
	30	05	05	06	06	04	03	01	01	02	04
	40	05	04	05	04	03	02	00	02	02	04
	50	05	07	08	07	06	07	07	07	09	09
07	00	10	10	10	12	11	12	13	14	15	16
	10	15	17	17	16	18	18	17	18	18	18
	20	17	16	16	13	11	10	09	09	09	09
	30	11	12	11	11	11	12	11	12	11	11
	40	11	11	11	12	11	12	11	12	13	13
	50	14	14	15	14	14	14	14	15	15	14
08	00	15	14	15	15	16	17	17	18	13	13
	10	12	11	13	13	14	14	14	10	09	10
	20	08	08	07	08	07	07	07	07	07	06
	30	07	05	04	05	05	06	06	05	05	00
	40	01	02	01	02	01	01	00	01	02	02
	50	02	03	03	05	05	06	08	09	09	10
09	00	11	13	13	13	14	15	17	17	18	18
	10	19	20	21	21	22	21	21	21	21	19
	20	20	21	21	20	20	18	11	03	08	21
	30	42	53	65	74	79	75	64	49	32	23
	40	14	08	04	03	08	14	21	17	14	10
	50	09	07	07	08	08	06	04	01	01	03
10	00	05	08	10	12	14	15	15	17	17	18

TABLE II (Continued)

φ S	0	1	2	3	4	5	6	7	8	9
10°00'	05	08	10	12	14	15	15	17	17	18
10	20	22	25	26	28	31	33	34	34	33
20	33	31	29	28	28	26	25	24	24	23
30	20	19	17	15	13	14	12	11	11	12
40	11	12	13	11	12	11	08	05	05	03
50	03	03	02	06	06	07	08	08	07	07
11 00	06	06	07	07	08	08	08	09	10	10
10	10	10	10	11	11	11	11	10	11	10
20	10	09	06	06	06	04	02	02	02	02
30	02	01	01	02	02	02	01	01	01	02
40	02	02	02	01	01	03	02	02	02	01
50	02	03	02	02	02	02	02	02	02	02
12 00	03	03	04	04	04	05	05	06	07	08
10	09	09	10	09	08	08	08	04	03	03
20	04	03	01	00	01	04	05	07	08	09
30	09	08	05	02	01	05	07	11	12	14
40	15	17	18	19	20	21	23	23	24	26
50	25	25	24	23	23	19	15	10	05	02
13 00	04	04	02	07	13	20	26	31	36	39
10	40	40	39	36	34	31	27	24	20	16
20	15	13	10	08	07	05	04	01	02	04
30	09	10	23	27	32	34	35	38	43	43
40	47	52	54	58	64	69	74	80	83	83
50	81	75	68	62	52	43	35	30	26	24
14 00	23	22	25	26	33	40	49	59	68	72
10	78	80	78	76	74	72	70	70	73	75
20	75	75	74	78	84	92	93	92	89	83
30	68	53	35	24	12	01	05†	12	17	23
40	26	30	32	33	34	35	35	33	33	31
50	30	29	27	27	26	24	23	23	23	22

15	00	23	23	24	23	23	23	21	19	18	18
	10	19	16	15	15	14	12	11	11	11	09
	20	08	09	10	11	09	09	10	11	09	09
	30	08	06	01	03	09	12	10	07	02	05
	40	08	10	11	11	11	09	08	10	11	12
	50	13	13	14	14	15	15	16	16	16	16
16	00	15	15	14	14	15	14	14	14	14	17
	10	16	16	17	19	20	19	19	18	20	20
	20	19	20	22	16	17	17	18	19	19	20
	30	22	22	22	23	22	20	18	18	18	17
	40	15	13	12	13	12	14	17	19	19	19
	50	20	20	20	20	19	19	18	18	17	18
17	00	17	18	18	20	21	22	21	19	18	14
	10	04	02	09	09	05	02	00	01	02	04
	20	07	09	11	14	18	22	29	36	41	44
	30	45	45	44	43	42	32	30	26	23	19
	40	17	14	11	07	04	03	02	02	01	01
	50	02	05	07	10	13	14	15	15	16	04
18	00	03	03	01	13	05	12	16	11	02	12
	10	23	31	35	36	36	36	35	35	34	33
	20	32	31	30	29	29	25	26	25	24	23
	30	22	20	19	15	13	12	13	15	16	17
	40	18	17	13	13	11	12	12	18	19	20
	50	19	15	12	12	16	21	23	24	25	26
19	00	25	23	20	18	16	10	10	11	15	16
	10	20	22	23	23	23	23	22	20	16	09
	20	05	01	01	01	02	07	11	15	16	18
	30	18	20	19	19	20	19	18	15	13	20
	40	08	08	09	10	12	15	16	19	20	21
	50	22	23	24	24	25	25	25	24	24	24
20	00	24	24	26	30	31	31	30	31	32	33

805

TABLE II (Continued)

φ S	0	1	2	3	4	5	6	7	8	9
20°00'	24	24	25	30	31	31	30	31	32	33
10	34	35	32	32	33	32	29	24	19	12
20	04	02	09	12	12	09	04	02	07	10
30	12	13	11	09	09	10	12	13	14	15
40	17	18	25	26	27	27	29	28	27	26
50	23	19	17	16	16	15	15	15	12	11
21 00	10	11	13	15	16	16	17	18	20	21
10	24	25	25	24	23	23	22	22	22	22
20	21	19	16	12	09	08	10	13	15	18
30	19	19	17	16	16	17	17	15	15	14
40	15	15	14	14	16	15	15	14	13	14
50	15	13	12	11	11	12	14	14	16	18
22 00	19	21	23	22	24	22	21	18	14	11
10	09	09	11	17	21	24	27	28	29	28
20	28	29	28	27	25	23	22	17	17	17
30	17	17	17	18	18	18	18	17	18	17
40	17	18	20	21	24	25	26	29	29	28
50	28	26	25	27	30	33	36	39	38	36
23 00	32	30	28	27	28	29	27	24	17	11
10	00	11	30	49	66	78	80	69	57	39
20	18	07	05	11	16	18	19	19	18	17
30	17	17	18	19	20	21	22	22	21	22
40	22	22	24	25	25	25	24	22	20	19
50	20	21	20	20	20	21	21	22	22	23
24 00	25	26	27	29	31	32	34	35	36	39
10	41	43	45	41	42	42	42	43	41	38
20	34	31	26	20	17	17	16	16	15	14
30	10	07	03	01	06	11	16	20	21	21
40	18	16	13	10	04	01	06	08	10	11
50	11	11	10	11	13	13	13	13	12	11

25	00	17	18	17	17	16	15	14	13	13	11
	10	11	11	12	13	15	16	17	17	17	16
	20	17	16	15	14	14	12	12	12	12	10
	30	10	09	09	07	05	05	04	02	03	02
	40	01	00	01	01	02	04	07	09	11	11
	50	12	12	12	12	12	12	12	11	10	09
26	00	08	08	07	07	06	04	05	04	04	03
	10	02	03	04	03	04	03	03	03	03	03
	20	03	02	03	03	03	03	04	05	05	06
	30	05	05	06	06	06	07	07	07	08	07
	40	07	08	08	09	10	09	11	13	13	14
	50	15	15	16	16	15	15	15	15	15	14
27	00	13	15	16	14	14	14	16	15	11	09
	10	07	07	06	04	03	03	03	03	04	03
	20	02	03	02	02	01	01	02	02	01	01
	30	02	02	01	01	00	01	01	01	00	03
	40	04	04	06	06	07	07	08	08	07	04
	50	01	02	01	01	02	05	09	15	19	24
28	00	30	34	36	37	35	30	22	15	08	04
	10	10	16	18	22	25	26	26	26	27	26
	20	25	23	19	16	12	09	06	03	00	04
	30	06	09	14	16	17	17	18	18	16	15
	40	12	09	06	04	05	04	05	04	05	04
	50	05	04	04	04	05	05	05	08	09	09
29	00	08	07	07	07	05	05	06	06	07	08
	10	08	07	05	02	01	02	04	06	08	09
	20	09	07	05	02	03	07	11	17	20	22
	30	26	27	26	24	22	20	16	14	11	07
	40	04	03	02	02	04	04	03	03	02	02
	50	04	06	07	09	09	10	10	10	10	09
30	00	10	09	09	09	10	12	12	14	14	14

TABLE II (Continued)

φ S	0	1	2	3	4	5	6	7	8	9
30°00'	10	09	09	09	10	12	12	14	14	14
10	13	11	09	06	04	02	*01*	*03*	*04*	*06*
20	*06*	*06*	*07*	*05*	*04*	*01*	01	05	11	13
30	14	13	09	05	01	*04*	*04*	*05*	*06*	*08*
40	*08*	*08*	*08*	*07*	*05*	*04*	*03*	*03*	*01*	01
50	00	00	*02*	*03*	*03*	*03*	*02*	*03*	*03*	*04*
31 00	*06*	*08*	*08*	*11*	*11*	*12*	*13*	*11*	*10*	*10*
10	*11*	*13*	*15*	*13*	*09*	*03*	03	08	09	11
20	10	06	03	02	02	00	01	00	01	02
30	04	14	16	18	19	18	17	16	14	09
40	06	03	01	*03*	*03*	*03*	*02*	*00*	*01*	01
50	02	01	02	01	00	00	*04*	*05*	*05*	*05*
32 00	*03*	*01*	*00*	*00*	*00*	*02*	*03*	*04*	*06*	*08*
10	*09*	*13*	*12*	*13*	*12*	*11*	*12*	*10*	*11*	*11*
20	*10*	*09*	*09*	*08*	*08*	*09*	*08*	*08*	*07*	*08*
30	*07*	*06*	*05*	*06*	*03*	*03*	*03*	*02*	*01*	*00*
40	01	02	04	04	04	04	04	03	03	01
50	*02*	*05*	*07*	*08*	*08*	*09*	*09*	*08*	*07*	*04*
33 00	*06*	*04*	*02*	*03*	*01*	*01*	*03*	*04*	*06*	*06*
10	*05*	*06*	*04*	*04*	*02*	*01*	*00*	02	04	04
20	05	06	08	09	07	07	06	04	04	03
30	02	02	01	02	03	01	01	*01*	*02*	*01*
40	*02*	*02*	*02*	*01*	*00*	*00*	01	01	00	02
50	01	03	03	03	03	03	04	05	05	05
34 00	06	06	06	01	01	01	00	01	00	02
10	02	02	03	04	06	05	06	06	05	07
20	07	06	07	06	05	05	05	06	04	05
30	05	04	04	04	05	05	03	03	00	00
40	*01*	*01*	*02*	*02*	*01*	*01*	*01*	*02*	*02*	*01*
50	*01*	*00*	01	01	01	00	00	00	*01*	*01*

35	00	03	02	02	03	01	01	01	01	01	03
	10	01	01	00	00	00	00	01	01	00	01
	20	01	00	02	01	01	02	02	02	02	03
	30	02	03	01	01	01	01	02	02	06	08
	40	09	09	08	06	04	02	01	00	02	02
	50	01	02	01	02	02	01	00	01	02	02
36	00	01	02	00	01	00	01	02	01	01	01
	10	01	01	01	01	01	01	03	03	03	02
	20	03	02	03	02	01	11	06	01	02	03
	30	02	03	01	01	02	02	03	03	02	04
	40	03	03	02	04	04	03	04	04	06	05
	50	05	06	06	06	06	08	06	08	08	09
37	00	11	11	10	10	12	11	07	08	10	10
	10	09	09	10	10	08	09	09	11	09	10
	20	09	09	10	10	10	11	11	15	16	16
	30	15	16	17	15	17	18	17	18	18	20
	40	17	14	15	13	15	13	12	10	09	08
	50	08	10	08	10	09	08	04	05	04	05
38	00	05	05	05	05	05	04	04	04	03	02
	10	03	03	04	03	04	04	04	05	04	03
	20	04	04	04	04	03	03	02	02	01	03
	30	02	03	04	04	04	04	05	03	03	04
	40	05	04	06	06	05	03	02	01	01	01
	50	01	03	02	06	07	09	09	10	09	07
39	00	05	06	08	07	07	08	09	10	10	10
	10	10	11	12	12	13	12	12	12	11	09
	20	08	08	08	09	07	08	07	07	07	07
	30	06	05	03	04	04	05	04	05	05	04
	40	05	04	04	04	04	03	04	03	03	02
	50	04	04	04	04	04	02	03	01	01	01
40	00	00	01	01	00	01	00	00	01	01	01

TABLE II (Continued)

φ S	0	1	2	3	4	5	6	7	8	9
40°00'	00	01	01	00	01	00	00	01	01	01
10	01	02	01	04	04	04	04	04	05	06
20	05	05	04	06	04	05	05	06	07	09
30	09	08	07	06	06	05	06	06	11	09
40	09	08	09	09	10	09	09	08	09	08
50	09	08	08	10	10	10	10	09	09	08
41 00	08	07	06	05	06	07	07	09	10	11
10	09	08	05	02	01	02	04	01	01	04
20	06	08	08	08	08	08	07	08	07	08
30	08	07	08	09	08	09	06	07	05	05
40	03	02	03	02	02	02	00	00	01	03
50	02	02	02	00	00	01	01	02	04	05
42 00	06	06	06	06	05	04	02	03	01	01
10	01	01	05	05	05	05	03	02	02	03
20	03	04	04	06	05	05	05	04	05	05
30	06	06	09	10	11	11	13	13	13	12
40	11	09	07	07	05	03	03	02	01	02
50	03	04	03	02	03	03	03	02	01	01
43 00	01	03	03	04	06	08	08	09	09	08
10	06	07	06	06	05	03	02	02	01	00
20	02	00	00	01	02	02	04	02	02	01
30	01	03	04	04	02	03	03	03	02	03
40	01	03	03	04	05	05	05	05	07	07
50	06	07	08	09	09	08	08	09	08	10
44 00	10	10	11	11	10	10	10	10	08	12
10	07	06	06	06	08	08	08	08	08	10
20	10	12	13	15	17	18	14	16	15	17
30	16	17	16	15	15	13	12	13	12	10
40	07	07	06	06	04	05	03	02	02	02
50	03	04	04	06	06	08	07	09	07	08

45	00	06	05	04	05	04	05	04	04	02	02
	10	00	02	01	02	05	03	04	04	06	05
	20	06	06	07	05	04	06	07	07	06	07
	30	07	07	05	06	08	05	07	08	08	06
	40	07	07	06	05	05	03	04	03	04	07
	50	08	09	10	08	09	08	11	11	13	12
46	00	09	10	10	09	10	10	10	07	07	02
	10	02	01	00	02	01	02	03	03	04	02
	20	02	02	00	01	00	01	00	00	00	00
	30	00	01	00	01	00	02	02	03	02	02
	40	01	01	00	01	03	03	05	08	12	13
	50	16	17	17	17	17	17	15	15	14	14
47	00	11	08	07	04	04	01	01	01	04	05
	10	06	09	08	07	06	04	02	02	00	01
	20	01	00	00	01	01	01	01	00	01	00
	30	01	01	02	01	01	02	00	00	00	00
	40	00	02	01	01	01	01	02†	03†	06†	10†
	50	14†	17†	18†	17†	14†	11†	07†	05†	03†	01†
48	00	00†	01†	03†	02†	03†	04†	05†	06†	08†	08
	10	09	09	10	10	10	11	11	11	12	13
	20	14	14	15	15	16	16	18	17	17	15
	30	16	16	17	16	17	18	18	17	18	17
	40	17	17	18	18	18	17	17	17	20	16
	50	17	16	16	17	19	20	22†	22†	23	25
49	00	27	28	28	29	25	20	14	08	04	00
	10	04	05	08	10	13	15	16	16	17	17
	20	19	20	21	22	25	25	24	22	23	22
	30	21	18	16	15	13	10	07	06	07	03
	40	01	01	05	05	07	07	08	08	11	12
	50	12	11	11	11	10	06	03	03	06	12
50	00	14	16	15	15	14	16	11	07	03	01

TABLE II (Continued)

φ S	0	1	2	3	4	5	6	7	8	9
50°00'	14	16	15	15	14	16	11	07	03	01
10	*02*	*04*	*06*	*12*	*12*	*13*	*11*	*09*	*08*	*07*
20	*06*	*05*	*04*	*03*	*02*	*02*	*00*	*00*	01	*03*
30	*02*	*02*	*02*	*02*	*01*	*01*	01	02	03	06
40	06	07	08†	09†	10†	10	10	10	09	09
50	08	08	06	03	*01*	*03*	*05*	*07*	*08*	*11*
51 00	*11*	*12*	*11*	*11*	*10*	*10*	*09*	*09*	*07*	*05*
10	*01*	01	02	03	05	07	09	10	09	09
20	09	09	08	08	07	07	05	05	02	01
30	00	*01*	*01*	*02*	*02*	*03*	*03*	*03*	*02*	*03*
40	*02*	*02*	*02*	*01*	*00*	01	00	01	00	00
50	00	02	01	02	02	03	01	00	00	*02*
52 00	*03*	*03*	*04*	*06*	*07*	*08*	*09*	*09*	*07*	*05*
10	*03*	*02*	*01*	*02*	*05*	*06*	*07*	*07*	*06*	*06*
20	*04*	*05*	*06*	*07*	*08*	*12*	*13*	*15*	*15*	*15*
30	*12*	*12*	*09*	*08*	*06*	*05*	*05*	*05*	*06*	*05*
40	*05*	*03*	*03*	*01*	01	04	10	11	13	13
50	11	07	05	04	04	05	04	05	06	07
53 00	07	08	06	06	05	05	07	08	10	09
10	09	08	06	05	04	01	00	*01*	*03*	*03*
20	*06*	*07*	*10*	*11*	*12*	*13*	*12*	*11*	*09*	*07*
30	*05*	*03*	*02*	01	02	01	*03*	*03*	*06*	*06*
40	*06*	*05*	*04*	*04*	*03*	*03*	*01*	*01*	01	02
50	02	03	04	05	10	16	20	22	22	18
54 00	12	05	01	00	*01*	*00*	*01*	*00*	*00*	*01*
10	*00*	*02*	*03*	*07*	*09*	*10*	*18*	*23*	*28*	*31*
20	*35*	*36*	*38*	*34*	*29*	*23*	*19*	*15*	*12*	*09*
30	*06*	*04*	*07*	*06*	*10*	*09*	*10*	*08*	*03*	*01*
40	03	04	06	07	09	08	08	08	08	09
50	10	10	10	09	08	07	08	07	04	05

55	00	04	03	03	02	03	03	03	01	02	04
	10	04	06	06	05	05	04	03	02	01	01
	20	*01*	*00*	01	02	03	05	04	03	03	01
	30	01	01	01	01	00	00	00	00	00	00
	40	00	00	*01*	*00*	*00*	02	04	06	08	06
	50	05	05	04	05	05	06	06	06	07	06
56	00	07	07	06	07	06	06	08	07	08	07
	10	11	09	08	08	08	08	08	06	06	06
	20	06	06	05	05	05	05	05	05	05	08
	30	07	05	03	00	*02*	*04*	*04*	*06*	*06*	*05*
	40	*06*	*08*	*10*	*12*	*14*	*13*	*11*	*08*	*04*	01
	50	04	03	*00*	*00*	*01*	*01*	*03*	*04*	*04*	*02*
57	00	*03*	*04*	*03*	*02*	*03*	*02*	*02*	*01*	01	00
	10	00	00	00	*02*	*02*	*01*	*00*	*00*	01	02
	20	02	03	05	04	05	04	04	06	05	05
	30	05	04	05	05	03	03	01	*01*	*00*	*02*
	40	*01*	*01*	*01*	*01*	*02*	01	01	01	01	01
	50	*02*	*00*	01	01	01	02	03	02	02	02
58	00	02	01	01	07	05	05	06	04	03	03
	10	03	02	03	03	04	04	04	06	05	05
	20	05	04	03	04	04	04	03	02	01	01
	30	00	00	01	00	01	01	00	01	01	00
	40	03	04	02	02	02	00	*01*	*01*	*02*	*01*
	50	*01*	*02*	*01*	*00*	*00*	04	07	08	05	04
59	00	02	01	00	00	00	*02*	*02*	*01*	02	04
	10	05	07	06	06	05	05	05	08	07	03
	20	03	04	05	06	06	07	10	08	07	05
	30	04	03	03	07	07	07	08	08	05	02
	40	*01*	*00*	*02*	*01*	*03*	*05*	*06*	*07*	*04*	*03*
	50	*00*	03	06	06	06	04	01	01	00	01
60	00	*05*	*05*	*09*	*08*	*03*	05	06	07	06	01

TABLE II (Continued)

φ S	0	1	2	3	4	5	6	7	8	9
60°00'	05	05	10	08	03	05	06	07	06	01
10	04	05	08	09	05	04	04	02	04	01
20	01	03	02	02	01	03	01	00	01	02
30	03	02	09	03	01	00	02	00	01	01
40	02	02	01	03	02	02	06	03	02	04
50	04	04	04	07	04	05	05	06	07	07
61 00	06	05	06	12	07	06	06	06	06	08
10	06	08	11	06	07	05	08	04	03	04
20	03	03	02	00	04	06	02	02	00	05†
30	10†	14	16	20	17	15	13	12	10	06
40	04	05	04	07	01	02	00	01	02	02
50	04	03	05	02	03	02	00	03	05	07
62 00	06	09	09	08	07	07	06	05	05	04
10	05	04	01	02	03	04	05	06	06	07
20	05	06	05	05	05	06	07	06	22	22
30	22	24	25	12	03	03	02	05	12	14
40	17	20	27	29	26	20	10	00	06	11
50	13	15	16	11	13					

TABLE III

Free Air Gravity Anomaly at Sea Level along 150°W Longitude
for each Minute of Latitude with reference to
the IAU Formula (1964) (Negative values in italics)

φ N									
0°	19	6°	12	12°	03	18°	09	24°	*09*
	18		11		03		08		*05*
	20		08		03		08		*05*
	21		06		06		08		*03*
	29		04		06		07		*02*
	25		13		05		04		*04*
	20		09		09		06		*07*
	18		12		09		04		*07*
	24		15		08		03		*02*
	20		17		04		*05*		*01*
1°	19	7°	08	13°	03	19°	*06*	25°	*06*
	17		04		00		*06*		*07*
	19		01		*04*		*04*		*09*
	13		17		*04*		04		02
	16		15		*01*		06		*03*
	17		15		01		07		09
	21		17		09		04		*09*
	19		17		11		06		*13*
	17		18		12		08		*14*
	17		21		04		11		*09*
2°	20	8°	24	14°	*15*	20°	12	26°	*09*
	20		20		*03*		09		*09*
	26		12		03		07		*09*
	16		10		00		05		*08*
	15		06		09		04		*09*
	13		03		09		18		*06*
	12		07		11		08		*06*
	14		08		16		08		*05*
	25		*03*		11		07		*04*
	33		*05*		06		*11*		*01*
3°	08	9°	*01*	15°	04	21°	*01*	27°	*01*
	01		01		02		*05*		*00*
	00		03		04		05		*05*
	03		16		06		08		*07*
	05		18		03		06		*08*
	09		14		03		05		*09*
	20		14		04		09		*07*
	32		10		06		06		*07*
	30		09		09		05		*05*
	24		01		11		02		*03*
4°	17	10°	03	16°	09	22°	01	28°	*03*
	18		*01*		07		08		*05*
	21		*02*		01		*07*		*07*
	30		*03*		*07*		*02*		*10*
	16		01		01		09		*07*
	11		01		16		06		*09*
	19		02		13		*05*		*07*
	23		03		07		*11*		*07*
	22		*04*		08		05		*05*
	17		*02*		05		04		01
5°	16	11°	*03*	17°	04	23°	03	29°	*03*
	17		*04*		03		03		*00*
	15		*02*		*01*		03		04
	09		*01*		04		04		06
	08		02		08		*02*		07
	08		04		09		03		13
	07		*04*		11		00		23
	09		*02*		08		00		14
	13		*00*		02		*02*		03
	15		06		07		*11*		*02*

TABLE III (Continued)

	φ N								
30°	25	36°	05	42°	11	48°	14	54°	31
	04		07		10		14		38
	04		01		08		02		54
	02		05		11		01		65
	03		07		14		00		80
	13		14		18		04		79
	07		16		19		06		61
	09		21		23		05		54
	16		19		17		06		48
	21		21		17		07		38
31°	17	37°	07	43°	17	49°	10	55°	33
	15		09		13		12		49
	11		09		09		04		27
	09		09		05		06		23
	05		20		07		08		21
	02		19		04		09		21
	03		17		05		11		12
	05		14		14		10		04
	04		16		18		05		11
	01		18		17		05		14
32°	02	38°	20	44°	11	50°	04	56°	17
	02		31		08		11		33
	00		39		05		14		36
	05		26		09		15		40
	03		10		11†		14		52
	07		07		11†		10		60
	10		07		12†		07		61
	11		10		13		07		53
	02		29		09		04		26
	05		32		06		04		09
33°	03	39°	12	45°	09	51°	08	57°	28
	05		06		09		16		53
	04		29		09		15		60
	00		30		07		18		70
	11		18		08		19		86
	13		15		09		20		90
	07		15		11		21		
	08		20		13		18		
	08		19		12		13		
	10		26		11		18		
34°	15	40°	37	46°	08	52°	41		
	17		34		08		39		
	09		27		07		32		
	14		06		06		30		
	17		08		04		23		
	17		04		05		40		
	14		03		02		19		
	15		01		03		23		
	15		02		03		86		
	15		03		05		76		
35°	14	41°	06	47°	07	53°	16		
	14		07		04		06		
	12		09		01		09		
	11		03		00		08		
	10		02		01		13		
	14		08		03		15		
	08		04		06		23		
	09		05		01		23		
	06		06		01		30		
	06		08		03		32		

TABLE III (Continued)

φ	S								
0°	19	6°	21	12°	14	18°	13	24°	*10*
	81		26		11		32		*19*
	18		17		06		*19*		*30*
	25		26		14		*18*		*26*
	23		21		18		*14*		*03*
	18		12		25		*06*		05
	25		16		09		03		31
	17		22		01		03		28
	17		15		*07*		03		05
	14		11		*06*		00		02
1°	19	7°	07	13°	21	19°	*09*	25°	*03*
	14		04		*09*		06		*00*
	18		00		*22*		*08*		02
	18		*01*		*03*		*00*		*03*
	18		05		10		13		*00*
	17		06		26		*02*		04
	18		06		52		*02*		10
	22		05		70		06		15
	22		04		99		*05*		03
	18		03		68		*09*		02
2°	17	8°	02	14°	39	20°	*08*	26°	06
	19		00		66		*14*		10
	18		04		94		*17*		11
	19		08		99		*04*		12
	21		10		101		27		11
	20		10		84		04		09
	20		12		11†		04		07
	20		18		*15*		*09*		07
	20		15		*17*		*11*		02
	22		12		*09*		*00*		*01*
3°	30	9°	06	15°	*07*	21°	*06*	27°	01
	28		00		*04*		01		*01*
	24		*04*		01		*09*		08
	25		*04*		06		*07*		18
	24		*04*		07		06		16
	26		58		08		*04*		16
	29		83		27		*02*		15
	29		21		05		01		20
	27		31		05		03		21
	26		24		01		04		17
4°	27	10°	11	16°	01	22°	*04*	28°	44
	29		01		02		*06*		37
	29		*08*		*01*		05		*04*
	27		*17*		*04*		*14*		*12*
	22		*11*		*01*		*10*		02
	19		*03*		*06*		*01*		20
	18		04		*02*		*03*		32
	13		04		04		*05*		20
	16		12		*03*		*14*		19
	15		10		*03*		*15*		19
5°	13	11°	11	17°	*01*	23°	*17*	29°	22
	05		09		*05*		*12*		20
	10		06		24		45		19
	21		06		18		72		06
	30		12		34		*01*		17
	46		15		61		*02*		40
	22		15		46		*07*		30
	10		15		27		*09*		15
	02		14		16		*06*		16
	15		15		03		*05*		23

TABLE III (Continued)

φ	S	φ	S	φ	S	φ	S	φ	S	φ	S
30°	24	36°	12	42°	05	48°	10†	54°	20	60°	02
	26		14		09		05†		07		13
	22		13		16		00		05		03
	09		16		13		*02*		*20*		03
	10		13		16		*06*		*21*		08
	28		15		17		*06*		02		04
	10		09		24		*08*		*01*		05
	06		10		18		*08*		14		07
	13		07		12		*10*		16		05
	11		06		14		*09*		16		03
31°	08	37°	01	43°	10	49°	*18*	55°	12	61°	01
	01		05		03		*05*		11		01
	01		02		05		17		14		*04*
	23		03		12		26		19		03
	16		02		13		34		11		11
	18		*03*		10		30		09		*03*†
	31		*05*		08		16		07		*07*
	13		*03*		08		04		07		03
	13		03		03		*02*		16		08
	14		03		01		*01*		13		10
32°	10	38°	07	44°	00	50°	23	56°	15	62°	00
	10		08		00		21		15		01
	01		08		04		03†		16		05
	02		08		02		01		14		01
	05		09		07		07		12		01
	07		10		06		07		15		*15*
	11		07		*02*		10		04		08
	17		06		04		17		*03*		33
	16		10		08		18		04		01
	05		05		04		08		07		*07*
33°	08	39°	07	45°	04	51°	*02*	57°	04		
	10		03		06		*00*		06		
	09		00		09		11		08		
	17		00		05		18		09		
	20		04		07		16		12		
	15		05		04		08		12		
	14		08		04		06		09		
	11		08		05		07		07		
	13		09		07		09		08		
	16		08		01		11		08		
34°	18	40°	12	46°	01	52°	05	58°	09		
	13		11		00		*01*		13		
	16		10		10		08		10		
	18		06		06		03		13		
	18		07		10		00		12		
	17		02		10		*04*		08		
	16		05		12		04		07		
	10		03		10		06		09		
	11		03		*02*		21		05		
	14		02		*07*		12		07		
35°	10	41°	04	47°	*01*	53°	16	59°	09		
	12		05		09		15		05		
	13		07		18		14		13		
	13		10		10		06		14		
	12		03		09		*04*		13		
	10		03		09		03		11		
	15		05		10		06		15		
	20		08		11		04		05		
	11		12		16†		09		03		
	10		11		24†		19		13		

MANDATORY DISTRIBUTION LIST
FOR UNCLASSIFIED TECHNICAL REPORTS, REPRINTS, & FINAL REPORTS
PUBLISHED BY OCEANOGRAPHIC CONTRACTORS
OF THE OCEAN SCIENCE AND TECHNOLOGY DIVISION
OF THE OFFICE OF NAVAL RESEARCH
(REVISED OCTOBER 1971)

DEPARTMENT OF DEFENSE

1 Office of the Secretary of Defense
Washington, D. C. 20301
ATTN: Office, Assistant Director
(E & LS)

NAVY

Office of Naval Research
Department of the Navy
Washington, D. C. 20360
2 Attn: Ocean Science & Technology
Div (Code 480)
1 Attn: Naval Applications & Analysis
Div (Code 460)
1 Attn: Earth Sciences Div (Code 410)

1 Office of Naval Research
Branch Office
495 Summer Street
Boston, Massachusetts 02210

1 LCDR T. L. Miller, (USN)
ONR Representative
Woods Hole Oceanographic Institution
Woods Hole, Massachusetts 02543

Director
Naval Research Laboratory
Washington, D. C. 20390
6 Attn: Library, Code 2029 (ONRL)
6 Attn: Library, Code 2000

Commander
Naval Oceanographic Office
Washington, D. C. 20390
1 Attn: Code 1640 (Library)
1 Attn: Code 70

OTHER GOVERNMENT AGENCIES

12 Defense Documentation Center
Cameron Station
Alexandria, Virginia 22314

1 Director
National Oceanographic Data Center
Bldg. 160
Navy Yard
Washington, D. C. 20390

Woods Hole Oceanographic Institution
Reference No. 71-68

HUDSON '70 GRAVITY OBSERVATIONS 62.9°S - 57.5°N ALONG 150°W by W. S. von Arx, D. C. Bowen, J. P. Dean, R. T. Haworth. 3 pages, 4 figures and tables I,II & III. November 1971. Contract No. N00014-66-C0241; NR 083-004.

To provide geoidal topography over the world oceans, a radar altimeter carried by earth satellite is planned. Ground truth calibration will be provided by a grid comprised of the equatorial belt and meridional traverses along the 30°W and 150°W meridians. Ground truth topography is derived from gravity values measured along these traverses. This report presents the free air gravity values and the computed free air anomalies obtained from 62.9°S to 57.5°N along the 150°W meridian.

1. HUDSON '70
2. 150°W Meridian
3. Gravity
4. Marine Geodesy

I. von Arx, W. S.

II. Bowen, D. C.

III. Dean, J. P.

IV. Haworth, R. T.

V. N00014-66-C0241; NR 083-004

This card is UNCLASSIFIED

Woods Hole Oceanographic Institution
Reference No. 71-68

HUDSON '70 GRAVITY OBSERVATIONS 62.9°S - 57.5°N ALONG 150°W by W. S. von Arx, D. C. Bowen, J. P. Dean, R. T. Haworth. 3 pages, 4 figures and tables I,II & III. November 1971. Contract No. N00014-66-C0241; NR 083-004.

To provide geoidal topography over the world oceans, a radar altimeter carried by earth satellite is planned. Ground truth calibration will be provided by a grid comprised of the equatorial belt and meridional traverses along the 30°W and 150°W meridians. Ground truth topography is derived from gravity values measured along these traverses. This report presents the free air gravity values and the computed free air anomalies obtained from 62.9°S to 57.5°N along the 150°W meridian.

1. HUDSON '70
2. 150°W Meridian
3. Gravity
4. Marine Geodesy

I. von Arx, W. S.

II. Bowen, D. C.

III. Dean, J. P.

IV. Haworth, R. T.

V. N00014-66-C0241; NR 083-004

This card is UNCLASSIFIED

Woods Hole Oceanographic Institution
Reference No. 71-68

HUDSON '70 GRAVITY OBSERVATIONS 62.9°S - 57.5°N ALONG 150°W by W. S. von Arx, D. C. Bowen, J. P. Dean, R. T. Haworth. 3 pages, 4 figures and tables I,II & III. November 1971. Contract No. N00014-66-C0241; NR 083-004.

To provide geoidal topography over the world oceans, a radar altimeter carried by earth satellite is planned. Ground truth calibration will be provided by a grid comprised of the equatorial belt and meridional traverses along the 30°W and 150°W meridians. Ground truth topography is derived from gravity values measured along these traverses. This report presents the free air gravity values and the computed free air anomalies obtained from 62.9°S to 57.5°N along the 150°W meridian.

1. HUDSON '70
2. 150°W Meridian
3. Gravity
4. Marine Geodesy

I. von Arx, W. S.

II. Bowen, D. C.

III. Dean, J. P.

IV. Haworth, R. T.

V. N00014-66-C0241; NR 083-004

This card is UNCLASSIFIED

Woods Hole Oceanographic Institution
Reference No. 71-68

HUDSON '70 GRAVITY OBSERVATIONS 62.9°S - 57.5°N ALONG 150°W by W. S. von Arx, D. C. Bowen, J. P. Dean, R. T. Haworth. 3 pages, 4 figures and tables I,II & III. November 1971. Contract No. N00014-66-C0241; NR 083-004.

To provide geoidal topography over the world oceans, a radar altimeter carried by earth satellite is planned. Ground truth calibration will be provided by a grid comprised of the equatorial belt and meridional traverses along the 30°W and 150°W meridians. Ground truth topography is derived from gravity values measured along these traverses. This report presents the free air gravity values and the computed free air anomalies obtained from 62.9°S to 57.5°N along the 150°W meridian.

1. HUDSON '70
2. 150°W Meridian
3. Gravity
4. Marine Geodesy

I. von Arx, W. S.

II. Bowen, D. C.

III. Dean, J. P.

IV. Haworth, R. T.

V. N00014-66-C0241; NR 083-004

This card is UNCLASSIFIED

UNCLASSIFIED
Security Classification

DOCUMENT CONTROL DATA - R&D
(Security classification of title, body of abstract and indexing annotation must be entered when the overall report is classified)

1. ORIGINATING ACTIVITY (Corporate author)
Woods Hole Oceanographic Institution
Woods Hole, Massachusetts

2a. REPORT SECURITY CLASSIFICATION
UNCLASSIFIED

2b. GROUP

3. REPORT TITLE
HUDSON '70 GRAVITY OBSERVATIONS 62.9°S - 57.5°N ALONG 150°W

4. DESCRIPTIVE NOTES (Type of report and inclusive dates)
Technical Report

5. AUTHOR(S) (Last name, first name, initial)
W. S. von Arx, D. C. Bowen, J. P. Dean, R. T. Haworth

6. REPORT DATE	7a. TOTAL NO. OF PAGES	7b. NO. OF REFS
November 1971	3	

8a. CONTRACT OR GRANT NO.	9a. ORIGINATOR'S REPORT NUMBER(S)
N00014-66-C0241; NR 083-004	REFERENCE NO. 71-68
b. PROJECT NO.	
c.	9b. OTHER REPORT NO(S) (Any other numbers that may be assigned this report)
d.	

10. AVAILABILITY/LIMITATION NOTICES

11. SUPPLEMENTARY NOTES

12. SPONSORING MILITARY ACTIVITY
Office of Naval Research
Ocean Science & Technology Division
Arlington, Virginia 22217

13. ABSTRACT

To provide geoidal topography over the world oceans, a radar altimeter carried by earth satellite is planned. Ground truth calibration will be provided by a grid comprised of the equatorial belt and meridional traverses along the 30°W and 150°W meridians. Ground truth topography is derived from gravity values measured along these traverses. This report presents the free air gravity values and the computed free air anomalies obtained from 62.9°S to 57.5°N along the 150°W meridian.

DD FORM 1473

14. KEY WORDS	LINK A		LINK B		LINK C	
	ROLE	WT	ROLE	WT	ROLE	WT
1. HUDSON '70						
2. 150°W Meridian						
3. Gravity						
4. Marine Geodesy						

INSTRUCTIONS

1. ORIGINATING ACTIVITY: Enter the name and address of the contractor, subcontractor, grantee, Department of Defense activity or other organization *(corporate author)* issuing the report.

2a. REPORT SECURITY CLASSIFICATION: Enter the overall security classification of the report. Indicate whether "Restricted Data" is included. Marking is to be in accordance with appropriate security regulations.

2b. GROUP: Automatic downgrading is specified in DoD Directive 5200.10 and Armed Forces Industrial Manual. Enter the group number. Also, when applicable, show that optional markings have been used for Group 3 and Group 4 as authorized.

3. REPORT TITLE: Enter the complete report title in all capital letters. Titles in all cases should be unclassified. If a meaningful title cannot be selected without classification, show title classification in all capitals in parenthesis immediately following the title.

4. DESCRIPTIVE NOTES: If appropriate, enter the type of report, e.g., interim, progress, summary, annual, or final. Give the inclusive dates when a specific reporting period is covered.

5. AUTHOR(S): Enter the name(s) of author(s) as shown on or in the report. Enter last name, first name, middle initial. If military, show rank and branch of service. The name of the principal author is an absolute minimum requirement.

6. REPORT DATE: Enter the date of the report as day, month, year; or month, year. If more than one date appears on the report, use date of publication.

7a. TOTAL NUMBER OF PAGES: The total page count should follow normal pagination procedures, i.e., enter the number of pages containing information.

7b. NUMBER OF REFERENCES: Enter the total number of references cited in the report.

8a. CONTRACT OR GRANT NUMBER: If appropriate, enter the applicable number of the contract or grant under which the report was written.

8b, 8c, & 8d. PROJECT NUMBER: Enter the appropriate military department identification, such as project number, subproject number, system numbers, task number, etc.

9a. ORIGINATOR'S REPORT NUMBER(S): Enter the official report number by which the document will be identified and controlled by the originating activity. This number must be unique to this report.

9b. OTHER REPORT NUMBER(S): If the report has been assigned any other report numbers *(either by the originator or by the sponsor)*, also enter this number(s).

10. AVAILABILITY/LIMITATION NOTICES: Enter any limitations on further dissemination of the report, other than those imposed by security classification, using standard statements such as:

(1) "Qualified requesters may obtain copies of this report from DDC."

(2) "Foreign announcement and dissemination of this report by DDC is not authorized."

(3) "U. S. Government agencies may obtain copies of this report directly from DDC. Other qualified DDC users shall request through _____."

(4) "U. S. military agencies may obtain copies of this report directly from DDC. Other qualified users shall request through _____."

(5) "All distribution of this report is controlled. Qualified DDC users shall request through _____."

If the report has been furnished to the Office of Technical Services, Department of Commerce, for sale to the public, indicate this fact and enter the price, if known.

11. SUPPLEMENTARY NOTES: Use for additional explanatory notes.

12. SPONSORING MILITARY ACTIVITY: Enter the name of the departmental project office or laboratory sponsoring *(paying for)* the research and development. Include address.

13. ABSTRACT: Enter an abstract giving a brief and factual summary of the document indicative of the report, even though it may also appear elsewhere in the body of the technical report. If additional space is required, a continuation sheet shall be attached.

It is highly desirable that the abstract of classified reports be unclassified. Each paragraph of the abstract shall end with an indication of the military security classification of the information in the paragraph, represented as *(TS), (S), (C), or (U)*.

There is no limitation on the length of the abstract. However, the suggested length is from 150 to 225 words.

14. KEY WORDS: Key words are technically meaningful terms or short phrases that characterize a report and may be used as index entries for cataloging the report. Key words must be selected so that no security classification is required. Identifiers, such as equipment model designation, trade name, military project code name, geographic location, may be used as key words but will be followed by an indication of technical context. The assignment of links, roles, and weights is optional.

Molluscan Fauna as Indicators of Late Pleistocene History, Southeastern Beaufort Sea

F. J. E. WAGNER,
Canada

ABSTRACT

One hundred and forty-nine grab samples were examined from the Beaufort Sea area bounded by latitudes 68°45′10″N and 71°34′18″N and longitudes 128°19′W and 140°-37′W. Of these, 97 were collected from CSS Hudson between August 26 and September 20, 1970; the remaining 52 samples were obtained on a helicopter operation during April 1971. Molluscs were obtained from 95 of these 149 samples. Fossil molluscs were picked from 8 of the 52 Hudson cores, and were also collected from four localities on Herschel Island and one locality at Kay Point, Yukon Territory. Molluscs from a depth of 10 to 30 cm in one core have been radiocarbon-dated at 700±180 years B.P., and from the 400- to 406-cm interval in another core gave an age of 3530±240 years B.P. A comparison of fossil molluscs from the cores with the recent fauna suggests that 3500 years ago sea level was approximately 270 m lower than at present, and 700 years ago it was approximately 15 m lower than now.

BETWEEN August 26 and September 20, 1970, 97 grab samples and 52 cores were obtained from CSS *Hudson* stations in the Beaufort Sea. Fifty-two additional grab samples were collected from stations on the ice during a helicopter operation in April 1971 (Fig. 1). Fossil molluscs were collected from four localities on Herschel Island and from one locality at Kay Point, Yukon Territory, and were picked from eight of the cores.

Environmental features of the area are presented in Figures 1 to 4, and are self-explanatory. Distribution of the benthonic molluscs (Fig. 5) is presented in terms of undisturbed and reworked specimens. Pelecypods with valves intact and undamaged gastropods were undoubtedly in living position when collected. Some specimens were alive when taken; others were recently dead. Single pelecypod valves and fragments of both pelecypod and gastropod shells indicate various degrees of reworking. All species found are listed in Table 1.

Thirty-three species of benthonic molluscs were found living or recently dead. One pelagic pelecypod, *Arctinula groenlandica*, a species hitherto not believed to inhabit the Beaufort Sea (MacNeil, 1967, p. 8), was collected alive. Thirteen of the 33 benthonic species were sufficiently abundant to be useful as ecologic indicators (Table 2).

A comparison of the molluscs found in the cores (Table 3) with those collected from the present sea bottom shows 16 species in common. Three other species are currently known in the area only from the cores. Six species from the cores appear in Table 2 and, of these, only *Portlandia intermedia* (Station 377), *P. lenticula* (Stations 377 and 427) and *Retusa umbilicata* (Stations 439 and 348)

Authors' addresses are given at the back of this book.

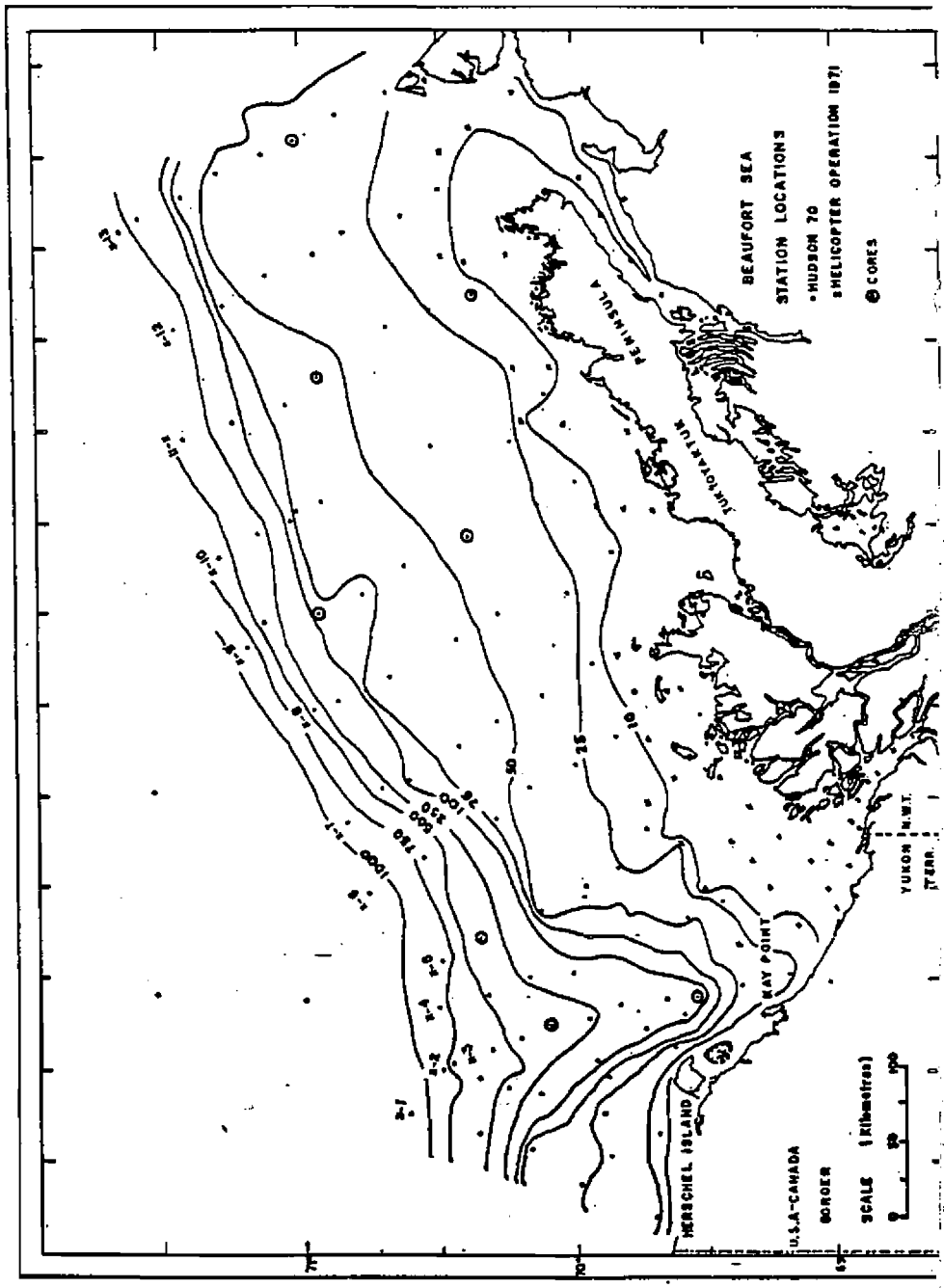


FIGURE 1 — Station locations and bathymetry. Cross-lines traversed are indica
thus: X-1, etc.

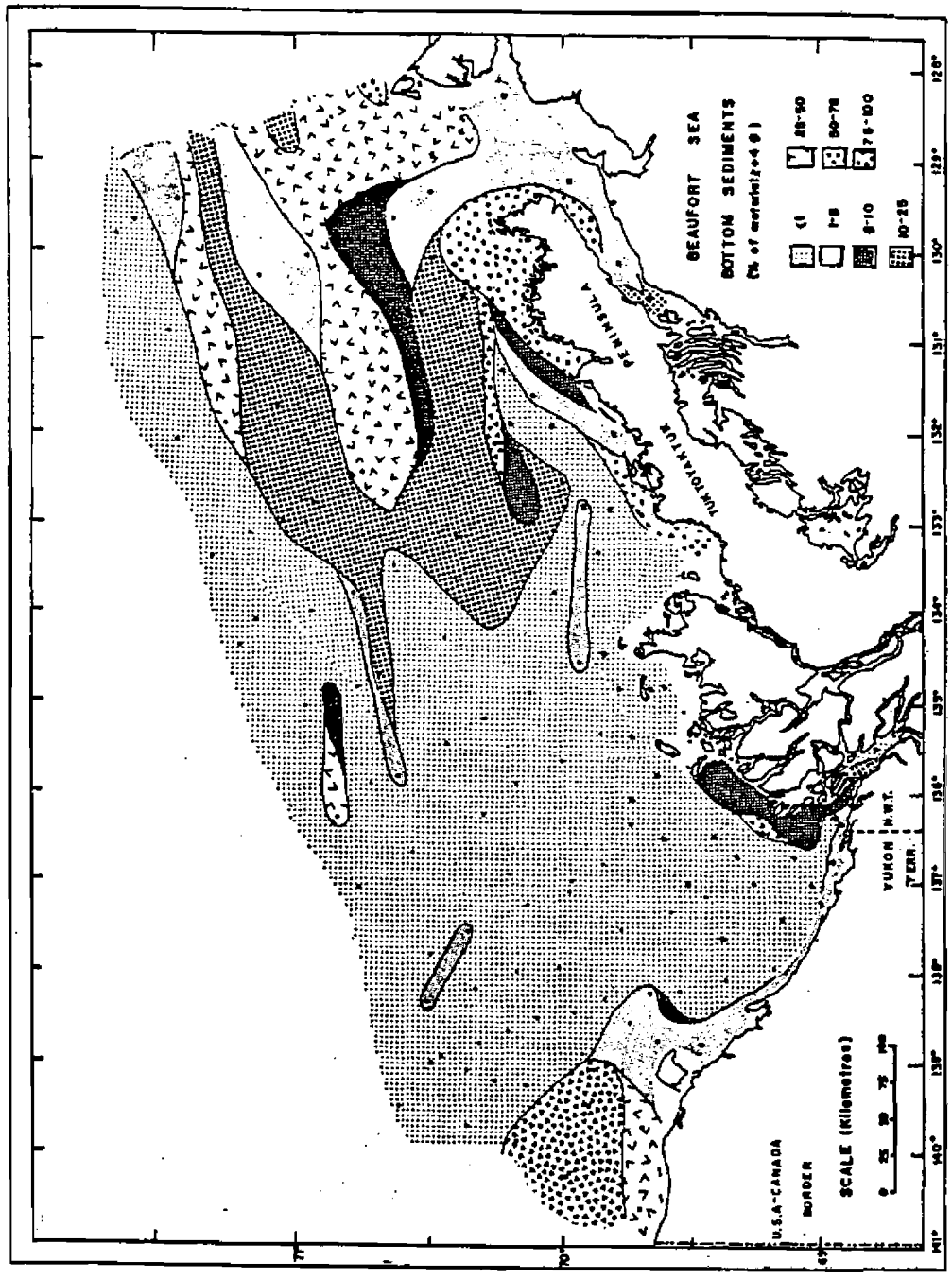


FIGURE 2 — Sediment distribution. The sediment texture is designated in terms of the percentage of material + 4 ϕ or coarser.

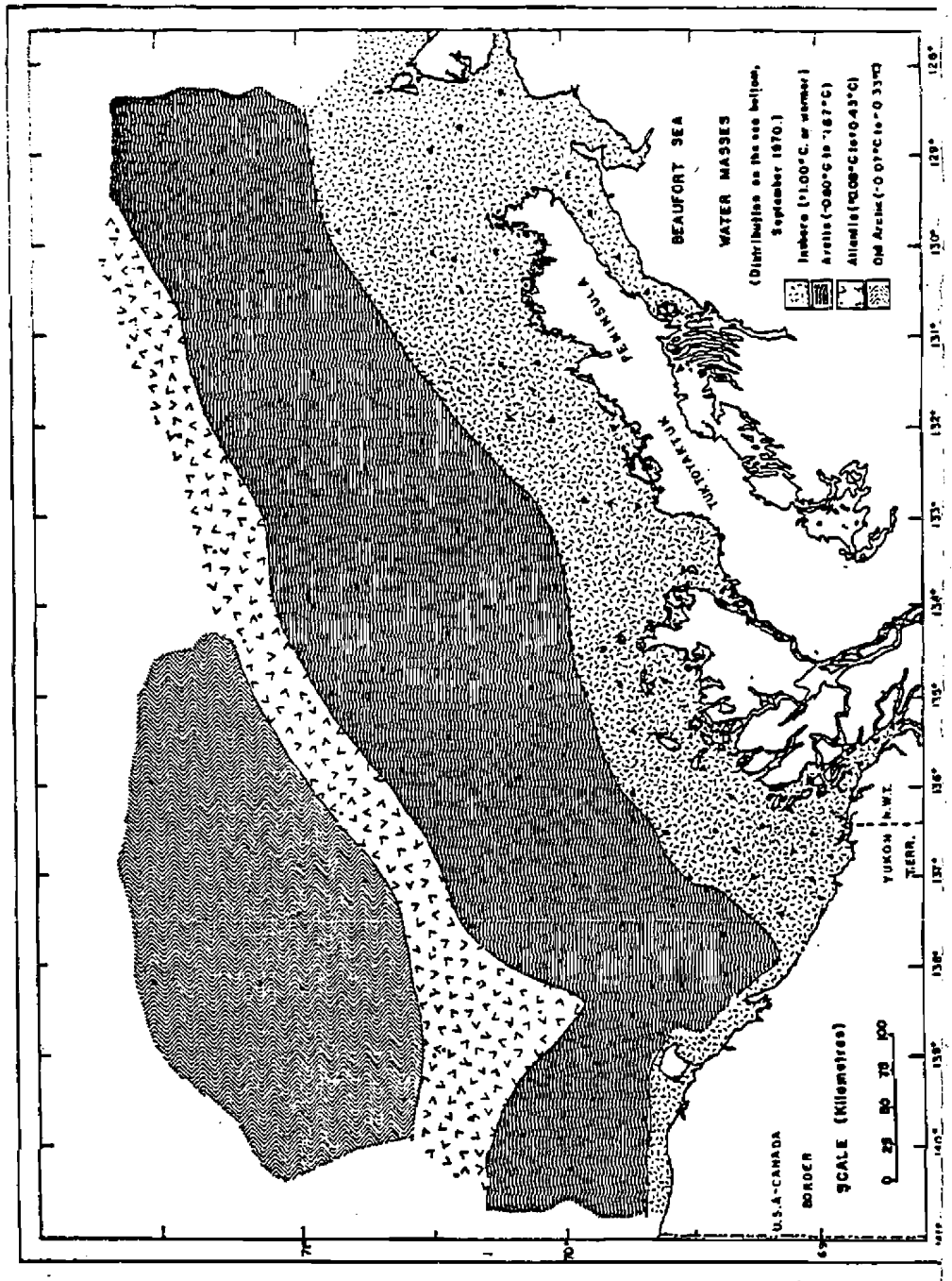


FIGURE 3 — Sea-bottom distribution of the various water masses differentiated ac cording to temperature, September 1970. The inshore water mass, with positive tem peratures, is probably replaced by Arctic waters during the major part of the year.

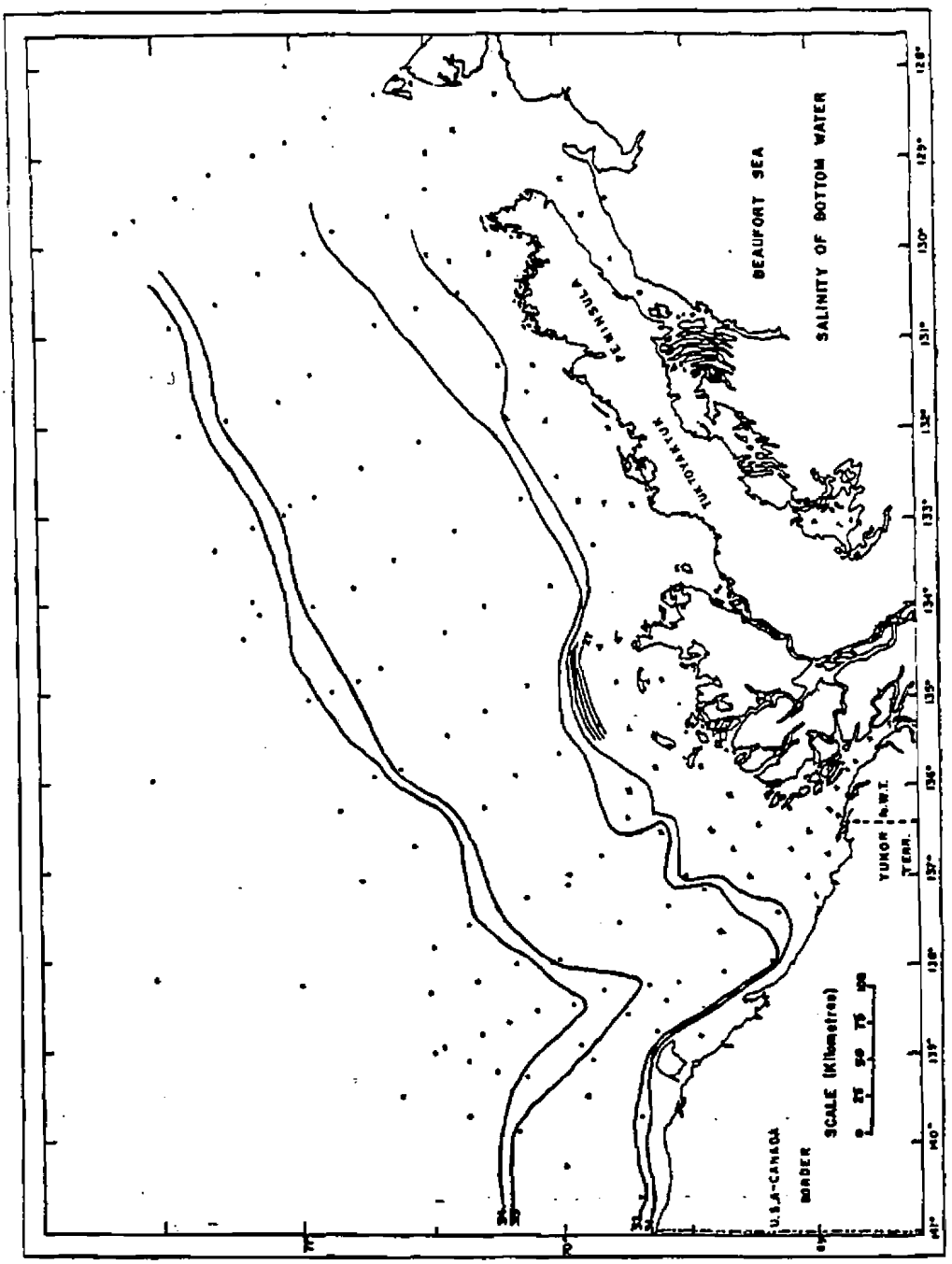


FIGURE 4 — Salinity (‰) of bottom waters, September 1970.

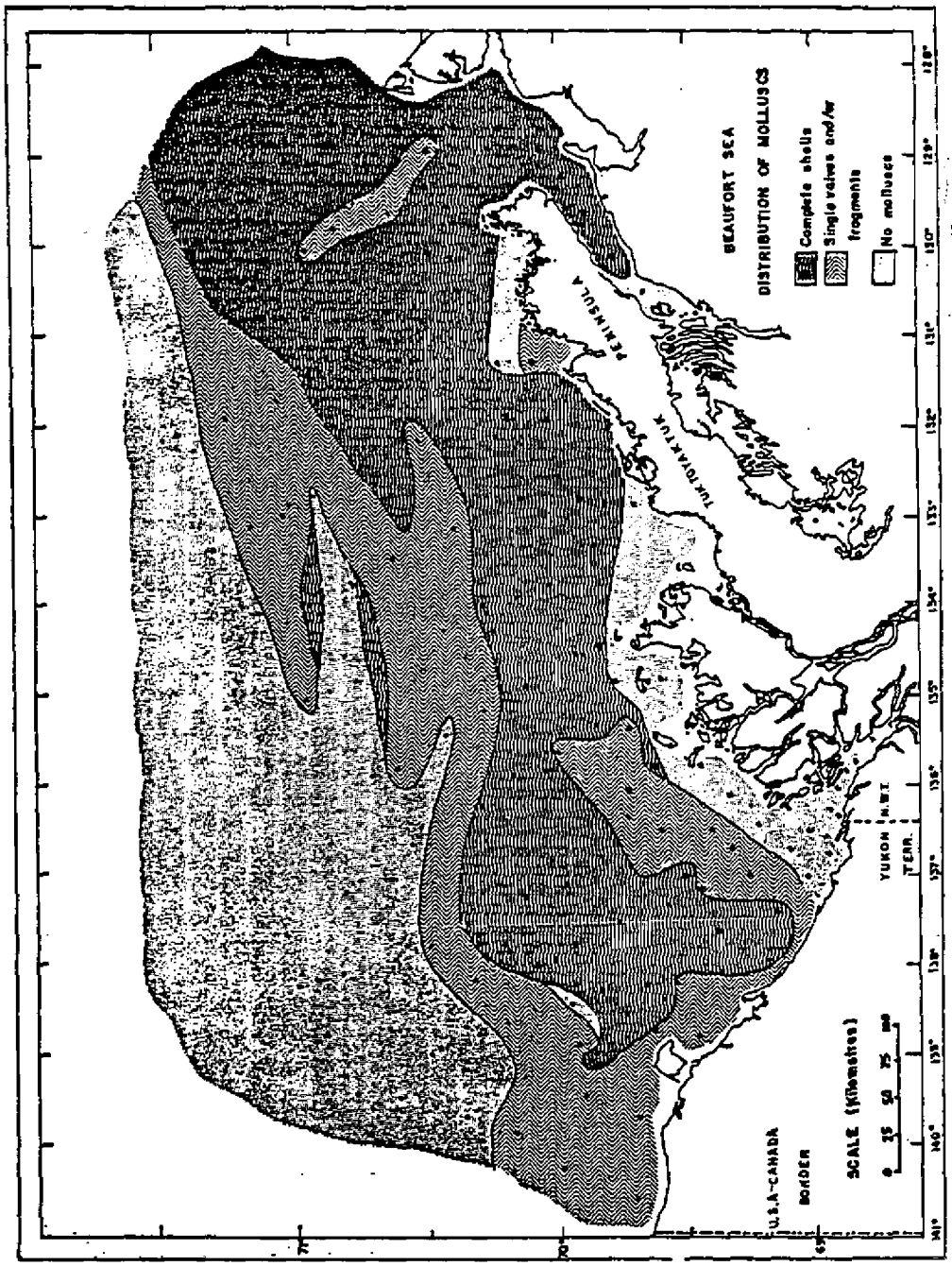


FIGURE 5 — Distribution of benthonic molluscs showing areas of occurrence of living specimens in relation to barren areas.

TABLE 1. — Mollusca from Grab and Dredge Samples, Beaufort Sea

Cross-Line	1	2	2-3*	3	4	5	6	7	8	9	10	11	12	13
Number of Stations in Cross-Line	5	5	6	10	7	6	6	7	8	8	8	7	7	7
Range in Depth (m)	26-69	15-211	48-187	33-390	24-421	18-346	16-57	16-87	16-457	19-80	17-346	18-109	16-62	29-69
Aretinula groenlandica (Sowerby)	2f	1f	2f 1c	5f 2s	2f 1s	2f 1s	1f		1f			1f		2f
Astarte sp.	1f	1f 1s		3f		1f						2f		
Nuculana sp.	1f			1f		1f					2f		1f	
Portlandia intermedia (M. Sars)	1f 1s	1f	1s 1c	2s 1c	2s 1c	2s 1c					1c			
Unidentifiable fragments		2f	2f	1f	1f						2f			
Astarte borealis Schumacher		1f 2s		1s						1f 1s	1f 1s			1s
Portlandia fraterna (Verrill and Bush)				1f3s1c	1s						1s 1c			
Bathyarca frielei (Jeffreys) Friele			1f1s1c		2f 2s	1f 1c		1c			2f			
Thyasira flexuosa sarsi Philippi			1c	2s 2c		1s				1 s				1c
Nucula (*Ennucula*) *tenuis* (Montagu)			1f	1c		1s 1c		1s 1c			2s		1c	
Tachyrhynchus erosum (Couthouy)			1c							1f		1f		1f
Portlandia arctica (Gray)			1c	2s 2c	2s 3c	1f3s2c	2f2s2c	1f2s1c	1f1e2c	1f1s2c	1e 2c	1s 2c	1f1s1c	
Astarte montagui striata (Leach)			1s	2s 2c										1f 1c
Macoma calcarea (Gmelin)				1c					1c	1f 1c			1f 3s	1s
Retusa umbilicata (Montagu)				1c		1c	1c					1c		
†*Oenopota* sp.				1f										
Portlandia frigida (Torell)				1c	2c	2s					1c			
Portlandia lenticula (Möller)				1c	2s	1f2s2c	1s	1s	1s 1c					
Macoma moesta (Deshayes)				1c									1s	
Cylichna occulta (Mighels)				1c	1c	2c	1c	1c	1c		1c	1c	1f	1c
Abanta sp.				1f	1c									

Lepeta caeca (Müller)					1c	1c						1f 2s		1c
Nuculana pernula (Müller)	1				1c									
Cingula castanea alaskana Dall					1c									
Onoposta cf. O. tenuicostata (G. O. Sars)					1c									
Bathyarca glacialis (Gray)						2s 1c								
Boreotrophon clathratus (Linné)						1c								
Pandora glacialis Leach						1s		1c				1f 2s	1f 1s	1s
Plicifusus sp.						1c								
Yoldia myalis (Couthouy)												2c	1f	1f 1s
Liocyma fluctuosa (Gould)												1s	1s	8c
Musculus niger (Gray)												1c	1f 1s	1c
Neptunea sp.												1f		
Astarte montagui warhami Hancock													1s 1c	
Clinocardium ciliatum (Fabricius)													2f 1c	3c
Mya truncata Linné													1f	1f
Trichotropis sp.														1f
Odostomia cassandra Dall														1c
Lunatia pallida (Broderip & Sowerby)														2c
Nuculana radiata (Krause)														1c
Thracia devexa G. O. Sars														2c
Neptunea ventricosa (Gmelin)														1c
Hiatella arctica (Linné)														1s 1c
Nuculana minuta (Fabricius)														1c
Serripes groenlandicus (Bruguière)														1f
Buccinum polare Gray (juvenile)														1c

c = complete shells; s = single valves; f = fragments

The number with each of the letters indicates the number of stations on the cross-line at which shells of each category were found, e. g., 1f3s1c means fragfragments were found at 1 station, single valves at 3 stations and complete shells at 1 station.

*Stations between cross-lines 2 and 3.

TABLE 2 — Most Common Benthonic Molluscs Living in Beaufort Sea

	Occurance Relative to Mackenzie Delta			Depth Range of Species (metres)								Bottom Sediment (% of Material +4ϕ or Coarser)							Bottom Salinity (‰)					Water Mass	
	W	N	E	0-25	26-50	51-75	76-100	101-125	126-150	151-175	176-200	< 1	1-5	5-10	10-25	25-50	50-75	> 75	< 31	31-32	32-33	33-34	> 34	Inshore	Arctic
Portlandia arctica Gray	25	26	23	30	24	18	25	25				36	26		14		40	17	29	22	23			19	21
Cylichna occulta (Mighels)	14	12	16	19	21							18	21		21				20	11	11			19	10
Portlandia lenticula (Möller)	4	12	3	4	10	6						9	5		7				5		8			4	7
Retusa umbilicata (Montagu)	4	3	5	4	7							7			7				2	11	4			4	8
Thyasira flexuosa sarsi Philippi	4	6	2		3				50		67	2	11			11					6	33			7
Portlandia frigida (Torell)	11		2		3	12		25				7				11					8				7
Portlandia intermedia (M. Sars)	11		2		3	6		25			33	4	5			11					8				7
Liocyma fluctuosa (Gould)			16	9	10								5		7	11		67	10	22	2			13	3
C inocardium ciliatum (Fabricius)			9		10	6									14	22					8				7
Nucula tenuis (Montagu)			9		14							7	5								8				7
Yoldia myalis (Couthouy)			5	2	3										14					11	2			2	2
Thracia devexa G.O. Sars			5		7										7			17		11	2			2	2
Musculus niger (Gray)			5		7											22				11	2			2	2

Above percentages derived as follows: $\frac{\text{total no. of stations at which species found living}}{\text{total no. of stations (see below)}} \times 100$

Total stations in each category	28	34	44	47	29	17	4	4	2	0	3	45	19	8	14	9	5	6	41	9	53	3	0	48	58

TABLE 3.— Mollusca in Beaufort Sea Cores

Station Number	430	439					412					427	409	868	848						877
Water Depth (m)	18	40					42					54	80	109	290						322
Depth in Core (cm)	235	30	50	0 — 7	100 — 110	230 — 235	99 — 100	180	299 — 301	499 — 501	549 — 551	10 — 30	44	249 — 251	670	690	699 — 701	899 — 901	949 — 951	1067	400 — 406
Portlandia arctica (Gray)	s									f			f								
Unidentifiable fragments	f	f	f								f										f
Arctinula groenlandica (Sowerby)		f				f						f	f								fs
Astarte montagui striata (Leach)		s			f	f															
Clinocardium ciliatum (Fabricius)			f		f	f															
Trichotropis sp.						c															
Retusa umbilicata (Montagu)						c													e		
Astarte borealis Schumacher							s					s									
Macoma sp.								f													
Musculus corrugatus (Stimpson)									f				f								
Balhygrra glacialis (Gray)												c			s	s	s	s			
Mya sp.												f									
Solariella sp.												c									
Portlandia lenticula (Möller)														s						s	sc
Nucula tenuis (Montagu)																					fs
Portlandia intermedia (M. Sars)																					sc
Tachyrhynchus erosum (Couthouy)																					c
Boreotrophon clathratus (Linné)																					s
†*Buccinum* sp.																					ft
†*Mollerla* sp.																					f

c = complete shells; s = single valves; f = fragments

*700 ± 180 years †3580 ± 240 years

TABLE 4. — Molluscs from Raised Marine Deposits, Herschel Is., Kay Pt., Y.T.

Locality Number	1	2	3	4	5
Longitude (west)	138°54'12"	138°54'15"	139°02'36"	139°04'00"	138°19'00"
Latitude (north)	69°35'00"	69°34'30"	69°36'15"	69°33'12"	69°15'00"
Elevation above sea level (m)	40 ±	25 ±	75 ±	25–30	15–25
Astarte borealis Schumacher	x	x	x	x	
Astarte montagui warhami Hancock	x	x		x	
Macoma balthica (Linné)	x				?
Bathyarca glacialis (Gray)		x			
Astarte montagui striata (Leach)		x	x	x	
Astarte montagui (Dillwyn) forma typica		x	x		
Tachyrhynchus erosum (Couthouy)		x		x	
Portlandia arctica (Gray)			x		
Neptunea heros (Gray)				x	
Astarte sp.					x

were probably in place. The writer's few observations on the ecological requirements of the other species that were apparently not reworked, i.e. *Bathyarca glacialis, Boreotrophon clathratus* and *Tachyrhynchus erosum*, have been augmented by information from MacGinitie (1959) and Ockelmann (1958).

Because of the paucity of unreworked material, precise depths at the time of deposition cannot be determined. However, general conclusions may be drawn, based on assemblages from four of the cores. Shells from a depth of 10 to 30 cm in the core from Station 427 (Lat. 70°56.5'N, Long. 131°24.7'W; depth 54 m) suggest a depth of about 40 m at the time of deposition (ref. Table 2). This depth is approximately 15 m shallower than at present. These shells have been dated by the Geological Survey of Canada at 700 ± 180 years B.P. At Station 439 (Lat. 71°01'N, Long. 128°49.5'W; depth 40 m), complete shells were found 230 to 235 cm down in the core. Past water depth has been determined at approximately 25 to 30 m (Table 2), or again about 15 m shallower than now. Thus during the period when at least 200 cm of sediment accumulated, sea level was apparently relatively constant at a depth about 15 m shallower than now, deepening to its present level during the past 700 years. Sufficient material for dating was obtained from the 400- to 406-cm interval at Station 377 (Lat. 70°21.5'N, Long. 137°33'W; depth 322 m); the date at this interval was 3530 ± 240 years B.P. When the dated molluscs were alive, the water depth is estimated to have been about 50 m (Table II). Therefore, some 3500 years ago the water at this site was approximately 270 m shallower than it is now. In the fourth core mentioned, that from Station 348 (Lat. 70°06.5'N, Long. 138°31'W; depth 290 m), a single specimen of *Retusa umbilicata* was found 950 cm below the surface of the sea floor. This species was found most commonly living in the 25- to 40-m depth range. A

comparison of this depth with the present depth of 290 m indicates an apparent deepening ranging between 240 and 265 m at this locality.

From the time of the earliest molluscs, that occur in situ in the cores, there has been a deepening of the water. The radiocarbon dates and the differences between past and present water depths suggest that the rate of deepening has slowed from 1 m in 13 years about 3500 years ago to 1 m in 46 years about 700 years ago. It is impossible to state, on the basis of the present evidence, the number of interruptions that took place during this progressive deepening. However, there was apparently one stillstand, as noted previously in discussion of the cores from Stations 427 and 439. Palynological evidence (Mackay and Terasmae, 1963) suggests that peat began accumulating in the Mackenzie Delta area between 8000 and 7000 years ago. Sea level then was probably considerably lower than at present, at least during the early period of peat accumulation. Currently, therefore, the marine molluscan record covers only about half the period of time of the pollen record, but both records are mutually consistent. Foraminiferal assemblages in the cores may enable extension and refinement of the marine record.

No dates are available for shells from the raised marine deposits (Table 4) of Herschel Island and Kay Point. However, other evidence would place their age at possibly between 35,200 years and 51,000 years B.P. (Dyck and Fyles, 1963, p. 29; Dyck, Lowdon, Fyles and Blake, 1966, p. 21). Three species found as fossils at these localities were not found among the recent fauna, and two of these, *Macoma balthica* and *Astarte montagui* forma typica, are indicative of somewhat more moderate temperatures.

REFERENCES

Dyck, W., and Fyles, J. G., 1963. Geological Survey of Canada radiocarbon dates I and II. Geol. Surv. Can., Pap. 63-21, p. 1-31.

Dyck, W., Lowdon, J. A., Fyles, J. G., and Blake, W., Jr., 1966. Geological Survey of Canada radiocarbon dates V. Geol. Surv. Can., Pap. 66-48, p. 1-32.

MacGinitie, N., 1959. Marine Mollusca of Point Barrow, Alaska. Proc. U.S. Nat. Mus., 109, p. 59-208, 27 pls.

Mackay, J. R., and Terasmae, J., 1963. Pollen diagrams in the Mackenzie Delta area, N.W.T. Arctic, 16, (4), p. 228-238.

MacNeil, F. S., 1967. Cenozoic pectinids of Alaska, Iceland and other northern regions. U.S. Geol. Surv. Prof. Pap. 553, p. 1-57, 25 pls.

Ockelmann, W. K., 1958. Marine Lamellibranchiata. Medd. om Grønn., 122, (4), p. 1-256, 3 pls.

SPINAL ULTRASTRUCTURE OF THE PLANKTONIC FORAMINIFERS *HASTIGERINA* THOMSON AND *GLOBIGERINELLA* CUSHMAN

DAVID A. WALKER AND GUSTAVS VILKS

Reprinted from JOURNAL OF FORAMINIFERAL RESEARCH
Vol. 3, No. 4, October 1973
p. 196–198
Made in the United States of America

Journal of Foraminiferal Research, v. 3, no. 4, p. 196–198, pl. 1, October 1973

SPINAL ULTRASTRUCTURE OF THE PLANKTONIC FORAMINIFERS *HASTIGERINA* THOMSON AND *GLOBIGERINELLA* CUSHMAN

DAVID A. WALKER AND GUSTAVS VILKS
Atlantic Geoscience Centre, Bedford Institute of Oceanography,
Dartmouth, Nova Scotia, Canada

ABSTRACT

Scanning electron microscopy of the planktonic foraminifer *Hastigerina pelagica* (d'Orbigny) has revealed the presence of spinal barbs along each of the edges of the triradiate spines. These structures were lacking on all *Globigerinella aequilateralis* (Brady) specimens examined, suggesting that the genus *Globigerinella* Cushman is valid and not a junior synonym of *Hastigerina* Thomson.

INTRODUCTION

The presence or absence of spines is often used as a criterion to separate taxa of planktonic foraminifera (Parker, 1962; Bé, 1967). With the aid of the scanning electron microscope it is now possible to take this approach a step further and investigate the various types of spines. The three basic types of spines reported in the literature to date have either (a) circular, (b) triangular, or (c) triradiate cross sections (Parker, 1962; Hemleben, 1969). We have observed the following associations of spines and genera: (a) circular cross section only in spinose species of *Globigerina* d'Orbigny, (b) circular to triangular cross section in *Globigerinoides* Cushman, (c) circular, triangular and triradiate cross section in *Orbulina* d'Orbigny, (d) both circular and triradiate in *Globigerinella* Cushman, and (e) only triradiate in *Hastigerina* Thomson. In the case of *Hastigerina*, the characteristic triradiate shape of the spines is consistent from proximal to distal ends, whereas in *Globigerinoides*, *Orbulina* and *Globigerinella* there is a gradual change in morphology from circular cross section at the base to triangular or triradiate toward the distal end. The three basic types of spines transgress generic boundaries in most instances, and these features may not be phylogenetically important. However, the triradiate spines of *Hastigerina pelagica* (d'Orbigny) possess additional features that may assist in separating *Hastigerina* from *Globigerinella*.

The purpose of the present study was to investigate Bé's (1969) comparison of the genera *Hastigerina* and *Globigerinella*, which was based on spinal morphology. Bé found that *Globigerinella aequilateralis* (Brady) (= *Globigerinella siphonifera* (d'Orbigny)) possesses both the circular and triradiate spines, the former being more common, whereas *Hastigerina pelagica* possesses only the triradiate type of spine. On the basis of these findings, Bé agreed to the suggestion of Bolli, Loeblich and Tappan (1957) and Banner and Blow (1960) to place *Globigerinella aequilateralis* with the genus *Hastigerina*.

MATERIALS AND METHODS

We observed 12 specimens of *Hastigerina pelagica* (pl. 1, figs. 1–5) and 7 specimens of *Globigerinella aequilateralis* (pl. 1, figs. 6, 7) by scanning electron microscopy. Samples were collected from the Atlantic and Pacific Oceans and the Caribbean Sea (table 1). Most specimens were collected from surface waters, either from 0–5 metres or 0–200 metres. A 202-micron

TABLE 1

Station locations of examined specimens.

Sample	Latitude	Longitude	*Hastigerina pelagica*	*Globigerinella aequilateralis*	Sampling Depth (m)
69–050VC–100	04°46.6′N	150°04.8′W	–	2	0–200
69–050VC–101	10°01.4′N	150°06.8′W	–	1	0–5
69–050VC–104	28°51.0′N	149°57.7′W	1	–	0–5
69–050VC–93	29°58.4′S	149°58.0′W	–	1	0–200
69–050VC–5	4°54.7′S	30°00.5′W	1	–	0–200
69–050VC–6	6°02.1′S	30°01.2′W	1	–	0–200
69–050VC–7	7°27.0′S	30°03.0′W	1	1	0–200
69–050VC–10	10°57.5′S	30°01.4′W	1	–	0–200
69–309VC–5	32°05.0′N	64°24′W	1	–	0–200
69–306VC–8	32°10.0′N	64°24′W	2	–	0–200
69–302VC–2	32°10.0′N	64°24′W	1	–	0–200
69–025–25–2	44°59.0′N	42°30.0′W	1	–	180–700
68–4–18	13°40.0′N	63°37.0′W	2	1	0–200
68–4–26–8	13°35.0′N	61°16.0′W	–	1	0–200

plankton net was used with a square mouth opening of 0.5 metres. The 0–5 metre tows were taken with the net suspended from the ship's bow. The deeper tows were taken by lowering the net to 200 metres from a stationary ship and retrieving not faster than 30m/min to preserve the delicate features of the foraminiferal tests. The samples were preserved in a 4% formaldehyde-seawater solution buffered with hexamethylene tetramine at pH 8.5.

In the laboratory organic matter was removed by oxidizing each sample with a Tracerlab low temperature asher (Vilks, 1970). Further preparation for the scanning electron microscope consisted of placing the specimens onto double-coated adhesive tape ("Sellotape") previously mounted on standard JEOL specimen blocks. Specimens were then coated with Au-Pd in an Edwards high-vacuum evaporator.

OBSERVATIONS

During this study our attention was focused on the microstructure of the spines. We observed the presence of secondary outgrowths, termed spinal barbs, along the edges of the triradiate spines of *Hastigerina pelagica* (pl. 1, figs. 2–5). These structures were lacking on all the *Globigerinella aequilateralis* specimens examined (pl. 1, fig. 7). The spinal barbs are consistently bifid (pl. 1, fig. 3), with the apices pointing distally (pl. 1, fig. 2). On some spines there is a textural discontinuity between the spine and spinal barbs (pl. 1, fig. 4). In some cases there may be a medial groove between the vertices (pl. 1, fig. 3). The spinal barbs illustrated in plate 1, figure 5 are basically similar to those in plate 1, figures 3 and 4 except that the former have more pointed apices, lack a medial groove, and have basal shoulders which are considerably longer and more continuous with the spine proper. Both types of spinal barbs may be present on the same specimen, however, only one type is present on a particular spine.

Measurements of spinal barbs were carried out on several specimens; however, it must be noted that comparable measurements are very difficult to obtain owing to the necessity of proper orientation of the spine being measured. The results presented in table 2 are reasonably representative and demonstrate statistically that the mean distance between apices is not significantly different, but that the mean length of the barbs is significantly different when comparing two spines on the same specimen. Generally, the spinal barbs appear about 20–25 μ from the proximal end of the spine, and continue to the distal end at intervals from 5–10 μ.

The basic morphology of the triradiate spines of

TABLE 2

Ratios of distances between apices (W) and length (L) of spinal barbs. Measurements were taken from the specimen of *Hastigerina pelagica* illustrated in plate 1 figure 1.

	Spine 1				Spine 2		
	W(μ)	L(μ)	W/L		W(μ)	L(μ)	W/L
	1.45	2.10	1.44		1.40	2.30	1.65
	1.13	1.61	1.43		1.23	1.78	1.44
	1.29	1.61	1.25		1.34	2.23	1.68
	1.13	1.61	1.43		1.35	2.52	1.87
	1.29	1.77	1.38		1.29	2.21	1.71
Mean	1.26	1.74	1.39	Mean	1.32	2.21	1.67

Globigerinella aequilateralis is similar to that of *Hastigerina pelagica*, except that on the former species the spines originate at the basal end with a circular cross section (pl. 1, fig. 7) and become triradiate at varying distances from the test. In both species spines often penetrate subsequent chambers and can be observed as triradiate spines without a shoulder and at a low angle to the surface of the test.

DISCUSSION

Our observations illustrate a difference between the triradiate spines of *Hastigerina pelagica* and *Gobigerinella aequilateralis*. The spinal barbs of *Hastigerina pelagica* are present on specimens from a wide geographic range, thus eliminating the possibility of (a) local environmental effects on test growth, or (b) additional polymorphism within the species.

Although we are dealing with only the skeletal remains of recently living animals, we would like to interpret the spinal barbs in terms of a biological function. Owing to experimental difficulties, natural histories of planktonic foraminifera have not been studied in the laboratory, other than a few observations of living specimens. Bé (1969) photographed a living *H. pelagica* primarily to show bubble-like capsules surrounding the test. Apparently, the gelatinous capsules are a characteristic peculiar to *H. pelagica*, and according to our observations so are the spinal barbs. Although Bé did not mention this in his text, spinal barbs are detectable in his plates, and it is possible to conceive a functional connection between the two features. Thus the spinal barbs of *H. pelagica* may be an inherent feature for a specific function in its natural history.

Bolli, Loeblich and Tappan (1957) and Banner and Blow (1960) emphasize that general test morphology is the main criterion to use in taxonomy, and based on similarities in chamber arrangement *Globigerinella* Cushman 1927 was considered a junior synonym of *Hastigerina* Thomson 1876. Lipps (1966) maintains that skeletal micromorphology of tests can be more effective in the interpretation of natural relationships between taxa than gross morphology, owing to evolutionary convergence of the latter in response to similar ecological stresses. Cushman (1927) erected *Globigerinella* on the basis of ". . . fine spines covering the test. . .", in contrast to the coarser and fewer spines of *Hastigerina*. On the basis of our findings we believe that *Globigerinella* is a valid genus and should be maintained.

ACKNOWLEDGMENTS

The authors extend their thanks to Drs. A. C. Grant, B. R. Pelletier and C. T. Schafer for critically reviewing the manuscript.

REFERENCES

BANNER, F. T., and BLOW, W. B., 1960, The taxonomy, morphology and affinities of the genera included in the subfamily *Hastigerininae*: Micropaleontology, v. 6, no. 1, p. 19–31.

BÉ, A. W. H., 1967, Foraminifera. Families *Globigerinidae* and *Globorotaliidae*: Fiches d'Identification du zooplankton, no. 108, Conseil Perm. Internat. Explor. Mer, Charlottenlund, Denmark, p. 2–9.

———, 1969, Microstructural evidence of the close affinity of *Globigerinella* Cushman to *Hastigerina* Thomson: Internat. Conf. Planktonic Microfossils. 1st. Geneva (1967) Proc., v. 1, p. 89–91.

BOLLI, H., LOEBLICH, A. R., and TAPPAN, H., 1957, Planktonic foraminiferal families *Hantkeninidae*, *Orbulinidae*, *Globorotaliidae* and *Globotruncanidae*: U.S. Natl. Mus. Bull. 215, p. 3–50.

CUSHMAN, J. A., 1927, An outline of a reclassification of the foraminifera: Cushman Lab. Foram. Research Contr., v. 3, pt. 1, no. 39.

HEMLEBEN, C., 1969, Ultramicroscopic shell and spine structure of some spinose planktonic foraminifera: Internat. Conf. Planktonic Microfossils 1st. Geneva (1967) Proc., v. 1, p. 254–256.

LIPPS, J. H., 1966, Wall structure, systematics, and phylogeny studies of Cenozoic planktonic Foraminifera: Jour. Paleontology, v. 40, n. 6, p. 1257–1273.

PARKER, F. L., 1962, Planktonic foraminiferal species in Pacific sediments: Micropaleontology, v. 8, n. 2, p. 219–250.

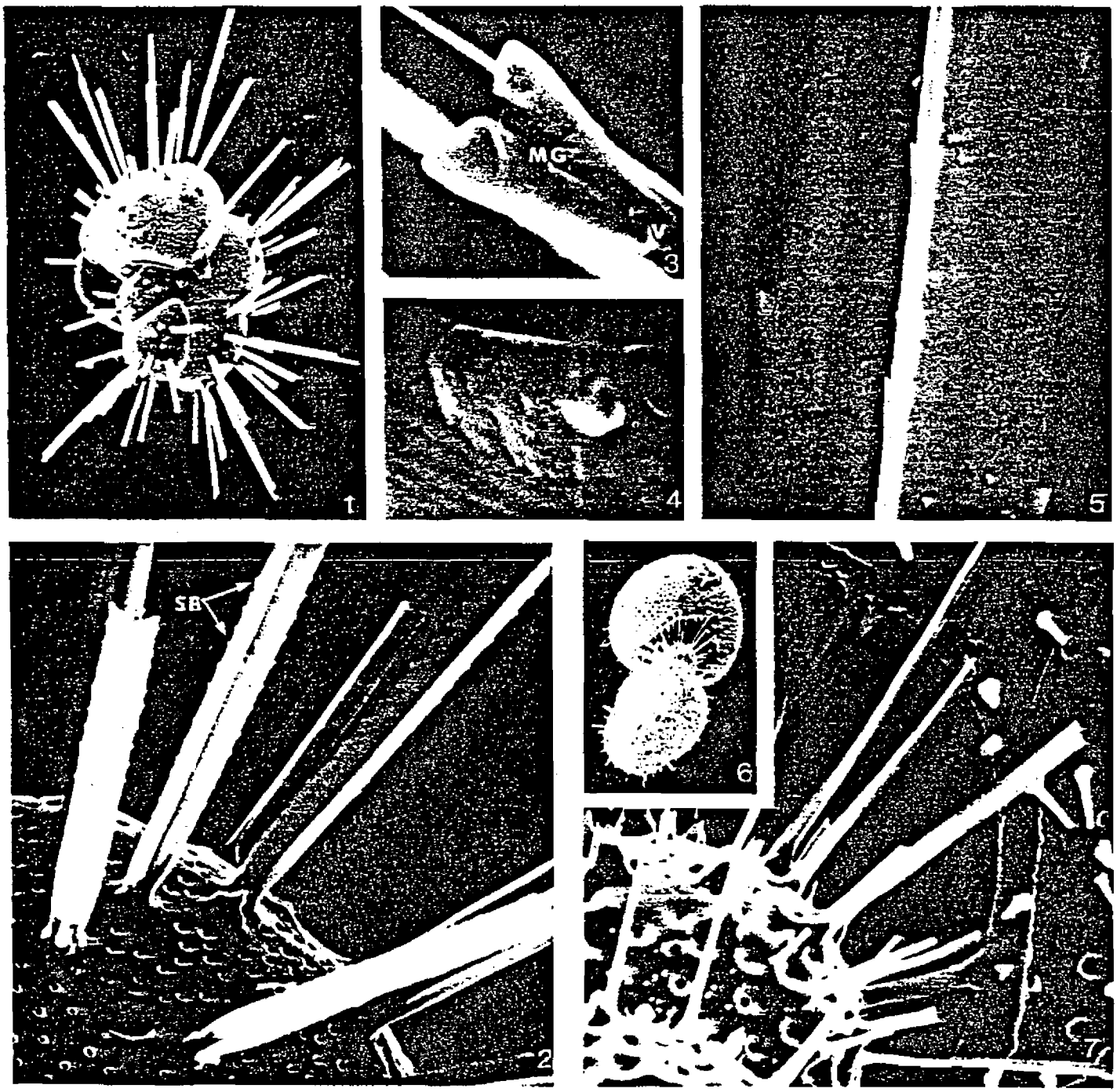
VILKS, G., 1970, New method for separation of skeletal material from a plankton sample: Maritime Sediments, v. 6, n. 2, p. 72–73.

Ms submitted January 1973

PLATE 1

1–5 *Hastigerina pelagica* (d'Orbigny) (1, 2, 4, 5. Sample 69–050VC–104; 3. Sample 69–302VC–2) 1. Whole test, ×100. 2. Enlarged portion of the test showing spinal barbs (SB) along the edges of the triradiate spines, ×700. 3. Individual spinal barb showing apices (A), medial groove (MG) and vertex (V), ×22,000. 4. Individual spinal barb illustrating the textural discontinuity between the spine and the spinal barb ×22,000. 5. A single triradiate spine with the alternate type of spinal barb, with the more pointed apices, no medial groove, and larger basal shoulder more continuous with the spine proper. ×3,000.

6–7 *Globigerinella aequilateralis* (Brady). (Sample 69–050VC–100.) 6. Whole test, ×100. 7. Enlarged portion of test illustrating lack of spinal barbs, ×1,000.


1
MG
V
3
4
5
SB
2
6
7

Deep-Sea Research, 1976, Vol. 23, pp. 457 to 465. Pergamon Press. Printed in Great Britain.

Particulate organic carbon in the Atlantic and Pacific oceans

PETER J. WANGERSKY*

(*Received* 7 *May* 1975; *in revised form* 29 *August* 1975; *accepted* 1 *September* 1975)

Abstract—When uniform methods of collection and analysis are employed, particulate organic carbon (POC) distributions in the South Atlantic, South Pacific, and North Pacific oceans are roughly comparable. All three regions display a logarithmic decrease in POC with depth, along with occasional anomalously high values.

INTRODUCTION

WHILE a large body of data has accumulated on the distribution of particulate organic carbon (POC) in the world oceans (BOGDANOV, 1965; BOGDANOV and OVCHINNIKOVA, 1965; BOGDANOV and SHAPOSHNIKOVA, 1971; DAL PONT and NEWELL, 1963; EHRHARDT, 1969; GORDON, 1971; GUNDERSEN, MOUNTAIN, TAYLOR, OHYE and SHEN, 1972; HOBSON, 1967; HOBSON and MENZEL, 1969; HOLM-HANSEN, STRICKLAND and WILLIAMS, 1966; JACOBS and EWING, 1969; KANE, 1967; MENZEL and RYTHER, 1968; NAKAJIMA, 1969; NEWELL and KERR, 1968; RILEY, 1963, 1970; RILEY, WANGERSKY and VAN HEMERT, 1964; SUSHCHENYA and FINENKO, 1966; WANGERSKY and GORDON, 1965; and many others), much of the work has been done by investigators using somewhat different methods of collection and analysis. Even within the body of work produced by a single investigator, development of methods has proceeded in parallel with data gathering. As yet unpublished work from this laboratory suggests that relatively minor differences in methodology can result in large differences in amounts of POC measured. Therefore, it has been difficult to compare POC values found for different regions of the oceans.

The *Hudson* 70 cruise around the Americas provided an opportunity to collect data along the 30th meridian in the South Atlantic, from the Equator to 54° 54·8′S, and in the Pacific, along the 150th meridian, from 62° 55·8′S to 54° 25′N. All of these samples were collected by the same group of scientists, treated in the same manner, and analyzed on the same instrument by the same analyst. They constitute the most uniform body of data on POC in the two oceans that has yet been produced, the major variables being the season of year and the location from which the samples were taken.

SAMPLING

The sampling stations were chosen at relatively even intervals over the vast area covered (Figs. 1 and 2, Tables 1 and 2). On the South Atlantic leg, stations were approximately 2°30′ apart until we neared the Antarctic Convergence. From 49 to 54°S, the stations were spaced at 1°30′ intervals until the station farthest south, at 54°54·8′S, was reached. We then ran a line of stations across the sill into the Argentine Basin, and another station well into the basin.

On the Pacific leg, the stations were generally spaced 5° apart until we reached 10°N. After that, because of limitations of time, the stations were 6° apart. A special surface cast was taken at the Equator in the Pacific.

SAMPLING METHODS

Samples were taken in 5-liter Niskin sampling bottles. A shallow and a deep cast were taken at each station. Generally, eight bottles were used on

*Department of Oceanography, Dalhousie University, Halifax, Nova Scotia, Canada.

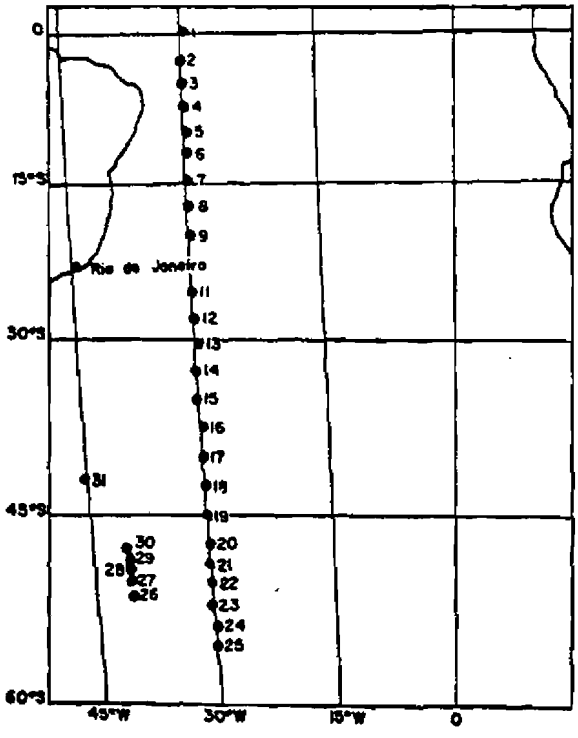


Fig. 1. Station positions, South Atlantic Ocean.

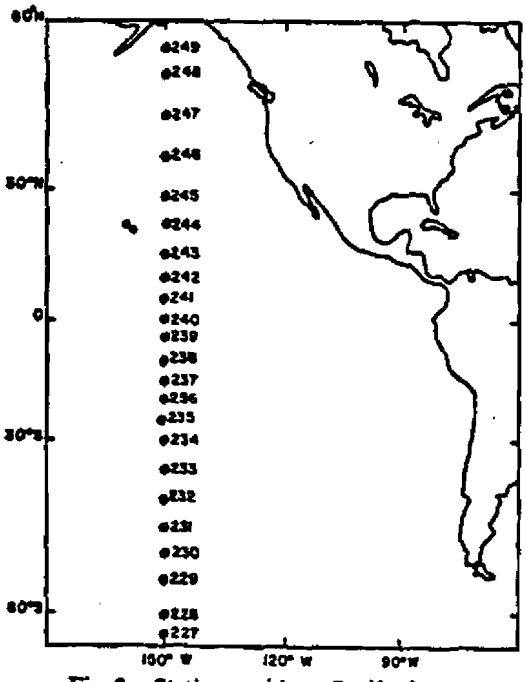


Fig. 2. Station positions, Pacific Ocean.

Table 1. Station positions, Atlantic Ocean.

Station No.	Latitude	Longitude	Date
1	0° 1.8'N	29°58.1'W	30 Nov. 1969
2	2°28.8'S	30° 4.3'W	1 Dec. 1969
3	4°54.7'S	30° 0.5'W	2 Dec. 1969
4	7°27.1'S	30° 3.2'W	3 Dec. 1969
5	9°58.6'S	30° 2.8'W	4 Dec. 1969
6	12°25.5'S	30° 6.8'W	5 Dec. 1969
7	14°54.7'S	30° 6.5'W	6 Dec. 1969
8	17°31.6'S	30° 1.2'W	7 Dec. 1969
9	20° 0.2'S	30° 0.2'W	8 Dec. 1969
11	25° 1.5'S	30° 1.6'W	10 Dec. 1969
12	27°31.6'S	30° 7.0'W	23 Dec. 1969
13	30° 4.3'S	29°56.4'W	24 Dec. 1969
14	32°25.1'S	30° 9.6'W	25 Dec. 1969
15	34°59.7'S	30° 4.7'W	26 Dec. 1969
16	37°28.4'S	29°59.2'W	27 Dec. 1969
17	39°55.0'S	29°53.0'W	28 Dec. 1969
18	42°29.9'S	29°57.5'W	29 Dec. 1969
19	45° 7.3'S	29°58.7'W	30 Dec. 1969
20	47°34.6'S	29°53.4'W	31 Dec. 1969
21	49° 3.4'S	29°48.7'W	1 Jan. 1970
22	50°33.3'S	29°35.4'W	2 Jan. 1970
23	52° 3.7'S	30° 3.7'W	3 Jan. 1970
24	53°27.2'S	29°59.5'W	4 Jan. 1970
25	54°54.8'S	29°23.2'W	5 Jan. 1970
26	51°27.9'S	39°57.3'W	8 Jan. 1970
27	49°59.0'S	39°57.8'W	9 Jan. 1970
28	48°58.9'S	39°52.4'W	9 Jan. 1970
29	47°58.9'S	39°59.6'W	10 Jan. 1970
30	47° 3.3'S	40° 4.6'W	11 Jan. 1970
31	41°46.5'S	46°26.4'W	13 Jan. 1970

the shallow cast and seven on the deep cast. In every case, the Niskin bottles were within 30 m of bottles carrying reversing thermometers. The depths given in this paper are therefore corrected depths. The Niskin bottles were spaced with reference to water mass structure reported from the area being sampled.

A 100-ml sample was taken from each bottle before filtration. The rest of the sample was filtered by gravity through a Selas Flotronic® silver filter of 0·8-μm pore size, held in a Sterilfil® polycarbonate filter holder. Before use, the silver filters were held at 450°C in an electric muffle furnace for 1 h, to reduce their organic carbon content. The 0·8-μm pore size was used in preference to the more customary 0·45 μm, because the manufacturer had informed us that when the 0·45-μm filters were heated to remove the large

Table 2. Station positions, Pacific Ocean.

Station No.	Latitude	Longitude	Date
227	62°55.8'S	149°57.9'W	27 April 1970
228	59°54.2'S	149°56.3'W	28 April
229	54°55.7'S	149°49.7'W	30 April
230	49°55.9'S	150° 1.3'W	1 May
231	44°54.9'S	150° 1.7'W	3 May
232	39°59.6'S	150° 1.4'W	4 May
233	35° 0.0'S	149°59.9'W	6 May
234	29°58.4'S	149°58.2'W	7 May
235	24°50.1'S	150° 0.7'W	9 May
236	19°57.8'S	150° 2.9'W	10 May
237	15° 3.1'S	149°59.7'W	17 May
238	9°50.0'S	150° 1.5'W	19 May
239	4°59.3'S	150° 8.3'W	20 May
240	0° 3.6'N	149°52.2'W	22 May
241	4°47.4'N	150° 0.2'W	23 May
242	10° 5.1'N	150° 3.8'W	25 May
243	16° 2.8'N	150° 5.7'W	26 May
244	22° 9.8'N	149°58.9'W	28 May
245	28°50.2'N	149°57.3'W	30 May
246	35°56.7'N	149°54.5'W	1 June
247	42°48.6'N	149°51.9'W	3 June
248	49° 9.0'N	150° 0.4'W	4 June
249	54°25.0'N	150° 4.6'W	6 June

and variable amounts of carbon they contained, their effective pore size increased to approximately 0·8 μm. The 0·8-μm filters were not appreciably changed in filtering characteristics by the heat-treatment.

After all of the sample had been filtered, the filters and filter holders were rinsed with two 25-ml rinses of distilled water, and the filters were stored in sealed Petri dishes in a freezer until analysis. The analytical technique, a dry combustion method, has already been described in detail (WANGERSKY, 1974), and will only be summarized here. In the laboratory the silver filters are folded and placed in quartz combustion tubes. To remove any inorganic carbon, 0·5 ml of 0·1N HCl is added, and the samples are dried under vacuum. The dry samples were then oxidized in a commercial micro-combustion furnace, using platinized asbestos as a catalyst, and the CO_2 evolved was measured with a non-dispersive infra-red CO_2 analyzer. For increased sensitivity, peak area rather than peak height was measured. This required a linearization of the output signal from the analyzer, followed by electronic integration.

Blanks were calculated from the analysis of filters that had undergone every step in the procedure, including the loading into filter holders, but had not had water drawn through them. We did not use the double-filter blank method suggested by MENZEL (1966) because both our own work and that of GORDON and SUTCLIFFE (1974) showed no significant absorption of dissolved organic carbon on the silver filters.

RESULTS

These data, almost 800 data points spread over two oceans, are almost too great to visualize in any simple form. Data of this kind are usually presented in the form of contoured sections. However, for reasons to be discussed in later sections of this paper, the data do not lend themselves to contouring, and I have chosen to present them by entering the data directly upon the sections (Figs. 3 to 5).

The reproducibility of the analytical method is good; the largest variable is the variability of the filter blank, which was ± 0·5 μg C l^{-1}. The real limitation on the interpretation of POC distribution is the inhomogeneity of the universe sampled. In an earlier paper (WANGERSKY, 1974) I found that the combined variability of sampling and analysis resulted in a standard deviation of ± 1·3 μg C l^{-1}. This standard deviation was calculated from replicates taken by rigging a Niskin rosette sampler to trip five bottles simultaneously at a given depth. Thus, for samples taken in 5-liter Niskin bottles and treated as described in this paper, a difference between two samples greater than 5 μg C l^{-1} suggested that they were drawn from regions of differing POC content.

In both oceans, the upper layers are regions of high POC values. Our shallowest samples were taken at 5 m to avoid contamination by organic materials coming from the ship; therefore we do not have true surface or sub-surface samples. The region of high POC always extended to the second bottle, usually at 25 m, but only occasionally to the third, somewhere below 100 m.

THE SOUTH ATLANTIC

The surface layer values in the South Atlantic

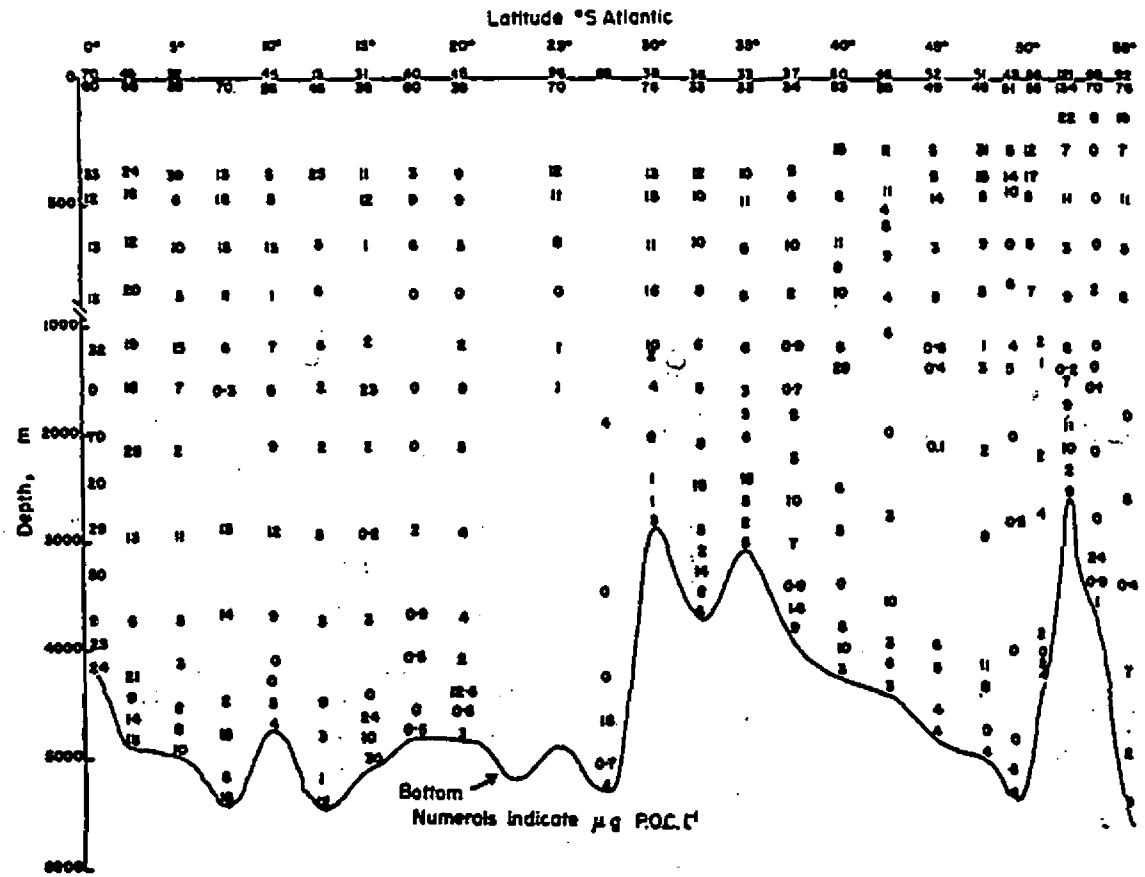


Fig. 3. Section from Equator to 55°S, along 30°W, South Atlantic Ocean.

were generally high and corresponded to well-known hydrographic features in their distribution. A region of higher values extended from the Equator to 10°S, and another was in the general region of 25°S. The latter region was not well defined on our samples because technical difficulties forced us to miss all of one station and parts of two others in this area. A region of low values extended from 30 to 37°S; south of this belt, the surface layer POC increased, reaching a peak at the Antarctic Convergence at 52°S. This series of samples is unusual in that although the first and last stations were occupied 2 months apart, they were all in essentially the same season, early summer. The high values at the southern end of the line were probably the remnants of the spring bloom. The contents of zooplankton tows taken at these stations demonstrated that we were still too early for the annual appearance of the krill.

The extension of the line, from Sta. 26 to 31, was designed to sample the deep water flowing into the Argentine Basin. The surface POC values were typical of surface values found in the region, away from the immediate area of the convergence.

The form of statistical summation used in this report is the frequency distribution of the logarithm of the concentration. This form serves to minimize the effect of the occasional high values; if the plots were of the actual, rather than the log concentration, all of the distributions would be skewed. At least some of the regularity in the frequency distributions shown results from the evenness of the sampling pattern and the condensation of sample range brought about by the use of the log transform.

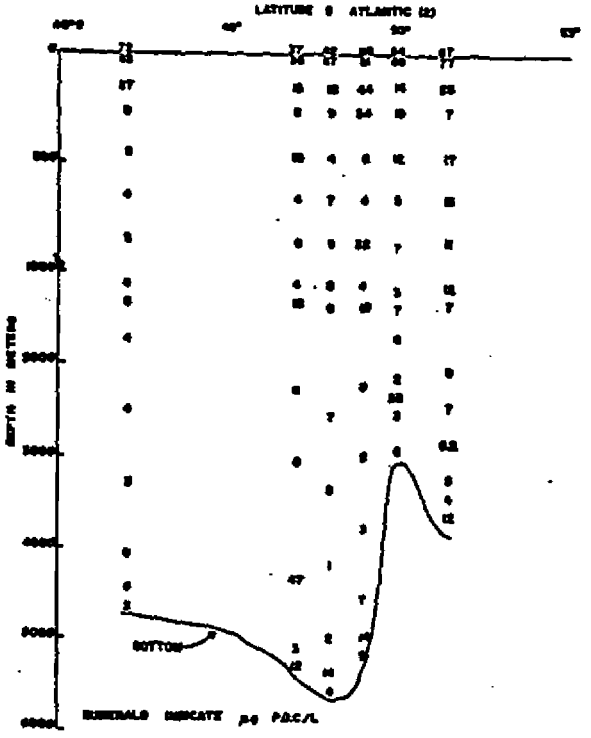


Fig. 4. Section across the sill into the Argentine Basin, South Atlantic Ocean.

The surface layer values range from a low of 13 μg C l^{-1}, at 12°25·5′S, 30°2·8′W, to a high of 134 μg C l^{-1} at the Antarctic Convergence. The overall surface layer average was 54 μg C l^{-1}. There is no consistent pattern of distribution with depth within this layer; the deeper sample is as often higher than the 5-m sample as it is lower. Both samples usually contain about the same amount of carbon. In only three stations are there large differences between the top two samples.

Ideally, the deeper water should be divided into regions determined by water mass distributions. However, some water masses, such as the Antarctic Intermediate Water, are represented by only a few samples in the Atlantic stations. It seemed more reasonable, therefore, to group the POC results by depth. The divisions used were 0 to 100 m, 100 to 500 m, 500 to 1000 m, 1000 to 3000 m, and > 3000 m. The Antarctic Intermediate Water would generally fall into the 100-to 500-m group, but it is seldom represented in the Atlantic samples. The 1000- to 3000-m group is principally Arctic Deep Water, while the > 3000-m group contains almost all of the Antarctic Bottom Water samples. The salinity and temperature data from this cruise are too voluminous to be included in this report, but can be obtained from the Bedford Institute of Oceanography.

When the POC values are so grouped, a steady decrease with depth can be demonstrated down to the Arctic Deep Water. The number of samples, average values, and other statistical parameters are given in Table 3. The averages of the log concentrations, rather than the average concentrations, are used to minimize the effects of the occasional large value on the average.

In the South Atlantic samples, the differences between the mean values of adjacent water layers are significant down to the 1000- to 3000-m group. A significant difference might have been demonstrated between the 1000- to 3000-m and the > 3000-m layers if the high values near the bottom of the first six stations, possibly part of a nepheloid layer, had been omitted. Even with these high values included, an overall inverse correlation with depth can be shown, with a correlation coefficient of − 0·76, significant at the 0·1% level. The regression is logarithmic rather than linear. A similar logarithmic decrease with depth was shown for particle number by SHELDON, PRAKASH and SUTCLIFFE (1972).

The amount of POC at any particular point in the ocean is a summation of processes of supply and utilization. At least three sources of supply must be considered: the descent through the water column of materials formed at the surface, the transport of material with the water mass in its descent from the surface, and the production of particles *in situ* by local events such as the death and decomposition of zooplankton or fish. In most cases, it is difficult to evaluate the relative importance of the first two sources. Most investigators have found little relationship between surface productivity and the standing crop of organic particulate matter in the waters directly below. The effect of high productivity can sometimes be seen one sample further down than usual, but never beyond that, in our stations. The

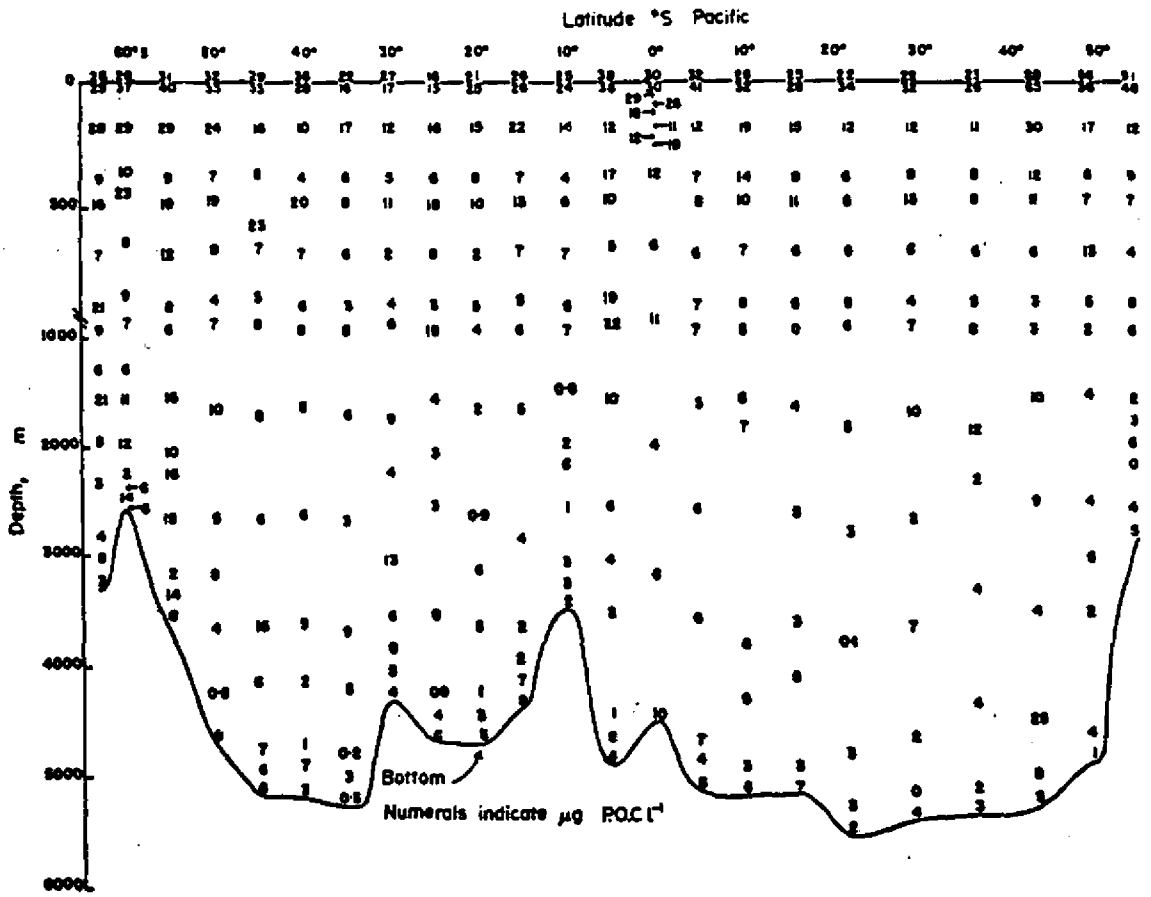


Fig. 5. Section along 150°W, from 65°S to 55°N, Pacific Ocean.

dominant effect on POC content in the deeper water seems to be the appearance of small regions of high POC content. In an earlier paper (WANGERSKY, 1974) a 5% frequency of unusually high samples was found in replicate samples taken by closing all of the bottles on a rosette sampler simultaneously. Such anomalous values occurred in approximately 7% of the South Atlantic samples. Because a decision as to whether a sample value is anomalous must be subjective when only a single sample is taken at any given depth, agreement with the earlier work is reasonably close.

At least some of the high values from deep water may not be anomalous. Over the interval from Sta. 1 to Sta. 6 there are high values in the bottom few bottles, possibly reflecting the presence of a nepheloid layer. In the Pacific, where our sampling line did not come close to a continental shelf, such regions of high POC near the bottom did not occur.

In the South Atlantic section, then, the dominant features of the POC distribution are: (1) in the surface waters, a regional variation correlated with primary productivity; (2) a logarithmic decrease with depth, at least down to 3000 m; (3) a possible contribution from a nepheloid layer in Sta. 1 to 6; and (4) a number of apparently random local high values scattered through an otherwise rather uniform background of particles in each of the deeper water masses.

THE PACIFIC SECTION

The correspondence between POC distributions in the two oceans is close. The major differences are in the surface values, where Pacific

samples are generally lower (Fig. 5), and in the absence of high values near the bottom. The lower surface values may well be due to seasonal effects; the samples from the southern section were taken in winter, while those from the South Atlantic were taken in early summer. The highest values in the Pacific were in the North Pacific and correspond to those taken in the South Atlantic at roughly the same season. However, the South Atlantic was sampled much more intensively, particularly in the regions of greatest productivity.

Below the surface layer, the distribution of POC in the two oceans is essentially the same, even to average values (Tables 3 and 4, Fig. 7). The Pacific seems to display fewer samples with zero values, but this may reflect a difference in the variability of the blank values of the lots of filters used. On the basis of this series of samples, we may safely conclude that there is no real difference in the POC content of the two oceans, when POC is defined by the sampling method described in this paper.

Table 3. Change in POC with depth, South Atlantic Ocean.

Depth range (m)	log POC	POC μg C/liter	D. F.	t
0 – 100	1.732	54		
			125	15.9
100 – 500	1.041	11		
			127	4.9
500 – 1000	0.638	4.6		
			185	1.8
1000 – 3000	0.479	3.0		
			231	0
>3000	0.482	3.0		

Table 4. Change in POC with depth, Pacific Ocean.

Depth range (m)	log POC	POC μg C/liter	D. F.	t
0 – 100	1.478	30		
			116	10.9
100 – 500	1.071	11.8		
			136	7.4
500 – 1000	0.799	6.3		
			127	2.1
1000 – 3000	0.690	4.9		
			144	1.94
>3000	0.558	3.6		

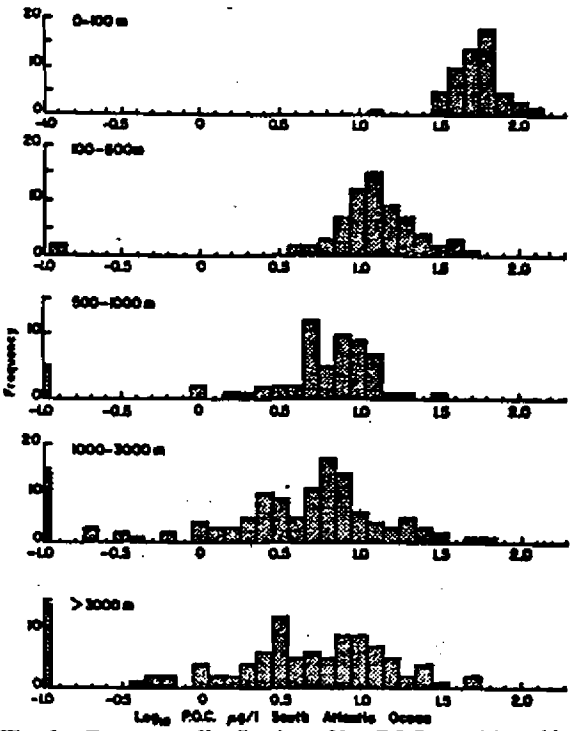


Fig. 6. Frequency distribution of log POC, partitioned by depth, South Atlantic Ocean.

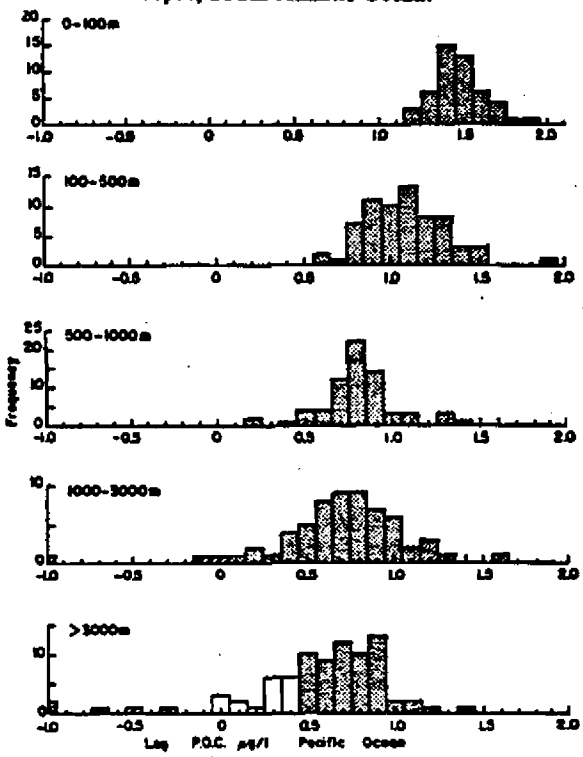


Fig. 7. Frequency distribution of log POC, partitioned by depth, Pacific Ocean.

The sampling pattern in the Pacific was such that a series of samples was taken in the Antarctic Intermediate Water, from our most southerly station, at 63°S, almost to the Equator. This water mass is generally near 500 m in this region. POC values in this water mass were uniformly higher than in the samples immediately above and below (Fig. 5). The water mass could be followed almost to the Equator by the elevated POC values alone.

A special cast, with samples at closer than normal intervals in the surface layer, was made at the Equator. POC decreased with depth within the layer.

The decrease in POC with depth in the Pacific follows the same pattern as in the Atlantic (Fig. 7), except that significant differences between layers can be found all the way to the bottom (Table 4). The regression of POC against depth accounts for about 80% of the variability in POC; the remaining 20% is presumably in the always more variable surface layers and in the isolated high values present in deeper water, which I have inferred to be the result of sampling small patches rich in organic carbon (WANGERSKY, 1974). If we accept the usual operational definition of POC as that part of the organic carbon caught by a filter of given pore size, then the decrease in POC with depth suggests either a utilization of POC all the way to the bottom or a shift in particle size out of the range sampled by our filtration system. It is not possible to distinguish between those possibilities on the basis of POC values alone. However, any agency bringing about such a shift in particle size distribution at these depths is probably biological, and would be expected to use some of the organic carbon as part of the process. This possibility can be examined by dividing the Pacific data into northern and southern groups at the Equator. If *in situ* utilization is occurring, the average value of the POC in the Antarctic Bottom Water should be higher in the younger southern section than in the northern half. This is the case; the average value for the southern half was 6·7 μg C l^{-1}, compared to 4·9 μg C l^{-1} for the northern portion. A paired *t*-test produces a value of $t = 1{\cdot}83$, with $D = 103$, the two means being significantly different at the 95% level.

As in the South Atlantic, anomalously high values of POC occurred in 7% of the samples. This phenomenon holds for both oceans, and appears to be a normal feature of all marine environments. In the most northerly stations the POC in the surface layers reflected the occurrence of the spring phytoplankton bloom. The effects of this bloom did not appear in the POC content of the deeper waters, although not enough samples were taken in the area of the bloom to determine whether an increase in the proportion of anomalously high values of POC might be found in the deeper layers.

CONCLUSIONS

1. When uniform collections and analytical treatments are employed, the POC values in the Atlantic and Pacific Oceans are essentially the same.
2. In the surface layers, the POC values are a function of productivity, and thus display a seasonal variation as well as a variability determined by the local hydrography.
3. POC content falls off logarithmically with depth, at a rate roughly comparable in the two oceans.
4. Superimposed on this distribution are occasional (~ 7%) patches considerably above the background values in POC.
5. There is some evidence for *in situ* utilization of POC in the deep water.

Acknowledgements—This research could not have been performed without the help of the Bedford Institute of Oceanography and the officers and men of the C.S.S. *Hudson*. The work was supported by grants from the National Research Council of Canada.

REFERENCES

BOGDANOV YU. A. (1965) Suspended organic matter in the Pacific. *Oceanology*, **5**, 77–85.

BOGDANOV YU. A. and L. I. OVCHINNIKOVA (1965) Procedure for determining bituminous substances in suspension. *Oceanology*, **5**, 137–141.

BOGDANOV YU. A. and M. G. SHAPOSHNIKOVA (1971) Concentrations of suspended organic matter in tropical Pacific water. *Oceanology*, **11**, 668–673.

DAL PONT G. and B. NEWELL (1963) Suspended organic matter in the Tasman Sea. *Australian Journal of Marine and Freshwater Research*, **14**, 155–165.

EHRHARDT M. (1969) The particulate organic carbon and nitrogen, and the dissolved organic carbon in the Gotland Deep in May 1968. *Kieler Meeresforschungen*, 25, 71–80.

GORDON D. C., JR. (1971) Distribution of particulate organic carbon and nitrogen at an oceanic station in the central Pacific. *Deep-Sea Research*, 19, 1127–1134.

GORDON, D. C., JR. and W. H. SUTCLIFFE, JR. (1974) Filtration of seawater using silver filters for particulate nitrogen and carbon analysis. *Limnology and Oceanography*, 19, 989–993.

GUNDERSEN K., C. W. MOUNTAIN, D. TAYLOR, R. OHYE and J. SHEN (1972) Some chemical and microbiological observations in the Pacific Ocean off the Hawaiian Islands. *Limnology and Oceanography*, 17, 524–531.

HOBSON L. A. (1967) The seasonal and vertical distribution of suspended particulate matter in an area of the northeast Pacific Ocean. *Limnology and Oceanography*, 12, 624–629.

HOBSON L. A. and D. W. MENZEL (1969) The distribution and chemical composition of organic particulate matter in the sea and sediments off the east coast of South America. *Limnology and Oceanography*, 14, 159–163.

HOLM-HANSEN O., J. D. H. STRICKLAND and P. M. WILLIAMS (1966) A detailed analysis of biologically important substances in a profile off Southern California. *Limnology and Oceanography*, 11, 548–561.

JACOBS M. B., and M. EWING (1969) Suspended particulate matter: concentration in the major oceans. *Science*, 163, 380–383.

KANE J. E. (1967) Organic aggregates in surface waters of the Ligurian Sea. *Limnology and Oceanography*, 12, 287–294.

MENZEL D. W. (1966) Bubbling of sea water and the production of organic particles: a re-evaluation. *Deep-Sea Research*, 13, 963–966.

MENZEL D. W. and J. H. RYTHER (1968) Organic carbon and the oxygen minimum in the South Atlantic Ocean. *Deep-Sea Research*, 15, 327–337.

NAKAJIMA K. (1969) Suspended particulate matter in the waters on both sides of the Aleutian Ridge. *Journal of the Oceanographical Society of Japan*, 25, 239–248.

NEWELL B. S. and J. D. KERR (1968) Suspended organic matter in the south-eastern Indian Ocean. *Australian Journal of Marine and Freshwater Research*, 19, 129–138.

RILEY G. A. (1963) Organic aggregates in seawater and the dynamics of their formation and utilization. *Limnology and Oceanography*, 8, 372–381.

RILEY G. A. (1970) Particulate organic matter in sea water. *Advances in Marine Biology*, 8, 1–118.

RILEY G. A., P. J. WANGERSKY and D. VAN HEMERT (1964) Organic aggregates in tropical and subtropical surface waters of the North Atlantic Ocean. *Limnology and Oceanography*, 9, 546–550.

SHELDON R. W., A. PRAKASH and W. H. SUTCLIFFE, JR. (1972) The size distribution of particles in the ocean. *Limnology and Oceanography*, 17, 327–340.

SUSHCHENYA L. M. and Z. Z. FINENKO (1966) Concentration of suspended organic matter in tropical Atlantic water and some quantitative relationships of its compounds. *Oceanology*, 6, 682–692.

WANGERSKY P. J. (1974) Particulate organic carbon: sampling variability. *Limnology and Oceanography*, 19, 980–984.

WANGERSKY P. J. and D. C. GORDON, JR. (1965) Particulate carbonate, organic carbon, and Mn^{++} in the open ocean. *Limnology and Oceanography*, 10, 544–550.

Deep Zonal Water Masses in the Equatorial Pacific Ocean Inferred from Anomalous Oceanographic Properties

C. S. WONG

Ocean Chemistry Division, Marine Sciences Directorate, Pacific Region
Water Management Service, Department of the Environment
Victoria, British Columbia, Canada

Two deep zonal water masses at approximately 5°S and 10°N from 170° to 130°W and a depth of 4–5 km were inferred from anomalous oceanographic properties, in particular potential temperature and dissolved oxygen.

Meridional deep circulation in the Pacific Ocean has been inferred from the distribution of oceanographic properties [*Wooster and Volkmann*, 1960; *Knauss*, 1962; *Bien et al.*, 1963; *Weyl*, 1965; *Lynn and Reid*, 1968]. At shallow depths in the equatorial waters, eastward zonal flows have been discovered in a similar way [*Cromwell et al.*, 1954; *Reid*, 1959].

I report evidence of possible zonal deep water masses in the equatorial Pacific Ocean suggested by anomalous oceanographic data of potential temperature, dissolved oxygen, potential density, and dissolved silicate based mainly on the unusual values observed on the Canadian *Hudson 70* cruise, after which supporting evidence was sought from other data. (The word anomaly is used to imply the value of an oceanographic parameter that deviates from that expected from the north-south trend of the parameter at a specific location. Anomalous values in the same cruise, rather than cruise-to-cruise changes, form the main basis of my deduction. At this stage with insufficient data the judgment on whether the data are anomalous or erroneous is rather marginal. The inability of scientists to discover the Cromwell undercurrent from the anomalous oceanographic properties in the *Challenger* expedition of 1874–1875 and in the expeditions previous to the chance discovery by Cromwell in 1954 suggests the utility of examining such values critically.) Figures 1–4 show these properties from 20°S to 30°N at depths below 3 km for *Southern Cross* [*Ocean Research Institute*, 1970*a*] along 170°W, *Hakuho Maru IBP* [*Ocean Research Institute*, 1970*b*] along 155°W, *Hudson 70* along 150°W, and *Downwind* [*Scripps Institution of Oceanography*, 1965] along about 130°W.

Copyright © 1972 by the American Geophysical Union.

Anomalies in potential temperature and dissolved oxygen are very distinct in the *Hudson 70* profile along 150°W. (Similar anomalies in alkalinity are observed in the unpublished *Hudson 70* data, and these will be discussed in a separate paper on the carbonate chemistry.) At 5°S, values of 0.9°C temperature and 4.3 ml/l oxygen at 4.5–5.0 km indicate a core that is relatively younger than that of the surrounding waters; a similar core with 0.96°C potential temperature and 4.1 ml/l oxygen exists at about 5 km at 10°N (dotted areas in Figure 3*a*, *b*). Supporting evidence of much more marginal values can be sought in the distributions of potential density and dissolved silicate, as can be seen in the dotted areas in Figure 3*c*, *d*. (Potential density is a better parameter than salinity for representing the actual stratification. Both are subjected to the uncertainties associated with the conductivity determinations.)

Evidence of the eastward extension of the two cores of deep waters with anomalous values can be seen in the *Downwind* data along 130°W (Figure 4). The effect of the southern core is reflected in the temperature low of about 1.06°C, the oxygen high of about 4.0 ml/l, and less obviously in the potential density high of 27.82 and the dissolved silicate low of about 135 μmole/l in the 4.0- to 4.5-km zone at about 7°S. The northern core, now between the rims of the Clipperton and Clarion fractures, shows a slight temperature low of about 1.08°C, an

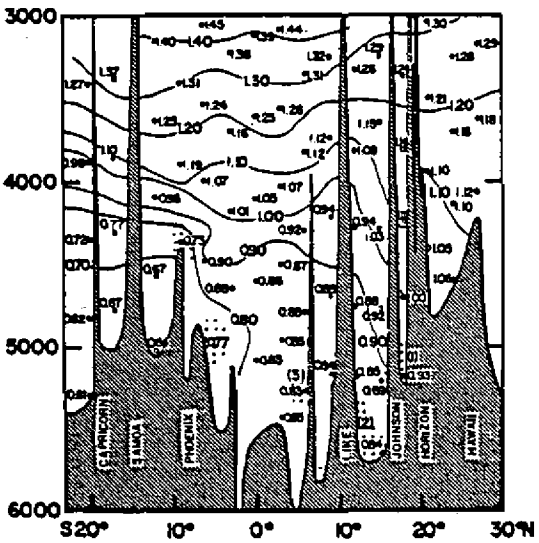


Fig. 1a.

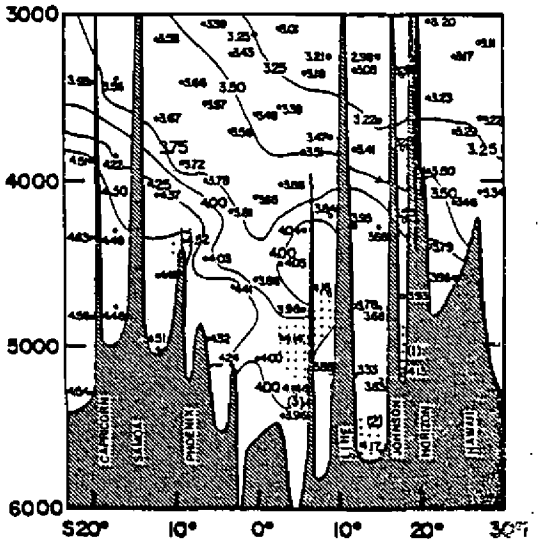


Fig. 1b.

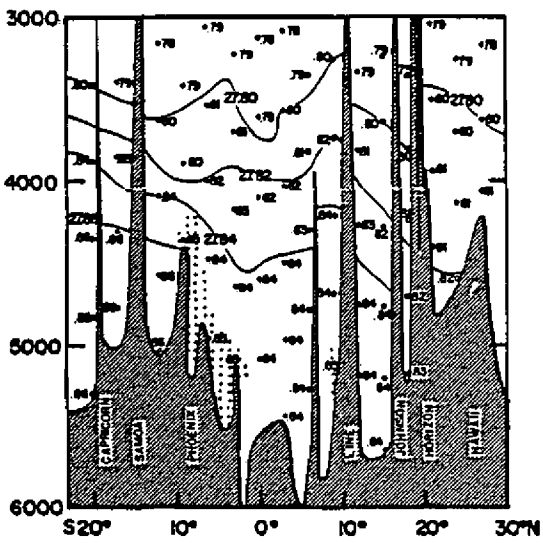


Fig. 1c.

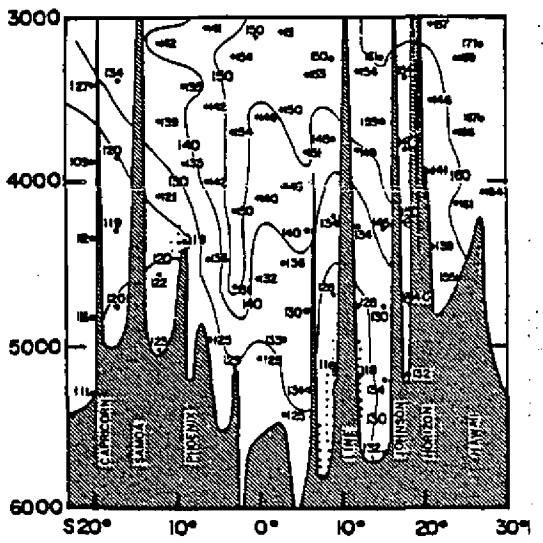


Fig. 1d.

Fig. 1. Along 170°W (*a*) potential temperature in degrees Celsius, (*b*) dissolved oxygen in milliliters per liter, (*c*) potential density in σ unit, and (*d*) dissolved silicate in micromoles per liter. The vertical scale is depth in meters.

oxygen high of about 3.75 ml/l, a potential density high of 27.82, and a dissolved silicate low of about 140 μmole/l at a depth below 4.0 km at 8°–11°N.

Effort to trace the cores in the oceanographic sections west of 150°W is hampered somewhat by the lack of deep data. In the *Hakuho Maru IBP* section at 155°W a northern core at about 10°N is quite evident from the occurrence of 0.97°C, 4.0 ml/l oxygen, and 141 μmole/l silicat and less obviously from the 27.83 density at 4.5-km depth. The southern core is difficult t pin point, because of a lack of data. Topo graphical evidence would suggest the passage a 8°S below 5 km to be the most likely place. Th temperature low of 0.99°C and the oxyge high of 4.2 ml/l at about 4.2 km for 10° would support the inference. The anomalies a

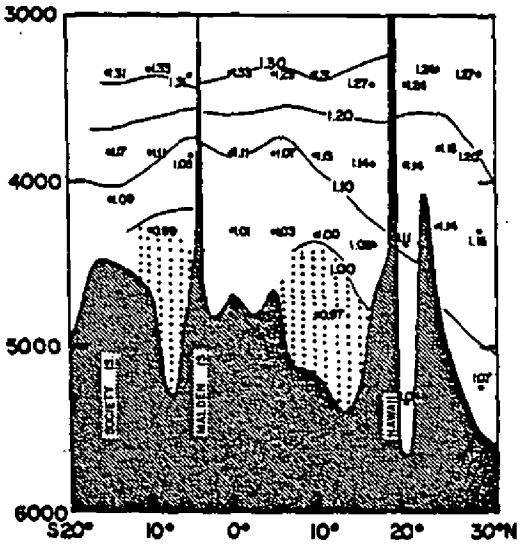


Fig. 2a.

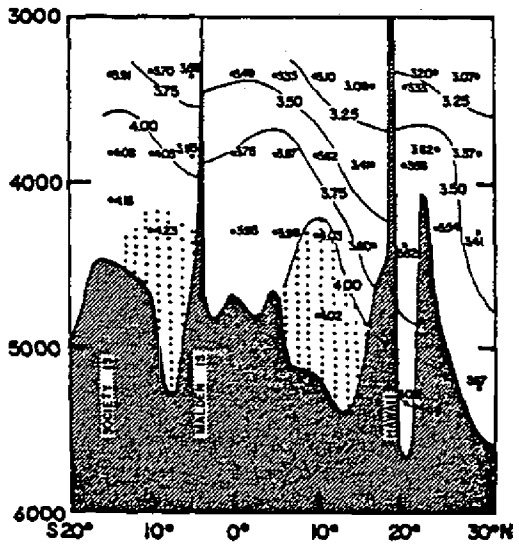


Fig. 2b.

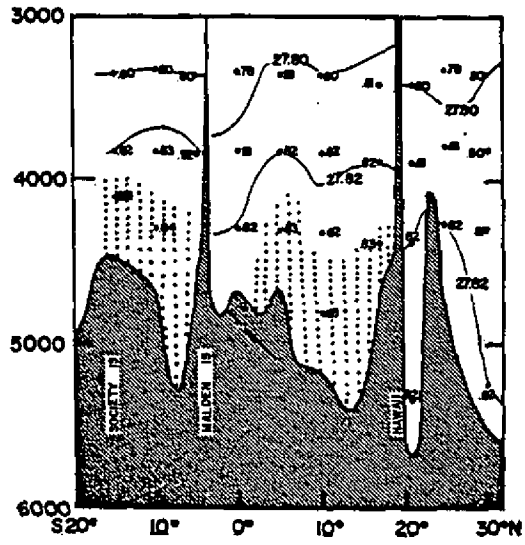


Fig. 2c.

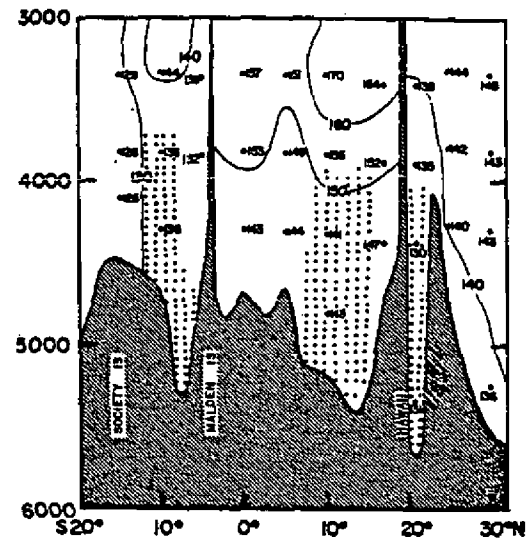


Fig. 2d.

Fig. 2. Along 155°W (*a*) potential temperature in degrees Celsius, (*b*) dissolved oxygen in milliliters per liter, (*c*) potential density in σ unit, and (*d*) dissolved silicate in micromoles per liter. The vertical scale is depth in meters.

21°N, just north of the Hawaiian Islands, belong to a different water mass moving around the island chain [*Edmond et al.*, 1971].

Three possible sets of anomalous values at 170°W would qualify as a source for the deep water in the northern core: (1) 4.13 ml/l oxygen and 0.93°C potential temperature at 18°N (station 13 of *Southern Cross*) at 5.2 km, (2) 4.17 ml/l oxygen and 0.84°C potential temperature at 15°N (station 14 of *Southern Cross*) at 5.7 km, and (3) 4.14 ml/l oxygen and 0.83°C potential temperature at 6°N (station 17 of *Southern Cross*). On the basis of a decrease of about 0.25 ml/l oxygen and a rise in potential temperature of about 0.13°C for a 20° longitude from 150° to 130°W, the source at 170°W should have an oxygen content of about 4.25 ml/l and a potential temperature of about

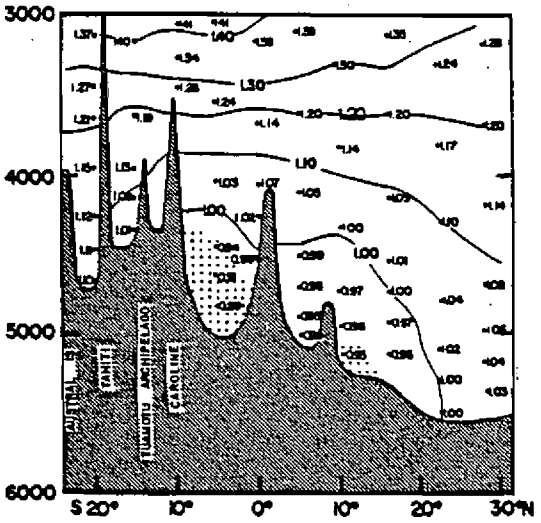


Fig. 3a.

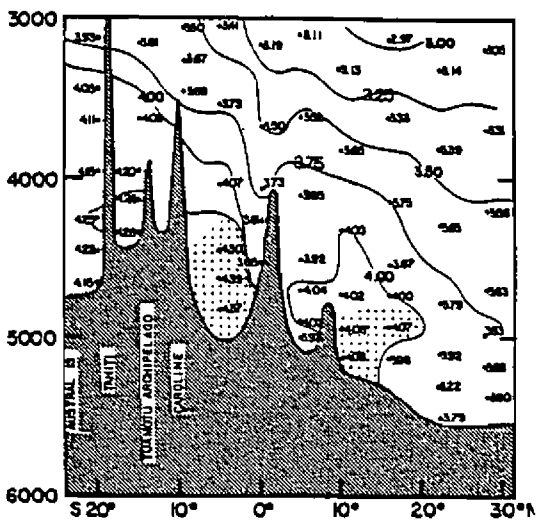


Fig. 3b.

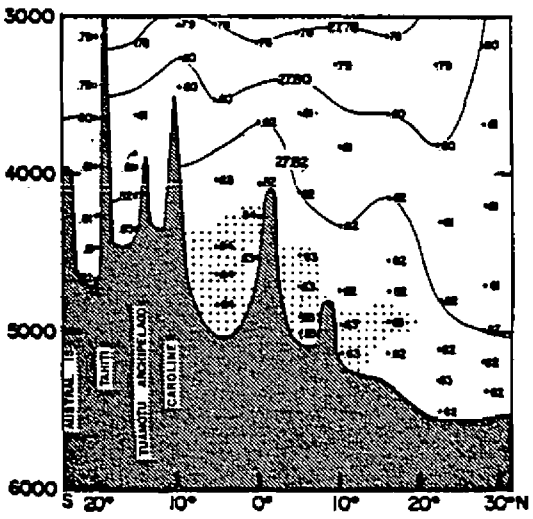


Fig. 3c.

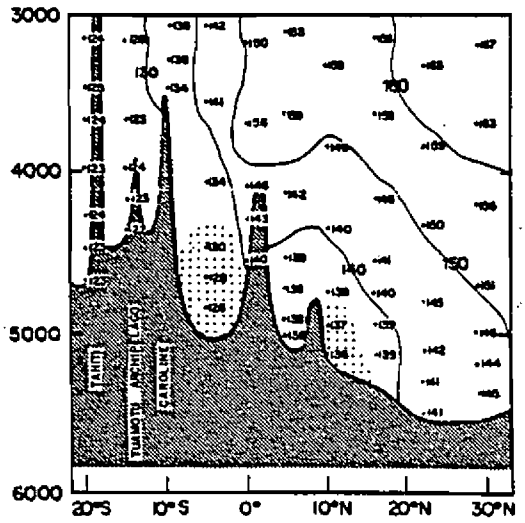


Fig. 3d.

Fig. 3. Along 150°W (*a*) potential temperature in degrees Celsius, (*b*) dissolved oxygen in milliliters per liter, (*c*) potential density in σ unit, and (*d*) dissolved silicate in micromoles per liter. The vertical scale is depth in meters.

0.84°C. Thus source 1 would be ruled out on the basis of too high a temperature. The topographical restraint of the Line Islands would rule out source 3. The most likely source of the northern core is the 15°N water at the entrance of the Clarion pass at 5.7 km with 4.2 ml/l oxygen and 0.84°C potential temperature.

A similar deduction applied to the southern core from a decrease of oxygen of about 0.3 ml/l and a potential temperature of 0.17° between 150° and 130°W would give values of 4.7 ml/l oxygen and 0.73°C potential temperature at 170°W. The most likely source is the water at 4.4 km at 9°S (station 22 of *Southern Cross*) with 0.73°C and 4.5 ml/l oxygen. The position is at the sill between the Samoa Islands and the Tokelau Islands. However, this would

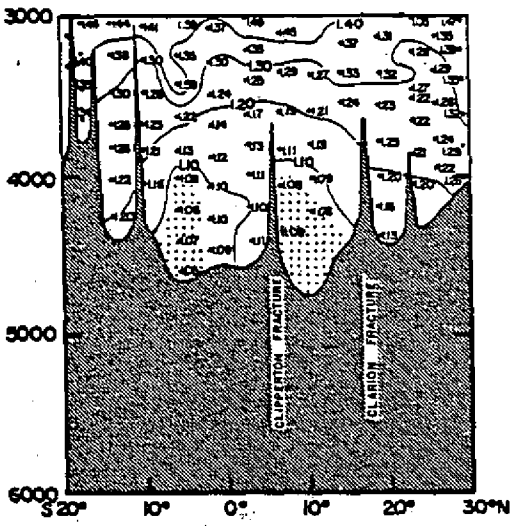


Fig. 4a.

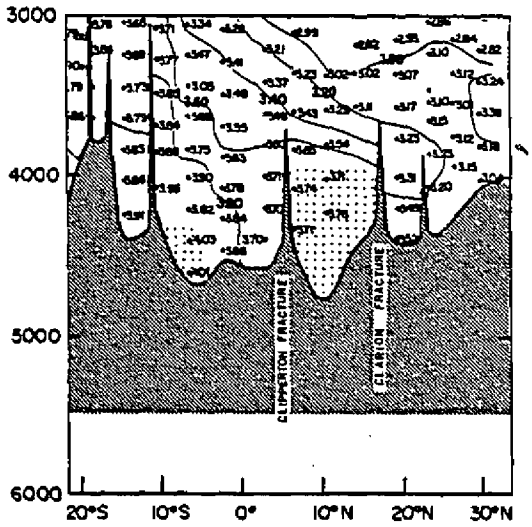


Fig. 4b.

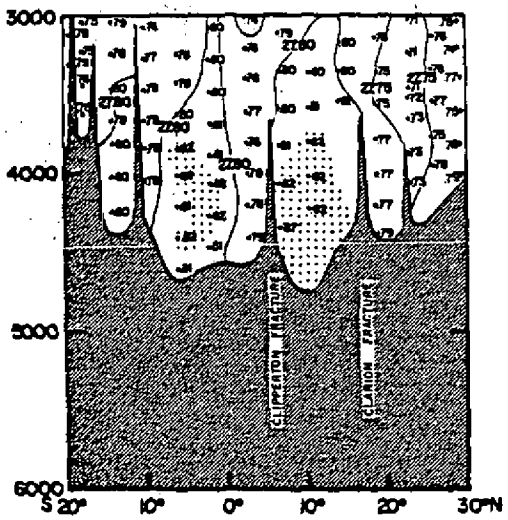


Fig. 4c.

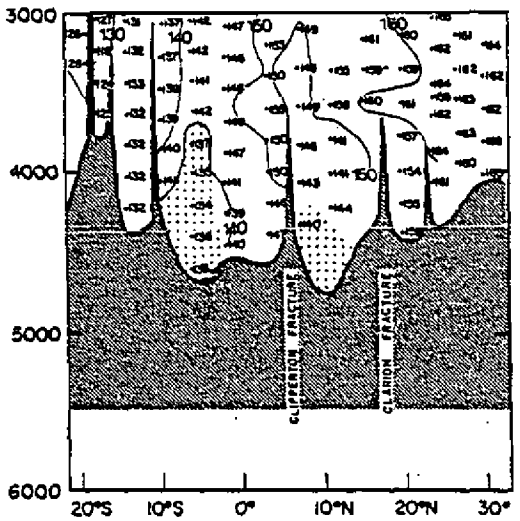


Fig. 4d.

Fig. 4. Along 130°W (*a*) potential temperature in degrees Celsius, (*b*) dissolved oxygen in milliliters per liter, (*c*) potential density in σ unit, and (*d*) dissolved silicate in micromoles per liter. The vertical scale is depth in meters.

not rule out the possibility that the southern core at 155°W may actually be at the sill between Tokelau Island and Cook Island or the Society Island chain. The most probable source of the southern core would be the 4.5-km water in the Southern basin, although the exact location of entry cannot be determined. The probable spreading of the cores is shown in Figure 5, and the possible values of the oceanographic properties of the cores are shown in Table 1.

Bottom topography [*Menard*, 1964; *Chase et al.*, 1971] appears to govern the spreading: the northern core is embayed against the southern rim of the North basin, i.e., between the Marcus-Necker rise and the Hawaii rise at 20°N and between the Line Island rise and the Clipperton extension at about 10°N, although the southern core is in the basin between the southern boundary of the Samoa-Tokelau rise, the Tuamotu archipelago, and the Marquesas rise at about 10°S and a northern boundary

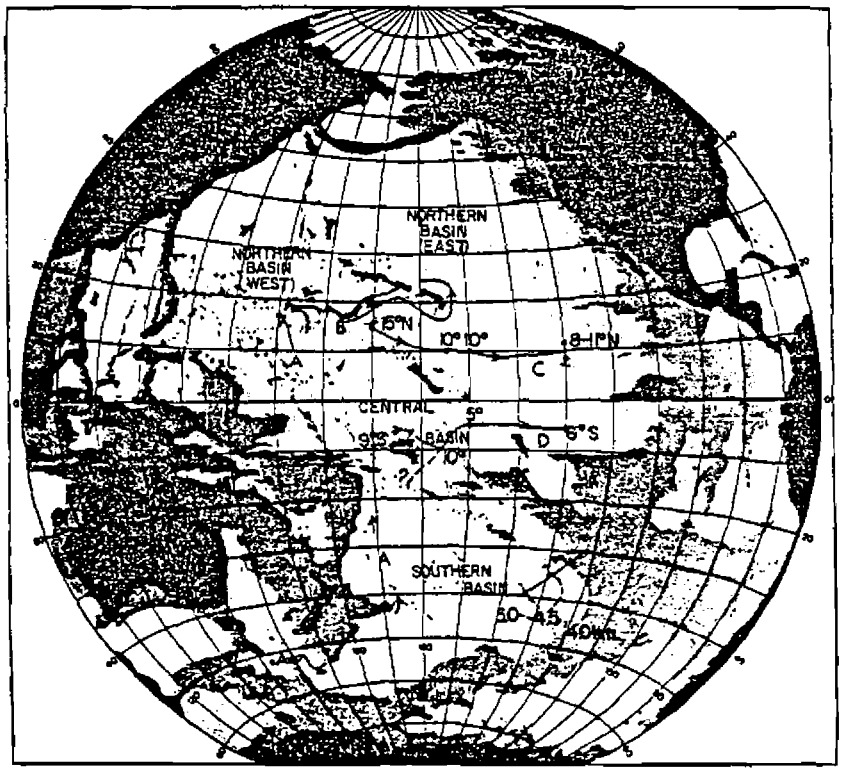


Fig. 5. Deep water masses in the Pacific Ocean. Arrows marked A indicate the Western Boundary current, and arrow B is the probable path of the eastern penetration of Pacific bottom water [*Edmond et al.*, 1971]. The dotted arrows indicate the probable spreading of the deep zonal water masses (C and D) inferred in this paper.

TABLE 1. Properties of the Zonal Cores

Properties	170°W	155°W	150°W	130°W
	Northern Core			
Latitude	15°N	10°N	10°N	8° to 11°N
Approximate depth, km	5.7	4.5	5.0	4.5
Potential temperature, °C	0.84	0.97	0.96	1.08
Dissolved oxygen, ml/l	4.2	4.0	4.1*	3.8
Potential density σ unit	27.84	27.83	27.83	27.82
Salinity, o/oo	34.71	34.71	34.70	34.70
Dissolved silicate, μmole/l	132	142	137	141
	Southern Core			
Latitude	9°S	10°S†	5°S	6°S
Approximate depth, km	4.4	4.3	4.8	4.3
Potential temperature, °C	0.73	0.99	0.90	1.06
Dissolved oxygen, ml/l	4.5	4.2	4.3*	4.0
Potential density σ unit	27.85	27.84	27.84	27.82
Salinity, o/oo	34.71	34.72	34.71	34.70
Dissolved silicate, μmole/l	119	136	127	136

*There is a discrepancy of 0.3 to 0.5 ml/l between the *Discovery* oxygen value in 1933 and the *Hudson 70* values. The *Hudson 70* oxygen values are on the high side [see *Duedall and Coote*, 1972].

†The trough at about 7°S and at 5.0-km depth is more likely to be the position of the central axis of the southern core, but, unfortunately, no oceanographic observations are available for this position.

formed by the Line Islands and the Galapagos Island extension at about 0° latitude. The presence of these two zonal deep water masses in the equatorial Pacific is consistent with the model of deep-water circulation proposed by *Stommel and Arons* [1960].

Acknowledgments. I thank Dr. Warren S. Wooster for reading the manuscript and for his comments, Dr. J. L. Reid for providing the potential density of the *Southern Cross* and the computer program for potential density, Dr. C. R. Mann for permission to use the *Hudson 70* data, and Mrs. V. M. Nadon for drafting the figures.

REFERENCES

Bien, G. S., N. W. Rakestraw, and H. E. Suess, Radiocarbon dating of deep water of the Pacific and Indian oceans, in *Radioactive Dating*, pp. 159–173, International Atomic Energy Agency, Vienna, 1963.

Chase, T. E., H. W. Menard, and J. Mammerickx, *Topography of North Pacific*, Institute of Marine Resources, University of California at San Diego, La Jolla, 1971.

Cromwell, T., R. B. Montgomery, and E. D. Stroup, Equatorial undercurrent in Pacific Ocean revealed by new methods, *Science, 119*, 648–649, 1954.

Duedall, I. W., and A. R. Coote, Oxygen distribution in the South Atlantic, *J. Geophys. Res., 77*, 496–498, 1972.

Edmond, J. M., Y. Chung, and J. G. Sclater, Pacific bottom water: Penetration east around Hawaii, *J. Geophys. Res., 76*, 8089–8097, 1971.

Knauss, J. A., On some aspects of the deep circulation of the Pacific, *J. Geophys. Res., 67*, 3943–3954, 1962.

Lynn, R. L., and J. L. Reid, Characteristics and circulation of deep and abyssal waters, *Deep Sea Res., 15*, 577–598, 1968.

Menard, H. W., *Marine Geology of the Pacific*, pp. 11–25, McGraw-Hill, New York, 1964.

Ocean Research Institute, University of Tokyo, Oceanographic data of KH-68-4 (*Southern Cross* cruise) of the *Hakuho Maru*, 67 pp., 1970*a*.

Ocean Research Institute, University of Tokyo, Preliminary report of the *Hakuho Maru* cruise KH-69-4 (*IBP* cruise), edited by R. Marumo, 68 pp., 1970*b*.

Reid, J. L., Jr., Evidence of a south equatorial countercurrent in the Pacific Ocean, *Nature, 184*, 209–210, 1959.

Scripps Institution of Oceanography, *Oceanic Observations of the Pacific: 1957*, 707 pp., University of California Press, Berkeley, 1965.

Stommel, H., and A. B. Arons, On the circulation of the world ocean, 1 and 2, *Deep Sea Res., 6*, 140–154, 217–233, 1960.

Weyl, P., On the oxygen supply of the deep Pacific Ocean, *Limnol. Oceanogr., 10*, 215–219, 1965.

Wooster, W. S., and G. H. Volkmann, Indications of deep Pacific circulation from the distribution of properties at 5 kilometers, *J. Geophys. Res., 65*, 1239–1248, 1960.

(Received August 9, 1972;
revised September 13, 1972.)

Diaphus hudsoni (Pisces: Myctophidae), a new lanternfish from the South Atlantic Ocean

R. E. ZURBRIGG

The Kingsway Animal Hospital, 3265 Bloor St. W., Etobicoke, Ont., Canada M8X 1E2

AND

W. B. SCOTT[1]

Royal Ontario Museum, Toronto, Ont., Canada M5S 2C6

Received January 22, 1976

ZURBRIGG, R. E., and W. B. SCOTT. 1976. *Diaphus hudsoni* (Pisces: Mycto dae), a new lanternfish from the South Atlantic Ocean. Can. J. Zool. 54: 1538–1541.

A new myctophid species, *Diaphus hudsoni*, was captured in the South Atlantic Ocean, and is described. It is similar to *Diaphus subtilis* Nafpaktitis, which occurs in the North Atlantic Ocean, but is definitely distinct with its slender, more numerous gill rakers (total 23–25), and non-continuous AOp–Prc series. The AO series numbers 5 + 5–6. The holotype is deposited in the Royal Ontario Museum, ROM 27569.

ZURBRIGG, R. E., et W. B. SCOTT. 1976. *Diaphus hudsoni* (Pisces: Myctophidae), a new lanternfish from the South Atlantic Ocean. Can. J. Zool. 54: 1538–1541.

Une nouvelle espèce de myctophidé, *Diaphus hudsoni*, a été capturée dans le sud de l'Océan Atlantique; on en trouvera ici la description. L'espèce *D. hudsoni* se rapproche de *Diaphus subtilis* Nafpaktitis qui habite l'hémisphère nord de l'Océan Atlantique, mais elle s'en distingue par ses branchiocténies plus nombreuses (23–25) et plus minces, et par sa série AOp–Prc non continue. La série AO compte 5 + 5–6. L'holotype a été déposé au Royal Ontario Museum, ROM 27569.

[Traduit par le journal]

Introduction

During the Hudson 70 Cruise made by the C.S.S. *Hudson* (Edmonds 1973), a number of myctophids were captured in the South Atlantic Ocean. Among these collections are some specimens of the genus *Diaphus* that are unlike any recorded by Fraser-Brunner (1949); they resemble *Diaphus subtilis* Nafpaktitis, 1968 and yet are distinctly different in a number of characters. These specimens are described here as representatives of a new species, *Diaphus hudsoni* (Fig. 1).

Materials and Methods

Dorsal (D) and anal fin (A) ray counts include the last two fin rays as one, the two having a common base. Pectoral (P) and ventral fin (V) ray counts exclude the rudimentary spine attached to the dorsal and outer ray of these fins respectively. All developed gill rakers are counted separately on the upper and lower limbs. The raker straddling the limbs was counted separately (Fig. 2).

Measurements were taken as follows: standard length (SL), from tip of snout to end of last entire vertebra (not to end of hypural); head length, from tip of snout to most posterior point of fleshy edge of operculum; eye diameter, width of iris; head depth, taken at a vertical from posterior tip of maxillary; body depth, taken at a vertical through the PLO; and caudal peduncle depth, least depth of peduncle.

The photophore nomenclature and the accompanying description is patterned after the method employed by Nafpaktitis (1968).

Specimens Examined

Holotype

ROM 27569, 58 mm SL; Hudson 70, station 30e, tow 35; 10 ft IKMT[2], 0–840 m; 44°14′ S 42°43′ W; 1032–1220 hours local time, 12/1/70; surface temperature 11.8 °C (Fig. 1).

Paratypes

ROM 27580, three specimens, 43, 47, 59 mm SL; Hudson 70, station 31*b*, tow 36; 10 ft IKMT, 0–250 m; 41°36′ S 46°49′13″ W; 2106–2225 hours local time, 13/1/70; surface temperature 17.4 °C.

National Museums of Canada, NMC 76-405, two specimens, 32.5, 43.5 mm SL; Hudson 70, station 17, tow 23; 10 ft IKMT, 0–590 m; 40°00′ S 30°00′ W; 0758–0930 hours local time, 28/12/69; surface temperature 15.2 °C.

[1]Present address: Huntsman Marine Laboratory, St. Andrews, N.B., Canada E0G 2X0.

[2]IKMT = Isaacs–Kidd Midwater Trawl.

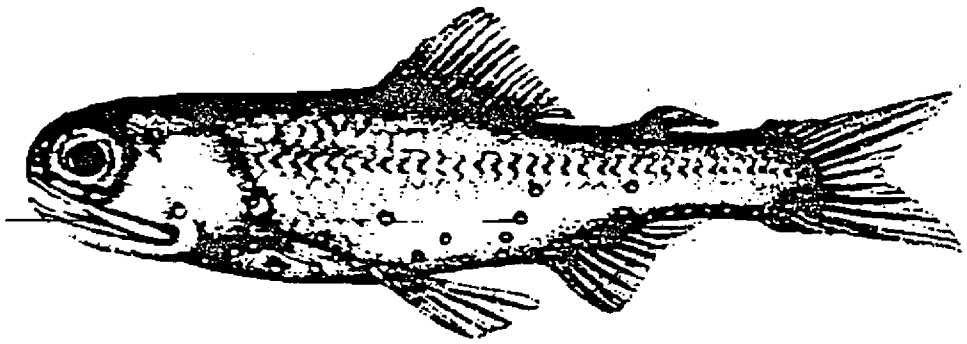


FIG. 1. *Diaphus hudsoni*, new species, holotype: 58 mm standard length; South Atlantic Ocean, 44°14′ S latitude, 42°43′ W longitude.

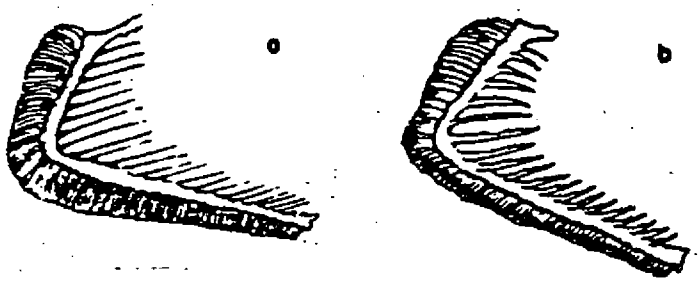


FIG. 2. (*a*) Right gill arch of *Diaphus hudsoni*, holotype. (*b*) Right gill arch of *Diaphus subtilis*.

***Diaphus hudsoni* sp.nov.**

Diagnosis

D 14(13); A 13(14); P 11; V 8; GR 7–8+1+15–16, total 23–25 (six specimens); AO 5+5 (four specimens), 5+6 (two specimens), total 10 or 11; LLS 35 or 36; vertebrae (excluding urostyle) 33.

A medium-sized myctophid fish; body heavy anteriorly, narrowing from origin of median fins to a relatively long and untapered, moderately deep caudal peduncle; head and anterior body evenly curved; head large; snout bluntly rounded, slightly overhanging upper jaw; inner row of teeth on posterior premaxillary large, broadly based, and recurved; vomer naked or almost so; length of upper jaw 65.2% (62.6–66.7%) of head length, extending well behind vertical through posterior margin of iris; maxillary not expanded posteriorly; eye very large, 35.5% (33.3–38.8%) of head length; pupil horizontally elliptical, larger than lens, aphakic space anterior to lens; a thin crescent of whitish tissue on iris posterodorsal to pupil; preopercular margin subvertical; operculum extending to PLO, its posterior margin truncate in large specimens but slightly pointed in young individuals; posterodorsal margin of operculum slightly angular.

Origin of dorsal fin at or somewhat *before* vertical through base of outer ray of ventral fin, midway between tip of snout and *fourth or fifth* AOp; origin of anal fin well behind vertical through end of dorsal fin base; base of adipose fin above *or behind* end of anal fin base; upper end of pectoral fin base on *or below* level of Op_2; pectoral rays extending to PO_3; ventral fin with rays extending to about the fourth anal fin ray.

The meristic data for the holotype are as follows: gill raker number 7+1+15; AO series 5 + 5; dorsal fin rays 14; anal fin rays 13; pectoral fin rays 11; pelvic fin rays 8; lateral line scales 35; vertebrae number (excluding urostyle) 33.

Proportions based on all six specimens, 32.5–59.0 mm standard length, and expressed as percentage of standard length (holotype given in square brackets): head length 31.9 (31.4–32.6) [31.4]; head depth 23.2 (22.0–24.2) [22.8]; iris diameter 11.3 (10.5–12.3) [10.9]; upper jaw length 20.6 (20.0–21.2) [20.5]; body depth 23.5 (22.0–24.4) [23.8]; caudal peduncle depth 11.0 (10.8–11.2) [10.9]; predorsal 48.6 (47.5–49.3) [48.3]; preanal 68.9 (67.2–71.3) [67.2]; prepectoral 31.4 (30.8–31.9) [30.9]; preventral 47.2 (45.8–48.0) [46.4]; preadipose 83.6 (80.7–84.9)

TABLE 1. Comparison of *Diaphus hudsoni* with three closely related Atlantic congeners

Character	*Diaphus hudsoni* (all 6 specimens)	*Diaphus subtilis* (Nafpaktitis (1968) and 4 specimens on loan from Woods Hole)	*Diaphus theta* (10 specimens, ROM 26430)	*Diaphus holti* (Nafpaktitis (1968) and 23 specimens from RHB 2050 and RHB 2534, on loan)
Gill rakers*	7–8+1+15–16 [23–25]	6–7+1+13–14 [20–22]	6–7+1+14–16 [21–23(24)]	5–7+1+12–14 [18–21]
Gill raker form	Long, slender	Medium length, broad	Medium length, broad	Short, broad
Dorsal rays	14(13)	13(12)	13(14)	(12)13 or 14
Eye/SL	11.3(10.5–12.3)	11.2(10.1–11.8) (loan specimens)	9.6(8.6–10.8)	11.4(10.3–12.2)
Lateral line scales	35 or 36	35 or 36	35–37	34 or 35
Caudal peduncle depth/SL	11.0(10.8–11.2)	10.6(10.0–11.2)	11.2(10.8–11.9)	12.5(12.0–12.9)
Vn, female	Longer than in *D. subtilis*; about equal in length to diameter of eye	Relatively short and deep; shorter than in *D. hudsoni*	As in *D. subtilis*	As in *D. hudsoni*
PLO position (PLO–LL/PLO–pectoral base)	1.3–2.0	1.5–2.0	2.2–3.6	2.0–2.5
Relative size of pectoral luminous patch	Medium (≥ one-half lens diameter)	Small (much less than one-half lens diameter)	Medium	Small
SAO_3 position	Over or before 1st anal fin ray base	Over 2nd–3rd anal fin ray bases	Over 2nd–4th anal fin ray bases	Over 2nd–3rd anal fin ray bases
AO counts	5+5–6	5(6)+6(5)	5(6)+5–6	5(4,6)+4(5)
AOp–Prc continuous?	Not†	Yes	No	No
Size at maturity	>60 mm SL	>60 mm SL	>60 mm SL	<60 mm SL

*A rudimentary gill raker was sometimes present on upper or lower arch but was not counted.
†One specimen with a tiny AOp_4 on left side, placed to make the AOp–Prc continuous.

[80.7]; length of dorsal fin base 18.5 (17.3–19.8) [17.9]; length of anal fin base 14.5 (13.6–15.4) [13.8].

Luminous Organs (Subadults)

A round forwardly directed Dn, one-half to three-quarters the size of nasal rosette, set in deep, cup-shaped recess above nasal apparatus; Vn along ventral border of eye, *slightly less in length than the diameter of iris*, probably larger in adult males (see following); anterior end of this organ wider than posterior and weakly bifurcating; a small roundish So inside pocket in dorsal end of a vertically elliptical structure, the latter protruding into the iris *well in front of* vertical through posterior margin of pupil and separated from Vn by a space equal to or greater than its own horizontal width; a continuous, thick strand of dark tissue extending from So, along dorsal aspect of Vn and anterior border of eye, reaching and fusing with dark tissue lining cup-shaped recess containing Dn.

A minute Op_1, close behind posterior tip of mouth; Op_2 a little larger than general body photophores, its anterior edge at a vertical from Op_1; Op_1 and Op_2 separated by a space 1.0 to 1.5 times Op_2 diameter.

PLO well behind vertical through uppermost ray of pectoral fin, nearer to latter than to lateral line, distance between PLO and lateral line from 1.3 to 2.0 times as great as that between PLO and upper end of pectoral fin base; PVO_1 below level of posterior tip of mouth and in an approximate line, midway between PO_1 and PVO_2 or slightly closer to PVO_2; PVO_2 on or slightly above level of posterior tip of mouth, *well in advance of vertical through anterior border of* PO_2, and immediately in front of bases of lower pectoral rays; first PO interspace between 1.5 and 2.0 times width of second, which is equal to or slightly smaller than that between PO_3 and PO_5; from ventral view often photophores of first PO pair or alternatively second PO pair markedly closer to each other than those of the

other PO pairs; PO_5 abruptly and widely divergent, situated about *1.0 to 1.5 times* its own diameter from, and anteromesial to, base of outermost ray of ventral fin; PO_4 above level of PVO_2, at or close behind vertical through centre of PO_3 and in an approximate straight line with PLO and PO_5; VLO behind vertical through base of outermost ray of ventral fin, midway between lateral line and ventral fin base or somewhat lower; VO_1 very near and mesad to base of innermost ray of ventral fin; VO_2 often nearer VO_1 than to VO_3, which is somewhat higher than a straight line connecting VLO with VO_5; SAO on a slightly angular line; SAO_1–SAO_2 interspace often distinctly narrower than that between SAO_2 and SAO_3; SAO_1 above and *slightly behind* VO_3; SAO_2 over anus or space between anus and origin of anal fin; SAO_3 *over or before anterior end of anal fin base* and 1.0 to 1.5 times its own diameter below lateral line; AOa_1 not at all or very slightly raised; AOa_5 elevated and *sometimes* AO_4 *elevated*, the posterior part of this series forming a gentle arc; *Pol at or behind vertical through centre of* AOa_5 and about 1.5 to 2.0 times its own diameter below lateral line; AOp evenly spaced, on a straight line, nearly always well separated from the Prc; first AOp behind end of anal fin base; *Prc forming an ascending arc; AOp–Prc interspace 1.5 to 2.5 times as wide as the first Prc interspace* (see footnote Table 1); Prc_4 2.0 to 3.0 times its own diameter below midlateral line.

A luminous scale at PLO, its width 2.0 to 3.0 times that of a general body photophore.

Unfortunately, none of the captured specimens are sexually mature. However, two specimens show a long, narrow, forward projection of luminous tissue from the ventral half of the Vn similar to that of young *D. subtilis* males (Nafpaktitis 1968, p. 94), and slightly thinner than that of *D. holti* Taning immature males at the same developmental stage.

The authors have found the VLO–ventral fin base measurement to be quite unreliable. The ventral fin base may be fixed in a range of vertical positions depending on a number of factors (e.g. condition of the fish, presence of food in gut, crushing of the fish's ventral profile during fixation, etc.).

Diaphus hudsoni derives its name from the C.S.S. *Hudson*, in honour of the Hudson 70 Cruise around the Americas.

Discussion

Diaphus hudsoni is similar to *D. subtilis*, and therefore, also to *D. holti* Taning in the Atlantic and *D. theta* Eigenmann and Eigenmann in the Pacific (Nafpaktitis 1968). However, *D. hudsoni* has longer and more slender gill rakers as well as a higher range of gill raker counts than any of these other species (Fig. 2) but *D. hudsoni* rakers are not more rugose. Some other differences, such as AOp–Prc separation, SAO_3 position, etc., are presented in concise form in Table 1. It is interesting to note that the three very closely related *Diaphus* species ring the Western Hemisphere with apparently mutually exclusive ranges: *Diaphus theta* (Pacific), *D. subtilis* (N Atlantic), and *D. hudsoni* (S Atlantic).

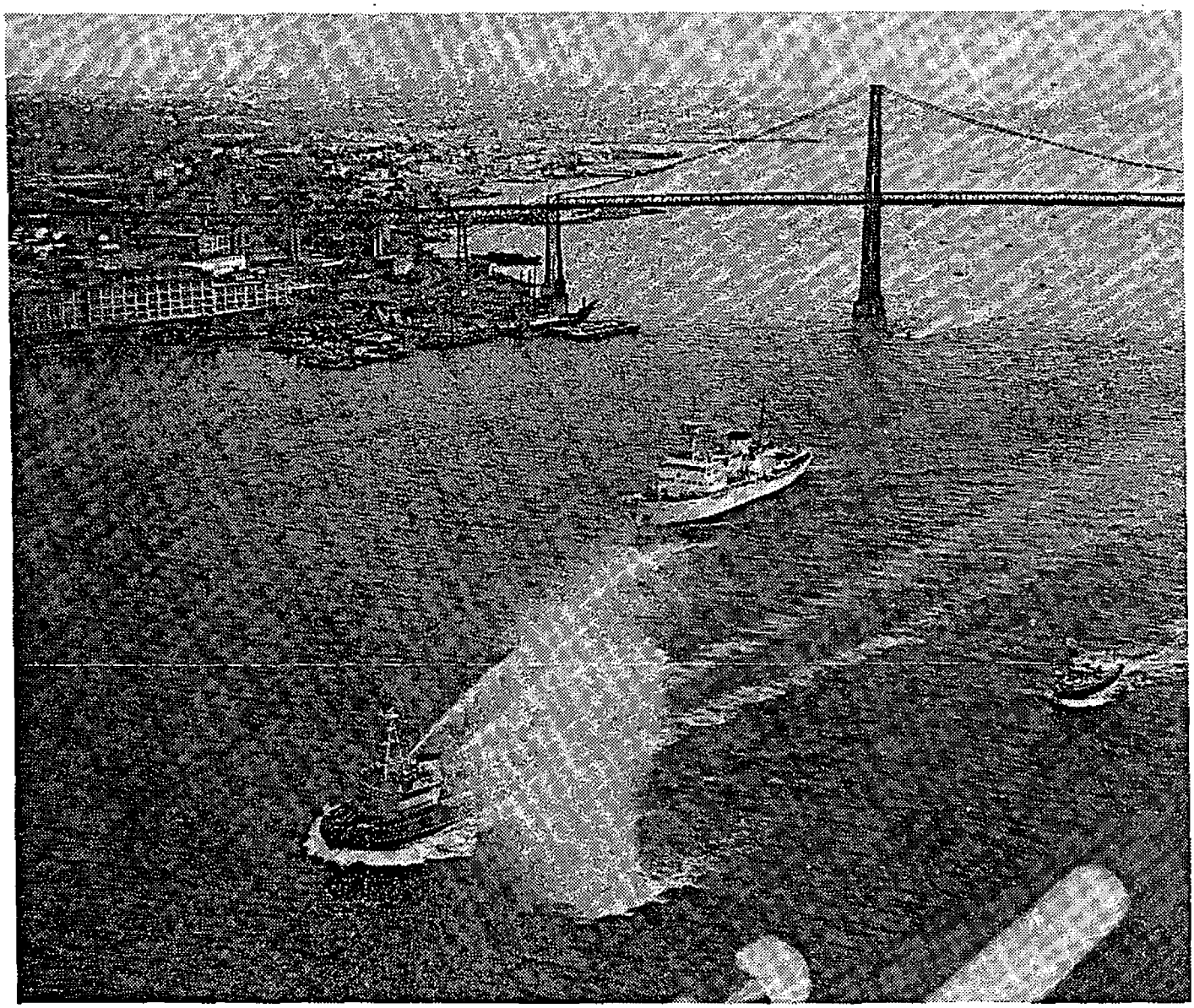
Acknowledgements

We thank Myvanwy M. Dick and J. E. Craddock for loan of specimens from Woods Hole Oceanographic Institution. We are grateful to the Department of Energy, Mines and Resources for the opportunity to participate in the Hudson 70 cruise. This work was made possible by a National Research Council of Canada grant (A-4284) to W. B. Scott.

Edmonds, A. 1973. Voyage to the edge of the world. McClelland and Stewart Limited, Toronto, Ontario.

Fraser-Brunner, A. 1949. A classification of the fishes of the family Myctophidae. Proc. Zool. Soc. London, 118(IV): 1019–1106.

Nafpaktitis, B. G. 1968. Taxonomy and distribution of the lanternfishes, genera *Lobianchia* and *Diaphus*, in the North Atlantic. Dana-Rep. Carlsberg Found. 73.



The expedition ends. It is nearly 1400 hrs.
on 16 October 1970 and the CSS Hudson,
her circumnavigation of the Americas completed,
steams into her home port and a waiting reception
at the Bedford Institute of Oceanography.